[Downloaded free from http://www.journalofdiabetology.org on Wednesday, November 2, 2022, IP: 49.205.98.146]

Original Article

Prediction and Risk Factor Analysis of Obesity-related Proteinuria among Individuals with Metabolic Syndrome

Syed Vaziha Tahaseen, P. Kiranmayi[1], Marni Rakshmitha[2], Bezawada Anusha[3]

Department of Biochemistry, SRR & CVR Govt. Degree College (A), Vijayawada, [1]Department of Biochemistry, Acharya Nagarjuna University, Guntur, [2]Department of Biochemistry, Gitam University, Visakhapatnam, [3]Department of Biotechnology, Acharya Nagarjuna University, Guntur, Andhra Pradesh, India

Abstract

Objective: In the present modern era of time, poor and frantic lifestyle has led to an enumerate increase in the number of people with obesity and metabolic syndrome (MS). Epidemiological studies have shown the incidence of chronic kidney disease (CKD) risk factors in individuals with obesity and MS; despite the nonclear evidence on the existing potential risk factors, it became important to reassess existing potential risk factors that are involved in disease progression and its further complications. The strongest risk factor of CKD, albumin-to-creatinine ratio (ACR) recognized as a marker of MS and obesity. This study was carried out to identify the association of obesity (body mass index [BMI]) as a risk factor for albuminuria and to observe the dependence and association with albuminuria of each critical and basic factor of MS. **Design:** We conducted the potential risk factor analysis on 913 subjects, including 398 females and 515 males, from various diabetic hospitals of Vijayawada, Andhra Pradesh from early 2013 to June 2015. The medical records of the patients followed up; the anthropometric measurements and clinical parameters were retrospectively collected. The total subjects were categorized as subjects with and without MS as per National Cholesterol Education Program Adult Treatment Panel (NCEP-ATPIII) and the subjects with BMI more than 30 kg/m^2 were defined as obese according to WHO classification. **Results:** Student's *t* test analysis indicates a significant difference for ACR with mean values of 39.5 ± 44.8 and 18.4 ± 24.3 ($P < 0.0001$) in subjects with MS and without MS, 43.4 ± 48.3 and 36.7 ± 42.5 ($P < 0.02$) in obese and nonobese subjects, respectively. Chi-square analysis showed a significant association ($P < 0.05$) between MS and ACR and correlation analysis manifested significant association ($P < 0.01$) between ACR and FBS, TG, B.P, and Age in subjects with MS. The subjects with high prevalence of albuminuria exhibited significant association with an odds ratio (OR) of 1 (referent) 1.9 (95% CI, 1.34–2.58, $P = 0.0002$), 1.5 (95% CI, 1.11–1.96, $P = 0.0082$) for FBS >110 mg/dL, and TG > 150 mg/dL, respectively. Although the subjects with obesity showed no correlation with albuminuria, the risk for albuminuria was 1.5 times (95%CI 1.03–2.40, $P = 0.03$) higher among obese male subjects compared to obese female subjects. **Conclusion:** Our study strongly supports that albuminuria is highly prevalent among the subjects, with MS showing a significant positive association between obesity (BMI) with albuminuria in males only.

Keywords: ACR, BMI, chronic kidney disease, FBS, HDL, metabolic syndrome, TG

Introduction

Chronic kidney disease (CKD) has become a major global health problem with an estimated worldwide affected population of 2 million. In this context, early detection of CKD is crucial to prevent the progression of CKD to end-stage renal disease (ESRD). The presence of persistently elevated albuminuria is an early clinical marker of CKD and a predictor for cardiovascular diseases (CVD) and mortality. The clinical manifestation of CKD includes albuminuria/proteinuria as an important diagnostic tool for primary treatment[1-3] and also considered in the definition of the metabolic syndrome (MS) by the World Health Organization.[4] The MS is defined as a

Received: 22-May-2020, **Revised:** 08-June-2020, **Accepted:** 09-June-2020, **Published:** 31-March-2021

Access this article online

Quick Response Code:

Website: www.journalofdiabetology.org

DOI: 10.4103/jod.jod_37_20

Address for correspondence: Dr. P. Kiranmayi, Department of Biochemistry, Acharya Nagarjuna University, Nagarjuna Nagar, Guntur 522510, Andhra Pradesh, India. E-mail: Kiranmayi.kodali@rediffmail.com

This is an open access journal, and articles are distributed under the terms of the Creative Commons Attribution-NonCommercial-ShareAlike 4.0 License, which allows others to remix, tweak, and build upon the work non-commercially, as long as appropriate credit is given and the new creations are licensed under the identical terms.

For reprints contact: wkhlrpmedknow_reprints@wolterskluwer.com

How to cite this article: Tahaseen SV, Kiranmayi P, Rakshmitha M, Anusha B. Prediction and risk factor analysis of obesity-related proteinuria among individuals with metabolic syndrome. J Diabetol 2021;12:140-5.

[Downloaded free from http://www.journalofdiabetology.org on Wednesday, November 2, 2022, IP: 49.205.98.146]

constellation of risk factors including obesity, impaired fasting glucose (FBS >110 mg/dL), increased triglycerides (TG>150 mg/dL), associated with insulin resistance, hypertension (systolic >140 mm Hg), low levels of high-density lipoprotein cholesterol (HDL< 40 mg/dL)[5] and chronic inflammation,[6] leads to composite metabolic derangements that contribute to CKD and coronary artery disease. As per the prior investigations, the relationship between albuminuria, and MS risk factors percentage of prevalence being reported to be 10%-42% in persons with type II diabetes, 11%-40% in people with hypertension and 5%-10% in those without diabetes, hypertension or cardiovascular disease.[7-9] Obesity has been pointed out as one of the critical factors of MS, and the body mass index (BMI) estimate of more than 30 kg/m^2 indicates obesity, and people with MS are at higher risk of many chronic diseases with reduced life expectancy. One of the molecular mechanisms underlying obesity-related CKD is the abnormal or excessive accumulation of fat, characterized by adipocytes hypertrophy. This phenomenon induces hypoxia,[10] promoting inflammation and secretion of adipokines such as leptin, which specifically binds to the receptors on glomerulus and show a direct effect on kidney by promoting excessive production of pro-fibrotic transforming growth factor beta (TGF-β) which further enhance the production of extracellular matrix (ECM) components leading to fibrosis.[11,12] In obesity, increased adipose storage or inflammation of adipocytes brings about insulin resistance conversely insulin sensitivity reduction by several intracellular mechanisms causing the onset of hyperglycemia facilitating renal fibrosis.[13]

In the studies with obesity, the possible existence of a relationship between the roles of obesity executed as BMI in routine clinical practice with kidney dysfunction remains controversial. Weisinger *et al.*[14] first reported that massive proteinuria is associated with obesity. Similarly, limited studies have systematically addressed the association between microalbuminuria with obesity or central obesity irrespective of gender and other predisposing conditions. Hoffmann *et al.* [15] conversely found that there is no difference in albuminuria levels in lean and obese glucose-tolerant subject's studies.[16] However, very fewer studies focused on microalbuminuria, especially in obese nondiabetic, no hypertensive subjects. Our study focused to predict the risk factors of CKD in obesity-associated albuminuria in the south Asian population having unique anthropometric body measurements and to substantiate the clinical practices in most of the hospitals where BMI usually considered as the only clinical parameter to determine obesity.

Materials and Methods

Study area and population

This study is a cross-sectional analysis carried out in Vijayawada, Krishna District, Andhra Pradesh, India, among subjects aged between 20 and 84 years. The study was conducted on 913 subjects including 398 females (43.6%) and 515 (56.4%) males during their hospital visit who underwent medical screening at various diabetic hospitals of Vijayawada from early 2013 to June 2015 and have undergone diagnosis. Majority of them had MS. The exclusion criteria of the study were pregnant women with MS and the patients who had other CKDs. The clinical diagnosis reports and anthropometric measurements regarding height and weight were collected with patient consent.

Sample size (n) was calculated as follows = z^2 p $(1–p)/d^2$. In this study, the sample size for obesity was calculated using prevalence P = 6.5%[17] and confidence level of 95% and the precision of 0.05, by adding 10% nonresponsive rate.The total sample size was n = 103. The sample size for obese was 258. Among them, 112 were males and 146 were females. For MS, the sample size was calculated using a 95% confidence level with the margin of error 0.05 and prevalence P = 20%[18] by adding 10% non-responsive rate, the total sample size should be n = 270, but a total number of 874 MS subjects included in the study.

Sampling technique and procedure

Laboratory findings

According to the "III Adult Treatment Panel" of the "National Cholesterol Education Program" (NCEP-ATPIII of 2001) principles, MS includes the evaluation of the following risk factors: (1) fasting serum glucose (FBS), (2) TG (triglycerides), and (3) HDL (high-density lipoproteins) with consideration of BMI >30 kg/m^2 and with systolic pressure > 130 mm Hg and diastolic pressure > 90 mm Hg. According to the National Kidney Foundation (NKF) guidelines (Joint National Committee on Prevention, Detection, Evaluation, and Treatment of High Blood Pressure, 1997),[19] the urinary albumin (μg/mL) to creatinine (mg/mL) ratios in an untimed urine specimen is a convenient way to assess albumin excretion. Albuminuria is classified based on severity as normal healthy category ACR <30 μg/mg and unhealthy albuminuria category ACR >30 μg/mg. Among the 913 subjects, 402 (44%) are unhealthy albuminuria subjects and 511 (56%) are healthy albuminuria subjects.

Physical examination and clinical data

The anthropometric measurements were carried out as per the hospital standard operating procedures, the height was measured using calibrated height meters with subjects standing bare-footed in erect position placing the feet together and weight measured with the calibrated weighing machine. BMI was calculated as weight in kilograms divided by a square of height in meters. Blood pressure (BP) was measure by trained nurses employing a standard mercury sphygmomanometer, while the subject sit in a chair with feet on the floor and arm reinforced elbow is at around heart level. The average of two readings was used

[Downloaded free from http://www.journalofdiabetology.org on Wednesday, November 2, 2022, IP: 49.205.98.146]

for the analysis. All participants' clinical data related to routine laboratory findings were collected from medical records of the respective hospitals.

Statistical analysis

We performed statistical analysis using the SPSS software package. The results summarized as percentages and as the mean ± standard deviation (SD). The Pearson chi-square test and Student's *t* test were used to compare the differences between categorical variables. An appropriate condition among each parameter tested using Spearman's correlation coefficient. A value of $P < 0.05$ was considered a statistically significant difference. We calculated odds ratios using a 2×2 table.

Ethical consideration

We conducted this study with the ethical consideration approval got from the institutional review board of Guntur Medical College and Government General Hospital, Guntur, Andhra Pradesh, India and approved by the Helsinki Declaration. (Application number GMC/IEC/120/2018).

Results

This cross-sectional study performed on 913 randomly selected individuals with the majority (874) participants having MS. Irrespective of their metabolic condition we categorized the total subjects into three different categories. Each time in this study, the total subjects were categorized individually following presence/absence of MS as with MS (95.7%) and without MS (4.3%), similarly with obesity (28%) and without obesity (72%) and with healthy albuminuria (56%) and unhealthy albuminuria (44%). The mean and SD values of the following risk factors such as anthropometric, BP, lipid profile, and blood

Table 1: Comparison of baseline characteristics in, without MS and with MS groups, without MA and with MA groups and without obesity and with obesity groups using Student's *t* test

	Metabolic syndrome (MS)				
	Without MS ($n = 39$)		With MS ($n = 874$)		
Risk factor	Mean	SD	Mean	SD	*P* Value
BMI	25.57	2.08	28.23	4.64	<0.0001*
FBS	91.00	5.69	147.73	50.79	<0.0001*
ACR	18.43	24.27	39.48	44.76	<0.0001*
TGs	112.72	29.74	174.70	89.91	<0.0001*
HDL	39.28	5.32	40.84	5.65	0.07
BP	125.00	16.37	128.26	17.77	0.22
Age	50.56	13.89	50.38	10.48	0.94
	Microalbumin (MA)				
	Without MA (albumin < 30) ($n = 402$)		With MA (albumin > 30) ($n = 511$)		
Risk factor	Mean	SD	Mean	SD	*P* Value
BMI	27.88	4.31	28.42	4.91	0.07
FBS	138.17	46.76	154.39	54.69	<0.0001*
ACR	12.21	7.86	72.09	48.67	<0.0001*
TGs	169.26	89.32	175.61	88.72	0.28
HDL	40.77	5.69	40.79	5.58	0.95
BP	126.75	16.36	129.87	19.18	<0.0001*
Age	50.17	10.25	50.66	11.12	0.48
	Obesity				
	Without obesity BMI < 30) $n = 655$		With obesity (BMI > 30) $n = 258$		
Risk factor	Mean	SD	Mean	SD	*P* Value
BMI	25.87	2.58	33.80	3.55	<0.0001*
FBS	145.62	52.21	144.52	47.95	0.76
ACR	36.68	42.47	43.38	38.58	0.02*
T. Gs	173.65	89.52	168.00	87.92	0.10
HDL	41.00	5.70	40.21	5.45	0.056
B. P	127.45	18.15	129.84	16.48	0.06
Age	50.33	10.92	50.55	9.90	0.77

SD = standard deviation, BMI = body mass index, FBS = fasting blood sugar, ACR= albumin creatinine ratio, HDL = high-density lipoproteins, BP = blood pressure

**P* value significant at <0.05

[Downloaded free from http://www.journalofdiabetology.org on Wednesday, November 2, 2022, IP: 49.205.98.146]

glucose measures are compared and ascertained [Table 1], similarly correlated with each parameter [Table 2].

Among all baseline characteristics, a significant difference was observed between the mean values of BMI, FBS, ACR, and TG in subjects with the prevalence and absence of MS [Tables 1 and 2] and in subjects with MS, albuminuria (ACR) is highly correlated with the incidence of FBS, TG, BP, and age ($P < 0.01$) [Table 2]. However, the frequency albuminuria is high with the FBS, BP, and TG in the study population and seems to be less associated with obesity [Tables 1 and 2] suggesting the least association between albuminuria and overweight. But we found a significant correlation between ACR with obesity in males ($P < 0.05$) [Tables 3 and 4] emphasizing the sexual dimorphism in adipose tissue distribution and associated comorbidities.

Discussion

The occurrence and severity of MS are followed by the association of the sum of critical risk factors that include obesity, hypertension, insulin resistance, dyslipidemia, and albuminuria. According to CJKN studies and NCEP ATP III, the relationship between kidney damage and MS is complex. It is also in debate whether the collective existence of all the risk factors of MS improves CKD beyond that afforded by individual risk factors. However, very fewer studies have been undertaken to incorporate the coexistence of risk factors associated with MS and CKD. The present study results targeted to recognize and correlate the strong integrated relationship of fasting blood glucose, hyper-triglyceridemia, and high systolic BP the three of the five risk factors of MS in association with albuminuria than each independent risk factor.

In this cross-sectional study, we observed a significant difference in albuminuria in obese and nonobese subjects [Table 1], but we observed gender difference in the association of BMI with albuminuria; BMI had a greater association with ACR in males, whereas in females BMI is not associated with ACR [Tables 3 and 4]. Many studies show that there is a strong, linear relationship between obesity and hypertension. Chang *et al.*[20] study reported that systolic BP is an independent risk factor of

Table 2: Correlation analysis of each parameter with baseline parameters in subjects with metabolic syndrome ($n = 874$), with unhealthy ACR ($n = 402$), and with obesity ($n = 258$)

With metabolic syndrome							
Risk factor	**BMI**	**FBS**	**ACR**	**TGs**	**HDL**	**BP**	**Age**
BMI	1.0	0.281	0.104	0.591	0.111	0.087	0.340
FBS	0.281	1.0	0.000*	0.001*	0.051	0.537	0.031*
ACR	0.104	0.000*	1.0	0.008*	0.939	0.001*	0.002*
T.Gs	0.591	0.001*	0.008*	1.00	0.000*	0.468	0.094
HDL	0.111	0.051	0.939	0.000*	1.00	0.150	0.037*
B.P	0.087	0.537	0.001*	0.468	0.150	1.00	0.000*
Age	0.340	0.031*	0.002*	0.094	0.037*	0.000*	1.00
With unhealthy ACR							
Risk factor	**BMI**	**FBS**	**ACR**	**TGs**	**HDL**	**BP**	**Age**
BMI	1.0	0.965	0.334	0.472	0.159	0.629	0.459
FBS	0.965	1.0	0.000*	0.010	0.658	0.267	0.189
ACR	0.334	0.000*	1.0	0.002*	0.936	0.020	0.000*
T.Gs	0.472	0.010*	0.002*	1.00	0.000*	0.430	0.080
HDL	0.159	0.658	0.936	0.001*	1.00	0.264	0.422
B.P	0.629	0.267	0.020*	0.430	0.264	1.00	0.000*
Age	0.459	0.189	0.000*	0.080	0.422	0.000*	1.00
With obesity							
Risk factor	**BMI**	**FBS**	**ACR**	**TGs**	**HDL**	**BP**	**Age**
BMI	1.0	0.501	0.232	0.600	0.854	0.130	0.230
FBS	0.501	1.0	0.018*	0.015*	0.767	0.308	0.043*
ACR	0.232	0.018*	1.0	0.003*	0.586	0.711	0.027*
TGs	0.600	0.015*	0.003*	1.00	0.197	0.759	0.820
HDL	0.854	0.767	0.586	0.197	1.00	0.333	0.193
BP	0.130	0.308	0.711	0.759	0.333	1.00	0.002*
Age	0.230	0.043*	0.027*	0.820	0.193	0.002*	1.00

*Correlation is significant at <0.05 level (two tailed)

[Downloaded free from http://www.journalofdiabetology.org on Wednesday, November 2, 2022, IP: 49.205.98.146]

microalbuminuria in euglycemic normotensive males. Our analysis also confirms this association between obesity and high BP. Yesmin *et al.*[21] report shows that there is no microalbuminuria in obese women without diabetes and/or hypertension suggesting in obese women and lean women; urinary albumin excretion was similar. A recent study on Japanese hypertensive patients showed that there were sex-related differences in the associations of insulin resistance and obesity to left ventricular hypertrophy.[22] Also Foster *et al.*[23] showed that in comparative Framingham heart study microalbuminuria is associated with visceral adipose tissue in men but not in women.

This study reports elucidate that in subjects with MS and unhealthy albuminuria [Table 2], coexistence of three of the five risk factors is strongly associated with the total conditions of the study. Age also shows a positive correlation with albuminuria. With these findings, our data analysis suggests that a gender difference may exist in the association between BMI and albuminuria. The difference might be due to gender-related specifications, such as the role of sex hormones on the inflammatory mechanism that links albuminuria to central obesity or it can be also predicted that the muscle mass in males is more than in females, which can warrant the creatinine levels and gender difference in interpretation.

The gender difference can be partly because of the prevalence of smoking in males, and the absence of smoking in females. In females, there is a highly significant relationship between anthropometric variables and albuminuria due to potential sex-based divergence in fat distribution pattern and renal outcomes for differential steroid hormone levels. The contradiction may be because of higher upper body adiposity and higher visceral fat for a given BMI in the Asian Indians. The study conducted by Wang *et al.*[24] on aboriginal people by receiver operating characteristic (ROC) analysis suggested that measuring body size-related diabetes waist circumference is the best method comparing a few more methods of body size measurement.

Conclusion

This study shows the relationship between obesity and the risk for CKD by gender-specific examination, which was measured clinically in the form of micro/macroalbuminuria that leads to proteinuria. Our findings suggest that BMI has an association with albuminuria in men showing that obesity calculated as BMI is a risk factor for kidney damage in males with a high prevalence of FBS, BP, TG, and age. However the contradictory results with females demonstrate that obesity calculated as BMI is not a high-risk factor for kidney harm in females, due to an account of gender specific variation in distribution of fat indicating men having a relatively more central allocation of fat giving the fact that male obese with hyperglycemia,

Table 3: Pearson chi-square analysis between risk factors and albuminuria

	Status of microalbumin				X^2 (df)	*P*	phi
	Healthy		Unhealthy				
	N	(%)	*N*	(%)			
Metabolic syndrome (MS							
Yes	481	55.0	393	45.0	7.26	0.005*	+0.09
No	30	76.9	9	23.1			
Obesity							
Yes	135	52.3	123	47.6	1.92	0.165	+0.05
No	377	57.4	280	42.6			
Obesity in males							
Yes	54	48.2	58	51.7	4.04	0.04*	+0.09
No	232	58.9	162	41.1			

Computed only for a 2 x 2 table

*Significant at $P < 0.05$

Table 4: Risk factors of microalbuminuria in the study population

Sex	Risk factors	OR (95% CI)	*P* Value*
Males	BMI > 30 kg/m^2	1.51(1.033–2.397)	0.03*
Females	BMI > 30 kg/m^2	0.98(0.65–1.47)	0.93
Both genders	FBS > 110 mg/dL	1.865(1.34–2.58)	0.0002*
Both genders	Triglycerides > 150 mg/dL	1.47(1.105–1.957)	0.0082*
Both genders	HDL < 40 mg/dL	0.99(0.746–1.328)	0.976
Both genders	BP > 130 mm Hg	1.29(0.971–1.71	0.078

OR = odds ratio

*Significant at $P < 0.05$

[Downloaded free from http://www.journalofdiabetology.org on Wednesday, November 2, 2022, IP: 49.205.98.146]

hypertension and hypertriglyceridemia are at high risk of developing CKD. The major limitation of this study is that it was conducted by not focusing on dietary patterns of the individuals that might influence the relationship between the severity of obesity and microalbuminuria and ignored alternative methods for the calculation of obesity.

Acknowledgement

We express a deep sense of gratitude to Dr. P. Anil Kumar, assistant professor at Department of Biochemistry, School of Life Sciences, University of Hyderabad, for his direction and suggestions in all aspects of my research work.

Financial support and sponsorship

Nil.

Conflicts of interest

There are no conflicts of interest.

References

1. National Kidney Foundation. K/DOQI clinical practice guidelines for chronic kidney disease: Evaluation, classification, and stratification. Am J Kidney Dis 2002;39: S1-S266.
2. Sarnak MJ, Levey AS, Schoolwerth AC, Coresh J, Culleton B, Hamm LL, *et al*.; American Heart Association Councils on Kidney in Cardiovascular Disease, High Blood Pressure Research, Clinical Cardiology, and Epidemiology and Prevention. Kidney disease as a risk factor for development of cardiovascular disease: A statement from the American Heart Association councils on kidney in cardiovascular disease, high blood pressure research, clinical cardiology, and epidemiology and prevention. Circulation 2003;108:2154-69.
3. Diercks GF, van Boven AJ, Hillege JL, de Jong PE, Rouleau JL, van Gilst WH. The importance of microalbuminuria as a cardiovascular risk indicator: A review. Can J Cardiol 2002;18:525-35.
4. Alberti KG, Zimmet PZ. Definition, diagnosis and classification of diabetes mellitus and its complications. Part 1: Diagnosis and classification of diabetes mellitus provisional report of a WHO consultation. Diabet Med 1998;15:539-53.
5. Alberti KG, Eckel RH, Grundy SM, Zimmet PZ, Cleeman JI, Donato KA, *et al*.; International Diabetes Federation Task Force on Epidemiology and Prevention; National Heart, Lung, and Blood Institute; American Heart Association; World Heart Federation; International Atherosclerosis Society; International Association for the Study of Obesity. Harmonizing the metabolic syndrome: A joint interim statement of the international diabetes federation task force on epidemiology and prevention; national heart, lung, and blood institute; American Heart Association; world heart federation; international atherosclerosis society; and international association for the study of obesity. Circulation 2009;120:1640-5.
6. Ramkumar N, Cheung AK, Pappas LM, Roberts WL, Beddhu S. Association of obesity with inflammation in chronic kidney disease: A cross-sectional study. J Ren Nutr 2004;14:201-7.
7. Deferrari G, Repetto M, Calvi C, Ciabattoni M, Rossi C, Robaudo C. Diabetic nephropathy: From micro- to macroalbuminuria. Nephrol Dial Transplant 1998;13:11-5.
8. Rosa TT, Palatini P. Clinical value of microalbuminuria in hypertension. J Hypertens 2000;18:645-54.
9. Jones CA, Francis ME, Eberhardt MS, Chavers B, Coresh J, Engelgau M, *et al*. Microalbuminuria in the US population: Third national health and nutrition examination survey. Am J Kidney Dis 2002;39:445-59.
10. Sun K, Kusminski CM, Scherer PE, Sun K, Kusminski CM, Scherer PE. Adipose tissue remodeling and obesity find the latest version : Review series Adipose tissue remodeling and obesity. J Clin Invest 2011;121:2094-101.
11. Tang J, Yan H, Zhuang S. Inflammation and oxidative stress in obesity-related glomerulopathy. Int J Nephrol 2012;2012:1-11.
12. Wolf G, Chen S, Han DC, Ziyadeh FN. Leptin and renal disease. Am J Kidney Dis 2002;39:1-11.
13. Anil Kumar P, Swathi Chitra P, Bhanuprakash Reddy G. Metabolic syndrome and associated chronic kidney diseases: Nutritional interventions. Rev Endocr Metab Disord 2013;14:273-86.
14. Weisinger JR, Kempson RL, Eldridge FL, Swenson RS. The nephrotic syndrome: A complication of massive obesity. Ann Intern Med 1974;81:440-7.
15. Hoffmann IS, Jimenez E, Cubeddu LX. Urinary albumin excretion in lean, overweight and obese glucose tolerant individuals: Its relationship with dyslipidaemia, hyperinsulinaemia and blood pressure. J Hum Hypertens 2001;15:407-12.
16. Nielsen S, Jensen MD. Relationship between urinary albumin e x c retion, body composition, and hyperinsulinemia in normotensive glucose - tolerant adults. Diabetes Care 1999;22:1728-33.
17. Schwartz GL, Sheps SG. A review of the sixth report of the joint national committee on prevention, detection, evaluation, and treatment of high blood pressure. Curr Opin Cardiol 1999;14:161-8.
18. Fouad M, Ismail MI, Gaballah A, Reyad E, ELdeeb S. Prevalence of obesity and risk of chronic kidney disease among young adults in Egypt. Indian J Nephrol 2016;26:413-8.
19. Singh AK, Kari JA. Metabolic syndrome and chronic kidney disease. Curr Opin Nephrol Hypertens 2013;22:198-203.
20. Chang Y, Yoo T, Ryu S, Huh BY, Cho BL, Sung E, *et al*. Abdominal obesity, systolic blood pressure, and microalbuminuria in normotensive and euglycemic Korean men. Int J Obes (Lond) 2006;30:800-4.
21. Yesim TE, Ugurlu S, Caglar E, Balci H, Ucgul A, Sarkis C, *et al*. Investigation of microalbuminuria in nondiabetic, normotensive obese women. Intern Med 2007;46:1963-5.
22. Shigematsu Y, Norimatsu S, Ogimoto A, Ohtsuka T, Okayama H, Higaki J. The influence of insulin resistance and obesity on left atrial size in Japanese hypertensive patients. Hypertens Res 2009;32:500-4.
23. Foster MC, Hwang SJ, Massaro JM, Hoffmann U, DeBoer IH, Robins SJ, *et al*. Association of subcutaneous and visceral adiposity with albuminuria: The Framingham heart study. Obesity (Silver Spring) 2011;19:1284-9.
24. Wang Z, Hoy WE. Body size measurements as predictors of type 2 diabetes in aboriginal people. Int J Obes Relat Metab Disord 2004;28:1580-4.

RESEARCH ARTICLE

SAMRIDDHI Volume 14, Issue 1, 2022 Print ISSN: 2229-7111 Online ISSN: 2454-5767

Synthesis and Spectral Characteristics of CoO mixed $ZnO\text{-}Bi_2O_3\text{-}B_2O_3$ Glasses

Bejjipurapu Chandrasekhar[1,3], Gunnam Nagarjuna[2], Sopinti Ramesh[1], B.V. Raghavaiah[3]*

[1]Department of Physics, Acharya Nagarjuna University, Nagarjuna Nagar, Guntur, 522510, Andhra Pradesh, India

[2]Department of Chemistry, SRR & CVR Government Degree College (A), Vijayawada, 520 004, Krishna District, Andhra Pradesh, India

[3]Department of Physics, RGUKT-Ongole Campus, Rajiv Gandhi University of Knowledge Technologies–AP, Ongole, 523001, Andhra Pradesh, India

Abstract

The conventional melt-quench process synthesized bismuth borate glasses containing ZnO and CoO. CoO is introduced up to a maximum of 0.8 mol% by replacing boric acid. All the prepared samples were tested by x-ray diffraction and scanning electron microscopy techniques. Characterization methods confirm the non-crystalline behavior of samples. The density of the samples was found to increase while molar volume diminishes against the content of cobalt oxide. UV-visible spectra have shown the necessary bands of divalent and trivalent cobalt ions. Infrared spectra display all characteristic vibrational bands of different molecular groups. Increasing structural degree of disorder is evidenced from the analyses of results, and details are presented.

Keywords: Bismuth, Borate glasses, Cobalt, Infrared, UV-visible absorption.

SAMRIDDHI : A Journal of Physical Sciences, Engineering and Technology (2022); DOI: 10.18090/samriddhi.v14i01.7

Introduction

Recently, a large amount of concentration has been paid to explore the spectral features of cobalt ions in different glass systems due to their significant visible and infrared emission that makes them potential materials for non-linear optical absorbers and fast switching devices.[1-3] When cobalt ions are added with heavy metal oxide like bismuth oxide enables them as prominent candidates for non-linear optical devices. Bi_2O_3 has the characteristic electron pair arrangement that opens pathways for large susceptibility coefficients, in turn, suitability for optical switches solid-state ionic devices.[4,5] Cobalt ions exhibit divalent and trivalent states, where divalent states give characteristic pink color to the glass samples. Based on the occupation symmetry of 'Co' ions in the fundamental borate structure would result in other colors. B_2O_3 is considered a very good network developer among various glass formers and could form glasses at low temperatures with high transparency.[6] The borate glass network allows cobalt and zinc ions and causes structural changes by conversion of BO_3 to BO_4along with non-bridging oxygens (NBOs). The structural degree of disorder is very much linked with oxygens and leads to changes in physical and spectroscopic properties of $ZnO\text{-}Bi_2O_3\text{-}B_2O_3$: CoO glasses. Limited numbers of studies are available on spectroscopic features of cobalt ions in zinc bismuth borate glass network. However, most of the investigations were focused on spectral features of 'Co' ions in borate glasses, silicate glasses without zinc oxide.[4,7] Hence, the current investigation is focused at the preparation of $ZnO\text{-}Bi_2O_3\text{-}B_2O_3$glasses doped with cobalt oxide and further characterization by XRD, SEM, absorption, and infrared studies to explore the usability of samples for optical switches applications because of their structural degree of disorder against replacement of zinc oxide by cobalt oxide. Attention is given to cobalt ions' oxidation conditions and their occupational symmetry in the borate glass system.

Corresponding Author: B.V. Raghavaiah, Department of Physics, RGUKT-Ongole Campus, Rajiv Gandhi University of Knowledge Technologies–AP, Ongole, 523001, Andhra Pradesh, India, e-mail: bv_raghavaiah@rediffmail.com

How to cite this article: Chandrasekhar, B., Nagarjuna, G., Ramesh, S., & Raghavaiah, B.V. (2022). Synthesis and Spectral Characteristics of CoO mixed $ZnO\text{-}Bi_2O_3\text{-}B_2O_3$ Glasses. *SAMRIDDHI : A Journal of Physical Sciences, Engineering and Technology,* 14(1), 44-47.

Source of support: Nil

Conflict of interest: None

Experimental Methods

A specific glass composition $ZnO\text{-}Bi_2O_3\text{-}B_2O_3$: CoO has been selected. Composition specifications of samples with their

© The Author(s). 2022 Open Access This article is distributed under the terms of the Creative Commons Attribution 4.0 International License (http://creativecommons.org/licenses/by/4.0/), which permits unrestricted use, distribution, and non-commercial reproduction in any medium, provided you give appropriate credit to the original author(s) and the source, provide a link to the Creative Commons license, and indicate if changes were made. The Creative Commons Public Domain Dedication waiver (http://creativecommons.org/publicdomain/zero/1.0/) applies to the data made available in this article, unless otherwise stated.

nomenclature are presented below. The glasses exhibited transparency up to 0.8 mol% of CoO; thereafter, glass nature was present but opaque in nature.

ZC_2: 19.8 ZnO- 25Bi_2O_3-55 B_2O_3: 0.2 CoO
ZC_4: 19.6 ZnO- 25 Bi_2O_3-55 B_2O_3: 0.4 CoO
ZC_6: 19.4 ZnO- 25 Bi_2O_3-55 B_2O_3: 0.6 CoO
ZC_8: 19.2 ZnO- 25 Bi_2O_3-55 B_2O_3:0.8 CoO

AR grade chemicals of Bi_2O_3, H_3BO_3, ZnO, and CoO powders in suitable amounts (all in mol%) had been very well jumbled using a mortar and liquefied in a platinum crucible withinside the temperature variety of 900 to 980°C in a PID temperature managed furnace for approximately1 hour. The resultant bubble-free melt was then poured in a brass mold and subsequently annealed at 300°C. After the annealing process, the samples prepared were ground and optical polished to the dimensions of 1 cm × 1 cm × 0.2 cm. Samples' solid-state nature is tested using an X-ray diffractometer with CuK_α radiation. Scanning Electron Microscope is used to verify the morphology of glasses. With Archimedes' principle and using o-xylene (99.99% pure), densities of samples were measured. Infrared transmission spectra were recorded on a JASCO-FT/IR–5300 spectrophotometer up to a resolution of 0.1 cm^{-1} in the spectral range 400–2000 cm^{-1}usingpotassium bromide pellets (300 mg) containing pulverized sample (1.5 mg). These pellets were pressed in a vacuum die at ~680MPa. The absorption spectra spanning from 300 to 1800 nm were carried out with a spectral resolution of 0.1 with a UV–vis–NIR spectrophotometer.

Results and Discussion

Before proceeding to spectroscopic properties, material features are calculated using experimental density values. Average molecular weight, density, cobalt ion concentration increase with the content of cobalt oxide. It could be due to the replacement of zinc oxide by cobalt oxide, whose molecular weight is higher than that of ZnO. The increase in density is associated explicitly with the cross-linkages with boron groups and other available transition metals along with interstitial positions/vacancies.[7,8] In another way, the interionic distance and polaron radius exhibited decrement with the rising content of CoO (Table 1). XRD patterns of ZnO-Bi_2O_3-B_2O_3: CoO glasses are shown in Figure 1. All X-ray scans of ZnO-Bi_2O_3-B_2O_3: CoO glasses have exhibited similar patterns, including a significant wide band from 20° to 30° that assures the non-crystalline behavior of glasses. Scanning electron microscopic pictures show no voids. However, tiny crystal granules are presented that could be due to the process of gradual cooling from a molten state to normal condition. The SEM images of two samples are presented in Figures 2 and 3.

UV-Visible-NIR spectra of all glass samples in the range 350 to 1800 nm are carried out. An interesting observation is that the absorption edges of all samples exhibited redshift against CoO content. Every sample has shown relevant bands; one small band in the range 520 to 550 nm assigned to $^4T_{1g}(F) \rightarrow {}^2T_{1g}(H)$ Co^{2+} ions occupied octahedrally, second peak is in the range 590 to 605 nm attributed to $^4A_2(^4F) \rightarrow {}^4T_1(^4P)$ and third peak in the range 1400 to 1450 nm attributing to transition $^4A_2(^4F) \rightarrow {}^4T_1(^4F)$ of divalent cobalt ions.[8] Another noteworthy observation is the very small absorption peak from 710 to 725 nm that could be due to transition $^5T_2 \rightarrow {}^2E$ corresponding octahedrally occupied trivalent cobalt ions.[9]

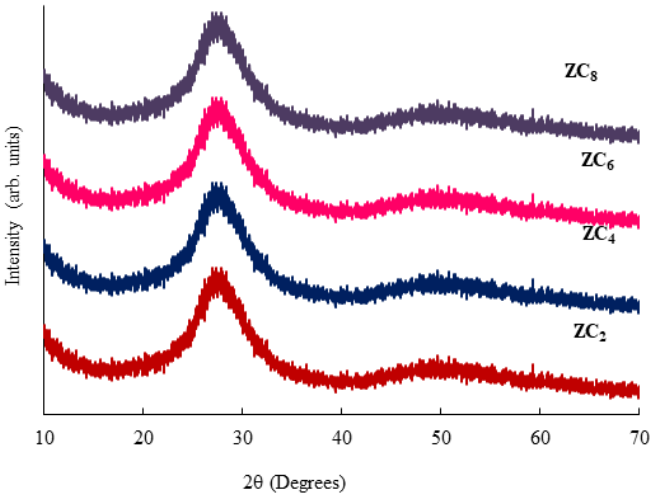


Figure 1: XRD patterns of ZnO-Bi_2O_3-B_2O_3: CoO glasses.

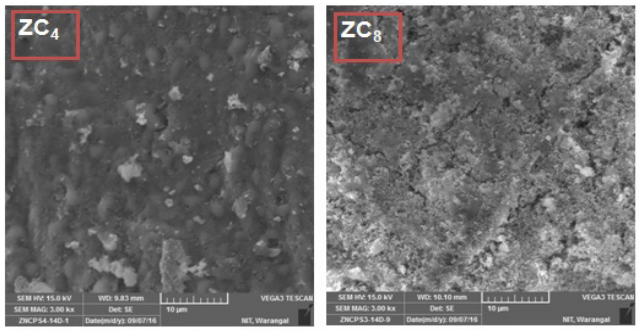


Figure 2: SEM images of ZC_4 and ZC_8 glasses.

Table 1: Experimental physical features of ZnO-Bi_2O_3-B_2O_3: CoO samples.

Glass	*Avg. Mol. Wt.*	*Density (g/cm^3)*	*Conc. of 'Co' ions N_i ($10^{21}/cm^3$)*	*Inter ionic distance of 'Co' ions $r_{i\,(A°)}$*	*Polaron radius $_{RP\,(A°)}$*
ZC_2	171.37	4.701	3.31	0.67	0.27
ZC_4	171.69	4.703	6.59	0.53	0.21
ZC_6	172.01	4.704	9.88	0.46	0.18
ZC_8	172.33	4.706	13.15	0.42	0.17

Table 2: IR spectral positions of $ZnO\text{-}Bi_2O_3\text{-}B_2O_3$: CoO glasses.

	Borate groups (cm^{-1})			
Glass	*BO_3*	*BO_4*	*B-O-B/B-OBi*	*Co-O groups (cm^{-1})*
ZC_2	1398	1072	731	---
ZC_4	1393	1079	733	659, 561
ZC_6	1386	1084	736	651, 553
ZC_8	1382	1087	739	640, 549

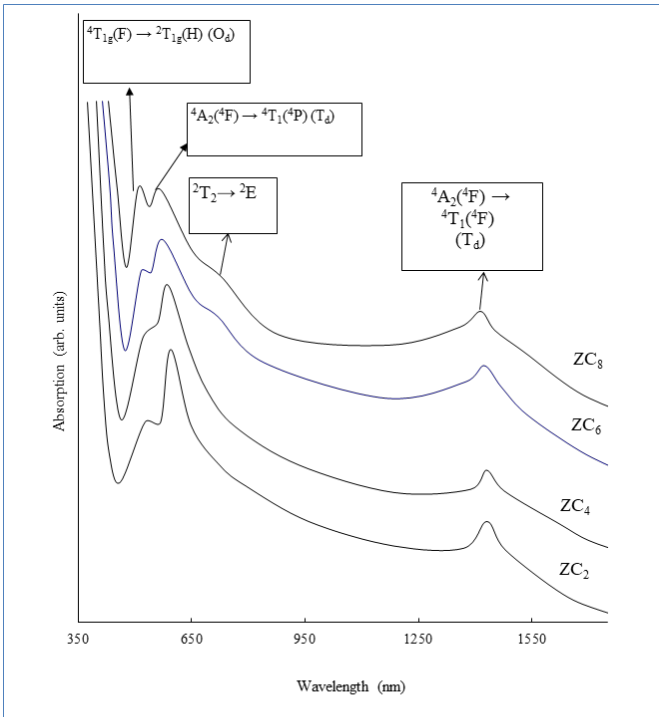


Figure 3: Optical absorption spectra of $ZnO\text{-}Bi_2O_3\text{-}B_2O_3$: CoO glasses recorded at room temperature.

The subsequent two bands were found to decrease at the expense of the first band.

An increasing dopant of CoO has resulted in a decrease in the half-width and the intensity of the bands in the range 590 to 1500 nm, whereas the 550 nm band has risen. These variations confirm the slow conversion of "Co" ions from the triangular pyramid to octahedral regularity. These ions, along with zinc ions, act as modifiers leading to NBOs, causing a blue shift in the bandgap.

Figure 4 depicts the infrared transmittance spectra of $ZnO\text{-}Bi_2O_3\text{-}B_2O_3$: CoO glasses. All the samples have evidenced the characteristic bands corresponding to all possible cross-connections among various structural clusters in the glass system. Pertaining to borate groups, BO_3 units in the range 1382 to 1398 cm^{-1}, BO_4 units in the range 1072 to 1087 cm^{-1}, and B-O-B bending vibrations & B-O-Bi in the range 731 to 739 cm^{-1} are observed.[10] Two tiny bands in the regions 549 to 561 cm^{-1} and 640 to 659 cm^{-1} are observed and attributed to Co-O linkages. The intensity of BO_3, B-O-B / B-O-Bi linkages, and Co-O bands is found to increase while the BO_4 band is found to decrease. The information on vibrational bands is

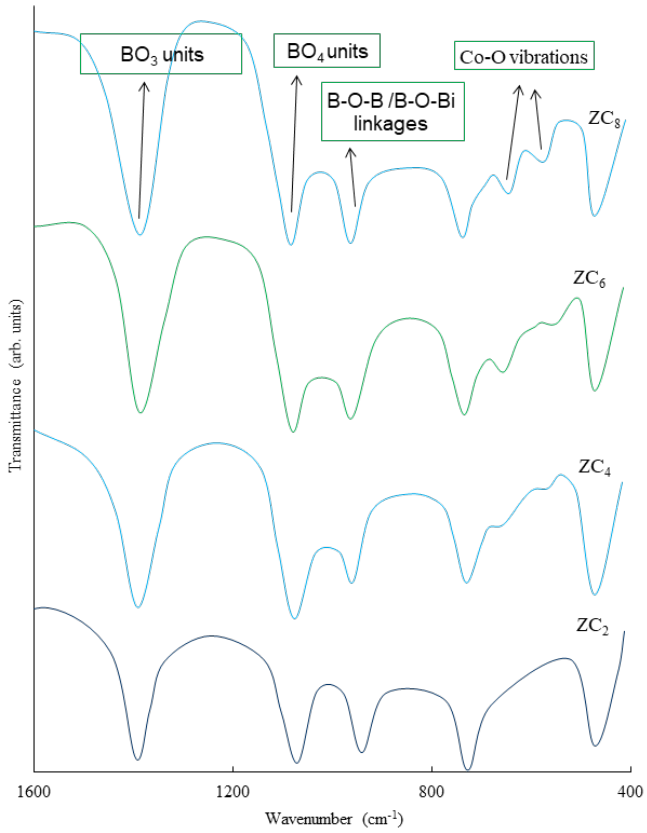


Figure 4: IR spectra of $ZnO\text{-}Bi_2O_3\text{-}B_2O_3$: CoO glass samples.

summarized in Table 2. When the content of CoO is low, i.e., 0.2 mol% (Sample ZC_2), no bands corresponding to Co^{III}-O bands are seen. Another band is located in the range 470 to 480 cm^{-1} that could be due to impurities or zinc oxide-related vibrational bands.

Conclusion

Preparation of $ZnO\text{-}Bi_2O_3\text{-}B_2O_3$: CoO glasses were done using the melt quenching method. The XRD studies show the broad halo, which is a characteristic non-crystalline nature. The scanning electron microscopic images indicated irregular shaping of samples. The IR studies have evidenced the presence of different borate, cobalt and bismuth linkages. From the analyses of IR results, it is very clear that the symmetrical structural vibrational groups diminished with the increasing dopant of CoO. The optical absorption spectra confirm conversational occupational symmetry and the

presence of cobalt ions' oxidation states. All the studies were directed to the fact of cobalt ions changing from tetrahedral to octahedral surroundings that might be the reason for more structural degree of disorder.

References

[1] Abhiram. J., Rajaramakrishna. R.,Rajashekara. KM, Jagannath. G., Vinayak. P., Venugopal RaoS., EraiahB., JagadeeshaA.V., Jakrapong, K., and Suchart, K.2020, Investigation on non-linear optical properties of gold nanoparticles doped fluoroborate Glasses for optical limiting applications,J. Non-Crys. Solid., 538, 120010.

[2] Johnson. B.,Chand. N. R. K., Sudhakar. B. K., and Srinivasa Rao. G., 2016, Chemical durability, thermal stability and spectroscopic studies of the influence of Ni^{2+} ions in oxyfluorophoshate glasses, J. Mat. Sc.: Mat. Ele., 27, pp 8833-8847.

[3] Abdelghany. A.M., El- Damrawi.G., Oraby. AH, andMadshal. MA, 2018, Optical and FTIR Structural Studies on CoO-Doped Strontium Phosphate Glasses, *J. Non-Crys.Solid.*, 499,pp153-158.

[4] Vinaya Teja. P.M., Rajyasree. Ch., Srinivasa Rao. P., Ramesh Babu. A., Tirupataiah. Ch., And Krishna Rao. D, 2012, Structural and electrical properties of ZnF_2-Bi_2O_3-GeO_2 glasses doped with CoO, J. Mol. Str., 1014, pp 119-125.

[5] Arti Yadav, Dahiya. MS, Hooda. A., Agarwal. A. and Khasa., 2018, Nano-Crystalline phase evolution and structural modification in Co/V substituted Li_2O-Bi_2O_3-B_2O_3 glasses, AIP Conf. Proc., 1953,090008.

[6] Satyanarayana. T., Gandhi. Y., Valente, A., Kityk. IV and Veeraiah. N., 2011, Influence of titanium ions on spectroscopic properties of TeO_2-Sb_2O_3-B_2O_3: TeO_2 glass ceramics, Phys. Status Solidi C-John Wiley & Sons, 11-12, pp 3082-3086.

[7] Satyanarayana. T., Valente, M.A., Nagarjuna. G., and Veeraiah. N., 2013, Spectroscopic Features of manganese doped tellurite borate glass ceramics, J. Phys. Chem. Solids, 74, pp 229-235.

[8] Sallum. O.I., Abdel Galil. A., Moussa. NL, 2021, Optimizing of optical and structure Characters of borate glasses by different concentration of CoO: Electron beam irradiation dosimetry, Mater, Chem. Phys., 269, 124767.

[9] Satyanarayana. T., Kityk. I.V., Piasecki. M., Brik. M. G., Gandhi. Y., and Veeraiah. N. 2009, Structural investigations on PbO-Sb_2O_3-B_2O_3: CoO glass-ceramics by means of spectroscopic and dielectric studies. J. Phy. Cond. Mat. (IOP-London), 21, 245104.

[10] Ravi Kumar. G., Srikumar. T., Rao. M. C., Venkat Reddy. P., and Srinivasa Rao. Ch., 2018, Influence of cobalt ions on spectroscopic and dielectric properties of Sb_2O_3 doped lithium fluoroboro phosphate glasses, Mater. Res. Exp., 5, 035203.

International Journal of Botany Studies
www.botanyjournals.com
ISSN: 2455-541X
Received: 04-08-2021, Accepted: 18-08-2021, Published: 08-09-2021
Volume 6, Issue 5, 2021, Page No. 19-26

HPLC Identification of active flavonoid and phenolic compounds from leaf extracts of *Diospyros chloroxylon* Roxb.

Nageswara Rao Naik B[1*], Jyothi D[2], Vishnuvardhan Z[3]
[1] Department of Environmental sciences, Acharya Nagarjuna University, Guntur, Andhra Pradesh, India
[2] Department of Botany SRR & CVR Govt. College Vijayawada Andhra Pradesh, India
[3] Department of Botany and Microbiology, Acharya Nagarjuna University, Guntur, Andhra Pradesh, India

Abstract
Diospyros is the most versatile genus belonging to family Ebanceae. It comprises more than 500 species distributed in tropical and warm temperate regions of the world. These species have been used in the traditional medical systems of several countries. Therefore, the *Diospyros* species drawn the attention of research investigators to analyze their phytochemical profile and biological activities. The present study relates to phytochemical screening of *Diospyros chloroxylon* leaf extracts through HPLC technique. Twelve phenolic and flavonoid compounds (*viz*., (1) Apigenin-6, 8-di-C-glucopyranoside (2) Kaempferol- 3, 7-di-O-rhamnosid (3) Kaempferol-7-O-rhamnoside (4) Isorhamnetin (5) Isorhamnetin-3-O-dihexoside (6) Scutellarein7-O-β-D-glucopyranoside (7) gallic acid (8) Quercetin (9) Kaempferol (10) Rutin (11) (−) epigallocatechine and (12) Epicatechin gallate) were identified in the aqueous and methanolic leaf extracts of *Diospyros chloroxylon*. The above compounds confirm the medicinal potential of *Diospyros chloroxylon* and emphasizes the need of further pharmacological studies in this species.

Keywords: phenoloics, flavonoids, HPLC protocols, medicinal plants, pharmacological importance

Introduction
Plants contain the bioactive compounds useful in many biological activities (Rahman *et al* 2018) [16]. Flavonoids are an important antioxidant agents. Phenolic compounds are the most commonly occurring group of phytochemicals and play a potential protective role against various kinds of oxidative diseases *viz*., antimutagenicity, anti-bacterial action, antiviral activity, anti-inflammatory and apoptotic actions (Glucin *et al* 2010 & 2011) [5, 6]. Natural flavonoids and phenols exhibited many protective therapeutic potential against dreadful diseases. Flavonoids present in fruits and leafy vegetables are responsible for useful health benefits through radical scavenging and chelating activity. Several studies have suggested that rutin, kaempferol, quercetin, apigenin etc., are well-known for their anti-inflammatory, anti-allergic, anti-thrombotic, hepatoprotective, anti-spasmodic and anticancer properties (Mahesh Kumar & Kerti 2012) [13]. The chromatographic techniques such as high performance liquid chromatography (HPLC), gas chromatography (GC), capillary electrophoresis (CE), nuclear magnetic resonance (NMR) and mass spectrometry have led to the identification of multitude of bioactive ingredients from many plant species (Sasidharan *et al* 2011, Katiyar *et al* 2012) [19, 8]. In recent times 'High performance liquid Chromatography (HPLC)' gained prominence for the analysis of plant extracts. This led to increasing interest in the isolation, identification and study of the biological activities of natural compounds. HPLC allows a high resolution rapid and reproducible determination of trace amounts of these compounds. The different naphthoquinens, anthroquinones, terpenoids, phenolic acids and flavonoids have been identified from *Diospyros* species (Rauf *et al* 2017) [17]. Because of the antioxidant, hepatoprotective, anti-inflammatory, analgesic, antipyretic, antihypertensive, antidiabetice, neuroprotective, antimicrobial, antiprotozal, fungicidal, antihelmintic, insecticidal, mollucidal, cytotoxicity, anti-tumor, multi drug resistance (MDR) reversal activities reported in *Diospyros* genus, the species have ever been considered as the most important medicinal species. Hence, the present study is aimed at the identification of some biological compounds (i.e, phenolics and flavonoids) from methanolic and aqueous leaf extracts.

Material and methods
HPLC instrument
Agilent 1100 series HPLC with Quaternary G1311 A pump, COLCOM G1316A thermostat column temperature control, Thermostatic auto sampler G 1329A with sample volume of 0. 1 – 1500 µL and variable programmable UV detector G 1314 A. The instrument was operated and integrated with Agilent chem. station LC software. High Performance Liquid Chromatographic (HPLC) protocols of Zang *et al* (2010) [23], Sait *et al* (2015) [18] and Hilal Bardakci *et al* (2018) [7] were used to identify different flavonoids in the aqueous leaf extracts of *Diospyros chloroxylon*. The HPLC protocols standardized by Adriana Skendi *et al* (2017) [2], Gini & Jothi (2018) [4] and Nadia Zeghad *et al* (2019) [14] were used for the identification of phenolic compounds in the methanolic leaf extracts of *Diospyros chloroxylon*.

Identification of flavonoid compounds through HPLC
Chemicals and Solvents
HPLC Grade Methanol is purchased from Thermo Fisher Scientific India private limited, Mumbai.
HPLC Grade Acetonitrile is purchased from Merck chemicals private limited, Mumbai.
HPLC Grade Water is purchased from Thermo Fisher Scientific India private limited, Mumbai other chemicals

used were of Laboratory reagent grade and were purchased from Merck chemicals, Mumbai.

Test method 1 (Zang *et al* 2010) [23].
Column: ZORBAX ODS C18 column (4.6 × 12.5 mm id, 5 µm).

Mobile phase: solvent A (0.1% formic acid aqueous, V/V, pH 2.6) and solvent B (acetonitrile).

Gradient program
0-10 min, linear gradient 10.0%-20.0% B; 10-20 min, isocratic 20.0% B 20-25 min, linear gradient 20.0%-30.0% B; 25-35 min, linear gradient 30.0%-33.0% B
35-40 min, linear gradient 33.0%-40.0% B; 40-60 min, linear gradient 40.0%-60.0% B

Mobile phase flow rate: 0.8 mL·min-1;
Sample volume: 20 µL; **Colum temperature:** 30°C; **Detector wavelength:** 254 nm

Test method 2 (Sait *et al* 2015**)** [18]**.**
Column: Ascentis C18 column (250 mm×4.6 mm I.D., 5 µm).
Mobile phase: (A) 0.1M HCOOH in H_2O and (B) ACN.

Gradient program
0-15 min from 10% to 20% B; 15-35 min from 20% to 30% B; 35-45 min from 30% to 50% B

Mobile phase flow rate: 1.0 mL·min-1
Sample volume: 20 µL;
Colum temperature: 30°C;
Detector wavelength: 352 nm

Test method 3 (Hilal Bardakci *et al* 2018**)** [7]**.**
Column: zorbax C18column (4.6 × 150 mm, 3.5 µm).
Mobile phase: Phase A was H2O, the mobile phase B was ACN both containing 0.02% acetic acid.

Gradient program
0 min 15% B; 10 min 20% B; 13 min 20% B; 15 min 25%B; 20 min 30% B; 25 min 30% B; 30 min 50% B.

Mobile phase flow rate: 1.0 mL·min-1; **Sample volume:** 20 µL; **Colum temperature:** 30°C

Detector wavelength: 340 nm

Identification of phenolic compounds through HPLC
Chemicals and Solvents
HPLC Grade Methanol is purchased from Thermo Fisher Scientific India private limited, Mumbai.
HPLC Grade Acetonitrile is purchased from Merck chemicals private limited, Mumbai.
HPLC Grade Water is purchased from Thermo Fisher Scientific India private limited, Mumbai.
Other chemicals used were of Laboratory reagent grade and were purchased from Merck chemicals, Mumbai.

Test method 1 (Gini and Jothi 2018**)** [4]
Column: ZORBAX ODS C18 column (4.6 × 12.5 mm id, 5 µm).
Mobile phase: Solvent A (acetonitrile) and solvent B (0.1% phosphoric acid in water).

Gradient program
92% of solvent B and was held at this concentration for 0–35 min, by 78% of solvent B for the next 35–50 min.

Mobile phase flow rate: 1.0 mL·min-1;
Sample volume: 20 µL; **Colum temperature:** 30°C

Detector wavelength: 280 nm,

Test method 2 (Adriana Skendi *et al* 2017**)** [2]
Column: Ascentis C18 column (250 mm×4.6 mm I.D., 5 µm); **Mobile phase:** (A)1% acetic acid in water, (B) acetonitrile and (C) methanol.

Gradient program
0 min, the A: B: C proportion was 90:0:0; 10 min, 80:4:16; at 25 min, 75:5:20;
30 min, 65:5:30; 31 min, 40:0:60;37 min, 35:20:45;50 min, 20:80:0.

Mobile phase flow rate: 1.5 mL·min-1; **Sample volume:** 20 µL,; **Colum temperature:** 30°C

Detector wavelength: 260 nm

Test method 3 (Nadia Zeghad *et al* 2019**)** [14]
Column: ZORBAX ODS C18 column (4.6 × 12.5 mm id, 5 µm).

Mobile phase: Trifluoroacetic acid 0.05% (v/v) in water to which methanol was added in a linear gradient from 95:5 to 5:95 (v/v) within 70 min.

Mobile phase flow rate: 1.0 mL·min-1; **Sample volume:** 20 µL; **Colum temperature:** 30°C,

Detector wavelength: 280 nm.

Results
The aqueous leaf extracts of *Diospyros chloroxylon* when subjected to HPLC method of Zang *et al* (2010) [23] resulted in the identification of four compounds. Figure 1 shows the chromatogram of leaf extract with 10 peaks. These peaks along with their retention time were compared with the retention time of flavonoid compounds available in literature. Peak number 4, 6, 8 and 10 were corresponded to Apigenin-6, 8-di-C-glucopyranoside (RT: 13.233 min), Kaempferol- 3, 7-di-O-rhamnoside (RT: 20.65 min), Kaempferol-7-O-rhamnoside (RT: 34.583 min) and Isorhamnetin (RT: 44.167) (table 1).
The chromatogram of aqueous leaf extract of *Diospyros chloroxylon* as per the protocol of Sait *et al* (2015) [18] gave seven peaks of which peak number four tallied with Isorhamnetin-3-*O*-dihexoside (RT: 18.33 min) and peak number seven was tallied with 'Isorhamnetin' (RT: 44.23 min) in the literature (Fig 2 & Table 2).
The chromatogram obtained with the leaf aqueous extract as per the protocol of Hilal Bardakci *et al* (2018) [7] is presented in figure 3. In the chromatogram six peaks were observed, of which peak number three (RT 10.56 min) was tallied with 'Scutellarein 7-O-β-D-glucopyranoside' (table 3). Hence, by the application of three different HPLC protocols to the leaf aqueous extracts of *Diospyros chloroxylon*, a total of six flavonoid compounds were identified in the leaf of *Diospyros chloroxylon* that include (i) Apigenin-6, 8-di-C-glucopyranoside (ii) Kaempferol- 3, 7-di-O-rhamnoside (iii) Kaempferol-7-O-rhamnoside (iv) Isorhamnetin (v) Isorhamnetin-3-O-dihexoside and (vi) Scutellarein 7-O-β-D-glucopyranoside (Table 4).
Methanolic leaf extracts of *Diospyros chloroxylon* were also analysed as per the HPLC protocol of Adriana Skendi *et al* (2017) [2]. The chromatogram exhibited nine peaks (figure 4), out of which peak one (Gallic acid RT: 4.5 min), peak three ((−) epigallocatechine RT: 10.0667 min), peak six (Rutin RT: 33.5667 min), peak seven (Quercetin RT:

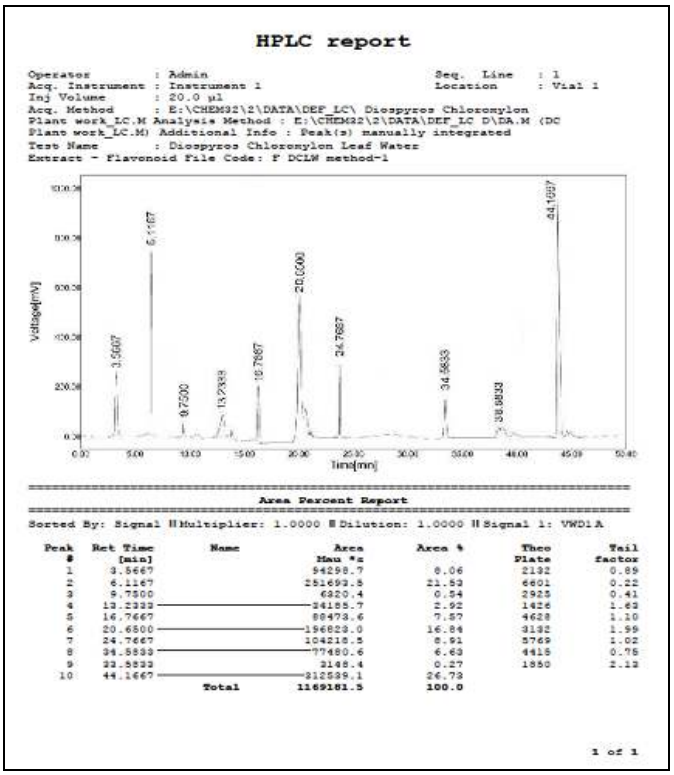
35.6667 min) and peak eight (Kaempferol RT: 37.90 min) were identified with the help of data available in literature (Table 5). Methanolic leaf extracts of *Diospyros chloroxylon* were subjected to HPLC analysis through the protocol developed by Gini & Jothi (2018) [4]. Figure 5 shows the chromatogram with eight (8) peaks out of which peak number two (Gallic acid RT: 5.983 min) and four (Quercetin RT: 13.8 min) were confirmed from the literature data (Table 6). The protocol of Nadia Zeghad *et al* (2019) [14] when used to the methanolic leaf extracts of *Diospyros chloroxylon* resulted in the identification of gallic acid and epicatechin gallate (Fig 6 & Tables 7). Hence, by the application of three different HPLC protocols to the aqueous leaf extracts of *Diospyros chloroxylon*, a total of six phenolic compounds were identified in the leaf that include (i) Gallic acid (ii) quercetin (iii) (-) -epigallocatechine (iv) rutin (v) kaempferol and (vi) epicatechin gallate (Table 8).

The adaption of six different HPLC protocols for aqueous and methanolic leaf extracts of *Diospyros chloroxylon* resulted in the identification of twelve different (phenolic and flavonoid) compounds in the leaf of *Diospyros chloroxylon* Roxb, which include (1) Apigenin-6, 8-di-C-glucopyranoside (2) Kaempferol- 3, 7-di-O-rhamnosid (3) Kaempferol-7-O-rhamnoside (4) Isorhamnetin (5) Isorhamnetin-3-O-dihexoside (6) Scutellarein7-O-β-D-glucopyranoside (7) gallicacid (8) Quercetin (9) Kaempferol (10) Rutin (11) (−) epigallocatechine and (12) Epicatechin gallate

Discussion

The phenolic and flavonoid compounds identified now from leaf of *Diospyros chloroxylon* were earlier found in the other *Diospyros* species. These compounds were considered as more important since they control many biological activities. Madlener *et al* (2007) [12] reported the anticancer activity of gallic acid. Vaquero *et al* (2007) [21] reported antimicrobial activity of quercetin, rutin and gallic acid isolated from different wine varieties. Li & Xu (2008) [10] also reported antimicrobial activity of quercetin. Zhang *et al* (2008) [24] studied the activities of kaempferol and quercetin isolated from straw berry. Kaempferol was found to inhibit the growth of ovarian cancer cell lines (Luo *et al* 2009) [11]. They noticed the inhibitory activity against human oral, colon and prostrate cancer cell lines. The quercetin, kaempferol, rutin and gallic acid isolated from *Zingiber officinale* were shown to inhibit the growth of human breast cancer cell lines (Ghasemzadeh & Jaafar 2011) [3]. Polyphenolics *viz*., epigallocatechine and catechins usually from wine extracts are with anti-cancer activity (Weisburg *et al* 2004) [22]. Catechines are bioactive molecules that provide protection from various ailments (Suzuki *et al* 2005) [20]. The epicatechin gallate, epigallocatechine and gallic acid were previously isolated from highly valued multi-purpose persimmon i.e *Diospyros kaki*. The above catechines were also reported by Achiwa *et al* (1997) [1] as possessed anticancer perspectives against various cancer cell lines. Park *et al* (2006) [15] reported that the catechines, kaempferol and quercetin from *Diospyros kaki* were with free radical scavenging and anti lipid peroxidation activity. Khaled Nabih Rashed *et al* (2013) [9] isolated kaempferol-3-O-α-rhamnoside, kaempferol, gallic acid and quercetin from *Diospyros lotus* and described it as a repertoire of phytochemicals beneficial to human health.

The important flavonoids and phenolic compounds identified now in *Diospyros chloroxylon* underline that it is also highly valued species containing many valuable bioactive molecules. The leaf of *Diospyros chloroxylon* might play a potential role for the preparation of herbal drugs to mitigate oxidative stress created health ailments. Further pharmacological investigations are required to understand the biological activities of the compounds now in *Diospyros chloroxylon*.



HPLC report

Operator : Admin
Acq. Instrument : Instrument 1
Inj Volume : 20.0 µl
Acq. Method : E:\CHEM32\2\DATA\DEF_LC\ Diospyros Chloroxylon
Plant work_LC.M Analysis Method : E:\CHEM32\2\DATA\DEF_LC D\DA.M (DC
Plant work_LC.M) Additional Info : Peak(s) manually integrated
Test Name : Diospyros Chloroxylon Leaf Water
Extract - Flavonoid File Code: F DCLW method-1
Seq. Line : 1
Location : Vial 1

Area Percent Report

Sorted By: Signal ‖ Multiplier: 1.0000 ‖ Dilution: 1.0000 ‖ Signal 1: VWD1 A

Peak #	Ret Time [min]	Name	Area Mau *s	Area %	Theo Plate	Tail factor
1	3.5667		54298.7	8.06	2132	0.89
2	6.1167		251693.8	21.53	6601	0.22
3	9.7500		6320.4	0.54	2923	0.41
4	13.2333		34185.7	2.92	1426	1.63
5	16.7667		88473.6	7.57	4628	1.10
6	20.6500		196823.0	16.84	3132	1.99
7	24.7667		104218.5	8.91	5769	1.02
8	34.5833		77480.6	6.63	4415	0.75
9	38.8833		2148.4	0.27	1850	2.12
10	44.1667		312539.1	26.73		
		Total	1169181.5	100.0		

1 of 1

Fig 1: HPLC chromatogram of *Diospyros chloroxylon* leaf aqueous extract showing peaks of flavonoid compounds (method-1: Zang *et al* 2010) [23].

Table 1: Flavonoids compounds identified from *Diospyros chloroxylon* Leaf aqueous extract (Method -1: Zang *et al* 2010) [23].

Peak. No	Ret Time [min]	Name identified
1	3.5667	-------
2	6.1167	-------
3	9.7500	-------
4	13.2333	Apigenin-6, 8-di-C glucopyranoside
5	16.7667	-------
6	20.6500	kaempferol- 3, 7-di-O-rhamnoside
7	24.7667	-------
8	34.5833	kaempferol-7-O-rhamnoside
9	33.5833	-------
10	44.1667	Isorhamnetin

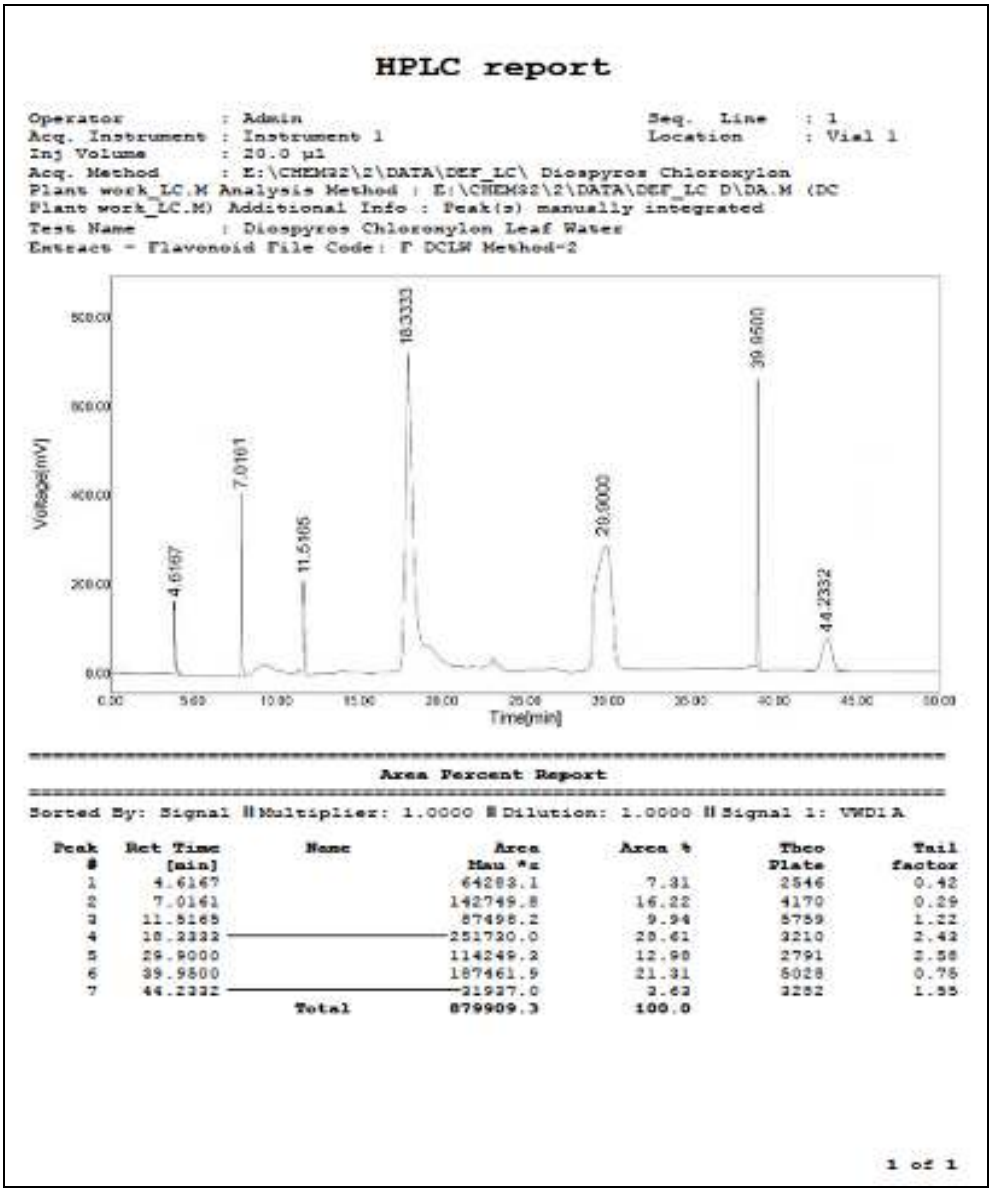
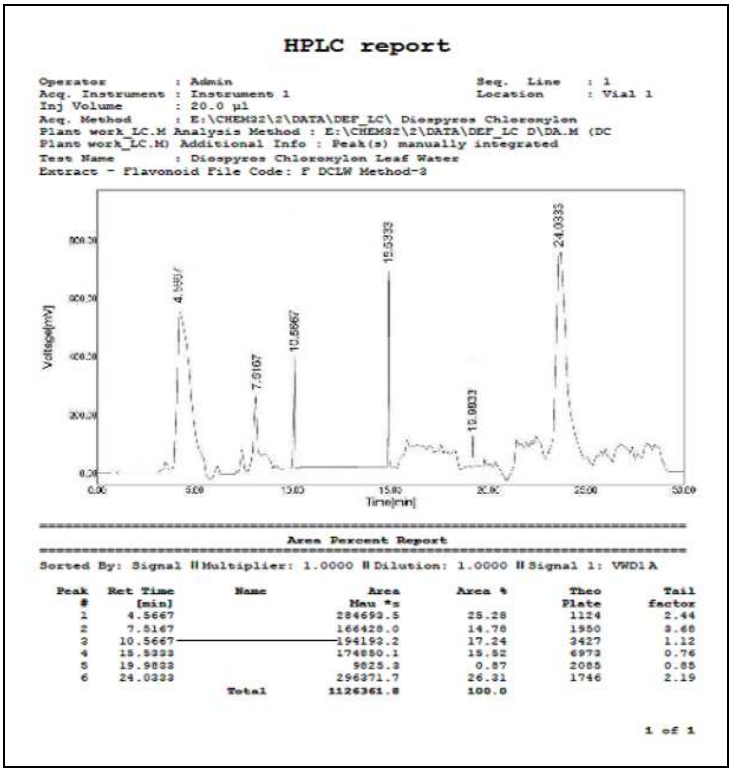


Fig 2: HPLC chromatogram of *Diospyros chloroxylon* leaf aqueous extract showing peaks of flavonoid compounds (method-2: Sait *et al* 2015) [18].

Table 2: Flavonoids compounds identified from *Diospyros chloroxylon* Leaf aqueous extract (Method-2: Sait *et al* 2015) [18]

Peak. No	Ret Time [min]	Name identified
1	4.6167	-------
2	7.0161	-------
3	11.5165	-------
4	18.3333	Isorhamnetin-3-*O*-dihexoside
5	29.9000	-------
6	39.9500	-------
7	44.2332	Isorhamnetin



HPLC report

Operator : Admin
Seq. Line : 1
Acq. Instrument : Instrument 1
Location : Vial 1
Inj Volume : 20.0 µl
Acq. Method : E:\CHEM32\2\DATA\DEF_LC\ Diospyros Chloroxylon
Plant work_LC.M Analysis Method : E:\CHEM32\2\DATA\DEF_LC D\DA.M (DC
Plant work_LC.M) Additional Info : Peak(s) manually integrated
Test Name : Diospyros Chloroxylon Leaf Water
Extract - Flavonoid File Code: F DCLW Method-3

Area Percent Report

Sorted By: Signal ‖Multiplier: 1.0000 ‖Dilution: 1.0000 ‖Signal 1: VWD1 A

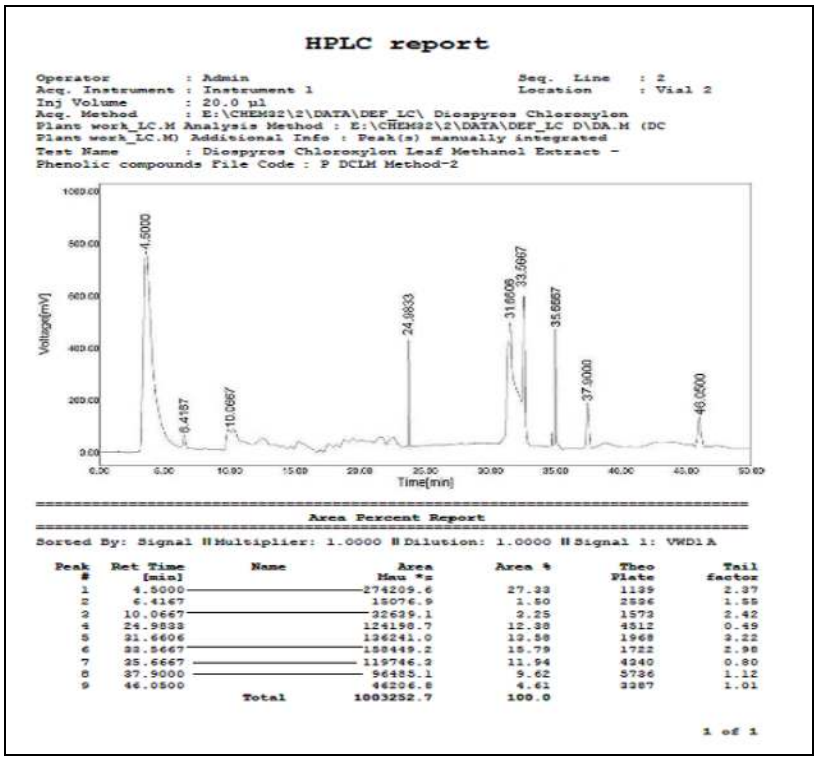
Peak #	Ret Time [min]	Name	Area Mau *s	Area %	Theo Plate	Tail factor
1	4.5667		284692.5	25.28	1124	2.44
2	7.5167		166428.0	14.78	1950	3.68
3	10.5667		194192.2	17.24	3427	1.12
4	15.5333		174880.1	15.52	6973	0.76
5	19.9833		9625.3	0.87	2085	0.85
6	24.0333		296371.7	26.31	1746	2.19
		Total	1126361.8	100.0		

1 of 1

Fig 3: HPLC chromatogram of *Diospyros chloroxylon* leaf aqueous extract showing peaks of flavonoid compounds (method-3: Hilal Bardakci *et al* 2018) [7]

Table 3: Flavonoid compounds identified from *Diospyros chloroxylon* Leaf aqueous extract (Method-3: Hilal Bardakci *et al* 2018) [7]

Peak. No	Ret Time [min]	Name identified
1	4.5667	-------
2	7.5167	-------
3	10.5667	Scutellarein 7-O-β-D-glucopyranoside
4	15.5333	-------
5	19.9833	-------
6	24.0333	-------



HPLC report

Operator : Admin
Seq. Line : 2
Acq. Instrument : Instrument 1
Location : Vial 2
Inj Volume : 20.0 µl
Acq. Method : E:\CHEM32\2\DATA\DEF_LC\ Diospyros Chloroxylon
Plant work_LC.M Analysis Method : E:\CHEM32\2\DATA\DEF_LC D\DA.M (DC
Plant work_LC.M) Additional Info : Peak(s) manually integrated
Test Name : Diospyros Chloroxylon Leaf Methanol Extract -
Phenolic compounds File Code : P DCLM Method-2

Area Percent Report

Sorted By: Signal ‖Multiplier: 1.0000 ‖Dilution: 1.0000 ‖Signal 1: VWD1 A

Peak #	Ret Time [min]	Name	Area Mau *s	Area %	Theo Plate	Tail factor
1	4.5000		274209.6	27.33	1139	2.37
2	6.4167		15076.9	1.50	2596	1.55
3	10.0667		22639.1	2.25	1573	2.42
4	24.9833		124198.7	12.38	4812	0.49
5	31.6606		136241.0	13.58	1968	3.22
6	33.5667		158449.2	15.79	1722	2.98
7	35.6667		119746.2	11.94	4240	0.80
8	37.5000		96455.1	9.62	5736	1.12
9	46.0500		46206.8	4.61	3287	1.01
		Total	1003252.7	100.0		

1 of 1

Fig 4: HPLC chromatogram of *Diospyros chloroxylon* leaf methanolic extract showing peaks of phenolic compounds (method-2: Adriana Skendi *et al* 2017) [2].

Table 4: Phenolic compounds identified from *Diospyros chloroxolyon* leaf methanol extract by the method of (Method -2) Adriana skendi *et al* 2017 [2].

Peak. No	Ret Time [min]	Name identified
1	4.5000	Gallic acid
2	6.4167	-------
3	10.0667	(−)-epigallocatechine
4	24.9833	--------
5	31.6606	--------
6	33.5667	Rutin
7	35.6667	Quercetin
8	37.9000	Kaempferol
9	46.0500	---------

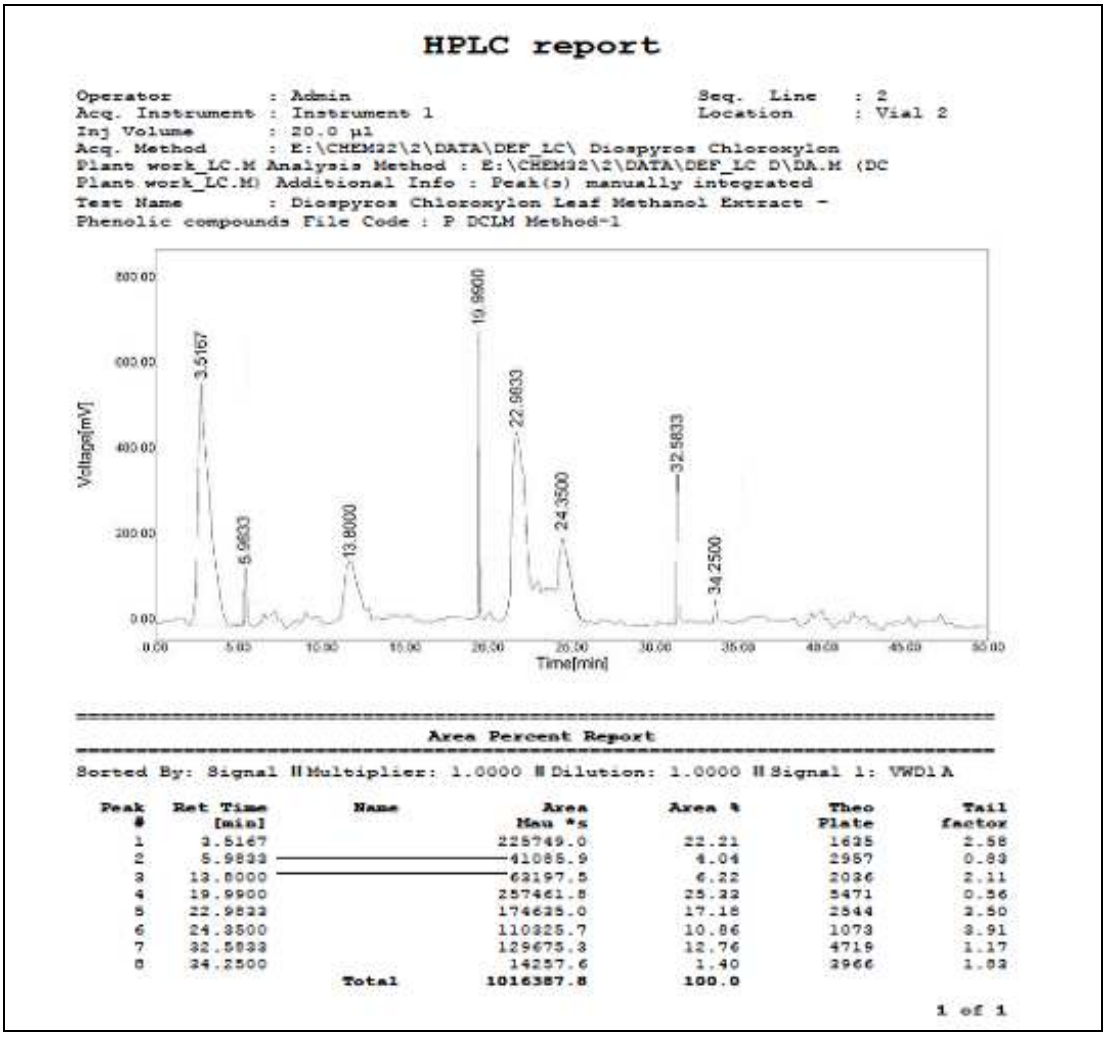
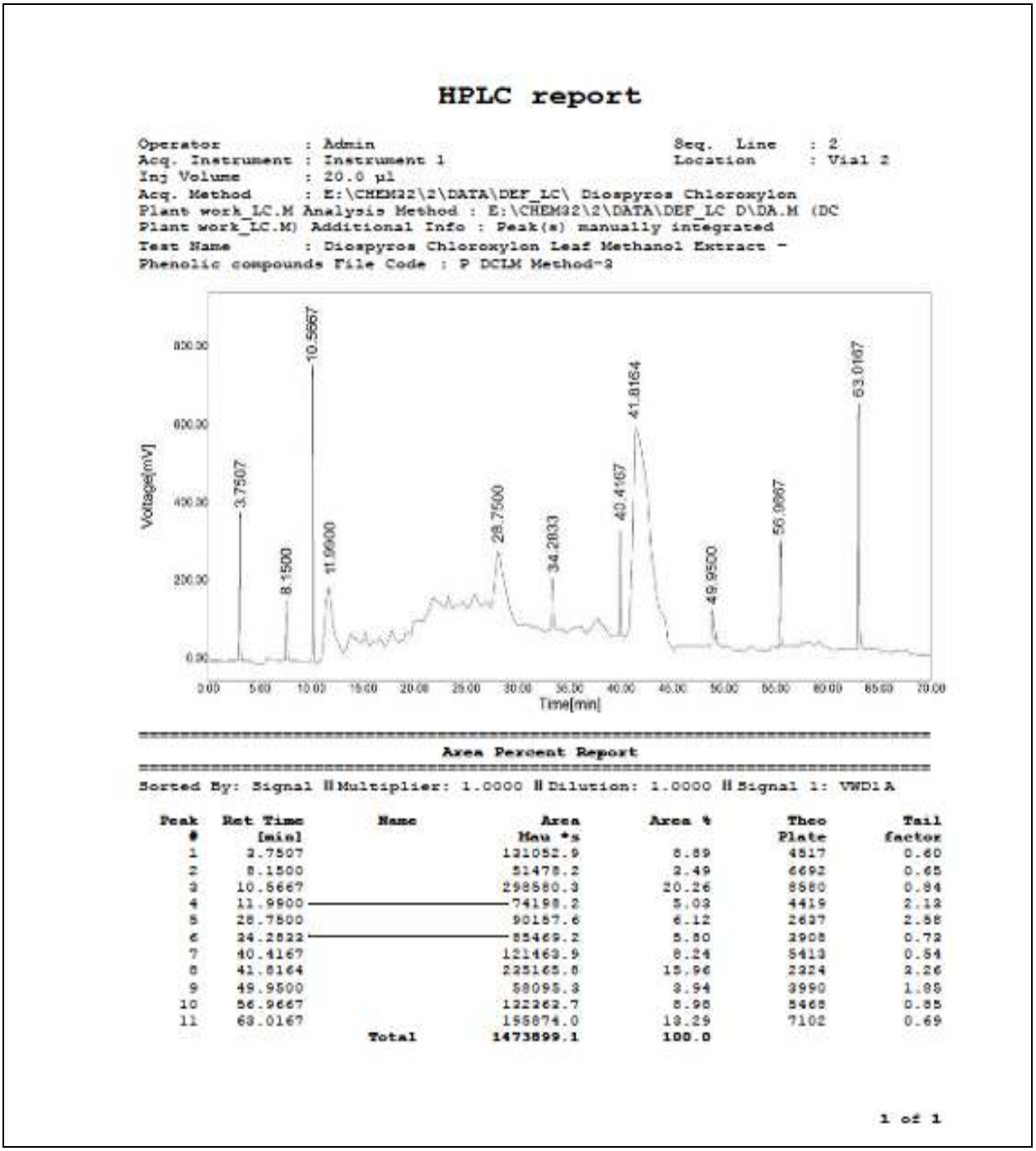


Fig 5: HPLC chromatogram of *Diospyros chloroxylon* leaf methanolic extract showing peaks of phenolic compounds (method-1: Gini TG and Jeya Jothi G 2018) [4].

Table 5: Phenolic compounds identified from *Diospyros chloroxolyon* leaf methanol extract by the method of (Method-1) Gini and Jeya Jothi 2018 [4]

Peak. No	Ret Time [min]	Name identified
1	3.5167	--------
2	5.9833	Gallic acid
3	13.8000	Quercetin
4	19.9900	--------
5	22.9833	---------
6	24.3500	---------
7	32.5833	----------
8	34.2500	----------



HPLC report

Operator : Admin
Acq. Instrument : Instrument 1
Inj Volume : 20.0 µl
Acq. Method : E:\CHEM32\2\DATA\DEF_LC\ Diospyros Chloroxylon
Plant work_LC.M Analysis Method : E:\CHEM32\2\DATA\DEF_LC D\DA.M (DC
Plant work_LC.M) Additional Info : Peak(s) manually integrated
Test Name : Diospyros Chloroxylon Leaf Methanol Extract -
Phenolic compounds File Code : P DCLM Method-2

Seq. Line : 2
Location : Vial 2

Area Percent Report

Sorted By: Signal ‖ Multiplier: 1.0000 ‖ Dilution: 1.0000 ‖ Signal 1: VWD1 A

Peak #	Ret Time [min]	Name	Area Mau *s	Area %	Theo Plate	Tail factor
1	3.7507		121052.9	8.89	4517	0.60
2	8.1500		51478.2	2.49	6692	0.65
3	10.5667		298580.3	20.26	8580	0.84
4	11.9900		74198.2	5.03	4419	2.13
5	28.7500		90157.6	6.12	2637	2.58
6	34.2833		85469.2	5.80	2908	0.72
7	40.4167		121463.9	8.24	5413	0.54
8	41.8164		225165.8	15.96	2324	2.26
9	49.9500		58095.3	3.94	3990	1.85
10	56.9667		122262.7	8.98	5468	0.85
11	63.0167		155874.0	10.29	7102	0.69
		Total	1473899.1	100.0		

1 of 1

Fig 6: HPLC chromatogram of *Diospyros chloroxylon* leaf methanolic extract showing peaks of phenolic compounds (method- 3: Nadia Zeghad *et al* 2019) [14]

Table 6: Phenolic compounds identified from *Diospyros chloroxolyon* leaf methanol extract by the method of (Method-3) Nadia Zeghad *et al* 2019 [14]

Peak. No	Ret Time [min]	Name identified
1	3.7507	-------
2	8.1500	-------
3	10.5667	-------
4	11.9900	Gallic acid
5	28.7500	-------
6	34.2833	Epicatechin gallate
7	40.4167	-------
8	41.8164	-------
9	49.9500	-------
10	56.9667	-------
11	63.0167	-------

Table 7: HPLC identification of different flavonoid compounds in *Dispyros chloroxylon* Roxb leaf aqueous extract (consolidated from Zang *et al* 2010 [23]; Sait *et al* 2015 [18]; Hilal Bardakci *et al* 2018) [7].

Peak. No	Name of the flavonoid compound	RT in Min
Method-1 (Zang *et al* 2010) [23]		
4	Apigenin-6, 8-di-C-glucopyranoside	13.233
6	kaempferol- 3, 7-di-O-rhamnoside	20.6500
8	kaempferol-7-O-rhamnoside	34.5833
10	Isorhamnetin	44.1667
Method-2 (Sait *et al* 2015) [18]		
4	Isorhamnetin-3-O-dihexoside	18.333
7	Isorhamnetin	44.2332
Method-3 (Hilal Bardakci *et al* 2018) [7]		
3	Scutellarein 7-O-β-D-glucopyranoside	10.5667

Table 8: HPLC identification of different phenolic compounds in *Dispyros chloroxylon* Roxb. leaf methanolic extract (consolidated from Gini and Jeya Jothi 2018 [4]; Adriana skendi *et al* 2017 [2]; Nadia Zeghad *et al* 2019) [14]

Peak. No	Name of the phenolic compound	RT in Min
Method-1 (Gini TG and Jeya Jothi G 2018) [4]		
2	Gallic acid	5.9833
3	Quercetin	13.8000
Method-2 (Adriana Skendi *et al* 2017) [2]		
1	Galic acid	4.5000
3	(−)-epigallocatechine	10.0667
6	Rutin	33.5667
7	Quercetin	35.6667
8	Kaempferol	37.9000
Method-3 (Nadia Zeghad *et al* 2019) [14]		
4	Gallic acid	11.9900
6	Epicatechin gallate	34.2833

References

1. Achiwa Y, Hibasami H, Katsuzaki H, Imai K, Komiya T. Inhibitory effects of persimmon (*Diospyros kaki*) extract and related polyphenol compounds on growth of human lymphoid leukemia cells. J. Biosci. Biotechnol. Biochem,1997:61:1099-1101.
2. Adriana Skendi, Maria Irakli, Paschalina Chatzopoulo. Analysis of phenolic compounds in Greek plants of Lamiaceae family by HPLC. J. Appli. Rese. on Medi. and Aromatic Plants,2017:6:62-69
3. Ghasemzadeh A, Jaafar HZE. Anticancer and antioxidant activities of Malaysian young ginger (zingiber officinale Roscoe) varieties grown under different CO2 concentration. J. Med. Plant Res,2011:5(14):3247-3255
4. Gini TG, Jeya Jothi G. Column chromatography and HPLC analysis of phenolic compounds in the fractions of *Salvinia molesta* Mitchell, Egyption. J. Basic and Applied Sci,2018:5(3):197-203
5. Gulcin I, Bursal E, Sehitoglu MH, Bilsel M,Goren A. Polyphenol contents and antioxidant activity of lyophilized aqueous extract of propolis from Erzurum, Turkey, Food Chem. Toxicol,2010:48:2227-2238.
6. Gulcin I, Topal F, Cakmakci R, Bilsel M, Goren AC, Erdogan U. Pomological features, nutritional quality, polyphenol content analysis and antioxidant properties of domesticated and three wild ecotype forms of raspberries (Rubus idaeus L.), J. Food Sci,2011:76:C585-C593.
7. Hilal Bardakci, Ebru Turkoz Acar, Hasan Kırmızıbekmez. Simultaneous quantification of six flavonoids in four Scutellaria taxaby HPLC-DAD method. J. Revista Brasileira de Farmacognosia,2018:29:17-23
8. Katiyar C, Gupta A, Kanjilal S, Katiyar S. Drug discovery from plants sources an integrated approach. J. Ayu,2012:33:10-19
9. Khaled Nabih Rashed, Randy Chi Fai Cheung, Tzi Bun Ng. Bio-active phytoconstituents from non-polar extracts of *Diospyros lotus* stems and demonstration of antifungal activity in the extracts. World. J. Pharmaceuti. Sci,2013:1(4):99-108
10. Li M, Xu Z. Quercetin in a lotus leaves extract may be responsible for antibacterial activity. J. Arch. Pharm. Res,2008:31:640-644
11. Luo H, Rankin GO, Liu L, Daddysman MK, Jiang BH, Chen YC. Kaempferol inhibits angiogenesis and VEGF expression through both HIF dependent and independent pathways in human ovarian cancer cells. J. Nutr. Cancer,2009:61:554-563
12. Madlener G, Bennett R, Bisignano G, Trombetta D, Saija A, Faulds C, et al. Antimicrobial activity of flavonoids extracted from bergamot (Citrus bergamia Risso) peel, a byproduct of the essential oil industry. J. Appl. Microbiol,2007:103:2056-2064
13. Mahesh kumar SK, Kirti SL. Determination of total flavonoids content and quantification of rutin in Momordica tuberosa (Roxb) Cogn. fruits by RP-HPLC. Asian Journal of Traditional Medicines,2012:7:220-25.
14. Nadia Zeghad, Ejaz Ahmed, Abdelmalik Belkhiri, Yvan Vander Heyden, Kristiaan Demeye. Antioxidant activity of *Vitis vinifera*, *Punica granatum*, *Citrus aurantium* and Opuntia *ficusindica* fruits cultivated in Algeria. J. Heliyon,2019:5:e01575. https://doi.org/10.1016/j.heliyon.2019.e01575
15. Park YS, Jung ST, Kang SG, Delgado-Licon E, Ayala ALM, Tapia MS. Drying of persimmons (*Diospyros kaki L.*) and the following changes in the studied bioactive compounds and the total radical scavenging activities. J. LWT-Food Sci. Technol,2006:039:748-755
16. Rahman TU, Zeb MA, Liaqat W, Sajid M, Hussain S, Choudhary MI. Phytochemistry and pharmacology of genusIndigofera: a review, Rec. Nat. Prod,2018:12:1-13.
17. Rauf A, Uddin G, Patel S, Khan A, Halim SA, Bawazeer S. Diospyros,an under-utilized, multi-purpose plant genus: A review. J. Biomed. Pharmacoth,2017:91:714-730
18. Sait S, Hamri-Zeghichi L, Boulekbache-Makhlouf K, Madani P, Rigou V, Brighenti F, *et al*. HPLC-UV/DAD and ESI-MSn analysis of flavonoids and antioxidant activity of an Algerian medicinal plant: *Paronychia argentea* Lam. J. Pharmacet. and Biomedical Analysis, (http://dx.doi.org/doi:10.1016/j.jpba.2015.03.027)
19. Sasidharan S, Chen Y, Saravanan D, Sundram KM, and Latha LY. Extraction, isolation and characterization of bioactive compounds from plants' extracts, Afr. J. Tradit. Complement. Altern. Med,2011:8:1-10
20. Suzuki T, Someya S, Hu F, Tanokura M. Comparative study of catechin compositions in five Japanese persimmons (Diospyros kaki) J. food Chem,2005:093:149-52
21. Vaquero-Rodríguez MJ, Alberto MR, Manca de Nadra MC. Antibacterial effect of phenolic compounds from different wines. J. Food Control,2007:18:93-101
22. Weisburg JH, Weissman DB, Sedaghat T, Babich H. *In vitro* cytotoxicity of epigallocatechin gallate and tea extracts to cancerous and normal cells from the human oral cavity. J. of. Basic Clin. Pharmacol. Toxicol,2004:95:191-200
23. Zang Ting-Ting, Zhou Jin-Song, Wang Qiang. HPLC Analysis of Flavonoids from the Aerial Parts of *Bupleurum* Species, Chinese J. Natu. Medici,2010:8(2):0107-0113
24. Zhang Y, Seeram NP, Lee R, Feng L, Hebe D. Isolation and identification of strawberry phenolics with antioxidant and human cancer cell antiproliferative properties. J. Agric. Food Chem,2008:56:670- 675

ResearchGate

See discussions, stats, and author profiles for this publication at: https://www.researchgate.net/publication/358261871

New synonymy in the genus Crotalaria L. (Fabaceae)

Article · January 2022

CITATIONS
0

READS
441

2 authors:



Ravi Kiran Arigela
Botanical Survey of India
75 PUBLICATIONS **79** CITATIONS
SEE PROFILE



Srinivasa Reddy Ch
SRR & CVR Government Degree College Vijayawada
7 PUBLICATIONS **13** CITATIONS
SEE PROFILE

Some of the authors of this publication are also working on these related projects:

Project Butterfly Conservation in Deccan Platue and Eastern ghats View project

Project Tropical montane forest-grassland ecosystems View project

All content following this page was uploaded by Ravi Kiran Arigela on 01 February 2022.

The user has requested enhancement of the downloaded file.

Species

23(71), 2022

New synonymy in the genus *Crotalaria* L. (Fabaceae)

Ravi Kiran Arigela[1] & **Ch. Srinivasa Reddy**[2]✉

ABSTRACT

Crotalaria lamelliformis P. Sivaramakrishna *et al*. and *C. gengmaensis* Z. Wei & C.Y. Yang are shown to be conspecific with *C. albida* B. Heyne ex Roth and are synonymised here. Similarly, *C. kanchiana* Gholave *et al*. found to be conspecific with *C. juncea* L. and reduced to synonym. Apart, the lectotype was designated here for the name *C. lamelliformis*.

Key words: *Crotalaria,* India, new species, new synonym and varieties.

To Cite:
Arigela RK, Reddy S. New synonymy in the genus *Crotalaria* L. (Fabaceae). *Species*, 2022, 23(71), 54-59

Author Affiliation:
[1]Botanical Survey of India (BSI), Deccan Regional Centre (DRC), Rooms 228–238, Kendriya Sadan, Sultan Bazar, Koti, Hyderabad - 500095, Telangana, India
[2]Department of Botany, SRR & CVR Govt. Degree College (A), Machavaram, Vijayawada - 520004, Andhra Pradesh, India

✉**Corresponding author:**
Email: reddybot@gmail.com

Peer-Review History
Received: 02 December 2021
Reviewed & Revised: 05/December/2021 to 25/January/2022
Accepted: 27 January 2022
Published: 29 January 2022

Peer-Review Model
External peer-review was done through double-blind method.

1. INTRODUCTION

The genus *Crotalaria* L. consists more than 700 species and widespread in Old and New World countries (POWO, 2021) including India with 116 taxa (Nandikar, 2018; Rokade *et al*., 2019, 2020; Dhatchanamoorthy *et al*., 2021). Unfortunately, some of newly described taxa were considered conspecific and synonymized with the older validated names (Arigela & Singh, 2018). We present below two another erroneously described species, *Crotalaria lamelliformis* P. Sivaramakrishna *et al*. and *C. kanchiana* Gholave *et al*., which are turned out to be conspecific with previously known taxa.

Taxonomic treatment

Crotalaria albida B. Heyne ex Roth, Nov. Pl. Sp.: 333. 1821.
Type: — Without locality, *s.d*., B. Heyne, *s.n*. (L barcode L0649895 [image!] lectotype designated by Turner, 2021)

Crotalaria lamelliformis P. Sivaramakrishna, P. Yugandhar & L.J. Singh in Phytotaxa 490 (1): 72. 2021, ***syn. nov.***
Type: — (Lectotype, designated here) *Crotalaria lamelliformis* P. Sivaramakrishna *et al*., in Phytotaxa 490 (1): 77. fig. 4, 2021.

Crotalaria albida B. Heyne ex Roth var. *kangrensis* A.A. Ansari, *Crotalaria* India: 157. 2008. (Singh & Garg, 2020)
Type: — India, Himachal Pradesh, Sihunta, Kangra, 16.10.1874, C.B. Clarke, 23655B (holotype CAL0000024597! Isotype CAL0000024572!)

Crotalaria gengmaensis Z. Wei & C.Y. Yang in Acta Phytotax. Sin. 20: 479. 1982. ***syn. nov.***
Type: — Yunnan. Gengmam Xian, alt. 1670 m, Apr. 1936, C.W. Wang 72861 (holotype PE - 2301193 - 01432515, isotype PE - 2301194 - 01432516)

DISCOVERY SCIENTIFIC SOCIETY
© 2022 Discovery Scientific Society. This work is licensed under a Creative Commons Attribution 4.0 International License.

© 2022 Discovery Scientific Society. All Rights Reserved. ISSN 2319–5746 EISSN 2319–5754 | OPEN ACCESS



Figure 1. *Crotalaria albida*; **A–E**: habit variations at different habitats.

Note: During botanical explorations at Deccan Plateau, Eastern Ghats, Indian Himalayan Range, Western Ghats, Aravalli Hills and the Thar Desert under various projects, *C. albida* has been observed and collected. Several morphological variations in the habit like, highly tufted decumbent habit to less branched erect (Fig. 1), leaf variations such as shape, size and indumentum, streaks colour on the standard petals from brownish to dark brown is observed (Fig. 2). Between 2012 and 2020, *C. albida* morphological variations were observed in the Kodaikanal Wildlife Sanctuary at elevations ranges 400–1900 m and collected specimens (*Kabeer & Ravi Kiran*

© 2022 Discovery Scientific Society. All Rights Reserved. ISSN 2319–5746 EISSN 2319–5754 I OPEN ACCESS

133181, 140914) deposited at MH, Coimbatore. We observed that, size of the plant depends on the aridity, moisture levels in the soil, altitude and temperature of habitat (Fig. 1).



Figure 2. *Crotalaria albida*; **A–B**: Leaf variations; **C–F**: Streaks variations on standard petal of flower.

© 2022 Discovery Scientific Society. All Rights Reserved. ISSN 2319–5746 EISSN 2319–5754 I OPEN ACCESS



Figure 3. *Crotalaria juncea*; **A–D**: Leaf variations; **E–H**: Close up of flower with streaks variations on standard petal; **I–K**: Ventral view of standard petal with colour variation; **L–M**: variations in pods.

Sivaramakrishna *et al.* (2021) described a new species *C. lamelliformis* and they were not submitted the type specimens to the Botanical Survey of India as stated in the protologue. Communication with the authors of *C. lamelliformis* revealed that, all the type specimens were spoiled and no original material available with them. It attracts the ICN (Turland *et al*., 2018) article 9.3 to designate nomenclatural type, thus we have designated the illustration from the protologue of the *C. lamelliformis* as lectotype. Furthermore, we have examined the live plants from the type locality and no plant is having the stipules, and authors of *C. lamelliformis*

© 2022 Discovery Scientific Society. All Rights Reserved. ISSN 2319–5746 EISSN 2319–5754 I OPEN ACCESS

considered the indumentum on petiole base as stipules. No petiole is visible in the figures given in the protologue of the *C. lamelliformis*. The diagnosis of the *C. lamelliformis* was erroneous and it is treated here as a synonym of *C. albida*.

Ansari (2008) described *C. albida* var. *kangrensis* and stated it is differ from *C. albida* by having shorter leaves, less number of flowered inflorescence and less hairy calyx. We observed these characters are driven by edaphic factors in the varied habitats and correctly synonymized by Singh & Garg (2020). Chun-Yu (1982) described *C. gengmaensis* and stated the new species is differing from *C. albida* by having elliptic leaf blade, adaxial calyx lobes acuminate at apex and 6–8-seeded legume. These characters exactly match with *C. albida* which grows in the Eastern Ghats and Western Ghats of India. After the study of protologue and type specimens of *C. gengmaensis* and *C. albida* var. *kangrensis* it is concluded that, they are ecotypes of *C. albida*. Therefore, *C. gengmaensis* is treated here as a synonym of *C. albida.*

Crotalaria juncea L., Sp. Pl. 2: 714. 1753.
Type: — India, without locality, *s.d*., C. Linnaeus, *s.n*. (Herb. Linn. No. 895.11 [Image!], lectotype designated by Fawcett & Rendle in *Fl. Jamaica* 4: 8. 1920)

Crotalaria kanchiana Gholave, Mane, Gore, Kambale & S.P. Gaikwad in Phytotaxa 409 (4): 234. 2019. ***syn. nov.***
Type:—India, Maharashtra, Osmanabad district, Barshi-Osmanabad road, near Hatlai Devi Temple, 530 m, 18°10′50″N, 76°0′45″E, 22 November 2018, A. R. Gholave, R. N. Mane & S. P. Gaikwad 700 (holotype CAL; isotype BSI, SUK)

Notes: *Crotalaria juncea* is native to India and commonly known as Sunn hemp, Indian hemp, Madras hemp and brown hemp (Bhandari *et al*., 2016). A good number of varieties of Sunn hemp have been developed and cultivated in many tropical and subtropical regions of world. Few cultivated variants of Sunn hemp escaped from cultivation and formed the colonies around the agriculture fields and the open forest in India and it is also considered as noxious weed in the USA (Sheahan, 2012). Nannajkar *et al.* (2016) explained the effect of different varieties and spacing on the yield attributes *viz*., number of pods per plant, pod length, diameter of pod, number of seeds pod and seed weight of *C. juncea*.

Gholave *et al.* (2019) stated "*C. kanchiana* morphologically resembles with *C. juncea* but differs in having 2–6 flowered inflorescence and 2–4 seeds in a pod". They have considered few characters like length of inflorescence, size of flower bud, size of flower and seed number in the pod which are regulated by edaphic factors. After 2 years field trials, Meagher *et al.* (2017) concluded of seasonality affected the numbers of racemes, flowers, numbers of plants with seed pods and number of seed pods per plant. During plant explorations in India, We have observed several morphological variations, colour variations in standard petals in the flowers of *C. juncea* (Fig. 3) and referred the several herbarium sheets of *C. juncea* ecotypes which are extant at Botanical Survey of India herbaria. After the study of protologue, type specimens and live specimens, *C. kanchiana* is reduced as synonym of *C. juncea*.

Acknowledgements
Authors are thankful to the Director, Botanical Survey of India, Kolkata, Head of Office, Botanical Survey of India, Deccan Regional Centre, Hyderabad and Principal, SRR & CVR Govt. Degree College, Vijayawada for facilities. We also thank Dr. K.N. Gandhi, Senior Nomenclatural Registrar, Harvard University Herbaria & Libraries and Dr. Mayur D. Nandikar for nomenclatural advice.

Funding
This study has not received any external funding.

Conflicts of interests
The authors declare that there are no conflicts of interests.

Data and materials availability
All data associated with this study are present in the paper.

REFERENCES AND NOTES

1. Ansari, A.A. (2008). *Crotalaria* L. in India. Dehra Dun: Bishen Singh Mahendra Pal Singh.
2. Arigela R.K. & Singh R.K. (2018). On the identity of *Crotalaria nallamalayana* Rasingam & J. Swamy (Fabaceae). *Phytotaxa* 374 (2): 177–177.

© 2022 Discovery Scientific Society. All Rights Reserved. ISSN 2319–5746 EISSN 2319–5754 I OPEN ACCESS

3. Bhandari H.R., Tripathi M.K., Chaudhary B. & Sarkar S.K. (2016). Sunnhemp breeding: Challenges and prospects. *Indian Journal of Agricultural Sciences* 86 (11): 1391–8.
4. Dhatchanamoorthy N, Noorunnisa Begum S, Patturaj R, Mahendra Nath Mitta. *Crotalaria leschenaultii* DC. (Fabaceae): A poorly known species rare and endemic Legumes from the Eastern Ghats, Southern India. *Species*, 2021, 22(70), 222-225
5. Gholave, A.R., Mane, R.N., Gore, R.D., Kambale, S.S. & Gaikwad, S.P. (2019). *Crotalaria kanchiana* (Fabaceae), a new species from Balaghat Ranges of Maharashtra, India. *Phytotaxa* 409 (4): 233–238. https://doi.org/10.11646/phytotaxa.409.4.6
6. Meagher Jr., R.L., Nagoshi, R. N., Brown, J.T., Fleischer, S.J., Westbrook, J.K. & Chase C.A. (2017). Flowering of the Cover Crop Sunn Hemp, *Crotalaria juncea* L. *Hort Science* 52 (7): 986–990. https://doi.org/10.21273/HORTSCI11981-17
7. Nandikar, M.D., Kishor, K.C. & Malpure, N.V. (2018). On the occurrence of *Crotalaria uncinella* subsp. *elliptica* (Fabaceae) in Andaman and Nicobar Islands, India. *Phytotaxa* 379 (1): 073–077. https://doi.org/10.11646/phytotaxa.379.1.7
8. Nannajkar, R.R., Sinare, B.T. & Ughade, S.R. (2016). Effect of different varieties and spacing on growth, yield and quality of sunnhemp (*Crotalaria juncea* L.). *Trends in Biosciences* 9(4): 231–235.
9. Rokade, K., Dalavi J.V., Gaikwad, S., Gaikwad, N. & Yadav, S. (2019). A new variety of *Crotalaria prostrata* Roxb. (Fabaceae) from the Northern Western Ghats, India. *Phytotaxa* 14 (1): 035–040. https://doi.org/10.11646/phytotaxa.414.1.4
10. Rokade, K., Dalavi, J.V., Gaikwad, S. & Gaikwad, N. (2020). *Crotalaria shrirangiana* (Fabaceae): A new rattlepod from the Western Ghats of India. *Phytotaxa* 449 (2): 188–194. DOI: https://doi.org/10.11646/phytotaxa.449.2.7
11. Sheahan, C.M. (2012). Plant guide for sunn hemp (*Crotalaria juncea*). USDA-Natural Resources Conservation Service, Cape May Plant Materials Center. Cape May, New Jersey. pp 1–4.
12. Singh, R.K., Garg, A. (2020) *Floristic diversity of Valmiki Tiger Reserve, West Champaran district, Bihar*. Today & Tomorrow's Printers and Publishers, New Delhi.
13. Sivaramakrishna, P. Yugandhar, P., Singh, L.J. (2021). *Crotalaria lamelliformis* (Fabaceae: Crotalarieae), a new species from Eastern Ghats of Andhra Pradesh, Peninsular India. *Phytotaxa* 490 (1): 071–081. https://doi.org/10.11646/phytotaxa.490.1.6
14. Turland, N.J., Wiersema, J.H., Barrie, F.R., Greuter, W., Hawksworth, D.L., Herendeen, P.S., Knapp, S., Kusber, W.-H., Li, D.-Z., Marhold, K., May, T.W., McNeill, J., Monro, A.M., Prado, J., Price, M.J. & Smith, G.F. (2018). *International Code of Nomenclature for algae, fungi, and plants (Shenzhen Code)*. Regnum Vegetabile 159. Koeltz Botanical Books, Glashütten.
15. Turner, I.M. (2021). Heyne, Roth, Roemer and Schultes, and the plant names published in Novae plantarum species praesertim Indiae orientalis. *Taxon* 70 (2): 365–428. https://doi.org/10.1002/tax.12449.

© 2022 Discovery Scientific Society. All Rights Reserved. ISSN 2319–5746 EISSN 2319–5754 I OPEN ACCESS

View publication stats

Asian Journal of Chemistry; Vol. 34, No. 10 (2022), 2478-2488

ASIAN JOURNAL OF CHEMISTRY

https://doi.org/10.14233/ajchem.2022.23904

REVIEW

A Comprehensive Review on Green Synthetic Approaches and Applications of 3*d*-Series Metal Oxide Nanoparticles

G. TEJASWINI[1,2], P. LAKSHMI KISHORE[3,*], V. NAGA LAKSHMI[4] and K. BHAGYA LAKSHMI[5]

[1]Department of Chemistry, Acharya Nagarjuna University, Guntur-522510, India
[2]Department of Chemistry, Government College (A), Rajamahendravaram-533105, India
[3]Department of Engineering Chemistry, S.R.K.R. Engineering College (A), Bhimavaram-534204, India
[4]Department of Chemistry, Ch. S.D. St. Theresa's College for Women (A), Eluru-534003, India
[5]Department of Chemistry, S.R.R. & C.V.R. Government Degree College (A), Vijayawada-520010, India

*Corresponding author: E-mail: lakshmikishorep@gmail.com

Received: 9 May 2022; *Accepted*: 21 July 2022; *Published online*: 19 September 2022; AJC-20948

Transition metal oxides have been studied by many workers of fields who want to find new ways to use them in medical devices and other fields. Researchers have done a lot of research on solid-state synthesis methods, which require high temperatures and make molecules that are thermodynamically stable. Transition metal oxides have been used for a wide range of things, from nanoparticles that deliver drugs to systems that store information in more than one state. In materials science and technology research and development, a new era of "green synthesis" methods is getting a great attention. Basically, green synthesis of materials and nanomaterials, which is done through a process of regulation, control, cleaning and remediation, will directly help make them more friendly to the environment. In this review, various green approaches for 3*d*-series metal oxide nanoparticles and their applications are discussed.

Keywords: Metal oxide, Green synthesis, Nanoparticles.

INTRODUCTION

Nanoscience is one of the most relevant and effective fields of study in modern science. In last few years, nanotechnology has become an advanced technology, with interdiscipline research taking place between various fields of study. Nanoparticles (NPs) are more interesting than bulk materials because of the enhanced surface Rayleigh scattering, plasmon resonance and enhanced surface Raman scattering of fine metals and their related metal oxides nanoparticles. Because of this, nanoparticle technology has a significant impact on the development of various chemical and biological sensors [1-7]. Nanoparticle materials made from metal and metal oxides with substantial surface modification are being studied for a wide range of applications, including medical, biological and electronic ones. Nanoparticle production can only be accomplished using a small number of harmful chemicals and solvents. The development of new green, non-toxic and safe technologies for synthesizing nanoparticle materials is accelerating [8]. The intrinsic qualities of inorganic materials are mostly governed by their composition, structure, crystallinity, size and shape. Developing new ways to make nanomaterials, which are safe for people to use is very important because of the problems that have been talked about [9]. Literature shows that there has been a rise in the use of biosynthesis or green synthesis of metal oxide nanoparticles [10,11].

Metal oxide nanoparticles: Microelectronic circuits, sensors, piezoelectric devices, fuel cells and corrosion catalysts are only few of the applications of metal oxides in materials science. Environmental pollutants can be absorbed by metal oxides, too. Due to their small size, oxide nanoparticles in nanotechnology may exhibit unusual chemical characteristics. A wide range of fields have been studied transition metal oxides in the hopes of finding new uses for them in medical devices and other fields. Solid-state synthesis methods, which demand high temperatures and produce thermodynamically stable

This is an open access journal, and articles are distributed under the terms of the Attribution 4.0 International (CC BY 4.0) License. This license lets others distribute, remix, tweak, and build upon your work, even commercially, as long as they credit the author for the original creation. You must give appropriate credit, provide a link to the license, and indicate if changes were made.

molecules, have been studied extensively. From drug delivery nanoparticles to multiple-state memory storage systems, transition metal oxides have also been used in a wide variety of applications [12,13].

Sc_2O_3 nanoparticles: Scandium(III) oxide adopts a cubic crystal structure (tetrahedral containing six-coordinated metal centres. Powder diffraction analysis shows Sc–O bond distances of 2.159-2.071 Å. Scandium oxide is an insulator with a band gap of 6.0 eV. Scandium sol-gel chemistry has had a significant impact on the development of scandium oxide as a dopant in garnet lasers [14] or as a stabilizer for zirconia [15,16]. Mixed nickel-copper oxides can also form materials that are sensitive to NO_2 [17]. The breakdown of propan-2-ol and the oxidation of CO on the surfaces of porous Sc_2O_3 bulk materials synthesized by precipitation in an aqueous solution have been explored as catalytic applications [18,19]. Materials with high refractive index, high transparency to emitted radiation and strong thermal stability are now being studied and developed in response to the possibility for UV lasers to be used in inertial confinement fusion (ICF). Among the high index materials coated using physical methods, scandia coatings generated by chemical vapour deposition demonstrate the best reflecting characteristics and laser damage resistance for multilayer UV-mirrors [20].

TiO_2 nanoparticles: Rutile is a mineral that is mostly made up of titanium dioxide (TiO_2) and it is the most common natural form of TiO_2. Anatase, akaogiite and brookite are some of the other rare polymorphs of TiO_2. Today, biosynthesis of nanoparticles has been used in a lot of different ways by making them with plants. The green method to make titanium oxide nanoparticles is better because it doesn't use a lot of chemicals [21,22]. TiO_2 is one of the metal oxide antimicrobial agents, which is both inert and durable. It can be used in a wide range of areas *viz*. optical, sensors, electronics, solar cells, gas sensing, magnetic, antibacterial and antifungal agents. TiO_2 contains high surface area, good surface morphology and is not harmful in nature. It has good activity on a wide range of bacteria [23-27].

V_2O_5 nanoparticles: Among the various vanadium oxide compositions that can be obtained, vanadium pentoxide (V_2O_5) possesses a unique set of properties as one of the most widely studied of the more stable phases of vanadium oxides. The vanadium pentoxide powders have been prepared mostly by dry processes such as vacuum evaporation [28,29] and sputtering [30], although wet processes such as electrodeposition and sol-gel method [31,32] seem to be more advantageous in producing large scale films. Recently, microbial cells have been proposed as inexpensive and environmentally friendly biotemplates to direct the deposition, assembly and patterning of inorganic nanoparticles and microstructures [33]. Both living and dead microorganism's cells are capable of directing the synthesis and assembly of crystalline inorganic materials due to their cell wall's active biomolecules. The synthesis of nanoparticles of metal oxides using yeasts as biological templates are reported [34-36].

The transition metal vanadium is highly sought after in a wide range of industrial applications. Potential applications include solar cells, sensors, batteries and catalysis [37-42] due to its oxides form. The valence electron state of vanadium can affect the structure of vanadium oxides form. In various VO, V_2O_3, VO_2 and V_2O_5 phases [43], the valence state of the metal fluctuates between the V^{2+} and V^{5+} range. The V_2O_5 is the most stable orthorhombic vanadium oxide and has the best electrical and optical characteristics of all vanadium oxides [44].

Cr_2O_3 nanoparticles: Because of their relevance in both science and technology, chromium oxides have recently gained a great deal of media interest. Chromium may create a variety of oxides due to its various stable oxidation states. When it comes to specific applications like high temperature resistance materials [45], corrosion resistance materials [46], liquid crystal displays [47,48], green pigments [49], catalysts [50,51], *etc*., researchers have paid close attention to the formation and properties of chromium oxide (Cr_2O_3). Many studies have been done on the synthesis of diverse Cr_2O_3 materials [52-54]. It is well-known that inorganic materials' intrinsic qualities are mostly governed by their composition, structure, crystallinity, size and morphology. The medical applications of nanoparticles for therapy and antibacterial action have been the focus of nanobiotechnology investigations. There are numerous uses for chromia (Cr_2O_3), such as high-temperature and corrosion-resistant materials; liquid crystal displays; green pigment; heterogeneous catalysts; coating materials, *etc*. [55-65].

MnO_2 nanoparticles: MnO_2 is one of the most promising transition metal oxides for catalytic applications due to its distinctive physical and chemical properties [66,67]. MnO_2 has the stable isomorph called pyrolusite, β-MnO_2. MnO_2 nanoparticles have been investigated through numerous applications in several fields like immobilization of proteins [68], sensitive biosensors [69], electrochemical capacitors [70], removal of dyes [71,72], lithium ion batteries [73], synthesis bioactive compound [74], analysis of neuro-behaviour of rats [75], biomimetic catalyst [76] and metal adsorption [77].

Fe_3O_4 nanoparticles: The separation and purification of dye, pharmaceutical and heavy metal contamination, as well as labelling and medication delivery systems, have all been made possible with iron oxide-based magnetic nanoparticles in recent years. Among iron oxide nanostructures, magnetite (Fe_3O_4) has drawn the most interest due to its exceptional magnetic and electrical properties [78]. Super-paramagnetism is one of the Fe_3O_4 nanoparticles' most noteworthy characteristics and supports that Fe_3O_4 nanoparticles behave like atomic paramagnets above the blocking temperature and act as a single magnetic domain. High saturation magnetization and high field irreversibility are the result of this sort of magnetism in Fe_3O_4 nanoparticles, making this iron oxide nanostructure more easily separable in external magnetic fields than other metal oxide nanoparticles.

The majority of iron oxide nanoparticle synthesis has utilized dangerous, costly and environmentally harmful laboratory compounds as reducing agents. Wet chemical, dry procedures and microbiological techniques can all be used to make iron oxide magnetic nanoparticles [79-84]. Many scientists have proposed an alternate and environmentally acceptable method for synthesizing nanoparticles: biogreen synthesis. Different magnetic nanocomposites can be made by putting high adsorption coatings on their surfaces [85-92]. Plant extracts,

particularly ferrous magnetic oxides, have been used in green nanoparticle manufacturing.

When compared to chemically produced Fe_3O_4 nanoparticles, green biosynthesized Fe_3O_4 nanoparticles can have better properties with improved biocompatibility and biodegradability. They can therefore be used in biomedical applications because of the distinctive surface coating of green materials, which is not only non-toxic and biocompatible but also allows targeted medication administration with Fe_3O_4 nanoparticles localization in a specific area. Because the green materials used to synthesize Fe_3O_4 nanoparticles are safe to consume, the toxicity to humans can be decreased, which is advantageous in biomedical applications [93]. Fe_3O_4 nanoparticles could be used in a variety of medical applications, including antimicrobial, tissue engineering and hyperthermia [94,95]. Fe_3O_4 nanoparticles can be employed in the fields of catalysts, water remediation and lithium-ion batteries [96-99]. Numerous studies have been done in order to maximise the potential use of Fe_3O_4 nanoparticles in various domains of application because of their intriguing properties, such as superparamagnetic. In addition, they serve as MRI contrast agents, photothermal therapy of malignancies, magnetofection agents, magnetic storage media, magnetic bioseparation and DNA molecule identification *via* targeted drug delivery systems. Due to their remarkable magnetic characteristics, Fe_3O_4 nanoparticles are becoming increasingly popular as a drug delivery system component [100-105].

Co_3O_4 nanoparticles: As a result of their wide range of applications in lithium ion batteries, cobalt oxide (Co_3O_4) nanoparticles with normal spinel structure have been extensively studied as promising types of multifunctional materials among the many transition metal oxides that have been extensively investigated because of their intriguing electronic and electrical properties as well as their catalytic and magnetic properties.

These nanoparticles have been synthesized using a variety of processes, including co-precipitation, sol-gel, sonochemical approach, chemical vapour deposition and thermal breakdown of cobalt precursors [106-112]. Co_3O_4 nanoparticles of various morphologies can be synthesized *via* hydrothermal techniques, chemical spray pyrolysis, combustion, mechanochemical processing, microwave irradiation and microemulsion methods [113-118]. However, the utilization of expensive equipments, complex synthesis stages, high temperatures, protracted reaction times and a high cost of synthesis have been associated with many of these synthesis approaches. These approaches are also not environmentally friendly. Toxic and hazardous chemicals used in the nanoparticle-synthesis technique have been reduced using green chemistry during the past two decades in both research and industry. Friendly environment materials can be used in a variety of contexts. It is therefore possible to reduce the use and environmental impact of some chemicals (capping agents, reducing agents and solvents) used in the production of various nanoparticles [119-129]. Biosynthesis utilizing plants is regarded the safest, most economically viable and environmentally benign strategy for synthesising nanoparticles. It also produces more stable nanoparticles more quickly. Co_3O_4 nanoparticles can be made using various plant extracts, such as *Calotropis gigantea* and *Aspalathus linearis* leaves [130,131], *Punica granatum* peal extract [132,133] and so on.

NiO nanoparticles: Recently, a lot of attention has been paid to nickel oxide nanomaterials, which have a large band gap (3.6-4.0 eV), p-type conductivity and can be used in a lot of different ways. There are a lot of different technologies that can be used to make smart windows, which include photocatalysis, antimicrobial, anti-ferromagnetic, electrochemical, photoelectronic, gas sensors, *etc*. Nanostructured NiO, on the other hand, has better properties than micro and macro-sized NiO particles in terms of volume, surface and quantum size [134]. A nanomaterial of NiO has been called a cheap semiconductor because of its long-term stability, availability and nontoxicity [134]. In addition, nickel nanoparticles have been found to have a superior antimicrobial impact to that of other metal nanoparticles. Jeyaraj *et al*. [135] reported that NiO nanostructures are better act as a antibaterial agent than silver nanostructures however, number of factors also depends upon the process and quantity.

A variety of methods may be used to produce NiO nanoparticles, including solvothermal process [136], chemical precipitation, thermal breakdown, sol-gel combustion [137], *etc.* These procedures, on the other hand, require special equipment, high temperatures and a long process. Plant extracts are used to make nanomaterials as a reducing agent and a capping agent instead of chemical and photochemical methods [138]. Moreover porous parts of plants also work as biotemplates to reduce metal ions to get the right shape [139].

CuO nanoparticles: Copper oxide nanoparticles have better biological and photocatalytic abilities than metal nanoparticles. It has been shown that copper oxide nanoparticles could be used in gas sensors, catalysis and batteries, as well as in agriculture [140-143]. They could also be used to remove dyes, remove field emission emitters and convert solar energy. CuO nanoparticles also have unique anticancer, antimicrobial and antioxidant properties, which makes them a good tool for biomedical applications [144,145].

Microwave irradiation, thermal decomposition, sol gel, colloidal thermal synthesis, sonochemical, hydrothermal and quick precipitation have all been used to make CuO nanoparticles that have the right morphologies and properties [146-152]. Phytosynthesis of CuO nanoparticles has been getting more attention recently because of its long-term sustain-ability, low cost and ease of use [153]. It has also been reported that different techniques can change their shape and its toxicity [154-157]. Using green methods, CuO nanoparticles act as both a reducing agent and a stabilizing agent, moreover, presence of biomolecules like flavonoids, saponins, tannins, starches and polypeptides help CuO nanoparticles less acidic and more stable [158].

Despite the fact that synthesizing nanoparticles from the microorganisms is beneficial for the environment, however, they too have some drawbacks, for example, the toxicity of some bacteria, the difficulties in separating them and the time it takes to grow them [159]. Nevertheless, plants are still the best source of metal and metal oxide nanoparticles, since they consists a fast reaction rate, contains a number of biomolecules, low-cost, stable and are easy to use [160].

ZnO nanoparticles: ZnO can be used in biosensors, cosmetics, drug carriers and antibacterial agents, because it has a wide band gap of 3.1-3.3 eV [161]. Synthesizing ZnO can be done in a number of different ways, which include sol-gel processing, homogeneous precipitation, mechanical milling and organometallic synthesis [162,163]. These kinds of methods usually use organic solvents and toxic reducing agents, most of which are highly reactive and corrosive. For the extraction of plant metabolites, mild solvents like water, alcohol and methanol were used [164-167] during the synthesis of zinc oxide nanoparticles using zinc salt solution.

Table-1 shows the summary of the several metal oxide nanoparticles prepared using various plant extracts.

Conclusion

In conclusion, the recent findings show that 3*d*-metal oxide nanoparticles are of substantial interest because of the prospective technological and therapeutic uses. The synthesis of 3*d*-metal oxides nanoparticles using traditional as well as greener, milder synthetic procedures that make use of plants, organisms and other natural products was also discussed. There are still many unanswered concerns regarding the operation of plant extracts, particularly plant leaf extracts, and how they produce even greener nanoparticles. Additionally, the molecular mechanism of plant nanoparticle interaction is still necessary for the bioreduction mechanism, the synthesis, growth,

TABLE-1
VARIOUS GREEN APPROACHES FOR SYNTHESIS OF 3d SERIES METAL OXIDE NANOPARTICLES AND THEIR APPLICATIONS

Plant	Size	Shape	Application	Ref
		TiO_2 nanoparticles		
Leaf extract *Aloe barbadensis* (aloevera)	~ 20 nm	Poly-dispersed, spherical	Antibiofilm potential against *Pseudomonas aeruginosa*	[168]
Flower aqueous extract of *Calotropis gigantea* (*C. gigantea*)	10.52 nm (XRD) 160-220 nm (SEM)	Aggregated and spherical	Acaricidal activity *Rhipicephalus microplus* and *Haemaphysalis bispinosa*	[169]
Leaf (KL), pod (KP), seed (KS) and seed shell (KSS) extracts of kola nut tree	25.00-191.41 nm	Spherical	Antimicrobial, dye degradation, antioxidant and anticoagulant activities	[170]
Echinacea purpurea herba extract	120 nm	Spherical agglomerated	Bio reductant	[171]
Aqueous leaf extract of *Psidium guajava*	32.58 nm	Spherical	Antibacterial and antioxidant activities *Staphylococcus aureus*	[172]
Leaf aqueous extract of *Mangifera indica* L	30 ± 5 nm	Spherical	Larvicidal activity, blood-feeding parasites	[173]
The root extract of with *Ania somnifera*	50-90 nm	Spherical and square	Broad-spectrum attenuation of biofilm and cytotoxic properties against HepG2 cell lines	[174]
Leaf aqueous extract of *Solanum trilobatum*	70 nm		To assess the antiparasitic efficacies	[175]
Aqueous leaf extracts of *Parthenium hysterophorus*	20-50 nm	Spherical	Larvicidal, antibacterial and photocatalytic efficacy	[176]
Leaf extract of *Morinda citrifolia*	15-19 nm	Quasi-spherical	Antimicrobial properties	[177]
		V_2O_5 nanoparticles		
Cotton fibres	19.21 nm	Orthorhombic	Catalytic activity for the degradation of 4-nitrophrnol	[178]
Tinospora cordifolia	10-40 nm	Orthorhombic nano rods	DNA cleaving and anti angiogenic agent	[179]
Phytomolecule isolated from *Phyllanthus amarus*	10-60 nm	Nano rods	High degree of cell viability with relatively less cytotoxicity for against breast cancer cell line MDA MB	[180]
Tannic acid is a type of green material which is extracted from natural tree bark and leaves	20-40 nm	Nanobelts	High electrochromic contrast	[181]
Daphne alpine (*D. alpine*) leaves extract	34-50 nm	Spherical	The degradation of methyl orange and picloram	[182]
Yeast *Saccharomyces cerevisiae* active dry yeast cells	40-50 nm	Nano disks	Comparison with different methods obtained different morphology	[183]
		Cr_2O_3 nanoparticles		
Tridax procumbens leaf extract	80-100 nm	Strips with rough surfaces	Antibacterial activity on *Escherichia coli*	[184]
Callistemon viminalis' red flower extract	~ 92.2 nm	A cubic-like platelet shape with sharp edge		[185]
Klebsiella pneumoniae	24 nm		Antibacterial activity pathogenic bacteria	[186]
Fungal extract of *Aspargillus niger*	36 nm	Hexagonal crystals		[187]
Leaf extract of *Rhamnus virgata* (RV)	~ 28 nm	Cubic	Anticancer, antileishmanial, antibacterial, antifungal, antioxidants, bio- compatibility,	[188]
Mukia maderaspatana or mulberry leaves	54 nm	Orthorhombic	Catalyst, pigment and antibacterial effect.	[189]

		MnO_2 nanoparticles		
Euphorbia heterophylla L. leaf extract	56.68 nm	Irregular		[190]
Orange peel and the extract of orange juice	12 nm	Fine interconnected nanowires	Storage electrode materials for supercapacitor	[191]
Yucca gloriosa leaf extract	32 nm	Spherical	Optimization	[192]
Gardenia resinifera leaves	17-35 nm	Spherical	Antimicrobial activity	[193]
Yucca gloriosa leaf extract	80 mm	Spherical	Photocatalytic activities for the dye degradation in the visible light region	[194]
		Fe_3O_4 nanoparticles		
Aqueous leaf extract of *Ficus hispida* L.	10.96 nm	Spherical	Adsorption of organic dye	[195]
Azadirachta indica leaf extract	3-8 nm			[196]
Seaweed *Kappaphycus alvarezii* (K. alvarezii)	14.7 nm	Spherical		[197]
Using natural rubber latex (NRL) extracted from *Hevea brasiliensis*				[198]
Rhus coriaria	53 nm	Spherical	Reusable catalyst for efficient synthesis of some new 2-naphthol *bis*-Betti bases	[199]
Clover leaf aqueous extract	14 nm	Spherical	Green synthesis of 1,3-benzoxazole derivatives	[200]
Couroupita guianensis Aubl. fruit extract for	17 ± 10 nm	Spherical	Antibacterial and cytotoxicity activities	[201]
Grape seed Proanthocyanidin	30 nm	Irregular		[202]
Perilla frutescens leaf extract	50 nm	Spherical	Synthesis of biologically interesting benzoxazinone and benzthioxazinone	[203]
Leaf extract of *Artemisia annua* (*A. annua*)	6 nm	Spherical	Biologically interesting benzoxazinone and benzthioxazinone derivatives	[204]
		Co_3O_4 nanoparticles		
Latex of *Calotropis procera*	10 nm	Spherical	Antibacterial activity for assessing eco-toxic effects	[205]
Ethanolic extract of *Trigonella foenumgraceum* (Fenugreek) leaves	13.2 nm	Spherical		[206]
Microbial induced precipitation (MIP) process using *Bacillus pasteurii*	10-31 nm	Non specific	Supercapacitor as applicable to energy sector.	[207]
Litchi chinensis		Elongated rod like morphology		[208]
Maltose	25 nm	emi-hexagonal nanoparticles	Potential hydrogen storage material	[209]
Punica granatum peel extract	40-80 nm	Spherical	Photo-catalytic activity	[210]
Four fungi were isolated from plant *Nothapodytes foetida*, *Aspergillus nidulans* (endophytic fungus *Aspergillus nidulans*)	20.29 nm	Spherical		[211]
Taraxacum officinale plant extract	50-100 nm	Spherical	Catalytic reduction of direct yellow-142 and methyl orange dyes	[212]
		NiO nanoparticles		
Solanum trilobatum extract	25-30 nm	Cylindrical and rod	Cytotoxicity, antibacterial and photocatalytic studies	[213]
Vicennia marina leaf extract in an aqueous medium	30-100 nm	Flacks like structure nano rods like structure		[214]
Leaves extract of a wild plant "*Calotropis gigantea*"	< 60 nm		Catalytic and antimicrobial potentials	[215]
Maize (*Zea mays* L.) dry silk extract	10-20 nm	Spherical and quasi spherical	Positive electrode material for electrochemical energy storage devices.	[216]
Terminalia chebula dried fruit extract	20-25 nm	FCC cubical structure	*In vitro* cytotoxicity, MMP and ROS activity against MCF-7 Cells	[217]
Phoenix dactylifera (Dates) extract	32 nm	Nanorod like morphology	Cytotoxic activity against A549 cell lines, antibacterial activity and photocatalytic degradation of 4-chlorophenol (4-CP)	[218]
E. heterophylla (L.) leaves extract	12-15 nm	Rhombohedra	Cytotoxicity against human lung cancer cell line (A549) and human hepatocarcinoma (HepG2) cell lines and anti bacterial activity	[219]
Fresh egg white (EW)		Cubic morphology	Cytotoxicity and photocatalytic activity	[220]

CuO nanoparticles				
Leaf extract of *Enicostemma axillare* (Lam.)	30 nm			[221]
Leaves extract of *Citrofortunella microcarpa* (Calamondin)	54-68 nm	Spherical	Rhodamin B (RhB) dye was degraded by photocatalytic activity	[222]
Peel extracts of *Banana musa* acuminate	50-60 nm	Rectangular	Toxicological profiling and sensing applications	[223]
Punica granatum peels extract	10-100 nm	Spherical	Mortality of Aphid 1st, 2nd, 3rd and 4th nymphal instars by 86% compared with control.	[224]
Rosa canina fruit extract	15-25 nm	Spherical	A recyclable and heterogeneous nanocatalyst for C-N Ullmann coupling reactions	[225]
ZnO nanoparticles				
Averrhoe carrambola (star) fruit extract	20 nm	The flake-like structure with sharp edges	Photocatalytic activity on Congo red dye	[226]
Hydnocarpus alpina aqueous alcoholic extract	38.84 nm	Spherical morphology	Screening of its antimicrobial, free radical scavenging and photocatalytic activity	[227]
Prunus dulcis (Almond gum)	25 nm	Spherical	Antimicrobial and supercapacitor applications	[228]
Tecoma castanifolia leaf extract	70-75 nm	Spherical	Antioxidant, bactericidal and anticancer activities	[229]
Cassia fistula plant extract	5-15 nm	Hexagonal wurtzite structure	Photodegradative, antioxidant and antibacterial activities	[230]
Aspalathus linearis's natural extract	1 to 8.5 nm	Non-agglomerated quasi-spherical		[231]
Agathosma betulina natural extract	15.8 nm	Quasi-spherical		[232]
Euphorbia Jatropa latex	15 nm	Hexagonal		[233]
Solanum nigrum leaf extract	29.79 nm	Quasi-spherical	Antibacterial activity	[234]
Banana peel crude extract, peels of medium ripe banana (*Musa sapientum*)	39-69 nm	Rod-like or sheet-like	Antibacterial activity and anticancer activity	[235]

and stabilization of metal oxide nanoparticles utilizing plant extracts.

CONFLICT OF INTEREST

The authors declare that there is no conflict of interests regarding the publication of this article.

REFERENCES

1. T.S. Wong and U. Schwaneberg, *Curr. Opin. Biotechnol.*, **14**, 590 (2003); https://doi.org/10.1016/j.copbio.2003.09.008
2. A. Ramanavicius, A. Kausaite and A. Ramanaviciene, *Biosens. Bioelectron.*, **20**, 1962 (2005); https://doi.org/10.1016/j.bios.2004.08.032
3. M.A.E. Aleem Ali El-Remaily, A.M. Abu-Dief and R.M. El-Khatib, *Appl. Organomet. Chem.*, **30**, 1022 (2016); https://doi.org/10.1002/aoc.3536
4. L.H. Abdel-Rahman, A.M. Abu-Dief, R.M. El-Khatib and S.M. Abdel-Fatah, *Bioorg. Chem.*, **69**, 140 (2016); https://doi.org/10.1016/j.bioorg.2016.10.009
5. A.M. Abu-Dief and W.S. Mohamed, *Mater. Res. Express*, **4**, 035039 (2017); https://doi.org/10.1088/2053-1591/aa6712
6. E.M.M. Ibrahim, L.H. Abdel-Rahman, A.M. Abu-Dief, A. Elshafaie, S.K. Hamdan and A.M. Ahmed, *Mater. Res. Bull.*, **99**, 103 (2018); https://doi.org/10.1016/j.materresbull.2017.11.002
7. A.A. Marzouk, A.M. Abu-Dief and A.A. Abdelhamid, *Appl. Organomet. Chem.*, **32**, 3794 (2018); https://doi.org/10.1002/aoc.3794
8. F. Buazar, M. Bavi, F. Kroushawi, M. Halvani, A. Khaledi-Nasab and S.A. Hossieni, *J. Exp. Nanosci.*, **11**, 175 (2016); https://doi.org/10.1080/17458080.2015.1039610
9. A.M. Awwad, B.A. Albiss and N.M. Salem, *SMU Med. J.*, **2**, 91 (2015).
10. M. Nasrollahzadeh, F. Ghorbannezhad, Z. Issaabadi and S.M. Sajadi, *Chem. Rec.*, **19**, 601 (2019); https://doi.org/10.1002/tcr.201800069
11. M. Nasrollahzadeh, S. Mahmoudi-Gom Yek, N. Motahharifar and M. Ghafori Gorab, *Chem. Rec.*, **19**, 2436 (2019); https://doi.org/10.1002/tcr.201800202
12. M. Ahangari, Z. Salouti, A.R. Heidari, A.A. Kazemizadeh and A.A. Safari, *Drug Deliv.*, **20**, 34 (2013); https://doi.org/10.3109/10717544.2012.746402
13. S.A. Wolf, D.D. Awschalom, R.aA. Buhrman, J.M. Daughton, S. Von Molnar, M.L. Roukes, A.Y. Chtchelkanova and D.M. Treger, *Science*, **294**, 1488 (2001); https://doi.org/10.1126/science.1065389
14. J.B. Gruber, M.E. Hills, M.D. Seltzer, S.B. Stevens and C.A. Morrison, *J. Appl. Phys.*, **72**, 5253 (1992); https://doi.org/10.1063/1.352008
15. S.D. Birmingham, *Am. Ceram. Soc. Bull.*, **73**, 121 (1994).
16. D.-S. Cheong and W.A. Sanders, *J. Am. Ceram. Soc.*, **75**, 3331 (1992); https://doi.org/10.1111/j.1151-2916.1992.tb04429.x
17. N. Imanaka, S. Banno and G. Adachi, *Chem. Lett.*, **23**, 319 (1994); https://doi.org/10.1246/cl.1994.319
18. K. Wojtera, *Pol. J. Chem.*, **57**, 947 (1983).
19. J. Fierro, S. Mendioroz and J. Sanz, *Colloid Surf. Sci*, **93**, 487 (1983); https://doi.org/10.1016/0021-9797(83)90432-0
20. I. Ladany, P.J. Zanzucchi, J.T. Andrews, J. Kane and E. DePiano, *Appl. Opt.*, **25**, 472 (1986); https://doi.org/10.1364/AO.25.000472
21. M. Nasrollahzadeh and S. Mohammad Sajadi, *J. Colloid Interface Sci.*, **465**, 121 (2016); https://doi.org/10.1016/j.jcis.2015.11.038
22. D. Baskar and G. Nallathambi, *Mater. Lett.*, **209**, 303 (2017); https://doi.org/10.1016/j.matlet.2017.08.038
23. I.-M. Chung, I. Park, K. Seung-Hyun, M. Thiruvengadam and G. Rajakumar, *Nanoscale Res. Lett.*, **11**, 40 (2016); https://doi.org/10.1186/s11671-016-1257-4
24. A.K.T. Bui, A. Bacic and F. Pettolino, *Phytochemistry*, **67**, 1271 (2006); https://doi.org/10.1016/j.phytochem.2006.04.023
25. M. Skocaj, M. Filipic, J. Petkovic and S. Novak, *Radiol. Oncol.*, **45**, 227 (2011); https://doi.org/10.2478/v10019-011-0037-0
26. P. Ravikumar and S. Sathish Kumar, *Int. J. Technol. Res. Appl.*, **2**, 108 (2014).

27. L. Inbathamizh, T.M. Ponnu and E.J. Mary, *J. Pharm. Res.*, **6**, 32 (2013); https://doi.org/10.1016/j.jopr.2012.11.010
28. M.A. Zoubi, H.K. Farag and F. Endres, *J. Mater. Sci.*, **44**, 1363 (2009); https://doi.org/10.1007/s10853-008-3004-4
29. N. Asim, S. Radiman, M.A. Yarmo and M.S. Banaye Golriz, *Micropor. Mesopor. Mater.*, **120**, 397 (2009); https://doi.org/10.1016/j.micromeso.2008.12.013
30. S. Kobayashi, T. Takemura and F. Kaneko, *Jpn. J. Appl. Phys.*, **26**, L1274 (1987); https://doi.org/10.1143/JJAP.26.L1274
31. Y. Fujita, K. Miyazaki and C. Tatsuyama, *Jpn. J. Appl. Phys.*, **24**, 1082 (1985); https://doi.org/10.1143/JJAP.24.1082
32. D. Wruck, S. Ramamurthi and M. Rubin, *Thin Solid Films*, **182**, 79 (1989); https://doi.org/10.1016/0040-6090(89)90245-9
33. B.B. Lakshmi, C.J. Patrissi and C.R. Martin, *Chem. Mater.*, **9**, 2544 (1997); https://doi.org/10.1021/cm970268y
34. B. Alonso and J. Livage, *J. Solid State Chem.*, **148**, 16 (1999); https://doi.org/10.1006/jssc.1999.8283
35. A.B. Sifontes, G. González, L.M. Tovar, F.J. Méndez, M.E. Gomes, E. Cañizales, G. Niño-Vega, H. Villalobos and J.L. Brito, *Mater. Res. Bull.*, **48**, 730 (2013); https://doi.org/10.1016/j.materresbull.2012.11.016
36. W. He, Z. Li, Y. Wang, X. Chen, X. Zhang, H. Zhao, S. Yan and W. Zhou, *J. Mater. Sci. Mater. Med.*, **21**, 155 (2010); https://doi.org/10.1007/s10856-009-3865-3
37. D. Li, C. Tong, W. Ji, Z. Fu, Z. Wan, Q. Huang, Y. Ming, A. Mei, Y. Hu, Y. Rong and H. Han, *ACS Sustain. Chem. & Eng.*, **7**, 2619 (2019); https://doi.org/10.1021/acssuschemeng.8b05653
38. A.K. Prasad, S. Dhara and S. Dash, *Sens. Lett.*, **15**, 552 (2017); https://doi.org/10.1166/sl.2017.3847
38. C. Niu, M. Huang, P. Wang, J. Meng, X. Liu, X. Wang, K. Zhao, Y. Yu, Y. Wu, C. Lin and L. Mai, *Nano Res.*, **9**, 128 (2016); https://doi.org/10.1007/s12274-015-0896-6
40. R. Berenguer, M.O. Guerrero-Pérez, I. Guzmán, J. Rodríguez-Mirasol and T. Cordero, *ACS Omega*, **2**, 7739 (2017); https://doi.org/10.1021/acsomega.7b01061
41. Á. Cunha, J. Martins, N. Rodrigues and F. Brito, *Int. J. Energy Res.*, **39**, 889 (2015); https://doi.org/10.1002/er.3260
42. R.R. Langeslay, D.M. Kaphan, C.L. Marshall, A.P. Sattelberger, P.C. Stair and M. Delferro, *Chem. Rev.*, **119**, 2128 (2019); https://doi.org/10.1021/acs.chemrev.8b00245
43. Y. Zhang, J. Zheng, Y. Zhao, T. Hu, Z. Gao and C. Meng, *Appl. Surf. Sci.*, **377**, 385 (2016); https://doi.org/10.1016/j.apsusc.2016.03.180
44. W. Jin, B. Dong, W. Chen, C. Zhao, L. Mai and Y. Dai, *Sens. Actuators B Chem.*, **145**, 211 (2010); https://doi.org/10.1016/j.snb.2009.11.059.
45. X. Yang, X. Peng, C. Xu and F. Wang, *J. Electrochem. Soc.*, **156**, C167 (2009); https://doi.org/10.1149/1.3082378
46. M. Ludwig, E. Sniezek, I. Jastrzebska, R. Prorok, Y. Li, N. Liao, M. Nath, J. Vlcek and J. Szczerba, *Materials*, **15**, 725 (2022); https://doi.org/10.3390/ma15030725
47. J.-Y. Hwang and D.-S. Seo, *J. Electrochem. Soc.*, **157**, J351 (2010); https://doi.org/10.1149/1.3473785
48. M. Freemantle, *Chemical Eng News Archive*, **76**, 8 (1998); https://doi.org/10.1021/cen-v076n006.p008
49. J.I. Fasick, N. Lee and D.D. Oprian, *Biochemistry*, **38**, 11593 (1999); https://doi.org/10.1021/bi991600h
50. H. Rotter, M.V. Landau, M. Carrera, D. Goldfarb and M. Herskowitz, *Appl. Catal. B*, **47**, 111 (2004); https://doi.org/10.1016/j.apcatb.2003.08.006
51. H. Rotter, M.V. Landau and M. Herskowitz, *Environ. Sci. Technol.*, **39**, 6845 (2005); https://doi.org/10.1021/es0500052
52. L. Chen, Z. Song, X. Wang, S.V. Prikhodko, J. Hu, S. Kodambaka and R. Richards, *Appl. Mater. Interf.*, **1**, 1931 (2009); https://doi.org/10.1021/am900334q
53. Y.-L. Bai, H.-B. Xu, Y. Zhang and Z.-H. Li, *J. Phys. Chem. Solids*, **67**, 2589 (2006); https://doi.org/10.1016/j.jpcs.2006.07.018
54. A.C. Santulli, M. Feygenson, F.E. Camino, M.C. Aronson and S.S. Wong, *Chem. Mater.*, **23**, 1000 (2011); https://doi.org/10.1021/cm102930z
55. D,-W. Kim, S.-I. Shin, J.-D. Lee and S.-G. Oh, *Mater. Lett.*, **58**, 189 (2004); https://doi.org/10.1016/j.matlet.2003.11.023
56. A.A. Ali, M. Madkour, F. Al Sagheer, M.I. Zaki and A.A. Nazeer, *Catalysts*, **10**, 105 (2020); https://doi.org/10.3390/catal10010105
57. T.M. Al-Saadi and N.A. Hameed, *Adv. Phys. Theor. Appl.*, **44**, 139 (2015).
58. P. Li, H.B. Xu, Y. Zhang, Z.H. Li, S.L. Zheng and Y.L. Bai, *Dyes Pigm.*, **80**, 287 (2009); https://doi.org/10.1016/j.dyepig.2008.07.016
59. T.V. Rao, Y. Yang and A. Sayari, *J. Mol. Catal. Chem.*, **301**, 152 (2009); https://doi.org/10.1016/j.molcata.2008.12.026
60. G. Wang, L. Zhang, J. Deng, H. Dai, H. He and C.T. Au, *Appl. Catal. A*, **355**, 192 (2009); https://doi.org/10.1016/j.apcata.2008.12.020
61. X. Pang, K. Gao, F. Luo, Y. Emirov, A.A. Levin and A.A. Volinsky, *Thin Solid Films*, **517**, 1922 (2009); https://doi.org/10.1016/j.tsf.2008.10.026
62. X. Hou and K.L. Choy, *Thin Solid Films*, **516**, 8620 (2008); https://doi.org/10.1016/j.tsf.2008.06.045
63. M. Abecassis-Wolfovich, H. Rotter, M.V. Landau, E. Korin, A.I. Erenburg, D. Mogilyansky and E. Garshtein, *Stud. Surf. Sci. Catal.*, **146**, 247 (2003); https://doi.org/10.1016/S0167-2991(03)80373-7
64. C.L. Li, H.X. Zhao, T. Takahashi and M. Matsumura, *Mater. Sci. Eng. A*, **308**, 268 (2001); https://doi.org/10.1016/S0921-5093(00)01976-6
65. M.V. Landau, G.E. Shter, L. Titelman, V. Gelman, H. Rotter, G.S. Grader and M. Herskowitz, *Ind. Eng. Chem. Res.*, **45**, 7462 (2006); https://doi.org/10.1021/ie0606744
66. Y. Meng, W. Song, H. Huang, Z. Ren, S.-Y. Chen and S.L. Suib, *J. Am. Chem. Soc.*, **136**, 11452 (2014); https://doi.org/10.1021/ja505186m
66. C. Wei, L. Yu, C. Cui, J. Lin, C. Wei, N. Mathews, F. Huo, T. Sritharan and Z. Xu, *Chem. Commun.*, **50**, 7885 (2014); https://doi.org/10.1039/c4cc02781g
68. Y. Lvov, B. Munge, O. Giraldo, I. Ichinose, S.L. Suib and J.F. Rusling, *Langmuir*, **16**, 8850 (2000); https://doi.org/10.1021/la000110j
69. X.-L. Luo, J.-J. Xu, W. Zhao and H.-Y. Chen, *Biosens. Bioelectron.*, **19**, 1295 (2004); https://doi.org/10.1016/j.bios.2003.11.019
70. M. Wayu, *Solids*, **2**, 232 (2021); https://doi.org/10.3390/solids2020015
71. A. Asfaram, M. Ghaedi, S. Hajati and A. Goudarzi, *RSC Adv.*, **5**, 72300 (2015); https://doi.org/10.1039/C5RA10815B
72. T.A. Abdullah, R.T. Rasheed, T. Juzsakova, N. Al-Jammal, M.A. Mallah, L.P. Cuong, A.D. Salman, E. Domokos, Z. Ali and I. Cretescu, *Int. J. Environ. Sci. Technol.*, **18**, 1499 (2021); https://doi.org/10.1007/s13762-020-02956-x
73. E. Moazzen, K. Kucuk, S. Aryal, E.V. Timofeeva and C.U. Segre, *J. Power Sources*, **448**, 227374 (2020); https://doi.org/10.1016/j.jpowsour.2019.227374
74. S. Nazir, H. Jan, G. Zaman, T. Khan, H. Ashraf, B. Meer, M. Zia, S. Drouet, C. Hano and B.H. Abbasi, *Artif. Cells, Nanomed. Biotechnol.*, **49**, 625 (2021); https://doi.org/10.1080/21691401.2021.1984935
75. T. Li, T. Shi, X. Li, S. Zeng, L. Yin and Y. Pu, *Int. J. Environ. Res. Public Health*, **11**, 7918 (2014); https://doi.org/10.3390/ijerph110807918
76. M.M. Najafpour, F. Rahimi, E.-M. Aro, S.I. Allakhverdiev and C.-H. Lee, *J. R. Soc. Interface*, **9**, 2383 (2012); https://doi.org/10.1098/rsif.2012.0412

77. D. Van-Phuc, L. Ngoc-Chung and N. Ngoc-Tuan, Removal of Copper(II) From Aqueous Solution by Adsorption onto MnO_2 Nanostructure: Equilibrium and Kinetic Studies, The 4th Academic Conference on Natural Science for Young Scientists, Master & Phd Students from Asean Countries, pp. 57-64 (2015).
78. A. Bahadur, S. Iqbal, A. Saeed, M.I. Bashir, M. Shoaib, M. Waqas, G. Shabir and A. Jabbar, *Chem. Pap.*, **71**, 1445 (2017); https://doi.org/10.1007/s11696-017-0138-3
79. D.L. Huber, *Small*, **1**, 482 (2005); https://doi.org/10.1002/smll.200500006
80. R.M. Cornell and U. Schwertmann, The Iron Oxides: Structure, Properties, Reactions, Occurrences and Uses, John Wiley & Sons, Ed.: 2 (2006).
81. S. Laurent, D. Forge, M. Port, A. Roch, C. Robic, L. Vander Elst and R.N. Muller, *Chem. Rev.*, **108**, 2064 (2008); https://doi.org/10.1021/cr068445e
82. A.S. Teja and P.-Y. Koh, *Prog. Cryst. Growth Charact. Mater.*, **55**, 22 (2009); https://doi.org/10.1016/j.pcrysgrow.2008.08.003
83. M. De Cuyper and M. Joniau, *Eur. Biophys. J.*, **15**, 311 (1988); https://doi.org/10.1007/BF00256482
84. S. Hasany, I. Ahmed, J. Rajan and A. Rehman, *Nanosci. Nanotechnol.*, **2**, 148 (2012); https://doi.org/10.5923/j.nn.20120206.01
85. Y. Cai, Y. Shen, A. Xie, S. Li and X. Wang, *J. Magn. Magn. Mater.*, **322**, 2938 (2010); https://doi.org/10.1016/j.jmmm.2010.05.009
86. N. Latha and M. Gowri, *Int. J. Scient. Res.*, **3**, 1551 (2014).
87. V.V. Makarov, S.S. Makarova, A.J. Love, O.V. Sinitsyna, A.O. Dudnik, I.V. Yaminsky, M.E. Taliansky and N.O. Kalinina, *Langmuir*, **30**, 5982 (2014); https://doi.org/10.1021/la5011924
88. S. Venkateswarlu, B.N. Kumar, B. Prathima, K. Anitha and N.V.V. Jyothi, *Phys B.*, **457**, 30 (2015); https://doi.org/10.1016/j.physb.2014.09.007
89. C. Prasad, S. Gangadhara and P. Venkateswarlu, *Appl. Nanosci.*, **6**, 797 (2016); https://doi.org/10.1007/s13204-015-0485-8
90. V. Niraimathee, V. Subha, R.E. Ravindran and S. Renganathan, *Int. J. Environ. Sustain. Dev.*, **15**, 227 (2016); https://doi.org/10.1504/IJESD.2016.077370
91. M. Martínez-Cabanas, M. López-García, J.L. Barriada, R. Herrero and M.E. Sastre de Vicente, *Chem. Eng. J.*, **301**, 83 (2016); https://doi.org/10.1016/j.cej.2016.04.149
92. W.H. Li and N. Yang, *Mater. Lett.*, **162**, 157 (2016); https://doi.org/10.1016/j.matlet.2015.09.064
93. M. Mahdavi, M.B. Ahmad, M.J. Haron, F. Namvar, B. Nadi, M.Z.A. Rahman and J. Amin, *Molecules*, **18**, 7533 (2013); https://doi.org/10.3390/molecules18077533
94. J.K. Patra, M.S. Ali, I.G. Oh and K.H. Baek, *Artif. Cells Nanomed. Biotechnol.*, **45**, 349 (2017); https://doi.org/10.3109/21691401.2016.1153484
95. S. Gil, C.R. Correia and J.F. Mano, *Adv. Healthc. Mater.*, **4**, 883 (2015); https://doi.org/10.1002/adhm.201400611
96. M.F. Horst, D.F. Coral, M.B. Fernández van Raap, M. Alvarez and V. Lassalle, *Mater. Sci. Eng.*, **74**, 443 (2017); https://doi.org/10.1016/j.msec.2016.12.035
97. D. Azarifar, O. Badalkhani and Y. Abbasi, *J. Sulfur Chem.*, **37**, 656 (2016); https://doi.org/10.1080/17415993.2016.1177055
98. K. Hardani, F. Buazar, K. Ghanemi and M. Kashisaz, *Am. Assoc. Sci. Technol. J. Nanosci.*, **1**, 11 (2015).
99. D. He, L. Li, F. Bai, C. Zha, L. Shen, H.H. Kung and N. Bao, *Chem. Eur. J.*, **22**, 4454 (2016); https://doi.org/10.1002/chem.201504429
100. W. Sun, S. Mignani, M. Shen and X. Shi, *Drug Discov. Today*, **21**, 1873 (2016); https://doi.org/10.1016/j.drudis.2016.06.028
101. J. Li, Y. Hu, J. Yang, P. Wei, W. Sun, M. Shen, G. Zhang and X. Shi, *Biomaterials*, **38**, 10 (2015); https://doi.org/10.1016/j.biomaterials.2014.10.065
102. W.M. Liu, Y.N. Xue, N. Peng, W.-T. He, R.-X. Zhuo and S.-W. Huang, *J. Mater. Chem.*, **21**, 13306 (2011); https://doi.org/10.1039/c1jm11460c
103. H. El Ghandoor, *Int. J. Electrochem. Sci.*, **7**, 5734 (2012).
104. Y. Sun, J. Li, Y. Wang, C. Ding, Y. Lin, W. Sun and C. Luo, *Spectrochim. Acta A Mol. Biomol. Spectrosc.*, **178**, 1 (2017); https://doi.org/10.1016/j.saa.2017.01.057
105. W. Lu, M. Ling, M. Jia, P. Huang, C. Li and B. Yan, *Mol. Med. Rep.*, **9**, 1080 (2014); https://doi.org/10.3892/mmr.2014.1906
106. T. Lai, Y. Lai, C. Lee, Y. Shu and C. Wang, *Catal. Today*, **131**, 105 (2008); https://doi.org/10.1016/j.cattod.2007.10.039
107. M. El Baydi, G. Poillerat, J.-L. Rehspringer, J.L. Gautier, J.-F. Koenig and P. Chartier, *J. Solid State Chem.*, **109**, 281 (1994); https://doi.org/10.1006/jssc.1994.1105
108. S.W. Oh, H.J. Bang, Y.C. Bae and Y.K. Sun, *J. Power Sources*, **173**, 502 (2007); https://doi.org/10.1016/j.jpowsour.2007.04.087
109. A.U. Mane, K. Shalini, A. Wohlfart, A. Devi and S.A. Shivashankar, *J. Cryst. Growth*, **240**, 157 (2002); https://doi.org/10.1016/S0022-0248(02)00860-6
110. A. Rumplecker, F. Kleitz, E.L. Salabas and F. Schüth, *Chem. Mater.*, **19**, 485 (2007); https://doi.org/10.1021/cm0610635
111. F. Mohandes, F. Davar and M. Salavati-Niasari, *J. Magn. Magn. Mater.*, **322**, 872 (2010); https://doi.org/10.1016/j.jmmm.2009.11.019
112. L. Ren, P. Wang, Y. Han, C. Hu and B. Wei, *Mater. Phys. Lett.*, **476**, 78 (2009); https://doi.org/10.1016/j.cplett.2009.06.015
113. L. Li, Y. Chu, Y. Liu, J.L. Song, D. Wang and X.W. Du, *Mater. Lett.*, **62**, 1507 (2008); https://doi.org/10.1016/j.matlet.2007.09.012
114. D.Y. Kim, S.H. Ju, H.Y. Koo, S.K. Hong and Y.C. Kang, *J. Alloys Compd.*, **417**, 254 (2006); https://doi.org/10.1016/j.jallcom.2005.09.013
115. F. Gu, C. Li, Y. Hu and L. Zhang, *J. Cryst. Growth*, **304**, 369 (2007); https://doi.org/10.1016/j.jcrysgro.2007.03.040
116. X. Wang, X.Y. Chen, L.S. Gao, H.G. Zheng, Z. Zhang and Y.T. Qian, *J. Phys. Chem. B*, **108**, 16401 (2004); https://doi.org/10.1021/jp048016p
117. A.S. Bhatt, D.K. Bhat, C.W. Tai and M.S. Santosh, *Mater. Chem. Phys.*, **125**, 347 (2011); https://doi.org/10.1016/j.matchemphys.2010.11.003
118. R.M. Wang, C.M. Liu, H.Z. Zhang, C.P. Chen, L. Guo, H.B. Xu and S.H. Yang, *Appl. Phys. Lett.*, **85**, 2080 (2004); https://doi.org/10.1063/1.1789577
119. H. Duan, D.Wang and Y. Li, *Chem. Soc. Rev.*, **44**, 5778 (2015); https://doi.org/10.1039/C4CS00363B
120. K. Elumalai, S. Velmurugan, S. Ravi, V. Kathiravan and G. Adaikala Raj, *Adv. Powder Technol.*, **26**, 1639 (2015); https://doi.org/10.1016/j.apt.2015.09.008
121. S.J. Hoseini, M. Darroudi, R. Kazemi Oskuee, L. Gholami and A. Khorsand Zak, *Adv. Powder Technol.*, **26**, 991 (2015); https://doi.org/10.1016/j.apt.2015.04.003
122. S. Iravani, *Green Chem.*, **13**, 2638 (2011); https://doi.org/10.1039/c1gc15386b
123. S.K. Kannan and M. Sundrarajan, *Adv. Powder Technol.*, **26**, 1505 (2015); https://doi.org/10.1016/j.apt.2015.08.009
124. A.K. Mittal, Y. Chisti and U.C. Banerjee, *Biotechnol. Adv.*, **31**, 346 (2013); https://doi.org/10.1016/j.biotechadv.2013.01.003
125. A.B. Samui, D.S. Patil, C.D. Prasad and N.M. Gokhale, *Adv. Powder Technol.*, **27**, 1879 (2016); https://doi.org/10.1016/j.apt.2016.06.010
126. B. Siripireddy and B.K. Mandal, *Adv. Powder Technol.*, **28**, 785 (2017); https://doi.org/10.1016/j.apt.2016.11.026
127. M. Sundrarajan, S. Ambika and K. Bharathi, *Adv. Powder Technol.*, **26**, 1294 (2015); https://doi.org/10.1016/j.apt.2015.07.001
128. M. Fazlzadeh, K. Rahmani, A. Zarei, H. Abdoallahzadeh, F. Nasiri and R. Khosravi, *Adv. Powder Technol.*, **28**, 122 (2017); https://doi.org/10.1016/j.apt.2016.09.003

129. J.K. Patra, Y. Kwon and K.-H. Baek, *Adv. Powder Technol.*, **27**, 2204 (2016); https://doi.org/10.1016/j.apt.2016.08.005
130. J.K. Sharma, P. Srivastava, G. Singh, M.S. Akhtar and S. Ameen, *Mater. Sci. Eng. B*, **193**, 181 (2015); https://doi.org/10.1016/j.mseb.2014.12.012
131. A. Diallo, A.C. Beye, T.B. Doyle, E. Park and M. Maaza, *Green Chem. Lett. Rev.*, **8**, 30 (2015); https://doi.org/10.1080/17518253.2015.1082646
132. I. Bibi, N. Nazar, M. Iqbal, S. Kamal, H. Nawaz, S. Nouren, Y. Safa, K. Jilani, M. Sultan, S. Ata, F. Rehman and M. Abbas, *Adv. Powder Technol.*, **28**, 2035 (2017); https://doi.org/10.1016/j.apt.2017.05.008
133. B. Sasi and K.G. Gopchandran, *Nanotechnology*, **18**, 115613 (2007); https://doi.org/10.1088/0957-4484/18/11/115613
134. K. Anandan and V. Rajendran, *Mater. Sci. Eng. B*, **199**, 48 (2015); https://doi.org/10.1016/j.mseb.2015.04.015
135. M. Jeyaraj, S. Gurunathan, M. Qasim, M.-H. Kang and J.-H. Kim, *Nanomaterials*, **9**, 1719 (2019); https://doi.org/10.3390/nano9121719
136. R. Hada, *Int. Res. J. Pure Appl. Chem.*, **3**, 111 (2013); https://doi.org/10.9734/IRJPAC/2013/2937
137. Y. Gangarajula and B. Gopal, *Appl. Catal A*, **475**, 211 (2014); https://doi.org/10.1016/j.apcata.2014.01.036
138. R. Veerasamy, T.Z. Xin, S. Gunasagaran, T.F.W. Xiang, E.F.C. Yang, N. Jeyakumar and S.A. Dhanaraj, *J. Saudi Chem. Soc.*, **15**, 113 (2011); https://doi.org/10.1016/j.jscs.2010.06.004
139. A. Kar and A.K. Ray, *Am. J. Nanosci. Nanotechnol.*, **2**, 17 (2014); https://doi.org/10.11648/j.nano.20140202.11
140. T. Jiang, Y. Wang, D. Meng and M. Yu, *Superlatt. Microstruct.*, **85**, 1 (2015); https://doi.org/10.1016/j.spmi.2015.05.014
141. A.F. Mohd Abd Fatah and N. A. Hamid, *Fund. Appl. Sci.*, **14**, 391 (2018); https://doi.org/10.11113/mjfas.v14n3.1220
142. S. Sundar, G. Venkatachalam and S.J. Kwon, *Nanomaterials*, **8**, E823 (2018); https://doi.org/10.3390/nano8100823
143. B.T. Sone, A. Diallo, X.G. Fuku, A. Gurib-Fakim and M. Maaza, *Arab. J. Chem.*, **13**, 160 (2020); https://doi.org/10.1016/j.arabjc.2017.03.004
144. Q. Maqbool, S. Iftikhar, M. Nazar, F. Abbas, A. Saleem, T. Hussain, R. Kausar, S. Anwaar and N. Jabeen, *IET Nanobiotechnol.*, **11**, 463 (2017); https://doi.org/10.1049/iet-nbt.2016.0125
145. W.M. Mohammed, T.H. Mubark and R.M.S. Al-Haddad, *Int. J. Appl. Eng. Res. Dev.*, **13**, 10559 (2018).
146. J. Emima Jeronsia, L. Allwin Joseph, P. Annie Vinosha, A. Jerline Mary and S. Jerome Das, *Mater. Today Proc.*, **8**, 214 (2019); https://doi.org/10.1016/j.matpr.2019.02.103
147. M.H. Koupaei, B. Shareghi, A.A. Saboury, F. Davar, A. Semnani and M. Evini, *RSC Adv.*, **6**, 42313 (2016); https://doi.org/10.1039/C5RA24862K
148. J. Sackey, A.C. Nwanya, A.K.H. Bashir, N. Matinise, J.B. Ngilirabanga, A.E. Ameh, E. Coetsee and M. Maaza, *Mater. Chem. Phys.*, **244**, 122714 (2020); https://doi.org/10.1016/j.matchemphys.2020.122714
149. K. Vishveshvar, M.A. Krishnan, K. Haribabu and S. Vishnuprasad, *BioNanoSci.*, **8**, 554 (2018); https://doi.org/10.1007/s12668-018-0508-5
150. S. Pourbeyram, J. Abdollahpour and M. Soltanpour, *Mater. Sci. Eng. C*, **94**, 850 (2019); https://doi.org/10.1016/j.msec.2018.10.034
151. M. Rafique, A.J. Shaikh, R. Rasheed, M.B. Tahir, S.S.A. Gillani, A. Usman, M. Imran, A. Zakir, Z.U.H. Khan and F. Rabbani, *J. Inorg. Organomet. Polym. Mater.*, **28**, 2455 (2018); https://doi.org/10.1007/s10904-018-0921-9
152. A. Azam, A.S. Ahmed, M. Oves, M. Khan and A. Memic, *Int. J. Nanomed.*, **7**, 3527 (2012); https://doi.org/10.2147/IJN.S29020
153. S.A. Akintelu and A.S. Folorunso, *J. Nanotechnol. Nanomed. Nanobiotechnol.*, **6**, 22 (2019); https://doi.org/10.24966/NTMB-2044/100022
154. K.D. Sirdeshpande, A. Sridhar, K.M. Cholkar and R. Selvaraj, *Appl. Nanosci.*, **8**, 675 (2018); https://doi.org/10.1007/s13204-018-0698-8
155. M. Saravanan, S.K. Barik, D.M. Ali, P. Prakash and A. Pugazhendhi, *Microb. Pathog.*, **116**, 221 (2018); https://doi.org/10.1016/j.micpath.2018.01.038
156. M.S. Samuel, S. Jose, E. Selvarajan, T. Mathimani and A. Pugazhendhi, *J. Photochem. Photobiol. B*, **202**, 111642 (2020); https://doi.org/10.1016/j.jphotobiol.2019.111642
157. M. Hosseini-Koupaei, B. Shareghi, A.A. Saboury, F. Davar, V.A. Sirotkin, M.H. Hosseini-Koupaei and Z. Enteshari, *Int. J. Biol. Macromol.*, **122**, 732 (2019); https://doi.org/10.1016/j.ijbiomac.2018.11.001
158. A.B. Rezaie, M. Montazer and M.M. Rad, *J. Photochem. Photobiol. B*, **176**, 100 (2017); https://doi.org/10.1016/j.jphotobiol.2017.09.021
159. S. Chand Mali, S. Raj and R. Trivedi, *Biochem. Biophys. Rep.*, **20**, 100699 (2019); https://doi.org/10.1016/j.bbrep.2019.100699
160. F. Duman, I. Ocsoy and F.O. Kup, *Mater. Sci. Eng. C*, **60**, 333 (2016); https://doi.org/10.1016/j.msec.2015.11.052
161. V. Srikant and D.R. Clarke, *J. Appl. Phys.*, **83**, 5447 (1998); https://doi.org/10.1063/1.367375
162. P.K. Stoimenov, R.L. Klinger, G.L. Marchin and K.J. Klabunde, *Langmuir*, **18**, 6679 (2002); https://doi.org/10.1021/la0202374
163. M. Roselli, A. Finamore, I. Garaguso, M.S. Britti and E. Mengheri, *J. Nutr.*, **133**, 4077 (2003); https://doi.org/10.1093/jn/133.12.4077
164. N.A.N. Mohamad, N.A. Arham, J. Jai and A. Hadi, *Adv. Mater. Res.*, **832**, 350 (2014); https://doi.org/10.4028/www.scientific.net/AMR.832.350
165. V.V. Makarov, A.J. Love, O.V. Sinitsyna, S.S. Makarova, I.V. Yaminsky, M.E. Taliansky and N.O. Kalinina, *Acta Naturae*, **6**, 35 (2014); https://doi.org/10.32607/20758251-2014-6-1-35-44
166. A.G. Ingale and A.N. Chaudhari, *J. Nanomed. Nanotechnol.*, **4**, 1 (2013); https://doi.org/10.4172/2157-7439.1000165
167. S.M. Roopan, V.D. Rajeswari, V.N. Kalpana and G. Elango, *Appl. Microbiol. Biotechnol.*, **100**, 1153 (2016); https://doi.org/10.1007/s00253-015-7190-0
168. J. Rajkumari, C.M. Magdalane, B. Siddhardha, M.V. Arasu, N.A. Al-Dhabi, J. Madhavan, G. Ramalingam, A.K.M. Ghilan, V. Duraipandiayan and K. Kaviyarasu, *J. Photochem. Photobiol. B*, **201**, 111667 (2019); https://doi.org/10.1016/j.jphotobiol.2019.111667
169. S. Marimuthu, A.A. Rahuman, C. Jayaseelan, T. Santhoshkumar, A.V. Kirthi, K. Velayutham, A. Bagavan, C. Kamaraj, G. Elango, M. Iyappan, C. Siva, L. Karthik and K.V. Rao, *Asian Pac. J. Trop. Med.*, **6**, 682 (2013); https://doi.org/10.1016/S1995-7645(13)60118-2
170. P.O. Akinola, A. Lateef, T.B. Asafa, L.S. Beukes, A.S. Hakeem and H.M. Irshad, *Heliyon*, **6**, e04610 (2020); https://doi.org/10.1016/j.heliyon.2020.e04610
171. R. Dobrucka, *Iran. J. Pharm. Res.*, **16**, 756 (2017).
172. T. Santhoshkumar, A.A. Rahuman, C. Jayaseelan, G. Rajakumar, S. Marimuthu, A.V. Kirthi, K. Velayutham, J. Thomas, J. Venkatesan and S.-K. Kim, *Asian Pac. J. Trop. Med.*, **7**, 968 (2014); https://doi.org/10.1016/S1995-7645(14)60171-1
173. G. Rajakumar, A.A. Rahuman, S.M. Roopan, I.M. Chung, K. Anbarasan and V. Karthikeyan, *Parasitol. Res.*, **114**, 571 (2015); https://doi.org/10.1007/s00436-014-4219-8
174. N.A. Al-Shabib, F.M. Husain, F.A. Qais, N. Ahmad, A. Khan, A.A. Alyousef, M. Arshad, S. Noor, J.M. Khan, P. Alam, T.H. Albalawi and S.A. Shahzad, *Front. Microbiol.*, **11**, 1680 (2020); https://doi.org/10.3389/fmicb.2020.01680.
175. G. Rajakumar, A.A. Rahuman, C. Jayaseelan, T. Santhoshkumar, S. Marimuthu, C. Kamaraj, A. Bagavan, A.A. Zahir, A.V. Kirthi, G. Elango, P. Arora, R. Karthikeyan, S. Manikandan and S. Jose, *Parasitol. Res.*, **113**, 469 (2014); https://doi.org/10.1007/s00436-013-3676-9
176. K. Thandapani, M. Kathiravan, E. Namasivayam, I.A. Padiksan, G. Natesan, M. Tiwari, B. Giovanni and V. Perumal, *Environ. Sci. Pollut. Res. Int.*, **25**, 10328 (2018); https://doi.org/10.1007/s11356-017-9177-0

177. M. Sundrarajan, K. Bama, M. Bhavani, S. Jegatheeswaran, S. Ambika, A. Sangili, P. Nithya and R. Sumathi, *J. Photochem. Photobiol. B*, **171**, 117 (2017); https://doi.org/10.1016/j.jphotobiol.2017.05.003
178. S. Alghool, H.F. Abd El-Halim and A.M. Mostafa, *J. Inorg. Organomet. Polym. Mater.*, **29**, 1324 (2019); https://doi.org/10.1007/s10904-019-01096-1
179. P. Deepika, H.M. Vinusha, B. Muneera, N.D. Rekha and K. Shiva Prasad, *Curr. Res. Green Sustainable Chem.*, **1-2**, 14 (2020); https://doi.org/10.1016/j.crgsc.2020.04.001
180. K.S. Prasad, C. Shivamallu, G. Shruthi and M. Prasad, *Chemistry Select*, **3**, 3860 (2018); https://doi.org/10.1002/slct.201800653
181. W. Kang, C. Yan, X. Wang, C.Y. Foo, A.W.M. Tan, K.J.Z. Chee and P.S. Lee, *J. Mater. Chem. C*, **2**, 4727 (2014); https://doi.org/10.1039/C4TC00158C
182. P. Rasheed, S. Haq, M. Waseem, S. Rehman, W. Rehman, N. Bibi and S.A.A. Shah, *Mater. Res. Expr.*, **7**, 2053 (2020); https://doi.org/10.1088/2053-1591/ab6fa2
183. N. Talavera, M. Navarro, A. Sifontes, Y. Díaz, H. Villalobos, G. Nino-Vega, A. Boada-Sucre and I. Gonzalez, Ed.: S.G. Padalai, Green Synthesis of Nanosized Vanadium Pentoxide using *Saccharomyces Cervisiae* as Biotemplate, In: Recent Research Developments in Materials Science, Kerala: Research Signpost, vol. 10, Chap. 5, pp. 89-102 (2013).
184. C. Ramesh, K.T. Mohan Kumar, N. Latha and V. Ragunathan, *Curr. Nanosci.*, **8**, 603 (2012); https://doi.org/10.2174/157341312801784366
185. B.T. Sone, E. Manikandan, A. Gurib-Fakim and M. Maaza, *Green Chem. Lett. Rev.*, **9**, 85 (2016); https://doi.org/10.1080/17518253.2016.1151083
186. P. Sangwan and H. Kumar, *Asian J. Pharm. Clin. Res.*, **10**, 206 (2017); https://doi.org/10.22159/ajpcr.2017.v10i2.15189
187. Z. Ahmad, A. Shamim, S. Mahmood, T. Mahmood and F. Khan, *Eng. Appl. Sci. Letts.*, **1**, 23 (2018); https://doi.org/10.30538/psrp-easl2018.0008
188. J. Iqbal, B.A. Abbasi, A. Munir, S. Uddin, S. Kanwal and T. Mahmood, *Microsc. Res. Technol.*, **83**, 706 (2020); https://doi.org/10.1002/jemt.23460
189. N. Gupta and S.P. Resmi, *Imp. J. Interdisciplin. Res.*, **2**, 532 (2016).
190. N.O.M. Dewi and Y. Yulizar, *Mater. Today: Proc.*, **22**, 199 (2020); https://doi.org/10.1016/j.matpr.2019.08.088
191. H.M. Abuzeid, S.A. Elsherif, N.A. Abdel Ghany and A.M. Hashem, *J. Energy Storage*, **21**, 156 (2019); https://doi.org/10.1016/j.est.2018.11.021
192. M. Souri, V. Hoseinpour, N. Ghaemi and A. Shakeri, *Int. Nano Lett.*, **9**, 73 (2019); https://doi.org/10.1007/s40089-018-0257-z
193. V. Kumar, K. Singh, S. Panwar and S.K. Mehta, *Int. Nano Lett.*, **7**, 123 (2017); https://doi.org/10.1007/s40089-017-0205-3
194. S.A. Khan, S. Shahid, B. Shahid, U. Fatima and S.A. Abbasi, *Biomolecules*, **10**, 785 (2020); https://doi.org/10.3390/biom10050785
195. A.V. Ramesh, B. Lavakusa, B.S. Mohan, Y.P. Kumar, D.R. Devi and K. Basavaiah, *IOSR J. Appl. Chem.*, **10**, 35 (2017); https://doi.org/10.9790/5736-1007013543
196. A.V. Samrot, P. Senthilkumar, S. Rashmitha, P. Veera and C.S. Sahithya, *J. Nanostruct. Chem.*, **8**, 343 (2018); https://doi.org/10.1007/s40097-018-0279-0
197. Y.P. Yew, K. Shameli, M. Miyake, N. Kuwano, N.B. Bt Ahmad Khairudin, S.E. Bt Mohamad and K.X. Lee, *Nanoscale Res. Lett.*, **11**, 276 (2016); https://doi.org/10.1186/s11671-016-1498-2
198. A. Azizi, *J. Inorg. Organomet. Polym.*, **30**, 3552 (2020); https://doi.org/10.1007/s10904-020-01500-1
199. A.A. Barzinjy, D.A. Abdul, F.H.S. Hussain and S.M. Hamad, *Inorg. Nano-Metal Chem.*, **50**, 620 (2020): https://doi.org/10.1080/24701556.2020.1723027
200. A. Azizi, *J. Inorg. Organomet. Polym. Mater.*, **30**, 3552 (2020); https://doi.org/10.1007/s10904-020-01500-1
201. G. Sathishkumar, V. Logeshwaran, S. Sarathbabu, P.K. Jha, M. Jeyaraj, C. Rajkuberan, N. Senthilkumar and S. Sivaramakrishnan, *Artif. Cells Nanomed. Biotechnol.*, **46**, 589 (2018); https://doi.org/10.1080/21691401.2017.1332635
202. S. Narayanan, B.N. Sathy, U. Mony, M. Koyakutty, S.V. Nair and D. Menon, *ACS Appl. Mater. Interfaces*, **4**, 251 (2012); https://doi.org/10.1021/am201311c
203. N. Basavegowda, K. Mishra and Y. Lee, *RSC Adv.*, **4**, 61660 (2014); https://doi.org/10.1039/C4RA11623B
204. N. Basavegowda, K.B. Somai Magar, K. Mishra and Y.R. Lee, *New J. Chem.*, **38**, 5415 (2014); https://doi.org/10.1039/C4NJ01155D
205. S. Dubey, J. Kumar, A. Kumar and Y.C. Sharma, *Adv. Powder Technol.*, **29**, 2583 (2018); https://doi.org/10.1016/j.apt.2018.03.009
206. N. Akhlaghi, G. Najafpour-Darzi and H. Younesi, *Adv. Powder Technol.*, **31**, 3562 (2020); https://doi.org/10.1016/j.apt.2020.07.004
207. C.-M. Hsu, Y.-H. Huang, H.-J. Chen, W.-C. Lee, H.-W. Chiu, J.P. Maity, C.-C. Chen, Y.-H. Kuo and C.-Y. Chen, *Mater. Today Commun.*, **14**, 302 (2018); https://doi.org/10.1016/j.mtcomm.2018.02.005
208. D.C. Onwudiwe, M.P. Ravele and E.E. Elemike, *Nano-Structures & Nano-Objects*, **23**, 100470 (2020); https://doi.org/10.1016/j.nanoso.2020.100470
209. F.S. Razavi, A. Sobhani, O. Amiri, M. Ghiyasiyan-Arani and M. Salavati-Niasari, *Int. J. Hydrogen Energy*, **45**, 17662 (2020); https://doi.org/10.1016/j.ijhydene.2020.04.273
210. I. Bibi, N. Nazar, M. Iqbal, S. Kamal, H. Nawaz, S. Nouren, Y. Safa, K. Jilani, M. Sultan, S. Ata, F. Rehman and M. Abbas, *Adv. Powder Technol.*, **28**, (2017); https://doi.org/10.1016/j.apt.2017.05.008
211. A.S. Vijayanandan and R.M. Balakrishnan, *J. Environ. Manage.*, **218**, 442 (2018); https://doi.org/10.1016/j.jenvman.2018.04.032
212. T. Rasheed, F. Nabeel, M. Bilal and H.M.N. Iqbal, *Biocatal. Agric. Biotechnol.*, **19**, 101154 (2019); https://doi.org/10.1016/j.bcab.2019.101154
213. A.A. Ezhilarasi, J.J. Vijaya, K. Kaviyarasu, X. Zhang and L.J. Kennedy, *Surf. Interfaces*, **20**, 100553 (2020); https://doi.org/10.1016/j.surfin.2020.100553
214. P. Karpagavinayagam, A. Emi Princess Prasanna and C. Vedhi, *Mater. Today Proc.*, **48**, 136 (2022); https://doi.org/10.1016/j.matpr.2020.04.183
215. M.I. Din, A.G. Nabi, A. Rani, A. Aihetasham and M. Mukhtar, *Environ. Nanotechnol. Monit. Manage.*, **9**, 29 (2018); https://doi.org/10.1016/j.enmm.2017.11.005
216. A.C. Nwanya, M.M. Ndipingwi, C.O. Ikpo, R.M. Obodo, S.C. Nwanya, S. Botha, F.I. Ezema, E.I. Iwuoha and M. Maaza, *J. Alloys Compd.*, **822**, 153581 (2020); https://doi.org/10.1016/j.jallcom.2019.153581
217. F. Ibraheem, M.H. Aziz, M. Fatima, F. Shaheen, S.M. Ali and Q. Huang, *Mater. Lett.*, **234**, 129 (2018); https://doi.org/10.1016/j.matlet.2018.09.075
218. A.A. Ezhilarasi, J.J. Vijaya, L.J. Kennedy and K. Kaviyarasu, *Mater. Chem. Phys.*, **241**, 122419 (2020); https://doi.org/10.1016/j.matchemphys.2019.122419
219. K. Lingaraju, H. Raja Naika, H. Nagabhushana, K. Jayanna, S. Devaraja and G. Nagaraju, *Arab. J. Chem.*, **13**, 4712 (2019); https://doi.org/10.1016/j.arabjc.2019.11.003
220. Z. Sabouri, A. Akbari, H.A. Hosseini, M. Khatami and M. Darroudi, *Polyhedron*, **178**, 114351 (2020); https://doi.org/10.1016/j.poly.2020.114351
221. S.C. Mali, S. Raj and R. Trivedi, *Biochem. Biophys. Rep.*, **20**, 100699 (2019); https://doi.org/10.1016/j.bbrep.2019.100699
222. M. Rafique, F. Shafiq, S.S. Ali Gillani, M. Shakil, M.B. Tahir and I. Sadaf, *Optik*, **208**, 164053 (2020); https://doi.org/10.1016/j.ijleo.2019.164053
223. S. Chaudhary, D. Rohilla, A. Umar, N. Kaur and A. Shanavas, *Ceram. Int.*, **45**, 15025 (2019); https://doi.org/10.1016/j.ceramint.2019.04.239

224. A.Y. Ghidan, T.M. Al-Antary and A.M. Awwad, *Environ. Nanotechnol. Monitor. Manage.*, **6**, 95 (2016); https://doi.org/10.1016/j.enmm.2016.08.002
225. S. Hemmati, L. Mehrazin, M. Hekmati, M. Izadi and H. Veisi, *Mater. Chem. Phys.*, **214**, 527 (2018); https://doi.org/10.1016/j.matchemphys.2018.04.114
226. S. Chakraborty, J.J. Farida, R. Simon, S. Kasthuri and N.L. Mary, *Surf. Interfaces*, **19**, 100488 (2020). https://doi.org/10.1016/j.surfin.2020.100488
227. M. Ganesh, S.G. Lee, J. Jayaprakash, M. Mohankumar and H.T. Jang, *Biocatal. Agric. Biotechnol.*, **19**, 101129 (2019); https://doi.org/10.1016/j.bcab.2019.101129
228. G.T. Anand, D. Renuka, R. Ramesh, L. Anandaraj, S.J. Sundaram, G. Ramalingam, C.M. Magdalane, A.K.H. Bashir, M. Maaza and K. Kaviyarasu, *Surf. Interfaces*, **17**, 100376 (2019); https://doi.org/10.1016/j.surfin.2019.100376
229. G. Sharmila, M. Thirumarimurugan and C. Muthukumaran, *Microchem. J.*, **145**, 578 (2019); https://doi.org/10.1016/j.microc.2018.11.022
230. D. Suresh, P.C. Nethravathi, H. Udayabhanu, H. Nagabhushana, H. Rajanaika and S.C. Sharma, *Mater. Sci. Semicond. Process.*, **31**, 446 (2015); https://doi.org/10.1016/j.mssp.2014.12.023
231. A. Diallo, B.D. Ngom, E. Park and M. Maaza, *J. Alloys Compd.*, **646**, 425 (2015); https://doi.org/10.1016/j.jallcom.2015.05.242
232. F.T. Thema, E. Manikandan, M.S. Dhlamini and M. Maaza, *Mater. Lett.*, **161**, 124 (2015); https://doi.org/10.1016/j.matlet.2015.08.052
233. M.S. Geetha, H. Nagabhushana and H.N. Shivananjaiah, *J. Sci.: Adv. Mater. Devices*, **1**, 301 (2016); https://doi.org/10.1016/j.jsamd.2016.06.015
234. M. Ramesh, M. Anbuvannan and G. Viruthagiri, *Spectrochim. Acta A Mol. Biomol. Spectrosc.*, **136**, 864 (2015); https://doi.org/10.1016/j.saa.2014.09.105
235. J. Ruangtong, J. T-Thienprasert and N.P. T-Thienprasert, *Mater. Today Commun.*, **24**, 101224 (2020); https://doi.org/10.1016/j.mtcomm.2020.101224

SRR & CVR Government Degree College (A) Vijayawada

Department of Mathematics

&

Department of Statistics

Report on

"Skill Enhancement Activity - Students Participation in 3-day Workshop on MATLAB at KBN College(A)"

(An Experiential & Peer Learning – Hands on Experience)

Dt: 28th to 30th April 2022

The Departments of Mathematics & Statistics encouraged the students of II & III year mathematics groups to participate in the 3-day workshop on MATLAB organised by the department of Mathematics & Statistics, KBN College(A), Vijayawada from 28-04-2022 to 30-04-2022. With the permission of the Principal Dr. K. Bhagya Lakshmi garu, HOD of the department of mathematics Smt. K.V Naga Lakshmi guided the students to attend the workshop. With the company of faculty members of the departments Sri M.Lakshmana Dasu, K.Ashok, P.Ramesh, Dr. K. Rajinikanth, Dr. K.V Rama Rao, a total of 25 students attended the workshop. The other faculty members are also involved in this activity.

The students learnt the basics of MATLAB and various topics (listed below) with hands on experience in the lab from the resource person of the workshop Dr. E. Vargil Kumar, Associate Professor, Gudlavalleru Engineering College,

Topics learnt in the workshop:

1. About MATLAB
2. MATLAB Tools
3. Some Math functions
4. Operations on vectors and matrices
5. Solution of equations using functions
6. MATLAB Built-in functions
7. Plotting graphs
8. About Unacademy APP

Learning Out Comes:

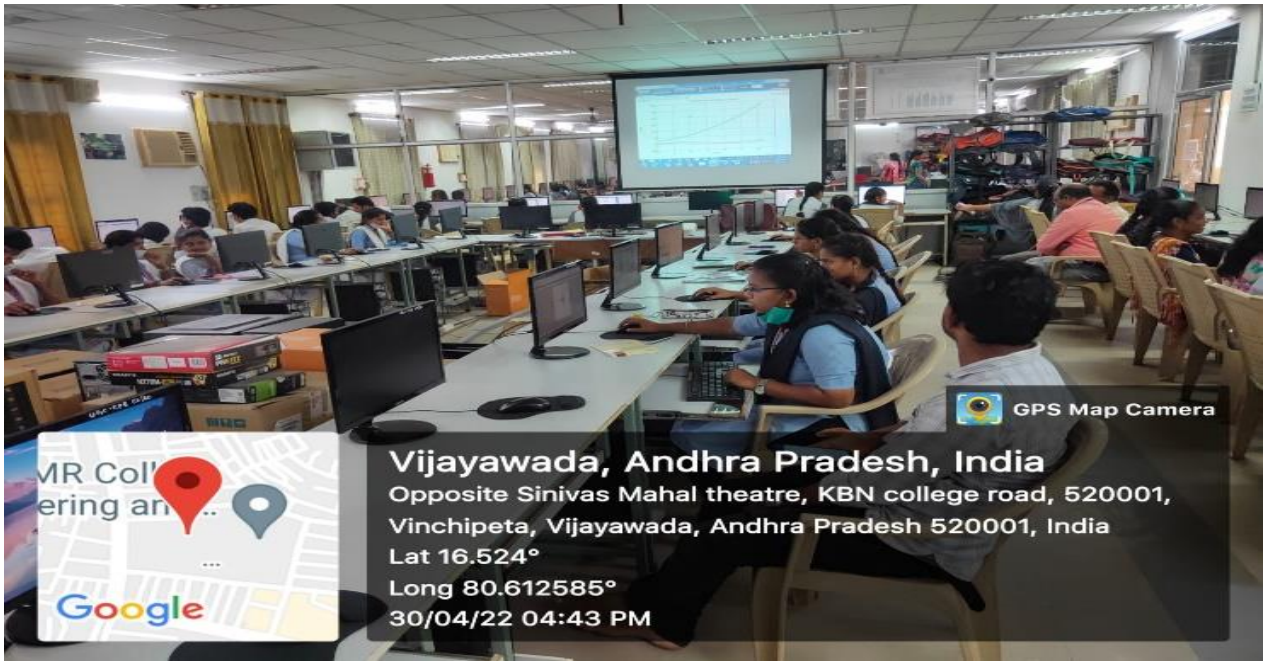
1. Students got awareness about MATLAB and its applications
2. Enriched on the usage of MATLAB to solve various mathematical problems with hands on experience.

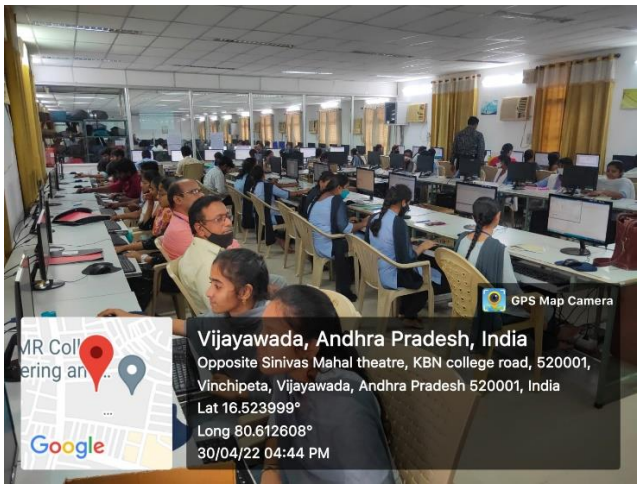
List of Students participated:

1. Ch. Sai Babu, III B.Sc MSCs
2. S. Jyothi, III B.Sc MSCs
3. G. Renuka Vyshnavi, III B.Sc MSCs
4. G. Venu, III B.Sc MSCs
5. M. Vaneswari, III B.Sc MSCs
6. P. Karishma, III B.Sc MSCs
7. G. Lakshmi, II B.Sc MSCs
8. P. Kiranmai, II B.Sc MSCs
9. T. Satya Kameswari, II B.Sc MSCs
10. N. Pratap Kumar, II B.Sc MSCs
11. P. Jishnu Suseela, II B.Sc MSCs
12. N. Priyanka, II B.Sc MSCs
13. PDVNR Shivani, II B.Sc MSCs
14. S. Ajay Kumar, II B.Sc MSCs
15. S. Uma Mahesh, II B.Sc MSCs

16. S. Abraham Lincoln, II B.Sc MSCs
17. B.Vivek, II B.Sc MSCs
18. D.Eswar Teja, II B.Sc MSCs
19. MD. Yasin Ali, II B.Sc MSCs
20. D. Karunakar, II B.Sc MSCs
21. M.Kusuma, II B.Sc MSCs
22. G. Jyothi, II B.Sc MSCs
23. B. Ravi Kiran, III B.Sc MPC
24. B. Yaswanth, III B.Sc MPC
25. M. Anil, III B.Sc MPC

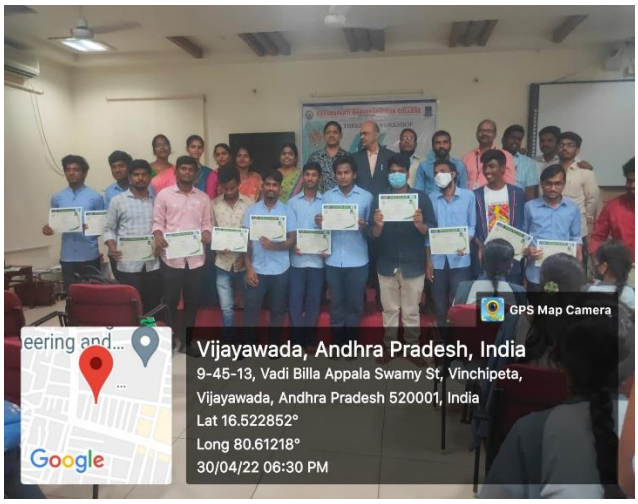



GPS Map Camera
Vijayawada, Andhra Pradesh, India
Opposite Sinivas Mahal theatre, KBN college road, 520001,
Vinchipeta, Vijayawada, Andhra Pradesh 520001, India
Lat 16.524°
Long 80.612585°
30/04/22 04:43 PM
Google


GPS Map Camera
Vijayawada, Andhra Pradesh, India
Opposite Sinivas Mahal theatre, KBN college road, 520001,
Vinchipeta, Vijayawada, Andhra Pradesh 520001, India
Lat 16.523999°
Long 80.612608°
30/04/22 04:44 PM
Google


vivo Y20G




GPS Map Camera
Vijayawada, Andhra Pradesh, India
9-45-13, Vadi Billa Appala Swamy St, Vinchipeta,
Vijayawada, Andhra Pradesh 520001, India
Lat 16.522852°
Long 80.61218°
30/04/22 06:30 PM
Google



[Certificates of all students]

Vijayawada,
Date: 27-04-2022

To

The Principal,
S.R.R & C.V.R GOVT Degree College (A),
Vijayawada.

Respected Principal Madam,

Sub:- Departments of Mathematics and Statistics - **Permission to send II B.Sc. & III B.Sc., Mathematics Students for attending MAT LAB Training Programme from 28-04-2022 to 30-04-2022 organising by K.B.N. College, Department of Mathematics, Vijayawada** – Reg.

***

I bring to kind notice that, K.B.N. College, Vijayawada is conducting MAT LAB Training Programme from 28-04-2022 to 30-04-2022 by the Department of Mathematics.

Hence I request you to kindly give permission for the students of II B.Sc. & III B.Sc. for attending the MAT LAB Training Programme from 28-04-2022 to 30-04-2022, which is useful to the Students. I am here with enclosing the List of the Participating Students & Broacher of the Programme.

Thanking you.

27.4.2022

Encl: 1) List of the Participating Students.

2) Broacher of the Programme

Yours faithfully,

27/4/2022.

(K.V. Naga Lakshmi)

In-charge of Mathematics Dept.

S.R.R. & C.V.R. GDC (A), Dept. of Chemistry :

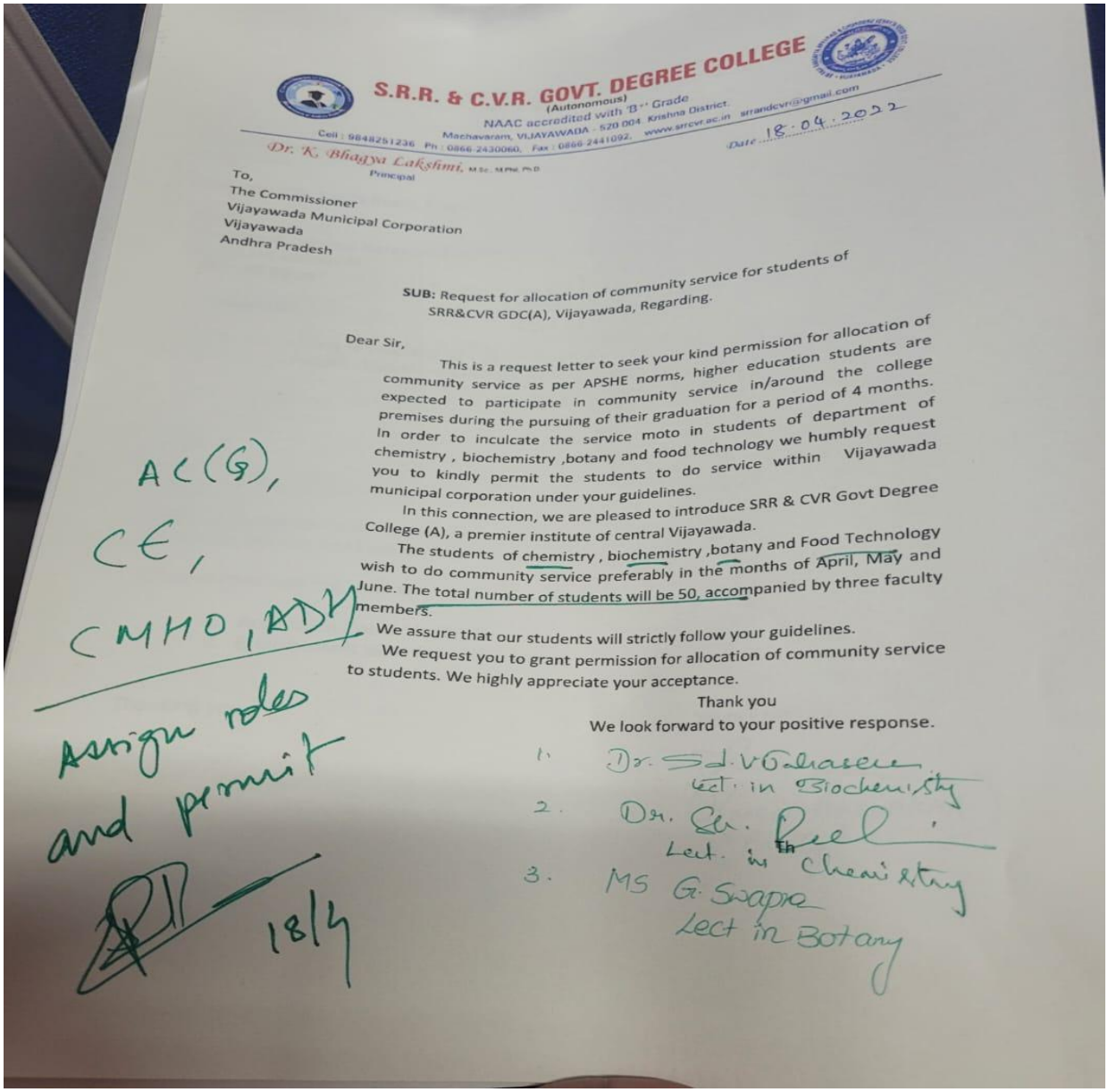
Parishubrata warotsavaalu in vijayawda

Outreach programme*- Swatch sarvekshan by II Year - M.P.C, M.B.C, B.Z.C and M.C.CS students*

21.04.2022 to 26.04.2022

Documentation by Dr. Sk. Beebi

Dept. of Chemistry joined with Dept. of Biochemistry, Dept. of Botany has planned an extension activity under the collaboration of Vijayawada Municipal corporation sensitised the students towards social responsibility in the Vijayawada city. Total 60 students participated in Swatch sarvekshan (Parisaralu parishuratha) programme conducted by Vijayawada Municipal Corporation from 21st April to 26th April, 2022 in different localities across the Eluru road.



S.R.R. & C.V.R. GOVT. DEGREE COLLEGE
(Autonomous)
NAAC accredited with 'B++' Grade
Machavaram, VIJAYAWADA - 520 004. Krishna District.
Cell : 9848251236 Ph : 0866-2430060, Fax : 0866-2441092. www.srrcvr.ac.in srrandcvr@gmail.com

Dr. K. Bhagya Lakshmi, M.Sc., M.Phil., Ph.D
Principal

Date 18.04.2022

To,
The Commissioner
Vijayawada Municipal Corporation
Vijayawada
Andhra Pradesh

SUB: Request for allocation of community service for students of SRR&CVR GDC(A), Vijayawada, Regarding.

Dear Sir,

This is a request letter to seek your kind permission for allocation of community service as per APSHE norms, higher education students are expected to participate in community service in/around the college premises during the pursuing of their graduation for a period of 4 months. In order to inculcate the service moto in students of department of chemistry , biochemistry ,botany and food technology we humbly request you to kindly permit the students to do service within Vijayawada municipal corporation under your guidelines.

In this connection, we are pleased to introduce SRR & CVR Govt Degree College (A), a premier institute of central Vijayawada.

The students of chemistry , biochemistry ,botany and Food Technology wish to do community service preferably in the months of April, May and June. The total number of students will be 50, accompanied by three faculty members.

We assure that our students will strictly follow your guidelines.

We request you to grant permission for allocation of community service to students. We highly appreciate your acceptance.

Thank you

We look forward to your positive response.

1. Dr. Sd. V Balasree, Lect. in Biochemistry
2. Dr. Sk. Beebi, Lect. in Chemistry
3. MS G. Swapna, Lect in Botany

AC(G), CE, CMHO, ADH
Assign roles and permit
18/4

The objective of this OUTREACH PROGRAMME by our students is to inculcate social responsibility and to understand the current day social problems and their remedies.

The programme is scheduled for 6 days., Each day with a separate theme of campaigning.

Day 1 : Monday – Don't throw waste on roads

Day 2 : Tuesday – Keep separate dustbin for wet waste and dry waste

Day 3: Wednesday – Cleaning and drying

Day 4 : Thursday – Ban plastic covers and plastic usage

Day 5 : Friday – Dry-day: Keep our surroundings' clean and dry

Day 6: Planting trees

The programme started on Monday by planting the trees and ended up by planting the trees.










vijayawada
విజయవాడ నగరపాలక సంస్థ
సుందర హరిత విజయవాడ
GPS Map Camera
Vijayawada, Andhra Pradesh, India
32-40/1-75A, Divine Nagar, Machavaram, Vijayawada, Andhra Pradesh 520004, India
Lat 16.519593°
Long 80.654958°
22/04/22 08:55 AM
Google


GPS Map Camera
Vijayawada, Andhra Pradesh, India
32-40-36, Yaram Vari St, Machavaram Down, Machavaram, Vijayawada, Andhra Pradesh 520004, India
Lat 16.518767°
Long 80.652434°
22/04/22 08:42 AM
Google


GPS Map Camera
Vijayawada, Andhra Pradesh, India
32-40-40A, Yaram Vari St, Machavaram, Vijayawada, Andhra Pradesh 520004, India
Lat 16.518233°
Long 80.652298°
22/04/22 08:39 AM
Google

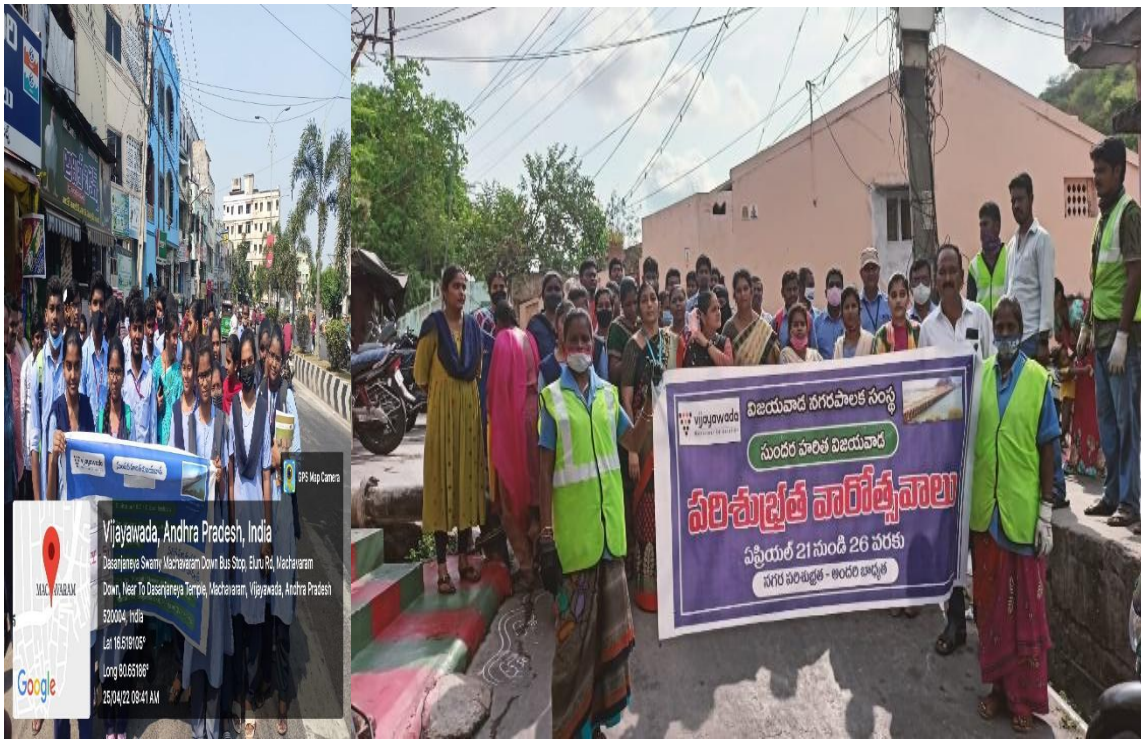

GPS Map Camera
Vijayawada, Andhra Pradesh, India
Dasanjaneya Swamy Machavaram Down Bus Stop, Eluru Rd, Machavaram Down, Near To Dasanjaneya Temple, Machavaram, Vijayawada, Andhra Pradesh 520004, India
Lat 16.519134°
Long 80.651877°
25/04/22 09:42 AM
Google
DAY - 5


ApolloPharmacy
vijayawada
సుందర హరిత విజయవాడ
Sanitation/ IEC / Citizen feedback
GPS Map Camera
MACH
75
Google
Vijayawada, Andhra Pradesh, India
GJ9X+FR6, Machavaram, Vijayawada, Andhra Pradesh 520004, India
Lat 16.518722°
Long 80.649586°
26/04/22 09:25 AM


ApolloPharmacy
vijayawada
సుందర హరిత విజయవాడ
Sanitation/ IEC / Citizen feedback
GPS Map Camera
MACH
75
Google
Vijayawada, Andhra Pradesh, India
GJ9X+FR6, Machavaram, Vijayawada, Andhra Pradesh 520004, India
Lat 16.518722°
Long 80.649586°
26/04/22 09:25 AM


vijayawada
సుందర హరిత విజయవాడ
Sanitation/ IEC / Citizen feedback
Zero garbage / IEC activities/ wall paintings/ plantation
Drain Cleaning
Plastic Ban
DAY-6
GPS Map Camera
Vijayawada, Andhra Pradesh, India
GJ9X+FR6, Machavaram, Vijayawada, Andhra Pradesh 520004, India
Lat 16.518722°
Long 80.649586°
26/04/22 09:25 AM
Google


MADINA
MUTTON CURRY
CHICKEN KEBAB
vijayawada
సుందర హరిత విజయవాడ
Sanitation/ IEC / Citizen feedback
GPS Map Camera
Vijayawada, Andhra Pradesh, India
32-26, 76/2, Eluru Rd, Machavaram, Vijayawada, Andhra Pradesh 520004, India
Lat 16.518589°
Long 80.64879°
25/04/22 09:23 AM
Masjid St
Google



Conclusion: This programme motivated our students towards cleanliness and inculcated the thought of clean and green environment which imply absence of pollution and a better quality of life. Everyone should think of its our God given duty to take care of our environment and keep it clean.

పారిశుద్ధ్య నిర్వహణకు ప్రాధాన్యత



విజయవాడ, మహానగర్

పారిశుద్ధ్య నిర్వహణకు ప్రభుత్వం అత్యంత ప్రాధాన్యతనిస్తోందని కార్పొరేటర్ అంబడిపూడి నిర్మలకుమారి పేర్కొన్నారు. నగర పాలక సంస్థ నిర్వహిస్తున్న ప్రత్యేక పారిశుద్ధ్య అవగాహన కార్యక్రమంలో భాగంగా శనివారం రెండో డివిజన్ పరిధిలో అవగాహన కార్యక్రమాలు నిర్వహించారు. ఎస్సారార్ కాలేజీ విద్యార్థులతో కలసి ప్లాస్టిక్ నిషేధం, పరిసరాల పరిశుభ్రత గురించి మాచవరం పరిసర ప్రాంతాల్లో అవగాహన కార్యక్రమం నిర్వహించారు. ఈ కార్యక్రమంలో కార్పొరేటర్ అంబడిపూడి నిర్మలకుమారి, స్పెషల్ ఆఫీసర్ చంద్రశేఖర్, డివిజన్ పరిధిలోని శానిటరీ సిబ్బంది, సచివాలయ సిబ్బంది, రెవెన్యూ సిబ్బంది పాల్గొన్నారు.

CERTIFICATE COURSE

LIFE SKILLS DEVELOPMENT TRAINING

in Association with

Barclays - Rubicon Foundation

DATE: 16-12- 2021 to 21-12-2021

No. of Participants : 127

Resource Persons : Jagadeesh & M. Sarkar (Rubicon Foundation Trainers)

DEPARTMENT OF PHYSICS & ELECTRONICS

SRR & CVR GOVERNMENT DEGREE COLLEGE(AUTONOMOUS)

Machavaram, Vijayawada - 520 004

BARCLAYS - RUBICON LIFESKILLS TRAINING PROGRAMME

Rubicon "Connect with work " " program supported by Barclays FinancialBank is conducted to the SRR & CVR GOVERNMENT DEGREE COLLEGE, VIJAYAWADA students in ONLINE mode.Under this training students are trained by corporate trainers . This enhanced their life skills which might increase their chances of succeeding in a job interview.

Objectives of the Training

To enhance one's ability to be fully self aware by helping oneself to overcome all fears and insecurities.
To set appropriate goals, manage stress and time effectively.
To adapt workplace environment.

Batch No	Date & Time	No. of Days	No. of students trained	Mode of Training	Trainer Name	Remarks
1&2	16 th to 21st December 2021 9AM - 2PM	6 days 30 hours	127	ONLINE	JAGADEESH & M. Sarkar	127 students received their certificates

Course outline (ONLINE)

New Hire Training/ Personality Development/ Employability Skills			
Sr. No.	Topic	Learning Objectives	Duration
1	Expectation setting	To learn Industry expectations from freshers	1
2	Ice breaking	To know more about the trainer & candidates	1
3	Organizational Structure	To learn Organizational structure	2
4	SWOT Analysis	To identify their Strength/Weakness/Opportunities/ Threat	2
5	Corporate Jargons	To learn most commonly used words in corporates	1
6	Public Speaking	To eliminate stage fear	2
7	Presentation Skills	To articulate your thoughts through Power point presentation	2
8	E-mail Etiquette	To learn E-mail writing skills	2
9	Grooming	Dress to impress/ Proximity/ Personal hygiene/	2

10	Body language	To learn positive body language	1
11	Telephone Etiquette	To handle telephonic round of interview/ To learn call mechanics	2
12	Group Discussion	To access candidates' public speaking skills	4
13	Personal Interview	To perform well during interviews	8
Total			**30hrs**

Permission letter.pdf

S.No	Student name	Class/ group
1	S.Jagadeesh	B.Sc - III Year
2	M.Gopi Krishna	B.Sc - III Year
3	Y.Sai Praveen	B.Sc - III Year
4	M. Krupa	B.Sc - III Year
5	A. Lavanya	B.Sc - III Year
6	N.Likhitha	B.Sc - III Year
7	M. Bhagya Lakshmi	B.Sc - III Year
8	D.Krishnaveni	B.Sc - III Year
9	D. Keerthi	B.Sc - III Year
10	M. Pushpa Latha	B.Sc - III Year
11	K.Keerthi	B.Sc - III Year
12	P. Dhanyasri	B.Sc - III Year
13	E. Nagarjuna	B.Sc - III Year
14	I.Nagavamsi	B.Sc - III Year
15	V.Hemanth Kumar	B.Sc - III Year
16	K Manikanta	B.Sc - III Year
17	K.Ganesh	B.Sc - III Year
18	Prudhvi	B.Sc - III Year
19	P.Yaswanth Kumar	B.Sc - III Year
20	Sk.Althaf	B.Sc - III Year
21	Chaitanya Kumar	B.Sc - III Year
22	R Naveen Naik	B.Sc - III Year
23	M.Sweety	B.Sc - III Year
24	V Mantru Naik	B.Sc - III Year
25	S. Bhavitha	B.Sc - III Year
26	A.Brahmaiah	B.Sc - III Year
27	K. Rajeswari	B.Sc - III Year
28	Md. Shahin	B.Sc - III Year
29	S.M.L Sireesha	B.Sc - III Year

30	Shaik Shahanaz	B.Sc - III Year
31	R.Roopesh	B.Sc - III Year
32	K.Teja	B.Sc - III Year
33	V.Narasimha Naidu	B.Sc - III Year
34	V.Vijay Kumar	B.Sc - III Year
35	G.V.Ajay Kumar	B.Sc - III Year
36	V.Durga Eshwar	B.Sc - III Year
37	M.Jaswanth	B.Sc - III Year
38	L.Subhashini	B.Sc - III Year
39	M.Siddartha	B.Sc - III Year
40	A.N.D Kalyani	B.Sc - III Year
41	Swarna Sri	B.Sc - III Year
42	V. Nagamani	B.Sc - III Year
43	S. Naga Seetha	B.Sc - III Year
44	K. Sravanthi	B.Sc - III Year
45	B.Hemalatha	B.Sc - III Year
46	B. Lakshmanrao	B.Sc - III Year
47	Venkataiah	B.Sc - III Year
48	A. Anantharaju	B.Sc - III Year
49	K. Venu	B.Sc - III Year
50	U. Anil Kumar	B.Sc - III Year
51	Alladi Manasa	B.Sc - III Year
52	G.Nagendrababu	B.Sc - III Year
53	R Pavan Kumar	B.Sc - III Year
54	K. Naveen	B.Sc - III Year
55	T Ganesh	B.Sc - III Year
56	Srinu	B.Sc - III Year
57	P.Pothuraju	B.Sc - III Year
58	K.Durgarao	B.Sc - III Year
59	D.Prudhvi	B.Sc - III Year
60	P. M. D. Sai Sandeep	B.Sc - III Year
61	Sk.Duran	B.Sc - III Year
62	J.Pavan Kumar	B.Sc - III Year
63	J.Pradeep	B.Sc - III Year
64	Y.Siva Sai Ram	B.Sc - III Year
65	S.Adi Narayana	B.Sc - III Year
66	K.Swami Sekhar	B.Sc - III Year
67	Rokesh.P	B.Sc - III Year
68	E.Veeranjaneyulu	B.Sc - III Year
69	B.Venkatesh	B.Sc - III Year
70	N.Premchend	B.Sc - III Year
71	R.Chandra Sekhar	B.Sc - III Year

Department of Physics & Electronics CVR GDC

72	M.Vijay Kumar	B.Sc - III Year
73	K.Suresh	B.Sc - III Year
74	S.Gopi Krishna	B.Sc - III Year
75	N.Jayanth	B.Sc - III Year
76	K.Akhil	B.Sc - III Year
77	M.Subba Rao Naik	B.Sc - III Year
78	Matta Samuel Paul	B.Sc - III Year
79	R.Venkatapathi Devaraya	B.Sc - III Year
80	B. Gopi Krishna Naik	B.Sc - III Year
81	K. Vinod Kumar	B.Sc - III Year
82	R.Sai Kumar	B.Sc - III Year
83	Y.Siva Narayana	B.Sc - III Year
84	P.Jagadeesh	B.Sc - III Year
85	Durga Prasad	B.Sc - III Year
86	P.Phanindra	B.Sc - III Year
87	S.Siddhardha	B.Sc - III Year
88	M.Anil	B.Sc - III Year
89	P.Kishore Reddy	B.Sc - III Year
90	R.Dinesh Sai Kumar	B.Sc - III Year
91	E.Sai Krishna	B.Sc - III Year
92	Sk.Sameer	B.Sc - III Year
93	P.Adi	B.Sc - III Year
94	I.Sandya Bhavani	B.Sc - III Year
95	Sowjanya	B.Sc - III Year
96	V.Hareesh	B.Sc - III Year
97	B. Lakshmanrao	B.Sc - III Year
98	B. Balaji	B.Sc - III Year
99	M.Meena Kumari	B.Sc - III Year
100	Kommu Venu	B.Sc - III Year
101	Adhi Lakshmi	B.Sc - III Year
102	K Venkat	B.Sc - III Year
103	A. Anantha Raju	B.Sc - III Year
104	P. Venkatesh	B.Sc - III Year
105	T. Varalakshmi	B.Sc - III Year
106	V. Mathew Babu	B.Sc - III Year
107	V. Raja	B.Sc - III Year
108	P. Jaswanth	B.Sc - III Year
109	R.Siva	B.Sc - III Year
110	K. Komali	B.Sc - III Year
111	M. Hima N	B.Sc - III Year
112	K. Nagarjuna	B.Sc - III Year
113	Vinod Kumar	B.Sc - III Year

PHYSICS & ELECTRONICS CVR GDC

114	Mohammed.Haseena	B.Sc - III Year
115	Kundeti.Anitha	B.Sc - III Year
116	Daggupati.Harileela	B.Sc - III Year
117	Korada.Suguna	B.Sc - III Year
118	Rowthu.Sirisha	B.Sc - III Year
119	Peddireddy.Leela R Mani	B.Sc - III Year
120	Uriviti.Sravana Lakshmi	B.Sc - III Year
121	Pothireddy.Ramya	B.Sc - III Year
122	Kommu.Hema Bhargavi	B.Sc - III Year
123	Gaddam. Divya	B.Sc - III Year
124	Gompa. Srinu	B.Sc - III Year
125	Sura. Nani	B.Sc - III Year
126	Katta Srinivasa Rao	B.Sc - III Year
127	Bevara Ganesh	B.Sc - III Year

Action Plan: 127 Students from MPC , MPCs , MECs streams from B.Sc are registered to this program through URL shared by Rubicon Team with their details like Aadhar ID, Name, College. A WhatsApp group is created to guide & instruct the students. Raagini – Rubicon (Business Executive) coordinated this program. Everyday at 8.50AM ZOOM link is shared to students group, only who registered are allowed to attend this program. Later Students joined in their respective Breakout sessions. The course is highly interactive & trainers tried to interact with each student. Assignments are given to students. students posted their assignments chat box / emailed to the Trainer. The entire training is coordinated by B. Nagamani, Lecturer in physics from SRR & CVR GDC, VJA.

CERTIFICATES_BARCLAYS_RUBICON SRR& CVR GDC PHYSICS DEPT



Student feedback

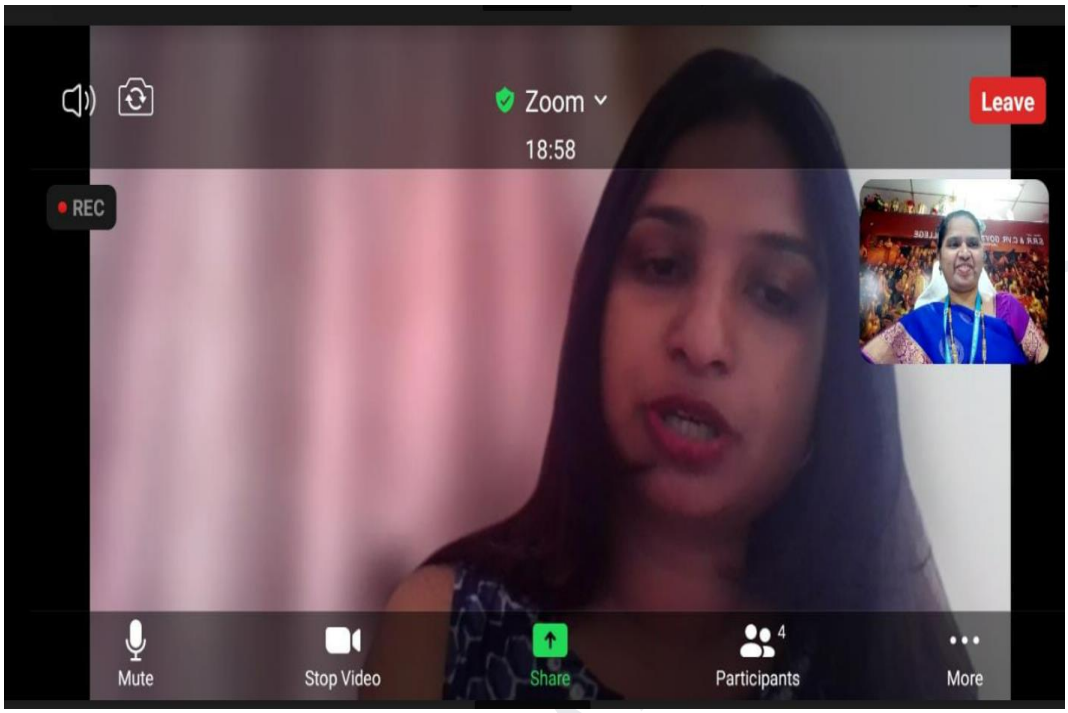
Before training students have issues with problem solving attitude, ability to express their thoughts, and when & how to start a conversation.

After training they overcome these challenges by curiosity, time management, self motivation and breaking their work process into small steps.

They are able to prepare their resume for a job interview. They developed skills like grooming, body language and communication skills , which are necessary for job interviews.

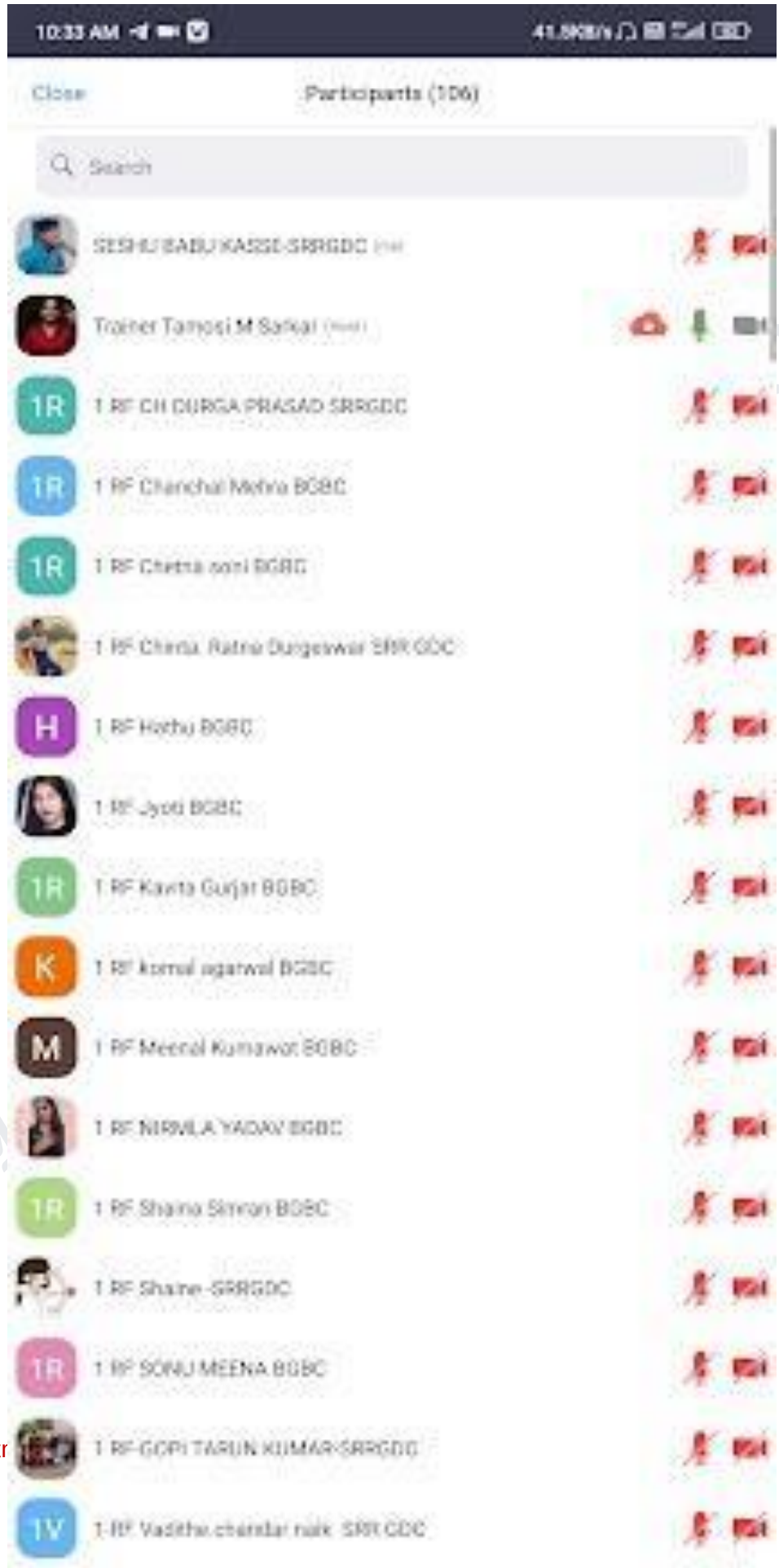
MURALIKRISHNA FEEDBACK

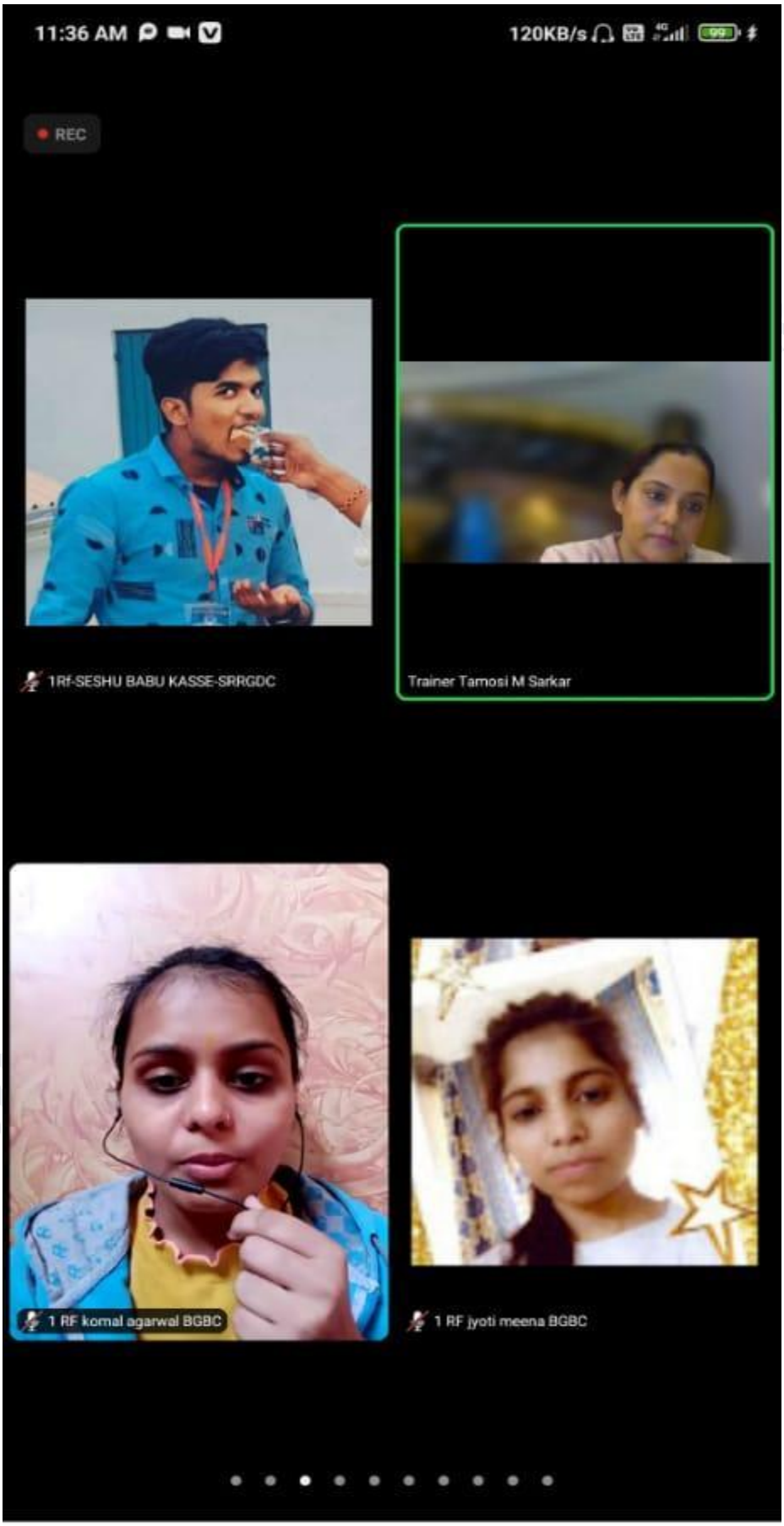
Dr. K. Bhagya Lakshmi, ,PRINCIPAL SRR & CVR GOVERNMENT DEGREE COLLEGE (A), VIJAYAWADA connected on Zoom meeting with rubicon CEO Dhanya Narayanan and gave feedback on 28 -02 -2022.

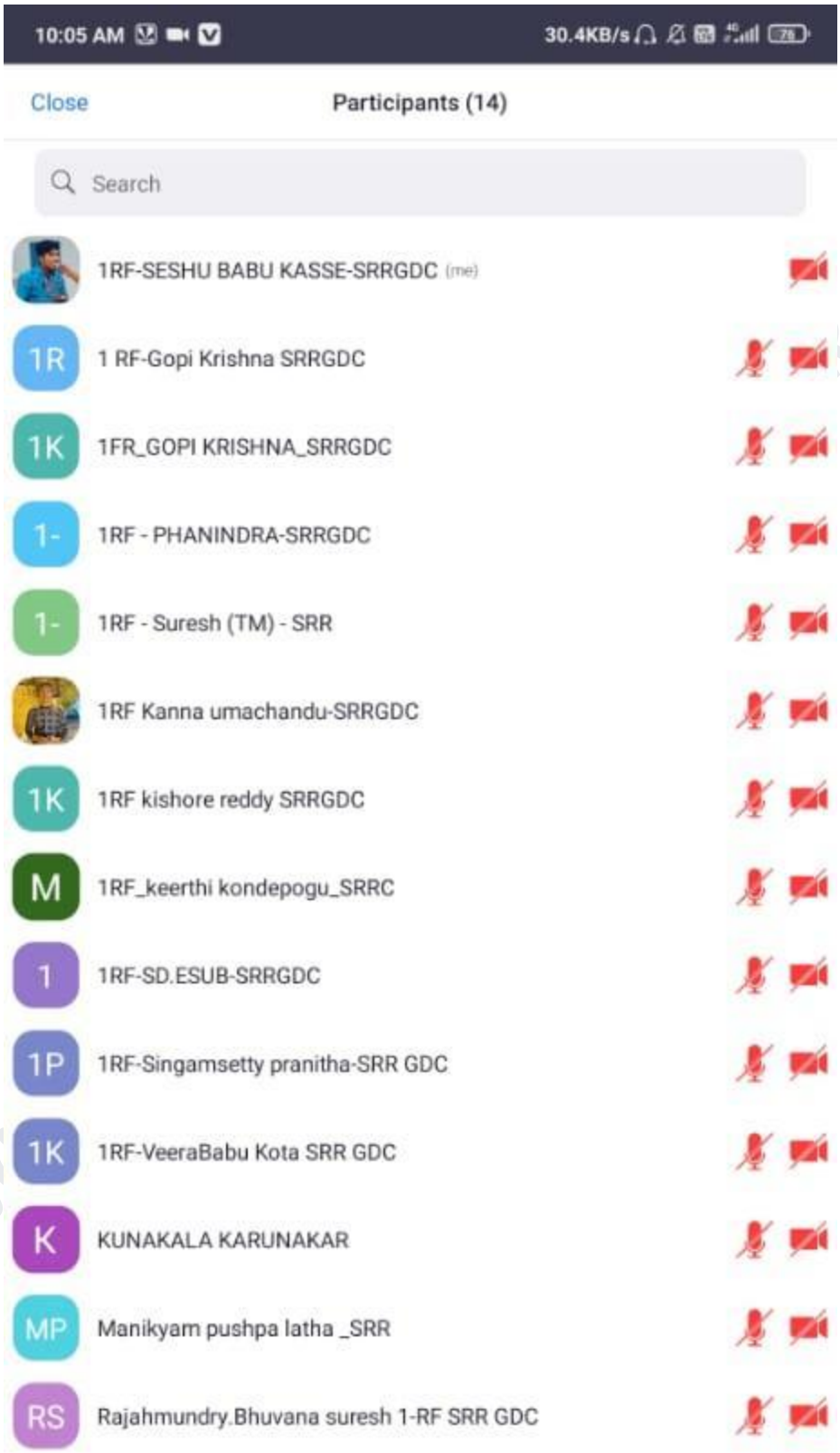


Learning Outcomes

- Build confidence both in spoken skills and for group collaboration and cooperation.
- Develop a greater sense of self-awareness
- Agility and adaptability to different roles and flexible working environments
- The ability to self-manage, solve problems and understand the business environment.


10:33 AM
Close
Participants (106)
Search
SESHU BABU KASSE-SRRGDC (Host)
Trainer Tanoshi M Sarkar (Host)
1R 1 RF CH DURGA PRASAD SRRGDC
1R 1 RF Chanchal Mehra BGBC
1R 1 RF Chetna soni BGBC
1 RF Chinta Ratna Durgeswar SRR GDC
H 1 RF Hathu BGBC
1 RF Jyoti BGBC
1R 1 RF Kavita Gurjar BGBC
K 1 RF komal agarwal BGBC
M 1 RF Meenal Kumawat BGBC
1 RF NIRMLA YADAV BGBC
1R 1 RF Shaina Simran BGBC
1 RF Shaine -SRRGDC
1R 1 RF SONU MEENA BGBC
1 RF GOPI TARUN KUMAR-SRRGDC
1V 1 RF Vadithe chandar naik SRR GDC


11:36 AM
120KB/s
REC
1Rf-SESHU BABU KASSE-SRRGDC
Trainer Tamosi M Sarkar
1 RF komal agarwal BGBC
1 RF jyoti meena BGBC



Department of


11:20 AM
19.4KB/s
Close
Participants (75)
Search
SESHU BABU KASSE-SRRGDC (me)
Trainer - Neeti Mudgal Sharma (Host)
Mothi Shaik-SRR GDC
1RF-Swarna Sri-SRRGDC
1 RF CH DURGA PRASAD SRRGDC
1 RF Ishwar Gadhe SVIT
1-RF-Akanksha Golesar-SVIT
1FR_GOPI KRISHNA_SRRGDC
1rf _MANIKYAM pushpa latha _SRR
1RF - PHANINDRA-SRRGDC
1RF - Ravi Naik- SRRGDC
1RF - suresh (tm) - srr&and
1RF -Rama G -SRR GDC
1RF chaitali tambe Svit
1RF Gayatri Varsale-SVIT
1rf Gopi Krishna naik srrGdc
1RF Hareesh Vempatapu-SRRGDC
1RF Kanna umachandu-SRRGDC
1RF kishore reddy SRRGDC
1RF Priyanka Borade SVIT
1RF Sandya immandhi SRRGDC
1RF Satya naga vara prasad Pujari SRR GDC
1RF V.VENKATESH-SRR GDC
1RF_CHANDRIKA E _SRRGDC
1RF_Ejaz_ SRR GDC
1RF_Ejaz_ SRR GDC
1RF_HEMALATHA BONU _SRRGDC
1RF_keerthi kondepogu_SRRC
1RF_Omkar Pandey_SVIT
1RF_RAJESWARI K_SRRC
1RF_SHAHIN MD_SRRC
1RF_SRAVANTHI K_SRRGDC
1RF-ADI PALLI-SRRC
1RF-Adilakshmi Ganduri SRRGDC

GOVT. DEGREE COLLEGE

AVANIGADDA-521121. KRISHNA DT. (A.P).

NAAC – B

gdcjkc.avanigadda@gmail.com
www.gdcavanigadda.ac.in

WINNERS ARE FORGED HERE

08671-272261
94-94-299418

Dr.D.Uma Rani, M.A,Ph.D.,
PRINCIPAL.

To
The Principal,
SRR & CVR Government degree College ,
Vijayawada.

Madam,

I request that Dr. A. Bhanu Prasad, lecturer in Hindi may be deputed to our college under faculty exchange program for 3 days, that is 8th 9th 10th of November 2021.

Thanking you,

Yours sincerely

PRINCIPAL
GOVT. DEGREE COLLEGE,
AVANIGADDA, Krishna Dist.

GOVT. DEGREE COLLEGE

AVANIGADDA-521121. KRISHNA DT. (A.P).

NAAC – B

gdcjkc.avanigadda@gmail.com
www.gdcavanigadda.ac.in

WINNERS ARE FORGED HERE

08671-272261
94-94-299418

Dr.D.Uma Rani, M.A.Ph.D.,
PRINCIPAL.

Attendance Certificate

This is to Certify that Dr.A.Bhanu Prasad, Lecturer in Hindi SRR & CVR Govt. Degree College, Vijayawada, has attended GDC-AVANIGADDA for Three Days i.e., 08/11/2021 to 10/11/2021.He has conducted Orientation Classes and Literary Activities during that period.

10/11/21

PRINCIPAL

PRINCIPAL
GOVT. DEGREE COLLEGE,
AVANIGADDA, Krishna Dist.

GOVT. DEGREE COLLEGE

AVANIGADDA-521121. KRISHNA DT. (A.P).

NAAC – B

gdcjkc.avanigadda@gmail.com
www.gdcavanigadda.ac.in

WINNERS ARE FORGED HERE

08671-272261
94-94-299418

FROM
Dr.D.Uma Rani,M.A ,P.hD
PRINCIPAL.

Date:-24/02/2022

TO
Principal,
SRR & CVR College(A), Vijayawada,
Vijayawada.

Respected Madam,

Sub:-Govt. Degree College, Avanigadda-DRC Resolution under Faculty Exchange Programme- Deputation of Sri.A.Bhanu Prasad Lecturer in Hindi, **SRR & CVR College(A), Vijayawada to our college for 2 Days - Request-Regarding.**

Ref:- 1.Resolutions in DRC Meeting held on 08-02-2022.

****

We request that Dr.A.Bhanu Prasad, Lecturer in Hindi may be deputed to our college on 25-02-2022 and 26-02-2022 under Faculty Exchange Programme.

Thank you Madam,

Yours Sincerely,

24/2/22

PRINCIPAL

PRINCIPAL
GOVT. DEGREE COLLEGE,
AVANIGADDA, Krishna Dist.

GOVERNMENT DEGREE COLLEGE

AVANIGADDA-521 121. KRISHNA DT.(A.P).

NAAC-B

gdcjkc.avanigadda@gmail.com
gdc-avg@rediffmail.com

08671- 272261
08671-273008

From
Dr. D.Uma Rani,
M.A, Ph.D.
Principal.

Attendance Certificate

This is to certify that Dr.A.Bhanu Prasad, Lecturer in Hindi, SRR & CVR Government Degree College (A), Vijayawada, has attended for Faculty Exchange Progremme at Government Degree College, Avanigadda on 25-02-2022 & 26-02-2022.

Principal
GOVT. DEGREE COLLEGE
AVANIGADDA, Krishna Dt. 521121.

GOVT. DEGREE COLLEGE ★AVANIGADDA★

Student Exchange programme on Nanoparticle preparations

S.R.R. & C.V.R. GDC (A) - Dept. of Chemistry

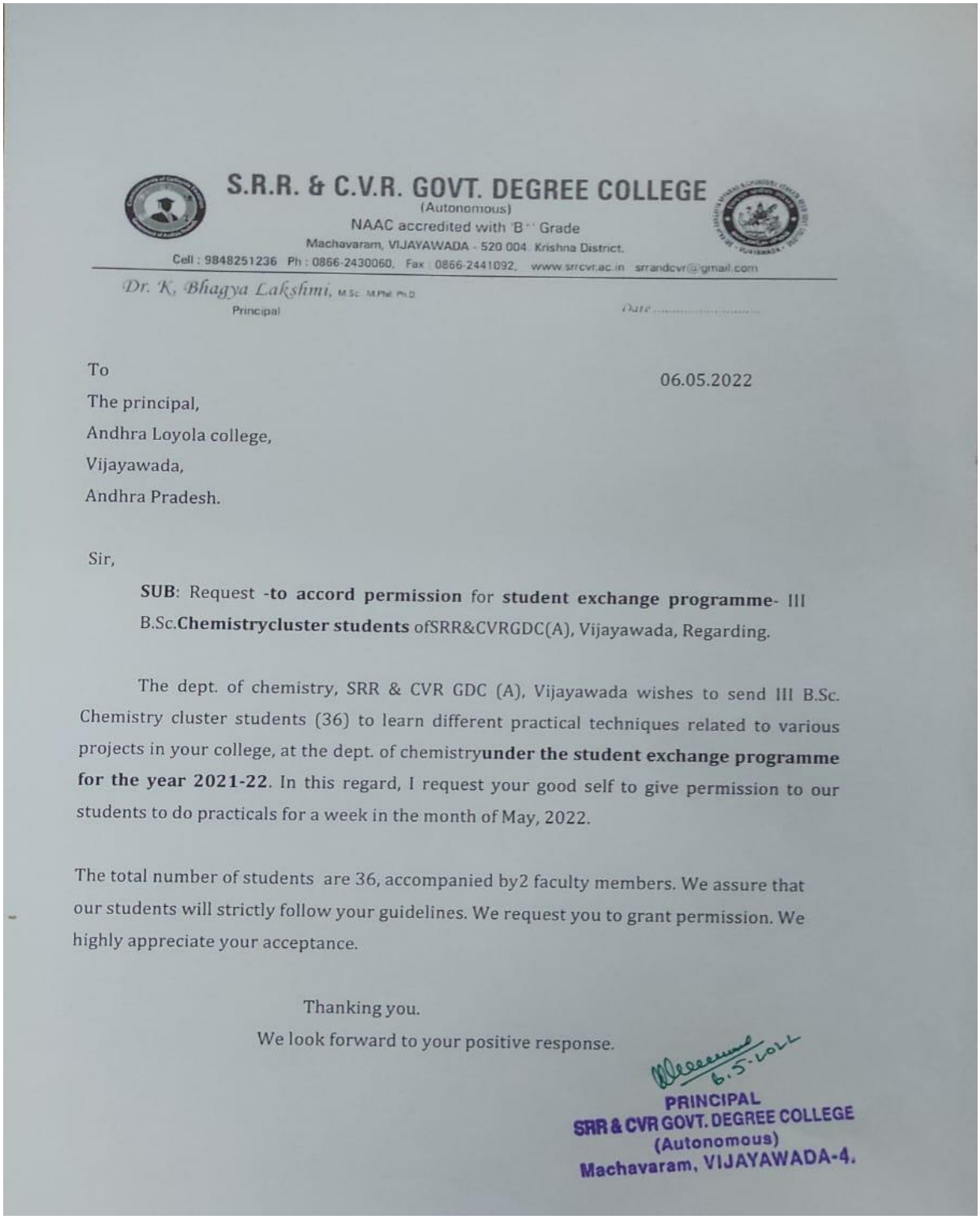
13.06.2022 to 17.06.2022 – ANDHRA LOYOLA COLLEGE, Vijaywada

****

As a part of Student exchange programme, Dept. of Chemistry has taken students to ANDHRA LOYOLA COLLEGE (A), Vijayawada for performing project (which is mandatory for cluster system in 8.3 practicals) during the period 13.06.2022 to 17.06.2022. 36 students of III-B.Sc Chemistry cluster accompanied by two faulty members – Dr. V. Srinivasa Rao, Incharge of Dept. of Chemistry and Dr. G. Nagarjuna have participated in this programme.

We have taken the prior permission and acceptance from the Principal, Andhra Loyola College (A), Vijayawada for student exchange programme in the month of May, 2022.

Our III B.Sc Chemistry Cluster batch of 36 students, (Final year students of 2021-2022) is participated in **Student Exchange Programme** at Department of Chemistry, Andhra Loyola College, Vijayawada. During this programme the students are carried out a project work on Green Synthesis of Nano materials like CuO, ZnO & mixture of CuO and ZnO with Peepal tree leaf extract , from 13/06/2022 to 17/06/2022 under the guidance of lecturers Dr. K. Rayapa Reddy, Dr. K.T.S. Thomas Raju and Dr.Y. Subba Reddy. The students are divided into three batches and carried out their chemistry cluster project work. Nanomaterials are prepared in a green synthetic approach and their characterization was done by XRD and UV-Visible Spectrometry. The faculty and laboratory staff of dept. of chemistry, Andhra Loyola College (A) has provided their assistance in terms of chemicals, lab equipment for the synthesis of nanomaterials.



S.R.R. & C.V.R. GOVT. DEGREE COLLEGE

(Autonomous)
NAAC accredited with 'B++' Grade
Machavaram, VIJAYAWADA - 520 004. Krishna District.
Cell : 9848251236 Ph : 0866-2430060, Fax : 0866-2441092, www.srrcvr.ac.in srrandcvr@gmail.com

Dr. K. Bhagya Lakshmi, M.Sc. M.Phil. Ph.D
Principal

Date .....

To
The principal,
Andhra Loyola college,
Vijayawada,
Andhra Pradesh.

06.05.2022

Sir,

SUB: Request -**to accord permission** for **student exchange programme**- III B.Sc.**Chemistrycluster students** ofSRR&CVRGDC(A), Vijayawada, Regarding.

The dept. of chemistry, SRR & CVR GDC (A), Vijayawada wishes to send III B.Sc. Chemistry cluster students (36) to learn different practical techniques related to various projects in your college, at the dept. of chemistry**under the student exchange programme for the year 2021-22**. In this regard, I request your good self to give permission to our students to do practicals for a week in the month of May, 2022.

The total number of students are 36, accompanied by2 faculty members. We assure that our students will strictly follow your guidelines. We request you to grant permission. We highly appreciate your acceptance.

Thanking you.
We look forward to your positive response.

6.5.2022

PRINCIPAL
SRR & CVR GOVT. DEGREE COLLEGE
(Autonomous)
Machavaram, VIJAYAWADA-4.

Permission letter for carrying out student exchange programme





Group of students participated in student exchange prograrmme



Induction programme on 13.06.2022 to students of SRR and CVR GDC (A), Vijayawada at Dept. of Chemistry, Andhra Layola College (A), Vijayawada.





Preparatory work for green synthesis of Nano particles



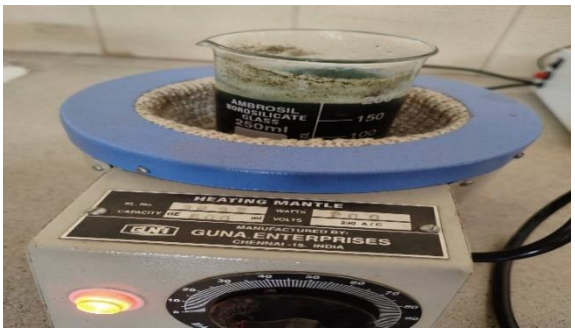


Synthesis of CuO- nano particles from Peepal tree leaf extract





Dr. Y. Subba Reddy garu explaining the procedure for synthesis of nano-materials

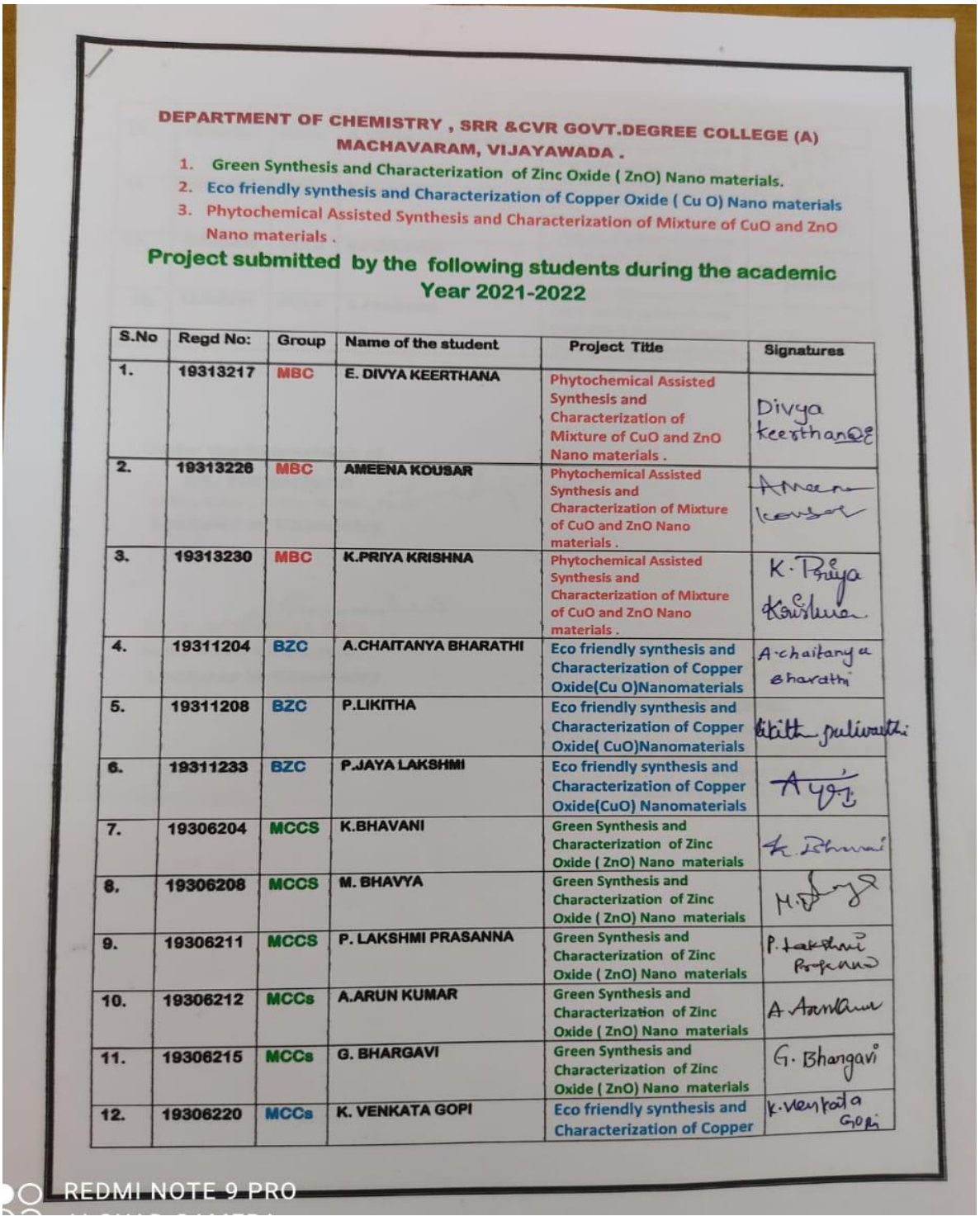








Student details and projects carried out in student exchange programme – June, 2022



DEPARTMENT OF CHEMISTRY , SRR &CVR GOVT.DEGREE COLLEGE (A)
MACHAVARAM, VIJAYAWADA .

1. Green Synthesis and Characterization of Zinc Oxide (ZnO) Nano materials.
2. Eco friendly synthesis and Characterization of Copper Oxide (Cu O) Nano materials
3. Phytochemical Assisted Synthesis and Characterization of Mixture of CuO and ZnO Nano materials .

Project submitted by the following students during the academic Year 2021-2022

S.No	Regd No:	Group	Name of the student	Project Title	Signatures
1.	19313217	MBC	E. DIVYA KEERTHANA	Phytochemical Assisted Synthesis and Characterization of Mixture of CuO and ZnO Nano materials .	Divya keerthana
2.	19313228	MBC	AMEENA KOUSAR	Phytochemical Assisted Synthesis and Characterization of Mixture of CuO and ZnO Nano materials .	Ameena kousar
3.	19313230	MBC	K.PRIYA KRISHNA	Phytochemical Assisted Synthesis and Characterization of Mixture of CuO and ZnO Nano materials .	K. Priya Krishna
4.	19311204	BZC	A.CHAITANYA BHARATHI	Eco friendly synthesis and Characterization of Copper Oxide(Cu O)Nanomaterials	A. chaitanya Bharathi
5.	19311208	BZC	P.LIKITHA	Eco friendly synthesis and Characterization of Copper Oxide(CuO)Nanomaterials	Likitha puliwarthi
6.	19311233	BZC	P.JAYA LAKSHMI	Eco friendly synthesis and Characterization of Copper Oxide(CuO) Nanomaterials	
7.	19306204	MCCS	K.BHAVANI	Green Synthesis and Characterization of Zinc Oxide (ZnO) Nano materials	K. Bhavani
8.	19306208	MCCS	M. BHAVYA	Green Synthesis and Characterization of Zinc Oxide (ZnO) Nano materials	M. Bhavya
9.	19306211	MCCS	P. LAKSHMI PRASANNA	Green Synthesis and Characterization of Zinc Oxide (ZnO) Nano materials	P. Lakshmi Prasanna
10.	19306212	MCCs	A.ARUN KUMAR	Green Synthesis and Characterization of Zinc Oxide (ZnO) Nano materials	A. Arun Kumar
11.	19306215	MCCs	G. BHARGAVI	Green Synthesis and Characterization of Zinc Oxide (ZnO) Nano materials	G. Bhargavi
12.	19306220	MCCs	K. VENKATA GOPI	Eco friendly synthesis and Characterization of Copper	K. Venkata Gopi

REDMI NOTE 9 PRO

13.	19306227	MCCs	B. VENKATAPATHI RAJU	Oxide(CuO)Nano materials Eco friendly synthesis and Characterization of Copper Oxide(CuO)Nano materials	B. Venkatapathi Raju
14.	19306228	MCCs	D.SUJATHA	Eco friendly synthesis and Characterization of Copper Oxide(CuO)Nano materials	D. Sujatha
15.	19306230	MCCs	G.PEDDANNA	Eco friendly synthesis and Characterization of Copper Oxide(CuO)Nano materials	G. peddanna
16.	19306231	MCCs	G.PRAVEEN	Eco friendly synthesis and Characterization of Copper Oxide(Cu O)Nanomaterials	G. Praveen.

Under the Supervision of

Dr. Nagarjuna
M.Sc., B.Ed ., M.Ed., M.Phil., Ph.D
Lecturer in Chemistry

Dr. V. SRINIVASA RAO,
M.Sc., B.Ed ., M.Phil., Ph.D
Lecturer in Chemistry

PRINCIPAL

PRINCIPAL
SRR & CVR GOVT. DEGREE COLLEGE
(Autonomous)
Machavaram, VIJAYAWADA-4.

DEPARTMENT OF CHEMISTRY , SRR &CVR GOVT.DEGREE COLLEGE (A)
MACHAVARAM, VIJAYAWADA .

1. Eco friendly synthesis and Characterization of Copper Oxide (Cu O) Nano particles
2. Phytochemical Assisted Synthesis and Characterization of Mixture of CuO and ZnO Nano materials .

Project submitted by the following students during the academic Year 2021-2022

S.No	Regd No.	Group	Name of the student	Project Title	Signature
17	19301003	MPC ™	K.VINOD KUMAR	Phytochemical Assisted Synthesis and Characterization of Mixture of CuO and ZnO Nano materials	K. Vinod Kumar
18	19301005	MPC ™	K.SRIKANTH	Phytochemical Assisted Synthesis and Characterization of Mixture of CuO and ZnO Nano materials	K. Srikanth
19	19301007	MPC ™	R. CHANDRA SEKHAR	Phytochemical Assisted Synthesis and Characterization of Mixture of CuO and ZnO Nano materials	R. Chandra Sekhar
20	19301012	MPC ™	K.SURESH	Eco friendly synthesis and Characterization of Copper Oxide (Cu O) Nano materials	K. Suresh
21	19301013	MPC ™	B.GOPI KRISHNA NAIK	Eco friendly synthesis and Characterization of Copper Oxide (Cu O) Nano materials	B. Gopi Krishna Naik
22	19301015	MPC ™	S. GOPI KRISHNA	Eco friendly synthesis and Characterization of Copper Oxide (CuO)Nano materials	S. Gopi Krishna

Under the Supervision of
Dr.V. SRINIVASA RAO,
M.Sc., B.Ed ., M.Phil., Ph.D
Lecturer in Chemistry

PRINCIPAL

PRINCIPAL
SRR & CVR GOVT. DEGREE COLLEGE
(Autonomous)
Machavaram, Vijayawada-4.

DEPARTMENT OF CHEMISTRY , SRR &CVR GOVT.DEGREE COLLEGE MACHAVARAM, VIJAYAWADA .

1. Green Synthesis and Characterization of Zinc Oxide (ZnO) Nano materials.
2. Eco friendly synthesis and Characterization of Copper Oxide (Cu O) Nano particles
3. Phytochemical Assisted Synthesis and Characterization of Mixture of CuO and ZnO Nano materials .

Project submitted by the following students during the academic Year 2021-2022

S.No.	Regd No:		Name of the student	Project Title	Signatures
23	19301202	MPC EM	P.JAGADEESH	Phytochemical Assisted Synthesis and Characterization of Mixture of CuO and ZnO Nano materials	P. Jagadeesh
24	19301207	MPC EM	V.LOKESH	Phytochemical Assisted Synthesis and Characterization of Mixture of CuO and ZnO Nano materials	V. Lokesh
25	19301208	MPC EM	P.ADI	Phytochemical Assisted Synthesis and Characterization of Mixture of CuO and ZnO Nano materials	
26	19301209	MPC EM	SAKEENA BANU	Phytochemical Assisted Synthesis and Characterization of Mixture of CuO and ZnO Nano materials	Sakeena
27	19301212	MPC EM	R.DINESH SAI KUMAR	Phytochemical Assisted Synthesis and Characterization of Mixture of CuO and ZnO Nano materials	R. Sai
28	19301216	MPC EM	M.JYOTHI	Eco friendly synthesis and Characterization of Copper Oxide (Cu O) Nano materials	M. Nagajyothi
29	19301218	MPC EM	CH. DURGA PRASAD	Eco friendly synthesis and Characterization of Copper Oxide (CuO) Nano materials	Ch. Durga Prasad
30	19301220	MPC EM	I.PARALOK	Eco friendly synthesis and Characterization of Copper Oxide (CuO) Nano materials	I. Paralok
31	19301225	MPC EM	E.SAI KRISHNA	Eco friendly synthesis and Characterization of Copper Oxide (CuO) Nano materials	E. Sai Krishna



32	19301234	MPC EM	R.SAI KUMAR	Eco friendly synthesis and Characterization of Copper Oxide (CuO) Nano materials	R. Sai
33	19301246	MPC EM	D. SUBHANI	Green Synthesis and Characterization of Zinc Oxide (ZnO) Nano materials	D. Subhani
34	19301250	MPC EM	V.HAREESH	Green Synthesis and Characterization of Zinc Oxide (ZnO) Nano materials	V. Hareesh
35	19301251	MPC EM	G.NANI BABU	Green Synthesis and Characterization of Zinc Oxide (ZnO) Nano materials	G. Nani Babu
36	19301254	MPC EM	Y.SIVA NARAYANA	Green Synthesis and Characterization of Zinc Oxide (ZnO) Nano materials	Y. Sivanarayana
37	20190308021	MPC EM	I.SANDYA BHAVANI	Green Synthesis and Characterization of Zinc Oxide (ZnO) Nano materials	I. Sandya

Dr. V. SRINIVASA RAO,
M.Sc., B.Ed ., M.Phil., Ph.D
Lecturer in Chemistry

PRINCIPAL
PRINCIPAL
SRR & CVR GOVT. DEGREE COLLEGE
(Autonomous)
Machavaram, VIJAYAWADA-4.

Acknowledgements: we extend our heartful thanks to the **principal, SRR and CVR GDC (A),** Vijayawada for her encouragement and the **principal, Andhra Loyola College (A)**, Vijayawada for giving permission. Our special thanks to **Dept. of Chemistry, Andhra Loyola College** for rendering their services in-terms of their time, chemicals and instruments. Special thanks to **Dr. Sk. Beebi**, Lecturer in chemistry, for documenting the programme and our colleagues in the dept. for supporting us.

Thanking you,

Dr. G. Nagarjuna, Dept. of Chemistry
Dr. V. Srinivasa Rao, Dept. of Chemistry
Principal, SRR and CVR GDC (A)

32	19301234	MPC EM	R.SAI KUMAR	Eco friendly synthesis and Characterization of Copper Oxide (CuO) Nano materials	R. Sai
33	19301246	MPC EM	D. SUBHANI	Green Synthesis and Characterization of Zinc Oxide (ZnO) Nano materials	D. Subhani
34	19301250	MPC EM	V.HAREESH	Green Synthesis and Characterization of Zinc Oxide (ZnO) Nano materials	V. Hareesh
35	19301251	MPC EM	G.NANI BABU	Green Synthesis and Characterization of Zinc Oxide (ZnO) Nano materials	G. Babu
36	19301254	MPC EM	Y.SIVA NARAYANA	Green Synthesis and Characterization of Zinc Oxide (ZnO) Nano materials	Y. Sivanarayana
37	20190308021	MPC EM	I.SANDYA BHAVANI	Green Synthesis and Characterization of Zinc Oxide (ZnO) Nano materials	I. Sandya

Dr. V. SRINIVASA RAO,
M.Sc., B.Ed., M.Phil., Ph.D
Lecturer in Chemistry

PRINCIPAL
PRINCIPAL
SRR & CVR GOVT. DEGREE COLLEGE
(Autonomous)
Machavaram, VIJAYAWADA-4.

Acknowledgements: we extend our heartful thanks to the **principal, SRR and CVR GDC (A),** Vijayawada for her encouragement and the **principal, Andhra Layola College (A)**, Vijayawada for giving permission. Our special thanks to **Dept. of Chemistry, Andhra Layola College** for rendering their services in-terms of their time, chemicals and instruments. Special thanks to **Dr. Sk. Beebi**, Lecturer in chemistry, for documenting the programme and our colleagues in the dept. for supporting us.

Thanking you,

Dr. G. Nagarjuna
Dept. of Chemistry

Dr. V. Srinivasa Rao
Dept. of Chemistry

Principal
SRR and CVR GDC (A)

SRR & CVR GOVT. DEGREE COLLEGE (A) VIJAYAWADA

DEPARTMENT OF MICROBIOLOGY









Internship

Scientific Beekeeping

In association with Krishi Vigyan Kendra, Ghantasala, Krishna (Dist.) Under National Bee Board (NBB) of Ministry of Agriculture Hyderabad

BSc Microbiology (MBC & MBF)

From 28th Feb To 7th March 2022



SRR & CVR GOVT DEGREE COLLEGE (a), VIJAYAWADA
DEPARTMENT OF MICROBIOLOGY

To

The Principal

SRR & CVR Govt. Degree College (A)

Vijayawada

Machavaram

Andhra Pradesh

Respected Madam,

Sub: - Department of Microbiology- Student Internship/Training programme - KVK, Ghantasala- Permission –Request – Regarding.

I submit to inform that the department of Microbiology has been planned 7 days student training programme /Internship on "Scientific Beekeeping" in association with Krishi Vigyan Kendra, Ghantasala, Krishna (Dist.), is one of the best organizations under National Bee Board (NBB) of Ministry of Agriculture, Hyderabad to be scheduled from 28th to 7 th March 2022. Since our students have industrial production, sources of Food spoilage and Food Preservation in their syllabus in the Course "Food and Industrial Microbiology" and field visit is a part of curriculum. I further inform that the host institute will provide TA, DA and Certification to the participants. Hence I request you to kindly permit 20 BSc (III & II MBC & MBF) students to attend training programme and teaching staff of Dr. D. Jyothi and Dr .K. Aruna, Department of Microbiology and kindly consider my absence as on-duty.

22.2.2022

Thanking you Madam,

Yours Sincerely

1. Dr. D. Jyothi 22/02/2022

2. Aruna

(Dr. K. ARUNA)

22/2/2022

List of Enclosures:

1. List of Students

SRR & CVR GOVT. DEGREE COLLEGE (A), VIJAYAWADA

DEPARTMENT OF MICROBIOLOGY

7 Day Training programme on "Scientific Beekeeping" Krishi Vigyan Kendra, Ghantasala, Krishna (Dist.) under National Bee Board (NBB) of Ministry of Agriculture, Hyderabad. From 28th Feb to 7th March 2022.

LIST OF STUDENTS:

S.NO	Name of the Student	Class	Signature
1	J. Chandini Priya	III BSc MBC	J. Chandini Priya
2	P. Sadhvika	III BSc MBC	P. Sadhvika
3	V. Rameswar Reddy	III BSc MBC	V. Rameswar Reddy
4	T. Durga Amal Prasad	III BSc MBC	T. Durga Amal Prasad
5	P. Ravi Teja	III BSc MBC	Ravi Teja
6	J. Venkateswaralu	III BSc MBC	J. Venkateswarlu.
7	K. Kinnera	III BSc MBC	K. Kinnera
8	G. Gopal Rao	III BSc MBC	G. Gopalarao
9	K. Vagdhan Babu	III BSc MBC	K. Vagdhan babu.
10	B. Aaron Wesly Paul	III BSc MBC	B. Aaron Wesley Paul.
11	Ch. Ramdevu	III BSc MBC	Ch. Ramdev
12	T. Bharathi	III BSc MBC	T. Bharathi
13	T. Teja	III BSc MBC	T. Teja
14	V. Vasanth Srinivas	II BSc MBF	
15	Ch. Pranoy Roy	II BSc MBF	Ch. Pranoy Roy.
16	G. Anil Kumar	I BSc MBF	G. Anil kumar
17	G. Revanth	I BSc MBF	G. Revanth
18	K. Vijay	I BSc MBC	K. Vijay
19	R. Sai Vardhani	I BSc MBC	R. Saivardhani
20	K. Naga Sriya	I BSc MBC	K. Naga Sriya
21	E Bhanu Teja	II BSc MBC	E. Bhanu Teja.
22	P. Rajya Lakshmi	II BSc MBC	P. Rajyalakshmi
23	Y. Muthyam	II BSc MBC	Y. Muthyam
24	N. Naga Lakshmi	II BSc MBC	N. Naga lakshmi
25	Sk. Refatunisa	II BSc MBC	Sk. Refatunnisa
26	Abdul Roshini	II BSc MBF	
27	R. Gopi Krishna	II BSc MBF	R. Gopikrishna
28	B. Sowmya	II BSc MBC	B. Sowmya

FACULTY ATTENDING:

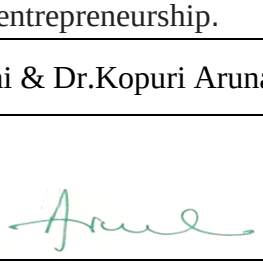
1	Dr. D. Jyothi	IN-CHARGE , DEPT. OF MICROBIOLOGY
2	Dr. Kopuri Aruna	LECTURER IN MICROBIOLOGY

SIGNATURE OF IN-CHARGE **PRINCIPAL**

SRR & CVR GOVT. DEGREE COLLEGE (A) Vijayawada

Department of Microbiology

Activity Register 2021-2022

Date	**From 28th Feb To 7th March 2022**
Conducted through (DRC/JKC/ELF/NCC/NSS/Departments etc.)	**Department of Microbiology**
Nature of Activity (Seminar/Workshop/Extn. Lecture etc.,)	**Internship**
Title of the Activity	**Scientific Beekeeping**
Name of the Department/Committee	Department of Microbiology
No. of students participated	28 BSc Microbiology MBC & MBF
Brief Report on the activity	The Department of Microbiology has been planned 7 days student training programme on "Scientific Beekeeping" in association with Krishi Vigyan Kendra, Ghantasala, Krishna (Dist.), is one of the best organizations under National Bee Board (NBB) of Ministry of Agriculture, Hyderabad to be scheduled from 28th to 6th March 2022. Since our students have industrial production, sources of Food spoilage and Food Preservation in their syllabus in the Course "Food and Industrial Microbiology". The training program emphasized on adopting the techniques of scientific beekeeping and developing entrepreneurship.
Name of the Lecturers who Planned & conducted the activity	Dr .D .Jyothi & Dr.Kopuri Aruna
Signature of the In- Charge	D. Jyothi 
Signature of the Principal	

DAY 1: INAUGURAL SESSION









WHY BEEKEEPING?

PRE EVALUATION

Day 1:

Session 1: Introduction to National Beekeeping and Honey Mission by Dr Sudha Jacob, Senior Scientist, Entomology, KVK Ghantasala

Govt. of India has approved a new Central Sector Scheme entitled "National Beekeeping & Honey Mission (NBHM)" for 2 years for overall promotion and development of scientific beekeeping in mission mode to achieve the goal of "Sweet Revolution" in the country by giving thrust on capacity building & trainings, specific focus on women, input support for promotion & production, setting up of Integrated Beekeeping Development Centres (IBDCs), other Infrastructures, Digitization /online registration, etc., processing, value addition, market support, etc. & R&D under 3 Mini Missions (MM s)-MM-1, MM-2 & MM-3.

Session 2: Types of Bees and Its importance by Dr Sudha Jacob, Senior Scientist, Entomology, KVK Ghantasala

Apis dorsata, the **giant honey bee**, is a honey bee of South and Southeast Asia, found mainly in forested areas. They are typically around 17–20 mm (0.7–0.8 in) long. Nests are mainly built in exposed places far off the ground, like on tree limbs, under cliff overhangs, and sometimes on buildings. These social bees are known for their aggressive defense strategies and vicious behavior when disturbed. Though not domesticating it, indigenous peoples have traditionally used this species as a source of honey and beeswax, a practice known as honey hunting

Session 3: Study on Bees by Dr Purnachandan Rao, Senior Scientist

- Colony initiation
- Colony migration and decline
- Mating
- Communication
- Foraging
- Worker policing
- Nest recognition and fidelity

Session 4: Practical Examination of Various Bees Dr Sudha Jacob,Senior Scientist, Entomology, KVK Ghantasala



DAY 2: SESSION 1



DR. SUDHA RANI, SENIOR SCIENTIST Honey Bee Managemennt



SESSION 2: DR. JHANSI, PROGRAME CO-ORDINATOR, KVK GHANTASALA

Pesticides and Disorders - Honeybee

SESSION 3:



MR. NAVEEN, Govt. Teacher, Chilakaluripeta,

Scientific beekeeping of Apis ceranea

- **Colony initiation**
- **Colony migration and decline**
- **Mating**
- **Communication**
- **Foraging**
- **Worker policing**
- **Nest recognition and fidelity**

DAY 3: SESSION 1



MR. CHINNA BABU, Honeybee farming

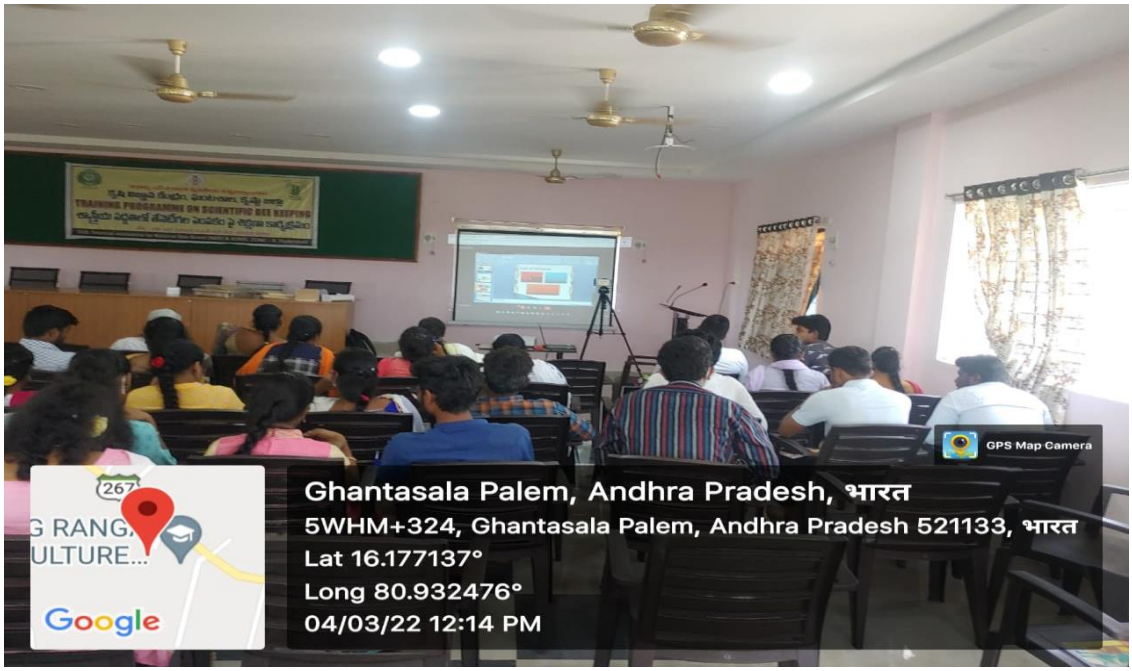
SESSION2:





Tools and Bee Box by Dr Sudha Jacob,Senior Scientist, Entomology, KVK Ghantasala

DAY 4 SESSION 1



ROLE OF POLLENATORS IN CROP YIELD INCREASE BY DR G A D GRACE, RARS, LAM, GUNTUR

SESSION 1



BEEKEEPIN MANAGEMENT

Dr. Mohan Rao, Principal scientist AICRP on Bees, Vijayarai

DAY 5: FIELD VISIT & HANDS ON TRANING AT AICRP ON BEES, VIJAYARAI





PREPARATION OF SUGAR SYRUP

OBSERVATION OF BROOD RACK







HONRY EXTRACTOR

BEEWAX FOUNDATION SHEET MACHINE

Ovoid brood cells and honey pots within a *Trigona laeviceps* nest



BEEHIVE BOX OBSERVATION

ARTIFICIAL BREEDING OF QUEEN BEE








ALL INDIA COORDINATED RESEARCH PROJECTON
HONEY BEES AND POLLINATORS
SRR & CVR GOVERNMENT DEGREE COLLEGE
DEPARTMENT OF MICROBIOLOG


GPS Map Camera
Ghantasala Palem, Andhra Pradesh, India
5WHM+324, Ghantasala Palem, Andhra Pradesh 521133, India
Lat 16.177489°
Long 80.93252°
05/03/22 11:07 AM







AICRP ON BEES, VIJAYARAI



PRESENTATION OF CERTIFICATES



PRESENTATION OF CERTIFICATES













PRESENTATION OF CERTIFICATES



PRESENTATION OF CERTIFICATES













INTERNSHIP "SCIENTIFIC BEEKEEPING"

In association with Krishi Vigyan Kendra, Ghantasala, Krishna (Dist.) Under National Bee Board (NBB) of Ministry of Agriculture Hyderabad

BSc Microbiology (MBC & MBF) SRR & CVR Govt. Degree College (A), Vijayawada

From 28th Feb To 7th March 2022

ACKNOWLEDGEMENTS

We express our deep sense of gratitude to Dr. K. Bhagya Lakshmi, Principal SRR & CVR Govt. Degree College Autonomous, and Vijayawada for her support and constant encouragement to upgrade the knowledge and skills of students.

We wish to express our sincere thanks Dr. K. Jhansi, Program Coordinator, KVK Ghantasala, Krishna District and Course Director, Dr Sudha Jacob, Senior Scientist, Entomology, KVK Ghantasala for providing internship to Microbiology students.

D. Jyothi

PRINCIPAL

ANGRAU

सत्यमेव जयते

NBB

भाकृअनुप
ICAR

Krishi Vigyan Kendra, Ghantasala, Krishna Dt.
Acharya N. G. Ranga Agricultural University

Certificate

This is to certify that Shri/Miss/Mrs J. Chandini Priya **has successfully completed 7 days training programme on 'Scientific Beekeeping' conducted at Krishi Vigyan Kendra, Ghantasala under Mini Mission-I under revised National Beekeeping and Honey Mission (NBHM) of National Bee Board (NBB) of Ministry of Agriculture and Farmers Welfare, Government of India through ICAR-Agricultural Technology Application Research Institute (ATARI), Zone-X, Hyderabad, from 28.02.2022 to 07.03.2022.**

Course Director

Programme Coordinator
KVK, Ghantasala

Place: Ghantasala

Date: 07.03.2022

ANGRAU

सत्यमेव जयते

NBB

भाकृअनुप
ICAR

Krishi Vigyan Kendra, Ghantasala, Krishna Dt.
Acharya N. G. Ranga Agricultural University

Certificate

This is to certify that Shri/Miss/Mrs .....P. Sadhvika..... has successfully completed 7 days training programme on 'Scientific Beekeeping' conducted at Krishi Vigyan Kendra, Ghantasala under Mini Mission-I under revised National Beekeeping and Honey Mission (NBHM) of National Bee Board (NBB) of Ministry of Agriculture and Farmers Welfare, Government of India through ICAR-Agricultural Technology Application Research Institute (ATARI), Zone-X, Hyderabad, from 28.02.2022 to 07.03.2022.

Course Director

Programme Coordinator
KVK, Ghantasala

Place: Ghantasala

Date: 07.03.2022

ANGRAU

सत्यमेव जयते

NBB

भाकृअनुप
ICAR

Krishi Vigyan Kendra, Ghantasala, Krishna Dt.
Acharya N. G. Ranga Agricultural University

Certificate

This is to certify that Shri/Miss/Mrs .....V. Rameswar Reddy..... has successfully completed 7 days training programme on 'Scientific Beekeeping' conducted at Krishi Vigyan Kendra, Ghantasala under Mini Mission-I under revised National Beekeeping and Honey Mission (NBHM) of National Bee Board (NBB) of Ministry of Agriculture and Farmers Welfare, Government of India through ICAR-Agricultural Technology Application Research Institute (ATARI), Zone-X, Hyderabad, from 28.02.2022 to 07.03.2022.

Course Director

Programme Coordinator
KVK, Ghantasala

Place: Ghantasala

Date: 07.03.2022

ANGRAU

सत्यमेव जयते

NBB

भाकृअनुप
ICAR

Krishi Vigyan Kendra, Ghantasala, Krishna Dt.
Acharya N. G. Ranga Agricultural University

Certificate

This is to certify that Shri/Miss/Mrs T. Durga Amal Prasad has successfully completed 7 days training programme on 'Scientific Beekeeping' conducted at Krishi Vigyan Kendra, Ghantasala under Mini Mission-I under revised National Beekeeping and Honey Mission (NBHM) of National Bee Board (NBB) of Ministry of Agriculture and Farmers Welfare, Government of India through ICAR-Agricultural Technology Application Research Institute (ATARI), Zone-X, Hyderabad, from 28.02.2022 to 07.03.2022.

Course Director

Programme Coordinator
KVK, Ghantasala

Place: Ghantasala

Date: 07.03.2022

ANGRAU

सत्यमेव जयते

NBB

भाकृअनुप
ICAR

Krishi Vigyan Kendra, Ghantasala, Krishna Dt.
Acharya N. G. Ranga Agricultural University

Certificate

This is to certify that Shri/Miss/Mrs P. Ravi Teja has successfully completed 7 days training programme on 'Scientific Beekeeping' conducted at Krishi Vigyan Kendra, Ghantasala under Mini Mission-I under revised National Beekeeping and Honey Mission (NBHM) of National Bee Board (NBB) of Ministry of Agriculture and Farmers Welfare, Government of India through ICAR-Agricultural Technology Application Research Institute (ATARI), Zone-X, Hyderabad, from 28.02.2022 to 07.03.2022.

Course Director

Programme Coordinator
KVK, Ghantasala

Place: Ghantasala

Date: 07.03.2022

ANGRAU

सत्यमेव जयते

NBB

भाकृअनुप
ICAR

Krishi Vigyan Kendra, Ghantasala, Krishna Dt.
Acharya N. G. Ranga Agricultural University

Certificate

This is to certify that Shri/Miss/Mrs ..... has successfully completed 7 days training programme on 'Scientific Beekeeping' conducted at Krishi Vigyan Kendra, Ghantasala under Mini Mission-I under revised National Beekeeping and Honey Mission (NBHM) of National Bee Board (NBB) of Ministry of Agriculture and Farmers Welfare, Government of India through ICAR-Agricultural Technology Application Research Institute (ATARI), Zone-X, Hyderabad, from 28.02.2022 to 07.03.2022.

P. Venkateswarlu

Course Director

Programme Coordinator
KVK, Ghantasala

Place: Ghantasala

Date: 07.03.2022

ANGRAU

सत्यमेव जयते

NBB

ICAR

Krishi Vigyan Kendra, Ghantasala, Krishna Dt.
Acharya N. G. Ranga Agricultural University

Certificate

This is to certify that Shri/Miss/Mrs .....K. kinnera..... has successfully completed 7 days training programme on 'Scientific Beekeeping' conducted at Krishi Vigyan Kendra, Ghantasala under Mini Mission-I under revised National Beekeeping and Honey Mission (NBHM) of National Bee Board (NBB) of Ministry of Agriculture and Farmers Welfare, Government of India through ICAR-Agricultural Technology Application Research Institute (ATARI), Zone-X, Hyderabad, from 28.02.2022 to 07.03.2022.

Course Director

Programme Coordinator
KVK, Ghantasala

Place: Ghantasala

Date: 07.03.2022

ANGRAU

सत्यमेव जयते

NBB

भाकृअनुप
ICAR

Krishi Vigyan Kendra, Ghantasala, Krishna Dt.
Acharya N. G. Ranga Agricultural University

Certificate

This is to certify that Shri/Miss/Mrs .....K. Vagdhan Babu..... has successfully completed 7 days training programme on 'Scientific Beekeeping' conducted at Krishi Vigyan Kendra, Ghantasala under Mini Mission-I under revised National Beekeeping and Honey Mission (NBHM) of National Bee Board (NBB) of Ministry of Agriculture and Farmers Welfare, Government of India through ICAR-Agricultural Technology Application Research Institute (ATARI), Zone-X, Hyderabad, from 28.02.2022 to 07.03.2022.

Course Director

Programme Coordinator
KVK, Ghantasala

Place: Ghantasala

Date: 07.03.2022

ANGRAU

सत्यमेव जयते

NBB

भाकृअनुप
ICAR

Krishi Vigyan Kendra, Ghantasala, Krishna Dt.
Acharya N. G. Ranga Agricultural University

Certificate

This is to certify that Shri/Miss/Mrs B. Aaron Wesly Paul has successfully completed 7 days training programme on 'Scientific Beekeeping' conducted at Krishi Vigyan Kendra, Ghantasala under Mini Mission-I under revised National Beekeeping and Honey Mission (NBHM) of National Bee Board (NBB) of Ministry of Agriculture and Farmers Welfare, Government of India through ICAR-Agricultural Technology Application Research Institute (ATARI), Zone-X, Hyderabad, from 28.02.2022 to 07.03.2022.

Course Director

Programme Coordinator
KVK, Ghantasala

Place: Ghantasala

Date: 07.03.2022

ANGRAU

सत्यमेव जयते

NBB

भाकृअनुप
ICAR

Krishi Vigyan Kendra, Ghantasala, Krishna Dt.
Acharya N. G. Ranga Agricultural University

Certificate

This is to certify that Shri/Miss/Mrs .....T. Bharathi..... has successfully completed 7 days training programme on 'Scientific Beekeeping' conducted at Krishi Vigyan Kendra, Ghantasala under Mini Mission-I under revised National Beekeeping and Honey Mission (NBHM) of National Bee Board (NBB) of Ministry of Agriculture and Farmers Welfare, Government of India through ICAR-Agricultural Technology Application Research Institute (ATARI), Zone-X, Hyderabad, from 28.02.2022 to 07.03.2022.

Course Director

Programme Coordinator
KVK, Ghantasala

Place: Ghantasala

Date: 07.03.2022

ANGRAU

सत्यमेव जयते

NBB

भाकृअनुप
ICAR

Krishi Vigyan Kendra, Ghantasala, Krishna Dt.
Acharya N. G. Ranga Agricultural University

Certificate

This is to certify that Shri/Miss/Mrs T. Teja has successfully completed 7 days training programme on 'Scientific Beekeeping' conducted at Krishi Vigyan Kendra, Ghantasala under Mini Mission-I under revised National Beekeeping and Honey Mission (NBHM) of National Bee Board (NBB) of Ministry of Agriculture and Farmers Welfare, Government of India through ICAR-Agricultural Technology Application Research Institute (ATARI), Zone-X, Hyderabad, from 28.02.2022 to 07.03.2022.

Course Director

Programme Coordinator
KVK, Ghantasala

Place: Ghantasala

Date: 07.03.2022

ANGRAU

सत्यमेव जयते

NBB

ICAR

Krishi Vigyan Kendra, Ghantasala, Krishna Dt.
Acharya N. G. Ranga Agricultural University

Certificate

This is to certify that Shri/Miss/Mrs V. Vasanth Srinivas has successfully completed 7 days training programme on 'Scientific Beekeeping' conducted at Krishi Vigyan Kendra, Ghantasala under Mini Mission-I under revised National Beekeeping and Honey Mission (NBHM) of National Bee Board (NBB) of Ministry of Agriculture and Farmers Welfare, Government of India through ICAR-Agricultural Technology Application Research Institute (ATARI), Zone-X, Hyderabad, from 28.02.2022 to 07.03.2022.

Course Director

Programme Coordinator
KVK, Ghantasala

Place: Ghantasala

Date: 07.03.2022

ANGRAU

सत्यमेव जयते

NBB

भाकृअनुप
ICAR

Krishi Vigyan Kendra, Ghantasala, Krishna Dt.
Acharya N. G. Ranga Agricultural University

Certificate

This is to certify that Shri/Miss/Mrs Ch. Pranoy Roy has successfully completed 7 days training programme on 'Scientific Beekeeping' conducted at Krishi Vigyan Kendra, Ghantasala under Mini Mission-I under revised National Beekeeping and Honey Mission (NBHM) of National Bee Board (NBB) of Ministry of Agriculture and Farmers Welfare, Government of India through ICAR-Agricultural Technology Application Research Institute (ATARI), Zone-X, Hyderabad, from 28.02.2022 to 07.03.2022.

Course Director

Programme Coordinator
KVK, Ghantasala

Place: Ghantasala

Date: 07.03.2022

ANGRAU

सत्यमेव जयते

NBB

भाकृअनुप
ICAR

Krishi Vigyan Kendra, Ghantasala, Krishna Dt.
Acharya N. G. Ranga Agricultural University

Certificate

This is to certify that Shri/Miss/Mrs ....U. Anil Kumar..... has successfully completed 7 days training programme on 'Scientific Beekeeping' conducted at Krishi Vigyan Kendra, Ghantasala under Mini Mission-I under revised National Beekeeping and Honey Mission (NBHM) of National Bee Board (NBB) of Ministry of Agriculture and Farmers Welfare, Government of India through ICAR-Agricultural Technology Application Research Institute (ATARI), Zone-X, Hyderabad, from 28.02.2022 to 07.03.2022.

Course Director

Programme Coordinator
KVK, Ghantasala

Place: Ghantasala

Date: 07.03.2022

ANGRAU

सत्यमेव जयते

NBB

भाकृअनुप
ICAR

Krishi Vigyan Kendra, Ghantasala, Krishna Dt.
Acharya N. G. Ranga Agricultural University

Certificate

This is to certify that Shri/Miss/Mrs .U. Revanth Kumar..... has successfully completed 7 days training programme on 'Scientific Beekeeping' conducted at Krishi Vigyan Kendra, Ghantasala under Mini Mission-I under revised National Beekeeping and Honey Mission (NBHM) of National Bee Board (NBB) of Ministry of Agriculture and Farmers Welfare, Government of India through ICAR-Agricultural Technology Application Research Institute (ATARI), Zone-X, Hyderabad, from 28.02.2022 to 07.03.2022.

Course Director

Programme Coordinator
KVK, Ghantasala

Place: Ghantasala

Date: 07.03.2022

ANGRAU

सत्यमेव जयते

NBB

भाकृअनुप
ICAR

Krishi Vigyan Kendra, Ghantasala, Krishna Dt.
Acharya N. G. Ranga Agricultural University

Certificate

This is to certify that Shri/Miss/Mrs ..... K. Vijay ..... has successfully completed 7 days training programme on 'Scientific Beekeeping' conducted at Krishi Vigyan Kendra, Ghantasala under Mini Mission-I under revised National Beekeeping and Honey Mission (NBHM) of National Bee Board (NBB) of Ministry of Agriculture and Farmers Welfare, Government of India through ICAR-Agricultural Technology Application Research Institute (ATARI), Zone-X, Hyderabad, from 28.02.2022 to 07.03.2022.

Course Director

Programme Coordinator
KVK, Ghantasala

Place: Ghantasala

Date: 07.03.2022

ANGRAU

सत्यमेव जयते

NBB

भाकृअनुप
ICAR

Krishi Vigyan Kendra, Ghantasala, Krishna Dt.
Acharya N. G. Ranga Agricultural University

Certificate

This is to certify that Shri/Miss/Mrs K. Sai Vardhani has successfully completed 7 days training programme on 'Scientific Beekeeping' conducted at Krishi Vigyan Kendra, Ghantasala under Mini Mission-I under revised National Beekeeping and Honey Mission (NBHM) of National Bee Board (NBB) of Ministry of Agriculture and Farmers Welfare, Government of India through ICAR-Agricultural Technology Application Research Institute (ATARI), Zone-X, Hyderabad, from 28.02.2022 to 07.03.2022.

Course Director

Programme Coordinator
KVK, Ghantasala

Place: Ghantasala

Date: 07.03.2022

ANGRAU

सत्यमेव जयते

NBB

भाकृअनुप
ICAR

Krishi Vigyan Kendra, Ghantasala, Krishna Dt.
Acharya N. G. Ranga Agricultural University

Certificate

This is to certify that Shri/Miss/Mrs K. Naga Sriya has successfully completed 7 days training programme on 'Scientific Beekeeping' conducted at Krishi Vigyan Kendra, Ghantasala under Mini Mission-I under revised National Beekeeping and Honey Mission (NBHM) of National Bee Board (NBB) of Ministry of Agriculture and Farmers Welfare, Government of India through ICAR-Agricultural Technology Application Research Institute (ATARI), Zone-X, Hyderabad, from 28.02.2022 to 07.03.2022.

Course Director

Programme Coordinator
KVK, Ghantasala

Place: Ghantasala

Date: 07.03.2022

ANGRAU

सत्यमेव जयते

NBB

भाकृअनुप
ICAR

Krishi Vigyan Kendra, Ghantasala, Krishna Dt.
Acharya N. G. Ranga Agricultural University

Certificate

This is to certify that Shri/Miss/Mrs E. Bhanu Teja **has successfully completed 7 days training programme on 'Scientific Beekeeping' conducted at Krishi Vigyan Kendra, Ghantasala under Mini Mission-I under revised National Beekeeping and Honey Mission (NBHM) of National Bee Board (NBB) of Ministry of Agriculture and Farmers Welfare, Government of India through ICAR-Agricultural Technology Application Research Institute (ATARI), Zone-X, Hyderabad, from 28.02.2022 to 07.03.2022.**

Course Director

Programme Coordinator
KVK, Ghantasala

Place: Ghantasala

Date: 07.03.2022

ANGRAU

सत्यमेव जयते

NBB

ICAR

Krishi Vigyan Kendra, Ghantasala, Krishna Dt.
Acharya N. G. Ranga Agricultural University

Certificate

This is to certify that Shri/Miss/Mrs P. Rajya Lakshmi has successfully completed 7 days training programme on 'Scientific Beekeeping' conducted at Krishi Vigyan Kendra, Ghantasala under Mini Mission-I under revised National Beekeeping and Honey Mission (NBHM) of National Bee Board (NBB) of Ministry of Agriculture and Farmers Welfare, Government of India through ICAR-Agricultural Technology Application Research Institute (ATARI), Zone-X, Hyderabad, from 28.02.2022 to 07.03.2022.

Course Director

Programme Coordinator
KVK, Ghantasala

Place: Ghantasala

Date: 07.03.2022

ANGRAU

सत्यमेव जयते

NBB

भाकृअनुप
ICAR

Krishi Vigyan Kendra, Ghantasala, Krishna Dt.
Acharya N. G. Ranga Agricultural University

Certificate

This is to certify that Shri/Miss/Mrs ....Y. Muthyam..... has successfully completed 7 days training programme on 'Scientific Beekeeping' conducted at Krishi Vigyan Kendra, Ghantasala under Mini Mission-I under revised National Beekeeping and Honey Mission (NBHM) of National Bee Board (NBB) of Ministry of Agriculture and Farmers Welfare, Government of India through ICAR-Agricultural Technology Application Research Institute (ATARI), Zone-X, Hyderabad, from 28.02.2022 to 07.03.2022.

Course Director

Programme Coordinator
KVK, Ghantasala

Place: Ghantasala

Date: 07.03.2022

ANGRAU

सत्यमेव जयते

NBB

भाकृअनुप
ICAR

Krishi Vigyan Kendra, Ghantasala, Krishna Dt.
Acharya N. G. Ranga Agricultural University

Certificate

This is to certify that Shri/Miss/Mrs ...N. NagaLakshmi... has successfully completed 7 days training programme on 'Scientific Beekeeping' conducted at Krishi Vigyan Kendra, Ghantasala under Mini Mission-I under revised National Beekeeping and Honey Mission (NBHM) of National Bee Board (NBB) of Ministry of Agriculture and Farmers Welfare, Government of India through ICAR-Agricultural Technology Application Research Institute (ATARI), Zone-X, Hyderabad, from 28.02.2022 to 07.03.2022.

Course Director

Programme Coordinator
KVK, Ghantasala

Place: Ghantasala

Date: 07.03.2022

ANGRAU

सत्यमेव जयते

NBB

भाकृअनुप ICAR

Krishi Vigyan Kendra, Ghantasala, Krishna Dt.
Acharya N. G. Ranga Agricultural University

Certificate

This is to certify that Shri/Miss/Mrs Sk. Refatunnisa has successfully completed 7 days training programme on 'Scientific Beekeeping' conducted at Krishi Vigyan Kendra, Ghantasala under Mini Mission-I under revised National Beekeeping and Honey Mission (NBHM) of National Bee Board (NBB) of Ministry of Agriculture and Farmers Welfare, Government of India through ICAR-Agricultural Technology Application Research Institute (ATARI), Zone-X, Hyderabad, from 28.02.2022 to 07.03.2022.

Course Director

Programme Coordinator
KVK, Ghantasala

Place: Ghantasala

Date: 7.3.2022

ANGRAU

सत्यमेव जयते

NBB

भाकृअनुप
ICAR

Krishi Vigyan Kendra, Ghantasala, Krishna Dt.
Acharya N. G. Ranga Agricultural University

Certificate

This is to certify that Shri/Miss/Mrs ....Abdul Roshini..... **has successfully completed 7 days training programme on 'Scientific Beekeeping' conducted at Krishi Vigyan Kendra, Ghantasala under Mini Mission-I under revised National Beekeeping and Honey Mission (NBHM) of National Bee Board (NBB) of Ministry of Agriculture and Farmers Welfare, Government of India through ICAR-Agricultural Technology Application Research Institute (ATARI), Zone-X, Hyderabad, from 28.02.2022 to 07.03.2022.**

Course Director

Programme Coordinator
KVK, Ghantasala

Place: Ghantasala

Date: 7.3.2022

ANGRAU

सत्यमेव जयते

NBB

भाकृअनुप
ICAR

Krishi Vigyan Kendra, Ghantasala, Krishna Dt.
Acharya N. G. Ranga Agricultural University

Certificate

This is to certify that Shri/Miss/Mrs ..K. Gopi Krishna..... has successfully completed 7 days training programme on 'Scientific Beekeeping' conducted at Krishi Vigyan Kendra, Ghantasala under Mini Mission-I under revised National Beekeeping and Honey Mission (NBHM) of National Bee Board (NBB) of Ministry of Agriculture and Farmers Welfare, Government of India through ICAR-Agricultural Technology Application Research Institute (ATARI), Zone-X, Hyderabad, from 28.02.2022 to 07.03.2022.

Course Director

Programme Coordinator
KVK, Ghantasala

Place: Ghantasala

Date: 7.3.2022

ANGRAU

सत्यमेव जयते

NBB

भाकृअनुप
ICAR

Krishi Vigyan Kendra, Ghantasala, Krishna Dt.
Acharya N. G. Ranga Agricultural University

Certificate

This is to certify that Shri/Miss/Mrs ..... B. Soumya ..... has successfully completed 7 days training programme on 'Scientific Beekeeping' conducted at Krishi Vigyan Kendra, Ghantasala under Mini Mission-I under revised National Beekeeping and Honey Mission (NBHM) of National Bee Board (NBB) of Ministry of Agriculture and Farmers Welfare, Government of India through ICAR-Agricultural Technology Application Research Institute (ATARI), Zone-X, Hyderabad, from 28.02.2022 to 07.03.2022.

Course Director

Programme Coordinator
KVK, Ghantasala

Place: Ghantasala

Date: 07.03.2022

CERTIFICATE COURSE

Basics on Electrical Appliances & Air Conditioning Mechanism

in Association with

INDUSTRIAL TRAINING INSTITUTE, VIJAYAWADA &

ANDHRA PRADESH STATE SKILL DEVELOPMENT CORPORATION

DATE: 15 - 03 - 2022 to 19 - 03- 2022 (30 Hours)

No. of participants :66

Instructors: Kishore, Murali, Surya Prakash

(ITI faculty, Hitachi company trainer)

DEPARTMENT OF PHYSICS & ELECTRONICS

SRR & CVR GOVERNMENT DEGREE COLLEGE(AUTONOMOUS), VIJAYAWADA

Basics on Electrical Appliances & Air Conditioning Mechanism

Objectives of the Training Program

- To get hands-on experience for "Electrical Appliances" paper introduced for 1st semester Science Students as a part of Skill Development Course.
- Fault detection and repairing of domestic appliances.

S.R.R. & C.V.R. GOVT. DEGREE COLLEGE
(Autonomous)
NAAC accredited with 'B+' Grade
Machavaram, VIJAYAWADA - 520 004. Krishna District.
Cell : 9848251236 Ph : 0866-2430060, Fax : 0866-2441092, www.srrcvr.ac.in srrandcvr@gmail.com

Dr. K. Bhagya Lakshmi, M.Sc., M.Phil, Ph.D.
Principal

Date .....

Dt: 03.03.2022,

From
Dr.K.Bhagya Lakshmi M.Sc., M.Phil., Ph.D.
Principal,
SRR & CVR Government Degree College (A)
Vijayawada

To
The Principal,
Government ITI College,
Vijayawada.

Respected Sir,

Sub: SRR & CVR Government Degree College (A), Vijayawada- Department of Physics& Electronics- Work shop on Electrical Appliances at your Institute- Permission-Request-Regarding.

I would like to request that to conduct a workshop on "Electrical Appliances" at your institute for the period of one week to our students. It would be very helpful for students to get hands-on experience for their skill development paper on "Electrical Appliances", which is introduced in 1st semester B.Sc course according to the norms of new NPE.The main focus of the workshop will be working and maintenance of Electrical Appliances.

At present 179 students are studying B.Sc Physics & Electronics course in our college. The duration of the workshop will be 10 to 12 PM for the period of 1 week at your convenient dates for 30 students per batch.

Hence, I request you to permit the students to get work experience at your institute as work shop.

Thanking you Sir,

Yours sincerely,

PRINCIPAL
SRR & CVR GOVT. DEGREE COLLEGE
(Autonomus)
Machavaram, VIJAYAWADA - 520 004.

Course outline

Date	Session	Content	Remarks
15-03-2022 10 - 1 PM& 2- 5 PM	1	Principles of working, parts and servicing of Electric fan,Electric Iron box,	2 batches , 33students per each Batch
16-03-2022 10 - 1PM& 2- 5 PM	2	Principles & working of Electric bulbs, CFL, LED lights, Testing Choke, Capacitor,	
17-03-2022 10-1 PM & 2- 5 PM	3	Principles & working of Electric Cooker, electric oven	
18-03-2022 10-1 PM & 2- 5 PM	4	Basic science of REFRIGERATION., Basics of air conditioning	
19-03-2022 10-1 PM & 2- 5 PM	5	electrical parts of air conditioner testing, function. electronic components.	

From All the sciences groups, MPCs, MECs, MPCA & MPC of 1st semester a total of 66 students had participated in this hands-on experience training Program.

Participated Students Details

SRR& CVR GDC (A) VIJAYAWADA - Electrical Appliances workshop at GOVT.ITI COLLEGE, VIJAYAWADA Batch - 2

	Name of the student	Class/ Group	contact number	Email ID	Batch No.	Date 15-03-2022	Date 16-03-2022	Date 17-03-2022	Date 18-03-2022	Date 19-03-2022
1	T. Siddu	1st BSC(MPCS)	6301515330	tiriveedhisiddu@gmail.com	II	P	P	P	P	P

SRR & CVR GDC(A), VIJAYAWADA, PHYSICS & ELECTRONICS

2	I.VAMSI KUMAR	1st BSC(MPCS)	7702864461	illurivamsikumar123@gmail.com	II	P	P	P	P	P
3	A.Abhishek	1st BSC(MPCS)	8074341878	abhishekanasuri123@gmail.com	II	P	P	P	P	P
4	Rajkumar	1st BSC(MPCS)	9346827545	rajkumar934683@gmail.com	II	P	P	P	P	P
5	Gopichand	1st BSC(MPCS)	6300488439	gopichandguduru9@gmail.com	II	P	P	P	P	P
6	S. Mahesh	1st BSC(MPCS)	7330631152	maheshsivalanke@gmail.cok	II	P	P	P	P	P
7	M.Rakesh kumar	1st BSC(MPCS)	7386522001	maheshyohusuva@gmail.com	II	P	P	P	P	P
8	K.Karunakar	1st BSC(MPCS)	6301993128	karthikkola98@gmail.com	II	P	P	P	P	P
9	P.Naveen	1st BSC(MPCS)	9100956527	naveen.peddhapurapu@gmail.com	II	P	P	P	P	P
10	T.Apparao	1st BSC(MPCS)	6300587516	tekuchinna152@gmail.com	II	P	P	P	P	P
11	S. Praveen	1st BSC(MPCS)	7569359703	spraveenkerry143@gmail.com	II	P	P	P	P	P
12	T.Mahesh Babu	1st BSC(MPCS)	9494543458	tumatimaheshbabu2@gmail.com	II	P	P	P	P	P
13	B.Altaf	1st BSC(MPCS)	7075690537	baigalthaf6@gmail.com	II	P	P	P	P	P
14	Ch. Harshavardhan	1st BSC(MPCS)	9704935685	harshavardhanchinthapalli@gmail.com	II	P	P	P	P	P
15	P. Murali Krishna	1st BSC(MPCS)	9398120531	**muralipalagarla@gmail. com**	II	P	P	P	P	P
16	K. Vamsi	1st BSC(MPCS)	9392500245	kvamsi9392@gmail.com	II	P	P	P	P	P
17	Ch. Arjun	1st BSC(MPCS)	9121732606	reddyarjun166@gmail.com	II	P	P	P	P	P

SPR & CVR GDCA, VIJAYAWADA, PHYSICS & ELECTRONICS

18	N.Pavan	1st BSC(MPCS)	7095282281	nallapavan713@gmail.com	II	P	P	P	P	P
19	E.Rakesh Kumar	1st BSC(MPCS)	8106087306	kumarrakesh05554@gmail.com	II	P	P	P	P	P
20	Sk. Zameer	1st BSC(MPCS)	9866790083	shaikzameer109@gmail.com	II	P	P	P	P	P
21	K. Ajay Kumar	1st BSC(MPCS)	9121187634	kumpatiajay84@gmail.com	II	P	P	P	P	P
22	Nageswara Rao	1st BSC(MPCS)	7093441692	nandhipatinageswararao@gmail.com	II	P	P	P	P	P
23	Md. Sameer	1st BSC(MPCS)	6302310841	ms253906@gmail.com	II	P	P	P	P	P
24	M. Narendra	1st B.Sc (MECS)	9381983396	munagapatinarendra9@gmail.com	II	P	P	P	P	P
25	B. G. M. Kalidas	1st B.Sc (MECS)	9848071567	bhogipatikalidas029@gmail.com	II	P	P	P	P	P
26	M. Chandrasekhar	1st B.Sc (MECS)	9390347992	chandrasekharmedasani@gamil.com	II	P	P	P	P	P
27	P. Omesh Durga ram	1st B.Sc (MECS)	8500363624	omeshdurgaram@gmail.com	II	P	P	P	P	P
28	GOLLURI MOHAN BABU	1st B.Sc (MECS)	7675918432	mohangolluri07@gmail.com	II	P	P	P	P	P
29	R.Mahesh babu	1st B.Sc (MECS)	6300852681	maheshbabu64545@gmail.com	II	P	P	P	P	P
30	K.Yelesh	1st B.Sc (MECS)	6305237486	yeleshkummarikunta@gmail.com	II	P	P	P	P	P
31	Y. Anil kumar Reddy	1st B.Sc (MECS)	9848608472	anilyanamala72@gmail.com	II	P	P	P	P	P
32	J. Vinayak	1st BSC(MPCS)	8309153674	vinayakarjun143@gmail.com	II	p	P	P	P	P
33	K.Anwesh	1st BSC(MPCS)	8106045615	anweshrockster@gmail.com	II	p	P	P	P	P

GRD & CVR GDC(A), VIJAYAWADA PHYSICS & ELECTRONICS

Instructors

Sri Kishore, Sri Anil from Electrical Department faculty of Government ITI, Vijayawada & Sri Surya Prakash from Hitachi Company staff through APSSDC.

Lab Equipment : Ceiling Fan windings, stator, rotor; Electric bulbs, Choke, capacitor, electric Cooker, Mixie Grinder , series Bulb connection for testing, Air conditioning trainer by Hitachi available at Government ITI, Vijayawada.
Electrical Department , Govt ITI Vijayawada is used as Training Room.

SRR& CVR GDC (A) VIJAYAWADA - Electrical Appliances workshop at GOVT.ITI COLLEGE, VIJAYAWADA ---- Batch 1

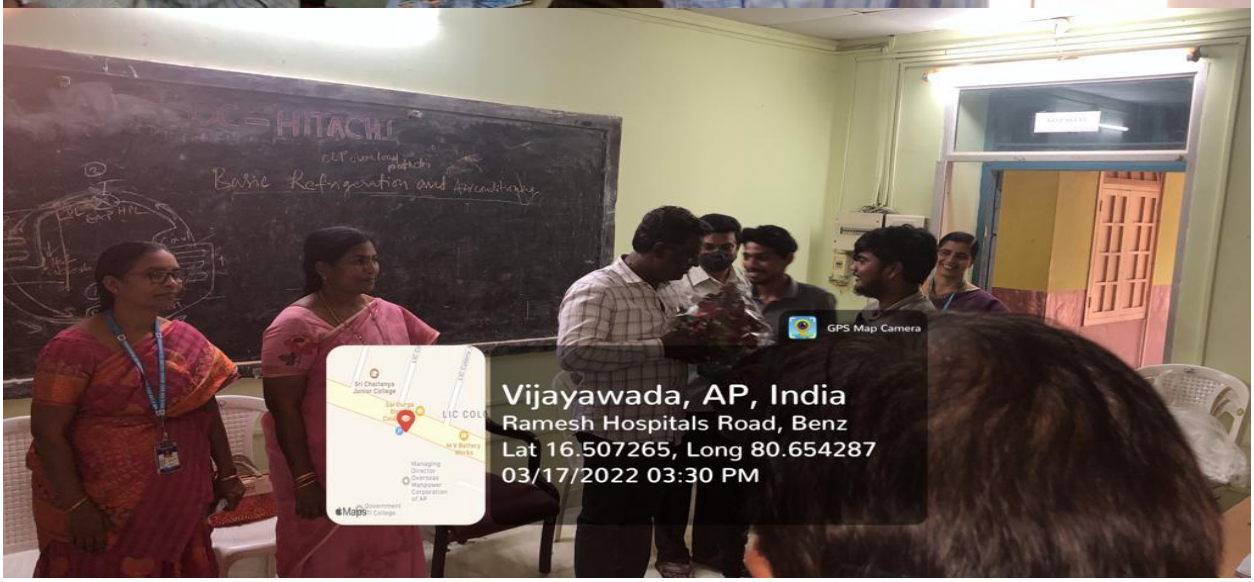
S.No	Name of the student	Group	contact number	emailID	Batch	Dt:15-03-	Dt:16-03-	Dt:17-03-	Dt: 19-03-
1	B.Praveen kumar	1B.SC (MPCA)	8712245876	praveenkumarbokinala2004@gmail.com	I	P	P	P	P
2	B. Vykunta vasu	1st BSC (MPC)	9390567989	bagusriramsriram@gmail.com	I	P	P	P	P
3	B.Crystal	1B.SC (MPCA)	6302626078	bandelacrystal2002@gmail.com	I	P	P	P	P
4	B.Satish	1B.SC (MPCA)	8919069394	budamparthi763@gmail.com	I	P	P	P	P
5	B.Vamsi	1st BSC (MPC)	9701765916	BEVARAVAMSI88@gmail.com	I	P	P	P	P
6	B.Vinay	1st BSC (MPC)	9182866878	akhilvinay@gmail.com	I	P	P	P	P
7	Ch.Jitendra	1B.SC (MPCA)	9391373141	chinthajitendra9391373141@gmail.com	I	P	P	P	P
8	D.Karteek	1st BSC (MPC)	8897992614	karthikxyz46@gmail.com	I	P	P	P	P
9	D.Sandeep	1B.SC (MPCA)	9705698073	sandeepdevarapalli2003@gmail.com	I	P	P	P	P
10	I.Pavan Kalyan naik	1B.SC (MPCA)	7036855368	pavankalyannaik98@gmail.com	I	P	P	P	P
11	K.Aditya	1B.SC (MPCA)	9100564390	aadityakomaravalli@gmail.com	I	P	P	P	P
12	K.Balaram	1st BSC (MPC)	9014994891	balaramkaparapu9@gmail.com	I	P	P	P	P
13	K.Kishore	1st BSC (MPC)	7997135524	kishorekoppu3@gmail.com	I	P	P	P	P

14	K.Kishore	1B.SC (MPCA)	9014932322	kishorekankipati9@gmail.com	I	P	P	P	P
15	K.Satish	1st BSC (MPC)	9550436304	satishsolo29@gmail com	I	P	P	P	P
16	M. Paul Devanth Kumar	1st BSC (MPC)	8978104701	devanthk87@gmail. com	I	P	P	P	P
17	M. Trinadh	1st BSC (MPC)	7729873358	maduputrinadh84@gmail.com	I	P	P	P	P
18	Bejjam vamsi krishna	1st BSC (MPC)	8790392640	vamsirowdy28@gmail.com	I	P	P	P	P
19	N.Deva Prasad	1st BSC (MPC)	8897275024	nallagatladevaprasad7@gmail.com	I	P	P	P	P
20	PJagadeesh	1B.SC (MPCA)	8919832761	pjagadeeshjagadeesh98@gmail.com	I	P	P	P	P
21	P.DurgaDinesh	1st BSC (MPC)	9666405707	durgadineshpathiripalli28@gmail.com	I	P	P	P	P
22	P.Suryateja	1st BSC (MPC)	7032152169	suryatejapolaki123@gmail.com	I	P	P	P	P
23	Sk. Hasan	1st BSC (MPC)	6304126715	hasanshaik6121@gmail.com	I	P	P	P	P
24	Sk.Subhan	1B.SC (MPCA)	9989879494	yashsubhan3 gmail.com	I	P	P	P	P
25	T.Sai Kiran	1B.SC (MPCA)	9701414886	saikirantaddisetti@gmail.com	I	P	P	P	P
26	T.Venkata Ramana	1st BSC (MPC)	9618396276	vr536313@gmail.com	I	P	P	P	P
27	V.Durga Prsasad	1st BSC (MPC)	7330936294	durgaprasadd164@gmali.com	I	P	P	P	P
28	S. Sai Teja	1st BSC (MPCs)	8074484599	saitejas975@gmail.com	I	P	P	P	P
29	B.Ravi Kumar	1st BSC (MPCs)	7036268299	ravibilugudi@gmail.com	I	P	P	P	P
30	Kambhampati Vamsi	1st BSC (MPC)	9392500245	kvamsi9392@gmail.com	I	P	P	P	P
31	K.Prabhu Kumar	1st BSC (MPC)	8688172218	kagithaprabhukumar@gmail.com	I	P	P	P	P
32	G.Karthik	1st BSC (MPC)	7386613196	mudhirajkarthik391@gmail.com	I	P	P	P	P
33	B.BhanuPrasad	1st BSC (MPC)	9492813882	prasadbhanu052@gmail.com	I	P	P	P	P
36	Sai Teja	1st BSC (MPCs)			I	P	P	P	P

VR & CVR (MPCA) VIJAYAWADA. PHYSICS & ELECTRONICS







DEPARTMENT OF PHYSICS & ELECTRONICS " **Basics of Electrical Appliances & Air Conditioning Mechanism"**





[Certificates Batch2]

[Certificates Batch1]

[Student feedback ITI electrical Appliances]

DEPARTMENT OF PHYSICS & ELECTRONICS " **Basics of Electrical Appliances & Air Conditioning Mechanism"**



CERTIFICATE OF TRAINING

ANDHRA PRADESH STATE SKILL DEVELOPMENT CORPORATION
in association with
GOVERNMENT INDUSTRIAL TRAINING INSTITUTE , VIJAYAWADA
&
SRR & CVR GOVERNMENT DEGREE COLLEGE
AN AUTONOMOUS & ISO 9001-2015 CERTIFIED INSTITUTION
RANKED BY NIRF 101-150 BAND at 2020 - NIRF & 151-200 BAND at 2021-NIRF
NAAC ACCREDITED INSTITUTION WITH B+ GRADE
VIJAYAWADA, KRISHNA(Dt), AP(State)
DEPARTMENT OF PHYSICS

This is to certify Mr. A.Abhishek, I B.Sc MPCS of SRR & CVR GOVERNMENT DEGREE COLLEGE (A), Vijayawada has successfully completed the course on "Basic of Electrical Appliances & Refrigeration Mechanism" conducted during 15-03-2022 to 19-03-2022 at Government INDUSTRIAL TRAINING INSTITUTE, VIJAYAWADA.

Principal, Govt. ITI, Vijayawada
Principal, SRR & CVR GDC(A)
Skill Development officer, APSSDC



CERTIFICATE OF TRAINING

ANDHRA PRADESH STATE SKILL DEVELOPMENT CORPORATION
in association with
GOVERNMENT INDUSTRIAL TRAINING INSTITUTE , VIJAYAWADA
&
SRR & CVR GOVERNMENT DEGREE COLLEGE
AN AUTONOMOUS & ISO 9001-2015 CERTIFIED INSTITUTION
RANKED BY NIRF 101-150 BAND at 2020 - NIRF & 151-200 BAND at 2021-NIRF
NAAC ACCREDITED INSTITUTION WITH B+ GRADE
VIJAYAWADA, KRISHNA(Dt), AP(State)
DEPARTMENT OF PHYSICS

This is to certify that Mr. Deva prasad I B.Sc MPC of SRR & CVR GOVERNMENT DEGREE COLLEGE, Vijayawada has successfully completed the course on " Basics of Electrical Appliances & Refrigeration Mechanism" conducted during " 15-03-2022 to 19-03-2022 at Government Industrial Training Institute, Vijayawada.

Principal, Govt. ITI, Vijayawada
Principal, SRR & CVR GDC(A)
Skill Development officer, APSSDC

Learning Outcomes

After attending this training, Students got Knowledge that how to test any electrical device like Bulb, grinder, choke coil, capacitor, electric cooker etc.

They are aware to check and repair any electrical device using safety measures.

Students got the knowledge of the mechanism that how refrigerants cool the environment etc.

SRR & CVR GOVERNMENT DEGREE COLLEGE (AUTONOMOUS)
MACHAVARAM, VIJAYAWADA-520004
DEPARTMENT OF ZOOLOGY

Name of the Activity	**ONE WEEK TRAINING PROGRAMME on Principles of Aquaculture, and Demonstration on aquaculture laboratory procedures**
Place	**Organized by state institute of fisheries technology SIFT, Kakinada, Andhra Pradesh**
Date	**21-3-2022 to 26-03-2022**





Students had Hands on Experience in STATE INSTITUTE OF FISHERIES TECHNOLOGY (SIFT) IN KAKINADA A.P by one week TRAINING PROGRAMME ON PRINCIPLES OF AQUACULTURE AND DEMONSTRATION OF AQUA LAB PROCEDURES (water and soil analysis, microbiology, feed analysis and PCR) in different parameters and sectors of aquaculture.

*****

SRR & CVR GOVERNMENT DEGREE COLLEGE (AUTONOMOUS)
MACHAVARAM, VIJAYAWADA-520004
DEPARTMENT OF ZOOLOGY

Name of the Activity	**SEVEN DAY TRAINING PROGRAMME ON SCIENTIFIC BEE KEEPING**
Place	**At Krishivigyan Kendra (KVK) Ghantasala Andhra Pradesh organised by ICAR Agriculture Technology**
Date	**25-03-2022 to 31-03-2022**





Students had Hands on Experience on scientific Bee Keeping, they learned about various species of Honey Bee and which species are economically beneficial for the process of Keeping Honey Bees. With these types of training programme students will be able to train themselves as future Entrepreneurs and help them for self-employments

*****.

S.R.R. & C.V.R. Government Degree College (A)

An Autonomous & ISO 9001: 2015 Certified Institution:: Ranked by NIRF in 101-150 band at NIRF-2020 & 151-200 band in NIRF 2019 NAAC accredited Institution with grade B+ with C.G.P.A 2.6 during March, 2017

Machavaram, Vijayawada, Krishna District, AP-520 004

ENTREPRENEURSHIP ACTIVITY
MUSHROOM CULTIVATION
MAY 2022



DEPARTMENT OF BOTANY

SRR & CVR Government Degree College

An Autonomous & ISO 9001: 2015 Certified Institution:: Ranked by NIRF in 101-150 band at NIRF-2020 & 151-200 band in NIRF 2019 NAAC accredited Institution with grade B+ with C.G.P.A 2.6 during March, 2017

Machavaram, Vijayawada, Krishna District, AP-520 004



DEPARTMENT OF BOTANY

Dates	**9.5.2022 to 13.5.2022**
Conducted through (DRC/JKC/ELF/NCC/NSS/ Departments etc.	**Department**
Nature of activity (seminar/Workshop/Extn. Lecture etc.	**Extension activity**
Title of the Activity	**Industrial training on Mushroom cultivation**
Name of the Department/Committee	**Department of Botany**
Details of Resource Persons (Name , Designation etc.,)	**B.SC BZC Students**
No of students participated	**45**
Name of the Lecturers who planned & conducted the activity	**Planned and Organized by** **G.Swapna** **Lecturer In Charge** **Mrs V.N Padmavathi Lecturer in Botany**
Remarks	**This training provided much needed exposure andon site experience to students on mushroom cultivation .**

Department of Botany SRR & CVR Govt DegreeCollege Organized Industrial training for 45 III BZC students from 9.5.2022 to 13.5.2022 for the Project work Paper in cluster which deals with industrial training .

Pre Preparation /Action Plan :

For Organizing this program the Department of Botany Faculty contacted Jyothi Mushrooms, a small scale Mushroom Entrepreneur , Nunna and formulated an action plan for arranging training with the encouragement and support from Principal Madam.

Motive of this program:

For FInal year students one of the Cluster papers in Botany cluster is completely about Project Work and Industrial training and one of the Cluster papers is entirely on Mushroom cultivation motivated us to organize this training .

Report of the training :

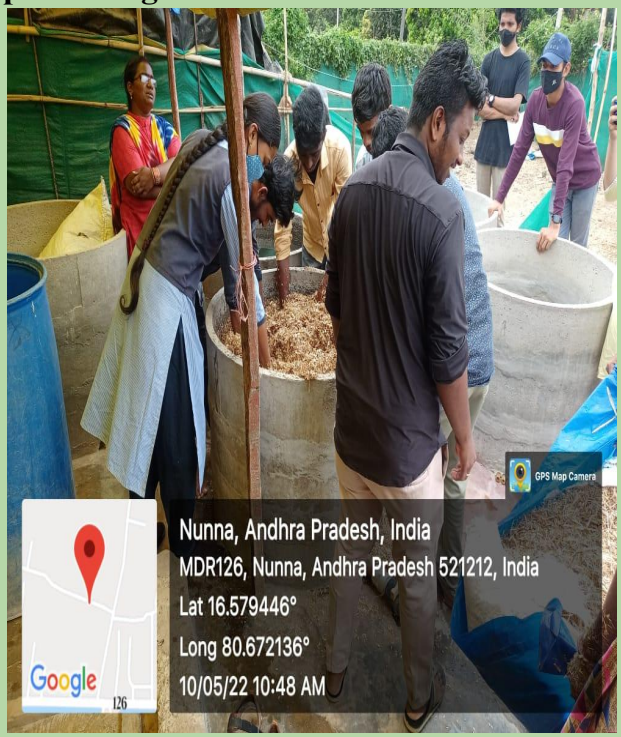
I Day training dated 9.5.2022 : On First day Jyothi Mushroom cultivation Entrepreneur explained to students about the stages of Mushroom cultivation, Significance of Grass used and the technique of Grass cutting and grass cutting machinery working principles . Students practiced Grass cutting on machines.





II Day training dated 10.5.2022

On the second day of training students got the training on Processing the grass physically and also with the help of grass processing machinery and the chemical substances used for processing .





<u>III Day training dated 11.5.2022 :</u> On the third day of training students got the training on Drying process and filling the mushroom polythene bags with grass and spawn .





<u>IV Day training dated 12.5.2022 :</u> On the fourth day of training students got the training on

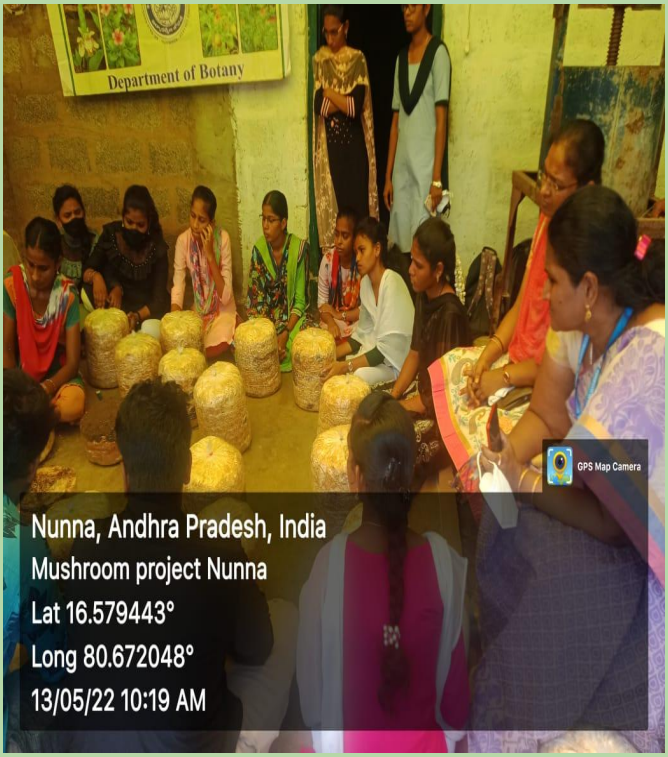
preparation of spawn, filling up of polythene covers with grass and spawn , drying casing etc





<u>V Day training dated 13.5.2022 :</u> On the fifth day of training students got the training on preparation of mushroom cases, storage methods , Marketing methods and financial process of mushroom culture industry.





Last day of the training explained all the aspects of Mushroom Culture Business .



Honorable principal madam congratulated the students and Faculty of Botany Department for successfully completing the training program and giving the certificates to students .



Press Clippings

చేశారు.

స్వయం ఉపాధి కోర్సులపై శిక్షణ

మాచవరం, న్యూస్‌టుడే: విద్యార్థులకు స్వయం ఉపాధి కోర్సులపై శిక్షణ ఇస్తున్నట్లు కళాశాల ప్రిన్సిపల్ డాక్టర్ కె. భాగ్యలక్ష్మి అన్నారు. మాచవరంలోని ఎస్సారార్ అండ్ సీవీఆర్ ప్రభుత్వ డిగ్రీ కళాశాల వృక్షశాస్త్ర విభాగం ఆధ్వర్యంలో కళాశాలలో బీఎస్‌సీ (బీజెడ్‌సీ) తృతీయ సంవత్సరం విద్యార్థులు గత అయిదు రోజులుగా నున్నలోని 'జ్యోతి మష్రూమ్స్'లో పుట్టగొడుగుల పెంపకం కేంద్రం వద్ద శిక్షణను విజయవంతంగా ముగించుకొని.. ఉత్తీర్ణులైన విద్యార్థులకు శుక్రవారం కళాశాలలో ఏర్పాటుచేసిన కార్యక్రమంలో ధ్రువపత్రాలను ఆమె అందజేశారు. ఈ సందర్భంగా ప్రిన్సిపల్ మాట్లాడుతూ.. శిక్షణలో భాగంగా నాణ్యమైన గడ్డి, మట్టి, పుట్టగొడుగుల రకం, స్పానింగ్, స్పాన్ రన్నింగ్, క్రోసింగ్, క్రాపింగ్ వంటి అంశాలను విద్యార్థులు చక్కగా నేర్చుకున్నారన్నారు. కార్యక్రమాన్ని చేపట్టిన కళాశాల వృక్షశాస్త్ర విభాగాధిపతి జి.స్వప్న, అధ్యాపకులు వి.నాగపద్మావతి, డాక్టర్ సీహెచ్ శ్రీనివాసరెడ్డి, ఐ.ప్రశాంతిలను అభినందించారు.



సాక్షి
విజయవాడ సిటీ

3/5

Advertisement

విద్యార్థులకు సర్టిఫికెట్ల ప్రదానం

మధురానగర్(విజయవాడ సెంట్రల్): విద్యార్థులు థియరీతోపాటు ప్రాక్టికల్ పరిజ్ఞానం పెంపొందించుకోవాలని ఎస్ఆర్ఆర్ అండ్ సీవీఆర్ ప్రభుత్వ కళాశాల ప్రిన్సిపల్ డాక్టర్ కె.భాగ్యలక్ష్మి తెలిపారు. మాచవరం ఎస్ఆర్ఆర్ ప్రభుత్వ కళాశాలలో శుక్రవారం వృక్షశాస్త్ర విభాగం ఆధ్వర్యాన పట్టభద్రుల పెంపకంపై శిక్షణ పూర్తి చేసుకున్న బీఎస్సీ తృతీయ సంవత్సరం విద్యార్థులకు సర్టిఫికెట్లు పంపిణీ చేశారు. ఈ సందర్భంగా ఆమె మాట్లాడుతూ అందివచ్చిన అవకాశాలను సద్వినియోగం చేసుకుని ఉన్నత స్థానాలకు చేరుకోవాలని సూచించారు. వృక్షశాస్త్ర విభాగాధిపతి జి.స్వప్న మాట్లాడుతూ శిక్షణలో నేర్చుకున్న అంశాలను క్షేత్రస్థాయిలో అమలు చేసేలా ప్రణాళికలు రూపొందించామని పేర్కొన్నారు. అధ్యాపకులు వి.నాగపద్మావతి, డాక్టర్ సీహెచ్ శ్రీనివాసరెడ్డి, ఐ.ప్రశాంతి తదితరులు పాల్గొన్నారు.

SRR & CVR Government Degree College

An Autonomous & ISO 9001: 2015 Certified Institution:: Ranked by NIRF in 101-150 band at NIRF-2020 & 151-200 band in NIRF 2019 NAAC accredited Institution with grade B+ with C.G.P.A 2.6 during March, 2017

Machavaram, Vijayawada, Krishna District, AP-520 004

DEPARTMENT OF BOTANY

సాక్షి
విజయవాడ సిటీ

విద్యార్థులకు సర్టిఫికెట్ల ప్రదానం



మదురానగర్(విజయవాడ సెంట్రల్): విద్యార్థులు థియరీతోపాటు ప్రాక్టికల్ పరిజ్ఞానం పెంపొందించుకోవాలని ఎస్ఆర్ఆర్ అండ్ సీవీఆర్ ప్రభుత్వ కళాశాల ప్రిన్సిపల్ డాక్టర్ కె.బాగ్యలక్ష్మి తెలిపారు. మాచవరం ఎస్ఆర్ఆర్ ప్రభుత్వ కళాశాలలో శుక్రవారం వృక్షశాస్త్ర విభాగం ఆధ్వర్యాన పుట్టగొడుగుల పెంపకంపై శిక్షణ పూర్తి చేసుకున్న బీఎస్సీ తృతీయ సంవత్సరం విద్యార్థులకు సర్టిఫికెట్లు పంపిణీ చేశారు. ఈ సందర్భంగా ఆమె మాట్లాడుతూ అందివచ్చిన అవకాశాలను సద్వినియోగం చేసుకుని ఉన్నత స్థానాలకు చేరుకోవాలని సూచించారు. వృక్షశాస్త్ర విభాగాధిపతి జి.స్వప్న మాట్లాడుతూ శిక్షణలో నేర్చుకున్న అంశాలను క్షేత్రస్థాయిలో అమలు చేసేలా ప్రణాళికలు రూపొందించామని పేర్కొన్నారు. అధ్యాపకులు వి.నాగసుధ్యావతి, డాక్టర్ సీహెచ్ శ్రీనివాసరెడ్డి, ఐ.ప్రశాంతి తదితరులు పాల్గొన్నారు.

SRR & CVR Government Degree College

Machavaram, Vijayawada, Krishna District, AP 520 004

DEPARTMENT OF BOTANY

LECTURER IN CHARGE
Dept. of Botany
SRR & CVR GOVT. DEGREE COLLEGE
VIJAYAWADA-4, Krishna Dist.

తేది: 7-12-2022.

స్థానిక SRR & CVR ప్రభుత్వ మహిళా కళాశాల వృక్షశాస్త్ర విభాగం ఆధ్వర్యంలో III-BSC-B2C యొక్క సప్లిమెంటరీ కోర్సులలో భాగంగా "పుట్టగొడుగుల పెంపకం" చేపట్టడం జరిగింది. విద్యార్థులు వృక్షశాస్త్ర అధ్యాపకులు డా॥ Ch. శ్రీనివాసరెడ్డి గారి దిశానిర్దేశంలో వ్యవసాయ వ్యర్థాలలో పింక్ ఆయిస్టర్ మష్రూమ్స్, మిల్కీ మష్రూమ్స్ పెంపకాన్ని సూక్ష్మజీవ రహిత పరిస్థితుల్లో పడకల తయారీ, విత్తనాలు చల్లడం, ఇంకుబేషన్, క్రాపింగ్ వంటి వివిధ దశలను దాటి ఫలసాయం సాధించడం జరిగింది.

తక్కువ పెట్టుబడితో ఎక్కువ లాభాలు పొందే అవకాశం వున్న పుట్టగొడుగుల పెంపకం స్వయం ఉపాధికి మరియు మార్గమని, నిరుద్యోగులు, గృహిణులు, రైతులు వీటి పెంపకాన్ని ఇంటిలోనే చేపట్టవచ్చునని, సమాజ అవసరాలకు తగిన స్థాయిలో తక్కువ సరఫరా తగ్గ పోవడంలో వీటి పెంపకం మంచి ఉపాధి వనరుగా పరిగణించవచ్చునని కళాశాల ప్రిన్సిపాల్ డా॥ కొడాలి శ్రీ. భూగ్రహలక్ష్మి సూచించారు.

పుట్టగొడుగులలో B విటమిన్ పుష్కలంగా వుంటుంది. వీటిని ఆహారంలో చేర్చుకోవడం వల్ల రోగనిరోధక శక్తి పెరుగుతుంది, వీటిలోని సెలీనియం క్యాన్సర్ రాకుండా చేస్తుంది, ఇవి స్థూలకాయుల బరువు తగ్గించడంలో తోడ్పడుతాయి, మధుమేహుల్లో చక్కెర స్థాయిలు నియంత్రణలో వుంటాయి-కాబట్టి వీటిని అందరూ తప్పనిసరిగా ఆహారంలో భాగంగా చేర్చుకోవాలని వృక్షశాస్త్ర విభాగాధిపతి అధ్యాపకురాలు శ్రీమతి వి. నాగ పద్మావతి స్పష్టం చేశారు. ఈ సందర్భంగా ఈ కార్యక్రమ విద్యార్థుల శ్రద్ధని అభినందించారు.

PRINCIPAL
SRR & CVR GOVT. DEGREE COLLEGE
(Autonomus)
Machavaram, VIJAYAWADA-520 004

III BSC BZC TM.

	Names	Mobile
1.	ch. Adhi lakshmi	- 9603975039
2.	K. Manga devi	- 9494196469
3.	B. Nagamani	- 6281729239
4.	B. Lakshman Rao	- 9347249294
5.	K. Monika	— 9642788395
6.	Ch. Venkataiah	- 9390767309
7.	R. Sandhya	- 7337240849
8.	K. Chandrika	- 7659807886
9.	A. Anantha raju	- 6281436654
10.	G. Satya priya	- 9346843701
11.	P. Venkatesh	- 9390673514
12.	B. Sai babu	- 7207406539
13.	B. Balaji	- 6305156258
14.	A. Annapurna Devi	- 7993658836
15.	K. Venu	— 9010426167
16.	V. Anil Kumar	- 9912167319
17.	M. Meena Kumari	- 8074177668
18.	K. Venkat	— 6303477913
19.	L. Gop.	— 7013794474

Name of student | III BZC [E.M] | Ph.NO:-

1. Narayana – 7997769926
2. Mastan – 7000923141
3. Nani – 9912882365
4. Ramya sri – 9553885527
5. Navya Jyothi – 9390796279
6. shankar – 9494667501
7. Durga prasad – 8008123134
8. Rex Dayan – 9676437728
9. Srinivasa Rao – 9390011606
10. M. preethi – 9398759599
11. T. venkat – 7995153568
12. K. Bhagya Ratna kumar – 7036878109
13. Ratshekar – 9405643790
14. Naveen – 9000571227
15. sony – 8309699334
16. Ramya sri. N – 9347039418
17. Mahendra – 8688013692
18. v. priya – 8125712911
19. Hema – 9440532850
20. Manikanta Deepak – 9247913345
21. Bhargavi – 9347284494
22. sonu. – 7671858702

CERTIFICATE

ACHIEVEMENT

JYOTHI MUSHROOMS, NUNNA, VIJAYAWADA

Skill Development Training / Project Work in Mushroom Cultivation

KANCHAPOGU. MAHENDRA

Student of III B.Sc, BZC E.M ..... S.R.R & C.V.R. Govt. Degree College (A)
Machavaram, Vijayawada

Has Successfully Completed 5 days Botany
Skill Development Training Program
{9.5.2022 to 13.5.2022} on Mushroom Cultivation
in the Academic year 2021-2022

JYOTHI MUSHROOMS

CERTIFICATE

ACHIEVEMENT

JYOTHI MUSHROOMS, NUNNA, VIJAYAWADA

Skill Development Training / Project Work in Mushroom Cultivation

K.manga devi

Student of III B.Sc, BZC ..... S.R.R & C.V.R. Govt. Degree College (A)
Machavaram, Vijayawada

Has Successfully Completed 5 days Botany
Skill Development Training Program
{9.5.2022 to 13.5.2022} on Mushroom Cultivation
in the Academic year 2021-2022

JYOTHI MUSHROOMS
VIJAYAWADA

JYOTHI
MASHROOMS

Scanned with OKEN Scanner

CERTIFICATE

ACHIEVEMENT

JYOTHI MUSHROOMS, NUNNA, VIJAYAWADA

Skill Development Training / Project Work in Mushroom Cultivation

M. Mounika

Student of III B.Sc, BZC ..... S.R.R & C.V.R. Govt. Degree College (A)
Machavaram, Vijayawada

Has Successfully Completed 5 days Botany
Skill Development Training Program
{9.5.2022 to 13.5.2022} on Mushroom Cultivation
in the Academic year 2021-2022

JY MUSHROOMS VIJAYAWADA

JYOTHI MASHROOMS

CERTIFICATE

ACHIEVEMENT

JYOTHI MUSHROOMS, NUNNA, VIJAYAWADA

Skill Development Training / Project Work in Mushroom Cultivation

VENKAt KARUMURI

Student of III B.Sc, BZC ..... S.R.R & C.V.R. Govt. Degree College (A)
Machavaram, Vijayawada

Has Successfully Completed 5 days Botany
Skill Development Training Program
{9.5.2022 to 13.5.2022} on Mushroom Cultivation
in the Academic year 2021-2022

JYOTHI MUSHROOMS

CERTIFICATE

ACHIEVEMENT

JYOTHI MUSHROOMS, NUNNA, VIJAYAWADA

Skill Development Training / Project Work in Mushroom Cultivation

Laharu. Gopi

Student of III B.Sc, BZC .T.M... S.R.R & C.V.R. Govt. Degree College (A)
Machavaram, Vijayawada

Has Successfully Completed 5 days Botany
Skill Development Training Program
{9.5.2022 to 13.5.2022} on Mushroom Cultivation
in the Academic year 2021-2022

JYOTHI MUSHROOMS
VIJAYAWADA

JYOTHI
MASHROOMS

CERTIFICATE

ACHIEVEMENT

JYOTHI MUSHROOMS, NUNNA, VIJAYAWADA

Skill Development Training / Project Work in Mushroom Cultivation

LANKA. REX DAYAN

Student of III B.Sc, BZC E.M. S.R.R & C.V.R. Govt. Degree College (A)
Machavaram, Vijayawada

Has Successfully Completed 5 days Botany
Skill Development Training Program
{9.5.2022 to 13.5.2022} on Mushroom Cultivation
in the Academic year 2021-2022

JYOTHI MUSHROOMS
VIJAYAWADA

JYOTHI
MASHROOMS

CERTIFICATE

ACHIEVEMENT

JYOTHI MUSHROOMS, NUNNA, VIJAYAWADA

Skill Development Training / Project Work in Mushroom Cultivation

M.Naveen

Student of III B.Sc, BZC ..... S.R.R & C.V.R. Govt. Degree College (A)
Machavaram, Vijayawada

Has Successfully Completed 5 days Botany
Skill Development Training Program
(9.5.2022 to 13.5.2022) on Mushroom Cultivation
in the Academic year 2021-2022

JYOTHI MUSHROOMS
VIJAYAWADA

JYOTHI
MUSHROOMS

CERTIFICATE

ACHIEVEMENT

JYOTHI MUSHROOMS, NUNNA, VIJAYAWADA

Skill Development Training / Project Work in Mushroom Cultivation

M.preethi

Student of III B.Sc, BZC ..... S.R.R & C.V.R. Govt. Degree College (A)
Machavaram, Vijayawada

Has Successfully Completed 5 days Botany
Skill Development Training Program
{9.5.2022 to 13.5.2022} on Mushroom Cultivation
in the Academic year 2021-2022

JYOTHI MUSHROOMS
VIJAYAWADA

JYOTHI
MASHROOMS

CERTIFICATE

ACHIEVEMENT

JYOTHI MUSHROOMS, NUNNA, VIJAYAWADA

Short Term Internship Training / Project Work in Mushroom Cultivation

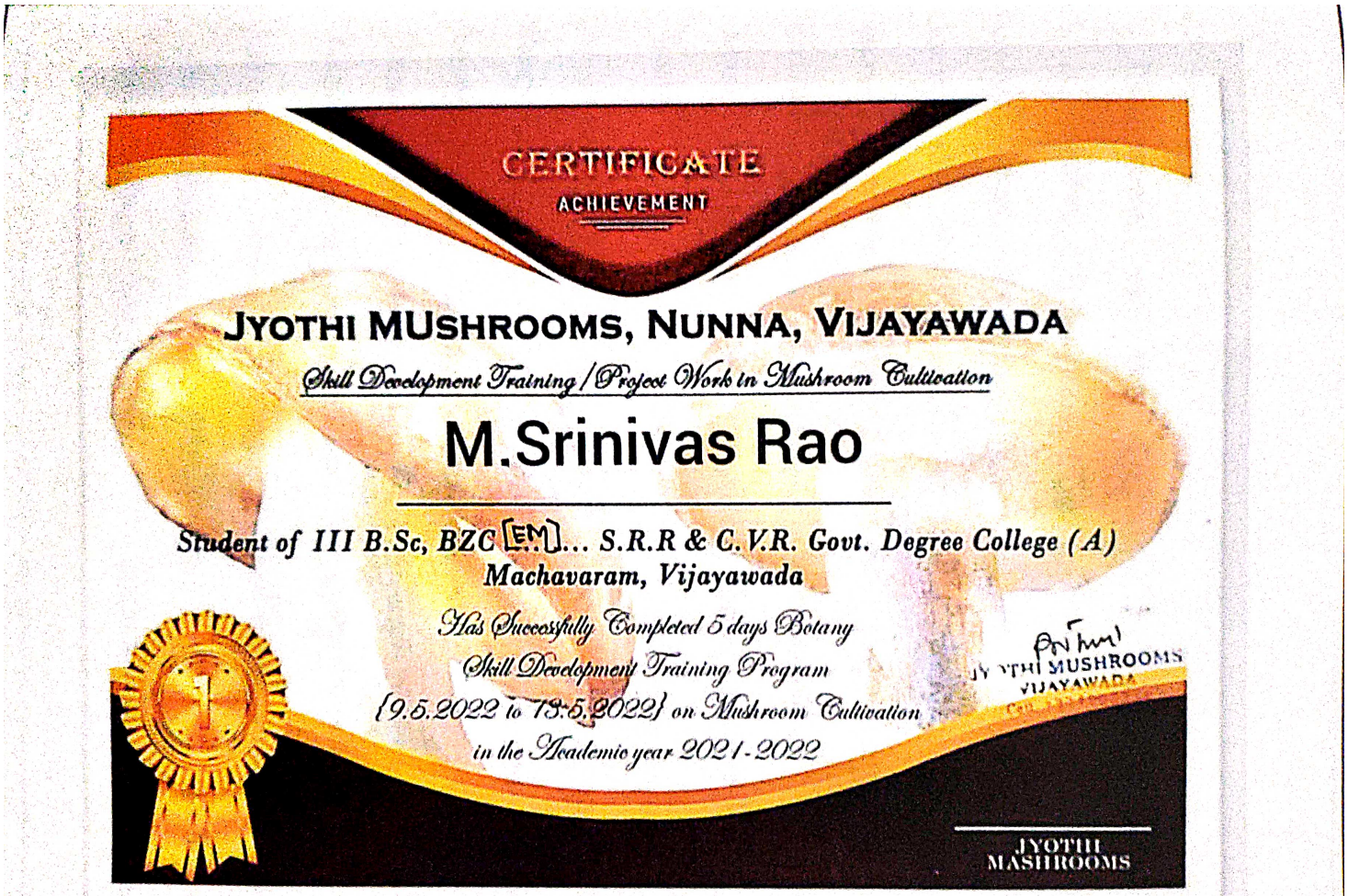
This is to certify that [illegible]

Student of III B.Sc. Botany, S.R.R & C.V.R. Govt. Degree College (A)
[illegible]ram, Vijayawada

has successfully Completed 5 days Botany
Short Term Internship Training Program
[01.08.2022 to 15.08.2022] on Mushroom Cultivation
in the Academic year 2021-2022

JYOTHI MUSHROOMS
VIJAYAWADA

JYOTHI


CERTIFICATE
ACHIEVEMENT
JYOTHI MUSHROOMS, NUNNA, VIJAYAWADA
Skill Development Training / Project Work in Mushroom Cultivation
M.Srinivas Rao
Student of III B.Sc, BZC [EM]... S.R.R & C.V.R. Govt. Degree College (A)
Machavaram, Vijayawada
Has Successfully Completed 5 days Botany
Skill Development Training Program
{9.5.2022 to 13.5.2022} on Mushroom Cultivation
in the Academic year 2021-2022
JYOTHI MUSHROOMS
VIJAYAWADA
JYOTHI
MASHROOMS

CERTIFICATE

ACHIEVEMENT

JYOTHI MUSHROOMS, NUNNA, VIJAYAWADA

Skill Development Training / Project Work in Mushroom Cultivation

Madduri Meena Kumari

Student of III B.Sc, BZC ..... S.R.R & C.V.R. Govt. Degree College (A)
Machavaram, Vijayawada

Has Successfully Completed 5 days Botany
Skill Development Training Program
{9.5.2022 to 13.5.2022} on Mushroom Cultivation
in the Academic year 2021-2022

JYOTHI MUSHROOMS
VIJAYAWADA

JYOTHI MUSHROOMS

CERTIFICATE

ACHIEVEMENT

JYOTHI MUSHROOMS, NUNNA, VIJAYAWADA

Skill Development Training / Project Work in Mushroom Cultivation

NEELAKANTI RAMYA SRI

Student of III B.Sc, BZC ..... S.R.R & C.V.R. Govt. Degree College (A)
Machavaram, Vijayawada

Has Successfully Completed 5 days Botany
Skill Development Training Program
{9.5.2022 to 13.5.2022} on Mushroom Cultivation
in the Academic year 2021-2022

JYOTHI MUSHROOMS
VIJAYAWADA
Cell

JYOTHI
MASHROOMS

CERTIFICATE

ACHIEVEMENT

JYOTHI MUSHROOMS, NUNNA, VIJAYAWADA

Skill Development Training / Project Work in Mushroom Cultivation

PARASU SONY

Student of III B.Sc, BZC ..... S.R.R & C.V.R. Govt. Degree College (A)
Machavaram, Vijayawada

Has Successfully Completed 5 days Botany
Skill Development Training Program
[9.5.2022 to 13.5.2022] on Mushroom Cultivation
in the Academic year 2021-2022



JYOTHI MUSHROOMS
VIJAYAWADA

CERTIFICATE

ACHIEVEMENT

JYOTHI MUSHROOMS, NUNNA, VIJAYAWADA

Skill Development Training / Project Work in Mushroom Cultivation

Puthi Venkatesh

Student of III B.Sc, BZC ..... S.R.R & C.V.R. Govt. Degree College (A)
Machavaram, Vijayawada

Has Successfully Completed 5 days Botany
Skill Development Training Program
{9.5.2022 to 13.5.2022 Mushroom Cultivation
in the Academic year 2022

JYOTHI MUSHROOMS
VIJAYAWADA
Cell

JYOTHI MUSHROOMS

CERTIFICATE

ACHIEVEMENT

JYOTHI MUSHROOMS, NUNNA, VIJAYAWADA

Skill Development Training / Project Work in Mushroom Cultivation

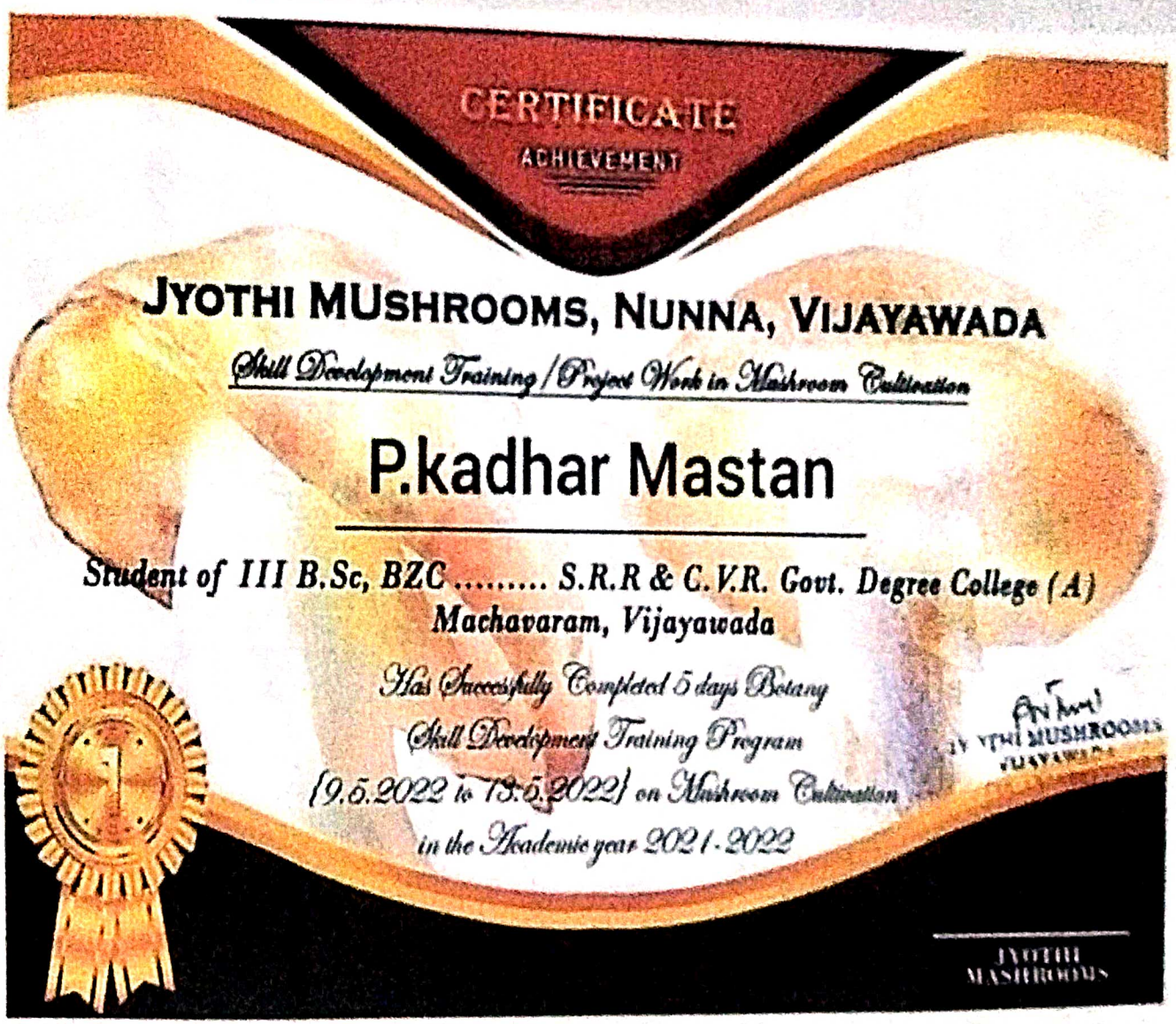
P. ANNA PURNA DEVI

Student of III B.Sc, BZC ..... S.R.R & C.V.R. Govt. Degree College (A)
Machavaram, Vijayawada

Has Successfully Completed 5 days Botany
Skill Development Training Program
{9.5.2022 to 13.5.2022} on Mushroom Cultivation
in the Academic year 2021-2022

JYOTHI MUSHROOMS
VIJAYAWADA

JYOTHI
MUSHROOMS


CERTIFICATE
ACHIEVEMENT
JYOTHI MUSHROOMS, NUNNA, VIJAYAWADA
Skill Development Training / Project Work in Mushroom Cultivation
P.kadhar Mastan
Student of III B.Sc, BZC ..... S.R.R & C.V.R. Govt. Degree College (A)
Machavaram, Vijayawada
Has Succesfully Completed 5 days Botany
Skill Development Training Program
{9.5.2022 to 13.5.2022} on Mushroom Cultivation
in the Academic year 2021-2022
JYOTHI MUSHROOMS

CERTIFICATE

ACHIEVEMENT

JYOTHI MUSHROOMS, NUNNA, VIJAYAWADA

Skill Development Training / Project Work in Mushroom Cultivation

THALAKAYALA VENKAT

Student of III B.Sc, BZC ..... E.M ..... S.R.R & C.V.R. Govt. Degree College (A)
Machavaram, Vijayawada

Has Successfully Completed 5 days Botany
Skill Development Training Program
{9.5.2022 to 13.5.2022} on Mushroom Cultivation
in the Academic year 2021-2022

JYOTHI MUSHROOMS
VIJAYAWADA

JYOTHI
MASHROOMS

CERTIFICATE

ACHIEVEMENT

JYOTHI MUSHROOMS, NUNNA, VIJAYAWADA

Skill Development Training / Project Work in Mushroom Cultivation

Ulliboina Anil Kumar

Student of III B.Sc, BZC ..... S.R.R & C.V.R. Govt. Degree College (A)
Machavaram, Vijayawada

Has Successfully Completed 5 days Botany
Skill Development Training Program
{9.5.2022 to 13.5.2022} on Mushroom Cultivation
in the Academic year 2021-2022

JYOTHI MUSHROOMS
VIJAYAWADA

JYOTHI MUSHROOMS

CERTIFICATE

ACHIEVEMENT

JYOTHI MUSHROOMS, NUNNA, VIJAYAWADA

Skill Development Training / Project Work in Mushroom Cultivation

Anantha Raju Avula

Student of III B.Sc, BZC ..... S.R.R & C.V.R. Govt. Degree College (A)
Machavaram, Vijayawada

has successfully Completed 1day Training
Skill Development Training Program
19.5.2022 to 19.5.2022 on Mushroom Cultivation
in the Academic year 2021-2022

JYOTHI MASHROOMS

CERTIFICATE

ACHIEVEMENT

JYOTHI MUSHROOMS, NUNNA, VIJAYAWADA

Skill Development Training / Project Work in Mushroom Cultivation

BANDARU. BHARGAVI

Student of III B.Sc, BZC **E.M** *..... S.R.R & C.V.R. Govt. Degree College (A)*
Machavaram, Vijayawada

Has Successfully Completed 5 days Botany
Skill Development Training Program
{9.5.2022 to 13.5.2022} on Mushroom Cultivation
in the Academic year 2021-2022

JYOTHI MUSHROOMS
VIJAYAWADA

JYOTHI
MASHROOMS

CERTIFICATE

ACHIEVEMENT

JYOTHI MUSHROOMS, NUNNA, VIJAYAWADA

Skill Development Training / Project Work in Mushroom Cultivation

Bhukya. Nagamani

Student of III B.Sc, BZC ..... S.R.R & C.V.R. Govt. Degree College (A)
Machavaram, Vijayawada

Has Successfully Completed 5 days Botany
Skill Development Training Program
...22 to 13.5.2022) on Mushroom Cultivation
Academic year 2021-2022

JYOTHI MUSHROOMS
VIJAYAWADA

JYOTIII
MASHROOMS

CERTIFICATE

ACHIEVEMENT

JYOTHI MUSHROOMS, NUNNA, VIJAYAWADA

Skill Development Training / Project Work in Mushroom Cultivation

Bhukya Sai babu

Student of III B.Sc, BZC ..... S.R.R & C.V.R. Govt. Degree College (A)
Machavaram, Vijayawada

Has Successfully Completed 5 days Botany
Skill Development Training Program
{9.5.2022 to 13.5.2022} on Mushroom Cultivation
in the Academic year 2021-2022

JYOTHI



CERTIFICATE
ACHIEVEMENT

JYOTHI MUSHROOMS, NUNNA, VIJAYAWADA

Skill Development Training / Project Work in Mushroom Cultivation

B. Lakshman Rao

Student of III B.Sc, BZC ..... S.R.R & C.V.R. Govt. Degree College (A)
Machavaram, Vijayawada

Has Successfully Completed 10days Theory
Skill Development Training Program
from 9.5.2022 to 18.5.2022 on Mushroom Cultivation
in the Academic year 2021-2022

JYOTHI MUSHROOMS

CERTIFICATE

ACHIEVEMENT

JYOTHI MUSHROOMS, NUNNA, VIJAYAWADA

Skill Development Training / Project Work in Mushroom Cultivation

Abi Lakshmi

Student of III B.Sc, BZC ..... S.R.R & C.V.R. Govt. Degree College (A)
Machavaram, Vijayawada

Has Successfully Completed 5 days Botany
Skill Development Training Program
{9.5.2022 to 13.5.2022} on Mushroom Cultivation
in the Academic year 2021-2022

JYOTHI MUSHROOMS
VIJAYAWADA

JYOTHI MUSHROOMS

CERTIFICATE

ACHIEVEMENT

JYOTHI MUSHROOMS, NUNNA, VIJAYAWADA

Skill Development Training / Project Work in Mushroom Cultivation

Ch.Jaya shankar

Student of III B.Sc, BZC ..... S.R.R & C.V.R. Govt. Degree College (A)
Machavaram, Vijayawada

Has Successfully Completed 5 days Botany
Skill Development Training Program
{9.5.2022 to 13.5.2022} on Mushroom Cultivation
in the Academic year 2021-2022

JYOTHI MUSHROOMS
VIJAYAWADA

JYOTHI
MASHROOMS

CERTIFICATE

ACHIEVEMENT

JYOTHI MUSHROOMS, NUNNA, VIJAYAWADA

Skill Development Training / Project Work in Mushroom Cultivation

CH. VENKATAIAH

Student of III B.Sc, BZC ..... S.R.R & C.V.R. Govt. Degree College (A)
Machavaram, Vijayawada

Has Successfully Completed 5 days Botany
Skill Development Training Program
[9.5.2022 to 13.5.2022] on Mushroom Cultivation
in the Academic year 2021-2022

JYOTHI MUSHROOMS

CERTIFICATE

ACHIEVEMENT

JYOTHI MUSHROOMS, NUNNA, VIJAYAWADA

Skill Development Training / Project Works in Mushroom Cultivation

CHIKKAVARAPU. MANIKANTA DEEPAK

Student of III B.Sc, BZC E.M S.R.R & C.V.R. Govt. Degree College (A)
Machavaram, Vijayawada

Has Successfully Completed 5 days Botany
Skill Development Training Program
{9.5.2022 to 13.5.2022} on Mushroom Cultivation
in the Academic year 2021-2022

JYOTHI MUSHROOMS

CERTIFICATE

ACHIEVEMENT

JYOTHI MUSHROOMS, NUNNA, VIJAYAWADA

Skill Development Training / Project Work in Mushroom Cultivation

Chettipogu.Navya jyothi [E-M]

Student of III B.Sc, BZC ..... S.R.R & C.V.R. Govt. Degree College (A)
Machavaram, Vijayawada

Has Successfully Completed 5 days Botany
Skill Development Training Program
{9.5.2022 to 13.5.2022} on Mushroom Cultivation
in the Academic year 2021-2022

JYOTHI MUSHROOMS
VIJAYAWADA

JYOTHI
MUSHROOMS

CERTIFICATE

ACHIEVEMENT

JYOTHI MUSHROOMS, NUNNA, VIJAYAWADA

Skill Development Training / Project Work in Mushroom Cultivation

DARELLI. NANI

Student of III B.Sc, BZC **E.M** *..... S.R.R & C.V.R. Govt. Degree College (A)*
Machavaram, Vijayawada

Has Successfully Completed 5 days Botany
Skill Development Training Program
{9.5.2022 to 13.5.2022} on Mushroom Cultivation
in the Academic year 2021-2022

JYOTHI MUSHROOMS

CERTIFICATE

ACHIEVEMENT

JYOTHI MUSHROOMS, NUNNA, VIJAYAWADA

Skill Development Training / Project Work in Mushroom Cultivation

ELLIPILLI. NARAYANA

Student of III B.Sc, BZC ..E.M.... S.R.R & C.V.R. Govt. Degree College (A)
Machavaram, Vijayawada

Has Successfully Completed 5 days Botany
Skill Development Training Program
{9.5.2022 to 13.5.2022} on Mushroom Cultivation
in the Academic year 2021-2022

JYOTHI MUSHROOMS
VIJAYAWADA

JYOTHI
MASHROOMS

CERTIFICATE

ACHIEVEMENT

JYOTHI MUSHROOMS, NUNNA, VIJAYAWADA

Skill Development Training / Project Work in Mushroom Cultivation

G.Durga prasad

Student of III B.Sc, BZC ..... S.R.R & C.V.R. Govt. Degree College (A)
Machavaram, Vijayawada

Has Successfully Completed 5 days Botany
Skill Development Training Program
{9.5.2022 to 13.5.2022} on Mushroom Cultivation
in the Academic year 2021-2022

JYOTHI MUSHROOMS
VIJAYAWADA

JYOTHI MASHROOMS

CERTIFICATE

ACHIEVEMENT

JYOTHI MUSHROOMS, NUNNA, VIJAYAWADA

Skill Development Training / Project Work in Mushroom Cultivation

G.satya priya

Student of III B.Sc, BZC ..... S.R.R & C.V.R. Govt. Degree College (A)
Machavaram, Vijayawada

Has Successfully Completed 5 days Botany
Skill Development Training Program
{9.5.2022 to 13.5.2022} on Mushroom Cultivation
in the Academic year 2021-2022

JYOTHI MUSHROOMS
VIJAYAWADA

JYOTHI
MASHROOMS

CERTIFICATE

ACHIEVEMENT

JYOTHI MUSHROOMS, NUNNA, VIJAYAWADA

Skill Development Training / Project Work in Mushroom Cultivation

JAMMALAMUDI RAJASHEKAR

Student of III B.Sc, BZC ..... S.R.R & C.V.R. Govt. Degree College (A)
Machavaram, Vijayawada

Has Successfully Completed 5 days Botany
Skill Development Training Program
{9.5.2022 to 13.5.2022} on Mushroom Cultivation
in the Academic year 2021-2022

JYOTHI MUSHROOM
VIJAYAWADA

CERTIFICATE

ACHIEVEMENT

JYOTHI MUSHROOMS, NUNNA, VIJAYAWADA

Skill Development Training / Project Work in Mushroom Cultivation

KOTA. BHAGYA RATNA KUMAR

Student of III B.Sc, BZC ..... E.M ..... S.R.R & C.V.R. Govt. Degree College (A)
Machavaram, Vijayawada

Has Successfully Completed 5 days Botany
Skill Development Training Program
{9.5.2022 to 13.5.2022} on Mushroom Cultivation
in the Academic year 2021-2022

JYOTHI MUSHROOMS
VIJAYAWADA

JYOTHI MUSHROOMS

CERTIFICATE

ACHIEVEMENT

JYOTHI MUSHROOMS, NUNNA, VIJAYAWADA

Skill Development Training / Project Work in Mushroom Cultivation

K.Chandrika

Student of III B.Sc, BZC ..... S.R.R & C.V.R. Govt. Degree College (A)
Machavaram, Vijayawada

Has Successfully Completed 5 days Botany
Skill Development Training Program
{9.5.2022 to 13.5.2022} on Mushroom Cultivation
in the Academic year 2021-2022

JYOTHI MUSHROOMS
VIJAYAWADA

JYOTHI MASHROOMS

CERTIFICATE

ACHIEVEMENT

JYOTHI MUSHROOMS, NUNNA, VIJAYAWADA

Skill Development Training / Project Work in Mushroom Cultivation

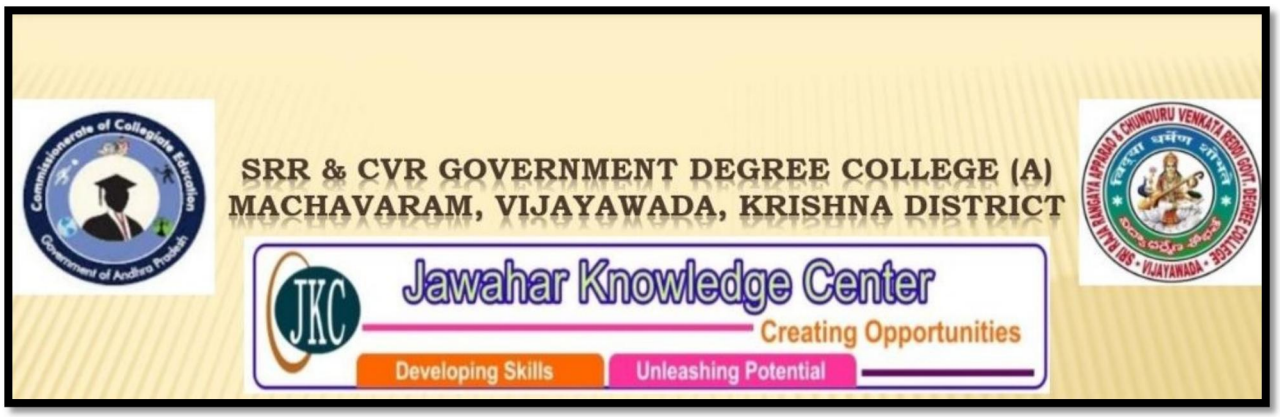
Kota Hema

Student of III B.Sc, BZC ..... S.R.R & C.V.R. Govt. Degree College (A)
Machavaram, Vijayawada

Has Successfully Completed 5 days Botany
Skill Development Training Program
(9.5.2022 to 13.5.2022) on Mushroom Cultivation
in the Academic year 2021-2022

JYOTHI MUSHROOMS
VIJAYAWADA

JYOTHI MASHROOMS



TRAINING IN SOFT SKILL DEVELOPMENT COURSE

by

APITA – NAANDI Foundation

DATES: 23-11-2021 TO 29-11-2021

Target Group: 100 students of II BCOM and II BA

APITA in association with Naandi Foundation conducted a training programme in soft skills on JKC Platform from 23.11.2021 to 29.11.2021 for 50 BA and 50 B.com students. The training was interactive and concentrated on themes like team work, time management and personality development. Students immensely benefitted from all sessions and requested inclusion of such training programmes. Naandi Foundation also issued certificates to students.

Gmail

Jawahar Knowledge Center Vijayawada <vijayawada.jkc@gmail.com>

Free Training Program on Soft Skills and Employability Skills by APITA and Naandi Foundation- reg

1 message

Satya Ratnam Marepalli <satyaratnam.m@ap.gov.in>
To: vijayawada jkc <vijayawada.jkc@gmail.com>
Sat, Nov 20, 2021 at 1:14 PM

Dear Madam,

Greetings From APITA !!

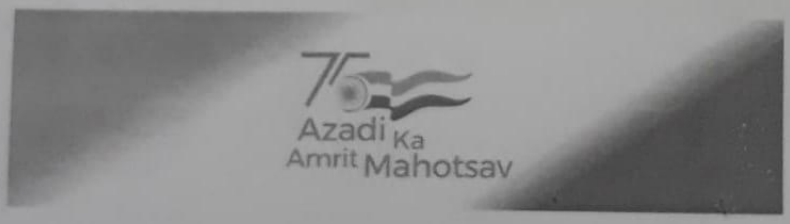
APITA had a MoU with Naandhi Foundation on various skilling programs to the students as a part of that they are providing free Employability and soft skills classes to the APITA registered college students 6 days program.

Offline Employability Skills 6 Days 42 Hours Any Students willing to Seek Job Immediately Classroom Training

Please find the attached 6 days schedule and give your willing to conduct the program at your college

Thanking you,

M. Satya Ratnam
District Development Manager
Krishna District
Andhra Pradesh Information Technology Academy
ITE & C Department , Govt of AP.
9989930766



Frame Work 42 Hours offline.xlsx
10K

SRR & CVR Government Degree College (A)
Vijayawada

JAWAHAR KNOLEDGE CENTRE (JKC)

22.11.2021

To
The Principal
SRR &CVR Govt. Degree College (A)
Vijayawada

Madam,

Sub: APITA Training in Soft Skills on JKC Platform - 23 – 29 November, 2021 – 50 BA students & 50 BCom students- Request for permission – Regarding

We submit that AP Information Technology Academy (APITA) in association with Naandhi Foundation is offering 6 Day Training in Soft Skills from 23 to 29 November 2021 from 9am to 1PM on JKC platform.

The copy of the mail and agenda is enclosed for your kind perusal and request your permission to conduct the training for 50 BA & 50 BCom students in our college.

The training is free of cost and JKC is asked to provide tea, snacks, water bottles and working lunch for two Trainers and workshop material like Charts, sketches and A4 bundles and water for students. The rooms 208 and 202 will be taken up for the training and are to be maintained clean on all 6 days.

The expenditure incurred for the training will be submitted with related bills and may be met from JKC funds of the college.

Thanking you

Yours faithfully

A. Rosaiah

JKC Coordinator

JKC committee

Approved

22.11.2021

PRINCIPAL
SRR & CVR GOVT. DEGREE COLLEGE
(Autonomous)
Machavaram, VIJAYAWADA - 520 004.

SRR & CVR Government Degree College (A), Vijayawada

Jawahar Knowledge Centre (JKC)

6 Days Training Programme in Soft Skills by AP Information Technology Academy (APITA) in association with Naandi Foundation for 100 II BA & II BCom students

Day 1		This is me + I am Unique
	23.11.2021	Body Language Grooming and Hyginene
		Yes we can
Day 2		Time Management
	24.11.2021	Social manners
		Point of view
Day3		Story Board
	25.11.2021	Goal Setting
		Money management
Day 4		Count Your blessings
	26.11.2021	Interview Preparation
		Interview Preparation
Day 5		Professional Ethics
	27.11.2021	Group Discussion
		Explaining a Process
Day 6		Skit Preparation
	29.11.2021	Skit Presentation
		Extempore Advance
Day 7		GD (How It Happens In real Interview)
	29.11.2021	Jam (How it Happens I real Interview
		Spreading happiness

Approved by Principal Madam **Dr.K.Bhagya Lakshmi**

JKC Coordinator Smt. A.Rosalind

JKC Committee Dr.D Ch.Appa Rao, Dept. of Commerce
Sri.Ajayi Babu, Dept. of History
Smt. V. Uma Lakshmi, Dept. of Physics
Dr.V. Lakshmi Sarvani, Dept. of Computer Science



Inauguration of the training programme



DATES: 23-11-2021 TO 28-11-2021
INAGURATION





JKC-APITA SOFT SKILLS SIX DAYS TRAINNING PROGRAMME
DATES: 23-11-2021 TO 28-11-2021

INAGURATION





JKC-APITA SOFT SKILLS SIX DAYS TRAINNING PROGRAMME

DATES: 23-11-2021 TO 28-11-2021
INAGURATION





JKC-APITA SOFT SKILLS SIX DAYS TRAINNING PROGRAMME
DATES: 23-11-2021 TO 28-11-2021
INAGURATION


23-Nov-2021 10:12:26 am
Vsn Street
Machavaram
Vijayawada
Krishna
Andhra Pradesh


Andhra Pradesh
Information Technology Academy (APITA)
APITA
Six Days Training Programme
on
Soft Skills
(23-11-2021 to 29-11-2021)
Naandi
Mahindra

DAY 1

Sessions on Self Introduction, Body Language and Self Confidence

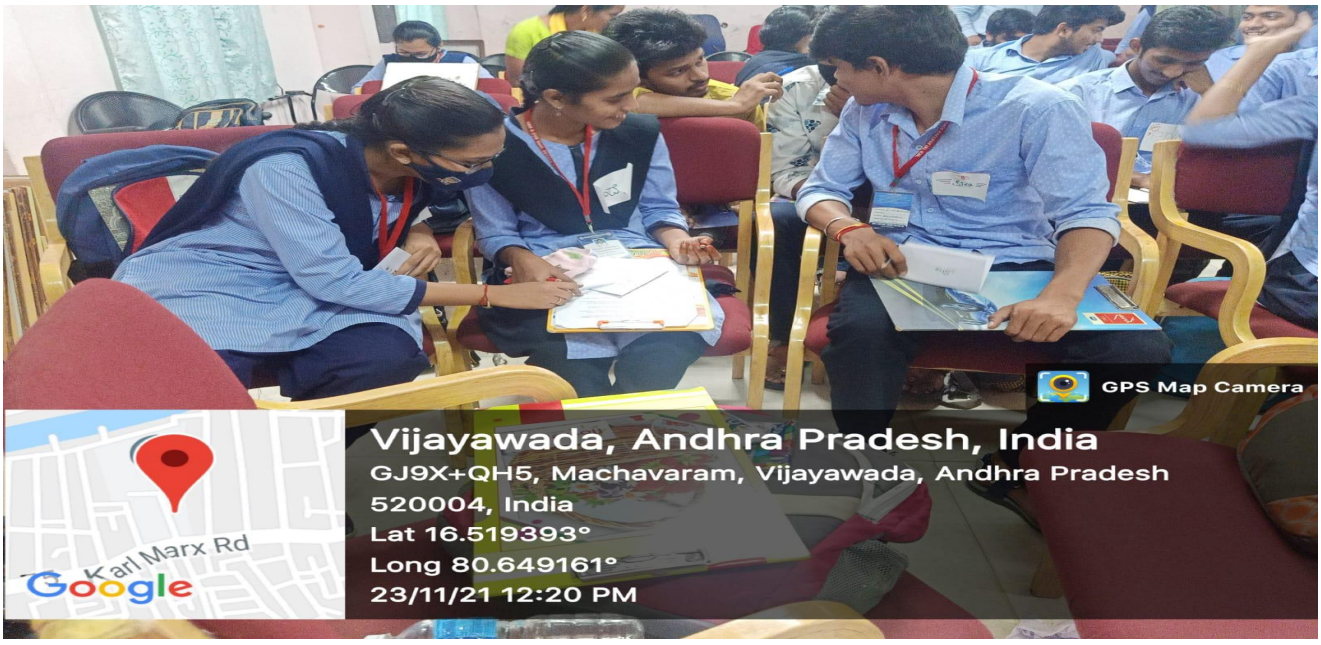
JKC-APITA SOFT SKILLS SIX DAYS TRAINNING PROGRAMME
DATES: 23-11-2021 TO 28-11-2021
DAY 1





JKC-APITA SOFT SKILLS SIX DAYS TRAINNING PROGRAMME
DATES: 23-11-2021 TO 28-11-2021
DAY 1





JKC-APITA SOFT SKILLS SIX DAYS TRAINNING PROGRAMME
DATES: 23-11-2021 TO 28-11-2021
DAY 1





JKC-APITA SOFT SKILLS SIX DAYS TRAINNING PROGRAMME
DATES: 23-11-2021 TO 28-11-2021
DAY 1





DATES: 23-11-2021 TO 28-11-2021
DAY 1



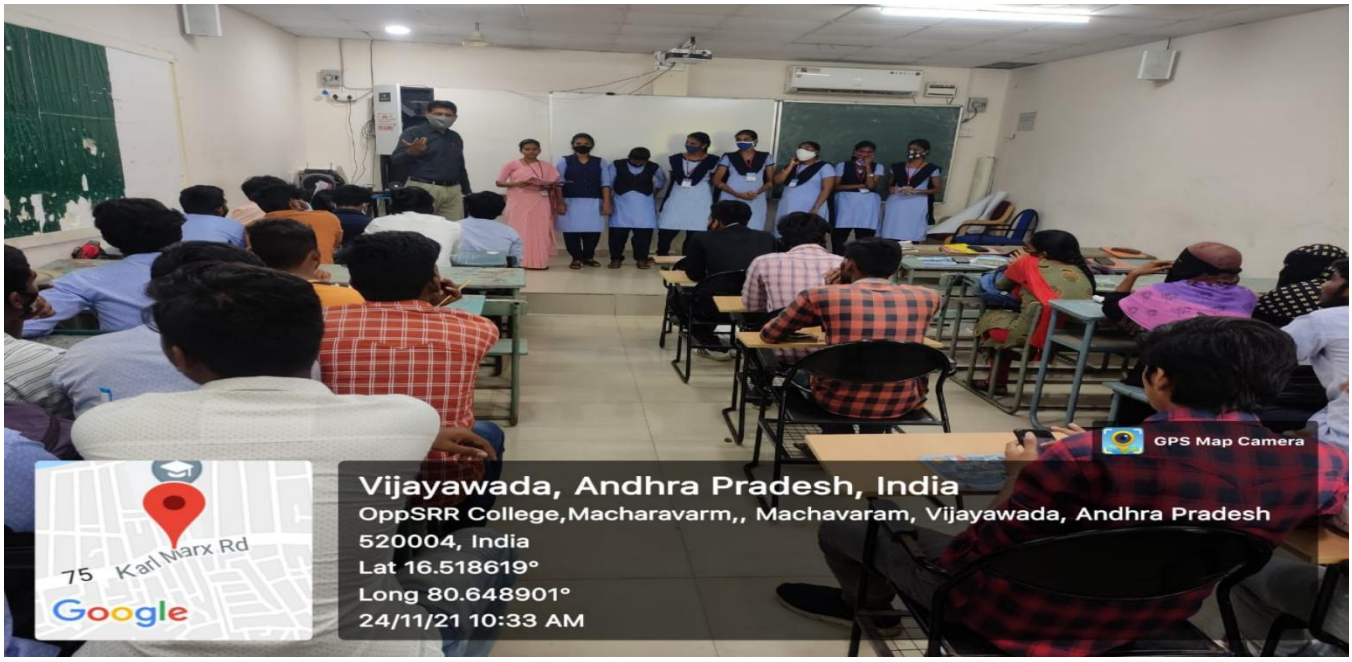


DAY 2

Sessions on Time Management and Social Manners


GPS Map Camera
Vijayawada, Andhra Pradesh, India
GJ9X+QH5, Machavaram, Vijayawada, Andhra Pradesh 520004, India
Lat 16.519391°
Long 80.649156°
24/11/21 10:26 AM
Karl Marx Rd
Google


GPS Map Camera
Vijayawada, Andhra Pradesh, India
GJ9X+JMP, Machavaram, Vijayawada, Andhra Pradesh 520004, India
Lat 16.519036°
Long 80.649129°
24/11/21 10:32 AM
75 Karl Marx Rd
Google


GPS Map Camera
Vijayawada, Andhra Pradesh, India
OppSRR College,Macharavarm,, Machavaram, Vijayawada, Andhra Pradesh 520004, India
Lat 16.518619°
Long 80.648901°
24/11/21 10:33 AM
75 Karl Marx Rd
Google


GPS Map Camera
Vijayawada, Andhra Pradesh, India
OppSRR College,Macharavarm,, Machavaram, Vijayawada, Andhra Pradesh 520004, India
Lat 16.518619°
Long 80.648901°
24/11/21 10:33 AM
75 Karl Marx Rd
Google


GPS Map Camera
Vijayawada, Andhra Pradesh, India
S.R.R. College Bus Stop, Eluru Rd, Near To My Home Complex, Machavaram, Vijayawada, Andhra Pradesh 520004, India
Lat 16.51873°
Long 80.648949°
24/11/21 10:33 AM
75 Karl Marx Rd
Google


GPS Map Camera
Vijayawada, Andhra Pradesh, India
OppSRR College,Macharavarm,, Machavaram, Vijayawada, Andhra Pradesh 520004, India
Lat 16.518665°
Long 80.648919°
24/11/21 10:33 AM
75 Karl Marx Rd
Google


GPS Map Camera
Vijayawada, Andhra Pradesh, India
GJ9X+QH5, Machavaram, Vijayawada, Andhra Pradesh 520004, India
Lat 16.519356°
Long 80.649148°
24/11/21 10:25 AM
Karl Marx Rd
Google


GPS Map Camera
Vijayawada, Andhra Pradesh, India
GJ9X+QH5, Machavaram, Vijayawada, Andhra Pradesh 520004, India
Lat 16.51938°
Long 80.649165°
24/11/21 10:26 AM
Karl Marx Rd
Google


GPS Map Camera
Vijayawada, Andhra Pradesh, India
31-10-7, Vsn St, Machavaram, Vijayawada, Andhra Pradesh 520004, India
Lat 16.519378°
Long 80.649171°
24/11/21 10:26 AM
Karl Marx Rd
Google


GPS Map Camera
Vijayawada, Andhra Pradesh, India
GJ9X+QH5, Machavaram, Vijayawada, Andhra Pradesh 520004, India
Lat 16.519391°
Long 80.649156°
24/11/21 10:26 AM
Karl Marx Rd
Google


GPS Map Camera
Vijayawada, Andhra Pradesh, India
31-10-7, Vsn St, Machavaram, Vijayawada, Andhra Pradesh 520004, India
Lat 16.519378°
Long 80.649171°
24/11/21 10:26 AM
Karl Marx Rd
Google


College
SRR & CVR
Sardar Patel St
Karl Marx Rd
Eluru Rd
Axis Bank
Mayor St
Bullemma St
75
Google
24-Nov-2021 2:26:32 pm
Machavaram
Vijayawada
Krishna
Andhra Pradesh


College
SRR & CVR
Sardar Patel St
Eluru Rd
Kari Marx Rd
Axis Bank
Mayor St
Google
24-Nov-2021 2:27:01 pm
Machavaram
Vijayawada
Krishna
Andhra Pradesh


GPS Map Camera
Vijayawada, Andhra Pradesh, India
#32-28-58,Macharavarm,Vijayawada, Machavaram,
Vijayawada, Andhra Pradesh 520004, India
Lat 16.518996°
Long 80.64911°
24/11/21 10:33 AM
75 Eluru Rd
Google

DAY 3

Sessions on Goal Setting and Money Management

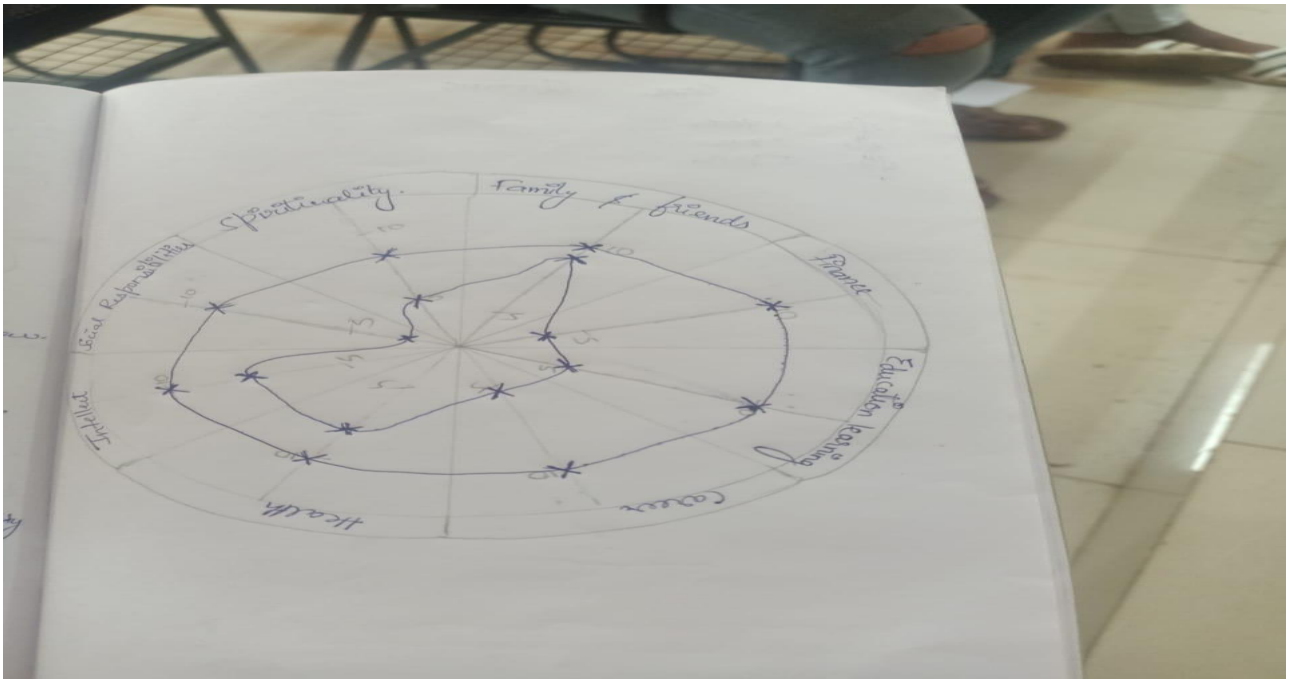



GPS Map Camera
Vijayawada, Andhra Pradesh, India
GJ9X+QH5, Machavaram, Vijayawada, Andhra Pradesh 520004, India
Lat 16.519411°
Long 80.649183°
25/11/21 11:12 AM
Karl Marx Rd
Google





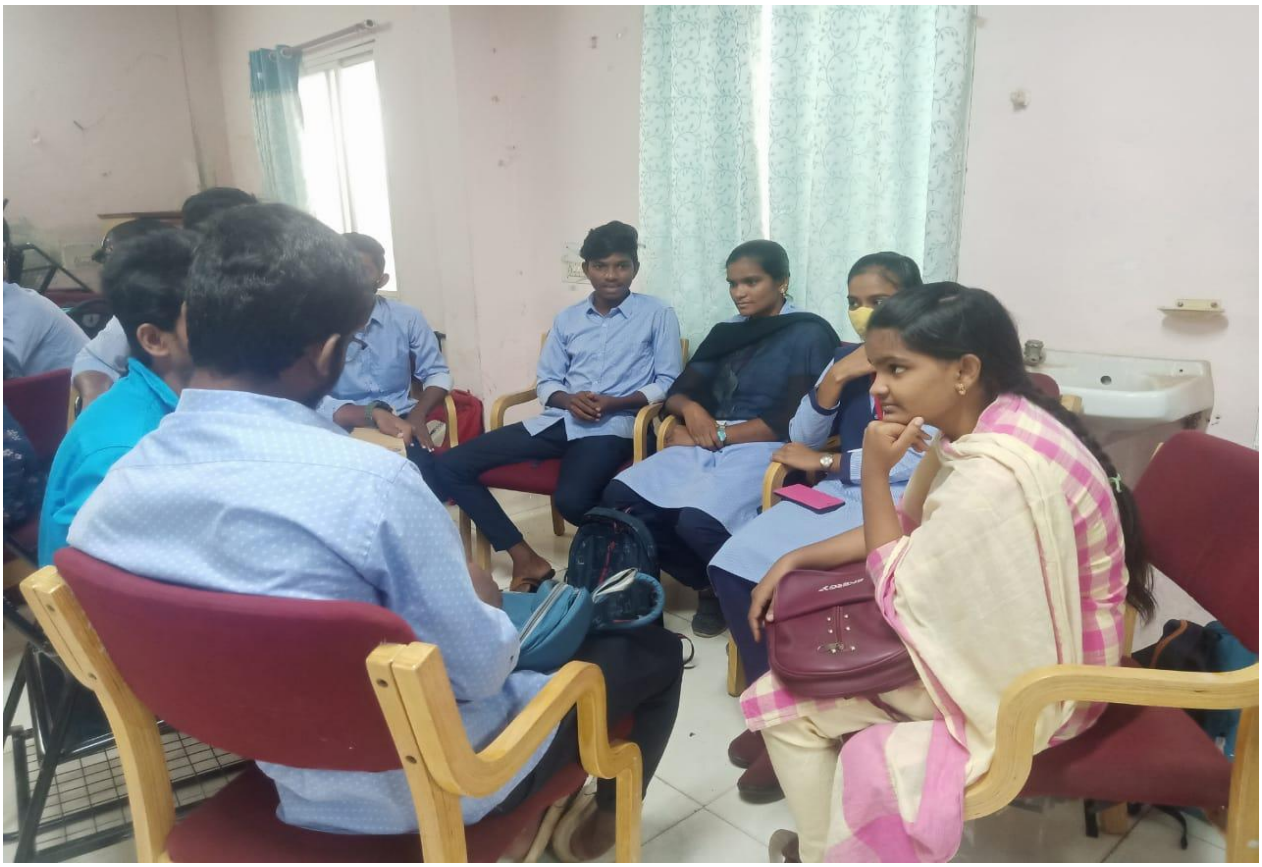



Spirituality
Family & friends
Finance
Education learning
Career
Health
Social Relationships
Spiritual







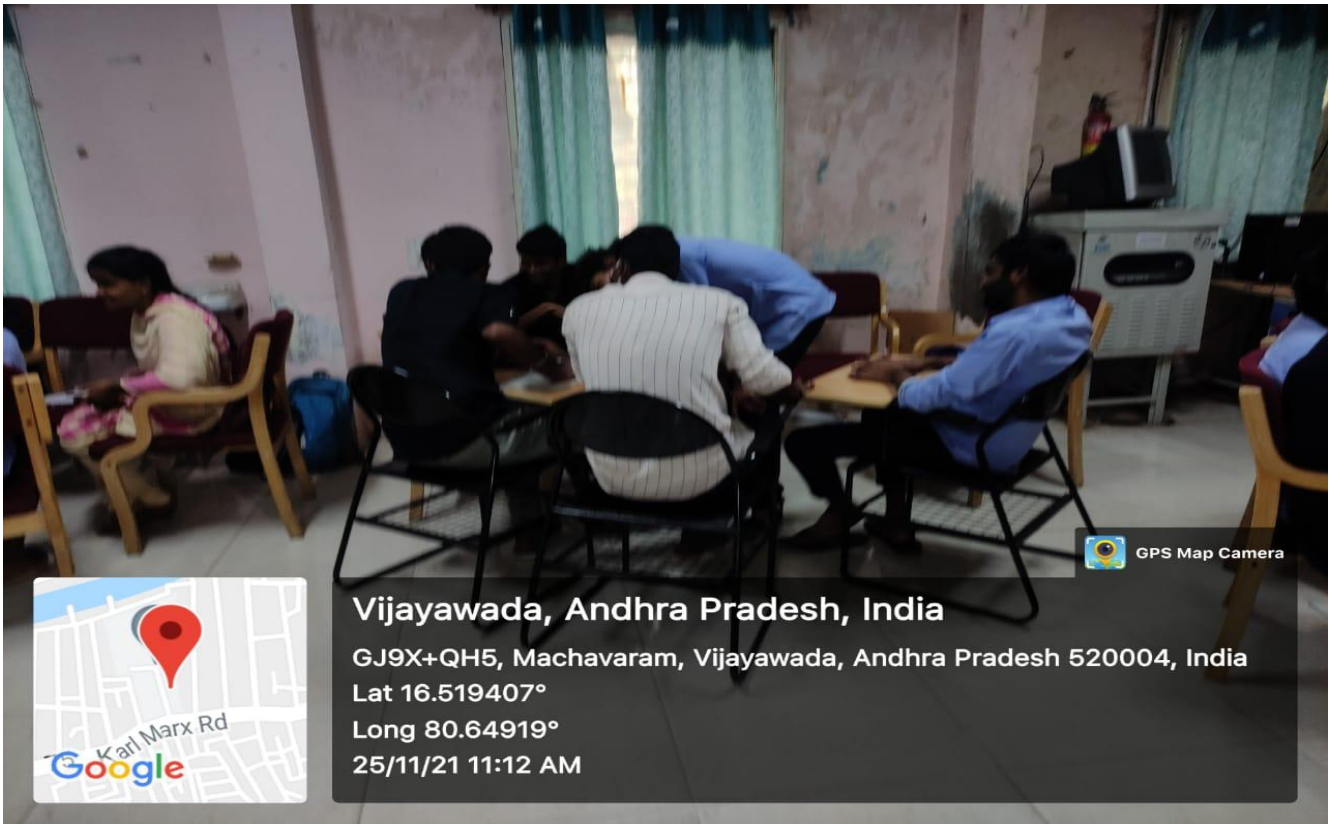



GPS Map Camera
Vijayawada, Andhra Pradesh, India
GJ9X+JMP, Machavaram, Vijayawada, Andhra Pradesh 520004, India
Lat 16.519035°
Long 80.649126°
25/11/21 11:15 AM
75 Karl Marx Rd
Google


GPS Map Camera
Vijayawada, Andhra Pradesh, India
GJ9X+QH5, Machavaram, Vijayawada, Andhra Pradesh 520004, India
Lat 16.519409°
Long 80.649178°
25/11/21 11:11 AM
Karl Marx Rd
Google


GPS Map Camera
Vijayawada, Andhra Pradesh, India
GJ9X+QH5, Machavaram, Vijayawada, Andhra Pradesh 520004, India
Lat 16.51941°
Long 80.649177°
25/11/21 11:12 AM
Karl Marx Rd
Google


GPS Map Camera
Vijayawada, Andhra Pradesh, India
GJ9X+QH5, Machavaram, Vijayawada, Andhra Pradesh 520004, India
Lat 16.519398°
Long 80.649186°
25/11/21 11:12 AM
Karl Marx Rd
Google


GPS Map Camera
Vijayawada, Andhra Pradesh, India
GJ9X+QH5, Machavaram, Vijayawada, Andhra Pradesh 520004, India
Lat 16.519407°
Long 80.64919°
25/11/21 11:12 AM
Karl Marx Rd
Google


GPS Map Camera
Vijayawada, Andhra Pradesh, India
GJ9X+JMP, Machavaram, Vijayawada, Andhra Pradesh 520004, India
Lat 16.519143°
Long 80.649171°
25/11/21 11:14 AM
Karl Marx Rd
Google


Save Girl Child

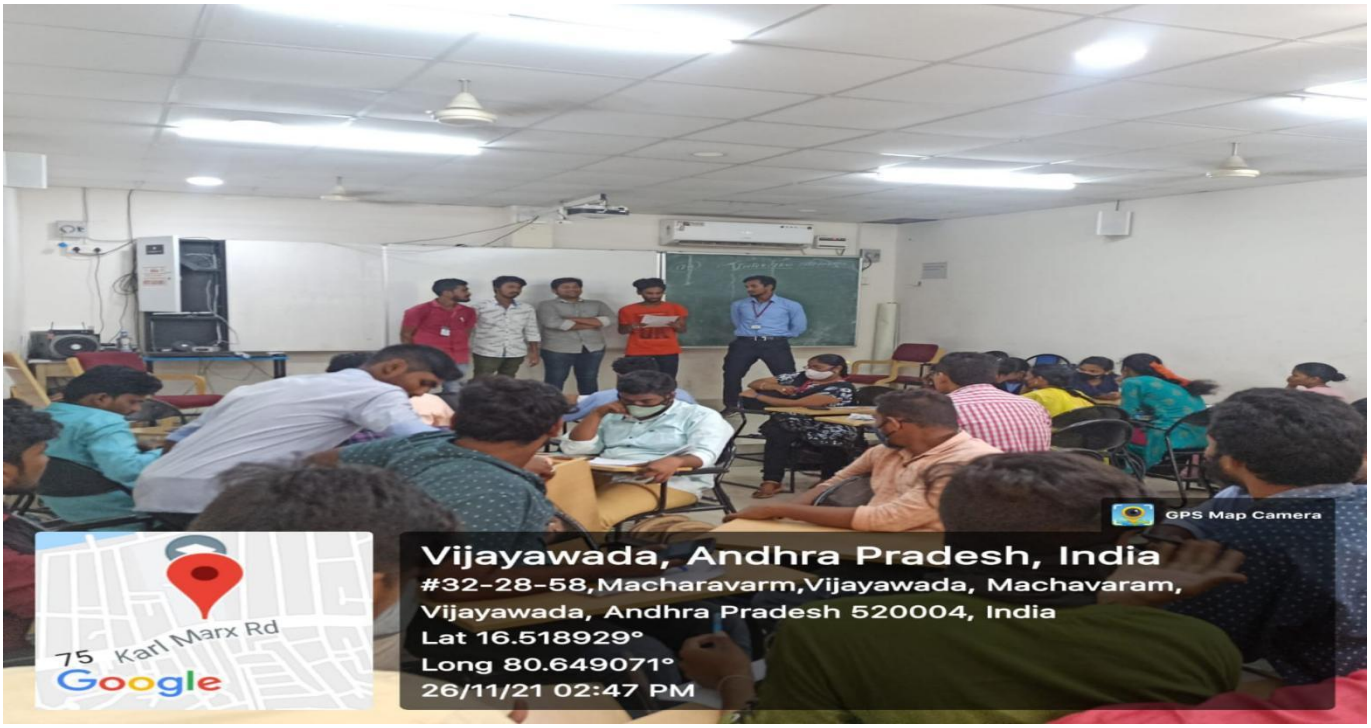

HOSPITAL
DO'S
DONT'S
BEACH
DO'S
DONT'S


SOCIAL
MANNERS
HOSPITAL
DO'S
DON'T'S
DO'S
DON'T'S

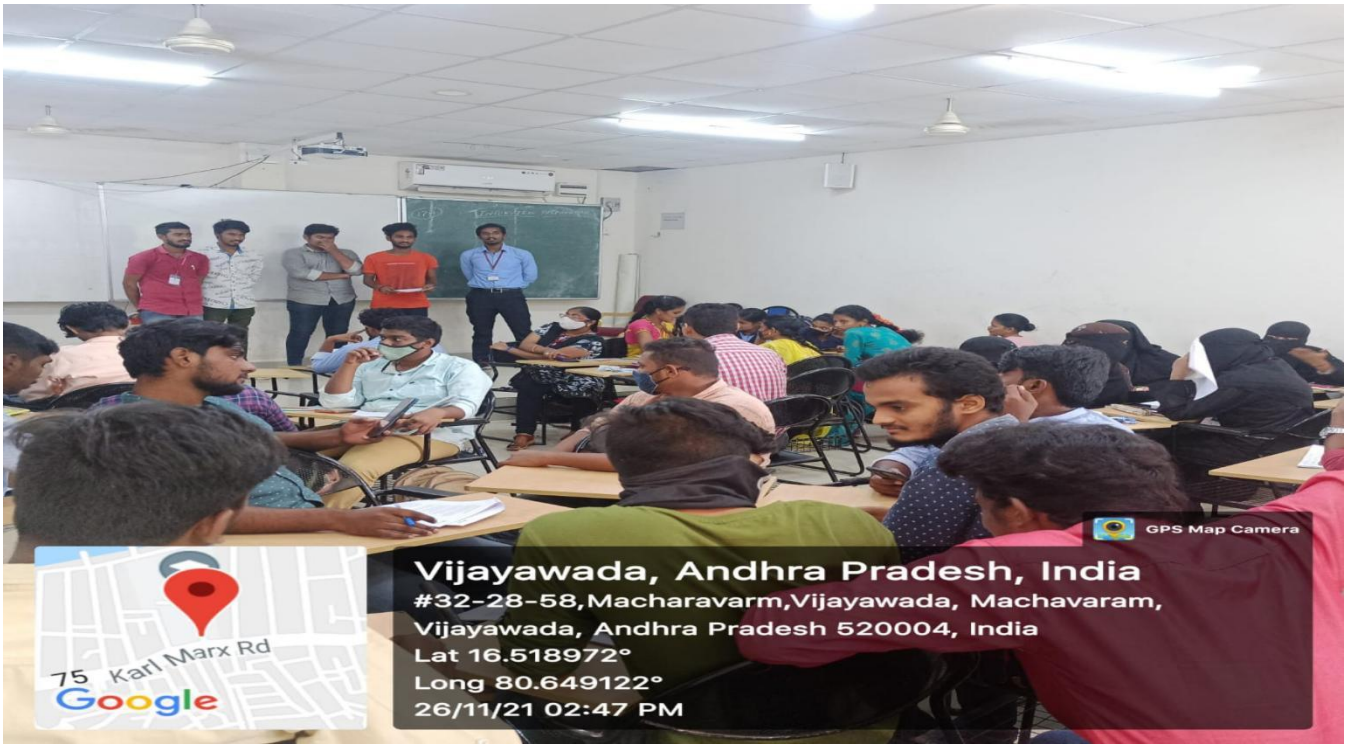

Group no:04
LIBRARY
HOSPITAL
✓ DO's
* Treat the Books with care
* Return Books On time
* Speak quietly
* Don't Disturb Others while Reading
* Ask for help if you can't find what you need
X DONTs
* Do Not bring Foods & Drinks Inside
* Don't Run Just walk
* Do not remove Furnitures to it's Proper place
* Don't take Phone Calls
✓ DO's
* Maintain Social distance
* Put your masks on
* Wash hands with Alchol based handrub
* Listen to health care wos Asks
* Limit the time you Spend in the Patient's Room
X DONTs
* Do not use the Patient's Toilet
* Do not Touch, hug & kiss the Patient
* Don't Smoke
* Maintain op
* Do not sit or Sleep on Patient Bed

DAY 4

Sessions on Count your Blessings and Interview Preparation


GPS Map Camera
Vijayawada, Andhra Pradesh, India
#32-28-58,Macharavarm,Vijayawada, Machavaram,
Vijayawada, Andhra Pradesh 520004, India
Lat 16.518929°
Long 80.649071°
26/11/21 02:47 PM
75 Karl Marx Rd
Google


GPS Map Camera
Vijayawada, Andhra Pradesh, India
Macharavarm, Machavaram, Vijayawada, Andhra Pradesh
520004, India
Lat 16.518909°
Long 80.648984°
26/11/21 11:11 AM
75 Karl Marx Rd
Google


GPS Map Camera
Vijayawada, Andhra Pradesh, India
#32-28-58,Macharavarm,Vijayawada, Machavaram,
Vijayawada, Andhra Pradesh 520004, India
Lat 16.518972°
Long 80.649122°
26/11/21 02:47 PM
75 Karl Marx Rd
Google


GPS Map Camera
Vijayawada, Andhra Pradesh, India
GJ9X+QH5, Machavaram, Vijayawada, Andhra Pradesh
520004, India
Lat 16.519433°
Long 80.649203°
26/11/21 10:36 AM
Karl Marx Rd
Google


GPS Map Camera
Vijayawada, Andhra Pradesh, India
GJ9X+QH5, Machavaram, Vijayawada, Andhra Pradesh
520004, India
Lat 16.519317°
Long 80.649157°
26/11/21 02:49 PM
Karl Marx Rd
Google


GPS Map Camera
Vijayawada, Andhra Pradesh, India
Macharavarm, Machavaram, Vijayawada, Andhra Pradesh
520004, India
Lat 16.518909°
Long 80.648984°
26/11/21 11:11 AM
75 Karl Marx Rd
Google


GPS Map Camera
Karl Marx Rd
Google
Vijayawada, Andhra Pradesh, India
GJ9X+QH5, Machavaram, Vijayawada, Andhra Pradesh
520004, India
Lat 16.51938°
Long 80.649158°
26/11/21 10:36 AM


GPS Map Camera
Karl Marx Rd
Google
Vijayawada, Andhra Pradesh, India
GJ9X+QH5, Machavaram, Vijayawada, Andhra Pradesh
520004, India
Lat 16.519308°
Long 80.64916°
26/11/21 02:49 PM




Andhra Pradesh
Information Technology Academy (APITA)
APITA
Six Days Training Programme
on

DAY 5

Sessions on Professional Ethics and Group Discussion


GPS Map Camera
Vijayawada, Andhra Pradesh, India
GJ9X+QH5, Machavaram, Vijayawada, Andhra Pradesh 520004, India
Lat 16.519423°
Long 80.649192°
27/11/21 03:33 PM
Karl Marx Rd
Google


GPS Map Camera
Vijayawada, Andhra Pradesh, India
GJ9X+QH5, Machavaram, Vijayawada, Andhra Pradesh 520004, India
Lat 16.519423°
Long 80.649192°
27/11/21 03:33 PM
Karl Marx Rd
Google


GPS Map Camera
Karl Marx Rd
Google
Vijayawada, Andhra Pradesh, India
GJ9X+QH5, Machavaram, Vijayawada, Andhra Pradesh 520004, India
Lat 16.519423°
Long 80.649192°
27/11/21 03:33 PM


GPS Map Camera
Karl Marx Rd
Google
Vijayawada, Andhra Pradesh, India
GJ9X+QH5, Machavaram, Vijayawada, Andhra Pradesh 520004, India
Lat 16.51931°
Long 80.649165°
27/11/21 03:04 PM


GPS Map Camera
Vijayawada, Andhra Pradesh, India
GJ9X+QH5, Machavaram, Vijayawada, Andhra Pradesh 520004, India
Lat 16.519368°
Long 80.649142°
27/11/21 10:47 AM
Karl Marx Rd
Google


GPS Map Camera
Vijayawada, Andhra Pradesh, India
SRR College Bus Stop, Eluru Rd, Machavaram, Vijayawada, Andhra Pradesh 520004, India
Lat 16.518822°
Long 80.648958°
27/11/21 10:41 AM
75 Karl Marx Rd
Google


GPS Map Camera
Vijayawada, Andhra Pradesh, India
SRR College Bus Stop, Eluru Rd, Machavaram, Vijayawada, Andhra Pradesh 520004, India
Lat 16.518829°
Long 80.648988°
27/11/21 10:41 AM
75 Karl Marx Rd
Google


GPS Map Camera
Vijayawada, Andhra Pradesh, India
Macharavarm, Machavaram, Vijayawada, Andhra Pradesh 520004, India
Lat 16.518836°
Long 80.648986°
27/11/21 10:41 AM
75 Karl Marx Rd
Google


GPS Map Camera
Vijayawada, Andhra Pradesh, India
SRR College Bus Stop, Eluru Rd, Machavaram, Vijayawada, Andhra Pradesh 520004, India
Lat 16.518829°
Long 80.648988°
27/11/21 10:41 AM
75 Karl Marx Rd
Google


GPS Map Camera
Vijayawada, Andhra Pradesh, India
SRR College Bus Stop, Eluru Rd, Machavaram, Vijayawada, Andhra Pradesh 520004, India
Lat 16.51883°
Long 80.648989°
27/11/21 10:41 AM
75 Karl Marx Rd
Google


GPS Map Camera
Vijayawada, Andhra Pradesh, India
GJ9X+QH5, Machavaram, Vijayawada, Andhra Pradesh 520004, India
Lat 16.519359°
Long 80.649154°
27/11/21 10:47 AM
Karl Marx Rd
Google


GPS Map Camera
Vijayawada, Andhra Pradesh, India
31-10-7, Vsn St, Machavaram, Vijayawada, Andhra Pradesh 520004, India
Lat 16.519341°
Long 80.649167°
27/11/21 03:04 PM
Karl Marx Rd
Google

DAY 6

Sessions on Skit Preparation

GD and GAM

















Feed Back from Students

Feedback on the Trainer for the training conducted by Andhra Pradesh Information Technology Academy

Training dates: 23Nov 2021 to 28 Nov 2021 *Training topic: Soft Skills* *Trainer Name:* T. MADHU BABU

College Name and district: SRR & CVR GOVT DEGREE COLLEGE, MACHAVARAM, VIJAYAWADA.

Note: Feedback may be given on the scale of 1 – 5; 1 – Poor, 2 – Below Average, 3 – Average, 4 – Good, 5 – Very Good

S.No	REG NO	FIRST NAME	MIDDLE NAME	LAST NAME	Topic Covered	Doubt Claification	Student Interaction	Subject Knowledge	Teaching ability	Overall Feedback
1	20101405	PATHAN	SARABI		5	5	5	5	5	5
2	20101414	SHAIK	NOORI		5	5	5	5	5	5
3	20101409	SHAIK	ASNATHUNNISA		5	5	5	5	5	5
4	20101415	SHAIK	RUKSANA		5	5	5	5	5	5
5	20101412	SHAIK	MUNNI		5	5	5	5	5	5
6	20101410	SHAIK	FATHIMUNNISA		5	5	5	5	5	5
7	20101417	SHAIK	ZEENATH		5	5	5	5	5	5
8	20106021	Rage	Ramalakshamamma		5	5	5	5	5	5
9	20106016	Parthakani	Rathnakumari		5	5	5	5	5	5
10	20101224	Kurra	Priya		5	5	5	5	5	5
11	20101282	Muthyalu	Harika		5	5	5	5	5	5
12	20101028	Yerninti	Yamuna		5	5	5	5	5	5
13	20205213	Tanuku	Thimothi		5	5	5	5	5	5

Feedback on the Trainer for the training conducted by Andhra Pradesh Information Technology Academy

Training dates: 23Nov 2021 to 28 Nov 2021 *Training topic: Soft Skills* *Trainer Name:* T. MADHU BABU

College Name and district: SRR & CVR GOVT DEGREE COLLEGE, MACHAVARAM, VIJAYAWADA.

Note: Feedback may be given on the scale of 1 – 5; 1 – Poor, 2 – Below Average, 3 – Average, 4 – Good, 5 – Very Good

S.No	REG NO	FIRST NAME	MIDDLE NAME	LAST NAME	Topic Covered	Doubt Claification	Student Interaction	Subject Knowledge	Teaching ability	Overall Feedback
1	20101003	Bukkavathu	Vamsi		5	5	5	5	5	5
2	20101027	Vadithya	Anjaneyulu		5	5	5	5	5	5
3	20101205	Baddigam Narendra	Narendra		5	5	5	5	5	5
4	20101013	Kanakkupudi	Yaswanth		5	5	5	5	5	5
5	20101204	Avula	Jallaiah		5	5	5	5	5	5
6	20101205	ARAVAPALLI	RAJA SEKHAR		5	5	5	5	5	5
7	20101401	KATIKALA	MAHESH		5	5	5	5	5	5
8	20101218	Jagga	Rishi	Sri Harsha	5	5	5	5	5	5
9	20101005	Budala	Kamal	Kiran	5	5	5	5	5	5
10	20101226	Madiki	Nagendra		5	5	5	5	5	5
11	20101227	Malapati	Srinu		5	5	5	4	5	5
12	20205204	G. Guvvalagu	Guravaiah		5	5	5	5	5	5
13	20202268	ROJA	Meduri		5	5	5	5	5	5

Feedback on the Trainer for the training conducted by Andhra Pradesh Information Technology Academy

Training dates: 23Nov 2021 to 28 Nov 2021 *Training topic: Soft Skills* *Trainer Name:* T. MADHU BABU

College Name and district: SRR & CVR GOVT DEGREE COLLEGE, MACHAVARAM, VIJAYAWADA.

Note: Feedback may be given on the scale of 1 – 5; 1 – Poor, 2 – Below Average, 3 – Average, 4 – Good, 5 – Very Good

S.No	REG NO	FIRST NAME	MIDDLE NAME	LAST NAME	Topic Covered	Doubt Claification	Student Interaction	Subject Knowledge	Teaching ability	Overall Feedback
1.	20205211	Pedasingu	Durga	Bhavani	5	5	5	5	5	5
2.	20101223	KURRA	Anusha	.	5	5	5	5	5	5
3.	20102009	Kanulla	Veera Naga	Durga	5	5	5	6	6	6
4.	20205215	[illegible]	Siva.	[illegible]	6	5	5	5	5	5

Feedback on the Trainer for the training conducted by Andhra Pradesh Information Technology Academy

Training dates: 23Nov 2021 to 28 Nov 2021 *Training topic: Soft Skills* *Trainer Name:* T. MADHU BABU

College Name and district: SRR & CVR GOVT DEGREE COLLEGE, MACHAVARAM, VIJAYAWADA.

Note: Feedback may be given on the scale of 1 – 5; 1 – Poor, 2 – Below Average, 3 – Average, 4 – Good, 5 – Very Good

S.No	REG NO H.T.No	FIRST NAME	MIDDLE NAME	LAST NAME	Topic Covered	Doubt Claification	Student Interaction	Subject Knowledge	Teaching ability	Overall Feedback
1	20102015	TEJAVATHU	RAMA KOTI		5	5	5	5	5	5
2.	20102004	GEDELA	HEMANTH ASHOK	KUMAR	5	5	5	5	5	5
3.	20205207	JARJANA	PAVAN KUMAR		5	5	5	5	5	5
4	20205206	Kumari	Sushma		5	5.	5	5	5	5
5	20101220	KAKUMANI	MAHESH	BABU	5	5	5	5	5	5
6	20101023	RENTAPALLI	PRASANTH	KUMAR	5	5	5	5	5	5
7	20101011	JALASUTRAM	VENKATA.	NAVEEN	5	5.	5	5	5	5
8	20106009	JALLU	VENKATA	RAMANA	5	5	5	5	5	5
9	20101004	BANDARU	VAMSI	KRISHNA	5	5	5	5	5	5
10	20102007	ISLAVATHU	DINESH	NAIK	5	5	5	5	5	5
11	20101404	MOPARTHY	SUNNY		5	5	5	5	5	5
12	20101213	DUDEKULA	ANEEF		5	5	5	5	5	5
13	20205208	KATARIAMUR	Akhil		5	5	5	5	5	5

Feedback on the Trainer for the training conducted by Andhra Pradesh Information Technology Academy

Training dates: 23Nov 2021 to 28 Nov 2021 *Training topic: Soft Skills* *Trainer Name:* Ramesh Sir

College Name and district: SRR & CVR GOVT DEGREE COLLEGE, MACHAVARAM, VIJAYAWADA.

Note: Feedback may be given on the scale of 1 – 5; 1 – Poor, 2 – Below Average, 3 – Average, 4 – Good, 5 – Very Good

S.No	REG NO	FIRST NAME	MIDDLE NAME	LAST NAME	Topic Covered	Doubt Clarification	Student Interaction	Subject Knowledge	Teaching ability	Overall Feedback
27	20202234	GATHEM	NAGAMANI	–	Yes	5	5	5	5	5
28	20202273	Natta	Gayathri	–	Yes	5	5	5	5	5
29	20202236	Gidukonda	Hemalatha	–	Yes	5	5	5	5	5
30	20202262	Madhu	M. KUSUMAHARI	–	Yes	5	5	5	5	5
31	20202225	Devalapalli	Dhanaraja	–	Yes	5	5	5	5	5 Satisfy
32	20202254	KOMIRI	RAJESH	–	Yes	5	5	5	5	5
33	20202233	Gupta	Srinivasarao	–	Yes	5	5	5	5	5

Feedback on the Trainer for the training conducted by Andhra Pradesh Information Technology Academy

Training dates: 23Nov 2021 to 28 Nov 2021 *Training topic: Soft Skills* *Trainer Name:* Ramesh Sir

College Name and district: SRR & CVR GOVT DEGREE COLLEGE, MACHAVARAM, VIJAYAWADA.

Note: Feedback may be given on the scale of 1 – 5; 1 – Poor, 2 – Below Average, 3 – Average, 4 – Good, 5 – Very Good

S.No	REG NO H.T NO	FIRST NAME	MIDDLE NAME	LAST NAME	Topic Covered	Doubt Clarification	Student Interaction	Subject Knowledge	Teaching ability	Overall Feedback
1	20202228	Dogupartha	Vali	–	Yes	5	5	5	5	5
2.	20202266	Masimukku	Vamsi	–	Yes	5	5	5	5	5
3.	20202308	Vempadapu	Ramya	Sree	Yes	5	5	5	5	5
4.	20202279	PUTTA.	Gowri	Sankara	Yes	5	5	5	5	5
5	20202263	Mallavarapu	Nani		Yes	5	5	5	5	5
6.	20202219	Burre	Japhanya		Yes	5	5	5	5	5
7.	20202255	Kommu	Anusha		Yes	5	5	5	5	5
8	20202251	Kanneboyina	Vasanthi		Yes	5	5	5	5	5
9.	20202283	Bavuthu	Sai	Kumari	Yes	5	5	5	5	5
10	20202208	Basetti	Bindhumadhavi		Yes	5	5	5	5	5
11	20202304	Vanukuru	Sarala		Yes	5	5	5	5	5
12	20202232	Bhanu	Ganji		Yes	5	5	5	5	5
13.	20202205	Aravapalli	Jayasree.		Yes	5	5	5	5	5

Feedback on the Trainer for the training conducted by Andhra Pradesh Information Technology Academy

Training dates: 23Nov 2021 to 29 Nov 2021 *Training topic: Soft Skills* *Trainer Name:*

College Name and district: SRR & CVR GOVT DEGREE COLLEGE, MACHAVARAM, VIJAYAWADA.

Note: Feedback may be given on the scale of 1 – 5; 1 – Poor, 2 – Below Average, 3 – Average, 4 – Good, 5 – Very Good

S.No	REG NO	FIRST NAME	MIDDLE NAME	LAST NAME	Topic Covered	Doubt Clarification	Student Interaction	Subject Knowledge	Teaching ability	Overall Feedback
14	20202250	Kandupotlu	Durga	Rao	Yes	5	5	5	5	5
15	20202305	Vasipalli	Anitha	-	Yes	5	5	5	5	5
16	20202230	Enjeti Spandana	Spandana	—	Yes	5	5	5	5	5
17	20202247	Kadiyka	Mounika	-	Yes	5	5	5	5	5
18	20202256	Kosuru	Leela	Chakradhar	Yes	5	5	5	5	5
19	20202286	Sarika	Naga	baby	Yes	5	5	5	5	5
20	20202212	Bhanam	manoj	kumar	yes	5	5	5	5	5
21	20202292	Shaik	Nazeer	-	Yes	5	5	5	5	5
22	20202282	Rambathu	Vara	Prasad	Yes	5	5	5	5	5
23	20202231	Galavilli	Siva	-	Yes	5	5	5	5	5
24	[illegible]	[illegible]	Aravind	kumar	yes	5	5	5	5	5
25	20202279	Patnala	Durga	Prasad	Yes	5	5	5	5	5
26	20202278	Pothuri	samuel	-	yes	5	5	5	5	5

Feedback on the Trainer for the training conducted by Andhra Pradesh Information Technology Academy

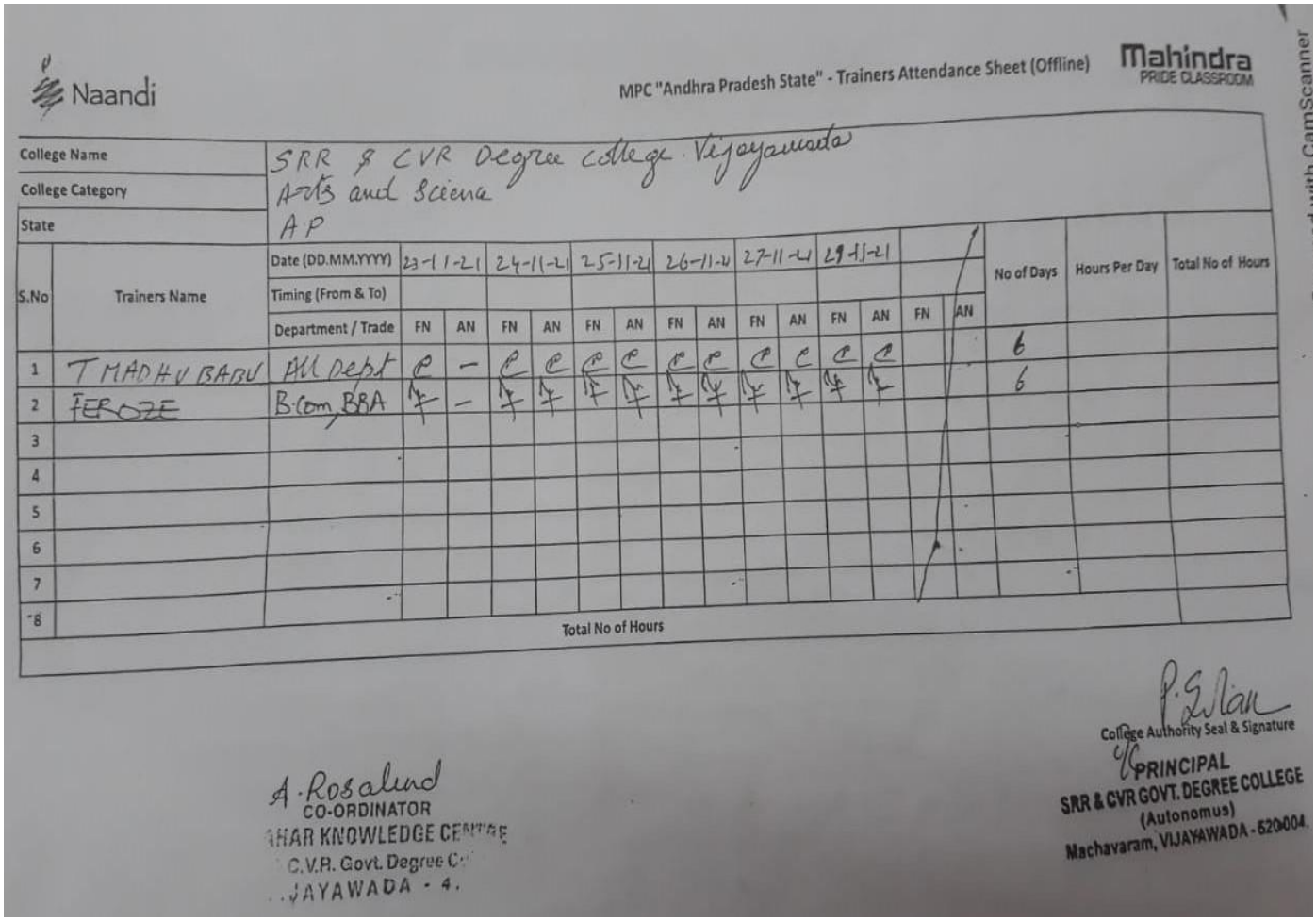
Training dates: 23Nov 2021 to 29 Nov 2021 *Training topic: Soft Skills* *Trainer Name:*

College Name and district: SRR & CVR GOVT DEGREE COLLEGE, MACHAVARAM, VIJAYAWADA.

Note: Feedback may be given on the scale of 1 – 5; 1 – Poor, 2 – Below Average, 3 – Average, 4 – Good, 5 – Very Good

S.No	REG NO	FIRST NAME	MIDDLE NAME	LAST NAME	Topic Covered	Doubt Clarification	Student Interaction	Subject Knowledge	Teaching ability	Overall Feedback
1	20203223	M. [illegible]	Rafi.		Yes	5	4	5	5	5
2	20203220	Md. Fairullah	Fairullah		Yes	5	5	5	4	4
3.	20203208	Ede. Abhigna	Bhabi		Yes	5	4	5	4	5
4.	20203210	G. Nandini	G. Nandini		Yes	4	5	5	4	5
5.	20203217	Shalini	Shalini		Yes	5	4	5	4	5
6.	20203231	Rabiya	Rashri		Yes	4	5	4	5	4
7.	20203215	K. Rani	Rani		Yes	5	4	4	5	5
8.	20203232	Syed Piyaz	Piyaz		Yes	4	5	5	5	5
9.	20203205	D. [illegible]	Koty		Yes	5	4	5	4	4
10.	20203204	B. Kavya	Kavya		Yes	4	5	5	4	5
11.	20203239	V Sanjay	Sanju		Yes	5	4	5	5	5
12.	20203213	K. [illegible]	[illegible]		Yes	4	5	5	4	5
13	20203221	M. Keerthi	[illegible]		Yes	5	5	4	5	5

Trainers Attendance



Naandi

MPC "Andhra Pradesh State" - Trainers Attendance Sheet (Offline)

Mahindra PRIDE CLASSROOM

College Name	SRR & CVR Degree college Vijayawada
College Category	Arts and Science
State	AP

S.No	Trainers Name	Date (DD.MM.YYYY)	23-11-21		24-11-21		25-11-21		26-11-21		27-11-21		29-11-21				No of Days	Hours Per Day	Total No of Hours
		Timing (From & To)																	
		Department / Trade	FN	AN	FN	AN	FN	AN	FN	AN	FN	AN	FN	AN	FN	AN			
1	T MADHU BABU	All Dept	P	–	P	P	P	P	P	P	P	P	P	P			6		
2	FEROZE	B.Com, BBA	P	–	P	P	P	P	P	P	P	P	P	P			6		
3																			
4																			
5																			
6																			
7																			
8																			

Total No of Hours

A. Rosalind
CO-ORDINATOR
GHAR KNOWLEDGE CENTRE
C.V.R. Govt. Degree C...
...JAYAWADA - 4.

College Authority Seal & Signature

PRINCIPAL
SRR & CVR GOVT. DEGREE COLLEGE
(Autonomus)
Machavaram, VIJAYAWADA - 520004.

Scanned with CamScanner

Certificates Issued



JKL

2

Training in Soft skill Development Course.

APITA in association with Naandi Foundation

S.No	Name of the student	Class	Hall Tic No	Signature
1	A.V.S.N.S Jayasree	B.Com (CA)	20202205	A. Jayasree.
2	B. Aranth kumar	B.com (CA)	20202213	B Aranthkumar
3	D. Vali	III B.Com (CA)	20202228	D. Vali
4	K. Mounika.	B.Com (CA)	20202247	K. Mounika
5	E. Spandana	B.Com (CA)	20202230	E. Spandana.
6	R. Sai kumari	B.Com (CA)	20202223	Sai kumari R.
7	B. Japhanya	B.Com (CA)	20202219	B. Japhanya,
8	V. Anitha	B.Com (CA)	20202305	V. Anitha.
9	G. Siva	B.Com (CA)	20202231	G. Siva
10	Y. Sumanth	B.Com (CA)	20202307	Y sumanth
11	P. Gowri Sankarao	B.Com (CA)	20202279	P Gowri sankarao
12	B. Manoj kumar	B.Com (CA)	20202212	B. Manoj kumar
	P. Durga prasanth	B.Com (CA)	20202275	P. Durga prasanth
13				
14	K. Vasanthi	B.Com (CA)	20202251	K. Vasanthi
15	G. Hemalatha.	B.Com (CA)	20202236	G. Hemalatha

S.NO	Name of the student	Class	Hall Tic NO	Signature
16	G. Bhanu	B.COM(CA)	20202232	G. Bhanu
17	V. Ramya Sree	B.com (CA)	20202308	V. Ramya Sree
18	V. Sarala	B.com (CA)	20202304	V. Sarala
19	Sk. Nazeer	B.Com(CA)	20202292	Sk. Nazeer
20	N. Gayathri	B.Com(C.A)	20202273	N. Gayathri
21	M. ROJA	B.com(CA)	20202268	M. Roja
22	K. Anusha	B.com (CA)	20202255	K. Anusha
23	G. Nandini	B.B.B 2nd	20203210	G. Nandini
24	K. Shalini	B.B.B 2nd	20203217	K. shalini
25	Sk. Rabiya Bashri	B.B.A IInd	20203231	Sk. Rabiya
26	Syed Riyaz	BBA IInd	20203232	Syed Riyaz
27	Sk. Degul Meera	B.B.A IInd	20203229	Sk. Degul Meera
28	M. John Abhishek Paul	BBA IInd	20203213	M. John Abhishek Paul
29	M. Keerthi	II BBA	20203221	M. Keerthi
30	K. Ravi	B BBA	20203215	K. Ravi

SNO	Name of the student	Class	Hall Tic No	Signature
31	E. Abhigna.	BBA II	20203208.	Abhigna
32	Md. Faizullah	BBA-II	20203220	Md. Faizullah
33	M. VAMSI	B.COM (CA)	20202266	M. Vamsi
34	P. Nageswara Rao	B.com(CA)	20202284	Nageswara Rao P.
35	R. Vara Prasad	BCom (CA)	20202282	R. Vara Prasad
36	B. Bindhu madhavi	B(com)CA	20202208	B. Bindhu madhavi
37	K. Leela chakradhar	B(COM)CA	20202256	K. L. chakradhar
38	K. Durga Rao	B(COM)CA	20202250	K. Durga Rao
39	P. Samuel	B(com) C.A	20202278	P. Samuel
40	K. Raju	B(Com)C.A	20202254	K. Raju
41	D. Janani Supraja	B.(Com)C.A	20202225	D. Janani Supraja
42	G. Naga Mani	B(Com) C.A	20202234	G. Naga Mani
43	P. Sanati	B.A (E.H.P) U/M	20101405	P. Sanati
44	Sk. ASMATHUNNISA	B.A[E.H.P]um	20101409	Sk. Asmathunnisa
45	K. MAHESH	B.A. EHP um	20101401	K. Mahesh

S NO	Name of the Student	Class	Hall TIC NO	Signature
46	SK. fathimunnisa	BA IInd EHP UM	20101410	SK. fathimunnisa
47	SK. Ruksana	BA IInd EHP UM	20101415	SK. Ruksana
48	Shaik Naari	BA 2nd EHP UM	20101414	SK. Naari
49	Shaik Munni	BA IInd EHP UM	20101412	SK Munni
50	Shaik. Jeenath	BA IInd EHP UM	20101417	SK
51	M. Sunny	BA EHP UM	20101404	M. Sunny
52	V. Sanjay Kumar	B.B.A IInd year	20203239	V. Sanjay Kumar
53	D. Koteswara Rao	B.B.A 2nd year	20203205	D. koteswarao
54	B. Harshivardhan	B.B.A 2nd year	20203204	B. Harshivardhan
55	K Jesu babu	B.B.A 2nd Year	20203213	K Jesu babu
56				
57				
58				
59				
60				

Thank you

S.R.R. & C.V.R. Government Degree College (A)

An Autonomous & ISO 9001: 2015 Certified Institution:: Ranked by NIRF in 101-150 band at NIRF-2020 & 151-200 band in NIRF 2019 NAAC accredited Institution with grade B+ with C.G.P.A 2.6 during March, 2017

Machavaram, Vijayawada, Krishna District, AP-520 004

SCHOOL TO LAB -28.2.2022

DEPARTMENT OF BOTANY

SRR & CVR Government Degree College

An Autonomous & ISO 9001: 2015 Certified Institution:: Ranked by NIRF in 101-150 band at NIRF-2020 & 151-200 band in NIRF 2019 NAAC accredited Institution with grade B+ with C.G.P.A 2.6 during March, 2017

Machavaram, Vijayawada, Krishna District, AP-520 004



DEPARTMENT OF BOTANY

Dates	**28.2.2022**
Conducted through (DRC/JKC/ELF/NCC/NSS/ Departments etc.	**Department**
Nature of activity (seminar/Workshop/Extn. Lecture etc.	**Extension activity**
Title of the Activity	**School to Lab**
Name of the Department/Committee	**Department of Botany**
Details of Resource Persons (Name , Designation etc.,)	**Department of Botany Faculty**
No of students participated	**250**
Name of the Lecturers who planned & conducted the activity	**Planned and Organized by** **Ms G.Swapna, Lecturer In Charge** **Mrs V.N.Padmavathi, Lecturer in Botany** **Dr Ch.Srinivasa Reddy, Lecturer in Botany** **Mrs I.Prasanthi, Lecturer in Botany**
Remarks	**This activity successfully conducted and reached its objectives**

Department of Botany SRR & CVR Govt DegreeCollege Organized School to Lab , an extension activity on National Science day.

Motive of this program:

- **To provide scientific exposure to school students**
- **To enhance subject matter and Develop scientific reasoning.**
- **For school students exploring college Laboratory experiences may enhance student understanding of specific scientific facts and concepts .**
- **Laboratory experiences may promote a school student's ability to identify questions and concepts that guide scientifically**
- **Cultivating interest in science and interest in learning science.**

Report of the activity :

SRR and CVR Govt Degree College Dept of Botany Organized National Science Day on 28.2.2022 . Faculty members contacted Government Schools namely "tamiri mallikarjuna rao chandramathi Nagara Palaka samstha unnatha patashala from Machavaram area and requested School Headmasters to send the school students to visit laboratories in our college to increase scientific awareness in students .

Head of the Institutions of Schools accepted the request and sent nearly 250 students of VIII, IX and X Class Students by 10.30 am to College.

Principal Madam Dr k.Bhagya Lakshmi Garu addressed the school students initially and explained to them about the Significance of National Science Day . She explained to them about the importance of Science, Discoveries and the Role of Science in Day to Day Human Life .

In this event various Science Departments like Botany , Zoology, Physics, Chemistry, Biochemistry Participated . Concerned Department incharges and Lecturers explained about their subject significance , Important scientific contributions , Scientists to High school students .

Later all 250 students from schools formed into batches class wise and visited all Department laboratories one by one accompanied by their teachers .



250 School students with their Teachers gathered at Auditorium



Principal Dr K. Bhagya Lakshmi Garu addressing the High school students on National Science Day " School to Lab" Program



Principal Dr K. Bhagya Lakshmi garu inaugurating the science exhibition at Botany Lab



High School students observing Plant Anatomy and Embryology Slides in the Botany Lab . They Observed all the Scientific Equipment in Botany Labs.

Department of Botany Faculty explained to the students about the working mechanism and significance of Laboratory equipment



Students in batches after visiting the Scientific Laboratories along with their teachers were asked to share their experiences . They Share their experiences on what they learnt and their overall experience on this Program. Teachers also gave their valuable feedback .

Principal and Various ScienceDepartments Faculty addressing the High school students



SRR & CVR Govt. Degree college, మాచవరం,
Dept. of Botany

28.02.2022.

జాతీయ సైన్స్ దినోత్సవాన్ని పురస్కరించుకొని

స్థానిక SRR & CVR ప్రభుత్వ కళాశాలలో

"పాఠశాల నుంచి ప్రయోగశాలకు" అనే కార్యక్రమం జరిగింది.

ఈ కార్యక్రమాన్ని కళాశాల ప్రిన్సిపల్ శ్రీమతి K. భాగ్యలక్ష్మి గారు వృక్ష శాస్త్ర విభాగంలో రిబ్బను కత్తిరించి ప్రారంభించి సైన్స్ దినోత్సవ ప్రాముఖ్యతను, ప్రేరణందిన జీవితంలో సైన్స్ పాత్రను సవివరంగా వివరించారు. ఈ కార్యక్రమంలో బోటనీ, జువాలజీ, ఫిజిక్స్, కెమిస్ట్రీ, బయోకెమిస్ట్రీ విభాగాలు పాల్గొన్నాయి. అయా ప్రయోగశాలల్లోని పరికరాలు, వాటి ప్రాముఖ్యతను కళాశాల విద్యార్థులు, అధ్యాపకులు పాఠశాల విద్యార్థులకు వివరించారు. తేమిరి మల్లిఖార్జునరావు శ్రీ-చంద్రమతి నగరపాలక సంస్థ ఉన్నత పాఠశాల, మాచవరం, విజయవాడకు చెందిన 8, 9 తరగతులకు చెందిన సుమారు 250 మంది విద్యార్థులు పాల్గొని ప్రయోగశాలలోని వివిధ పరికరాలను, నమూనాలను గురించి క్షుణ్ణంగా తెలుసుకున్నారు. ఈ కార్యక్రమంలో కళాశాల వైస్ ప్రిన్సిపల్ శ్రీమతి P. శైలజ, ఇతర విభాగాధిపతులు, అధ్యాపకులు పాల్గొన్నారు. కార్యక్రమం విజయవంతంగా ముగిసింది.

28.2.2022

PRINCIPAL
SRR & CVR GOVT. DEGREE COLLEGE
(Autonomus)
Machavaram, VIJAYAWADA - 520.004.

Department of Botany Faculty explained to the students about the working mechanism and significance of Laboratory equipment



Students in batches after visiting the Scientific Laboratories along with their teachers were asked to share their experiences . They Share their experiences on what they learnt and their overall experience on this Program. Teachers also gave their valuable feedback .

Principal and Various ScienceDepartments Faculty addressing the High school students



PRINCIPAL
SRR & CVR GOVT. DEGREE COLLEGE
(Autonomus)
Mecharvaram, VIJAYAWADA-520 004

LECTURER IN CHARGE
Dept. of Botany
SRR & CVR GOVT. DEGREE COLLEGE
VIJAYAWADA-4, Krishna Dist.

STUDENT SIGNATURES AND FEEDBACK

S.No	Date	Class	Roll no/ Reg no	Signature	Remarks
1.	28/2/22	8th class	2131	T. Mrudula Angel	Beneficiead
2.	28/2/22	7th class	2.	K. Mouli	useful
3	28/2	10th class	213172/2	P. Vijay	Good.
4	28/2/22	4th class	213172201	Prathamika	very useful
5	28/2/22	8th class		P. Siddhu	useful
6	28/2/22	8th class		G. Praveen	very useful
7	28/2/22	8th class		T. Gayatri	good
8	28/2/22	9th class		K. Sreathe	Benificiead
9	28/2/22	7th class		S. K. Sony	Very useful
10	28/2/22	10th class		P. Sanjay	Good
11	28/2/22	7th class		K. Rohit	Good
12	28/2/22	8th class		K. Ratood	satisfactory
13	28/2/22	9th class		M. Akhila	Very good
14	28/2/22	10th class		B. Poorna	useful
15	28/2/22	9th class		S. Sunitha	Good
16	28/2/22	10th class		V. Hasthagiri	Good

STUDENT SIGNATURES AND FEEDBACK

S.No	Date	Class	Roll no/ Reg no	Signature	Remarks
17	28/2/22	10th class		K. prathibha	useful
18	28/2/22	9th class		S. pavani	good
19	28/2/22	8th class		M. Divya.	Beneficial
20	28/2/22	7th class		L. Renuka	useful
21	28/2/22	7th class		P. Jaswitha	Good
22	28/2/22	10th class		G. Venkat	very useful
23	28/2/22	9th class		E. Tharun	Good
24	28/2/22	7th class		M. Ramesh	useful
25	28/2/22	10th class		K. Abhishek	Beneficial
26	28/2/22	9th class		L. Santhosh	very good
27	28/2/22	10th class		V. Ramya	Good
28	28/2/22	7th class		D. Bhanu	useful
29	28/2/22	8th class		S. Vishnu	Beneficial
30	28/2/22	9th class		K. Vandhana	good
31	28/2/22	8th class		K. Nandini	Very useful
32	28/2/22	9th class		K. Bhavani	useful

STUDENT SIGNATURES AND FEEDBACK

S.No	Date	Class	Roll no/ Reg no	Signature	Remarks
17.	28/2/22	7 class		S. Jayasudha	Good
18.	28/2/22	7 class		K. Divyamma	Very good
19.	28/2/22	7 class		K. Vallisri	Useful
20.	28/2/22	8 class		K. Radharani	Very helpful
21.	28/2/22	10 class		M. Ashajyothi	Satisfaction
22.	28/2/22	10 class		S.K. Reshma	Good
23.	28/2/22	10 class		P. Mrudula	Very Good
24.	28/2/22	9 class		G. Uday Kishan	Useful
25.	28/2/22	10 class		K. Sudheer	Very helpful
26.	28/2/22	9 class		S.K. Ayesha	Good
27.	28/2/22	7 class		M. Prashanthi	Very Useful
28.	28/2/22	8 class		K. Rameshbabu	Very helpful
29.	28/2/22	7 class		A. Rakesh	Good
30.	28/2/22	8 class		B. Rajkumar	Satisfied
31.	28/2/22	10 class		K. Hemanth	Useful
32.	28/2/22	10 class		Sk. Subani	Good

STUDENT SIGNATURES AND FEEDBACK

S.No	Date	Class	Roll no/ Reg no	Signature	Remarks
1	28/2/22	8 Class		S.K. Hafiza	Beneficial
2.	28/2/22	7 class		P. Jyothsna	Good
3	28/2/22	7 class		M. Krishnaveni	useful
4	28/2/22	8 class		N. Preethi	Good
5.	28/2/22	7 class		G. Adharsh	Beneficial
6.	28/2/22	9. class		S. Praveen	Not bad
7.	28/2/22	7. class		M. Thrisha	helpful
8.	28/2/22	10 class		K. Kiran	Very Good
9.	28/2/22	10 class		G. Sriia	Beneficial
10.	28/2/22	10 class		S. Siva	useFull
11.	28/2/22	9 class		M. Sujatha	Very Good
12.	28/2/22	8 class		K. Suneetha	Beneficial
13.	28/2/22	9 class		M. Jyothi	Good
14.	28/2/22	7. class		K. Balavathi	Beautiful
15.	28/2/22	8 class		R. Manjula	Very Good
16.	28/2/22	10 class		D. Baji	Good

SRR & CVR GOVERNMENT DEGREE COLLEGE (A)
MACHAVARAM, VIJAYAWADA, KRISHNA DISTRICT

Jawahar Knowledge Center
Creating Opportunities
Developing Skills | Unleashing Potential

JKC-Calligraphy Training Report

2021-2022

SRR & CVR GOVT. DEGREE COLLEGE
(AUTONOMOUS)
PHONE NO : 0866-2430080
FAX NO : 0866-2441092
NAAC : B+ (III CYCLE WITH CGPA : 2.60) - ESTD: 1937
WEBSITE : www.srrcvr.org
EMAIL : srrandcvr@gmail.com

SRR & CVR GOVERNMENT DEGREE COLLEGE (A)VIJAYAWADA: ANDHRA PRADESH

JKC-calligraphy training

2021-2022

Concept:

Handwriting is important and legible handwriting reflects clarity of mind. Students with neat and clear handwriting skills are fast learners and use learning opportunities around them and improve academically. Now, most employment situations will involve at least some handwriting and many require the communication of critical information (e.g. analysis, assessments, medical notes, prescriptions).

Quotes on Handwriting:

I saw that bad handwriting should be regarded as a sign of an imperfect education.

Mahatma Gandhi

Hand writing causes thinking - the repetition of writing your goal everyday willincrease your awareness. The true purpose of a goal is to help you grow.

Bob Proctor

Objectives:

To encourage students to write neatly
To develop clarity in expression and presentation skills
To help students understand the importance of written forms of communication

Focus areas:

Holding the Pencil Correctly. Teaching the correct posture
Handwriting exercises
Writing legibly. Focus on writing that can be read, to communicate a message tothe reader

Resource Persons:

1. Smt.Veerla Kanaka Durga

2.Smt.Kasibhotla Radha

Resolution 129 2.3.2022

The members of the IKC committee under the chairmanship of the Principal discussed and approved the follow agenda point related to calligraphy training to students.

Agenda:

1. Introduction of training in calligraphy to all students.

Discussed the importance of improving handwriting in students and welcomed the idea of professional trainers providing training to students free of cost.

Resolution :-

1) It is resolved to permit Limra Rural Development Society Regd No 84/2010 (Non Govt. Organization) to conduct free training in calligraphy to all students of this college in batches of 30hrs per batch with the help of two trainers Smt Veerla Kanak Durga and Kasibhotla Radha. from 2.3.2022 onwards.

2. Resolved to start the training for final year students first and continue the training for 2nd year and 1st year students.

3. Resolved to request the Limra Rural Development

Society to provide certificates to students after conducting exam at the end of the 30hr course.

4. The guidelines and expenditure details of certificates will be discussed with Limra in the next meeting.

JKC Chairman :-

JKC coordinator

PRINCIPAL
SRR & CVR GOVT. DEGREE COLLEGE
(Autonomus)
Machavaram, VIJAYAWADA - 520 004.
A. Rosalind
CO-ORDINATOR
JAWAHAR KNOWLEDGE CENTRE
S.R.R. & C.V.R. Govt. Degree College (A)
VIJAYAWADA-4.

JKC Committee:

1. Dr. D.Ch. Apparao.
Dept of Commerce
2/3/22

2. Sri Ajay Baby.
Dept of History.
2/3/22

3. Smt. Uma Lakshmi
Dept of Physics
2/3/22

4. Smt. Saevani
Dept of Computer Science
N. Saevani
2/03/2022

LIMRA

Rural Development Society
Regd No. : 84/2010
(Non Government Organization)

Chairman & CEO
Shaik Karimulla, M.A., B.Ed., Calligraper (Govt of India)
Cell : 8019292425, 9866025252

Address : D.No.12-17-10,
Prakash Nagar,Opp : Town Hall,
NARASARAOPET - 522 601.
Email : limrardos@gmail.com

Ref :

Date.....

Date: 02.03.2022.

To

The Principal,
SRR & CVR Govt. Degree College,
Karl Marx Road, Machavaram,
Vijayawada,
Andhra Pradesh – 522 004, India.

Sub: Request to accept our trainee person in your Calligraphy Training Centre – Reg.

Respected Sir,

I, Sk. Karimulla from the Calligraphy and Graphici Designing Trainining Center. I am pleased to accept my student for starting the caligraphy training with your college from date 02.03.2022.

Thank you for the opportunity for acccepting Calligraphy Training in our college. I am sending student **Veerla Kanaka Durga** to your college for giving the trainng. Please accept her as Calligraphy trainer in your college.

If thre is any future inforamton or paper work you need me to complete, please let me know and I will arrange it soon as spossible.

(SK. KARIMULLA)
Calligraphy and
Graphic Design Training Centre

CENTRE INCHARGE
N.C.P.U.L.'S
CALLIGRAPHY & GRAPHIC DESIGN
TRAINING CENTRE
Ministry of H.R.D. Govt. of India
Limra Rural Development Society
Narasaraopet - 522 601. A.P.

LIMRA

Rural Development Society
Regd No. : 84/2010
(Non Government Organization)

Chairman & CEO
Shaik Karimulla, M.A., B.Ed., Calligraper (Govt of India)
Cell : 8019292425, 9866025252

Address : D.No.12-17-10,
Prakash Nagar,Opp : Town Hall,
NARASARAOPET - 522 601.
Email : limrardos@gmail.com

Ref :

Date.....

Date: **02.03.2022**

Dear Veerla Kanaka Durga,

Sub: Appointment for the post of Trainee Calligrapher

Dear Veerla Kanaka Durga,

This letter is to advice you that the following Institute official has been appointment to serve as our Calligraphy trainer. We are pleased to offer you the position of Trainee Calligrapher with Calligraphy and training center on the following terms and conditions

Your employment will be effective, as of (02.03.2022)

Your job title will be Trainee Calligrapher and you will be reporting to Mrs. Bindu, Senior Calligrapher and to Head of the Institute Sk. Karimulla.

You will be posted at Vijayawada. You may however be required to work at any place of training which the company has, or may later acquire.

We congratulate you on your appointment and wish you a long career with us. We assure you have a great journey and get our full support for your professional growth and development Calligraphy and Graphic Designing Training Center.

Calligraphy and
Graphic Designing Training Center

CENTRE INCHARGE
N.C.P.U.I.'S
CALLIGRAPHY & GRAPHIC DESIGN
TRAINING CENTRE
Limra Rural Development Society
Narasaraopet - 522 601. A.P.

LIMRA

Rural Development Society
Regd No. : 84/2010
(Non Government Organization)

Chairman & CEO
Shaik Karimulla, M.A., B.Ed., Calligraper (Govt of India)
Cell : 8019292425, 9866025252

Address : D.No.12-17-10,
Prakash Nagar,Opp : Town Hall,
NARASARAOPET - 522 601.
Email : limrardos@gmail.com

Ref :

Date.....

Date: 02.03.2022.

To

The Principal,
SRR & CVR Govt. Degree College,
Karl Marx Road, Machavaram,
Vijayawada,
Andhra Pradesh – 522 004, India.

Sub: Request to accept our trainee person in your Calligraphy Training Centre – Reg.

Respected Sir,

I, Sk. Karimulla from the Calligraphy and Graphici Designing Trainining Center. I am pleased to accept my student for starting the caligraphy training with your college from date 02.03.2022.

Thank you for the opportunity for acccepting Calligraphy Training in our college. I am sending student **Kasibhotla Radha** to your college for giving the trainng. Please accept her as Calligraphy trainer in your college.

If thre is any future inforamton or paper work you need me to complete, please let me know and I will arrange it soon as spossible.

(SK. KARIMULLA)
Calligraphy and
Graphic Design Training Centre

CENTRE INCHARGE
N.C.P.U.L.'S
CALLIGRAPHY & GRAPHIC DESIGN
TRANING CENTRE
Ministry of H.R.D. Govt. of India
Limra Rural Development Society
Narasaraopet - 522 601. A.P.

LIMRA

Rural Development Society
Regd No. : 84/2010
(Non Government Organization)

Chairman & CEO
Shaik Karimulla, M.A., B.Ed., Calligraper (Govt of India)
Cell : 8019292425, 9866025252

Address : D.No.12-17-10,
Prakash Nagar,Opp : Town Hall,
NARASARAOPET - 522 601.
Email : limrardos@gmail.com

Ref :

Date.....

Date: **02.03.20-22**

Dear Kasibhotla Radha,

Sub: Appointment for the post of Trainee Calligrapher

Dear Kasibhotla Radha,

This letter is to advice you that the following Institute official has been appointment to serve as our Calligraphy trainer. We are pleased to offer you the position of Trainee Calligrapher with Calligraphy and training center on the following terms and conditions

Your employment will be effective, as of (02.03.2022)

Your job title will be Trainee Calligrapher and you will be reporting to Mrs. Bindu, Senior Calligrapher and to Head of the Institute Sk. Karimulla.

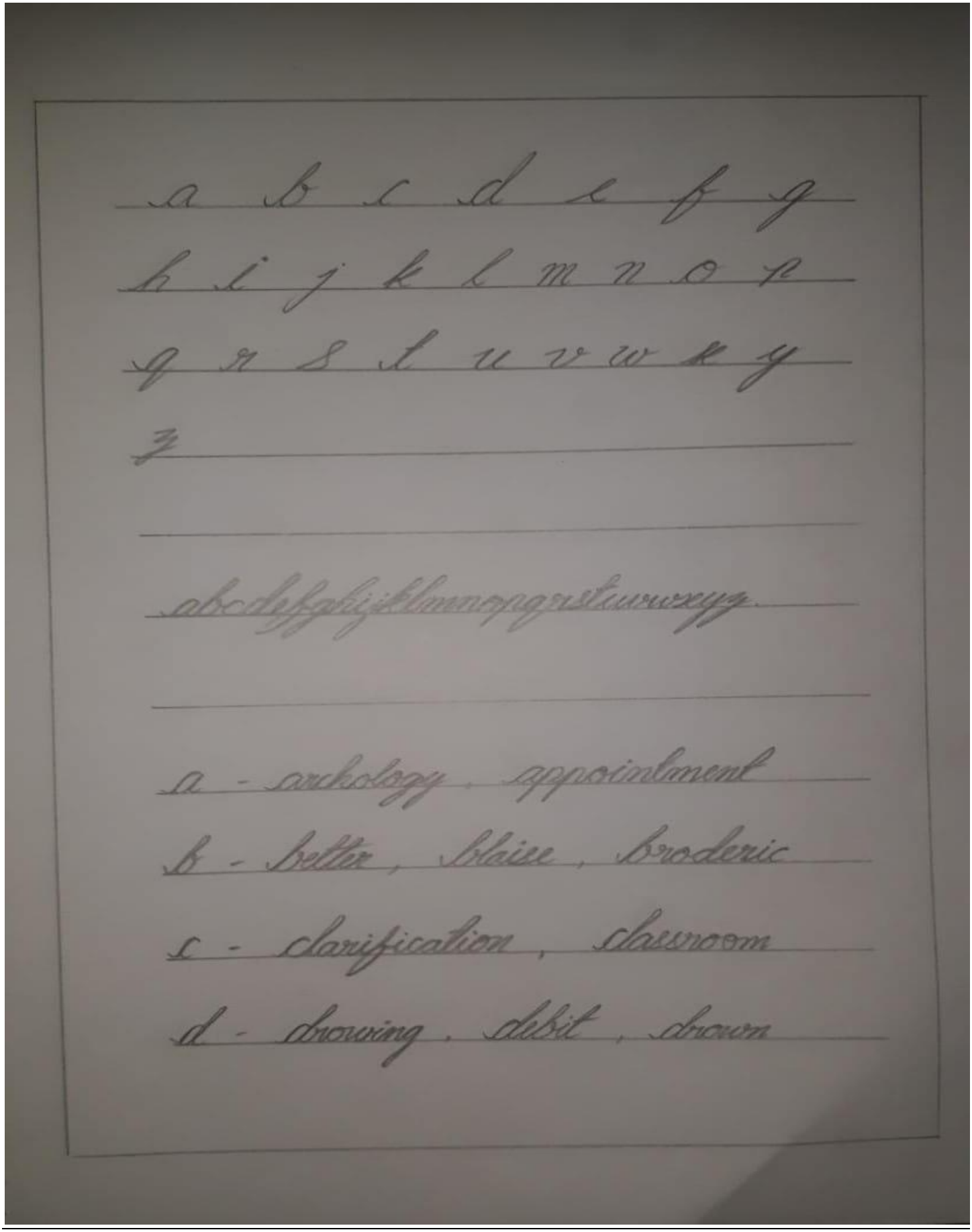
You will be posted at Vijayawada. You may however be required to work at any place of training which the company has, or may later acquire.

We congratulate you on your appointment and wish you a long career with us. We assure you have a great journey and get our full support for your professional growth and development Calligraphy and Graphic Designing Training Center.

Calligraphy and
Graphic Designing Training Center

CENTRE INCHARGE
N.C.P.U.L.'S
CALLIGRAPHY & GRAPHIC DESIGN
TRAINING CENTRE
Ministry of H.R.D. Dept of S.E. Govt of India
Limra Rural Development Society
Narasaraopet - 522 601. A.P.

Syllabus:


a b c d e f g
h i j k l m n o p
q r s t u v w x y
z
abcdefghijklmnopqrstuvwxyz.
a - archology, appointment
b - better, blaise, broderic
c - clarification, classroom
d - drowning, debit, drown

e - effective, ethos, establishment

f - frances, flamingo, flash

g - grow, glamour, grammer

h - habit, happy, horse

i - imagine, illustrate, india

j - jack, jackson, jocker

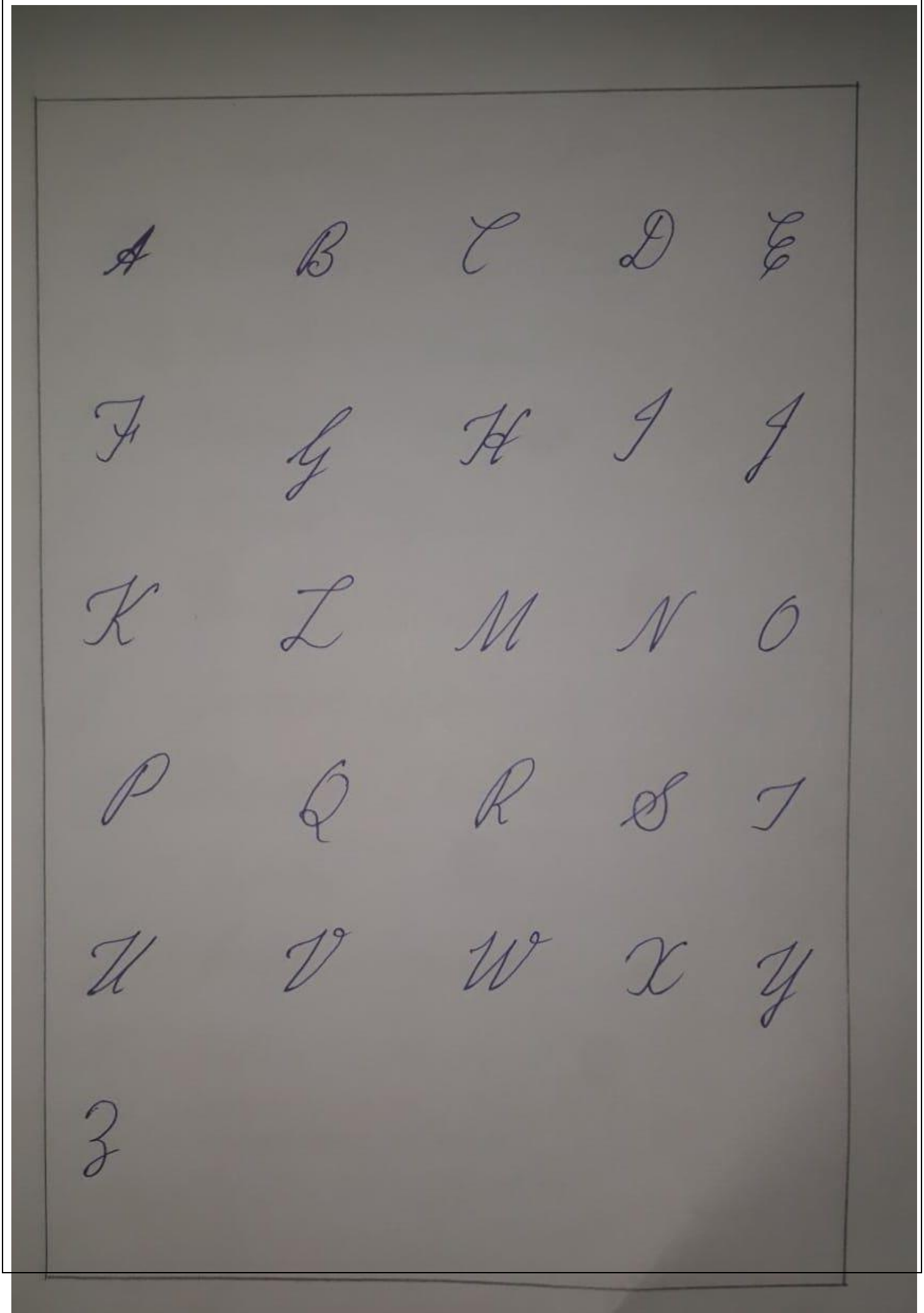
k - killing, kilometer, koria

l - loyality, liberity, listern

m - medium, mango, media

n - narrative, narrow, net

o - openiness, orange, operate


A B C D E
F G H I J
K L M N O
P Q R S T
U V W X Y
Z

A - Anesthesia , Alphabet

B - Bonemarrow , Buccal-Cavity

C - Clavicle , Camphore

D - Diclofinac , Doctorate

E - Elegant , Enema

F - Fevastin , Ferric

G - Germophobia , Global

H - Harmones , Homocide

I - Intestine , Iliac

J - Jersey , Jaundice

K - Ketones , Keyboard

L - Lymphona , Lungs

M - Malaria , Meningitis

N - Norovirus , Neonates

O - Organs , Origami

P - Psychosis , Psychology

Q - Quadriceps , Quantum

R - Romatic-fever , Romania

S - Schezophrenia , Stomach

T - Tumour , Tuberculosis

U - Urology , Ulcer

V - Venom , Vericosis

W - Wills disease , Women

X - Xanthoma , Xaviar

Y - Yolksack , Yack

Z - Zomato , Zerodol

Cognitive Behavioral Therapy is a form of talking therapy which can be used to treat people with a wide range of mental health problems. CBT is based on idea that how we think (Cognition), how we feel (Emotions) and how we act (Behavior) all interact together. Aims to help people become aware of when they make negative interpretations, and of behaviors which reinforce the distorted the thinking. CBT helps people to develop alternate ways of thinking and behaving which aim to reduce their psychological distress. Two of the earliest forms of Cognitive Behavioral Therapy were "REBT" and Cognitive Therapy.

SRR AND CVR Government Degree College(A), Vijayawada

Central Inst. For calligraphy and Graphic Design

01	Company		Registered	Completed
	Central Inst. For calligraphy and Graphic Design	calligraphy	All Final years	60

B.Sc MPCS Students

S No	Student Name	Roll No	Course
1	Ampolu Lavanya	19302209	3rd B.Sc(MPCS)
2	Kaza Rajeswari	19302250	3rd B.Sc(MPCS)
3	M. Pushpa Latha	19302264	3rd B.Sc(MPCS)
4	M.Sweety	19302208	3rd B.Sc(MPCS)
5	B. Hema Latha	19302273	3rd B.Sc(MPCS)
6	N.PremChand	19302234	3rd B.Sc(MPCS)
7	Dubbaku Keerthi	19302240	3rd B.Sc(MPCS)
8	D. Krishna Veni	19302222	3rd B.Sc(MPCS)
9	MD. Shahin	19302242	3rd B.Sc(MPCS)

BA EPJ Students

S No	Student Name	Roll No	Course
1	K Sai Ramya	19103205	3rd BA (EPJ)
2	N.S.S.R Krishna	19103242	3rd BA (EPJ)
3	Kolli Pujitha	19103225	3rd BA (EPJ)
4	A.Magadevi	19103203	3rd BA (EPJ)
5	S.Sujatha	19103211	3rd BA (EPJ)
6	Shaik. Sharmi	19103240	3rd BA (EPJ)
7	J.Vijay Madhuri	19103238	3rd BA (EPJ)
8	Rentala Ajay kumar	19103230	3rd BA (EPJ)
9	Gampa Hema Latha	19103204	3rd BA (EPJ)
10	Namagiri Bhanu	19103207	3rd BA (EPJ)
11	Y.S.P Akhilandeswari	19103223	3rd BA (EPJ)
12	T N Vasantha	19103202	3rd BA (EPJ)
13	T Renu Sri	19103218	3rd BA (EPJ)
14	G Siva	19103208	3rd BA (EPJ)
15	Y Ejhwarvyas	19103243	3rd BA (EPJ)
16	E Ruthu	19103212	3rd BA (EPJ)
17	P Sravya	19103201	3rd BA (EPJ)
18	P Suguna	19103213	3rd BA (EPJ)
19	T.V.P Sai kishore	19103222	3rd BA (EPJ)

B.com CA Section A

S No	Student Name	Roll No	Course
1	M Naga Haritha	19202241	3rd B.com CA
2	K Anitha	19202209	3rd B.com CA
3	Md. Haseena	19202225	3rd B.com CA
4	P Leela Ratna Mani	19202230	3rd B.com CA
5	Katta Jagadish	19202229	3rd B.com CA
6	K suguna	19202254	3rd B.com CA
7	Shaik Iliyaz	19202251	3rd B.com CA
8	K Srinivasa rao	19202232	3rd B.com CA
9	P Durga Bhavani	19202226	3rd B.com CA
10	R Lokesh	19202239	3rd B.com CA
11	L Rakesh		3rd B.com CA
12	K Raghu Nadh	19202238	3rd B.com CA
13	P Ramya	19202205	3rd B.com CA
14	Gampa Srinu	19202217	3rd B.com CA
15	K Hema Bhargavi	19202234	3rd B.com CA
16	D Venkatesh	19202220	3rd B.com CA
17	L Ajay krishna	19202228	3rd B.com CA
18	T Lokesh Reddy	19202213	3rd B.com CA
19	Dasari Yaswanth Paul	19202221	3rd B.com CA
20	R Sirisha	19202249	3rd B.com CA
21	U Sravani	19202224	3rd B.com CA
22	SK Baji	19202231	3rd B.com CA
23	P Adilakshmi	19202201	3rd B.com CA
24	V Sruthi	19202237	3rd B.com CA
25	D Harileela	19202248	3rd B.com CA

B.com CA Section B

S No	Student Name	Roll No	Course
1	Jyothirmai	19202312	3rd B.com CA
2	P Prem Sagar	19202307	3rd B.com CA
3	Ch Eswari	19202308	3rd B.com CA
4	P Rama Krishna	19202288	3rd B.com CA
5	Rajeswari	19202327	3rd B.com CA
6	K Manasa	19202315	3rd B.com CA
7	V Krupa Indu	19202285	3rd B.com CA
8	Sayyad Habiba	19202282	3rd B.com CA

Attendance:

S.R.R. & C.V.R. GOVT. DEGREE COLLEGE, Vijayawada

III B.A (EPJ) Spl Eng

Month : March - 2024

S.No.	Name of the Student	1	2	3	4	5	6	7	8	9	10	11	12
1.	T. Vasantha.	x	x	x	x	x	SUNDAY	x	WOMENS DAY CELEBRATIONS	x	x	x	SATURDAY
2.	A. Mahadevi.	x	x	x	x	x		x		x	x	x	
3.	G. Hemalatha.	x	a	x	x	x		x		x	x	a	
4.	K. Ramya.	x	x	x	x	a		a		x	x	x	
5.	N. Bhanu.	x	x	x	x	x		x		x	x	x	
6.	G. Siva.	a	x	x	x	x		a		x	x	x	
7.	S. Sujatha.	x	x	x	x	x		x		x	x	x	
8.	E. Ruthu.	a	x	a	x	x		x		x	x	a	
9.	T. Renu Sri	x	x	x	x	x		x		x	x	x	
10.	T. Kishore.	x	x	x	x	x		x		x	x	x	
11.	Y Akhila.	x	x	x	a	x		x		x	x	x	
12.	K. Pujitha.	x	a	x	x	a		x		x	x	x	
13.	R. Ajay Kumar.	x	x	x	x	x		x		x	x	x	
14.	J. V. Madhuri	x	x	x	x	x		x		x	x	x	
15.	SK. Sharmi	x	x	x	x	x		x		x	x	x	
16.	N. Sai Siva Rama Krishna.	x	x	a	x	x		x		x	x	x	
17.	Y. Eshwar Vyas.	x	x	x	x	x		x		x	x	x	
	IV B.Sc (MPCs)												
18.	M. Sweety.	x	x	x	x	x		x		x	x	x	
19.	A. Lavanya.	x	x	a	x	x		x		x	x	x	
20.	D. Krishnaveni.	x	x	x	x	x		x		x	x	x	
21.	N. Premachend.	x	x	x	a	x		x		x	x	a	
22.	D. Keerthi.	x	x	x	x	x		x		x	x	x	
23.	Md. Shahin.	x	x	x	x	x		x		x	x	x	
24.	K. Rajeswari	a	x	x	x	x		x		x	x	x	
25.	M. Pushpa Latha.	x	x	a	x	x		x		x	x	x	
26.	B. Hemalatha.	x	x	x	x	x		x		x	x	x	
27.	K. S. Bhavitha.	x	x	x	x	a		x		x	x	x	

S.R.R. & C.V.R. GOVT. DEGREE COLLEGE, Vijayawada

Month :

13	14	15	16	17	18	19	20	21	22	23	24	25	26	27	28	29	30	31	Remarks
		X	a	X		X		X	X	X	X	X	X		X	X	a	X	
		X	X	X		X		X	X	X	X	X	X		X	X	X	X	
		X	X	X		X		X	X	X	X	X	X		X	X	X	a	
		X	X	X		a		X	X	X	X	X	X		X	X	X	X	
		X	X	X		X		X	X	X	X	X	X		X	X	X	X	
		X	X	X		X		X	X	X	X	a	X		X	X	X	X	
		X	X	X		X		X	X	X	X	X	X		X	X	X	a	
		X	X	X		a		X	a	X	X	X	X		X	X	X	X	
	G.	X	X	X		X		X	X	X	X	X	X		X	X	X	X	
	ETHN	X	X	X		X		X	X	X	X	X	X		X	X	X	X	
SUNDAY	M	a	X	X		X		X	X	X	X	X	X		X	X	X	X	
		X	X	X		X		X	X	X	X	X	X		X	X	X	X	
		X	X	X		X		X	X	X	X	X	X		X	X	X	X	
		X	a	X		X		X	X	X	X	X	X		X	X	X	X	
SU		X	X	X	HOLI	X	SUNDA	X	X	X	X	X	X	SUNDA	X	X	X	X	
		X	X	X		X		X	X	X	X	X	X		X	X	X	X	
	GUNTUR																		
		X	X	X		X		X	X	X	X	X	X		X	X	X	X	
		X	X	X		X		X	X	X	X	X	X		X	X	X	X	
		a	X	X		X		X	X	X	X	X	X		X	X	X	X	
		X	X	X		X		X	X	X	X	X	X		X	X	X	X	
		X	a	X		X		X	X	X	X	X	X		X	X	X	X	
		X	X	X		X		X	X	X	X	X	X		X	X	a	X	
		X	X	X		X		X	X	X	X	a	X		X	X	X	X	
		X	X	X		X		X	X	X	X	X	X		X	X	X	X	
		X	X	X		X		X	X	X	X	X	X		X	X	X	X	
		X	X	X		X		X	X	X	X	X	X		X	X	X	X	

S.R.R. & C.V.R. GOVT. DEGREE COLLEGE, Vijayawada

III B.Com (A & B Sec.) Month : March-2022

S.No.	Name of the Student	1	2	3	4	5	6	7	8	9	10	11	12	13
28.	K. Raghunadh.	x	x	a	x	x		x		x	x	a		
29.	K. Srinivas.	x	x	x	x	x		x		x	x	x		
30.	D. Venkatesh	x	x	x	x	x		x		x	a	x		
31.	SK. Iliyaz	a	x	x	x	x		x		x	x	x		
32.	L. Rakesh.	x	x	x	x	a		x		x	x	x		
33.	SK. Baji.	x	x	x	x	x		x		x	x	x		
34.	L. Ajay Krishna.	x	x	x	a	x		x		x	x	x		
35.	D. Yaswanth.	x	x	x	x	x		x		x	x	x		
36.	K. Hema Bhargavi.	x	x	x	x	x		x		x	x	x		
37.	K. Anitha.	x	a	x	x	x		x		a	x	x		
38.	P. Adi Lakshmi.	x	x	x	x	a		x		x	x	x		
39.	Lokesh.	a	x	x	x	x		x		x	x	x		
40.	P. Leela Ratna Mani.	x	x	x	x	x		x		x	x	x		
41.	P. Durga Bhavani.	x	x	a	x	x		x		a	x	x		
42.	V. Sruthi.	x	x	x	x	x		x		x	x	x		
43.	U. Sravani.	x	x	x	x	x		x		x	x	x		
44.	M. Naga Haritha.	x	x	x	x	x		x		x	x	x		
45.	D. Hari Leela.	x	a	x	x	x		x		x	a	x		
46.	K. Jagadish.	x	x	x	x	x		x		x	x	x		
47.	P. Ramya.	x	x	x	x	x		x		x	x	x		
48.	R. Sirisha.	x	x	x	x	x		x		x	x	x		
49.	G. Srinu.	x	x	x	a	x		x		x	x	x		
50	K. Suguna.	x	x	x	x	x		a		x	x	x		
51.	Haseena.	x	x	x	x	x		x		x	x	x		
52.	R. Lokesh.	x	x	x	x	x		x		x	x	x		
53.	B. Rajeswari.	x	x	x	x	x		x		x	x	x		
54.	Sd. Habiba.	x	a	x	x	x		x		x	x	x		
55.	Ch. Eswari	x	x	x	x	x		a		x	x	x		
56.	J. Jyothirmai.	x	x	x	x	x		x		x	x	a		

SUNDAY CELEBRATIONS

WOMENS DAY CELEBRATIONS

S.R.R. & C.V.R. GOVT. DEGREE COLLEGE, Vijayawada

Month :

13	14	15	16	17	18	19	20	21	22	23	24	25	26	27	28	29	30	31	Remarks
		x	x	x		x		x	x	x	x	x	x		x	x	x	x	
		x	x	x		a		x	x	x	x	a	x		x	x	a	x	
		x	x	x		x		x	x	x	x	x	x		x	x	x	x	
		a	x	x		x		x	x	x	x	x	x		x	x	x	x	
		x	x	x		x		x	x	x	x	x	x		x	x	a	x	
		x	x	x		x		x	x	a	x	x	x		x	x	x	x	
		x	x	x		x		x	x	x	x	x	x		x	a	x	x	
G.		x	x	x		x		a	x	x	x	x	x		x	x	x	x	
N		x	x	x		x		x	x	x	x	x	x		x	x	x	x	
E T		x	x	x		x		x	x	x	x	x	x		a	x	x	x	
M		x	x	x		a		x	x	x	x	x	x		x	x	x	x	
A Y		x	x	x		x		x	x	x	x	x	x		a	x	x	x	
D		x	x	x	T	x		x	x	x	x	x	x		x	x	x	x	
N A		x	x	x	L	x		x	x	x	x	x	x		x	x	a	x	
U S		a	x	x	O	x		x	x	x	x	x	x		x	x	x	x	
R		x	x	x	H	x		x	x	x	a	x	x		x	a	x	x	
U		x	x	x		x		x	x	x	x	x	a		x	x	x	x	
T		x	x	x		x		x	x	x	x	x	x		a	x	x	x	
N		x	x	x		x		x	x	x	x	x	x		x	x	x	x	
U		x	x	x		x		x	x	x	x	x	x		x	x	x	x	
G		x	x	x		x		a	x	x	x	x	x		x	a	x	x	
		x	x	x		x		x	x	x	x	x	x		x	x	x	x	
		x	x	x		x		x	x	x	x	x	x		x	x	x	x	
		x	x	x		x		x	a	x	x	x	x		x	x	x	x	
		x	a	x		x		x	x	x	x	x	x		a	x	x	x	
		x	x	x		x		x	x	a	x	x	x		x	x	x	x	
		x	x	x		x		x	x	x	x	x	x		x	x	x	a	
		x	x	x		x		x	x	x	x	x	x		x	x	x	x	
		x	x	x		x		x	x	x	x	x	x		x	x	x	x	

S.R.R. & C.V.R. GOVT. DEGREE COLLEGE, Vijayawada

Month : March -2022

S.No.	Name of the Student	1	2	3	4	5	6	7	8	9	10	11	12
57.	V. Indhu.	x	x	x	x	a	SUNDAY	x	WOMENSDAYCELEBRATIONS	x	x	x	SECOND SATURDAY
58.	K. Manasa.	x	x	x	x	x		x		x	x	x	
59.	P. Prem Sagar.	a	x	x	x	x		x		x	x	x	
60.	P. Rama Krishna	a	x	x	x	x		x		x	x	x	

S.R.R. & C.V.R. GOVT. DEGREE COLLEGE, Vijayawada

Month : April - 2022

II B.A (EPJ) Spl Eng.

S.No.	Name of the Student	1	2	3	4	5	6	7	8	9	10	11	12	13
1.	T. Vasantha.	x			x	x	x	x	x	x		x		x
2.	A. Mahadevi.	x			x	x	x	x	x	x		x		x
3.	G. Hemalatha.	x			x	a	x	x	x	x		x		x
4.	K. Ramya.	x			x	x	x	x	x	x		x		x
5.	N. Bhanu.	x			x	x	x	x	x	x		x		x
6.	G. Siva.	x			a	x	x	x	x	x		x		x
7.	S. Sujatha.	x			x	x	x	x	x	a		x		x
8.	E. Ruthu.	a			x	x	x	x	x	x		x		x
9.	T. Renu Sri.	x			x	x	x	x	x	x		x		x
10.	T. Kishore.	x			a	x	x	x	x	x		x		x
11.	Y. Akhila.	x			x	x	x	x	x	x		x		
12.	K. Pujitha.	x			x	x	x	x	x	x		x	a	
13.	R. Ajay Kumar.	x			x	x	x	a	x	x		x		
14.	J.V. Madhuri.	x			x	x	x	x	x	x		x		
15.	Sk. Sharmi.	x			x	x	x	x	x	x		x		
16.	N. Sai Siva Rama Krishna.	x			x	x	x	x	x	x		x		
17.	Y. Eshwar Vyas.	x			x	x	x	x	x	x		x		

II B.Sc (MPCs)

18.	M. Sweety.	x			x	x	x	x	x	x		a	x	
19.	A. Lavanya.	x			x	x	x	x	x	x		x		
20.	D. Krishnaveni.	x			x	x	a	x	x	x		x	a	
21.	N. Premachend	x			x	x	x	a	x	x		x		
22.	D. Keerthi.	x			a	x	x	x	x	a		x		
23.	Md. Shahin.	x			x	a	x	x	x	x		x		
24.	K. Rajeswari.	x			x	x	x	x	x	x		x		
25.	M. Pushpa Latha.	x			x	x	x	x	x	x		x		
26.	B. Hemalatha.	x			x	x	x	x	x	x		x		
27.	S. Bhavitha.	x			x	a	x	x	x	x		x		

S.R.R. & C.V.R. GOVT. DEGREE COLLEGE, Vijayawada

Month :

13	14	15	16	17	18	19	20	21	22	23	24	25	26	27	28	29	30	31	Remarks
x					x	x	x	a	x	x		x	x	x	x	x	x		
x					x	x	x	x	x	x		x	x	a	x	x	x		
x					x	x	x	x	x	x		x	x	x	a	x	x		
x					x	x	x	x	a	x		x	x	x	x	x	x		
x					x	x	x	x	x	x		x	x	x	x	x	x		
x					x	x	x	x	x	x		x	x	x	x	x	x		
x					x	x	x	x	x	x		x	x	x	x	x	x		
x					x	x	x	x	x	x		x	x	x	x	x	x		
x					x	x	x	x	x	x		x	x	x	x	x	x		
x					a	x	x	x	x	x		x	x	x	x	x	x		
x					x	x	x	x	x	x		x	x	x	x	x	x		
x					x	x	x	x	x	x		x	a	x	x	x	x		
x					x	x	a	x	x	x		x	x	x	x	x	x		
x					x	x	x	x	x	x		x	x	x	x	x	a		
x					x	x	x	x	x	x		x	x	x	x	x	x		
x					x	x	x	x	x	x		x	x	x	x	x	x		
x					x	a	x	x	x	x		x	a	x	x	x	x		
x					x	x	x	x	x	x		x	x	a	x	x	x		
x					x	x	x	x	x	x		x	x	x	x	x	x		
x					x	x	x	x	a	x		x	x	x	x	x	x		
x					x	x	x	x	x	x		x	x	x	x	x	x		
x					x	x	x	x	x	x		x	x	x	x	x	x		
x					x	x	x	x	x	x		x	x	x	x	a	x		
x					x	x	x	x	x	x		x	x	x	x	x	x		
x					x	x	x	x	x	x		x	x	x	x	x	x		
x					x	x	x	a	x	x		x	x	x	x	x	x		

AMBEDKAR JAYANTHI
GOOD FRIDAY
OPTIONAL HOLIDAY
SUNDAY
SUNDAY

S.R.R. & C.V.R. GOVT. DEGREE COLLEGE, Vijayawada

(II) B.Com (A x B Sec)

Month : April-2022

S.No.	Name of the Student	1	2	3	4	5	6	7	8	9	10	11	12
28.	K. Raghunadh.	a	SUNDAY	SUNDAY	x	x	x	x	x	x	SUNDAY	x	x
29.	K. Srinivas.	x			x	x	x	x	x	x		x	x
30.	D. Venkatesh.	x			x	x	a	x	x	x		x	x
31.	SK. Iliyaz	x			x	x	x	a	x	x		x	x
32.	L. Rakesh.	x			x	a	x	x	x	x		x	x
33.	Sk. Baji	x			x	x	x	x	x	x		x	x
34.	L. Ajay Krishna.	x			x	x	x	x	x	x		x	x
35.	D. Yaswanth.	x			x	x	x	x	a	x		x	x
36.	K. Hema Bhargavi.	x			x	x	x	x	x	x		x	x
37.	K. Anitha.	x			x	x	x	x	x	x		x	x
38.	P. Adi Lakshmi.	x			x	x	x	x	x	x		x	x
39.	. Lokesh.	x			x	x	x	x	x	x		x	x
40.	P. Leela Ratna Mani.	x			x	x	x	x	x	x		x	x
41.	P. Durga Bhavani.	x			x	x	x	x	x	x		x	x
42.	V. Sruthi.	x			x	x	x	x	x	x		x	x
43.	U. Sravani.	x			x	x	x	x	x	x		x	x
44.	M. Naga Havitha.	x			x	x	x	x	a	x		x	x
45.	D. Hari Leela.	x			x	x	x	x	x	x		x	x
46.	K. Jagadish.	x			x	x	x	x	a	x		x	x
47.	P. Ramya.	x			x	x	x	x	x	x		x	x
48.	R. Sirisha.	x			x	x	x	x	x	x		x	a
49.	G. Srinu.	x			x	x	x	x	x	x		x	x
50.	K. Suguna.	x			x	x	x	x	x	x		x	x
51.	. Haseena.	x			x	x	x	x	x	x		x	x
52.	R. Lokesh.	x			x	x	x	x	x	x		x	x
53.	B. Rajeswari	x			x	x	x	x	x	x		a	x
54.	Sd. Habiba.	x			x	x	x	x	x	x		x	a
55.	Ch. Eswari.	x			x	x	x	x	x	x		x	x
56.	J. Jyothirmai.	x			x	x	x	x	x	a		x	x

S.R.R. & C.V.R. GOVT. DEGREE COLLEGE, Vijayawada

Month :

13	14	15	16	17	18	19	20	21	22	23	24	25	26	27	28	29	30	31	Remarks
x					x	a	x	x	x	x		a	x	x	x	x	a		
x					x	x	a	x	x	x		x	x	x	x	a	x		
x					x	x	x	x	x	x		x	a	x	x	x	x		
x					x	a	x	x	x	a		x	x	x	x	x	x		
x					a	x	x	x	x	x		x	x	x	x	x	x		
x					x	x	x	x	x	x		x	x	a	x	x	x		
x					x	x	x	x	x	x		x	x	x	x	a	x		
x					x	x	x	x	x	x		x	x	x	x	x	a		
x					x	x	x	x	x	x		x	x	x	x	x	x		
x					x	a	x	x	x	x		a	x	x	x	x	x		
x					x	x	x	x	x	x		x	x	x	x	x	x		
x					x	x	x	x	x	x		x	x	x	x	x	x		
x					a	x	x	x	x	a		x	x	x	x	x	x		
x					x	x	x	x	x	x

S.R.R. & C.V.R. GOVT. DEGREE COLLEGE, Vijayawada

Month : ఆగస్టు -20

S.No.	Name of the Student	1	2	3	4	5	6	7	8	9	10	11	12
57.	V. Indhu.	x			x	x	x	x	x	x		x	x
58.	K. Manasa.	x			x	a	x	x	x	x		x	x
59.	P. Prem Sagar.	x			x	x	x	x	a	x		x	x
60.	P. Rama Krishna.	x			x	x	x	x	x	x		x	a

UGADI
SUNDAY

SUNDAY

S.R.R. & C.V.R. GOVT. DEGREE COLLEGE, Vijayawada

Month :

13	14	15	16	17	18	19	20	21	22	23	24	25	26	27	28	29	30	31	Remarks
x					x	x	x	x	x	x		x	x	x	x	x	a		
x					x	x	x	x	x	x		x	x	a	x	x	x		
x					x	x	x	x	a	x		x	a	x	x	a	x		
a					x	x	x	x	x	x		x	x	x	x	x	a		

— AMBEDKAR JAYANTHI
— GOOD FRIDAY
— OPTIONAL HOLIDAY
— SUNDAY
— SUNDAY.

Exam

DATE: 23-06-2022 TELUGU K. Jagadish.
FATHER NAME: Kotaiah. katta Calligraphy. III rd B.Com (A)
A SECTION
Exam HALL TICKET NO: 19202229

ఉపాంత ప్రతిస్థాపన రేటును అనే నిర్వచించుము ధర
సూత్రం యొక్క పాముఖ్యతను విశ్లేషించుము క్షీణ
పాముఖ్యతను విశ్లేషించుము వింత తరహానునుసరించి పై
అంతర్గత ఆదాలకు గల కారణాలను పరిశీలించుము
వివరించుము ప్రక్రతి పరంగా ఉచితంగా సప్లై ధర
లేనపుడు వస్తువులు ఉచిత పైవన్నియు సాధరణం
విషయంలో మరియు వస్తువు డిమాండ్ మధ్య ధర
పై సంబంధం ఉంటుంది ధనాత్మక రుణాత్మక పై
రెండు వేవి కావు ప్రక్రతి పరంగా ఉచితంగా వేవి
చేయుబడి ధర లేనటువంటి క్రింది విధంగా అంటారు
ప్రైవేటు ధర ఉచిత వస్తువులు సాధారణ వస్తువు
డిమాండ్ పరిమాణం ఏ మధ్య రేఖ యొక్క
యాలు మూలానికి పూటాకారంగా ఉంటుంది
అక్షానికి సమాంతరంగా ఉంటుంది లంబంగా పై
ఉంటుంది తరహానునుసరించిన ఈ అనుబంధాలం.

K.Anitha B.com(CA)-ASection 19202209

There was a village near a jungle. Village cows used to go upto the the jungle in Search of food. In the forest there lived a wicked lion. He used to kill a crow in now and then and her. This was happening for quite Sometime The cows were frightened. One day all the cows held a meeting. In An old cow said. "Listen every body the lion eats one of us only because go into jungle our seperately, from now on we all together. All chased him away.

Hall Ticket NO:- 19202241

M. Naga Haritha
B.com III year (C.A)

(A-2)

When I had the pleasure of my
One never can find one to comprae us
With mother for true loving and caring.
Mother is only personally who love and
Care to her childs without a single or
Hidden personal intention. A child is a
Actual property for a mother. She teach
Us unigue methods of life to pass if
Through hard time. She bar heard for us.
She bear with us and listen us where as
We say good or bad. She don't make any
Boundaries to restrict us but she always
Teach in soft and sweat manner. Her
Motivations are enough for us to make
Different good and bad things.

D. Harileela B.Com(CA) 'A' Section 19202248

A lion was once sleeping in the jungle when a mouse started running upon and down his body just for fun. The disturbed the lion's sleep, and on he woke up quite angry. He was about to eat the mouse when the mouse desperately requested the lion to set him free. "I promice you, an I will be of great help to you someday if you save me." The lion laughed at the mouse's confidence and let him go. One day, a few hun-ters came into the forest and is took the lion with them. They tied him up against a tree. The lion was struggling to get out and started.

23/06/22 Calligraphy exam (A-Sec)

R. Sirisha.
19202249.
B.Com (CA) III rd year

Ability of an Organisation to prosper arises for its competitive advantage over the other Organisation operating its market sector.

The ability of the Organisation to be survive requires that is competitive is position is not significantly less than to the other firms operatings the market sector. Cost leadership is simple to be able to sell the goods or provide the it service at a price that is lower than to that of the competing products even by though the competition may have a some lower price. Information and communication technologies can have a considerable part to paly in competative strategy. ability.

Date: 22-6-2022

Calligraphy exam

Shaik Sleya
III^rd BCom Computers (A section)
172022251

Decides grain of wheat in the express the idea that, before a seed can grow into a new plant, It must first day out and sacrifice its own life. Grains uses flashbacks throught the novel's present event. In the beginning the kenyans welcomed the British but they became suspicious when they saw how much of their land was being taken from then and started registered them leading to kenyan independence. Thomson drops at the party represents kenya

Date: 22-6-2022

Calligraphy exam

Shaik Shyaz
III^rd B.Com.Computers (A section)
172022251

Decides grain of wheat in the express the idea that, before a seed can grow into a new plant, It must first day out and sacrifice its own life. Grains uses flashbacks throught the novel's present event. In the beginning the kenyans welcomed the British but they became suspucious when they saw how much of their land was being taken from them and started registered them leading to kenyan independence. Thomson drops at the party represents kenya

S. Bhavitha
30/6/22

CALLIGRAPHY EXAM

1930225g
IIIrd B.Sc - MPCs

Nature is the creation of natural material and physical world on earth independent of human of activity. The beauty and richness is of nature is diverse and massive. Nature provides us with several and delicacies to enjoy and is our life is support system. Our basic needs like food, shelter, water and air are of the gifts from nature. Humans have a strong connection and interrelation with nature. Escaping away in the best nature heals the mind and body and soothes our soul and mind.

S. Bhavitha 19302259
30/6/22 III rd B.Sc - MPCs

CALLIGRAPHY EXAM

Nature is the creation of natural material and physical world on earth independent of human of activity. The beauty and richness is of nature is diverse and massive. Nature provides us with several and delicacies to enjoy and is our life is support system. Our basic needs like food, shelter, water and air are of the gifts from nature. Humans have a strong connection and interrelation with nature. Escaping away in the lest nature heals the mind and body and soothes our soul and mind.

Class Work Photos

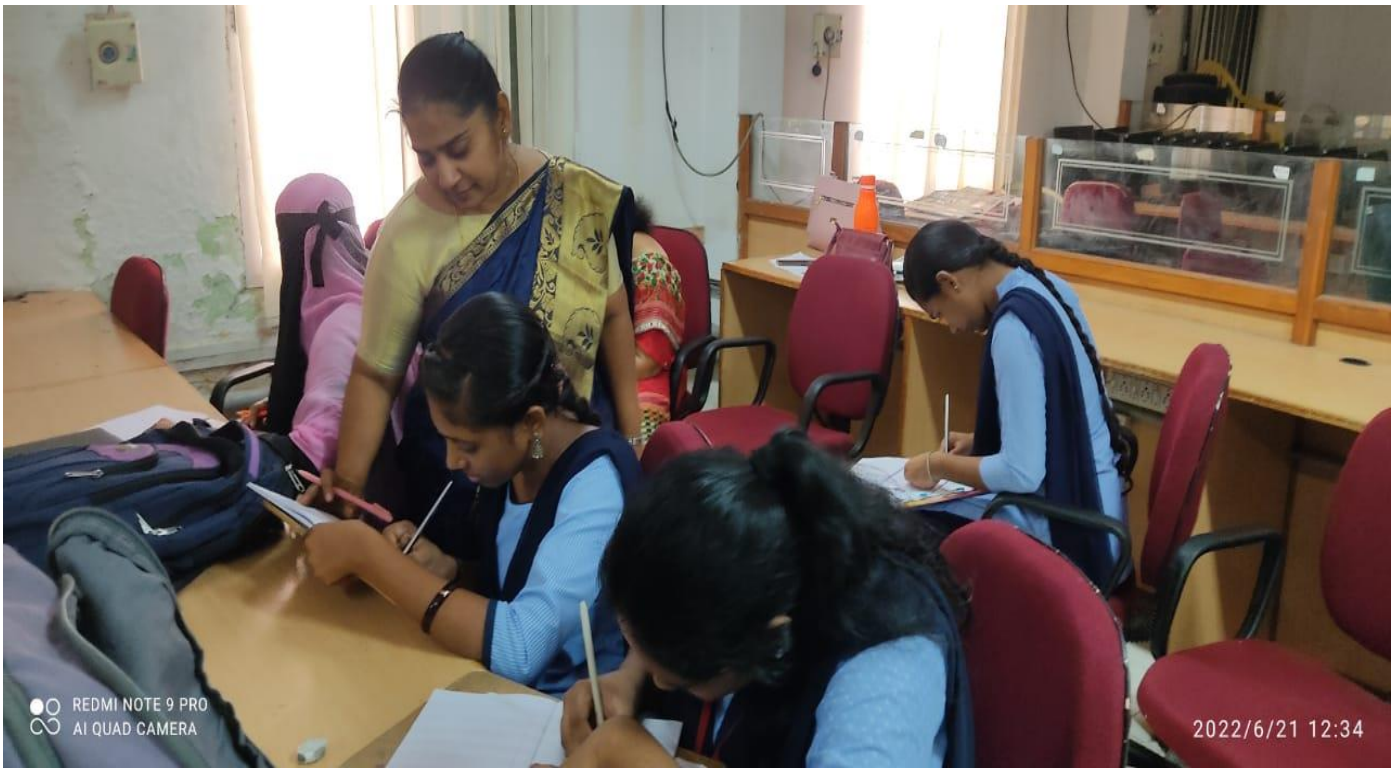


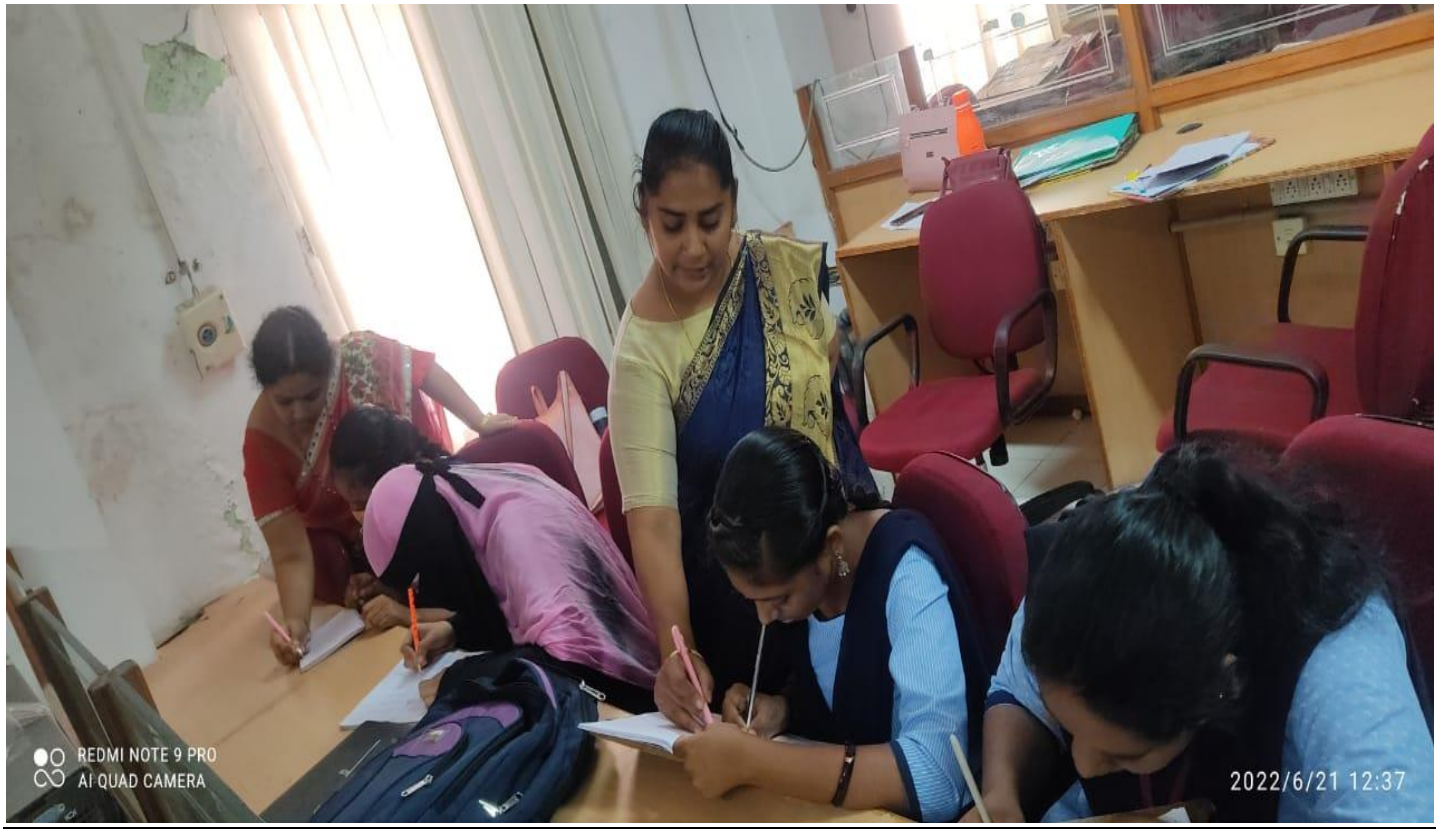




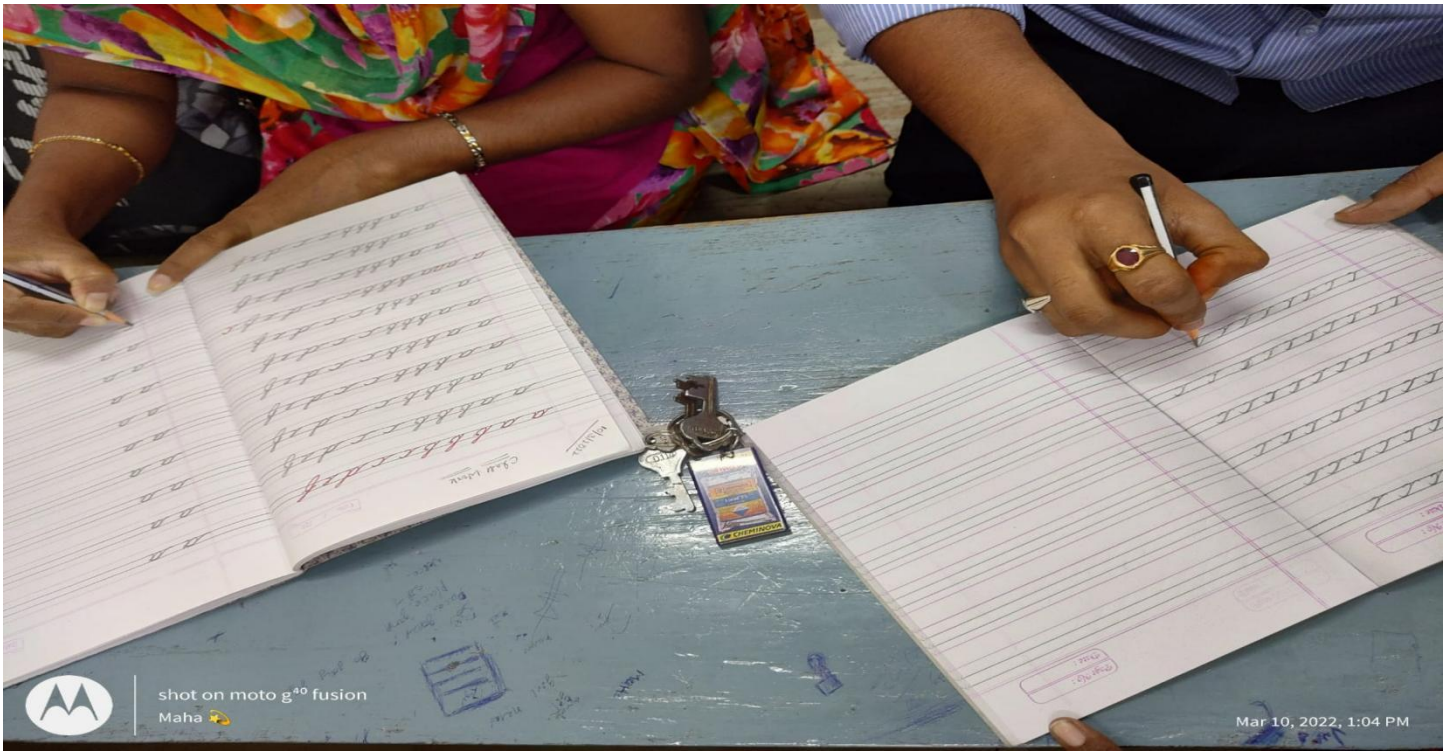




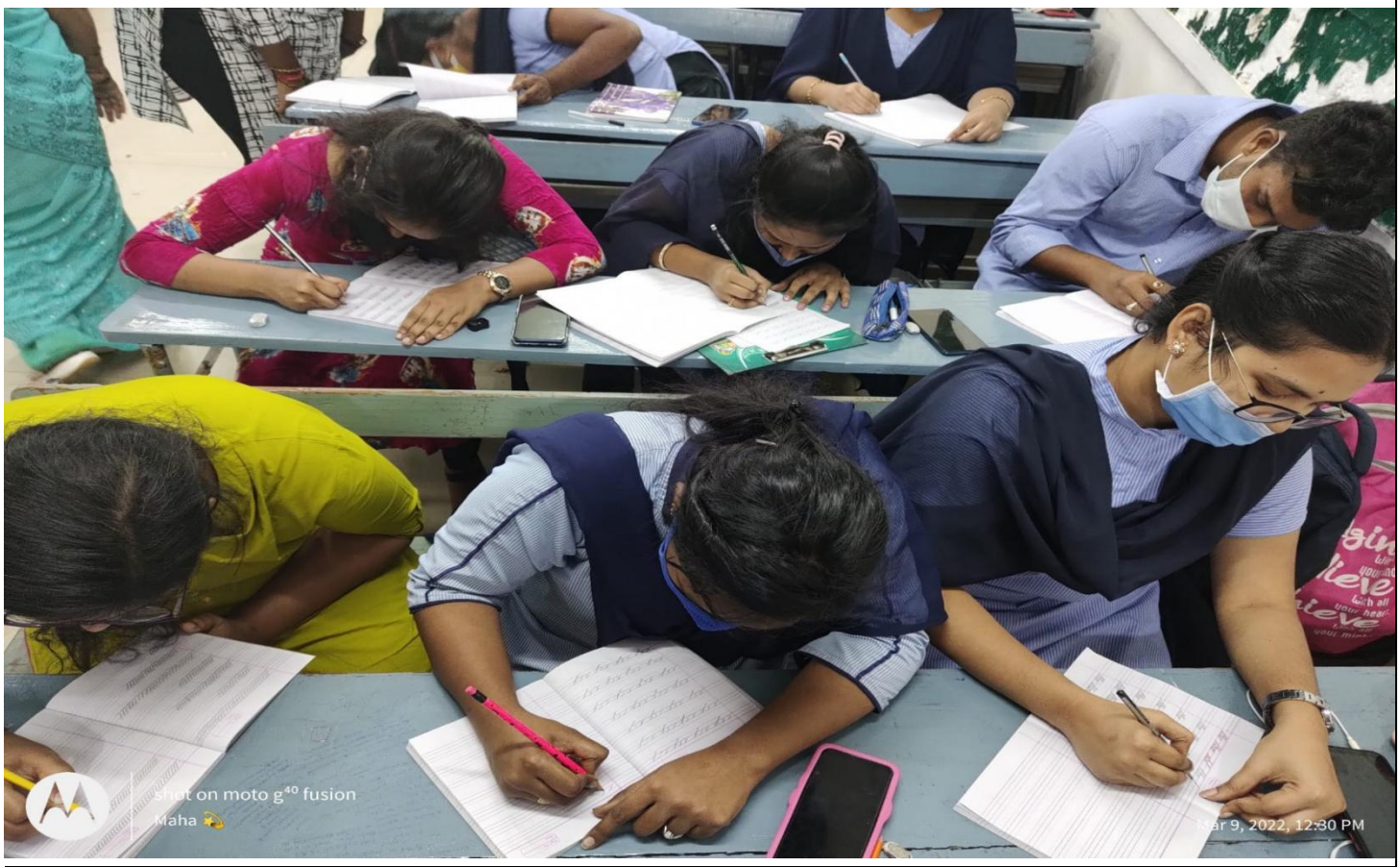

REDMI NOTE 9 PRO
AI QUAD CAMERA
2022/6/21 12:34


REDMI NOTE 9 PRO
AI QUAD CAMERA
2022/6/21 12:37



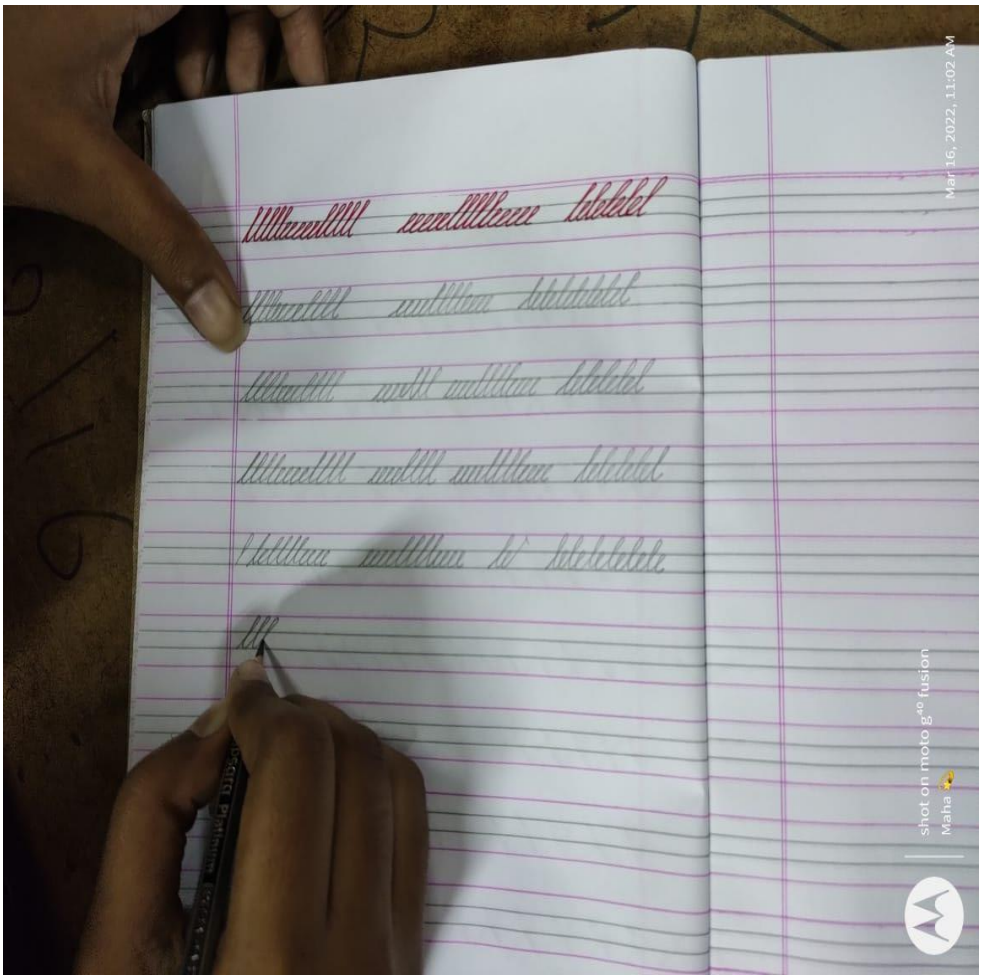

shot on moto g40 fusion
Maha
Mar 10, 2022, 1:04 PM


shot on moto g40 fusion
Maha
Mar 10, 2022, 1:05 PM


shot on moto g40 fusion
Maha
Mar 9, 2022, 12:30 PM


shot on moto g40 fusion
Maha
Mar 9, 2022, 12:28 PM

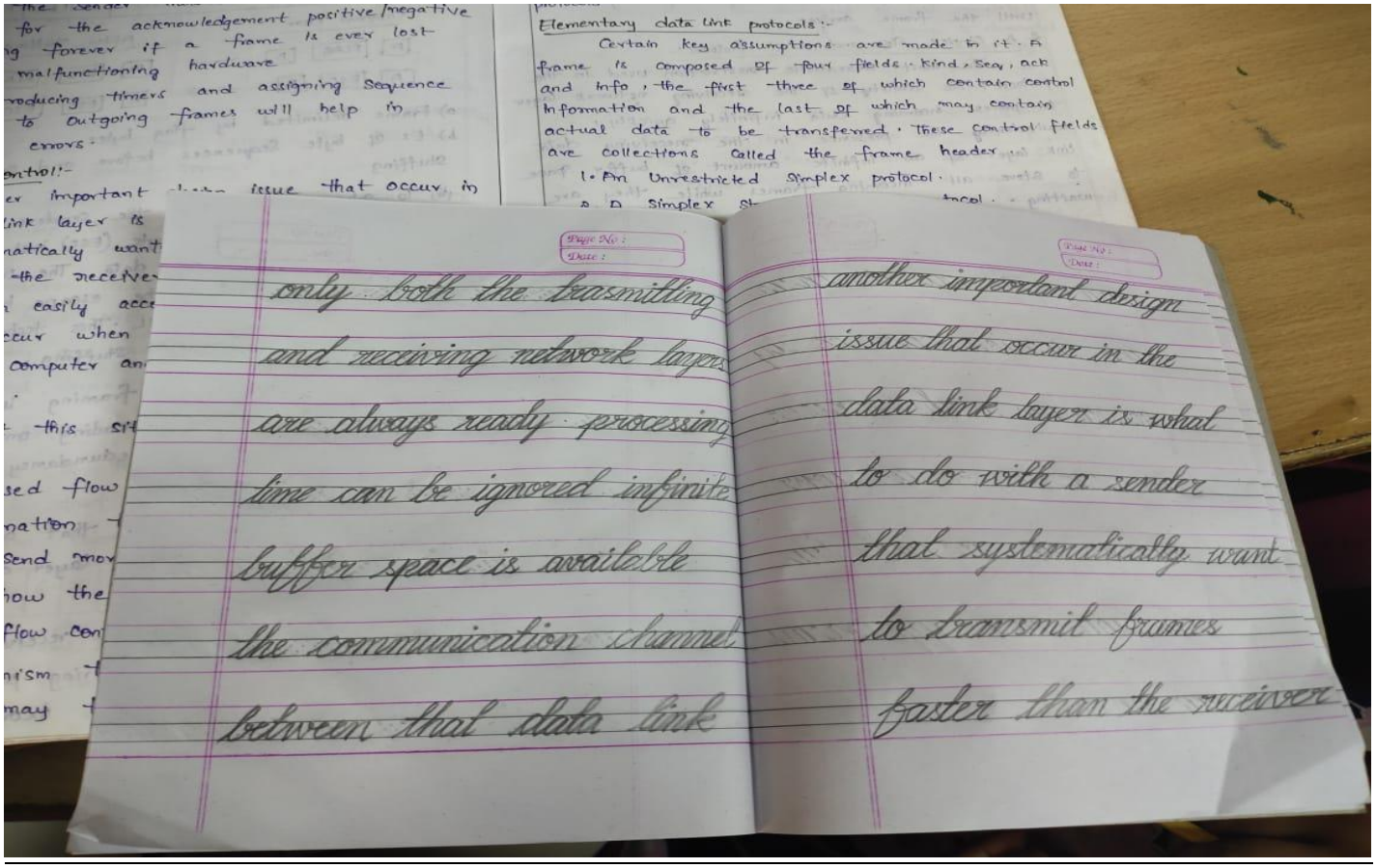

shot on moto g40 fusion
Maha
Mar 11, 2022, 1:02 PM


Mar 16, 2022, 11:02 AM
shot on moto g40 fusion
Maha


shot on moto g40 fusion
Maha
Mar 16, 2022, 10:59 AM


shot on moto g40 fusion
Maha
Mar 25, 2022, 12:13 PM

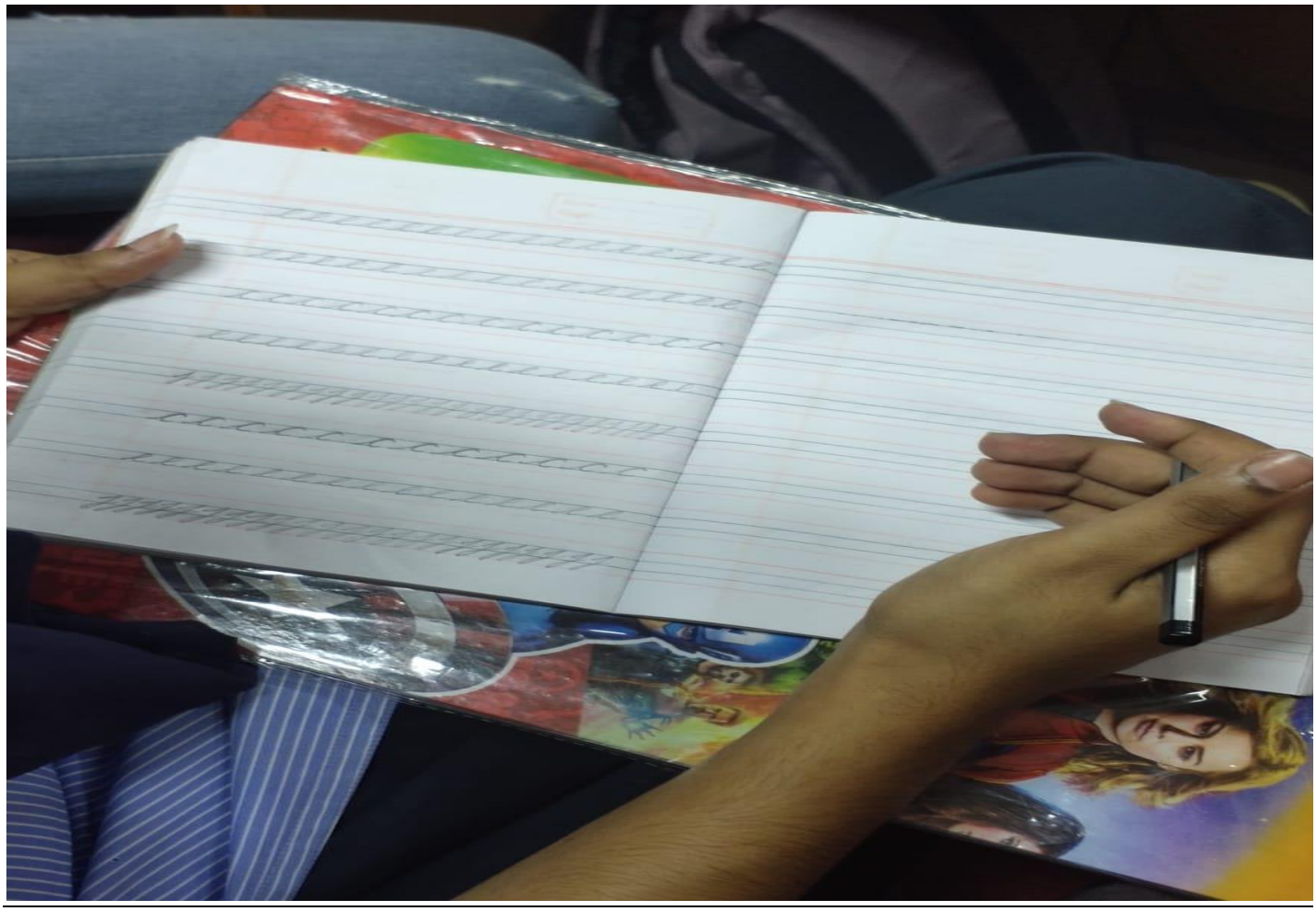

shot on moto g⁴⁰ fusion
Maha
Mar 21, 2022, 1:02 PM

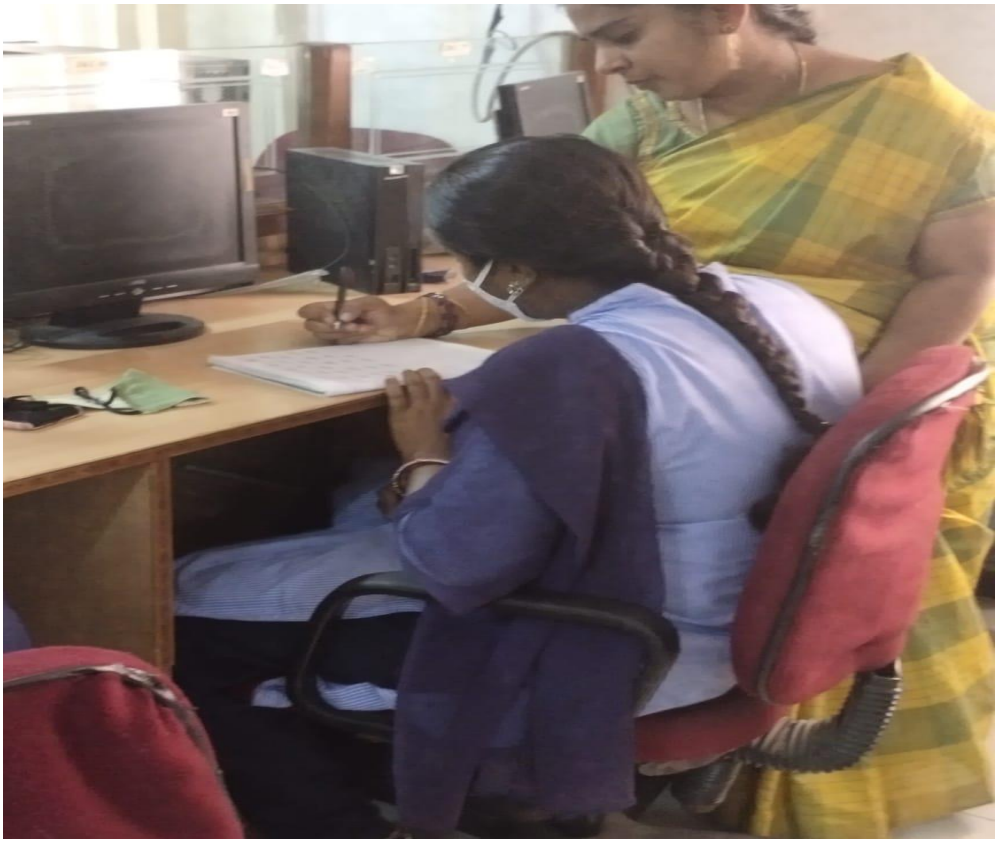

for the acknowledgement positive/negative
forever if a frame is ever lost
malfunctioning hardware
producing timers and assigning sequence
to outgoing frames will help in
errors.
Elementary data link protocols:-
Certain key assumptions are made in it. A
frame is composed of four fields: kind, seq, ack
and info, the first three of which contain control
information and the last of which may contain
actual data to be transferred. These control fields
are collections called the frame header.
1. An Unrestricted Simplex protocol.
only both the trasmitting
and receiving network layers
are always ready processing
time can be ignored infinite
buffer space is available
the communication channel
between that data link
another important design
issue that occur in the
data link layer is what
to do with a sender
that systematically want
to transmit frames
faster than the receiver


shot on moto g40 fusion
Maha
Mar 17, 2022, 1:06 PM


shot on moto g40 fusion
Maha
Mar 17, 2022, 1:04 PM







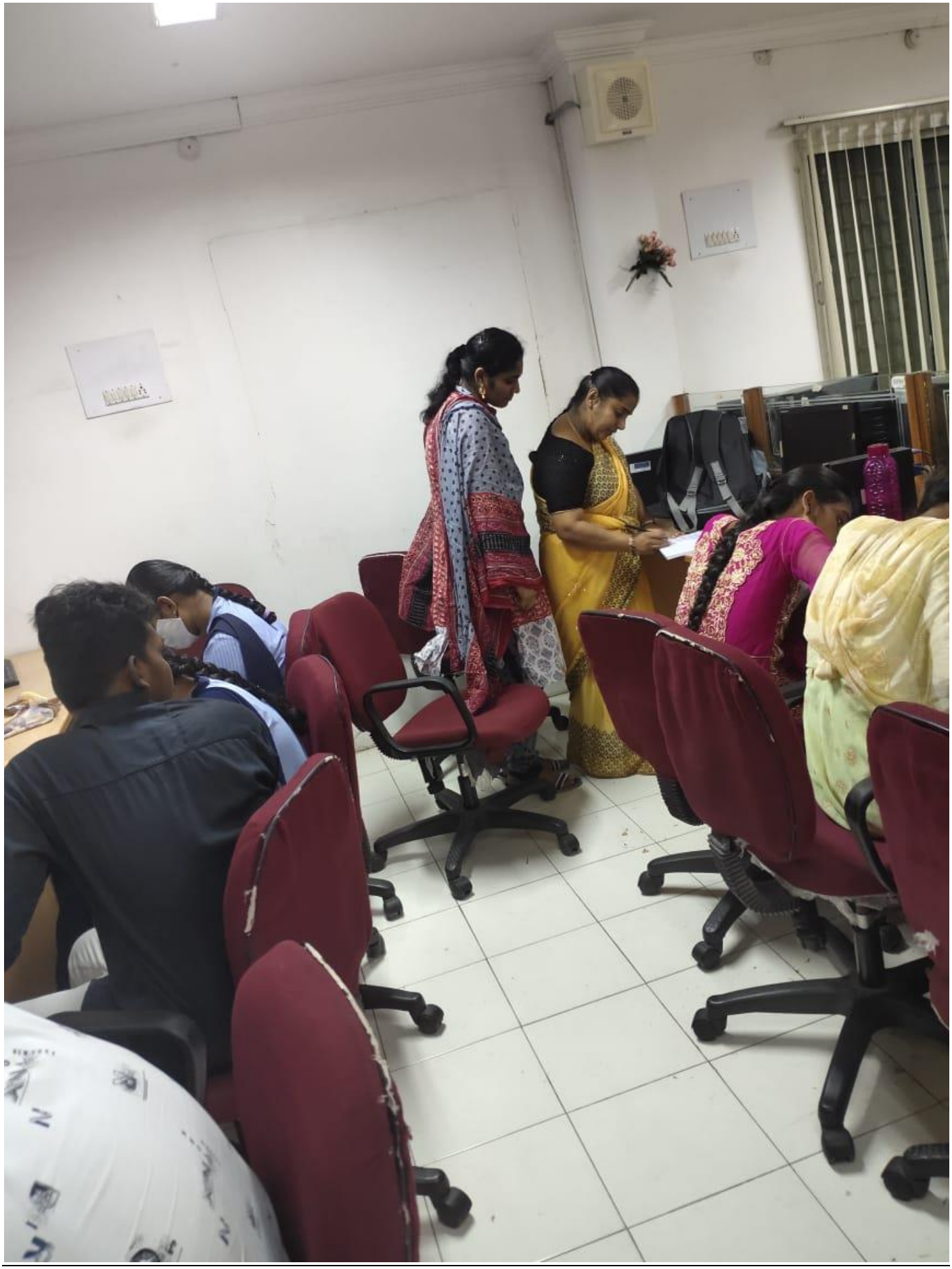
-

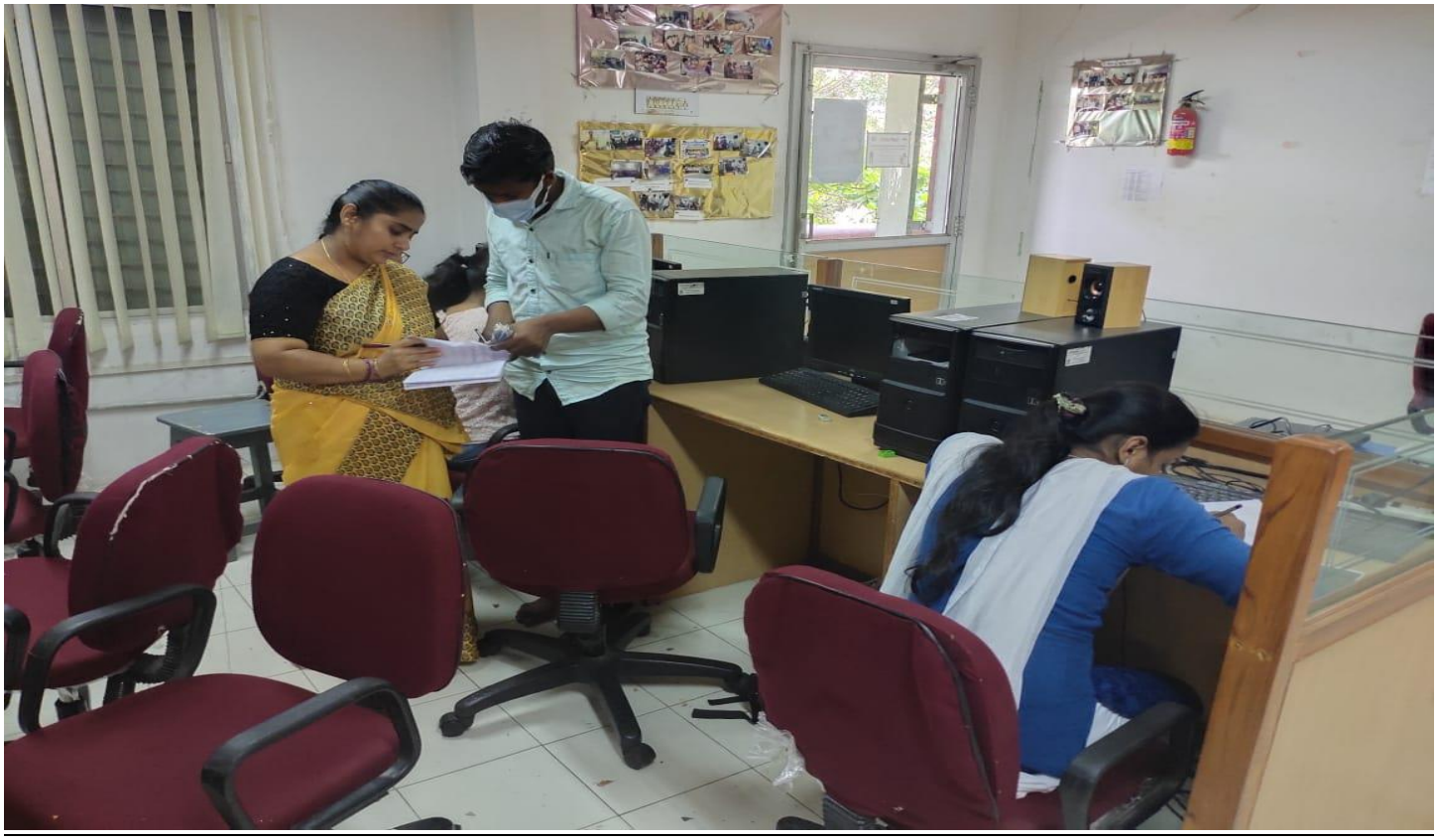


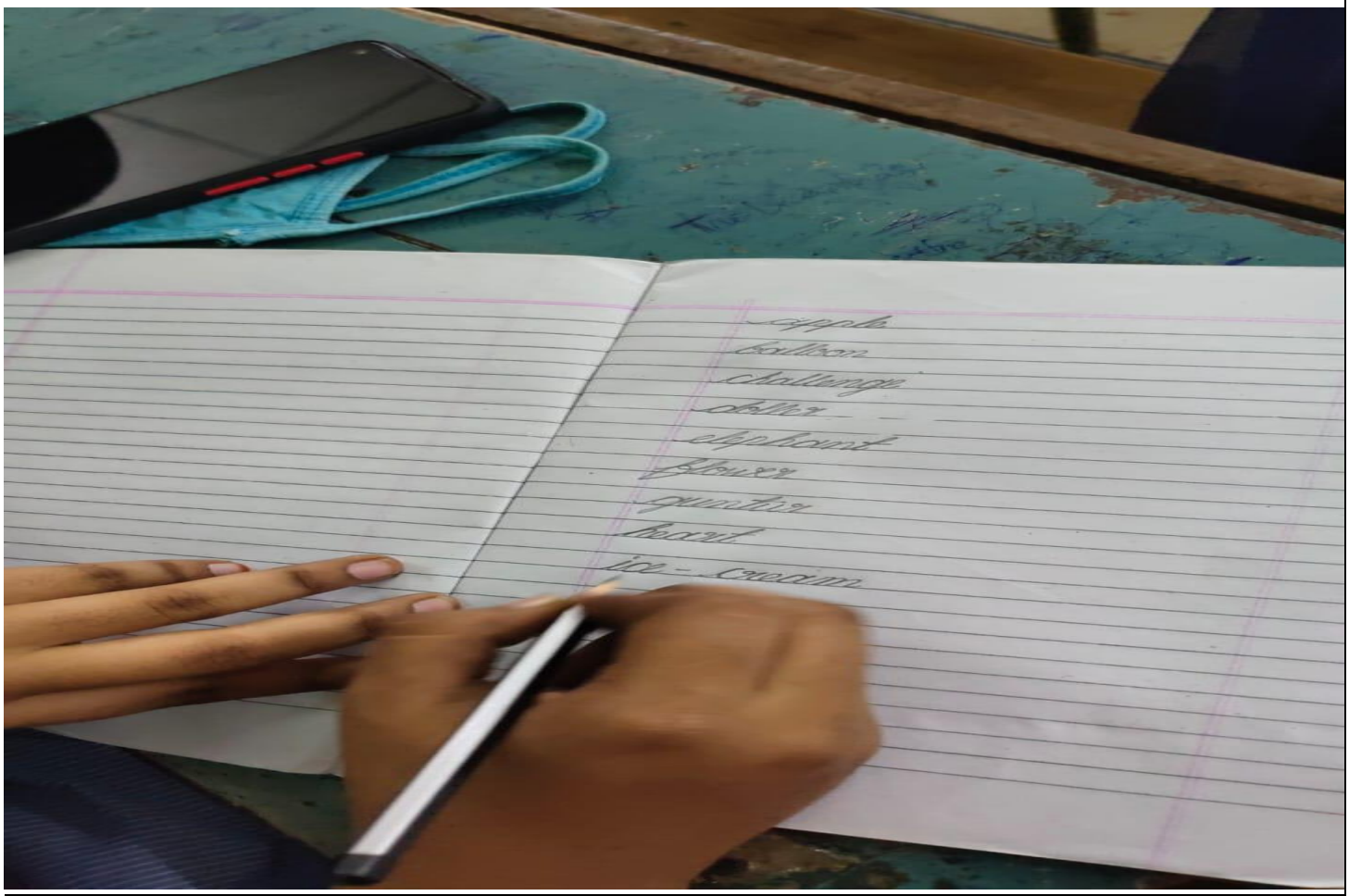






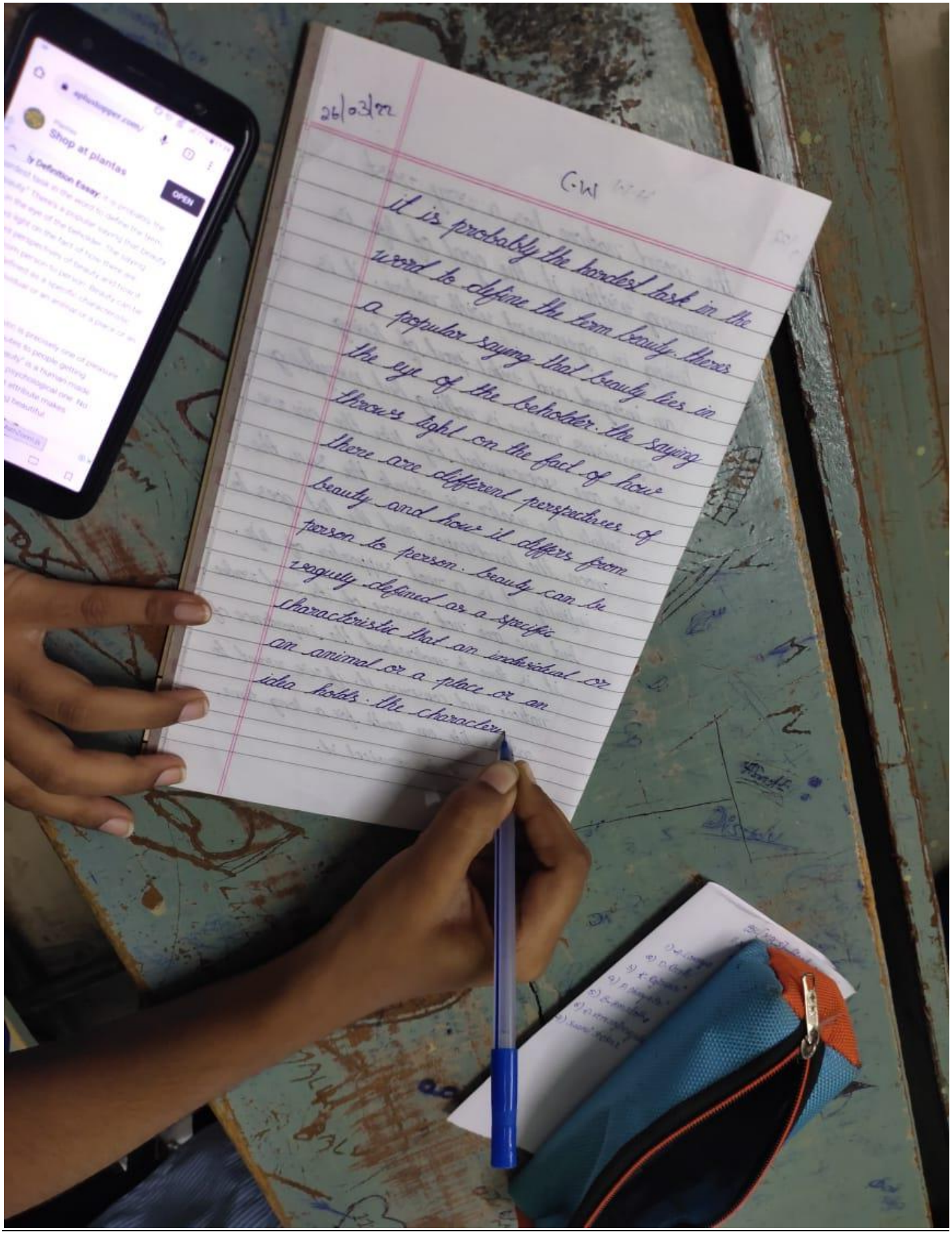


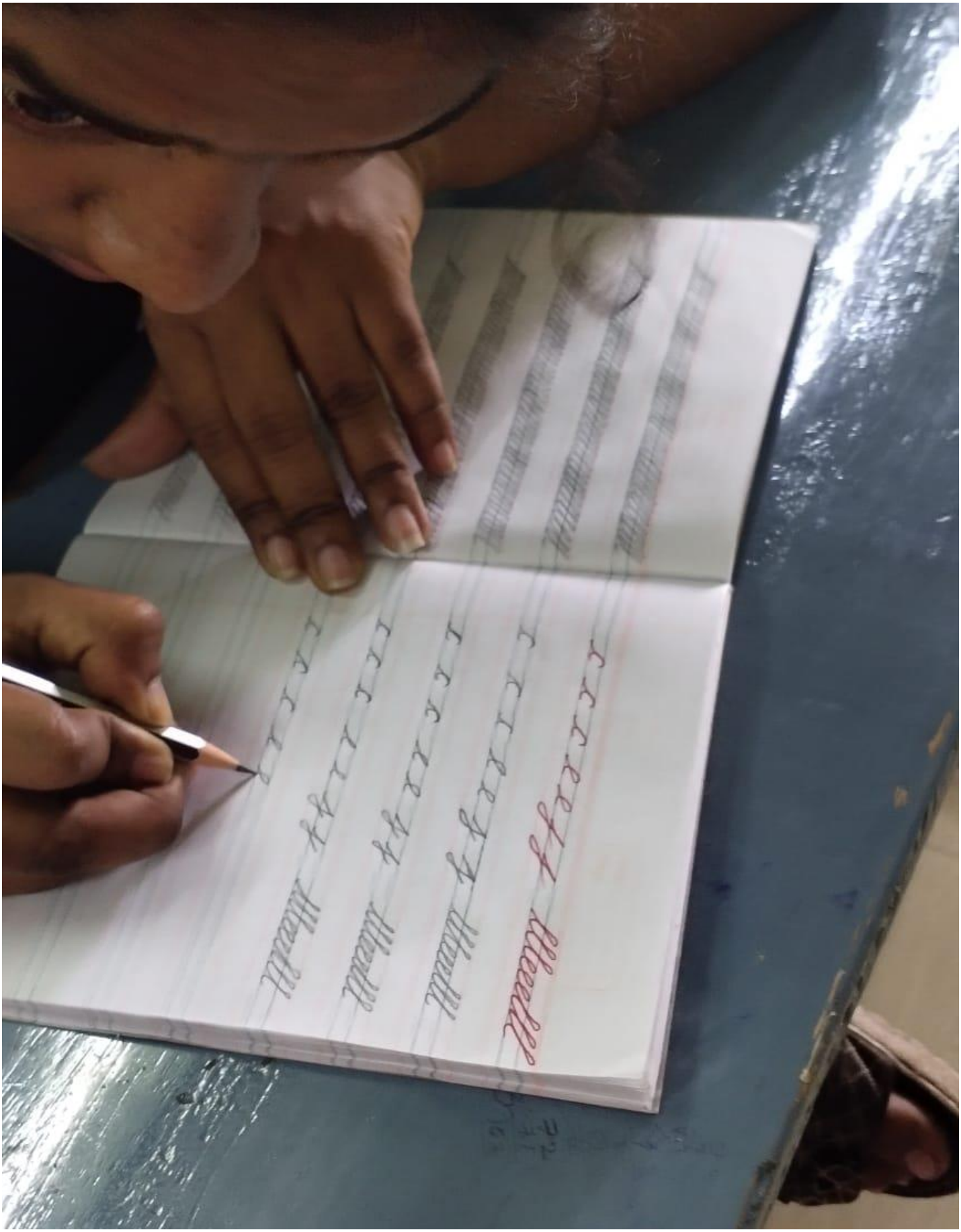


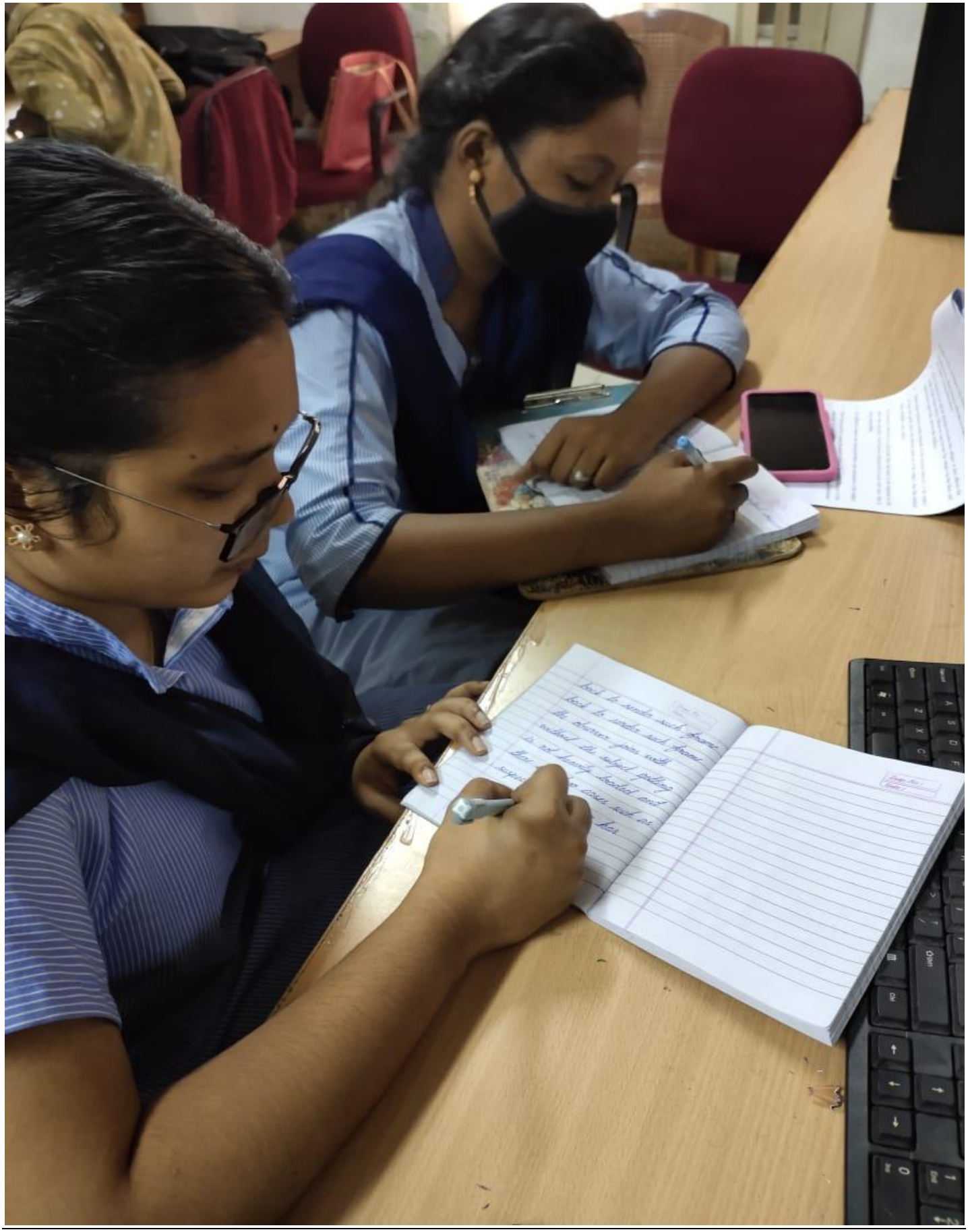




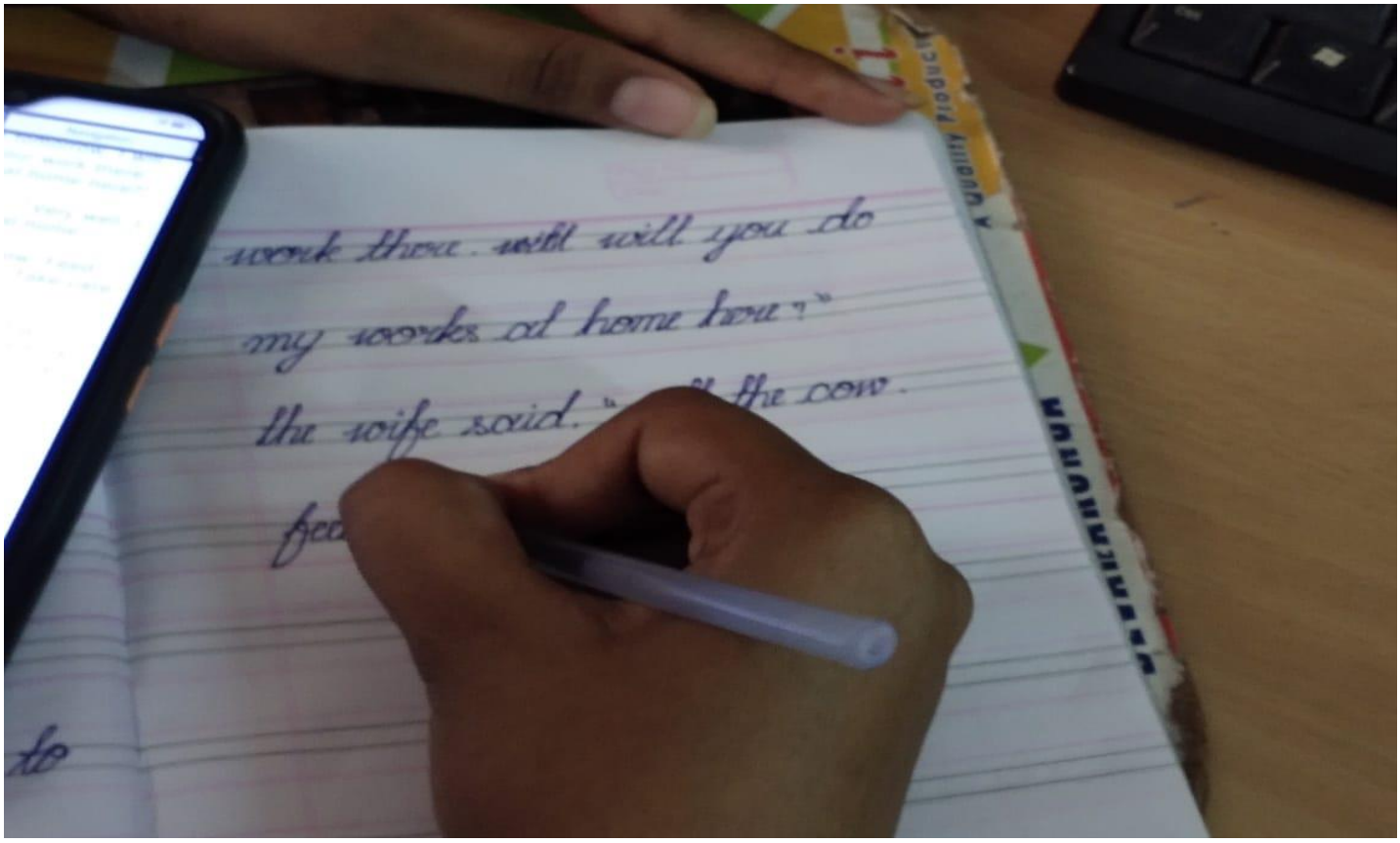



26/03/22
C.W
it is probably the hardest task in the
word to define the term beauty. there's
a popular saying that beauty lies in
the eye of the beholder. the saying
throws light on the fact of how
there are different perspectives of
beauty and how it differs from
person to person. beauty can be
vaguely defined as a specific
characteristic that an individual or
an animal or a place or an
idea holds. the character
Shop at plantas
OPEN





the following maps the flowchart into a corresponding flow graph in the flow graph each circle called a flow) flow graph node represented one or more procedural statements.


work there. will will you do
my works at home here?"
the wife said. "
the cow.
fee
to




REDMI NOTE 9 PRO
AI QUAD CAMERA
2022/7/5 11:14


REDMI NOTE 9 PRO
AI QUAD CAMERA
2022/7/5 11:57


REDMI NOTE 9 PRO
AI QUAD CAMERA
2022/7/5 11:59


REDMI NOTE 9 PRO
AI QUAD CAMERA
2022/4/8 12:22

Calligraphy Exhibition on August 15/2022










(AUTONOMOUS)



Calligraphy Certificates

Calligraphy and Graphic Design
Training Centre - New Delhi

Regd.No.: 418 / 2016

ISO 9001 : 2008 Certified Organization

Certificate course in Hand Writing

This is certificate that Ms./Mrs./Mr. Rentala. Ajay. Kumar.....

S/o, D/o... Rentala. Madhu Babu.... has successfully completed

Hand Writing course during the Academic

Student Class III. B.A [EPJ].

Year ..2022.....

SRR & CVR Government Degree College[A], Vijayawada.

Instructor - Calligraphy

LIMRA INSTITUTE OF CALLIGRAPHY
& GRAPHIC DESIGN TRAINING CENTRE
HYDERABAD - 500 012.

Director

Calligraphy and Graphic Design
Training Centre - New Delhi

Regd.No.: 418 / 2016

ISO 9001 : 2008 Certified Organization

Certificate course in Hand Writing

This is certificate that Ms./Mrs./Mr. Alla Mahadevi

S/o, D/o. Alla Srinivasa Reddy has successfully completed

Hand Writing course during the Academic

Student Class III B.A [EPS]

Year 2022

SRR & CVR Government Degree College [A], Vijayawada.

Instructor - Calligraphy

LIMRA INSTITUTE OF CALLIGRAPHY
& GRAPHIC DESIGN TRAINING CENTRE
HYDERABAD 500 012.

Director

Calligraphy and Graphic Design
Training Centre - New Delhi

Regd.No.: 418 / 2016

ISO 9001 : 2008 Certified Organization

Certificate course in Hand Writing

This is certificate that Ms./Mrs./Mr. Bhanu Namagiri

S/o, D/o. Namagiri V. Satyanarayana has successfully completed

Hand Writing course during the Academic

Student Class ~~III~~ B.A. [EPJ]

Year ~~2022~~

SRR & CVR Government Degree College [A] Vijayawada.

Instructor - Calligraphy

LIMRA INSTITUTE OF CALLIGRAPHY
& GRAPHIC DESIGN TRAINING CENTRE
HYDERABAD - 500 012.

Director

Calligraphy and Graphic Design
Training Centre - New Delhi

Regd.No.: 418 / 2016

ISO 9001 : 2008 Certified Organization

Certificate course in Hand Writing

This is certificate that Ms./Mrs./Mr. Malladi.....Sweety.....

S/o, D/o. Malladi...Sankara Rao.....has successfully completed

Hand Writing course during the Academic

Student Class III. B.Sc [MPCs]

Year .....2022.....

SRR & CVR Government Degree College [A], Vijayawada.

Instructor - Calligraphy

Director

UMRA INSTITUTE OF CALLIGRAPHY
& GRAPHIC DESIGN TRAINING CENTRE
HYDERABAD - 500 012.

Calligraphy and Graphic Design Training Centre - New Delhi

Regd.No.: 418 / 2016

ISO 9001 : 2008 Certified Organization

Certificate course in Hand Writing

This is certificate that Ms./Mrs./Mr. Y. Sri. Pujitha Akhilandeswari.

S/o, D/o. Yerragadda Srinath ..... has successfully completed

Hand Writing course during the Academic

Student Class III B.A [EPJ]

Year ...2022.....

SRR & CVR Government Degree College[A], Vijayawada.

Instructor - Calligraphy

LIMRA INSTITUTE OF CALLIGRAPHY
& GRAPHIC DESIGN TRAINING CENTRE
HYDERABAD - 500 012.

Director

Calligraphy and Graphic Design
Training Centre - New Delhi

Regd.No.: 418 / 2016

ISO 9001 : 2008 Certified Organization

Certificate course in Hand Writing

This is certificate that Ms./Mrs./Mr. Tenneti. Sai Kishore

S/o, D/o. Tenneti. Srinivas Rao *has successfully completed*

Hand Writing course during the Academic

Student Class III B.A [EPJ]

Year 2022

SRR & CVR Government Degree College[A], Vijayawada.

Instructor - Calligraphy

LIMRA INSTITUTE OF CALLIGRAPHY
& GRAPHIC DESIGN TRAINING CENTRE
HYDERABAD - 500 012.

Director

Calligraphy and Graphic Design
Training Centre - New Delhi

Regd.No.: 418 / 2016

ISO 9001 : 2008 Certified Organization

Certificate course in Hand Writing

This is certificate that Ms./Mrs./Mr. Gampa Hemalathar

S/o, D/o. Gampa Subba Rao has successfully completed

Hand Writing course during the Academic

Student Class III B.A [EPS]

Year 2022

SRR & CVR Government Degree College[A] Vijayawada

LIMRA INSTITUTE OF CALLIGRAPHY
& GRAPHIC DESIGN TRAINING CENTRE
HYDERABAD - 500 012.

Instructor - Calligraphy

Director

August 15/2022

Calligraphy and Graphic Design Training Centre - New Delhi

Regd.No.: 418 / 2016

ISO 9001 : 2008 Certified Organization

Certificate course in Hand Writing

This is certificate that Ms./Mrs./Mr. Byneedu. Rajeswari.....

S/o, D/o. Byneedu. Venkateswara Rao has successfully completed

Hand Writing course during the Academic

Student Class III. B.Com. Computer Applications.

Year 2022.....

SRR & CVR Government Degree College [A], Vijayawada.

Instructor - Calligraphy

LIMRA INSTITUTE OF CALLIGRAPHY
& GRAPHIC DESIGN TRAINING CENTRE
HYDERABAD - 500 012.

Director

Calligraphy and Graphic Design Training Centre - New Delhi

Regd.No.: 418 / 2016

ISO 9001 : 2008 Certified Organization

Certificate course in Hand Writing

This is certificate that Ms./Mrs./Mr. Rowthu Sirisha

S/o, D/o. Rowthu Ramana has successfully completed

Hand Writing course during the Academic

Student Class III B.Com. Computer Application.

Year 2022

SRR & CVR Government Degree College(A), Vijayawada

Instructor - Calligraphy

LIMCA INSTITUTE OF CALLIGRAPHY & GRAPHIC DESIGN TRAINING CENTRE HYD.

Director

Calligraphy and Graphic Design
Training Centre - New Delhi

Regd.No.: 418 / 2016

ISO 9001 : 2008 Certified Organization

Certificate course in Hand Writing

This is certificate that Ms./Mrs./Mr. Salluri Sujatha

S/o, D/o. Salluri Venkatapathi has successfully completed

Hand Writing course during the Academic

Student Class III B.A. [EPJ]

Year 2022

SRR&CVR Government Degree College [A], Vijayawada.

LIMRA INSTITUTE OF CALLIGRAPHY
& GRAPHIC DESIGN TRAINING CENTRE
HYDERABAD - 500 012.

Instructor - Calligraphy

Director

Calligraphy and Graphic Design
Training Centre - New Delhi

Regd.No.: 418 / 2016

ISO 9001 : 2008 Certified Organization

Certificate course in Hand Writing

This is certificate that Ms./Mrs./Mr. Maroju. Naga Haritha.....

S/o, D/o. M. Gnana Parvathi Kumar has successfully completed

Hand Writing course during the Academic

Student Class III. B.Com. Computer Applications.

Year 2022.....

SRR & CVR Government Degree College[A], Vijayawada.

Instructor - Calligraphy

LIMRA INSTITUTE OF CALLIGRAPHY
& GRAPHIC DESIGN TRAINING CENTRE
HYDERABAD - 500 012.

Director

Calligraphy and Graphic Design
Training Centre - New Delhi

Regd.No.: 418 / 2016

ISO 9001 : 2008 Certified Organization

Certificate course in Hand Writing

This is certificate that Ms./Mrs./Mr. Nallathoti...Premchend.....

S/o, D/o. Nallathoti...Srinivas.....has successfully completed

Hand Writing course during the Academic

Student Class III B.Sc [MPCS]

Year .....2022.....

SRR&CVR Government Degree College[A], Vijayawada

Instructor - Calligraphy

Director

Calligraphy and Graphic Design
Training Centre - New Delhi

Regd.No.: 418 / 2016

ISO 9001 : 2008 Certified Organization

Certificate course in Hand Writing

This is certificate that Ms./Mrs./Mr. Manikyam. Pushpa. Latha.....

S/o, D/o. Manikyam. Pushpa Raju ... has successfully completed

Hand Writing course during the Academic

Student Class III B.Sc [MPCS]

Year ...2022.....

SRR&CVR Government Degree College[A], Vijayawada.

Instructor - Calligraphy

Director

LIMCA INSTITUTE OF CALLIGRAPHY & GRAPHIC DESIGN TRAINING CENTRE HYDERABAD - 500 012.

Calligraphy and Graphic Design
Training Centre - New Delhi

Regd.No.: 418 / 2016

ISO 9001 : 2008 Certified Organization

Certificate course in Hand Writing

This is certificate that Ms./Mrs./Mr. Dubbaku. Keerthi.....

S/o, D/o. Dubbaku. Adiramudu.....has successfully completed

Hand Writing course during the Academic

Student Class III. B.Sc [MPCs]

Year .....2022.....

SRR & CVR Government Degree College [A], Vijayawada.

Instructor - Calligraphy

LIMRA INSTITUTE OF CALLIGRAPHY
& GRAPHIC DESIGN TRAINING CENTRE
500 012.

Director

Calligraphy and Graphic Design
Training Centre - New Delhi

Regd.No.: 418 / 2016

ISO 9001 : 2008 Certified Organization

Certificate course in Hand Writing

This is certificate that Ms./Mrs./Mr. Kaza Rajeswari

S/o, D/o. Kaza Siva Sankara Rao ...has successfully completed

Hand Writing course during the Academic

Student Class III B.Sc [MPCs]

Year 2022

SRR & CVR Government Degree College [A], Vijayawada.

Instructor - Calligraphy

LIMRA INSTITUTE OF CALLIGRAPHY & GRAPHIC DESIGN TRAINING CENTRE HYDERABAD - 500 012.

Director

Calligraphy and Graphic Design
Training Centre - New Delhi

Regd.No.: 418 / 2016

ISO 9001 : 2008 Certified Organization

Certificate course in Hand Writing

This is certificate that Ms./Mrs./Mr. Ampolu. Lavanya.....

S/o, D/o. Ampolu. Appala Naidu.....has successfully completed

Hand Writing course during the Academic

Student Class III B.Sc [MPCs]

Year .....2022.....

SRR&CVR Government Degree College (A), Vijayawada.

Instructor - Calligraphy

LIMRA INSTITUTE OF CALLIGRAPHY
& GRAPHIC DESIGN TRAINING CENTRE
HYDERABAD - 500 012.

Calligraphy and Graphic Design
Training Centre - New Delhi

Regd.No.: 418 / 2016

ISO 9001 : 2008 Certified Organization

Certificate course in Hand Writing

This is certificate that Ms./Mrs./Mr. Kammuri. Sai Ramya.....

S/o, D/o. Kammuri. Narasimha Rao has successfully completed

Hand Writing course during the Academic

Student Class III. B.A. [EPS]

Year ..2022.....

SRR & CVR Government Degree College [A] Vijayawada.

Instructor - Calligraphy

LIMRA INSTITUTE OF CALLIGRAPHY
& GRAPHIC DESIGN TRAINING CENTRE
HYDERABAD - 500 012.

Director

Calligraphy and Graphic Design
Training Centre - New Delhi

Regd.No.: 418 / 2016

ISO 9001 : 2008 Certified Organization

Certificate course in Hand Writing

This is certificate that Ms./Mrs./Mr. Mohammad. Shahin

S/o, D/o. Mohammad. Basheer has successfully completed

Hand Writing course during the Academic

Student Class III B.Sc [MPCs]

Year 2022

SRR & CVR Government Degree College [A], Vijayawada.

Instructor - Calligraphy

LIMRA INSTITUTE OF CALLIGRAPHY & GRAPHIC DESIGN TRAINING CENTRE HYDERABAD 500 012.

Director



Calligraphy and Graphic Design
Training Centre - New Delhi

Regd.No.: 418 / 2016

ISO 9001 : 2008 Certified Organization

Certificate course in Hand Writing

This is certificate that Ms./Mrs./Mr. Sampara Bhavitha

S/o, D/o... Sampara Satyanarayana has successfully completed

Hand Writing course during the Academic

Student Class III B.Sc [MPCS]

Year 2022

SRR & CVR Government Degree College [A] Vijayawada.

Instructor - Calligraphy

LIMRA INSTITUTE OF CALLIGRAPHY & GRAPHIC DESIGN TRAINING CENTRE Hyderabad-500 012.

Director

OPPO F11 Pro · ©smile😉
2022/10/28 13:00

Calligraphy and Graphic Design
Training Centre - New Delhi

Regd.No.: 418 / 2016

ISO 9001 : 2008 Certified Organization

Certificate course in Hand Writing

This is certificate that Ms./Mrs./Mr. Bonu. Hemalatha.....

S/o, D/o. Bonu. Chinnaiah.....has successfully completed

Hand Writing course during the Academic

Student Class III. B.Sc [MPCS].

Year ..2022.....

SRR & CVR Government Degree College [A], Vijayawada.

Instructor - Calligraphy

LIMRA INSTITUTE OF CALLIGRAPHY
& GRAPHIC DESIGN TRAINING CENTRE
HYDERABAD - 500 012.

Director

Calligraphy and Graphic Design Training Centre - New Delhi

Regd.No.: 418 / 2016

ISO 9001 : 2008 Certified Organization

Certificate course in Hand Writing

This is certificate that Ms./Mrs./Mr. Shaik. Iliyaz

S/o, D/o. Shaik. Ismail has successfully completed

Hand Writing course during the Academic

Student Class III. B. Com. Computer Applications.

Year 2022

SRR & CVR Government Degree College [A], Vijayawada.

Instructor - Calligraphy

LIMRA INSTITUTE OF CALLIGRAPHY
& GRAPHIC DESIGN TRAINING CENTRE
HYDERABAD-500 012.

Director

Calligraphy and Graphic Design
Training Centre - New Delhi

Regd.No.: 418 / 2016

ISO 9001 : 2008 Certified Organization

Certificate course in Hand Writing

This is certificate that Ms./Mrs./Mr. Katti.....Manasa.....

S/o, D/o...Katti.....Ravindra Kumar. *has successfully completed*

Hand Writing course during the Academic

Student Class III..B..Com. Computer Applications.

Year ..2022.....

SRR&CVR Government Degree College[A] Vijayawada

Instructor - Calligraphy

LIMRA INSTITUTE OF CALLIGRAPHY
& GRAPHIC DESIGN TRAINING CENTRE
HYDERABAD - 500 012.

Director

Calligraphy and Graphic Design
Training Centre - New Delhi

Regd.No.: 418 / 2016

ISO 9001 : 2008 Certified Organization

Certificate course in Hand Writing

This is certificate that Ms./Mrs./Mr. Daggupati Harileela

S/o, D/o. Daggupati Gauruvardhan Rao has successfully completed

Hand Writing course during the Academic

Student Class III B.Com Computer Applications.

Year 2012

SRR & CVR Government Degree College [A], Vijayawada

Instructor - Calligraphy

UMRA INSTITUTE OF CALLIGRAPHY & GRAPHIC DESIGN TRAINING CENTRE HYDERABAD - 500 012.

Director

Calligraphy and Graphic Design
Training Centre - New Delhi

Regd.No.: 418 / 2016

ISO 9001 : 2008 Certified Organization

Certificate course in Hand Writing

This is certificate that Ms./Mrs./Mr. Dulla. Venkatesh

S/o, D/o. Dulla Srinu has successfully completed

Hand Writing course during the Academic

Student Class III B.Com. Computer Applications.

Year 2022

SRR&CVR Government Degree College[A] Vijayawada.

Instructor - Calligraphy

LIMRA INSTITUTE OF CALLIGRAPHY & GRAPHIC DESIGN TRAINING CENTRE HYD 012.

Director

Calligraphy and Graphic Design
Training Centre - New Delhi

Regd.No.: 418 / 2016

ISO 9001 : 2008 Certified Organization

Certificate course in Hand Writing

This is certificate that Ms./Mrs./Mr. Nandi: Sai Siva Rama Krishna.

S/o, D/o. Nandi: Srinivas Rao ..... has successfully completed

Hand Writing course during the Academic

Student Class III B.A [EPS]

Year .... 2022 .....

SRR & CVR Government Degree College[A], Vijayawada.

Instructor - Calligraphy

LIMRA INSTITUTE OF CALLIGRAPHY
& GRAPHIC DESIGN TRAINING CENTRE
HYDERABAD-500 012.

Director

Calligraphy and Graphic Design
Training Centre - New Delhi

Regd.No.: 418 / 2016

ISO 9001 : 2008 Certified Organization

Certificate course in Hand Writing

This is certificate that Ms./Mrs./Mr. Jamandlamudi Vijaya Madhuri

S/o, D/o Jamandlamudi Kumar Vijay ..... has successfully completed

Hand Writing course during the Academic

Student Class III B.A. [EPS]

Year ....2022.....

SRR & CVR Government Degree College [A], Vijayawada.

Instructor - Calligraphy

LIMRA INSTITUTE OF CALLIGRAPHY
& GRAPHIC DESIGN TRAINING CENTRE
HYDERABAD - 500 012.

Director

Calligraphy and Graphic Design
Training Centre - New Delhi

Regd.No.: 418 / 2016

ISO 9001 : 2008 Certified Organization

Certificate course in Hand Writing

This is certificate that Ms./Mrs./Mr. Shaik Sharmi

S/o, D/o. Shaik Babji has successfully completed

Hand Writing course during the Academic

Student Class III B.A [EPJ]

Year 2022

SRR & CVR Government Degree College [A], Vijayawa

Calligraphy and Graphic Design Training Centre - New Delhi

Regd.No.: 418 / 2016

ISO 9001 : 2008 Certified Organization

Certificate course in Hand Writing

This is certificate that Ms./Mrs./Mr...Kundeti...Anitha.....

S/o, D/o...Kundeti..VenkataRatnam.has successfully completed

Hand Writing course during the Academic

Student Class III..B.Com. Computer Applications.

Year ...2022.....

SRR&CVR Government Degree College[A], Vijayawada

Instructor - Calligraphy

Director

LIMRA INSTITUTE OF CALLIGRAPHY
& GRAPHIC DESIGN TRAINING CENTRE
HYDERABAD - 500 012.

Calligraphy and Graphic Design
Training Centre - New Delhi

Regd.No.: 418 / 2016

ISO 9001 : 2008 Certified Organization

Certificate course in Hand Writing

This is certificate that Ms./Mrs./Mr. Mahammed Haseena.....

S/o, D/o. Mahammed Haneef.....has successfully completed

Hand Writing course during the Academic

Student Class III B.Com Computer Applications.

Year ....2022.....

SRR&CVR Government Degree College [A], Vijayawada.

Instructor - Calligraphy

LIMRA INSTITUTE OF CALLIGRAPHY & GRAPHIC DESIGN TRAINING CENTRE HYDERABAD - 500 012.

Director

Calligraphy and Graphic Design Training Centre - New Delhi

Regd.No.: 418 / 2016

ISO 9001 : 2008 Certified Organization

Certificate course in Hand Writing

This is certificate that Ms./Mrs./Mr. Kodali Raghunadh

S/o, D/o. K. Venkata Satyanarayana ....has successfully completed

Hand Writing course during the Academic

Student Class III B.Com. Computer Applications.

Year 2022

SRR & CVR Government Degree College [A], Vijayawada

Instructor - Calligraphy

LIMRA INSTITUTE OF CALLIGRAPHY & GRAPHIC DESIGN TRAINING CENTRE HYDERABAD - 500 012.

Director

Calligraphy and Graphic Design
Training Centre - New Delhi

Regd.No.: 418 / 2016

ISO 9001 : 2008 Certified Organization

Certificate course in Hand Writing

This is certificate that Ms./Mrs./Mr...Korada...Suguna.....

S/o, D/o...Korada...Ramu.....has successfully completed

Hand Writing course during the Academic

Student Class III B.Com Computer Applications.

Year .....

SRR & CVR Government Degree College [A], Vijayawada

Instructor - Calligraphy

LIMRA INSTITUTE OF CALLIGRAPHY
& GRAPHIC DESIGN TRAINING CENTRE
HYDERABAD - 500 012.

Director

Calligraphy and Graphic Design
Training Centre - New Delhi

Regd.No.: 418 / 2016

ISO 9001 : 2008 Certified Organization

Certificate course in Hand Writing

This is certificate that Ms./Mrs./Mr. Katta. Jagadish.....

S/o, D/o. Katta. Kotaiah.....has successfully completed

Hand Writing course during the Academic

Student Class III. B. Com Computer Applications.

Year ....2022.....

SRR&CVR Government Degree College [A], Vijayawada.

Instructor - Calligraphy

LIMRA INSTITUTE OF CALLIGRAPHY
& GRAPHIC DESIGN TRAINING CENTRE
HYDERABAD - 500 012.

Director

Calligraphy and Graphic Design Training Centre - New Delhi

Regd.No.: 418 / 2016

ISO 9001 : 2008 Certified Organization

Certificate course in Hand Writing

This is certificate that Ms./Mrs./Mr. P. Rama Krishna Reddy.

S/o, D/o. P. Janardhana Reddy. has successfully completed

Hand Writing course during the Academic

Student Class III B.Com - Computer Applications.

Year 2022

SRR & CVR Government Degree College [A], Vijayawada

Instructor - Calligraphy

LIMRA INSTITUTE OF CALLIGRAPHY & GRAPHIC DESIGN TRAINING CENTRE HYDERABAD-500 012.

Director

Calligraphy and Graphic Design
Training Centre - New Delhi

Regd.No.: 418 / 2016

ISO 9001 : 2008 Certified Organization

Certificate course in Hand Writing

This is certificate that Ms./Mrs./Mr. Jampani. Jyothirmai .....

S/o, D/o. Jampani ... Srinivas .....*has successfully completed*

Hand Writing course during the Academic

Student Class III. B.Com Computer Applications

Year ...2022.....

SRR & CVR Government Degree College[A], Vijayawada

Instructor - Calligraphy

LIMRA INSTITUTE OF CALLIGRAPHY
& GRAPHIC DESIGN TRAINING CENTRE
HYDERABAD - 500 012.

Director

Calligraphy and Graphic Design
Training Centre - New Delhi

Regd.No.: 418 / 2016

ISO 9001 : 2008 Certified Organization

Certificate course in Hand Writing

This is certificate that Ms./Mrs./Mr...Chevuri...Eswari.....

S/o, D/o...Chevuri...Apparao.....has successfully completed

Hand Writing course during the Academic

Student Class III..B.Com. Computer Applications.

Year ...2022.....

SRR & CVR Government Degree College [A] Vijayawada.

Instructor - Calligraphy

LIMRA INSTITUTE OF CALLIGRAPHY
& GRAPHIC DESIGN TRAINING CENTRE
Hyderabad-500 012.

Director

Calligraphy and Graphic Design
Training Centre - New Delhi

Regd.No.: 418 / 2016

ISO 9001 : 2008 Certified Organization

Certificate course in Hand Writing

This is certificate that Ms./Mrs./Mr. Sayyad Habiba

S/o, D/o. Sayyad Hussain has successfully completed

Hand Writing course during the Academic

Student Class III B.Com. Computer Applications.

Year 2022

SRR & CVR Government Degree College (A), Vijayawada.

Instructor - Calligraphy

Director

LIMRA INSTITUTE OF CALLIGRAPHY
& GRAPHIC DESIGN TRAINING CENTRE
HYDERABAD - 500 012.

Calligraphy and Graphic Design
Training Centre - New Delhi

Regd.No.: 418 / 2016

ISO 9001 : 2008 Certified Organization

Certificate course in Hand Writing

This is certificate that Ms./Mrs./Mr. Tummuru Lokesh Reddy.

S/o, D/o. Tummuru Siva Satyanarayana *has successfully completed*

Hand Writing course during the Academic

Student Class III B.Com. Computer Applications.

Year 2022

SRR&CVR Government Degree College [A], Vijayawada.

Instructor - Calligraphy

LIMRA INSTITUTE OF CALLIGRAPHY
& GRAPHIC DESIGN TRAINING CENTRE
HYDERABAD - 500 012.

Director

Calligraphy and Graphic Design
Training Centre - New Delhi

Regd.No.: 418 / 2016

ISO 9001 : 2008 Certified Organization

Certificate course in Hand Writing

This is certificate that Ms./Mrs./Mr. Yarasi...Eshwar...Vyas.....

S/o, D/o..... Yarasi...Haripsthuluru.....*has successfully completed*

Hand Writing course during the Academic

Student Class III...B.A [EPJ]

Year 2022.....

SRR & CVR Government Degree College [A], Vijayawada.

Instructor - Calligraphy

LIMRA INSTITUTE OF CALLIGRAPHY
& GRAPHIC DESIGN TRAINING CENTRE
HYD 012.

Director

Calligraphy and Graphic Design
Training Centre - New Delhi

Regd.No.: 418 / 2016

ISO 9001 : 2008 Certified Organization

Certificate course in Hand Writing

This is certificate that Ms./Mrs./Mr. Uriviti. Sravana Lakshmi

S/o, D/o. Uriviti. Srinivas Rao has successfully completed

Hand Writing course during the Academic

Student Class III. B.Com. Computer Applications.

Year ...2022.....

SRR&CVR Govenmet Degree College[A], Vijayawada

Instructor - Calligraphy

UMA INSTITUTE OF CALLIGRAPHY & GRAPHIC DESIGN TRAINING CENTRE HYDERABAD-500 012.

Director

Calligraphy and Graphic Design
Training Centre - New Delhi

Regd.No.: 418 / 2016

ISO 9001 : 2008 Certified Organization

Certificate course in Hand Writing

This is certificate that Ms./Mrs./Mr. Uriviti Sravana Lakshmi.

S/o, D/o. Uriviti Srinivas Rao has successfully completed

Hand Writing course during the Academic

Student Class III B.Com. Computer Applications.

Year 2022

SRR&CVR Govenrmet Degree College[A], Vijayawada

Instructor - Calligraphy

LIMRA INSTITUTE OF CALLIGRAPHY & GRAPHIC DESIGN TRAINING CENTRE HYDERABAD-500 012.

Director

Calligraphy and Graphic Design
Training Centre - New Delhi

Regd.No.: 418 / 2016

ISO 9001 : 2008 Certified Organization

Certificate course in Hand Writing

This is certificate that Ms./Mrs./Mr. Uriviti. Sravana Lakshmi.

S/o, D/o. Uriviti. Srinivas Rao has successfully completed

Hand Writing course during the Academic

Student Class III. B.Com. Computer Applications.

Year 2022

SRR&CVR Govermet Degree College[A], Vijayawada

Instructor - Calligraphy

LIMRA INSTITUTE OF CALLIGRAPHY & GRAPHIC DESIGN TRAINING CENTRE HYDERABAD-500 012.

Director

Calligraphy and Graphic Design
Training Centre - New Delhi

Regd.No.: 418 / 2016

ISO 9001 : 2008 Certified Organization

Certificate course in Hand Writing

This is certificate that Ms./Mrs./Mr. K. Hema Bhargavi

S/o, D/o. K. Adi Narayan has successfully completed

Hand Writing course during the Academic

Student Class III B.Com - Computer Applications.

Year 2022

SRR & CVR Government Degree College (A), Vijayawada

Instructor - Calligraphy

Director

LIMRA INSTITUTE OF CALLIGRAPHY
& GRAPHIC DESIGN TRAINING CENTRE
HYDERABAD - 500 012.

Calligraphy and Graphic Design
Training Centre - New Delhi

Regd.No.: 418 / 2016

ISO 9001 : 2008 Certified Organization

Certificate course in Hand Writing

This is certificate that Ms./Mrs./Mr. Velupukonda. Krupa Indu...

S/o, D/o. Velupukonda. Veerachari. has successfully completed

Hand Writing course during the Academic

Student Class III. B. Com. Computer Applications.

Year ....2022.....

SRR & CVR Government Degree College[A] Vijayawada

Instructor - Calligraphy

LIMRA INSTITUTE OF CALLIGRAPHY
& GRAPHIC DESIGN TRAINING CENTRE
HYD 012.

Director

Calligraphy and Graphic Design
Training Centre - New Delhi

Regd.No.: 418 / 2016

ISO 9001 : 2008 Certified Organization

Certificate course in Hand Writing

This is certificate that Ms./Mrs./Mr. Gentela. Siva

S/o, D/o. Gentela. Venkatesh has successfully completed

Hand Writing course during the Academic

Student Class III. B.A [EPS]

Year 2022

SRR & CVR Government Degree College [A], Vijayawada.

Instructor - Calligraphy

UMRA INSTITUTE OF CALLIGRAPHY
& GRAPHIC DESIGN TRAINING CENTRE
HYDERABAD - 500 012.

Director

Calligraphy and Graphic Design
Training Centre - New Delhi

Regd.No.: 418 / 2016

ISO 9001 : 2008 Certified Organization

Certificate course in Hand Writing

This is certificate that Ms./Mrs./Mr. Rauthu Lokesh

S/o, D/o. Rauthu Chinni has successfully completed

Hand Writing course during the Academic

Student Class III B.Com. Computer Applications.

Year 2022

SRR&CVR Government Degree College[A] Vijayawada.

Instructor - Calligraphy

LIMRA INSTITUTE OF CALLIGRAPHY
& GRAPHIC DESIGN TRAINING CENTRE
HYDERABAD - 500 012.
Director

Calligraphy and Graphic Design
Training Centre - New Delhi

Regd.No.: 418 / 2016

ISO 9001 : 2008 Certified Organization

Certificate course in Hand Writing

This is certificate that Ms./Mrs./Mr. Pothureddy ..... Ramya .....

S/o, D/o. P. Malleswara Rao ..... has successfully completed

Hand Writing course during the Academic

Student Class III B.Com. Computer Applications.

Year 2022 .....

SRR & CVR Government Degree College [A], Vijayawada

Instructor - Calligraphy

LIMRA INSTITUTE OF CALLIGRAPHY
& GRAPHIC DESIGN TRAINING CENTRE
HYDERABAD - 500 012.

Director

Calligraphy and Graphic Design
Training Centre - New Delhi

Regd.No.: 418 / 2016

ISO 9001 : 2008 Certified Organization

Certificate course in Hand Writing

This is certificate that Ms./Mrs./Mr. Pilleli Adilakshmi

S/o, D/o. Pilleli ArjunaRao has successfully completed

Hand Writing course during the Academic

Student Class III B.Com. Computer Applications.

Year 2022

SRR & CVR Government Degree College[A], Vijayawada.

Instructor - Calligraphy

LIMRA INSTITUTE OF CALLIGRAPHY & GRAPHIC DESIGN TRAINING CENTRE HYDERABAD - 500 012

Director

Calligraphy and Graphic Design
Training Centre - New Delhi

Regd.No.: 418 / 2016

ISO 9001 : 2008 Certified Organization

Certificate course in Hand Writing

This is certificate that Ms./Mrs./Mr. P. Leela Ratna Mani

S/o, D/o. Peddi Reddy Raghava has successfully completed

Hand Writing course during the Academic

Student Class III B.Com Computer Applications.

Year 2022

SRR & CVR Government Degree College[A], Vijayawada

Instructor - Calligraphy

LIMRA INSTITUTE OF CALLIGRAPHY
& GRAPHIC DESIGN TRAINING CENTRE
HYDERABAD - 500 012.

Director

Calligraphy and Graphic Design
Training Centre - New Delhi

Regd.No.: 418 / 2016

ISO 9001 : 2008 Certified Organization

Certificate course in Hand Writing

This is certificate that Ms./Mrs./Mr. Lingapagu Rakesh

S/o, D/o. L. Rajini Kanth has successfully completed

Hand Writing course during the Academic

Student Class III B.Com. Computer Applications

Year 2022

SRR & CVR Government Degree College[A], Vijayawada.

Instructor - Calligraphy

LIMRA INSTITUTE OF CALLIGRAPHY & GRAPHIC DESIGN TRAINING CENTRE HYDERABAD - 500 012.

Director

Calligraphy and Graphic Design
Training Centre - New Delhi

Regd.No.: 418 / 2016

ISO 9001 : 2008 Certified Organization

Certificate course in Hand Writing

This is certificate that Ms./Mrs./Mr. Tenke. Naga. Vasantha.....

S/o, D/o. Tenke. Satyanarayana. has successfully completed

Hand Writing course during the Academic

Student Class III. B.A [EPS].

Year ...2022.....

SRR & CVR Government Degree College[A], Vijayawada.

Instructor - Calligraphy

LIMRA INSTITUTE OF CALLIGRAPHY
& GRAPHIC DESIGN TRAINING CENTRE
HYDERABAD - 500 012.

Director

Calligraphy and Graphic Design
Training Centre - New Delhi

Regd.No.: 418 / 2016

ISO 9001 : 2008 Certified Organization

Certificate course in Hand Writing

This is certificate that Ms./Mrs./Mr. Shaik. Baji.

S/o, D/o. Shaik. Meeravali. has successfully completed

Hand Writing course during the Academic

Student Class III. B.Com Computer Applications.

Year 2022

SRR & CVR Government Degree College[A], Vijayawada.

Instructor - Calligraphy

LIMRA INSTITUTE OF CALLIGRAPHY
& GRAPHIC DESIGN TRAINING CENTRE
HYDERABAD 500 012.
Director

Calligraphy and Graphic Design
Training Centre - New Delhi

Regd.No.: 418 / 2016

ISO 9001 : 2008 Certified Organization

Certificate course in
Hand Writing

This is certificate that Ms./Mrs./Mr. Depalli. Krishna. Veni.....

S/o, D/o. Depalli. Krishna. *has successfully completed*

Hand Writing course during the Academic

Student Class III. B.Sc [MPCs]

Year ....2022.....

SRR & CVR Goverment Degree College(A), Vijayawada.

Instructor - Calligraphy

LIMRA INSTITUTE OF CALLIGRAPHY & GRAPHIC DESIGN TRAINING CENTRE HYD. *Director* 012.

THANK YOU

International Journal of Advanced Research in Engineering and Technology (IJARET)
Volume 11, Issue 10, October 2020, pp.28-35, Article ID: IJARET_11_10_003
Available online at http://iaeme.com/Home/issue/IJARET?Volume=11&Issue=10
ISSN Print: 0976-6480 and ISSN Online: 0976-6499
DOI: 10.34218/IJARET.11.10.2020.003

© **IAEME** Publication **Scopus** Indexed

FUZZY REGULAR SUBSEMIGROUPS OF PARTIALLY ORDERED Γ- SEMIGROUPS

Srinivas Telikepalli*
Dept. of Mathematics, QIS INSTITUTE OF TECHNOLOGY, Ongole, India

A. Gangadhara Rao
Dept. of Mathematics, V.S.R. & N.V.R. College, Tenali, India

K.V. Naga Lakshmi
Dept. of Mathematics, SRR & CVR Govt Degree College, Vijayawada, India

A. Anjaneyulu
Dept. of Mathematics, V.S.R. & N.V.R. College, Tenali, India

Corresponding Authors*

ABSTRACT

In this paper, the terms Fuzzy regular Γ-Subsemigroup, λ-Cut, Fuzzy left and right regular Γ-Subsemigroup, Fuzzy intra regular Γ-Subsemigroup, Fuzzy completely Regular Γ-subsemigroup, ideal generated by the ordered fuzzy point a_λ, fuzzy semi simple in a PO Gamma semigroup are introduced. It is proved that (1) If f is fuzzy regular Γ-subsemigroup of S then f is fuzzy Idempotent,(2) If f is fuzzy completely regular then f is regular, left regular and right regular, (3) If a_λ is fuzzy regular then a_λ is fuzzy semi simple, (4) If an orderd fuzzy point a_λ of S is left(right) regular Γ-semigroup then a_λ is fuzzy semi simple, (5) If a_λ is fuzzy intra regular Gamma semigroup then $a_\lambda$is fuzzy semi simple.

Mathematical Subject Classification (2010): 20M12; 20M17; 20N25.

Keywords: Fuzzy regular Γ-subsemigroup, fuzzy completely regular Γ-subsemigroup, fuzzy intra regular Γ -sub semigroup, fuzzy semisimple

Cite this Article: Srinivas Telikepalli, A. Gangadhara Rao, K.V. Naga Lakshmi and A. Anjaneyulu, Fuzzy Regular Subsemigroups of Partially Ordered Γ- Semigroups, *International Journal of Advanced Research in Engineering and Technology (IJARET),* 11(10), 2020, pp.28-35,
http://iaeme.com/Home/issue/IJARET?Volume=11&Issue=10

1. INTRODUCTION

The algebraic theory of semigroups has been extensively studied by CLIFFORD [2],[3],PETRICH [5] and LJAPIN [4]. *Anjaneyulu* [1] puts forward the ideal theory in general semigroups. In this article, we introduce the concepts of fuzzy regular elements, fuzzy completely regular elements and fuzzy intra regular elements in Po-Γ-semigroup. *Lzadeh* proposes the concept of fuzzy subset in 1965. Since then, a series of studies on fuzzy sets results fuzzy logic, fuzzy set theory, fuzzy algebra, etc. we Introduced fuzzy regular Γ-subsemigroup, fuzzy completely regular Γ-subsemigroup, Fuzzy intra regular semigroups and fuzzy semisimple concepts.

2. PRELIMINARIES

Definition 2.1: A **Γ -** semigroup S with an ordered relation $\leq$ is said to be po - **Γ-** semigroup if S is a partially ordered set such that $a \leq b \Rightarrow a\gamma c \leq b\gamma c$ and $c\gamma a \leq c\gamma b$ for all a, b, c ∈ S and ∀ γ ∈ Γ .

DEFINITION 2.2: A function f from S to the closed interval [0,1] is called a ***fuzzy subset*** of S. The po- **Γ**-semigroup S itself is a fuzzy subset of S such that S(x)=1, $\forall x \in S$. It is denoted by S or 1.

DEFINITION 2.3: Let A be a non-empty subset of S. We denote f_A, ***the characteristic mapping*** **of A**. i.e., The mapping of S into [0,1] defined by

$f_A(x)=\begin{cases}1 \; if \; x \in A \\ 0 \; if \; x \notin A\end{cases}$ **then f_A is fuzzy subset of S**

DEFINITION 2.4: Let f and g be two fuzzy subsets of po semigroup S. Then ***the inclusion relation*** f⊆g is defined by f(x)≤g(x),∀x∈ S and $f \cup g$, $f \cap g$ are defined by

$(f \cup g)(x) = max\{f(x), g(x)\} = f(x) \vee g(x), \forall x \in S$,

$(f \cap g)(x) = min\{f(x), g(x)\} = f(x) \wedge g(x), \forall x \in S.$

DEFINITION 2.5: ([13]) Let (S, ≤) be a po- Γ- semigroup and f,g be two fuzzy subsets of S. For $x \in S$ **the product** $f \Gamma g$ is defined by $(f \Gamma g)(x) = \begin{cases} V_{x \leq y\gamma z} \; f(y) \wedge g(z), & if \; x \leq y\gamma z \\ 0 & otherwise \end{cases}$

DEFINITION 2.6: Let S be a po- **Γ-** semigroup. For H⊆ S

we define **(H]**={t∈S / t≤ h for some h∈H}. For H={a} we write (a]= ({a}] = { t∈S / t ≤a}

DEFINITION 2.7: ([14]) **A** fuzzy subset f of a po- **Γ-** semigroup S is called

fuzzy Γ-subsemigroup of S if $f(x\gamma y) \geq f(x) \wedge f(y)$, ∀x, y ∈ S and $\gamma \in \Gamma$.

PROPOSITION 2.8: ([15]) **A fuzzy subset f of a** po- **Γ-** semigroup **S is fuzzy**

Γ-**subsemigroup of S⇔** $f\Gamma f \subseteq f$.

DEFINITION 2.9: A fuzzy subset f of a po- Γ- semigroup S is called ***fuzzy po*** Γ-***subsemigroup*** of S if (i) $x \leq y$ then $f(x) \geq f(y)$ (ii) $f(x\gamma y) \geq f(x) \wedge f(y)$, $\forall x, y \in S, \forall \gamma \in \Gamma$.

DEFINITION 2.10:[16]Let S be a po- Γ- semigroup . A fuzzy subset f of S is called a ***fuzzy left ideal*** of S if (i) $x \leq y$ *then* $f(x) \geq f(y)$ (ii) $f(x\gamma y) \geq f(y), \forall x, y \in S, \forall \gamma \in \Gamma$.

LEMMA 2.11: [16] Let S be a po- Γ- semigroup and f be a fuzzy subset of S. Then f is a fuzzy left ideal of S if and only if f satisfies that (i) x ≤ y then f(x) ≥ f(y) ∀ x,y∈S (ii) S**Γ**f ⊆ f.

DEFINITION 2.12: [16] Let S be a po- Γ- semigroup. A fuzzy subset f of S is called a f***uzzy right ideal*** of S if (i) x≤y then f(x)≥f(y) (ii) f(xγy) ≥ f(x), ∀ x,y∈S,∀$\gamma \in \Gamma$.

LEMMA 2.13: [16] Let S be a po- Γ- semigroup and f be a fuzzy subset of S. Then f is a fuzzy right ideal of S if and only if f satisfies that (i) $x \leq y$ **then** $f(x) \geq f(y)$ ∀ $x,y \in S$ **(ii)** f

$\Gamma s \subseteq f$. **DEFINITION 2.14:** [16]Let S be a po- Γ- semigroup . A fuzzy subset f of S is called a ***fuzzy ideal*** of S if (i) $x \leq y$ *then* $f(x) \geq f(y)$ (ii) $f(x\gamma y) \geq f(y)$, $f(x\gamma y) \geq f(x)$, $\forall\, x,y \in S, \forall \gamma \in \mathbf{\Gamma}$.

Example 1. Let S be the set of all non positive integers without zero and **Γ**

be the set of all non positive even integers without zero. Then S is a **Γ** -semigroup

if aγb denotes the usual multiplication of integers a, γ , b where a, b ∈ S and $\gamma \in \mathbf{\Gamma}$. Again with respect to usual ≤ of Z, S becomes a po- **Γ** -semigroup. Let f be a fuzzy subset of S, defined as follows

$$f(x) = \begin{cases} 0.1 & if\ x = -1 \\ 0.3 & if\ x = -2 \\ 0.5 & if\ x < -2 \end{cases}$$ Then f becomes a fuzzy ideal of S".

LEMMA 2.15: [16] Let S be a po- Γ- semigroup and f be a fuzzy subset of S. Then f is a fuzzy ideal of S if and only if f satisfies that (i) $x \leq y$ *then* $f(x) \geq f(y)$ $\forall\, x,y \in S$

(ii) $f\,\Gamma s \subseteq f$ *and* $s\,\Gamma f \subseteq f$.

DEFINITION 2.16: Let S be a po- Γ- semigroup . A fuzzy ideal f of S is called ***idempotent*** if

$f^2 = f\Gamma\, f\, = f$.

3. SPECIAL ELEMENTS IN FUZZY REGULAR SUBSEMIGROUP OF PO –Γ- SEMIGROUP:

DEFINITION 3.1: An element 'a' of a po- Γ- semigroup S is said to be ***regular*** if there exist

$x \in$S such that a≤ a$\alpha x\beta$a for some $x \in$A and α,β∈Γ.

DEFINITION 3.2: A po- Γ- semigroup S is said to be ***regular semigroup*** provided every element is regular.

DEFINITION 3.3: Let S be a po- Γ- semigroup and $x \in$S, α, β∈Γ. Define

$R_x = \{x'/x' \in s, x \leq x\alpha x'\beta x\}$. Let f be a fuzzy Γ- subsemigroup of S if $\forall\, x \in S$ there exist

$x' \in R_x$ such that $f\ (x) \leq f\ (x')$ provided $f(x) \neq 0$ then f is called ***fuzzy regular*** Γ-***subsemigroup*** of S.

THEOREM 3.4: Let A be a non-empty subset of po- Γ- semigroup S . A is regular

Γ**-subsemigroup of S if and only if** f_A**, the characteristic function of A is a fuzzy regular Γ-subsemigroup of S.**

***Proof*:** Suppose A is regular Γ- subsemigroup of S . Let x,y∈A and γ ∈ Γ ⇒ xγy∈A. Therefore$f_A\ (x\gamma y) \geq f_A\ (x) \wedge f_A\ (y)$.

Let x∈A ⇒ $f_A\ (x) = 1$. Then from the regularity of A there exists $x^1 \in R_x$ such that $x^1 \in A$ and $f_A\ (x') = 1$. ⇒ $f_A\,(x) \leq f_A\ (x')$. Therefore f_A is a fuzzy regular Γ-subsemigroup of S.

Conversely suppose that f_A is a fuzzy regular Γ - subsemigroup of S. Let $\gamma \in \Gamma$ and x,y ∈A ⇒ $f_A\ (x) = f_A\,(y) = 1$ and f_A is fuzzy regular-subsemigroup of S.

⇒ $f_A(x\gamma y) \geq f_A(x) \wedge f_A(y) = 1 \Rightarrow f_A(x\gamma y) = 1 \Rightarrow x\gamma y \in A \Rightarrow$ A is a Γ-subsemigroup of S.

Let x∈A ⇒ $f_A\ (x) = 1$. Since f_A is a fuzzy regular, there exists$x^1 \in R_x$such that

$f_A\,(x) \leq f_A\,(x')$. ⇒ $f_A\ (x') \geq 1 \Rightarrow x^1 \in A$

Therefore A is regular Γ –subsemigroup of S.

DEFINITION 3.5: Let f be a fuzzy subset of a po- Γ- semigroup S. Let $\lambda \in [0,1]$. Define

$f_\lambda = \{x \in S/f\ (x) \geq \lambda\}$ is the ***λ-cut of f.***

THEOREM 3.6: Let S be a po- Γ- semigroup. f is fuzzy Γ- subsemigroup of S if and only if $\forall\ \boldsymbol{\lambda} \in [\mathbf{0}, \mathbf{1}]$, $\boldsymbol{f_\lambda}$ is a Γ-subsemigroup of S.

***Proof*:** Assume that f is a fuzzy Γ-subsemigroup of S.

Let $\gamma \in \Gamma$ *and* $a, b \in f_\lambda \Rightarrow f(a) \geq \lambda, f(b) \geq \lambda$

Since $f(a\gamma b) \geq f(a) \wedge f(b) \geq \lambda \wedge \lambda = \lambda \Rightarrow f(a\gamma b) \geq \lambda \Rightarrow a\gamma b \in f_\lambda$

$\Rightarrow f_\lambda$ is Γ- subsemigroup of S.

Conversely suppose that f_λ is a Γ-subsemigroup of S.

Suppose there exists one $x_1, y_1 \in f_\lambda$ *and* $\gamma \in \boldsymbol{\Gamma}$ **s**uchthat

$f(x_1\gamma y_1) < f(x_1) \wedge f(y_1) < f(x_1) \Rightarrow f(x_1\gamma y_1) < f(x_1)$

Define $\lambda = \frac{1}{2}[f(x_1) - f(x_1\gamma y_1)]$ then $\lambda \in (0,1]$

and $0 \leq f(x_1\gamma y_1) < \lambda \leq 1$, $0 < \lambda < f(x_1) \leq 1$so that $x_1 \in f_\lambda$, similarly $y_1 \in f_\lambda \Rightarrow x_1\gamma y_1 \in f_\lambda \Rightarrow f(x_1\gamma y_1) \geq \lambda$

But $f(x_1\gamma y_1) < \lambda$ which is a contradiction.

Therefore $f(x\gamma y) \geq f(x) \wedge f(y), \forall x, y \in S, \gamma \in \boldsymbol{\Gamma} \Rightarrow f_\lambda$ is Γ- subsemigroup of S.

THEOREM 3.7: Let f be a fuzzy subset of a po- Γ- semigroup S. f is a fuzzy regular Γ-subsemigroup of S if and only if $\forall\ \boldsymbol{\lambda} \in (\mathbf{0}, \mathbf{1}]$, $\boldsymbol{f_\lambda}$ is a regular Γ-subsemigroup of S provided $\boldsymbol{f_\lambda} \neq \emptyset$.

***Proof*:** Assume that f is fuzzy regular Γ-subsemigroup of S. From theorem 3.6, f_λ is Γ-subsemigroup of S.

Let $x \in f_\lambda$ since f is fuzzy regular $\exists\ x' \in R_x$ such that $f(x) \leq f(x') \Rightarrow f(x') \geq \lambda$

$\Rightarrow x' \in f_\lambda$.

Therefore $\forall x \in f_\lambda \exists\ x' \in f_\lambda$and α, β∈**Γ** such that $x \leq x\alpha x'\beta x \Rightarrow f_\lambda$is a regular Γ-subsemigroup of S.

Conversely, suppose that f_λ is a regular **Γ**-subsemigroup of S provided $f_\lambda \neq \emptyset$

Assume that f is not fuzzy regular ⇒ there exists $x \in S$ such that f(x)≠ 0 and$\forall\ x' \in R_x$,

$f(x) > f(x')$. Set $\lambda = f(x)$, clearly $x \in f_\lambda$ and $\forall\ x' \in R_x \Rightarrow \lambda = f(x) > f(x') \Rightarrow x' \notin f_\lambda$

Which is a contradiction, since f_λ is regular. Therefore *f* is fuzzy regular Γ -subsemigroup of S.

THEOREM 3.8: Let S be a po- Γ- semigroup. If *f is* fuzzy regular Γ-subsemigroup of S then $\boldsymbol{f\Gamma f = f}$.

Proof: Let f be a fuzzy subset of S .

From [2.8] If f is a fuzzy Γ-subsemigroup of S if and only if $f\Gamma f \subseteq f$.

Let $x \in S$ if f(x) =0 then $(f\Gamma f)(x) \leq f(x) \Rightarrow (f\Gamma f)(x) = f(x) = 0$

if $f(x) \neq 0$ then $\exists\ x' \in R_x$ such that $f(x) \leq f(x')$,since f is fuzzy regular

Now$(f\ \boldsymbol{\Gamma} f)(x) =$

$= \underset{x \leq y\gamma z}{V} [f(y) \wedge f(z)] \qquad = \underset{x \leq x\ \alpha x'\ \beta x}{V} [f(x) \wedge f(x'\beta x)] \geq f(x) \wedge f(x') \wedge f(x)$

$= f(x), \forall x \in S$

$f \subseteq f\Gamma f.$

Therefore $f\ \Gamma f = f$ if f is fuzzy regular.

COROLLARY 3.9: Let S be a po- Γ- semigroup and f is fuzzy ideal of S. If f is fuzzy regular Γ-subsemigroup of S then f is fuzzy idempotent.

DEFINITION 3.10: [9] Let f be a fuzzy subset of a po- Γ- semigroup S. We define $(f]$ by $(f](x) = \bigvee_{x \le y} f(y), \forall x \in S$

NOTE 3.11: Clearly $f \subseteq (f]$.

DEFINITION 3.12: [9]Let S be a po- Γ- semigroup , $a \in S$ and $\lambda \in [0,1]$. An ***ordered fuzzy point a***

: $S \to [0,1]$ defined by

$$a_\lambda(x) = \begin{cases} \lambda & if\ x \in (a] \\ 0 & if\ x \notin (a] \end{cases}$$

clearly a_λ is a fuzzy subset of S.

LEMMA 3.13: [9] If a_λ is an ordered fuzzy point of S then $a_\lambda = (a_\lambda]$.

NOTE 3.14: Let f be a fuzzy subset of a po- Γ- semigroup S then $(f] = \bigcup_{y_\lambda \in (f]} y_\lambda$

DEFINITION 3.15: Let f be a fuzzy subset of a po- Γ- semigroup S. Then $\forall x \in S$, **the fuzzy**

Subset $(x\alpha f\beta x)$ of S is defined by $\forall y \in S$, $(x\alpha f\beta x](y) = \begin{cases} \bigvee_{y \le x\alpha s\beta x} f(s) & if\ \exists y \le x\alpha s\beta x \\ 0 & otherwise \end{cases}$

THEOREM 3.16: If f is a fuzzy Γ- subsemigroup of po- Γ- semigroup S. Then f is fuzzy regular if and only if $\forall x \in S$, $(x\alpha f\beta x](x) \ge f(x)$ provided $f(x) \ne 0$

Proof: Suppose f is fuzzy regular.

Consider $(x\alpha f\beta x](x) = \bigvee_{x \le x\alpha s\beta x} f(s) = \bigvee_{x \le x\alpha x^1\beta x} f(x') \ge f(x') \ge f(x)$,

Since f is fuzzy regular $\Rightarrow (x\alpha f\beta x)(x) \ge f(x)\ \forall x \in S$.

Conversely assume that $\forall x \in S$, $(x\alpha f\beta x)(x) \ge f(x)$.

Since $f(x) \le (x\alpha f\beta x](x) = \bigvee_{x \le x\alpha x^1\beta x} f(x') = \bigvee_{x \le x\alpha x^1\beta x} f(x')\ provided\ f(x) \ne 0$

That is $\forall x \in S\ \exists$ at least one x' such that $x \le x\alpha x'\beta x\ and\ f(x) \le f(x')\ since\ f(x) \ne 0$

$\Rightarrow f$ is fuzzy regular.

COROLLARY 3.17: If an ordered fuzzy point a_λ of a po- Γ- semigroup S is regular if and only if $\forall x \in S$, $(x\alpha a_\lambda\beta x](x) \ge a_\lambda(x)$ provided $a_\lambda(x) \ne 0$.

***Proof*:** Proof follows from the Theorem 3.14.

DEFINITION 3.18: Let S be a po- Γ- semigroup and $x \in S$, $\alpha, \beta \in \Gamma$.

Define $LR_x = \{x' \in S / x \le x\alpha x\beta x'\}$.

Let f be a fuzzy Γ-subsemigroup of S. For every $\alpha, \beta \in \Gamma$, $x \in S$, $\exists\ x' \in LR_x \ni f(x) \le f(x')$ provided f(x)≠ 0 then f is called ***fuzzy left regular*** Γ- ***subsemigroup*** of S.

DEFINITION 3.19: Let S be a po- Γ- semigroup and $x \in S$, $\alpha, \beta \in \Gamma$. Define $RR_x = \{x' \in S / x \le x'\alpha x\beta x\}$. Let f be a fuzzy Γ-subsemigroup of S.

For every $x \in Sand, \alpha, \beta \in \Gamma\ \exists\ x' \in RRx \ni f(x) \leq f(x')$ provided f(x)≠ 0 then f is called ***fuzzy right regular*** Γ-***subsemigroup***of S.

DEFINITION 3.20: Let S be a po- Γ- semigroup and $\alpha, \beta, \gamma \in \Gamma, x \in S$,

define$IR_x = \{x' \in S / x \leq x_1 \alpha a \beta a \gamma x_2\}$. Let f *be* a fuzzy Γ-subsemigroup of S. For every

$x \in S\ \exists\ (x1, x2) \in IRx \ni f(x) \leq f(x1) \wedge f(x2)$ provided f(x) ≠ 0 then f is called fuzzy Intraregular Γ-subsemigroupof S.

DEFINITION 3.21: Let S be a po- Γ- semigroup and $x \in S$, α,β∈Γ.

Define $R_x = \{x'/x' \in s, x \leq x\alpha x'\beta x\}$and $C_x = \{x' \in S/x\alpha x' = x'\beta x\}$.Let f be a fuzzy Γ-subsemigroup of S and for every $x \in S\ \exists x' \in R_x \cap C_x$

$\ni f(x) \leq f(x')$ provided f(x)≠ 0 then f is called fuzzy completely regular Γ-subsemigroup of S.

THEOREM3.22: Let S be a po- Γ- semigroup and f is a fuzzy Γ-subsemigroup of S. If f is fuzzy completely regular then f is regular, left regular and right regular.

***Proof*:** Suppose that f is completely regular.

Then for every α, β ∈ Γ, $x \in S\ \exists x' \in Rx \cap Cx \ni f(x) \leq f(x')$ provided f(x)≠ 0 . Since $x' \in Rx \Rightarrow x \leq x\alpha x'\beta x$ and $f(x) \leq f(x')$, f(x)≠ 0

⇒ f is fuzzy regular.

Now for every $x \in S\ \exists x' \in Rx \cap Cx \ni f(x) \leq f(x')$ provided f(x)≠ 0 .

$\Rightarrow x \leq x\alpha x'\beta x$ and $x\alpha x' = x'\beta x$.

Consider $x \leq x\alpha x'\beta x = x\alpha x\alpha x' = (x\alpha)^2 x' \Rightarrow x \leq (x\alpha)^2 x'$and $f(x) \leq f(x')$

⇒ f is fuzzy left regular.

Also $x \leq x\alpha x'\beta x = x'\beta x\beta x = x'(x\beta)^2$. Therefore f is fuzzy right regular.

DEFINITION 3.23: Let$a \in S, \lambda \in (0,1]$. Define ***ideal generated by the ordered fuzzy point*** a_λ

of S by $< a_\lambda >(x) = \begin{cases} \lambda, & \text{if } x \in (a) = (a \cup a\Gamma S \cup S\Gamma a \cup S\Gamma a\Gamma S] = (s'as') \\ 0, & \text{othewise} \end{cases}$

DEFINITION 3.24: An ordered fuzzy element a_λ of a po- Γ- semigroup S is said to be ***fuzzy semisimple*** if $a_\lambda \subseteq < a_\lambda >^2$**.**

NOTE 3.25: Clearly $a_\lambda \subseteq < a_\lambda >$

THEOREM 3.26: Let S be a po- Γ- Semi group and a_λ is a fuzzy Γ- subsemigroup of S. If a_λ is fuzzy regular then a_λ is fuzzy semisimple.

Proof: Suppose a_λ is fuzzy regular.

Consider $< a_\lambda >^2(x) = \bigvee_{x \leq yyz} [< a_\lambda > (y) \wedge < a_\lambda > (z)]$

$$\geq < a_\lambda > (y) \wedge < a_\lambda > (z)$$
$$\geq < a_\lambda > (x\alpha x') \wedge < a_\lambda > (x)$$
$$\geq a_\lambda(x\alpha x') \wedge a_\lambda(x) \geq a_\lambda(x) \wedge a_\lambda(x') \wedge a_\lambda(x)$$
$$\geq a_\lambda(x) \wedge a_\lambda(x) \wedge a_\lambda(x) = a_\lambda(x) \forall x \in S$$

$\Rightarrow a_\lambda \subseteq < a_\lambda >^2$

Therefore a_λ is fuzzy semisimple.

THEOREM 3.27: Let S be a po- Γ- Semi group. If an ordered fuzzy point $a_\lambda$of S is left(right) regular semigroup then a_λ is fuzzy semisimple.

***Proof*:** Suppose $a^{\lambda}$is fuzzy left regular. Then ∀ x∈S $\exists x^{'} \in LR^{x}$ such that
$a_\lambda(x) \leq a_\lambda(x^{'})$ provided $a_\lambda(x) \neq 0$.

Consider $< a_\lambda >^2 (x) = \bigvee_{x \leq y\gamma z}[< a_\lambda > (y) \wedge < a_\lambda > (z)]$

$\geq < a_\lambda > (y) \wedge < a_\lambda > (z)$

$\geq < a_\lambda > (x\alpha x) \wedge < a_\lambda > (x^{'})$

$\geq a_\lambda(x) \wedge a_\lambda(x) \wedge a_\lambda(x^{'})$

$\geq a_\lambda(x) \wedge a_\lambda(x^{'}) = a_\lambda(x)$

$\Rightarrow a_\lambda \subseteq < a_\lambda >^2$

Therefore a_λ is fuzzy semisimple.

Similarly if a_λ is fuzzy right regular semigroup then a_λ is fuzzy semisimple.

THEOREM 3.28: Let $\boldsymbol{a_\lambda}$ be an ordered fuzzy point of a po - Γ- semigroup S. If $\boldsymbol{a_\lambda}$ is fuzzy intra regular semigroup then $\boldsymbol{a_\lambda}$ is fuzzy semisimple.

***Proof*:** Let $a_\lambda$is fuzzy intra regular.

∀ x∈S ∃ $(x_1, x_2) \in IR_x \ni a_\lambda(x) \leq a_\lambda(x_1) \wedge a_\lambda(x_2)$ provided $a_\lambda(x) \neq 0$.

Consider $< a_\lambda >^2$(x) = $(< a_\lambda > o < a_\lambda >)(x)$

$$= \bigvee_{x \leq y\gamma z} |< a_\lambda > (y) \wedge < a_\lambda(z)|$$

$$\geq < a_\lambda > (y) \wedge < a_\lambda > (z)$$

$$\geq < a_\lambda > (x_1) \wedge < a_\lambda > (x\beta x\gamma x_2)$$

$$\geq a_\lambda(x_1) \wedge a_\lambda(x) \wedge a_\lambda(x\gamma x_2)$$

$$\geq a_\lambda(x_1) \wedge a_\lambda(x) \wedge a_\lambda(x_2)$$

$$\geq a_\lambda(x) \wedge a_\lambda(x) \wedge a_\lambda(x) = a_\lambda(x), \forall x \in S$$

$$\Rightarrow a_\lambda \subseteq < a_\lambda >^2$$

Therefore a_λ is fuzzy semi simple.

5. CONCLUSION

The objective of this paper is describing fuzzy completely regular and fuzzy regular and also establish the relation between them. The ordered fuzzy points of an ordered gamma semigroup S are key tools to describe the algebraic subsystems of S .we established the relation between fuzzy regular and fuzzy semi simple also fuzzy intra regular and fuzzy semi simple. We hope that the research along this direction can be continued, and in fact, some results in this paper have already constituted a platform for further discussion concerning the future development of ordered gamma semi groups. Hopefully, some new results in these topics can be obtained in the forthcoming paper.

ACKNOWLEDGEMENTS

The authors wish to express their sincere thanks to the referees for the valuable suggestions which lead to an improvement of this paper.

REFERENCES

[1] ANJANEYULU A., Structure and ideal theory of semigroups – Thesis, ANU (1980).

[2] Clifford A.H and Preston G.B., The algebroic theory of semigroups ,vol – I American Math. Society, Province (1961).

[3] Clifford A.H and Preston G.B., The algebroic theory of semigroups ,vol – II American Math. Society, Province (1967).

[4] LJAPIN E. S., Semigroups, American Mathematical Society, Providence, RhodeIsland (1974).

[5] Petrch.M. Introduction to semigroups ,Merril publishing company, Columbus Ohio(1973)

[6] W.M.Wu, Normal fuzzy subsemigroups, Fuzzy Math1(1).21-30(1981)

[7] T.M.G. Ahsanullah and F.A. AI-Thukair, Conditions on a semigroup to be a fuzzy neighborhood group, Fuzzy Sets and Systems, 55(1993), 333-340.

[8] J. N. Mordeson, D. S. Malik, N. Kuroki, Fuzzy Semigroups Springer-Verlag Berlin Heidelberg GmbH ISBN 978-3-642-05706-9 ISBN 978-3-540-37125-0 (eBook)

[9] DOI 10.1007/978-3-540-37125-0

[10] Xiang-Yun Xie,, Jian Tang, Fuzzy radicals and prime fuzzy ideals of ordered semigroups, Information Sciences 178 (2008), 4357–4374.

[11] N.Kehayopulu,M.Tsingelis, Fuzzy sets in ordered groupoids, Semigroup Forum 65(2002), 128-132

[12] Jizhongshen,On fuzzy Regular Subsemigroups of a semigroup, Information Sciences 51,111-120(1990)

[13] T.K. Dutta, N.C. Adhikari, on partially ordered Γ -semigroup, South East Asian Bull. Math., 28, No. 6 (2004), 1021-1028.

[14] S. K. Mujemder and S. K. Sardar, On properties of fuzzy ideals in PO-G-Semigroups, Armenian Journal of Mathematics. Vol. 2(2)(2009), 65.72.

[15] W. J. Lie, Fuzzy invariant subgroups and fuzzy ideals, Fuzzy sets syst. 8 (1982), 130.139.

[16] T.Nagaiah ,K.Vijay kumara Study of fuzzy ideals in PO-Gamma semigroupsPalestine Journal of Marhematics,Vol.6(2)(2017),591-597

[17] A. Iampan, Characterizing fuzzy sets in ordered G-Semigroups, Journal of Matematics Research,2(4)(2010), 52.60.

[18] Sen, M.K., Seth, A.: On po- Γ-semigroups. Bull. Calcutta Math. Soc. 85, 445–450 (1993)

IJPSR (2020), Volume 11, Issue 9 (Research Article)

INTERNATIONAL JOURNAL OF PHARMACEUTICAL SCIENCES AND RESEARCH

Received on 02 October 2019; received in revised form, 21 March 2020; accepted, 23 March 2020; published 01 September 2020

A VALIDATED LCMS METHOD FOR THE ANALYSIS OF ISOPROTERENOL – A β ADRENORECEPTOR AGONIST IN SPIKED HUMAN PLASMA

V. S. Singh Gaddala [*1], R. S. Reddy Dachuru [2] and E. Divakar Tella [3]

Department of Chemistry [1], SRR & CVR Government Degree College (A), Vijayawada - 520004, Andhra Pradesh, India.
Department of Chemistry [2], Krishna University, Machilipatnam - 521001, Andhra Pradesh, India.
Department of Chemistry [3], Noble College (A), Machilipatnam - 521001, Andhra Pradesh, India.

Keywords:

Isoproterenol, LCMS Analysis, Plasma extraction, Stability studies

Correspondence to Author:
Vijaya Swaroop Singh Gaddala

Lecturer,
Department of Chemistry, SRR & CVR Government Degree College (A), Vijayawada - 520004, Andhra Pradesh, India.

E-mail: vijayssgaddala@gmail.com

ABSTRACT: A simple, sensitive, and rapid Liquid Chromatography-Mass Spectroscopy method was developed and validated for the quantification of Isoproterenol in human plasma using Dobutamine as an internal standard. The method utilized simple liquid-liquid extraction using a mixture of diethyl ether and dichloromethane for the sample preparation involved prior to LCMS analysis. The analytes were chromatographed on Prontosil ODS C18 Column with isocratic elution using methanol, Acetonitrile and Tri ethyl-amine in the ratio of 60:25:15 (v/v) at pH 6.3 as the mobile phase at a flow rate of 0.9 mL/min and the UV detector response of the column eluents were recorded at a wavelength of 248 nm. Quantification was performed in multiple-reaction-monitoring mode with the ion transitions m/z 212.19 → 135.21 for Isoproterenol, m/z 302.19 → 107.05 for Dobutamine. Good linearity was obtained in the range of 0.50–300 ng/mL (r^2 = 0.999). The method was fully validated with accuracy, precision, matrix effects, recovery and stability. The results of the stability study confirm that the method was found to be stable. The validated data have met the acceptance criteria in FDA guidelines. This study could be readily applied in therapeutic drug monitoring of Isoproterenol in patients receiving such drug combinations.

INTRODUCTION: Isoproterenol (IPTN) is a non-selective β-adrenoreceptor agonist [1] prescribed for the treatment of slow heart rate (bradycardia), heart block and rarely for asthma. IPTN increases the heart rate and cardiac output by affecting the β1 adrenergic receptors in the myocardium. IPTN causes smooth muscle relaxation by affecting the β2 adrenergic receptors in bronchiolar and vascular smooth muscle [2, 3].

QUICK RESPONSE CODE

DOI: 10.13040/IJPSR.0975-8232.11(9).4567-74

This article can be accessed online on www.ijpsr.com

DOI link: http://dx.doi.org/10.13040/IJPSR.0975-8232.11(9).4567-74

IPTN has unwanted side effects on cardiac and metabolic functions, central nervous system, and motility of the gastrointestinal tract [4]. Limited experience with isoprenaline (Isoproterenol) does not show adverse effects on embryonic and fetal development [5].

The drug IPTN is available as several brands in the market and is widely used for the treatment of bradycardia and heart block. But in the literature, only one analytical HPLC method for the estimation of IPTN in pharmaceutical formulations [6], one HPLC method for the synthesis and characterization of IPTN and its process impurities [7] were reported. Hence, the present work is aimed to develop a validated HPLC tandem mass spectrophotometer method for the quantification of

IPTN in spiked human plasma. In the analysis of IPTN **Fig. 1A** in spiked plasma, a similar class of drug Dobutamine **Fig. 1B** was used as an internal standard (IS).

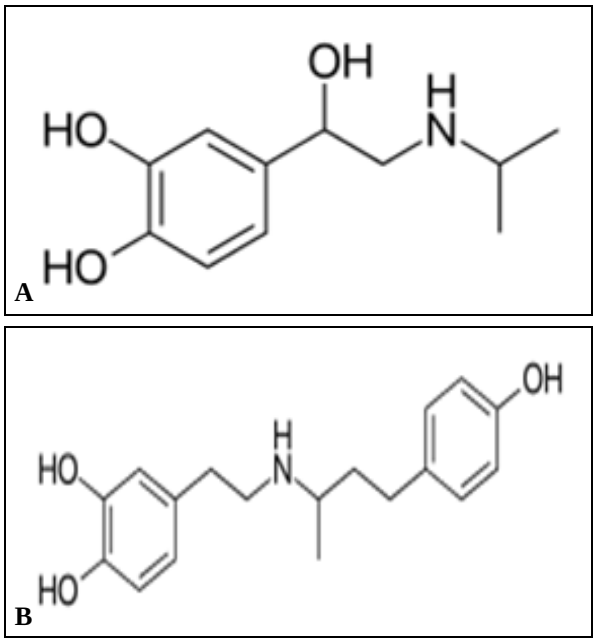


FIG. 1: MOLECULAR STRUCTURE OF STANDARD IPTN (1A) AND IS (1B)

MATERIALS AND METHODS:

Instrumentation: Agilent 1100 series HPLC with Quaternary G1311 A pump, COLCOM G1316A thermostat column temperature control, Thermo-static autosampler G 1329A with a sample volume of 0.1 - 1500 µL and variable programmable UV detector G 1314 A was used. The instrument was operated and integrated with Agilent chem. station LC software.

The HPLC system was coupled with Waters ZQ Mass Detector (model LAA 1369) with Waters Empower software. The mass spectra were taken in ESI (Turbo Ion Spray) positive mode in the mass range of 40-1000 amu and analyzed in the triple quadrupole analyzer. The nitrogen gas (300Psi) was used as a carrier gas in mass spectral analysis with fixed MS tune (3.0 kV capillary, 40V cone, 3V extractor)

Chemicals and Materials: Reference standards of IPTN (99.21%) and IS (99.17%) were obtained from Samarth Pharma Private Limited. (Mumbai, India). HPLC-grade methanol and acetonitrile were procured from Merck chemicals, Mumbai. Water used in the study was prepared from a Milli-Q water purification system from Millipore (Bangalore, India). Blank human plasma in K_3EDTA was obtained from a local diagnostic center, Guntur, and was stored at -20 °C until use.

Extraction of Drug from Plasma: A simple liquid-liquid extraction was used for the extraction of IS and IPTN from the plasma matrix. Prior to the analysis, the freeze and thaw plasma matrix were stored at -20 °C. In the liquid-liquid extraction process, 100 µl of plasma, 100 µl aliquot of working standard solution of IPTN and IS was added in polypropylene centrifuge tubes and then 600 µl of Diethyl ether and 400 µl of dichloromethane were added. Then tubes were centrifuged for 10 min at 3000 rpm. The clear supernatant layer was transferred into another conical glass tube, and the organic layer was completely evaporated at room temperature. Then it was reconstructed using the mobile phase. The solution was used for the analytical method development and validation study.

Preparation of Calibration Solutions: 10 mg each of standard drug IPTN and IS were weighed and dissolved in 10 mL of methanol separately in a 10 ml volumetric flask. A standard stock solution of 1000 µg/mL was obtained. Required calibration concentrations of IPTN and 100 µg/mL of IS were prepared separately.

0.5 - 300 ng/mL calibration curve standards of IPTN and 100 ng/mL of IS were spiked to human plasma and were extracted using liquid-liquid extraction. In the calibration range, a concentration of 25 ng/mL, 100 ng/mL, and 300 ng/mL were considered as low-quality control (LQC), middle-quality control (MQC) and high-quality control (HQC) standards respectively.

Method Development: Different compositions of the mobile phase, with different organic and pH modifiers, were studied for the separation and analysis of IPTN and IS. The separation was carried on different configurations of stationary phases, and eluents were recorded using a UV detector coupled with a mass spectrophotometer. The conditions that produce valid system suitability were studied for validation.

Method Validation: Method validation for the analysis of IPTN in the presence of IS in human plasma was done following the USFDA guidelines

[8]. The method was validated for selectivity, interference check, carryover, linearity, precision and accuracy, reinjection reproducibility, recovery, ion suppression/enhancement, matrix effect, stability, dilution integrity, and ruggedness.

Test for selectivity was carried out in 10 different batches of blank human plasma, including haemolysed & lipemic plasma collected with K_3EDTA as an anticoagulant. From each of the batch, two replicates each of 100 µL was spiked with 100 µL of methanol and deionized water (50:50, v/v). In the first set, the blank human plasma was directly injected after extraction (without analyte and IS), while the other set was spiked with only IS before. Further, one system suitability sample at PSCC - 10 concentration and two replicates of LLOQ concentration (PSCC-1) were prepared by spiking 100 µL blank human plasma with 100 µL of aqueous standards of IPTN and IS, respectively. The acceptance criterion requires that at least 90% of selectivity samples should be free from any interference at the retention time of analyte and IS.

The linearity of the method was determined by an analysis of ten calibration curves containing ten non-zero concentrations. The area ratio response for IPTN/IS obtained from multiple reaction monitoring was used for regression analysis. The calibration curve was analyzed individually by using the least square weighted ($1/x^2$) linear regression. The lowest standard on the calibration curve was accepted as the LLOQ, if the analyte response was at least ten times more than that of drug-free (blank) extracted plasma.

For determining the accuracy and precision, replicate analysis of plasma samples of analytes was performed on the same day for intraday and three different days for inter-day precision and accuracy. The run consisted of a calibration curve and six replicates of LQC, MQC and HQC samples. The deviation at each concentration level from the nominal concentration was expected to be within ±15%.

The relative recovery and matrix effect were assessed at HQC, MQC, and LQC levels in six replicates. Relative recovery was calculated by comparing the mean area response of pre-spiked samples (spiked before extraction) to that of extracts with post-spiked samples (spiked after extraction) at each QC level. The % recovery and the % RSD of the recovery were calculated.

The stability of the bioanalytical method developed was evaluated by measuring the area response of stability samples against freshly prepared comparison standards at LQC, MQC, and HQC levels. Stock solutions of IPTN and IS were checked for short term stability at room temperature (25 °C) and long term (benchtop) stability at 2-8 °C. Freeze-thaw stability was studied after three freeze, and thaw cycles of plasma matrix spiked with IPTN and IS at LQC, MQC and HQC levels. The CV (%) and accuracy (%) should be within ±15 %, and also, at least 2/3 quality control samples should meet the criteria of ±15% of nominal concentration is the acceptance criteria for the stability studies.

RESULTS AND DISCUSSION:

LCMS Analysis of IPTN: In the LCMS analysis of IPTN in the spiked human plasma, the mass spectra of column eluents were recorded in both positive and negative ion modes in electrospray ionization (ESI) detector.

The standard drug IPTN is having polar groups in the molecular structure that gives good mass spectrometric response in the negative mode. The molecule IPTN contains one basic and three acidic functional groups in the molecular structure with pKa of 9.81 (Strongly Acidic) and 8.96 (Strongly Basic). During the method development stage, the mass spectra of IPTN and IS was analyzed in ESI, and APCI (Atmospheric Pressure Chemical Ionization) by direct infusion of 50ng/mL solution of the analytes and the results confirm that ESI provided better ionization efficiency than APCI for both the analytes and hence further study was carried in ESI mode.

The observed mass spectra in the positive ion mode showed predominant protonated molecular ions [M-H]- at m/z 212.19 for IPTN and 312.19 for IS. The collision-induced dissociation of [M-H]- ions gave intense fragment/product ion at m/z of 194.57, 170.10, 135.21, and 72.09 for IPTN **Fig. 2A** and 284.25, 258.03, 137.48, and 107.05 for IS **Fig. 2B** respectively.

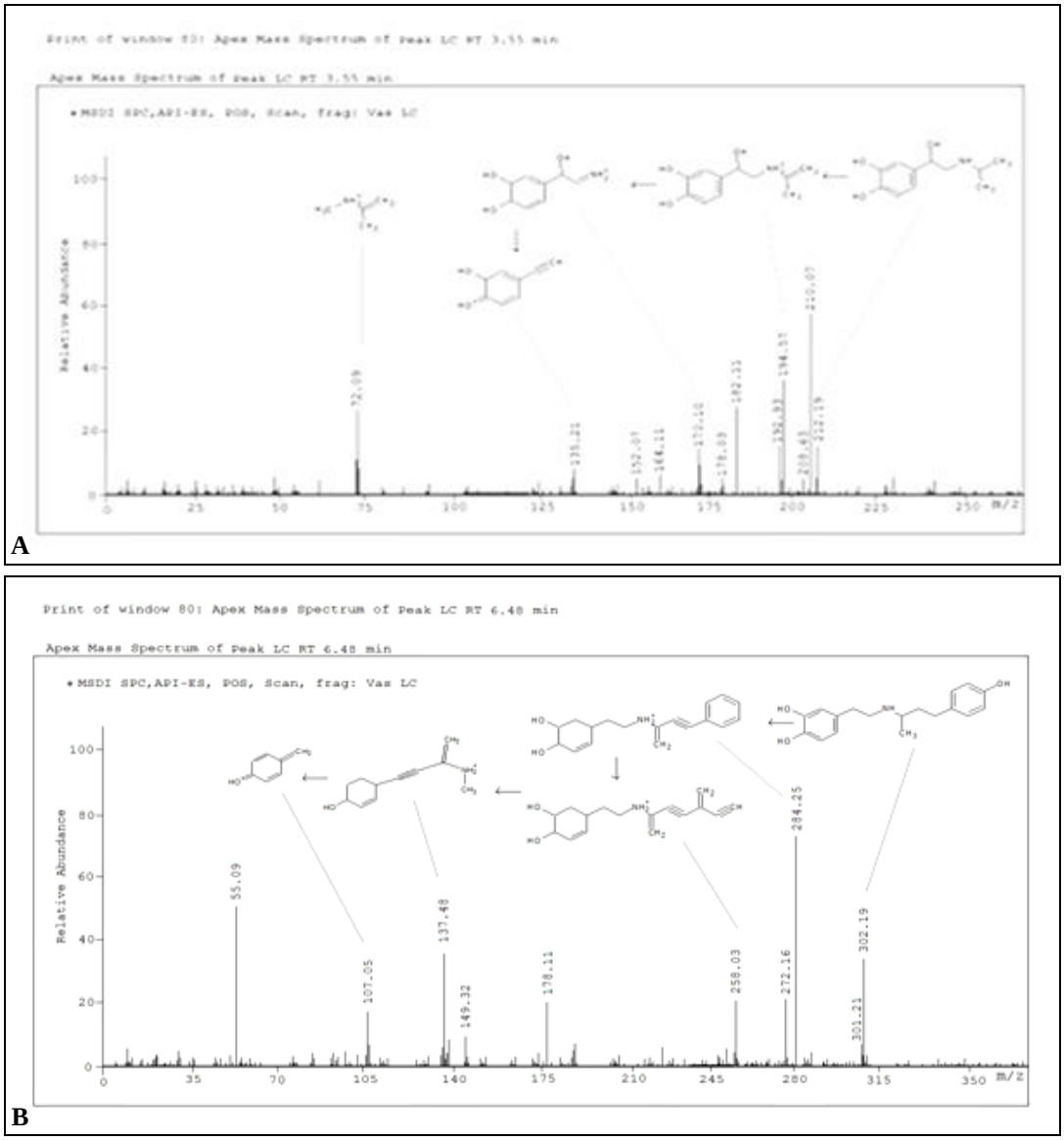


FIG. 2: ESI ION-CHROMATOGRAMS OF BLANK PLASMA SPIKED WITH IPTN AND IS. A) MASS SPECTRA OF IPTN AT THE RETENTION TIME OF 3.55 min. B) MASS SPECTRA OF IS AT THE RETENTION TIME OF 6.48 min

HPLC Optimized Conditions: In the optimization of LC conditions for the analysis of IPTN in spiked plasma samples, several reversed-phase columns with different configurations like Hypersil Gold C18 (50/100 mm × 3.0 mm, 5 µm), Gemini C18 (50/100 mm × 4.6 mm, 5.0 µm) and Prontosil ODS C18 Column (250 × 4.6 mm, 5 µm) were tested. For chromatographic separation of IPTN and IS from the plasma matrix, various combinations of methanol, acetonitrile in combination with different buffers in different pH ranges (3.5-6.5) were studied in order to obtain symmetrical peak shapes, suitable retention and adequate signal-to-noise ratio leading to lower limits of quantization. Compared to individual solvent mixtures, the combination of methanol and acetonitrile helped in providing higher sensitivity and sharp peaks shapes.

Another important observation was that a higher proportion (>75%) of organic diluents was necessary for the optimum resolution of the drugs. Both the peaks observed for IPTN and IS were satisfactorily resolved (Resolution factor ≥2) on all columns studied using Methanol, Acetonitrile and Triethylamine in the ratio of 60:25:15 (v/v) at pH 6.3 as the mobile phase at a flow rate of 0.9 mL/min and the UV detector response of the column eluents were recorded at a wavelength of 248 nm. The peak area response was not adequate on Hypersil Gold C18, and the peak shapes were not acceptable with Gemini C18 column. Nevertheless, the best chromatographic conditions were achieved on Prontosil ODS C18 Column (250 × 4.6 mm, 5µm) with an adequate response, resolution (Resolution factor ≥2), symmetric peak

shape, baseline separation within 2.0 min **Fig. 3**. The retention time of IPTN and IS were found to be 3.5 and 4.6 min, respectively. The use of labeled internal standards that had identical chromatographic behavior helped to achieve acceptable method performance.

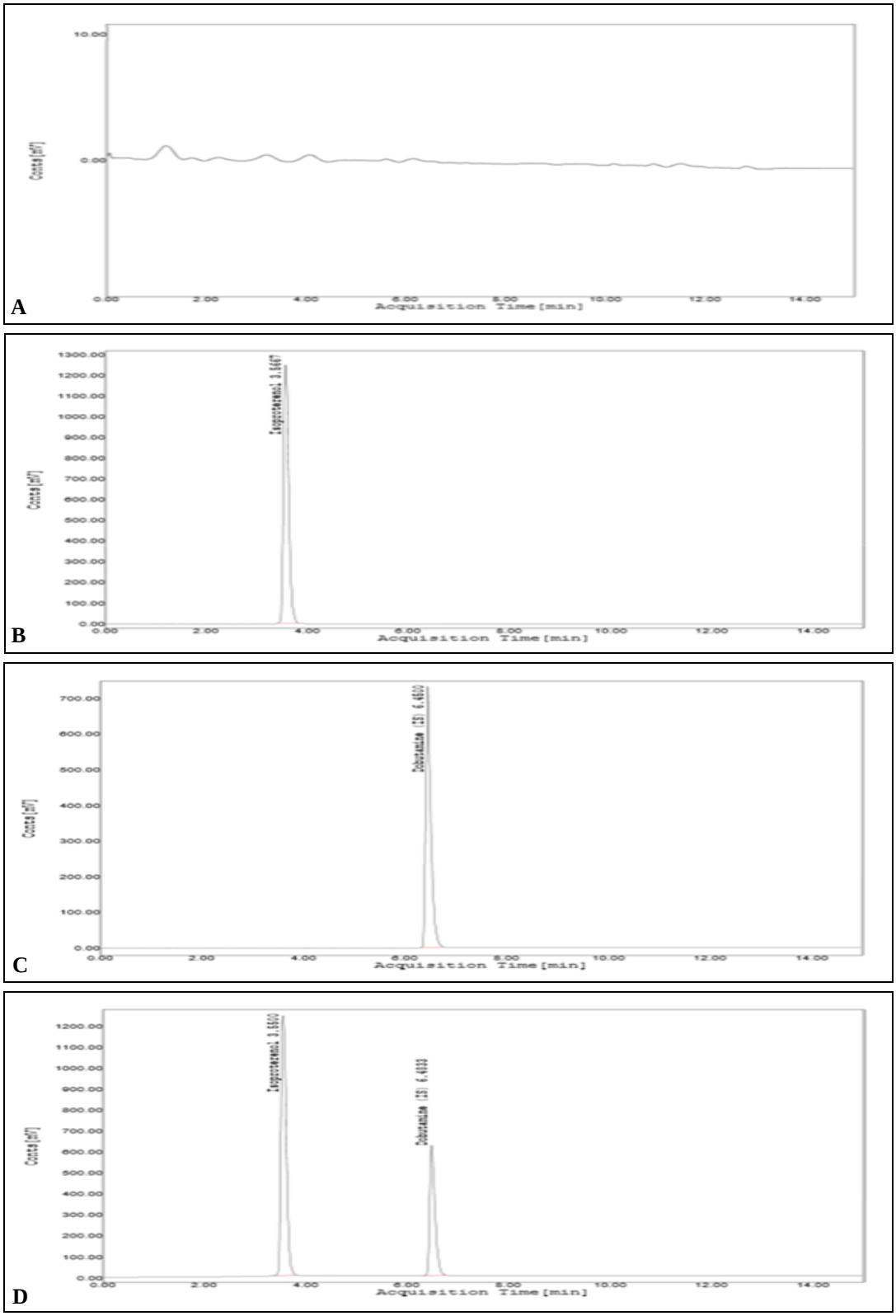


FIG. 3: SYSTEM SUITABILITY CHROMATOGRAM OF IPTN IN THE DEVELOPED METHOD. A) PLASMA SPIKED BLANK CHROMATOGRAM. B) CHROMATOGRAM OF BLANK PLASMA MATRIX SPIKED WITH IPTN. C) CHROMATOGRAM OF BLANK PLASMA MATRIX SPIKED WITH IS. D) STANDARD CHROMATOGRAM OF PLASMA SPIKED IPTN AND IS

The plasma spiked calibration curve for peak area ratio of IPTN and IS against the IPTN concentration prepared showed a linear relationship over a concentration range of 0.5-300 ng/mL. The regression equation for IPTN in the developed method was found to be y = 0.010x + 0.085, with a correlation coefficient (r^2) of 0.999 indicates the good linearity of the method. The results of the linearity study of IPTN in the developed method were given in **Table 1,** and the calibration curve was shown in **Fig. 4**.

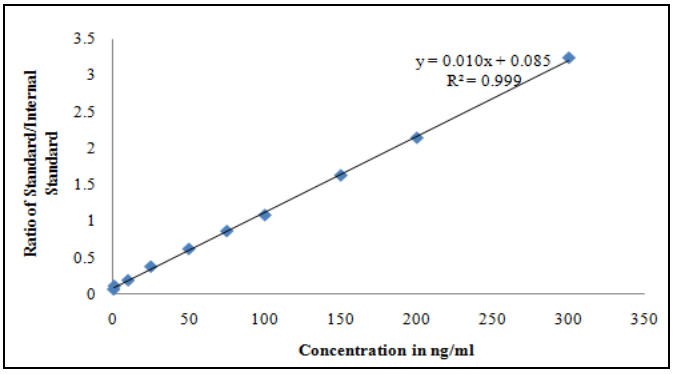


FIG. 4: CALIBRATION CURVE OF IPTN

TABLE 1: CALIBRATION CURVE RESULTS OF IPTN IN THE DEVELOPED METHOD

S. no.	Sample Id	Concentration in ng/ml	Peak Area observed for		Ratio of Standard/IS
			Isoproterenol - Standard	Dobutamine - IS	
1	PSCC 1	0.5	10143	150469	0.067
2	PSCC 2	1	17486	151171	0.116
3	PSCC 3	10	28947	150964	0.192
4	PSCC 4	25	57601	151769	0.380
5	PSCC 5	50	94295	151528	0.622
6	PSCC 6	75	130240	150361	0.866
7	PSCC 7	100	164963	151958	1.086
8	PSCC 8	150	247491	151822	1.630
9	PSCC 9	200	323884	151036	2.144
10	PSCC 10	300	491746	151739	3.241

The precision and accuracy of the method developed for IPTN were analyzed in three independent occasions in the calibration curve. The intra-assay coefficient of variation was found to be 0.143%, 0.828%, and 0.119% for HQC, MQC, and LQC, respectively, and trueness ranged from 98.665 to 99.913%. The inter-assay coefficients of variation ranged from 0.089% 0.837% and 0.119 for HQC, MQC, and LQC, respectively, and trueness ranged from 98.066% to 100.058% indicating that the assay method was sufficiently reliable and reproducible within the required analytical range. The results indicated that the matrix component in human plasma did not significantly affect response, and the method was found to be precise. **Table 2** shows the precision and accuracy results of the method developed for IPTN.

TABLE 2: PRECISION AND ACCURACY RESULTS

S. no.	Parameter	Intra-assay (n = 6)			Inter-assay (n = 6)		
		HQC	MQC	LQC	HQC	MQC	LQC
1	Concentration studied (ng/mL)	300 ng/ml	100 ng/ml	25 ng/ml	300 ng/ml	100 ng/ml	25 ng/ml
2	Concentration observed (ng/mL)	299.740	98.665	24.951	300.173	98.066	24.951
3	Peak Area	491320	162563	57487	492030	161576	57487
4	%CV	0.143	0.828	0.119	0.089	0.837	0.119
5	Trueness (%)	99.913	98.665	99.803	100.058	98.066	99.803
6	RE (%)	0.087	1.335	0.197	0.058	1.934	0.197

* CV = Coefficient of Variation; RE = Relative Error

Recovery and Matrix Effect: The absolute recovery IPTN and IS in the developed method was determined by comparing the peak area responses of QC samples (LQC, MQC, and HQC, n = 6) extracted in spiked plasma with corresponding standard concentrations prepared in reconstitution solvents. The % recovery was found to be 89.082, 93.431, and 84.80 for HQC, MQC, and LQC, respectively. The high recovery observed for both standard and IS and the % recovery of more than 85% and less than

115% observed confirms that the matrix effect was not observed. The result of the recovery study **Table 3** confirms that the method was found to be acceptable.

TABLE 3: RECOVERY RESULTS

S. no.	Parameter	HQC	MQC	LQC
1	Concentration studied (ng/mL)	300	100	25
2	Concentration observed (ng/mL)	267.25	93.431	21.20
3	Peak Area	542331	178446	67396
4	%CV	0.058	0.169	0.386
5	Recovery (%)	89.082	93.431	84.801
6	RE (%)	10.918	6.569	15.199

* n=6; CV = coefficient of variation; RE = relative error

The stability of both analyte and internal standard in the developed method was evaluated by short term stability, long term stability, and freeze-thaw stability. The % stability in all the stability studies was found to be 99.907, 97.555, and 87.461 for short term stability, 96.351, 93.362, and 87.461 for long term stability and 98.128, 96.126 and 88.919 for freeze-thaw stability in HQC, MQC and LQC respectively.

The results of the three stability studies **Table 4** confirms that the method was found to be stable and is suitable for the analysis of IPTN in biological samples.

TABLE 4: RECOVERY RESULTS

S. no	Parameter	HQC	MQC	LQC
	Short Term Stability			
1	Concentration studied (ng/mL)	300 ng/ml	100 ng/ml	25 ng/ml
2	Concentration observed (ng/mL)	299.721	97.555	21.865
3	Peak Area	491289	160734	50378
4	%CV	0.182	0.406	0.324
5	Stability (%)	99.907	97.555	87.461
6	RE (%)	0.093	2.445	12.539
	Long Term Stability			
7	Concentration studied (ng/mL)	300 ng/ml	100 ng/ml	25 ng/ml
8	Concentration observed (ng/mL)	289.053	93.362	21.865
9	Peak Area	473802	153825	50378
10	%CV	0.720	1.141	0.324
11	Stability (%)	96.351	93.362	87.461
12	RE (%)	3.649	6.638	12.539
	Freeze Thaw Stability			
13	Concentration studied (ng/mL)	300 ng/ml	100 ng/ml	25 ng/ml
14	Concentration observed (ng/mL)	294.384	96.126	22.229
15	Peak Area	482540	158381	51218
16	%CV	0.491	0.214	0.392
17	Stability (%)	98.128	96.126	88.919
18	RE (%)	1.872	3.874	11.081

* n=6; CV = coefficient of variation; RE = relative error

CONCLUSION: A simple and novel LCMS method was developed for the identification and quantification of IPTN in spiked human plasma samples. The method is applicable for the high throughput bio-analysis of IPTN owing to a run time of 15 min per sample.

The assay performance studies like linearity, accuracy, precision, and recovery were satisfactory for routine pharmacokinetic applications. Hence, the current LCMS method provides a valuable tool to improve the efficacy and safety of IPTN therapy.

ACKNOWLEDGEMENT: I am thankful for my authorities concerned for the permission accorded and coauthors for their valuable suggestions and guidance in carrying out this work.

CONFLICTS OF INTEREST: I declare that to the best of my knowledge and belief, neither my coauthors nor I have any interests which might conflict.

REFERENCES:

1. Osborn DA: Hemodynamics and Cardiology: Neonatology Questions and Controversies, Elsevier Academic Press, Cambridge, Massachusetts 2008: 229-65.
2. Arbuthnott G and Munoz MG: Companion to Psychiatric Studies Elsevier Academic Press, Cambridge, Massachusetts Edition 8, 2010: 45-76.
3. Mozayani A and Raymon L: Handbook of Drug Interactions: A Clinical and Forensic Guide. Springer Science & Business Media 2003: 541-42.
4. Jalba MS: Three Generations of Ongoing Controversies Concerning the Use of Short Acting Beta-Agonist Therapy in Asthma: A Review. Journal of Asthma 2008; 45(1): 9-18.

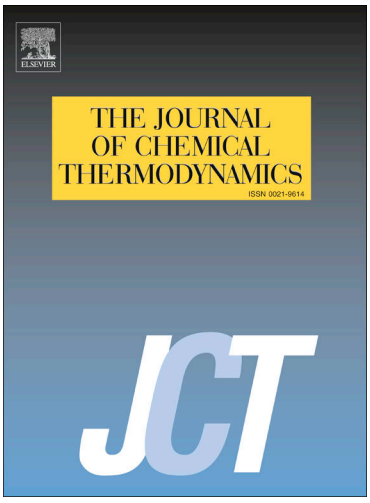
5. Garbis H: Drugs During Pregnancy and Lactation Elsevier Academic Press, Cambridge, Massachusetts: Elsevier Academic Press, Second Edition 2007: 63-77.
6. Muneer S, Hindustan AA and Chandrasekhar KB: Stability Indicating method development and validation for the quantification of Isoproterenol HCl in bulk and its formulation by RP-HPLC using PDA detection, Journal of Pharmaceutical and Scientific Innov 2018; 7(5): 183-87.
7. Kumar N, Rao DS, Reddy GP, Dubey SK and Kumar P: Synthesis, isolation, identification and characterization of new process-related impurity in isoproterenol hydrochloride by HPLC, LC/ESI-MS and NMR. Journal of Pharmaceutical Analysis 2017; 7(6): 394-400.
8. Guidance for Industry, Bioanalytical Method Validation, U. S. Department of Health and Human Services, Food and Drug Administration, Centre for Drug Evaluation and Research (CDER), Centre for Veterinary Medicine (CVM), 2001.

How to cite this article:
Gaddala VSS, Dachuru RSR and Tella ED: A validated LCMS method for the analysis of isoproterenol – A β adrenoreceptor agonist in spiked human plasma. Int J Pharm Sci & Res 2020; 11(9): 4567-74. doi: 10.13040/IJPSR.0975-8232.11(9).4567-74.

All © 2013 are reserved by the International Journal of Pharmaceutical Sciences and Research. This Journal licensed under a Creative Commons Attribution-NonCommercial-ShareAlike 3.0 Unported License.

This article can be downloaded to **Android OS** based mobile. Scan QR Code using Code/Bar Scanner from your mobile. (Scanners are available on Google Play store)

Journal Pre-proofs



A molecular interactions study between 1-butyl-3-methylimidazolium hexafluorophosphate ([Bmim][PF_6]) and N-methylpyrrolidone

Sowjanya Prathipati, Srinivasa Rao Vipparla, Srinivasa Reddy Munnangi, Md Nayeem Sk, Hari Babu Bollikolla

PII: S0021-9614(20)30593-0
DOI: https://doi.org/10.1016/j.jct.2020.106330
Reference: YJCHT 106330

To appear in: *J. Chem. Thermodynamics*

Received Date: 20 May 2020
Revised Date: 21 October 2020
Accepted Date: 23 October 2020

Please cite this article as: S. Prathipati, S. Rao Vipparla, S. Reddy Munnangi, M. Nayeem Sk, H. Babu Bollikolla, A molecular interactions study between 1-butyl-3-methylimidazolium hexafluorophosphate ([Bmim][PF_6]) and N-methylpyrrolidone, *J. Chem. Thermodynamics* (2020), doi: https://doi.org/10.1016/j.jct.2020.106330

This is a PDF file of an article that has undergone enhancements after acceptance, such as the addition of a cover page and metadata, and formatting for readability, but it is not yet the definitive version of record. This version will undergo additional copyediting, typesetting and review before it is published in its final form, but we are providing this version to give early visibility of the article. Please note that, during the production process, errors may be discovered which could affect the content, and all legal disclaimers that apply to the journal pertain.

© 2020 Elsevier Ltd.

A molecular interactions study between 1-butyl-3-methylimidazolium hexafluorophosphate ([Bmim][PF_6]) and N-methylpyrrolidone

Sowjanya Prathipati[a], Srinivasa Rao Vipparla[a,b], Srinivasa Reddy Munnangi[c], Md Nayeem Sk[d], Hari Babu Bollikolla[a*]

[a]*Department of Chemistry, Acharya Nagarjuna University, Nagarjunanagar–522 510, A.P., India*

[b]*Department of Chemistry, Govt. Degree College , Avanigadda-521 121, A.P., India.*

[c]*Department of Chemistry, TRR Govt. Degree College, Kandukur-523 105, A.P., India.*

[d]*Department of Physics, KRK Govt. Degree College, Addanki-523 201, A.P., India.*

ABSTRACT:

The work entitled results from initial determination of physical parameters, density (ρ), speed of sound (u), refractive index of [Bmim][PF_6]/ N-methylpyrrolidone and their binaries at all compositions at atmospheric pressure and at task temperatures ranging from (303.15 - 323.15) K. The experimental results were utilized for computation of molar volumes (V_m^E)/partial molar volumes ($\overline{V}_m^E$)/ partial molar volumes at infinite dilution ($\overline{V}_m^{E,\infty}$)/isentropic compressibility (κ_s^E)/ free length (L_f^E)/ speeds of sound (u^E) and isobaric thermal expansion coefficient (α_P^E) of the binary system. Further, the binary coefficients and the standard deviations were deduced by fitting the excess properties in Redlich-Kister equation. A fortitude of these parameters indicated strong intermolecular interactions and likewise increases with increase of temperature. Furthermore, molecular properties were also evaluated using Sehgal's relation on non-linear parameters of Hartmann-Balizar and Ballou semiempirical relations at all temperatures. Moreover, the activity coefficients were calculated by Margules/Porter/Wilson/NRTL relations at temperature 308.15 K. The results of Prigogine–Flory–Patterson (PFP) theory of excess molar volume and IR spectra were supported the deduced strong interactions.

Key words: [Bmim][PF_6]; N-methylpyrrolidone; PFP theory; speed of sound; IR spectra; thermodynamic parameters.

* Corresponding Author:dr.b.haribabu@gmail.com

Phone: +91-8500338866

Journal Pre-proofs

1. Introduction

Today Ionic Liquids (ILs) have attracted significant consideration for the reason of their distinctive properties, *viz.* thermal stability, non-volatility and reuse [1,2]. ILs can be selected to have various cations and anions, in order to shape Ionic Liquids with preferred properties. Besides, ILs have been recognized for quite a while, yet their wide utility as solvents in catalysis and processes design for chemical synthesis in recent times happen to be noteworthy. ILs have potential applications in many areas but real applications must be investigated further. However, the much cost of the ILs and more viscous nature than conventional organic solvents restricted their use in multiple applications.

Researchers are becoming more interested in IL mixtures with molecular organic solvents, as the resulting liquid mixtures provide many advantages than individual IL and organic solvent. The properties of such mixtures are dependent on the proportion of mixing. Mixing of IL with organic molecular solvents is one of the alternatives for reducing the use of costly ILs and also save the time in preparing new ILs of wanted properties [3], fortunately the mixtures also have reduced viscosity without loss in their advantages as green solvents. Meticulously, the mixing of co-solvents with polar nature may have a significant effect on physical and chemical properties of the IL's[4]. Recently it has been shown that specific (IL + molecular organic solvent) binary systems have better performance than pure ILs. These were also found to be useful in various advanced applications, *viz.* in super capacitors, bio-catalysed processes, as a medium for the solvation of biopolymers, *etc.* [5 17]. In recent years, therefore, the thermo-physical study of IL + molecular solvents has received increased attention. In view of the fact that these data are important for industrial applications, the prospective of the new systems can be exploited by examining their physicochemical properties.

The selection of the studied IL 1-butyl-3-methylimidazolium hexafluorophosphate, ([Bmim] [PF_6]) is based on its ability as a green plasticizer for poly (L-lactide) [18], in Tussah silk dyeing [19], RP HPLC [20], in organic synthesis [21], in separatión technology [22] and also used in enzymatic catalysis [23]. On the other hand, NMP (N-methylpyrrolidone) solvent is unique in its properties with low volatility compared to most of the organic liquids, and high polarity. Its commercial uses are in petrochemical and plastic industries, taking advantage of its

non-volatility and their capability to dissolve various materials[24]. Further, NMP is also used in drugs formulation and in the manufacture of lithium ion batteries.

Physico-chemical properties between [Bmim] [PF_6] with organic solvents such as dimethyl formamide [37], methyl methacrylate [25], butanol, acetone [38], THF, DMSO, methanol, acetonitrile [39], ethanol, benzene [40], 2-propoxyethanol [30], 2, 2, 2-trifluoroethanol [41], 2-Pyrrolidone [42], N-vinyl-2-pyrrolidinone [43], N-Methylaniline [26] and ethyl acetate [44] were found so far in literature. Feng *etal* [45] has reported density only at (298.15 - 313.15) K for the binary mixture under study. So, in this article, the authors made an attempt to fortitude the molecular interactions between ([Bmim][PF_6]) and N-methylpyrrolidone binary system using a comprehensive study on volumetric, acoustic, optical and their derived parameters at temperatures (303.15 - 323.15) K along with spectral studies.

On the basis of our initial experiments, the selected IL in all proportions completely miscible with NMP. Therefore, in this analysis, we propose to calculate the density, speed of sound and refractive index of [Bmim][PF_6] binary mixtures with NMP between 303.15 K - 323.15 K temperatures across all compositions and at atmospheric pressure. We calculated the deviation / excess properties based on the measured values, and these properties were fitted using Redlich-Kister polynomial equation for their possible application in industrial processes. Additionally, IR spectroscopy sought to understand the contact behavior between the two liquids in the mixture. Finally, the experimental excess molar volume data was contrasted with the theory of Prigogine-Flory-Patterson (PFP).

2. Experimental

2.1. Materials and methods

The [Bmim] [PF_6] (CAS 174501-64-5) with a mass fraction purity of 0.99 was bought from Iolitec GmBH (Germany); Sigma Aldrich supplied the NMP (CAS 872-50-4), with a mass fraction purity of 0.995. The chemicals used in this work were well purified using known methods [46,47]. Karl Fisher titrator was used to determine the water content in IL and NMP (Metrohm, 890 Titrando). All samples were dried under reduced pressure (0.1 bar) at moderate temperature for at least 72 h before taking each measurement (starting at room temperature and

Journal Pre-proofs

gradually rising to 333 K). The water content of all samples was further checked, and was found less than 170 ppm, a much lower value than the pre-evacuation analysis, which showed values of around 210 ppm. The NMP solvent was further purified by distillation and [Bmim] [PF_6] was used without further purification (See Table S1, **SI** for other procedures and equipment). Further, the purities were checked by comparing measured density, speed of sound and refractive index with the literature values given in **Table 1**.

Measurement of density and speed of sound

Densities and speed of sound are measured with an Anton Paar DSA-5000M vibrating tube density and sound velocity meter. The density meter is calibrated with doubly distilled degassed water, and with dry air at atmospheric pressure. The temperature of the apparatus is controlled to within ±0.01 K by a built-in Peltier device. Measured density and speed of sound values (at frequency approximately 3 MHz) are precise to $5x10^{-3}$ $kg.m^{-3}$and $5x10^{-1}m.s^{-1}$respectively. The standard uncertainties associated with the measurements of temperature, density and speed of sound are estimated to be ±0.01 K, 1.0 kg m^{-3} and ±0.5 m s^{-1} respectively.

Measurement of refractive index

The refractive indices are determined using an automatic refractometer (Anton Paar Dr Krenchen Abbemat (WR-HT)) which has also a temperature controller that keeps the samples at working temperature. The uncertainties in the temperature and refractive index values are ±0.01K and $±5x10^{-4}$ respectively. The apparatus is calibrated by measuring the refractive index of Millipore quality water and tetrachloroethylene (supplied by the company) before each series of measurements according to manual instructions. The calibration is checked with pure liquids by known refractive index.

Measurement of infrared spectra

Infrared transmittance is measured by using Shimadzu Fourier transform infrared (FT-IR) spectrometer (IRAffinity-1S**)** equipped with attenuated total reflectance (ATR) accessories. The spectral region is (650-4000) cm^{-1} with resolution of 2 cm^{-1} and 100 scans. At least five repeated measurements are performed for each sample.

3. Results and discussion

Experimental density (ρ), speed of sound (u), refractive index (n_D), for binary mixtures of [Bmim] [PF_6] with NMP with respect to the mole fraction (x_1), of [Bmim][PF_6] at scrutinizing

temperatures were given in **Table 2**. The densities of the mixtures of this work have been graphically compared (**Figure 1**) with those of Feng *et al.* [45]. There are clear deviations of densities of pure solvents. This might be due to that Feng *et al.* [45] used NMP with mass fraction purity of 0.99 and didn't mention the purity of [Bmim][PF_6]. In this work, we not only used the solvents with high purity but also more sophisticated equipment for accuracy.Both [Bmim][PF_6] and N-methyl pyrrolidine are considered polar, which contributes to the full miscibility of themselves in all proportions and at temperatures. A close look density in **Table 2** clearly demonstrates a linear decrease when temperature rises due to expansiveness of volume. The thermal expansion coefficient (α_p) is a measure of the fluid expansion or contraction with temperature in all directions. The resulting values of [Bmim][PF_6] were smaller than NMP, which means that the IL expands or contracts less than NMP at a predetermined temperature.

From the above experimental data the authors computed the excess properties, molar volume (V_m^E), isentropic compressibility (κ_s^E), free length (L_f^E), velocity of sound (u^E) and isobaric thermal expansion coefficient (α_p^E) using thermodynamic equations (**S1-S11; SI**). The Plots of excess molar volume (V_m^E) against mole fraction of IL in the mixture with NMP at studied temperatures **(**303.15 to 323.15) K were shown in **Figure 2**. Excess molar volumes at all investigated temperatures were found negative for the mixtures and the more negative value was found to be -0.79x10^{-6}m^{3}mol^{-1} at x_1 = 0.1894 and T= 303.15 K. At upper temperatures the minimum of V_m^E further decreased (more negative) and changes were marginally to higher mole fraction of IL. Imidazolium ILs can also form hydrogen bonds at suitable conditions, as these act as both donor and acceptor of protons. So, the H-bonds between the [Bmim][PF_6] and NMP can therefore be assumed to be responsible for a significant contraction of the mixture volume. Moreover, the complimentary fitting of smaller NMP solvent molecules (at T=303.15 K, V_m= 96.94x10^{-6} m^{3}mol^{-1}) into cavities formed by larger [Bmim][PF_6] molecules (at T=303.15 K, V_m= 208.26x10-6 m^{3}mol^{-1}) is also considerable for these tough interactions. For other temperatures a similar pattern may also be observed and the effect is more predominant at upper temperature. This is owing to the reason that smaller NMP molecules are more favourably fitted into the cavities produced by larger [Bmim][PF_6] molecules, thus sinking the volume of the mixture to a greater degree, ensuing in more negative values with increasing temperature. In terms of

temperature, the order of interaction forces is (323.15>318.15>313.15>308.15>303.15) K. The polynomial coefficients of the Redlich-Kister and the corresponding standard deviations were given in **Table 3**.

The molecular interactions that occur in the system reflect well on the properties of partial molar volumes ($\overline{V}_m^E$). The ($\overline{V}_m^E$) of component 1 ([Bmim][PF_6]) and 2 (NMP) in the mixtures were calculated using equations **S12-S17 (**See **SI**) and the values were given in **Table 4**. From this table it can be found that the $\overline{V}_{m,1}$ values for [Bmim][PF_6] in the mixtures were almost lower than their individual molar volumes in their pure states, suggesting that the volume contraction occurs by combining [Bmim][PF_6] and NMP under any temperature. The **Figures 3** and **4** shows the discrepancy of excess partial molar volumes of ([Bmim][PF_6]) and (NMP) in the binary system at T = (303.15, 308.15, 313.15, 318.15 and 323.15) K respectively. The negative pattern of these properties found at all temperatures also supports the resultant negative excess molar volumes. A scrutiny of this data not only shows the presence of strong interactions between the different molecules but also supports conclusions drawn from excess molar volumes.

The partial molar volumes [Bmim][PF_6] and NMP denoted as $\overline{V}_{m,1}^{\infty}, \overline{V}_{m,2}^{\infty}$ and excess partial molar volumes at infinite dilution $\overline{V}_{m,1}^{E,\infty}, \overline{V}_{m,2}^{E,\infty}$ were computed from the known equations (**S18** and **S19** of **SI**). The computed values at all investigated temperatures of $\overline{V}_{m,1}^{\infty}, \overline{V}_{m,2}^{\infty}$ and $\overline{V}_{m,1}^{E,\infty}, \overline{V}_{m,2}^{E,\infty}$ were given in **Table 5.** The values of $\overline{V}_{m,1}^{E,\infty}$ were found negative and also become more negative with increased temperatures. This signify that the molecular association effect is larger than the dissociation for [Bmim][PF_6] IL system. On the other side the excess partial molar volumes at infinite dilution for NMP ($\overline{V}_{m,2}^{E,\infty}$) are positive at all temperatures determined. This is for the reason that of ion solvation process and extinction of ion-ion interactions in [Bmim][PF_6] [48]. This is observed in the case of V_m^E values which reproduce well from the computed parameters of partial molar volumes at infinite dilution at all temperatures calculated.

For [Bmim][PF_6] + NMP system, the excess isoentropic compressibility (κ_s^E) behavior is very likely to the $V_{\mathrm{m}}^{\mathrm{E}}$ that was shown in the **Figure 5**. It was also found negative in the entire

region of investigated temperatures and composition ratios and becomes more negative with rise in temperature. The negative values of κ_s^E mean that the mixtures are more compressible than the respective ideal mixtures [49]. Therefore, it is assumed that the decrease in free volume is making the mixture more compressible than the ideal mixture, which eventually results in negative values for excess isoentropic compressibility. The disparity of excess free length (L_f^E) against mole fraction of IL is shown in **Figure 6**. The negative values of excess free length suggested the presence of specific interactions between different molecules as well as structural adjustments in the liquid mixture leading to closer molecular packaging.

At all investigated temperatures the clearly **Figure 7** illustrates that the speeds of sound (u^E) values were positive for the current binary system over the whole compositions. The positive deviations are a sign of increase interactions between the component molecules of the binary liquid mixtures [50]. The deviations in refractive index ($\Delta_\phi n_D$) against mole fraction were plotted in **Figure 8** and the values were found positive in the studied composition ratios of the binary mixture. This further supported the existence of strong interaction forces among the component molecules [51]. **Figure 9** indicates negative values of α_P^E for the binary mixture over the entire composition and at all investigated temperatures. This further supported the presence of tough interactions between the component molecules [52].

3.1. Infrared spectral studies

The observed interactions from the above inferences of excess parameters in the system were well supported by the IR spectral data. The unique nature of imidazolium cations is demonstrated well by their electronic structure (**Figure 10**). Because of the less electron density on the C=N bond, the hydrogen in C_2-H has more acidic nature than C_4-H, and C_5-H. These hydrogens' resulting acidity is important for understanding the properties of the current ILs. The 'H' on the C_2 carbon (C_2–H) was shown to be normally associate with solvent molecules [53].

The infrared absorbance was recorded between 650 cm^{-1} to 4000 cm^{-1} wavelength (**Figure 11** and **Table 6**) to know the outcome of molecular interactions. For [Bmim][PF_6], signals can be divided into two different parts, the signals between 3000 cm^{-1} and 3200 cm^{-1} may be endorsed mainly to the C-H vibrational modes of aromatic imidazolium ring [54]. Further, the

Journal Pre-proofs

signals from 2800 cm^{-1} to 3000 cm^{-1} are mainly due to aliphatic C-H stretchings in the methyl and butyl moieties [55–57]. Since for its stronger acidic character, the C_2-H vibrational frequency (3124.3 cm^{-1}) was found to be moved to a lower frequency by around 44.9 cm^{-1} compared to C_4-H and C_5-H stretchings (3169.2 cm^{-1}). The C_2-H and $C_{4,5}$-H stretching frequencies of the IL cation were examined (**Figure 12**) along with C=O stretching area of NMP (**Figure 13**). It was also found that the red shift is very predominant in C_2-H frequencies compared to $C_{4,5}$-H stretching frequencies, implying that more acidic C_2-H plays a most important role in the formation of H-bond with carbonyl oxygen of NMP (**Figure 13**). At the same time, a strong red shift is observed for C=O Sym Stretch frequencies in NMP, as the mole fraction of IL increases. This evidently demonstrated the formation of intermolecular hydrogen bonds between the 'H'-atoms of aromatic imidazolium ring and NMP carbonyl oxygen.

ATR-FTIR studies suggested the key role of hydrogen in miscibility and stability of the binary system. Hence it can be assumed that the hydrogen bonds in the system are also accountable for the existing tough interactions and contractions in the mixtures volumes.

3.2. Prigogine-Flory-Patterson statistical theory for excess molar volume V_m^E

The Prigogine-Flory-Patterson (PFP) theory was used to check and compare experimental excess molar volumes of binary mixtures [58–62]. At T = (303.15-323.15) K, we compared 'V_m^E' of the titled binary mixture utilizing the PFP theory over the whole mole fractions range. The calculation of various parameters of this theory is based on relevant equations reported in literature [63–67]. The parameters of pure components for the PFP theory were listed in **Table 7**. In the absence of experimental excess molar enthalpy (H_m^E), the Flory contact interaction parameter χ_{12}, the only adjustable parameter required in the PFP theory, was obtained from experimentally determined values of V_m^E. It was found that for all the investigated temperatures, the Flory contact interaction parameter χ_{12} was found negative. The values of said 3 contributions, V_{int}^E,$V_{fv}^E and V_{P^*}^E$, to V_m^E(PFP) at equimolar composition were given in **Table 8.** The first term V_{int}^E is negative, indicating the tough interactions occur in the mixture. For all measured temperatures the connecting forces contributions were observed negative. The second term V_{fv}^E was also found to be negative as V_{fv}^E is proportional to $-(\tilde{V}_1 - \tilde{V}_2)^2$ [59,68]. The degree of negative values of V_{fv}^E depends on difference in Flory's reduced volumes of the

components. Negative values in the magnitude of V_{fv}^{E} increase further with rise in temperature as more free volume becomes available in [Bmim][PF_6] to accommodate the smaller NMP molecules which resulted in more negative V_{m}^{E}. The third term, i.e. characteristic pressure V_{P*}^{E}, was found positive at investigated temperatures, the *P** effect which depends on the relative cohesive energy of the expanded and less expanded component. Further, it is proportional to $(\tilde{V}_1 - \tilde{V}_2)(P_1^* - P_2^*)$ and can have both the negative and positive sign depending upon the magnitude of P_i^* and $\widetilde{V_i^*}$ of unlike components [59,68]. For the system [Bmim][PF_6] + NMP, V_{P*}^{E} was found positive which was related to the structure-braking consequence of the solvent NMP on the electrostatic interactions between [Bmim][PF_6] ions and so the NMP molecules can be placed around the $[Bmim]^+$ and $[PF_6]^-$ ions[68]. V_{int}^{E} and V_{fv}^{E} were found to be negative in the present system while V_{P*}^{E} were found to be positive which indicates that the interaction and free volume contributions are responsible for the strong interactions between solute and solvent particles. We may summarize that the volumetric behavior of the binary mixture of {[Bmim][PF_6] + NMP} can be explained very effectively through the application of this PFP theory.

4. Conclusions

Density, speed of sound and refractive index for binary liquid mixtures of [Bmim][PF_6] with NMP were experimentally determined at atmospheric pressure and at temperatures 303.15 K, 308.15 K, 313.15 K, 318.15 K and 323.15 K over the whole compositions. From the experimental results the excess properties, V_m^E, κ_S^E, L_f^E, u^E, α_P^E and $\Delta_\phi n_D$ were calculated. The excess and deviation parameters were fitted to the Redlich-Kister polynomial, and the corresponding standard deviations were also determined. The observed excess values in the current binary liquid system [Bmim][PF_6] and NMP clearly indicated the predominance of strong attractive forces. Using Sehgal 's relationship on Hartmann-Balizar and Ballou semiempirical relations, molecular properties were determined at all temperatures. Activity coefficients determined by the NRTL relation showed low standard deviation at 308.15 K compared to other models. The inferences from excess properties were also supported by the IR spectral study. With reasonable success the PFP theory was applied to well explain the volumetric behavior of the studied system.

Journal Pre-proofs

Acknowledgements

The first author thank DST for providing an INSPIRE fellowship (F.No-DST/INSPIRE Fellowship/2018/IF180782, dated 25.09.2019) and all the authors thank KTSS Raju, Dept. of Chemistry, A. L. College, Vijayawada, for help in instrumental support.

References:

[1] T.L. Greaves, C.J. Drummond, Chem. Rev. 115 (2015) 11379–11448.

[2] F. Guo, S. Zhang, J. Wang, B. Teng, T. Zhang, M. Fan, Curr. Org. Chem. 19 (2015) 455–468.

[3] A.A. Shamsuri, R. Daik, Rev. Adv. Mater. Sci 40 (2015) 45–59.

[4] C. Comminges, R. Barhdadi, M. Laurent, M. Troupel, J. Chem. Eng. Data 51 (2006) 680–685.

[5] M.D. Bhatt, C. O'Dwyer, Phys. Chem. Chem. Phys. 17 (2015) 4799–4844.

[6] C.J. Allen, S. Mukerjee, E.J. Plichta, M.A. Hendrickson, K.M. Abraham, J. Phys. Chem. Lett. 2 (2011) 2420–2424.

[7] S. Park, R.J. Kazlauskas, Curr. Opin. Biotechnol. 14 (2003) 432–437.

[8] M. Sureshkumar, C.-K. Lee, J. Mol. Catal. B Enzym. 60 (2009) 1–12.

[9] M. Moniruzzaman, K. Nakashima, N. Kamiya, M. Goto, Biochem. Eng. J. 48 (2010) 295–314.

[10] J. V Rodrigues, D. Ruivo, A. Rodríguez, F.J. Deive, J.M.S.S. Esperança, I.M. Marrucho, C.M. Gomes, L.P.N. Rebelo, Green Chem. 16 (2014) 4520–4523.

[11] M. da Graça Nascimento, J.M.R. da Silva, J.C. da Silva, M.M. Alves, J. Mol. Catal. B Enzym. 112 (2015) 1–8.

[12] P. Lozano, T. de Diego, D. Carrié, M. Vaultier, J.L. Iborra, Chem. Commun. (2002) 692–693.

[13] M.B. Turner, S.K. Spear, J.D. Holbrey, D.T. Daly, R.D. Rogers, Biomacromolecules 6 (2005) 2497–2502.

[14] M.B. Turner, S.K. Spear, J.D. Holbrey, R.D. Rogers, Biomacromolecules 5 (2004) 1379–1384.

[15] S.S.Y. Tan, D.R. MacFarlane, J. Upfal, L.A. Edye, W.O.S. Doherty, A.F. Patti, J.M. Pringle, J.L. Scott, Green Chem. 11 (2009) 339–345.

Journal Pre-proofs

[16] M. Gericke, T. Liebert, T. Heinze, Macromol. Biosci. 9 (2009) 343–353.

[17] M. Gericke, J. Schaller, T. Liebert, P. Fardim, F. Meister, T. Heinze, Carbohydr. Polym. 89 (2012) 526–536.

[18] P. Zhang, L. Peng, W. Li, E-Polymers 8 (2008).

[19] J. Lin, Y. Teng, Y. Lu, S. Lu, X. Hao, D. Cheng, CLEAN–Soil, Air, Water 42 (2014) 799–803.

[20] J. Flieger, Anal. Lett. 42 (2009) 1632–1649.

[21] H. Zhao, S. V Malhotra, Aldrichimica Acta. 35 (2002) 75-83.

[22] D. Han, K.H. Row, Molecules 15 (2010) 2405–2426.

[23] M. Erbeldinger, A.J. Mesiano, A.J. Russell, Biotechnol. Prog. 16 (2000) 1129–1131.

[24] A.L. Harreus, R. Backes, J.O. Eichler, R. Feuerhake, C. Jäkel, U. Mahn, R. Pinkos, R. Vogelsang, Pyrrole 30 (2000) 615–618.

[25] W. Fan, Q. Zhou, J. Sun, S. Zhang, J. Chem. Eng. Data 54 (2009) 2307–2311.

[26] B. Goddu, M.M. Tadavarthi, V.K. Tadekoru, J.N. Guntupalli, J. Chem. Eng. Data 64 (2019) 2303–2319.

[27] M.A.A. Rocha, F.M.S. Ribeiro, A.I.M.C.L. Ferreira, J.A.P. Coutinho, L.M. Santos, J. Mol. Liq. 188 (2013) 196–202.

[28] M.G. Montalbán, C.L. Bolívar, F.G. Diaz Banos, G. Víllora, J. Chem. Eng. Data 60 (2015) 1986–1996.

[29] A.B. Pereiro, J.L. Legido, A. Rodrı, J. Chem. Thermodyn. 39 (2007) 1168–1175.

[30] T.S. Krishna, K. Raju, M. Gowrisankar, A.K. Nain, B. Munibhadrayya, J. Mol. Liq. 216 (2016) 484–495.

[31] J. Troncoso, C.A. Cerdeiriña, Y.A. Sanmamed, L. Romaní, L.P.N. Rebelo, J. Chem. Eng. Data 51 (2006) 1856–1859.

[32] T.S. Krishna, K. Narendra, M.G. Sankar, A.K. Nain, B. Munibhadrayya, J. Chem. Thermodyn. 98 (2016) 262–271.

[33] A. García-Abuín, D. Gomez-Diaz, M.D. La Rubia, J.M. Navaza, J. Chem. Eng. Data 56 (2011) 646–651.

[34] N. V Živković, S.S. Šerbanović, M.L. Kijevčanin, E.M. Zivkovic, J. Chem. Eng. Data 58 (2013) 3332–3341.

[35] J.-Y. Wu, Y.-P. Chen, C.-S. Su, J. Solution Chem. 44 (2015) 395–412.

Journal Pre-proofs

[36] M. Mundhwa, S. Elmahmudi, Y. Maham, A. Henni, J. Chem. Eng. Data 54 (2009) 2895–2901.

[37] G. Yanfang, W. Tengfang, Y.U. Dahong, P. Changjun, L.I.U. Honglai, H.U. Ying, Chinese J. Chem. Eng. 16 (2008) 256–262.

[38] A. Zhu, J. Wang, L. Han, M. Fan, Chem. Eng. J. 147 (2009) 27–35.

[39] M.T. Zafarani-Moattar, R. Majdan-Cegincara, J. Chem. Eng. Data 52 (2007) 2359–2364.

[40] Y. Qiao, F. Yan, S. Xia, S. Yin, P. Ma, J. Chem. Eng. Data 56 (2011) 2379–2385.

[41] M.R. Currás, M.M. Mato, P.B. Sánchez, J. García, J. Chem. Thermodyn. 113 (2017) 29–40.

[42] V.S. Rao, M.S. Reddy, K.T.S.S. Raju, B.L. Rani, B.H. Babu, J. Solution Chem. 47 (2018) 430–448.

[43] P. Suneetha, T.S. Krishna, M. Gowrisankar, M.S. Reddy, D. Ramachandran, J. Therm. Anal. Calorim. 134 (2018) 1151–1167.

[44] P.R. Rao, T.S. Krishna, D. Ramachandran, J. Chem. Thermodyn. 141 (2020) 105906.

[45] F. Qi, H. Wang, J. Chem. Thermodyn. 41 (2009) 265–272.

[46] W.L.F. Armarego, C.L.L. Chai, Purification of laboratory chemicals.(7thedn) (2013).

[47] E. Scholz, Karl Fischer Titration, Springer-Verlag, Berlin, 1984.

[48] M.B. Vraneš, S. Dožić, V. Djerić, S.B. Gadžurić, J. Chem. Eng. Data 58 (2013) 1092–1102.

[49] M.S. Reddy, S.M. Nayeem, K. Raju, B.H. Babu, J. Therm. Anal. Calorim. 124 (2016) 959–971.

[50] M.S. Reddy, K.T.S.S.S. Raju, S.M. Nayeem, I. Khan, K.B.M.M. Krishana, B.H. Babu, J. Solution Chem. 45 (2016) 675–701.

[51] S. Reddy, M.N. Sk, K. Raju, J. Mol. Liq. 218 (2016) 83–94.

[52] M.S. Reddy, I. Khan, K.T.S.S. Raju, P. Suresh, B.H. Babu, J. Chem. Thermodyn. 98 (2016) 298–308.

[53] A. Aggarwal, N.L. Lancaster, A.R. Sethi, T. Welton, Green Chem. 4 (2002) 517–520.

[54] V. Znamenskiy, M.N. Kobrak, J. Phys. Chem. B 108 (2004) 1072–1079.

[55] N.R. Dhumal, H.J. Kim, J. Kiefer, J. Phys. Chem. A 115 (2011) 3551–3558.

[56] J.-C. Lassègues, J. Grondin, D. Cavagnat, P. Johansson, J. Phys. Chem. A 113 (2009) 6419–6421.

Journal Pre-proofs

[57] J.-C. Lassegues, J. Grondin, D. Cavagnat, P. Johansson, J. Phys. Chem. A 114 (2010) 687–688.

[58] E. Vercher, F.J. Llopis, M.V. González-Alfaro, A. Martínez-Andreu, J. Chem. Eng. Data 55 (2010) 1377–1388.

[59] D. Patterson, G. Delmas, Discuss. Faraday Soc. 49 (1970) 98–105.

[60] M.T. Zafarani-Moattar, H. Shekaari, J. Chem. Thermodyn. 38 (2006) 1377–1384.

[61] M. Srinivasa Reddy, K.T.S.S.S. Raju, S. Md Nayeem, K. Bala Murali Krishna, H.B. Bollikolla, Phys. Chem. Liq. 55 (2017) 775–795.

[62] M. SrinivasaReddy, G.S. Rao, S.K.M. Nayeem, K. Raju, B.H. Babu, J. Therm. Anal. Calorim. 132 (2018) 725–739.

[63] R.B. Tôrres, M.I. Ortolan, P.L.O. Volpe, J. Chem. Thermodyn. 40 (2008) 442–459.

[64] P.J. d Flory, J. Am. Chem. Soc. 87 (1965) 1833–1838.

[65] A. Abe, P.J. Flory, J. Am. Chem. Soc. 87 (1965) 1838–1846.

[66] E. Vercher, A.V. Orchilles, P.J. Miguel, A. Martínez-Andreu, J. Chem. Eng. Data 52 (2007) 1468–1482.

[67] A. Kumar, T. Singh, R.L. Gardas, J.A.P. Coutinho, J. Chem. Thermodyn. 40 (2008) 32–39.

[68] Z.S. Vaid, U.U. More, S.B. Oswal, N.I. Malek, Thermochim. Acta 634 (2016) 38–47.

Highlights

- The studied binary systems is {**[Bmim][PF_6]+1-methylpyrrolidone**}
- Density, speed of sound and refractive index are measured at various temperatures
- The interactions in the system are analyzed in terms of excess parameters
- The existing interactions are well explained with the help of IR spectral studies
- Observed experimental results are correlated with PFP theory

Journal Pre-proofs

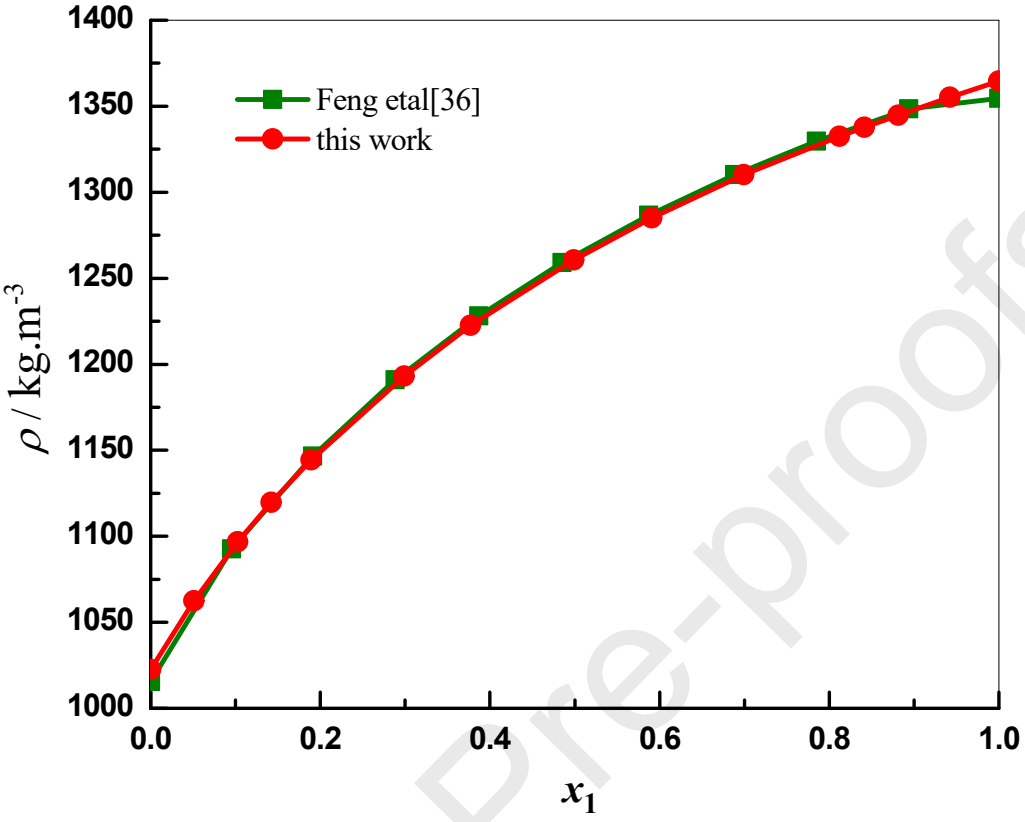


Fig. 1 Plots of experimental densities of Feng etal[36] and this work of the binary mixtures of [Bmim][PF_6] with NMP against mole fraction of [Bmim][PF_6] at 303.15 K.

Journal Pre-proofs

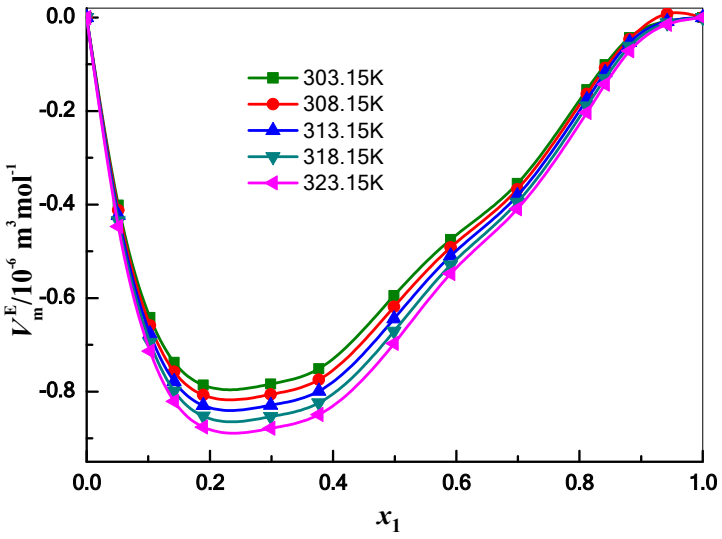


Fig. 2 Plots of excess molar volume (V_m^E) against mole fraction of [Bmim][PF_6] in the mixture with NMP at different temperatures**.**

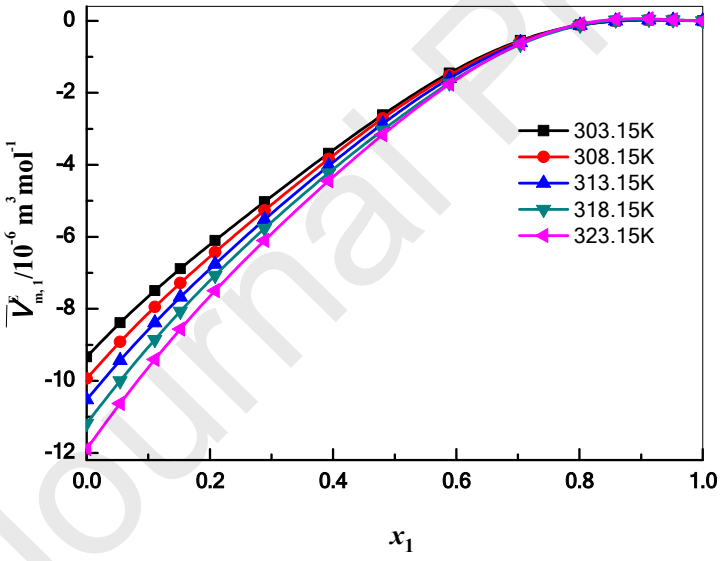


Fig. 3 Plots of excess partial molar volume ($\overline{V}_{m,1}^E$) against mole fraction of [Bmim][PF_6] in the mixture with NMP at different temperatures.

Journal Pre-proofs

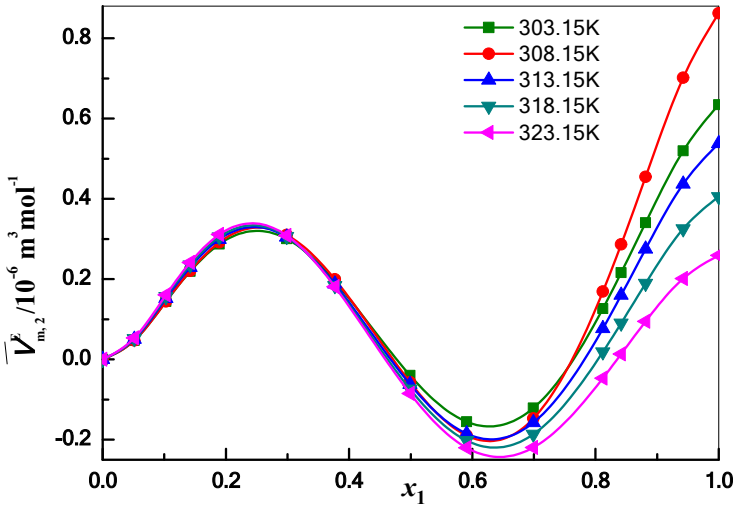


Fig. 4 Plots of excess partial molar volume ($\overline{V}^{E}_{m,2}$) against mole fraction of [Bmim][PF_6] in the mixture with NMP at different temperatures.

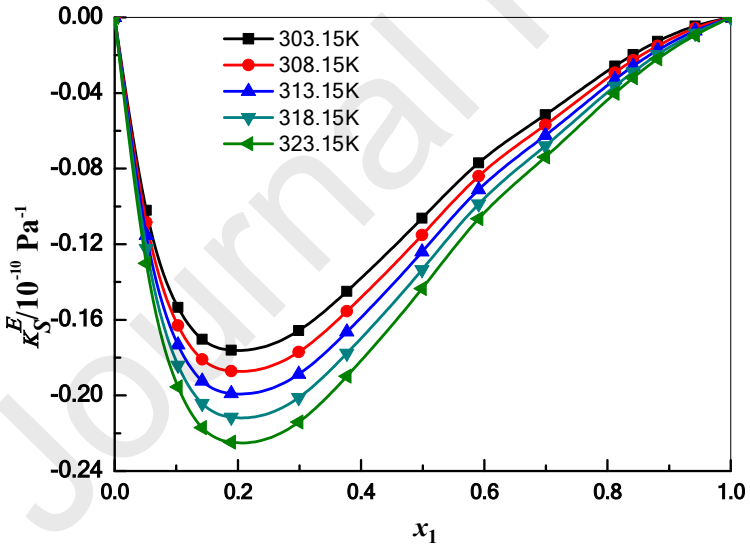


Fig. 5 Plots of excess isentropic compressibility (κ^{E}_{S}) against mole fraction of [Bmim][PF_6] in the mixture with NMP at different temperatures.

Journal Pre-proofs

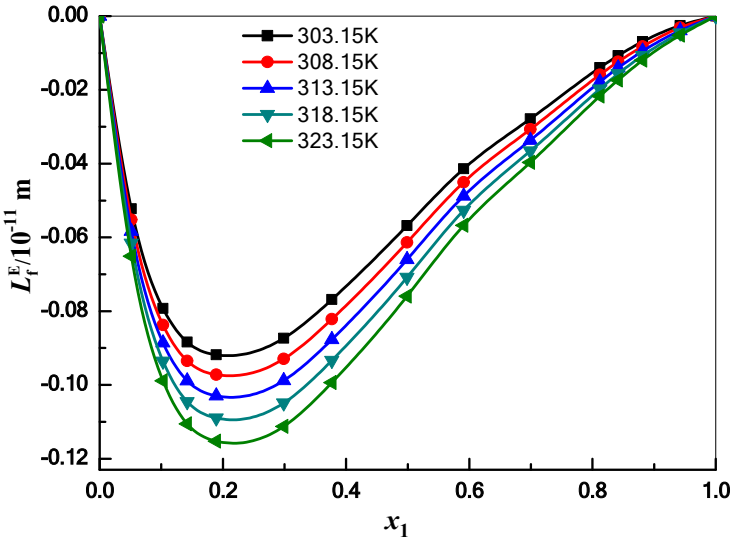


Fig. 6 Plots of excess free length (L_f^E) against mole fraction of [Bmim][PF_6] in the mixture with NMP at different temperatures.

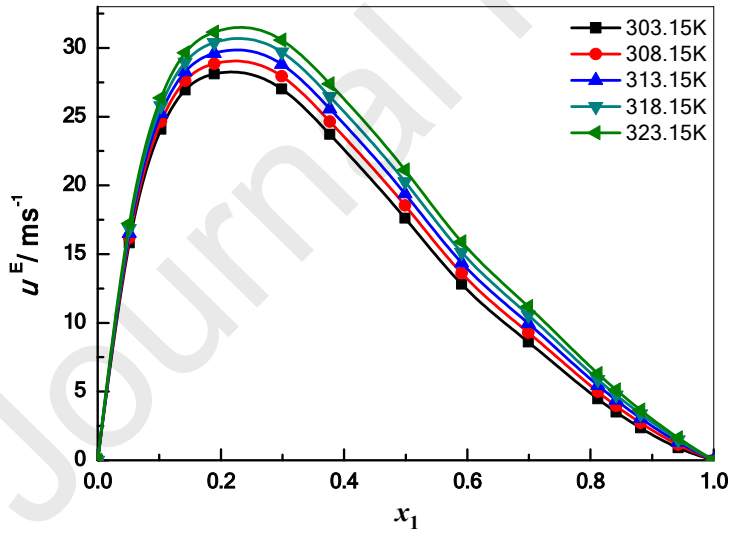


Fig.7 Plots of Excess ultrasonic speed of sounds (u^E) against mole fraction of [Bmim][PF_6] in the mixture with NMP at different temperatures.

Journal Pre-proofs

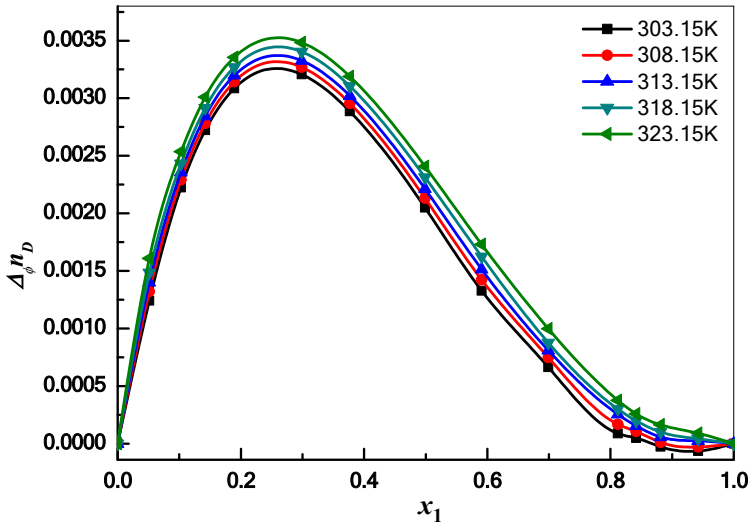


Fig. 8 Plots of deviation in refractive index ($\Delta_\emptyset n_D$) against mole fraction of [Bmim][PF_6] in the mixture with NMP at different temperatures.

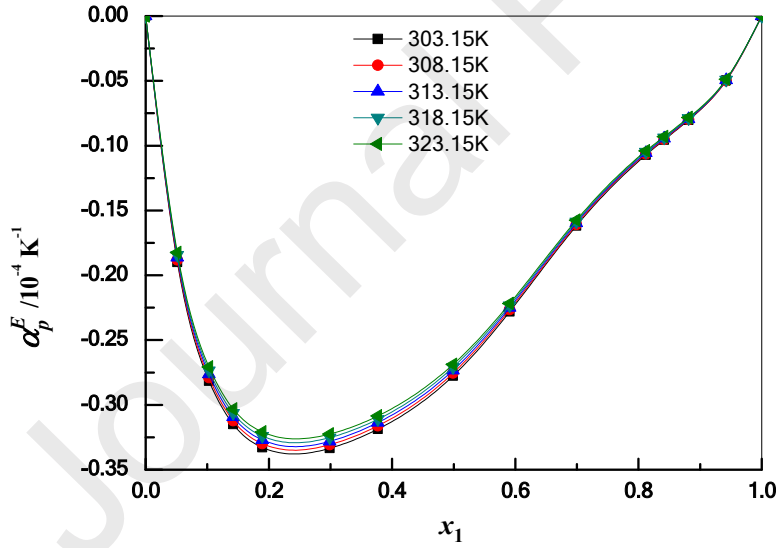
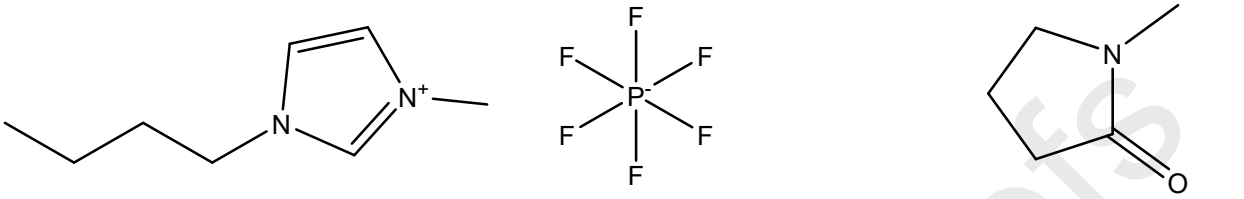


Fig. 9 Plots of Excess isobaric thermal expansion coefficient (α_P^E) against mole fraction of [Bmim][PF_6] in the mixture with NMP at different temperatures.

Journal Pre-proofs



1-butyl-3-methylimidazolium hexafluorophosphate

1-methyl-2-pyrrolidone

Fig.10 Chemical Structures of [Bmim][PF_6] and NMP.

Journal Pre-proofs

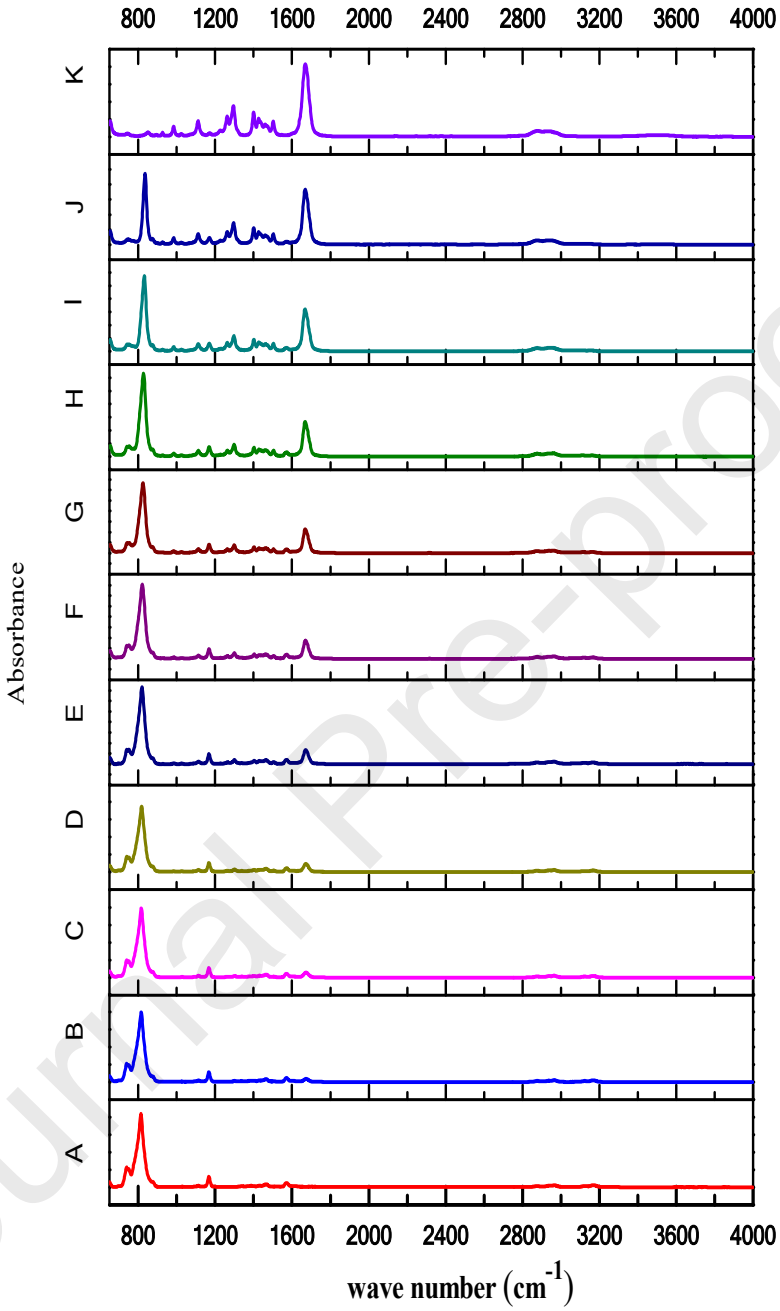


Fig.11 Infrared spectra (650 cm^{-1}-4000 cm^{-1}) of (A) Pure IL [Bmim][PF_6],(B) 0.8812; (C) 0.8120; (D) 0.6991; (E) 0.5910; (F0.4990; (G) 0.3771; (H) 0.2988; (I) 0.1894; (J) 0.1028 and (K) Pure NMP. (B), (C), (D), (E), (F), (G), (H), (I), (J) represents mole fraction of [Bmim][PF_6] in the mixture with NMP.

Journal Pre-proofs

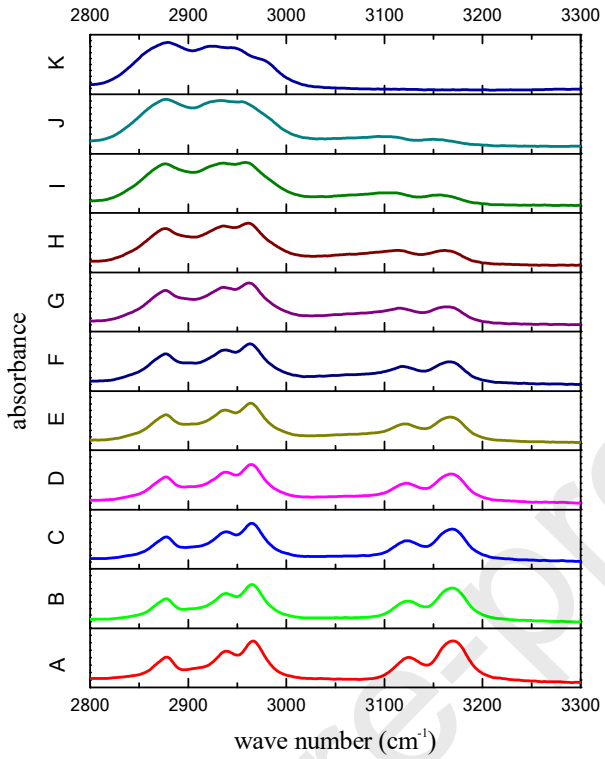


Fig.12 Infrared spectra (2800 cm^{-1}-3300 cm^{-1}) of (A) Pure IL [Bmim][PF_6];(B) 0.8812; (C) 0.8120; (D) 0.6991; (E) 0.5910; (F0.4990; (G) 0.3771; (H) 0.2988; (I) 0.1894; (J) 0.1028 and (K) Pure NMP. (B), (C), (D), (E), (F), (G), (H), (I), (J) represents mole fraction of [Bmim][PF_6] in the mixture with NMP.

Journal Pre-proofs

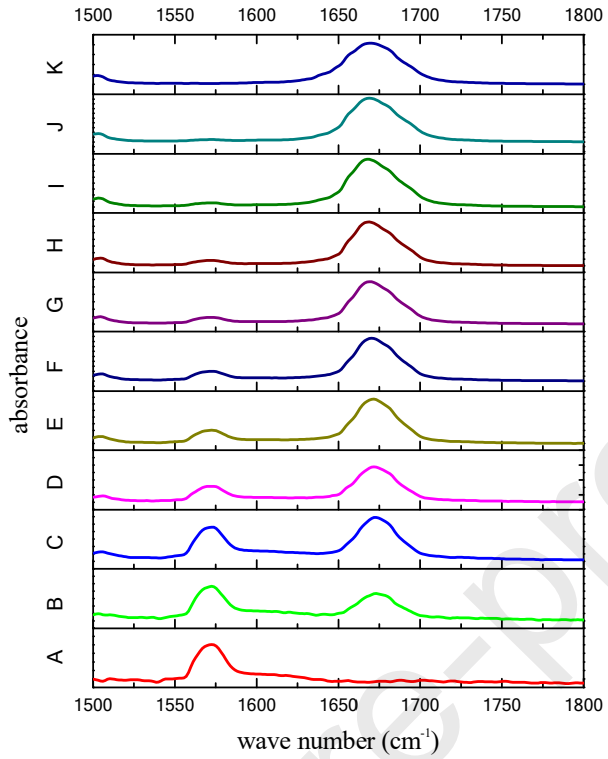


Fig.13 Infrared spectra (1500 cm^{-1}-1800 cm^{-1}) of (A) Pure IL [Bmim][PF_6];(B) 0.8812; (C) 0.8120; (D) 0.6991; (E) 0.5910; (F0.4990; (G) 0.3771; (H) 0.2988; (I) 0.1894; (J) 0.1028 and (K) Pure NMP. (B), (C), (D), (E), (F), (G), (H), (I), (J) represents mole fraction of [Bmim][PF_6] in the mixture with NMP.

Table 1 Comparison of experimental values of density, ρ, speed of sound, u, refractive index, n_D, and specific heat, C_p, of pure liquids with the corresponding literature values at different temperatures and at atmospheric pressure P = 101.3 kPa.

Liquid	Temp / (K)	ρ /(kg m^{-3})		u/(m s^{-1})		n_D		C_p/(J K^{-1} mol^{-1})
		Expt.	Lit.	Expt.	Lit.	Expt.	Lit.	Lit.
[Bmim][PF_6]	303.15	1364.6	1363.277 [25] 1363.08[26]	1431.7	1430.6 [29] 1431.9[2	1.4082 3	1.40746 [30] 1.40812[2	410.33 [31]

Journal Pre-proofs

			1363.2[27] 1362.36[28]		6]		7] 1.4080[28]	
	308.15	1360.4	1359.191 [25] 1358.91[26] 1359.0[27]	1419.8	1419.0 [29] 1420.1[26]	1.40691	1.40585 [30] 1.40679[27]	413.14 [31]
	313.15	1356.2	1355.087 [25] 1354.74[26] 1354.9[27] 1353.99[28]	1408.2	1406.4 [29] 1408.5[26]	1.40556	1.40468 [30] 1.40546[27] 1.4055[28]	415.98 [31]
	318.15	1352.1	1350.980 [25] 1350.58[26] 1350.8[27]	1396.8	1395.0 [29] 1397.1[26]	1.40414	1.40352 [30] 1.40413[27]	418.91 [31]
	323.15	1348.0	1346.874 [25] 1346.41[26] 1346.8[27] 1345.70[28]	1385.6	1385.15 [29] 1385.9[26]	1.40276	1.40243 [30] 1.4030[28]	421.88 [31]
1-Methyl-2-pyrrolidinone	303.15	1022.6	1022.64 [32] 1023.95[33] 1023.925[34] 1023.70[35]	1524.3	1524.32 [32] 1526.5[33]	1.46638	1.46626 [32] 1.4664[33] 1.46520[34]	166 [36]
	308.15	1018.2	1018.18 [32] 1019.462[34]	1505.0	1504.96 [32]	1.46428	1.46412 [32] 1.46306[34]	167 [36]
	313.15	1013.7	1013.72 [32] 1015.03[33] 1015.000[34] 1014.78[35]	1485.7	1485.74 [32] 1487.8[33]	1.46219	1.46199 [32] 1.4621[33] 1.46095[34]	168 [36]
	318.15	1009.3	1009.25 [32] 1010.533[34]	1466.7	1466.67 [32]	1.46008	1.45983 [32] 1.45891[34]	169 [36]
	323.15	1004.8	1004.78 [32] 1006.10[33]	1447.8	1447.76 [32] 1450.2[3	1.45796	1.45571 [32] 1.4576[33]	170 [36]

Journal Pre-proofs

	1006.061[34] 1005.85[35]	3]	1.45680[34]

Standard uncertainties u are: $u(\rho)$ = 1.0 kg ·m^{-3},$u(u)$ = 0.5 ms^{-1}, $u(n_D)$ = 0.0005,u (I) = 0.01 K and $u(P)$=0.5kPa

Table 2 Experimental density (ρ), speed of sound (u), refractive index (n_D), molar volume (V_m),Isentropic compressibility(κ_S),free length (L_f)and isobaric thermal expansion coefficient (α_p) with mole fraction (x_1) of [Bmim][PF_6] in the binary liquid mixture of {[Bmim][PF_6]+ 1-Methyl-2-pyrrolidinone} from T/K = 303.15 to 323.15 at pressure P = 101.3 kPa.

x_1	ρ / (kg m^{-3})	u / (m s^{-1})	n_D	V_m/ (10^{-6}m^3 mol^{-1})	κ_S / (10^{-10}Pa^{-1})	L_f /(10^{-11}m)	α_p /10^{-4} K^{-1}
303.15 K							
0.0000	1022.6	1524.3	1.46638	96.94	4.21	4.258	8.73
0.0513	1062.4	1522.2	1.46171	102.24	4.06	4.183	8.27

0.1028	1096.7	1516.1	1.45724	107.74	3.97	4.134	7.93
0.1422	1119.8	1510.0	1.45396	112.03	3.92	4.108	7.72
0.1894	1144.5	1502.2	1.45018	117.23	3.87	4.084	7.52
0.2988	1193.2	1485.8	1.44196	129.41	3.80	4.044	7.14
0.3771	1222.6	1474.9	1.43656	138.17	3.76	4.025	6.92
0.4990	1260.6	1460.7	1.42898	151.89	3.72	4.002	6.66
0.5910	1285.0	1451.8	1.42391	162.25	3.69	3.988	6.51
0.6991	1310.2	1444.3	1.41867	174.41	3.66	3.970	6.37
0.8120	1332.4	1437.9	1.41403	187.18	3.63	3.954	6.25
0.8415	1337.7	1436.6	1.41296	190.51	3.62	3.950	6.21
0.8812	1344.7	1434.9	1.41161	194.99	3.61	3.945	6.17
0.9423	1355.2	1432.9	1.40974	201.83	3.59	3.935	6.12
1.0000	1364.6	1431.7	1.40823	208.26	3.58	3.925	6.10
308.15 K							
0.0000	1018.2	1505.0	1.46428	97.36	4.34	4.361	8.77
0.0513	1058.0	1503.9	1.45966	102.67	4.18	4.281	8.31
0.1028	1092.3	1498.8	1.45526	108.17	4.08	4.228	7.97
0.1422	1115.4	1493.2	1.45203	112.46	4.02	4.199	7.76
0.1894	1140.2	1486.0	1.44830	117.67	3.97	4.174	7.55
0.2988	1189.0	1470.9	1.44020	129.88	3.89	4.129	7.17
0.3771	1218.3	1460.6	1.43488	138.65	3.85	4.108	6.95
0.4990	1256.4	1447.2	1.42741	152.40	3.80	4.083	6.69
0.5910	1280.8	1438.8	1.42241	162.78	3.77	4.067	6.54
0.6991	1306.0	1431.7	1.41723	174.97	3.74	4.048	6.40
0.8120	1328.2	1425.8	1.41265	187.77	3.70	4.030	6.27
0.8415	1333.5	1424.5	1.41159	191.11	3.70	4.026	6.23
0.8812	1340.5	1423.0	1.41025	195.60	3.68	4.020	6.19
0.9423	1350.9	1421.1	1.40840	202.47	3.67	4.010	6.14
1.0000	1360.4	1419.8	1.40691	208.90	3.65	3.999	6.11
313.15 K							
0.0000	1013.7	1485.7	1.46219	97.79	4.47	4.467	8.81
0.0513	1053.6	1485.8	1.45764	103.10	4.30	4.381	8.34
0.1028	1088.0	1481.6	1.45329	108.60	4.19	4.324	8.01
0.1422	1111.1	1476.6	1.45011	112.90	4.13	4.293	7.80
0.1894	1135.9	1470.0	1.44643	118.12	4.07	4.265	7.59
0.2988	1184.7	1456.0	1.43845	130.35	3.98	4.216	7.20
0.3771	1214.1	1446.4	1.43320	139.14	3.94	4.193	6.98
0.4990	1252.2	1433.9	1.42582	152.91	3.88	4.165	6.71
0.5910	1276.6	1425.9	1.42088	163.32	3.85	4.148	6.56

Journal Pre-proofs

0.6991	1301.8	1419.4	1.41577	175.54	3.81	4.126	6.42
0.8120	1324.1	1413.8	1.41123	188.36	3.78	4.107	6.29
0.8415	1329.4	1412.6	1.41018	191.71	3.77	4.103	6.26
0.8812	1336.3	1411.2	1.40886	196.21	3.76	4.096	6.21
0.9423	1346.8	1409.4	1.40703	203.09	3.74	4.085	6.16
1.0000	1356.2	1408.2	1.40556	209.54	3.72	4.074	6.13
318.15 K							
0.0000	1009.3	1466.7	1.46008	98.22	4.61	4.575	8.85
0.0513	1049.2	1467.8	1.45559	103.53	4.42	4.484	8.38
0.1028	1083.6	1464.5	1.45130	109.04	4.30	4.422	8.04
0.1422	1106.8	1460.1	1.44816	113.34	4.24	4.389	7.84
0.1894	1131.6	1454.1	1.44453	118.57	4.18	4.358	7.63
0.2988	1180.4	1441.3	1.43666	130.82	4.08	4.305	7.24
0.3771	1209.8	1432.4	1.43148	139.62	4.03	4.279	7.02
0.4990	1248.0	1420.7	1.42419	153.42	3.97	4.248	6.74
0.5910	1272.4	1413.2	1.41931	163.86	3.94	4.229	6.59
0.6991	1297.6	1407.1	1.41426	176.10	3.89	4.206	6.45
0.8120	1319.9	1402.0	1.40977	188.95	3.85	4.185	6.31
0.8415	1325.2	1400.9	1.40873	192.31	3.85	4.180	6.28
0.8812	1332.2	1399.6	1.40742	196.82	3.83	4.173	6.23
0.9423	1342.6	1398.0	1.40561	203.71	3.81	4.162	6.18
1.0000	1352.1	1396.8	1.40414	210.19	3.79	4.150	6.15
323.15 K							
0.0000	1004.8	1447.8	1.45796	98.66	4.75	4.686	8.89
0.0513	1044.8	1450.1	1.45353	103.97	4.55	4.588	8.42
0.1028	1079.3	1447.6	1.44930	109.48	4.42	4.522	8.08
0.1422	1102.5	1443.8	1.44620	113.79	4.35	4.486	7.87
0.1894	1127.3	1438.4	1.44261	119.02	4.29	4.453	7.66
0.2988	1176.1	1426.7	1.43483	131.29	4.18	4.395	7.27
0.3771	1205.6	1418.5	1.42972	140.11	4.12	4.366	7.05
0.4990	1243.9	1407.6	1.42253	153.93	4.06	4.332	6.77
0.5910	1268.2	1400.6	1.41772	164.40	4.02	4.312	6.61
0.6991	1293.4	1395.1	1.41274	176.67	3.97	4.286	6.47
0.8120	1315.8	1390.3	1.40831	189.54	3.93	4.264	6.33
0.8415	1321.1	1389.3	1.40729	192.91	3.92	4.259	6.30
0.8812	1328.1	1388.1	1.40600	197.43	3.91	4.251	6.25
0.9423	1338.5	1386.6	1.40421	204.34	3.89	4.239	6.20
1.0000	1348.0	1385.6	1.40276	210.83	3.86	4.227	6.17

Journal Pre-proofs

	T/K	A_0	A_1	A_2	A_3	A_4	σ
	303.15	-2.4072	2.2409	-1.5853	2.9412	-0.5551	0.0132

Journal Pre-proofs

Standard uncertainties u are: u (x_1) = 0.0005, u (ρ) = 1 kg·m^{-3},u (u) = 0.5 m s^{-1}, u (n_D) = 0.0005, u (T) = 0.01 K and u(P)= 0.5 kPa Combined uncertainties (Confidence level, 95%).: U_c (V_m) = ± 0.1 x 10^{-6} m^3 mol^{-1},U_c(κ_S) = ± 0.05 x10^{-10} Pa^{-1},U_c (L_f) = ± 0.05 x10^{-11} m, U_c(α_p) = ± 0.06 x10^{-4} K^{-1}. All the experiments were carried out at atmospheric pressure.

Table 3 Redlich-Kister coefficients of deviation/excess properties and corresponding standard deviations (σ) for the system at different temperatures

V_m^E /(10^{-6}m^{3}mol^{-1})	308.15	-2.4870	2.2507	-1.7358	3.1317	-0.2971	0.0128
	313.15	-2.5847	2.3292	-1.5966	3.0718	-0.6820	0.0132
	318.15	-2.6796	2.3766	-1.6045	3.1027	-0.7898	0.0133
	323.15	-2.7732	2.4264	-1.6244	3.1294	-0.8987	0.0135
κ_s^E /(10^{-10} Pa^{-1})	303.15	-0.4256	0.5814	-0.4516	0.6023	-0.4404	0.0023
	308.15	-0.4604	0.6102	-0.4731	0.6364	-0.4763	0.0025
	313.15	-0.4963	0.6419	-0.4948	0.6713	-0.5205	0.0027
	318.15	-0.5338	0.6758	-0.5187	0.7098	-0.5617	0.0028
	323.15	-0.5733	0.7108	-0.5426	0.7545	-0.6087	0.0031
u^E/ (ms^{-1})	303.15	69.39	-94.57	71.93	-84.42	61.72	0.35
	308.15	73.50	-96.18	72.33	-84.78	64.61	0.36
	313.15	77.42	-97.80	73.48	-85.73	66.46	0.38
	318.15	81.30	-99.62	74.30	-86.60	68.17	0.38
	323.15	85.21	-101.29	74.89	-88.13	70.31	0.39
L_f^E/(10^{-11} m)	303.15	-0.2246	0.3037	-0.2329	0.2979	-0.2098	0.0012
	308.15	-0.2439	0.3184	-0.2434	0.3126	-0.2254	0.0013
	313.15	-0.2439	0.3184	-0.2434	0.3126	-0.2254	0.0013
	318.15	-0.2844	0.3518	-0.2651	0.3436	-0.2628	0.0014
	323.15	-0.3061	0.3694	-0.2764	0.3627	-0.2829	0.0015
α_P^E (10^{-4} K^{-1})	303.15	-1.1080	0.8704	-0.1379	0.8614	-1.8421	0.0024
	308.15	-1.1001	0.8638	-0.1304	0.8454	-1.8364	0.0022
	313.15	-1.0915	0.8551	-0.1325	0.8371	-1.8095	0.0022
	318.15	-1.0830	0.8472	-0.1295	0.8260	-1.7919	0.0022
	323.15	-1.0745	0.8393	-0.1256	0.8142	-1.7745	0.0021
$\Delta_\phi n_D$	303.15	0.00812	-0.01538	0.00680	-0.00016	-0.00190	0.00002
	308.15	0.00812	-0.01538	0.00680	-0.00016	-0.00190	0.00002
	313.15	0.00883	-0.01487	0.00575	-0.00143	0.00144	0.00001
	318.15	0.00925	-0.01472	0.00492	-0.00215	0.00331	0.00001
	323.15	0.00968	-0.01430	0.00443	-0.00344	0.00536	0.00002

Journal Pre-proofs

Table 4 Partial molar volumes of component-1 ($\overline{V}_{m,1}$) ([Bmim][PF_6])and component-2($\overline{V}_{m,2}$) (1-Methyl-2-pyrrolidinone) with mole fraction (x_1) of [Bmim][PF_6] in the binary liquid mixture from T/K =303.15 to 323.15 at pressure P = 101.3 kPa.

	303.15 K		308.15 K		313.15 K		318.15 K		323.15 K	
x_1	$\overline{V}_{m,1}$	$\overline{V}_{m,2}$	$\overline{V}_{m,1}$	$\overline{V}_{m,2}$	$\overline{V}_{m,1}$	$\overline{V}_{m,2}$	$\overline{V}_{m,1}$	$\overline{V}_{m,2}$	$\overline{V}_{m,1}$	$\overline{V}_{m,2}$
	/ 10^{-6} m^3 mol^{-1}		/ 10^{-6} m^3 mol^{-1}		/ 10^{-6} m^3 mol^{-1}		/ 10^{-6} m^3 mol^{-1}		/ 10^{-6} m^3 mol^{-1}	
0.0000	198.53	96.94	199.00	97.36	199.28	97.79	199.63	98.22	199.98	98.66
0.0513	199.62	96.98	200.10	97.41	200.43	97.84	200.82	98.27	201.21	98.71
0.1028	200.83	97.08	201.31	97.50	201.71	97.94	202.14	98.38	202.56	98.82
0.1422	201.75	97.15	202.24	97.58	202.69	98.02	203.15	98.46	203.61	98.90
0.1894	202.82	97.22	203.31	97.65	203.82	98.09	204.31	98.53	204.80	98.97
0.2988	204.91	97.24	205.45	97.67	206.02	98.09	206.58	98.53	207.13	98.97
0.3771	206.01	97.13	206.58	97.56	207.18	97.98	207.76	98.41	208.34	98.84
0.4990	207.09	96.90	207.71	97.30	208.31	97.73	208.92	98.15	209.52	98.57
0.5910	207.54	96.78	208.17	97.17	208.77	97.60	209.39	98.02	210.01	98.44
0.6991	207.83	96.81	208.46	97.21	209.09	97.63	209.72	98.03	210.36	98.44
0.8120	208.04	97.06	208.67	97.53	209.32	97.87	209.96	98.24	210.60	98.61
0.8415	208.09	97.15	208.72	97.65	209.37	97.95	210.01	98.31	210.66	98.67
0.8812	208.15	97.28	208.78	97.81	209.43	98.06	210.08	98.41	210.72	98.75
0.9423	208.23	97.45	208.87	98.06	209.51	98.23	210.16	98.55	210.80	98.86
1.0000	208.26	97.57	208.90	98.22	209.54	98.33	210.19	98.63	210.83	98.92

Combined uncertainties (Confidence level, 95%):$U(\overline{V}_{m,1}) = \pm 0.1 \times 10^{-6}$ m^3 mol^{-1}, $U(\overline{V}_{m,2}) = \pm 0.1 \times 10^{-6}$ m^3 mol^{-1}

Journal Pre-proofs

Table 5 Partial molar volumes at infinite dilution ($\overline{V}^{\infty}_{m,1}$, $\overline{V}^{\infty}_{m,2}$) and excess partial molar volumes at infinite dilution ($\overline{V}^{E,\infty}_{m,1}$, $\overline{V}^{E,\infty}_{m,2}$) of [Bmim][PF_6] and 1-Methyl-2-pyrrolidinone T = (303.15, 308.15, 313.15, 318.15 and 323.15) K.

T/ K	$\overline{V}^{\infty}_{m,1}$	$\overline{V}^{E,\infty}_{m,1}$	$\overline{V}^{\infty}_{m,2}$	$\overline{V}^{E,\infty}_{m,2}$
	/(10^{-6} m^3mol^{-1})		/(10^{-6} m^3mol^{-1})	
303.15	198.53	-9.73	97.57	0.63
308.15	199.00	-9.90	98.22	0.86
313.15	199.28	-10.26	98.33	0.54
318.15	199.63	-10.55	98.63	0.41
323.15	199.98	-10.85	98.92	0.26

Standard uncertainties u are: u (x_1) = 0.0002, u (T) = 0.01 K and u(P)=0.5 kPa

Combined uncertainties (Confidence level, 95%):$U(\overline{V}^{E,\infty}_{m,1})$ = ± 0.1 x 10^{-6} m^3 mol^{-1}, $U(\overline{V}^{E,\infty}_{m,2})$ = ± 0.1 x 10^{-6} m^3 mol^{-1}

Journal Pre-proofs

Table 6 Infrared absorbance wave numbers (cm^{-1}) between 2800 to 3200 of [Bmim][PF_6] in NMP at room temperature and atmospheric pressure P = 101.3 kPa.

Infrared absorbance wave numbers /(cm^{-1})

Mole fraction of [Bmim][PF_6]	Mole fraction of NMP	C_2-H stretching	$C_{4,5}$-H stretching	C=O Stretch
1.0000	0.0000	3124.3	3169.2	-
0.8812	0.1188	3123.3	3168.3	1672.7
0.8120	0.1880	3122.2	3168.2	1672.7
0.6991	0.3009	3121.2	3168.2	1671.7
0.5910	0.4090	3120.2	3167.2	1671.7
0.4990	0.5024	3119.2	3166.2	1670.7
0.3771	0.6229	3116.1	3164.1	1669.7
0.2988	0.7012	3113.3	3161.8	1668.5
0.1894	0.8106	-	-	1667.8
0.1028	0.8972	-	-	1668.9
0.0000	1.0000	-	-	1669.3

Journal Pre-proofs

Table 7 Characteristic and reduced parameters for the pure components used in PFP theory at various temperatures.

T/(K)	$\tilde{V}$	V_1^* /(10^{-6}m^3.mol^{-1})	P_1^* /(10^6 J.mol^{-1})
[Bmim][PF$_6$]			
303.15	1.1642	178.88	604.01
308.15	1.1671	178.99	606.90
313.15	1.1699	179.11	609.77
318.15	1.1728	179.22	612.62
323.15	1.1757	179.33	615.42
NMP			
303.15	1.2242	79.18	713.79
308.15	1.2282	79.27	712.94
313.15	1.2322	79.36	711.85
318.15	1.2361	79.46	710.53
323.15	1.2401	79.56	708.99

Table 8 PFP interaction parameter, χ_{12}, and calculated values of the three contributions from the PFP theory at equimolar composition for ([Bmim][PF$_6$] + NMP) system at *T*=(303.15-323.15) K

T /K	χ_{12} /(10^6 J m^{-3})	$V_m^E(int)$ /(10^{-6} m^3 mol^{-1})	$V_m^E(fv)$ /(10^{-6} m^3 mol^{-1})	$V_m^E(ip)$ /(10^{-6} m^3 mol^{-1})
303.15	-56.5832	-0.7253	-0.1598	0.2833
308.15	-56.1203	-0.7346	-0.1654	0.2782
313.15	-55.9229	-0.7474	-0.1711	0.2722
318.15	-55.5898	-0.7584	-0.1768	0.2654
323.15	-55.1682	-0.7684	-0.1827	0.2578

Journal of Genetic Engineering and Biotechnology

RESEARCH Open Access

Antioxidant potential and optimization of production of extracellular polysaccharide by *Acinetobacter indicus* M6

Ch. Ravi Teja[1], Abraham P. Karlapudi[2], Neeraja Vallur[3], K. Mamatha[1], D. John Babu[2], T. C. Venkateswarulu[2] and Vidya Prabhakar Kodali[1*]

Abstract

Background: Extracellular polysaccharides (ECPs) produced by biofilm-producing marine bacterium have great applications in biotechnology, pharmaceutical, food engineering, bioremediation, and bio-hydrometallurgy industries. The ECP-producing strain was identified as *Acinetobacter indicus* M6 species by 16S rDNA analysis. The polymer produced by the isolate was quantified and purified and chemically analyzed, and antioxidant activities have been studied. The face-centered central composite design (FCCCD) was used to design the model.

Results: The results have clearly shown that the ECP was found to be endowed with significant antioxidative activities. The ECP showed 59% of hydroxyl radical scavenging activity at a concentration of 500 μg/mL, superoxide radical scavenging activity (72.4%) at a concentration of 300 μg/mL, and DPPH$^{\bullet}$ radical scavenging activity (72.2%) at a concentration of 500 μg/mL, respectively. Further, HPLC and GC-MS results showed that the isolated ECP was a heteropolymer composed of glucose as a major monomer, and mannose and glucosamine were minor monomers. Furthermore, the production of ECP by *Acinetobacter indicus* M6 was increased through optimization of nutritional variables, namely, glucose, yeast extract, and $MgSO_4$ by "Response Surface Methodology". Moreover the production of ECP reached to 2.21 g/L after the optimization of nutritional variables. The designed model is statistically significant and is indicated by the R^2 value of 0.99. The optimized medium improved the production of ECP and is two folds higher in comparison with the basal medium.

Conclusions: *Acinetobacter indicus* M6 bacterium produces a novel and unique extracellular heteropolysaccharide with highly efficient antioxidant activity. GC-MS analyses elucidated the presence of quite uncommon (1→4)-linked glucose, (1→4)-linked mannose, and (→4)-GlcN-(1→) glycosidic linkages in the backbone. The optimized medium improved the production of ECP and is two folds higher in comparison with the basal medium. The newly optimized medium could be used as a promising alternative for the overproduction of ECP.

Keywords: Extracellular polysaccharide, Antioxidant activity, Response surface methodology, Monosaccharide composition

* Correspondence: kodalividyaprabhakar@gmail.com
[1]Department of Biotechnology, Vikrama Simhapuri University, Kakutur, Nellore A.P-524320, India
Full list of author information is available at the end of the article

Springer Open

© The Author(s). 2021 **Open Access** This article is licensed under a Creative Commons Attribution 4.0 International License, which permits use, sharing, adaptation, distribution and reproduction in any medium or format, as long as you give appropriate credit to the original author(s) and the source, provide a link to the Creative Commons licence, and indicate if changes were made. The images or other third party material in this article are included in the article's Creative Commons licence, unless indicated otherwise in a credit line to the material. If material is not included in the article's Creative Commons licence and your intended use is not permitted by statutory regulation or exceeds the permitted use, you will need to obtain permission directly from the copyright holder. To view a copy of this licence, visit http://creativecommons.org/licenses/by/4.0/.

Background

Acinetobacter species produce medicinally and commercially important diverse group of molecules [1]. Extracellular polysaccharides (ECPs) are one of such important molecules. ECPs are long-chain, high molecular-mass polymers which have been reported to show antiulcer, immunomodulatory, antiviral, antioxidant, and various other biological activities [2, 3]. These ECPs are the alternative class of biothickeners and also proved to have good emulsifying property apart from the texture-promoting property in various foods [4]. In some countries of the European Union (EU) and the United States of America (USA), where addition of synthetic texture-promoting agents in food and dairy products is prohibited, ECPs can successfully be used as food additives to enhance texture [5]. The ECPs are economically important because they can impart functional effects to foods. Depending on the monosaccharide composition, ECPs can be classified into homo (HoPSs) and heteropolysaccharides (HePSs). HoPSs consist of only one type of monosaccharide.

Recently, studies have been focused on antioxidant polysaccharides that can find potential applications in food industries [6]. Free radicals such as superoxide radical anion ($O_2^{\cdot-}$), hydroxyl radical (OH·), and other reactive oxygen species (ROS) are considered to be highly potent oxidants that can react with all biomacromolecules in living cells, and they may associate with carcinogenesis and mutagenesis [7]. ECPs were reported to have free radical scavenging activities [8]. Bacterial polysaccharides isolated from *Pantoea agglomerans* and *Microbacterium terregens* [9] showed pronounced antioxidant activities.

Considering the antioxidant activity and other therapeutic importance of the ECP, it is important to characterize the ECP structurally. Therefore, the monomeric composition of the ECP was identified by HPLC, and glycosidic linkages of the ECP were determined by GC-MS. HPLC is frequently used for both the qualitative and quantitative analysis of liberated monosaccharides after acid hydrolysis. HPLC with an ultraviolet (UV) detector or refractive index (RI) is an alternative method for quantitative determination of saccharides. Due to low sensitivity and inapplicability to gradient elution, HPLC with RI detector is less commonly used [10]. The alternative approach is HPLC with UV detector, which is highly sensitive and widely used for analysis and quantification of monomers. GC attached to a mass spectrometer is an efficient and widely applicable method for linkage analysis of methylated polysaccharides. Methylation analysis is an essential step for studying the linkage pattern of sugar residues. Depending on the mass spectra obtained, the glycosidic linkages are analyzed [11, 12].

The production of polymers is highly influenced by different factors such as nutritional variables and physical variables of the process, namely, temperature, pH, RPM, dissolved oxygen concentration, and RPM [9]. Studies also reported that the growth and development of film formation depend on surface area, smoothness, flow velocity, and nutrients [13]. Very few reports are available on design fermentation medium through response surface methodology (RSM) optimization studies for production of ECPs [13]. Therefore, the present study aimed to design the low-cost fermentation medium for enhanced production of the ECP using RSM.

Considering the tremendous reported therapeutic and commercial potentials, the ECP molecule may be developed as a potential drug molecule in the near future. Establishing the structure-function relationship of the ECP molecule by elucidating its complete molecular structure on further chemical derivatizations and enzymatic digestions (with glucosidases) will enable to identify the right fragments of the large ECP molecule, responsible for important bioactive properties of therapeutic and commercial interests. This would also help to use the small fragments for specific therapeutic purposes, instead of using the whole molecule.

Methods

Extraction, purification, and quantification of extracellular polysaccharide

ECP-producing organism was isolated and identified as mentioned previously [14]. Ten milliliters of overnight culture was centrifuged, and 30 mL alcohol (95%) was added to the supernatant. The mixture was shaken thoroughly and kept at 4 °C for overnight. The precipitated polymer was separated by centrifugation and dried to get crude ECP. The dried and crude powder (10 mg) was dissolved in 1 mL 0.2 M NaCl buffer to a concentration of 10 g/L and was filtered through a 0.22-μm membrane filter, loaded onto a Sephadex G-100 column (Sigma Aldrich, St Louis, USA-50 × 1.5 cm). The column was eluted with the same buffer at a flow rate of 0.5 mL/min, and 0.5 mL of fractions was collected. Total carbohydrate content of the fractions was determined by phenol-sulfuric acid method, and the carbohydrate content was measured by phenol sulfuric acid method [15].

Antioxidant activity of the ECP

The antioxidant potential of ECP was studied by superoxide radical scavenging assay by phenazine methosulfate (PMS)-nicotinamide adenine dinucleotide (NADH)-Nitroblue tetrazolium chloride (NBT) system, 1,1-diphenyl-2-picrylhydrazyl (DPPH) radical scavenging activity [16]. Vitamin C was used as a positive control.

Hydroxyl radical scavenging activity of the ECP

The hydroxyl radical scavenging activity of ECP was measured according to Liu et al. and Ren et al. [17, 18]. The hydroxyl radicals were generated in the L-ascorbic acid-$CuSO_4$ system by reduction of Cu^{2+} and were assayed by the oxidation of cytochrome C. In this experiment, hydroxyl radicals were generated in 3 mL of 0.15 mM sodium phosphate buffer (pH 7.4), which included 100 μM L-ascorbic acid, 100 μM $CuSO_4$, 12 μM cytochrome C, and the samples to be tested at different concentrations. The mixture was incubated at 25 °C for 90 min. The color change of cytochrome C was measured at 550 nm. Thiourea was used as control, and glucose was used as negative control.

The inhibition rate of hydroxyl radical generation by thiourea was taken as 100%.

The inhibition rate was calculated using the following equation:

$$\text{Inhibition rate } (\%) = \left[\frac{T - T_2}{T - T_1}\right] \text{x}100$$

where T is the transmittance of hydroxyl radical ($OH^{\cdot}$) generation system and T_1 and T_2 are the transmittance of control and test sample systems respectively.

Superoxide ($O_2^{\cdot}$) radical scavenging activity of the ECP

Measurement of superoxide radical scavenging activity was done based on the method described by Ren et al. [18] and Nishimiki et al. [19]. To 1 mL of NBT solution (156 μM NBT in 100 mM phosphate buffer, pH 7.4), 1 mL NADH solution (468 μM in 100 mM phosphate buffer, pH 7.4) and 0.1 ml of ECP in water were added and mixed well. The reaction was started by adding 100 μL of PMS solution (60 μM PMS in 100 mM phosphate buffer, pH 7.4) to the mixture. The reaction mixture was incubated at 25 °C for 5 min, and the absorbance was measured at 560 nm against blank samples using a spectrophotometer, and vitamin C was used as positive control. Decreased absorbance of the reaction mixture indicated increased superoxide anion-scavenging activity.

The scavenging activity of superoxide radical (%) was calculated from the following equation:

$$\text{Superoxide radical scavenging activity } (\%) = \left[1 - \frac{A_{Sample}}{A_{Blank}}\right] \text{x}100$$

where A_{Blank} is the absorbance of the control reaction (containing all reagents except the test compound) and A_{Sample} is the absorbance of the test compound.

DPPH radical scavenging activity

The free radical scavenging activity of ECP was measured by DPPH free radical scavenging assay. To 1 mL of 0.1 mM solution of DPPH in ethanol, 3 ml of ECP in water was added in different concentrations. After 30 min, absorbance was measured at 517 nm against blank. Radical scavenging activity was expressed as percentage inhibition of DPPH and estimated by the following equation [20]:

$$\text{DPPH free radical scavenging activity } (\%) = \left[1 - \frac{A_{Sample}}{A_{Blank}}\right] \text{x}100$$

where A_{Blank} is the absorbance of the control reaction (containing all reagents except the test compound) and A_{Sample} is the absorbance of the test compound. Vitamin C was used as the positive control. All determinations were performed in triplicate. Decrease in the absorbance indicated the antioxidant activity.

Compositional analysis of ECP

HPLC analysis is a commonly used method to determine the monosaccharide composition of polysaccharides. The polysaccharides are hydrolyzed to get individual monomers and then labeled with anthranilic acid to increase the florescence for easy and accurate identification [21]. The sugar composition of the ECP was studied by high-performance liquid chromatography (HPLC) [7]. For specific determination of monosaccharides with high sensitivity, ECP was acid hydrolyzed and then derivatized in a simple step with excess anthranilic acid (2-aminobenzoic acid) in the presence of sodium cyanoborohydride to give highly fluorescent-stable derivatives. The monosaccharide derivatives were completely separated from the excess reagent and from each other by HPLC on a C_{18} reversed-phase column using a butylamine-phosphoric acid-tetrahydrofuran mobile phase [2].

Acid hydrolysis of ECP

ECP isolated from 36 h culture was dissolved in deionized water and dialyzed against deionized water using 12 kDa membrane at 4 °C for 24 h and then lyophilized. Ten milligrams of lyophilized ECP was hydrolyzed with 2 M trifluoroacetic acid (TFA) for 6 h at 100 °C. TFA was removed using rotary vacuum evaporator [22].

Derivatization of monosaccharides with anthranilic acid

The hydrolysates were derivatized by anthranilic acid reagent [21, 22]. Briefly, anthranilic acid reagent was prepared by dissolving anthranilic acid (30 mg) and sodium cyanoborohydride in 1 mL of acetate-boric acid-methanol solution. The ECP hydrolysates were dissolved

Table 1 Carbohydrate and protein contents of crude and pure ECP

S.No	Fraction	Total carbohydrate (%)	Protein (%)
1.	Crude ECP[a]	92 ± 2	0.9 ± 0.3
2.	Purified ECP[b]	98 ± 1	0

[a]Alcohol-precipitated ECP
[b]Purified ECP by gel filtration chromatography

in 100 μL of 1% sodium acetate, and an aliquot of 50 μL was transferred to a new screw-cap freeze vial. Samples were mixed with 100 μL of anthranilic acid and capped tightly. Vials were heated at 80 °C for 60 min. After cooling, the samples were made up to 1 mL with solvent A (2% 1-butylamine, 0.5% phosphoric acid, and 1% tetrahydrofuran) for analysis in HPLC.

HPLC analysis of anthranilic acid-monosaccharide derivatives

Monosaccharide derivatives were analyzed in Agilent 1000 series HPLC (Agilent Technologies, Model No.1100). A reversed-phase C_{18} column (ZORBAX 300 SB-C18, 5 μm, 4.6 × 250 mm, USA) and 1-butylamine-phosphoric acid-tetrahydrofuran mobile phase system consisting of solvents A and B were used for this analysis. Solvent A comprises of 0.2% 1-butylamine, 0.5% phosphoric acid, and 1% tetrahydrofuran in water, and solvent B consisted of equal parts of solvent A and acetonitrile. The separations were carried out at 24 °C using a flow rate of 1 mL/min, and 20 mL of each sample was injected. An UV detector was used to detect the derivatized monosaccharides. The gradient program was used according to [21].

Determination of monosaccharide linkage analysis of the ECP molecule

GC-MS methylation analysis

A solution of ECP (5 mg) in dimethyl sulfoxide (0.5 mL) was permethylated by adding finely powdered NaOH (20 mg) and methyl iodide (0.1 mL). Then, the mixture was sonicated for 15 min. The permethylated ECP was extracted with $CHCl_3$ (1 mL) and H_2O (3 mL). $CHCl_3$ phase was separated and dried under N_2 and hydrolyzed in 2 M TFA at 100 °C for 1 h. The hydrolyzed ECP was reduced with 50 mM $NaBH_4$ at room temperature for 4 h and evaporated three times from a mixture of acetic acid/methanol (1:1) followed by acetylation with 50:50 acetic anhydride/pyridine at 100 °C for 90 min. Alditol acetates of the methylated sugars were analyzed by Shimadzu GCMS-QP2010. The temperature program and other column conditions were used according to Kim et al. [23, 24].

Optimization studies of ECP production

Production of ECP in shake flask

Luria Bertani medium was inoculated with *Acinetobacter indicus* M6, incubated for 48 h at 160 rpm at room temperature. Effect of salt, carbon, and nitrogen source on ECP production has been studied by varying

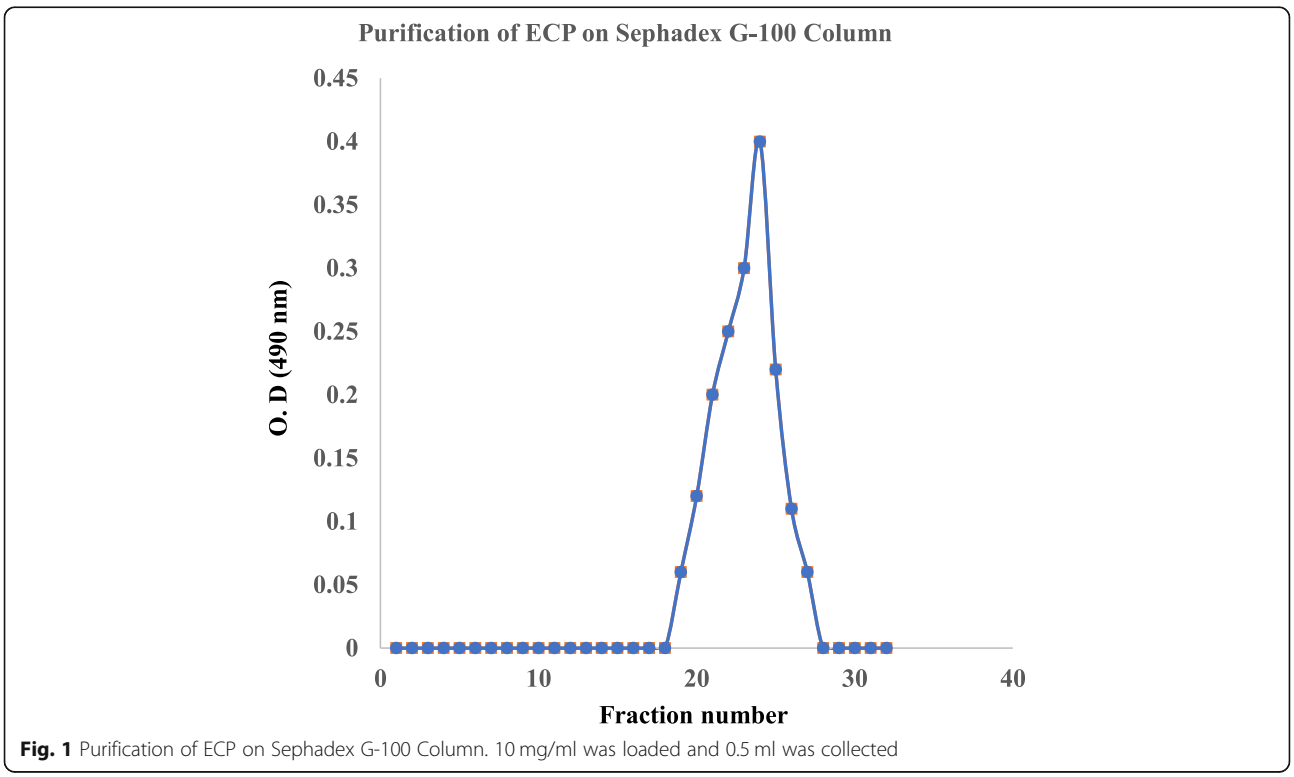


Fig. 1 Purification of ECP on Sephadex G-100 Column. 10 mg/ml was loaded and 0.5 ml was collected

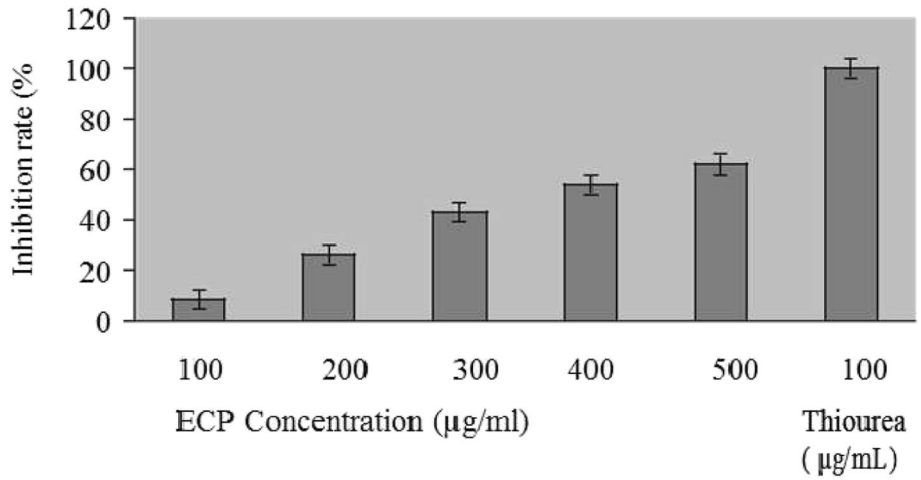


Fig. 2 OH radical scavenging activity of the ECP. Values are means of triplicates ± SD. The rate of inhibition of hydroxyl radical generation by thiourea (100 µg/ml) was taken 100%

concentrations of $MgSO_4$, glucose, and yeast extract. ECP production was expressed in terms of total carbohydrate concentration spectrophotometrically (490 nm) [18]. ECP extraction method was followed as mentioned above.

Optimization of nutritional variables by RSM

Response surface methodology (RSM) is a more convenient tool for designing experiments, plotting models, evaluating the effects of factors, and exploring optimum conditions of factors for significant responses. RSM is also used for optimization of prominent varieties of fermentation media and studying interactions among various bioprocess parameters with the minimum number of experiments [25, 26]. In the present experimentation, production of ECP in shake flask culture with *Acinetobacter indicus* M6 was found to be higher when compared to other bacterial species. Therefore, this strain has been considered as a potential bacterium for ECP production and hence it has been aimed to develop a suitable medium for enhanced production of ECP through optimization of nutrient component concentrations by response surface methodology (RSM). Fermentation medium variables such as glucose (A), yeast extract (B), and $MgSO_4$ (C) were optimized using the Design Expert software (Version 7.0.0, Stat-Ease Inc., Minneapolis, USA). The variables range from low (−1) to high (+ 1) used in the study are presented in Table 1.The impact of nutritional components on production and regression analysis of experimental data was carried out; further, the three-dimensional surface plots were drawn. The model was validated through the conduction of an experiment at predicted variables as suggested by the designed statistical model [27].

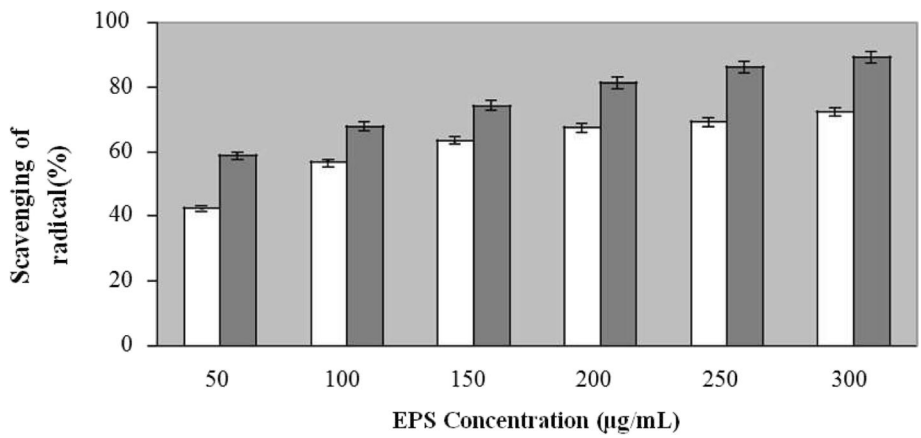


Fig. 3 Scavenging activity of ECP against superoxide radical generated in PMS/NADH system with vitamin C used as positive control. Values are means of triplicates ± SD. White bar indicates ECP, Black bar indicates Vitamin C

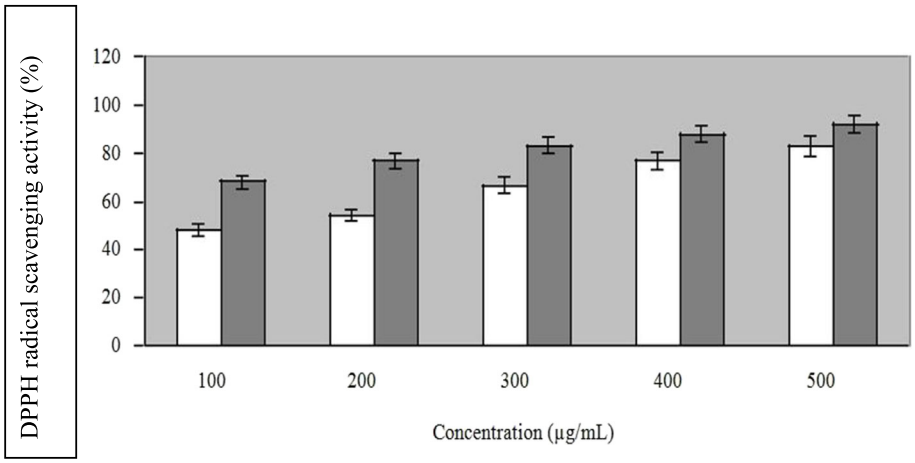


Fig. 4 Scavenging effects of ECP against 1, 1-diphenyl-2-picryl hydrazyl radical with vitamin C used as positive control. Values are means of triplicates ± SD. White bar indicates ECP, Black bar indicates Vitamin C

Results

Extraction, purification, and quantification of the ECP

The ECP produced by *Acinetobacter indicus* M6 was extracted as described previously and then purified. The gel filtration chromatogram (Fig. 1) showed that the elution of the ECP starts at the 18th fraction and ended at the 28th fraction. There was no protein content in polysaccharide fractions, indicating that the ECP had no associated proteins. The carbohydrate and protein contents of the crude and purified ECP are listed in Table 1. While the total sugar content (%, w/w) of the ECP was found to increase by 6% on purification, the % content of the contaminating proteins decreased to zero from a value of 0.9%. The total carbohydrate and protein concentrations were observed to be 380 µg/mL and 150 µg/mL respectively.

Antioxidant activity of the ECP

Hydroxyl radical scavenging assay of the ECP

The hydroxyl radical scavenging activity of ECP (ranging from 100 to 500 µg/mL) by ascorbic acid-Cu^{2+}-cytochrome C system is shown in Fig. 2. The

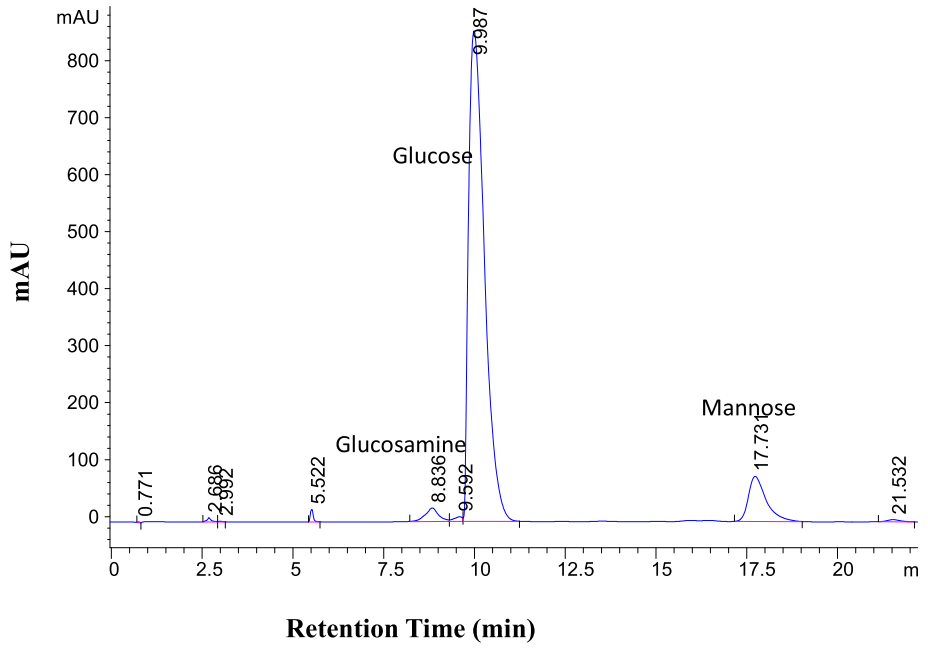


Fig. 5 HPLC analysis of hydrolyzed ECP. (Glucose is a major monomeric unit; mannose and glucosamine are the minor units)

Table 2 Results of the analysis of GC-MS

Fragments[a]	Mode of Linkage
1,2,4-tri-*O*-acetyl-3,6-di-*O*-methyl-D-mannitol	(→1, 2)-Man-(4→
1,4-di-*O*-acetyl-2,4,6-tri-*O*-methyl-D-glucitol	(→1)-Glc-(4→
1,4,6-di-*O*-acetyl-3-mono-*O*-methyl-2-amino-D-glucitol	(→1, 4)-GlcN-(6→

[a]Alditol acetates generated after methylation and reduction of monomers

scavenging activity of the ECP when correlated with its concentration showed that the activity increased till a concentration of 500 μg/mL and remained stable thereafter. ECP showed considerable hydroxyl radical scavenging activity of 59% at the concentration of 500 μg/mL. Here, in these experiments, the rate of inhibition of hydroxyl radical generation by thiourea (as a positive control) at a concentration of 100 μg/mL was taken as 100%, and glucose was used as negative control.

Superoxide ($O_2^{\cdot -}$) radical anion scavenging activity of the ECP

The decrease in absorbance at 560 nm with the addition of ECP indicates the consumption of superoxide radical in the reaction mixture (Fig. 3). The ECP showed noticeable superoxide radical scavenging activity with increasing concentration ranging from 50 to 300 μg/mL. The maximum scavenging activity of the ECP was estimated to be 72.4% where reference compound vitamin C showed 90% at concentration of 300 μg/mL.

DPPH free radical scavenging activity

This method is based on the reduction of methanolic DPPH$^{\cdot}$ solution in the presence of a hydrogen-donating antioxidant, due to the formation of the non-radical form DPPH-H by the reaction. DPPH$^{\cdot}$ is a stable free radical and accepts an electron or hydrogen radical to become a stable diamagnetic molecule [21, 22]. The antioxidant of ECP was determined by DPPH$^{\cdot}$ radical scavenging activity assay. Vitamin C was used as standard. Figure 4 illustrates the DPPH$^{\cdot}$ radical scavenging ability of ECP which increased with increasing concentration of ECP ranging from 100 to 500 μg/mL. Vitamin C and ECP showed 92% and 72.2% DPPH$^{\cdot}$ radical scavenging activity respectively at 500 μg/mL concentration. In terms of this antioxidant activity, the antioxidant activity of the ECP and the standard were comparable.

Compositional analysis of the ECP

The ECP after being hydrolyzed and derivatized with anthranilic acid was analyzed for its sugar composition by HPLC. The HPLC chromatogram (Fig. 5) showed that the ECP was a heteropolysaccharide, composed of glucose and glucosamine [22]. In terms of peak area, glucose (retention time 9.9 min) was the major monosaccharide, whereas glucosamine (retention time 8.8 min), and mannose (retention time 17.7) were the minor ones.

Determination of linkages between the monosaccharide units

The sugar linkages in alditol acetates of the methylated sugars of the ECP were elucidated by GC-MS analysis. Methylation analysis is a widely used method for determining polysaccharide structure [28, 29]. However, reductive cleavage depolymerization has several advantages compared to standard methylation analysis, and it is an effective method for structural characterization of complex carbohydrates, which have different sugar residues [27]. The alditol derivatives were 1,2,4-tri-*O*-acetyl-3,6-tri-*O*-methyl-D-mannitol; 1,4-di-*O*-acetyl-2,4,6-tri-*O*-methyl-D-glucitol; 1,4,6-di-*O*-acetyl-3-mono-*O*-methyl-2-amino-D-glucitol (Tables 2 and 3), revealed that (1→4)-linked glucose, (1→4) linked mannose, (→4)-GlcN-(1→). The linkages between the monosaccharides were predicted according to Bjorndal et al. [12, 27]. Based on the HPLC and GC-MS data, the probable structure of the ECP is given in Figs. 6 and 7.

Optimization studies of ECP production

Central composite design for medium optimization

Response surface methodology (RSM) is a collection of mathematical and statistical techniques widely used to determine the effects of several variables and to optimize different biotechnological processes [26]. The central composite design (CCD) was adopted for optimization of medium components such as glucose, yeast extract, and $MgSO_4$. The experimental results of CCD for enhancing the yield of ECP are shown in Table 4.

The response (Y) fitted with the second-order polynomial equation

Table 3 GC data showing the number of peak traces

Fragments	Mode of linkage	Major mass fragments (m/z) peak traces
1,2,4-tri-*O*-acetyl-3,6-di-*O*-methyl-D-mannitol	(→1, 2)-Man-(4→	104, 113, 129, 147, 161, 181, 191, 197
1,4-di-*O*-acetyl-2,4,6-tri-*O*-methyl-D-glucitol	(→1)-Glc-(4→	103, 119, 130, 151, 177, 193, 196
1,4,6-di-*O*-acetyl-3-mono-*O*-methyl-2-amino-D-glucitol	(→1, 4)-GlcN-(6→	110, 117, 131, 147, 163, 181, 191, 197

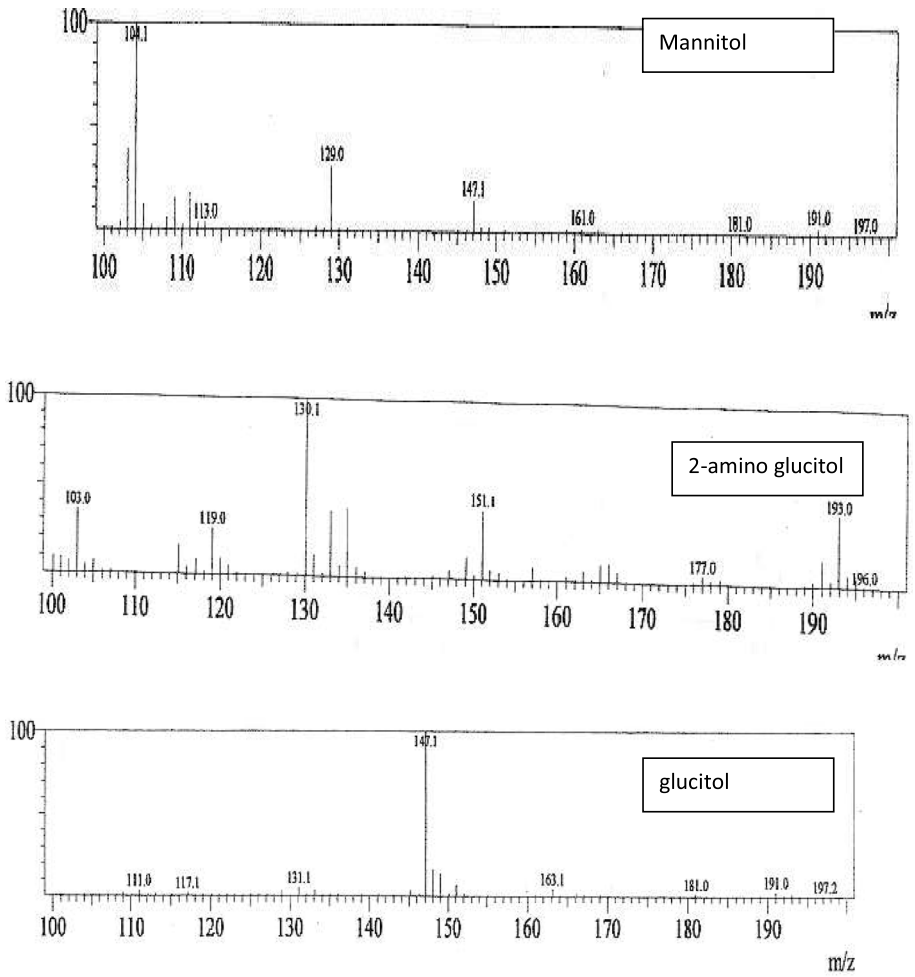


Fig. 6 Mass spectra obtained by GC-MS analysis obtained by Shimadzu GC-MS QP 2010 using ZB-1 column

$$R_1 = +2.54 + 0.14\,A - 0.032B - 0.083\,C + 0.014A\,B - 0.13\,\mathrm{AC} - 0.079\,BC - .59A^2 - 1.23\,B^2 - 0.11C^2$$

R_1 represents the response for ECP production, whereas glucose, yeast extract, and $MgSO_4$ are represented by variables A, B, and C, respectively, and the R^2 coefficient value of 0.99 suggested that predicted model was significant (Table 5). The Model F-value of 154.37 implies the model is significant. In this case, A, C, AC, A^2, and B^2 are significant model terms (Table 6). The combinational effect of

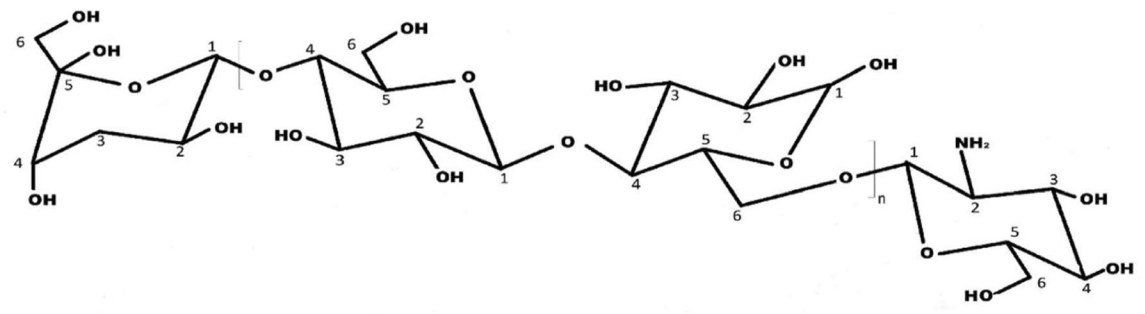


Fig. 7 The probable structure of ECP

Table 4 The nutritional variables selected for optimization study

S.No.	Nutritional variables	[a]Range in g/L
1	Glucose (A)	5–15
2	Yeast extract (B)	5–10
3	$MgSO_4$ (C)	0.2–0.4

[a]Concentration ranges

nutritional variables on the production of ECP was analyzed from the 3-D response surface curves as shown in Fig. 8.

Validation of RSM model

The RSM model is validated by conducting an experiment at best-predicted solution for production of ECP. Under optimized conditions, the ECP yield reached 2.21 g/L from *Acinetobacter indicus* M6, which is almost near to the RSM predicted value (Table 7).

Discussion

Acinetobacter M6 produces ECP in substantial quantities (2.21 g/L). This quantity is considerably higher when compared to other reported bacterial ECPs. As far as our knowledge, there is no report available on ECP from *Acinetobacter indicus* M6 bacterium. ECP from this marine bacterium may be beneficial because few of the ECPs have been reported to have emulsification property which can find potential applications in the reduction of marine water pollution [27, 28]. The purified ECP shows significant antioxidant activities when compared to the standard antioxidant active compound (Vit C). Free radicals such as superoxide radical, hydroxyl radical, and other reactive oxygen species (ROS) are associated with multistage carcinogenesis and mutagenesis [29, 30]. The results of present study have demonstrated that ECP was effective in scavenging superoxide, hydroxyl, and DPPH radicals in a concentration-dependent fashion. There are very few reports available on antioxidant activities of bacterial ECPs. However, this is the first report on antioxidant and free radical scavenging activities of an ECP from *Acinetobacter indicus* M6. Hence, the ECP may be developed as a potential antioxidant molecule after studying various toxicological studies. The monosaccharides in the ECPs are actually potent reductive agents as they have a hidden aldehyde moiety [31]. The antioxidant mechanism of polysaccharides may thus be attributed to the reductive nature of the monosaccharides owing to the presence of –CHO group as these polysaccharides such as ECPs are not proton-donors. The mechanism of free-radical scavenging of polysaccharides is still not fully understood. The results of the present

Table 5 Actual data for design of experiments

S.No.	Glucose	Yeast extract	$MgSO_4$	Production of biosurfactant in g/L	
				Experimental[a]	Predicted[b]
1.	15	10	0.3	1.95	2.1
2.	5	15	0.4	0.36	0.39
3.	10	10	0.3	2.51	2.54
4.	15	15	0.2	1.08	1.03
5.	5	5	0.4	0.63	0.64
6.	10	10	0.3	2.54	2.54
7.	10	10	0.4	2.36	2.34
8.	10	10	0.3	2.63	2.54
9.	10	5	0.3	1.22	1.34
10.	15	5	0.4	0.66	0.63
11.	10	15	0.3	1.25	1.28
12.	5	15	0.2	0.46	0.45
13.	10	10	0.3	2.65	2.54
14.	15	5	0.2	0.98	0.91
15.	10	10	0.3	2.56	2.54
16.	5	10	0.3	1.8	1.81
17.	10	10	0.3	2.65	2.54
18.	5	5	0.2	0.42	0.38
19.	15	15	0.4	0.44	0.44
20.	10	10	0.2	2.34	2.51

[a]Experimental result of biosurfactant production at the mentioned nutrient concentrations
[b]RSM predicted value of biosurfactant production at the mentioned nutrient concentrations

Table 6 ANOVA for response surface quadratic model

Source	Sum of squares	df	Mean square	F-value	*p*-value Prob > *F*	
Model	15.38	9	1.71	154.37	< 0.0001	**Significant**[a]
A-glucose	0.21	1	0.21	18.73	0.0015	
B-yeast extract	0.01	1	0.01	0.92	0.3589	
C-$MgSO_4$	0.07	1	0.07	6.22	0.0318	
AB	0.00	1	0.00	0.14	0.7194	
AC	0.14	1	0.14	12.92	0.0049	
BC	0.05	1	0.05	4.48	0.0604	
A^2	0.95	1	0.95	85.92	< 0.0001	
B^2	4.15	1	4.15	374.61	< 0.0001	
C^2	0.04	1	0.04	3.18	0.1048	
Residual	0.11	10	0.01			
Lack of fit	0.09	5	0.02	4.95	0.0519	**Not significant**
Pure error	0.02	5	0.00			
Cor total	15.50	19				

[a]If *p*-value of a parameter is < 0.05, the effect of that parameter is significant

study have demonstrated that ECP is effective in scavenging superoxide, hydroxyl, and DPPH radicals in a concentration-dependent fashion. There are a very few reports available on antioxidant activities of bacterial ECPs. However, this is the first report on antioxidant and free radical scavenging activities of an ECP from *Acinetobacter indicus* M6. HPLC analysis indicated that ECP was a heteropolymer composed of glucose, mannose, and glucosamine. The presence of these monomers makes the heteropolymer unique, and this monomeric combination was not found in any other reported ECPs. GC-MS data of alditol derivatives revealed that (1→4)-linked glucose, (1→4)-linked mannose, and (→4)-GlcN-(1→) were present in the ECP. Presence of these linkages also makes our ECP unique and novel, and the predicted structure is given in Fig. 7 [32]. ECP from *Acinetobacter indicus* M6 was found to be a structurally complex but novel molecule for its unique

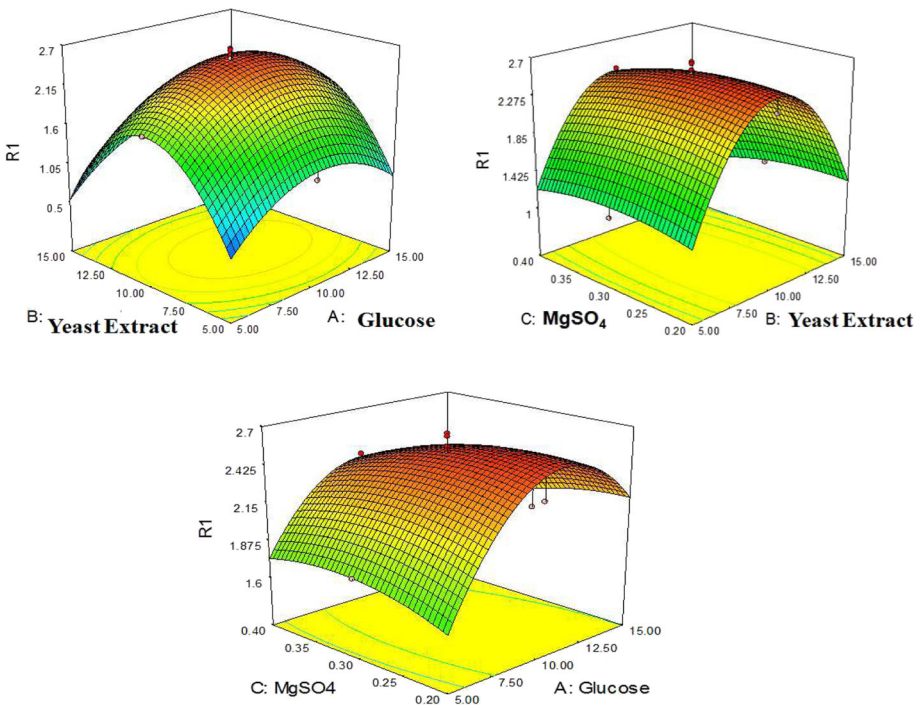


Fig. 8 3D graphs showing the combinational interaction of variables on production of ECP

Table 7 Validation of RSM model for ECP production

S.No.	Glucose (A), g/L	Yeast extract (B), g/L	$MgSO_4$ (C), g/L	ECP production (R_1), g/L	
				RSM model predicted	Experimental
1	15	10.12	0.2	2.19	2.21

monosaccharide composition and the glycosidic linkages between the monomeric units. This unique combination of the monosaccharides and unusual glycosidic linkages between them make our ECP novel. To undertake a holistic approach towards critically establishing the structure-function relationship of the ECP molecule by elucidating its complete molecular structure on further chemical derivatizations and enzymatic digestions (with glucosidases), so as enable us to identify the right fragments of the large ECP molecule, responsible for each of its important bioactive properties of therapeutic and commercial interests [27, 33]. This would also help us to use the small fragments for specific therapeutic purposes, instead of using the whole molecule [34, 35]. However, the complete structural elucidation may be performed by other sophisticated techniques like NMR and ESI-MS which is the scope of the present study. The optimized medium improved the production of ECP and is two folds higher in comparison with the basal medium.

Conclusion

ECP produced by marine bacterium was purified and found to be a heteropolymer composed of glucose as a major monomer, and mannose and glucosamine were minor monomers, and this makes ECP unique in terms of its composition. GC-MS analyses elucidated the presence of quite uncommon (1→4)-linked glucose, (1→4)-linked mannose, and (→4)-GlcN-(1→) glycosidic linkages in the backbone. The purified ECP has shown significant antioxidant activity. The detailed mechanisms of actions of the ECP molecule for its significant antioxidant activities need to be elucidated to develop the whole ECP molecule or the suitable fragments of it into prospective drug candidates. This requires a lot of basic research inputs. The production of ECP reached 2.21 g/L after the optimization of nutritional variables. The designed model is statistically significant and is indicted by the R^2 value of 0.99. The optimized medium improved the production of ECP and is two folds higher in comparison with the basal medium. As a long-term future scope and perspective, it would be prudent to scale the optimal process up to a pilot plant scale for consistent production of this important bioactive ECP molecule in large quantities. Though there are reports available on bacterial ECPs, this is the first report on ECP from *Acinetobacter indicus* M6. Unique monosaccharide composition and the glycosidic linkages between the monomeric units of the ECP markedly differ with the reported ECPs.

Considering the unique monosaccharide composition and significant antioxidant activity, the ECP may be developed as a drug molecule. The ECP is a promising antioxidant, and it can be used as an additive in food, pharmaceutical, and cosmetic preparations. The relationship between structure of ECP and antioxidant activity and also elucidation of its antioxidant mechanism at the molecular level will improve its biological activities by chemical modifications, one of the important implications of this study.

Abbreviations

ECP: Extracellular polysaccharide; DPPH: 1,1-diphenyl-2 picryl hydrazyl; RSM: Response surface methodology

Acknowledgements

Prof. G. Vijay Ananda Kumar Babu, Head, Department of Biotechnology, VSU for providing the facilities.

Authors' contributions

RTCh carried out the isolation and purification of the ECP. APK studied the antioxidant activity of the ECP. NV is involved in the HPLC analysis. VTC and MK helped in GC-MS part of the structural analysis. JBD is involved in optimization studies. VPK is the main author involved in the design and analysis of the whole study. All authors have read and approved the manuscript.

Funding

Department of Biotechnology (DBT), Ministry of Science and Technology, Govt. of India for financial support (F. No. BT/PR/7952/AAQ/3/642/2013) and DST-FIST-LSI-595 (LSI-026) for providing facility.

Availability of data and materials

The data is available and it will be provided to the editor if required.

Declarations

Ethics approval and consent to participate

This work is not involved in animal or human models. Hence, ethical approval is not required.

Consent for publication

Not applicable.

Competing interests

The authors declare no competing interest.

Author details

[1]Department of Biotechnology, Vikrama Simhapuri University, Kakutur, Nellore A.P-524320, India. [2]Department of Biotechnology, VFSTR University, Vadlamudi, Guntur A.P-522213, India. [3]SRR and CVR Government Degree College, Machavaram, Vijayawada A.P-520010, India.

Received: 23 July 2020 Accepted: 16 February 2021
Published online: 12 March 2021

References

1. Shabtai Y (1990) Production of exopolysaccharides by *Acinetobacter* strains in a controlled fed-batch fermentation process using soap stock oil (SSO) as carbon source. Int J Biol Macromol 12(2):145–152
2. Welman AD, Maddox IS (2003) Exopolysaccharides from lactic acid bacteria: perspectives and challenges. Trends Biotechnol 21(6):269–274
3. Naidu AS, Bidlack WR, Clemens RA (1999) Probiotic spectra of lactic acid bacteria (LAB). Crit Rev Food Sci Nutr 39(1):13–126
4. Ashtaputre AA, Shah AK (1995) Emulsifying property of a viscous exopolysaccharide from *Sphingomonas paucimobilis*. World J Microbiol Biotechnol 11:219–222
5. De Vuyst L, Bart D (1999) Heteropolysaccharides from lactic acid bacteria. FEMS Microbiol Rev 23:153–177
6. Kishk YFM, Al-Sayed HMA (2007) Free-radical scavenging and antioxidative activities of some polysaccharides in emulsions. LWT Food Sci Technol 40: 270–277
7. Sun C, Wang JW, Fang L, Gao XD (2004) Free radical scavenging and antioxidant activities of EPS2, an exopolysaccharide produced by a marine filamentous fungus *Keissleriella sp.YS* 4108. Life Sci 75:1063–1073
8. Halliwell B, Gutteridge JMC (1986) Oxygen free radicals and iron in relation to biology and medicine: some problems and concepts. Arch Biochem Biophys 246:501–514
9. Reddy AR, Peele KA, Krupanidhi S, Kodali VP, Venkateswarulu TC (2018) Production of polyhydroxybutyrate from *Acinetobacter nosocomialis* RR20 strain using modified mineral salt medium: a statistical approach. Int J Environ Sci Technol 16(3):6447–6452
10. Wang QJ, Fang YZ (2004) Analysis of sugars in traditional Chinese drugs. J Chromatogr B 812:309–324
11. Donlan RM, Costerton JW (2002) Biofilms: survival mechanisms of clinically relevant microorganisms. Clin Microbiol Rev 15(2):167–193
12. Bjorndal H, Hellerqvist CG, Lindberg B, Svensson SA (1970) Gas-liquid chromatography and mass spectrometry in methylation analysis of polysaccharides. Chem Int 9(8):610–618
13. Gruter M, Leeflang BR, Kuiper J, Kamerling JP, Vliegenthart JF (1993) Structural characterisation of the exopolysaccharide produced by *Lactobacillus delbrückii* subspecies bulgaricus rr grown in skimmed milk. Carbohydr Res 239:209–226
14. Peele KA, Ch VRT, Kodali VP (2016) Emulsifying activity of a biosurfactant produced by a marine bacterium. 3Biotech 6(2):177–180
15. Dubois M, Gilles KA, Hamilton JK, Pebers PA, Smith F (1956) Calorimetric method for determination of sugars and related substances. Anal Chem 28: 350–356
16. Wang H, Dong X, Zhou GC, Cai L, Yao WB (2008) In vitro and in vivo antioxidant activity of aqueous extract from *Choerospondias axillaris* fruit. Food Chem 106:888–895
17. Liu F, Ng TB (2000) Antioxidative and free radical scavenging activities of selected medicinal herbs. Life Sci 66:725–735
18. Ren D, Jiao Y, Yang X, Yuan L, Guo J, Zhao Y (2015) Antioxidant and antitumor effects of polysaccharides from the fungus *Pleurotus abalonus*. Chem Biol Interact 237:166–174
19. Nishimiki M, Rao NA, Yagi K (1972) The occurrence of superoxide anion in the reaction of reduced phenazine methosulfate and molecular oxygen. Biochem Biophys Res Commun 46:849–853
20. Sokmena M, Angelovab M, Krumovab E, Pashovab S (2005) In vitro antioxidant activity of polyphenol extracts with antiviral properties from Geranium sanguineum L. Life Sci 76:2981–2993
21. Anumula KR (1994) Quantitative determination of monosaccharides in glycoproteins by high-performance liquid chromatography with highly sensitive fluorescence detection. Anal Biochem 220(2):275–283
22. Anumula KR, Dhume ST (1998) High resolution and high sensitivity methods for oligosaccharide mapping and characterization by normal phase high performance liquid chromatography following derivatization with highly fluorescent anthranilic acid. Glycobiol 8(7):685–694
23. Kim SJ, Kim BG, Parka HU, Yim JH (2016) Cryoprotective properties and preliminary characterization of exopolysaccharide (P-Arcpo 15) produced by the Arctic bacterium *Pseudoalteromonas elyakovii* Arcpo 15. Prep Biochem Biotechnol 46:261–266
24. Maheswari P, Mahendran S, Sankaralingam S, Sivakumar N (2019) In vitro antioxidant activity of exopolysaccharide extracted from marine sediment soil bacteria. Res J Pharm Tech 12(9)
25. Bomfim VB, Neto JHL, Leite KS, Vieira EA (2020) Partial characterization and antioxidant activity of exopolysaccharides produced by Lactobacillus plantarum CNPC003. Food Sci Tech 127:109349
26. Lin SM, Baek CY, Jung JH, Kim WS, Song HY, Lee JH, Ji HJ, Zhi Y, Kang BS, Bahn YS, Seo HS, Lim S (2020) Antioxidant activities of an exopolysaccharide (DeinoPol) produced by the extreme radiation-resistant bacterium *Deinococcus radiodurans*. Nat Sci Rep 63(10):55
27. Yasuda T, Inaba A, Ohmori M, Endo T (2000) Urinary metabolites of gallic acid in rats and their radical scavenging effect on DPPH. J Nat Prod 63: 1444–1446
28. Cheng BH, Chan JYW, Chan BCL (2014) Structural characterization and immunomodulatory effect of a polysaccharide HCP-2 from *Houttuynia cordata*. Carbohydr Polym 103:244–249
29. Venkateswarulu TC, Kodali VP, Kumar RB (2017) Optimization of nutritional components of medium by response surface methodology for enhanced production of lactase. 3 Biotech 7(3):202
30. Soares JR, Dins TCP, Cunha AP, Ameida LM (1997) Antioxidant activity of some extracts of *Thymus zygis*. Free Radic Res 26:469–478
31. Haschemie KK, Renger A, Steinhart H (1996) A comparison between reductive-cleavage and standard methylation analysis for determining structural features of galactomannans. Carbohydr Polym 30(1):31–35
32. Knight J (1998) Free radicals: their history and current status in aging and disease. Ann Clin Lab Sci 28:331–346
33. Sun T, Powers JR, Tang J (2007) Evaluation of the antioxidant activity of asparagus, broccoli and their juices. Food Chem 105:101–106
34. Kodali VP, Das S, Sen R (2009) An exopolysaccharide from a probiotic: biosynthesis dynamics, composition and emulsifying activity. Food Res Int 42:695–699
35. Venkateswarulu TC, Prabhakar KV, Kumar RB, Krupanidhi S (2017) Modeling and optimization of fermentation variables for enhanced production of lactase by isolated *Bacillus subtilis* strain VUVD001 using artificial neural networking and response surface methodology. 3 Biotech 7(3):1–9

Publisher's Note

Springer Nature remains neutral with regard to jurisdictional claims in published maps and institutional affiliations.

Submit your manuscript to a SpringerOpen journal and benefit from:

- ► Convenient online submission
- ► Rigorous peer review
- ► Open access: articles freely available online
- ► High visibility within the field
- ► Retaining the copyright to your article

Submit your next manuscript at ► springeropen.com

Nature Environment and Pollution Technology
An International Quarterly Scientific Journal

p-ISSN: 0972-6268
(Print copies up to 2016)
e-ISSN: 2395-3454

Vol. 19 | No. 5 (Suppl) | pp. 1821-1829 | 2020

Original Research Paper

https://doi.org/10.46488/NEPT.2020.v19i05.005

Open Access Journal

Biochemical Changes Induced by Cartap Hydrochloride (50% SP), Carbamate Insecticide in Freshwater Fish *Cirrhinus mrigala* (Hamilton, 1822)

G. Vani*†, K. Veeraiah, M. Vijaya Kumar*, Sk. Parveen* and G.D.V. Prasad Rao*****

*Department of Zoology, SRR & CVR Government Degree College (A), Vijayawada, Andhra Pradesh, India

**Department of Zoology and Aquaculture, Acharya Nagarjuna University, Nagarjunanagar-522 510, Guntur, Andhra Pradesh, India

***Department of Zoology SGS College, Jaggaiahpet, Andhra Pradesh, India

†Corresponding author: G. Vani; gandhamvanipradeep@gmail.com

Nat. Env. & Poll. Tech.
Website: www.neptjournal.com

Received: 08-11-2019
Revised: 25-11-2019
Accepted: 03-01-2020

Key Words:
Cartap hydrochloride
Cirrhinus mrigala
LC_{50}
Glycogen
Total proteins
Nucleic acids

ABSTRACT

The freshwater fish *Cirrhinus mrigala* was exposed to Cartap hydrochloride (50% SP) for 24, 48, 72 and 96 h. The LC_{50} values were found to be 0.436, 0.419, 0.394 and 0.376 mg^{-1} in static method and 0.399, 0.371, 0.361 and 0.339 $mg.L^{-1}$ in continuous flow-through system. The static LC_{50} values are higher than the continuous flow-through method. The LC_{50} values showed a decreasing trend with an increase in time of exposure in both the methods. The decrease was more in a continuous flow-through method than in the static method. The fish were exposed to sub-lethal ($1/10^{th}$ of 96 h LC_{50} value 0.0376 $mg.L^{-1}$) and lethal (96 h LC_{50} value 0.376 $mg.L^{-1}$) concentrations of the pesticide for 24 and 96 hours to study the alterations in glycogen, total proteins and nucleic acids (DNA & RNA) contents of various tissues viz., gill, brain, liver, kidney and muscle. Glycogen, total proteins and nucleic acids (DNA & RNA) content values decreased in all the tissues of exposed fish and the per cent decrease is more apparent in lethal concentrations than in sub-lethal concentrations. From the present study, it can be concluded that Cartap hydrochloride caused a decline in the glycogen, total protein and nucleic acids (DNA, RNA) content in *Cirrhinus mrigala* and the changes are more pronounced in lethal exposure than in sub-lethal exposure.

INTRODUCTION

Indiscriminate use of pesticides is one of the main reasons for the pollution of aquatic ecosystems. These toxic pesticides are causing deleterious effects on aquatic organisms. They are causing stress to aquatic organisms which are reflected as biochemical changes in their body (Mayers 1977). Fish acts as a bioindicator species and can be used for monitoring of water pollution as they accumulate the contaminants from polluted water and diet (Chaudary & Jabeen 2011, Kafilzadeh et al. 2012). Fish accumulate these pollutants directly or indirectly from polluted waters and food chain (Jabeen et al. 2016, Chaudary & Jabeen 2011). Carbamates are extensively used water-soluble pesticides in agricultural practices. In India, Cartap hydrochloride is a Carbamate pesticide which is considered as nereistoxin analog is extensively used in rice and sugarcane crops to control pests. The present investigation is aimed to study the toxic effects of Cartap hydrochloride in sub-lethal and lethal concentrations at 24 and 96 hours of exposure period on glycogen, total protein, DNA and RNA contents of freshwater fish *Cirrhinus mrigala* (Hamilton 1822).

MATERIALS AND METHODS

The fingerlings of the test fish *Cirrhinus mrigala* size 6-8 ± ½ cm and weight 6-7 ± ½ g were procured from local fish hatcheries of Nandivelugu, Tenali Mandal, Guntur district, Andhra Pradesh. The fish were acclimated at (28 ± 2°C)) in the laboratory conditions for two weeks. All the precautions laid down by APHA et al. (1998) were followed. During the acclimation period, the fish were fed with rice bran and groundnut cake. One day before the experimentation feeding was stopped. Cartap hydrochloride (50% SP) commercial grade was purchased from Mangalagiri, Guntur District. The stock solution was prepared with water as a solvent. The acclimatized fish were exposed to static sub-lethal (0.376 $mg.L^{-1}$) and lethal concentrations (3.76 $mg.L^{-1}$) of Cartap hydrochloride (50% SP) for 24 and 96 h. The hydrographical properties of water were estimated by the modified method followed by Golterman & Claimo (1969) method. Finney's probit analysis (Finney 1971) as reported by Roberts % Boyce (1972) was followed to calculate the LC_{50} value. The 95% confidence limits of the LC_{50} values for each test were also calculated for different time periods

by using SPSS software. At the end of the exposure periods, the tissues like gill, brain, liver, kidney and muscle were taken out from exposed and control fish and processed for the estimation of glycogen, total proteins and nucleic acids (DNA & RNA). Glycogen was estimated by the method of Kemp et al. (1954), total protein by Lowry et al. (1951) and DNA and RNA by the methods of Searchy & Maclinnis (1970a & 1970b).

The data obtained in the present work were expressed as means of four observations ± SD (standard deviation) and were statistically analysed using student "t" test (Pillai & Sinha 1968) to compare means of treated data against their controls and the result was considered significant at ($P < 0.05$) level.

RESULTS AND DISCUSSION

Glycogen, total proteins and nucleic acids (DNA & RNA) decreased in various tissues, viz. gill, brain, liver, kidney and muscle of *Cirrhinus mrigala* exposed to sub-lethal and lethal concentrations of cartap hydrochloride for 24 and 96 hours were graphically represented in Fig. 1 to Fig. 8. In exposed fish per cent decrease is more apparent in lethal concentrations than at sub-lethal concentrations.

Glycogen

The changes in glycogen content observed in the various tissues of *Cirrhinus mrigala* after the Cartap hydrochloride exposure along with the control are graphically represented in Fig .1 and Fig. 2.

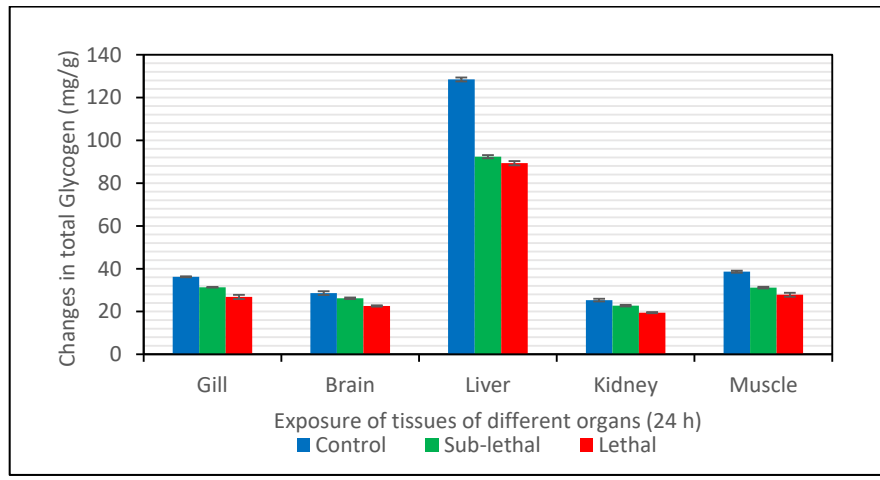


Fig.1: Changes in the glycogen content (mg/g wet weight of the tissue) in the tissue of fish *Cirrhinus mrigala* on exposure to sub-lethal and lethal concentration of Cartap hydrochloride (50%SP) for 24 hours.

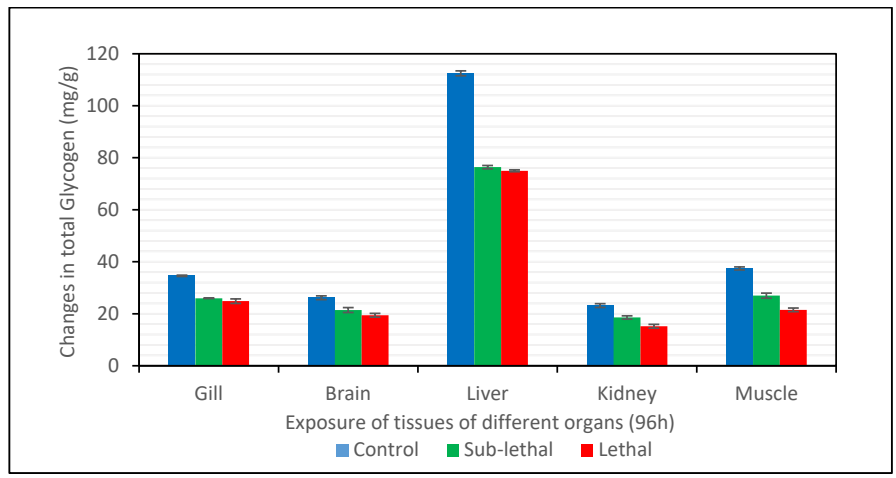


Fig. 2: Changes in the glycogen content (mg/g wet weight of the tissue) in the tissue of fish *Cirrhinus mrigala* on exposure to sub-lethal and lethal concentration of Cartap hydrochloride (50% SP) for 96 hours.

In the tissues of control fish, *Cirrhinus mrigala* glycogen content was in the order of:

Liver > Muscle > Gill > Brain > Kidney

Under exposure to sub-lethal and lethal concentrations of Cartap hydrochloride for 24 and 96 hours, the amount of glycogen was found to decrease in all the tissue of *Cirrhinus mrigala*. The lyotropic gradation series in terms of per cent decrement at 24 h and 96 h exposure was:

Sub-lethal -24 h: Liver > Muscle > Gill > Kidney > Brain

Lethal -24 h: Liver > Muscle > Gill > Kidney > Brain

Sub-lethal 96 h: Liver > Muscle > Gill > Kidney > Brain

Lethal-96 h: Muscle > Kidney > Liver > Gill > Brain

Exposure of *Cirrhinus mrigala* to Cartap hydrochloride for 24 hours caused a maximum decrease of glycogen in the liver (sub-lethal 28.117, lethal 30.453). For 96 h maximum decrease was found in the liver (sub-lethal 32.073) and muscle (lethal 42.570). In the present study under Cartap hydrochloride 24 h sub-lethal and lethal exposure minimum percentage of depletion was in the brain (8.595) and (20.96). For 96 h exposure minimum depletion was found in the brain (sub-lethal 18.056, lethal 25.707).

Srivastava & Singh (2013) observed reduction in glycogen content in different tissues of freshwater fish *Clarius batrachus* exposed to 80% of LC_{50} (22.87 $mg.L^{-1}$) of Mancozeb at different time intervals of 24 and 96 h. Sastry et al. (1982) reported decreased glycogen content of liver and muscles decreased when *Channa punctatus was exposed to* sub-lethal concentration of the carbamate pesticide, Sevin (1.05 $mg.L^{-1}$) for 15, 30 and 60 days. Veeraiah et al. (2013a) observed that exposure to sub-lethal and lethal concentrations of cadmium chloride in the fish *Cirrhinus mrigala* for 96 h caused changes in the total glycogen level which may be attributed to toxic stress, resulting in the disruption of enzymes associated with carbohydrate metabolism. Bantu & Rathnamma (2013) reported that there is a decrease in the amount of glycogen in the fish *Labeo rohita* exposed to sub-lethal and lethal concentrations of Dimethoate for 8 days. Priya et al. (2013) observed depletion of glycogen in the liver of freshwater teleost *Channa punctatus* (Bloch) when exposed to various concentrations of Imidacloprid (0.002 ppm, 0.00 ppm, 0.006 ppm, 0.008 ppm and 0.01 ppm) for 96 h suggesting the possibility of an alter from aerobic to anaerobic mode of energy metabolism of the liver. Dhanalakshmi (2013) noticed decrement in the tissue glycogen concentration in fish *Cirrhinus mrigala* when exposed to 0.25 ppm concentration of the metal chromium sulphate for 24, 48, 72 h and 10, 20 and 30 days which may be due to its enhanced utilization, since glycogen forms the immediate source of energy to meet energy demands under metallic stress caused by test toxicant.

Tataji & Kumar (2016) reported a decline in glycogen content of freshwater fish *Channa punctatus* exposed for 8 days to 1/5th of LC_{50} 96 hours of both Butachlor technical grade and Machete (50% EC), i.e. 32 ppb and 71.2 ppb for both technical and 50% EC respectively. Reduction in glycogen content was also noticed by Naik et al. (2016) in all the tissues of *Labeo rohita* when exposed to sub-lethal concentrations of cypermethrin for 1, 2 and 3 weeks. Exposure of sub-lethal doses (40% and 80 % of LC_{50} of 24 h) of glyphosate for 24 or 96 h against the freshwater non-target fish *Channa punctatus* caused significant ($P < 0.05$) alteration in biochemical parameters in liver and muscle tissues of the fish *Channa punctatus* (Bloch) was reported by Singh et al. (2017). Veeraiah et al. (2018) observed that exposure to lethal and sub-lethal concentrations of cyhalothrin 2.5% EC, in the fish *Ctenopharyngdon idellus* for 24 and 96 hours caused a decrease in glycogen content in all tissues.

According to Dezwaan & Zandee (1973) depletion of glycogen in tissues may be due to direct utilization of the compound for energy generation, a demand caused by pesticide-induced hypoxia. Under hypoxia condition, the fish derives its energy from anaerobic breakdown of glucose which is available to the cell by increased glycogenolysis (Chandravathy & Reddy 1996, Rajamannar & Manohar 1998, Rajamanickam 1992). Reduction in glycogen is probably due to its more rapid break down for energy requirement of fish (Muley et al.1996).

Liver suggested as an organ for detoxification. During exposure to Cartap hydrochloride exposure fishes came under stress condition and need more energy to cope with the toxicants. glycogen serves as reserve material. It is utilized when the body came under stress condition. Depletion of glycogen in liver and tissues may be due to increment in the glycolysis pathway. During stress conditions, the glycogen reserves depleted to meet energy demand (Rawat et al. 2002). Fall in glycogen levels indicates its rapid utilization to meet the enhanced energy demands intoxicant treated animals through glycolysis or hexose monophosphate pathway as observed by Cappon & Nicholas (1975). The above findings support the alterations of glycogen in the present study.

Proteins

The changes in protein content observed in the various tissues of *Cirrhinus mrigala* after Cartap hydrochloride exposure along with the control was graphically represented in Fig. 3 and Fig. 4.

The Protein content in different tissues in control fish *Cirrhinus mrigala* was in the order of:

Muscle > Liver > Brain > Kidney > Gill

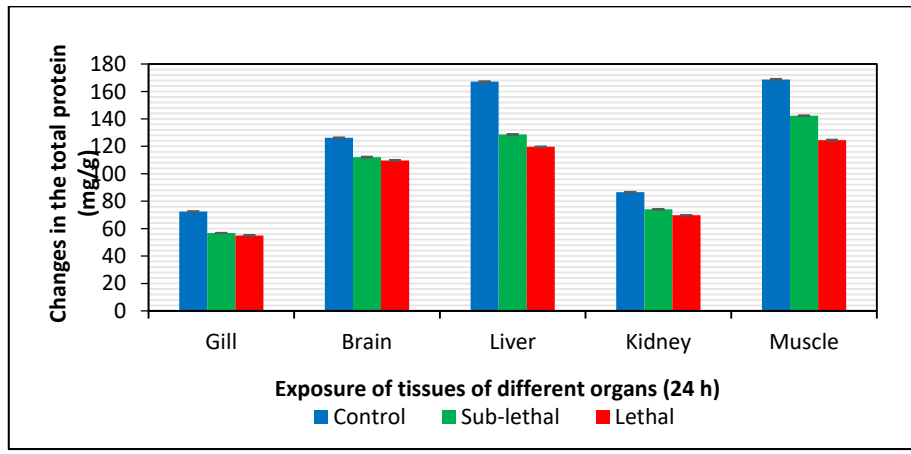


Fig. 3: *Changes* in protein content (mg/g wet wt of the tissue) in different tissues of fish *Cirrhinus mrigala* (Hamilton) on exposure to sub-lethal and lethal concentration of Cartap hydrochloride (50% SP) for 24 hours.

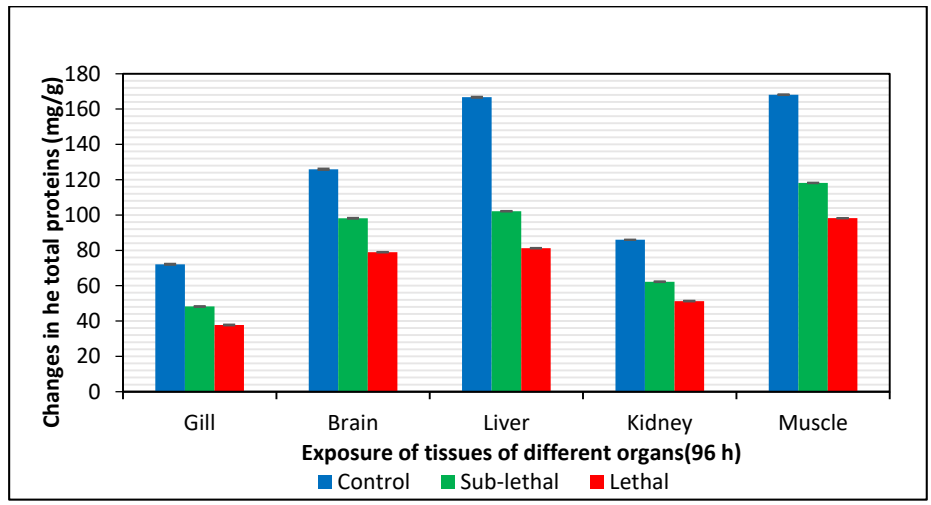


Fig. 4: Changes in protein content (mg/g wet wt of the tissue) in different tissues of fish *Cirrhinus mrigala* (Hamilton) on exposure to sub-lethal and lethal concentration of Cartap hydrochloride (50% SP) for 96hours.

Under exposure of sub-lethal and lethal concentrations of Cartap hydrochloride for 24 h, the amount of protein was found to decrease in all the tissue of *Cirrhinus mrigala.*

The lyotropic gradation series in terms of per cent decrement at 24 h and 96 h exposure was:

Sub-lethal -24 h: Liver > Gill > Muscle > Kidney > Brain

Lethal-24 h- Liver > Muscle > Gill > Kidney > Brain

Sub-lethal -96 h: Liver > Gill > Muscle > Kidney > Brain

Lethal-96 h: Liver > Gill > Muscle > Kidney > Brain

For 24 h exposure maximum per cent of the decrease in total protein was observed in the liver (sub-lethal 23.05, lethal 28.33). For 24 h exposure minimum percentage of depletion of total protein was found in the brain (sub-lethal 11.18, lethal 13.13). For 96 h the percentage of decrease was maximum in the liver (sub-lethal 38.72, lethal 51.27). Similarly, for 96 h minimum percentage of decrease was noticed in the brain (sub-lethal 22.06, lethal 37.30).

Protein is the most primary biochemical ingredient present in large quantities in the body of fish. Liver is rich in protein and centre for various metabolism of the fish. In the present study maximum decrease of total protein in the liver is due to the increased rate of proteolytic activity or repeated break down of protein to yield energy due to stress caused due to pesticide exposure. Anitha & Rathnamma (2016) noticed decreased protein levels in all the tissues like liver, kidney, brain, gill and muscle of *Labeo rohita* exposed to lethal and sub-lethal concentrations of Pyraclostrobin 20%

WG (carbamate) for 24 h and sub-lethal concentrations for 5 and 10 days. A decline in the protein content was noticed by Kumari et al. (2014) in the liver of *Clarias batrachus* when exposed to sub-lethal concentrations (2 and 4 $mg.L^{-1}$) of the Carbaryl for 96 h. A decrease in protein may be due to the impairment of protein synthesis or an increase in the rate of its degradation to amino acids. Exposure to Carbryl for 4 and 24 days, decreased protein content in liver and muscle of fish *Mugil cephalus*, when exposed to the lethal and sub-lethal concentration of Carbaryl for 4 days and 21 days respectively was reported by Shivanagouda et al. (2013). Kumar et al. (2017) reported a reduction in proteins in the liver and kidney of freshwater fish, *Channa punctatus* exposed to different sub-lethal concentrations of pesticide Carbaryl for a period of 15, 30, 45, 60, 75 and up to 90 days. Muddassir (2015) observed significant decrease value in Total protein in the liver of *Channa punctatus* was treated with 0.1 mL Carbofuran and 0.09 mL Malathion pesticides at different time intervals 7, 14, 21 and 28 days. The decrement of total protein may be due to the inhibition of RNA synthesis disturbing the protein metabolism or this may be due to liver damage where most protein synthesis usually occurs, these results agreed with that of Singh & Sharma (1998). The depletion of protein might also be attributed to spontaneous utilization of amino acids in various catabolic reactions inside the organism to combat the stress condition (Borah & Yadav 1996). Wankhedkar & Bhavsar (2015) found that total protein content significantly decreased in foot and hepatopancreas in land snail *C. moussonianus* when treated with Cartap hydrochloride and Imidacloprid at lowest concentration i.e. LC_{50} 0.41ppm and LC_{50} 0.54 ppm respectively. Veeraiah et al. (2018) observed a decrease in protein content in all tissues exposed to lethal and sub-lethal concentrations of cyhalothrin 2.5% EC, in the fish *Ctenopharyngdon idellus* for 24 and 96 h.

Proteins are important organic constituents of the animal cells. Understanding the protein components of the cell becomes necessary in the light of the radical changes taking place in protein profiles during pesticide intoxication (Anitha & Rathnamma 2016). The decreased trend of the protein content as observed in the present study in most of the fish tissues may be due to metabolic utilization of the ketoacids through gluconeogenesis pathway for the synthesis of glucose or due to the directing of free amino acids for the synthesis of necessary proteins, or for the maintenance of osmotic and ionic regulation (Schmidt Neilson 1975).

Nucleic Acids (DNA & RNA)

The changes in DNA content observed in the various tissues of *Cirrhinus mrigala* after the Cartap hydrochloride exposure along with the control was graphically represented in Fig. 5 and Fig. 6.

In control fish, DNA content present in different organs was in the order of:

Muscle > Gill > Brain > Liver > Kidney.

Under exposure to sub-lethal and lethal concentrations of Cartap hydrochloride, for 24 h the amount of DNA was found to decrease in all the tissue of *Cirrhinus mrigala.* The lyotropic gradation series in terms of per cent decrement at 24 h and 96 h exposure was:

Sub-lethal -24 h: Gill > Liver > Muscle > Brain > Kidney

Lethal-24 h-Gill > Liver > Muscle > Brain > Kidney

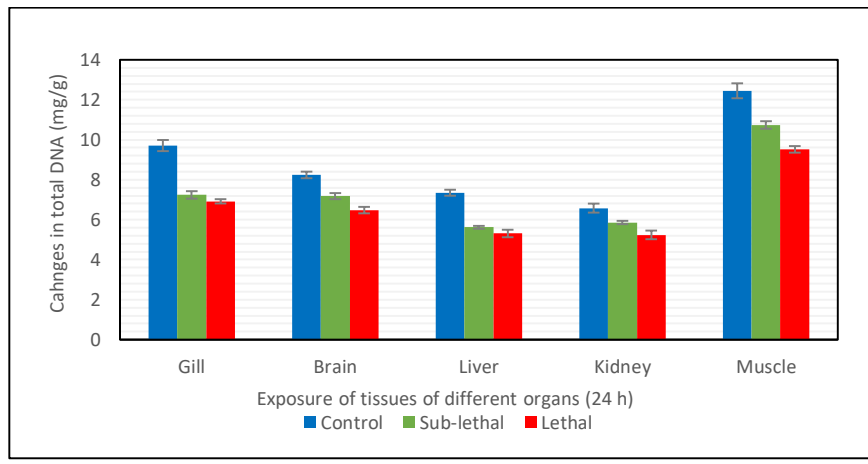


Fig. 5: Changes in the amount of deoxyribonucleic acid (DNA) (mg/g wet weight of the tissue) in different tissues of the fish, *Cirrhinus mrigala* on exposure to sub-lethal and lethal concentration of Cartap hydrochloride (50% SP) for 24 h.

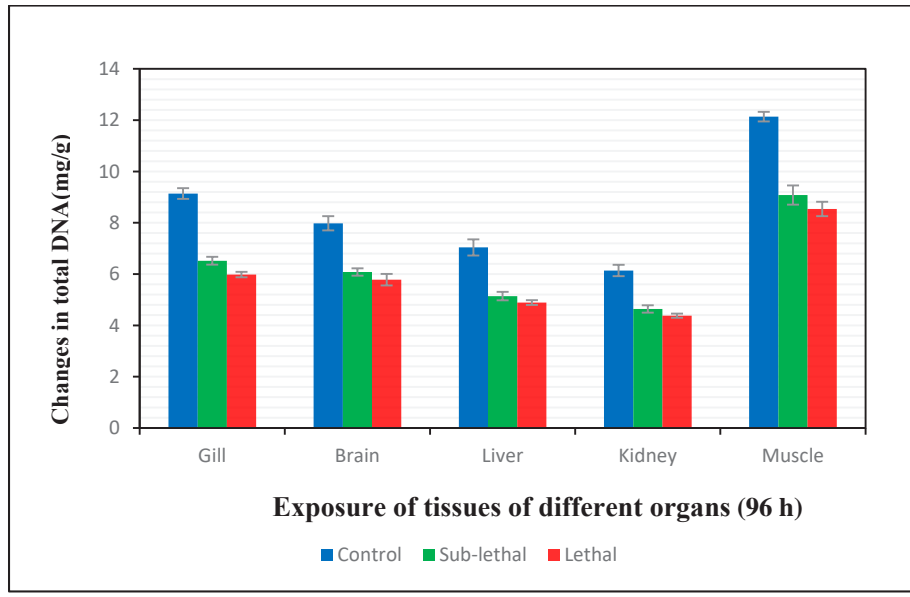


Fig. 6: Changes in the amount of deoxyribonucleic acid (DNA) (mg/g wet wt of the tissue) in different tissues of the fish *Cirrhinus mrigala* on exposure to sub-lethal and lethal concentration of Cartap hydrochloride (50% SP) for 96 h.

Sub-lethal-96 h: Gill > Liver > Muscle > Kidney > Brain

Lethal-96 h: Gill > Liver > Muscle > Kidney > Brain

In the present study under Cartap hydrochloride exposure for 24 h, maximum percentage of depletion in amount of DNA was noticed in Gill (sub-lethal 25.44, lethal 28.74). Minimum percentage of depletion was exhibited in the Kidney (sub-lethal 10.95, lethal 20.37). Under exposure to sub-lethal and lethal concentrations of Cartap hydrochloride for 96 h, maximum percentage of depletion was seen in Gill (sub-lethal 28.67, lethal 34.58) and minimum percentage of depletion was noticed in the brain (sub-lethal 23.81, lethal 27.57).

The changes in RNA content observed in the various tissues of *Cirrhinus mrigala* after Cartap hydrochloride exposure along with the control was graphically represented in Fig. 7 and Fig. 8.

The RNA content in different tissues in control fish *Cirrhinus mrigala* was in the order of:

Muscle > Brain > Gill > Liver > Kidney.

Under exposure to lethal and sub-lethal concentrations of Cartap hydrochloride, for 24 and 96 h, the amount of RNA was found to decrease in all the tissues. The lyotropic gradation series in terms of per cent decrement at 24 h and 96 h exposure was:

Sub-lethal -24h: Muscle > Gill > Kidney > Brain > Liver

Lethal-24h: Muscle > Gill > Kidney > Liver > Brain

Sub-lethal -96h: Gill > Muscle > Kidney > Liver > Brain

Lethal-96h: Gil l > Muscle > Liver > Kidney > Brain

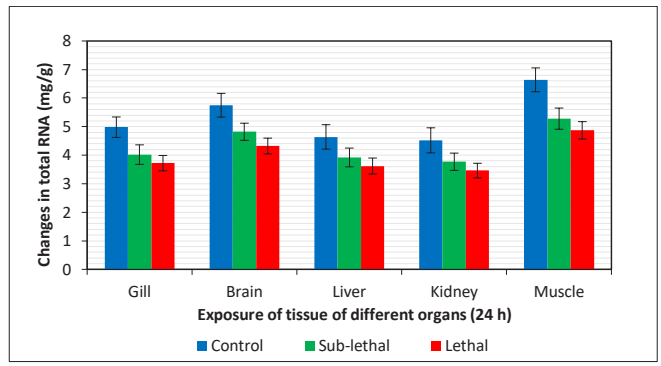


Fig. 7: Changes in the amount of ribonucleic acid (RNA) (mg/g wet wt of the tissue) in different tissues of the fish, *Cirrhinus mrigala* on exposure to sub-lethal and lethal concentration of Cartap hydrochloride (50% SP) for 24 h.

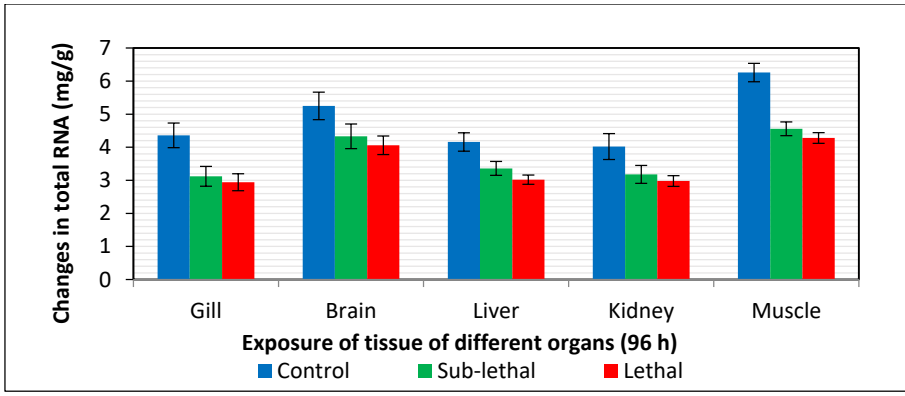


Fig. 8: Changes in the amount of ribonucleic acid (RNA) (mg/gm wet wt of the tissue) in different tissues of the fish, *Cirrhinus mrigala* on exposure to sub-lethal and lethal concentration of Cartap hydrochloride (50% SP) for 96 h.

After 24 h of exposure maximum percentage of decrease in the amount of RNA was found in muscle (sub-lethal 20.48, lethal 26.65). Minimum per cent of the decrease in RNA was found in the liver (15.51) in sub-lethal concentration and brain (19.65) in lethal concentration. After 96h of exposure maximum percentage of decrease in the amount of RNA was found in Gill (sub-lethal 28.44, lethal 32.56). Minimum percentage of decrease in RNA was found in brain(sub-lethal 17.52, lethal 22.66).

The results indicated that the DNA and RNA content in all the tissues of test fish were decreased compared to controls and the decreasing trend was more pronounced in lethal concentrations than in sub-lethal concentrations. In maintaining the physiological configuration of the fish Nucleic acids play a vital role. As Nucleic acid and protein play the main role in regulating different activities of cells they are regarded as important biomarkers of the metabolic potential of cells (Veeriah et al 2013a).

The decrease in nucleic acid content in the present study was in accordance with Vivek (2015) in fingerlings of *Labeo rohita* exposed to sub-lethal concentrations of Cartap hydrochloride for 24, 48, 72 and 96 h. Similar results were also found by Dasu (2014) in fingerlings of *Labeo rohita* were exposed to Thiocarb (Larvin 75% WP) a thiocarbamate pesticide. Anitha & Rathnamma (2016) noticed decreased DNA and RNA levels in all the tissues like liver, kidney, brain, gill and muscle of *Labeo rohita* exposed to lethal and sub-lethal concentrations of Pyraclostrobin 20%WG (carbamate) for 24 h and sub-lethal concentrations for 5 and 10 days.

Tilak et al. (2009) noticed a decreased level of DNA and RNA content in Alachlor treated freshwater fish, *Channa punctatus* (Bloch). The decrease of RNA may be due to inhibiting the function of RNA polymerase or due to interference in the incorporation of precursor in the nucleic acid synthesis. The alterations in DNA levels may be due to disturbances in DNA synthesis and its turnover rate besides degenerative changes caused by pesticides.

From the present study, it can be concluded that exposure of *Cirrhinus mrigala* to Cartap hydrochloride caused a decline in the glycogen, total protein and Nucleic acids (DNA, RNA) content which is more pronounced in lethal exposure than in sub-lethal exposure. The alterations caused during pesticide exposure may be due to the decreased catabolism of the biomolecules to meet the energy demand of test organism under stress or their reduced synthesis due to impaired tissue function. Therefore, the results of this study suggest a serious concern towards the potential danger of Cartap hydrochloride for the aquatic environment and organisms suggesting judicious and careful use of this pesticide in the agricultural area.

ACKNOWLEDGEMENTS

The authors are thankful to the UGC SAP-DRS-III for extending the infrastructure facilities to carry out the present work in the Laboratories of the Deptt. of Zoology & Aquaculture and thank the Head, Department of Zoology and Aquaculture for permitting to do the work.

REFERENCES

Anitha, A. and Rathnamma, V.V. 2016. Toxicity Evaluation and Protein Levels of Fish Labeo rohita Exposed to Pyraclostrobin 20% Wg (Carbamate). International Journal of Advanced Research, 4(3): 967-974.

APHA 1998. Standard Method for the Examination of Water and Wastewater, A.D. Eaton, L.S. Clesceri and A.E. Greenberg (Eds.), 20th edition. American Public Health Association, AWWA and WEF, Washington D.C.

Bantu, N. and Rathnamma Vakita 2013. Effect of dimethoate on mortality and biochemical changes of freshwater fish *Labeo rohita* (Hamilton). Journal of Biology and Today's World, 2(10): 456-470.

Borah, S. and Yadav, R.N.S. 1996. Effect of Rogor (30% w/w dimethoate) on the activity of lactate dehydrogenase, acid and alkaline phosphatase in muscle and gill of a freshwater fish, *Heteropneustes fossilis*. Journal of Environmental Biology, 17(4): 279-283.

Cappon, I.D. and Nicholls, D.M. 1975. Factors involved in increased protein synthesis in liver Microsomes after administration of DDT. Pestic. Biochem. Physiol., 5: 109-118.

Chandravathy, V.M. and Reddy, S.L.N. 1996. Lead nitrate exposure changes in carbohydrate metabolism of freshwater fish. Journal of Environmental Biology, 17: 75-79.

Chaudhry, A.S. and Jabeen, F. 2011. Assessing metal, protein, and DNA profiles in *Labeo rohita* from the Indus River in Mianwali, Pakistan. Environ. Monit. Assess., 174(1-4): 665-679.

Dasu, P.M. 2014. Thiocarb 75 % wp a carbamate insecticide induced toxicity biochemical and histopathological changes in the freshwater Indian major carp *Labeo rohita* Hamilton, Ph.D. Thesis, Acharya Nagarjuna University, Nagarjuna Nagar, Guntur, A.P, India

Dezwaan, A. and Zandee, D.I. 1973. Body distribution and seasonal changes in glycogen content of the common sea mussel, *Mytilus edulis*. Comp. Biochem. Physiol., 43: 53-55.

Dhanalakshmi, B. 2013. Acute and chronic toxicity of chromium on biochemical composition of the freshwater major carp *Cirrhinus mrigala* (Hamilton). Asian J. Sci. Technol., 4: 021-026.

Finney, D.J. 1971. Probit Analysis, 3rd edition. Cambridge University Press.

Golterman, H. and Claimo, R.S. 1969. Methods for Chemical Analysis of Freshwater. Blackwell Sci. Pub., 166 pp.

Jabeen, F., Chaudhry, A.S., Manzoor, S. and Shaheen, T. 2016. Carbamates and neonicotenoids in fish, water and sediments from the Indus River for potential health risks. Environ. Monit. Assess., 187(2): 29.

Kafilzadeh, F., Shiva, A.H., Malekpour, R. and Azad, H.N. 2012. Determination of organochlorine pesticide residues in water, sediments and fish from Lake Parishan, Iran. World J. Fish. Mar. Sci., 4(2): 150-154.

Kemp, A. and and Van Heijningen, A.J.K. 1954. A colorimetric method for the determination of glycogen in tissues. Bio. Chem. J., 56: 646-648.

Kumar, A., Singh, S. and Sharma, H.N. 2017. Changes in total protein in Liver and Kidney of freshwater fish, *Channa punctatus* (Bloch.) after intoxication of Carbaryl. Journal of Advanced Laboratory Research in Biology, 8(2): 41-43.

Kumari, A., Srivastava, A. and Jha, M.M. 2014. Carbaryl Induced alteration in histology and certain biochemical parameter in liver of *Clarias batrachus*. Global Journal of Bioscience and Biotechnology, 3(3): 259-263.

Lowry, O.H., Rosebrough, N.J., Farr, A.L. and Randall, R.J.1951. Protein measurement with the Folin Phenol Reagent. J. boil. Chem., 193: 265-275

Mayers, P. A. 1977. In: Review of Physiological Chemistry, 16th edition. Eds: Harper H A. Rodwell U V and Mayers P.A. Large Medical Publications, California.

Muddassir, A.T. 2015. Comparative study of biochemical alterations induced by carbofuran and malathion on *Channa punctatus* (Bloch.). International Research Journal of Biological Sciences, 4(9): 61-65.

Muley, D.V., Kamble, G.B. and Gaikwad, P.T. 1996. Endosulfan toxicity in the freshwater fish *Tilapia mossambica*. Journal of Aquatic Biology, 11: 61-66.

Naik, B. R., Rao, G. N. and Neelima, P. 2016. Sub-lethal toxicity of cyperkill (a synthetic pyrethroid pesticide) on glycogen content in the tissues of *Labeo rohita.* Int. J. Curr. Res. Aca. Rev., 4(12): 127-134.

Pillai, S.K. and Sinha, H.C.1968. Statistical Methods for Biological Works. Ramprasad and Sons, Agra.

Prasada Rao, G. D. V., Veeraiah, K., Krishna, Ch., Rajeswari, A. and Sindhoori, E. 2018. Cyhalothrin induced bio-chemical alterations in the grass carp *Ctenopharyngodon idellus* (Valenciennes). European Journal of Biomedical and Pharmaceutical Sciences, 5(9): 525-536.

Priya, B.P. and Maruthi, Y.A. 2013. Imidacloprid toxicity on biochemical constituents in liver tissue of fresh water teleost *Channa punctatus*. International Journal of Pharma and Bio Sciences, 4(4b): 50-54.

Rajamanickam, C. 1992. Effects of Heavy Metal Copper on the Biochemical Contents, Bioaccumulation and Histology of the Selected Organs in the Freshwater Fish, *Mystus Vittatus* (Bloch). Ph.D. Thesis, Annamalai University, India.

Rajamannar, K. and Manohar, L. 1998. Sublethal toxicity of certain pesticides on carbohydrates, proteins and amino acids in *Labeo rohita*. J. Ecobiol., 10(3): 185-191.

Rawat, D.K., Bais, V.S. and Agrawal, N.C. 2002. A correlative study on liver glycogen and endosulfan toxicity in *Heterpneustes fossilis*. J. Environ. Biol., 23: 205-207.

Roberts, M. and Boyce, C.B.C. 1972. In Methods in Microbiology. 7-A Edition. (eds: J.R. Norris and D.W. Ribbows). Academic Press, New York, pp 479.

Sastry, K.V. and Abad A Siddiqui. 1982. Chronic toxic effects of the carbamate pesticide Sevin on carbohydrate metabolism in a freshwater snakehead fish, *Channa punctatus*. Toxicology Letters, 14(1-2): 123-130.

Schmidt Nielson, B. 1975. Osmoregulation: Effect of salinity and heavy metal. Fed. Proc., 33: 2137-2146.

Searchy, D.G. and MacLennis, A.J. 1970a. Determination of DNA by the Barton Diphenylanine technique. In: Experiments and Techniques in Parasitology. (eds: A.J. Mac Lnnis and M. Voge) W.H. Freeman and Co, San-Franscisco, 190-191 pp.

Searchy, D.G. and MacLennis, A.J. 1970b. Determination of RNA by Dische orcinol technique. In: Experiments and Techniques in Parasitology. (eds: A.J. Mac Lennis and M. Voge). W.H. Freeman and Co, San-Francisco, pp. 189-190.

Shivanagouda, N., Sanagoudra and Bhat, U.G. 2013. Carbaryl induced changes in the protein and cholesterol contents in the liver and muscle of marine benthic fish, *Mugil cephalus*. American Journal of Biochemistry, 3(2): 29-33.

Singh, A. and Singh, A. 2017. Studies on toxicity stress, behavioural alterations and biochemical changes induced by glyphosate herbicide on the freshwater fish, *Channa punctatus* (Bloch). Int. J. Food Agricul. Veter. Sci., 7(3): 39-48.

Singh, R.K. and Sharma B. 1998. Carbofuran induced biochemical changes in *Clarias batrachus*. J. Pestic. Sci., 53: 285-290.

Srivastava, P. and Singh, A. 2013. In vivo study of effects of dithiocarbamates fungicide (mancozeb) and its metabolite ethylene thiourea (ETU) on freshwater fish *Clarius batrachus*. Journal of Biology and Earth Sciences, 3(2): B228-B235.

Tataji, P.B. and Kumar, M.V. 2016. Biochemical changes induced by Butachlor and Machete 50% EC to the freshwater fish *Channa punctata* (Bloch). International Journal of Science and Research, 5: 2048-2052.

Tilak, K.S., Raju, P.W. and Butchiram, M.S. 2009. Effects of alachlor on biochemical parameters of the freshwater fish, *Channa punctatus* (Bloch). J. Environ. Biol., 30(3): 421-426.

Veeraiah, K., Venkatrao, G., Vivek, Ch. and Hymaranjani, G. 2013a. Heavy metal, cadmium chloride induced biochemical changes in the Indian major *Cirrhinus mrigala* (Hamilton). Int. J. Bioassays, 2(07): 1028-1033.

Veeraiah, K., Vivek, Ch., Srinivas Rao, P. and Venkatrao, G. 2013b. Biochemical changes induced by Cypermethrin (10% EC), a pyrethroid compound in sub-lethal and lethal concentrations to the freshwater fish

Cirrhinus mrigala (Hamilton). J. Atoms and Molecules, 3(6): 625-634.
Vivek, Ch. 2015. Impact of Cartap Hydrochloride (50% SP) on Biochemical, Haematological and Enzymatic Activities of the Freshwater Fish, *Labeo Rohita* (Hamilton). Ph.D. Thesis submitted to Acharya Nagarjuna University, Nagarjuna Nagar, Guntur, A.P, India.
Wankhedkar, P. T. and Bhavsar, S.S. 2015. Effect of Cartap hydrochloride and Imidacloprid on biochemical parameters of *Cerastus moussonianus*. Biolife, 3(1): 125-131.

Eco. Env. & Cons. 26 (August Suppl. Issue) : 2020; pp. (S127-S131)
Copyright@ EM International
ISSN 0971–765X

Effect of Cartap hydrochloride (50% SP) insecticide on gill histology of the fish, *Cirrhinus mrigala* (Hamilton)

G. Vani[1]*, K. Veeraiah [2], M. Vijaya Kumar[1] and S.K. Parveen[1]

[1]Department of Zoology, SRR & CVR Government Degree College (A), Vijayawada 520 004, Krishna District, A.P., India
[2]Department of Zoology and Aquaculture, Acharya Nagarjuna University, Nagarjunanagar 522 510, Guntur, A.P., India

Received 26 October, 2019; accepted 3 February, 2020)

ABSTRACT

The fish, *Cirrhinus mrigala,* Indian major carp was exposed to Cartap hydrochloride and the static LC_{50}values for 24,48,72 and 96 hours were found to be 0.436, 0.419, 0.394 and 0.376 mg^{-1} and 0.399, 0.371, 0.361 and 0.339 mg^{-1} in Continuous flow-through system. The gills which are the primary organs to get exposed to foreign contaminants and pesticides were studied for histological changes. The following histological changes like epithelial lifting, degeneration of primary and secondary gill lamellae, curling of secondary gill filaments, atrophy of secondary gill lamellae, congestion of secondary lamellae, fusion of secondary gill filaments were observed. The results obtained were discussed at length with the available literature. By studying the histological deformities, it was concluded that the pesticide caused enough damage to the gills of the fish and can influence on the survival of the fish

Key words : *Cartap hydrochloride, Cirrhinus mrigala, Gill histopathology*

Introduction

Indiscriminate and extensive use of pesticides in modern agricultural practices globally for achieving increased food production is one of the major sources of water pollution. Presence of pesticide in aquatic bodies is largely due to outfall from pesticide manufacturing factories and the runoff from agricultural fields (Ganeshwade, 2012). Pesticides are not highly selective but are generally toxic to macrophytes, non-target organisms such as fish (Ayoola, 2008 and Franklin *et al*., 2010).

Fish accumulate these pollutants directly or indirectly from polluted waters and food chain (Jabeen *et al*., 2016). In India, Cartap hydrochloride, a carbamate pesticide is extensively used in rice, sugarcane cabbage and cauliflower crops to control pests. In fish, the gill is the major organ for respiration, excretion and osmotic regulation. Gills are appropriate for the assessment of environmental impact as they are considered as a good tissue indicator of the water quality (Fanta, 2003). Histopathological analysis is a very sensitive parameter and is helpful in determining cellular damage that may occur in target organs (Altinok and Capkin, 2007). In this viewpoint an attempt was made to study the effect of sublethal and lethal concentrations of Cartap hydrochloride on gill histopathology of freshwater fish, *Cirrhinus mrigala* exposed for 24 and 96 hours.

Materials and Methods

The fingerlings of the test fish *Cirrhinus mrigala* of size 6-8 ± ½ cm and weight 6-7 ± ½ gm were pro-

cured from local fish hatcheries of Nandivelugu, Tenali mandal, Guntur district, Andhra Pradesh. The fish were acclimated at (28±2°C)) in the laboratory conditions for two weeks. All the precautions laid down on recommendations of the toxicity tests to aquatic organisms were followed (Annon, 1975). Fish were regularly fed with rice bran and one day prior to the experimentation feeding was stopped. Fingerlings were exposed to sub-lethal ($1/10^{th}$ of 96 h LC_{50} value 0.0376 mg^{-1}) and lethal (96 hours LC_{50} value 0.376 mg^{-1}) concentrations of Cartap hydrochloride for 24 and 96 hrs.

Gills were processed in laboratory for routine histological characterization by the double staining method using Haematoxylene and Eosin. All samples were fixed in 10% phosphate- buffered formalin for about 24 hrs. The specimens were dehydrated in a series of graded ethanol (50%, 70% and 90%) and then after embedded in paraffin. Five-micron sections were cut using an ultramicrotome (Leica, Japan) and deparaffinized by means of xylol. The sections were dehydrated in 90%, 70% and 50% ethanol followed by a 10 min wash in water and further stained with Hematoxylin and Eosin (HE). Sections were observed in digital microscope (Intel Play QX3) at 400 x magnification.

Results

The transverse section of gill tissue of normal fish shows branches from the central axis called the primary gill lamellae. Each of the primary gill lamella further divides into secondary gill lamellae or filaments. Within each division of the gills are the adjacent afferent vessels and efferent vessels with hemocytes. A thin septum separates the primary and secondary gill filaments. The secondary non branching filament lamella possesses epithelial pillar cells separated by large lacunae Fig. 1.

Cartap hydrochloride has induced marked pathological changes in gills of fish *Cirrhinus mrigala*. In the current study, it was observed that with the increase in the time of exposure the histopathological alterations increased in the gills of fish, *Cirrhinus mrigala*.

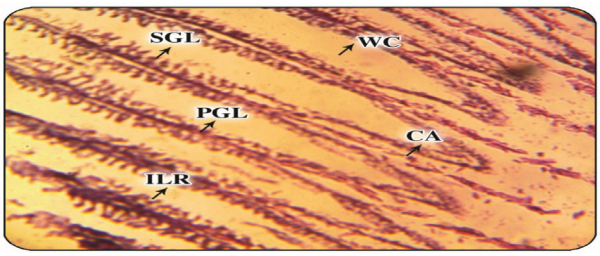


Fig. 1. Normal Gill tissue of *Cirrhinus mrigala*, H.E x 400

CA-Central Axis, PGL-Primary gill lamellae, SGL-Secondary gill lamellae, ILR-Inter lamellar space, WC-Water channel, FSG-Fusion of secondary lamellae, CSG-Curling of secondary lamellae, DPGL-Degenerated primary gill lamellae, DSGL-Degenerated secondary gill lamellae, BC-Blood congestion, EL-Epithelial lifting, LF-Lamellar fusion, ASL-Atrophy of secondary lamellae.

In the control group, no pathological changes were observed in the gills (Fig.1). After treatment with cartap hydrochloride for 24hrs at sublethal concentrationsepithelial lifting,curling of secondary gill filaments,fusion of secondary lamellae and degeneration of secondary gill lamellaestarted to appear (Fig. 2). Degenerative changes like lamellar fusion, epithelial lifting, degenerative secondary gill lamellae and curling of secondary gill filaments were observed after exposure to lethal concentration for 24hrs (Fig. 3). Similar more pronounced degenerative changes like curling of secondary gill filaments, epithelial lifting, degenerative primary and secondary gill lamellae, blood congestion, atrophy of secondary lamellae, mucous secretionwere no-

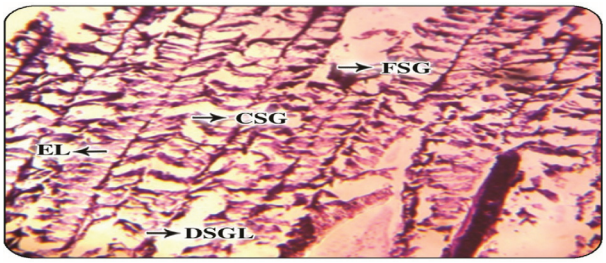


Fig. 2. Gill tissue of *Cirrhinus mrigala*exposed to sublethal concentration of Cartap hydrochloride for 24 hours, H.E x 400

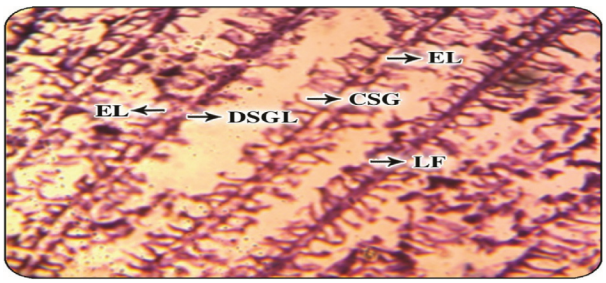


Fig. 3. Gill tissue of *Cirrhinus mrigala* exposed to lethal concentration of Cartap hydrochloride for 24 hours, H.E x 400

ticed in gill exposed to sublethal concentration of cartap hydrochloride for 96 hrs (Fig. 4). Damage in the gills exposed to lethal concentration of cartap hydrochloride for 96 hrs was much extensive with severe degeneration in primary and secondary gill lamellae, hemorrhage between gill filaments, separation of epithelial cells from the basement membrane, collapsed pillar cell, fusion of secondary gill lamellae, lamellar disorganization, atrophy of secondary lamellae, necrosis, blood congestion, mucous secretion, hyperplasia and epithelial lifting (Fig. 5). Thus, the lethal concentration of Cartap hydrochloride has produced significant histopathological changes in comparison to sublethal concentration in *Cirrhinus mrigala*.

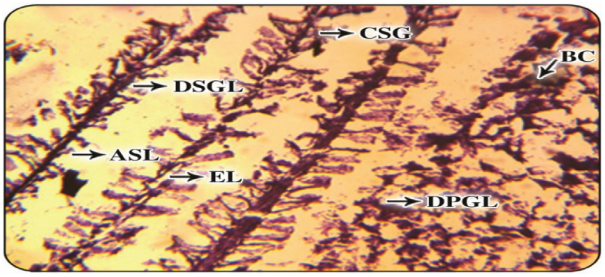


Fig. 4. Gill tissue of *Cirrhinus mrigala* exposed to sublethal concentration of cartap hydrochloride for 96 hours, H.E x 400

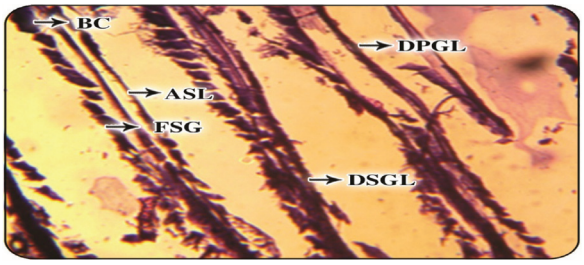


Fig. 5. Gill tissue of *Cirrhinus mrigala* exposed to lethal concentration of cartap hydrochloride for 96 hours, H.E x 400

Discussion

Several authors observed similar degenerative changes in gill when exposed to carbamate pesticides. Vivek *et al.*, (2016) observed fusion of primary and secondary lamellae, epithelial hyperplasia, curling of secondary lamellae, degeneration of lamellae in gills of *Labeo rohita* exposed to sublethal concentrations of cartap hydrochloride for 24,48,72 and 96hrs. Mariya dasu (2014) observed bulging of tips of primary gill filaments, curling of secondary gill filaments, necrosis, fusion of secondary gill lamellae, hyperplasia, hypertrophy of nuclei, pyknotic nuclei, lifting of epithelium in *Labeo rohita* exposed to Thiocarb, a thiocarbamate pesticide in both sublethal and lethal concentrations. Anitha (2015) observed necrosis, curling and fusion of secondary gill filaments, atrophy, degeneration of primary and secondary gill lamella, blood conjunction, epithelial hyperplasia, lamellar telangiectesis, in gills of *Labeo rohita* exposed to sublethal concentrations of Pyraclostrobin for 24 hrs, 5 days and 10 days and to lethal concentration for 24 hrs. Ali Taheri Mirghaed *et al*., (2018) noticed edema, lamellar curling, hyperplasia, lamellar fusion in the gill of *Cyprinus carpio* treated with 0.75 mg/L, 1.5 mg/L, and 3 mg/Lof indoxacarb for 7, 14 and 21 days. The histopathological changes observed in the present study were in accordance with the above studies.

Similar histopathological changes in gills were reported in *Channa punctatus* exposed to Imidacloprid (Pawara *et al.,* 2019), in *Labeo rohita* exposed to phenol (Butchiram *et al.,* 2013), in *Labeo rohita* exposed to cadmium (Saravanan *et al*., 2019), in *Oreochromis niloticus*exposed to heavy metals (Shameem Rani, 2018), in *Labeo rohita* exposed to tannery industrial effluent (Diana Handa and Gurinder Kaur Walia, 2019), in *Puntius sophore* treated with Acephate (Gavit and Patil, 2019), *in Cirrhinus mrigala* exposed to cement factory effluent (Juginu and Sujila, 2019) in *Cirrhinus mrigala*exposed to lead arsenate (Vanitha *et al.,* 2017), in *Labeo rohita* exposed to dimethoate (Dey and Saha, 2014), In *Cirrhinus mrigala* exposed to cypermythrin (Sree Veni and Veeraiah, 2014).

In fish, gill is the major organ for respiration, excretion and osmotic regulation. Gills are appropriate for the assessment of environmental impact as they are considered as a good tissue indicator of the water quality (Fanta, 2003). The lifting of lamellar epithelium in the present studymay be induced by the incidence of severe Oedema (Pane *et al.,* 2004). Swelling in gill epithelium leads to decreased efficiency of gases exchange and oxygen consumption. (Sudhasaravanan and Binukumari, 2015).

The first line of defense to metal/ toxicant exposure in the gills is mucus secretion and by fusion of lamellae it can temporarily protect the underlying epithelium from injury (Handy and Maunder, 2009). Pronounced secretion of mucus layer over the gill lamellae curtails the diffusion of oxygen (David *et al.*, 2002 and Rudragouda Marigoudar *et al*., 2009) which may ultimately reduce the oxygen consump-

tion by the animal (Kalavathy *et al*., 2001). All metabolic pathways depend upon the efficiency of the gills for their energy supply as gills are the major respiratory organs and damage to these vital organs lead to respiratory distress. The present histological studies clearly indicate that the damage in gills of *Cirrhinus mrigala* decreases the uptake of oxygen which results in histotoxic anoxia. Due to this the gill tissue suffers from oxygen debt and losses the capacity to remove CO_2 from blood which is in accordance with (Sathivel *et al*., 1991).

In the present study the observed alterations such as partial fusion of secondary lamellae, lifting of epithelial cells and proliferation of the epithelial cells, act as defense mechanisms towards toxicants. These alterations increase the distance between the external environment and the blood in the gills which serves as a barrier for the entry of contaminants. (Fernandes and Mazon, 2003 and Mallatt, 1985). When any type of toxicants meets gills, lamellar fusion in gills occur which is a protective measure as it diminishes the amount of vulnerable gill surface area in fish (Mallatt, 1985). when gills come in contact withany types of toxicants oedema appears to be a common feature of the gill pathology. Due to disturbance in branchial Na+, K+-ATPase pump by toxicants, solute accumulation in the epithelial cells occur and disturb the osmotic influx of water. This exchange protects the lamellar epithelial cells and prevents the entry of waterborne pollutants into the bloodstream (Arellano *et al*., 1999).

Conclusion

The results of the present study suggest that the changes in gill histomorphology of *Cirrhinus mrigala* may serve as a rapid biological 7monitor to assess the impact of Cartap hydrochloride on other biotic communities in the water body. The results of the present study also stress on the diligent usage of the pesticide product to prevent the environmental pollution.

Acknowledgements

The authors are thankful to the UGC SAP-DRS-III for extending the infrastructure facilities to carry out the present work in the Laboratories of the Dept. of Zoology & Aquaculture. They also thank the Head, Department of Zoology and Aquaculture for permitting to do the work.

References

Ali Taheri Mirghaed., Melika Ghelichpour., Seyed Saeed Mirzargar., Hamidreza Joshaghani. and Hoseinali Ebrahimzadeh Mousavi, 2018. Toxic effects of indoxacarb on gill and kidney histopathology and biochemical indicators in common carp (*Cyprinus carpio*). *Aquaculture Research*. 49(4) : 616-1627.

Altinok, I. and Capkin, E. 2007. Histopathology of rainbow trout exposed to sublethal concentrations of methiocarb or endosulfan. *Toxicol Pathol*. 35 : 405–10.

Anitha, A. 2015. *Pyraclostrobin (20%WG) induced toxicity and biochemical aspects of freshwater fish Labeo rohita* (Hamilton) Ph.D. Acharya Nagarjuna University. Nagarjuna Nagar, Guntur, A.P, India.

Annon, 1975. Committee on methods of toxicity tests with fish macro invertebrates and amphibians. EPA. Oregon: 61.

Arellano, J. M., Storch, V. and Sarasquete, C. 1999. Histological changes and copper accumulation in liver and gills of the *Senegales sole, Solea senegalensis. Ecotoxicology and Environmental Safety*. 44 : 62-72.

Ayoola, S.O. 2008. Toxicity of glyphosate herbicide on Nile tilapia (*Oreochromis niloticus*) juvenile. *Afr. J. Agric. Res*. 3 (12): 825-834.

Butchiram, M.S., Vijaya Kumar, M. and Tilak, K.S. 2013. Studies on the histopathological changes in selected tissues of fish *Labeo rohita* exposed to phenol. *Journal of Environmental Biology*. 34: 247-51.

David, M., Mushigari, S. B. and Prashanth, M. S. 2002. Toxicity of fenvalerate to the freshwater fish. *Labeo rohita. Geobios*. 29 : 25-28.

Dey Chandrimaand Saha Samir Kumar, 2014. Dimethoate (30% EC) induced toxicities on the tissues of the Indian major carp: *Labeo rohita* (Hamilton). *International Journal of Fisheries and Aquatic Studies*. 1(6) : 232-236.

Diana Handa. and Gurinder Kaur Walia. 2019.Quantitative and Semi-quantitative analysis on Gills of a freshwater fish, *Labeo rohita* (Hamilton-Buchanan, 1822) exposed to Tannery industrial effluent using histopathology as biomarker. *IJRAR*. 6(1): 980-981.

Fanta, E., Rios, F.S., Romao, S., Vianna, A.C.C. and Freiberger, S. 2003. Histopathology of the fish *Corydoras paleatus* contaminated with sublethal levels of organophosphorus in water and food. *Ecotoxicology and Environmental Safety*. 54(2) : 119-130.

Fernandes, M.N. and Mazon, A.F. 2003. Environmental Pollution and Fish Gill Morphology. In: Val, A.L. and Kapoor, B.G., Eds., Fish Adaptation. Science Publishers, Enfield: 203-231.

Franklin R. K., Loo, H. S. and Osumanu, H. A. 2010.Incorporation of Bentazone with Exserohilumrostratum for Controlling *Cyperusiria. Am. J. Agri. Biol. Sci*. 5: 210-214.

Gavit, P. J. and Patil, R. D. 2019. Effect of Acephate (Organophosphate) on Gill Histology of the Fresh Water Fish *Puntius sophore* (Hamilton). *IJRAR*. 6(1): 338-342.

Ganeshwade, R.M. 2012. Histopathological changes in the gills of *Puntius Ticto* (Ham) under dimethoate toxicity. *The BioScan*.7(3) : 423-426.

Handy, R. D. and Maunder, R. J. 2009. The biological roles of mucus: Importance for osmoregulation and osmoregulatory disorders of fish health. In: *Osmoregulation and Ion Transport: Integrating Physiological, Molecular and Environmental Aspects*. Society for Experimental Biology Press, London. I: 203- 235.

Jabeen, F., Chaudhry, A.S., Manzoor, S. and Shaheen, T. 2016. Carbamates and neonicotenoids in Fish, water and sediments from the Indus River for potential health risks. *Environ. Monit. Assess*. 187 (2) : 29.

Juginu, M. S. and Sujila, T. 2019. Histopathological responses of gill, liver and kidney in the freshwater fish, *Cyrrhinus mrigala* exposed to cement factory effluent. *Wjpps*. 8 (8) : 1511-1530.

Kalavathy, K., Siva Kumar, A.A. and Chandran, R. 2001. Toxic effects of the pesticide dimethoate on the fish, *Sarotherodon mossambicus*. *J. Ecol. Res Bio*. 2 : 27-32.

Mallatt, J. 1985. Fish gill structural changes induced by toxicants and other irritants: a statistical review. *Canadian Journal of Fisheries and Aquatic Science*. 42(4): 630-648.

Mariya Dasu, P. 2014. *Thiocarb 75 percentage WP a carbamate insecticide induced toxicity biochemical and histopathological changes in the freshwater Indian major carp Labeo rohita* Hamilton, Ph.D. Thesis, Acharya Nagarjuna University, Nagarjuna Nagar, Guntur, A.P, India.

Pane, E.F., Haque, A. and Wood, C.M. 2004. Mechanistic analysis of acute, induced respiratory toxicity in the rainbow trout, *Oncorhynchus mykiss*: an exclusively branchial phenomenon. *Aquatic Toxicology*. 69 : 11-24.

Pawara., Ravindra, H., Patel Nisar, G. and Sarvade Raju, C. 2019.Study on the effect of Imidacloprid on gill tissue of the fish *Channa punctatus* (Perciformes: Channidae) (Bloch.). *IJRAR*. 6 (1): 372-378.

Rudragouda Marigoudar, S., Nazeer Ahmed, R. and David, M. 2009. Cypermethrin induced respiratory and behavioral responses of the freshwater teleost, *Labeo rohita* (Hamilton). *Veterinarski Arhive*. 79(6): 583-590.

Sakthivel., Sampath, K. and Pandian, T.J. 1991. Sublethal effects of textile dye stuff effluent on selected oxidative enzymes and tissue respiration of *Cyprinus carpio* (Linn). *Indian J. Expt. Biol*. 29 : 979-981.

Saravanan, K., Mohanambal, R. and Iyyappan, A. 2019. Effect of cadmium on the histology of gill, liver and hepatopancreas of freshwater fish *Labeo rohita* (Hamilton, 1822). *IJRAR*. 6 (1) : 1255-1263.

Shameem Rani, K. 2018. Histological studies and heavy metal accumulation in the gills and muscles of tilapia fish from Vellar estuary, South East Coast of India, Tamilnadu. *IJRAR*. 5(3) : 298-304.

Sree Veni, S.M. and Veeraiah, K. 2014. Effect of Cypermethrin (10%EC) on Oxygen Consumption and Histopathology of Freshwater Fish *Cirrhinus mrigala*(Hamilton). *IOSR J. Environ. Sci., Toxicol. Food Technol*. 8(10) : 12–20.

Sudhasaravanan, R. and Binukumari, S. 2015. Effects of different concentartions of detergent on dissolved oxygen consumption in *Lepidocephalichythyes thermalis*. *World Journal of Pharmaceutical Research.* (2): 940-945.

Vanitha, S., Amsath,A., Shanthi,P. and Muthukumaravel, K. 2017. Sublethal effects of lead Arsenate on histology of selected organs of freshwater fish, *Cirrhinus mrigala*. *International Journal of Zoology and Applied Biosciences*. 2(5): 250-257.

Vivek, Ch., Veeraiah, K., Padmavathi, P. Dhilleswara Rao, H. and Bramhachari, P.V. 2016. Acute toxicity and residue analysis of cartap hydrochloride pesticide: Toxicological implications on the fingerlings of freshwater fish *Labeo rohita*. *Biocatalysis and Agricultural Biotechnology*. 7 : 193-201.

Eco. Env. & Cons. 27 (November Suppl. Issue) : 2021; pp. (S218-S225)
Copyright@ EM International
ISSN 0971–765X

Acute toxicity and effect of Flubendiamide (39.35% SC) on the oxygen consumption of the Fish, *Catla catla* (Hamilton)

S.K. Parveen*[1], K. Veeraiah[2], G. Vani[1] and M. Vijaya Kumar[1]

[1]Department of Zoology, SRR & CVR Government Degree College (A), Vijayawada 520 004, Krishna District, A.P., India
[2]Department of Zoology and Aquaculture, Acharya Nagarjuna University, Nagarjunanagar 522 510, Guntur, A.P., India

(Received 10 March, 2021; Accepted 18 May, 2021)

ABSTRACT

The fish *Catla catla* fingerlings were exposed to the test toxicant an insecticide Flubendiamide for 24, 48, 72 and 96 hrs and the LC_{50} values were calculated and were reported to be 3.566, 3.456, 3.0221 and 2.892 mg5^{-1} respectively for 24, 48, 72 and 96 hrs. After determination of LC_{50} values the fish were exposed to sub-lethal concentration ($1/10^{th}$ of 96 hrs LC_{50} value i.e., 0.289 mg5′¹) for 24, 48, 72, 96 hrs and 8 days and the changes in oxygen uptake of the Indian major carp *Catla catla* was studied. Fingerlings were exposed to sub-lethal (0.289 mg5^{-1}) and lethal (2.892 mg5′¹) concentrations of flubendiamide for 24 hrs, 48 hrs, 96 hrs and only to the sub-lethal concentration exposed for 8 days. In both sub-lethal and lethal concentrations for all exposed periods *Catla catla* showed an increase in oxygen consumption during the initial time of exposure and a gradual decrease during the subsequent periods of exposures. This initial increase was from 0-6 hours in 24, 48 and 96 hrs where as in 8 days exposed fish the initial increase is only up to 0-4 hours. Alterations in oxygen consumption may be due to respiratory distress as a consequence of impaired oxidative metabolism. In the present study it was observed that flubendiamide has altered respiratory metabolism in the test fish *Catla catla* which can be used as a bio-indicator for assessing pesticide induced alterations in the uptake of oxygen in the fish. Fish in the sub-lethal concentration were found under stress, but that was not fatal. The results obtained in all were discussed with the available literature.

Key words: *Flubendiamide, Catla catla, LC_{50} Values, and Oxygen consumption.*

Introduction

After green revolution during sixties especially in India, pesticides emerged as knight armours for crops (Srivastava and Singh, 2014). Pesticides has credited with economic potential to enhance production of food and fibre and ameliorated in vector-borne diseases, the long-term use has caused effects on human health and the environment including aquatic ecosystem that evolved new branch of aquatic toxicology (Igbedioh, 1991; Forget, 1993; Aktar *et al.*, 2009). Pesticides have been found to be highly toxic not only to fish but also to the other organisms which constitute the food chain. Agricultural run-off from near water bodies is the major cause of deposition of pesticides in aquatic ecosystem. The qualitative and quantitative chemical usage is of great concern ecologically. The discriminate use of chemicals is for the control of insect pests by elimination of target species whereas indiscrimi-

nate usage posed the problem on non-target organisms including man.

Wide and indiscriminate use of pesticides in modern agricultural practices throughout the world has indirectly created problem of pollution of aquatic ecosystems (Ganeshwade, 2012). These chemicals impair water quality which becomes unsuitable for all aquatic organisms due to their toxicity, persistence, bioaccumulation, and biomagnifications in food chain and ecological balance (Subramani Lavanya *et al.*, 2011). Fish accumulate these pollutants directly or indirectly from polluted waters and food chain (Jabeen *et al*., 2016).

Mass mortality of fish due to pesticide exposure is rare, and results only from accidents or direct spraying of the water bodies. Fish are the most often tested aquatic organisms because they are the most conspicuous as predominant and are economically important to man because they are linked in the food chain. Evaluation of LC_{50} is the pioneer step in toxicological assessment of any chemical. It helps to select sub-lethal concentrations to carry out several toxicity tests. Therefore, this knowledge is essential for exploring impacts of any chemical on physical and physiological status of exposed organisms.

In India, flubendiamide, a rynoid pesticide is extensively used in rice and pulse crops to control pests. The excess pesticides used in the farms reach the water bodies by the surface run off and are known to cause ill effects on aquatic organisms. One of the indicators of the health status of a fish is its total oxygen consumption. It helps in evaluating the susceptibility or resistance potential useful to assess the physiological condition of an organism and to correlate the behaviour of the animal, which ultimately serve as predictors of functional disruptions of population. Hence, the analysis of total oxygen consumption can be used as a tool of bio-indicator system to evaluate the basic damage caused to the animal which could either decrease or increase the oxygen uptake (Maharajan *et al.,* 2013). In this viewpoint an attempt was made to study the effect of sub-lethal and lethal concentrations of flubendiamide on oxygen consumption of freshwater fish, *Catla catla* exposed for 24, 48, 96 hrs, and only sub-lethal concentration for 8 days.

Materials and Methods

The fingerlings of the test fish *Catla catla* of size 6-8 ± ½ cm and weight 6-7 ± ½ gm were procured from local fish hatcheries of Nandivelugu, Tenali mandal, Guntur district, Andhra Pradesh. The fish were acclimated at (28±2°C) in the laboratory conditions for two weeks. All the precautions laid down on recommendations of the toxicity tests to aquatic organisms were followed (Annon, 1975). Fish were regularly fed with rice bran and one day prior to the experimentation feeding was stopped. Experiments on the oxygen consumption of the fish *Catla catla* was carried out in a respiratory apparatus developed by Job (1955). Fish were exposed to sub-lethal ($1/10^{th}$ of 96 hrs LC_{50} value 0.289 $mg5^{\sim 1}$) and lethal (96 hrs LC_{50} value 2.892 $mg5^{\sim 1}$) concentrations of Flubendiamide for 24, 48, 72 and 96 hrs and only for sub-lethal concentration for 8 days. The samples for estimation of oxygen, consumption were taken from the respiratory chamber, at alternate hours of intervals for 24 hrs. The amount of dissolved oxygen consumption was calculated per gram body weight per hour. The dissolved oxygen content was estimated by modified Winkler's method as described by Golterman and Clymo (1969). The difference in the dissolved oxygen content between initial and final water samples represents the amount of oxygen consumed by the fish. Students, "t-test" was employed to calculate the significance of the differences between control and experimental means. P values of 0.05 or less were considered statistically significant (Fisher, 1950).

Results

Toxicity

The calculated LC_{50} values for 24, 48, 72 and 96 hrs to the test fish *Catla catla* were presented in Table 1 and graphically represented in Figure 1. The LC_{50} values obtained were 3.566, 3.456, 3.0221 and 2.892 $mg5^{\sim 1}$ respectively for 24, 48, 72 and 96 hrs. The LC_{50} values decreased with the increase in the period of exposure.

The toxicity may be influenced by exposure conditions, source and size of fish, formulation, and water quality. The ground water used for acclimatization of fish and experimental purpose was clear and unchlorinated. The hydrographical properties of water were estimated by the modified methods of Golterman and Clymo, (1969).

Oxygen Consumption

Determination of oxygen consumption by the fish is

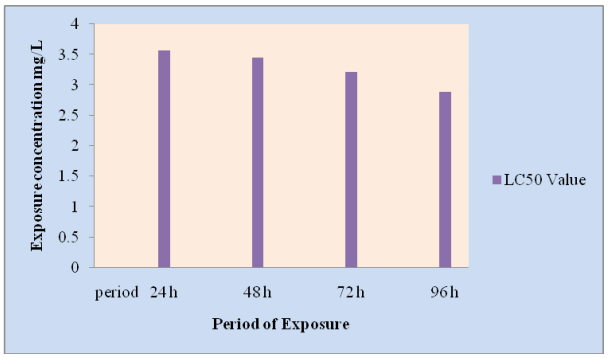


Fig. 1. Calculated LC_{50} values for flubendiamide to the fish *Catla catla* under static exposure for 24, 48, 72 and 96 hrs.

an important indicator which reflects physiological state of animal and is useful for assessment of lethal effects (Tilak *et al.*, 2007). One of the indicators of the health status of a fish is its total oxygen consumption. It helps in evaluating the susceptibility or resistance potential useful to assess the physiological condition of an organism and to correlate the behavior of the animal, which ultimately serves as predictors of functional disruptions of population (Maharajan *et al.*, 2013). Oxygen consumption is an important physiological parameter which can be used as a useful measure of toxic effects of pesticides in sub-lethal and lethal concentrations because energy processes are indicators of overall physiological state of organism. Changes in the respiratory activity in fish have been used by several investigators as indicator of response to environmental stress (Ram Nayan Singh, 2014; Sudhasaravanan and Binukumari, 2015; Neelima *et al.*, 2016; Adnan Amin *et al.*, 2017).

Exposure to sub-lethal concentrations of toxicant is reported to increase respiratory activity, leading to increased ventilation and hence increased uptake of the toxicant. The comparative data of the whole animal oxygen consumption in control and experimental fish, *Catla catla* calculated per gram body weight per hour in sub-lethal and lethal concentrations of flubendiamide for 24, 48, and 96 hrs and 8 days were given in the Tables 2 and 3 and graphically represented in Figures 2 and 3.

The results of the experimental and control fish values are graphically represented in Figures 2 and 3 by taking hours of exposure on X axis and the amount of oxygen consumed per gram body weight per hour on Y axis. In sub-lethal concentrations of flubendiamide, it was observed that the fish showed increase in oxygen consumption during the initial time of exposure i.e., 0-6 hours in 24 and 48 hrs treated fish and 0-4 hours in 96 hrs and 8 days exposed fish and thereafter a gradual decrease was observed in the subsequent periods of exposure. The

Table. 1. Calculated LC_{50} values of flubendiamide to the fish *Catla catla* under static exposure for 24, 48, 72 and 96 hrs

S. No.	Test Fish	Exposure period	Concentration in mg/L	Log Conc.	No. of fish exposed	Percent mortality	Probit Mortality	LC_{50} Value
1	*Catla catla*	24 h	3.20	0.51	10	20	4.16	3.566
2			3.40	0.53	10	30	4.48	
3			3.60	0.56	10	60	5.25	
4			3.80	0.58	10	70	5.52	
5			4.00	0.60	10	80	5.84	
6		48 h	3.00	0.48	10	20	4.16	3.456
7			3.20	0.51	10	30	4.48	
8			3.40	0.53	10	50	5.00	
9			3.60	0.56	10	60	5.25	
10			3.80	0.58	10	70	5.52	
11		72 h	2.80	0.45	10	10	3.72	3.221
12			3.00	0.48	10	30	4.48	
13			3.20	0.51	10	50	5.00	
14			3.40	0.53	10	70	5.52	
15			3.60	0.56	10	80	5.84	
16		96 h	2.60	0.41	10	20	4.16	2.892
17			2.80	0.45	10	40	4.75	
18			3.00	0.48	10	60	5.25	
19			3.20	0.51	10	80	5.84	
20			3.40	0.53	10	90	6.28	

Table 2. Changes in oxygen consumption of the fish *Catla catla* under exposure to lethal and sub-lethal concentrations of flubendiamide for 24 and 48 hrs.

Hours	Control	24 Sub-lethal	24 Lethal	48 Sub-lethal	48 Lethal
0	0.795±0.0032	0.886±0.0038	0.874±0.0042	0.83±0.0040	0.846±0.0026
2	0.781±0.0045	1.436±0.0036	1.482±0.0046	1.428±0.0038	1.576±0.0048
4	0.770±0.0035	1.424±0.0042	1.454±0.0042	1.454±0.0042	1.592±0.0042
6	0.761±0.0041	1.406±0.0044	1.436±0.0040	1.474±0.0046	1.602±0.0044
8	0.754±0.0045	0.988±0.0044	0.922±0.0046	0.988±0.0046	0.932±0.0042
10	0.742±0.0043	0.83±0.0036	0.864±0.0044	0.892±0.0038	0.856±0.0038
12	0.736±0.0040	0.678±0.0040	0.688±0.0046	0.658±0.0036	0.626±0.0042
14	0.734±0.0044	0.548±0.0038	0.444±0.0038	0.454±0.0038	0.396±0.0038
16	0.732±0.0036	0.534±0.0036	0.42±0.0040	0.436±0.0044	0.364±0.0044
18	0.730±0.0042	0.515±0.0042	0.398±0.0042	0.388±0.0044	0.326±0.0046
20	0.725±0.0034	0.488±0.0034	0.378±0.0034	0.368±0.0046	0.292±0.0036
22	0.720±0.0044	0.466±0.0044	0.356±0.0044	0.356±0.0044	0.266±0.0044

Results are mean values of four observations
Standard Deviation is indicated as (±)
Values are significant at $p < 0.05$

Table 3. Changes in oxygen consumption of the fish *Catla catla* under exposure to lethal and sub-lethal concentrations of flubendiamide for 96 hrs and only for sub-lethal concentration for 8 days.

Hours	Control	96 h Sub -lethal	96 Lethal	8 d Sub-lethal
0	0.757±0.0032	0.829±0.0048	0.846±0.0026	0.456±0.0040
2	0.782±0.0046	0.846±0.0038	0.788±0.0046	0.460±0.0038
4	0.770±0.0035	0.857±0.0049	0.850±0.0042	0.388±0.0042
6	0.761±0.0041	0.634±0.0046	0.606±0.0040	0.407±0.0046
8	0.753±0.0046	0.784±0.0048	0.726±0.0046	0.394±0.0046
10	0.741±0.0044	0.594±0.0036	0.556±0.0034	0.386±0.0038
12	0.736±0.0042	0.564±0.0040	0.526±0.0036	0.401±0.0036
14	0.735±0.0045	0.456±0.0038	0.398±0.0038	0.378±0.0038
16	0.733±0.0034	0.439±0.0046	0.366±0.0040	0.356±0.0044
18	0.730±0.0042	0.288±0.0042	0.284±0.0042	0.309±0.0044
20	0.725±0.0034	0.266±0.0046	0.290±0.0034	0.298±0.0046
22	0.719±0.0044	0.256±0.0044	0.256±0.0044	0.276±0.0044

Results are mean values of four observations
Standard Deviation is indicated as (±)
Values are significant at $p < 0.05$

presence of sub-lethal concentration of toxicant is aquatic environment is inevitable. The toxicant stress on oxygen consumption along with depletion in oxygen in aquaculture practices makes fish less fit and reduces their growth due to lack of proper metabolism (Hyma Ranjani, 2015 and Bantu *et al*., 2017). In lethal concentrations of flubendiamide, it was observed that a gradual increase in oxygen consumption during the initial time of exposure i.e., 0 to 6 hours in 24 and 48 hrs treated fish and 0 to 4 hours in 96 hrs and 8 days exposed fish and a gradual decline is observed during the later periods of exposure. In control fish the rate of oxygen consumption gradually decreased and this might be due to starved conditions and the reduced metabolic rates of the starved fish (Anitha, 2015). From the present study it is clear that the flubendiamide affected oxygen consumption of *Catla catla* under all hours of exposure in both sub-lethal and lethal concentrations.

Discussion

Several authors have reported the effect of Rynoid pesticides on the oxygen consumption in fish. Mariya Dasu (2014) observed initial increase in oxy-

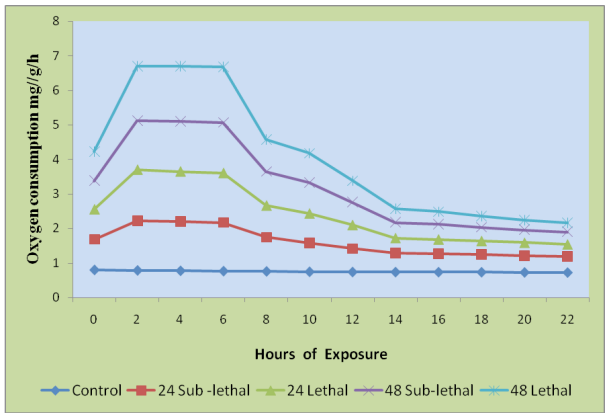


Fig. 2. Changes in oxygen consumption of the fish *Catla catla* under exposure to lethal and sub-lethal concentrations of flubendiamide for 24 and 48 hrs.

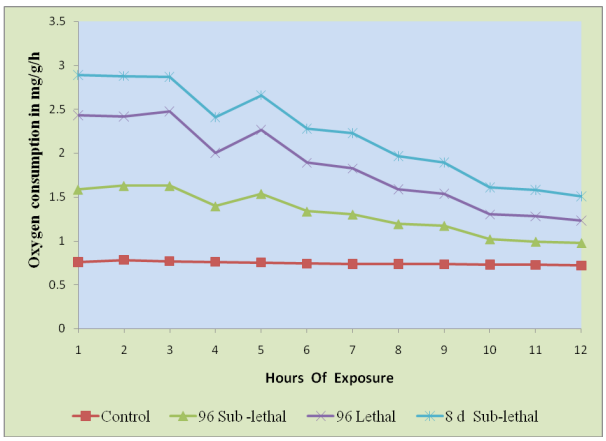


Fig. 3. Changes in oxygen consumption of the fish *Catla catla* under exposure to lethal and sub-lethal concentrations of flubendiamide for 96 hrs and sub-lethal concentration for 8 days.

gen consumption in *Labeo rohita* exposed to Thiocarb. Anitha (2015) also observed increase in oxygen consumption during the initial time of exposures, i.e. 1 to 6 hours and a gradual decrease was observed during the subsequent period of study in *Labeo rohita* exposed to Pyraclostrobin. In lethal concentrations the rate of oxygen consumption showed a decreasing trend from the beginning to the end. Bantu *et al.*, (2017) observed increase in oxygen consumption during the initial time of exposures i.e., 1 to 4 hours and a gradual decrease during the subsequent period in *Labeo rohita* exposed to sublethal concentrations of Indoxacarb for 24 hrs and 8 days. Oxygen consumption decreased in *Labeo* during exposure to lethal concentrations of indoxacarb for 24 hrs.

The initial increase in oxygen consumption in the present study is in agreement with Neelima *et al.*, (2016) in *Cyprinus carpio* exposed to cypermethrin. Jothinarendiran (2012) in *Channa punctatus* exposed to dimethoate, Bantu *et al.*, (2017) in *Labeo rohita* exposed Indoxacarb, Tilak and Vijaya Kumar (2009) in *Channa punctatus* exposed to Quinaphos, Veeraiah (2001) in *Labeo rohita* exposed to Cypermethrin, Hyma Ranjani (2015) in *Catla catla* exposed to Glyphosate. The present work coincides with the reports of the same. The initial increase in oxygen uptake in sub-lethal concentration might be the reflection of an augmented physiological activity for elimination acting the chemical stress (Tilak and Vijaya kumar, 2009). Due to stress, muscular activity increases which results in an increased demand for oxygen. The increase in activity might boost up oxidative metabolism which results in increased supply of energy to combat the chemical stress (David *et al.*, 2003). Sree Veni and Veeraiah (2014) reported that due to stress there is increased respiratory activity resulting in increased ventilation and increased uptake of the toxicant in *Cirrhinus mrigala* exposed to cypermethrin. Several authors (Veenethkumar and David, 2008; Shereena *et al.*, 2009; Logaswamy and Remia, 2009) reported that alteration in whole animal oxygen consumption is due to the disturbance in oxidative metabolism in different species of fish exposed to pesticides. During the initial hours of exposure elevation in the rate of respiration could be explained in terms of acceleration of oxidative metabolism, as a result of sudden response to the toxic stimulus of the pesticide. With the onset of symptoms of poisoning, probably due to acclimatization to the chemical environment the rate decreased in the later periods of exposure. Similar observations were also made by Neelima *et al.* (2016) and Jothinarendiran (2012). Vani *et al.* (2020) also reported that their is an initial increase in oxygen consumption of fish *Cirrhinus mrigala* (Hamilton) with the effect of carbamate Cartap hydrochloride (50% SP) and gradually decreased. The results of the present study agree with above findings.

As the pesticides stimulate the peripheral nervous system, the activity of fish increases which requires more oxygen to fulfill the energy demand. This could be the reason for initial elevation in the rate of oxygen consumption (Rao, 1989). In sub lethal medium, in the subsequent period of exposure the respiration rate of fish decreased which might be

due to acclimatization of the fish in the chemical environment (Rao, 1989 and Neelima *et al.,* 2016). Under toxic conditions, the oxygen in take decreases and a number of poisons become more toxic, so the amount of poison being exposed to the animal also increases. Fish breath more rapidly and the amplitude of respiratory movements will increase (Vakita Venkata Rathnamma and Nagaraju Bantu, 2014). By triggering the process of detoxification, the fish might have overcome the pesticide toxicity. In the later period the decrease in oxygen consumption appears to be a protective measure to ensure that there is low intake of the toxic substances which agrees with the findings of Tilak and Vijaya Kumar (2009). Subsequent decrease in oxygen consumption may be due to increased entry of flubendiamide molecules or their accumulation in the body of fish as a function of time. In sub-lethal concentrations of the flubendiamide the decrease in oxygen consumption appears to be mainly due to lowering down of energy requirements which can be considered as adaptive and even strategic this is in accordance with findings of Tilak and Vardhan, (2002). Depletion in the oxygen consumption is due to disorganization of the respiratory action caused by rupture in the respiratory epithelium of the gill tissue and also secretion of mucus over the gill curtails the diffusion of oxygen (Neelima *et al*., 2016).

Decreased oxygen consumption was observed by Maharajan *et al.,* (2013) in *Catla catla* exposed to Profenofos, by Vakita Venkata Rathnamma and Nagaraju Bantu (2014) in *Labeo rohita* exposed to Chlorantraniliprole, by Jipsa *et al.,* (2014) in *Tilapia mossambica* exposed to Cypermethrin, by Anthony Reddy (2015) in *Labeo rohita* exposed to Spinosad. Joshi and Kulkarni (2007) reported that *Garra mullya* (Skyes) when exposed to Cypermethrin and Fenvalerate, oxygen consumption increased in the initial period in both lethal and sub lethal concentrations and thereafter decreased. They concluded that alteration in oxygen consumption increased and later decreased which is a bio-indicator for assessing the pesticide toxicity, which can be correlated with the present study.

Mucus secretion in fish forms a barrier between the body irritating effects, or to eliminate it through epidermal mucus. Similar observations were made by Rao *et al*. (2003) and Parma De Croux *et al.* (2002) in *Prochilodus lineatus* under monocrotophos stress. Opercular movements increased initially in all exposure periods but decreased later steadily in lethal compared to sub lethal exposure periods. The increased opercular gill movements observed initially may possibly compensate for increased physiological activity under stressful conditions (Shivakumar and David, 2004). Gulping of air at the surface, swimming on the water surface, disrupted shoaling behaviour and easy predation was seen on the first day itself in lethal and sub-lethal exposure periods and continued the same more intensely, which is in accordance with the observations made by Ural and Simsek (2006). Gulping of air may help to avoid contact with the toxic medium. Surfacing phenomenon i.e., significant preference of upper layers the exposure period (Katja *et al.,* 2005). Finally fish sank to the bottom with the least opercular movements and died with their mouths open.

Under sub-lethal exposure, the fish bodies became lean towards the abdomen position compared to the control fish and they were found to be under stress, but this was not fatal. Leanness in fish indicates a reduced amount of dietary protein consumed by the fish under pesticide stress which is immediately utilized and not stored as body mass (Kalavathy *et al.,* 2001).

From the above results and discussion, it can be concluded that decrease in oxygen consumption in fish in response to the toxic stress is the cumulative effect of several stages at which the toxicant act. From the results obtained, it is clearly evident that flubendiamide affect the oxygen consumption of *Catla catla* in all exposed concentrations.

Conclusion

In conclusion, the analysis of data from the present investigation demonstrated that flubendiamide had a profound impact on respiration in *Catla catla* in both sub-lethal and lethal concentrations. Variation in the oxygen consumption in flubendiamide exposed fish was probably due to impaired oxidative metabolism and pesticide induced stress. Changes in gill architecture under flubendiamide stress would alter the diffusing capacity of gill with consequent hypoxic or anoxic conditions thus respiration may become a problematic task for the fish. These results suggest that the altered rates of respiration in *Catla catla* may also serve as a rapid biological monitor to assess the impact of pesticides such as flubendiamide on other biotic communities in the water body. This study also stresses the diligent use of pesticides to prevent environmental pollution.

Acknowledgements

The authors are thankful to the UGC for extending the infrastructure facilities to carry out the present work in the laboratories of the Dept. of Zoology & Aquaculture under UGC SAP DRS Phase-III and also thankful to the Head, Department of Zoology and Aquaculture for permitting to do the work.

References

Adnan Amin, Ramachandra Naik, A.T., Nilma Priyadarshini, Harsha Nayak and Sruthi Sree, C. 2017. Toxic effect of heavy metal lead on oxygen consumption of rohu (*Labeo rohita*) fingerlings. *Biochem. Cell. Arc,*. 17(1) : 225-228.

Aktar, W., Sengupta, D. and Chowdhury, A. 2009. Impact of pesticides use in agriculture their benefits and hazards. Interdiscip. *Toxicol.* 2 : 1-12.

Anon, 1975. Committee on methods of toxicity tests with fish macro invertebrates and amphibians. *EPA, Oregon.* 61.

Anitha, A. 2015. *Pyraclostrobin (20% WG) induced toxicity and biochemical aspects of freshwater fish Labeo rohita* (Hamilton). *Ph.D. Thesis,* submitted to Acharya Nagarjuna University. Nagarjuna Nagar, Guntur, A.P, India.

Anthony Reddy, P. 2015. *Impact of Spinosad (45% SC, Tracer) a biopesticide compound on freshwater fish, Labeo rohita* (Hamilton) *Ph.D. Thesis*, submitted to Acharya Nagarjuna University, Nagarjuna Nagar, Guntur, A.P, India.

Bantu, N., Hagos, Z. and Krishna, C., Gopla Krishnan; Abaynew; Rathnamma and Ravibabu. 2017. Acute toxicity and respiratory responses in freshwater fish, *Labeo rohita* exposed to an agrochemical Indoxacarb. *Algerian Journal of Environmental Science and Technology.* 3(3-B) : 595-603.

David, M., Shivakumar, H.B., Shivakumar, R. Mushigeri, S.B. and Ganti, B.H. 2003. Toxicity evaluation of cypermethrin and its effect on oxygen consumption of the freshwater fish , *Tilapia mossambica. Indian J. of Environ. Toxicol.* 13 : 99-102.

Fisher, R.A. 1950. *Statistical Methods for Research Workers.* 11th edition, Edinburgh UK: Oliver and Boyd Ltd.

Forget, G. 1993. Balancing the need for pesticides with the risk to human health. In: *Impact of Pesticide Use on Health in Developing Countries* (eds. Forget G, Goodman T and De Villiers A.): 2-16. IDRC, Ottawa.

Ganeshwade, R.M. 2012. Histopathological changes in the gills of *Puntius Ticto* (Ham) under dimethoate toxicity. *The Bio Scan.* 7(3) : 423–426.

Golterman, H. and Clymo. 1969. Methods for Chemical Analysis of Fresh Water. *Black well Scientific Publication.* 166.

Hyma Ranjani, G. 2015. *Glyphosate (Glycil 41% SL) a systemic herbicide impact on biochemical and histopathological changes in the freshwater fish Catla catla* (Hamilton). *Ph.D Thesis,* submitted to Acharya Nagarjuna University. Nagarjuna Nagar, Guntur, A.P, India.

Igbedioh, S.O. 1991. Effects of agricultural pesticides on humans, animals and higher plants in developing countries. Arch. *Environ. Hlth.* 46 : 218-224.

Jabeen, F., Chaudhry, A.S., Manzoor, S. and Shaheen, T. 2016. Carbamates and neonicotenoids in fish, water and sediments from the Indus River for potential health risks. *Environ. Monit. Assess.* 187 (2): 29.

Jipsa, J.R., Kalavathi, R., Dhanya, P.Y., and Logaswamy, S. 2014. Studies on the impact of a Cypermethrin insecticide on oxygen consumption and certain biochemical constituents of a fish *Tilapia mossambica*. *International Journal of Fisheries and Aquatic Studies.* 1(5) : 93-97.

Job, S.V. 1955. The oxygen consumption of *Salvelinus fontinalis*. *Univ. Toronto Biol. Ser*. No. 61; Ont. Fish. Res. Lab. Publ. 73 : 1-39.

Joshi, P.P. and Kulkarni, G.K. 2007. Change in the oxygen consumption of a freshwater fish *Garra mulya* (Sykes) exposed to cypermethrin and fenvalerate. *Himalayan J. Environ. Zool*. 21(1): 7–13.

Jothinarendiran, N. 2012. Effect of dimethoate pesticide on oxygen consumption and gill histology of the fish, *Channa punctatus* (Hamilton). *Current Biotica*. 5 (4) : 500-507.

Kalavathy, K., Siva Kumar, A.A. and Chandran, R. 2001. Toxic effect of the pesticide Dimethoate on the fish *Sarotherodon mossambicus*. *J. Ecol. Res. Bioconserv.* 2(1-2): 27-32.

Katja, S., Georg, B.O.S., Stephan, P. and Christian, E.W.S. 2005. Impact of PCB mixture (Aroclor 1254) and TBT and a mixture of both on swimming behavior, body growth and enzymatic biotransformation activities (GST) of young carp ,*Cyprinus carpio*. *Aqua. Toxicol*. 71: 49-59.

Logaswamy, S. and Remia. K.M. 2009. Impact of Cypermethrin and Ekalux on respiratory and some biochemical activities of a freshwater fish. *Tilapia Mossambica*. *Current Biotica*. 3 : 65-73.

Maharajan, A., Usha, R., Paru Ruckmani, P.S., Vijaykumar, B.S., Ganapiriya, V. and Kumarasamy, P. 2013. Sublethal effect of Profenofos on oxygen consumption and gill histopathology of the Indian major carp, *Catla catla* (Hamilton). *Int. J. Pure Appl. Zool.* 1 (1) : 196-204.

Mariya Dasu, P. 2014. *Thiodicarb 75 percentage wp a carbamate insecticide induced toxicity biochemical and histopathological changes in the freshwater Indian major carp Labeo rohita* (Hamilton). *Ph.D Thesis*, submitted to Acharya Nagarjuna University, Nagarjuna Nagar, Guntur, A.P, India.

Neelima, P., Gopala Rao, N., Srinivasa Rao, G. and Chandra Sekhara Rao, J. 2016. A study on oxygen consumption in a freshwater fish *Cyprinus carpio* exposed to lethal and sublethal concentrations of cypermethrin (25% EC). *Int. J. Curr. Microbiol. App. Sci.* 5 (4) : 338-346.

Parma de Croux, M.J., Loteste, A. and Cazenave, J. 2002. Inhibition of plasma cholinesterase and acute toxicity of monocrotophos in Neotropical fish, *Prochilodus lineatus* (Pisces, Curimatidae). *Bull. Environ. Contam. Toxicol.* 69 : 356-362.

Ram Nayan Singh. 2014. Effects of Dimethoate (EC 30%) on Gill Morphology, Oxygen Consumption and Serum Electrolyte Levels of Common Carp, *Cyprinus Carpio* (Linn). *International Journal of Scientific Research in Environmental Sciences*. 2(6) : 192-198.

Rao, D.M.R. 1989. Studies on the relative toxicity of Endosulphan to the Indian major carp *Catla catla* with special reference to some biochemical changes induced by the pesticide. *Pest. Biol. Phy*. 33 : 220-229.

Rao, J.V. 2003. Rani, C.H.S., Kavitha, P., Rao, R.N. and Madhavendra, S.S.Toxicity of chlorpyrifos to the fish, *Oreochromis mossambicus*. *Bull. Environ. Contam. Toxicol.* 70 : 985-992.

Sree Veni, S.M. and Veeraiah, K. 2014. Effect of Cypermethrin (10%EC) on Oxygen Consumption and Histopathology of Freshwater Fish *Cirrhinus mrigala* (Hamilton). *IOSR J. Environ. Sci., Toxicol. Food Technol.* 8(10): 12–20.

Srivastava, P. and Singh, A .2014. Fate of fungicides on fish, *Clarias batrachus*- a complete study. *LAP LAMBERT Academic Publishing*, Germany. 134 p

Shereena, K.M., Logaswamy, S. and Sunitha, P. 2009. Effect of an organo phosphorous pesticides (Dimethoate) on oxygen consumption of the fish *Tilapia Mossambica*. *Recent Res. Sci. Technol*. 1: 4-7.

Shivakumar, R. and David, M. 2004. Toxicity of endosulfan to the freshwater fish, *Cyprinus carpio*. *Indian J. Ecol*. 31 : 27–29.

Subramani Lavanya, Mathan Ramesh, Chokkalingam Kavitha, and Annamalai Malarvizhi, 2011. Haematological, biochemical and ion regulatory responses of Indian major carp *Catla catla* during chronic sub-lethal exposure to inorganic arsenic. *Chemosphere*. 82 : 977-985.

Sudhasaravanan, R. and Binukumari, S. 2015. Effects of different concentartions of detergent on dissolved oxygen consumption in *Lepidocephalichythyes thermalis*. *World Journal of Pharmaceutical Research*. (2): 940-945.

Tilak, K.S. and Vardhan, S.K. 2002. Effect of fenvalerate on oxygen consumption and haematological parameters in the fish. *Channa punctatus* (Bloch). *J. Aquatic Biol*. 17 : 81–86.

Tilak, K. S., Veeraiah, K., Bhaskara Thathaji, P. and Butchiram, M. S. 2007. Toxicity studies of butachlor to the freshwater fish *Channa punctatus* (Bloch). *Journal of Environmental Biology*. 28 (2) : 485-487.

Tilak, K. S. and Vijaya Kumar, M. 2009. Effect of Quinaphos technical grade and commercial grade (25%EC) formulations on oxygen consumption in freshwater fish *Channa punctatus* (Bloch). *ANU Journal of Natural Sciences*. 39-45.

Ural, M. S. and Simsek, K. S. 2006. Acute toxicity of dichlorvos on fingerling of European catfish, *Silurus glanis*. *Bulletin of Environmental Contamination and Toxicology*. 76 : 871-876.

Vakita Venkata Rathnamma and Nagaraju Bantu, 2014. The effect of Chlorantraniliprole on the oxygen consumption of the freshwater fish *Labeo rohita* (Hamilton). *Frontiers of Biological and Life Sciences*. 5-7.

Vani, G., Veeraiah, K., Vijaya Kumar, M. and Parveen, S.K. 2020. Effect of Cartap hydrochloride (50%) on oxygen consumption of freshwater, *Cirrhinus mrigala*. (Hamilton). *Poll. Res.* 39 (2) : 368-372.

Veeraiah, K. and Durga Prasad, M. K. 2001. Studies on ventilatory patterns of fish under normal and stressed conditions using indigenously designed electronic recording instrument. *Proc. Intern. Conf. ICIPACT* -2001.

Vineetkumar, K. Patil and David, M. 2008. Behavior and respiratory dysfunction as an index of Malathion toxicity in the freshwater fish *Labeo rohita*. (Hamilton). *Turkish Journal of Fisheries and Aquatic Sciences.* 8 : 233-237.

Journal of Molecular Structure 1243 (2021) 130784

Contents lists available at ScienceDirect

Journal of Molecular Structure

journal homepage: www.elsevier.com/locate/molstr

Luminescence investigations on Dy^{3+} doped CdO-PbF_2 phosphate glass-ceramics

Ch. Nageswara Rao[a,g], P. Vasudeva Rao[a,g], R. Kameswari[b], R. Ramesh Raju[c], G. Chandana[d], K. Samatha[d], M.V.V.K. Srinivas Prasad[e], M. Venkateswarlu[e], A. Naveen[e,f], G.G. Dhar[g,*]

[a] Department of Physics, Acharya Nagarjuna University, Guntur, A.P., India
[b] Department of Physics, SRR & CVR Government Degree college (Autonomous), Vijayawada, A.P., India
[c] Department of Chemistry, Acharya Nagarjuna University, Guntur, A.P., India
[d] Department of Physics, Andhra University, Visakhapatnam, A.P., India
[e] Department of Physics, Koneru Lakshmaiah Education Foundation, Vaddeswaram, Guntur, A.P., India
[f] Department of Physics and Electronics, Chaitanya Deemed to be University, Hanamkonda, Telangana, India
[g] Department of Nanotechnology, Acharya Nagarjuna University, Guntur, A.P., India

ARTICLE INFO

Article history:
Received 18 December 2020
Revised 24 May 2021
Accepted 25 May 2021
Available online 31 May 2021

Keywords:
Phosphate glass
Glass ceramics
Nanocrystals
Luminescence

ABSTRACT

This paper reports the structural and photoluminescence investigations on Dy^{3+} doped transparent CdO-PbF_2 phosphate glass/glass ceramics with SrO. Upon heat treatment, the nanocrystals occurred in glass ceramics are spherical in shape in the sizes of 10nm to 20nm. The luminescence intensities were strongly dependent on nanocrystallinity and showing the same kinetics as efficient luminescent hosts. In the present host, well incorporation of Dy^{3+} ions in nanocrystals and low energy transfer to Dy^{3+} ions due to existence of other crystalline phases, both the mechanisms occurred. The consequent variations in luminescence intensities also observed.

© 2021 Elsevier B.V. All rights reserved.

1. Introduction

Search for new optical materials has always had considerable interest to cater to the requirements in telecommunication, solid-state lasers, optical amplifiers as well as up-conversion fibers [1]. Controlled nucleation and growth of crystalline phase cause the glass ceramic formation which has a polycrystalline structure [2]. These glass-ceramics are useful in many current applications like liquid crystal displays, photonic devices and solar concentrator cells [3]. In glass-ceramics, nanocrystals can enhance luminescence efficiency by conquering a decrease in absorption coefficient [4–8].

In recent years, many researchers are working on glass ceramics based on the glass transition temperatures to achieve both transparence and improvement in luminescence properties of rare-earth ions in glass ceramics [9–12]. Studies on Na_2O-CaF_2-P_2O_5 glasses/glass ceramics reported the dependence of optical properties on structural arrangement upon heat treatment in the glass network [13]. In glass ceramics, the formed nanocrystals will improve the local field around the rare-earth ions and result in an enhancement in absorption cross section and luminescent intensity [14–16]. Therefore, to understand the luminescence enhancement mechanism, a thorough study is required on the interactions between doped activators and formed nanocrystals in the glass ceramics.

Among Rare Earth(RE) ions, trivalent dysprosium (Dy^{+3}) is useful for white light emission in both glass and glass-ceramics [17–22]. Dy^{3+} ion shows intense emission bands at blue (at 486 nm, $^4F_{9/2} \rightarrow {}^6H_{15/2}$) and yellow (at 575 nm, $^4F_{9/2} \rightarrow {}^6H_{13/2}$) regions upon suitable excitation. Here, in the yellow region, $^4F_{9/2} \rightarrow {}^6H_{13/2}$ the transition of Dy^{3+} is hypersensitive and its intensity strongly depends on the host [23–25]. The transition $^4F_{9/2} \rightarrow {}^6H_{15/2}$ in the blue region is a magnetic dipole allowed transition and is less sensitive to the host matrix. Therefore, the intensity ratio of these transitions (Yellow/Blue) determines the generation of white light in the host matrix. Besides that, lead content in the glasses leads to high transparency and shows more stability over atmospheric moisture [26]. PbF_2 content in glasses can increase the refractive index and can be useful as a core material in optical fibers [27]. Rare-earth doped glasses with PbF_2 content reported high luminescence emission with large radiative transition probabilities. Further, a high refractive index leads to an increase in the local field on dopant ions [28–30]. Further, one of the effective ways to improve the chemical durability of phosphate glasses is the addition

* Corresponding author.
E-mail address: drggiridhar@rediffmail.com (G.G. Dhar).

https://doi.org/10.1016/j.molstruc.2021.130784
0022-2860/© 2021 Elsevier B.V. All rights reserved.

of various oxides to phosphate glasses. Here, SrO addition to the host improves the strength of the phosphate network by decreasing the non-bridging oxygens. Sr^{2+} has higher field strength than other alkali earth ions like Ca^{2+} and Mg^{2+} results an improvement in the glass network strength [31–34].

Previous reports on Dy^{3+} ions doped hosts for high performance white light generation explained through various aspects like concentration variation of activator, co-doped, tri-doped and energy transfer mechanisms [11,19,35–46]. Besides, activator behavior in the host, an additional structural information is also required in well establishment of luminescence efficiency. In view of that, we made an attempt in the present phosphate glass matrix.

The aim of the present study is to find out the growth of lead fluoride nanocrystals in Dy^{3+} doped cadmium phosphate glass upon heat treatment and their effect on structural, luminescence properties for a wide variety of lighting applications. Variations in luminescence intensities observed due to the existence of multiple nanocrystalline phases. Further, Glass-ceramics showed higher emission intensity over glass whereas GC5 (5h annealed) had a higher emission than all other glass and glass-ceramics.

2. Experimental

The basic composition of the present glass matrix (as-melted) used in this study was 49.5 P_2O_5 – 20 CdO – 25 PbF_2 -5 SrO – 0.5 Dy_2O_3. The raw materials used were obtained from Loba Chemicals pvt ltd in high purity. Glass was prepared by using the well known melt quenching technique. All the chemicals were mixed in a mortar and thoroughly grinded for 1 hour. The resultant mixture was taken into a porcelain crucible and kept in an electrical furnace at 200 °C for 1h to remove the excess gasses. This was further heated at 950 °C for 1.5h. At that stage, the mixture was in melt form and was poured on a pre heated brass plate, then immediately placed in high temperature furnace at 250 °C to overcome the cracks due to thermal strain. The resultant samples were cut and polished into the glass samples with a thickness of ~1.5 mm and was denoted as GS. To obtain glass ceramics, the samples were annealed at slightly above the glass transition (T_g) point 380 ± 5°C for a duration of 2h, 5h and 10h continuously and thereafter were cooled to room temperature. Attained samples were denoted as GC2, GC5 and GC10 respectively.

Physical properties of the current glasses were measured as per our previous reports [47] in different methods. Shimadzu DTG-60H was used for DTA (Differential Thermal Analysis) measurement. The sample was taken in powder form in aluminium crucible and experiment done at a rate of 10 °C/min in air. BRUKER FTIR spectrometer was used and recorded the FTIR spectra of KBr associated samples in the frequency range 400±1400 cm^{-1} at room temperature with 2 cm^{-1} resolution.

Thermo scientific spectrophotometer was used to study the emission and excitation properties. Lifetime measurements were carried out by using Edinburgh Instruments FLSP 920 system to study the decay mechanism. All the spectral recordings were done at room temperature only.

3. Results and discussion

3.1. TG-DTA analysis

Fig. 1 shows the differential thermal analysis curves for the CdO-PbF2 phosphate glass and glass-ceramics. From the DTA curves, both glass transition temperatures (T_g – 380 °C) and an exothermic peak or crystallization peak at temperatures (T_c – 470 °C) of the glass sample was estimated. The samples were annealed at slightly above the T_g as partial and controlled crystallization gives glass ceramic. At this point, one can get the glass ceramics with good mechanical stability due to less internal mechanical stress. This heat treatment was done for the duration of 2h, 5h and 10h continuously for resultant glass ceramic samples containing fluoride nanophase. A Small increase in both T_g and T_c takes

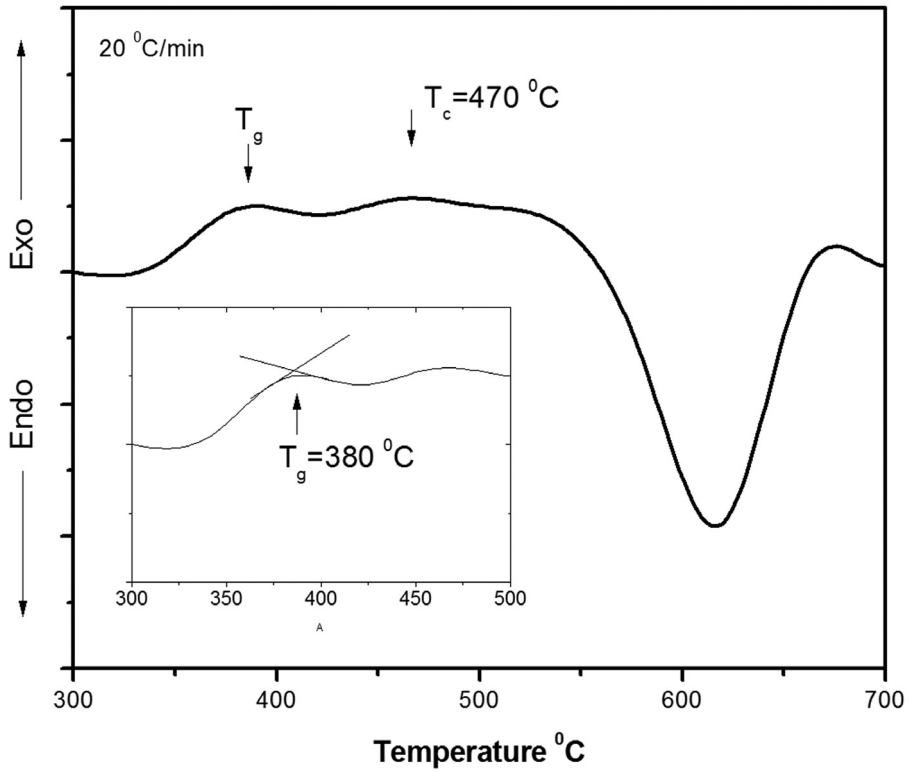


Fig. 1. T_g-DTA graph of GS sample

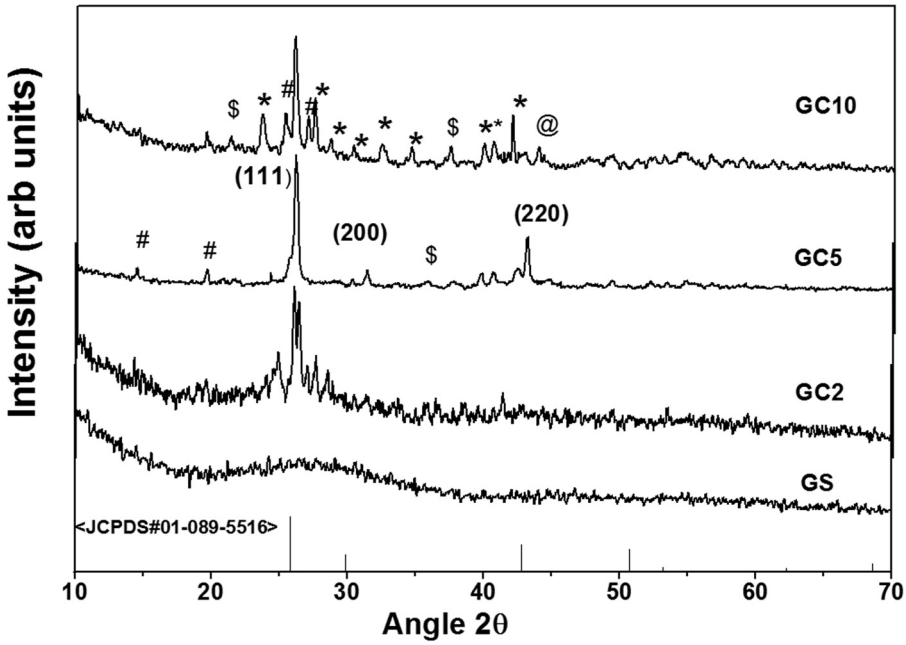


Fig. 2. XRD spectra of CdO-P2O5 glass and Glass Ceramics

place as annealing time increases from 2h to 10h. This is because of becoming strong network connectivity on heat treatment.

3.2. X-Ray diffraction studies

The X-ray diffraction (XRD) spectra of the cadmium phosphate glass and glass-ceramics (GS-GC10) have been recorded in the range of $10° \leq \theta \leq 80°$ to bring the proper understanding of the effect of heat treatment on structural evolution.

The resultant diffraction spectra did not show a sharp peak except for widespread scattering at low angles. This confirms the amorphous nature of the base glass. Glass ceramic samples (GC2, GC5 and GC10) are showing considerable peaks indicating the crystalline phases. Both glass and glass ceramics XRD spectra are shown in Fig. 2.

These diffraction peaks are matched with the standard powder diffraction data and reveal the formation of PbF_2 and metal phosphate crystals. Besides, existence of other phosphate phases and the enhancement in peak intensity was observed. Grain size was calculated by using Scherrer's formula,

$$D_{hkl} = \frac{k}{\beta cos\theta}$$

where D_{hkl} is the grain size at the vertical direction of (h k l), λ, θ and β are the wavelength of X-ray, angle of diffraction and the full-width half-maximum of the diffraction peak, respectively. Here the shape factor and/or proportionality constant is k = 0.90 as most of the grains are in spherical in shape. The evaluated average grain size is 25-38 nm. Further, upon increasing annealing time, the crystallization process is stabilized and nearly similar grain sizes observed in GC10 glass-ceramic. Other cadmium phosphate phases were raised as annealing time increased(*-$Cd_3(PO4)_2$ #-$Cd(PO_3)_2$ $-$Sr(PO_3)_2$ and @-$Cd_2P_6O_{17}$).

3.3. TEM analysis

Fig. 3 (a-GS; b- GC5 c-GC10) shows the transmission electron micrograph of GC10 sample only. No dark crystallites were observed in the glassy matrix to represent any kind of crystal nature. In case of 10 hours heat treated sample (c1 and c2), one can clearly distinguish dark crystallites and the light background of the glassy matrix, which resembles the homogeneous distribution of crystallites. These images are processed by Image J software and particle size estimated by using the formula

$$d_i = \sqrt{\frac{4}{\pi}A_i}$$

where Ai area of each particle, d_i an average diameter [48].

The crystallite size distribution of GC10 is shown in Fig. 4. 50 crystallites are analyzed and found that the mean diameter is (7.3 ± 0.1) nm, which shows a narrow crystallite size with polydispersity or the degree of non-uniformity, is only 2%. This is near and supports the calculated crystallite size from XRD spectra by using Scherrer's formula.

3.4. FTIR- analysis

Fourier Transform Infrared (FTIR) spectra of present CdO-PbF_2 phosphate glass and glass ceramics are shown in Fig. 5. P_2O_5 glass contains extended network of the [PO_4] tetrahedral; each tetrahedral shares three corners. The sharing will be through P-O-P linkage. Here the unshared oxygen ion has a double bond with phosphorous ion due to its pentavalence [49–51]. The vibrational bands depend on the concentration of network former. In the present glass system, the major building units are Q_2 and Q_3 because of higher P_2O_5 concentration. The remaining metal oxides can be positioned with phosphorus linkage.

FTIR spectra show nearly twelve bands as characteristics of the phosphorus–oxygen networks in the present glass and glass ceramics.

The asymmetric and symmetric stretching of O-P-O band is observed at ~ 1261 cm^{-1} and ~ 1058 cm^{-1}respectively. It indicates the formation of Q_2 phosphate tetrahedral long chain along with asymmetric stretching of P-O-P mode vibration observed at ~ 910 cm^{-1} [52–55].

The band at ~ 749 cm^{-1} is attributed to symmetric stretching of P-O-P groups [56]. The remaining bands observed in the range 600-400 cm^{-1} are P-O-P bending and P-O-P stretching modes [57,58]. Here one can observe the peak shifts with in this range

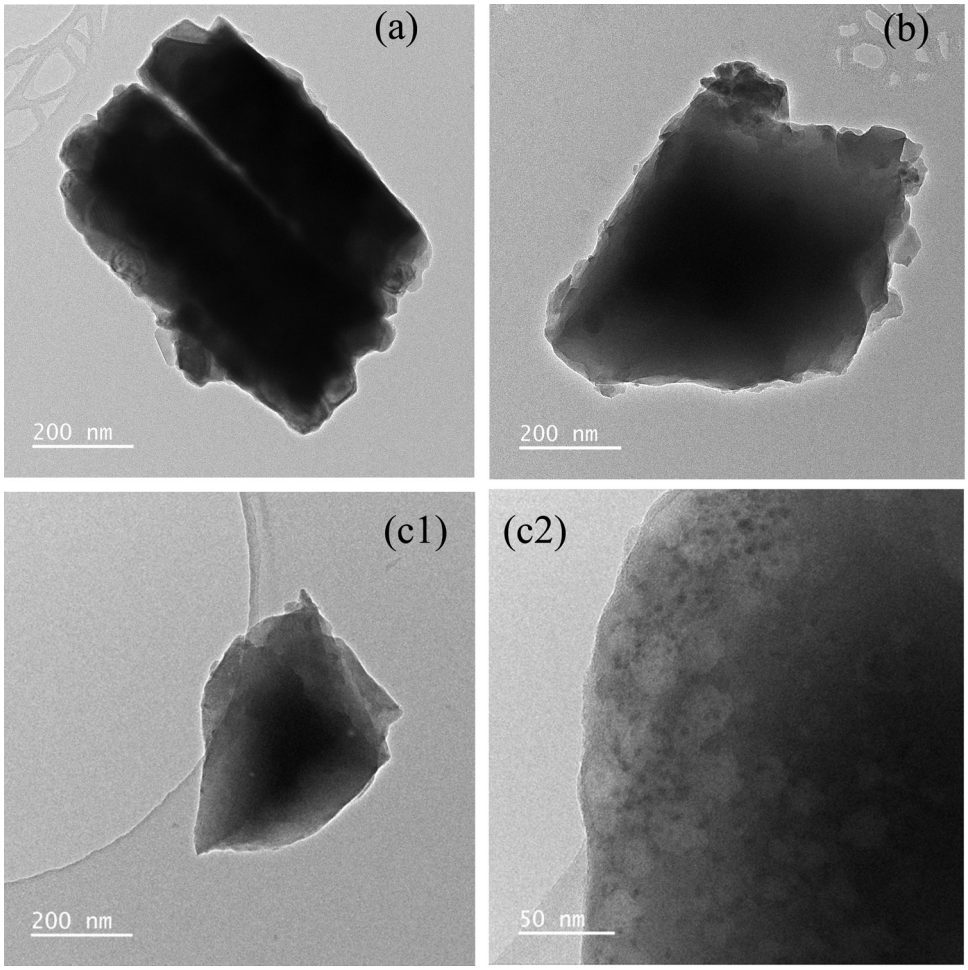


Fig. 3. TEM images of GC10

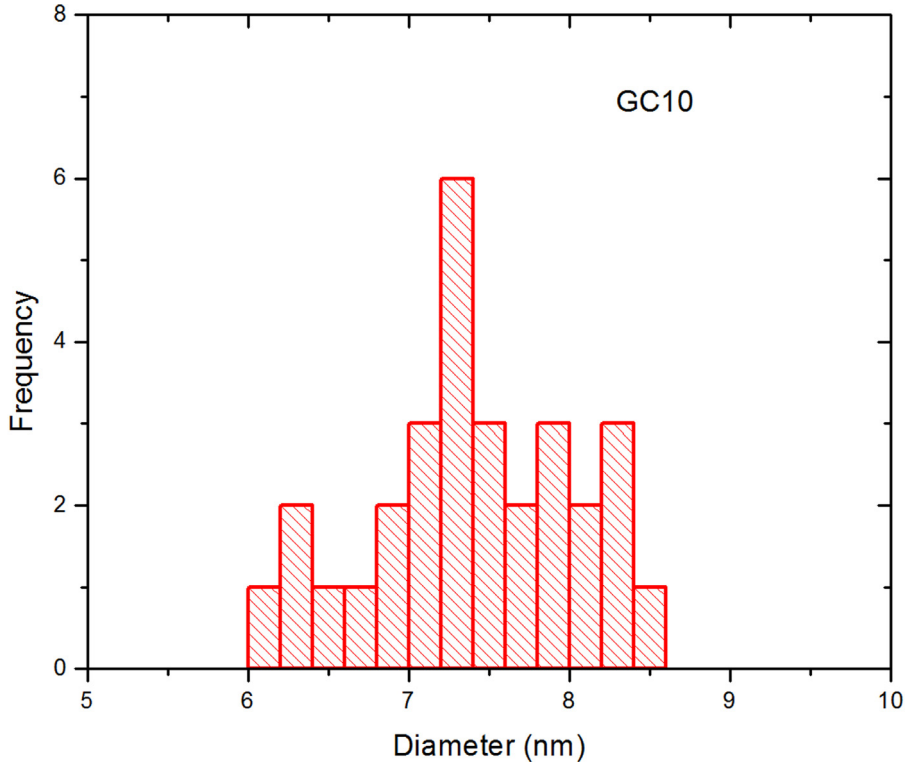


Fig. 4. Crystallite size distribution of GC10 sample (10h heat treated)

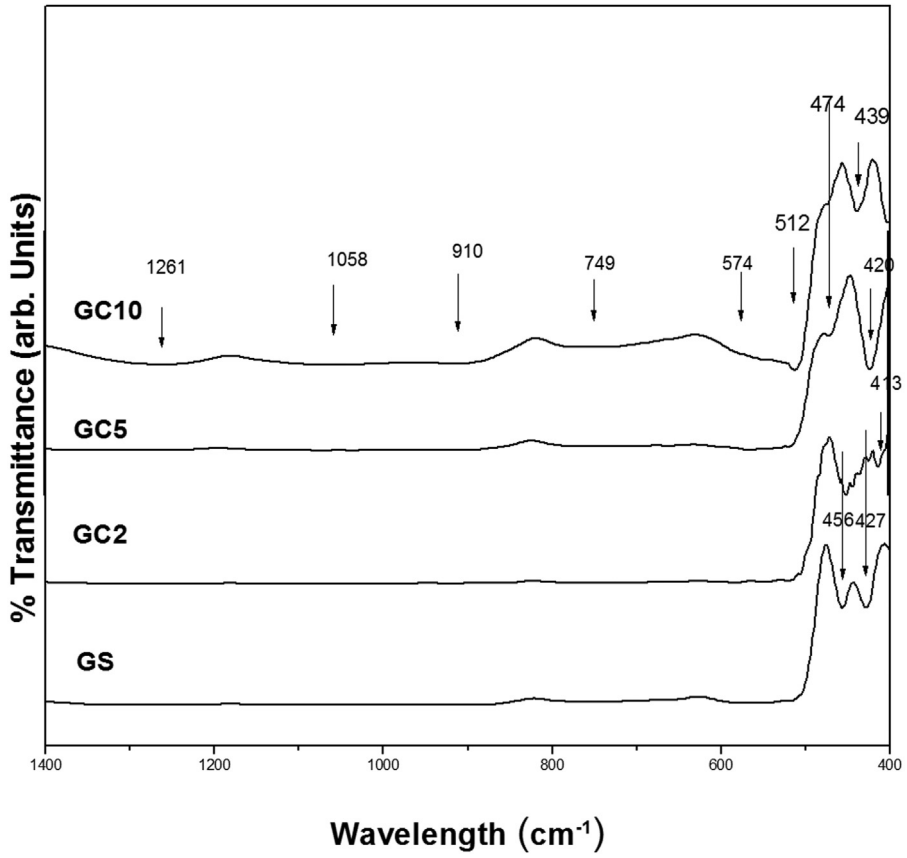


Fig. 5. FTIR spectra of Cadmium Phosphate glass and glass ceramics

when compared to glass (GS) with glass ceramics samples (GC2, GC5 and GC10). Because of the heat treatment, it is clear that prominent changes occurred in PO_4 structural units in terms of position, bandwidth and intensity. Therefore upon heat treatment, more other ions coupled with P-O bonds [59]. The existence of other crystalline phases in the heat treated samples evidenced that Cd-O-P or Sr-O-P type bonds formed in the structure. These structural changes are well connected with X-ray diffraction studies as it shows the other crystalline phases upon heat treatment.

3.5. Emission and excitation

Fig 6 (a,b) shows the excitation and emission spectra of the precursor glass and glass ceramic under respective emission and excitation wavelengths. In all the spectra, spectral shape look alike but in case of glass ceramics, the luminescence intensity is strong and higher in order than the base glass.

Fig 6a illustrates the excitation spectrum of GC10 glass ceramic in the range of 320–500 nm with λ_{em} = 574nm ($^4F_{9/2}\rightarrow{}^6H_{13/2}$ transition) recorded at room temperature. Nearly seven intense peaks were identified and assigned to the transitions from $^6H_{15/2}$ -the ground state to different excited states of Dy^{3+} ions. At 322 nm, 348 nm, 363nm, 385 nm, 424 nm, 451 nm and 472 nm bands were assigned to $^6H_{15/2}\rightarrow{}^4K_{15/2}+(^4D,^4G)_{5/2}$, $^6H_{15/2}\rightarrow{}^6P_{7/2}+(^4M,^4I)_{15/2}$, $^6H_{15/2}\rightarrow{}^6P_{5/2}+{}^4I_{11/2}$, $^6H_{15/2}\rightarrow{}^4M_{21/2}+{}^4K_{17/2}+{}^4M_{11/2}+(^4P,^4D)_{3/2}$, $^6H_{15/2}\rightarrow{}^4G_{11/2}+{}^4F_{7/2}+{}^4I_{13/2}$, $^6H_{15/2}\rightarrow{}^4I_{15/2}$ and $^6H_{15/2}\rightarrow{}^4F_{9/2}$ transitions respectively [12,60,61].

The emission spectra were recorded for present glass, glass ceramics with selected high intense excitation wavelength 348 nm in the spectral region 450–700 nm. The resultant spectra (shown in Fig 6b) reveals that the emitted peaks at 482 and 574 nm are very strong and at 663 nm is feeble and were assigned to $^4F_{9/2}\rightarrow{}^6H_{15/2}$ (blue) and $^4F_{9/2}\rightarrow{}^6H_{13/2}$ (yellow-hypersensitive) and $^4F_{9/2}\rightarrow{}^6H_{11/2}$ (red) transitions in visible region respectively.

Further, it is observed that emission intensities were varied upon heat treatment. To analyze the change in the intensities one can estimate the asymmetric intensity ratio (AIR) which is the ratio between the electric dipole and the magnetic dipole transitions. But in case of Dy^{3+} ions, estimation of the Yellow to Blue (Y/B) ratio is appropriate as relative fluorescence intensity and it is inversely proportional to local ion symmetry. That is the degree of distortion from the inversion symmetry of the local environment of Dy^{3+} in the lattice [39,62,63]. Therefore to estimate the Y/B ratio, the intense electric dipole transition (in yellow region- 574nm) and the magnetic dipole transitions (in blue region-472nm) were taken into account and the values are 1.08, 1.18, 1.05 and 1.22 for GS, GC2, GC5 and GC10 respectively. The variation in the intensity ratio values reflects the substitution of Dy^{3+}, in place of the element with same valence, minute variation; or in place of the element with different valence, considerable variation due to formation of defects in the host matrix. So, Y/B ratio is dependent on site asymmetry or environmental variations in the vicinity of the Dy^{3+} ion [18].

However, the yellow emission is more prominent than blue which suggests that there is no centre of symmetry around the Dy^{3+} ions due to the charge separation [64,65] in both the glass and glass ceramics. In GC10, higher the Y/B ratio may be due to higher degree of covalancy between Dy-O than others.

Here the change in Y/B ratio strongly influenced by the local environment of the rare earth ions. Therefore the varied values of Y/B ratio in glass ceramics than glass, clearly represents the structural

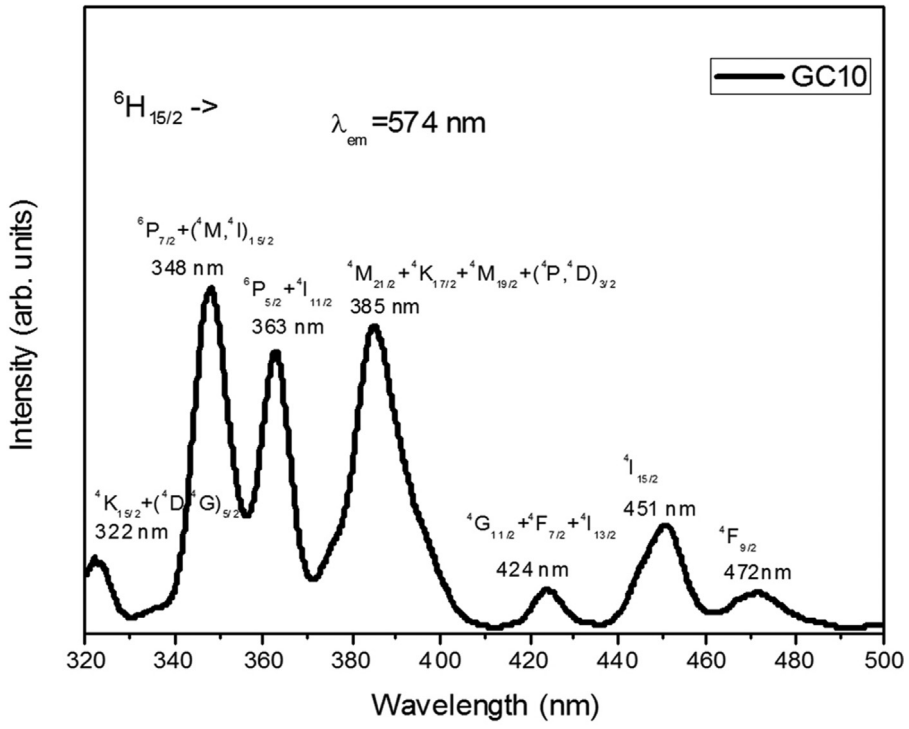


Fig. 6. a Excitation spectrum of GC10 sample. b Emission spectra of CdO-P2O5 glasses

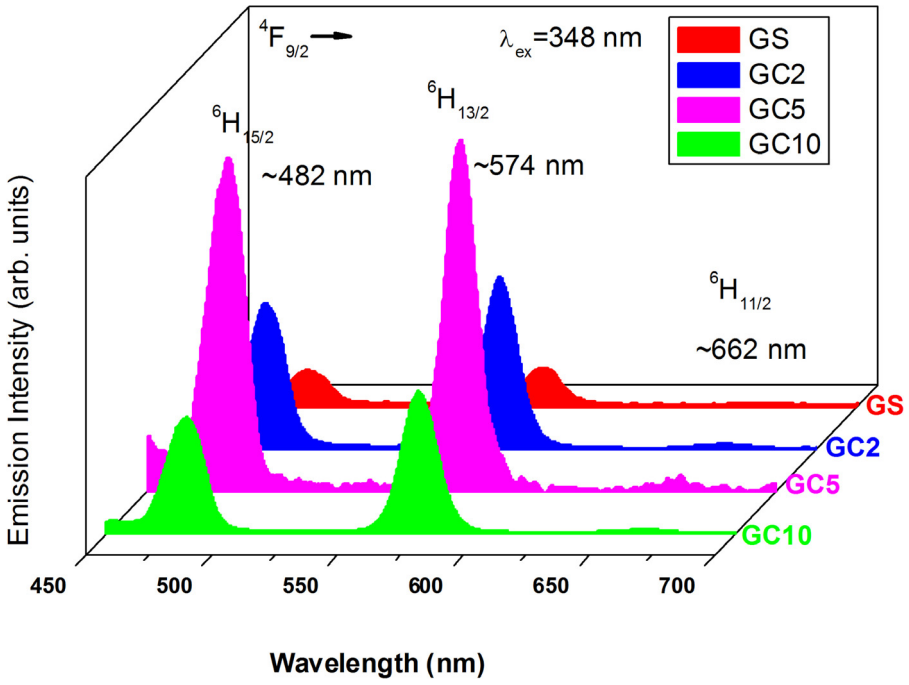


Fig. 6. Continued

changes as Dy^{3+} ions incorporated into PbF_2 nanocrystals. In other words changes in the local environment around the Dy^{3+} ions can control the white light emission.

The yellow band at 574 nm is more intense than the blue band (Fig. 4b), suggests that the Dy^{3+} ion is in lower symmetry local site [24]. Further, heat treatment gives enhancement in emission intensities in present glass ceramics under study from GC2 to GC5.

The GC5 shows 10 times more enhancement in emission intensity when compared untreated glass (GS glass). In addition, there was an increase in intensity from GS to GC5 as Dy^{3+} ions are well incorporated in PbF_2 nanocrystals; it is to note that the fluoride nanocrystals have low phonon energies than oxide. In case of GC10, intensity decreased. It suggests that, after 10h heat treatment, there are considerable structural changes in the host. In spite of the fact that Dy^{3+} ions are incorporated in PbF_2 nanocrystals, due to superimposition of other cadmium phases, excitation energy was fully not transferred to Dy^{3+} ions from PbF_2 crystallites [17,18].

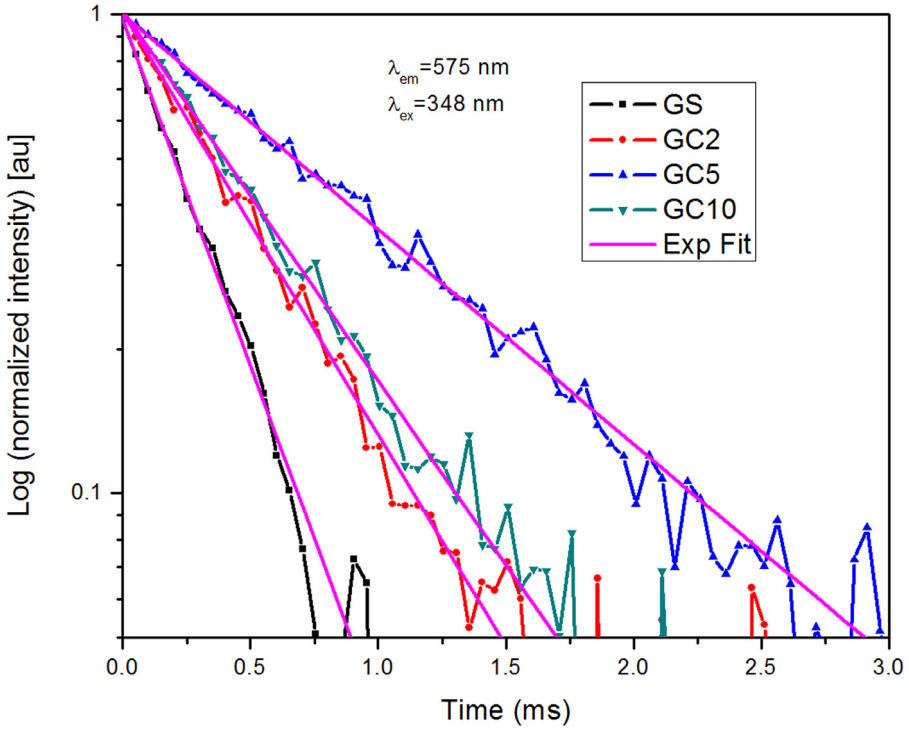


Fig. 7. Decay profiles of CdO-PbF_2 phosphate glass and Glass-Ceramics for $^4F_{9/2}$

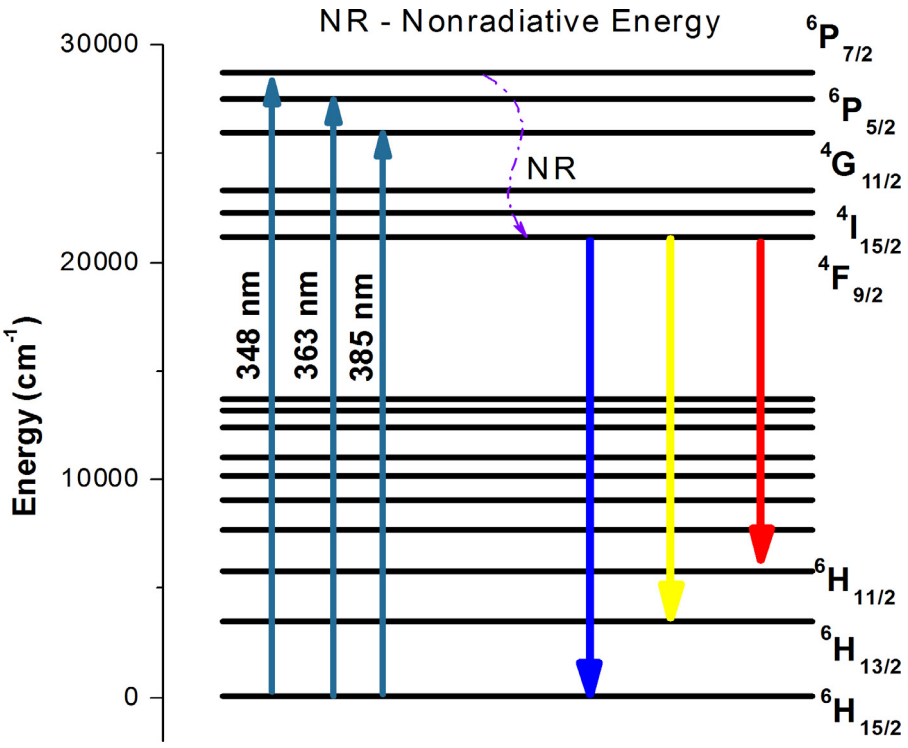


Fig. 8. Energy Level diagram representing excitation and emission mechanisms

The decay curves of CdO-PbF_2 phosphate glass and Glass-Ceramics doped with Dy^{3+} were measured and fitted by single exponential curves (Fig. 7). The measured lifetimes (in mille seconds) are 0.37 ms, 0.53 ms, 0.86 ms and 0.59 ms for GS, GC2, GC5 and GC10 respectively. An Energy level diagram for Dy^{3+} ions in the present glass host matrix is shown in Fig. 8. It illustrates the excitation and emission processes pertaining to radiative and non-radiative transitions in the present phosphate glasses.

Colorcalculator v.7.77 was used to analyze the experimental emission data of CdO-PbF2 phosphate glass, glass ceramics in terms of CIE 1931 (Commission Internationale de l'Eclairage) colour coordinates to characterize the colour rendering. The obtained values were presented in Table 1 with correlated color temperatures (CCT) values and shown in Fig. 9.

The coordinates were well placed in the white light region. The CCT values indicate that these materials were emitting cool white

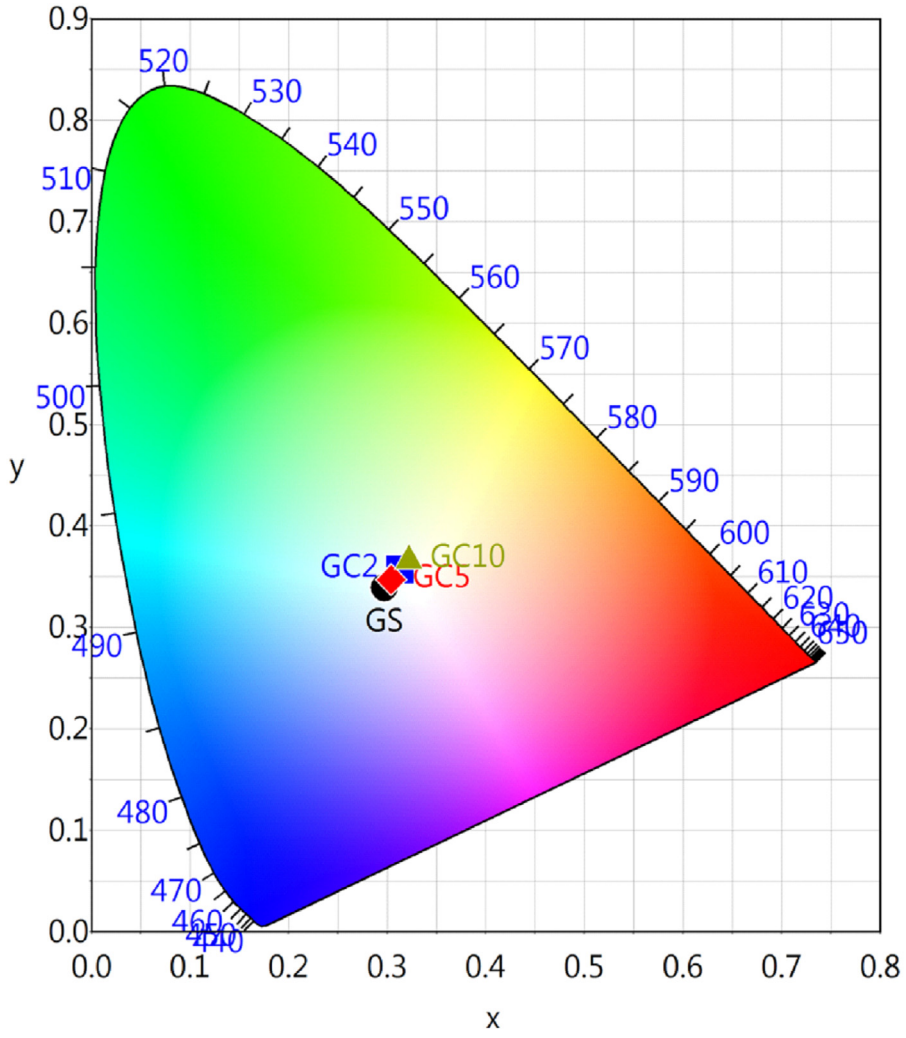


Fig. 9. CIE diagram for CdO-PbF2 phosphate glass and glass ceramics

Table 1
CIE co-ordinates and CCT values for CdO-PbF2 phosphate glass and glass ceramics

Glass/Glass Ceramic sample	x	y	CCT (K)
GS	0.297	0.339	7258
GC2	0.313	0.357	6317
GC5	0.304	0.347	6805
GC10	0.322	0.367	5908

light and can be useful for security lights, offices and/or retail locations. Therefore, these prepared glass and glass ceramics with PbF_2 nanocrystals are efficient and useful to cater the needs of efficient white light generating device applications.

4. Conclusion

CdO-PbF_2 phosphate glass, glass-ceramics doped with Dy^{3+} ion were prepared by using most familiar melt quenching method. Glass transition temperature was obtained from DTA measurement. At slightly above (+5 °C) the T_g, samples were annealed and obtained glass ceramics. Structural information was confirmed as polycrystalline from X-Ray diffraction spectra. The diffraction pattern confirmed the existence of PbF_2 and other crystalline phases in glass ceramics together with other cadmium phosphate phases in GC10 (maximum annealing time of 10h). The crystallite size distribution in the glass ceramic (GC10) is homogeneous with an average size of 7.3 ± 0.1 nm. The enhancement in Dy^{3+} characteristic luminescent emission intensity upon excitation was obtained in host glass ceramics than glass. Such enhancement was due to the well placement of Dy^{3+} ions into PbF_2 nanocrystals in GC2 and GC5. But in case of 10h annealed GC10 glass ceramic the emission intensity was decreased. This is due to the superimposition of other cadmium phosphate phases. So, sufficient excitation energy was not transferred from PbF_2 crystallites to Dy^{3+} ions. Therefore, structural feasibility is also an important element for efficient light emission. FTIR spectra show the distinct changes in phosphate structural units of Glass and glass-ceramics. So, the results of the present glass, glass ceramics are clearly indicating that, excess heat treatment undeniably influences emission intensity with the inducement of other crystallite phases. The CIE co-ordinates were well placed in the cool white light region. Hence, these glass/glass ceramics are useful in light emission and as well as promising candidates for white light emission devices.

Declaration of Competing Interest

The authors declare that they have no known competing financial interests or personal relationships that could have appeared to influence the work reported in this paper.

CRediT authorship contribution statement

Ch. Nageswara Rao: Data curation, Methodology, Writing - original draft, Writing - review & editing. **P. Vasudeva Rao:** Data curation, Methodology, Writing - original draft, Writing - review & editing. **R. Kameswari:** Data curation, Methodology, Writing - review & editing. **R. Ramesh Raju:** Methodology, Writing - original draft, Writing - review & editing. **G. Chandana:** Data curation, Methodology, Writing - original draft, Writing - review & editing. **K. Samatha:** Methodology, Writing - original draft, Writing - review & editing. **M.V.V.K. Srinivas Prasad:** Data curation, Methodology, Writing - original draft, Writing - review & editing. **M. Venkateswarlu:** Data curation, Methodology, Writing - review & editing. **A. Naveen:** Methodology, Writing - original draft, Writing - review & editing. **G.G. Dhar:** Conceptualization, Data curation, Methodology, Writing - original draft, Writing - review & editing.

References

[1] K.A. Bashar, G. Lakshminarayana, S.O. Baki, A.-B. Mohammed, U. Caldiño, A.N. Meza-Rocha, V. Singh, I.V Kityk, M.A. Mahdi, Tunable white-light emission from Pr3+/Dy3+ co-doped B2O3-TeO2 PbO-ZnO Li2O-Na2O glasses, Opt. Mater. (Amst). 88 (2019) 558–569.

[2] R. Narro-García, H. Desirena, T. López-Luke, J. Guerrero-Contreras, C.K. Jayasankar, R. Quintero-Torres, E. De la Rosa, Spectroscopic properties of Eu3+/Nd3+ co-doped phosphate glasses and opaque glass–ceramics, Opt. Mater. (Amst). 46 (2015) 34–39.

[3] K.V. Krishnaiah, Y. Ledemi, C. Genevois, E. Veron, X. Sauvage, S. Morency, E.S. de Lima Filho, G. Nemova, M. Allix, Y. Messaddeq, Ytterbium-doped oxyfluoride nano-glass-ceramic fibers for laser cooling, Opt. Mater. Express. 7 (2017) 1980–1994.

[4] S.P. Singh, B. Karmakar, Photoluminescence enhancement of Eu 3+ by energy transfer from Bi 2+ to Eu 3+ in bismuth glass nanocomposites, RSC Adv. 1 (2011) 751–754.

[5] J. Qian, Q. Luo, D. Zhao, S. Cui, X. Qiao, X. Fan, X. Zhang, Preparation and photoluminescence properties of fluorosilicate glass ceramics containing CeOF: Dy3+ nanocrystals, Opt. Mater. (Amst). 34 (2012) 700–704.

[6] A. Antuzevics, M. Kemere, G. Krieke, R. Ignatans, Electron paramagnetic resonance and photoluminescence investigation of europium local structure in oxyfluoride glass ceramics containing SrF2 nanocrystals, Opt. Mater. (Amst). 72 (2017) 749–755.

[7] B. Ghaemi, G. Zhao, G. Jie, H. Xi, X. Li, J. Wang, G. Han, A study of formation and photoluminescence properties of ZnO quantum dot doped zinc-alumino-silicate glass ceramic, Opt. Mater. (Amst). 33 (2011) 827–830.

[8] A. Tarafder, A.R. Molla, S. Mukhopadhyay, B. Karmakar, Fabrication and enhanced photoluminescence properties of Sm3+-doped ZnO–Al2O3–B2O3–SiO2 glass derived willemite glass–ceramic nanocomposites, Opt. Mater. (Amst). 36 (2014) 1463–1470.

[9] Y. Chen, G.H. Chen, X.Y. Liu, T. Yang, Enhanced up-conversion luminescence and optical thermometry characteristics of Er3+/Yb3+ co-doped transparent phosphate glass-ceramics, J. Lumin. 195 (2018) 314–320.

[10] D. Chen, Y. Wang, K. Zheng, T. Guo, Y. Yu, P. Huang, Bright upconversion white light emission in transparent glass ceramic embedding Tm 3+/ Er 3+/ Yb 3+: β-YF 3 nanocrystals, Appl. Phys. Lett. 91 (2007) 251903.

[11] M. Kemere, U. Rogulis, J. Sperga, Luminescence and energy transfer in Dy3+/Eu3+ co-doped aluminosilicate oxyfluoride glasses and glass-ceramics, J. Alloys Compd. 735 (2018) 1253–1261.

[12] S. Kaur, O.P. Pandey, C.K. Jayasankar, N. Chopra, Spectroscopic, thermal and structural investigations of Dy3+ activated zinc borotellurite glasses and nano-glass-ceramics for white light generation, J. Non. Cryst. Solids. 521 (2019) 119472, doi:10.1016/j.jnoncrysol.2019.119472.

[13] M.A. Marzouk, N.A. Ghoneim, Gamma irradiation and crystallization effects on the photoluminescence properties of soda lime fluorophosphates host glass activated with Ce4+, Dy3+ or Pr3+ ions, Radiat. Phys. Chem. (2020) 108893, doi:10.1016/j.radphyschem.2020.108893.

[14] A.A. Cabral, R. Balda, J. Fernández, G. Gorni, J.J. Velázquez, L. Pascual, A. Durán, M.J. Pascual, Phase evolution of KLaF 4 nanocrystals and their effects on the photoluminescence of Nd 3+ doped transparent oxyfluoride glass-ceramics, CrystEngComm 20 (2018) 5760–5771.

[15] G. Lakshminarayana, R. Yang, M. Mao, J. Qiu, I.V Kityk, Photoluminescence of Sm3+, Dy3+, and Tm3+-doped transparent glass ceramics containing CaF2 nanocrystals, J. Non. Cryst. Solids. 355 (2009) 2668–2673.

[16] N. Pawlik, B. Szpikowska-Sroka, T. Goryczka, W.A. Pisarski, Photoluminescence investigation of sol-gel glass-ceramic materials containing SrF2: Eu3+ nanocrystals, J. Alloys Compd. 810 (2019) 151935.

[17] J. Pisarska, R. Lisiecki, W. Ryba-Romanowski, T. Goryczka, W.A. Pisarski, Unusual luminescence behavior of Dy3+-doped lead borate glass after heat treatment, Chem. Phys. Lett. 489 (2010) 198–201.

[18] J. Pisarska, L. Żur, W.A. Pisarski, Optical spectroscopy of Dy3+ ions in heavy metal lead-based glasses and glass–ceramics, J. Mol. Struct. 993 (2011) 160–166.

[19] L.L. Martin, P. Haro-González, I.R. Martín, Optical properties of transparent Dy3+ doped Ba2TiSi2O8 glass ceramic, Opt. Mater. (Amst). 33 (2011) 738–741.

[20] K. Swapna, S. Mahamuda, A.S. Rao, M. Jayasimhadri, T. Sasikala, L.R. Moorthy, Visible fluorescence characteristics of Dy3+ doped zinc alumino bismuth borate glasses for optoelectronic devices, Ceram. Int. 39 (2013) 8459–8465.

[21] L. Wang, Z. Guo, S. Wang, H. Zhang, H. Lv, T. Wang, C. Su, Luminescence properties of Dy3+ doped glass ceramics containing Na3Gd (PO4) 2, J. Non. Cryst. Solids. 543 (2020) 120091.

[22] K. Linganna, C.S. Rao, C.K. Jayasankar, Optical properties and generation of white light in Dy3+-doped lead phosphate glasses, J. Quant. Spectrosc. Radiat. Transf. 118 (2013) 40–48.

[23] S. Damodaraiah, V. Reddy Prasad, Y.C. Ratnakaram, Structural and luminescence properties of Sm3+-doped bismuth phosphate glass for orange-red photonic applications, Luminescence 33 (2018) 594–603, doi:10.1002/bio.3451.

[24] M. Vijayakumar, K. Viswanathan, K. Marimuthu, Structural and optical studies on Dy3+:Tb3+ co-doped zinc leadfluoro-borophosphate glasses for white light applications, J. Alloys Compd. 745 (2018) 306–318, doi:10.1016/j.jallcom.2018.02.211.

[25] N. Chanthima, Y. Tariwong, T. Sareein, J. Kaewkhao, N.W. Sangwaranatee, Investigation of Luminescence Properties of Dy3+ Doped Alkaline Earth Oxides Barium Phosphate Glasses, Appl. Mech. Mater., Trans Tech Publ (2018) 27–31.

[26] K. Jha, M. Jayasimhadri, Spectroscopic investigation on thermally stable Dy3+ doped zinc phosphate glasses for white light emitting diodes, J. Alloys Compd. 688 (2016) 833–840.

[27] M. Braglia, J. Kraus, S. Mosso, Core/clad compositions with high numerical aperture for single-mode fluoride fibres, J. Non. Cryst. Solids. 201 (1996) 237–245.

[28] S. Todoroki, K. Hirao, N. Soga, Local structure around rare-earth ions in indium-and lead-based fluoride glasses with high upconversion efficiency, J. Non. Cryst. Solids. 143 (1992) 46–51.

[29] L. Niu, A.R. Kortan, N. Kopylov, P.H. Citrin, Local structural study of Pb-induced instability in ZBLAN glass, J. Non. Cryst. Solids. 213 (1997) 358–362.

[30] G. Chandana, C.N. Rao, P.V. Rao, M.J.S. Al-Musawi, K. Samatha, G.G. Dhar, Luminescent properties of Sm3+ doped metal fluoro phosphate glasses, Optik (Stuttg) (2019) 163909.

[31] A. Moguš-Milanković, A. Šantić, A. Gajović, D.E. Day, Spectroscopic investigation of MoO3–Fe2O3–P2O5 and SrO–Fe2O3–P2O5 glasses. Part I, J. Non. Cryst. Solids. 325 (2003) 76–84, doi:10.1016/S0022-3093(03)00362-4.

[32] S. Li, H. Liu, F. Wu, Z. Chang, Y. Yue, Effects of alkaline-earth metal oxides on structure and properties of iron phosphate glasses, J. Non. Cryst. Solids. 434 (2016) 108–114, doi:10.1016/j.jnoncrysol.2015.12.004.

[33] E.A. Abou Neel, W. Chrzanowski, D.M. Pickup, L.A. O'Dell, N.J. Mordan, R.J. Newport, M.E. Smith, J.C. Knowles, Structure and properties of strontium–doped phosphate-based glasses, J. R. Soc. Interface. 6 (2009) 435–446.

[34] P.-Y. Shih, H.-M. Shiu, Properties and structural investigations of UV-transmitting vitreous strontium zinc metaphosphate, Mater. Chem. Phys. 106 (2007) 222–226.

[35] E.F. Huerta, A.N. Meza-Rocha, R. Lozada-Morales, A. Speghini, S. Bordignon, U. Caldiño, White, yellow and reddish-orange light generation in lithium-aluminum-zinc phosphate glasses co-doped with Dy3+/Tb3+ and tri-doped with Dy3+/Tb3+/Eu3+, J. Lumin. 219 (2020) 116882.

[36] B.H. Babu, V.V.R.K. Kumar, Warm white light generation in γ-irradiated Dy3+, Eu3+ codoped sodium aluminoborate glasses, J. Lumin. 169 (2016) 16–23.

[37] L.Q. Yao, G.H. Chen, H.J. Zhong, S.C. Cui, F. Li, J.Y. Gan, Enhanced Luminescent Properties in Tm3+/Dy3+ Co-doped Transparent Phosphate Glass Ceramic, in: MATEC Web Conf, EDP Sciences, 2016, p. 4005.

[38] D. Valiev, S. Stepanov, O. Khasanov, E. Dvilis, E. Polisadova, V. Paygin, Synthesis and optical properties of Tb3+ or Dy3+-doped MgAl2O4 transparent ceramics, Opt. Mater. (Amst). 91 (2019) 396–400.

[39] P.R. Rani, M. Venkateswarlu, S. Mahamuda, K. Swapna, N. Deopa, A.S. Rao, Spectroscopic studies of Dy3+ ions doped barium lead alumino fluoro borate glasses, J. Alloys Compd. 787 (2019) 503–518.

[40] G.V. Prakash, Absorption spectral studies of rare earth ions (Pr3+, Nd3+, Sm3+, Dy3+, Ho3+ and Er3+) doped in NASICON type phosphate glass, Na4AlZnP3O12, Mater. Lett. 46 (2000) 15–20.

[41] U. Caldiño, A. Lira, A.N. Meza-Rocha, I. Camarillo, R. Lozada-Morales, Development of sodium-zinc phosphate glasses doped with Dy3+, Eu3+ and Dy3+/Eu3+ for yellow laser medium, reddish-orange and white phosphor applications, J. Lumin. 194 (2018) 231–239.

[42] J. An, Z. Zhang, Y. Qiu, Z. Fu, Y. Zhou, F. Zeng, Luminescence properties of borosilicate glass doped with Ce3+/Dy3+/Eu3+ under ultraviolet excitation for white LED, J. Non. Cryst. Solids. 503 (2019) 208–213.

[43] C. Ming, F. Song, Y. Qin, X. Ren, L. An, M (Tm3+, Tb3+, Ho3+, Dy3+, Mn2+)-doped transparent fluorophosphate glasses for white light-emitting–diodes, Opt. Commun. 321 (2014) 195–197.

[44] Y. Liu, G. Liu, J. Wang, X. Dong, W. Yu, Single-component and warm-white-emitting phosphor NaGd (WO4) 2: Tm3+, Dy3+, Eu3+: synthesis, luminescence, energy transfer, and tunable color, Inorg. Chem. 53 (2014) 11457–11466.

[45] N.P. Rajesh, G. Subalakshmi, C.K. Jayasankar, Investigations on energy transfer and tunable luminescence spectra for single, co-doped and tri-doped RE3+ (RE3+= Dy3+, Sm3+ and Eu3+) activated Sr1. 99Bi0. 01CeO4 phosphors, Opt. Mater. (Amst). 85 (2018) 464–473.

[46] Y. Yu, F. Song, C. Ming, J. Liu, W. Li, Y. Liu, H. Zhao, Color-tunable emission and energy transfer in Tm3+/Dy3+/Sm3+ tri-doped phosphate glass for white light emitting diodes, Opt. Commun. 303 (2013) 62–66.

[47] V.R. Kumar, G. Giridhar, V. Sudarsan, N. Veeraiah, Influence of red lead on the intensity of green and orange emissions of Sm3+ and Ho3+ co-doped ZnO–SrO–P2O5 glass system, J. Alloys Compd. 695 (2017) 668–681.
[48] C. Bocker, S. Bhattacharyya, T. Höche, C. Rüssel, Size distribution of BaF2 nanocrystallites in transparent glass ceramics, Acta Mater 57 (2009) 5956–5963, doi:10.1016/j.actamat.2009.08.021.
[49] Y.M. Moustafa, K. El-Egili, Infrared spectra of sodium phosphate glasses, J. Non. Cryst. Solids. 240 (1998) 144–153.
[50] A.H. Hammad, A.M. Abdelghany, Optical and structural investigations of zinc phosphate glasses containing vanadium ions, J. Non. Cryst. Solids. 433 (2016) 14–19.
[51] J. Wong, C.A. Angell, Glass: structure by spectroscopy, M. Dekker New York, 1976.
[52] A. Shaim, M. Et-Tabirou, Role of titanium in sodium titanophosphate glasses and a model of structural units, Mater. Chem. Phys. 80 (2003) 63–67.
[53] G.Le Saout, P. Simon, F. Fayon, A. Blin, Y. Vaills, Raman and infrared study of (PbO) x (P2O5)(1−glasses, J. Raman Spectrosc. 33 (2002) 740–746.
[54] P.K. Jha, O.P. Pandey, K. Singh, FTIR spectral analysis and mechanical properties of sodium phosphate glass-ceramics, J. Mol. Struct. 1083 (2015) 278–285, doi:10.1016/j.molstruc.2014.11.027.
[55] M. Karabulut, A. Popa, G. Borodi, R. Stefan, An FTIR and ESR study of iron doped calcium borophosphate glass-ceramics, J. Mol. Struct. 1101 (2015) 170–175, doi:10.1016/j.molstruc.2015.08.004.
[56] A. Chahine, M. Et-Tabirou, J.L. Pascal, FTIR and Raman spectra of the Na2O–CuO–Bi2O3–P2O5 glasses, Mater. Lett. 58 (2004) 2776–2780.
[57] A.M. Abdelghany, G. El-Damrawi, A.H. Oraby, M.A. Madshal, Optical and FTIR structural studies on CoO-doped strontium phosphate glasses, J. Non. Cryst. Solids. 499 (2018) 153–158, doi:10.1016/j.jnoncrysol.2018.07.022.
[58] A. Okasha, A.M. Abdelghany, S.K. Mohamed, S.Y. Marzouk, H.A. El-Batal, M.S. Gaafar, Gamma ray interactions with samarium doped strontium phosphate glasses, J. Mater. Sci. Mater. Electron. 29 (2018) 20907–20913, doi:10.1007/s10854-018-0234-3.
[59] S. Rada, E. Culea, FTIR spectroscopic and DFT theoretical study on structure of europium-phosphate-tellurate glasses and glass ceramics, J. Mol. Struct. 929 (2009) 141–148, doi:10.1016/j.molstruc.2009.04.021.
[60] W.T. Carnall, P.R. Fields, K. Rajnak, Electronic energy levels in the trivalent lanthanide aquo ions. I. Pr3+, Nd3+, Pm3+, Sm3+, Dy3+, Ho3+, Er3+, and Tm3+, J. Chem. Phys. 49 (1968) 4424–4442.
[61] I.I. Pm, W.T. Carnall, P.R. Fields, K. Rajnak, Spectral Intensities of the Trivalent Lanthanides and Actinides in Solution. II. Pm3+, Sm3+, Eu3+, Gd3+, Tb3+, Dy3+, and Ho3+, 4412 (1968). doi:10.1063/1.1669892.
[62] M. Kaur, A. Singh, V. Thakur, L. Singh, Thermal, optical and structural properties of Dy3+ doped sodium aluminophosphate glasses, Opt. Mater. (Amst). 53 (2016) 181–189.
[63] D.V. Rao, C.M. Kumar, G. Srinivas, R. Manepalli, R.R. Raju, G. Giridhar, Spectroscopic properties of Dy3+ doped MgO-LiF-CdO-P2O5 glasses, Optoelectron. Adv. Mater. Commun. 11 (2017) 691–696.
[64] K. Anilkumar, S. Damodaraiah, S. Babu, V.R. Prasad, Y.C. Ratnakaram, Emission spectra and energy transfer studies in Dy3+ and Dy3+/Eu3+ co-doped potassium fluorophosphate glasses for white light applications, J. Lumin. 205 (2019) 190–196.
[65] T.R. Raman, Y.C. Ratnakaram, Concentration dependent Dy3+ activated LiPbB5O9 phosphor: Structure and luminescence studies for white LED applications, Opt. Mater. (Amst). 99 (2020) 109515.

Volume 65, Issue 3, 2021
Journal of Scientific Research
Institute of Science,
Banaras Hindu University, Varanasi, India.

Glomerulotubular Injury and Phenotypic Switch of Kidney Cells in Diabetic Nephropathy

Syed Vaziha Tahaseen[1,2], Manga Motrapu[3], Rajkishor Nishad[3] and Kiranmayi Peddi[*2]

[1]Department of Biochemistry, SRR & CVR College, Vijayawada-520004, India. vazeehatahaseensuraj@gmail.com
[2]Department of Biochemistry, Acharya Nagarjuna University, Guntur-522510, India. kiranmayi.kodali@rediffmail.com*
[3]Department of Biochemistry, University of Hyderabad, Hyderabad- 500046, India. biochemistry1520@gmail.com

Abstract: **The increased prevalence of diabetes mellitus (T2DM), and one of the complications, diabetic nephropathy (DN), constitutes a significant health care burden worldwide. Nephron, the kidney's structural and functional unit, includes two principal regions: glomerulus and tubule. Glomerular dysfunction and podocyte injury are significant factors in the development and progression of DN. Nevertheless, emerging evidence suggests that kidney tubular damage also contributes significantly to the pathogenesis of DN. To assess the contribution of both glomerular and tubular damage in DN's pathogenesis, we evaluated the functional and histochemical parameters and immunohistochemistry of the kidney biopsy specimens for EMT and fibrosis markers from 11 patients with confirmed diabetic nephropathy. Histopathological analysis revealed that besides significant glomerulosclerosis, kidneys are presented with tubular injury. These patients' glomeruli showed decreased epithelial markers' expression while expressing a more considerable number of mesenchymal markers. On the other hand, the tubular region displays an enhanced expression of the fibroblastic marker. Pathogenesis and proteinuria in DN patients could be contributed by the morphometric transformation of podocytes into mesenchymal form, tubular epithelial cells into fibroblasts. Our observations are significantly relevant for identifying novel therapeutics for both diagnosing and treating DN.**

Index Terms: **Diabetes, EMT, Fibroblast, Glomerulus, Nephropathy, Podocytes.**

I. INTRODUCTION

Vertebrate kidneys contribute to the body's homeostasis by regulating electrolyte, acid-base, and water balance with millions of nephrons' collective effort. The glomerulus and tubule are two regions of the nephron, while the former responsible for permselectivity, latter ensures selective reabsorption. Thus, the collective effort of the glomerulus and tubule determines the final composition of urine. The kidney's potential to excrete ultrafiltrated urine devoid of large molecules, including protein, is primarily determined by a three-layered glomerular filtration barrier (GFB). The three layers of GFB are the fenestrated endothelium of glomerular capillaries, glomerular basement membrane (GBM), and glomerular podocytes.

Podocytes are considered highly imperative for the normal function of GFB over the other components. Podocytes are visceral epithelial cells of the glomerulus, presented with a giant cell body and characteristic primary and secondary foot processes. With the help of foot processes, podocytes provide epithelial coverage to the capillaries. Podocytes injury is expected to impair the efficiency of glomerular permselectivity and is manifested by sclerosis and varying degree of albuminuria. Simultaneously, the kidney tubule is a layer of elongated tubular epithelial cells connected with the kidney capsule wall. The kidney tubular epithelial cells constitute the tubule's outer layer that plays a crucial role in absorbing glucose, amino acids, and primary urine proteins. At the same time, tubular cells elicit several essential functions such as regulating water, electrolyte, acid, and alkali balance. Injury to the kidney cells, including podocytes and tubular epithelial cells, during clinical conditions such as diabetic nephropathy (DN), compromise both kidney architecture and function.

DN is one of the most common complications in diabetic patients and the primary cause of end-stage kidney failure (ESKD) and is associated with increased mortality. 30-40% of diabetic patients (both type 1 and type2) develop DN, whereas a significant proportion of DN cases progresses to end-stage kidney disease (ESKD).

Although early stages of DN are asymptomatic, end-stage is being treated by either dialysis or kidney transplantation. DN'spathophysiological features include glomerulosclerosis, interstitial and tubular fibrosis, inflammation, thickening of GBM, decreased glomerular filtration rate (GFR), and overt proteinuria. Progressive proteinuria is a hallmark of DN, whereas patients initially show microalbuminuria (30-300 mg/24 hr) for an extended period (5-10 years), followed by

* Corresponding Author

DOI: 10.37398/JSR.2021.650313

macroalbuminuria (≥300 mg/ 24 hr). A proteinuric condition during DN suggests both impaired glomerular permselectivity and tubular reabsorption. Despite microalbuminuria or proteinuria, diabetic patients might have a standard glomerular structure with or without tubulointerstitial and arteriolar abnormalities (Rockwell,1994) .The clinical manifestations of DN are strongly related to the degree of mesangial expansion. Microscopic morphometric analysis has described both structural changes and the structural-functional relationships of DN. These structural changes may include injury to both podocytes and tubular epithelial cells. Podocytes (visceral epithelial cells) may undergo phenotypic conversion to mesenchymal cells and become motile and detach from GBM. Alternatively, tubular epithelial cells may transform into fibroblasts due to various noxious stimuli in the T2DM. Nevertheless, the simultaneous occurrence of both events was not demonstrated earlier in the glomeruli from DN subjects.

Since podocyte contributes to the glomerular permselectivity and integrity of GBM, any insult to podocytes could contribute to altered glomerular morphology and proteinuria. Simultaneously, tubular injury and impaired reabsorption could also be anticipated during damage to tubular cells. This study demonstrated the phenotypic switch of podocytes (glomerular regions) and tubular epithelial cells (kidney tubule) in biopsy sections from T2DM patients.

II. METHODOLOGY

A. *Enrollment of Patients:*

We enrolled 11 patients with T2DM undergoing biopsy as recommended by the nephrologist. Inclusion criteria are diabetes with more than 15 years, persistently inadequate glycemic control, and proteinuria above 300 mg/24 hr. Exclusion criteria were hematuria, clinical and laboratory findings suggestive of non-diabetic glomerulopathy, and secondary renal damage due to hypertension. For the enrolled patients, 24 hours of urine and early morning spot urine were collected, and proteinuria was determined. Kidney biopsies of these 11 DN patients were collected and performed histopathological analysis. Biopsy specimens from kidney cancer patients who underwent nephrectomy for a localized kidney tumor were considered non-diabetic. The non-affected part of the kidney tissue was utilized for histopathological examinations. The kidney biopsy serial sections (4 μm) from paraffin-embedded tissues were prepared to perform morphometric analysis. The Institutional Review Board approved the study of GunturMedical College, Guntur, Andhra Pradesh, India (#GMC/IEC/120/2018). Our studies abide by the Declaration of Helsinki principle.

B. *Clinical Examination:*

Anthropometric measurements were recorded for the patients; Body mass index (BMI) was calculated using the formula: weight in kg and height in m^2. Blood pressure (BP) was checked thrice by a digital oscillometer (Omron Healthcare Co. Ltd.). Fasting blood glucose (FBG) was assessed in the whole blood using a glucometer (Accu-Chek Aviva, Roche *Diagnostics GmbH, Germany). HbA1c was estimated in whole blood using a bio-rad D-10 analyzer. Urinary albumin (number COD11573) and creatinine (number COD11502) levels were estimated using existing assay kits (Biosystems).*

C. *Morphometric analysis:*

For histological analysis, kidney cortical samples were fixed with 4% neutral buffered paraformaldehyde before embedding in paraffin. Paraffin-embedded tissues were sliced longitudinally into four μm thick sections, subjected to staining with haematoxylin and eosin for general evaluation of the cellular structure, periodic acid–Schiff (PAS) staining applied to provides excellent definitions for glomerular basement membrane, tubular basement membrane, and mesangium. Masson's trichrome staining is used to observe the extracellular mesangial volume, interstitial fibrosis percentage, and tubular atrophy (IFTA). At least 15 glomeruli per stained biopsy had to be counted for the measurement to be considered valid. The diagnosis and histological scoring for kidney damage were evaluated based on Tervaert et al.(2010). At least six glomeruli were captured for each biopsy sample and quantified for histopathological changes. We took images with a BX51 light microscope (Olympus, Tokyo) with appropriate filters. Histological positive staining intensity was quantified using software (Image J 1.44, NIH, USA) (Nishad et al., 2019; Kudose et al., 2018; Meyer, 2003).

D. *Nephroseq analysis:*

To validate the observations found in biopsy specimens holds with the existing database generated with data from human, we analysed the expression of the same set of genes Nephroseq database (https://nephroseq.org). The source for Nephroseq database is the University of Michigan O'Brien Renal Centre, Michigan, Ann Arbor, MI.

E. *Statistical analysis*:

Data are presented as mean±SD. For the statistical difference between the two groups of the data, Student's t-test was used to generate the P-values ($p \leq 0.05$). Statistical analyses were performed using GraphPad Prism V.6.0.

III. RESULTS

A. *Impaired renal function in diabetic subjects:*

Mean age of 11 diabetic patients was 61±5 years, BMI 29.7 ± 5.6, and HbA1c 9.1 ± 2%. Fasting glucose of diabetic patients significantly high (Fig.1A). Similarly, urinary albumin (302±71.87mg/24hrs.) and serum creatinine (3.87± 2.52 mg/dL)), and eGFR values (34.9±11.9ml/min/1.73m^2) suggests kidney functional parameters were in the progressive DN pathological range (Fig.1B-D). High fasting and postprandial

glucose levels and HbA1c (%) indicate poor glycemic control in these patients. These patients have ~15 yrs of diabetic history, and they are high overt proteinuria, suggesting that kidney function has been compromised and suffering from progressive DN.

Figure 1

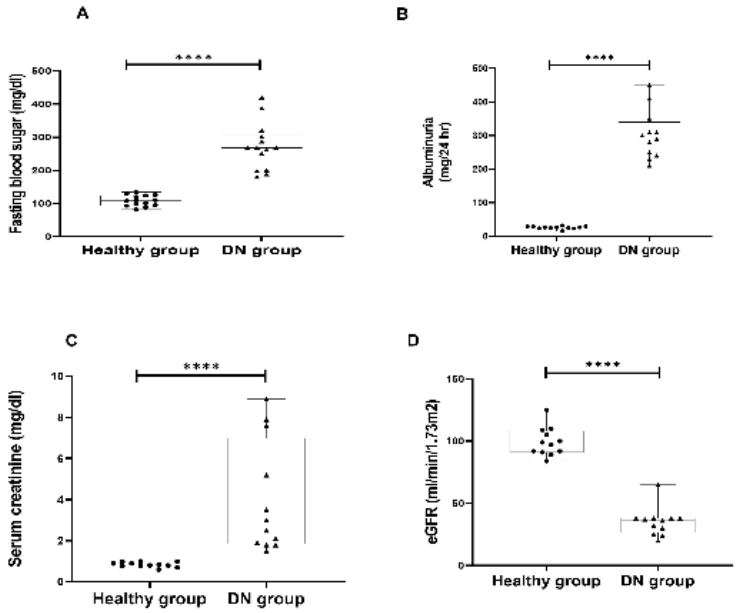


Figure 1: The kidney functional parameters in patients enrolled in the study:(A) Fasting blood glucose levels of healthy volunteers and patients with DN. (B) Albumin levels were measured in healthy volunteers and DN patients. (B) Creatinine levels were estimated in serum. (C) Glomerular filtration rate (GFR) was calculated in healthy volunteers and DN patients. Data from the DN group is significantly different from the Healthy group. ($p < 0.001$).

Figure 2

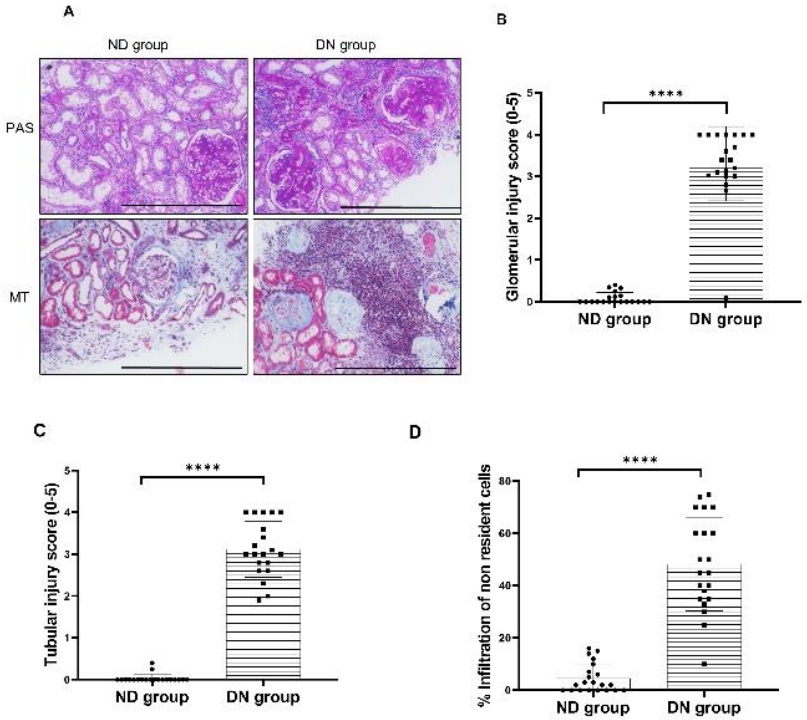


Figure 2: Quantification of kidney injury in DN patients. (A) Representative images of periodic acid Schiff's stain and Mason's trichrome staining of kidney sections from non-diabetic (ND) and diabetic nephropathy (DN) subjects. Glomerular injury score (B) and tubular injury score (C) were quantified in biopsy sections (n= 20). (D) % of infiltrated cells was quantified in ND and DN patients' specimens. Data from DN is significantly different from ND subjects ($p < 0.001$).

Figure 3

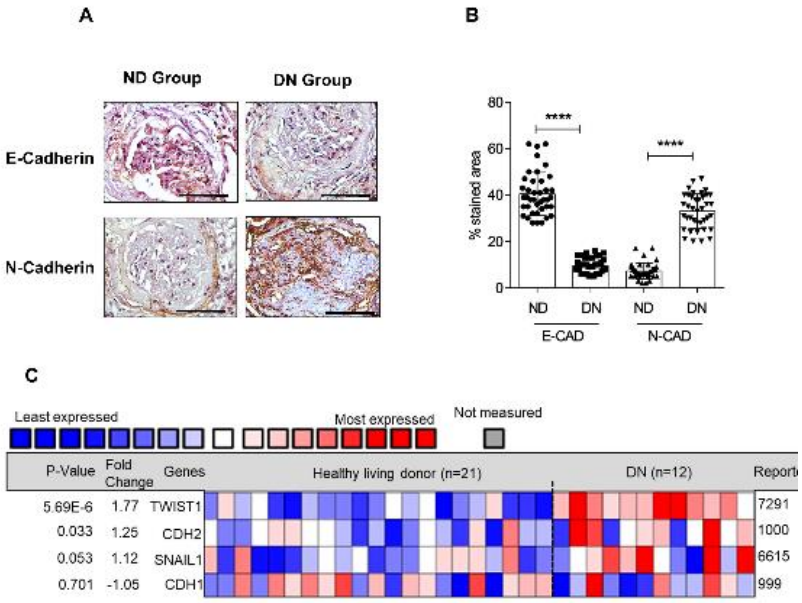


Figure 3: Quantification of epithelial-mesenchymal markers in glomerulus from DN patients, A) Staining for E-cadherin (epithelial marker) and N-cadherin (mesenchymal marker) in the glomerular region of non-diabetic (ND) and diabetic nephropathy (DN) subjects. (B) Staining intensity for E-cad and N-cad was quantified using Image-J (NIH, USA) and presented as a bar diagram (n= ~40 sections) (p <0.001). (C) Expression of EMT markers in glomeruli from healthy living donors vs. DN patents (Data mining in the Nephroseq database (University of Michigan O'Brien renal center, Ann Arbor, USA).

Figure 4

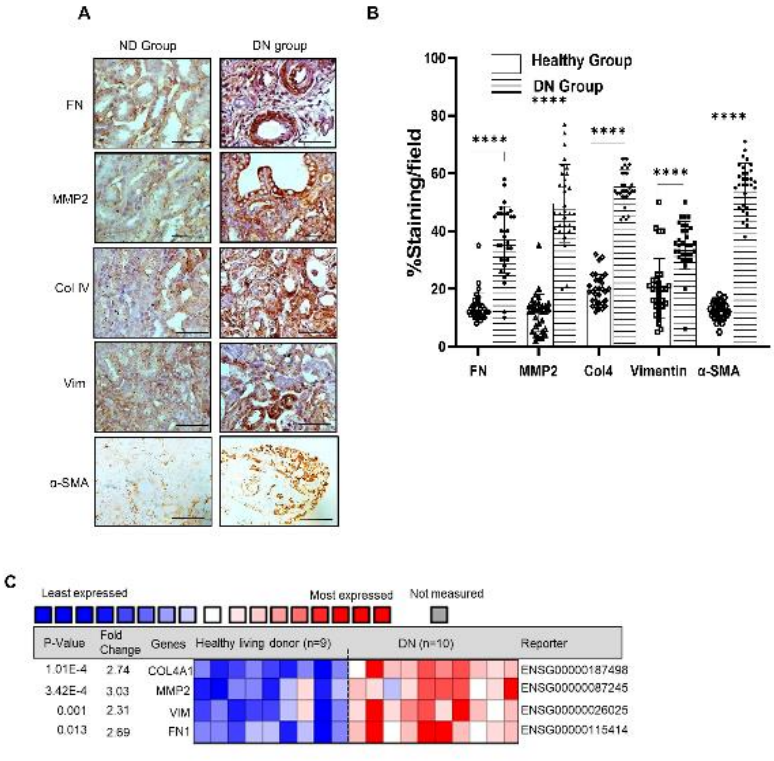


Figure 4*:* Quantification of fibroblast markers in the tubular region from DN patients**.** (A), (B), Representative images of staining for fibronectin (FN), MMP2, Collagen IV (Col IV), Vimentin (Vim), and α-Smooth Muscle Actin (SMA) in a tubular region of non-diabetic (ND) and diabetic nephropathy (DN) subjects. Staining intensity was quantified using Image-J (NIH, USA) and presented as a bar diagram (n= ~40 sections) (p <0.001). (C) Expression of fibroblastic markers from healthy living donors vs. DN patents (Data mining in the Nephroseq database, U of Michigan O'Brien renal center, Ann Arbor, USA).

B. Severe glomerular and tubular injury in DN patients:

Since diabetic patients showed macroalbuminuria, we wanted to perform a histological examination to assess nephropathy intensity. We performed PAS and Mason's trichrome stainings (Fig.2A) and evaluated both glomerular and tubular injury in these patients. One of the characteristic features of DN is the infiltration of non-resident cells into glomeruli. Therefore, we

counted % of in filtered cells into the glomeruli of these patients and found that ~50% of glomerular cells are non-resident cells compared with ~5% of non-resident cells in non-diabetic individuals (Fig.2D)

C. Attenuated expression of epithelial markers in glomerular regions in DN patients:

As discussed in the introduction, the appearance of protein in the urine indicates a structural and functional artifact, particularly in the glomerular area. Podocytes are the primary cell type and account for ~40% of all glomerular cells. In response to injury, Podocytes undergo a morphologic switch known as epithelial to mesenchymal transition (EMT), during which they attain an embryonic form by shedding their epithelial features. It is conceivable that podocytes, undergone EMT, abandon their complex architecture and relinquish their specialized functions, leading to proteinuria. Since we observed proteinuria in these patients and few resident cells in the glomerulus, we suspect that podocytes might have undergone EMT. When we stained for E-cadherin, a putative epithelial marker, we observed decreased staining (Fig.3A).

On the other hand, N-cadherin (a mesenchymal marker) expression enhanced, suggesting loss of epithelial features and gain of mesenchymal features (Fig.3A&B). We also performed a meta-analysis of the Nephroseq database for EMT markers. Nephroseq analysis (Fig.3C) reveals a marginally decreased expression of E-cadherin (CDH1; -1.05) but an enhanced expression of N-cadherin (CDH2; 1.25), SNAIL1 (1.12), and TWIST. (1.77). Together Nephroseq analysis and histochemical data suggest podocytes undergo EMT in DN patients.

D. Elevated fibrotic markers in tubular regions in diabetic patients:

Recent studies suggest that increased glomerular leakage and impaired tubular reabsorption are accountable for albuminuria in the early DN(Zeni et al., 2017). Further, tubulocentric pathology and treatment for DN were proposed(Zeni et al., 2017). Since we observed tubular injury in these patients (Fig2C), we investigated whether tubular cells have undergone any phenotypic transformation. Interestingly, we observed enhanced expression of fibrotic markers such as fibronectin (FN), MMP2, collagen IV, vimentin, and α-SMA in both proximal and distal tubules (Fig.4A&B). Thesignificantinduction of these markers suggests that the transformation of tubular cells to fibroblasts. We also performed a meta-analysis using the Nephroseq database for fibroblasts markers. Nephroseq analysis (Fig.4C) reveals the significant induction of the above-mentioned fibrotic markers suggesting our biopsy data correlates with data mined from the database (Fig.4B vs. Fig.4C). Together our data suggest tubular cells from DN patients could transform into fibroblasts.

DISCUSSION

Diabetes is presented with high morbidity and often progresses to chronic kidney disease and accounts for significant ESKD and dialysis cases. With the increasing prevalence of T2DM, its complications DN impose a tremendous burden on individuals, families, and the health care sector. Although there is extensive information on diagnosis and biomarkers of diabetic kidney diseases, it is still increasingly clear whether the glomerulus or tubules are more critical in DN's development and progression. Glomerulosclerosis was considered a primary event of the pathogenesis in DN. Other glomerular changes such as thickening of the basement membrane and mesangial expansion, and podocytopathy are prominent manifestations during DN.Although glomerular centric pathological events undoubtedly contribute to DN's pathology, there is growing evidence to suggest a significant role for the proximal tubules as drivers of proteinuria and other clinical manifestations of DN. In the present, we noticed that DN patients showed both glomerular and tubular injury, as evidenced by PAS and Mason's trichrome staining. Indeed, we saw the loss of epithelial markers and mesenchymal markers in glomerular cells and fibrotic markers in tubular cells. This evidence of both glomerular cells and tubular cells' transition to mesenchymal and fibrotic phenotype, respectively, provides a new perspective on the pathophysiology of DN. This novel observation provides new diagnosis and therapeutic approaches by targeting both glomerular epithelial cells and tubular cells in DN.

Both glomerular filtration barrier (consist of podocytes, basement membrane, and endothelium) and tubular epithelium work in concert to ensure the ultrafiltration of plasma and reabsorption of primary urine, respectively, from becoming urine. Thus, both glomerulus and tubule regulate the final composition of urine. Besides being a part of the filtration apparatus, glomerular podocytes elicit several functions to maintain the glomerular function's integrity. Podocytes provide epithelial coverage to the glomerular capillaries and oppose hydrostatic pressure to facilitate glomerular filtration and are thus indispensable to renal filtration. However, podocytes are exposed to a myriad of hematological agents and noxious stimuli due to diabetes. A body of experimental data demonstrated high glucose, glucose-derived advanced glycation end-products (AGEs), activation of sorbitol, RAAS, Growth hormone (GH), and TGF-β, etc., were contributed to the altered signaling events thus pathology of DN. Accumulating evidence suggests that glomerular podocytes undergo EMT during various insults such as high glucose, AGEs, GH, and TGF-β (Anil Kumar et al., 2014). Podocytes

might majorly contribute to the EMT phenomenon; we observed glomeruli from DN patients as they are the glomerulus' predominant epithelial cells. EMT of podocytes might compromise their ability to offer epithelial coverage to the capillaries and oppose hydrostatic pressure, resulting in impaired glomerular filtration.EMT of podocytes could be a reason for podocytes' appearance in urine from patients with advanced DN (Reidy & Susztak, 2009). The two parts of the kidney tubule, proximal and distal, have specialized functions. The proximal part is concerned with the reabsorption of several primary urine components to maintain homeostasis; in contrast, the distal tubule is associated with complete water, electrolyte, and acid-base balance regulation. Recent studies suggest that in addition to increased glomerular leakage, impaired tubular reabsorption is also accountable for DN's albuminuria(Zeni et al., 2017). DN's tubular manifestations include tubular atrophy, interstitial fibrosis, and thickening of the tubular basement membrane, correlated with kidney dysfunction and proteinuria. It is noteworthy that the proximal tubule injury can trigger glomerular dysfunction and such retrograde trafficking has implications in the progression of DN(Hasegawa et al., 2013).Glomerular podocytes and proximal tubular cells work in association with complementing each other's biology. Hasegawa et al. demonstrated that proximal tubules communicate with podocytes by releasing nicotinamide mononucleotide(Hasegawa et al., 2013).Proximal tubule-specific Sirt1 helps maintain glomerular NMN concentrations, thus preserving the glomerular podocyte function and offering protection against diabetic kidney disease(Hasegawa et al., 2013). These observations suggest that the injury to tubular cells significantly affects the glomerular function and promotes DN progression.

Additionally, the injured proximal tubule epithelium triggers the inflammatory response, which leads to tubulointerstitial fibrosis, tubular atrophy that, in turn, promotes secondary glomerulosclerosis(Lee et al., 2012). Therefore, the observed tubular and glomerular injury in DN patients from our study reveals that DN's pathological evaluation needs to be comprehensive and evaluate the tubular injury and not only glomerulus. In summary, our study provides evidence for significant tubular damage in addition to glomerular injury. It suggests a need for diagnostic evaluation and therapeutic advances in DN towards both glomerulus and tubule.

ACKNOWLEDGMENTS

Authors thank Guntur Medical College and Dr. Srilatha .V, nephrologist, NRI hospital, patients, and their families, for their support during this study.

REFERENCES

Anil Kumar, P., Welsh, G.I., Saleem, M.A., Menon, R.K. (2014) Molecular and cellular events mediating glomerular podocyte dysfunction and depletion in diabetes mellitus. *Front Endocrinol (Lausanne)*, 5(SEP),1-10.

Hasegawa, K., Wakino, S., Simic, P., et al. (2013) Renal tubular sirt1 attenuates diabetic albuminuria by epigenetically suppressing claudin-1 overexpression in podocytes. *Nat Med*, 19(11), 1496-1504.

Kudose, S., Hoshi, M., Jain, S., Gaut, J,P. (2018) Renal Histopathologic Findings Associated with Severity of Clinical Acute Kidney Injury. *Am J Surg Pathol*, 42(5), 625-635.

Lee, P.T., Chou, K.J., Fang, H.C. (2012) Are tubular cells not only victims but also perpetrators in renal fibrosis. *Kidney Int*, 82(2), 128-130.

Meyer, T.W. (2003) Tubular injury in glomerular disease. *Kidney Int*, 63(2), 774-787.

Nishad, R., Mukhi, D, Tahaseen, S.V., Mungamuri, S.K., Pasupulati, A.K. (2019) Growth hormone induces Notch1 signaling in podocytes and contributes to proteinuria in diabetic nephropathy. *J Biol Chem*, 294(44), 16109-16122.

Reidy, K., Susztak, K. (2009) Epithelial-Mesenchymal Transition and Podocyte Loss in Diabetic Kidney Disease. *Am J Kidney Dis*, 54(4), 590-593.

Rockwell, R. (1994) Interview with the Executive Director. *ICPSR Bull*, 15(2), 1-6.

Tervaert, T,W,C., Mooyaart, AL., Amann, K., et al. (2010) Pathologic classification of diabetic nephropathy. *J Am Soc Nephrol*, 21(4), 556-563.

Zeni, L., Norden, A.G.W., Cancarini, G., Unwin, R.J. (2017) A more tubulocentric view of diabetic kidney disease. *J Nephrol*, 30(6), 701-717.

***

[Downloaded free from http://www.journalofdiabetology.org on Wednesday, November 2, 2022, IP: 49.205.107.68]

Original Article

Prediction and Risk Factor Analysis of Obesity-related Proteinuria among Individuals with Metabolic Syndrome

Syed Vaziha Tahaseen, P. Kiranmayi[1], Marni Rakshmitha[2], Bezawada Anusha[3]

Department of Biochemistry, SRR & CVR Govt. Degree College (A), Vijayawada, [1]Department of Biochemistry, Acharya Nagarjuna University, Guntur, [2]Department of Biochemistry, Gitam University, Visakhapatnam, [3]Department of Biotechnology, Acharya Nagarjuna University, Guntur, Andhra Pradesh, India

Abstract

Objective: In the present modern era of time, poor and frantic lifestyle has led to an enumerate increase in the number of people with obesity and metabolic syndrome (MS). Epidemiological studies have shown the incidence of chronic kidney disease (CKD) risk factors in individuals with obesity and MS; despite the nonclear evidence on the existing potential risk factors, it became important to reassess existing potential risk factors that are involved in disease progression and its further complications. The strongest risk factor of CKD, albumin-to-creatinine ratio (ACR) recognized as a marker of MS and obesity. This study was carried out to identify the association of obesity (body mass index [BMI]) as a risk factor for albuminuria and to observe the dependence and association with albuminuria of each critical and basic factor of MS. **Design:** We conducted the potential risk factor analysis on 913 subjects, including 398 females and 515 males, from various diabetic hospitals of Vijayawada, Andhra Pradesh from early 2013 to June 2015. The medical records of the patients followed up; the anthropometric measurements and clinical parameters were retrospectively collected. The total subjects were categorized as subjects with and without MS as per National Cholesterol Education Program Adult Treatment Panel (NCEP-ATPIII) and the subjects with BMI more than 30 kg/m^2 were defined as obese according to WHO classification. **Results:** Student's *t* test analysis indicates a significant difference for ACR with mean values of 39.5 ± 44.8 and 18.4 ± 24.3 ($P < 0.0001$) in subjects with MS and without MS, 43.4 ± 48.3 and 36.7 ± 42.5 ($P < 0.02$) in obese and nonobese subjects, respectively. Chi-square analysis showed a significant association ($P < 0.05$) between MS and ACR and correlation analysis manifested significant association ($P < 0.01$) between ACR and FBS, TG, B.P, and Age in subjects with MS. The subjects with high prevalence of albuminuria exhibited significant association with an odds ratio (OR) of 1 (referent) 1.9 (95% CI, 1.34–2.58, $P = 0.0002$), 1.5 (95% CI, 1.11–1.96, $P = 0.0082$) for FBS >110 mg/dL, and TG > 150 mg/dL, respectively. Although the subjects with obesity showed no correlation with albuminuria, the risk for albuminuria was 1.5 times (95%CI 1.03–2.40, $P = 0.03$) higher among obese male subjects compared to obese female subjects. **Conclusion:** Our study strongly supports that albuminuria is highly prevalent among the subjects, with MS showing a significant positive association between obesity (BMI) with albuminuria in males only.

Keywords: ACR, BMI, chronic kidney disease, FBS, HDL, metabolic syndrome, TG

Introduction

Chronic kidney disease (CKD) has become a major global health problem with an estimated worldwide affected population of 2 million. In this context, early detection of CKD is crucial to prevent the progression of CKD to end-stage renal disease (ESRD). The presence of persistently elevated albuminuria is an early clinical marker of CKD and a predictor for cardiovascular diseases (CVD) and mortality. The clinical manifestation of CKD includes albuminuria/proteinuria as an important diagnostic tool for primary treatment[1-3] and also considered in the definition of the metabolic syndrome (MS) by the World Health Organization.[4] The MS is defined as a

Received: 22-May-2020, **Revised:** 08-June-2020, **Accepted:** 09-June-2020, **Published:** 31-March-2021

Access this article online

Quick Response Code:

Website: www.journalofdiabetology.org

DOI: 10.4103/jod.jod_37_20

Address for correspondence: Dr. P. Kiranmayi, Department of Biochemistry, Acharya Nagarjuna University, Nagarjuna Nagar, Guntur 522510, Andhra Pradesh, India. E-mail: Kiranmayi.kodali@rediffmail.com

This is an open access journal, and articles are distributed under the terms of the Creative Commons Attribution-NonCommercial-ShareAlike 4.0 License, which allows others to remix, tweak, and build upon the work non-commercially, as long as appropriate credit is given and the new creations are licensed under the identical terms.

For reprints contact: wkhlrpmedknow_reprints@wolterskluwer.com

How to cite this article: Tahaseen SV, Kiranmayi P, Rakshmitha M, Anusha B. Prediction and risk factor analysis of obesity-related proteinuria among individuals with metabolic syndrome. J Diabetol 2021;12:140-5.

[Downloaded free from http://www.journalofdiabetology.org on Wednesday, November 2, 2022, IP: 49.205.107.68]

constellation of risk factors including obesity, impaired fasting glucose (FBS >110 mg/dL), increased triglycerides (TG>150 mg/dL), associated with insulin resistance, hypertension (systolic >140 mm Hg), low levels of high-density lipoprotein cholesterol (HDL< 40 mg/dL)[5] and chronic inflammation,[6] leads to composite metabolic derangements that contribute to CKD and coronary artery disease. As per the prior investigations, the relationship between albuminuria, and MS risk factors percentage of prevalence being reported to be 10%-42% in persons with type II diabetes, 11%-40% in people with hypertension and 5%-10% in those without diabetes, hypertension or cardiovascular disease.[7-9] Obesity has been pointed out as one of the critical factors of MS, and the body mass index (BMI) estimate of more than 30 kg/m^2 indicates obesity, and people with MS are at higher risk of many chronic diseases with reduced life expectancy. One of the molecular mechanisms underlying obesity-related CKD is the abnormal or excessive accumulation of fat, characterized by adipocytes hypertrophy. This phenomenon induces hypoxia,[10] promoting inflammation and secretion of adipokines such as leptin, which specifically binds to the receptors on glomerulus and show a direct effect on kidney by promoting excessive production of pro-fibrotic transforming growth factor beta (TGF-β) which further enhance the production of extracellular matrix (ECM) components leading to fibrosis.[11,12] In obesity, increased adipose storage or inflammation of adipocytes brings about insulin resistance conversely insulin sensitivity reduction by several intracellular mechanisms causing the onset of hyperglycemia facilitating renal fibrosis.[13]

In the studies with obesity, the possible existence of a relationship between the roles of obesity executed as BMI in routine clinical practice with kidney dysfunction remains controversial. Weisinger *et al.*[14] first reported that massive proteinuria is associated with obesity. Similarly, limited studies have systematically addressed the association between microalbuminuria with obesity or central obesity irrespective of gender and other predisposing conditions. Hoffmann *et al.* [15] conversely found that there is no difference in albuminuria levels in lean and obese glucose-tolerant subject's studies.[16] However, very fewer studies focused on microalbuminuria, especially in obese nondiabetic, no hypertensive subjects. Our study focused to predict the risk factors of CKD in obesity-associated albuminuria in the south Asian population having unique anthropometric body measurements and to substantiate the clinical practices in most of the hospitals where BMI usually considered as the only clinical parameter to determine obesity.

Materials and Methods

Study area and population

This study is a cross-sectional analysis carried out in Vijayawada, Krishna District, Andhra Pradesh, India, among subjects aged between 20 and 84 years. The study was conducted on 913 subjects including 398 females (43.6%) and 515 (56.4%) males during their hospital visit who underwent medical screening at various diabetic hospitals of Vijayawada from early 2013 to June 2015 and have undergone diagnosis. Majority of them had MS. The exclusion criteria of the study were pregnant women with MS and the patients who had other CKDs. The clinical diagnosis reports and anthropometric measurements regarding height and weight were collected with patient consent.

Sample size (n) was calculated as follows = z^2 p $(1–p)/d^2$. In this study, the sample size for obesity was calculated using prevalence P = 6.5%[17] and confidence level of 95% and the precision of 0.05, by adding 10% nonresponsive rate.The total sample size was n = 103. The sample size for obese was 258. Among them, 112 were males and 146 were females. For MS, the sample size was calculated using a 95% confidence level with the margin of error 0.05 and prevalence P = 20%[18] by adding 10% non-responsive rate, the total sample size should be n = 270, but a total number of 874 MS subjects included in the study.

Sampling technique and procedure

Laboratory findings

According to the "III Adult Treatment Panel" of the "National Cholesterol Education Program" (NCEP-ATPIII of 2001) principles, MS includes the evaluation of the following risk factors: (1) fasting serum glucose (FBS), (2) TG (triglycerides), and (3) HDL (high-density lipoproteins) with consideration of BMI >30 kg/m^2 and with systolic pressure > 130 mm Hg and diastolic pressure > 90 mm Hg. According to the National Kidney Foundation (NKF) guidelines (Joint National Committee on Prevention, Detection, Evaluation, and Treatment of High Blood Pressure, 1997),[19] the urinary albumin (μg/mL) to creatinine (mg/mL) ratios in an untimed urine specimen is a convenient way to assess albumin excretion. Albuminuria is classified based on severity as normal healthy category ACR <30 μg/mg and unhealthy albuminuria category ACR >30 μg/mg. Among the 913 subjects, 402 (44%) are unhealthy albuminuria subjects and 511 (56%) are healthy albuminuria subjects.

Physical examination and clinical data

The anthropometric measurements were carried out as per the hospital standard operating procedures, the height was measured using calibrated height meters with subjects standing bare-footed in erect position placing the feet together and weight measured with the calibrated weighing machine. BMI was calculated as weight in kilograms divided by a square of height in meters. Blood pressure (BP) was measure by trained nurses employing a standard mercury sphygmomanometer, while the subject sit in a chair with feet on the floor and arm reinforced elbow is at around heart level. The average of two readings was used

[Downloaded free from http://www.journalofdiabetology.org on Wednesday, November 2, 2022, IP: 49.205.107.68]

for the analysis. All participants' clinical data related to routine laboratory findings were collected from medical records of the respective hospitals.

Statistical analysis

We performed statistical analysis using the SPSS software package. The results summarized as percentages and as the mean ± standard deviation (SD). The Pearson chi-square test and Student's *t* test were used to compare the differences between categorical variables. An appropriate condition among each parameter tested using Spearman's correlation coefficient. A value of $P < 0.05$ was considered a statistically significant difference. We calculated odds ratios using a 2×2 table.

Ethical consideration

We conducted this study with the ethical consideration approval got from the institutional review board of Guntur Medical College and Government General Hospital, Guntur, Andhra Pradesh, India and approved by the Helsinki Declaration. (Application number GMC/IEC/120/2018).

Results

This cross-sectional study performed on 913 randomly selected individuals with the majority (874) participants having MS. Irrespective of their metabolic condition we categorized the total subjects into three different categories. Each time in this study, the total subjects were categorized individually following presence/absence of MS as with MS (95.7%) and without MS (4.3%), similarly with obesity (28%) and without obesity (72%) and with healthy albuminuria (56%) and unhealthy albuminuria (44%). The mean and SD values of the following risk factors such as anthropometric, BP, lipid profile, and blood

Table 1: Comparison of baseline characteristics in, without MS and with MS groups, without MA and with MA groups and without obesity and with obesity groups using Student's *t* test

	Metabolic syndrome (MS)				
	Without MS ($n = 39$)		With MS ($n = 874$)		
Risk factor	Mean	SD	Mean	SD	*P* Value
BMI	25.57	2.08	28.23	4.64	<0.0001*
FBS	91.00	5.69	147.73	50.79	<0.0001*
ACR	18.43	24.27	39.48	44.76	<0.0001*
TGs	112.72	29.74	174.70	89.91	<0.0001*
HDL	39.28	5.32	40.84	5.65	0.07
BP	125.00	16.37	128.26	17.77	0.22
Age	50.56	13.89	50.38	10.48	0.94
	Microalbumin (MA)				
	Without MA (albumin < 30) ($n = 402$)		With MA (albumin > 30) ($n = 511$)		
Risk factor	Mean	SD	Mean	SD	*P* Value
BMI	27.88	4.31	28.42	4.91	0.07
FBS	138.17	46.76	154.39	54.69	<0.0001*
ACR	12.21	7.86	72.09	48.67	<0.0001*
TGs	169.26	89.32	175.61	88.72	0.28
HDL	40.77	5.69	40.79	5.58	0.95
BP	126.75	16.36	129.87	19.18	<0.0001*
Age	50.17	10.25	50.66	11.12	0.48
	Obesity				
	Without obesity BMI < 30) $n = 655$		With obesity (BMI > 30) $n = 258$		
Risk factor	Mean	SD	Mean	SD	*P* Value
BMI	25.87	2.58	33.80	3.55	<0.0001*
FBS	145.62	52.21	144.52	47.95	0.76
ACR	36.68	42.47	43.38	38.58	0.02*
T. Gs	173.65	89.52	168.00	87.92	0.10
HDL	41.00	5.70	40.21	5.45	0.056
B. P	127.45	18.15	129.84	16.48	0.06
Age	50.33	10.92	50.55	9.90	0.77

SD = standard deviation, BMI = body mass index, FBS = fasting blood sugar, ACR= albumin creatinine ratio, HDL = high-density lipoproteins, BP = blood pressure

**P* value significant at <0.05

[Downloaded free from http://www.journalofdiabetology.org on Wednesday, November 2, 2022, IP: 49.205.107.68]

glucose measures are compared and ascertained [Table 1], similarly correlated with each parameter [Table 2].

Among all baseline characteristics, a significant difference was observed between the mean values of BMI, FBS, ACR, and TG in subjects with the prevalence and absence of MS [Tables 1 and 2] and in subjects with MS, albuminuria (ACR) is highly correlated with the incidence of FBS, TG, BP, and age ($P < 0.01$) [Table 2]. However, the frequency albuminuria is high with the FBS, BP, and TG in the study population and seems to be less associated with obesity [Tables 1 and 2] suggesting the least association between albuminuria and overweight. But we found a significant correlation between ACR with obesity in males ($P < 0.05$) [Tables 3 and 4] emphasizing the sexual dimorphism in adipose tissue distribution and associated comorbidities.

Discussion

The occurrence and severity of MS are followed by the association of the sum of critical risk factors that include obesity, hypertension, insulin resistance, dyslipidemia, and albuminuria. According to CJKN studies and NCEP ATP III, the relationship between kidney damage and MS is complex. It is also in debate whether the collective existence of all the risk factors of MS improves CKD beyond that afforded by individual risk factors. However, very fewer studies have been undertaken to incorporate the coexistence of risk factors associated with MS and CKD. The present study results targeted to recognize and correlate the strong integrated relationship of fasting blood glucose, hyper-triglyceridemia, and high systolic BP the three of the five risk factors of MS in association with albuminuria than each independent risk factor.

In this cross-sectional study, we observed a significant difference in albuminuria in obese and nonobese subjects [Table 1], but we observed gender difference in the association of BMI with albuminuria; BMI had a greater association with ACR in males, whereas in females BMI is not associated with ACR [Tables 3 and 4]. Many studies show that there is a strong, linear relationship between obesity and hypertension. Chang *et al.*[20] study reported that systolic BP is an independent risk factor of

Table 2: Correlation analysis of each parameter with baseline parameters in subjects with metabolic syndrome ($n = 874$), with unhealthy ACR ($n = 402$), and with obesity ($n = 258$)

With metabolic syndrome							
Risk factor	**BMI**	**FBS**	**ACR**	**TGs**	**HDL**	**BP**	**Age**
BMI	1.0	0.281	0.104	0.591	0.111	0.087	0.340
FBS	0.281	1.0	0.000*	0.001*	0.051	0.537	0.031*
ACR	0.104	0.000*	1.0	0.008*	0.939	0.001*	0.002*
T.Gs	0.591	0.001*	0.008*	1.00	0.000*	0.468	0.094
HDL	0.111	0.051	0.939	0.000*	1.00	0.150	0.037*
B.P	0.087	0.537	0.001*	0.468	0.150	1.00	0.000*
Age	0.340	0.031*	0.002*	0.094	0.037*	0.000*	1.00
With unhealthy ACR							
Risk factor	**BMI**	**FBS**	**ACR**	**TGs**	**HDL**	**BP**	**Age**
BMI	1.0	0.965	0.334	0.472	0.159	0.629	0.459
FBS	0.965	1.0	0.000*	0.010	0.658	0.267	0.189
ACR	0.334	0.000*	1.0	0.002*	0.936	0.020	0.000*
T.Gs	0.472	0.010*	0.002*	1.00	0.000*	0.430	0.080
HDL	0.159	0.658	0.936	0.001*	1.00	0.264	0.422
B.P	0.629	0.267	0.020*	0.430	0.264	1.00	0.000*
Age	0.459	0.189	0.000*	0.080	0.422	0.000*	1.00
With obesity							
Risk factor	**BMI**	**FBS**	**ACR**	**TGs**	**HDL**	**BP**	**Age**
BMI	1.0	0.501	0.232	0.600	0.854	0.130	0.230
FBS	0.501	1.0	0.018*	0.015*	0.767	0.308	0.043*
ACR	0.232	0.018*	1.0	0.003*	0.586	0.711	0.027*
TGs	0.600	0.015*	0.003*	1.00	0.197	0.759	0.820
HDL	0.854	0.767	0.586	0.197	1.00	0.333	0.193
BP	0.130	0.308	0.711	0.759	0.333	1.00	0.002*
Age	0.230	0.043*	0.027*	0.820	0.193	0.002*	1.00

*Correlation is significant at <0.05 level (two tailed)

[Downloaded free from http://www.journalofdiabetology.org on Wednesday, November 2, 2022, IP: 49.205.107.68]

microalbuminuria in euglycemic normotensive males. Our analysis also confirms this association between obesity and high BP. Yesmin *et al.*[21] report shows that there is no microalbuminuria in obese women without diabetes and/or hypertension suggesting in obese women and lean women; urinary albumin excretion was similar. A recent study on Japanese hypertensive patients showed that there were sex-related differences in the associations of insulin resistance and obesity to left ventricular hypertrophy.[22] Also Foster *et al.*[23] showed that in comparative Framingham heart study microalbuminuria is associated with visceral adipose tissue in men but not in women.

This study reports elucidate that in subjects with MS and unhealthy albuminuria [Table 2], coexistence of three of the five risk factors is strongly associated with the total conditions of the study. Age also shows a positive correlation with albuminuria. With these findings, our data analysis suggests that a gender difference may exist in the association between BMI and albuminuria. The difference might be due to gender-related specifications, such as the role of sex hormones on the inflammatory mechanism that links albuminuria to central obesity or it can be also predicted that the muscle mass in males is more than in females, which can warrant the creatinine levels and gender difference in interpretation.

The gender difference can be partly because of the prevalence of smoking in males, and the absence of smoking in females. In females, there is a highly significant relationship between anthropometric variables and albuminuria due to potential sex-based divergence in fat distribution pattern and renal outcomes for differential steroid hormone levels. The contradiction may be because of higher upper body adiposity and higher visceral fat for a given BMI in the Asian Indians. The study conducted by Wang *et al.*[24] on aboriginal people by receiver operating characteristic (ROC) analysis suggested that measuring body size-related diabetes waist circumference is the best method comparing a few more methods of body size measurement.

Conclusion

This study shows the relationship between obesity and the risk for CKD by gender-specific examination, which was measured clinically in the form of micro/macroalbuminuria that leads to proteinuria. Our findings suggest that BMI has an association with albuminuria in men showing that obesity calculated as BMI is a risk factor for kidney damage in males with a high prevalence of FBS, BP, TG, and age. However the contradictory results with females demonstrate that obesity calculated as BMI is not a high-risk factor for kidney harm in females, due to an account of gender specific variation in distribution of fat indicating men having a relatively more central allocation of fat giving the fact that male obese with hyperglycemia,

Table 3: Pearson chi-square analysis between risk factors and albuminuria

	Status of microalbumin				X^2 (df)	*P*	phi
	Healthy		Unhealthy				
	N	(%)	*N*	(%)			
Metabolic syndrome (MS							
Yes	481	55.0	393	45.0	7.26	0.005*	+0.09
No	30	76.9	9	23.1			
Obesity							
Yes	135	52.3	123	47.6	1.92	0.165	+0.05
No	377	57.4	280	42.6			
Obesity in males							
Yes	54	48.2	58	51.7	4.04	0.04*	+0.09
No	232	58.9	162	41.1			

Computed only for a 2 x 2 table

*Significant at $P < 0.05$

Table 4: Risk factors of microalbuminuria in the study population

Sex	Risk factors	OR (95% CI)	*P* Value*
Males	BMI > 30 kg/m^2	1.51(1.033–2.397)	0.03*
Females	BMI > 30 kg/m^2	0.98(0.65–1.47)	0.93
Both genders	FBS > 110 mg/dL	1.865(1.34–2.58)	0.0002*
Both genders	Triglycerides > 150 mg/dL	1.47(1.105–1.957)	0.0082*
Both genders	HDL < 40 mg/dL	0.99(0.746–1.328)	0.976
Both genders	BP > 130 mm Hg	1.29(0.971–1.71	0.078

OR = odds ratio

*Significant at $P < 0.05$

[Downloaded free from http://www.journalofdiabetology.org on Wednesday, November 2, 2022, IP: 49.205.107.68]

hypertension and hypertriglyceridemia are at high risk of developing CKD. The major limitation of this study is that it was conducted by not focusing on dietary patterns of the individuals that might influence the relationship between the severity of obesity and microalbuminuria and ignored alternative methods for the calculation of obesity.

Acknowledgement

We express a deep sense of gratitude to Dr. P. Anil Kumar, assistant professor at Department of Biochemistry, School of Life Sciences, University of Hyderabad, for his direction and suggestions in all aspects of my research work.

Financial support and sponsorship

Nil.

Conflicts of interest

There are no conflicts of interest.

References

1. National Kidney Foundation. K/DOQI clinical practice guidelines for chronic kidney disease: Evaluation, classification, and stratification. Am J Kidney Dis 2002;39: S1-S266.
2. Sarnak MJ, Levey AS, Schoolwerth AC, Coresh J, Culleton B, Hamm LL, *et al*.; American Heart Association Councils on Kidney in Cardiovascular Disease, High Blood Pressure Research, Clinical Cardiology, and Epidemiology and Prevention. Kidney disease as a risk factor for development of cardiovascular disease: A statement from the American Heart Association councils on kidney in cardiovascular disease, high blood pressure research, clinical cardiology, and epidemiology and prevention. Circulation 2003;108:2154-69.
3. Diercks GF, van Boven AJ, Hillege JL, de Jong PE, Rouleau JL, van Gilst WH. The importance of microalbuminuria as a cardiovascular risk indicator: A review. Can J Cardiol 2002;18:525-35.
4. Alberti KG, Zimmet PZ. Definition, diagnosis and classification of diabetes mellitus and its complications. Part 1: Diagnosis and classification of diabetes mellitus provisional report of a WHO consultation. Diabet Med 1998;15:539-53.
5. Alberti KG, Eckel RH, Grundy SM, Zimmet PZ, Cleeman JI, Donato KA, *et al*.; International Diabetes Federation Task Force on Epidemiology and Prevention; National Heart, Lung, and Blood Institute; American Heart Association; World Heart Federation; International Atherosclerosis Society; International Association for the Study of Obesity. Harmonizing the metabolic syndrome: A joint interim statement of the international diabetes federation task force on epidemiology and prevention; national heart, lung, and blood institute; American Heart Association; world heart federation; international atherosclerosis society; and international association for the study of obesity. Circulation 2009;120:1640-5.
6. Ramkumar N, Cheung AK, Pappas LM, Roberts WL, Beddhu S. Association of obesity with inflammation in chronic kidney disease: A cross-sectional study. J Ren Nutr 2004;14:201-7.
7. Deferrari G, Repetto M, Calvi C, Ciabattoni M, Rossi C, Robaudo C. Diabetic nephropathy: From micro- to macroalbuminuria. Nephrol Dial Transplant 1998;13:11-5.
8. Rosa TT, Palatini P. Clinical value of microalbuminuria in hypertension. J Hypertens 2000;18:645-54.
9. Jones CA, Francis ME, Eberhardt MS, Chavers B, Coresh J, Engelgau M, *et al*. Microalbuminuria in the US population: Third national health and nutrition examination survey. Am J Kidney Dis 2002;39:445-59.
10. Sun K, Kusminski CM, Scherer PE, Sun K, Kusminski CM, Scherer PE. Adipose tissue remodeling and obesity find the latest version : Review series Adipose tissue remodeling and obesity. J Clin Invest 2011;121:2094-101.
11. Tang J, Yan H, Zhuang S. Inflammation and oxidative stress in obesity-related glomerulopathy. Int J Nephrol 2012;2012:1-11.
12. Wolf G, Chen S, Han DC, Ziyadeh FN. Leptin and renal disease. Am J Kidney Dis 2002;39:1-11.
13. Anil Kumar P, Swathi Chitra P, Bhanuprakash Reddy G. Metabolic syndrome and associated chronic kidney diseases: Nutritional interventions. Rev Endocr Metab Disord 2013;14:273-86.
14. Weisinger JR, Kempson RL, Eldridge FL, Swenson RS. The nephrotic syndrome: A complication of massive obesity. Ann Intern Med 1974;81:440-7.
15. Hoffmann IS, Jimenez E, Cubeddu LX. Urinary albumin excretion in lean, overweight and obese glucose tolerant individuals: Its relationship with dyslipidaemia, hyperinsulinaemia and blood pressure. J Hum Hypertens 2001;15:407-12.
16. Nielsen S, Jensen MD. Relationship between urinary albumin e x c retion, body composition, and hyperinsulinemia in normotensive glucose - tolerant adults. Diabetes Care 1999;22:1728-33.
17. Schwartz GL, Sheps SG. A review of the sixth report of the joint national committee on prevention, detection, evaluation, and treatment of high blood pressure. Curr Opin Cardiol 1999;14:161-8.
18. Fouad M, Ismail MI, Gaballah A, Reyad E, ELdeeb S. Prevalence of obesity and risk of chronic kidney disease among young adults in Egypt. Indian J Nephrol 2016;26:413-8.
19. Singh AK, Kari JA. Metabolic syndrome and chronic kidney disease. Curr Opin Nephrol Hypertens 2013;22:198-203.
20. Chang Y, Yoo T, Ryu S, Huh BY, Cho BL, Sung E, *et al*. Abdominal obesity, systolic blood pressure, and microalbuminuria in normotensive and euglycemic Korean men. Int J Obes (Lond) 2006;30:800-4.
21. Yesim TE, Ugurlu S, Caglar E, Balci H, Ucgul A, Sarkis C, *et al*. Investigation of microalbuminuria in nondiabetic, normotensive obese women. Intern Med 2007;46:1963-5.
22. Shigematsu Y, Norimatsu S, Ogimoto A, Ohtsuka T, Okayama H, Higaki J. The influence of insulin resistance and obesity on left atrial size in Japanese hypertensive patients. Hypertens Res 2009;32:500-4.
23. Foster MC, Hwang SJ, Massaro JM, Hoffmann U, DeBoer IH, Robins SJ, *et al*. Association of subcutaneous and visceral adiposity with albuminuria: The Framingham heart study. Obesity (Silver Spring) 2011;19:1284-9.
24. Wang Z, Hoy WE. Body size measurements as predictors of type 2 diabetes in aboriginal people. Int J Obes Relat Metab Disord 2004;28:1580-4.

Antioxidant Activity Evaluation of Methanolic Leaf Extracts of Krishna Estuary Mangroves, Andhra Pradesh., India

P Suneeta*[1], Nageswara Rao Naik B[2], D Jyothi[3], Z Vishnuvardhan[4]

1. *Department of Microbiology, Government College (Autonomous), Rajahmundry, Andhra Pradesh.*
2. *Department of Environmental sciences, Acharya Nagarjuna University, Guntur, Andhra Pradesh.*
3. *Department of Botany SRR & CVR Govt.college Vijayawada Andhra Pradesh.*
4. *Department of Botany and Microbiology, Acharya Nagarjuna University, Guntur, Andhra Pradesh.*

Abstract: *Antioxidants are vital substances that protect the body from damages caused by free radical-induced oxidative stress. A variety of natural antioxidants are found in plants. The present study is aimed at assessment of relative antioxidative potential of methanolic leaf extracts of eight mangrove species. Four different assays have been used to determine the best mangrove with superior antioxidant capacity. B. gymnorrhiza is adjudged as the best species. E. agallocha, A. marina, A. officinalis and A. rotundifolia exhibited moderate activity, where as less antioxidant activity is recorded in A. corniculatum, R. apiculata and B. cylindrica.*

Key words: *Krishna Estuary mangroves, phenolic content, Reducing power, Oxidative stress, Antioxidants.*

1. INTRODUCTION

Free radicals/oxidants are being produced with enhanced rate during oxidative stress in organisms. The family of free radicals generated from the oxygen is known as 'Reactive Oxygen Species (ROS) and responsible for many diseases. Antioxidants are important since they offer protection to organisms from damage caused by free radical ROS. The antioxidants present in plants offer considerable resistance to oxidative damage caused by ROS. Mangrove plants are rich in phytochemicals capable of removing free radicals before they cause damage. Therefore the present study is aimed at evaluation of antioxidant potential of eight mangrove species. Antioxidant potential of mangrove species is assessed through four different assays evaluation of viz., i) DPPH free radical scavenging ii) reducing power iii) total phenolic content and iv) total antioxidant activity.

2. Materials and Methods

Eight mangrove species were collected from Krishna estuary, Nagayalanka, Andhra Pradesh, India which is located between latitude $15^{0}15^{1}$ - $15^{0}55$N and $80^{0}45^{1}$-81^{1}00E longitude. The plant material were identified to their species level with the help of available flora. The plant specimens were preserved in the dept. of Botany & Microbiology, Acharya Nagarjuna University. Methanolic leaf extracts of eight mangrove species constitute the materials for the present study.

Preparation of plant extract

Leaves of eight mangroves were air dried at room temperature to constant weights. The dried plant materials were ground separately to powder. 100 gms of each ground plant materials were shaken separately in methanol for 48 hrs on an orbital shaker. Extracts were filtered using a

whatman No. 1 filter paper. Each filtrate was concentrated by soxhlet apparatus and each extract was resuspended in methanol to make 100 mg/ml stock solution.

DPPH free radical activity

Diphenyl Picryl Hydrozyl radical scavenging assay was determined by Bamionuri *et al*., 2010. Briefly, 5 ml of DPPH solution (0.004%) in methanol was added to 50 µl of plant extract. After 30 minutes of incubation period at room temperature, the absorbance was read against a blank containing sample and methanol at 517 nm. Control containing the buffer and reagent was carried out. Similarly positive controls were treated in the same way as test sample replaced by positive control. Butyl Hydroxyl Touline (BHT) used as positive control. Inhibition (I) of Diphenyl Picryl Hydroxyl radical was calculated in the following way.

$$\text{Percentage of inhibition (I)} = \frac{\text{Absorbance of control} - \text{Absorbance of test}}{\text{Absorbance of control}} \times 100$$

Total Phenolic compounds estimation

The total phenolic contents in the extract, was determined by Bomaniri *et al*., 2010 with minor modifications, including gallic acid as standard and Folincioculteau reagent. To 2.5 ml of 10% Folincioculteau reagent 2 ml of Na_2CO_3 (2%, w/v) was added to 0.1 ml of each sample (3 replicates) of plant extract solution (1 mg/ml). The resulting mixture was incubated at 45^0C with shaking for 15 minutes. The absorbance of the sample was measured at 765 nm using Uv/visible light. Results were expressed as mgs of Gallic acid (20-100 µg/ml) dissolved in water.

Reducing Power assay (RP)

The reducing power of the extracts was determined according to the method of Oyaizu (1986). Extracts (100 ml) of mangrove plant parts were mixed with phosphate buffer (2.5ml, 0.2M, pH 6.6) and 1% Potassium Ferricyanide (2.5 ml). The mixture was incubated at 50^0C for 20 minutes. Aliquots of 10% trichloroacetic acid (2.5 ml) were added to the mixture, which was then centrifuged at 3000 rpm for 10 minutes. The upper layer of the solution (2.5 ml) was mixed with distilled water (2.5 ml) and freshly prepared ferric chloride solution (0.5 ml, 0.1%). The absorbance was measured to 700 nm. Reducing power in given in ascorbic acid equivalent (AAE) in milligram per gram of dry material.

Total Antioxidant activity

It is determined by the conjugated diene method of Lingnert *et al* (1979). The extract is mixed with 2 ml of 10 mN linoleie acid emulsion in 0.2 M sodium phosphate buffer (P^H 6.6) and kept in dark at $37^{0C.}$ After 15 hrs of incubation, 0.1 ml from each tube is mixed with 7.0 ml of 80% methanol. The absorbance is read at 234 nm against blank in spectrophotometer. Antioxidant activity (%) = $\frac{AO-A1}{AO} \times 100$ where AO is the absorbance of control-A1 is the absorbance of test. Phenol is the positive control.

3. Results and Discussion

Total phenolic content and total antioxidant activity of methanolic leaf extracts of eight mangrove species are presented in table1. Leaf extract concentrations raging from 100µg to 500 µg were subjected to above assessment. 100 µg methanolic extract of *B. cylindrica* contained less

amount of phenolic substances (34.26 µg) and it was proportionately increased with an increase in extract concentration up to 500 µg in all the species. 500 µg leaf extract of *B. gymnorrhiza* contained the maximum quantity (95.62 µg) of phenolics followed by *E. agalloch* (84 µg), *A. marina* (82.78 µg), *A. rotundifolia* (82.62 µg), *A. officinalis* (79.09 µg), *A. corniculatum* (63.03 µg) *R. apiculata* (62.32 µg) and *B. cylindrica* (52.97 µg).

Total antioxidant activity of 500 µg extract of *B. gymnorrhiza* was found be maximum (93.24%) and it was minimum in *B. cylindrica* extract (52.87%). The other species viz., *E. agallocha, A. rotundifolia* and *A. marina* were rated next to *B. gymnorrhiza* with the range of antioxidant activity between 79.42 to 84.48%.

The DPPH free radical scavenging activity of eight mangroves is presented in table 2. Free radical inhibition percent of mangrove extracts was increased steadly with an increase in extract concentration of mangroves from 100 µg to 500 µg. The free radical scavenging activity of *B. gymnorrhiza* 500 µg extract of excelled other species with 93.15% inhibition *A. corniculatum* extract (500µg) showed the minimum inhibition (62.97%) of DPPH radical while the other six species manifested the DPPH radical scavenging in the range from 72.09% to 75.3%.

Reducing power of the mangroves extracts was presented in the table2. 500µg extract of *A. corniculatum* has the lowest percent (65.82) of reducing power, where as *B. gymnorrhiza* expressed the highest percent (89.71%) of reducing power. The remaining six mangroves exhibited moderate reducing power rangining between 80.41% and 86.48%.

Discussion

Plants serve as a reservoir of effective chemotherapentants. Organisms are equipped with antioxidant system via many natural compounds and enzymes. In addition to the inherent mechanisms, exist in organisms, they must be sometimes supplemented through diet. In this context natural antioxidants from plants appear to be the solution to mitigate the effects of oxidative stress. Hence, there is growing demand for antioxidants from plants. The plant based antioxidants belong to different classes ranging from carotenoids, flavonoids, polyphenols, galic acid derivatives, tannins and catechins.

According to Miles *et al* (1998) mangroves have been considered as great source for chemical compounds of potential value. The flavonoids and polyphenolic compounds are powerful antioxidants due to the presence of C_4-C_7 hydroxyl groups that act as hydrogen donors. The phenolic compounds and flavonoids have positive correlation with free radical scavenging activity (Cushnie &Andrew 2005; Bandini *et al* 2006; Deepanjan *et al* 2008).

The results of present study comprehensively revealed that *B. gymnorrhiza* possess greater antioxidant potential since its extract contain the highest DPPH free radical scavenging activity, reducing power, phenolic content and total antioxidants. Mldadulal Haq *et al* (2011) and Kiran Kumar & Sitaram (2013) also found the highest antioxidant activity in *B. gymnorrhiza.* Moderate antioxidant activity was found in *E. agalloch, A. marina*, *A. officinalis* and *A. rotundifolia*. Relatively less antioxidant activity was recorded in *A. corniculatum*, *R. apiculata* and *B. cylindrica.* In the mangroves of present study Suneeta (2020) reported the presence of flvonoids, terpenoids and hydrocarbons (alkanes and alkenes). Hence, the compounds may be responsible for the antioxidant activity of eight mangrove species in the present study.

Table 1: Total phenolic content and Antioxidant activity of methanolic leaf extracts of eight mangrove species

S.No	Name of the Mangrove species	PHENOLIC CONTENT (µg)					TOTAL ANTIOXIDANT ACTIVITY (%)				
		Extract conc. in µg					Extract conc. in µg				
		100	200	300	400	500	100	200	300	400	500
1	***A.corniculatum***	49.20	54.16	56.92	60.91	63.03	48.09	54.90	59.72	62.27	63.23
2	***A. Marina***	42.76	51.37	68.78	73.23	82.78	33.06	45.21	54.31	76.09	79.42
3	***A. officinalis***	44.02	64.21	65.62	68.78	79.09	23.53	34.06	57.71	59.23	64.34
4	***A. rotundifolia***	51.32	66.42	67.53	73.09	82.62	32.05	49.62	52.23	71.64	82.32
5	***B. cylindrica***	34.26	38.04	49.82	50.20	52.97	33.09	42.32	48.08	51.03	52.87
6	***B. gymnorrhiza***	42.03	73.92	77.62	81.93	95.62	15.87	32.34	50.27	71.14	93.24
7	***E. agallocha***	41.05	57.42	73.92	78.09	84.00	26.52	38.32	59.15	72.62	84.48
8	***R. apiculata***	42.26	54.31	56.42	59.51	62.32	35.57	39.61	42.62	57.43	62.21

Table. 2 : DPPH free radical scavenging and Reducing Power (RP) activity of methanolic leaf extracts of eight mangrove species.

S.No	Name of the Mangrove species	DPPH (%)					REDUCING POWER (%)				
		Extract conc. in µg					Extract conc. in µg				
		100	200	300	400	500	100	200	300	400	500
1	***A. corniculatum***	12.50	21.03	35.01	54.19	62.97	43.23	56.32	58.78	59.04	65.82
2	***A. Marina***	10.90	21.23	34.20	49.52	73.12	42.34	56.28	69.31	74.71	80.41
3	***A. officinalis***	15.25	29.36	46.97	61.06	72.80	42.26	58.29	73.34	78.62	86.48
4	***A. rotundifolia***	13.23	19.31	34.90	47.73	75.30	43.03	50.52	66.25	79.62	82.02
5	***B. cylindrica***	11.08	23.32	35.03	52.13	69.16	46.56	59.23	62.31	71.52	72.09
6	***B. gymnorrhiza***	15.76	32.73	50.35	71.92	93.15	32.98	55.73	62.35	74.82	89.71
7	***E. agallocha***	12.90	26.23	38.20	51.00	75.12	44.06	74.12	74.51	81.32	84.41
8	***R. apiculata***	9.27	20.00	35.23	43.41	72.09	50.62	62.59	74.26	76.31	85.23

References

[1] Bamoniri A, Ebrahimabadi AH, Mazochi A, Behpour M, Kashi FJ and Batooli H (2010). Antioxidant and Antimicrobial activity evaluation and essential oil analysis of Semenovia tragioides Bioss. From Iran. *Food Chem*. 122 ; 553-8.

[2] Bandini A and Cerrestanil Pizolante L (2006). Phenol content related to Antimicrobial and antioxidant activity of *Passiflora* species Extracts. *European Food Research Technology* 223: 102-109.

[3] Cushnie TPT and Andrew JL (2005). Antimicrobial activity of flavonoids. *International Journal of antimicrobial agents* 26: 343-356.

[4] Deepanjan Banerjee, Shrabana Chakrabarti, Alok K Hazra, Shivaji Banerjee, Jharna Ray and Biswapati Mukherjee(2008). Antioxidant activity and total phenolics of some mangroves in Sundarbans. *African Journal of Biotechnology Vol.* 7(6): pp. 805-810.

[5] Kiran Kumar, Mundla and Sitaram, B (2013). Comparative Study of Phytochemical, Antimicrobial, Cytotoxic and antioxidant Activities in *Blepharis genus* plant Seeds. *IJSIT*. 2(1): 07-20.

[6] Miles DH, Kokpal U, Chittawong V, Tip-Pyang S, Tunsuwan K and Nguyen C (1998). Mangrove forests – The importance of conservation as a bioresource for ecosystem diversity and utilization as a source of chemical constituents with potential medicinal and agricultural value. *IUPAC* 70 (11): 1-9.

[7] Mldadul Haq, Wirakarnain Sani, Hossain ABMS, Rosna Mat Taha and Monneruzzaman KM (2011). Total phenolic contents, antioxidant and antimicrobial activities of *Bruguiera gymnorrhiza. Journal of Medicinal Plants Research* Vol. 5(17): 4112-4118.

[8] Suneeta .P (2010).Ph. D Thesis entitled Antibacterial, Antioxidant and phytochemical studies of certain mangroves of Krishna district, Andhra Pradesh.

SRR & CVR GOVERNMENT DEGREE COLLEGE(A) VIJAYAWADA

DEPARTMENT OF POLITICAL SCIENCE & PUBLIC ADMINISTRATION

WORKSHOP ON IMPLEMENTATION OF RTI ACT 2005

7th March 2021

The Department of Political Science & Public Administration conducted one day workshop to create awareness on the Right To Information Act 2005 (RTI 2005) and changes brought recently. The council for citizen's rights, civil and human rights protection Non-Government Organisation has also participated to air their views and issues.

The AP Chief Information Officer Rtd. Sri Ramesh Kumar IAS and AP Information Officer Sri Srinivasu attended the workshop and addressed the RTI activists of 13 districts across Andhra Pradesh. Activists of 126 from 13 districts participated enthusiastically and expressed their own experiences. Dr.Illa Ravi, principal of the college spoke on the awareness and importance campaign on the Right to Information.





Dr.DSVS.Balasubrahmanyam, Associate Professor of the Political science department welcomed the dignitaries and spoke about the importance of the RTI Act with examples of his own experience. The Right to Information Act, simply known as RTI, is a revolutionary act that aims to promote transparency in government institutions in India. The Act came into existence in 2005, after sustained efforts of anti-corruption activists. RTI or Right to Information Act is a fundamental right and is an aspect of Article 19 (1)(a) of the Indian Constitution.

Right to Information replaced the Freedom of Information Act, 2002. Grounds for Rejection of RTI There are only three possible grounds on which information can be denied: The organisation is not a Public authority - eg. a Cooperative Society, or a Private corporate or Institution, not substantially financed or controlled by the Government.



The AP Chief Information Officer Rtd. Sri Ramesh Kumar IAS addressed the workshop. He informed the various provisions and sections of RTI Act sub-section (1) of section 4, sub-sections (1) and (2) of section 5, sections 12, 13, 15,16, 24, 27 and 28 shall come into force at once, and the remaining provisions of this Act shall come into force on the one hundred and twentieth day of its enactment. Issue of Enforceability as he said the Act does not give adequate authority to the Information Commissions to enforce their decisions. Information commissions can give directions to public authorities to take the steps necessary to comply with the Act but are not empowered to take any action if such directions are ignored. Situations for filing First Appeals and prescribed Time Limits. 1. PIO did not respond within 30 days from receipt of RTI Application in his office. After 30 (+7 days for postal transit time) but within 60 days from the date of receipt of RTI Application at PIO's Office. You may only ask for specific information under the RTI Act, 2005 rather than questioning the action of public authority. ' The RTI act does not state that queries must not be answered, nor does it stipulate that prefixes such as 'why, what, when and whether' cannot be used.

స.హ.చట్టాన్ని వినియోగించుకోవాలి

మధురానగర్(విజయవాడ సెంట్రల్): సమాచార హక్కు చట్టాన్ని సమాజ హితం, సమాజ అభివృద్ధి కోసం వినియోగించుకోవాలని రాష్ట్ర ముఖ్య సమాచార కమిషనర్ పీ రమేష్‌కుమార్ సూచించారు. స్థానిక మాచవరం ఎస్ఆర్ఆర్ అండ్ సీవీఆర్ ప్రభుత్వ డిగ్రీ కళాశాలలో కౌన్సిల్ ఫర్ సిటిజన్ రైట్స్ పౌర, మానవ హక్కుల స్వచ్ఛంద సంస్థ సహకారంతో సమాచార హక్కు చట్టంపై అవగాన సదస్సు శనివారం నిర్వహించారు. కార్యక్రమంలో ఆయన ముఖ్య అతిథిగా పాల్గొని సమాచార హక్కు చట్టం గురించి వివరించారు. ఆర్‌టీఐ యాక్ట్ ప్రకారం ఐఏఎస్, ఐపీఎస్ తరహాలో రికార్డులు తనిఖీ చేయవచ్చని, గ్రామ పరిధి నుంచి రాష్ట్ర కేంద్ర స్థాయి వరకు సహ చట్టాన్ని వినియోగించి సమాచారం తీసుకోవచ్చని తెలిపారు. ఏపీ సమాచార కమిషనర్ రేపాల శ్రీనివాస్, ఎన్.హరినాథ్, మంచికట్ల అనిల్‌కుమార్, కళాశాల ప్రిన్సిపాల్ డాక్టర్ ఇళ్ల రవి మాట్లాడారు. కార్యక్రమాన్ని రాజనీతి శాస్త్ర విభాగం అధ్యాపకులు డాక్టర్ డీఎస్‌వీఎస్ బాలసుబ్రహ్మణ్యం, అధ్యాపకులు పర్యవేక్షించారు.



అవగాహన సదస్సులో వక్తలు

సాక్షి Sun, 07 March 2021
https://epaper.sakshi.com/c/58923625

The RTI act influence on people and impact on Indian Administration in greater Transparency in functioning of public authorities: disclosure of information regarding government rules, regulations and decisions, every public authority is mandated to 'maintain all records duly catalogued and indexed. “Improving Transparency and Accountability in Government through effective implementation of Right to Information

It was published in the paper that the CIO stressed that the RTI Act was promulgated in October 2005 to ensure transparency and good governance in the country. Based on content analysis and depth interviews with a few bureaucrats and activists, the paper indicates that RTI Act has succeeded in reducing information asymmetries and exposing corruption.

In the last 15 years, at least 86 people who had filed RTI applications have been killed while 175 others have been attacked. At least seven applicants committed suicide while 184 applicants reported being harassed.

అవినీతి రహిత భారతదేశానికి ఆర్టిఐ యాక్ట్ ఓ ఆయుధం

(వార్తామండలి ప్రతినిధి)

విజయవాడ: రాష్ట్రంకానీ దేశంకానీ అవినీతి రహితంగా నిలబడడానికి ఆర్టిఐ యాక్ట్ ఆయుధంగా ఉపయోగపడుతుందని రాష్ట్ర ముఖ్య సమాచార కమిషనర్ విశ్రాంత ఐ ఏ ఎస్ అధికారి పి. రమేష్ కుమార్ అన్నారు. కౌన్సిల్ ఫర్ సిటిజెన్ రైట్స్ ఆధ్వర్యంలో విజయవాడ నగరంలోని ఎస్ ఆర్ ఆర్ అండ్ సివిఆర్ కళాశాలలో అవగాహన సదస్సు సి సి ఆర్ అధికార ప్రతినిధి వ్యవస్థాపకులు మాచి కట్ల అనిల్ కుమార్ అధ్యక్షతన జరిగింది. ముఖ్య అతిథి రమేష్ కుమార్ మాట్లాడుతూ కళాశాల ప్రిన్సిపాల్ అధ్యాపక ఉపాధ్యాయులు ఆర్ టి ఐ యోధులను తయారుచేయడం అభినందనీయమన్నారు. ఆర్టిఐ యాక్ట్ సద్వినియోగం వలన ఎన్నో ఫలితాలు ఉంటాయన్నారు. అదే ఆర్టిఐ యాక్ట్ ను దుర్వినియోగం చేస్తే ఆర్టిఐ యాక్ట్ నిర్వీర్యం అవుతుందన్నారు.ఆర్ టి ఐ అవగాహన సదస్సు విజయవంతం అవడం అభినందనీయ మన్నారు. మరో ముఖ్య అతిథి రేపాక శ్రీనివాసరావు, ఎన్ హరినాథ్ ఆర్టిఐ చట్టం విధివిధానాలను అవగాహన సదస్సులో వివరించారు, ఈ కార్యక్రమంలో కళాశాల ప్రిన్సిపాల్ డాక్టర్ రవిని జ్ఞాపికతో సన్మానించారు. అవగాహన సదస్సుకు వచ్చిన అతిథులకు షీల్డులు బహుకరించారు. ఆర్టిఐ కార్యకర్తలకు సర్టిఫికెట్లు ప్రధానోత్సవం చేశారు. అవగాహన సదస్సులో హైకోర్టు అడ్వకేట్, సి సి ఆర్ లీగల్ అడ్వైజర్ అనిల్ వైద్య ప్రసంగించారు. కెట్టీ రామకృష్ణ, పావులూరి కోటేశ్వరరావు, ఇ లక్ష్మీ ప్రశాంత్, బి మహేష్, శ్రీనివాస రావు సభా నిర్వాహకులుగా వ్యవహరించారు. ఈ కార్యక్రమంలో విద్యార్థినీ విద్యార్థులు ఉపాధ్యాయులు తదితరులు పాల్గొన్నారు.



SRR & CVR GOVERNMENT DEGREE COLLEGE(A) VIJAYAWADA

DEPARTMENT OF POLITICAL SCIENCE & PUBLIC ADMINISTRATION

WORKSHOP ON IMPLEMENTATION OF RTI ACT 2005

7th March 2021

The department of Political Science & Public Administration conducted one day workshop to create awareness on the Right To Information Act 2005 (RTI 2005) and changes brought recently. The council for citizen's rights, civil and human rights protection Non-Government Organisation has also participated to air their views and issues.

The AP Chief Information Officer Rtd. Sri Ramesh Kumar IAS and AP Information Officer Sri Srinivasu attended the workshop and addressed the RTI activists of 13 districts across Andhra Pradesh. Activists of 126 from 13 districts participated enthusiastically and expressed their own experiences. Dr.Illa Ravi, principal of the college spoke on the awareness and importance campaign on the Right to Information.





Dr.DSVS.Balasubrahmanyam, Associate Professor of the Political science department welcomed the dignitaries and spoke about the importance of the RTI Act with examples of his own experience. The Right to Information Act, simply known as RTI, is a revolutionary Act that aims to promote transparency in government institutions in India. The Act came into existence in 2005, after sustained efforts of anti-corruption activists. RTI or Right to Information Act is a fundamental right and is an aspect of Article 19 (1)(a) of the Indian Constitution. Right to Information replaced the Freedom of Information Act, 2002. Grounds for Rejection of RTI There are only three possible grounds on which information can be denied: The organisation is not a Public authority - eg. a Cooperative Society, or a Private corporate or Institution, not substantially financed or controlled by the Government.



The AP Chief Information Officer Rtd. Sri Ramesh Kumar IAS addressed the workshop. He informed the various provisions and sections of RTI Act sub-section (1) of section 4, sub-sections (1) and (2) of section 5, sections 12, 13, 15,16, 24, 27 and 28 shall come into force at once, and the remaining provisions of this Act shall come into force on the one hundred and twentieth day of its enactment. Issue of Enforceability as he said the Act does not give adequate authority to the Information Commissions to enforce their decisions. Information commissions can give directions to public authorities to take the steps necessary to comply with the Act, but are not empowered to take any action if such directions are ignored.

Situations for filing First Appeals and prescribed Time Limits. 1. **PIO did not respond within 30 days from receipt of RTI Application in his office**. After 30 (+7 days for postal transit time) but within 60 days from the date of receipt of RTI Application at PIO's Office. You may only ask for **specific information** under RTI Act, 2005 rather than questioning the action of public authority. ' The RTI act does not state that queries must not be answered, nor does it stipulate that prefixes such as 'why, what, when and whether' cannot be used.



స.హ.చట్టాన్ని వినియోగించుకోవాలి

మధురానగర్(విజయవాడ సెంట్రల్): సమాచార హక్కు చట్టాన్ని సమాజ హితం, సమాజ అభివృద్ధి కోసం వినియోగించుకోవాలని రాష్ట్ర ముఖ్య సమాచార కమిషనర్ పీ రమేష్‌కుమార్ సూచించారు. స్థానిక మాచవరం ఎస్‌ఆర్‌ఆర్ అండ్ సీవీఆర్ ప్రభుత్వ డిగ్రీ కళాశాలలో కౌన్సిల్ ఫర్ సిటిజన్ రైట్స్ పౌర, మానవ హక్కుల స్వచ్ఛంద సంస్థ సహకారంతో సమాచార హక్కు చట్టంపై అవగాన సదస్సు శనివారం నిర్వహించారు. కార్యక్రమంలో ఆయన ముఖ్య అతిథిగా పాల్గొని సమాచార హక్కు చట్టం గురించి వివరించారు. ఆర్‌టీఐ యాక్ట్ ప్రకారం ఐఏఎస్, ఐపీఎస్ తరహాలో రికార్డులు తనిఖీ చేయవచ్చని, గ్రామ పరిధి నుంచి రాష్ట్ర కేంద్ర స్థాయి వరకు సహ చట్టాన్ని వినియోగించి సమాచారం తీసుకోవచ్చని తెలిపారు. ఏపీ సమాచార కమిషనర్ రేపాల శ్రీనివాస్, ఎన్‌మారి

అవగాహన సదస్సులో వక్తలు

నాథ్, మంచికట్ల అనిల్‌కుమార్, కళాశాల ప్రిన్సిపాల్ డాక్టర్ ఇళ్ల రవి మాట్లాడారు. కార్యక్రమాన్ని రాజనీతి శాస్త్ర విభాగం అధ్యాపకులు డాక్టర్ డీఎస్‌వీఎస్ బాలసుబ్రహ్మణ్యం, అధ్యాపకులు పర్యవేక్షించారు.

సాక్షి Sun, 07 March 2021
https://epaper.sakshi.com/c/58923625



అవినీతి రహిత భారతదేశానికి ఆర్టిఐ యాక్ట్ ఓ ఆయుధం

(వార్తామండలి ప్రతినిధి)

విజయవాడ: రాష్ట్రంకానీ దేశంకానీ అవినీతి రహితంగా నిలబడడానికి ఆర్టిఐ యాక్ట్ ఆయుధంగా ఉపయోగపడుతుందని రాష్ట్ర ముఖ్య సమాచార కమిషనర్ విక్రాంత్ ఐ ఏ ఎస్ అధికారి పి. రమేష్ కుమార్ అన్నారు. కౌన్సిల్ ఫర్ సిటిజన్ రైట్స్ ఆధ్వర్యంలో విజయవాడ నగరంలోని ఎస్ ఆర్ ఆర్ అండ్ సివిఆర్ కళాశాలలో అవగాహన సదస్సు సి సి ఆర్ అధికార ప్రతినిధి వ్యవస్థాపకులు మాచి కట్ల అనిల్ కుమార్ అధ్యక్షతన జరిగింది. ముఖ్య అతిథి రమేష్ కుమార్ మాట్లాడుతూ కళాశాల ప్రిన్సిపాల్ అధ్యాపక ఉపాధ్యాయులు ఆర్ టి ఐ యోధులను తయారుచేయడం అభినందనీయమన్నారు. ఆర్టిఐ యాక్ట్ సద్వినియోగం వలన ఎన్నో ఫలితాలు ఉంటాయన్నారు. అదే ఆర్టిఐ యాక్ట్ ను దుర్వినియోగం చేస్తే ఆర్టిఐ యాక్ట్ నిర్వీర్యం అవుతుందన్నారు.ఆర్ టి ఐ అవగాహన సదస్సు విజయవంతం అవడం అభినందనీయ మన్నారు. మరో ముఖ్య అతిథి రేపాక క్రీనివాసరావు, ఎన్ హరినాథ్ ఆర్టిఐ చట్టం విధివిధానాలను అవగాహన సదస్సులో వివరించారు, ఈ కార్యక్రమంలో కళాశాల ప్రిన్సిపాల్ డాక్టర్ రవిని జ్ఞాపికతో సన్మానించారు. అవగాహన సదస్సుకు వచ్చిన అతిథులకు పీట్లులు బహుకరించారు. ఆర్టిఐ కార్యకర్తలకు సర్టిఫికెట్లు ప్రధానోత్సవం చేశారు. అవగాహన సదస్సులో హైకోర్టు అడ్వకేట్, సి సి ఆర్ లీగల్ అడ్వైజర్ అనిల్ వైద్య ప్రసంగించారు. శెట్టి రామకృష్ణ, పావులూరి కోటేశ్వరరావు, ఇ లక్ష్మీ ప్రశాంత్, బి మహేష్, శ్రీనివాస రావు సభా నిర్వాహకులుగా వ్యవహరించారు. ఈ కార్యక్రమంలో విద్యార్థినీ విద్యార్థులు ఉపాధ్యాయులు తదితరులు పాల్గొన్నారు.

KINETICS OF OXIDATION OF P-PHENYLENE DIAMINE BY 2,6-DICHLORO QUININE-4-CHLORO-IMIDE

Dr. Neeraja Valluru

Dept . of chemistry ,SRR &CVR Government Degree College (A) , Vijayawada.
Email: neeraja2812@gmail.com

Sailaja Valluru

Dept. of ChemsitryP.BSiddartha College of Arts & Science (A) Vijayawada.

Received: Jan. 2020 Accepted: Feb. 2020 Published: Feb. 2020

Abstract: Gibbs reagent 2,6-dichloroquinone -4-chloro-imide (DCQCI) has been utilised for the estimation of phenols and pyridoxine for a quite number of years. Para-phenylene diamine (p-PDA) having two (1,4)-diamino functions attached to a benzene nucleus is well known to undergo a variety of oxidation or oxidative hydrolytic reactions in the presence of electron acceptors.The investigation mainly deals with the oxidation of p-phenylene diamine in aqueous AcOH – $HClO_4$ mixtures by 2,6-dichloroquinone-4-chloro-imide. The reaction is found to be first order in oxidising agent. The reaction is found to be second order in substrate. The reaction rate decreases with increasing the concentration of perchloric acid.

The most probable mechanistic scheme envisaged is that precursor intermediate complex being formed between the oxidant species and a molecule of unprotonated substrate species which in a rate determining step condenses with another molecule of the substrate to give intermediate product which in fast step gives final product.

Introduction and Scope: Gibbs reagent 2,6-dichloroquinone -4-chloro-imide (DCQCI) has been utilised for the estimation of phenols and pyridoxine for a quite number of years. The main reaction has been a coupling process leading to colour changes and thus colorimetry was extensively used for the assay of these compounds.Para-phenylene diamine (p-PDA) having two (1,4)-diamino functions attached to a benzene nucleus is well known to undergo a variety of oxidation or oxidative hydrolytic reactions in the presence of electron acceptors. The actual products of the reaction depend upon the reaction conditions employed: concentration, the nature of the oxidant, the acidity of the medium, the solvent system besides the relative ratios of the oxidant and substrate concentrations. The reactions of para-phenylene diamine are very complicated due to the availability of two donar nitrogen sites, and due to the subsequent reactions of the intermediate products not to mention of the additional complication of electrophilic attack at the nitrogen sites and at the nucleus.

P-Phenylene Diamine: The investigation mainly deals with the oxidation of p-phenylene diamine in aqueous AcOH – $HClO_4$ mixtures by 2,6-dichloroquinone-4-chloro-imide.

a) Dependence on Oxidant: The reaction is found to be first order in oxidising agent. Plot of log(a-x) vs time is linear up to three half lives of the reaction indicating first order dependence on oxidising agent .The kinetic data is given in Table 1.

Table 1

[p–PDA] = 12.5 x 10^{-3} M $[H^+]$ = 0.1 M
AcOH – H_2O = 10% - 90%(v/v) Temp = 35°C

Variant	[Variant] x 10^4 M	k_1 x 10^2 min^{-1}
DCQCI	2.5	10.7
	5.0	9.2
	10.0	10.1

b) Dependence on Substrate: The reaction is found to be second order in substrate. Plot of log k_1 vs log [S] is linear with slope two indicating second order dependence. The observation that the plot of $\frac{[S]}{k_1}$ vs $\frac{1}{[S]}$ is linear and passes through origin also confirms the second order dependence on substrate. Such second order dependence has been observed in the oxidation of p-phenylene diamine with I_3^-. The kinetic data is given Table -2.

Table 2:

[DCQCl] = 5.0×10^{-4} M $[H^+]$ = 0.1 M
AcOH – H_2O = 10% - 90%(v/v) Temp = 35°C

Variant	[Variant] x 10^3 M	$k_1 \times 10^2$ min^{-1}
p-phenylene diamine	3.1	0.25
	6.2	1.56
	12.5	9.23
	25.0	47.74

c) Dependence on Acid Concentration: The reaction rate decreases with increasing the concentration of perchloric acid. The reaction is found to be inverse mixed order. Plot of log k_1 vs log$[H^+]$ is linear with a slope of 1.5 . Plot of k_1 $[H^+]$ vs $\frac{1}{[H^+]}$ gives an intercept and slope . The intercept corresponds to first order component and slope corresponds to second order component. This explains the observed mixed order kinetics. The combination of first order kinetics and second order kinetics giving inverse dependence on $[H^+]$ gives resultant inverse 1.5 order on H^+. The kinetic data is given in Table: 3.

Table 3:

[DCQCl] = 5.0×10^{-4} M [p-PDA] = 12.5×10^{-3}M
AcOH – H_2O = 10% - 90% (v/v) Temp = 35°C

Variant	[Variant] x 10^2 M	$k_1 \times 10^2$ min^{-1}
$HClO_4$	5.0	33.2
	10.0	9.2
	20.0	6.0
	40.0	1.6

Effect of Varying Solvent Composition: The reactions have been carried out at varying solvent compositions to find the effect of change in dielectric constant. The reaction rate decreases with increase in concentration of acetic acid. This reaction essentially involves $H_2O\overset{+}{C}l$ and the dipolar molecule of the amine. This requires an increase in rate with decrease in dielectric constant. But the observation is reverse. Thus specific solvent effects probably are causing this observation. Probably the following factors like solvation, acidic or basic nature of the solvent, effect of solvent on molecular dispersion, non random distribution of the component of mixed solvent are responsible. Plot of log k_1 vs $\frac{1}{D}$ is linear (Fig.6). The kinetic data is given in Table-4.

Table 4:

[DCQCl] = 5.0×10^{-4} M $[H^+]$ = 0.1 M
[p-PDA] = $12.5\ 10^{-3}$ M Temp = 35°C

Variant	% of Variant	$k_1 \times 10^2$ min^{-1}
AcOH	5	10.5
	10	9.2
	20	6.1
	40	4.5

Effect of Temperature: The reactions are carried out at three different temperatures i.e., 35°C, 45°C and 55°C to compute various activation parameters. Plot of log k_1 vs $\frac{1}{T}$ is linear (Fig.7). The kinetic data is given in Table-5.

Table 5:

$[DCQCI] = 5.0 \times 10^{-4}$ M $[H^+] = 0.1$ M

$[p\text{-}PDA] = 12.5 \times 10^{-3}$ M AcOH - H_2O = 10% - 90% (v/v)

Variant	Change in Variant °C	$k_1 \times 10^2$ min^{-1}
Temperature	35	9.2
	45	13.8
	55	29.0

The derived Arrhenius parameters are given in Table 6.

Table 6:

Arrhenius Parameters at 308°K:

Compound	$\Delta E^{\neq}$ KJ/mole	$\Delta H^{\neq}$ KJ/mole	$-\Delta S^{\neq}$ JK^{-1} / mole	$\log_{10} P_Z$	$\Delta G^{\neq}$ KJ/mole.
p-phenylene diamine	44.18	41.4	130.44	6.45	81.65

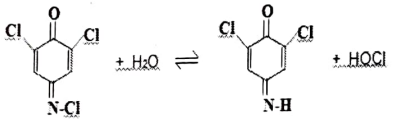
The kinetic features and net activation parameters do not provide any clue whether or not this reaction involves termolecular interactions.

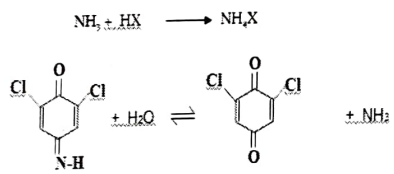
In as much the oxidant DCQCI is well known to function as a two electron oxidant. It is reasonable to assume that this reaction does not go through step wise one electron transfer which would mean that this reaction should go through radical path way. It appears that this mechanistic speculation involving radicals would impose large energy barrier, since a large number of nuclei-rearrangement should be required for radical formation and hence it is most unlikely that this reaction would proceed through radical path way.

The possibility that the rapid electron transfer from one of the substrate species to the oxidant species followed by rate determining condensation of the redox intermediate thus produced with the second substrate species is also unlikely as this mechanistic supposition would involve too many ionic species in an equilibrium step, and there should be much larger retardation with increase in H^+ than what has been observed experimentally.

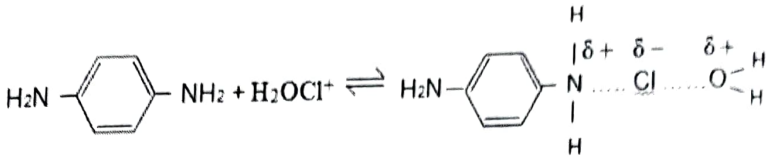
Mechanism and Rate Law: The most probable mechanistic scheme envisaged is that precursor intermediate complex being formed between the oxidant species and a molecule of unprotonated substrate species which in a rate determining step condenses with another molecule of the substrate to give intermediate product which in fast step gives final product.

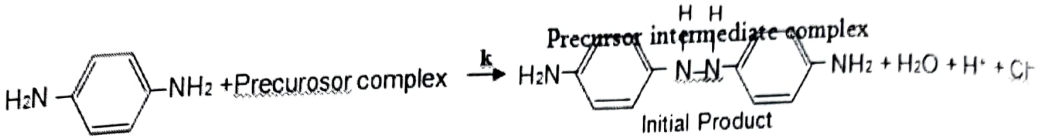
The sequence of reactions may be represented as follows.

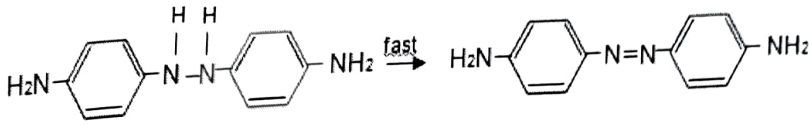




The most active species H_2OCl^+ produced in first hydrolytic step. The mechanistic path way involving the main oxidant species and substrate are given below.







The relevant rate law is derived as follows. The sequence of reactions of hydrolysis of DCQCI are given below.

2-6-dichloroquionone-4-chloro-imide + $H_2O \underset{}{\overset{Kh_1}{\rightleftharpoons}}$ 2,6-dichloroquionone-imide + HOCl

$$H^+ + HOCl \overset{K_p}{\rightleftharpoons} H_2O\overset{+}{Cl}$$

$$S + H^+ \overset{K_1}{\rightleftharpoons} SH^+$$

$$SH^+ + H^+ \overset{K_2}{\rightleftharpoons} SH^{+2}$$

$$S + H_2O\overset{+}{Cl} \overset{KC_1}{\rightleftharpoons} \text{Complex}_1$$

$$\text{Complex}_1 + S \xrightarrow[\text{slow}]{k} \text{Products}$$

$$\therefore \text{Rate} = k\,[C_1]\,[S]$$

$$= k.KC_1.[S]\,[S]\,[H_2O\overset{+}{Cl}]$$

$$= k.KC_1.K_p\,[S]^2\,[H^+]\,[HOCl]$$

$$S_T = S + SH^+ + SH^{+2}$$

$$= S + K_1\,[S]\,[H^+] + K_1.K_2[S]\,[H^+]^2$$

$$= S\,[1 + K_1H^+] + K_1K_2\,[S]\,[H^+]^2$$

by neglecting Square terms

$$S_T = S\,[1 + K_1H^+]$$

$$\therefore \text{Rate} = \frac{kKC_1K_p[S_T]^2[HOCl][H^+]}{[1+K_1H^+]^2}$$

$$= \frac{kKC_1K_p[S_T]^2[HOCl][H^+]}{[1+2K_1H^+ + K_1H^{+^2}]}$$

$$= \frac{kKC_1K_p[S_T]^2[HOCl]_T[H^+]}{[1+2K_1H^+ + K_1H^{+^2}][1+K_pH^+]}$$

Replacing $[HOCl]_T$ by DCQCI

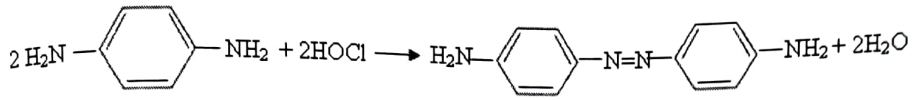
$$\therefore \text{Rate} = \frac{Kh_1kKC_1K_p[S_T]^2[DCQCl][H^+]}{\{1+2K_1H^+ + K_1H^{+2}\}\{1+K_pH^+\}}$$

If $1 < K_pH^+$ neglecting the second term in the denominator we get

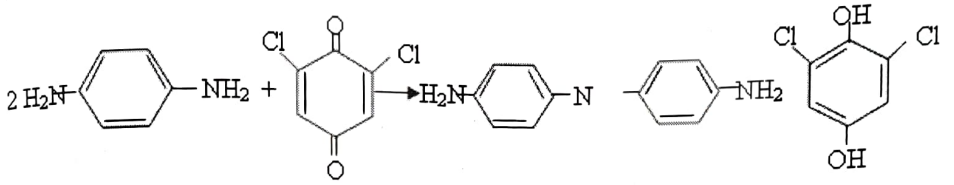
$$\therefore \text{Rate} = \frac{kKC_1[S_T]^2[DCQCl]}{\{1+2K_1H^+ + K_1H^{+2}\}}$$

The rate law explains the observed first order in oxidant, second order in substrate, and a mixed order in H^+ involving both first order component of H^+ and second order component in H^+ resulting in inverse 1.5 order in H^+.

Stoichiometric Studies: The product studies under the given set of conditions were performed and worked up as follows. The ratio of substrate-oxidant was maintained as 1:10. The reactants were mixed and the mixture was allowed to react over night. It has been found that two oxidant species HOCl and 2,6-dichloro benzoquinone interact causing oxidation to the products in a ratio 2:1 indicating that both the species interact finally giving.



Similarly



The experimental procedure is as follows.

The contents were treated with solid sodium bicarbonate until there was no evolution of carbon dioxide gas. The resultant mixture was extracted with diethyl ether, the solvent was evaporated from the ether layer and a minimum quantity of dilute HCl was added $(pH \sim 3)$.

The green colour solution was evaporated over a water bath to get a dirty green solid. This crude product was crystallized from absolute ethanol and filtered. The HCl from this salt was neutralized by treatment with a saturated solution of $NaHCO_3$, the green solid was filtered, washed well with water, recrystallised from absolute ethanol, vaccum-dried and desiccated.

References:

1. J.C. Panigrahy Ph.D.Thesis, Berhampur Univerity and references cited therein (1990)
2. L.N.Palo Ph.D.Thesis, Berhampur University and references cited therein (1990)
3. M.S.Ramachandran, T.S.Vivekanandam, N.R.Subbaratnam and N.Raja ram, Indian J.Chem., **22**, (1983) 895.
4. G.Grampp and W.Jaenicke, J.Chem.Soc., Faraday Trans-II **81**, (1985)1035.
5. A.Hunig and R.Richter, Chem Ber., **91**, (1958) 442; E.A.Burns, Anal.Chem., **32**, (1960) 1800; G.W.Ewing In '*Instrumental Methods of Chemical Analysis*'. 3rd ed., Mc.Graw Hill Kogakusha Ltd., Tokyo (1969) P.102.

***

Optik - International Journal for Light and Electron Optics 205 (2020) 164236

Contents lists available at ScienceDirect

Optik

journal homepage: www.elsevier.com/locate/ijleo

Original research article

Optical, electrical and photoluminescence studies on Al_2O_3 doped PVA capped ZnO nanoparticles for optoelectronic device application

Ravindranadh Koutavarapu[a], R.K.N.R. Manepalli[b], B.T.P. Madhav[c], T. Satyanarayana[d], G. Nagarjuna[e], Jaesool Shim[a,*], M.C. Rao[f,*]

[a] School of Mechanical Engineering, Yeungnam University, Gyeongsan, 712-749, Republic of Korea
[b] Department of Physics, The Hindu College, Machilipatnam, 521001, India
[c] LCRC-R&D, Department of ECE, Koneru Lakshmaiah Education Foundation, Guntur, 522502, India
[d] Department of EIE, Lakireddy Bali Reddy College of Engineering, Mylavaram, 521230, India
[e] Department of Physics, S.R.R. & C.V.R. Govt. Degree College, Vijayawada, 520004, India
[f] Department of Physics, Andhra Loyola College, Vijayawada, 520008, India

ARTICLE INFO

Keywords:
ZnO
Co-precipitation
XRD
SEM
Optical
DC conductivity
I-V
PL

ABSTRACT

ZnO is a significant I I-V I n-type direct bandgap semiconductor material which has shown great attention because of its applications in light-transmitting diodes and photograph detectors. In the present investigation, Al_2O_3 doped ZnO nanoparticles were prepared by co-precipitation technique utilizing PVA as a host polymer. X-ray diffraction studies revealed the cubic structure of nanoparticles. The determined normal crystallite size of Al_2O_3 doped PVA capped ZnO nanoparticles was around 12 nm. SEM image showed that the nanoparticles were distributed uniformly with small sized grains consisting of nano dots like tips due to the agglomeration of particles. FTIR demonstrated the trademark vibrational modes of constituent components in the host matrix. The optical studies of all samples displayed close band edge retention at 351 nm (3.26 eV). From the DC studies the conductivity was found to be 3.24×10^{-3} S/cm. EPR studies revealed the crystalline structure and coordination/neighbourhood site evenness of Al_2O_3 doped ZnO in the host lattice. Photoluminescence studies of Al_2O_3 doped PVA capped ZnO nanoparticles demonstrated two groups at 416 and 619 nm. The main band was seen in violet and other band in blue region. These studies revealed that the Al_2O_3 doped PVA capped ZnO nanoparticles materials can be used as LEDs, electroluminescence boards and plasma devices.

1. Introduction

Zinc oxide (ZnO) material possesses a large number of properties when compared to the IV group elements, because of wide energy bandgap of 3.37 eV. It has stable wurtzite structure. When compared to the other materials, ZnO has emerged an attractive material for its different kind of properties and flexible application like reflection coatings, anode materials, solar cells, optoelectronic devices, antibacterial specialist and sensor applications [1,2]. Silicon based transistors are used in many devices. But their energy bandgap is low. In order to fulfil the drawback, ZnO based materials are used as a thin film transistors (TFTs). Owing to its wide energy bandgap and high electrical properties, it is used in optoelectronic and photovoltaic devices. ZnO exhibits high UV

* Corresponding authors.
E-mail addresses: jshim@ynu.ac.kr (J. Shim), raomc72@gmail.com (M.C. Rao).

https://doi.org/10.1016/j.ijleo.2020.164236
Received 2 December 2019; Accepted 16 January 2020
0030-4026/ © 2020 Elsevier GmbH. All rights reserved.

transmitting radiation and gets more stabilized at room temperature, even when compared to the phosphorus and GaN [3]. By using ZnO nanopowders acoustic wave filters which are mostly used in audio and video frequency circuits have been developed [4]. A few creators have announced high photoluminescence efficiencies in ZnO nanostructures [5]. Additionally ZnO is a domain well disposed material, which is uniquely attractive for bio-applications.

Several techniques have been used to prepare the nanomaterials such as spin coating method, CVD technique, thermal decomposition, co-precipitation method etc. Among these co-precipitation method is chosen to prepare the nanoparticles, due to the cost effectiveness as well as the stability in environment conditions such as ambient temperatures, pressure variance etc [6]. Due to these properties, the prepared nanoparticles showed the tremendous change in their size, shapes as well as optical properties. Moreover, the properties can be additionally improved in nano-ZnO structures, nanoparticles, nanowires, which upgrade the exciton oscillator quality and quantum efficiency [7]. In optoelectronic applications, the ZnO particles demonstrated a wide unmistakable photoluminescence in the blue-green locale i.e. 470–550 nm. The obvious outflow is ascribed to deformities, for example, oxygen opening which are accepted to be situated close to the surface region [8]. The properties of ZnO can be customized for spintronic applications however doping diverse progress metal particles such as Co, Al, Mn, V, Fe, etc. into the ZnO lattice. Much exertion has been paid to the natural attractive trade collaborations of ZnO frameworks. So as to address the real instrument of attractive cooperation's in these frameworks, it is similarly critical to have an essential comprehension of various nanoscaled stage development and their outcomes on optical properties [9]. Size consistency and substance dependability in nanosized particles are the primary issues that influence attraction and are stayed to be a test in the field of weakened attractive semiconductors and optoelectronic applications [10].

In this present examination, Al_2O_3 doped PVA capped ZnO nanoparticles were prepared by co-precipitation method. The aim of this work is to prepare the nanosized particles which show a great influence on optoelectronic applications. Until now, based on these aluminium doped ZnO nanoparticles, no proper literature has been found on optoelectronic applications. Due to the insertion of aluminium oxide in the zinc oxide a large number of oxygen vacancies are generated. As a result a wide energy bandgap is obtained. It shows tremendous change on optical properties. The novelty of this present work is to prepare Al_2O_3 doped PVA capped ZnO nanoparticles with cost effective co-precipitation method. The prepared nanomaterials can be used for extensively obtaining the novel materials with different properties, because through this process nanosize grain particles have been deposited with high purity than those reported by other methods. The prepared nanoparticles can give the output which can be utilized in many applications like luminescence, optoelectronic and display devices.

2. Experimental

2.1. Preparation of Al_2O_3 doped PVA capped ZnO nanoparticles

Zinc Oxide (ZnO) and polyvinyl alcohol (PVA) with 98 % purity were obtained from Sigma Aldrich Ltd., India. Cleaned refined water was utilized as a dissolvable. In the present exploratory technique, 50 mL of two fold refined water was taken in a 100 mL of measuring flask. 2.6 g of PVA and 0.050 g of Zinc Oxide were included. The homogenous solution was left for 48 h at room temperature to swell. Later the arrangement was warmed up to 80 °C by steady working as long as 6 h until precipitate was formed. 1.5 mL of sodium hydrogen telluride (NaHTe) and 0.02 mol % nickel oxide were added drop wise to the arrangement. Following couple of minutes a straightforward arrangement was framed. The readied arrangement was thrown on level glass plate dishes and permitted to vanish the dissolvable followed by putting in tourist oven. Al_2O_3 doped PVA capped ZnO nanoparticles were obtained.

2.2. Characterization

XRD pattern was recorded on PANalytical X'Pert Pro X-beam powder diffractometer utilizing CuK_α (1.54060 Å) radiation. Size and morphology of nanoparticles were observed by using Hitachi S-3400 N Scanning electron microscope. FTIR spectrum of the sample was recorded on a Bruker-Alpha FTIR spectrophotometer. The optical transmission spectrum was measured on Hitachi Make UV-VIS spectrometer-3900 in the wavelength range $200-800$ nm. DC conductivity measurement was done by using standard four-probe technique. EPR spectrum of the sample was performed on JEOL JES-FA200 EPR spectrometer. I–V and surface resistance of the prepared nanoparticles were measured using Keithley 2400 Source-Meter. Photoluminescence spectra was recorded on Horiba Jobin-Yvon Fluorolog-3 spectrofluorimeter with Xe continuous (450 W) and pulsed (35 W) lamps as excitation sources. The CIE chromaticity was calculated by using Horiba Jobin-Yvon flouorolog-3 spectrofluorimeter.

3. Results and discussion

3.1. XRD analysis

XRD is utilized to decide the level of crystalline nature of Al_2O_3 doped PVA capped ZnO utilizing Debye-Scherrer's condition. As the particle size increases the intensity of XRD peaks decreases. As a result the FWHM of broadening peaks increases. The low intensity XRD peaks indicate that the films consist of coarsely fine grains (nanocrystalline) and/or are amorphous in nature. The diffraction peaks are observed close to $2\theta = 21.2^\circ, 38.2^\circ, 42.1^\circ$ and 53.6° are attributed to (1 1 0), (2 1 1), (3 2 0), and (4 1 0) planes, which are shown in Fig. 1. The obtained peaks are compared to the JCPDS card no. 80-0075. The films are highly oriented along (1 1 0) and (2 0 1) planes. The significant improvement in crystallinity is due to sintering of nanocrystals into effectively larger crystals after the annealed process [11]. The crystalline size data is acquired from FWHM and the normal crystalline size can be determined

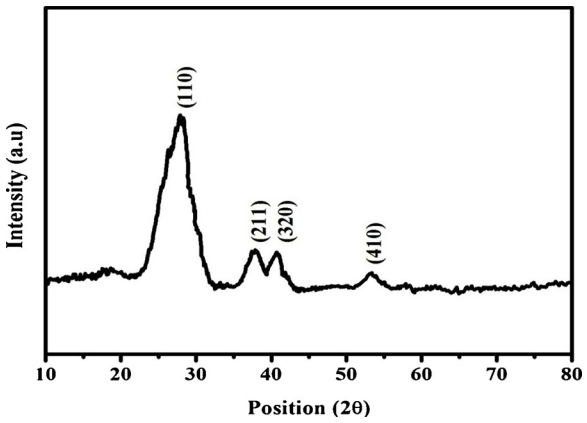


Fig. 1. XRD pattern of Al_2O_3 doped PVA capped ZnO nanoparticles.

by Debye-Scherrer equation.

$$D = (K \lambda / \beta \cos \theta) \quad (1)$$

where

D is the mean crystallite size,
K = 0.9 is Scherrer's constant,
λ is the wavelength of the occurrence pillar,
θ is the diffraction edge,
β is the full width half greatest power of the diffraction top.
From the XRD pattern, the determined estimation of normal crystallite size was 12 nm.

3.2. SEM analysis

Surface morphology and grain size of Al_2O_3 doped PVA capped ZnO nanoparticles were shown in Fig. 2. The prepared nanoparticles were annealed to remove the impurities because the nanoparticles are distributed uniformly with small sized grains consisting of nano dots like tips. This may be due to the agglomeration of particles [12]. At some regions the fusion of agglomerated walls is also observed. The SEM image has been taken at 200 nm resolution. The higher surface harshness is formed due to the capping of PVA polymer and dispersion is plotted at the inset of Fig. 2. The rest of agglomeration of particles are the combination of ZnO doped Al particles which is plotted in the inset of Fig. 2. Figure speaks to the run of the mill SEM micrograph of ZnO-Al nanopowder installed in PVA framework. It has been seen that ZnO-Al nanoparticles like structures lie inside the PVA grid. This micrograph showed that this small concentration of PVA doping in ZnO lattice causes growth of sized grains in some regions which result in porous surface [13]. The bigger ionic radii of aluminium ions distort crystal structure due to ionic radii mismatch which increases grains/particles growth activity of ZnO and formation of bigger particles.

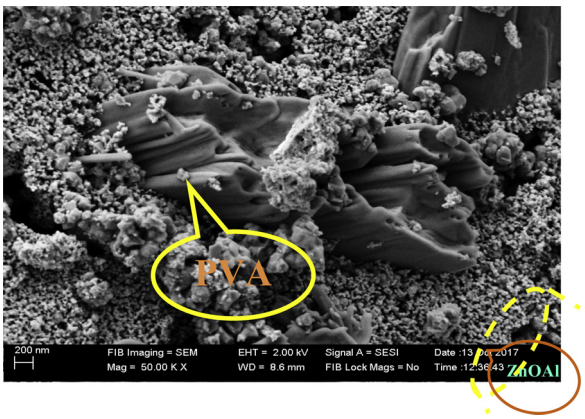


Fig. 2. SEM image of Al_2O_3 doped PVA capped ZnO nanoparticles.

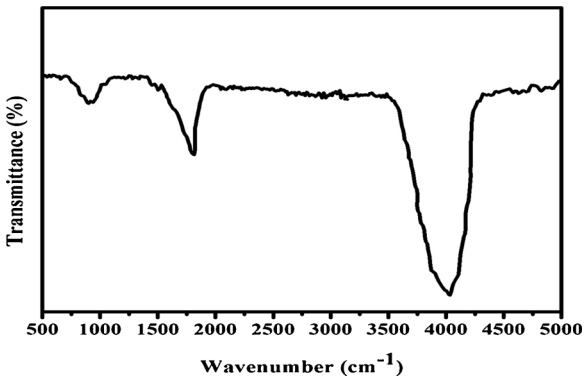


Fig. 3. FTIR spectrum of Al_2O_3 doped PVA capped ZnO nanoparticles.

3.3. FT-IR studies

The characterization peaks of surface useful gatherings of Al_2O_3 doped PVA capped ZnO nanoparticles in the wavenumber range $500-5000\,cm^{-1}$ at room temperature were shown in Fig. 3. The characteristic groups in the FTIR range were formed because of stretching vibrations of Al-O, C═O and C—H, gatherings. The absorption peaks formed at $870\,cm^{-1}$ were expected to C═O extending vibration. The peaks formed at $1700\,cm^{-1}$ were allocated to C—H extending vibration. Moreover, the characteristic peaks of Al-O gatherings were shown at $4800\,cm^{-1}$ viewed as the related aluminium bond among the particles [14]. Hence once again it was confirmed that aluminium oxide decomposes followed by the dissolution of Al^{+} ions within ZnO host lattice by occupying most probably Al^{2+} sites.

3.4. Optical properties

The UV-VIS absorbance spectra in the locale 200–800 nm for Al_2O_3 doped PVA capped ZnO nanoparticles were appeared in Fig. 4. It is obvious from the figure that the assimilation spectrum of the particles is diminished with expanding wavelength. From the figure it is observed that the ingestion expanded with expanding doping convergence of ZnO in PVA matrix [15], as per Beer-lamberts law; the assimilation is corresponding to the quantity of engrossing atoms [16]. Arrangement of new peaks for the sample in the wake of doping and furthermore widening of those peaks with expanding ZnO demonstrate a significant collaboration among PVA and ZnO [17]. This figure shows that the transmittance power increments with the expanding of the wavelength and as the convergence of doped material nano ZnO builds, the transmittance diminishes. The explanation behind this nature is that the increments of grouping of ZnO lead to expanding the limited state of thickness which lessens the transmittance values. The transmission range increments and it is roughly steady at lower absorbance value. It is seen that the composite nanoparticles after doping of aluminium nanoparticles have new peaks were shown in the short wavelengths.

Diffuse reflectance spectrum of prepared nanopowders is shown in Fig. 5. The spectra of all samples display close band edge retention at 351 nm (3.26 eV). Fig. 4 shows the UV–noticeable room temperature optical ingestion spectra of the PVA-ZnO-Al_2O_3 composites. The common place close to band edge ingestion of mass ZnO (3.26 eV) is plainly observed for the sample. It may be seen that the ingestion peaks of the composite containing the bigger size is not standard fit as a fiddle likely because of the arrangement of totals. On account of the particles having size of 200 nm the state of the assimilation peaks are smaller.

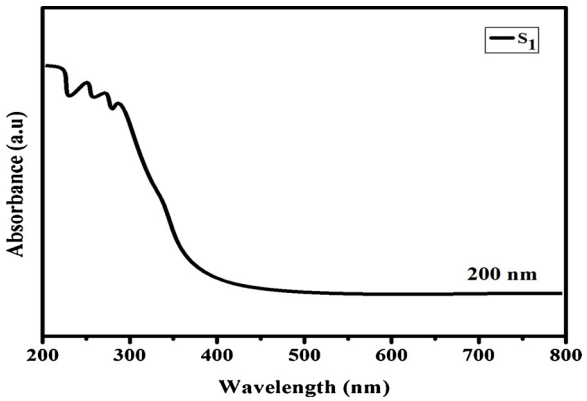


Fig. 4. Optical absorption spectrum of Al_2O_3 doped PVA capped ZnO nanoparticles.

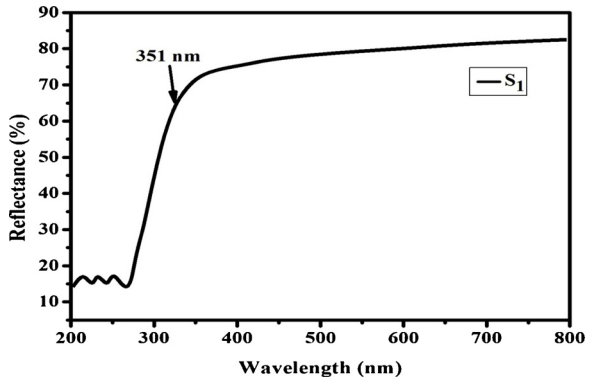


Fig. 5. Reflectance vs wavelength of Al_2O_3 doped PVA capped ZnO nanoparticles.

3.5. DC electrical conductivity studies

The DC electrical conductivity of Al_2O_3 doped PVA capped ZnO nanoparticles were shown in Fig. 6. DC electrical conductivity estimations have been done in the temperature range 200–373 K. The electrical resistivity is calculated by the following equation

$$\rho = \frac{\pi t}{\ln 2}\left(\frac{V}{I}\right) \tag{2}$$

where ρ is the resistivity (Ω-cm), t is the sample thickness (cm), V is the applied voltage and I is the source current (A).

The above plot shows an expansion in conductivity with respect to temperature. This might be because of the hopping mechanism between planning sides, nearby structure unwinding and segmental movement of the polymer. This plot seem to be Arrhenius conduct, with two areas (I & II) with initiation vitality gives above and beneath the dissolving locale 2.9–3.2 K of the polymer. In locale I, the conductivity increments gradually while in area II, it increments at higher rate. The last might be because of the adjustment in stage from a semi- crystalline to an indistinct state at the dissolving point. Further the shapeless area dynamically increments in district II because of which polymer chain gains quicker inward modes for which bond pivot produce segmental movement. This favours bouncing of particles with in the middle of the chains and thus the conductivity turns out to be high [18]. Comparable reports have likewise been accounted for electrolytes dependent on PVA.

The temperature reliance of the DC resistivity can be shown by the outstanding Arrhenius condition. Micheletti and Mark evaluated the intergranular boundary stature (φ_b) from the accompanying condition:

$$\mu = \mu_0 \exp(-\varphi_b/KT) \tag{3}$$

where each one of the terms have their typical implications. The estimation of (φ_b) acquired from plot Fig. 6, log (ρ) versus $1/T$ is 0.61 eV. Charge bearer versatility μ is resolved from the relation given by

$$\mu = \sigma/ne, \text{ (3)} \tag{4}$$

Where n is electron thickness and σ is the conductivity. It infers the semiconducting idea of the example since conductivity increments with increment in working temperature because of increasing of transport of ions. From the plot the calculated conductivity was found to be at 3.24×10^{-3} S/cm. The expansion conductivity with increment of temperature demonstrates total undefined stage and is like similar in daintily doped PVA film. It was recommended that a variable range jumping conduction model can be applied for

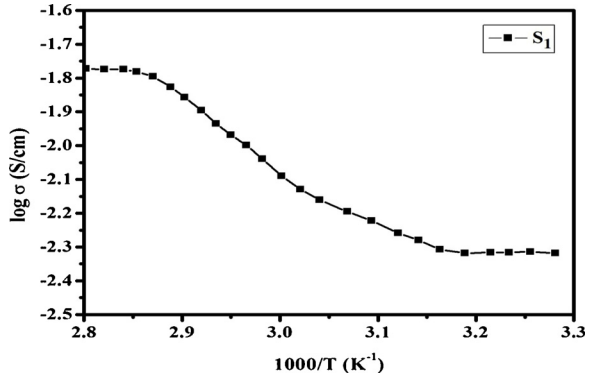


Fig. 6. DC conductivity of Al_2O_3 doped PVA capped ZnO nanoparticles.

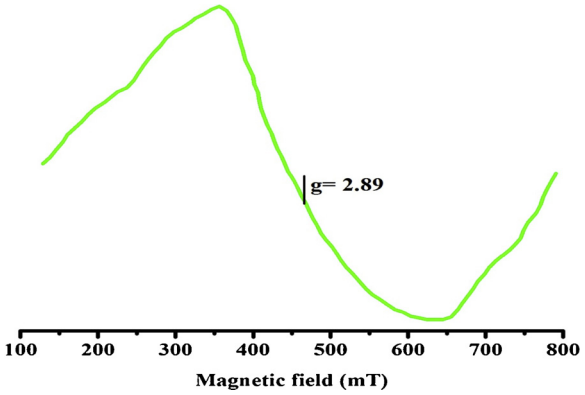


Fig. 7. EPR spectrum of Al_2O_3 doped PVA capped ZnO nanoparticles.

such situation where the conductivity is estimated.

3.6. EPR studies

EPR spectrum of Al_2O_3 doped PVA capped ZnO nanoparticles were measured on JEOL JES-FA200 having 100 kHz field regulation at room temperature was shown in Fig. 7. The reverberation sign was determined at g = 2.89 for 100 K temperature. The variation in the magnetic field was observed due to the insertion of Al^+ ions in the ZnO crystal lattice. The insertion of Al^+ ions in a host polymer induced the magnetic behaviour in the ZnO nanoparticles and also exhibit ferromagnetic nature at room temperature [19]. The Al_2O_3 doping may change the perfect ZnO structure to make it possible for forming defects and holes which could be regarded as additional charge carriers. It was clear that Al^+ (d6) particles have octahedral coordination and orbital singlet $^3A_{2g}$ has the most reduced vitality level, which split in to 3 F ground state as an outcome of crystal field. Turn Hamiltonian is utilized to speak to the EPR range of Al^+ particle for an isotropic g factor. An isotropic line is acquired which relates to the |0–1' | ± 1' attractive dipole changes. The turn - Hamiltonian can be represented as,

$$H = g\beta BS + SAI + SDS \quad (5)$$

where g is the isotropic factor,
β is the Bohr magnetron,
B is the external magnetic field,
S is the vector operator of the electron spin momentum,
A is the hyperfine interaction parameter,
I is the vector operator of nuclear spin momentum,
and D is the zero field splitting parameter.

From the above relations the accompanying parameters can be determined. The isotropic factor 'g' esteem is 2.89. The Δ worth is 9532 cm^{-1} in the wavelength of λ = 353 cm^{-1}. The communication with the electric field segment of the proper recurrence of electromagnetic radiation can start a change between the two states and results in the assimilation of photons. The fundamental rule in the EPR method is the ingestion of concoction substance in the vitality levels, which may reach out over a wide wavelength run in an outer attractive field. By EPR and UV-noticeable investigations the ionic parameter, α^2 can be assessed by,

$$g = 2.0023 - (\alpha^2 8\lambda/\Delta) \quad (6)$$

The ionic parameter lies in the middle of 0.2 and 1.5 which means the readied nanoparticles contain ionic and covalent holding. The acquired ionic parameter estimation of α^2 is 0.84. This unequivocally recommends that there exists a covalent holding between doped Al^+ particles and its ligands presence in the host lattice [20].

3.7. I–V characteristics

I–V characteristics of the prepared nanoparticles were shown in Fig. 8. The basic principle includes in I–V qualities is the charge move of electrons upgrade through the doped sample. Consequently the ionic conduction happens in the sample. Al^+ doped particles get quickly circulated over the stick gaps in the sample. At the point when the temperature of the sample should be brought up in the conduction phenomenon, at that point the charge transport is conceivable through the nanoparticles in the host material [21]. From the obtained plot, it clearly shows that the prepared nanoparticles possess the semi-conduction behaviour. Fig. 8 plainly demonstrates the voltage required for current and is obtained above the + ve side indicates the bright light. It is obvious that the voltage necessary for current is obtained below the + ve side indicates the dark light [22]. It is also obviously clear that the Al_2O_3 doped PVA capped ZnO nanoparticles, is a perfect material which is utilized for semiconducting applications. The dull current in the turnaround inclination is exceptionally close to zero and it could be considered a perfect case for diode qualities.

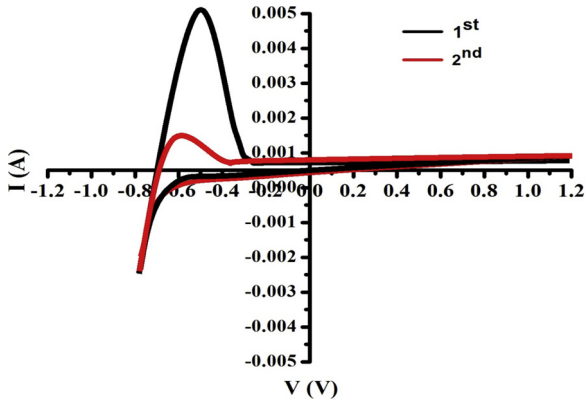


Fig. 8. Current- voltage characteristics of Al_2O_3 doped PVA capped ZnO nanoparticles.

3.8. Photoluminescence studies

The photoluminescence spectrum of Al_2O_3 doped PVA capped ZnO was shown in Fig. 9. Blue emission states are attributed to surface defects. These are hidden in the crystalline surface, whereas the bond formation and their respective boundaries are additionally perceived. Band twisting will bring about formation of a consumption district at the grain limits and it will influence the ionization condition of the deformities inside the exhaustion locale. Since the annealed sample comprises of fine particles with an enormous surface territory and bunches of grain limits, the green outflow likely to begin from contributor acceptor changes, where benefactor and additionally acceptor imperfections are situated at surfaces or grain limits [23,24]. From the figure, it is seen that, annealed sample has showed two excitation peaks at 416 and 619 nm. Everything happens because of excitation wavelength of 353 nm at room temperature. The acquired groups demonstrate the shading organized in the unmistakable district and furthermore the locale demonstrates that the main band is seen in violet area and the subsequent band in blue locale [25]. In this way the readied nanoparticles are valuable in the showcase gadget applications.

CIE color chromaticity is framed by the interesting combination of three coordinates which are green, blue and red with proper proportions. The light emission radiated by Xe source has monochromatic wavelength which is incident on the sample. The yield of the sample blower recognizes the approaching radiation. The subsequent radiation is sifted by an outflow monochromator which results in to a sign of a photomultiplier identifier [26]. CIE 1931 chromaticity directions are observed to be at x = 0.2053 and y = 0.1453. The related CIE outline is appeared in Fig. 10. The CIE chromaticity, organized locale for the readied nanoparticles is found in blue region.

4. Conclusions

Al_2O_3 doped PVA dopped ZnO nanoparticles were obtained by co-precipitation method. From the XRD pattern, the diffraction peaks observed close to 2θ = 21.2°, 38.2°, 42.1°, and 53.6° were attributed to the (1 1 0), (2 1 1), (3 2 0), and (4 1 0) planes. The

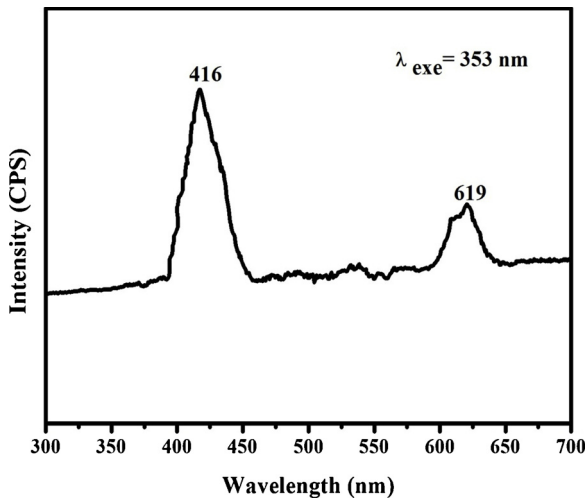


Fig. 9. Photoluminescence spectrum of Al_2O_3 doped PVA capped ZnO nanoparticles.

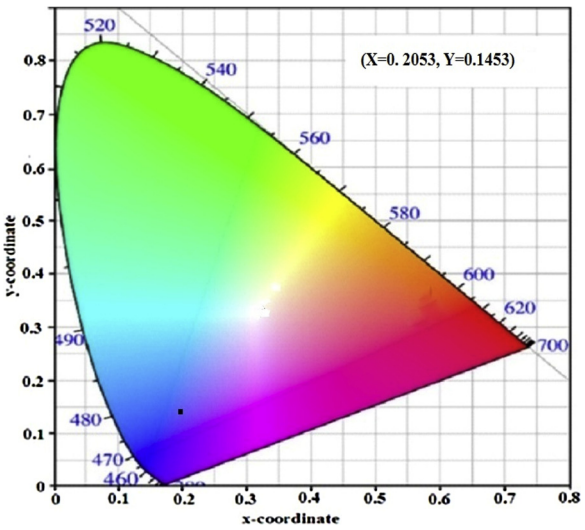


Fig. 10. Chromaticity diagram of Al_2O_3 doped PVA capped ZnO nanoparticles.

normal crystallite size was 12 nm. SEM image showed that the nanoparticles are distributed uniformly with small sized grains consisting of nano dots like tips due to the agglomeration of particles. The characteristic groups in the FTIR range were formed due to stretching vibrations of Al-O, C═O and C−H, gatherings. The absorption peaks formed at 870 cm^{-1} were expected to C═O extending vibration. The optical spectrum of all examples displays close band edge retention at 351 nm (3.26 eV). From the DC plot the calculated conductivity was found to be at 3.24×10^{-3} S/cm. The expansion in conductivity with increment of temperature demonstrates total undefined stage and is like similar in daintily doped PVA film. The voltage required for current was obtained above the + ve side indicated as bright light and the voltage below the + ve side indicated as dark light. Photoluminescence studies revealed that the annealed sample have showed two excitation peaks at 416 and 619 nm. CIE chromaticity of the readied nanoparticles was found in blue region. These studies revealed that the prepared nanoparticles can be utilized in many applications like luminescence, optoelectronic and display devices.

Role of the funding sources

There are no funding sources for this article work.

Declaration of Competing Interest

The authors declare that there is no conflict of interest regarding the publication of this paper.

References

[1] A. Van Dijken, E.A. Meulenkamp, D. Vanmaekelbergh, A. Meijerink, J. Lumin. 454 (2000) 87–89.
[2] I. Shalish, H. Temkin, V. Narayananmurti, Phys. Rev. B 69 (2004) 245401.
[3] M. Ghosh, A.K. Raychaudhuri, Appl. Phys. Lett. 93 (2008) 123113.
[4] S. Deka, P.A. Joy, Solid State Commun. 142 (2007) 190–194.
[5] A. Debernardi, M. Fanciulli, Physica B 401–402 (2007) 451–453.
[6] A.J. Chen, X.M. Wu, Z.D. Sha, L.J. Zhug, Y.D. Meng, J. Phys. D 39 (2006) 4762.
[7] Y.Q. Wang, S.L. Yuan, P. Liu, X.X. Lan, Z.M. Tian, J.H. He, S.Y. Yin, J. Magn. Magn. Mater. 320 (2008) 1423–1426.
[8] S. Bachiv, C. Sandouly, J. Kossanyi, J.C. Ranford-Haret, J. Phys. Chem. Solids 57 (1996) 1869–1879.
[9] M. Naeem, S.K. Hasanain, M. Kobayashi, Y. Ishida, A. Fujimori, S. Buzby, S.I. Shah, Nanotech 17 (2006) 2675–2680.
[10] M. Naeem, S.K. Hasanain, A. Mumtaz, J. Phys. Condens. Mater 20 (2008) 025210.
[11] A.K. Srivastava, M. Deepa, N. Bahadur, M.S. Goyat, Mater. Chem. Phys. 114 (2009) 194–198.
[12] N. Bouropoulos, G.C. Psarras, N. Moustakas, A. Chrissanthopoulos, S. Baskoutas, Phys Stat Sol 205 (2008) 2033–2037.
[13] J. Lee, E.M. Bourim, W. Lee, J. Park, M. Jo, S. Jung, J. Shin, H. Hwang, Appl. Phys. Lett. 97 (2010) 172105.
[14] R. Viswanatha, S. Sapra, S.S. Gupta, B.B. Satpati, P.V. Satyam, B.N. Dev, D.D. Sarma, J. Phys. Chem. B 108 (2004) 6303–6310.
[15] A.S. Roy, S. Gupta, S. Sidhu, A. Praveen, C. Ramamurthy, Compos. Part B Eng. 47 (2013) 314–319.
[16] A. Wasan, T. Mohammed, K. Tagreed, J. Baghdad Sci. 8 (2011) 543–550.
[17] M. Hamed, H. Sabah, A. Sarkawt, Asian Trans. Sci. Tech. 1 (2012) 16–20.
[18] A. Kurt, Turkish J. Chem. 34 (2010) 67–79.
[19] J. Antony, S. Pendyala, D.E. McCready, M.H. Engelhard, D. Meyer, A. Sharma, Y. Qiang, IEEE Trans. Magn. 42 (2006) 2697–2699.
[20] Y.Y. Tay, S. Li, C.Q. Sun, P. Chen, Appl. Phys. Lett. 88 (2006) 173118.
[21] K.J. Albert, N.G. Lewis, C.L. Sahauer, G.A. Sotzing, S.E. Stizel, T.P. Vaid, D.R. Walt, Chem. Rev. 100 (2000) 2595–2626.
[22] B. Ashkenov, N. Mbenkum, C. Bundesmann, V. Riede, M. Lorenz, D. Spemann, M. Kaidashev, A. Kasic, M. Schubert, M. Grundmann, G. Wagner, H. Neumann, V. Darakchieva, H. Arwin, B. Monemar, J. Appl. Phys. 93 (2003) 126–133.
[23] G. Xiong, U. Pal, J.D. Serrano, J. Appl. Phys. 101 (2007) 024317.

[24] F. Decremps, J.P. Porres, A.M. Saitta, J.C. Chervin, A. Polian, Phys. Rev. B 65 (2002) 092101.
[25] V.A. Fonoberov, A.A. Balandin, Phys. Rev. B 70 (2004) 233205.
[26] J. Yang, X. Liu, L. Yang, Y. Wang, Y. Zhang, L. Lang, M. Gao, B. Feng, J. Alloys Compd. 477 (2009) 632–635.

Preparation and structural characterization of P_2O_5-CaO-Na_2O: CuO glasses

SATYANARAYANA TALAM[a,*], RAMBABU BUSI[a], NAGARJUNA GUNNAM[b], P. SYAM PRASAD[c], VENKATESWARA RAO PENUGONDA[d]
[a]*Department of EIE, Lakireddy Bali Reddy College of Engg. (A), Mylavaram-521230, Krishna, A.P., India*
[b]*Department of Chemistry, S.R.R. & C.V.R. Govt. Degree College, Vijayawada – 520004, India*
[c]*Department of Physics, National Institute of Technology (NIT), Warangal-506 004, Telangana State, India*
[d]*Department of Physics, The University of the West Indies, Mona Campus, Kingston 7, Jamaica*

Glasses of particular composition (65-x) P_2O_5-23CaO-12Na_2O: x CuO ($0.5 \le x \le 2.0$) mol% was synthesized. Further, the samples were characterized by X-Ray Diffraction (XRD), Scanning Electron Microscopy (SEM), Differential Thermal Analyses (DTA), Fourier Transform Infrared, optical Absorption and luminescence spectroscopy techniques.The XRD patterns recorded at room temperature have confirmed the non-crystalline nature to all glass samples which was also supported by SEM pictures. Shifting of glass transition temperature (T_g) towards lower temperature with the CuO addition is observed from the DTA scans.This observation is an indication of more disorder of glass network. Basic phosphate bands and possible cross linkages with CuO addition have been observed in FTIR spectra of all samples. Optical absorption spectra exhibted two bands in the regions about 335 and 795 nm. Luminescence spectra has exhibited two emission peaks corresponding to the transition of $^3D_1 \rightarrow {}^1S_0$ single Cu^+ centers and Cu^+-Cu^+ pairs respectively. From all the results, the sample with high content of CuO found to exhibit more degree of disorder. The reasons for more disorder have been discussed in detail by means of spectroscopic properties.

(Received April 21, 2018; accepted August 20, 2019)

*Keywords:*Phosphate glasses, XRD, DTA, Optical absorption, Copper ions

1. Introduction

Phosphate based glasses have been extensively investigated because of their superior properties [1-3]. High refractive index and low dispersion properties enable phosphate glasses to act as suitable hosts for different lasing ions than that of conventional borate and silicate glasses [4]. It also has been demonstrated that metal containing phosphate glasses can be considered as promising materials for a variety of photonic applications [4-6]. In addition, phosphate glasses may be considered as bioactive materials since they exhibit high dissolution with controlled rate in aqueous solutions [7]. Introducing transition metals into phosphate glass network would result in improving chemical durability and stability against devitrification and moisture [4-6]. Basically, phosphate network consisting of phosphate tetrahedra with different numbers of bridging oxygens, including cross-linked networks (Q^3), polymer-like chains (Q^2+Q^1) or small pyro(Q^1) and orthophosphate groups (Q^0) [7].

Semiconducting copper ion, one of the interesting transition metal ions in various glasses. Usually, copper exists in two stable states viz., Cu^+ which does not produce colouring and Cu^{2+} ions create colour centres [8]. Lot of attention has been given to the investigations on copper ions in different glass systems to provide structure-physical properties relation. It is found that copper ions have strong impact on spectral and electric features of various glass systems. The addition of CuO and Na_2O to phosphate glass network would modify the phosphate network resulting in change of physical properties as these properties depending on metal oxide dopant concentration and coordination environments. A large number of studies on copper ions in different glass systems are available; still there is a scope to investigate the structural changes resulting from addition of CuO in phosphate glasses. Hence, a considerable interest is attached on structure-properties relation of copper doped phosphate glasses. In this scenario, to explore the structural modifications in phosphate glass network with CuO, a particular glass system P_2O_5-CaO-Na_2O: CuO has been chosen and investigated.

2. Experimental

The nominal glass composition of the present study is selected as (65-x) P_2O_5-23CaO-12Na_2O: x CuO ($0.5 \le x \le 2.0$) and the samples are labelled with the following:

PC_5: 64.5 P_2O_5-23CaO-12Na_2O: 0.5 CuO
PC_{10}: 64.0 P_2O_5-23CaO-12Na_2O: 1.0 CuO
PC_{15}: 63.5 P_2O_5-23CaO-12Na_2O: 1.5 CuO
PC_{20}: 63.0 P_2O_5-23CaO-12Na_2O: 2.0 CuO

P_2O_5, a strong glass former was introduced in the glass composition in a form of $NH_4H_2PO_4$ while CaO and Na_2O were added in their natural form of anhydrous carbonates. The hygroscopic nature of P_2O_5 is controlled by adding suitable metal oxides. It is also expected that de-

polymerization of the phosphate network for the formation of P-OH bonds. CuO chemical powder was directly taken as per mol%. The chemical composition of the studied glass is chosen such that contents of Na_2O and CaO remain constant while the contents of P_2O_5 and CuO vary from 64.5 to 63 mol% and 0.5 to 2.0 mol% respectively. The present glasses were prepared using the melt quenching method. For preparing the glasses, powders of constituents corresponding to mol% were weighed using an electronic balance and the contents thoroughly mixed homogeneously in an agate pestle-mortar. The mixture was then poured into an aluminium crucible and placed in Termolab 1800 - Shimaden FP21 Controlled high temperaturefurnace set at the 1000 ºC for approximately one hour. Halfway during the melting period, the mixture would be stirred to allow for proper mixing of compounds. After one hour completed, the mixture was then poured into graphite moulds and placed in an annealing furnace set at the 300 ºC for approximately six hours. The glass samples were grounded and optical polished to the dimensions of 1.2 cm x 1.2 cm x 0.2 cm. The amorphous nature of the prepared glass samples was confirmed by the X-ray diffractometer (XRD, Rigaku D/Max ULTIMA III) and HITACHI S-3400N Scanning Electron Microscope. The glass transition temperature and temperatures of crystallization were determined by using the Netzsch Simultaneous DSC/TG Thermal Analyser STA409C. The densities of the samples were calculated using the Archimedes principle. Infrared absorption spectra were noted on a JASCO-FT/IR–5300 spectrophotometer up to a resolution of 0.1 cm^{-1} in the spectral range 400–4000cm^{-1} using potassium bromide pellets (300 mg) containing pulverized sample (1.5 mg). These pellets were pressed in a vacuum die at ~680MPa.Optical absorption spectra of the glasses were recorded at room temperature in the wavelength range 250-1000 nm with a resolution of 0.1nm using UV-3092 spectrophotometer. The photoluminescence spectra of glass samples were carried out using F-2500 FL Spectrophotometer, Hitachi.

3. Results and discussion

At first, calculation of physical parameters was done as they provide very important information about structural changes in the glasses with rise in CuO content. The density values of all samples were measured by Archimedes principle. Addition of CuO in place of P_2O_5 results little increase in density that might be due to slightly larger molecular weight and density of copper oxide than calcium oxide, sodium oxide. Degree of structural packaging, change in coordination& position of phosphate ions were assumed as few reasons for density changes. It is also observed that the values of average molecular weight found to decrease with the content of copper oxide while ion concentration found to increase. It could be due to replacing by CuO with P_2O_5 of high molecular weight [9].

Using the measured density and average molecular weight M of glasses, other essential physical parameters viz., copper ion concentration N_i, mean copper ion separation r_i and polaron radius r_p have been evaluated and presented in Table 1. Another interesting observation is that the decreasing trend of interionic distancer_i and polaron radius $r_p$with CuO content which supports the loosely packed glass network resulting more structural degree of disorder.

Fig. 1 presents the X-ray diffraction patterns of P_2O_5-CaO-Na_2O: CuO glasses recoreded at room temperature. These patterns did not show any sharp peaks except wide ranging halo that confirms non-crystalline nature to the samples. The broad halo observed was the characterisitc peak of glass samples. This result also supports the abscence of signs of crystalization tendency that might be occured sometimes during quenching process.

Table 1. Physical parametersof P_2O_5-CaO-Na_2O: CuO glasses

Sample	Avg. Mol. Wt. (g/mol)	Density (g/cm^3)	Conc. of 'Cu' ions N_i ($10^{21}/cm^3$)	Interionic distance of 'Cu' ions $r_{i\,(A°)}$	Polaron radius $r_{p\,(A°)}$
PC_5	203.8	2.616	3.85	6.38	2.57
PC_{10}	202.7	2.635	7.80	5.04	2.03
PC_{15}	201.8	2.658	11.84	4.38	1.77
PC_{20}	200.5	2.679	15.98	3.97	1.59

Another interesting study is recording of scanning electron microscopic pictures which reveal the morphological details of glass samples. Fig. 2 displays the SEM images of PC_{10} and PC_{20} recorded at room temperature with magnification of 20 μm. These pictures clearly indicating the absence of micro-crystals those usually might occurred due to quenching process. Thus it confirms non-crystalline nature and also supports the XRD patterns.

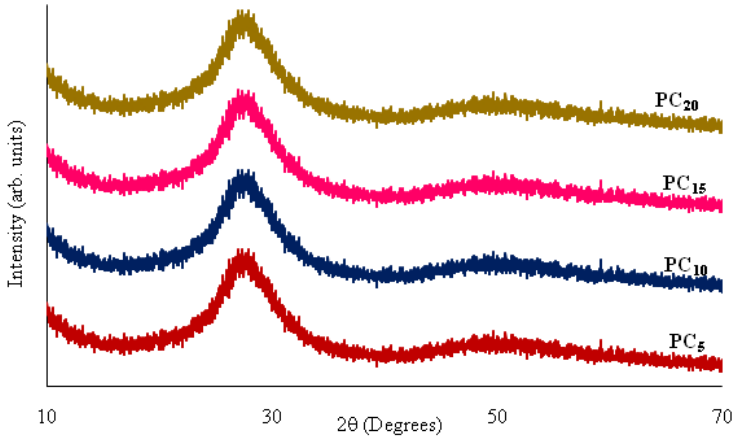


Fig. 1. XRD patterns of P_2O_5-CaO-Na_2O: CuO glasses.

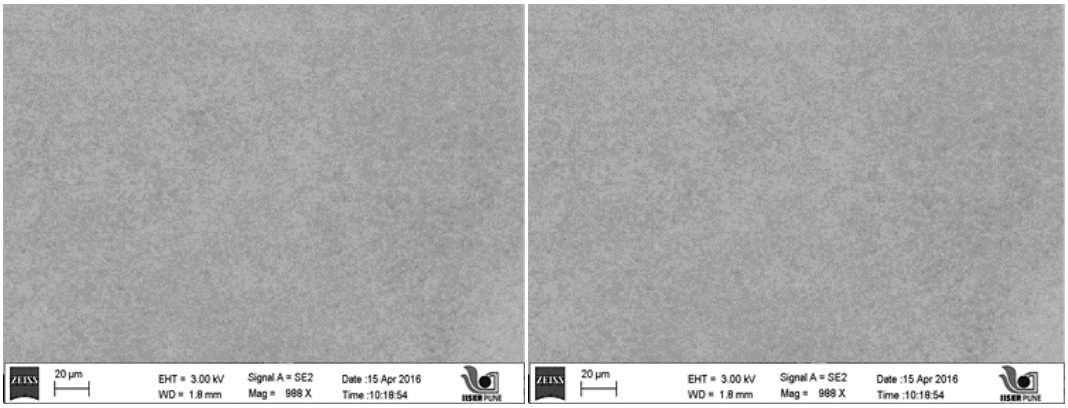


Fig. 2. Scanning Electron Microscopic pictures of P_2O_5-CaO-Na_2O: CuO glasses.

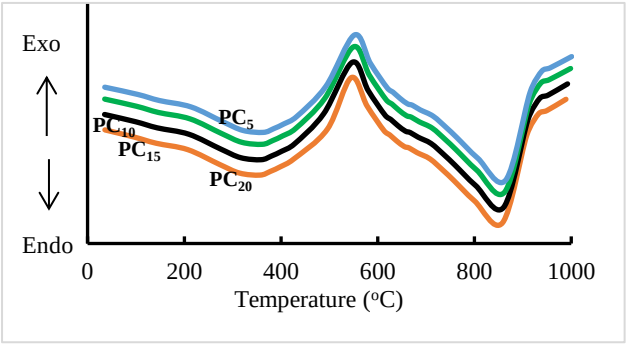


Fig. 3. DTA traces of P_5O_5-CaO-Na_2O: CuO glasses

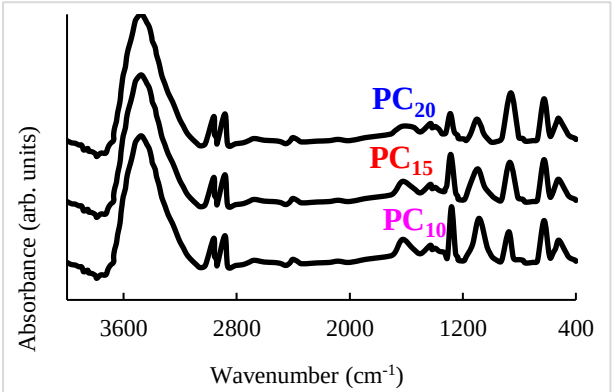


Fig. 4. FT-IR absorption spectra of P_2O_5- CaO- Na_2O: CuO glasses.

Differential thermal analysis (DTA) traces of P_2O_5-CaO-Na_2O: CuO glasses are presented in Fig. 3. The traces indicating broad range endothermic and exothermic peaks that confirms homogeneity of glass samples. It is observed that the addition of copper oxide resulted decrease in glass transition and melting temperatures. DTA trace of PC_{20} glass exhibits glass transition at about 375ºC which was small among other samples. From the traces, it was very clear that the glass transition Tg and melting temperature shift towards lower temperature region with copper oxide addition. Divalent copper ions act as modifiers and make the phosphate glass network weak by inducing many non-bridging oxygens leading to more structural network disorder. This could be the reason for above thermal changes [9].

The prepared glass samples are mixtures of glass network former (P_2O_5), intermediate oxides and modifiers (CaO& Na_2O). Phosphorous pentaoxide is one of the strong glass network formers and possesses PO_4 tetrahedron network structure. With bridging oxygens, PO_4 tetrahedrons forming chains through covalent bonding. Modifier calcium oxide enters the phosphate glass network by breaking P–O–P bonds that causing bonding defects leading to network disorder. Na_2O is considered to be incipient glass network formers which can form glass with the help of modifier oxides like CaO [10, 11].

Table 2. Summary of data on optical absorption spectra of P_2O_5-CaO-Na_2O: CuOglasses

Sample	Cut-off wavelength (nm)	$^2B_{1g} \rightarrow {}^2B_{2g}$(nm)	Optical band gap E_o (eV)
PC_5	325	752	2.88
PC_{10}	329	757	2.82
PC_{15}	336	759	2.76
PC_{20}	339	764	2.70

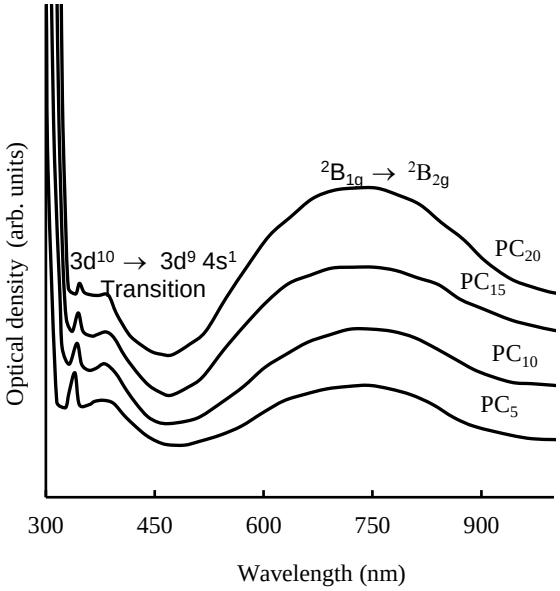


Fig. 5. Optical absorption spectra of P_2O_5-CaO-Na_2O: CuO glasses.

To investigate the structural changes in P_2O_5-CaO-Na_2O: CuO glasses,FTIR absorbance spectra is recorded and shown in Fig. 4. The positions of spectral bands for samples PC_5 and PC_{10} almost ensemble the same due to low concentration of CuO. Hence, the Fig.4 has shown only three IR traces corresponding to samples PC_{10}, PC_{15} and PC_{20}. Various characteristic absorption bands corresponding to P-O-P stretching, $\mathbf{PO_4^{3-}}$group, P-O-P asymmetric bending and pyrophosphate groups ($P_2O_7^{4-}$) in the wavenumber regions 1265-1286, 1057-1085 and 887-893 cm^{-1} have been observed in the spectra of all samples [2, 12-15]. Another interesting observation is that the small band located in the region 1600-1640 cm^{-1} could be due to the deformation mode of water molecule. Stretching mode vibrations of hydroxyl groups were also observed in the region 3140 to 3740 cm^{-1}. One more interesting vibrational band located in the region 440–610 cm^{-1} was identified and assigned to Na^+ and Ca^{2+} modifier cations [16]. With rise in the content of CuO, $\mathbf{PO_2^-}$ vibrational bands observed to grow and bending mode of $\mathbf{PO_4^{3-}}$ tetrahedron groups found to decrease. Reduction in wavenumber of vibrational bands corresponding to O–P–O vibrations and $\mathbf{PO_4^{3-}}$ tetrahedral groups clearly supports the more structural degree of disorder around phosphate groups. From these observations, the glass sample with high amount of CuO found to exhibit high degree of disorder due to more loosely cross-linked phosphate glass network with cations and it also supports DTA results.

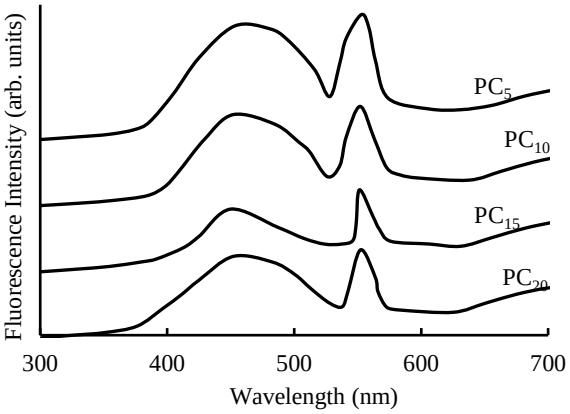


Fig. 6. Luminescence spectra of P_2O_5-CaO-Na_2O: CuO

Room temperature UV-visible absorption spectra of CuO doped P_2O_5-CaO-Na_2O glasses is presented as Fig.5. One strong absorption band and another small kink located at about 335 and 375nm assigned to $3d^{10} \rightarrow 3d^9\ 4s^1$ transitions observed in the spectrum of every glass sample [17, 18]. The CuO content rise in sample has shown that intensity and half-width of these bands found to decrease which caused by the larger existence of monovalent copper ions. One more broad absorption band centered at 794nm assigned to the transition $^2B_{1g} \rightarrow {}^2B_{2g}$ of divalent copper ions in octahedral coordination. [17, 19, 20]. Increase in CuO content has resulted in changing of absorption edge from higher wavenumber to lower wavenumber side. Interesting observation is that increase of intensity and half-width of broad absorption band with CuO rise at the expense of primary two bands. It is strongly felt that there exists conversion of Cu^+ ions to Cu^{2+} ions into octahedral environment. There was decrease in optical band gap with rise of CuO content.

Divalent octahedrally coordinated copper ions act as modifiers leading to growth of non-bridging oxygens (NBOs) that resulting prominent rise in donor centres by localized electrons. This rise moves the absorption edge to higher wavelength side by causing decrease in optical band gap (Table 2).

Fig. 6 shows the luminescence spectra of P_2O_5-CaO-Na_2O: CuO glasses excited with their corresponding absorption edges recorded in the wavelength region 300 to 900 nm at room temperature.

The spectra exhibited two emission peaks; one broad band at about 484 nm and another sharp peak at 595 nm. Both the bands are assigned to $^3D_1 \rightarrow {}^1S_0$ single Cu^+ centres and Cu^+-Cu^+ pairs transitions respectively [20]. Interesting detail is that the intensity and half width of these emission peaks found to diminish with CuO. This could be due to the fact that the conversion of Cu^+ ions into octahedrally coordinated Cu^{2+} ions. From the fluorescence results, it is clear that the sample PC_5 exhibit high emission intensity due to the presence of more Cu^+ ions [8]. With increase in the content of CuO, there is a change in the glass structure and was observed by FTIR , which also supports the conversion of Cu^+ to Cu^{2+}.

4. Conclusion

Glasses of particular composition P_2O_5-CaO-Na_2O: CuO were synthesized by melt quenching. Later, characterization of samples by XRD, SEM, DTA, optical absorption, FTIR and photoluminescence spectra. Absence of sharp peaks in XRD confirming amorphous nature, but characteristic glassy broad halo was observed. SEM pictures indicating signs of absence of micro-crystals which also supports XRD results. DTA traces have clearly indicated that glass transition and melting temperatures move close to lower temperature with CuO reveals decrease in rigidity of glass network that supports FTIR result. Infrared spectra have shown various distinctive phosphate vibrational bands and possible cross linkages. The sample PC_{20} found to exhibit more structural degree of disorder. Optical absorption spectra indicated the characteristic copper absorption transitions and decrease in band gap due to the larger concentrations of donor centres. Luminescence spectra has exhibited two emission peaks; one broad band at about 484 nm and another sharp peak at 595 nm corresponding to the transition of $^3D_1 \rightarrow {}^1S_0$ single Cu^+ centres and Cu^+-Cu^+ pairs respectively.

Acknowledgements

One of the authors Dr. T. Satyanarayana would like to acknowledge Science and Engineering Research Board (SERB)-DST, Govt. of India for the financial assistance (Ref. No.: SB/FTP/PS-044/2014).

References

[1] D. Bellucci, A. Sola, I. Cacciotti, C. Bartoli, M. Gazzarri, A. Bianco, F. Chiellini, V. Cannillo, Mater. Sci. Eng.C**42,**312 (2014).
[2] T. Satyanarayana, T. Kalpana, N. Veeraiah, J. Lumin. **130**, 498 (2010).
[3] D. E. Day, Z. Wu, C. S. Ray, P. Hrma, J. Non-Cryst. Solids **241**, 1 (1998).
[4] S. Shailajha, K. Geetha, P. Vasantharani, Mater Sci. **39**, 1001 (2016).
[5] M. Chemnitz, J. Wei, Ch. Jain, P. B. Rodrigues, T. Wieduwilt, J. Kobelke, L. Wondraczek, A. M. Schmidt, Optics Letters **41**(15), 3519 (2016**)**.
[6] I. Konidakis, S. Pissadakis, Materials**7**(8), 5735 (2014).
[7] D. A. Magdas, R. Stefan, D. Toloman, N. S. Vedeanu, J. Mol**.** Structure**1056–1057**, 314 (2014).
[8] A. Samir, M.A. Hassan, A. Abokhadra, L. I. Soliman, M. Elokr, Opt. Quant. Electron. **51**, 123 (2019).
[9] T. Satyanarayana, M. A. Valente, G. Nagarjuna, N. Veeraiah, J. Phys. and Chem. of Solids **74**, 229 (2013).
[10] T. Satyanarayana, Tilak Mukherjee, G. Nagarjuna, J. Optoelectron. Adv. M. **18**(9-10), 827 (2016).
[11] S. V. G. V. A. Prasad, M. Srinivasa Reddy,

V. Ravi Kumar, N. Veeraiah, J. Lumin.**127**, 637 (2007).
[12] D. Palles, I. Konidakis, C. P. E. Varsamis, E. I. Kamitsos, RSC Adv. **6**(20), 16697 (2016).
[13] P. Stoch, W. Szczerba, W. Bodnar, M. Ciecinska, A. Stoch, E. Burkel, Phys. Chem. Chem. Phys. **16**, 19917 (2014).
[14] M. A. Marzouk, H. A. ElBatal, A. M. Abdel Ghany, F. M. EzzEldin, J. Mol. Struct. **997**, 94 (2011).
[15] R. K. Brow, J. Non-Cryst. Solids **263-264**, 1 (2000).
[16] M. A. Ouis, A. M. Abdelghany, H. A. ElBatal, Processing and Applications of Ceram. **6**(3), 141 (2012).
[17] L. Srinivasa Rao, M. Srinivasa Reddy, D. Krishna Rao, N. Veeraiah, Solid State Sci. **11**, 78 (2009).
[18] H. A. El-Batal, Z. S. El-Mandouh, H. A. Zayed, S. Y. Marzouk, G. M. El-Komy, A. Hosny, Indian J. of Pure & Appl. Phys. **50**, 398 (2012).
[19] T. Satyanarayana, K. Srinivasa Rao, N. T. V. Naga Lakshmi, G. Nagarjuna, Solid State Phenomena **207**, 55 (2014).
[20] B. Padlyak, W. Ryba-Romanowski, R. Lisiecki, I. M. Teslyuk, J. Non-Crystalline Solids **356**, 2033 (2010).

*Corresponding author:drtsatyam@gmail.com

Send Orders for Reprints to reprints@benthamscience.net

Letters in Organic Chemistry, 2020, *17*, 000-000

RESEARCH ARTICLE

Design, Synthesis and Anticancer Evaluation of Acetamides Comprising 1,2,3-triazole, 1,3,4-thiadiazole and Isothiazolo[4,3-*b*]pyridine Rings

Shaik Shahinshavali[1,2], Nuthalapati Poojith[2], Venkat Rao Guttikonda[3], Reddymasu Sreenivasulu[4], and Mandava Venkata Basaveswara Rao[1,*]

[1]*Department of Chemistry, Krishna University, Machilipatnam, Andhra Pradesh, 521001 India;* [2]*Sri Ramachandra Institute of Higher Education and Research, Ramachandra Nagar, Porur, Chennai, 600116, Tamilnadu, India;* [3]*Department of Chemistry, SRR and CVR Government Degree College (Autonomous), Vijayawada, Andhra Pradesh, 520004 India;* [4]*Department of Chemistry, University College of Engineering (Autonomous), Jawaharlal Nehru Technological University, Kakinada, Andhra Pradesh, 533003 India*

ARTICLE HISTORY

Received: June 29, 2019
Revised: January 07, 2020
Accepted: January 30, 2020

DOI:
10.2174/1570178617666200225102939

Abstract: We have synthesized a library of new 1,2,3-triazole incorporated 1,3,4-thiadiazole-isothiazolo[4,3-*b*]pyridine derivatives **12a-j** and have screened these products for their anticancer activities against four human cancer cell lines such as MCF-7 (breast cancer), A549 (lung cancer), DU-145 (prostate cancer), and MDA MB-231 (breast cancer) using MTT assay with etoposide as a positive control. Among them, compound **12e** has shown excellent activities against MCF-7, A549, DU-145, and MDA-MB-231 with IC_{50} values of 0.53±0.055 µM, 0.18±0.077 µM, 0.10±0.082 µM, and 0.92±0.041 µM, respectively.

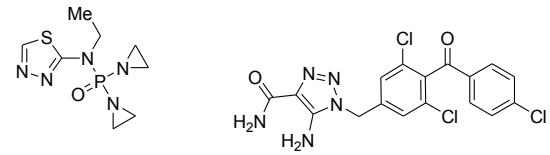
Keywords: 1,2,3-triazole, 1,3,4-thiadiazole, anticancer activity, azetepa, Carboxyamido triazole (CAI), isothiazolo[4,3-*b*]pyridine.

1. INTRODUCTION

Cancer is the second leading cause of death in both developing as well as undeveloped countries [1]. It is a very dangerous disease with rapid growth and uncontrolled spread of abnormal cells. Cancer can be due to several factors such as environment, diet, tobacco, radiations, *etc*. [2, 3]. Cancer cell lines can be destroyed by three different ways such as surgery, radiation therapy and chemotherapy. Among them, chemotherapy is a potent treatment for the inhibition of cancer cells. Most of the nitrogen-containing heterocyclic moieties act as cytotoxic agents in cancer chemotherapy [4-25].

1,3,4-thiadiazole constitutes a significant class of five-membered heterocyclic compounds and are extensively used in medicinal chemistry, organic synthesis, and material chemistry [26, 27]. The structure of –N=C=S in 1,3,4-thiadiazole derivatives can work as the active centre, chelate certain metal ions *in vivo,* and show good tissue permeability [28]. Recently, several 1,3,4-thiadiazole derivatives have been reported with different types of biological properties such as anticancer [29], antileishmanial [30], antihistamine [31], antibacterial [32], antioxidant [33], antiviral [34], anti-psychotic [35], anti-inflammatory [36], antihypertensive [37], analgesic [38], antimicrobial [39], antihepatitis B [40] and antidiabetic activities [41]. Some of the drugs such as azetepa (**1**, Fig. **1**), has 1,3,4-thiadiazole unit as a part of the structure and showed antineoplastic activity [42].

On the other hand, 1,2,3-triazoles are among the most privileged *N*-heterocyclic pharmacophores and are also able to form hydrogen bonds with suitable targets [43, 44]. There is a common method for the synthesis of triazoles *via* copper-catalyzed azide-alkyne cycloaddition, a "click-chemistry" reaction firstly introduced by Sharpless [45, 46]. The 1,2,3-triazole containing compounds have been reported to demonstrate a broad spectrum of biological activities including anticancer [47], antineoplastic [48], antitubercular [49], antibacterial [50], antiHIV [51], antifungal [52], antimalarial [53], antidiabetic [54], anti-inflammatory [55], glycosidase inhibitors [56], and antiplatelet properties [57]. The carboxyamidotriazole (CAI, **2**) is an anticancer agent containing 1,2,3-triazole ring as a part of the structure [58-60] (Fig. **1**).



Azepeta (1) **CAI (2)**

Fig. (1). Structures of azepeta (1) and CAI (20).

*Address correspondence to this author at the Department of Chemistry, Krishna University, Machilipatnam, Andhra Pradesh, 521001 India;
E-mail: professormandava@gmail.com

1570-1786/20 $65.00+.00 © 2020 Bentham Science Publishers

Based on the above-mentioned reports on noteworthy biological significances of 1,3,4-thiadiazole and 1,2,3-triazole derivatives, it appeared that these frameworks could be the key moieties responsible for a wide range of biological properties. Indeed, we were particularly interested in knowing the anticancer properties of combined moieties (*i.e.* 1,3,4-thiadiazole and 1,2,3-triazole) in a single molecular entity. Accordingly, we have designed and synthesized a series of new acetamides **12a-j** including 1,2,3-triazole, 1,3,4-thiadiazole, and isothiazolo[4,3-b]pyridine rings. Furthermore, all the synthesized compounds (12) have been screened for their anticancer activity against human cancer cell lines.

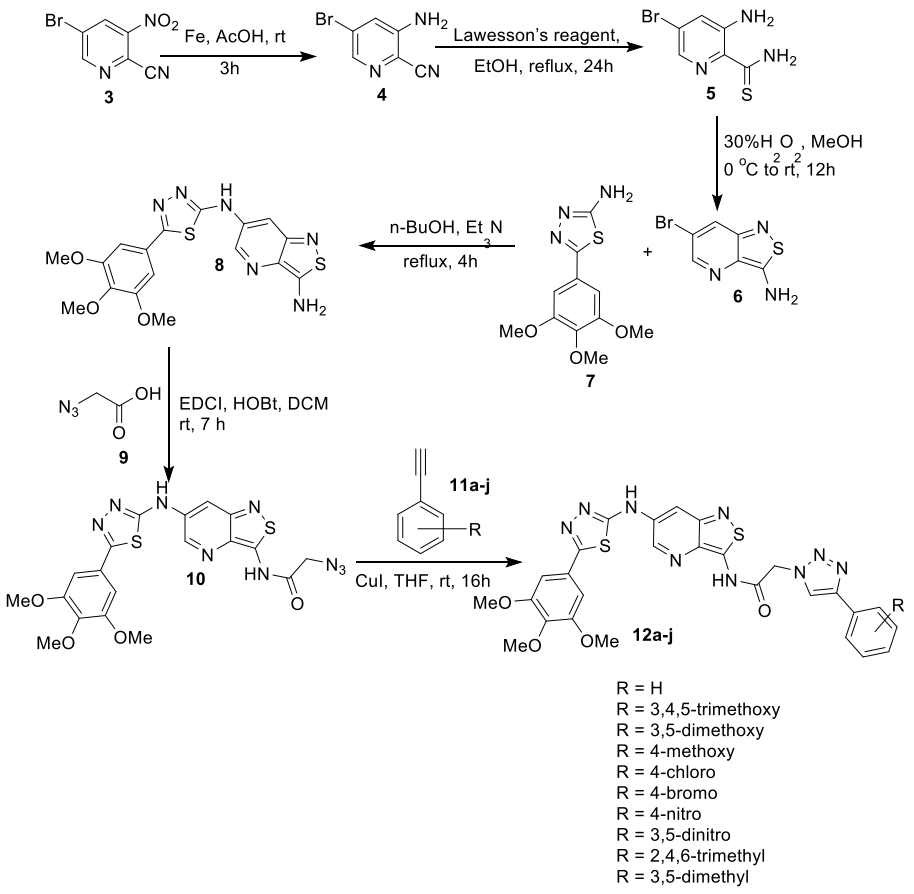
2. RESULTS AND DISCUSSION

2.1. Chemistry

The synthetic route for the preparation of a series of new 2-(4-aryl-1*H*-1,2,3-triazol-1-yl)-*N*-[6-[[5-(3,4,5-trimethoxyphenyl)-1,3,4-thiadiazol-2-yl]amino]isothia zolo[4,3-*b*]pyridin-3-yl]acetamides **12a-j** is shown in Scheme (**1**). Compounds **3-7, 9, 11** are known, while **8, 10,** and **12** have not been previously reported in the literature. The starting compound **3 [61]** was submitted to reduction with iron in acetic acid (AcOH) at room temperature (rt) over 3 h time period to afford the amino derivative **4** [61, 62]. This amino derivative **4** was refluxed with Lawesson's reagent [2,4-bis(4-methoxyphenyl)-1,3,2,4-dithiadiphosphetane 2,4-disulfide] in ethanol (EtOH) for 24 h to afford pure carbothio amide **5** [62]. This thioamide derivative **5** underwent cyclization by reaction with 30% H_2O_2 in methanol (MeOH) at rt over 12 h time period then afforded pure 6-bromoisothiazolo[4,3-*b*]pyridin-3-amine (**6**) [62]. Product 6 was refluxed with 5-(3,4,5-trimethoxy phenyl)-1,3,4-thiadiazol-2-amine (**7**) [63] in the presence of triethyl amine (Et_3N) in 1-butanol for 4 h time period then afforded isothiazolo pyridinamine derivative **8**. It underwent coupling with 2-azidoacetic acid (**9**) in the presence of EDCI [N^3-(ethylcarbonimidoyl)-N^1,N^1-dimethyl-1,3-propanediamine hydrochloride (1:1)], and HOBt (1-hydroxy-1*H*-benzotriazole) in anhydrous CH_2Cl_2 (DCM) at rt over 7 h time period then afforded pure azido derivative **10**. Finally, product 10 underwent clik-chemistry reaction with differently substituted ethynylbenzenes **11a-j** in the presence of CuI in anhydrous tetrahydrofuran (THF) for 16 h to give target compounds **12a-j**.

2.2. Biological Evaluation: *In vitro* Cytotoxicity

All these derivatives **12a-j** were examined for their anticancer activity against four human cancer cell lines [MCF-7 (breast cancer), A549 (lung cancer), DU-145 (prostate cancer) and MDA-MB-231 (breast cancer)] by the use of MTT [2-(4,5-dimethyl-2-thiazolyl)-3,5-diphenyl-2*H*-tetrazolium bromide (1:1)] assay and etoposide as positive reference drug. The obtained results are incorporated in Table **1** and most of the synthesized derivatives **12** exhibited better anticancer activity than the positive control. Derivatives **12** showed IC_{50} (half maximal inhibitory concentration) values



Scheme (1). Synthesis of 2-(4-aryl-1*H*-1,2,3-triazol-1-yl)-*N*-[6-[[5-(3,4,5-trimethoxyphenyl)-1,3,4-thiadiazol-2-yl]amino]isothiazolo[4,3-*b*]pyridin-3-yl]acetamides **12a-j**.

Table 1. ***In vitro*** **cytotoxicity of synthesized compounds 12a-j with IC_{50} in µM.**

Compound	MCF-7[a]	A549	DU-145	MDA-MB-231
12a	3.76±1.85	2.18±1.09	4.77±2.44	ND[b]
12b	0.67±0.093	0.22±0.034	0.11±0.071	1.09±0.83
12c	1.87±0.56	1.23±0.47	2.03±1.20	1.94±0.39
12d	2.98±1.77	2.12±1.32	4.76±2.60	3.16±1.94
12e	0.53±0.055	0.18±0.077	0.10±0.082	0.92±0.041
12f	2.44±2.03	7.43±2.30	3.08±1.88	ND
12g	1.32±0.12	1.49±0.48	2.10±1.56	2.77±1.70
12h	5.14±3.45	ND	ND	2.56±3.20
12i	8.12±4.56	10.2±4.10	6.29±3.86	2.64±1.99
12j	ND	12.4±4.65	14.7±6.21	3.72±2.66
Etoposide	2.11 ± 0.024	3.08 ± 0.135	1.97 ± 0.45	1.91 ± 0.84

[a]MCF-7: human breast cancer cell lines; A549: human lung cancer cell lines; DU-145: human prostate cancer cell lines; MDA-MB-231: human breast cancer cell lines.

[b]ND = Not determined.

in the range of 0.10±0.082 to 14.7±6.21 µM, and positive control in the range of 1.91±0.84 to 3.08±0.135 µM. Among all the synthesized **12**, four derivatives **12b,c,e**,**g** exhibited more potent activity. Structure-activity relationship results indicated that compound **12b** with 3,4,5-trimethoxy electron-donating substitution on phenyl ring showed better anti-cancer activity on four cell lines (MCF-7 0.67±0.093 µM, A549 0.22±0.034 µM, DU-145 0.11±0.071 µM and MDA-MB-231 1.09±0.83 µM) than the positive control, while compound **12c**, having 3,5-dimethoxy substitution, exhibited lower activity (MCF-7 1.87±0.56 µM, A549 1.23±0.47 µM, DU-145 2.03±1.20 µM and MDA-MB-231 1.94±0.39 µM) than **12b.** Compound **12d** with 4-methoxy substitution demonstrated much less activity (MCF-7 2.98±1.77 µM, A549 2.12±1.32 µM, DU-145 4.76±2.60 µM and MDA-MB-231 3.16±1.94 µM) than that of compounds **12b**,**c**. From the above results, we deduced that the decrease of electron-donating methoxy substituents should decrease the activity. Replacement of 4-methoxy with 4-chloro substituent yielded compound **12e** which showed the most promising activity (MCF-7 0.53±0.055 µM, A549 0.18±0.077 µM, DU-145 0.10±0.082 µM and MDA-MB-231 0.92±0.041 µM) compared to all the other compounds **12**, whereas compound **12g**, having 4-nitro substitution, displayed lesser activity (MCF-7 1.32±0.12 µM, A549 1.49±0.48 µM, DU-145 2.10±1.56 µM and MDA-MB-231 2.77±1.70 µM) in comparison with **12e.** The other compounds **12f**,**h**, showing electron-withdrawing substitution, exhibited moderate activity (MCF-7 = 2.44±2.03µM, A549 = 7.43±2.30µM, DU-145 = 3.08±1.88µM) and (MCF-7 = 5.14±3.45 µM, MDA-MB-231 = 2.56±3.20 µM) respectively in comparison with both compounds **12e,12g**. The compounds **12i**,**j**, with 2,4,6-trimethyl and 3,5-dimethyl substitution, showed very poor activity.

3. EXPERIMENTAL SECTION

All chemicals and reagents were obtained from Aldrich (Sigma–Aldrich, St. Louis, MO, USA), Lancaster (Alfa Aesar, Johnson Matthey Company, Ward Hill, MA, USA), and were used without further purification. Reactions were monitored by TLC, performed on silica gel 60 F_{254} glass plates, and visualization on TLC was achieved by UV light or iodine indicator. ^{1}H spectra were recorded on Brucker advance – 1 300 MHz and Brucker advance HD 400 MHz NMR spectrometer and ^{13}C NMR spectra were recorded on Brucker advance HD 400 MHz NMR spectrometer. Chemical shifts (δ) were reported in ppm downfield from internal TMS standard. ESI spectra were recorded on Micromass Quattro LC spectrometer using ESI+ software with capillary voltage 3.98 kV and MS (FAB) and MS (ESI) mode positive ion trap detector. Melting points were determined with an electrothermal melting point apparatus, and are uncorrected.

3.1. 3-Amino-5-bromo-2-pyridinecarbonitrile (4) [61,62]

5-Bromo-3-nitro-2-pyridinecarbonitrile (**3**) [61, 62] (13 g, 57.017 mmol) in one portion was added to a stirred solution of iron powder (6.4 g, 114.603 mmol) in AcOH (50 mL) at rt. The resulting reaction mixture was allowed to stir over 3 h time period. After completion of the reaction, ethyl acetate (65 mL) was added and the reaction mixture was filtered through a paper filter. The filtered cake was washed thoroughly with ethyl acetate (30 mL) and the filtrate was evaporated under reduced pressure. The crude product was purified by flash silica gel column chromatography with DCM to afford pure compound **4** (7.4 g, 37.370 mmol, 66% yield). ^{1}H NMR (300 MHz, DMSO-d_6): δ 6.57 (bs, 2H), 7.27-7.36 (m, 1H), 7.66-7.70 (m, 1H); MS (FAB): 197 $[M]^+$.

3.2. 3-Amino-5-bromo-2-pyridinecarbothioamide (5)

Lawesson's reagent (28.6 g, 70.710 mmol) was added to a solution of 3-amino-5-bromo pyridine-2-carbonitrile (**4)** (7 g, 35.350 mmol) in absolute EtOH (50 mL) [62]. This reaction mixture was allowed to stir at reflux temperature over 24 h time period. After completion of the reaction confirmed

by TLC, the solvent was evaporated under reduced pressure. The residue was redissolved in water (100 mL) and extracted three times with DCM (3 X 20 = 60 mL). The combined organic layers were evaporated under reduced pressure. The crude product was purified by flash silica gel column chromatography with heptane/acetone 6:4 to afford pure compound **5** (7 g, 30.159 mmol, 85% yield). ^{1}H NMR (300 MHz, DMSO-d_6) δ 6.96 (bs, 2H), 7.28 (d, 1H, *J* = 1.95 Hz), 7.89 (d, 1H, *J* = 1.95 Hz), 9.39 (bs, 2H); ^{13}C NMR (100 MHz, DMSO-d6) *δ* 129.3, 139.6, 141.7, 144.6, 147.3, 179.6; MS (FAB): 233 $[M+2H]^+$.

3.3. 6-Bromoisothiazolo[4,3-b]pyridin-3-amine (6)

30% aqueous H_2O_2 solution (2 mL, 19.6 mmol) was added dropwise to a solution of 3-amino-5-bromopyridine-2-carbothioamide (**5**) (6 g, 25.851 mmol) in MeOH (30 mL) at 0°C. The reaction mixture was stirred at rt overnight. After consumption of the starting material, the reaction mass was cooled to 0 °C. The precipitate was filtered off and washed with cold MeOH (4 mL) to afford pure compound **6** (3.1 g, 13.473 mmol, 52% yield). ^{1}H NMR (300 MHz, DMSO-d_6): δ 8.04 (d, 1H, *J* = 2.0 Hz), 8.08 (bs, 2H), 8.30 (d, 1H, *J* = 2.0 Hz); ^{13}C NMR (100 MHz, DMSO-d6): δ 109.6, 120.8, 138.9, 146.1, 155.8, 159.0; MS (FAB): 231$[M+2H]^+$.

3.4. *N*^{6}-[5-(3,4,5-Trimethoxyphenyl)-1,3,4-thiadiazol-2-yl)isothiazolo[4,3-b]pyridine-3,6-diamine (8)

The compound 6-bromoisothiazolo[4,3-*b*]pyridin-3-amine (**6**) (10 g, 43.461 mmol) was heated with 5-(3,4,5-trimethoxyphenyl)-1,3,4-thiadiazol-2-amine (**7**) [63] (11.6 g, 43.397 mmol) in anhydrous 1-butanol (50 mL). To this, Et_3N (12.1 mL, 86.753 mmol) was added dropwise to the reaction mixture under stirring conditions and refluxed for 4 h. After completion of the reaction, water (70 mL) was added and the crude product was extracted using ethyl acetate (3 X 10 = 30 mL). The compound was purified by silica gel column chromatography using ethyl acetate/hexane 4:6 to afford **8** (12.6 g, 30.254 mmol, 70% yield). Mp;163-164 ^{o}C. ^{1}H NMR (300 MHz, DMSO-d_6): δ 3.87 (s, 6H), 3.90 (s, 3H), 7.34 (s, 2H), 7.91 (d, 1H, *J* = 2.1 Hz), 8.07 (bs, 2H), 8.23 (s, 1H), 8.27 (d, 1H, *J* = 2.1 Hz); ^{13}C NMR (100 MHz, DMSO-d_6): δ 56.8, 60.3, 106.7, 115.3, 121.6, 134.7, 144.7, 149.3, 149.9, 150.1, 151.1, 154.7, 156.7, 163.2; MS (ESI): 417 $[M+H]^+$. Anal. Calcd for $C_{17}H_{16}N_6O_3S_2$: C, 49.03; H, 3.87; N, 20.18; found: C, 49.18; H, 4.01; N, 20.07%.

3.5. 2-Azido-*N*-[6-[[5-(3,4,5-trimethoxyphenyl)-1,3,4-thiadiazol-2-yl]amino]isothiazolo[4,3-*b*]pyridin-3-yl) acetamide (10)

Compound **8** (12 g, 28.813 mmol), EDCI (10.5 g, 54.773 mmol), HOBt (38 mg, 0.281 mmol) were dissolved in 50 mL anhydrous DCM and stirred at 0 ^{o}C for 1 h. 2-Azidoacetic acid (**9**) (2.2 mL, 29.388 mmol) was then added into the mixture and stirred at rt for 7 h (Reaction time of 7 h is reported in Scheme **1**). After completion of the reaction, the mixture was washed with saturated sodium bicarbonate solution. The organic layer was evaporated under reduced pressure to afford the pure compound **10** (11.6 g, 23.222 mmol, 81% yield). Mp;181-183 ^{o}C ^{1}H NMR (300 MHz, DMSO-d_6): δ 3.87 (s, 6H), 3.91 (s, 3H), 4.68 (s, 2H), 7.34 (s, 2H), 7.90 (d, 1H, *J* = 2.2 Hz), 8.28 (d, 1H, *J* = 2.2 Hz), 10.54 (s, 1H), 12.85 (bs, 1H); ^{13}C NMR (100 MHz DMSO-d_6): δ 47.8, 56.7, 60.1, 105.9, 115.3, 133.8, 144.3, 147.6, 148.7, 150.1, 152.3, 156.7, 157.8, 163.1, 168.2; MS (ESI): 500 $[M+H]^+$. Anal. Calcd for $C_{19}H_{17}N_9O_4S_2$: C, 45.68; H, 3.43; N, 25.24; found: C, 45.54; H, 3.58; N, 25.05%.

3.6. *N*-[6-[[5-(3,4,5-Trimethoxyphenyl)-1,3,4-thiadiazol-2-yl]amino]isothiazolo[4,3-*b*]pyridin-3-yl]-2-(4-phenyl-1*H*-1,2,3-triazol-1-yl)acetamide (12a)

The azide **10** (300 mg, 0.601 mmol) and 1-ethynylbenzene (**11a**) (0.067 mL, 0.601 mmol) were dissolved in 15 mL of anhydrous THF and CuI (0.6 mg, 0.5 mol%, 0.003 mmol) was added. The mixture was stirred vigorously at rt for 16 h. After completion of the reaction, THF was evaporated in vacuum and the crude product was handled with ethyl acetate (3 × 30 mL = 90 mL). The organic phase was washed with water (3 × 30 mL = 90 mL) and dried over with Na_2SO_4. After removal of the solvent in vacuum the crude product was purified by silica gel column chromatography with ethyl acetate/hexane 4:6 to obtain pure compound **12a** (143.4 mg, 0.238 mmol, 40% yield). Mp: 201-203^{o}C; ^{1}H NMR (400 MHz, DMSO-d_6): δ 3.88 (s, 6H), 3.91 (s, 3H), 4.81 (s, 2H), 7.33 (s, 2H), 7.45-7.57 (m, 3H), 7.66 (d, 2H, *J* = 7.8 Hz), 7.91 (d, 1H, *J* = 2.3 Hz), 7.96 (s, 1H), 8.34 (d, 1H, *J* = 2.3 Hz), 10.53 (s, 1H), 13.44 (bs, 1H); ^{13}C NMR (100 MHz, DMSO-d_6): δ 45.4, 57.6, 61.8, 106.3, 114.8, 116.3, 126.8, 128.4, 129.3, 131.2, 134.7, 143.2, 144.5, 148.5, 149.3, 150.5, 154.6, 155.7, 156.8, 157.8, 162.6, 169.8; MS (ESI): 602 $[M+H]^+$. Anal. Calcd for $C_{27}H_{23}N_9O_4S_2$: C, 53.90; H, 3.85; N, 20.95; found: C, 54.04; H, 3.98; N, 20.99%.

3.7. *N*-[6-[[5-(3,4,5-Trimethoxyphenyl)-1,3,4-thiadiazol-2-yl]amino]isothiazolo[4,3-*b*]pyridin -3-yl]-2-[4-(3,4,5-trimethoxyphenyl)-1*H*-1,2,3-triazol-1-yl]acetamide (12b)

Compound **12b** was prepared by the method described for **12a**, employing **10** (300 mg, 0.601 mmol) which was dissolved in 15 mL of THF, followed by the addition of 5-ethynyl-1,2,3-trimethoxybenzene (**11b**) (115 mg, 0.598 mmol) and CuI (0.6 mg, 0.5 mol%, 0.003 mmol). The crude product was purified by silica gel column chromatography with ethyl acetate/hexane 6:4 to afford pure compound **12b** (139.6 mg, 0.202 mmol, 34% yield). Mp: 256-258^{o}C; ^{1}H NMR (400 MHz, DMSO-d_6): δ 3.85 (s, 6H), 3.88 (s, 6H), 3.91 (s, 3H), 3.95 (s, 3H), 4.78 (s, 2H), 7.33 (s, 2H), 7.40 (s, 2H), 7.90 (d, 1H, *J* = 2.1 Hz), 7.95 (s, 1H), 8.33 (d, 1H, *J* = 2.1 Hz), 10.54 (s, 1H), 13.45 (bs, 1H); ^{13}C NMR (100 MHz, DMSO-d_6): δ 45.5, 56.7, 57.8, 61.4, 62.6, 105.7, 110.5, 114.3, 116.8, 127.3, 134.2, 143.4, 144.6, 145.6, 148.3, 149.4, 150.2, 154.6, 155.3, 156.7, 157.3, 157.8, 162.7, 170.2; MS (ESI): 692 $[M+H]^+$. Anal. Calcd for $C_{30}H_{29}N_9O_7S_2$: C, 52.09; H, 4.23; N, 18.22; found: C, 52.24; H, 4.11; N, 18.39%.

3.8. *N*-[6-[[5-(3,4,5-Trimethoxyphenyl)-1,3,4-thiadiazol-2-yl]amino]isothiazolo[4,3-*b*]pyridin-3-yl]-2-[4-(3,5-dimethoxyphenyl)-1*H*-1,2,3-triazol-1-yl]acetamide (12c)

Compound **12c** was prepared by the method described for **12a**, employing **10** (300 mg, 0.601 mmol) which was

dissolved in 15 mL of THF, followed by the addition of 1-ethynyl-3,5-dimethoxybenzene (**11c**) (97 mg, 0.598 mmol) and CuI (0.6 mg, 0.5 mol%, 0.003 mmol). The crude product was purified by silica gel column chromatography with ethyl acetate / hexane 6:4 to afford pure compound **12c** (131.7 mg, 0.199 mmol, 33% yield). Mp: 230-232°C; ^{1}H NMR (400 MHz, DMSO-d_6): δ 3.79 (s, 6H), 3.88 (s, 6H), 3.91 (s, 3H), 4.80 (s, 2H), 7.09 (s, 1H), 7.34 (s, 2H), 7.39 (s, 2H), 7.91 (d, 1H, *J* = 2.0 Hz), 7.96 (s, 1H), 8.35 (d, 1H, *J* = 2.0 Hz), 10.54 (s, 1H), 13.44 (bs, 1H); ^{13}C NMR (100 MHz, DMSO-d_6): δ 45.6, 57.4, 58.3, 61.8, 99.4, 106.4, 110.6, 114.5, 116.3, 132.4, 134.5, 143.7, 145.6, 148.3, 149.2, 150.4, 154.6, 155.4, 156.7, 157.8, 162.4, 164.6, 169.7; MS (ESI): 662 $[M+H]^+$. Anal. Calcd for $C_{29}H_{27}N_9O_6S_2$: C, 52.64; H, 4.11; N, 19.05; found: C, 52.49; H, 4.01; N, 18.02%.

3.9. *N*-[6-[[5-(3,4,5-Trimethoxyphenyl)-1,3,4-thiadiazol-2-yl]amino]isothiazolo[4,3-*b*]pyridin-3-yl]-2-[4-(4-methoxyphenyl)-1*H*-1,2,3-triazol-1-yl]acetamide (12d)

Compound **12d** was prepared by the method described for **12a**, employing **10** (300 mg, 0.601 mmol) which was dissolved in 15 mL of THF, followed by the addition of 1-ethynyl-4-methoxybenzene (**11d)** (0.077 mL, 0.587 mmol) and CuI (0.6 mg, 0.5 mol%, 0.003 mmol). The crude product was purified by silica gel column chromatography with ethyl acetate / hexane 6:4 to afford pure compound **12d** (112.8 mg, 0.179 mmol, 30% yield). Mp: 199-201°C; ^{1}H NMR (400 MHz, DMSO-d_6): δ 3.76 (s, 3H), 3.89 (s, 6H), 3.92 (s, 3H), 4.83 (s, 2H), 7.18 (d, 2H, *J* = 7.6 Hz), 7.34 (s, 2H), 7.44 (d, 2H, *J* = 7.6 Hz), 7.91 (d, 1H, *J* = 2.2 Hz), 7.95 (s, 1H), 8.34 (d, 1H, *J* = 2.2 Hz), 10.43 (s, 1H), 13.45 (bs, 1H); ^{13}C NMR (100 MHz, DMSO-d_6): δ 45.6, 57.5, 58.2, 61.8, 106.5, 114.5, 115.8, 116.4, 124.3, 127.6, 134.5, 141.4, 143.6, 148.7, 149.3, 150.5, 154.3, 156.7, 157.2, 157.8, 160.4, 162.5, 169.8; MS (ESI): 632 $[M+H]^+$. Anal. Calcd for $C_{28}H_{25}N_9O_5S_2$: C, 53.24; H, 3.99; N, 19.96; found: C, 53.09; H, 4.14; N, 20.13%.

3.10. 2-[4-(4-Chlorophenyl)-1*H*-1,2,3-triazol-1-yl]-*N*-[6-[[5-(3,4,5-trimethoxyphenyl)-1,3,4-thiadiazol-2-yl]amino]isothiazolo[4,3-*b*]pyridin-3-yl]acetamide (12e)

Compound **12e** was prepared by the method described for **12a**, employing **10** (300 mg, 0.601 mmol) which was dissolved in 15 mL of THF, followed by the addition of 1-chloro-4-ethynylbenzene (**11e)** (82 mg, 0.600 mmol) and CuI (0.6 mg, 0.5 mol%, 0.003 mmol) and the crude product was purified by silica gel column chromatography with ethyl acetate / hexane 4:6 to afford pure compound **12e** (191.6 mg, 0.301 mmol, 50% yield). Mp: 266-268°C; ^{1}H NMR (400 MHz, DMSO-d_6): δ 3.88 (s, 6H), 3.92 (s, 3H), 4.90 (s, 2H), 7.34 (s, 2H), 7.52 (d, 2H, *J* = 7.9 Hz), 7.67 (d, 2H, *J* = 7.9 Hz), 7.90 (d, 1H, *J* = 2.3 Hz), 7.98 (s, 1H), 8.35 (d, 1H, *J* = 2.3 Hz), 10.44 (s, 1H), 13.48 (bs, 1H); ^{13}C NMR (100 MHz, DMSO-d_6): δ 45.7, 57.8, 61.9, 106.5, 114.7, 116.8, 128.6, 130.3, 130.8, 133.4, 134.9, 143.5, 144.2, 148.7, 149.7, 150.3, 154.4, 156.7, 157.1, 157.6, 162.7, 170.4; MS (ESI): 636 $[M+H]^+$. Anal. Calcd for $C_{27}H_{22}ClN_9O_4S_2$: C, 50.98; H, 3.49; N, 19.82; found: C, 51.12; H, 3.61; N, 19.66%.

3.11. 2-[4-(4-Bromophenyl)-1*H*-1,2,3-triazol-1-yl]-*N*-[6-[[5-(3,4,5-trimethoxyphenyl)-1,3,4-thiadiazol-2-yl]amino]isothiazolo[4,3-*b*]pyridin-3-yl]acetamide (12f)

Compound **12f** was prepared by the method described for **12a**, employing **10** (300 mg, 0.601 mmol) which was dissolved in 15 mL of THF, followed by the addition of 1-bromo-4-ethynylbenzene (**11f**) (108 mg, 0.597 mmol) and CuI (0.6 mg, 0.5 mol%, 0.003 mmol). The crude product was purified by silica gel column chromatography with ethyl acetate / hexane 5:5 to afford pure compound **12f** (159.4 mg, 0.234 mmol, 39% yield). Mp: 259-261°C; ^{1}H NMR (400 MHz, DMSO-d_6): δ 3.89 (s, 6H), 3.92 (s, 3H), 4.93 (s, 2H), 7.33 (s, 2H), 7.57 (d, 2H, *J* = 8.0 Hz), 7.69 (d, 2H, *J* = 8.0 Hz), 7.92 (d, 1H, *J* = 2.4 Hz), 7.99 (s, 1H), 8.36 (d, 1H, *J* = 2.4 Hz), 10.44 (s, 1H), 13.50 (bs, 1H); ^{13}C NMR (100 MHz, DMSO-d_6): δ 45.8, 57.8, 61.6, 106.7, 114.5, 116.7, 122.4, 128.5, 130.5, 132.6, 134.8, 143.5, 144.7, 148.2, 149.6, 150.2, 154.6, 156.7, 157.3, 157.9, 162.7, 170.2; MS (ESI): 680 $[M+H]^+$. (The exact mass of **12f** is 679.04. Is this line M+3?) Anal. Calcd for $C_{27}H_{22}BrN_9O_4S_2$: C, 47.65; H, 3.26; N, 18.52; found: C, 47.51; H, 3.42; N, 18.67%.

3.12. *N*-[6-[[5-(3,4,5-Trimethoxyphenyl)-1,3,4-thiadiazol-2-yl]amino]isothiazolo[4,3-*b*]pyridin-3-yl]-2-[4-(4-nitrophenyl)-1*H*-1,2,3-triazol-1-yl]acetamide (12g)

Compound **12g** was prepared by the method described for **12a**, employing **10** (300 mg, 0.601 mmol) which was dissolved in 15 mL of THF, followed by the addition of 1-ethynyl-4-nitrobenzene (**11g**) (88 mg, 0.598 mmol) and CuI (0.6 mg, 0.5 mol%, 0.003 mmol). The crude product was purified by silica gel column chromatography with ethyl acetate / hexane 4:6 to afford pure compound **12g** (178.2 mg, 0.276 mmol, 46% yield). Mp: 280-282°C; ^{1}H NMR (400 MHz, DMSO-d_6): δ 3.89 (s, 6H), 3.92 (s, 3H), 4.97 (s, 2H), 7.34 (s, 2H), 7.72 (d, 2H, *J* = 8.1 Hz), 7.92 (d, 1H, *J* = 2.3 Hz), 8.01 (s, 1H), 8.28-8.40 (m, 3H), 10.44 (s, 1H), 13.53 (bs, 1H); ^{13}C NMR (100 MHz, DMSO-d_6): δ 46.3, 57.8, 61.8, 106.5, 114.8, 116.8, 125.3, 130.8, 134.6, 135.8, 143.4, 144.7, 147.3, 148.6, 149.2, 150.3, 154.6, 156.7, 157.4, 157.8, 162.8, 170.4; MS (ESI): 647 $[M+H]^+$. Anal. Calcd for $C_{27}H_{22}N_{10}O_6S_2$: C, 50.15; H, 3.43; N, 21.66; found: C, 50.32; H, 3.61; N, 21.83%.

3.13. *N*-[6-[[5-(3,4,5-Trimethoxyphenyl)-1,3,4-thiadiazol-2-yl]amino]isothiazolo[4,3-*b*]pyridin-3-yl]-2-[4-(3,5-dinitrophenyl)-1*H*-1,2,3-triazol-1-yl]acetamide (12h)

Compound **12h** was prepared by the method described for **12a**, employing **10** (300 mg, 0.601 mmol) which was dissolved in 15 mL of THF, followed by the addition of 1-ethynyl-3,5-dinitrobenzene (**11h**) (115 mg, 0.599 mmol) and CuI (0.6 mg, 0.5 mol%, 0.003 mmol). The crude product was purified by silica gel column chromatography with ethyl acetate / hexane 5:5 to afford pure compound **12h** (210.5 mg, 0.304 mmol, 51% yield). Mp: 290-292°C; ^{1}H NMR (400 MHz, DMSO-d_6): δ 3.88 (s, 6H), 3.92 (s, 3H), 4.98 (s, 2H), 7.33 (s, 2H), 7.92 (d, 1H, *J* = 2.3 Hz), 8.04 (s, 1H), 8.34 (d, 1H, *J* = 2.3 Hz), 8.47 (s, 2H), 8.86 (s, 1H), 10.44 (s, 1H), 13.56 (bs, 1H); ^{13}C NMR (100 MHz, DMSO-d_6): δ 46.8, 57.8, 61.7, 106.5, 114.8, 115.8, 118.4, 133.4, 134.2, 134.6, 143.6, 147.3, 147.8, 148.3, 149.6, 150.3, 154.6, 156.3, 157.5,

157.9, 162.7, 170.6; MS (ESI): 692 $[M+H]^+$. Anal. Calcd for $C_{27}H_{21}N_{11}O_8S_2$: C, 46.89; H, 3.06; N, 22.28; found: C, 46.72; H, 3.19; N, 22.44%.

3.14. *N*-[6-[[5-(3,4,5-Trimethoxyphenyl)-1,3,4-thiadiazol-2-yl]amino]isothiazolo[4,3-*b*]pyridin-3-yl]-2-[4-(2,4,6-trimethylphenyl)-1*H*-1,2,3-triazol-1-yl)acetamide (12i)

Compound **12i** was prepared by the method described for **12a**, employing **10** (300 mg, 0.601 mmol) which was dissolved in 15 mL of THF, followed by the addition of 2-ethynyl-1,3,5-trimethylbenzene (**11i**) (0.09 mL, 0.573 mmol) and CuI (0.6 mg, 0.5 mol%, 0.003 mmol). The crude product was purified by silica gel column chromatography with ethyl acetate / hexane 4:6 to afford pure compound **12i** (166.8 mg, 0.259 mmol, 45% yield). Mp: 210-212°C; ^{1}H NMR (400 MHz, DMSO-d_6): δ 2.46 (s, 3H), 2.64 (s, 6H), 3.89 (s, 6H), 3.91 (s, 3H), 4.78 (s, 2H), 6.98 (s, 2H), 7.33 (s, 2H), 7.91 (d, 1H, J = 2.2 Hz), 7.95 (s, 1H), 8.33 (d, 1H, J = 2.2 Hz), 10.42 (s, 1H), 12.67 (bs, 1H); ^{13}C NMR (100 MHz, DMSO-d_6): δ 24.8, 27.6, 45.6, 57.7, 61.6, 106.5, 114.7, 116.8, 129.4, 130.5, 134.2, 136.7, 138.2, 143.2, 144.6, 148.4, 149.7, 150.4, 154.6, 156.8, 157.3, 157.8, 162.7, 169.6; MS (ESI): 644 $[M+H]^+$. Anal. Calcd for $C_{30}H_{29}N_9O_4S_2$: C, 55.97; H, 4.54; N, 19.58; found: 56.11; H, 4.42; N, 19.41%.

3.15. *N*-[6-[[5-(3,4,5-Trimethoxyphenyl)-1,3,4-thiadiazol-2-yl]amino]isothiazolo[4,3-*b*]pyridin-3-yl]-2-[4-(3,5-dimethylphenyl)-1*H*-1,2,3-triazol-1-yl]acetamide (12j)

Compound **12j** was prepared by the method described for **12a**, employing **10** (300 mg, 0.601 mmol) which was dissolved in 15 mL of THF, followed by the addition of 1-ethynyl-3,5-dimethylbenzene (**11j**) (0.08 mL, 0.571 mmol) and CuI (0.6 mg, 0.5 mol%, 0.003 mmol). The crude product was purified by silica gel column chromatography with ethyl acetate/hexane 4:6 to afford pure compound **12j** (152.7 mg, 0.242 mmol, 42% yield). Mp: 205-207°C; ^{1}H NMR (400 MHz, DMSO-d_6): δ 2.55 (s, 6H), 3.89 (s, 6H), 3.92 (s, 3H), 4.77 (s, 2H), 7.09 (s, 1H), 7.24 (s, 2H), 7.34 (s, 2H), 7.91 (d, 1H, J = 2.1 Hz), 7.96 (s, 1H), 8.32 (d, 1H, J = 2.1 Hz), 10.43 (s, 1H), 12.68 (bs, 1H); ^{13}C NMR (100 MHz, DMSO-d_6): δ 26.5, 45.7, 57.6, 61.8, 106.4, 114.8, 116.4, 129.6, 131.5, 134.2, 135.8, 140.4, 143.8, 146.3, 148.4, 149.6, 150.4, 154.6, 156.7, 157.4, 157.8, 162.7, 169.8; MS (ESI): 630 $[M+H]^+$. Anal. Calcd for $C_{29}H_{27}N_9O_4S_2$: C, 55.31; H, 4.32; N, 20.02; found: C, 55.14; H, 4.46; N, 20.17%.

3.16. MTT Assay

Each datum is represented as mean ±SD (standard deviation) value from three different experiments performed in triplicates. Individual wells of a 96-well tissue culture microtiter plate were inoculated with 100 µL of complete medium containing 10^4 cells. The plates were incubated at 37°C in a humidified 5% CO_2 incubator for 18 h prior to the experiment. After medium removal, 100 µL of fresh medium containing the test compounds and etoposide at different concentrations such as 0.5, 1, and 2 µM was added to each well and incubated at 37°C for 24 h. Then the medium was discarded and replaced with 10 µL MTT dye. Plates were incubated at 37°C for 2 h. The resulting formazan (diazene carboxaldehyde hydrazone) crystals were solubilized in 100 µL extraction buffer. The optical density was read at 570 nm with a microplate reader (Thermo Scientific Varioskan LUX Multimode instrument). The percentage of DMSO in the medium never exceeded 0.25%.

CONCLUSION

In summary, we have reported a series of new acetamides **12a-j** incorporating 1,2,3-triazole, 1,3,4-thiadiazole, and isothiazolo[4,3-*b*]pyridine rings. Their chemical structures were confirmed by elemental analyses, ^{1}H NMR, ^{13}C NMR, and mass spectral data. Furthermore, these derivatives **12** were tested for their anticancer activity towards four human cancer cell lines [MCF-7 (breast cancer), A549 (lung cancer), DU-145 (prostate cancer) and MDA-MB-231 (breast cancer)] by the use of MTT assay. Etoposide was used as a positive control and all the synthesized derivatives **12** displayed good to moderate activity. Among them, compounds **12b,c,e,g** showed more potent activity. Compound **12e** showed excellent anticancer activity on all cell lines.

CONSENT FOR PUBLICATION

Not applicable.

AVAILABILITY OF DATA AND MATERIALS

The authors confirm that the data supporting the findings of this research are available within the article and its supplementary materials.

FUNDING

None.

CONFLICT OF INTEREST

The authors declare no conflict of interest, financial or otherwise.

ACKNOWLEDGEMENTS

Declared none.

SUPPLEMENTARY MATERIAL

Supplementary material is available on the publisher's website along with the published article.

REFERENCES

[1] Eckhardt, S. *Curr. Med. Chem. Anticancer Agents,* **2002**, *2*(3), 419-439. http://dx.doi.org/10.2174/1568011024606389 PMID: 12678741

[2] Anand, P.; Kunnumakkara, A.B.; Sundaram, C.; Harikumar, K.B.; Tharakan, S.T.; Lai, O.S.; Sung, B.; Aggarwal, B.B. *Pharm. Res.,* **2008**, *25*(9), 2097-2116. http://dx.doi.org/10.1007/s11095-008-9661-9 PMID: 18626751

[3] Vogelstein, B.; Kinzler, K.W. *The Genetic Basis of Human Cancer*; McGraw-Hill Education / Medical, **2005**.

[4] Hatti, I.; Sreenivasulu, R.; Jadav, S.S.; Ahsan, M.J.; Raju, R.R. *Monatsh. Chem.,* **2015**, *146*, 1699-1705. http://dx.doi.org/10.1007/s00706-015-1448-1

[5] Hatti, I.; Sreenivasulu, R.; Jadav, S.S.; Jayaprakash, V.; Kumar, C.G.; Raju, R.R. *Med. Chem. Res.,* **2015**, *24*, 3305-3313. http://dx.doi.org/10.1007/s00044-015-1375-z

[6] Ahsan, M.J.; Choudhary, K.; Jadav, S.S.; Yasmin, S.; Ansari, M.Y.; Sreenivasulu, R. *Med. Chem. Res.,* **2015**, *24*, 4166-4180. http://dx.doi.org/10.1007/s00044-015-1457-y

[7] Reddy, N.B.; Burra, V.R.; Ravindranath, L.K.; Sreenivasulu, R.; Kumar, V.N. *Monatsh. Chem.,* **2016**, *147*, 593-598. http://dx.doi.org/10.1007/s00706-016-1685-y

[8] Reddy, N.B.; Burra, V.R.; Ravindranath, L.K.; Kumar, V.N.; Sreenivasulu, R.; Sadanandam, P. *Monatsh. Chem.,* **2016**, *147*, 599-604. http://dx.doi.org/10.1007/s00706-016-1684-z

[9] Sreenivasulu, R.; Sujitha, P.; Jadav, S.S.; Ahsan, M.J.; Kumar, C.G.; Raju, R.R. *Monatsh. Chem.,* **2017**, *148*, 305-314. http://dx.doi.org/10.1007/s00706-016-1750-6

[10] Madhavi, S.; Sreenivasulu, R.; Raju, R.R. *Monatsh. Chem.,* **2017**, *148*, 933-938. http://dx.doi.org/10.1007/s00706-016-1790-y

[11] Agarwal, M.; Singh, V.; Sharma, S.K.; Sharma, P.; Ansari, M.Y.; Jadav, S.S.; Yasmin, S.; Sreenivasulu, R.; Hassan, M.Z.; Saini, V.; Ahsan, M.J. *Med. Chem. Res.,* **2016**, *25*, 2289-2303. http://dx.doi.org/10.1007/s00044-016-1672-1

[12] Madhavi, S.; Sreenivasulu, R.; Yazala, J.P.; Raju, R.R. *Saudi Pharm. J.,* **2017**, *25*(2), 275-279. http://dx.doi.org/10.1016/j.jsps.2016.06.005 PMID: 28344479

[13] Madhavi, S.; Sreenivasulu, R.; Ansari, Md. *Lett. Org. Chem.,* **2016**, *13*, 682-692. http://dx.doi.org/10.2174/1570178613666161021105317

[14] Sreenivasulu, R.; Durgesh, R.; Jadav, S.S.; Sujitha, P.; Kumar, C.G.; Raju, R.R. *Chem. Pap.,* **2018**, *72*, 1369-1378. http://dx.doi.org/10.1007/s11696-017-0372-8

[15] Subramanyam, M.; Sreenivasulu, R. *Lett. Drug Des. Discov.,* **2018**, *15*, 1299-1307. http://dx.doi.org/10.2174/1570180815666180219165119

[16] Rudavath, D.; Sreenivasulu, R.; Pinapati, S.R.; Raju, R.R. *J. Indian Chem. Soc.,* **2018**, *95*, 433-438.

[17] Suma, V.R.; Sreenivasulu, R.; Subramanyam, M.; Rao, K.R.M. *Russ. J. Gen. Chem.,* **2019**, *89*, 499-504. http://dx.doi.org/10.1134/S1070363219030228

[18] Shahinshavali, S.; Sreenivasulu, R.; Guttikonda, V.R.; Kolli, D.; Rao, M.V.B. *Russ. J. Gen. Chem.,* **2019**, *89*, 324-329. http://dx.doi.org/10.1134/S1070363219020257

[19] Spandana, Z.; Sreenivasulu, R.; Rao, M.V.B. *Lett. Org. Chem.,* **2019**, *16*, 662-667. http://dx.doi.org/10.2174/1570178616666181211094526

[20] Spandana, Z.; Sreenivasulu, R.; Rekha, T.M.; Rao, M.V.B. *Lett. Drug Des. Discov.,* **2019**, *16*, 656-662. http://dx.doi.org/10.2174/1570180816666181031125946

[21] Devi, E.R.; Sreenivasulu, R.; Rao, K.P.; Nadh, R.V.; Sireesha, M. *Lett. Org. Chem.,* **2020**, *17*, 54-60. http://dx.doi.org/10.2174/1570178616666190528095548

[22] Reddy, K.T.; Sreenivasulu, R.; Raju, R.R. *J. Indian Chem. Soc.,* **2019**, *96*, 1085-1090.

[23] Murthy, I.S.; Sreenivasulu, R.; Alluraiah, G.; Raju, R.R. *Russ. J. Gen. Chem.,* **2019**, *89*, 1718-1723. http://dx.doi.org/10.1134/S1070363219080279

[24] Rao, B.V.D.; Sreenivasulu, R.; Rao, M.V.B. *Russ. J. Gen. Chem.,* **2019**, *89*, 2115-2120. http://dx.doi.org/10.1134/S1070363219100207

[25] Yakantham, T.; Sreenivasluu, R.; Raju, R.R. *Russ. J. Gen. Chem.,* **2019**, *89*, 1485-1490. http://dx.doi.org/10.1134/S1070363219070181

[26] Sayed, A.R. *Tetrahedron,* **2012**, *68*, 2784-2789. http://dx.doi.org/10.1016/j.tet.2012.02.011

[27] Shahcheragh, S.M.; Habibi, A.; Khosravi, S. *Tetrahedron Lett.,* **2017**, *58*, 855-859. http://dx.doi.org/10.1016/j.tetlet.2017.01.057

[28] Luo, Z.; Chen, B.; He, S.; Shi, Y.; Liu, Y.; Li, C. *Bioorg. Med. Chem. Lett.,* **2012**, *22*(9), 3191-3193. http://dx.doi.org/10.1016/j.bmcl.2012.03.043 PMID: 22483583

[29] Aliabadi, A.; Eghbalian, E.; Kiani, A. *Iran. J. Basic Med. Sci.,* **2013**, *16*(11), 1133-1138. PMID: 24494064

[30] Poorrajab, F.; Ardestani, S.K.; Emami, S.; Behrouzi-Fardmoghadam, M.; Shafiee, A.; Foroumadi, A. *Eur. J. Med. Chem.,* **2009**, *44*, 1758-1762. http://dx.doi.org/10.1016/j.ejmech.2008.03.039 PMID: 18485538

[31] Gupta, J.K.; Yadav, R.K.; Dudhe, R.; Sharma, P.K. *Int. J. Pharm. Tech. Res.,* **2010**, *2*, 1493-1507.

[32] Li, P.; Shi, L.; Gao, M-N.; Yang, X.; Xue, W.; Jin, L-H.; Hu, D-Y.; Song, B-A. *Bioorg. Med. Chem. Lett.,* **2015**, *25*(3), 481-484. http://dx.doi.org/10.1016/j.bmcl.2014.12.038 PMID: 25563889

[33] Gür, M.; Muglu, H.; Çavus, M.S.; Güder, A.; Sayiner, H.S.; Kandemirli, F. *J. Mol. Struct.,* **2017**, *1134*, 40-50. http://dx.doi.org/10.1016/j.molstruc.2016.12.041

[34] Chen, Z.; Xu, W.; Liu, K.; Yang, S.; Fan, H. *Molecules,* **2010**, *15*, 9046-9056. http://dx.doi.org/10.3390/molecules15129046 PMID: 21150824

[35] Kaur, H.; Kumar, S.; Vishwakarma, P.; Sharma, M.; Saxena, K.K.; Kumar, A. *Eur. J. Med. Chem.,* **2010**, *45*(7), 2777-2783. http://dx.doi.org/10.1016/j.ejmech.2010.02.060 PMID: 20392546

[36] Hafez, H.N.; Hegab, M.I.; Ahmed-Farag, I.S.; El-Gazzar, A.B.A. *Bioorg. Med. Chem.,* **2008**, *18*, 4538-4543. http://dx.doi.org/10.1016/j.bmcl.2008.07.042

[37] Turner, S.; Myers, M.; Gadie, B.; Nelson, A.J.; Pape, R.; Saville, J.F.; Doxey, J.C.; Berridge, T.L. *J. Med. Chem.,* **1988**, *31*, 902-906. http://dx.doi.org/10.1021/jm00400a003 PMID: 3361578

[38] Ragab, F.A.; Heiba, H.I.; El-Gazzar, M.G.; Abou-Seri, S.M.; El-Sabbagh, W.A.; El-Hazek, R.M. *J. Photochem. Photobiol. B,* **2017**, *166*, 285-300. http://dx.doi.org/10.1016/j.jphotobiol.2016.12.007 PMID: 28013183

[39] El-Gohary, N.S.; Shaaban, M.I. *Eur. J. Med. Chem.,* **2013**, *63*, 185-195. http://dx.doi.org/10.1016/j.ejmech.2013.02.010 PMID: 23474904

[40] Balaji, K.; Bhatt, P.; Mallika, D.; Jha, A. *Int. J. Pharm. Pharm. Sci.,* **2015**, *7*, 145-149.

[41] Pattan, S.R.; Kekare, P.; Dighe, N.S.; Nirmal, S.A.; Musmade, D.S.; Parjane, S.K.; Daithankar, A.V. *J. Chem. Pharm. Res.,* **2009**, *1*, 191-198.

[42] Choy, D.S.; Arandia, J.; Rosenbaum, I. *Int. J. Cancer,* **1967**, *2*(2), 189-193. http://dx.doi.org/10.1002/ijc.2910020213 PMID: 6039768

[43] Dalvie, D.K.; Kalgutkar, A.S.; Khojasteh-Bakht, S.C.; Obach, R.S.; O'Donnell, J.P. *Chem. Res. Toxicol.,* **2002**, *15*(3), 269-299. http://dx.doi.org/10.1021/tx015574b PMID: 11896674

[44] Horne, W.S.; Yadav, M.K.; Stout, C.D.; Ghadiri, M.R. *J. Am. Chem. Soc.,* **2004**, *126*(47), 15366-15367. http://dx.doi.org/10.1021/ja0450408 PMID: 15563148

[45] Kolb, H.C.; Finn, M.G.; Sharpless, K.B. *Angew. Chem. Int. Ed.,* **2001**, *40*, 2004-2021. http://dx.doi.org/10.1002/1521-3773(20010601)40:11<2004::AID-ANIE2004>3.0.CO;2-5

[46] Kolb, H.C.; Sharpless, K.B. *Drug Discov. Today,* **2003**, *8*(24), 1128-1137. http://dx.doi.org/10.1016/S1359-6446(03)02933-7 PMID: 14678739

[47] Cho, S.; Oh, S.; Um, Y.; Jung, J-H.; Ham, J.; Shin, W-S.; Lee, S. *Bioorg. Med. Chem. Lett.,* **2009**, *19*(2), 382-385. http://dx.doi.org/10.1016/j.bmcl.2008.11.067 PMID: 19081249

[48] Al-Masoudi, N.A.; Al-Soud, Y.A. *Tetrahedron Lett.,* **2002**, *43*, 4021-4022. http://dx.doi.org/10.1016/S0040-4039(02)00733-5

[49] Kumar, K.K.; Seenivasan, S.P.; Kumar, V.; Das, T.M. *Carbohydr. Res.,* **2011**, *346*, 2084-2090. http://dx.doi.org/10.1016/j.carres.2011.06.028 PMID: 21767828

[50] Lal, K.; Kaushik, C.P.; Kumar, A. *Med. Chem. Res.,* **2015**, *24*, 3258-3271. http://dx.doi.org/10.1007/s00044-015-1378-9

[51] da Silva, F.C.; de Souza, M.C.B.V.; Frugulhetti, I.I.P.; Castro, H.C.; Souza, S.L.O.; de Souza, T.M.L.; Rodrigues, D.Q.; Souza, A.M.T.; Abreu, P.A.; Passamani, F.; Rodrigues, C.R.; Ferreira, V.F. *Eur. J. Med. Chem.,* **2009**, *44*, 373-383. http://dx.doi.org/10.1016/j.ejmech.2008.02.047 PMID: 18486994

[52] Costa, M.S.; Boechat, N.; Rangel, E.A.; da Silva, Fde.C.; de Souza, A.M.T.; Rodrigues, C.R.; Castro, H.C.; Junior, I.N.; Lourenço, M.C.S.; Wardell, S.M.S.V.; Ferreira, V.F. *Bioorg. Med. Chem.,* **2006**, *14*(24), 8644-8653. http://dx.doi.org/10.1016/j.bmc.2006.08.019 PMID: 16949290

[53] Kumar, K.; Pradines, B.; Madamet, M.; Amalvict, R.; Kumar, V. *Eur. J. Med. Chem.,* **2014**, *86*, 113-121. http://dx.doi.org/10.1016/j.ejmech.2014.08.053 PMID: 25147153

[54] Bokor, E.; Docsa, T.; Gergely, P.; Somsák, L. *Bioorg. Med. Chem.,* **2010**, *18*(3), 1171-1180. http://dx.doi.org/10.1016/j.bmc.2009.12.043 PMID: 20080412

[55] Biagi, G.; Dell'Omodarme, G.; Ferretti, M.; Giorgi, I.; Livi, O.; Scartoni, V.; Tiscione, E. *Farmaco,* **1990**, *45*(11), 1181-1192. PMID: 2128450

[56] Ferreira, S.B.; Sodero, A.C.R.; Cardoso, M.F.C.; Lima, E.S.; Kaiser, C.R.; Silva, F.P., Jr; Ferreira, V.F. *J. Med. Chem.,* **2010**, *53*(6), 2364-2375. http://dx.doi.org/10.1021/jm901265h PMID: 20170190

[57] Cunha, A.C.; Figueiredo, J.M.; Tributino, J.L.M.; Miranda, A.L.P.; Castro, H.C.; Zingali, R.B.; Fraga, C.A.M.; de Souza, M.C.B.V.; Ferreira, V.F.; Barreiro, E.J. *Bioorg. Med. Chem.,* **2003**, *11*, 2051-2059. http://dx.doi.org/10.1016/S0968-0896(03)00055-5 PMID: 12670656

[58] Felder, C.C.; Ma, A.L.; Liotta, L.A.; Kohn, E.C. *J. Pharmacol. Exp. Ther.,* **1991**, *257*(3), 967-971. PMID: 1646332

[59] Kohn, E.C.; Sandeen, M.A.; Liotta, L.A. *Cancer Res.,* **1992**, *52*(11), 3208-3212. PMID: 1591730

[60] Wasilenko, W.J.; Palad, A.J.; Somers, K.D.; Blackmore, P.F.; Kohn, E.C.; Rhim, J.S.; Wright, G.L., Jr; Schellhammer, P.F. *Int. J. Cancer,* **1996**, *68*(2), 259-264. http://dx.doi.org/10.1002/(SICI)1097-0215(19961009)68:2<259::AID-IJC20>3.0.CO;2-4 PMID: 8900438

[61] Berrie, A.H.; Newbold, G.T.; Spring, F.S. *J. Chem. Soc.,* **1952**, 2042-2046. http://dx.doi.org/10.1039/jr9520002042

[62] Kovackova, S.; Chang, L.; Bekerman, E.; Neveu, G.; Barouch-Bentov, R.; Chaikuad, A.; Heroven, C.; Šála, M.; De Jonghe, S.; Knapp, S.; Einav, S.; Herdewijn, P. *J. Med. Chem.,* **2015**, *58*(8), 3393-3410. http://dx.doi.org/10.1021/jm501759m PMID: 25822739

[63] Rao, V.R.; Srinivasan, V.R. *Indian J. Chem.,* **1970**, *8*, 509-513.

Growth hormone induces Notch1 signaling in podocytes and contributes to proteinuria in diabetic nephropathy

Received for publication, April 19, 2019, and in revised form, August 28, 2019 Published, Papers in Press, September 11, 2019, DOI 10.1074/jbc.RA119.008966

Rajkishor Nishad[‡], **Dhanunjay Mukhi**[‡], **Syed V. Tahaseen**[§], **Sathish Kumar Mungamuri**[¶], **and Anil K. Pasupulati**[‡1]

From the [‡]*Department of Biochemistry, School of Life Sciences, University of Hyderabad, Hyderabad, India 500046, the* [§]*Department of Biochemistry, SRR & CVR Degree College, Vijayawada, India 520010, and the* [¶]*Division of Food Safety, National Institute of Nutrition, Hyderabad, India 500007*

Edited by Jeffrey E. Pessin

Growth hormone (GH) plays a significant role in normal renal function and overactive GH signaling has been implicated in proteinuria in diabetes and acromegaly. Previous results have shown that the glomerular podocytes, which play an essential role in renal filtration, express the GH receptor, suggesting the direct action of GH on these cells. However, the exact mechanism and the downstream pathways by which excess GH leads to diabetic nephropathy is not established. In the present article, using immortalized human podocytes *in vitro* and a mouse model *in vivo*, we show that excess GH activates Notch1 signaling in a γ-secretase–dependent manner. Pharmacological inhibition of Notch1 by γ-secretase inhibitor DAPT (*N*-[*N*-(3,5-Difluorophenacetyl)-L-alanyl]-*S*-phenyl glycine *t*-butylester) abrogates GH-induced epithelial to mesenchymal transition (EMT) and is associated with a reduction in podocyte loss. More importantly, our results show that DAPT treatment blocks cytokine release and prevents glomerular fibrosis, all of which are induced by excess GH. Furthermore, DAPT prevented glomerular basement membrane thickening and proteinuria induced by excess GH. Finally, using kidney biopsy sections from people with diabetic nephropathy, we show that Notch signaling is indeed up-regulated in such settings. All these results confirm that excess GH induces Notch1 signaling in podocytes, which contributes to proteinuria through EMT as well as renal fibrosis. Our studies highlight the potential application of γ-secretase inhibitors as a therapeutic target in people with diabetic nephropathy.

Renal interstitial fibrosis is the hallmark of progressive chronic kidney disease, which correlates well with renal failure (1). Renal fibrosis is characterized by myofibroblast proliferation and activation, epithelial cell dysfunction, leukocyte migration, excessive production, and deposition of extracellular matrix (2). In response to kidney damage, there will be infiltration of mature myofibroblasts from various sources including interstitial fibroblasts, pericytes, endothelial cells, and circulating fibrocytes (2). Previous studies have shown that multiple pathways such as the transforming growth factor-β (TGF-β)[2]/Smad2/3 and Notch signaling are involved in epithelial cell dysfunction and fibroblast activation, which leads to the progression of kidney fibrosis (2).

In the early glomerular development, particularly at the S-shaped body formation, podocyte fate determination is regulated by the highly conserved Notch signaling, which transduces short-range signals between neighboring cells (3–6). The Notch pathway comprises 4 transmembrane Notch receptors (Notch 1–4) and 5 Notch ligands (Delta-like 1, 3, and 4, and Jagged 1 and 2). After ligand binding, Notch receptors undergo a series of cleavages catalyzed by the ADAM proteases and γ-secretase complex, which results in the release of the Notch intracellular domain (NICD, Fig. S1); this process can be inhibited by the γ-secretase inhibitor and dibenzoazepine (7). The resulting NICD translocates into the nucleus (8), wherein it forms a ternary complex by associating with the DNA-binding protein, retinol-binding protein-jk and the coactivator, Mastermind-like protein 1 and activates expression of target genes (9–12).

Vooijs *et al.* (13) have reported that Notch1 is highly active in the developing kidney; however, in the mature kidney detection of active Notch1 is very little. Inhibition of Notch signaling during early development of the mouse kidney results in a severe deficiency of glomerular podocytes, indicating the importance of Notch signaling during kidney development (3). On the other hand, persistent activation of Notch signaling in the mature kidney leads to podocyte damage and subsequent kidney failure (14). Further studies had also shown that ectopic Notch activation in terminally differentiated podocytes is correlated with both diffuse mesangial sclerosis and focal segmental glomerulosclerosis, which are associated with *de novo* Pax2 expression and p53-induced podocyte apoptosis, respectively (14, 15). It was also observed that the genetic deletion of the

This work was supported by Science and Engineering Research Board Grant EMR/2015/2076 (to A. K. P.), Research Fellowships from the University Grants Commission, India (to R. N. and D. M.), and a Ramanujan Fellowship from Department of Science and Technology - Science and Engineering Research Board Grant (to S. K. M.). The authors declare that they have no conflicts of interest with the contents of this article.

This article contains Figs. S1–S5.

The microarray data reported in this paper have been submitted to the Gene Expression Omnibus (GEO) database under GEO accession no. GSE21327.

[1] To whom correspondence should be addressed. Tel.: 91-40-23134519; E-mail: pasupulati.anilkumar@gmail.com.

[2] The abbreviations used are: TGF-β, transforming growth factor β; NICD, Notch intracellular domain; GH, growth hormone; GBM, glomerular basement; EMT, epithelial to mesenchymal transition; qRT, quantitative RT; DAPT, *N*-[*N*-(3,5-difluorophenacetyl)-L-alanyl]-*S*-phenylglycine *t*-butyl ester; UACR, urinary albumin-creatinine ratio; GFR, glomerular filtration rate; DN, diabetic nephropathy; PAS, periodic acid-Schiff; TEM, transmission electron microscope; DAPI, 4′,6-diamidino-2-phenylindole; α-SMA, α-smooth muscle actin.

© 2019 Nishad et al. Published under exclusive license by The American Society for Biochemistry and Molecular Biology, Inc.

Notch pathway in tubular epithelial cells ameliorates renal fibrosis in the unilateral ureteral obstruction murine model and folic acid-induced renal fibrosis (16). These data reveal that Notch signaling plays an essential role in the fibrotic pathogenesis. However, the precise underlying cellular mechanisms are not fully understood.

Although many studies show that the role of Notch1 signaling in glomerular diseases (17–19), the correlation between activated Notch1 signaling and diabetic proteinuria remains to be elucidated. Elevated levels of circulating growth hormone (GH) are associated with the development of nephropathy in "type 1 diabetes" and "acromegaly" (20, 21). Conditions of elevated GH are typified by hyperfiltration, glomerulosclerosis, and albuminuria. On the other hand, both decreased GH secretion and action can protect from glomerular complications (22). Previously, we have established the role of GH on glomerular cells, particularly on podocytes (23, 24). Our present study demonstrates that excess GH activates Notch signaling in human podocytes as well as in the murine kidneys. Blocking the activated Notch signaling through pharmacological inhibition of γ-secretase function reverted the excess GH-induced kidney fibrosis, interstitial infiltration of plasma-lymphocytic cells and proteinuria, hindered the glomerular basement membrane (GBM) thickening with severe foot process effacement in mice as well as epithelial to mesenchymal transition (EMT) and fibrotic marker expression of podocytes. Our present study demonstrates that an elevated level of circulatory GH after embryonic development may compromise the podocyte function by activation of Notch signaling and could represent a new pharmacological target.

Results

GH induces Notch1 activation in immortalized human podocytes

To identify the biochemical pathways downstream of GH signaling that are hyperactivated in podocytes in response to excess GH, we previously performed microarray analysis (GEO accession number GSE21327) on immortalized human podocytes treated with GH and identified transcriptional activation of EMT regulator "ZEB2" (24). By reanalyzing the same microarray data, we now identified that in response to GH treatment, Notch1 signaling is up-regulated in human podocytes (Fig. S2). To reconfirm the up-regulation of Notch signaling pathway by GH in podocytes, we also analyzed the expression of Notch1 and its targets Hes1 and Jag1 in nondiabetic mouse kidney ($n = 18$) *versus* diabetic nephropathy mouse kidney ($n = 21$) in the Hodgin diabetes mouse glomerulus data set available at Nephroseq (https://nephroseq.org),[3] which shows that diabetic nephropathy kidneys overexpress Notch1 and its target genes, *Hes1* and *Jag1* (Fig. 1*A*). Next, to validate the data obtained in our microarray analysis as well as that from Nephroseq, we measured the mRNA levels of both Notch1 and its target genes by quantitative RT (qRT)-PCR, and as expected, the levels of Notch1 (full-length) and its targets were up-regulated with GH treatment in the human podocytes (Fig. 1*B*). GH had induced the expression of activated Notch1 (NICD1) and its target proteins in both concentration (Fig. 1*C*) and time-dependent (Fig. 1*D*) manners. γ-Secretase is an intramembrane protease that cleaves many membrane proteins including Notch1, which generates the NICD1 (25). Accordingly, we also observed a time-dependent increase in γ-secretase activity with GH treatment in human podocytes (Fig. 1*E*). All these data suggests that Notch1 signaling is up-regulated in response to GH treatment in human podocytes.

γ-Secretase activity is required for GH-mediated Notch activation

To confirm the role of γ-secretase in GH-induced Notch1 activation, we next treated the human podocytes with GH in the absence or presence of well-established γ-secretase inhibitor, DAPT (*N*-[*N*-(3,5-difluorophenacetyl)-L-alanyl]-*S*-phenylglycine *t*-butyl ester). As expected, DAPT treatment to the GH-exposed human podocytes has decreased the γ-secretase activity in a time-dependent manner (Fig. 2*A*). GH was not able to induce the expression of Notch1 or its target genes (*Hes1* and *Hey1*) in the presence of DAPT in human podocytes as measured by qRT-PCR (Fig. 2*B*), Western blotting (Fig. 2*C*), and immunofluorescence (Fig. 2*D*). Furthermore, we continued our quest of understanding the effect of GH on Notch signaling *in vivo*. Similar to the observations *in vitro*, GH treatment led to the induction of NICD1, Jag1, and NICD targets: Hes1 and Hey1 in glomerular sections from mice as measured with immunostaining (Fig. 3, *A–D*) and Western blotting (Fig. 3, *E* and *F*). DAPT inhibited NICD1 accumulation and induction of its targets in glomerular sections (Fig. 3, *A*, *C*, and *D*), glomerular lysates (Fig. 3*E*), and primary podocytes (Fig. 3*F*) isolated from GH-treated mice. However, the expression of Jag1 was unaffected by DAPT treatment (Fig. 3, *B*, *E*, and *F*). It should be noted that the data from isolated podocytes corroborate with that from glomerular lysate (Fig. 3, *E* and *F*). Together, the data confirm that GH stimulates NICD1 expression in glomeruli and podocytes, and functional γ-secretase is required to activate GH-dependent Notch1 signaling.

Activated Notch signaling is required for GH-induced EMT in podocytes

Previously, we established that excess GH elicits EMT in podocytes (24). Thus, we analyzed the influence of Notch signaling in GH-induced EMT in podocytes. GH treatment induced the EMT markers (E-Cad, N-Cad, Snail, Slug, ZEB2, Vimentin, and α-SMA) in human podocytes and mouse glomerulus as shown at both mRNA (Fig. 4*A*) and protein levels (Fig. 4, *B* and *C*). DAPT treatment abrogated this effect of GH in human podocytes (Fig. 4, *A* and *B*) and mouse glomerulus (Fig. 4*C*).

Remodeling of actin filaments is necessary for EMT (26). To confirm the physiological function of EMT induced by GH, we next performed the phalloidin staining of the podocytes treated with GH, with or without DAPT treatment. The results presented in Fig. 4*D* suggests that there is complete disorganization of the actin filaments in the podocytes treated with GH, and can be rescued by co-treatment with DAPT (Fig. 4*D*). Quantification of F-actin stress fiber distribution revealed a sig-

[3] Please note that the JBC is not responsible for the long-term archiving and maintenance of this site or any other third party hosted site.

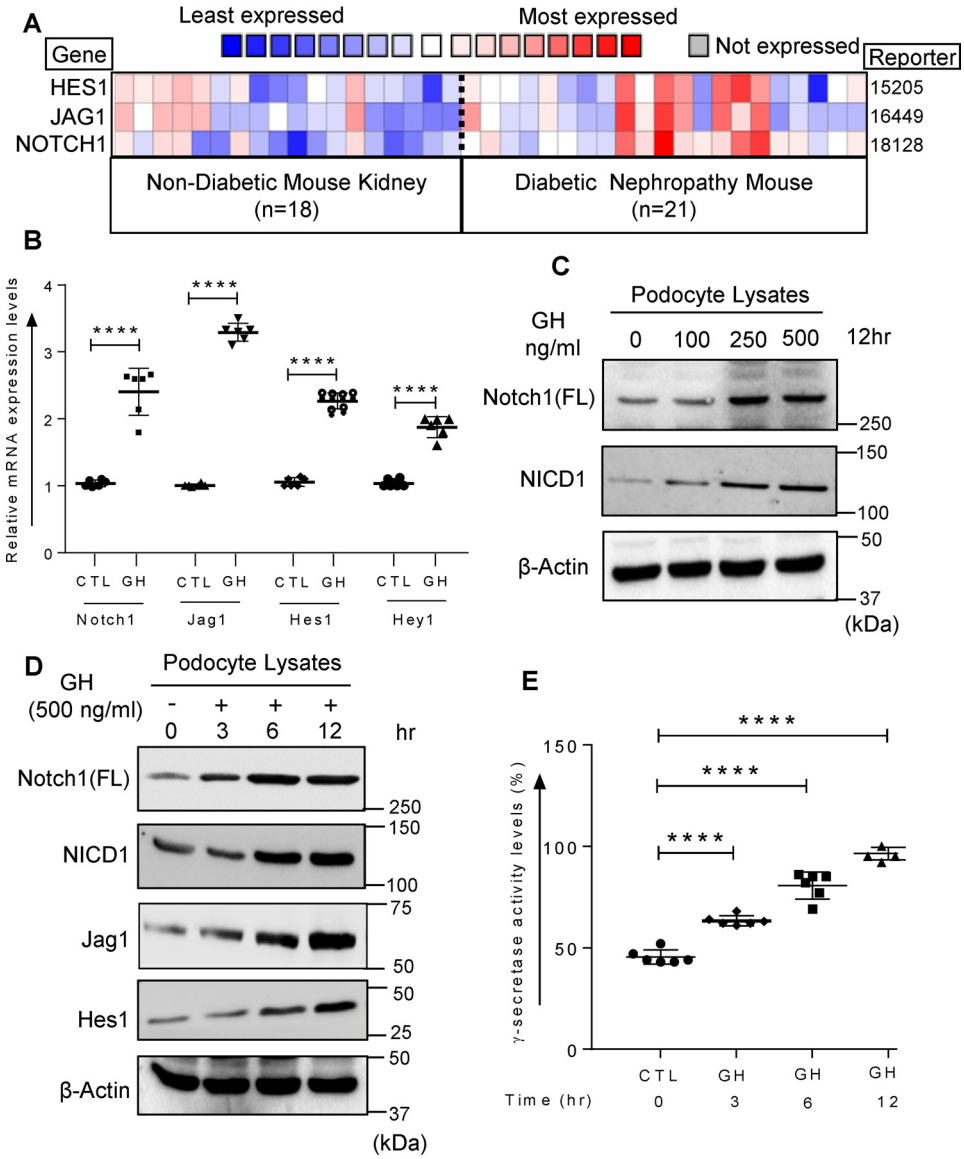


Figure 1. GH induces Notch1 activation in immortalized human podocytes. *A*, Nephroseq (University of Michigan O'Brien Renal Center, Michigan, Ann Arbor, MI) analysis comparing *HES1*, *JAG1*, and *NOTCH1* expression levels from nondiabetic mouse kidney ($n = 18$) *versus* diabetic nephropathy mouse kidney ($n = 21$) in Hodgin diabetes mouse glomerulus. Data indicate that expression of these genes increased >1.5-fold in the diabetic group. *B*, qRT-PCR analysis showing the expression of Notch pathway genes (*Notch1*, *Jag1*, *Hes1*, and *Hey1*) in human podocytes treated with GH (500 ng/ml) or without GH (*CTL*) for 30 min. mRNA levels were normalized to β-Actin levels and presented as fold-change on the *y* axis. ****, $p < 0.0001$. *C*, immunoblotting analysis showing the expression of Notch1 full-length (*FL*), active Notch1 (NICD1), and β-Actin in human podocytes treated with GH (100 to 500 ng/ml) for 12 h. *D*, immunoblotting analysis showing the expression of Notch1 (*FL*), NICD1, Jag1, Hes1, and β-Actin in human podocytes treated with GH (500 ng/ml) or the indicated time intervals (0 to 12 h). *E*, γ-secretase activity in human podocytes treated with or without GH (500 ng/ml) for 0–12 h. ****, $p < 0.0001$. Data represent the mean ± S.D. ($n = 6$) and statistical significance was analyzed by Student's *t* test.

nificant loss (60 ± 5%) of stress fibers in podocytes exposed to GH, whereas DAPT ameliorated GH-induced injury to the actin stress fibers (Fig. 4*E*).

Furthermore, to confirm the role of Notch1 signaling in GH-induced EMT in the podocytes, we also performed the cell migration assay. Although GH treatment alone to the podocytes completely covered the wound by 12 h, DAPT treatment abrogated this GH-induced phenotype (Fig. 4*F*). Quantification of wound coverage in response to CTL, GH, and GH + DAPT exposure, GH solely enhanced the migration of podocytes (90 ± 8%, Fig. 4*G*). All these results confirm that excess GH induces EMT in the podocytes and activated Notch signaling is essential for GH-induced EMT in podocytes.

Activated Notch signaling is required for GH-induced interstitial infiltration of plasma-lymphocytic cells and fibrosis in kidneys

Diabetes is characterized by mild, but significant glomerulosclerosis, and GH has been shown to contribute to the glomerulosclerosis (27). Next, we treated the mice with GH and prepared the paraffin-embedded kidney sections to look for interstitial infiltration of plasma-lymphocytic cells. As previously noted, our hematoxylin and eosin staining of the kidney sections showed interstitial infiltration of plasma-lymphocytic cells in mice treated with the GH (Fig. 5*A*). We also observed enhanced fibrosis in the mice kidneys treated with the GH, as analyzed by both periodic acid-Schiff (PAS) (Fig. 5*B*) and Mas-

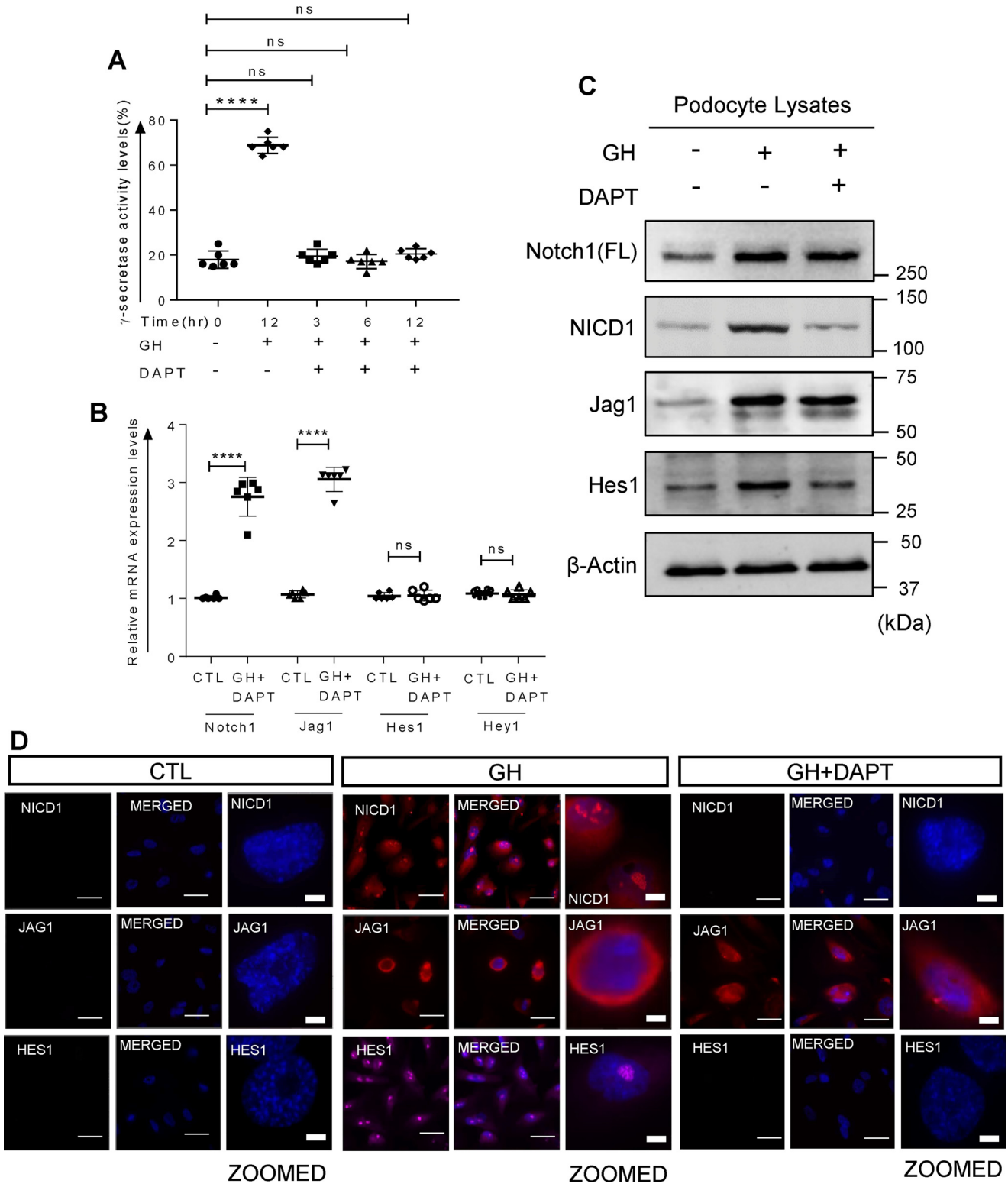


Figure 2. DAPT limits the hyperactive Notch signaling in human podocytes by inhibiting the γ-secretase activity. *A*, γ-secretase activity in human podocytes treated with GH or GH + DAPT for the indicated time intervals (3–12 h). ****, $p < 0.0001$, *ns*, not significant. *B*, qRT-PCR analysis showing the expression of *Notch1*, *Jag1*, *Hes1*, and *Hey1* in human podocytes treated with GH (500 ng/ml) + DAPT (5 μg/ml). β-Actin was used as an internal control. ****, $p < 0.0001$. *C*, immunoblotting analysis showing the expression of Notch1 (*FL*), NICD1, Jag1, and Hes1 in CTL, GH, and GH + DAPT-treated (12 h) human podocytes. *D*, immunofluorescence analysis for NICD1, Jag1, and Hes1 in CTL, GH, and GH + DAPT treated (12 h) human podocytes (×630). *Scale bar* = 20 μm. Data presented as mean ± S.D. ($n = 6$) and statistical significance was analyzed by Student's *t* test.

son's trichrome (Fig. S3*A*) stainings. Quantification of the Masson's trichrome-stained area revealed that GH enhanced glomerular fibrosis (50 ± 10%, Fig. S3*B*). These data also correlated with increased expression of cytokines (Fig. 5*C*) and fibrotic marker in GH-treated mice, as measured at both mRNA and protein (Fig. S3, *C* and *D*) levels.

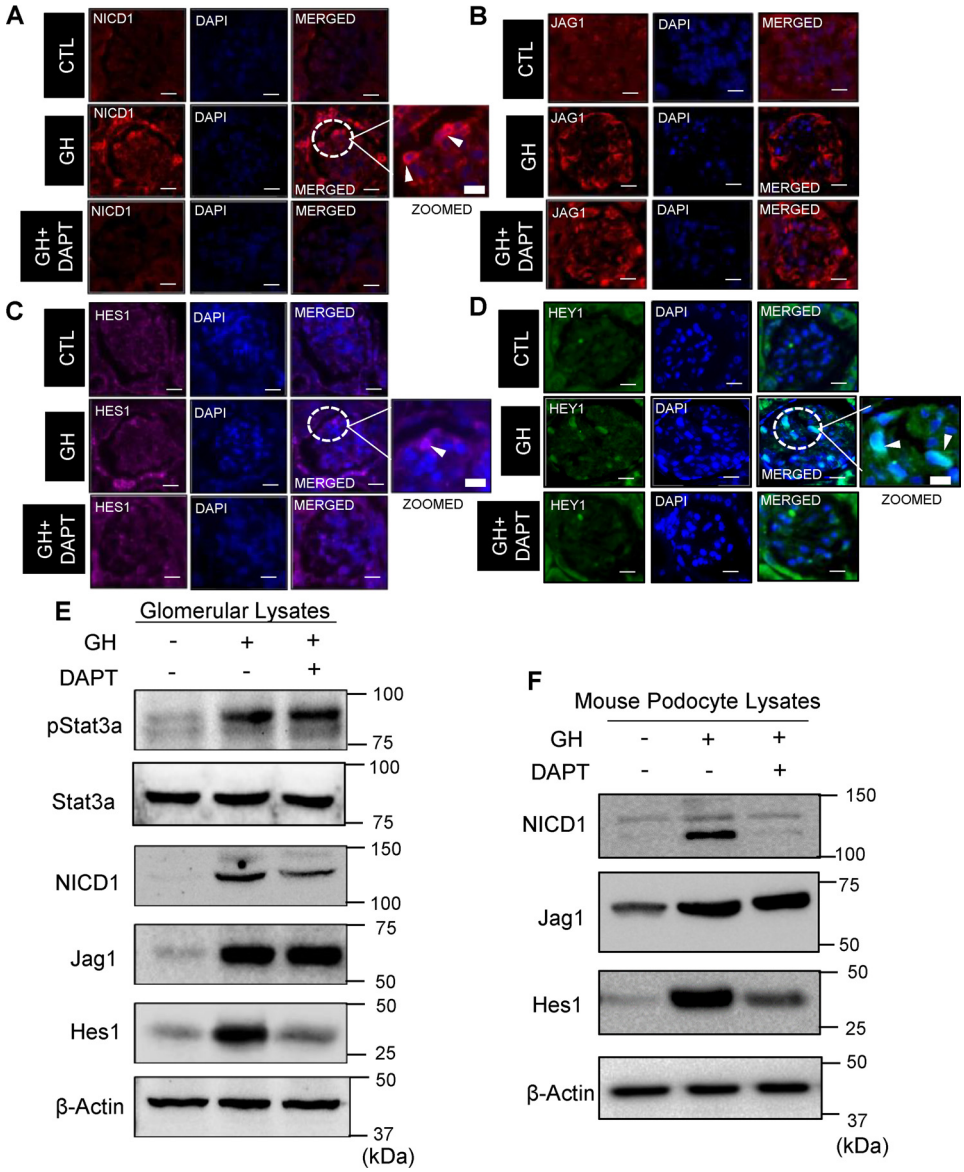
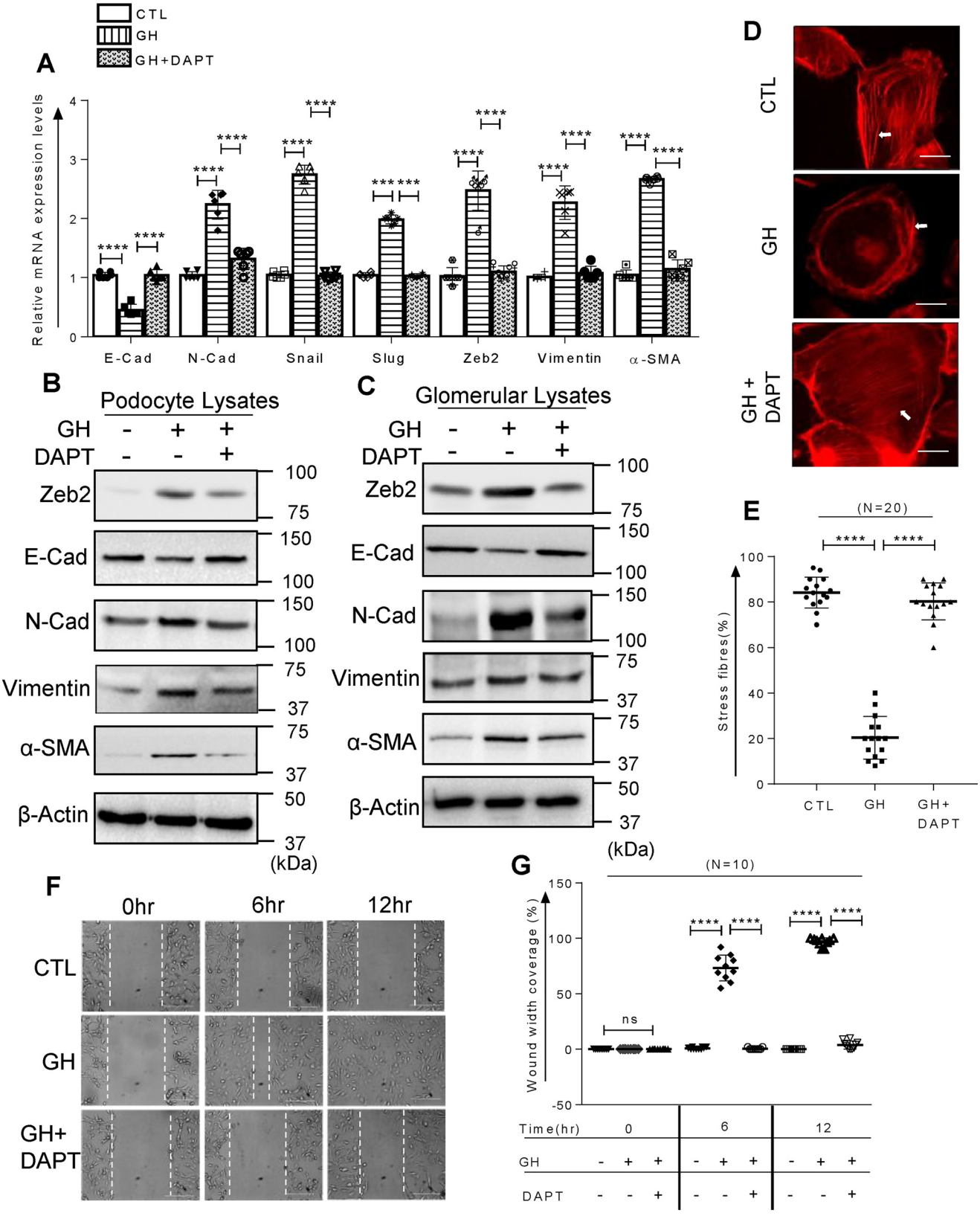


Figure 3. GH induces Notch signaling in glomerulus of mice kidney. *A–D*, representative images of immunostaining for NICD1 (*A*), Jag1 (*B*), Hes1 (*C*), and Hey1 (*D*) in glomeruli from CTL, GH, and GH + DAPT mice ($n = 6$). We employed DyLight 594-conjugated secondary antibody for NICD1 and Jag1; Cy5-conjugated secondary antibody for Hes1; and DyLight 488-conjugated secondary antibody for Hey1. These sections were counterstained with DAPI. *Scale bars* = 20 μm (×630). *E*, Western blot analysis showing the expression of pStat3a, total Stat3a, NICD1, Jag1, and Hes1 from CTL, GH, and GH + DAPT-treated mice glomerular lysates ($n = 6$). Expression of β-Actin was used as an internal control. *F*, Western blot analysis showing the expression of NICD1, Jag1, and Hes1 in primary mouse podocytes isolated from CTL, GH, and GH + DAPT- treated mice. Expression of β-Actin was used as an internal control. Data are presented as mean ± S.D. and statistical significance was calculated by using Student's *t* test.

Indeed, treatment of mice with DAPT had reversed the GH-induced nonresident cell infiltration into the kidneys (Fig. 5*A*) and was able to reverse the fibrosis as evidenced by periodic acid-Schiff (Fig. 5*B*) and Masson's trichrome (Fig. S3*A*) stainings. Mesangial expansion and glomerular damage score were found elevated with GH treatment (Fig. 5, *C* and *D*). DAPT treatment also inhibited the GH-induced cytokine and fibrotic gene induction (Fig. 5*E*); and reversed podocyte-specific marker genes expression as measured at both mRNA and protein levels (Fig. S3, *C* and *D*). To further evaluate whether the cytokines released from these podocytes are indeed functional, and DAPT blocked the function of these cytokines, we next performed classical chemotaxis assay using J774A.1 macrophages. As expected, the macrophages were able to fill the gap, when treated with conditioned medium collected from podocytes treated with the GH, whereas this function was completely blocked when similar conditioned medium from podocytes treated with GH + DAPT was used (Fig. S4*A*). The conditioned medium from the untreated podocytes was used as a control. Quantification of the wound coverage in response to CTL, GH, GH + DAPT, and C5a exposure, GH-treated spent medium solely enhanced the migration of J774A.1 macrophages (70 ± 10% increase, $p < 0.001$, Fig. S4*B*).

Kidney fibrosis leads to thickening of the GBM, which consequently results in podocyte foot process effacement (28). To confirm whether a similar phenomenon also happens in our GH-induced proteinuria mice model, we next performed transmission EM studies to analyze the structural changes in the

GBM as well as podocyte foot processes in mice kidney samples. Our results show that whereas GH treatment in the mice leads to GBM thickening and podocyte foot process effacement, similar treatment of GH along with DAPT completely abrogated this effect (Fig. 5, *F* and *G*). All these results confirm that excess GH activates Notch1 signaling, which in turn leads to infiltration of circulating cells in the kidneys and leading to its fibrosis.



Blocking activated Notch1 signaling abrogates GH-induced proteinuria

Previously, we showed that GH treatment to rodents induces loss of podocyte number (23). GH-treated mice kidney sections were probed for WT1, which specifically express in podocytes. Our data reconfirm that GH treatment results in depletion of podocytes (Fig. 6, *A* and *B*). We also confirmed that GH treatment reduced the physiological functional ability of the kidneys in the mice as analyzed by an increase in urinary albumin-creatinine ratio (UACR) (Fig. 6*C*), and decrease in glomerular filtration rate (GFR) (Fig. 6*D*). We also assessed the extent of proteinuria in GH-treated mice by analyzing the urinary protein content on SDS-PAGE and staining with silver nitrate. GH treatment had increased the amount of protein in urine. Co-treatment of mice with DAPT has rescued the decrease in podocyte number induced by the GH (Fig. 6, *A* and *B*). We also observed that DAPT ameliorated GH-induced UACR (Fig. 6*C*) and GH-induced loss of GFR (Fig. 6*D*). Finally, DAPT also blocked the proteinuria induced by the GH in these mice (Fig. 6*E*). Albumin influx assay (*in vitro*) revealed that DAPT has prevented GH-induced albumin leakage across podocyte monolayer (Fig. 6*F*). Together the data suggest that excess GH impair the podocyte function and induces proteinuria through activated Notch1 signaling.

Notch signaling is hyperactivated in people with diabetic nephropathy

Finally, to confirm the results obtained so far that excess GH induces activated Notch1 signaling in humans, we evaluated the extent of NICD1 expression in people with diabetic nephropathy (DN). As expected, urine from these people showed higher albumin (Fig. S5*A*) and elevated serum creatinine (Fig. S5*B*) levels and decreased glomerular filtration rate (Fig. S5*C*). We observed that there is more urinary protein in these patients as observed by Coomassie Brilliant Blue staining of the urine samples (Fig. 7*A*). Immunohistochemical analysis of the kidney sections from people with diabetes showed increased NICD1, Jag1, and Hes1 expression compared with the healthy controls (Fig. 7*B*). Furthermore, we observed elevated expression of EMT markers α-SMA, N-Cad, and Vimentin in glomerulus in patients with diabetic nephropathy (Fig. 7, *C–F*). All these data confirm that people with diabetic nephropathy have elevated functional Notch signaling in their kidney glomeruli and enhanced expression of EMT markers.

Discussion

In the present article, we show that GH activates Notch1 signaling in podocytes and pharmacological inhibition of γ-secretase blocks the GH-induced EMT induction, infiltration of nonresident cells, fibrosis, GBM thickening, and podocyte foot-process effacement. Glomerular sclerosis and albuminuria are associated with failure of the normal kidney functions. GH induces the albuminuria, whereas the γ-secretase inhibitor treatment under similar conditions kept a constant check on these parameters and thus protects the mice kidneys from fibrosis. More importantly, GH treatment in mice leads to proteinuria, a common symptom associated with diabetic nephropathy, which was successfully abrogated with the γ-secretase inhibitor treatment.

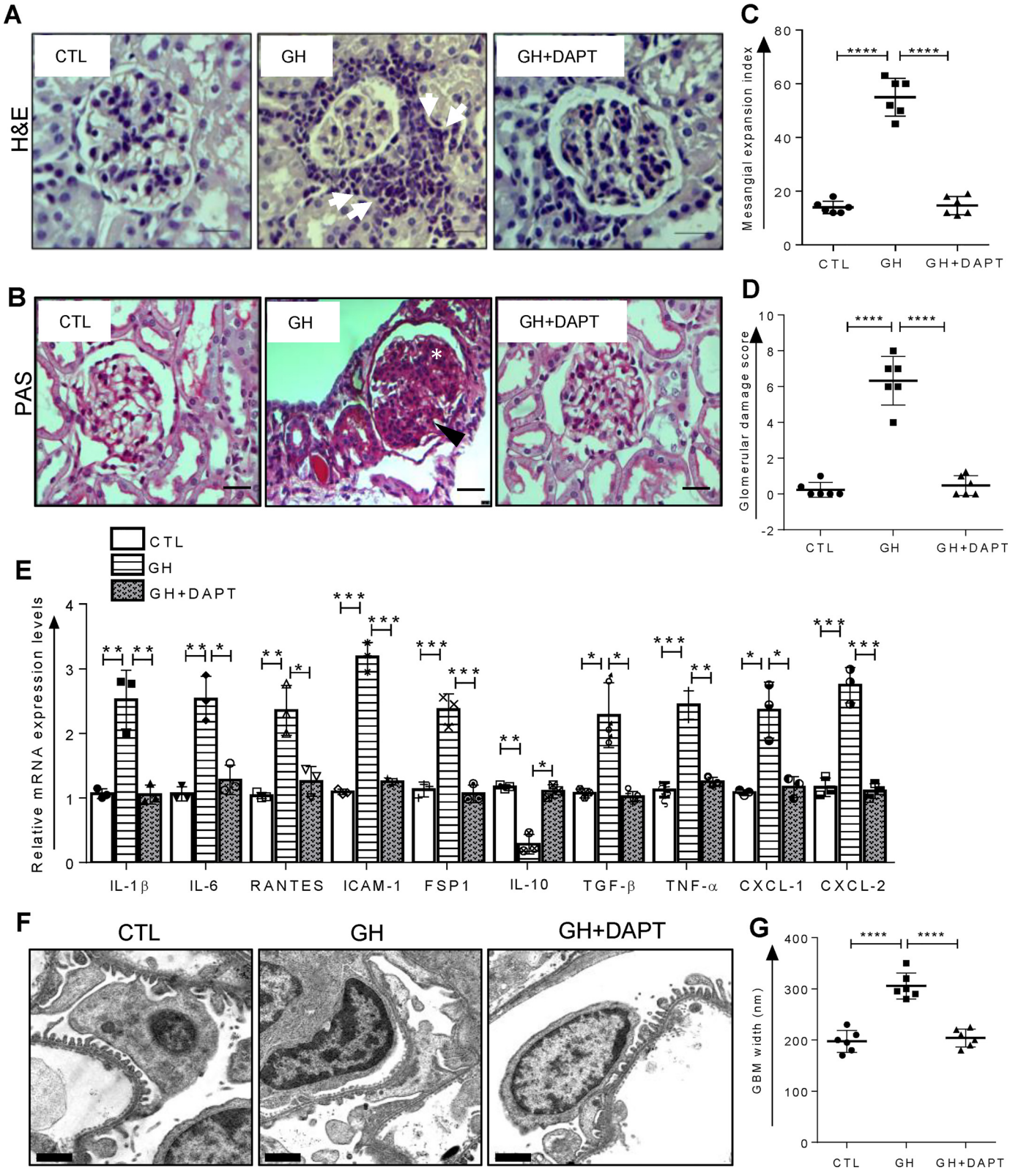
Notch signaling is essential during nephrogenesis, *i.e.* during the embryonic development of glomerular podocytes and proximal tubules (29). On the contrary, Notch signaling is not required for podocyte formation, beyond the stage of the S-shaped body (29, 30). Although, Niranjan *et al.* (14) showed that NICD1 induces apoptosis in rat podocytes, whereas in the experiments performed by Waters *et al.* (15) show that the podocyte-specific expression of NICD1 promoted severe proteinuria and showed evidence of foot-process effacement and progressive glomerulosclerosis. The differences in these two reports can be attributed toward different mice strains used in their studies. Lasagni *et al.* (31) demonstrated that persistent activation of Notch signaling results in mitotic catastrophe and inhibition of the Notch pathway in renal progenitors is prerequisite for the differentiation toward podocyte lineage. Expression of Notch was undetectable in the glomeruli from healthy adult kidneys, whereas a strong up-regulation was observed in podocytes in patients affected by glomerular disorders. Inhibition of Notch signaling in mouse models of focal segmental glomerulosclerosis reduced podocyte loss and improved proteinuria (31). Mice with podocyte-specific deletion of Notch1 were shown to be protected from DN (32). Similarly, podocyte-specific deletion of retinol-binding protein-jk, which is an important downstream component of canonical Notch signaling, has lowered the severity of proteinuria and reduced the podocyte injury in DN rodent model (14). However, the mechanism by which NICD1 is induced during the DN conditions is not yet known. The data presented in our study confirms that excess GH, commonly observed during the DN (33), activates Notch signaling in the podocytes and inhibition of this signaling by γ-secretase inhibitor blocks GH-induced proteinuria and foot-process effacement in mice.

EMT, as well as renal fibrosis, are the shared pathological hallmarks of progressive chronic kidney disease, which comes with diverse etiologies. Hyperglycemia was demonstrated to provoke podocyte EMT through several molecular mechanisms, including activation of Notch signaling (34). Podocyte-specific Notch activation leads to dedifferentiation and its shedding (14, 15). In different models, either treatment with

Figure 4. Activated Notch signaling is required for GH-induced EMT in podocytes. *A*, qRT-PCR analysis showing the expression of EMT markers (E-Cad, N-Cad, Snail, Slug, Zeb2, Vimentin, and α-SMA) in human podocytes treated with GH in the presence or absence of DAPT. β-Actin was used as an internal control. ****, $p < 0.0001$. *B* and *C*, Western blot analysis showing the expression of Zeb2, E-Cad, N-Cad, Vimentin, and α-SMA in (*B*) human podocytes and (*C*) mice glomerular lysates (CTL, GH, and GH + DAPT treatments). *D*, phalloidin staining of podocytes showing F-actin arrangement and changes in stress fibers (indicated by *white arrow*). *E*, phalloidin-stained F-actin stress fibers in podocytes are quantified by ImageJ and data are presented as mean ± S.D. ($n = 20$). ****, $p < 0.0001$. *Scale bars* = 20 μm (×630). *F*, wound healing assay was performed to determine the extent of motility of podocytes from CTL, GH, and GH + DAPT groups and images were captured at the indicated times (0–12 h) using an Olympus inverted microscope (×100) and *scale bar* = 100 μm. *G*, the % area of wound covered by cells was quantified by ImageJ. ****, $p < 0.0001$. Data are presented as mean ± S.D. and statistical significance was analyzed by Student's *t* test. Results shown are representative of three independent experiments.

γ-secretase inhibitors or reducing Notch transcriptional binding protein levels showed a significant amelioration of glomerular injury and fibrosis, demonstrating the role of Notch signaling in podocyte EMT (35, 36). Several upstream master regulators like Wnt and TGF-β etc., are shown to increase the Notch activity (37–39).

Our data indicate that GH induces activated Notch1 signaling in podocytes, and since during DN, GH is up-regulated (20), and we observed increased NICD1 in people with DN, we presume that during DN, GH activates Notch signaling in podocytes. In mice treated with GH, we have shown enhanced glomerulosclerosis and more importantly, DAPT treatment had



reduced the GH-induced glomerulosclerosis in these mice. Furthermore, our data indicate that activated Notch1 regulates the GH-induced EMT of the podocytes. We had shown previously that GH induces the expression of the EMT transcription factor, ZEB2, which transcriptionally down-regulates P- and E-cadherin expressions in the podocytes (24, 40). In the present article, we show that GH induces NICD1, and treatment of podocytes with γ-secretase inhibitor blocks GH-induced ZEB2 and thus EMT in podocytes.

TGF-β1 is a pro-sclerotic cytokine and it is accepted that TGF-β1 and its downstream SMAD signaling is involved in the development and progression of renal fibrosis in people with DN (41, 42). Studies from our laboratory report that GH regulates the bioavailability of TGF-β1 via regulating the expression of transforming growth factor-β-induced protein (TGFBIp) (23) and induces the expression of Smad-interacting protein, SIP1 (24). Recently, we identified that GH directly stimulates TGF-β expression in podocytes.[4] Whereas DAPT treatment successfully abrogated GH-induced Notch signaling, our data shows that DAPT was not able to reverse GH-induced Jag1 expression. TGF-β1 has been shown to independently regulate Jag1 and Hey1 expression in renal epithelial cells (43, 44). Furthermore, TGF-β–induced EMT can be inhibited by silencing either Hey1 or Jag1 as well as by chemical inactivation of Notch signaling (44). All these data suggest that there is a significant cross-talk between Notch and TGF-β signaling in fine-tuning the EMT phenomenon. How this cross-talk is specifically modulated during GH-depandant podocyte EMT and renal fibrosis needs further studies.

Preclinical studies have shown that DAPT could suppress the Notch signaling and also selective antibodies to preferentially target Notch receptors and ligands have proven successful (44). Based on our data that people with DN show stronger NICD1 staining in the podocytes, as well as blocking NICD1 function through γ-secretase inhibitor abrogates the proteinuria in mice, we believe that proteinuria and glomerulosclerosis in DN can be repressed using γ-secretase inhibitors. However, for the utilization of γ-secretase inhibitors, there are clinical concerns remaining over normal organ homeostasis and significant pathology in multiple organs. Because Notch signaling is not essential for the podocytes after embryonic development, we believe that tissue-specific administration of such inhibitors may offer protection against diabetic nephropathy.

[4] Mukhi D, Nishad R, Singh AK, Mungamuri SK and Pasupulati AK; unpublished data.

Experimental procedures

Reagents

The primary antibodies are as following: anti-activated Notch1 (ab8925), anti-WT-1(ab212951), anti-pSTAT3a (ab76315), anti-t-STAT3a (ab5073), anti-cleaved Notch1 (ab8925), anti-FSP1 (ab41532), and anti-HEY1 (ab154077) were purchased from Abcam (Cambridge, MA). Notch1 Full-length (FL) (number 3608), anti-E-Cadherin (number 3195), anti-N-Cadherin (number 13116), anti-αSMA (number 19245), anti-cleaved Notch1 (number 4147S), anti-ICAM-1 (number 4915), and anti-Actin (number 4970) were purchased from Cell Signaling Technology (Danvers, MA). The anti-HES1 (sc-166410) and anti-ZO-1 (sc-33725) were obtained from Santa Cruz Biotechnology (Dallas, TX). Anti-Vimentin (PAB040Hu01), anti-Col4 (PAA180Hu01), anti-Fibronectin (PAA037Hu01), and anti-JAG1 (PAB807Hu01) were purchased from Cloud-clone (Houston, TX). Anti-ZEB2 (PA5–20980) was purchased from Thermo Fisher Scientific. DAPT (D5942), SIGMAFAST DAB with Metal Enhancer Tablet Set (D0426), phalloidin fluorescein isothiocyanate labeled (P5282), and glutaraldehyde solution (G5882) were obtained from Sigma. Pink pre-stained marker protein (ABIN5662611, Nippon Genetics Europe), Precision Plus Protein Dual Color Standards (Bio-Rad, Hercules, CA), and ProLong™ Diamond Antifade Mountant (P36961) were purchased from Molecular Probes Life Technologies and DyLight 488 and DyLight 564, and Cy5-conjugated secondary antibody were obtained from Vector Laboratories (Burlingame, CA). Primers used in this study procured from Integrated DNA Technologies (Coralville, IA). cDNA reverse transcription kit and SYBR Green Master Mix reagents were obtained from Bio-Rad. All other reagents used were of analytical grade and obtained from Sigma.

Animals and tissues

All the experimental procedures for the animals were pre-approved by the Institutional Animal Ethics Committee of the University of Hyderabad, India. 8-Week-old Swiss Webster male mice weighing nearly 30 ± 5 g were used in this study. The mice were randomly assigned to three groups (6 mice per group): 1) control group (CTL), 2) GH-treated group, and 3) GH + DAPT-treated group. Experimental mice received a single i.p. dose of hGH (1.5 mg/kg/day), whereas control mice have received an equal volume of saline for 4 weeks. The inhibitor groups were received DAPT (10 mg/kg of body weight) per day prior to the GH treatment. After 4 weeks of the experimental period, the mice were placed in individual metabolic cages for collecting 24-h urine to estimate albumin and creatinine. An

Figure 5. Activated Notch signaling is required for GH-induced immune cell infiltration and fibrosis in kidneys. *A*, representative images of H&E staining in glomerular sections from CTL, GH, and GH + DAPT-treated mice. Interstitial infiltration of plasma-lymphocytic cells can be noticed in the GH-treated group (*white arrows*). *Scale bars* indicate 20 μm (×630). *B*, representative images of PAS staining in glomeruli from CTL, GH, and GH + DAPT-treated mice ($n = 6$). *Scale bars* = 20 μm (×630). *C*, mesangial expansion index from PAS-stained images was quantified using ImageJ. Each *dot* represents the average value of 20 glomeruli from a single animal of each group ($n = 6$). ***, $p < 0.004$. *D*, glomerular damage score was derived from PAS-stained images by summing the mesangial expansion (*asterisks*), glomerular capillary blockage, and adhesin of glomerular tuft to Bowman's capsule (*black arrowhead*). Each *dot* represents the average value of 20 glomeruli from a single animal from each group ($n = 6$). ***, $p < 0.004$. *E*, expression of cytokines and chemokines in human podocytes (CTL, GH, and GH + DAPT) was analyzed qRT-PCR. Expression of β-Actin was used as an internal control. *, $p < 0.05$; **, $p < 0.01$; and ***, $p < 0.004$. *F*, TEM images of glomeruli from CTL, GH, and GH + DAPT mice ($n = 6$). Thickening of GBM and effacement of podocyte foot processes was noticed predominantly in GH-treated mice. *Scale bars* indicate 0.5 μm. *G*, thickness of GBM was quantified as described under "Experimental procedures." Data are presented as mean ± S.D. and statistical significance were analyzed by Student's *t* test.

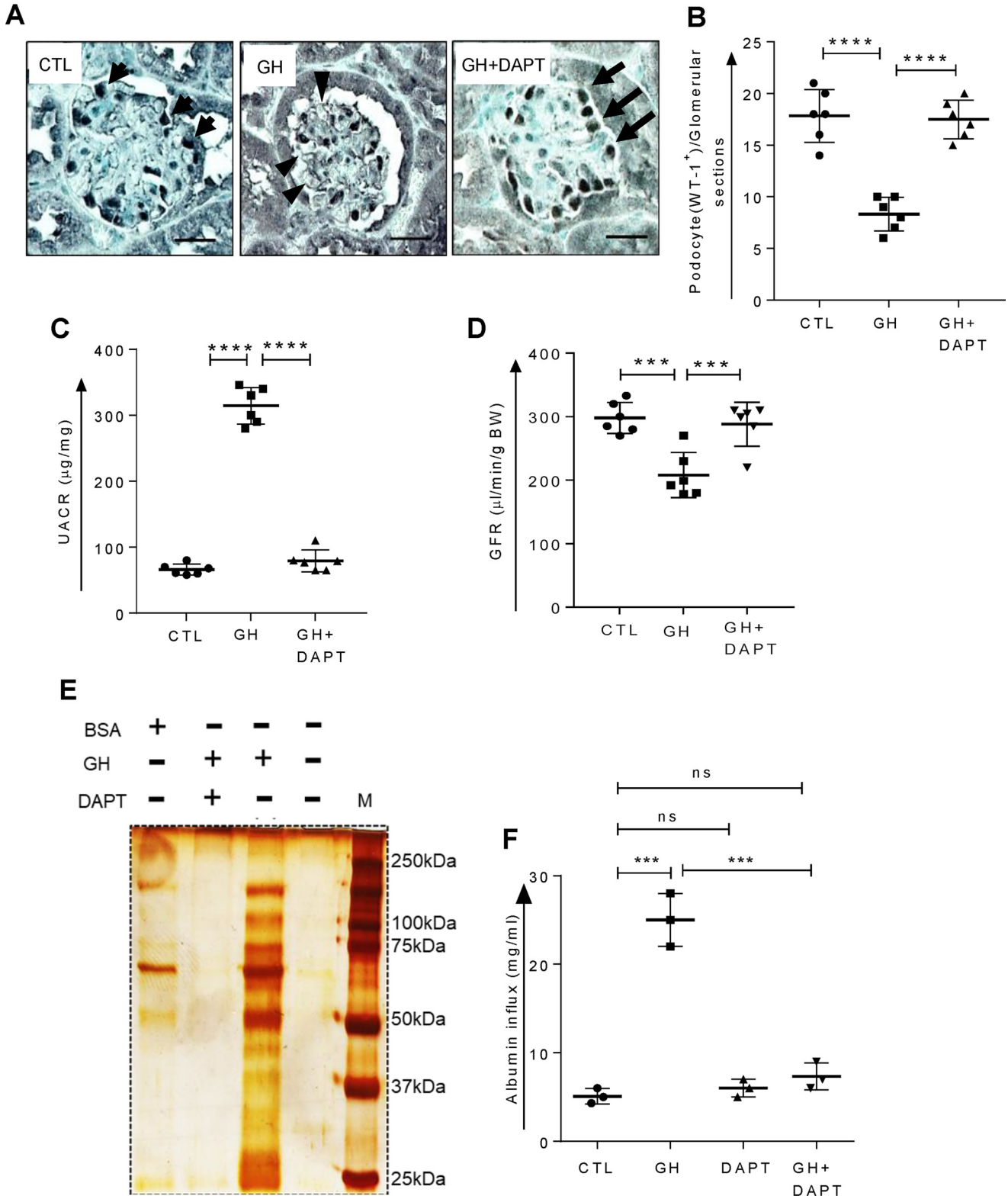


Figure 6. Blockade of Notch signaling protect mice from GH-induced proteinuria. *A*, representative images of immunohistochemical staining for WT1 (podocyte) in glomerulus from CTL, GH, and GH + DAPT-treated mice. *Scale bars* indicate 20 μm. *Arrow* indicates the podocyte and the arrow head indicates loss of podocyte. *B*, average number of $WT1^+$ cells from each mouse from CTL, GH, and GH + DAPT groups. ($n = 6$) **, $p < 0.01$ and ***, $p < 0.004$. We analyzed 20 glomeruli in each mouse for WT^+ cells. *C*, UACR was estimated in CTL, GH, and GH + DAPT-treated mice ($n = 6$). ***, $p < 0.004$; ***, $p < 0.004$. *D*, GFR in CTL, GH, and GH + DAPT-treated mice ($n = 6$). ***, $p < 0.004$. *E*, urinary samples from CTL, GH, and GH + DAPT group mice were subjected to SDS-PAGE and silver stained as described under "Experimental procedures." BSA was used as a standard. *F*, quantification of albumin influx across human podocyte monolayer after 4 h followed by treatment with GH, DAPT, and GH + DAPT for 12 h. ***, $p < 0.004$; *ns*, not significant. Data are presented as mean ± S.D. ($n = 3$) and statistical significance were analyzed by Student's *t* test.

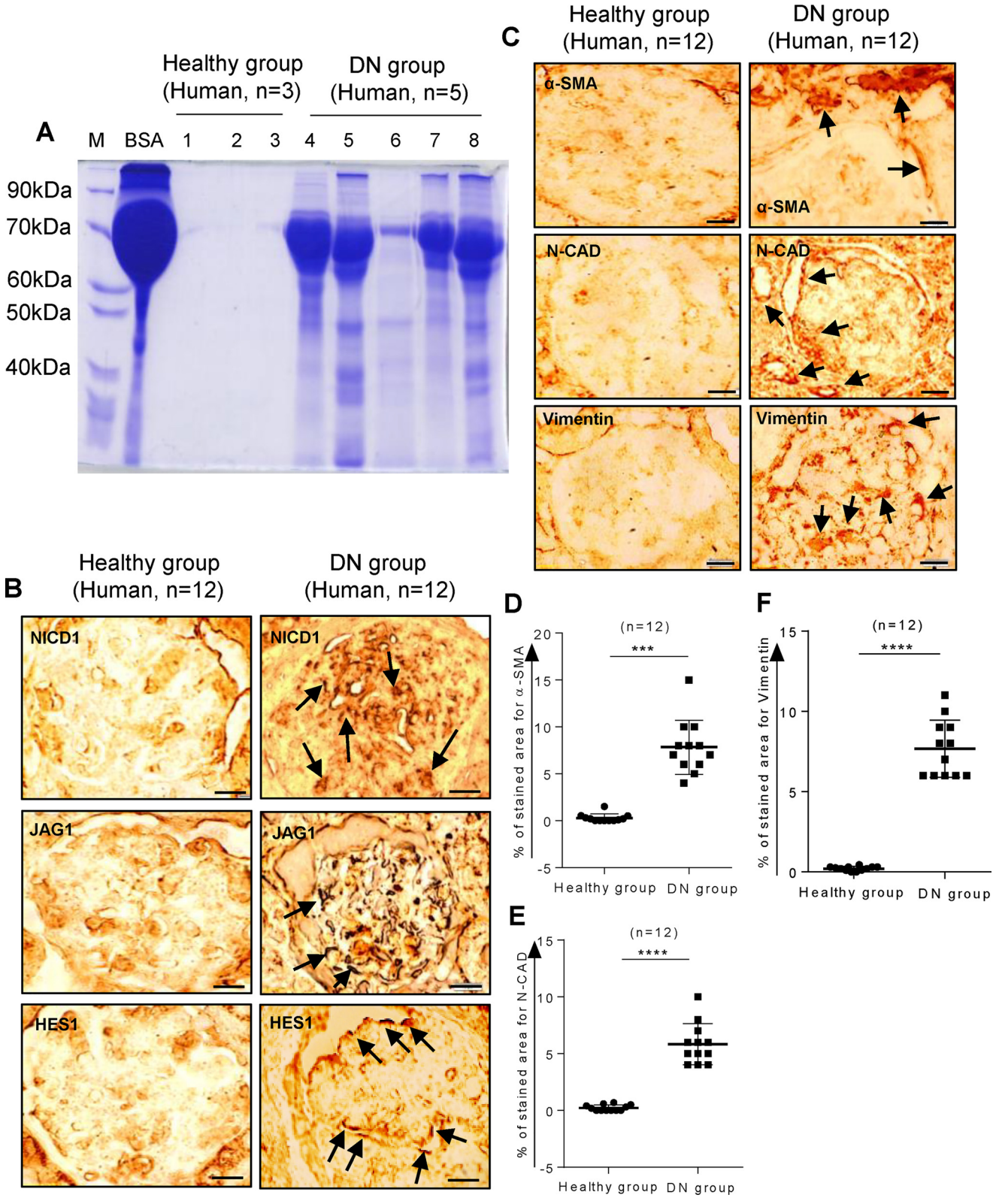


Figure 7. Elevated Notch pathway and EMT in podocytes and proteinuria in people with DN. *A*, urine samples from people with DN ($n = 5$) and healthy volunteers ($n = 3$) were resolved on SDS-PAGE and stained with Coomassie Blue. *B*, representative images of immunohistochemical staining for NICD1, Jag1, and Hes1 in glomerular sections from people with or without DN. *Scale bars* indicate 20 μm (×630). *C*, representative images of immunohistochemical staining for α-SMA, N-Cad, and Vimentin in glomerular sections from people with or without DN. *Scale bars* indicate 20 μm (×630). Quantification of expression of α-SMA (*D*), N-Cad (*E*), and Vimentin (*F*) in 20 glomeruli from each individual with DN compared with people without DN using ImageJ. Data are presented as mean ± S.D. ***, $p < 0.004$ and ****, $p < 0.0001$.

aliquot of urine from mice was subjected to SDS-PAGE gel and silver staining was performed to visualize proteins in the urine (40). We have also estimated GFR in these mice, as described previously (40). We performed immunohistochemistry and Western blotting for analyzing the expression of several markers. For Western blotting, kidneys were collected, and glomeruli were isolated. Protein and RNA were prepared from the glomerular lysate. For histological analysis, kidney cortex was fixed with 4% paraformaldehyde before embedding in paraffin. Paraffin-embedded tissues were sliced longitudinally into 3-μm thick sections, subjected to staining with hematoxylin and eosin, PAS, and Masson's trichrome stainings. Transmission electron microscopic (TEM) images were obtained for glomerular sections from experimental mice groups as described earlier (45).

Human kidney specimens

Kidney specimens were collected without patient identifiers from archived kidney biopsies at Guntur Medical College and Government General Hospital, Andhra Pradesh, India. We selected cases with biopsy-proven diabetic nephropathy and significant proteinuria. The study was approved by the Institutional Review Board of Guntur Medical College and Government General Hospital, Guntur, Andhra Pradesh, India (application number GMC/IEC/120/2018). Our studies abide by the Declaration of Helsinki principles.

Morphological studies

All histological quantifications were evaluated in a blinded manner by two independent investigators. Using kidney sections from these mice ($n = 6$ each group), 20 consecutive glomeruli per mouse were examined for evaluation of glomerular mesangial expansion and an average value of 120 glomeruli from each group presented as a dot plot. The index of the mesangial expansion was defined as the ratio of the mesangial area/glomerular tuft area. The mesangial area was determined by the assessment of the PAS-positive and nucleus-free area in the mesangium using ImageJ (NIH). Ultrastructure of glomerulus was recorded using TEM. For measurement of GBM thickness, we have randomly selected 6 glomeruli per animal ($n = 6$ each group). In each glomerulus, we have selected 6 spots and assessed the thickness of GBM using ImageJ. In the dot plot, each dot represents the average thickness of GBM from a single animal.

Estimation of glomerular filtration rate

GFR in mice was performed at 8 weeks of age using a FIT GFR Test Kit for Inulin according to the manufacturer's instructions (BioPal, Worcester, MA). Briefly, 5 mg/kg of inulin was injected intraperitoneally, followed by serial saphenous bleeds at 30, 60, and 90 min. Next, serum isolation was done and quantified on a inulin ELISA kit. Serum inulin clearance estimation was performed by the nonlinear regression method using a one-phase exponential decay formula ($y = Be - bx$), and GFR was calculated (GFR $= ((I)/(B/b))/KW$, where I is the amount of inulin delivered by the bolus injection, B is y intercept, b is the decay constant, x is time, and KW is kilo weight of the animal). Urinary albumin (number COD11573) and creatinine (number COD11502) levels were estimated using available assay kits (Biosystems, Barcelona, Spain).

Podocyte culture and experimentation

Conditionally immortalized HPC were cultured as described earlier (24). Differentiated podocytes were maintained for 12–16 h in serum-free medium before treating with hGH (Pfizer, NY), pegvisomant (Pfizer), and DAPT (Sigma). Unless otherwise mentioned all the experimental conditions for podocyte cells were given for 12 h. The cell lysate was prepared for RNA isolation or immunoblotting. For immunofluorescence, cells were cultured on coverslips, followed by treatment as mentioned above, subsequent fixation with paraformaldehyde (4%), and blocking with PBS containing normal BSA (5%) before incubation with primary antibodies. The next day, the samples were incubated with Alexa Fluor-conjugated secondary antibodies, and DAPI for 1 h. Images were acquired using a confocal microscope (Zeiss). Albumin influx assay across podocyte monolayer was performed as described earlier (23). Primary podocytes were isolated from mice kidney as described earlier (46).

Immunoblotting

Glomerular lysate from kidney or human podocytes was prepared with lysis buffer (150 mM NaCl, 1% Nonidet P-40, 0.1% SDS, 2 μg/ml of aprotinin, 1 mM PMSF) for 30 min at 4 °C. The homogenate was centrifuged at 12,000 $\times$ g for 25 min at 4 °C and supernatant was collected. An equal amount of protein from different groups was electrophoresed through 10 to 15% SDS-PAGE gel and Western blotting was performed with corresponding primary and secondary antibodies. Blots were developed using the ECL Western blotting substrate (number 1705060, Bio-Rad) and chemiluminescence device (Bio-Rad Versa Doc 5000 MFP).

RNA extraction and qRT-PCR

The total transcripts were extracted by using TRIzol reagent (Invitrogen) and isolated using RNA isolation kit (Qiagen). Next, 1 μg of total RNA was reverse transcribed using the cDNA synthesis kit (Thermo Fisher Scientific). qPCR analysis was performed by the QuantStudio 3 system (Applied Biosystem) with SYBR Green (KAPPABIOSYSTEM, USA) Master Mix using three-step standard cycling conditions with sequence-specific primers. To ensure a single PCR product was amplified, we examined the melting curve for each primer. mRNA expression of each gene was normalized using the expression of β-actin.

Enzyme-linked immunosorbent assay

γ-Secretase activity was quantified by fluorescent microscopy using a γ-secretase activity kit according to the manufacturer's instructions (ImmunoTag, G-Biosciences, St. Louis, MO). Briefly, the γ-secretase activity was determined by quantification of human APH1A (Gamma-Secretase subunit APH-1A) with biotin-conjugated anti-APH1A antibody as a detection antibody. The cleavage-dependent release was measured at 450 nm by using a fluorescent microplate reader (Multiskan GO Microplate Spectrophotometer, Thermo Scientific).

Chemotaxis assay

J774A.1 macrophages were cultured as a monolayer and were scratched using the sterile 10-μl tip and washed with PBS to remove cell debris. Conditioned media from podocytes treated with GH, GH + DAPT, or naive to any treatment was added to J774A.1 macrophage. C5a was used as a positive control with a concentration of 10 ng/ml (47). After the scratch, the images of the wounded area were captured at different time intervals to monitor J774A.1 macrophage migration into the wounded area. The migratory abilities were quantified by measuring the distance between cells in the scratch zone.

F-actin staining

Phalloidin staining for F-actin was performed to visualize the distribution of stress fibers in differentiated podocytes as described previously (48). Briefly, the cells were fixed in 4% paraformaldehyde at room temperature for 15 min after washing, and then permeabilized for 15 min with 0.3% Triton X-100 in PBS followed by 5% BSA blocking. Cells were incubated with rhodamine-phalloidin (Invitrogen Corp.) for 15 min at room temperature to stain F-actin. The slides were examined using confocal laser scanning microscopy. Fifty cells per group were counted to calculate the ratio of cells retaining distinct F-actin fibers. The slides were examined by Leica Microsystems trinocular or Zeiss confocal microscopy.

Wound healing assay

The phenomenon of EMT in podocyte cells was assessed using a wound healing migration assay. A confluent monolayer of podocytes in 6-well plates was wounded with a 10-μl pipette tip following two perpendicular diameters, giving rise to two acellular clear areas per well. After washing with PBS, podocyte cells were treated with GH and GH + DAPT and incubated for 0–12 h and images were captured at different time intervals. The extent of migration of cells to cover wounded area was determined by ImageJ.

Statistical analysis

The data are presented as mean ± S.D. of at least 6 independent experiments unless otherwise mentioned. Prism software (GraphPad Software Inc.) was used to analyze the data. Statistical differences between the groups made using Student's *t* test. Statistical significance was determined as $p < 0.05$.

Author contributions—R. N., D. M., S. V. T., and S. K. M. data curation; R. N., D. M., and S. V. T. methodology; R. N., S. K. M., and A. K. P. writing-original draft; R. N., S. K. M., and A. K. P. writing-review and editing; D. M., S. V. T., S. K. M., and A. K. P. formal analysis; S. K. M. and A. K. P. conceptualization; S. K. M. and A. K. P. supervision; A. K. P. funding acquisition; A. K. P. validation; A. K. P. investigation; A. K. P. visualization; A. K. P. project administration.

Acknowledgment—We acknowledge Prof. Ram K. Menon (University of Michigan, Ann Arbor) for sharing microarray data.

References

1. Nath, K. A. (1992) Tubulointerstitial changes as a major determinant in the progression of renal damage. *Am. J. Kidney Dis.* **20,** 1–17 CrossRef
2. Liu, Y. (2011) Cellular and molecular mechanisms of renal fibrosis. *Nat. Rev. Nephrology* **7,** 684–696 CrossRef Medline
3. Cheng, H. T., Miner, J. H., Lin, M., Tansey, M. G., Roth, K., and Kopan, R. (2003) Gamma-secretase activity is dispensable for mesenchyme-to-epithelium transition but required for podocyte and proximal tubule formation in developing mouse kidney. *Development* **130,** 5031–5042 CrossRef Medline
4. Cheng, H. T., Kim, M., Valerius, M. T., Surendran, K., Schuster-Gossler, K., Gossler, A., McMahon, A. P., and Kopan, R. (2007) Notch2, but not Notch1, is required for proximal fate acquisition in the mammalian nephron. *Development* **134,** 801–811 CrossRef Medline
5. Liu, Z., Chen, S., Boyle, S., Zhu, Y., Zhang, A., Piwnica-Worms, D. R., Ilagan, M. X., and Kopan, R. (2013) The extracellular domain of Notch2 increases its cell-surface abundance and ligand responsiveness during kidney development. *Dev. Cell* **25,** 585–598 CrossRef Medline
6. Chung, E., Deacon, P., and Park, J. S. (2017) Notch is required for the formation of all nephron segments and primes nephron progenitors for differentiation. *Development* **144,** 4530–4539 CrossRef Medline
7. Milano, J., McKay, J., Dagenais, C., Foster-Brown, L., Pognan, F., Gadient, R., Jacobs, R. T., Zacco, A., Greenberg, B., and Ciaccio, P. J. (2004) Modulation of notch processing by γ-secretase inhibitors causes intestinal goblet cell metaplasia and induction of genes known to specify gut secretory lineage differentiation. *Toxicol. Sci.* **82,** 341–358 CrossRef Medline
8. Hayward, P., Kalmar, T., and Arias, A. M. (2008) Wnt/Notch signalling and information processing during development. *Development* **135,** 411–424 CrossRef Medline
9. Zhao, Y., Katzman, R. B., Delmolino, L. M., Bhat, I., Zhang, Y., Gurumurthy, C. B., Germaniuk-Kurowska, A., Reddi, H. V., Solomon, A., Zeng, M. S., Kung, A., Ma, H., Gao, Q., Dimri, G., Stanculescu, A., *et al.* (2007) The notch regulator MAML1 interacts with p53 and functions as a coactivator. *J. Biol. Chem.* **282,** 11969–11981 CrossRef Medline
10. Del Bianco, C., Aster, J. C., and Blacklow, S. C. (2008) Mutational and energetic studies of Notch 1 transcription complexes. *J. Mol. Biol.* **376,** 131–140 CrossRef Medline
11. Liu, Z. J., Xiao, M., Balint, K., Soma, A., Pinnix, C. C., Capobianco, A. J., Velazquez, O. C., and Herlyn, M. (2006) Inhibition of endothelial cell proliferation by Notch1 signaling is mediated by repressing MAPK and PI3K/Akt pathways and requires MAML1. *FASEB J.* **20,** 1009–1011 CrossRef
12. McCright, B. (2003) Notch signaling in kidney development. *Curr. Opin. Nephrol. Hypertens.* **12,** 5–10 CrossRef Medline
13. Vooijs, M., Ong, C. T., Hadland, B., Huppert, S., Liu, Z., Korving, J., van den Born, M., Stappenbeck, T., Wu, Y., Clevers, H., and Kopan, R. (2007) Mapping the consequence of Notch1 proteolysis in vivo with NIP-CRE. *Development* **134,** 535–544 Medline
14. Niranjan, T., Bielesz, B., Gruenwald, A., Ponda, M. P., Kopp, J. B., Thomas, D. B., and Susztak, K. (2008) The Notch pathway in podocytes plays a role in the development of glomerular disease. *Nat. Med.* **14,** 290–298 CrossRef Medline
15. Waters, A. M., Wu, M. Y., Onay, T., Scutaru, J., Liu, J., Lobe, C. G., Quaggin, S. E., and Piscione, T. D. (2008) Ectopic notch activation in developing podocytes causes glomerulosclerosis. *J. Am. Soc. Nephrol.* **19,** 1139–1157 CrossRef Medline
16. Bielesz, B., Sirin, Y., Si, H., Niranjan, T., Gruenwald, A., Ahn, S., Kato, H., Pullman, J., Gessler, M., Haase, V. H., and Susztak, K. (2010) Epithelial Notch signaling regulates interstitial fibrosis development in the kidneys of mice and humans. *J. Clin. Invest.* **120,** 4040–4054 CrossRef Medline
17. Murea, M., Park, J. K., Sharma, S., Kato, H., Gruenwald, A., Niranjan, T., Si, H., Thomas, D. B., Pullman, J. M., Melamed, M. L., and Susztak, K. (2010) Expression of Notch pathway proteins correlates with albuminuria, glomerulosclerosis, and renal function. *Kidney Int.* **78,** 514–522 CrossRef Medline
18. Walsh, D. W., Roxburgh, S. A., McGettigan, P., Berthier, C. C., Higgins, D. G., Kretzler, M., Cohen, C. D., Mezzano, S., Brazil, D. P., and Martin, F. (2008) Co-regulation of Gremlin and Notch signalling in diabetic nephropathy. *Biochim. Biophys. Acta* **1782,** 10–21 CrossRef Medline

19. Niranjan, T., Murea, M., and Susztak, K. (2009) The pathogenic role of Notch activation in podocytes. *Nephron Exp. Nephrol.* **111,** e73–79 CrossRef Medline
20. Pasupulati, A. K., and Menon, R. K. (2019) Growth hormone and chronic kidney disease. *Curr. Opin. Nephrol. Hypertens.* **28,** 10–15 CrossRef Medline
21. Mukhi, D., Nishad, R., Menon, R. K., and Pasupulati, A. K. (2017) Novel actions of growth hormone in podocytes: implications for diabetic nephropathy. *Front. Med.* **4,** 102 CrossRef Medline
22. Kumar, P. A., Brosius F. C., 3rd, Menon, R. K. (2011) The glomerular podocyte as a target of growth hormone action: implications for the pathogenesis of diabetic nephropathy. *Curr. Diabetes Rev.* **7,** 50–55 CrossRef Medline
23. Chitra, P. S., Swathi, T., Sahay, R., Reddy, G. B., Menon, R. K., and Kumar, P. A. (2015) Growth hormone induces transforming growth factor-β-induced protein in podocytes: implications for podocyte depletion and proteinuria. *J. Cell. Biochem.* **116,** 1947–1956 CrossRef Medline
24. Kumar, P. A., Kotlyarevska, K., Dejkhmaron, P., Reddy, G. R., Lu, C., Bhojani, M. S., and Menon, R. K. (2010) Growth hormone (GH)-dependent expression of a natural antisense transcript induces zinc finger E-box-binding homeobox 2 (ZEB2) in the glomerular podocyte: a novel action of GH with implications for the pathogenesis of diabetic nephropathy. *J. Biol. Chem.* **285,** 31148–31156 CrossRef Medline
25. Beel, A. J., and Sanders, C. R. (2008) Substrate specificity of γ-secretase and other intramembrane proteases. *Cell. Mol. Life Sci.* **65,** 1311–1334 CrossRef Medline
26. Haynes, J., Srivastava, J., Madson, N., Wittmann, T., and Barber, D. L. (2011) Dynamic actin remodeling during epithelial-mesenchymal transition depends on increased moesin expression. *Mol. Biol. Cell* **22,** 4750–4764 CrossRef Medline
27. Whitney, J. L., Bilkan, C. M., Sandberg, K., Myers, A. K., and Mulroney, S. E. (2013) Growth hormone exacerbates diabetic renal damage in male but not female rats. *Biol. Sex Differ.* **4,** 12 CrossRef Medline
28. Song, K., Fu, J., Song, J., Herzog, B. H., Bergstrom, K., Kondo, Y., McDaniel, J. M., McGee, S., Silasi-Mansat, R., Lupu, F., Chen, H., Bagavant, H., and Xia, L. (2017) Loss of mucin-type *O*-glycans impairs the integrity of the glomerular filtration barrier in the mouse kidney. *J. Biol. Chem.* **292,** 16491–16497 CrossRef Medline
29. Cheng, H. T., and Kopan, R. (2005) The role of Notch signaling in specification of podocyte and proximal tubules within the developing mouse kidney. *Kidney Int.* **68,** 1951–1952 CrossRef Medline
30. Asanuma, K., Oliva Trejo, J. A., and Tanaka, E. (2017) The role of Notch signaling in kidney podocytes. *Clin. Exp. Nephrol.* **21,** 1–6 CrossRef Medline
31. Lasagni, L., Ballerini, L., Angelotti, M. L., Parente, E., Sagrinati, C., Mazzinghi, B., Peired, A., Ronconi, E., Becherucci, F., Bani, D., Gacci, M., Carini, M., Lazzeri, E., and Romagnani, P. (2010) Notch activation differentially regulates renal progenitors proliferation and differentiation toward the podocyte lineage in glomerular disorders. *Stem Cells (Dayton, OH)* **28,** 1674–1685 CrossRef Medline
32. Sweetwyne, M. T., Gruenwald, A., Niranjan, T., Nishinakamura, R., Strobl, L. J., and Susztak, K. (2015) Notch1 and Notch2 in podocytes play differential roles during diabetic nephropathy development. *Diabetes* **64,** 4099–4111 CrossRef Medline
33. Press, M., Tamborlane, W. V., and Sherwin, R. S. (1984) Importance of raised growth hormone levels in mediating the metabolic derangements of diabetes. *New Engl. J. Med.* **310,** 810–815 CrossRef Medline
34. Ying, Q., and Wu, G. (2017) Molecular mechanisms involved in podocyte EMT and concomitant diabetic kidney diseases: an update. *Ren. Fail.* **39,** 474–483 CrossRef Medline
35. Ahn, S. H., and Susztak, K. (2010) Getting a notch closer to understanding diabetic kidney disease. *Diabetes* **59,** 1865–1867 CrossRef Medline
36. Lin, C. L., Wang, F. S., Hsu, Y. C., Chen, C. N., Tseng, M. J., Saleem, M. A., Chang, P. J., and Wang, J. Y. (2010) Modulation of notch-1 signaling alleviates vascular endothelial growth factor-mediated diabetic nephropathy. *Diabetes* **59,** 1915–1925 CrossRef Medline
37. Wang, Y., and Zhou, B. P. (2011) Epithelial-mesenchymal transition in breast cancer progression and metastasis. *Chin. J. Cancer* **30,** 603–611 CrossRef Medline
38. Collu, G. M., and Brennan, K. (2007) Cooperation between Wnt and Notch signalling in human breast cancer. *Breast Cancer Res.* **9,** 105 CrossRef Medline
39. Leong, K. G., Niessen, K., Kulic, I., Raouf, A., Eaves, C., Pollet, I., and Karsan, A. (2007) Jagged1-mediated Notch activation induces epithelial-to-mesenchymal transition through Slug-induced repression of E-cadherin. *J. Exp. Med.* **204,** 2935–2948 CrossRef Medline
40. Nakuluri, K., Mukhi, D., Nishad, R., Saleem, M. A., Mungamuri, S. K., Menon, R. K., and Pasupulati, A. K. (2019) Hypoxia induces ZEB2 in podocytes: Implications in the pathogenesis of proteinuria. *J. Cell. Physiol.* **234,** 6503–6518 CrossRef Medline
41. Hills, C. E., and Squires, P. E. (2011) The role of TGF-beta and epithelial-to mesenchymal transition in diabetic nephropathy. *Cytokine Growth Factor Rev.* **22,** 131–139 Medline
42. Sutariya, B., Jhonsa, D., and Saraf, M. N. (2016) TGF-β: the connecting link between nephropathy and fibrosis. *Immunopharmacol. Immunotoxicol.* **38,** 39–49 CrossRef Medline
43. Zavadil, J., Cermak, L., Soto-Nieves, N., and Böttinger, E. P. (2004) Integration of TGF-β/Smad and Jagged1/Notch signalling in epithelial-to-mesenchymal transition. *EMBO J.* **23,** 1155–1165 CrossRef Medline
44. Geling, A., Steiner, H., Willem, M., Bally-Cuif, L., and Haass, C. (2002) A gamma-secretase inhibitor blocks Notch signaling *in vivo* and causes a severe neurogenic phenotype in zebrafish. *EMBO Rep.* **3,** 688–694 CrossRef Medline
45. Nakuluri, K., Mukhi, D., Mungamuri, S. K., and Pasupulati, A. K. (2018) Stabilization of hypoxia-inducible factor 1α by cobalt chloride impairs podocyte morphology and slit-diaphragm function. *J. Cell. Biochem.* 10.1002/jcb.28041 CrossRef
46. Katsuya, K., Yaoita, E., Yoshida, Y., Yamamoto, Y., and Yamamoto, T. (2006) An improved method for primary culture of rat podocytes. *Kidney Int.* **69,** 2101–2106 CrossRef Medline
47. Das, D., Barnes, M. A., and Nagy, L. E. (2014) Anaphylatoxin C5a modulates hepatic stellate cell migration. *Fibrogenesis Tissue Repair* **7,** 9 CrossRef Medline
48. Zhou, H., Tian, X., Tufro, A., Moeckel, G., Ishibe, S., and Goodwin, J. (2017) Loss of the podocyte glucocorticoid receptor exacerbates proteinuria after injury. *Sci. Rep.* **7,** 9833 CrossRef Medline

ASBMB

Indian Journal of Research in Pharmacy and Biotechnology (IJRPB)
ISSN: 2321-5674 (Print), 2320-3471 (Online)

CrossRef DOI: https://doi.org/10.31426/ijrpb **Indexed in CAS and CABI, Impact Factor: 0.64**

A Validated Reversed Phase HPLC Method Development for the Assay of Ciprofloxacin in Oral Suspension

Bathula Sivannarayana[1], Modugula Jyosthna[1], Dr Dasi Jeevan Mani Babu[1], Mekala Sunil[1], Choppavarapu Dorcas Anand[2], Dr M. Manoranjani[3]

[1]St.Xavier Institute of Pharmacy, Phirangipuram, Guntur. A.P., India
[2]SRR & CVR Govt. (A) Degree College, Vijayawada, A.P., India
[3]Dept. of Chemistry, PB Siddartha College of Arts and Sciences, Vijayawada, A.P., India

E-Mail: drjeevanbabu@gmail.com

Keywords:
Ciprofloxacin, RP-HPLC

ABSTRACT

A simple Reverse phase liquid chromatographic method has been developed and subsequently validated for the determination of Ciprofloxacin in oral suspension. The separation was carried out using a mobile phase consisting of buffer of pH 2.0 and Acetonitrile in the ratio of 87: 13. The column used was Inertsil ODS-3 4.6×250mm, 5µ. with a flow rate of 1.5 ml / min by detection at 278 nm. The described method was linear over a concentration range of 25-150%. The retention time of Ciprofloxacinwas found to be 9.4min. Results of analysis were validated statistically and by recovery studies. The results of the study showed that the proposed RP-HPLC method is simple, rapid, precise and accurate, which is useful for the routine determination of Ciprofloxacinin its pharmaceutical dosage forms.

1. INTRODUCTION

Ciprofloxacin is a broad-spectrum antimicrobial carboxyfluoroquinoline. The bactericidal action of ciprofloxacin results from inhibition of the enzymes topoisomerase II (DNA gyrase) and topoisomerase IV, which are required for bacterial DNA replication, transcription, repair, strand supercooling repair, and recombination. [1]

Indian Journal of Research in Pharmacy and Biotechnology (IJRPB)
ISSN: 2321-5674 (Print), 2320-3471 (Online)

CrossRef DOI: https://doi.org/10.31426/ijrpb **Indexed in CAS and CABI, Impact Factor: 0.64**

Ciprofloxacin is a broad-spectrum anti-infective agent of the fluoroquinolone class. Ciprofloxacin has in vitro activity against a wide range of gram-negative and gram-positive microorganisms. The mechanism of action of quinolones, including ciprofloxacin, is different from that of other antimicrobial agents such as beta-lactams, macrolides, tetracyclines, or aminoglycosides; therefore, organisms resistant to these drugs may be susceptible to ciprofloxacin. There is no known cross-resistance between ciprofloxacin and other classes of antimicrobials. Notably the drug has 100 times higher affinity for bacterial DNA gyrase than for mammalian. The bactericidal action of ciprofloxacin results from inhibition of the enzymes topoisomerase II (DNA gyrase) and topoisomerase IV, which are required for bacterial DNA replication, transcription, repair, strand supercooling repair, and recombination.

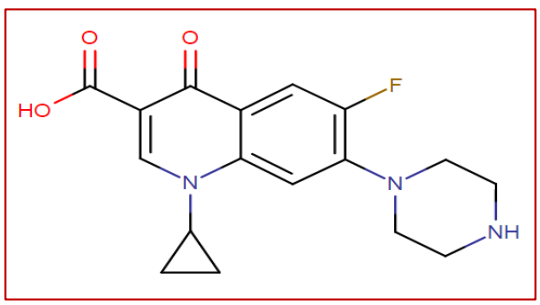


Figure. 1. Molecular structure of Ciprofloxacin

2. Materials and Methods:

2.1 Chemicals and Reagents:

Standard bulk drug sample Ciprofloxacin was provided by Chandra labs, Hyderabad. All the chemicals used were of analytical and HPLC grade procured from Qualigens, India Ltd. The chemicals used for this study were Acetonitrile (HPLC grade), Methanol (HPLC grade), Water (HPLC grade), Ortho phosphoric acid (Analytical grade). Waters HPLC 2695with UV detector was used for the analysis.

2.2. Preparation of Mobile Phase:

Mobile phase-A: (Buffer) Pipette out 10ml of Methanol in to 1000ml of and mix. Adjust to pH 2.0 with Orthophosphoric acid, then filter through 0.45µ filter paper and sonicate for 2minutes.

Mobile phase-B: Acetonitrile

Preparation of Mobile Phase:

Mix the mobile phase-A and mobile phase-B in the ratio in the ratio 87:13%v/v.

Indian Journal of Research in Pharmacy and Biotechnology (IJRPB)
ISSN: 2321-5674 (Print), 2320-3471 (Online)

CrossRef DOI: https://doi.org/10.31426/ijrpb **Indexed in CAS and CABI, Impact Factor: 0.64**

2.3. Preparation of Stock and Standard Solutions:

Preparation of Standard solution:

Weigh and transfer 25mg ciprofloxacin working standard into a 50mL volumetric flask. Add 7ml of acetonitrile andsonicate for 2minutes then add 30ml of pH2.00buffer, sonicate for 10minutes then make up to the mark with diluent. Further pipette out 5ml of the above solution in to 20ml volumetric flask, add 2.8ml of acetonitrile mix well, then add 12ml of pH2.00 buffer, then make up to the mark with diluent.

Preparation of Test Solution:

Shake the bottle 10minutes immediately prior to sampling in order to accomplish homogeneity of suspension. Weigh and transfer 5.5g ciprofloxacin suspension into a 500mL volumetric flask. Add 70ml of acetonitrile sonicate for 10 minutes, then add 250ml of pH 2.00 buffer, sonicate for 20minutes then make up to the mark with diluent. Further pipette out 5ml of the above solution in to 20ml volumetric flask, add 2.8ml of acetonitrile mix well, then add 12ml of pH2.00 buffer, then make up to the mark with diluent.

2.4. Optimized Chromatographic Conditions:

Column: Inertsil ODS-3 4.6×250mm, 5µ.

Flow rate : 1.5 mL /min.

Wavelength : 278 nm

Column temperature : 40°C

Injection Volume : 10 µL

Run Time : 15 minutes

Retention time: Ciprofloxacin, RT about 9.4min

3. Method Validation Parameters:

Linearity:

A series of Ciprofloxacin solutions were prepared in the concentration ranging from 25% to 150% of specification level and injected into the HPLC system as per the test method. The square of the correlation coefficient, intercept and residual sum of squares were calculated.

Indian Journal of Research in Pharmacy and Biotechnology (IJRPB)
ISSN: 2321-5674 (Print), 2320-3471 (Online)

CrossRef DOI: https://doi.org/10.31426/ijrpb **Indexed in CAS and CABI, Impact Factor: 0.64**

Accuracy:

A series of solutionswereprepared in triplicatetest preparation at the specification limit in the range of about 25%to 150% of test concentration and injected into HPLC system and analyzed as per the test method. Individual % recovery, mean % recovery, %RSD and linearity of the testmethodwere calculated at each level.

Intermediate Precision:

To evaluate the intermediate precision for assay method, six samples were prepared and analyzed as per test method by using different column, by different analysts on different days. Intermediate precision was calculated and found to be within the acceptable limits. The overall % RSD of six samples in method precision, intermediate precision (n=6 and n=12) were calculated.

Filter Validation:

A study was conducted to evaluate the filter suitability by using two different types of filters namely0. 45 µm PVDF and 0.45µm Nylon filters. Standard solution was prepared in single and test solution was prepared in duplicate as per the test method. Portion of standard and test solutions were filtered through 0.45 µm PVDF, 0.45 µm nylon filter and some portion of standard and sample solutions were centrifuged and analyzed as per test method.

Robustness:

Flow Rate Variation:

A study was conducted to determine the effect of variation in flow rate. Blank, Standard and sample (at the specification level) were prepared as per the test method and injected into the HPLC system with flow rates of 1.4ml/minute and 1.6ml/minute. The system suitability parameters sample was evaluated and found to be within the specified limits as per test method.

Column Oven Temperature Variation:

A study was conducted to determine the effect of variation in Column oven Temperature. Standard and test preparations (at the specification level) were prepared as per the test method and injected into the HPLC system with a column oven temperature of 35°C and 45°C. System suitability parameters and sample were evaluated and found to be within the specified limits as per test method.

Indian Journal of Research in Pharmacy and Biotechnology (IJRPB)
ISSN: 2321-5674 (Print), 2320-3471 (Online)
CrossRef DOI: https://doi.org/10.31426/ijrpb **Indexed in CAS and CABI, Impact Factor: 0.64**

Effect of Variation In Mobile Phase Composition:

A study was conducted to determine the effect of variation in mobile phase composition. Two different mobile phases of Buffer and Acetonitrile were prepared in the ratio of 855:145%v/v and 885:115%v/v as per the test method. Standard and test preparations with specification level were prepared as per the test method and injected into the HPLC system.

Effect of pH Variation in Mobile Phase:

A study was conducted to determine the effect of variation in pH in the mobile phase. Two mobile phases of pH 2.80 and 3.20 were prepared as per the test method. Blank, Standard and test preparations were prepared as per the test method and injected into the HPLC system with System suitability parameters and sample were evaluated and found to be within the specified limits as per test method.

The Effect of Wavelength Variation:

A study was conducted to determine the effect of variation in wavelength. Standard and test preparations (at the specification level) were prepared as per the test method and injected into the HPLC system with wavelength of -Ciprofloxacin280nm and 276nm.System suitability parameters and sample were evaluated and found to be within the specified limits as per test method.

4. Results and Discussion:

The solution of Ciprofloxacin was scanned in the range of 200-400nm and 278nm was selected as detection wavelength by RP-HPLC method with an isocratic elution technique. The optimization was done by changing the composition of the mobile phase, ratio and flow rate. Finally the mobile phase with buffer (pH 2): ACN in the ratio 87:13v/v% was optimized for the estimation of Ciprofloxacin and the column used for separation is Inertsil ODS-3 4.6×250mm,5µ. [2]

The chromatographicparameters of system suitability such as %RSD, standard recovery, Tailing factor, Theoretical plates were found to be satisfactory. The values of these parameters are tabulated in Table-1.

Indian Journal of Research in Pharmacy and Biotechnology (IJRPB)
ISSN: 2321-5674 (Print), 2320-3471 (Online)
CrossRef DOI: https://doi.org/10.31426/ijrpb **Indexed in CAS and CABI, Impact Factor: 0.64**

Table.1. System suitability data for Ciprofloxacin

System suitability parameters for Ciprofloxacin	Method Precision	Intermediate precision	Acceptance Criteria
%RSD	0.3	0.3	Not more than 2.0
Standard recovery (%)	101.4	99.5	Between 98.0 to 102.0
Tailing factor	1.1	1.1	Not more than 2.0
Theoretical plates	9925	9271	Not less than 2000

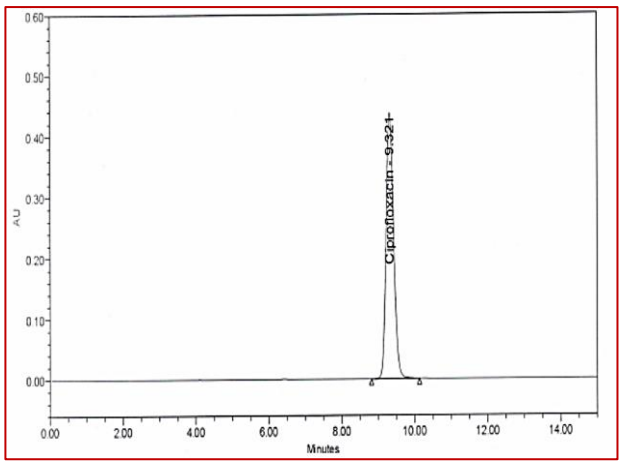


Figure.2.Typical chromatogram of Standard solution

The linearity of the developed method was determined by analyzing different concentrations of the standard solution containing a concentration range from 25% to 150%. The response factor of the standard solutions was calculated. The ratio of peak areas of ciprofloxacin was plotted against the concentration to obtain the calibration graph (Fig. 3) and was found to be linear over the concentration range from 25% to 150%. The data were analyzed by linear regression, least-squares method and the corresponding equation are given by Y = BX + c, where 'Y' is the ratio of the peak areas values of Ciprofloxacin, 'b' is the slope, 'c' is the intercept and 'X' is the concentration of the analyte. Linear regression, least squares fit data are given in (Table 2). [3] The percentage purity was found to be 99.3%. The precision of the method was confirmed by the repeatability of formulation for six times. The accuracy of the method was confirmed by recovery studies and the data was given by (Table 3). [4] Similarity factors were calculated for the filtered standards against unfiltered standard (Centrifuged) and found to be within the specified limit. The difference in the % between unfiltered (centrifuged) and filtered samples were calculated and found to be

Indian Journal of Research in Pharmacy and Biotechnology (IJRPB)
ISSN: 2321-5674 (Print), 2320-3471 (Online)
CrossRef DOI: https://doi.org/10.31426/ijrpb **Indexed in CAS and CABI, Impact Factor: 0.64**

meeting the acceptable limit. Both PVDF and Nylon filters were suitable for the intended purpose.

Table.2.Linearity of detector response for Ciprofloxacin

% Linearity level	Concentration (ppm)	Response	Acceptance criteria
25	31.0875	1536480	Square of Correlation co-efficient should not be less than 0.999
50	62.175	3107355	
75	93.2625	4623963	
100	124.35	6039873	
150	186.525	9110398	
Square of correlation coefficient : 0.999 Slope: 48483.76574 Intercept : 60448.78378 Residual sum of squares: 45710.56736			

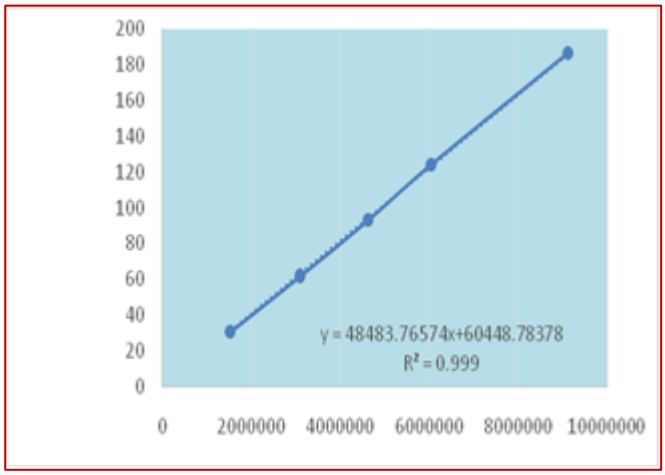


Figure.3.Linearity of detector response graph for Ciprofloxacin.

Indian Journal of Research in Pharmacy and Biotechnology (IJRPB)
ISSN: 2321-5674 (Print), 2320-3471 (Online)
CrossRef DOI: https://doi.org/10.31426/ijrpb **Indexed in CAS and CABI, Impact Factor: 0.64**

Table.3.Accuracy data of Ciprofloxacin

S. No.	% spike level	Amount added (%w/w)	Amount recovered (%w/w)	% Recovery	% Mean recovery	% RSD
1.	25%	62.1229	62.37308	100.4	99.8	0.6
2.		63.0287	62.40228	99.0		
3.		63.0885	62.62924	99.3		
4.		63.1979	62.72669	99.3		
5.		62.2424	62.36469	100.2		
6.		62.3220	62.55297	100.4		
1.	100%	250.8408	247.83270	98.8	99.3	0.4
2.		248.9894	247.87577	99.6		
3.		249.1088	247.78317	99.5		
1.	150%	378.5307	377.14133	99.6	100.6	0.5
2.		374.4894	377.08205	100.7		
3.		374.7781	377.28255	100.7		
4.		373.8921	377.45520	101.0		
5.		373.2252	376.76809	101.0		
6.		374.1609	376.10577	100.5		

Specificity:

Chromatogram of blank and placebo should not show any peak at the retention time of Ciprofloxacin peak and known impurity peaks.

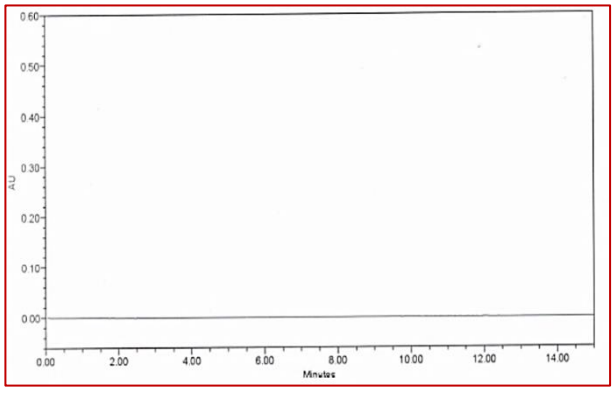


Figure.4.Typical chromatogram of Blank

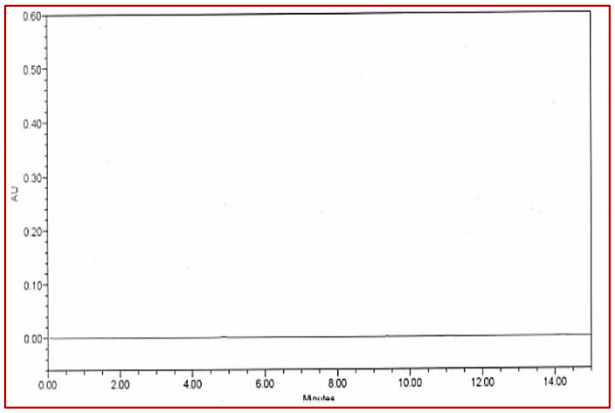


Figure.5.Typical chromatogram of placebo

Indian Journal of Research in Pharmacy and Biotechnology (IJRPB)
ISSN: 2321-5674 (Print), 2320-3471 (Online)

CrossRef DOI: https://doi.org/10.31426/ijrpb **Indexed in CAS and CABI, Impact Factor: 0.64**

Table.4.Method Precision data for Ciprofloxacin

Sample No.	Ciprofloxacin content (%)
1	100.9
2	100.2
3	100.0
4	99.4
5	101.1
6	100.5
Mean	**100.4**
% RSD	**0.6**

5. Conclusion:

This study showed that the antibiotic drug, Ciprofloxacin can be precisely and accurately determined in pure and pharmaceutical dosages. The proposed method is simple and requires less time for analysis. System performance parameters revealed that the method is ideal for the assay ofCiprofloxacin.

Hence, the developed chromatography method was applied for routine analysis and can be used for the intended purpose.

References:

1) Tripathi KD. Essentials of medical pharmacology; sixth edition 2008: 688
2) Abdel-Hay MH, Hassan EM, Gazy AA, Belal TS. Kinetic spectrophotometric analysis and spectrofluorimetric analysis of ciprofloxacin hydrochloride and norfloxacin in pharmaceutical preparations using 4-Chloro-7-nitrobenzo-2-oxa-1,3-diazole (NBD-Cl). J Chin ChemSoc 2008; 55(4): 818-827
3) Gummadi S, Thota D, Varri SV, Vaddi P, Jillella VLNSR. Development and validation of UV spectroscopic methods for simultaneous estimation of ciprofloxacin and tinidazole in tablet formulation.Intcurr Pharm j 2012; 1(10): 317-321
4) El-Brashy AM, El-Sayed MM, El-Sepai FA. Spectrophotometric determination of some fluoroquinoloneantibacterials through charge-transfer and ion-pair complexation reactions. Bul Korean ChemSoc2004; 25(3): 365
5) Safwan A, Mouhammed K. Kinetic Spectrophotometric method for the quantitative analysis of pravastatin sodium (PVS) in pure and pharmaceutical formulations. Arabian J Chem 2012; 4(3): 299-305
6) Chaudhari BG, Patel NM, Shah PB. Determination of simvastatin, pravastatin, rosuvastatin calcium in tablet

Indian Journal of Research in Pharmacy and Biotechnology (IJRPB)
ISSN: 2321-5674 (Print), 2320-3471 (Online)

CrossRef DOI: https://doi.org/10.31426/ijrpb **Indexed in CAS and CABI, Impact Factor: 0.64**

dosage form. Int j pharm sci 2007; 69(10): 130-132

7) Kadikar HK, Shah R. Simultaneous UV spectrophotometry of pravastatin and co-enzyme Q10 in their formulation combined dosage forms and synthetic mixtures. IJPR 2012; 1(4): 112-127
8) D'Silva T, Olivera MA, De'Oliveira RB, Soares CDV. Development and validation of a simple and fast hplc method for determination of lovastatin, pravastatin and simvastatin. J ChromatogrSci2010; 50(9): 831-832
9) Maha F, Abdel-Aziz O, Reham N, Abdel-Fattah L. Validated spectrophotometric methods for determination of some anti-hyperlipidemic drugs. J Med Res 2010; 2(3): 202-211
10) Safwan A, Husni N, Soulafa O. Quantitative determination of pravastatin in pharmaceutical dosage forms by high-performance liquid chromatography with ultraviolet detection. Int J Biomed sci 2011; 4(1): 84-90

Poll Res. 39 (2) : 368-372 (2020)
Copyright © EM International
ISSN 0257–8050

EFFECT OF CARTAP HYDROCHLORIDE (50% SP) ON OXYGEN CONSUMPTION OF FRESH WATER FISH, *CIRRHINUS MRIGALA* (HAMILTON)

G. VANI[1], K. VEERAIAH [2], M. VIJAYA KUMAR [1] AND S.K. PARVEEN [1,]

[1]Department of Zoology, SRR & CVR Government Degree College, (A), Vijayawada 520 004, Krishna District. A.P., India
[2]Department of Zoology and Aquaculture, Acharya Nagarjuna University, Nagarjunanagar 522 510, Guntur, A.P., India

(Received 23 October, 2019; accepted 3 February, 2020)

ABSTRACT

Effect of Cartap hydrochloride on oxygen consumption of the Indian major carp, *Cirrhinus mrigala* was studied. Fingerlings were exposed to sub-lethal (0.0376 mg^{-1}) and lethal (0.376 mg^{-1}) concentrations of Cartap hydrochloride for 24,48,72 and 96hrs. In both sublethal and lethal concentrations for all exposed hours *Cirrhinus mrigala* showed an increased tendency in oxygen consumption during the initial time of exposure and a gradual decrease during the subsequent study period. Alterations in oxygen consumption may be due to respiratory distress as a consequence of impaired oxidative metabolism. Present study showed that Cartap hydrochloride altered respiratory metabolism in *Cirrhinus mrigala* which can be used as bio-indicator for assessing pesticide toxicity to fish.

KEYWORDS: Cartap hydrochloride, *Cirrhinus mrigala,* Oxygen consumption.

INTRODUCTION

Wide and indiscriminate use of pesticides in modern agricultural practices throughout the world has indirectly created problem of pollution of aquatic ecosystems. (Ganeshwade, 2012). These chemicals impair water quality which become unsuitable for all aquatic organisms due to their toxicity, persistence, bioaccumulation, and biomagnification in food chain and ecological balance (Subramani Lavanya *et al.,* 2011). Fish accumulate these pollutants directly or indirectly from polluted waters and food chain (Jabeen *et al*., 2016). In India, Cartap hydrochloride a carbamate pesticide is extensively used in rice and sugarcane crops to control pests. One of the indicators of the health status of a fish is its total oxygen consumption. It helps in evaluating the susceptibility or resistance potential useful to assess the physiological condition of an organism and to correlate the behavior of the animal, which ultimately serve as predictors of functional disruptions of population. Hence the analysis of total oxygen consumption can be used as a biodetectory system to evaluate the basic damage caused to the animal which could either decrease or increase the oxygen uptake (Maharajan *et al.,* 2013). In this viewpoint an attempt was made to study the effect of sublethal and lethal concentrations of Cartap hydrochloride on oxygen consumption of freshwater fish, *Cirrhinus mrigala* exposed for 24,48,72 and 96hrs.

MATERIALS AND METHODS

Experiment on the oxygen consumption of the fish *Cirrhinus mrigala* was carried out in a respiratory apparatus developed by Job (1955). The fingerlings of the test fish *Cirrhinus mrigala* of size 6-8 ± ½ cm and weight 6-7 ± ½ g were procured from local fish hatcheries of Nandivelugu, Tenali mandal, Guntur district, Andhra Pradesh. The fish were acclimated at (28±2 °C) in the laboratory conditions for two

weeks. All the precautions laid down on recommendations of the toxicity tests to aquatic organisms were followed (Annon, 1975). Fish were regularly fed with rice bran and one day prior to the experimentation feeding was stopped. Fish were exposed to sub-lethal ($1/10^{th}$ of 96 h LC_{50} value 0.0376 mg^{-1}) and lethal (96 h LC_{50} value 0.376 mg^{-1}) concentrations of Cartap hydrochloride for 24,48,72 and 96 hrs. The samples for estimation of oxygen consumption were taken from the respiratory chamber, at alternate hours of intervals for 24hours. The amount of dissolved oxygen consumption was calculated per gram body weight per hour. The dissolved oxygen content was estimated by modified Winkler's method as described by Golterman and Clymo (1969). The difference in the dissolved oxygen content between initial and final water samples represents the amount of oxygen consumed by the fish.

Student·s t-test was employed to calculate the significance of the differences between control and experimental means. P values of 0.05 or less were considered statistically significant (Fisher, 1950).

RESULTS

The results of the experimental and control fish values are graphically represented in Figures 1,2,3 and 4 by taking hours of exposure on X axis and the amount of oxygen consumed per gram body weight per hour on Y axis.

In sublethal concentrations of Cartap hydrochloride it was observed that the fish showed increase in oxygen consumption during the initial time of exposure i.e., 0-6 hours in 24 and 48 hour treated fish and 0 to 4 hour in 72 and 96 hour treated fish and a gradual decrease was observed in the subsequent periods of study. The presence of sub

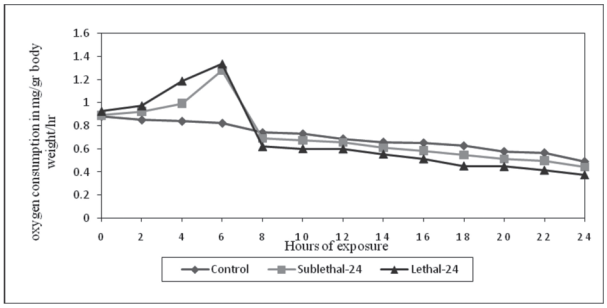


Fig. 1. The amount of oxygen consumed in mg/g body weight/hr of Cirrhinus mrigala exposed to sublethal and lethal concentrations of Cartap hydrochloride for 24 hrs

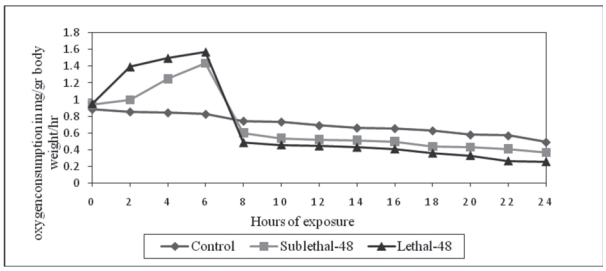


Fig. 2. The amount of oxygen consumed in mg/g body weight/hr of *Cirrhinus mrigala* exposed to sublethal and lethal concentrations of Cartap hydrochloride for 48 hrs.

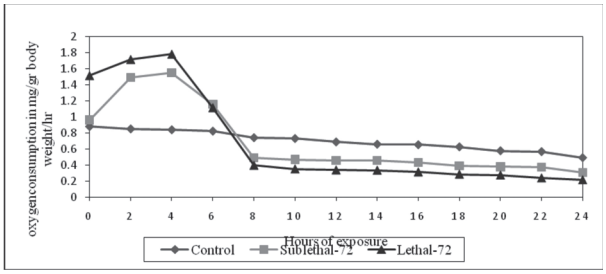


Fig. 3. The amount of oxygen consumed in mg/g body weight/hr of *Cirrhinus mrigala* exposed to sublethal and lethal concentrations of Cartap hydrochloride for 72 hrs.

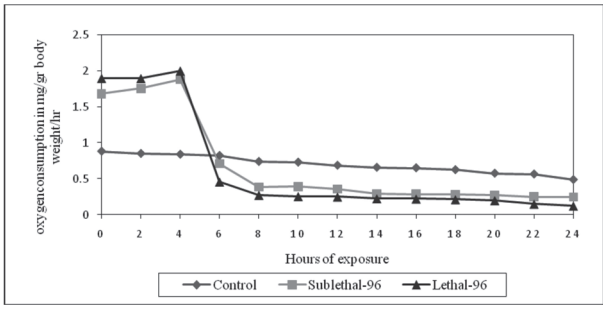


Fig. 4. The amount of oxygen consumed in mg/g body weight/hr of *Cirrhinus mrigala* exposed to sublethal and lethal concentrations of Cartap hydrochloride for 96 hrs.

lethal concentration of toxicants is aquatic environment is inevitable. The toxicant stress on oxygen consumption along with depletion in oxygen in aquaculture practices makes fish less fit and reduces their growth due to lack of proper metabolism (Hyma Ranjani, 2015 and Bantu *et al*., 2017). In lethal concentrations of Cartap hydrochloride it was noticed that a gradual increase in oxygen consumption during the initial time of exposure i.e., 0-6 hours in 24 and 48 hour treated fish and 0 to 4 hour in 72 and 96 hour exposed fish and a gradual decline is observed during the later

periods of study. In control fish the rate of oxygen consumption gradually decreased, and this might be due to starved conditions and the reduced metabolic rates of the starved fish (Anitha, 2015). From the present study it is clear that the Cartap hydrochloride affected oxygen consumption of *Cirrhinus mrigala* under all hours of exposure in both sublethal and lethal concentrations.

DISCUSSION

Several authors reported the effect of carbamate pesticides on the oxygen consumption in fish. Mariya Dasu (2014) observed initial increase in oxygen consumption in *Labeo rohita* exposed to Thiocarb. Anitha (2015) also observed increase in oxygen consumption during the initial time of exposures, i.e. 1 to 6 hours and a gradual decrease was observed during the subsequent period of study in *Labeo rohita* exposed to Pyraclostrobin. In lethal concentrations the rate of oxygen consumption showed a decreasing trend from the beginning to the end. Bantu *et al.,* (2017) observed increase in oxygen consumption during the initial time of exposures i.e., 1 to 4 hours and a gradual decrease during the subsequent ṗeriod in *Labeo rohita* exposed to sublethal concentrations of Indoxacarb for 24hrs and 8 days. Oxygen consumption decreased in *Labeo* during exposure to lethal concentrations of indoxacarb for 24 hours.

The initial increase in oxygen consumption in the present study is in agreement with Neelima *et al.,* (2016) in *Cyprinus carpio* exposed to cypermethrin, Jothinarendiran (2012) in *Channa punctatus* exposed to dimethoate, Bantu *et al.,* (2017) in *Labeo rohita* exposed Indoxacarb, Tilak and Vijaya kumar (2009) in *Channa punctatus* exposed to Quinaphos, Veeraiah (2001) in *Labeo rohita* exposed to Cypermethrin. Hyma Ranjani (2015) in *Catla catla* exposed to Glyphosate. The present work coincides with the report of the same.

The initial increase in oxygen uptake in sublethal concentration might be the reflection of an augmented physiological activity for elimination acting the chemical stress (Tilak and Vijaya kumar, 2009). Due to stress, muscular activity increases which results in an increased demand for oxygen. The increase in activity might boost up oxidative metabolism which results in increased supply of energy to combat the chemical stress (David *et al.,* 2003). Sree Veni and Veeraiah (2014) reported that due to stress there is increased respiratory activity, resulting in increased ventilation and increased uptake of the toxicant in *Cirrhinus mrigala* exposed to cypermethrin.

Several authors (Veenethkumar and David, 2008; Shereena *et al.*, 2009; Logaswamy and Remia, 2009) reported that alteration in whole animal oxygen consumption is due to the disturbance in oxidative metabolism in different species of fish exposed to pesticides. During the initial hours of exposure elevation in the rate of respiration could be explained in terms of acceleration of oxidative metabolism, as a result of sudden response to the toxic stimulus of the pesticide. With the onset of symptoms of poisoning, probably due to acclimatization to the chemical environment the rate decreased in the later periods of exposure. Similar observations were also made by Neelima *et al.,* (2016) and Jothinarendiran (2012). The results of the present study agree with above findings.

As the pesticides stimulate the peripheral nervous system, the activity of fish increases which requires more oxygen to fulfill the energy demand. This could be the reason for initial elevation in the rate of oxygen consumption (Rao, 1989). In sub lethal medium, in the subsequent period of exposure the respiration rate of fish decreased which might be due to acclimatization of the fish in the chemical environment (Rao, 1989 and Neelima *et al.,* 2016). Under toxic conditions, the oxygen in take decreases and a number of poisons become more toxic, so the amount of poison being exposed to the animal also increases. Fish breath more rapidly and the amplitude of respiratory movements will increase (Vakita Venkata Rathnamma and Nagaraju Bantu, 2014). By triggering the process of detoxification, the fish might have overcome the pesticide toxicity.,

In the later period the decrease in oxygen consumption appears to be a protective measure to ensure that there is low intake of the toxic substances which agrees with Tilak and Vijaya Kumar (2009). Subsequent decrease in oxygen consumption may be due to increased entry of Cartap hydrochloride molecules or their accumulation in the body of fish as a function of time. In sub lethal concentrations of the Cartap hydrochloride the decrease in oxygen consumption appears to be mainly due to lowering down of energy requirements which can be considered as adaptive and even strategic which is in accordance with findings of Tilak and Vardhan, (2002). Depletion in the oxygen consumption is due to disorganization of the respiratory action caused by

rupture in the respiratory epithelium of the gill tissue and also secretion of mucus over the gill curtails the diffusion of oxygen (Neelima *et al*., 2016).

Decreased oxygen consumption was observed by Maharajan *et al.,* (2013) in *Catla catla* exposed to Profenofos, by Vakita Venkata Rathnamma and Nagaraju Bantu (2014) in *Labeo rohita* exposed to Chlorantraniliprole, by Jipsa *et al.,* (2014) in *Tilapia mossambica* exposed to Cypermethrin, by Anthony reddy (2015) in *Labeo rohita* exposed to Spinosad. Joshi and Kulkarni (2007) reported that *Garramullya* (Skyes) when exposed to Cypermethrin and Fenevelerate, oxygen consumption increased in the initial period in both lethal and sublethal concentrations and thereafter decreased. They concluded that alteration in oxygen consumption increased and later decreased which is a bioindicator for assessing the pesticide toxicity, which can be correlated with the present study.

From the above results and discussion, it can be concluded that decrease in oxygen consumption in fish in response to the toxic stress is the cumulative effect of several stages at which the toxicant act. From the results obtained, it is clearly evident that Cartap hydrochloride affect the oxygen consumption of *Cirrhinus mrigala* in all exposed concentrations.

CONCLUSION

In conclusion, the analysis of data from the present investigation demonstrated that Cartap hydrochloride had a profound impact on respiration in *Cirrhinus mrigala* in both sublethal and lethal concentrations. Variation in the oxygen consumption in Cartap hydrochloride exposed fish was probably due to impaired oxidative metabolism and pesticide induced stress. Changes in gill architecture under Cartap hydrochloride stress would alter the diffusing capacity of gill with consequent hypoxic or anoxic conditions thus, respiration may become a problematic task for the fish. These results suggest that the altered rates of respiration in *Cirrhinus mrigala* may also serve as a rapid biological monitor to assess the impact of pesticides such as Cartap hydrochloride on other biotic communities in the water body. This study also stresses the diligent use of pesticides to prevent environmental pollution.

ACKNOWLEDGEMENTS

The authors are thankful to the UGC SAP-DRS-III for extending the infrastructure facilities to carry out the present work in the laboratories of the Dept. of Zoology & Aquaculture and also thank the Head, Department of Zoology and Aquaculture for permitting to do the work.

REFERENCES

Anon. 1975. Committee on methods of toxicity tests with fish macro invertebrates and amphibians. EPA, Oregon, 61.

Anitha, A. 2015. Pyraclostrobin (20% WG) induced toxicity and biochemical aspects of freshwater fish *Labeo rohita* (Hamilton) Ph.D. Thesis, Acharya Nagarjuna University. Nagarjuna Nagar, Guntur, A.P, India.

Anthony Reddy, P. 2015. *Impact of Spinosad (45% SC, Tracer) a biopesticide compound on freshwater fish, Labeo rohita* (*Hamilton*) Ph.D. Thesis, Acharya Nagarjuna University, Nagarjuna Nagar, Guntur, A.P, India.

Bantu, N., Hagos, Z., Krishna, C., Goplakrishnan, Abaynew, Rathnamma and Ravibabu, 2017. Acute toxicity and respiratory responses in freshwater fish, *Labeo rohita* exposed to an agrochemical Indoxacarb. *Algerian Journal of Environmental Science and Technology*. 3(3-B) : 595-603.

David, M., Shivakumar, H.B., Shivakumar, R. Mushigeri, S.B. and Ganti, B.H. 2003. Toxicity evaluation of cypermethrin and its effect on oxygen consumption of the freshwater fish , *Tilapia mossambica*, *Indian J. of Environ. Toxicol.*13: 99-102.

Fisher, R.A. 1950. *Statistical Methods for Research Workers,* 11th edition, (Edinburgh UK: Oliver and Boyd Ltd.).

Ganeshwade, R.M. 2012. Histopathological changes in the gills of *Puntius Ticto* (Ham) under dimethoate toxicity. *The BioScan*. 7(3) : 423-426.

Golterman, H. and Clymo, 1969. *Methods for Chemical Analysis of Fresh Water.* Black well Scientific Publication, 166.

Hyma Ranjani, G. 2015. *Glyphosate (Glycil 41% SL) a systemic herbicide impact on biochemical and histopathological changes in the freshwater fish Catla catla (Hamilton)*. Ph. D. Thesis, Acharya Nagarjuna University. Nagarjuna Nagar, Guntur, A.P, India.

Jabeen, F., Chaudhry, A.S., Manzoor, S. and Shaheen, T. 2016. Carbamates and neonicotenoids in Fish, water and sediments from the Indus River for potential health risks. *Environ. Monit. Assess*. 187 (2): 29.

Jipsa, J.R., Kalavathi, R., Dhanya, P.Y. and Logaswamy, S. 2014. Studies on the impact of a Cypermethrin insecticide on oxygen consumption and certain biochemical constituents of a fish *Tilapia mossambica. International Journal of Fisheries and*

Aquatic Studies. 1(5) : 93-97.

Job, S.V. 1955. The oxygen consumption of *Salvelinus fontinalis*. Univ. Toronto Biol. Ser. No. 61; *Ont. Fish. Res. Lab. Publ*. 73 : 1-39.

Joshi, P.P. and Kulkarni, G.K. 2007. Change in the oxygen consumption of a freshwater fish *Garra mulya* (Sykes) exposed to cypermethrin and fenvalerate. *Himalayan J. Environ. Zool.* 21(1): 7-13.

Jothinarendiran, N. 2012. Effect of dimethoate pesticide on oxygen consumption and gill histology of the fish, *Channa punctatus*. *Current Biotica*. 5 (4) : 500-507.

Logaswamy, S. and Remia. K.M. 2009. Impact of Cypermethrin and Ekalux on respiratory and some biochemical activities of a freshwater fish. *Tilapia Mossambica*. *Current Biotica*. 3 : 65-73.

Maharajan.A., Usha, R., Paru Ruckmani, P.S., Vijaykumar, B.S., Ganapiriya, V. and Kumarasamy, P.2013. Sublethal effect of Profenofos on oxygen consumption and gill histopathology of the Indian major carp, *Catla catla* (Hamilton). *Int. J. Pure Appl. Zool*. 1 (1) : 196-204.

Mariya Dasu, P. 2014. Thiodicarb 75 percentage wp a carbamate insecticide induced toxicity biochemical and histopathological changes in the freshwater Indian major carp *Labeo rohita* Hamilton, Ph.D. Thesis, Açharya Nagarjuna University, Nagarjuna Nagar, Guntur, A.P, India.

Neelima, P., Gopala Rao, N., Srinivasa Rao, G. and Chandra Sekhara Rao, J. 2016. A study on oxygen consumption in a freshwater fish *Cyprinus carpio* exposed to lethal and sublethal concentrations of cypermethrin (25% EC). *Int. J. Curr. Microbiol. App. Sci*. 5 (4) : 338-346.

Rao, D.M.R. 1989. Studies on the relative toxicity of Endosulphan to the Indian major carps *Catla catla* with special reference to some biochemical changes induced by the pesticide. *Pest. Biol. Phy*. 33 : 220-229.

Sree Veni, S.M. and Veeraiah, K. 2014. Effect of Cypermethrin (10%EC) on Oxygen Consumption and Histopathology of Freshwater Fish *Cirrhinus mrigala* (Hamilton). *IOSR J. Environ. Sci., Toxicol. Food Technol*. 8(10): 12-20.

Shereena, K.M., Logaswamy, S. and Sunitha, P. 2009. Effect of an organo phosphorous pesticides (Dimethoate) on oxygen consumption of the fish *Tilapia Mossambica*. *Recent Res. Sci. Technol*. 1: 4-7.

Subramani Lavanya, Mathan Ramesh, Chokkalingam Kavitha and Annamalai Malarvizhi, 2011. Hematological, biochemical and ion regulatory responses of Indian major carp *Catla catla*during chronic sublethal exposure to inorganic arsenic. *Chemosphere*. 82 : 977-985.

Tilak, K.S. and Vardhan, S.K. 2002. Effect of fenvalerate on oxygen consumption and hematological parameters in the fish. *Channa punctatus* (Bloch). *J. Aquatic Biol*. 17 : 81-86.

Tilak, K. S. and Vijaya Kumar, M. 2009. Effect of Quinaphos technical grade and commercial grade (25%EC) formulations on oxygen consumption in freshwater fish *Channa punctatus* (Bloch). *ANU Journal of Natural Sciences*: 39-45.

Vakita Venkata Rathnamma and Nagaraju Bantu. 2014. The effect of Chlorantraniliprole on the oxygen consumption of the freshwater fish *Labeo rohita* (Hamilton). *Frontiers of Biological and Life Sciences*. 5-7.

Veeraiah, K. and Durga Prasad, M. K. 2001. Studies on ventilatory patterns of fish under normal and stressed conditions using indigenously designed electronic recording instrument. *Proc. Intern. Conf. ICIPACT* -2001.

Vineetkumar, K. Patil and David, M. 2008. Behavior and respiratory dysfunction as an index of Malathion toxicity in the freshwater fish. *Labeo rohita* (Hamilton). *Turkish Journal of Fisheries and Aquatic Sciences*. 8 : 233-237.

Eco. Env. & Cons. 26 (August Suppl. Issue) : 2020; pp. (S127-S131)
Copyright@ EM International
ISSN 0971–765X

Effect of Cartap hydrochloride (50% SP) insecticide on gill histology of the fish, *Cirrhinus mrigala* (Hamilton)

G. Vani[1]*, K. Veeraiah [2], M. Vijaya Kumar[1] and S.K. Parveen[1]

[1]Department of Zoology, SRR & CVR Government Degree College (A), Vijayawada 520 004, Krishna District, A.P., India
[2]Department of Zoology and Aquaculture, Acharya Nagarjuna University, Nagarjunanagar 522 510, Guntur, A.P., India

Received 26 October, 2019; accepted 3 February, 2020)

ABSTRACT

The fish, *Cirrhinus mrigala,* Indian major carp was exposed to Cartap hydrochloride and the static LC_{50}values for 24,48,72 and 96 hours were found to be 0.436, 0.419, 0.394 and 0.376 mg^{-1} and 0.399, 0.371, 0.361 and 0.339 mg^{-1} in Continuous flow-through system. The gills which are the primary organs to get exposed to foreign contaminants and pesticides were studied for histological changes. The following histological changes like epithelial lifting, degeneration of primary and secondary gill lamellae, curling of secondary gill filaments, atrophy of secondary gill lamellae, congestion of secondary lamellae, fusion of secondary gill filaments were observed. The results obtained were discussed at length with the available literature. By studying the histological deformities, it was concluded that the pesticide caused enough damage to the gills of the fish and can influence on the survival of the fish

Key words : *Cartap hydrochloride, Cirrhinus mrigala, Gill histopathology*

Introduction

Indiscriminate and extensive use of pesticides in modern agricultural practices globally for achieving increased food production is one of the major sources of water pollution. Presence of pesticide in aquatic bodies is largely due to outfall from pesticide manufacturing factories and the runoff from agricultural fields (Ganeshwade, 2012). Pesticides are not highly selective but are generally toxic to macrophytes, non-target organisms such as fish (Ayoola, 2008 and Franklin *et al*., 2010).

Fish accumulate these pollutants directly or indirectly from polluted waters and food chain (Jabeen *et al*., 2016). In India, Cartap hydrochloride, a carbamate pesticide is extensively used in rice, sugarcane cabbage and cauliflower crops to control pests. In fish, the gill is the major organ for respiration, excretion and osmotic regulation. Gills are appropriate for the assessment of environmental impact as they are considered as a good tissue indicator of the water quality (Fanta, 2003). Histopathological analysis is a very sensitive parameter and is helpful in determining cellular damage that may occur in target organs (Altinok and Capkin, 2007). In this viewpoint an attempt was made to study the effect of sublethal and lethal concentrations of Cartap hydrochloride on gill histopathology of freshwater fish, *Cirrhinus mrigala* exposed for 24 and 96 hours.

Materials and Methods

The fingerlings of the test fish *Cirrhinus mrigala* of size 6-8 ± ½ cm and weight 6-7 ± ½ gm were pro-

cured from local fish hatcheries of Nandivelugu, Tenali mandal, Guntur district, Andhra Pradesh. The fish were acclimated at (28±2°C)) in the laboratory conditions for two weeks. All the precautions laid down on recommendations of the toxicity tests to aquatic organisms were followed (Annon, 1975). Fish were regularly fed with rice bran and one day prior to the experimentation feeding was stopped. Fingerlings were exposed to sub-lethal ($1/10^{th}$ of 96 h LC_{50} value 0.0376 mg^{-1}) and lethal (96 hours LC_{50} value 0.376 mg^{-1}) concentrations of Cartap hydrochloride for 24 and 96 hrs.

Gills were processed in laboratory for routine histological characterization by the double staining method using Haematoxylene and Eosin. All samples were fixed in 10% phosphate- buffered formalin for about 24 hrs. The specimens were dehydrated in a series of graded ethanol (50%, 70% and 90%) and then after embedded in paraffin. Five-micron sections were cut using an ultramicrotome (Leica, Japan) and deparaffinized by means of xylol. The sections were dehydrated in 90%, 70% and 50% ethanol followed by a 10 min wash in water and further stained with Hematoxylin and Eosin (HE). Sections were observed in digital microscope (Intel Play QX3) at 400 x magnification.

Results

The transverse section of gill tissue of normal fish shows branches from the central axis called the primary gill lamellae. Each of the primary gill lamella further divides into secondary gill lamellae or filaments. Within each division of the gills are the adjacent afferent vessels and efferent vessels with hemocytes. A thin septum separates the primary and secondary gill filaments. The secondary non branching filament lamella possesses epithelial pillar cells separated by large lacunae Fig. 1.

Cartap hydrochloride has induced marked pathological changes in gills of fish *Cirrhinus mrigala*. In the current study, it was observed that with the increase in the time of exposure the histopathological alterations increased in the gills of fish, *Cirrhinus mrigala*.

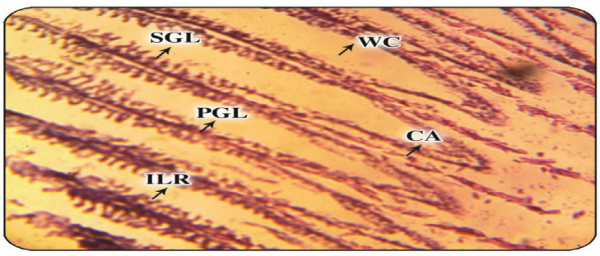


Fig. 1. Normal Gill tissue of *Cirrhinus mrigala*, H.E x 400

CA-Central Axis, PGL-Primary gill lamellae, SGL-Secondary gill lamellae, ILR-Inter lamellar space, WC-Water channel, FSG-Fusion of secondary lamellae, CSG-Curling of secondary lamellae, DPGL-Degenerated primary gill lamellae, DSGL-Degenerated secondary gill lamellae, BC-Blood congestion, EL-Epithelial lifting, LF-Lamellar fusion, ASL-Atrophy of secondary lamellae.

In the control group, no pathological changes were observed in the gills (Fig.1). After treatment with cartap hydrochloride for 24hrs at sublethal concentrationsepithelial lifting,curling of secondary gill filaments,fusion of secondary lamellae and degeneration of secondary gill lamellaestarted to appear (Fig. 2). Degenerative changes like lamellar fusion, epithelial lifting, degenerative secondary gill lamellae and curling of secondary gill filaments were observed after exposure to lethal concentration for 24hrs (Fig. 3). Similar more pronounced degenerative changes like curling of secondary gill filaments, epithelial lifting, degenerative primary and secondary gill lamellae, blood congestion, atrophy of secondary lamellae, mucous secretionwere no-

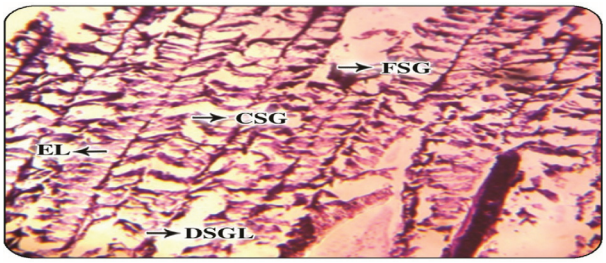


Fig. 2. Gill tissue of *Cirrhinus mrigala*exposed to sublethal concentration of Cartap hydrochloride for 24 hours, H.E x 400

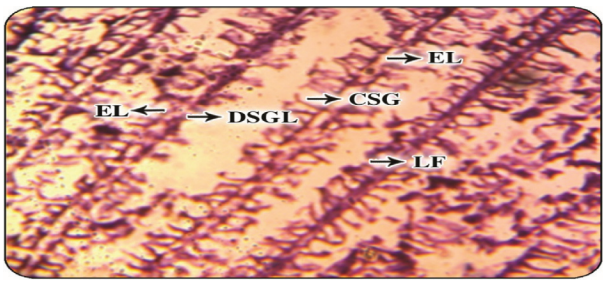


Fig. 3. Gill tissue of *Cirrhinus mrigala* exposed to lethal concentration of Cartap hydrochloride for 24 hours, H.E x 400

ticed in gill exposed to sublethal concentration of cartap hydrochloride for 96 hrs (Fig. 4). Damage in the gills exposed to lethal concentration of cartap hydrochloride for 96 hrs was much extensive with severe degeneration in primary and secondary gill lamellae, hemorrhage between gill filaments, separation of epithelial cells from the basement membrane, collapsed pillar cell, fusion of secondary gill lamellae, lamellar disorganization, atrophy of secondary lamellae, necrosis, blood congestion, mucous secretion, hyperplasia and epithelial lifting (Fig. 5). Thus, the lethal concentration of Cartap hydrochloride has produced significant histopathological changes in comparison to sublethal concentration in *Cirrhinus mrigala*.

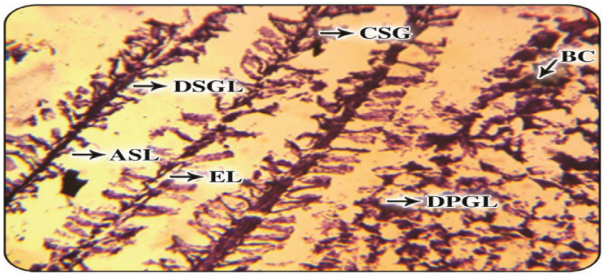


Fig. 4. Gill tissue of *Cirrhinus mrigala* exposed to sublethal concentration of cartap hydrochloride for 96 hours, H.E x 400

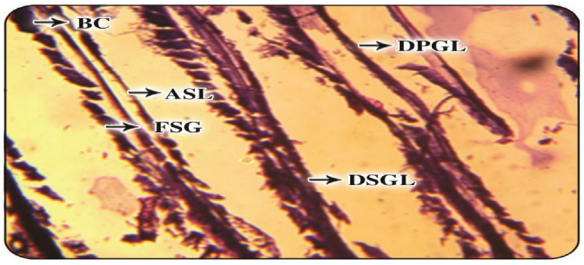


Fig. 5. Gill tissue of *Cirrhinus mrigala* exposed to lethal concentration of cartap hydrochloride for 96 hours, H.E x 400

Discussion

Several authors observed similar degenerative changes in gill when exposed to carbamate pesticides. Vivek *et al.*, (2016) observed fusion of primary and secondary lamellae, epithelial hyperplasia, curling of secondary lamellae, degeneration of lamellae in gills of *Labeo rohita* exposed to sublethal concentrations of cartap hydrochloride for 24,48,72 and 96hrs. Mariya dasu (2014) observed bulging of tips of primary gill filaments, curling of secondary gill filaments, necrosis, fusion of secondary gill lamellae, hyperplasia, hypertrophy of nuclei, pyknotic nuclei, lifting of epithelium in *Labeo rohita* exposed to Thiocarb, a thiocarbamate pesticide in both sublethal and lethal concentrations. Anitha (2015) observed necrosis, curling and fusion of secondary gill filaments, atrophy, degeneration of primary and secondary gill lamella, blood conjunction, epithelial hyperplasia, lamellar telangiectesis, in gills of *Labeo rohita* exposed to sublethal concentrations of Pyraclostrobin for 24 hrs, 5 days and 10 days and to lethal concentration for 24 hrs. Ali Taheri Mirghaed *et al*., (2018) noticed edema, lamellar curling, hyperplasia, lamellar fusion in the gill of *Cyprinus carpio* treated with 0.75 mg/L, 1.5 mg/L, and 3 mg/Lof indoxacarb for 7, 14 and 21 days. The histopathological changes observed in the present study were in accordance with the above studies.

Similar histopathological changes in gills were reported in *Channa punctatus* exposed to Imidacloprid (Pawara *et al.,* 2019), in *Labeo rohita* exposed to phenol (Butchiram *et al.,* 2013), in *Labeo rohita* exposed to cadmium (Saravanan *et al*., 2019), in *Oreochromis niloticus*exposed to heavy metals (Shameem Rani, 2018), in *Labeo rohita* exposed to tannery industrial effluent (Diana Handa and Gurinder Kaur Walia, 2019), in *Puntius sophore* treated with Acephate (Gavit and Patil, 2019), *in Cirrhinus mrigala* exposed to cement factory effluent (Juginu and Sujila, 2019) in *Cirrhinus mrigala*exposed to lead arsenate (Vanitha *et al.,* 2017), in *Labeo rohita* exposed to dimethoate (Dey and Saha, 2014), In *Cirrhinus mrigala* exposed to cypermythrin (Sree Veni and Veeraiah, 2014).

In fish, gill is the major organ for respiration, excretion and osmotic regulation. Gills are appropriate for the assessment of environmental impact as they are considered as a good tissue indicator of the water quality (Fanta, 2003). The lifting of lamellar epithelium in the present studymay be induced by the incidence of severe Oedema (Pane *et al.,* 2004). Swelling in gill epithelium leads to decreased efficiency of gases exchange and oxygen consumption. (Sudhasaravanan and Binukumari, 2015).

The first line of defense to metal/ toxicant exposure in the gills is mucus secretion and by fusion of lamellae it can temporarily protect the underlying epithelium from injury (Handy and Maunder, 2009). Pronounced secretion of mucus layer over the gill lamellae curtails the diffusion of oxygen (David *et al.*, 2002 and Rudragouda Marigoudar *et al*., 2009) which may ultimately reduce the oxygen consump-

tion by the animal (Kalavathy *et al*., 2001). All metabolic pathways depend upon the efficiency of the gills for their energy supply as gills are the major respiratory organs and damage to these vital organs lead to respiratory distress. The present histological studies clearly indicate that the damage in gills of *Cirrhinus mrigala* decreases the uptake of oxygen which results in histotoxic anoxia. Due to this the gill tissue suffers from oxygen debt and losses the capacity to remove CO_2 from blood which is in accordance with (Sathivel *et al*., 1991).

In the present study the observed alterations such as partial fusion of secondary lamellae, lifting of epithelial cells and proliferation of the epithelial cells, act as defense mechanisms towards toxicants. These alterations increase the distance between the external environment and the blood in the gills which serves as a barrier for the entry of contaminants. (Fernandes and Mazon, 2003 and Mallatt, 1985). When any type of toxicants meets gills, lamellar fusion in gills occur which is a protective measure as it diminishes the amount of vulnerable gill surface area in fish (Mallatt, 1985). when gills come in contact withany types of toxicants oedema appears to be a common feature of the gill pathology. Due to disturbance in branchial Na+, K+-ATPase pump by toxicants, solute accumulation in the epithelial cells occur and disturb the osmotic influx of water. This exchange protects the lamellar epithelial cells and prevents the entry of waterborne pollutants into the bloodstream (Arellano *et al*., 1999).

Conclusion

The results of the present study suggest that the changes in gill histomorphology of *Cirrhinus mrigala* may serve as a rapid biological 7monitor to assess the impact of Cartap hydrochloride on other biotic communities in the water body. The results of the present study also stress on the diligent usage of the pesticide product to prevent the environmental pollution.

Acknowledgements

The authors are thankful to the UGC SAP-DRS-III for extending the infrastructure facilities to carry out the present work in the Laboratories of the Dept. of Zoology & Aquaculture. They also thank the Head, Department of Zoology and Aquaculture for permitting to do the work.

References

Ali Taheri Mirghaed., Melika Ghelichpour., Seyed Saeed Mirzargar., Hamidreza Joshaghani. and Hoseinali Ebrahimzadeh Mousavi, 2018. Toxic effects of indoxacarb on gill and kidney histopathology and biochemical indicators in common carp (*Cyprinus carpio*). *Aquaculture Research*. 49(4) : 616-1627.

Altinok, I. and Capkin, E. 2007. Histopathology of rainbow trout exposed to sublethal concentrations of methiocarb or endosulfan. *Toxicol Pathol*. 35 : 405–10.

Anitha, A. 2015. *Pyraclostrobin (20%WG) induced toxicity and biochemical aspects of freshwater fish Labeo rohita* (Hamilton) Ph.D. Acharya Nagarjuna University. Nagarjuna Nagar, Guntur, A.P, India.

Annon, 1975. Committee on methods of toxicity tests with fish macro invertebrates and amphibians. EPA. Oregon: 61.

Arellano, J. M., Storch, V. and Sarasquete, C. 1999. Histological changes and copper accumulation in liver and gills of the *Senegales sole, Solea senegalensis. Ecotoxicology and Environmental Safety*. 44 : 62-72.

Ayoola, S.O. 2008. Toxicity of glyphosate herbicide on Nile tilapia (*Oreochromis niloticus*) juvenile. *Afr. J. Agric. Res*. 3 (12): 825-834.

Butchiram, M.S., Vijaya Kumar, M. and Tilak, K.S. 2013. Studies on the histopathological changes in selected tissues of fish *Labeo rohita* exposed to phenol. *Journal of Environmental Biology*. 34: 247-51.

David, M., Mushigari, S. B. and Prashanth, M. S. 2002. Toxicity of fenvalerate to the freshwater fish. *Labeo rohita. Geobios*. 29 : 25-28.

Dey Chandrimaand Saha Samir Kumar, 2014. Dimethoate (30% EC) induced toxicities on the tissues of the Indian major carp: *Labeo rohita* (Hamilton). *International Journal of Fisheries and Aquatic Studies*. 1(6) : 232-236.

Diana Handa. and Gurinder Kaur Walia. 2019.Quantitative and Semi-quantitative analysis on Gills of a freshwater fish, *Labeo rohita* (Hamilton-Buchanan, 1822) exposed to Tannery industrial effluent using histopathology as biomarker. *IJRAR*. 6(1): 980-981.

Fanta, E., Rios, F.S., Romao, S., Vianna, A.C.C. and Freiberger, S. 2003. Histopathology of the fish *Corydoras paleatus* contaminated with sublethal levels of organophosphorus in water and food. *Ecotoxicology and Environmental Safety*. 54(2) : 119-130.

Fernandes, M.N. and Mazon, A.F. 2003. Environmental Pollution and Fish Gill Morphology. In: Val, A.L. and Kapoor, B.G., Eds., Fish Adaptation. Science Publishers, Enfield: 203-231.

Franklin R. K., Loo, H. S. and Osumanu, H. A. 2010.Incorporation of Bentazone with Exserohilumrostratum for Controlling *Cyperusiria. Am. J. Agri. Biol. Sci*. 5: 210-214.

Gavit, P. J. and Patil, R. D. 2019. Effect of Acephate (Organophosphate) on Gill Histology of the Fresh Water Fish *Puntius sophore* (Hamilton). *IJRAR*. 6(1): 338-342.

Ganeshwade, R.M. 2012. Histopathological changes in the gills of *Puntius Ticto* (Ham) under dimethoate toxicity. *The BioScan*.7(3) : 423-426.

Handy, R. D. and Maunder, R. J. 2009. The biological roles of mucus: Importance for osmoregulation and osmoregulatory disorders of fish health. In: *Osmoregulation and Ion Transport: Integrating Physiological, Molecular and Environmental Aspects*. Society for Experimental Biology Press, London. I: 203- 235.

Jabeen, F., Chaudhry, A.S., Manzoor, S. and Shaheen, T. 2016. Carbamates and neonicotenoids in Fish, water and sediments from the Indus River for potential health risks. *Environ. Monit. Assess*. 187 (2) : 29.

Juginu, M. S. and Sujila, T. 2019. Histopathological responses of gill, liver and kidney in the freshwater fish, *Cyrrhinus mrigala* exposed to cement factory effluent. *Wjpps*. 8 (8) : 1511-1530.

Kalavathy, K., Siva Kumar, A.A. and Chandran, R. 2001. Toxic effects of the pesticide dimethoate on the fish, *Sarotherodon mossambicus*. *J. Ecol. Res Bio*. 2 : 27-32.

Mallatt, J. 1985. Fish gill structural changes induced by toxicants and other irritants: a statistical review. *Canadian Journal of Fisheries and Aquatic Science*. 42(4): 630-648.

Mariya Dasu, P. 2014. *Thiocarb 75 percentage WP a carbamate insecticide induced toxicity biochemical and histopathological changes in the freshwater Indian major carp Labeo rohita* Hamilton, Ph.D. Thesis, Acharya Nagarjuna University, Nagarjuna Nagar, Guntur, A.P, India.

Pane, E.F., Haque, A. and Wood, C.M. 2004. Mechanistic analysis of acute, induced respiratory toxicity in the rainbow trout, *Oncorhynchus mykiss*: an exclusively branchial phenomenon. *Aquatic Toxicology*. 69 : 11-24.

Pawara., Ravindra, H., Patel Nisar, G. and Sarvade Raju, C. 2019.Study on the effect of Imidacloprid on gill tissue of the fish *Channa punctatus* (Perciformes: Channidae) (Bloch.). *IJRAR*. 6 (1): 372-378.

Rudragouda Marigoudar, S., Nazeer Ahmed, R. and David, M. 2009. Cypermethrin induced respiratory and behavioral responses of the freshwater teleost, *Labeo rohita* (Hamilton). *Veterinarski Arhive*. 79(6): 583-590.

Sakthivel., Sampath, K. and Pandian, T.J. 1991. Sublethal effects of textile dye stuff effluent on selected oxidative enzymes and tissue respiration of *Cyprinus carpio* (Linn). *Indian J. Expt. Biol*. 29 : 979-981.

Saravanan, K., Mohanambal, R. and Iyyappan, A. 2019. Effect of cadmium on the histology of gill, liver and hepatopancreas of freshwater fish *Labeo rohita* (Hamilton, 1822). *IJRAR*. 6 (1) : 1255-1263.

Shameem Rani, K. 2018. Histological studies and heavy metal accumulation in the gills and muscles of tilapia fish from Vellar estuary, South East Coast of India, Tamilnadu. *IJRAR*. 5(3) : 298-304.

Sree Veni, S.M. and Veeraiah, K. 2014. Effect of Cypermethrin (10%EC) on Oxygen Consumption and Histopathology of Freshwater Fish *Cirrhinus mrigala*(Hamilton). *IOSR J. Environ. Sci., Toxicol. Food Technol*. 8(10) : 12–20.

Sudhasaravanan, R. and Binukumari, S. 2015. Effects of different concentartions of detergent on dissolved oxygen consumption in *Lepidocephalichythyes thermalis*. *World Journal of Pharmaceutical Research.* (2): 940-945.

Vanitha, S., Amsath,A., Shanthi,P. and Muthukumaravel, K. 2017. Sublethal effects of lead Arsenate on histology of selected organs of freshwater fish, *Cirrhinus mrigala*. *International Journal of Zoology and Applied Biosciences*. 2(5): 250-257.

Vivek, Ch., Veeraiah, K., Padmavathi, P. Dhilleswara Rao, H. and Bramhachari, P.V. 2016. Acute toxicity and residue analysis of cartap hydrochloride pesticide: Toxicological implications on the fingerlings of freshwater fish *Labeo rohita*. *Biocatalysis and Agricultural Biotechnology*. 7 : 193-201.

Nature Environment and Pollution Technology
An International Quarterly Scientific Journal

p-ISSN: 0972-6268
(Print copies up to 2016)
e-ISSN: 2395-3454

Vol. 19 | No. 5 (Suppl) | pp. 1821-1829 | 2020

Original Research Paper

https://doi.org/10.46488/NEPT.2020.v19i05.005

Open Access Journal

Biochemical Changes Induced by Cartap Hydrochloride (50% SP), Carbamate Insecticide in Freshwater Fish *Cirrhinus mrigala* (Hamilton, 1822)

G. Vani*†, K. Veeraiah, M. Vijaya Kumar*, Sk. Parveen* and G.D.V. Prasad Rao*****

*Department of Zoology, SRR & CVR Government Degree College (A), Vijayawada, Andhra Pradesh, India

**Department of Zoology and Aquaculture, Acharya Nagarjuna University, Nagarjunanagar-522 510, Guntur, Andhra Pradesh, India

***Department of Zoology SGS College, Jaggaiahpet, Andhra Pradesh, India

†Corresponding author: G. Vani; gandhamvanipradeep@gmail.com

Nat. Env. & Poll. Tech.
Website: www.neptjournal.com

Received: 08-11-2019
Revised: 25-11-2019
Accepted: 03-01-2020

Key Words:
Cartap hydrochloride
Cirrhinus mrigala
LC_{50}
Glycogen
Total proteins
Nucleic acids

ABSTRACT

The freshwater fish *Cirrhinus mrigala* was exposed to Cartap hydrochloride (50% SP) for 24, 48, 72 and 96 h. The LC_{50} values were found to be 0.436, 0.419, 0.394 and 0.376 mg^{-1} in static method and 0.399, 0.371, 0.361 and 0.339 $mg.L^{-1}$ in continuous flow-through system. The static LC_{50} values are higher than the continuous flow-through method. The LC_{50} values showed a decreasing trend with an increase in time of exposure in both the methods. The decrease was more in a continuous flow-through method than in the static method. The fish were exposed to sub-lethal ($1/10^{th}$ of 96 h LC_{50} value 0.0376 $mg.L^{-1}$) and lethal (96 h LC_{50} value 0.376 $mg.L^{-1}$) concentrations of the pesticide for 24 and 96 hours to study the alterations in glycogen, total proteins and nucleic acids (DNA & RNA) contents of various tissues viz., gill, brain, liver, kidney and muscle. Glycogen, total proteins and nucleic acids (DNA & RNA) content values decreased in all the tissues of exposed fish and the per cent decrease is more apparent in lethal concentrations than in sub-lethal concentrations. From the present study, it can be concluded that Cartap hydrochloride caused a decline in the glycogen, total protein and nucleic acids (DNA, RNA) content in *Cirrhinus mrigala* and the changes are more pronounced in lethal exposure than in sub-lethal exposure.

INTRODUCTION

Indiscriminate use of pesticides is one of the main reasons for the pollution of aquatic ecosystems. These toxic pesticides are causing deleterious effects on aquatic organisms. They are causing stress to aquatic organisms which are reflected as biochemical changes in their body (Mayers 1977). Fish acts as a bioindicator species and can be used for monitoring of water pollution as they accumulate the contaminants from polluted water and diet (Chaudary & Jabeen 2011, Kafilzadeh et al. 2012). Fish accumulate these pollutants directly or indirectly from polluted waters and food chain (Jabeen et al. 2016, Chaudary & Jabeen 2011). Carbamates are extensively used water-soluble pesticides in agricultural practices. In India, Cartap hydrochloride is a Carbamate pesticide which is considered as nereistoxin analog is extensively used in rice and sugarcane crops to control pests. The present investigation is aimed to study the toxic effects of Cartap hydrochloride in sub-lethal and lethal concentrations at 24 and 96 hours of exposure period on glycogen, total protein, DNA and RNA contents of freshwater fish *Cirrhinus mrigala* (Hamilton 1822).

MATERIALS AND METHODS

The fingerlings of the test fish *Cirrhinus mrigala* size 6-8 ± ½ cm and weight 6-7 ± ½ g were procured from local fish hatcheries of Nandivelugu, Tenali Mandal, Guntur district, Andhra Pradesh. The fish were acclimated at (28 ± 2°C)) in the laboratory conditions for two weeks. All the precautions laid down by APHA et al. (1998) were followed. During the acclimation period, the fish were fed with rice bran and groundnut cake. One day before the experimentation feeding was stopped. Cartap hydrochloride (50% SP) commercial grade was purchased from Mangalagiri, Guntur District. The stock solution was prepared with water as a solvent. The acclimatized fish were exposed to static sub-lethal (0.376 $mg.L^{-1}$) and lethal concentrations (3.76 $mg.L^{-1}$) of Cartap hydrochloride (50% SP) for 24 and 96 h. The hydrographical properties of water were estimated by the modified method followed by Golterman & Claimo (1969) method. Finney's probit analysis (Finney 1971) as reported by Roberts % Boyce (1972) was followed to calculate the LC_{50} value. The 95% confidence limits of the LC_{50} values for each test were also calculated for different time periods

by using SPSS software. At the end of the exposure periods, the tissues like gill, brain, liver, kidney and muscle were taken out from exposed and control fish and processed for the estimation of glycogen, total proteins and nucleic acids (DNA & RNA). Glycogen was estimated by the method of Kemp et al. (1954), total protein by Lowry et al. (1951) and DNA and RNA by the methods of Searchy & Maclinnis (1970a & 1970b).

The data obtained in the present work were expressed as means of four observations ± SD (standard deviation) and were statistically analysed using student "t" test (Pillai & Sinha 1968) to compare means of treated data against their controls and the result was considered significant at ($P < 0.05$) level.

RESULTS AND DISCUSSION

Glycogen, total proteins and nucleic acids (DNA & RNA) decreased in various tissues, viz. gill, brain, liver, kidney and muscle of *Cirrhinus mrigala* exposed to sub-lethal and lethal concentrations of cartap hydrochloride for 24 and 96 hours were graphically represented in Fig. 1 to Fig. 8. In exposed fish per cent decrease is more apparent in lethal concentrations than at sub-lethal concentrations.

Glycogen

The changes in glycogen content observed in the various tissues of *Cirrhinus mrigala* after the Cartap hydrochloride exposure along with the control are graphically represented in Fig .1 and Fig. 2.

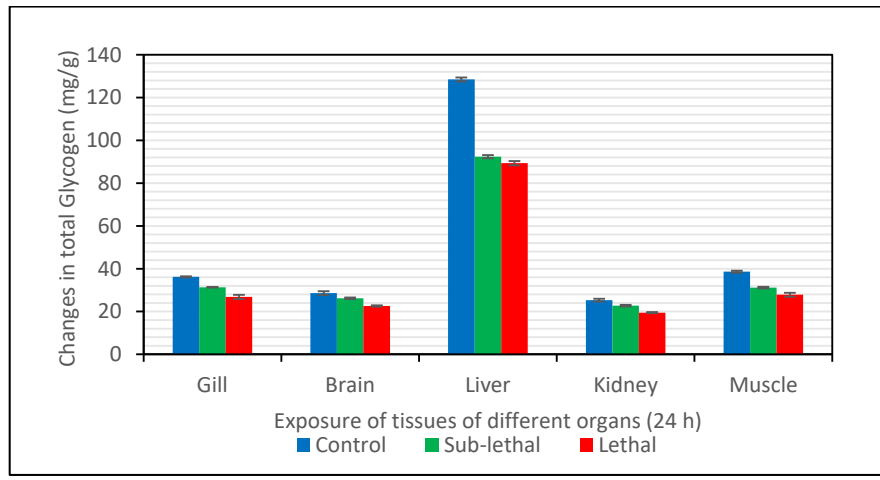


Fig.1: Changes in the glycogen content (mg/g wet weight of the tissue) in the tissue of fish *Cirrhinus mrigala* on exposure to sub-lethal and lethal concentration of Cartap hydrochloride (50%SP) for 24 hours.

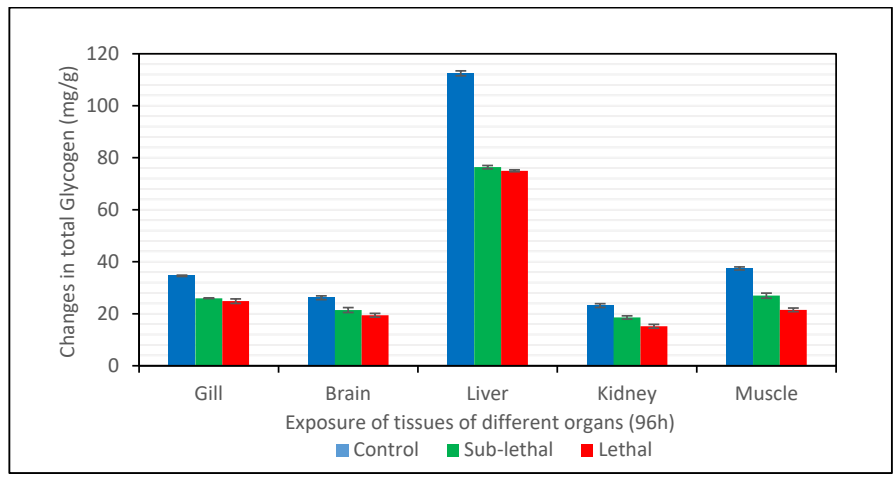


Fig. 2: Changes in the glycogen content (mg/g wet weight of the tissue) in the tissue of fish *Cirrhinus mrigala* on exposure to sub-lethal and lethal concentration of Cartap hydrochloride (50% SP) for 96 hours.

In the tissues of control fish, *Cirrhinus mrigala* glycogen content was in the order of:

Liver > Muscle > Gill > Brain > Kidney

Under exposure to sub-lethal and lethal concentrations of Cartap hydrochloride for 24 and 96 hours, the amount of glycogen was found to decrease in all the tissue of *Cirrhinus mrigala*. The lyotropic gradation series in terms of per cent decrement at 24 h and 96 h exposure was:

Sub-lethal -24 h: Liver > Muscle > Gill > Kidney > Brain

Lethal -24 h: Liver > Muscle > Gill > Kidney > Brain

Sub-lethal 96 h: Liver > Muscle > Gill > Kidney > Brain

Lethal-96 h: Muscle > Kidney > Liver > Gill > Brain

Exposure of *Cirrhinus mrigala* to Cartap hydrochloride for 24 hours caused a maximum decrease of glycogen in the liver (sub-lethal 28.117, lethal 30.453). For 96 h maximum decrease was found in the liver (sub-lethal 32.073) and muscle (lethal 42.570). In the present study under Cartap hydrochloride 24 h sub-lethal and lethal exposure minimum percentage of depletion was in the brain (8.595) and (20.96). For 96 h exposure minimum depletion was found in the brain (sub-lethal 18.056, lethal 25.707).

Srivastava & Singh (2013) observed reduction in glycogen content in different tissues of freshwater fish *Clarius batrachus* exposed to 80% of LC_{50} (22.87 $mg.L^{-1}$) of Mancozeb at different time intervals of 24 and 96 h. Sastry et al. (1982) reported decreased glycogen content of liver and muscles decreased when *Channa punctatus was exposed to* sub-lethal concentration of the carbamate pesticide, Sevin (1.05 $mg.L^{-1}$) for 15, 30 and 60 days. Veeraiah et al. (2013a) observed that exposure to sub-lethal and lethal concentrations of cadmium chloride in the fish *Cirrhinus mrigala* for 96 h caused changes in the total glycogen level which may be attributed to toxic stress, resulting in the disruption of enzymes associated with carbohydrate metabolism. Bantu & Rathnamma (2013) reported that there is a decrease in the amount of glycogen in the fish *Labeo rohita* exposed to sub-lethal and lethal concentrations of Dimethoate for 8 days. Priya et al. (2013) observed depletion of glycogen in the liver of freshwater teleost *Channa punctatus* (Bloch) when exposed to various concentrations of Imidacloprid (0.002 ppm, 0.00 ppm, 0.006 ppm, 0.008 ppm and 0.01 ppm) for 96 h suggesting the possibility of an alter from aerobic to anaerobic mode of energy metabolism of the liver. Dhanalakshmi (2013) noticed decrement in the tissue glycogen concentration in fish *Cirrhinus mrigala* when exposed to 0.25 ppm concentration of the metal chromium sulphate for 24, 48, 72 h and 10, 20 and 30 days which may be due to its enhanced utilization, since glycogen forms the immediate source of energy to meet energy demands under metallic stress caused by test toxicant.

Tataji & Kumar (2016) reported a decline in glycogen content of freshwater fish *Channa punctatus* exposed for 8 days to 1/5th of LC_{50} 96 hours of both Butachlor technical grade and Machete (50% EC), i.e. 32 ppb and 71.2 ppb for both technical and 50% EC respectively. Reduction in glycogen content was also noticed by Naik et al. (2016) in all the tissues of *Labeo rohita* when exposed to sub-lethal concentrations of cypermethrin for 1, 2 and 3 weeks. Exposure of sub-lethal doses (40% and 80 % of LC_{50} of 24 h) of glyphosate for 24 or 96 h against the freshwater non-target fish *Channa punctatus* caused significant ($P < 0.05$) alteration in biochemical parameters in liver and muscle tissues of the fish *Channa punctatus* (Bloch) was reported by Singh et al. (2017). Veeraiah et al. (2018) observed that exposure to lethal and sub-lethal concentrations of cyhalothrin 2.5% EC, in the fish *Ctenopharyngdon idellus* for 24 and 96 hours caused a decrease in glycogen content in all tissues.

According to Dezwaan & Zandee (1973) depletion of glycogen in tissues may be due to direct utilization of the compound for energy generation, a demand caused by pesticide-induced hypoxia. Under hypoxia condition, the fish derives its energy from anaerobic breakdown of glucose which is available to the cell by increased glycogenolysis (Chandravathy & Reddy 1996, Rajamannar & Manohar 1998, Rajamanickam 1992). Reduction in glycogen is probably due to its more rapid break down for energy requirement of fish (Muley et al.1996).

Liver suggested as an organ for detoxification. During exposure to Cartap hydrochloride exposure fishes came under stress condition and need more energy to cope with the toxicants. glycogen serves as reserve material. It is utilized when the body came under stress condition. Depletion of glycogen in liver and tissues may be due to increment in the glycolysis pathway. During stress conditions, the glycogen reserves depleted to meet energy demand (Rawat et al. 2002). Fall in glycogen levels indicates its rapid utilization to meet the enhanced energy demands intoxicant treated animals through glycolysis or hexose monophosphate pathway as observed by Cappon & Nicholas (1975). The above findings support the alterations of glycogen in the present study.

Proteins

The changes in protein content observed in the various tissues of *Cirrhinus mrigala* after Cartap hydrochloride exposure along with the control was graphically represented in Fig. 3 and Fig. 4.

The Protein content in different tissues in control fish *Cirrhinus mrigala* was in the order of:

Muscle > Liver > Brain > Kidney > Gill

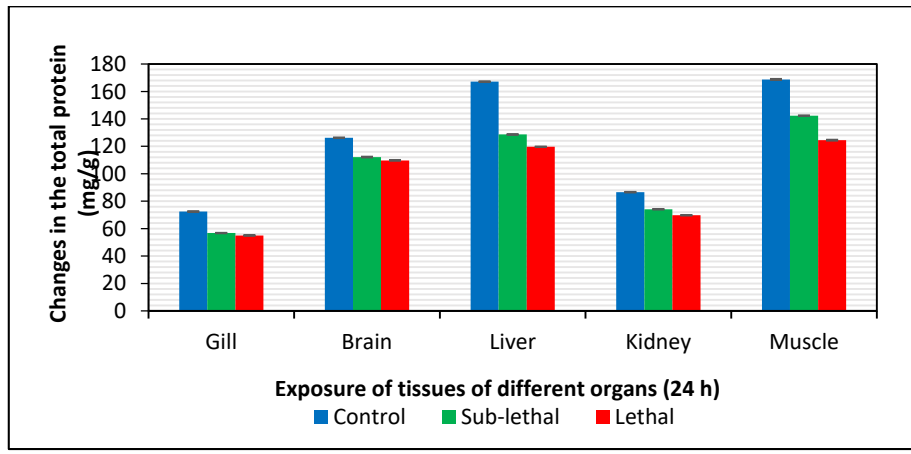


Fig. 3: *Changes* in protein content (mg/g wet wt of the tissue) in different tissues of fish *Cirrhinus mrigala* (Hamilton) on exposure to sub-lethal and lethal concentration of Cartap hydrochloride (50% SP) for 24 hours.

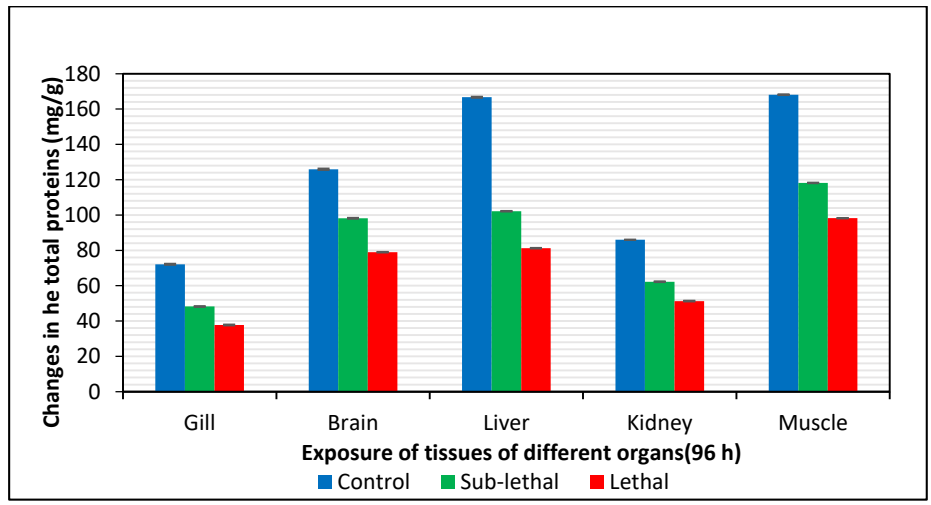


Fig. 4: Changes in protein content (mg/g wet wt of the tissue) in different tissues of fish *Cirrhinus mrigala* (Hamilton) on exposure to sub-lethal and lethal concentration of Cartap hydrochloride (50% SP) for 96hours.

Under exposure of sub-lethal and lethal concentrations of Cartap hydrochloride for 24 h, the amount of protein was found to decrease in all the tissue of *Cirrhinus mrigala.*

The lyotropic gradation series in terms of per cent decrement at 24 h and 96 h exposure was:

Sub-lethal -24 h: Liver > Gill > Muscle > Kidney > Brain

Lethal-24 h- Liver > Muscle > Gill > Kidney > Brain

Sub-lethal -96 h: Liver > Gill > Muscle > Kidney > Brain

Lethal-96 h: Liver > Gill > Muscle > Kidney > Brain

For 24 h exposure maximum per cent of the decrease in total protein was observed in the liver (sub-lethal 23.05, lethal 28.33). For 24 h exposure minimum percentage of depletion of total protein was found in the brain (sub-lethal 11.18, lethal 13.13). For 96 h the percentage of decrease was maximum in the liver (sub-lethal 38.72, lethal 51.27). Similarly, for 96 h minimum percentage of decrease was noticed in the brain (sub-lethal 22.06, lethal 37.30).

Protein is the most primary biochemical ingredient present in large quantities in the body of fish. Liver is rich in protein and centre for various metabolism of the fish. In the present study maximum decrease of total protein in the liver is due to the increased rate of proteolytic activity or repeated break down of protein to yield energy due to stress caused due to pesticide exposure. Anitha & Rathnamma (2016) noticed decreased protein levels in all the tissues like liver, kidney, brain, gill and muscle of *Labeo rohita* exposed to lethal and sub-lethal concentrations of Pyraclostrobin 20%

WG (carbamate) for 24 h and sub-lethal concentrations for 5 and 10 days. A decline in the protein content was noticed by Kumari et al. (2014) in the liver of *Clarias batrachus* when exposed to sub-lethal concentrations (2 and 4 $mg.L^{-1}$) of the Carbaryl for 96 h. A decrease in protein may be due to the impairment of protein synthesis or an increase in the rate of its degradation to amino acids. Exposure to Carbryl for 4 and 24 days, decreased protein content in liver and muscle of fish *Mugil cephalus*, when exposed to the lethal and sub-lethal concentration of Carbaryl for 4 days and 21 days respectively was reported by Shivanagouda et al. (2013). Kumar et al. (2017) reported a reduction in proteins in the liver and kidney of freshwater fish, *Channa punctatus* exposed to different sub-lethal concentrations of pesticide Carbaryl for a period of 15, 30, 45, 60, 75 and up to 90 days. Muddassir (2015) observed significant decrease value in Total protein in the liver of *Channa punctatus* was treated with 0.1 mL Carbofuran and 0.09 mL Malathion pesticides at different time intervals 7, 14, 21 and 28 days. The decrement of total protein may be due to the inhibition of RNA synthesis disturbing the protein metabolism or this may be due to liver damage where most protein synthesis usually occurs, these results agreed with that of Singh & Sharma (1998). The depletion of protein might also be attributed to spontaneous utilization of amino acids in various catabolic reactions inside the organism to combat the stress condition (Borah & Yadav 1996). Wankhedkar & Bhavsar (2015) found that total protein content significantly decreased in foot and hepatopancreas in land snail *C. moussonianus* when treated with Cartap hydrochloride and Imidacloprid at lowest concentration i.e. LC_{50} 0.41ppm and LC_{50} 0.54 ppm respectively. Veeraiah et al. (2018) observed a decrease in protein content in all tissues exposed to lethal and sub-lethal concentrations of cyhalothrin 2.5% EC, in the fish *Ctenopharyngdon idellus* for 24 and 96 h.

Proteins are important organic constituents of the animal cells. Understanding the protein components of the cell becomes necessary in the light of the radical changes taking place in protein profiles during pesticide intoxication (Anitha & Rathnamma 2016). The decreased trend of the protein content as observed in the present study in most of the fish tissues may be due to metabolic utilization of the ketoacids through gluconeogenesis pathway for the synthesis of glucose or due to the directing of free amino acids for the synthesis of necessary proteins, or for the maintenance of osmotic and ionic regulation (Schmidt Neilson 1975).

Nucleic Acids (DNA & RNA)

The changes in DNA content observed in the various tissues of *Cirrhinus mrigala* after the Cartap hydrochloride exposure along with the control was graphically represented in Fig. 5 and Fig. 6.

In control fish, DNA content present in different organs was in the order of:

Muscle > Gill > Brain > Liver > Kidney.

Under exposure to sub-lethal and lethal concentrations of Cartap hydrochloride, for 24 h the amount of DNA was found to decrease in all the tissue of *Cirrhinus mrigala.* The lyotropic gradation series in terms of per cent decrement at 24 h and 96 h exposure was:

Sub-lethal -24 h: Gill > Liver > Muscle > Brain > Kidney

Lethal-24 h-Gill > Liver > Muscle > Brain > Kidney

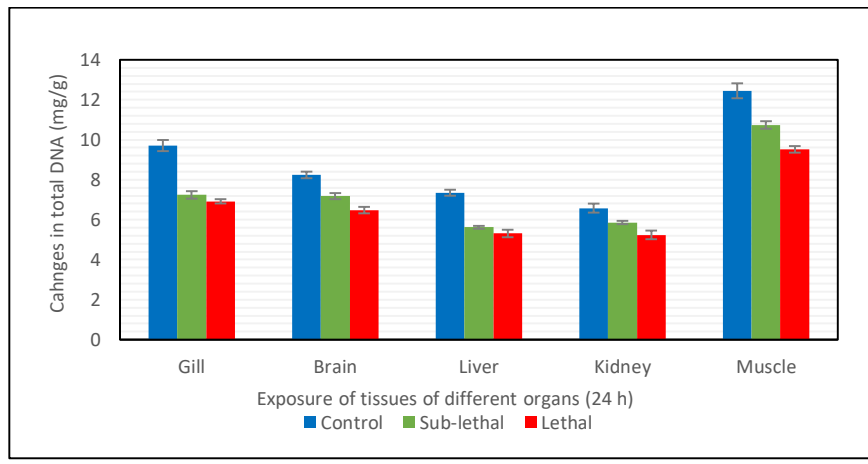


Fig. 5: Changes in the amount of deoxyribonucleic acid (DNA) (mg/g wet weight of the tissue) in different tissues of the fish, *Cirrhinus mrigala* on exposure to sub-lethal and lethal concentration of Cartap hydrochloride (50% SP) for 24 h.

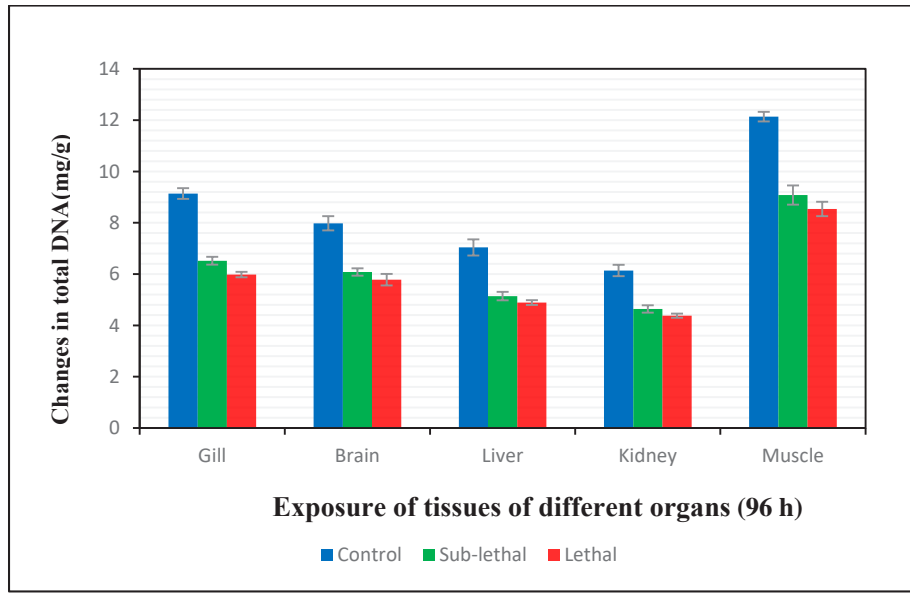


Fig. 6: Changes in the amount of deoxyribonucleic acid (DNA) (mg/g wet wt of the tissue) in different tissues of the fish *Cirrhinus mrigala* on exposure to sub-lethal and lethal concentration of Cartap hydrochloride (50% SP) for 96 h.

Sub-lethal-96 h: Gill > Liver > Muscle > Kidney > Brain

Lethal-96 h: Gill > Liver > Muscle > Kidney > Brain

In the present study under Cartap hydrochloride exposure for 24 h, maximum percentage of depletion in amount of DNA was noticed in Gill (sub-lethal 25.44, lethal 28.74). Minimum percentage of depletion was exhibited in the Kidney (sub-lethal 10.95, lethal 20.37). Under exposure to sub-lethal and lethal concentrations of Cartap hydrochloride for 96 h, maximum percentage of depletion was seen in Gill (sub-lethal 28.67, lethal 34.58) and minimum percentage of depletion was noticed in the brain (sub-lethal 23.81, lethal 27.57).

The changes in RNA content observed in the various tissues of *Cirrhinus mrigala* after Cartap hydrochloride exposure along with the control was graphically represented in Fig. 7 and Fig. 8.

The RNA content in different tissues in control fish *Cirrhinus mrigala* was in the order of:

Muscle > Brain > Gill > Liver > Kidney.

Under exposure to lethal and sub-lethal concentrations of Cartap hydrochloride, for 24 and 96 h, the amount of RNA was found to decrease in all the tissues. The lyotropic gradation series in terms of per cent decrement at 24 h and 96 h exposure was:

Sub-lethal -24h: Muscle > Gill > Kidney > Brain > Liver

Lethal-24h: Muscle > Gill > Kidney > Liver > Brain

Sub-lethal -96h: Gill > Muscle > Kidney > Liver > Brain

Lethal-96h: Gil l > Muscle > Liver > Kidney > Brain

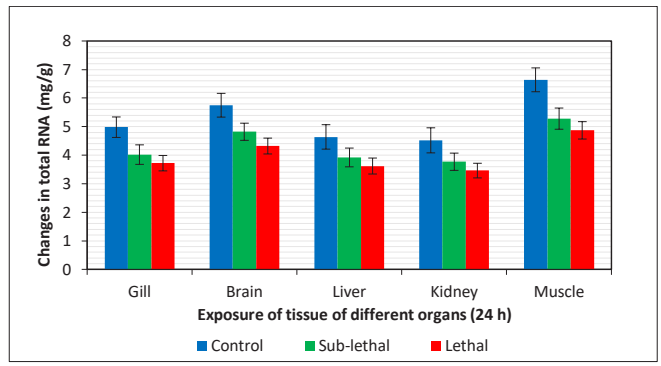


Fig. 7: Changes in the amount of ribonucleic acid (RNA) (mg/g wet wt of the tissue) in different tissues of the fish, *Cirrhinus mrigala* on exposure to sub-lethal and lethal concentration of Cartap hydrochloride (50% SP) for 24 h.

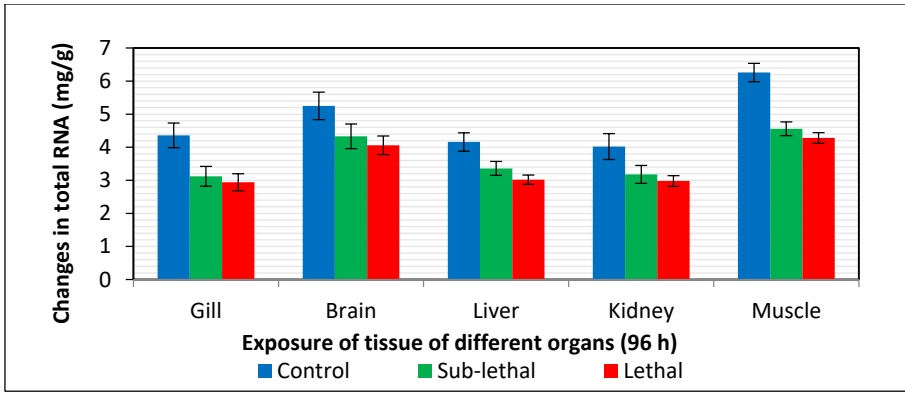


Fig. 8: Changes in the amount of ribonucleic acid (RNA) (mg/gm wet wt of the tissue) in different tissues of the fish, *Cirrhinus mrigala* on exposure to sub-lethal and lethal concentration of Cartap hydrochloride (50% SP) for 96 h.

After 24 h of exposure maximum percentage of decrease in the amount of RNA was found in muscle (sub-lethal 20.48, lethal 26.65). Minimum per cent of the decrease in RNA was found in the liver (15.51) in sub-lethal concentration and brain (19.65) in lethal concentration. After 96h of exposure maximum percentage of decrease in the amount of RNA was found in Gill (sub-lethal 28.44, lethal 32.56). Minimum percentage of decrease in RNA was found in brain(sub-lethal 17.52, lethal 22.66).

The results indicated that the DNA and RNA content in all the tissues of test fish were decreased compared to controls and the decreasing trend was more pronounced in lethal concentrations than in sub-lethal concentrations. In maintaining the physiological configuration of the fish Nucleic acids play a vital role. As Nucleic acid and protein play the main role in regulating different activities of cells they are regarded as important biomarkers of the metabolic potential of cells (Veeriah et al 2013a).

The decrease in nucleic acid content in the present study was in accordance with Vivek (2015) in fingerlings of *Labeo rohita* exposed to sub-lethal concentrations of Cartap hydrochloride for 24, 48, 72 and 96 h. Similar results were also found by Dasu (2014) in fingerlings of *Labeo rohita* were exposed to Thiocarb (Larvin 75% WP) a thiocarbamate pesticide. Anitha & Rathnamma (2016) noticed decreased DNA and RNA levels in all the tissues like liver, kidney, brain, gill and muscle of *Labeo rohita* exposed to lethal and sub-lethal concentrations of Pyraclostrobin 20%WG (carbamate) for 24 h and sub-lethal concentrations for 5 and 10 days.

Tilak et al. (2009) noticed a decreased level of DNA and RNA content in Alachlor treated freshwater fish, *Channa punctatus* (Bloch). The decrease of RNA may be due to inhibiting the function of RNA polymerase or due to interference in the incorporation of precursor in the nucleic acid synthesis. The alterations in DNA levels may be due to disturbances in DNA synthesis and its turnover rate besides degenerative changes caused by pesticides.

From the present study, it can be concluded that exposure of *Cirrhinus mrigala* to Cartap hydrochloride caused a decline in the glycogen, total protein and Nucleic acids (DNA, RNA) content which is more pronounced in lethal exposure than in sub-lethal exposure. The alterations caused during pesticide exposure may be due to the decreased catabolism of the biomolecules to meet the energy demand of test organism under stress or their reduced synthesis due to impaired tissue function. Therefore, the results of this study suggest a serious concern towards the potential danger of Cartap hydrochloride for the aquatic environment and organisms suggesting judicious and careful use of this pesticide in the agricultural area.

ACKNOWLEDGEMENTS

The authors are thankful to the UGC SAP-DRS-III for extending the infrastructure facilities to carry out the present work in the Laboratories of the Deptt. of Zoology & Aquaculture and thank the Head, Department of Zoology and Aquaculture for permitting to do the work.

REFERENCES

Anitha, A. and Rathnamma, V.V. 2016. Toxicity Evaluation and Protein Levels of Fish Labeo rohita Exposed to Pyraclostrobin 20% Wg (Carbamate). International Journal of Advanced Research, 4(3): 967-974.

APHA 1998. Standard Method for the Examination of Water and Wastewater, A.D. Eaton, L.S. Clesceri and A.E. Greenberg (Eds.), 20th edition. American Public Health Association, AWWA and WEF, Washington D.C.

Bantu, N. and Rathnamma Vakita 2013. Effect of dimethoate on mortality and biochemical changes of freshwater fish *Labeo rohita* (Hamilton). Journal of Biology and Today's World, 2(10): 456-470.

Borah, S. and Yadav, R.N.S. 1996. Effect of Rogor (30% w/w dimethoate) on the activity of lactate dehydrogenase, acid and alkaline phosphatase in muscle and gill of a freshwater fish, *Heteropneustes fossilis*. Journal of Environmental Biology, 17(4): 279-283.

Cappon, I.D. and Nicholls, D.M. 1975. Factors involved in increased protein synthesis in liver Microsomes after administration of DDT. Pestic. Biochem. Physiol., 5: 109-118.

Chandravathy, V.M. and Reddy, S.L.N. 1996. Lead nitrate exposure changes in carbohydrate metabolism of freshwater fish. Journal of Environmental Biology, 17: 75-79.

Chaudhry, A.S. and Jabeen, F. 2011. Assessing metal, protein, and DNA profiles in *Labeo rohita* from the Indus River in Mianwali, Pakistan. Environ. Monit. Assess., 174(1-4): 665-679.

Dasu, P.M. 2014. Thiocarb 75 % wp a carbamate insecticide induced toxicity biochemical and histopathological changes in the freshwater Indian major carp *Labeo rohita* Hamilton, Ph.D. Thesis, Acharya Nagarjuna University, Nagarjuna Nagar, Guntur, A.P, India

Dezwaan, A. and Zandee, D.I. 1973. Body distribution and seasonal changes in glycogen content of the common sea mussel, *Mytilus edulis*. Comp. Biochem. Physiol., 43: 53-55.

Dhanalakshmi, B. 2013. Acute and chronic toxicity of chromium on biochemical composition of the freshwater major carp *Cirrhinus mrigala* (Hamilton). Asian J. Sci. Technol., 4: 021-026.

Finney, D.J. 1971. Probit Analysis, 3rd edition. Cambridge University Press.

Golterman, H. and Claimo, R.S. 1969. Methods for Chemical Analysis of Freshwater. Blackwell Sci. Pub., 166 pp.

Jabeen, F., Chaudhry, A.S., Manzoor, S. and Shaheen, T. 2016. Carbamates and neonicotenoids in fish, water and sediments from the Indus River for potential health risks. Environ. Monit. Assess., 187(2): 29.

Kafilzadeh, F., Shiva, A.H., Malekpour, R. and Azad, H.N. 2012. Determination of organochlorine pesticide residues in water, sediments and fish from Lake Parishan, Iran. World J. Fish. Mar. Sci., 4(2): 150-154.

Kemp, A. and and Van Heijningen, A.J.K. 1954. A colorimetric method for the determination of glycogen in tissues. Bio. Chem. J., 56: 646-648.

Kumar, A., Singh, S. and Sharma, H.N. 2017. Changes in total protein in Liver and Kidney of freshwater fish, *Channa punctatus* (Bloch.) after intoxication of Carbaryl. Journal of Advanced Laboratory Research in Biology, 8(2): 41-43.

Kumari, A., Srivastava, A. and Jha, M.M. 2014. Carbaryl Induced alteration in histology and certain biochemical parameter in liver of *Clarias batrachus*. Global Journal of Bioscience and Biotechnology, 3(3): 259-263.

Lowry, O.H., Rosebrough, N.J., Farr, A.L. and Randall, R.J.1951. Protein measurement with the Folin Phenol Reagent. J. boil. Chem., 193: 265-275

Mayers, P. A. 1977. In: Review of Physiological Chemistry, 16th edition. Eds: Harper H A. Rodwell U V and Mayers P.A. Large Medical Publications, California.

Muddassir, A.T. 2015. Comparative study of biochemical alterations induced by carbofuran and malathion on *Channa punctatus* (Bloch.). International Research Journal of Biological Sciences, 4(9): 61-65.

Muley, D.V., Kamble, G.B. and Gaikwad, P.T. 1996. Endosulfan toxicity in the freshwater fish *Tilapia mossambica*. Journal of Aquatic Biology, 11: 61-66.

Naik, B. R., Rao, G. N. and Neelima, P. 2016. Sub-lethal toxicity of cyperkill (a synthetic pyrethroid pesticide) on glycogen content in the tissues of *Labeo rohita.* Int. J. Curr. Res. Aca. Rev., 4(12): 127-134.

Pillai, S.K. and Sinha, H.C.1968. Statistical Methods for Biological Works. Ramprasad and Sons, Agra.

Prasada Rao, G. D. V., Veeraiah, K., Krishna, Ch., Rajeswari, A. and Sindhoori, E. 2018. Cyhalothrin induced bio-chemical alterations in the grass carp *Ctenopharyngodon idellus* (Valenciennes). European Journal of Biomedical and Pharmaceutical Sciences, 5(9): 525-536.

Priya, B.P. and Maruthi, Y.A. 2013. Imidacloprid toxicity on biochemical constituents in liver tissue of fresh water teleost *Channa punctatus*. International Journal of Pharma and Bio Sciences, 4(4b): 50-54.

Rajamanickam, C. 1992. Effects of Heavy Metal Copper on the Biochemical Contents, Bioaccumulation and Histology of the Selected Organs in the Freshwater Fish, *Mystus Vittatus* (Bloch). Ph.D. Thesis, Annamalai University, India.

Rajamannar, K. and Manohar, L. 1998. Sublethal toxicity of certain pesticides on carbohydrates, proteins and amino acids in *Labeo rohita*. J. Ecobiol., 10(3): 185-191.

Rawat, D.K., Bais, V.S. and Agrawal, N.C. 2002. A correlative study on liver glycogen and endosulfan toxicity in *Heterpneustes fossilis*. J. Environ. Biol., 23: 205-207.

Roberts, M. and Boyce, C.B.C. 1972. In Methods in Microbiology. 7-A Edition. (eds: J.R. Norris and D.W. Ribbows). Academic Press, New York, pp 479.

Sastry, K.V. and Abad A Siddiqui. 1982. Chronic toxic effects of the carbamate pesticide Sevin on carbohydrate metabolism in a freshwater snakehead fish, *Channa punctatus*. Toxicology Letters, 14(1-2): 123-130.

Schmidt Nielson, B. 1975. Osmoregulation: Effect of salinity and heavy metal. Fed. Proc., 33: 2137-2146.

Searchy, D.G. and MacLennis, A.J. 1970a. Determination of DNA by the Barton Diphenylanine technique. In: Experiments and Techniques in Parasitology. (eds: A.J. Mac Lnnis and M. Voge) W.H. Freeman and Co, San-Franscisco, 190-191 pp.

Searchy, D.G. and MacLennis, A.J. 1970b. Determination of RNA by Dische orcinol technique. In: Experiments and Techniques in Parasitology. (eds: A.J. Mac Lennis and M. Voge). W.H. Freeman and Co, San-Francisco, pp. 189-190.

Shivanagouda, N., Sanagoudra and Bhat, U.G. 2013. Carbaryl induced changes in the protein and cholesterol contents in the liver and muscle of marine benthic fish, *Mugil cephalus*. American Journal of Biochemistry, 3(2): 29-33.

Singh, A. and Singh, A. 2017. Studies on toxicity stress, behavioural alterations and biochemical changes induced by glyphosate herbicide on the freshwater fish, *Channa punctatus* (Bloch). Int. J. Food Agricul. Veter. Sci., 7(3): 39-48.

Singh, R.K. and Sharma B. 1998. Carbofuran induced biochemical changes in *Clarias batrachus*. J. Pestic. Sci., 53: 285-290.

Srivastava, P. and Singh, A. 2013. In vivo study of effects of dithiocarbamates fungicide (mancozeb) and its metabolite ethylene thiourea (ETU) on freshwater fish *Clarius batrachus*. Journal of Biology and Earth Sciences, 3(2): B228-B235.

Tataji, P.B. and Kumar, M.V. 2016. Biochemical changes induced by Butachlor and Machete 50% EC to the freshwater fish *Channa punctata* (Bloch). International Journal of Science and Research, 5: 2048-2052.

Tilak, K.S., Raju, P.W. and Butchiram, M.S. 2009. Effects of alachlor on biochemical parameters of the freshwater fish, *Channa punctatus* (Bloch). J. Environ. Biol., 30(3): 421-426.

Veeraiah, K., Venkatrao, G., Vivek, Ch. and Hymaranjani, G. 2013a. Heavy metal, cadmium chloride induced biochemical changes in the Indian major *Cirrhinus mrigala* (Hamilton). Int. J. Bioassays, 2(07): 1028-1033.

Veeraiah, K., Vivek, Ch., Srinivas Rao, P. and Venkatrao, G. 2013b. Biochemical changes induced by Cypermethrin (10% EC), a pyrethroid compound in sub-lethal and lethal concentrations to the freshwater fish

Cirrhinus mrigala (Hamilton). J. Atoms and Molecules, 3(6): 625-634.
Vivek, Ch. 2015. Impact of Cartap Hydrochloride (50% SP) on Biochemical, Haematological and Enzymatic Activities of the Freshwater Fish, *Labeo Rohita* (Hamilton). Ph.D. Thesis submitted to Acharya Nagarjuna University, Nagarjuna Nagar, Guntur, A.P, India.
Wankhedkar, P. T. and Bhavsar, S.S. 2015. Effect of Cartap hydrochloride and Imidacloprid on biochemical parameters of *Cerastus moussonianus*. Biolife, 3(1): 125-131.

SRR & CVR GOVERNMENT DEGREE COLLEGE (AUTONOMOUS)
MACHAVARAM, VIJAYAWADA-520004
DEPARTMENT OF ZOOLOGY

Name of the Activity	**Training Programme attended by B.Sc. AT.Z.C Final year and Second year Aquaculture Technology students**
Place	**SIFT State Institute of Fisheries Technology Kakinada**
Date	**26/8/2019 to 31/8/2019**



As per the curriculum students go to SIFT STATE INSTITUTE OF FISHERIES TECHNOLOGY (SIFT) IN KAKINADA A.P and will have Hands on Experience in for one week TRAINING PROGRAMME ON PRINCIPLES OF AQUACULTURE AND DEMONSTRATION OF AQUA LAB PROCEDURES (water and soil analysis, microbiology, feed analysis and PCR) in different parameters and sectors of aquaculture.



In the training period, they are taken to different aquaculture ponds to understand the farming techniques, feeding management, disease identification in the ponds and water quality management in field area. Through these types of training programmes students will be exposed to practical approach in the field areas also.

*****

WORKSHOP

Printed Circuit Board (PCB) Designing

DATE: 13-03-2020

No. of Participants : 44

Instructor: Ch. Veera Arjuna Rao

CMOS Lab, Vijayawada

DEPARTMENT OF PHYSICS & ELECTRONICS

SRR & CVR GOVERNMENT DEGREE COLLEGE(A)

MACHAVARAM, VIJAYAWADA

PCB Circuit Design

Objective:

Training in Printed Circuit Board (PCB) Designing to enhance students' creativity.

This Training also help them to choose a career in PCB Designing.

A workshop on "PCB circuit Design " is arranged to MECs students by Department of Physics & Electronics.

Dr. Velaga Joshi, Principal; RJD, Guntur had chaired this program & mentioned consistently like these training programs are organised by Physics & Electronics department. These will trigger the creativity in students.

PCB Designing is an integral part of any Electronic Gadget or Robotics. A printed circuit board (PCB) mechanically supports and electrically connects electronic components using conductive tracks from copper sheets laminated onto a non-conductive substrate. Capacitors, resistors or active devices are soldered on the PCB.

Hands on experience to design electronic circuit with screen printing technique is demonstrated to students by Trainer from CMOS Lab, Vijayawada, **Ch. Veera Arjuna Rao**. Students prepared PCB & soldered electronic circuits used in their regular Lab's needs.

A total of 44 students from MECs had trained in this 1 Day training program with faculty.

Smt. Sailaja, HoD , Physics & Electronics Department encouraged students to learn PCB design and educated them the career opportunities in it.

Outcome:

Students are well trained in PCB fabrication, Circuit Design, Soldering, Screen Printing.

They got the knowledge of software tools available to build PCB.

They manufactured PCB & soldered electronic circuits used in their regular Lab's needs.

They educated about the further career opportunities available in PCB design.

Student Details who participated in PCB DESIGN workshop

SRR & CVR GOVERNMENT DEGREE COLLEGE(A)

DEPARTMENT OF PHYSICS & ELECTRONICS

Printed Circuit Board Designing Workshop

Dt : 13-03-2020

S.No.	Regd. No.	Name of the Student	Signature
1	19303201	Allacheruvu Brahmaiah	A. Brahmaiah.
2	19303202	Yetuvu Ramesh	Y. Ramesh
3	19303203	Shaik Ejaz	S. Ejaz
4	19303204	Perla Yaswanth Kumar	P. Yaswanth Kumar
5	19303206	Varanasi Hemanth Kumar	V. Hemanth Kumar
6	19303207	Kona Mani Kanth	K. mani Kanth
7	19303208	Shaik Abdul Shail	Shaik. Abdul Shail.
8	19303209	Lingam Subhashini	L. Subhashini
9	19303210	Matta Jaswanth	M. Jaswanth
10	19303211	Vaddipalli Navasimha Naidu	V. N. Naidu
11	19303212	Kollipara Teja	K. Teja
12	19303213	Ila Naga Vamsi	I. Naga Vamsi
13	19303214	Peluri Ramana	P. Ramana

14	19303215	Mattipalli Anantha Sai Krishna	M. A. Sai Krishna
15	19303216	Marangi Paul Diwakar	Marangi Paul Diwakar
16	19303217	Alluri Naga Divya Kalyani	A. N. Divya Kalyani
17	19303218	Chekka Swarna Sri	Chekka Swarna Sri
18	19303219	Jagannadham Avinash	J. Avinash.
19	19303220	Vemula Vijay Kumar	V. Vijay Kumar
20	19303221	Gannavarapu Lokesh Babu	Gannavarapu Lokesh Babu
21	19303224	Shaik Shahanaz	Sk. Shahanaz.
22	19303225	Mahanti Siddhartha	M. siddartha
23	19303228	Saladi Mahalakshmi Sireesha	S.M. Sireesha
24	19303230	Kolaboni Ganesh	K. Ganesh
25	19303231	Meka Bharadwaj Sai Krishna	M. Bharadwaj sai krishna
26	19303232	Kasarelli Veera Bhadra Rao	R. Veera Bhadra
27	19303233	Kosuri Naveen	K. Naveen
28	19303234	Vittanala Josesh	V. Josesh.
29	19303235	Chintra Chaitanya Kumar	C. C. Kumar
30	19303236	Shaik Althaf	G. Sai Teja
31	19303237	Tallapragada Manasa	T. Manasa.
32	19303238	Barlapudi Ajay	B. Ajay
33	19303239	Ramavath Naveen Naik	R. Naveen Naik

34	19303240	Vankadavathu Mantru Naik	Vankadavathu Mantru Naik
35	19303241	Vavilapalli Naga Mani	V. Naga Mani
36	19303242	Namalikanth Ramesh Babu	N. Ramesh Babu
37	19303243	Nadakuditi Ravi Varma	N. Ravi Varma
38	19303246	Gundala Venkata Ajay Kumar	G. Venkata Ajay Kumar
39	19303247	Ravada Sreedhar	Ravada Sreedhar
40	19303249	Shaik Duran	Shaik Duran
41	19303251	Kuthada Naga Venkateswara Rao	K.N. Venkateswara Rao
42	19303253	Pakkurthi Sai Ram	P. Sai Ram
43	19303254	Challari Venkata Mahesh	C. Venkata Mahesh
44	19303256	Mopidevi Venkata Vamsi Krishna	M. Venkata Vamsi Krishna





సాంకేతిక పరిజ్ఞానాన్ని పెంపొందించుకోవాలి

మధురానగర్: విద్యార్థులు ఎప్పటికప్పుడు మారుతున్న సాంకేతిక పరిజ్ఞానాన్ని పెంపొందించుకోవాలని అప్పుడే నిర్దేశించుకున్న లక్ష్యాలు సులభంగా చేరుకోగలమని ఆర్జేడీ డాక్టర్ వెలగా జోషి సూచించారు. స్థానిక మాచవరం ఎస్ఆర్ఆర్ అండ్ సీవీఆర్ ప్రభుత్వ డిగ్రీ కళాశాలలో శుక్రవారం ఫిజిక్స్, ఎలక్ట్రానిక్స్ విభాగం ఆధ్వర్యంలో ప్రింటెడ్ సర్క్యూట్ బోర్డ్ డిజైనింగ్ వర్క్‌షాప్ జరిగింది. కార్యక్రమంలో ఆయన ముఖ్య అతిథిగా పాల్గొని వర్క్‌షాప్‌ను ప్రారంభించారు. ఈ సందర్భంగా ఆయన మాట్లాడుతూ విద్యార్థుల్లోని సృజనాత్మకతను వెలికితీయటానికి ఇటువంటి వర్క్‌షాప్‌లు దోహదపడతాయన్నారు. విద్యార్థులు పరిశోధనకు ప్రాధాన్యత ఇవ్వాలని సూచించారు. అనంతరం రిసోర్స్ పర్సన్‌లు సీఎంఓఎస్ రీసెర్చ్ ల్యాబ్ విజయవాడ నుంచి సీహెచ్ వీర అర్జునరావు ప్రింటెడ్ సర్క్యూట్ బోర్డ్ డిజైనింగ్, షోల్డరింగ్, సర్క్యూట్ తయారీ, స్క్రీన్ ప్రింటింగ్ తదితర అంశాలను వివరించారు. కార్యక్రమాలను ఫిజిక్స్ అండ్ ఎలక్ట్రానిక్స్ విభాగాధిపతి పి. శైలజ పర్యవేక్షించగా, అధ్యాపకులు నయోమి, కనకాల సాయిబలరామ్ సమన్వయపరిచారు.

కాలానుగుణంగా విద్యాబోధన మారాలి

మధురానగర్: మారుతున్నకాలం, పరిస్థితులకు నుగుణంగా విద్యాబోధన చేసి విద్యార్థులను ఉన్నత పౌరులుగా తీర్చిదిద్దాల్సిన బాధ్యత అధ్యాపకులపై ఉందని ఆర్జేడీ, కళాశాల ప్రిన్సిపల్ డాక్టర్ వెలగా జోషి అన్నారు. స్థానిక



ప్రింటెడ్ సర్క్యూట్ బోర్డ్ డిజైనింగ్ వర్క్‌షాప్‌లో ప్రయోగాలు చేస్తున్న విద్యార్థులు



మాట్లాడుతున్న ప్రిన్సిపల్ డాక్టర్ వెలగా జోషి

మాచవరం ఎస్ఆర్ఆర్ అండ్ సీవీఆర్ ప్రభుత్వ డిగ్రీ కళాశాలలో శుక్రవారం ఇంటర్నల్ క్వాలిటీ ఎష్యూరెన్స్ సెల్ ఆధ్వర్యంలో ఇన్ఫర్మేషన్ అండ్ కమ్యునికేషన్ టెక్నాలజీ టీచింగ్ మెథడాలజీపై ఫ్యాకల్టీ డెవలప్‌మెంట్ వర్క్‌షాప్ జరిగింది. కార్యక్రమంలో పాల్గొన్న ఆయన మాట్లాడుతూ బోధనా పద్ధతుల్లోని మెలకువలను తెలియజేసేందుకు జిల్లాలోని వివిధ డిగ్రీ కళాశాల అధ్యాపకులకు వర్క్‌షాప్‌ను నిర్వహిస్తున్నట్లు తెలిపారు.

సాక్షి Sat, 14 March 2020
https://epaper.sakshi.com/c/49928543

సాంకేతిక పరిజ్ఞానాన్ని పెంపొందించుకోవాలి





ప్రింటెడ్ సర్క్యూట్ బోర్డ్ డిజైనింగ్ వర్క్‌షాప్‌లో ప్రయోగాలు చేస్తున్న విద్యార్థులు; మాట్లాడుతున్న ప్రిన్సిపల్ డాక్టర్ వెలగా జోషి

మధురానగర్: విద్యార్థులు ఎప్పటికప్పుడు మారుతున్న సాంకేతిక పరిజ్ఞానాన్ని పెంపొందించుకోవాలని అప్పుడే నిర్దేశించుకున్న లక్ష్యాలు సులభంగా చేరుకోగలమని ఆర్జేడీ డాక్టర్ వెలగా జోషి సూచించారు. స్థానిక మాచవరం ఎస్ఆర్ఆర్ అండ్ సీవీఆర్ ప్రభుత్వ డిగ్రీ కళాశాలలో శుక్రవారం ఫిజిక్స్, ఎలక్ట్రానిక్స్ విభాగం ఆధ్వర్యంలో ప్రింటెడ్ సర్క్యూట్ బోర్డ్ డిజైనింగ్ వర్క్‌షాప్ జరిగింది. కార్యక్రమంలో ఆయన ముఖ్య అతిథిగా పాల్గొని వర్క్‌షాప్‌ను ప్రారంభించారు. ఈ సందర్భంగా ఆయన మాట్లాడుతూ విద్యార్థుల్లోని సృజనాత్మకతను వెలికితీయటానికి ఇటువంటి వర్క్‌షాప్‌లు దోహదపడతాయన్నారు. విద్యార్థులు పరిశోధనకు ప్రాధాన్యత ఇవ్వాలని సూచించారు. అనంతరం రిసోర్స్ పర్సన్‌లు సీఎంఓఎస్ రీసెర్చ్ ల్యాబ్ విజయవాడ నుంచి సీహెచ్ వీర అర్జునరావు ప్రింటెడ్ సర్క్యూట్ బోర్డ్ డిజైనింగ్, షోల్డరింగ్, సర్క్యూట్ తయారీ, స్క్రీన్ ప్రింటింగ్ అంశాలను వివరించారు. కార్యక్రమాలను ఫిజిక్స్ అండ్ ఎలక్ట్రానిక్స్ విభాగాధిపతి పి. శైలజ పర్యవేక్షించగా, అధ్యాపకులు నయోమి, కనకాల సాయిబలరామ్ సమన్వయపరిచారు.

కాలానుగుణంగా విద్యాబోధన మారాలి

మధురానగర్: మారుతున్నకాలం, పరిస్థితులకు నుగుణంగా విద్యాబోధన చేసి విద్యార్థులను ఉన్నత పౌరులుగా తీర్చిదిద్దాల్సిన బాధ్యత అధ్యాపకులపై ఉందని ఆర్జేడీ, కళాశాల ప్రిన్సిపల్ డాక్టర్ వెలగా జోషి అన్నారు. స్థానిక మాచవరం ఎస్ఆర్ఆర్ అండ్ సీవీఆర్ ప్రభుత్వ డిగ్రీ కళాశాలలో శుక్రవారం ఇంటర్నల్ క్వాలిటీ ఎష్యూరెన్స్ సెల్ ఆధ్వర్యంలో ఇన్ఫర్మేషన్ అండ్ కమ్యునికేషన్ టెక్నాలజీ టీచింగ్ మెథడాలజీపై ఫ్యాకల్టీ డెవలప్‌మెంట్ వర్క్‌షాప్ జరిగింది. కార్యక్రమంలో పాల్గొన్న ఆయన మాట్లాడుతూ బోధనా పద్ధతుల్లోని మెలకువలను తెలియజేసేందుకు జిల్లాలోని వివిధ డిగ్రీ కళాశాల అధ్యాపకులకు వర్క్‌షాప్‌ను నిర్వహిస్తున్నట్లు తెలిపారు. అనంతపూర్ ప్రభుత్వ కళాశాల జువాలజీ అసోసియేట్ ప్రొఫెసర్ డాక్టర్ జి. రాజశేఖర్ రిసోర్స్ పర్సన్‌గా వ్యవహరించారు. కార్యక్రమంలో వర్క్‌షాప్ కోఆర్డినేటర్ ఎం. శ్యాంబాబు పాల్గొన్నారు.

సాక్షి Sat, 14 March 2020
https://epaper.sakshi.com/c/49928596

WORKSHOP

NANO MATERIALS PREPARATION

DATE: 12-12-2019

RESOURCE PERSON : **Dr.G.GIRIDHAR**

Asst. Professor, Department of Nano Technology

Acharya Nagarjuna University, Nagarjuna Nagar

No of Students Participated: **40**

DEPARTMENT OF PHYSICS & ELECTRONICS

SRR & CVR GOVERNMENT DEGREE COLLEGE (AUTONOMOUS),

Machavaram, Vijayawada - 520 004

NANO MATERIALS PREPARATION

The Department of Physics & Electronics had conducted a one day workshop on "Preparation of NanoMaterials" in Collaboration with NanoTechnology Department Acharya Nagarjuna University , Nagarjuna Nagar , Guntur.

Objectives of Workshop

- To create interest in students on research in Material Science & enrich their knowledge on new technologies.
- To acknowledge students about Easy & low cost equipment methods to prepare nanoparticles in UG labs.
- Students are able to do Nano particle preparation as their future Project work.

S.R.R. & C.V.R. GOVT. DEGREE COLLEGE
(Autonomous)
NAAC accredited with 'B+' Grade
Machavaram, VIJAYAWADA - 520 004. Krishna District.
Cell : 94922 34488 Ph : 0866-2430060, Fax : 0866-2441092, www.srrcvr.org, srrandcvr@gmail.com

Dr. Velaga Joshi, Principal
M.A. (Phil.), M.A. (His.), M.A., (M.C.J.), B.L., M.Phil., Ph.D.,

Date 11 DEC 2019

To,
Dr. G. Giridhar,
Assistant Professor,
Dept. of Nano Technology,
Acharya Nagarjuna University,
Nagarjuna Nagar,
Guntur District.

Respected Sir,

Sub: Invitation to conduct Workshop on Preparation of Nano Materials For Final B.Sc., Students of SRR & CVR Govt. Degree College (A), Vijayawada on 12th December, 2019 – Regarding.

* * *

The Department of Physics/Electronics, SRR & CVR Govt. Degree College (A), Vijayawad is going to conduct Workshop on preparation of Nano Materials for Final B.Sc., Students on 12th December, 2019.

Hence, I request you sir, kindly come and conduct the workshop as a resource person on 12th December, 2019 in our college for which we are grateful to you sir.

Thanking You Sir,

Yours Sincerely,

Dr. Velaga Joshi, Principal
Principal
SRR & CVR Govt. COLLEGE
VIJAYAWADA.

As per the request forwarded by The Department of Physics & Electronics, SRR & CVR GDC(A), Vijayawada, Dr. G. Giridhar , Assistant Professor , Nanotechnology arranged a workshop at Physics Lab , SRR & CVR GDC(A) on Dt. 12-12-2019.

Dr. Giridhar demonstrated the experimental procedure to synthesise Zinc, manganese, Silver nanoparticles in a lab using chemicals and magnetic stirrer.

He discussed the precautions that should be taken to prepare superior metal nanoparticles.

He explained the various other methods, characterization techniques & applications of these Nanoparticles.

Students interacted with the resource person & refined their knowledge on nano materials.

Dr. Velaga Joshi , Principal , RJD(FAC), Guntur felicitated Dr. Giridhar & appreciated both staff , students of Physics & Electronics Department.

Dr. Joshi said such workshops are arranged by Physics & Electronics Department from time to time to inculcate & develop new technologies to students.

Profile of Resource Person : Dr.G.GIRIDHAR

Dr. Giridhar Published 30 (international)+ 2 (national) journal Publication in various research topics of material sciences.

He also guided 11 students for CSIR-SRTP-2020 . Under his guidance 1 Ph.D & 1 M. Phil. is successfully awarded.

Outcomes

Students had hands on experience on nano particles preparation which is the part of their Curriculum in Modern Physics.

It enhanced their knowledge about the application of nano particles of normal metals they use in their daily life.

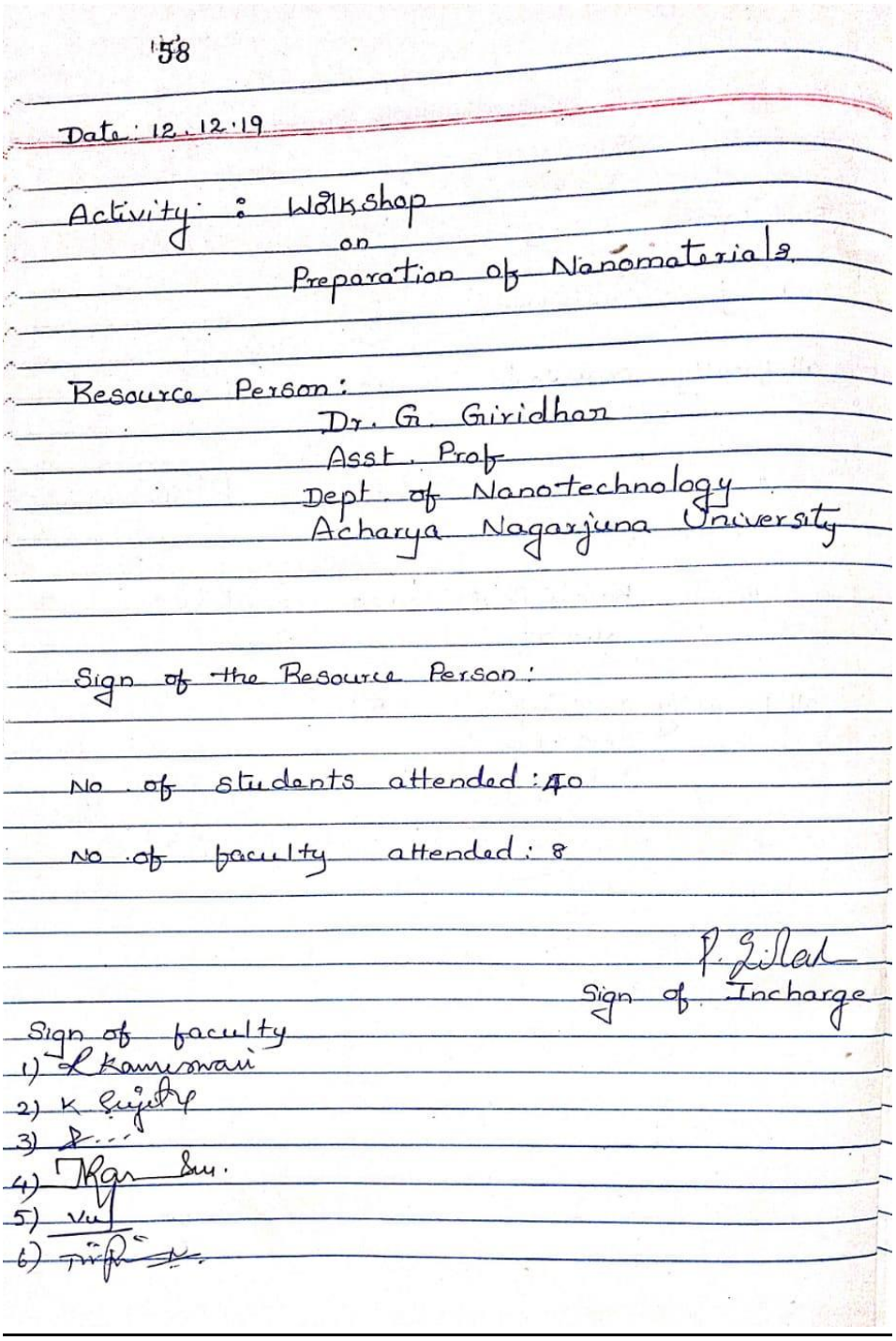
Few students got much interest to continue their higher studies in Physics & nano Technology.






Zn Nano Particle
Mn - Nano Particle
Cu - Nano Particle

COLLEGE ACTIVITY REGISTER



158

Date: 12.12.19

Activity : Workshop
on
Preparation of Nanomaterials

Resource Person:
Dr. G. Giridhar
Asst. Prof
Dept. of Nanotechnology
Acharya Nagarjuna University

Sign of the Resource Person:

No. of students attended: 40

No. of faculty attended: 8

P. Lillah
Sign of Incharge

Sign of faculty
1) K Kameswari
2) K Sujatha
3) ...
4) Rgr Sw.
5) Vu
6) ...

STUDENTS ATTENDANCE

S.R.R. & C.V.R. GOVT. DEGRE COLLEGE (A)

Machavaram, Vijayawada – 520004, Krishna District, A.P.

DEPARTMENT OF PHYSICS

All the B.Sc final year Students attended the WORK-SHOP On "Preparation of Nano Materials" on 12th December 2019 in final year B.Sc Physics lab from 10 A.M to 5 P.M. Dr.G.Giridhar, Asist. Professor in Nano Technology, Acharya Nagarjuna University, Guntur is a Resource Person.

Student Attendance

Sl.No	Name of the Students	Signature of the students
1.	A.Pedda Anantha Raju.	A.P.A. Raju.
2.	M. Prabhukiran	M. Prabhu Kiran.
3.	M. Venkaiah	M. Venkaiah
4.	SHABANA FATHIMA	Shabana Fathima
5.	V. VAISHNAVI	V. Vaishnavi
6	M. Siva	M. Siva
7.	T. Durga Vasi	T. Vasi
8.	B. Kranthi Koti	B. Kranthi Koti
9.	L. Thaubi	L. Thoubi
10.	D. Purnachandra Rao	D. Purna.
11.	T. Bhargav	T. Bhargav
12.	B. sudheer	B. Sudheer
13.	G. naveen kumar	Gnaveen
14.	M. venkaiah	
15.	A. Kondalu	A. Kondalu
16.	K.V. Krishna Reddy	K.V. Reddy
17	K. Mounika	K. Mounika
18	K. Prasanna Gopal	K. Prasanna Gopal
19.	V. Samatha	V. Samatha
20	Sk. Nazma	Sk. Nazma
21	G. Prathima	G. Prathima.
22	P. Vinod kumar	P. Vinod kumar

Sl.No	Name of the Students	Signature of the students
23	R. Vijaya Kumar	R Vijaya Kumar
24.	G. Rama Kalyan	G. Ramakalyan
25	P. Aravind	P. Aravind
26.	K. Antaryami	K. Antaryami Rao
27.	L. Uday Kiran	Udaykiran
28.	V. Narasimha	V. Narasimha Rao
29.	K. Jagadish	K. Jagadesh
30.	~~Subramanyam~~	
31.	A. Subrahmanyam	A. Subrahmanyam
32.	M. Gopi Chandana	M. Gopi Chandana C.
33.	V. Uma Maheswari	V. Uma Maheswari
34.	P Sarathi	P Sarathi
35.	T. Sai S.V.D Jyothi	T. Sai S.V.D Jyothi
36.	T. Damayanthi	T. Damayanthi
37.	P. Rohini	P. Rohini
38.	D. Renuka	D. Renuka
39.	K. Shamitha	K. Shamitha
40.	B. Shanmukha Sai	B. Shanmukha Sai
	B. Nagaraju	B. Nagaraju

Scanned with CamScanner

PAPER CLIPPINGS

'ఎస్ఆర్ఆర్'లో నానో టెక్నాలజీపై వర్క్‌షాప్

మధురానగర్: మాచవరం ఎస్ఆర్ఆర్ అండ్ సీవీఆర్ ప్రభుత్వ డిగ్రీ కళాశాలలో కళాశాల భౌతిక శాస్త్రం, ఎలక్ట్రానిక్స్ విభాగం ఆధ్వర్యంలో నానో టెక్నాలజీ రంగంలోని నానో మెటీరియల్స్, నానో పదార్థాల తయారీపై గురువారం వర్క్‌షాప్ జరిగింది. ఆచార్య నాగార్జున యూనివర్సిటీ అసిస్టెంట్ ప్రొఫెసర్ డాక్టర్ జి.గిరిధర్ నానో టెక్నాలజీ గురించి విద్యార్థులకు వివరించారు. జింక్, కాపర్, మెగ్నీషియం పదార్థాలను వినియోగించి నానో పదార్థాల తయారీని ప్రయోగాత్మకంగా విద్యార్థుల చేత చేయించారు. ఈ సందర్భంగా విద్యార్థులు అడిగిన పలు ప్రశ్నలకు ఆయన సమాధానం ఇచ్చారు. విద్యార్థులు వర్క్‌షాప్‌ను సద్వినియోగం చేసుకుని నైపుణ్యాలను మెరుగు పరుచుకోవాలని సూచించారు. ఆర్జేడీ డాక్టర్ వెలగా జోషి మాట్లాడుతూ విద్యార్థులలో నైపుణ్యాలను, సాంకేతికతను పెంపొందించేందుకు తాము వర్క్‌షాప్‌లు ఏర్పాటు చేస్తున్నట్లు తెలిపారు. అనంతరం డాక్టర్ గిరిధర్‌ను ఘనంగా సత్కరించారు. కార్యక్రమాలను వర్క్‌షాప్ కో-ఆర్డినేటర్ డాక్టర్ ఆర్.కామేశ్వరి, విభాగాధిపతి పి.శైలజ, అధ్యాపకులు కె.సుజాత, ఉమాలక్ష్మి, టీవీ రాంబాబు, కె.సాయిబలరామ్, ఎండీ ఇక్బాల్ పాష, రాజశేఖర్ తదితరులు పర్యవేక్షించారు.

సాక్షి Fri, 13 December 2019
https://epaper.sakshi.com/c/46802066

ఈనాడు అమరావతి

శుక్రవారం 13 డిసెంబరు 2019 20 పేజీలు

నానో పదార్థాల తయారీపై కార్యశాల



విద్యార్థులకు అవగాహన కల్పిస్తున్న డాక్టర్ గిరిధర్

మాచవరం, న్యూస్‌టుడే : స్థానిక ఎస్సార్ అండ్ సీవీఆర్ ప్రభుత్వ డిగ్రీ కళాశాల భౌతికశాస్త్రం, ఎలక్ట్రానిక్స్ విభాగాల సంయుక్త ఆధ్వర్యంలో గురువారం నానో సాంకేతిక రంగంలోని నానో పదార్థాల తయారీపై కార్యశాల నిర్వహించారు. ఆచార్య నాగార్జున విశ్వవిద్యాలయం సహాయ ఆచార్యుడు డాక్టర్ జి.గిరిధర్ హాజరై నానో టెక్నాలజీపై అవగాహన కల్పించారు. జింక్, కాపర్ (రాగి), మెగ్నీషియం పదార్థాలను ఉపయోగించి విద్యార్థులతో నానో పదార్థాలను తయారు చేయించారు. డాక్టర్ ఆర్.కామేశ్వరి సమన్వయకర్తగా వ్యవహరించారు. భౌతికశాస్త్ర విభాగాధిపతి పి.శైలజ, డాక్టర్ కె.సుజాత, యు.ఉమాలక్ష్మి, డిగ్రీ, పీజీ విద్యార్థులు పాల్గొన్నారు.

International Journal of Applied Engineering Research ISSN 0973-4562 Volume 13, Number 18 (2018) pp. 13428-13438
© Research India Publications. http://www.ripublication.com

r-Generalization of Phi Functions For The Subsets Of {m,m+1,…,n}

G.Lalitha[1*] and G.Kamala[2]

[1]SRR&CVR Govt Degree College, Vijayawada, Andhrapradesh, India.
[2]Department of mathematics, Osmania university, Hyderabad, Telangana, India.

Abstract

A nonempty finite set A of positive integers is r-relatively prime if greatest r[th] power common divisor of elements of A is 1. In this case we write $\gcd_r(A)=1$. Let $f^{(r)}(m,n)$ be the number of r-relatively prime subsets of $\{m,\ m+1,\ ...,\ n\}$ and the number of sets in $f^{(r)}(m,n)$ of cardinality k is $f_k^{(r)}(m,n)$. The number of nonempty subsets which are r-relatively prime to n is $\Phi^{(r)}(m,n)$ and the number of sets in $\Phi^{(r)}(m,n)$ of cardinality k is $\Phi_k^{(r)}(m,n)$. We obtained exact formulae and asymptotic estimates for these functions $f^{(r)}(m,n)$, $f_k^{(r)}(m,n)$, $\Phi^{(r)}(m,n)$ and $\Phi_k^{(r)}(m,n)$ in [4]. In this paper we find simple explicit formulae for these four functions which simplify the results in [4] and also find the asymptotic estimates for these functions.

AMS Subject Classification : 11BXX , 11B75

Keywords: r-relatively prime sets; $f^{(r)}(m,n)$; $f_k^{(r)}(m,n)$; $\Phi^{(r)}(m,n)$; $\Phi_k^{(r)}(m,n)$

INTRODUCTION

Let A be a nonempty subset of {1,2,…,n}. The greatest common divisor of elements of A is denoted as $\gcd(A)$. We say that A is relatively prime if $\gcd(A)=1$, and that A is relatively prime to n if $\gcd(A\cup n)=1$. Nathanson [1] defined $f(n)$ is the number of relatively prime subsets of {1,2,…,n} and for $k\geq 1$, $f_k(n)$ is the number of sets in $f(n)$ of cardinality k. The number of nonempty subsets which are relatively prime to n is $\Phi(n)$ and the number of sets in $\Phi(n)$ of cardinality k is $\Phi_k(n)$. M.El.Bachraoui[3] generalized these four functions for the set $\{m,\ m+1,\ ...,\ n\}$. The set A is r-relatively prime if the greatest r[th] power common divisor of elements of A is 1. In this case we write $\gcd_r(A)=1$. The set A is r-relatively prime to n if the greatest r[th] power common divisor of elements of A and n is 1. In this case we write $(\gcd_r(A),n)_r=1$. In [5] we defined the following functions:

$$f^{(r)}(n)=\#\{A\subseteq\{1,2,...,n\}: A\neq\phi,\gcd_r(A)=1\}$$

$$f_k^{(r)}(n)=\#\{A\subseteq\{1,2,...,n\}:\#A=k,\gcd_r(A)=1\}$$

$$\Phi^{(r)}(n)=\#\{A\subseteq\{1,2,...,n\}: A\neq\phi,(\gcd_r(A),n)_r=1\}$$

$$\Phi_k^{(r)}(n)=\#\{A\subseteq\{1,2,...,n\}:\#A=k,(\gcd_r(A),n)_r=1\}$$

and obtained the exact formulae and asymptotic estimates for these functions in [5]. We generalized these four functions for the set $\{m,\ m+1,\ ...,\ n\}$ where $n\geq m$, and obtained exact formulae for the functions $f^{(r)}(m,n)$, $f_k^{(r)}(m,n)$, $\Phi^{(r)}(m,n)$ and $\Phi_k^{(r)}(m,n)$ in [4]. In the present paper we further simplify the exact formulae which are obtained in [4] and find the asymptotic estimates for these four functions.

DEFINITIONS

$$f^{(r)}(m,n)=\#\{A\subseteq\{m,m+1,...,n\}: A\neq\phi,\gcd_r(A)=1\}$$
$$f_k^{(r)}(m,n)=\#\{A\subseteq\{m,m+1,...,n\}:\#A=k,\gcd_r(A)=1\}$$

$$\Phi^{(r)}(m,n)=\#\{A\subseteq\{m,m+1,...,n\}: A\neq\phi,(\gcd_r(A),n)_r=1\}$$

$$\Phi_k^{(r)}(m,n)=\#\{A\subseteq\{m,m+1,...,n\}:\#A=k,(\gcd_r(A),n)_r=1\}$$

We obtain the explicit formulae and asymptotic estimates for these four functions. The following inequality is used.

$$[x]-[y]\leq[\,x-y\,]+1$$

Theorem 1 : Let m,n be non-negative integers. Then for $m < n$,

(i) $$f^{(r)}(m,\ n) = \sum_{1 \le d^r \le n} \mu_r\left(d^r\right)\left(2^{\left\lfloor \frac{n}{d^r} \right\rfloor - \left\lfloor \frac{m-1}{d^r} \right\rfloor} - 1\right)$$

(ii) $$0 \le 2^{n-m+1} - 2^{\left\lfloor \frac{n}{2^r} \right\rfloor - \left\lfloor \frac{m-1}{2^r} \right\rfloor} - f^{(r)}(m,\ n) \le 2n \cdot 2^{\left\lfloor \frac{n-m+1}{3^r} \right\rfloor}$$

if $\{m,\ m+1,\ ...,\ n\}$ contains multiplies of 2^r, and

$$0 \le -2^{n-m+1} - f^{(r)}(m,\ n) \le 2n \cdot 2^{\left\lfloor \frac{n-m+1}{3^r} \right\rfloor} + 2^{\left\lfloor \frac{n}{2^r} \right\rfloor - \left\lfloor \frac{m-1}{2^r} \right\rfloor}$$

if $\{m,\ m+1,\ ...,\ n\}$ has no multiplies of 2^r.

Proof **: (i)** We have proved in [4], that

$$f^{(r)}(m,\ n) = \sum_{1 \le d^r \le n} \mu_r\left(d^r\right)\left(2^{\left\lfloor \frac{n}{d^r} \right\rfloor} - 1\right) - \sum_{i=1}^{m-1}\left(\sum_{d^r \mid i} \mu_r\left(d^r\right) 2^{\left\lfloor \frac{n}{d^r} \right\rfloor - \left\lfloor \frac{i}{d^r} \right\rfloor}\right)$$

Which can be written as

$$f^{(r)}(m,\ n) = \sum_{1 \le d^r \le n} \mu_r\left(d^r\right)\left(2^{\left\lfloor \frac{n}{d^r} \right\rfloor} - 1\right) - \sum_{1 \le d^r \le m-1} \mu_r\left(d^r\right) 2^{\left\lfloor \frac{n}{d^r} \right\rfloor} \sum_{i=1}^{m-1} 2^{-\frac{i}{d^r}}$$

$$= \sum_{1 \le d^r \le n} \mu_r\left(d^r\right)\left(2^{\left\lfloor \frac{n}{d^r} \right\rfloor} - 1\right) - \sum_{1 \le d^r \le m-1} \mu_r\left(d^r\right) 2^{\left\lfloor \frac{n}{d^r} \right\rfloor}\left(\sum_{j=1}^{\left\lfloor \frac{m-1}{d^r} \right\rfloor} 2^{-j}\right)$$

$$= \sum_{1 \le d^r \le n} \mu_r\left(d^r\right) 2^{\left\lfloor \frac{n}{d^r} \right\rfloor}\left(1 - \sum_{j=1}^{\left\lfloor \frac{m-1}{d^r} \right\rfloor} 2^{-j}\right) - \sum_{1 \le d^r \le n} \mu_r\left(d^r\right)$$

Note that $\left\lfloor \frac{m-1}{d^r} \right\rfloor = 0$ if $m \le d^r \le n$

$$= \sum_{1 \le d^r \le n} \mu_r\left(d^r\right) 2^{\left\lfloor \frac{n}{d^r} \right\rfloor}\left(1 - \left(1 - 2^{-\left\lfloor \frac{m-1}{d^r} \right\rfloor}\right)\right) - \sum_{1 \le d^r \le n} \mu_r\left(d^r\right)$$

$$= \sum_{1\le d^r \le n} \mu_r\left(d^r\right)\left(2^{\left\lfloor \frac{n}{d^r}\right\rfloor - \left\lfloor \frac{m-1}{d^r}\right\rfloor} - 1\right).$$

(ii) Let $1 \le d^r \le n.$ Then $m \le a \le n$ and $d^r \mid a$ if and only if

$$\left\lceil \frac{m}{d^r} \right\rceil \le \frac{a}{d^r} \le \left\lfloor \frac{n}{d^r} \right\rfloor.$$

Which gives that $A \subseteq \{m,\ m+1,\ ...,\ n\}$ and $\gcd_r(A) = d^r$ if and only if

$A^1 = \frac{1}{d^r} * A \subseteq \left\{\left\lceil \frac{m}{d^r} \right\rceil,\ \left\lceil \frac{m}{d^r} \right\rceil + 1,\ ...,\ \left\lfloor \frac{n}{d^r} \right\rfloor\right\}$ and $\gcd_r\left(A^1\right) = 1.$ Therefore

$$2^{n-(m-1)} - 1 = \sum_{1\le d^r \le n} f^{(r)}\left(\left\lceil \frac{m}{d^r} \right\rceil,\ \left\lfloor \frac{n}{d^r} \right\rfloor\right).$$

$$\Rightarrow 2^{n-(m-1)} - 1 = f^{(r)}(m,\ n) + f^{(r)}\left(\left\lceil \frac{m}{2^r} \right\rceil,\ \left\lfloor \frac{n}{2^r} \right\rfloor\right) + \sum_{3\le d^r \le n} f^{(r)}\left(\left\lceil \frac{m}{d^r} \right\rceil,\ \left\lfloor \frac{n}{d^r} \right\rfloor\right)$$

$$\Rightarrow 2^{n-(m-1)} - 1 \le f^{(r)}(m,\ n) + \left(2^{\left\lfloor \frac{n}{2^r}\right\rfloor - \left\lceil \frac{m-1}{2^r}\right\rceil} - 1\right) + \sum_{3\le d^r \le n} 2^{\left(\left\lfloor \frac{n}{d^r}\right\rfloor - \left\lceil \frac{m-1}{d^r}\right\rceil\right)}$$

$$\Rightarrow 2^{n-(m-1)} \le f^{(r)}(m,\ n) + 2^{\left\lfloor \frac{n}{2^r}\right\rfloor - \left\lceil \frac{m-1}{2^r}\right\rceil} + n \cdot 2^{\left\lfloor \frac{n}{3^r}\right\rfloor - \left\lceil \frac{m-1}{3^r}\right\rceil}$$

$$\le f^{(r)}(m,\ n) + 2^{\left\lfloor \frac{n}{2^r}\right\rfloor - \left\lceil \frac{m-1}{2^r}\right\rceil} + n \cdot 2^{\left\lfloor \frac{n-m+1}{3^r}\right\rfloor + 1}$$

Since $\lfloor x \rfloor - \lceil y \rceil \le \lfloor x - y \rfloor + 1.$

$$2^{n-m+1} - 2^{\left\lfloor \frac{n}{2^r}\right\rfloor - \left\lceil \frac{m-1}{2^r}\right\rceil} - 2n \cdot 2^{\left\lfloor \frac{n-m+1}{3^r}\right\rfloor} \le f^{(r)}(m,\ n) \qquad \text{..... (1)}$$

and hence the lower bound for $f^{(r)}(m,\ n)$ is obtained.

The upper bound for $f^{(r)}(m,\ n)$ is obtained as follows :

If the set $\{m,\ m+1,\ ...,\ n\}$ contains multiples of $2^r,$ then

$$f^{(r)}(m,\ n) \le 2^{n-m+1} - 2^{\left\lfloor \frac{n}{2^r} \right\rfloor - \left\lfloor \frac{m-1}{2^r} \right\rfloor}$$

$$\Rightarrow 0 \le 2^{n-m+1} - 2^{\left\lfloor \frac{n}{2^r} \right\rfloor - \left\lfloor \frac{m-1}{2^r} \right\rfloor} - f^{(r)}(m,\ n). \qquad \text{..... (2)}$$

From equations (1) and (2)

$$\Rightarrow 0 \le 2^{n-m+1} - 2^{\left\lfloor \frac{n}{2^r} \right\rfloor - \left\lfloor \frac{m-1}{2^r} \right\rfloor} - f^{(r)}(m,\ n) \le 2n \cdot 2^{\left\lfloor \frac{n-m+1}{3^r} \right\rfloor}$$

If the set $\{m,\ m+1,\ ...,\ n\}$ has no multiples of 2^r, then

$$f^{(r)}(m,\ n) \le 2^{n-m+1}.$$

Hence

$$0 \le 2^{n-m+1} - f^{(r)}(m,\ n) \le 2n \cdot 2^{\left\lfloor \frac{n-m+1}{3^r} \right\rfloor} + 2^{\left\lfloor \frac{n}{2^r} \right\rfloor - \left\lfloor \frac{m-1}{2^r} \right\rfloor}$$

$$\le 2n \cdot 2^{\left\lfloor \frac{n-m+1}{3^r} \right\rfloor} + 2 \cdot 2^{\left\lfloor \frac{n-m+1}{2^r} \right\rfloor}$$

$$= 2\left\lfloor n \cdot 2^{\left\lfloor \frac{n-m+1}{3^r} \right\rfloor} + 2^{\left\lfloor \frac{n-m+1}{2^r} \right\rfloor} \right\rfloor.$$

Theorem 2 : Let m,n be non-negative integers. Then for $m < n$, $k \ge 1$,

(i) $$f_k^{(r)}(m,\ n) = \sum_{1 \le d^r \le n} \mu_r\left(d^r\right) \binom{\left\lfloor \frac{n}{d^r} \right\rfloor - \left\lfloor \frac{m-1}{d^r} \right\rfloor}{k}$$

(ii) $$0 \le \binom{n-m+1}{k} - \binom{\left\lfloor \frac{n}{2^r} \right\rfloor - \left\lfloor \frac{m-1}{2^r} \right\rfloor}{k} - f_k^{(r)}(m,\ n) \le n \binom{\left\lfloor \frac{n-m+1}{2^r} \right\rfloor + 1}{k}$$

if $\{m,\ m+1,\ ...,\ n\}$ contains multiplies of 2^r and

$$0 \le \binom{n-m+1}{k} - f_k^{(r)}(m,\ n) \le n \binom{\left\lfloor \frac{n-m+1}{2^r} \right\rfloor + 1}{k}$$

if $\{m,\ m+1,\ ...,\ n\}$ does not contain multiples of 2^r.

Proof : (i) In [4] we have proved that

$$f_k^{(r)}(m,\ n) = \sum_{1\le d^r \le n} \mu_r\left(d^r\right)\binom{\left\lfloor \frac{n}{d^r}\right\rfloor}{k} - \sum_{i=1}^{m-1}\sum_{d^r \mid i} \mu_r\left(d^r\right)\binom{\left\lfloor \frac{n}{d^r}\right\rfloor - \frac{i}{d^r}}{k-1}$$

For $K \ge 1$ and $0 \le M \le N$,we have

$$\binom{N}{K} - \sum_{j=1}^{M}\binom{N-j}{K-1} = \binom{N-M}{\mathrm{K}}$$

$$f_k^{(r)}(m,\ n) = \sum_{1\le d^r \le n} \mu_r\left(d^r\right)\binom{\left\lfloor \frac{n}{d^r}\right\rfloor}{k} - \sum_{1\le d^r \le m-1} \mu_r\left(d^r\right)\sum_{\substack{i=1 \\ d^r \mid i}}^{m-1}\binom{\left\lfloor \frac{n}{d^r}\right\rfloor - \frac{i}{d^r}}{k-1}$$

$$= \sum_{1\le d^r \le n} \mu_r\left(d^r\right)\binom{\left\lfloor \frac{n}{d^r}\right\rfloor}{k} - \sum_{1\le d^r \le m-1} \mu_r\left(d^r\right)\sum_{j=1}^{\left\lfloor \frac{m-1}{d^r}\right\rfloor}\binom{\left\lfloor \frac{n}{d^r}\right\rfloor - j}{k-1}$$

$$= \sum_{1\le d^r \le m-1} \mu_r\left(d^r\right)\left[\binom{\left\lfloor \frac{n}{d^r}\right\rfloor}{k} - \sum_{j=1}^{\left\lfloor \frac{m-1}{d^r}\right\rfloor}\binom{\left\lfloor \frac{n}{d^r}\right\rfloor - j}{k-1}\right] + \sum_{m\le d^r \le n} \mu_r\left(d^r\right)\binom{\left\lfloor \frac{n}{d^r}\right\rfloor}{k}$$

$$= \sum_{1\le d^r \le m-1} \mu_r\left(d^r\right)\binom{\left\lfloor \frac{n}{d^r}\right\rfloor - \left\lfloor \frac{m-1}{d^r}\right\rfloor}{k} + \sum_{m\le d^r \le n} \mu_r\left(d^r\right)\binom{\left\lfloor \frac{n}{d^r}\right\rfloor - \left\lfloor \frac{m-1}{d^r}\right\rfloor}{k}$$

Note that $\left\lfloor \frac{m-1}{d^r}\right\rfloor = 0$ if $m \le d^r \le n$.

$$= \sum_{1\le d^r \le n} \mu_r\left(d^r\right)\binom{\left\lfloor \frac{n}{d^r}\right\rfloor - \left\lfloor \frac{m-1}{d^r}\right\rfloor}{k}.$$ Which proves (i).

(ii) The upper bound for $f_k^{(r)}(m,\ n)$ is obtained by deleting k-element sets of multiples of 2^r if they belong to the set $\{m,\ m+1,\ ...,\ n\}$. If the set contains multiples of 2^r, then the upper bound for $f_k^{(r)}(m,\ n)$ is obtained by deleting sets of order k from the set

$$\left\{\left\lfloor \frac{m}{2^r}\right\rfloor,\ \left\lfloor \frac{m+1}{2^r}\right\rfloor,\ ...,\ \left\lfloor \frac{n}{2^r}\right\rfloor\right\}$$

Hence

$$f_k^{(r)}(m,\ n) \le \binom{n-m+1}{k} - \binom{\left\lfloor \frac{n}{2^r} \right\rfloor - \left\lfloor \frac{m-1}{2^r} \right\rfloor}{k}$$

The lower bound for $f_k^{(r)}(m,\ n)$ is obtained as follows:

$$\binom{n-m+1}{k} = \sum_{1 \le d^r \le n} f_k^{(r)}\left(\left[\frac{m}{d^r}\right], \left[\frac{n}{d^r}\right]\right)$$

$$\le f_k^{(r)}(m,\ n) + \binom{\left\lfloor \frac{n}{2^r} \right\rfloor - \left\lfloor \frac{m-1}{2^r} \right\rfloor}{k} + \sum_{3^r \le d^r \le n} \binom{\left\lfloor \frac{n}{d^r} \right\rfloor - \left\lfloor \frac{m-1}{d^r} \right\rfloor}{k}$$

$$\le f_k^{(r)}(m,\ n) + \binom{\left\lfloor \frac{n}{2^r} \right\rfloor - \left\lfloor \frac{m-1}{2^r} \right\rfloor}{k} + n\binom{\left\lfloor \frac{n-m+1}{3^r} \right\rfloor + 1}{k}$$

$$\therefore\ 0 \le \binom{n-m+1}{k} - \binom{\left\lfloor \frac{n}{2^r} \right\rfloor - \left\lfloor \frac{m-1}{2^r} \right\rfloor}{k} - f_k^{(r)}(m,\ n) \le n\binom{\left\lfloor \frac{n-m+1}{3^r} \right\rfloor + 1}{k}.$$

If the set $\{m,\ m+1,\ ...,\ n\}$ does not contain multiples of 2^r, then

$$f_k^{(r)}(m,\ n) \le \binom{n-m+1}{k} \Rightarrow\ 0 \le \binom{n-m+1}{k} - f_k^{(r)}(m,\ n).$$

Also

$$\binom{n-m+1}{k} = \sum_{1 \le d^r \le n} f_k^{(r)}\left(\left[\frac{m}{d^r}\right], \left[\frac{n}{d^r}\right]\right)$$

$$= f_k^{(r)}(m,\ n) + \sum_{2 \le d^r \le n} f_k^{(r)}\left(\left[\frac{m}{d^r}\right], \left[\frac{n}{d^r}\right]\right)$$

$$\le f_k^{(r)}(m,\ n) + n\binom{\left\lfloor \frac{n}{2^r} \right\rfloor - \left\lfloor \frac{m-1}{2^r} \right\rfloor}{k}$$

$$\le f_k^{(r)}(m,\ n) + n\binom{\left\lfloor \frac{n-m+1}{2^r} \right\rfloor + 1}{k}$$

$$\therefore\ 0 \le \binom{n-m+1}{k} - f_k^{(r)}(m,\ n) \le n \binom{\left\lfloor \frac{n-m+1}{2^r} \right\rfloor + 1}{k}.$$

Which proves (ii).

***Theorem* 3:** Let m,n be non-negative integers. Then for, $m < n$

(i) $$\Phi^{(r)}(m,\ n) = \sum_{d^r \mid n} \mu_r\left(d^r\right) \binom{2^{\frac{n}{d^r}} - \left\lfloor \frac{m-1}{d^r} \right\rfloor}{}$$

(ii) If p is the smallest prime such that $p^r \mid n$, then

$$0 \le 2^{n-m+1} - 2^{\frac{n}{p^r} - \left\lfloor \frac{m-1}{p^r} \right\rfloor} - \Phi^{(r)}(m,\ n) \le 2n \cdot 2^{\left\lfloor \frac{n-m+1}{p^r} \right\rfloor}.$$

***Proof* : (i)** In [4] we obtained

$$\Phi^{(r)}(m,\ n) = \sum_{d^r \mid n} \mu_r\left(d^r\right) 2^{\frac{n}{d^r}} - \sum_{i=1}^{m-1} \sum_{d^r \mid \gcd_r(i,\ n)} \mu_r\left(d^r\right) 2^{\frac{n-i}{d^r}}.$$

Which can be written as

$$\Phi^{(r)}(m,\ n) = \sum_{d^r \mid n} \mu_r\left(d^r\right) 2^{\frac{n}{d^r}} - \sum_{d^r \mid n} \mu_r\left(d^r\right) \sum_{i=1}^{m-1} 2^{\frac{n-i}{d^r}}$$

$$= \sum_{d^r \mid n} \mu_r\left(d^r\right) 2^{\frac{n}{d^r}} - \sum_{d^r \mid n} \mu_r\left(d^r\right) 2^{\frac{n}{d^r}} \sum_{i=1}^{m-1} 2^{\frac{-i}{d^r}}$$

$$= \sum_{d^r \mid n} \mu_r\left(d^r\right) 2^{\frac{n}{d^r}} - \sum_{d^r \mid n} \mu_r\left(d^r\right) 2^{\frac{n}{d^r}} \sum_{j=1}^{\left\lfloor \frac{m-1}{d^r} \right\rfloor} 2^{-j}$$

$$= \sum_{d^r \mid n} \mu_r\left(d^r\right) 2^{\frac{n}{d^r}} \left(1 - \sum_{j=1}^{\left\lfloor \frac{m-1}{d^r} \right\rfloor} 2^{-j}\right)$$

$$= \sum_{d^r \mid n} \mu_r\left(d^r\right) 2^{\frac{n}{d^r}} \left(1 - \left(1 - 2^{-\left\lfloor \frac{m-1}{d^r} \right\rfloor}\right)\right)$$

$$= \sum_{d^r \mid n} \mu_r\left(d^r\right)\left(2^{\frac{n}{d^r}} \cdot 2^{-\left\lfloor \frac{m-1}{d^r} \right\rfloor}\right)$$

$$= \sum_{d^r \mid n} \mu_r\left(d^r\right) 2^{\frac{n}{d^r} - \left\lfloor \frac{m-1}{d^r} \right\rfloor}$$

which proves (i).

(ii) For the smallest prime divisor p of n such that $p^r \mid n$, if we delete all subsets of $\{m,\ m+1,\ \ldots,\ n\}$ whose elements are multiples of p^r, we get

$$\Phi^{(r)}(m,\ n) \le 2^{n-(m-1)} - 2^{\frac{n}{p^r} - \left\lfloor \frac{m-1}{p^r} \right\rfloor}$$

$$\Rightarrow\ 0 \le 2^{n-(m-1)} - 2^{\frac{n}{p^r} - \left\lfloor \frac{m-1}{p^r} \right\rfloor} - \Phi^{(r)}(m,\ n).$$

The lower bound for $\Phi^{(r)}(m,\ n)$ can be obtained as follows:

$$\Phi^{(r)}(m,\ n) = \sum_{d^r \mid n} \mu_r\left(d^r\right)\left(2^{\frac{n}{d^r} - \left\lfloor \frac{m-1}{d^r} \right\rfloor}\right)$$

$$= \mu_r(1) 2^{n-(m-1)} + \mu_r\left(p^r\right) 2^{\frac{n}{p^r} - \left\lfloor \frac{m-1}{p^r} \right\rfloor} + \sum_{\substack{d^r \mid n \\ d > p}} \mu_r\left(d^r\right)\left(2^{\frac{n}{d^r} - \left\lfloor \frac{m-1}{d^r} \right\rfloor}\right)$$

$$\Phi^{(r)}(m,\ n) = 2^{n-m+1} - 2^{\frac{n}{p^r} - \left\lfloor \frac{m-1}{p^r} \right\rfloor} + \sum_{\substack{d^r \mid n \\ d > p}} \mu_r\left(d^r\right)\left(2^{\frac{n}{d^r} - \left\lfloor \frac{m-1}{d^r} \right\rfloor}\right)$$

$$\Phi^{(r)}(m,\ n) - 2^{n-m+1} + 2^{\frac{n}{p^r} - \left\lfloor \frac{m-1}{p^r} \right\rfloor} = \sum_{\substack{d^r \mid n \\ d > p}} \mu_r\left(d^r\right)\left(2^{\frac{n}{d^r} - \left\lfloor \frac{m-1}{d^r} \right\rfloor}\right)$$

$$\geq \sum_{\substack{d^r \mid n \\ d>p}} (-1)\, 2^{\frac{n}{d^r} - \left\lfloor \frac{m-1}{d^r} \right\rfloor}$$

$$\geq (-1)\, n \cdot 2^{\left\lfloor \frac{n-m+1}{p^r} \right\rfloor + 1}$$

$$= -2n \cdot 2^{\left\lfloor \frac{n-m+1}{p^r} \right\rfloor}$$

$$\Rightarrow\ 2^{n-m+1} - 2^{\frac{n}{p^r} - \left\lfloor \frac{m-1}{p^r} \right\rfloor} - \Phi^{(r)}(m,\ n) \leq 2n \cdot 2^{\left\lfloor \frac{n-m+1}{p^r} \right\rfloor}$$

$$\therefore\ 0 \leq 2^{n-m+1} - 2^{\frac{n}{p^r} - \left\lfloor \frac{m-1}{p^r} \right\rfloor} - \Phi^{(r)}(m,\ n) \leq 2n \cdot 2^{\left\lfloor \frac{n-m+1}{p^r} \right\rfloor}.$$

which proves (ii).

Theorem 4 : Let m,n be non-negative integers. Then for $m < n$,

(i) $$\Phi_k^{(r)}(m,\ n) = \sum_{d^r \mid n} \mu_r\left(d^r\right) \binom{\frac{n}{d^r} - \left\lfloor \frac{m-1}{d^r} \right\rfloor}{k}$$

and

(ii) $$0 \leq \binom{n-m+1}{k} - \binom{\frac{n}{p^r} - \left\lfloor \frac{m-1}{p^r} \right\rfloor}{k} - \Phi_k^{(r)}(m,\ n) \leq n \binom{\left\lfloor \frac{n-m+1}{p^r} \right\rfloor + 1}{k}$$

Proof **: (i)** Let *p* be the smallest prime such that $p^r \mid n$. In [4] , we obtained

$$\Phi_k^{(r)}(m,\ n) = \sum_{d^r \mid n} \mu_r\left(d^r\right) \binom{\frac{n}{d^r}}{k} - \sum_{d^r \mid n} \mu_r\left(d^r\right) \sum_{\substack{i=1 \\ d^r \mid i}}^{m-1} \binom{\frac{n-i}{d^r}}{k-1}$$

$$= \sum_{d^r \mid n} \mu_r\left(d^r\right) \left(\binom{\frac{n}{d^r}}{k} - \sum_{j=1}^{\left\lfloor \frac{m-1}{d^r} \right\rfloor} \binom{\frac{n}{d^r} - j}{k-1} \right)$$

$$= \sum_{d^r \mid n} \mu_r\left(d^r\right)\binom{\frac{n}{d^r} - \left\lfloor \frac{m-1}{d^r} \right\rfloor}{k}$$

Note that $\binom{N}{K} - \sum_{j=1}^{M}\binom{N-j}{K-1} = \binom{N-M}{\mathrm{K}}$

which proves (i).

(ii) Consider

$$\Phi_k^{(r)}(m,\ n) = \sum_{d^r \mid n} \mu_r\left(d^r\right)\binom{\frac{n}{d^r} - \left\lfloor \frac{m-1}{d^r} \right\rfloor}{k}$$

$$\geq \mu_r(1)\binom{n-(m-1)}{k} - \binom{\frac{n}{p^r} - \left\lfloor \frac{m-1}{p^r} \right\rfloor}{k} - \sum_{\substack{d^r \mid n \\ d>p}}\binom{\frac{n}{d^r} - \left[\frac{m-1}{d^r}\right]}{k}$$

$$\geq \binom{n-(m-1)}{k} - \binom{\frac{n}{p^r} - \left\lfloor \frac{m-1}{p^r} \right\rfloor}{k} - \sum_{\substack{d^r \mid n \\ d>p}}\binom{\left[\frac{n-m+1}{d^r}\right]+1}{k}$$

$$\geq \binom{n-(m-1)}{k} - \binom{\frac{n}{p^r} - \left\lfloor \frac{m-1}{p^r} \right\rfloor}{k} - n\cdot\binom{\left\lfloor \frac{n-m+1}{p^r} \right\rfloor+1}{k}.$$

The upper bound is obtained by deleting k -element sets of $\{m,\ m+1,\ \ldots,\ n\}$ whose elements are multiples of p^r, we get

$$\Phi_k^{(r)}(m,\ n) \leq \binom{n-(m-1)}{k} - \binom{\frac{n}{p^r} - \left\lfloor \frac{m-1}{p^r} \right\rfloor}{k}.$$

$$\Rightarrow\ 0 \leq \binom{n-(m-1)}{k} - \binom{\frac{n}{p^r} - \left\lfloor \frac{m-1}{p^r} \right\rfloor}{k} - \Phi_k^{(r)}(m,\ n) \leq n\binom{\left\lfloor \frac{n-m+1}{p^r} \right\rfloor+1}{k}$$

which proves (ii).

REFERENCES

[1] Melvyn B.Nathanson , *Affine Invariants , relatively prime sets, and phi function for subsets of* $\{1,2,...,n\}$ *,Integers,(2007),A1,7pp (electronic).*

[2] Melvyn B.Nathanson, *Asymptotic Estimates for Phi Functions for Subsets of* $\{M, M+1, ..., N\}$*, Integers,7(2007), A54,7pp (electronic).*

[3] Mohamed El.Bachraoui ,*The Number of relatively prime subsets and phi functions for* $\{m, m+1, ..., n\}$ *,Integers,7(2007), A43,8pp (electronic).*

[4] G.Kamala, G.Lalitha, *The Number Of r-Relatively Prime Subsets And Their Phi Functions for* $\{m, m+1, ..., n\}$ *-Its r-Generalization, Annals of pure and Applied Mathematics , vol. 14, No.3,581-592 .*

[5] G.Kamala, G.Lalitha, *r-Relatively prime Sets And r-Generalization of Phi Functions for Subsets of* $\{1,2,...,n\}$*, Annals Of pure And Applied Mathematics, Vol. 14, No.3, 497-508.*

Toxicity and Behavioural Studies on the Earthworm, *Lampito mauritii* (Kinberg) Exposed to Organophosphate Insecticide Monocrotophos

M.Ramakrishna[1] , M.VijayaKumar [2],G.Mathew Srirangam[3]
[1,2,3]Assistant Professor, Department of Zoology,
[1]SMBTAV & SN Degree College, Veeravasaram, West Godavari District,
[2]SRR & CVR Government Degree College (A), Vijayawada, Krishna District,
[3]Andhra Loyola College (A), Vijayawada, Krishna District,
Andhra Pradesh, India

Abstract: Earthworms have long been recognized as a 'friend of the farmer'. They plough, aerate and manure the soil ecosystem. Such a defense less friendly creature deserves attention and protection from the onslaught through the irrational use of pesticides. Indiscriminate use of pesticides is bound to disturb the ecological balance of the soil ecosystem. *Lampito mauritii*, a common earthworm in the West Godavari District has been chosen to study the influence of an organophosphate monocrotophos compound which is most commonly used in this area. On calculation the LC_{50} values for 24, 48, 72, 96 hrs were found to be 6.75, 6.25, 5.25 and 4.50 ppm respectively. During the present studies the changes in their morphological features and the patterns of behaviour were observed when exposed to monocrotophos pesticide. The changes were noticed to depend on the experimental periods and concentration levels of the pesticide compounds of the experimental media. The colour of the worms changed from brown to pale brown and mucous material was secreted by the worms. When exposed to monocrotophos the amount of mucous produced was comparatively high at higher concentration and low at low concentration. At higher concentration, *Lampito mauritii* developed swellings, sores and even rupture develop in the entire body when exposed to monocrotophos. Further, protrusion of internal visceral parts through ruptured regions on the body wall became visible in the monocrotophos exposed worms. The data obtained from LC_{50} calculation and the observed behavioural changes were discussed in the light of available literature.
Keywords: *Lampito mauritii,* monocrotophos, LC_{50}, behavioural changes.

INTRODUCTION

One of the major sources of pollution in the terrestrial environment is through indiscriminate and extensive use of biocidal chemicals which are collectively known as pesticides in agricultural operations. It has been now been increasingly realized that the pesticides play an important role in the soil ecosystem. The soil, therefore, acts as a reservoir of pesticides used in the eradication of pests. These pesticides, although primarily aimed at combating pests on crops reach soil system and slowly degrade, gradually spread and possibly get translocated to other environments as well as in the neighborhood through water or air. The rate of degradation of these toxic substances depends upon the constitution of the chemical used. In the above process of dissipation, persistence may result. The pesticides normally become transformed, modified or perhaps magnified through bio-concentrations at different tropic levels in soil ecosystems. Pesticides have been widely used all over the world to control insects, pests and disease vectors and they are one of the most potentially harmful chemicals introduced into the environment. Though they have contributed considerably to human welfare, their adverse effects on non-target organisms are significant.

The determination of LC_{50} values is useful in the evaluation of safe level of tolerance of pollutant and moreover it provides fundamental data to design more complex disposal modes of toxicity to the exposed animals. It is suggested that the chronic test, aiming at sublethal effects, is more sensitive and is a more realistic approach for the prediction of environmental effects because in the field, the exposure concentration of pesticides are usually quite low (Rombke *et al*., 2007). Toxicity test are basic tools for ecological risk assessment of toxic compounds. Earthworms are important biocomponents of ecosystem, although not numerically dominant in soil but their large size makes them major contributors to total biomass. They are extremely important in soil formation, principally through their activities in consuming organic matter, fragmenting and mixing it intimately with mineral particles to form aggregates. Pesticides

are either directly applied to the soil to control soil borne pests or deposited on soil as runoff from foliar application. The pesticides residues will impair the physiological functions of earthworms leading to their mortality (Ahmed, 1991). Riepert, (2009) reported that the acute earthworm test is part of the basic test set, but the earthworm reproduction test is considered ecologically more relevant.

Several workers have also investigated the effects of organophosphate insecticides on earthworms' populations. Azinphosmethyl did not affect earthworm populations (Hopkins and Krik, 1957) but carbofuran did (Kring, 1969; Thompson, 1971) Chlorfenvinphos had slight effects (Edwards 1967). Parathion has been reported as moderately toxic to earthworms, particularly in large doses (Heungens, 1966). Senapati (1987) observed the impact of malathion on the population of the earthworms and reported its stressful effect on earthworm in agroecosystem. The earthworms when exposed to organophosphate pesticides showed increased ureotelic and ammonotellic activity (Patnaik and Madhab, 1991). In the same animal Kulkarni (1989) observed that fenvalerate produced pronounced changes in the behavior, and physiology bycausing hormonal and enzymatic imbalance. Goven (1993) have studied the cellular biomarkers for measuring toxicity of xenobiotics. Effect of polychlorinated biphenyls on the coelomocytes of earthworm *Lumbricus terrestris*. From the foregoing account it is clear that the work done on the effects of pesticides on earthworms is scanty. This is especially true in regard to earthworms in India. As mentioned earlier India in general and Andhra Pradesh, in particular, agriculture is the main occupation of a majority of the people.

Lampito mauritii, a common earthworm in the West Godavari District has been chosen to study the influence of one of the pesticide which is most commonly used in the area. The pesticide selected for the present study is organophosphate compound namely, monocrotophos (MCP), commonly known as Azodrin, is an extensively used, potent and highly toxic organophosphate insecticide with and acaricides belonging to the vinyl phosphate group and having a wide range of applications in agriculture (Kavitha and Rao, 2007). This is now in active use in agricultural practices in Lankalakoderu village, Palakol mandal, West Godavari District, Andhra Pradesh in India. *Lampito mauritii*is one of the most common terrestrial oligochaete inhabiting the upper horizon of soils in the southern parts of the Indian sub-continent. Since the use of insecticides has gone up by leaps and bounds now-a-days, it is thought that a study of toxicity of the commonly used organophosphate compounds to *Lampito mauritii* is worthwhile. It is reasonable to expect that the organophosphate compounds even at moderate doses exercise an immediate kill of the earthworm populations. Hence, the present investigations are designed to evaluate the dose-mortality levels of selected organophosphate insecticide namely monocrotophos.

MATERIALS AND METHODS

The earthworm specimens of *Lampito mauritii* were dug-out from the kitchen gardens of residential localities in Lankalakoderu village, Palakol mandal, West Godavari District. They were conveyed to laboratory in wide mouthed plastic jars along with some amount of damp soil collected from their habitat usually within an hour after their collections. After reaching the laboratory they were carefully isolated with a pair of brushes from the soil and gently washed in aerated freshwater. Only healthy, uninjured nearly equal sized worms weighing about 1.0 to 1.5g were selected and acclimated to the laboratory conditions (30 ± 1°C).Since overcrowding causes mortality of the worms, they were maintained in small numbers in batches in number of glass troughs containing fresh water. The media were periodically aerated. The fresh water used for maintenance analyzed to insure that the worms were in a medium of normal composition and therefore under normal physicochemical conditions. They were acclimated for 3 to 4 days to laboratory conditions. They were not fed either during acclimation or experimentation. Lest sudden and or large variations in temperatures should exercise deleterious effects on their survival, both acclimation and the experimentation on the worms were done at constant temperatures. Healthy, active and equal sized worms were chosen for toxicity studies. Standard renewal techniques recommended by (APHA *et al.*, 1998) have been adapted in the present exposure experiments. The renewal techniques followed here were simple and easy to follow in the laboratory.

The media, to which the specific toxicants were added, were freshly prepared. Accumulation excretory products which resulted in deoxygenation and other secondary effects were prevented by frequent renewal of experimental media. Simultaneously control experiments were also made by adding appropriate amounts distilled water to aqueous media. The distilled water added to the control experiments is identical to the quantities used at the maximum toxicant – concentration – exposures. Hence, it was thought fit

simultaneously run controls at the same time. pH and dissolved oxygen content of water media are 7.1 to 7. 5 and 5.6 to 6.5 ml/litre respectively. Preliminary pilot experiments were conducted of exploratory nature to arrive at the broad concentration ranges of pesticides with in which the percentage mortality varied between 5 and 95percent. The concentrations resulting below 5 and above 95 percent mortalities were ignored for the final experiments. The pesticidal concentrations thus selected were used for the final experiments with *Lampito mauritii*. The glassware used was thoroughly cleaned and dried. Filtered and sufficiently aerated pond water was taken in uniform quantities into the various experimental troughs containing worms. Then, appropriate quantities of the stock solution were added to yield the desired concentrations at which the experiments were conducted. The concentration ranges used in the final experiments were in an increasing order at equal intervals of time. Exactly 200ml of water was provided per animal. The toxic media were repeatedly renewed in the experimental chambers as suggested by Environment Protect Agency (EPA, 1975). Periodically the oxygen levels in the experimental media were checked to insure that sufficient oxygen level were maintained.

Immediately after the subjection of the worms to experimental media they were continuously observed hour after hour. Indication of immobility when a touch or mild prick by an entomological pin is given to the posterior part of the worm was considered as dead. The mortalities encountered in each experimental chamber were recorded periodically. In the dose mortality study the total kill observed at the end of each 24hrs period was taken into account for a period of 96hrs. Experiments were conducted in aqueous media to find out LC_{50} values for 24, 48, 72 and 96hrs exposure of the worms to the insecticide monocrotophos. All the experiments were repeated several times to register the constancy of the toxicity of each pesticide. After scoring the mortalities of the worms at various test concentrations, the data were processed employing unweighted regression method as suggested by Finney (1971) to evaluate the LC_{50} (Median Lethal concentrations). The data were recorded and calculated mortalities obtained in these investigations were further subject to heterogeneity test employing chi-square analysis (Finney, 1971). The dose-mortalities obtained in the present study were plotted on a probit graph paper against the calculated dose-mortalities at various concentrations.

RESULTS

The data obtained for *Lampito mauritii* on exposure to organophosphate Insecticide monocrotophos are presented in Table -1. The dose mortalities obtained for *Lampito mauritii* on exposure to 24 hrs to the concentration range of 2.5 to 11.0 ppm of monocrotophos showed 50 percent deaths at a concentration range of 5.90 to 7.59 ppm. On calculation the LC_{50} value for 24hrs obtained was found to be 6.75ppm for monocrotophos, similarly the LC_{50} value for 48hrs was also determined by exposing the worm to a concentration range of 2.0 to 10 ppm of at intervals of 1ppm and the LC_{50} pesticidal concentration for 48hrs was 6.25 ppm. The results indicate that the LC_{50}value for 72 hrs with the concentration range of 1 to 10 ppm was found to be 5.25 ppm. In 96hrs exposure study the pesticide concentration in the test media varied from 0.5 to 9.0ppm at a concentration of 4.50ppm, 50 percent of the test animals died in 96hrs. Hence the LC50 value for 96hrs exposure was found to be 4.50 ppm in Table 1& Fig -1.Concentrations below the LC_{50} concentration level are expressed as sub-lethal concentration. But in the present study a concentration which is 1/5th of the LC_{50} concentration has been considered. The sub- lethal concentration values were 1.35, 1.25, 1.05 and 0.90 ppm for 24, 48, 72 and 96 hrs respectively in Table1 and Fig.1. The results obtained on dose mortality studies of an organophosphate insecticide monocrotophos to *Lampito mauritii* reveal clearly that the worm reacted differently to pesticide concentrations in the present study.

Table 1: Toxicity of monocrotophos to the earth worm *Lampito mauritii*

Exp. Period (hrs)	$^{LC}50$ concentration in ppm	95% Fiducial Limit	1/5th Of $^{LC}50$ Values	95% Fiducial Limit
24	6.75	5.90 -7.59	1.35	1.08-1.62
48	6.25	5.46 -7.03	1.25	1.0-1.50
72	5.25	4.59 -5.90	1.05	0.84-1.26
96	4.50	3.93 -5.06	0.90	0.72-1.08

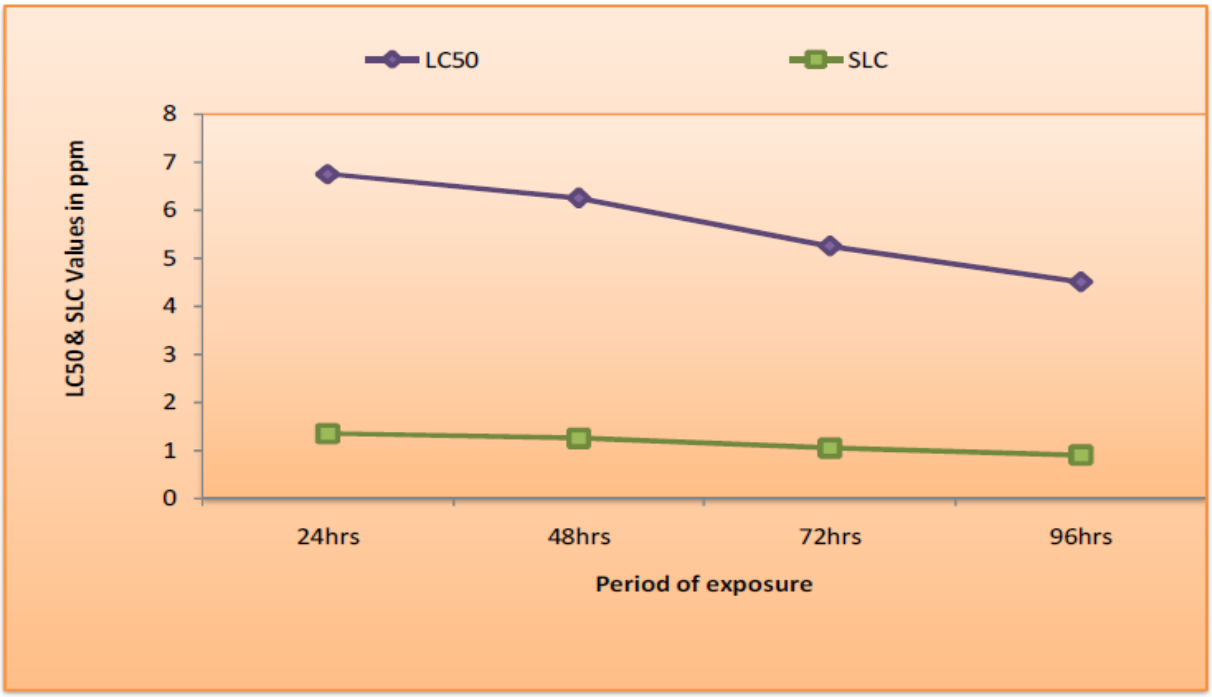


Fig -1: Regression lines showing dose mortality relationship of *L. mauritii* subjected to Monocrotophos for test periods in water medium.

BEHAVIOUR OF WORMS

The present studies revealed the changes in their morphological features and in the patterns of behaviour, when exposed to monocrotophos pesticide. The changes were noticed to depend on the experimental periods and concentration levels of the pesticide compounds of the experimental media. The colour of the worm's changed from brown to pale brown, mucous material was secreted by the worms. When exposed to monocrotophos the amount of mucous produced was comparatively high at higher concentration and low at low concentration. A gradual reduction was noticed in the quantity of mucous secreted with the increase in time of exposure to the pesticide. The intense coiling of the worm noticed after their exposure to toxic media monocrotophos is more effective, as noticed in the present studies, as evidence by the quick and haphazard moments of the worms. After two to three days of exposure the worms became lethargic and moribund and also become immobile and remained curled in a semicircular fashion.

At higher concentration, *Lampito mauritii* developed swellings; sores and even rupture develop in the entire body when exposed to monocrotophos. Further, protrusion of internal visceral parts through ruptured regions on the body wall became visible in the monocrotophos exposed worms (Plate 1-4). In general it was observed that the movement of the worm released in water, containing pesticide, the movements of the worms was invariably quick and erratic in behaviour obviously, as a reaction to toxic action of the chemical. However, this apparent activity of the worms gradually became dissipated with increasing exposure periods of time and concentration.

Moderately large swellings appeared in the anterior parts of the body in the first 3 to 4 segments covering the esophageal region (Plate 1- 4). On certain occasions the worms showed swellings at the clitellar region. The swellings in the posterior segments were less frequently noticed in pesticide exposed worms. It may be mentioned, however, that although observation on the behaviour of the worms indicate the relative levels of toxic influence of the pesticide in the experimental media from the moment they are released into the above media, their movements and/ other changes in the worms noticed at short intervals of time could be made out as it was not possible to quantify the observed differences.



Plate-1: Coiling of the worm



Plate-2: Mucous secretion of the body



Plate-3: Reddening of the entire body



Plate-4: Swelling of the entire body

DISCUSSION

The present studies were principally aimed at investigating the 24, 48, 72 and 96 hrs LC_{50} values on exposure to monocrotophos. The differences between observed and calculated values were tested for significance using chi-square test which showed that the difference was not significant at P = 0.05 level at concentrations 6.75, 6.25, 5.25 and 4.50 ppm respectively. The experimental data clearly indicate the relative toxicity of the insecticide monocrotophos to *Lampito mauritii* under the laboratory conditions.

The results indicate that the worms showed higher mortality rate, even at lower concentrations of monocrotophos high mortality in water may be due to two reasons. The pesticide in medium of water diffuses into body easily through body wall. As there is no food supply, naturally the animal will starve. The test animal being terrestrial animal and soft skinned, possible a quicker exchange of the toxicant is possible and there by neurotoxicity effects may ensure since the quantity of toxicant in water medium may directly enter more readily through the body openings resulting in reddening and in the appearance of swellings in the anterior segments in the worms within two days after their exposure to insecticide (Plates 1 & 2). Similar effects were reported in the case of *Lumbricus terrestris, Lumbricus rubellus, Eisenia foetida, Aporrectodea caligilosa, Allobophora chlorotica, Lampito mauritii* and *Parvularcula bermudensis* when exposed to variety of organophosphate, organochlorine and carbamate insecticides (Vijayalakshmi, 1980; Janardhanarao, 1984). In general it was the movements of the worm released in water containing pesticide, the movements of the worms were invariably quick and erratic in behaviour, obviously as a reaction to toxic action of the chemical. However, this apparent activity of the worms gradually became dissipated with increasing exposure periods of time and concentration. Moderately large swellings appeared in the anterior parts of the body in the first 3 to 4 segments covering the esophageal region. On certain occasions the worms showed swellings at the clitellar region. The swellings in the posterior segments were less frequently noticed in the toxic media exposed worms (Sattibabu, 2013; Rakesh, 2014). Stenersen et.al., (1973) is of the opinion that most of the carbamate insecticides like carbaryl, carbofuran are highly toxic to the earthworms like *Lumbricus terrestris* Cathey, (1973); Kring, (1969); Gilman & Vardanis (1974) on exposure. The pesticides were reported to cause characteristic sores and tumor-like swellings in earthworms. Like organophosphate insecticides and several carbamates were also found to be neurotoxic producing systemic changes in a number of aquatic and terrestrial organisms (Vijayalakshmi, 1980).At higher concentration,

Lampito mauritii developed swelling in the entire body when exposed to dichlorvos. Protrusion of internal visceral parts through ruptured regions on the body wall became visible in the dichlorvos exposed worms.

At times the worms showed swellings at the clitellar region (Bharathi and Subba Rao, 1987). Immediately after exposure to pentachlorophenol *Lampito mauritii* have become highly agitated and slowly curled-up into horse shoe and circular shapes followed by arresting their movements. In course of time the anterior part of the worms turned pale and characteristic wounds and sores appeared on different regions of the body. In higher concentration the worms became rigid similar to that reported in *Lumbricus terrestris* exposed to carbofuran and carbaryl (Stenersen, 1973). The present investigation on the worm involving organophosphate compound showed (Plate 1 & 2) similar changes with slight variations in the characteristic sores, swellings, cuts etc., in the pesticide exposed worms. Although the toxicity levels of the insecticide are different to *Lampito mauritii* the characteristic abnormalities found were nearly similar. The reddening, swellings, sores, cuts, blister, etc., in worms noticed in exposed in test media.

In the light of the present findings of comprehensive assessment of the toxicity levels (LC_{50} values) of insecticide and the effects on the earthworms is of a great value. A perusal of literature dealing with assessment of LC_{50} values of insecticide in respect of earthworms indicate that a quite a large number of publications appeared dealing with the toxicity levels of several agro chemicals based on field studies (Doane, 1962; Edwards *et al*., 1968; Thompson, 1973; Vijayalakshmi, 1980; Bharathi,1983; Sattibabu, 2013; Rakesh, 2014). These reports indicate the toxic nature of a number of organochlorine, organophosphate and carbamate compounds to a variety of non-target organisms including earth worms. Very few investigations are available dealing with the toxicity of pesticides to terrestrial oligochaete species under laboratory conditions (Martin and Wiggans, 1959; Stenersen *et al*., 1973, Chio and Sanborn, 1978; Stenersen, 1979a; Stenersen and Oien, 1980, Vijayalakshmi,1980; Bharathi,1983; Sattibabu, 2013; Rakesh, 2014).

In the case of monocrotophos, concentration levels above 1.0 ppm were noticed to be toxic to the aquatic oligochaete *Tubifex tubifex*. In the present instance *Lampito mauritii* being longer in size tolerated a high concentration of monocrotophos shows LC_{50} value as 0.85 ppm for 96 hrs exposure. Kale and Krishnamoorthy (1979) reported 30 day LC_{50} value for carbaryl compound Sevin as 375 ppm in *Pontoscolex corethrurus*. They reported higher concentrations of the carbamate compounds inhibiting release of castings, resulting loss in weight, survivability and retarded growth. They further felt that higher concentration of these pesticides might as well reduce populations in the ecosystem. Cathey (1973) made a valuable contribution in the field of oligochaete toxicology in his study on the toxic effects of carbamate pesticides to *Lumbricus terrestris*, she reported that a 21 day LC_{50} was 20 µg of carbaryl to *Lumbricus terrestris* in addition a good number of behavioral changes such as withdrawal response i.e., extensive coiling, bodily constrictions, swellings, blisters and reddening of anterior parts consequent to carbaryl treatment were also notice in *Lumbricus terrestris.*

A critical examination of the effects of the chemicals chosen reveals that *Lampito mauritii* exhibited initial hyperactivity at low pesticidal concentrations and developed lethargy at higher concentration of the organophosphate compound. The insecticide presently used is systemic in nature and neurotoxic like any other organophosphates or carbamates as reported by Cathey (1973), Stenersen *et al*., (1973), Stenersen (1979b), Kale and Krishnamurthy (1979), Vijayalakshmi (1980), Bharathi (1983), Sattibabu (2013), Rakesh (2014). Based on laboratory studies, Richards and Cutkomp (1946) and Martin and Wiggans (1959) showed that the DDT in water could survive amounts of at least 1: 10,000. The present findings also showed that at lower concentration the pesticide was stimulatory to the worm rather than inhibitory because the pesticide does act on central nervous system. The hyperactivity at low pesticide concentration and the lethargy developed by the worm at high concentration positively affect changes in population of the worms. Capacities for bioaccumulation and transformation by earthworms on repeated applications of the pesticides have been amply demonstrated (Stenersen *et al*., 1973). In the present study *Lampito mauritii* showed that the toxicity increased with exposure period. This suggests that the toxicity is associated with accumulation of monocrotophos in excess amounts that may be metabolized and prove injurious to the earthworms.

REFERENCES

1. Ahmed, Y.M. 1991. Kinetic study on inhibition of earthworm acetylcholinestrease by carbamate insecticides. Journal of the Egyptian Society of Parasitology, 21: 283-292.
2. Bharathi, Ch.1983. Studies on the effects of organophosphate insecticides, phosphamidon, monocrotophos and dichlorvos on some aspects of physiology of the earthworm, *Lampito mauritii* (Kinberg). Ph. D. Thesis Dept. Zool. Andhra University. pp: 186.
3. Bharathi, Ch. and Subba Rao, B. S. S. R. 1987. Some observation on behavioural and morphological changes in the earthworm *Lampito mauritii* to insecticidal exposure. Aspects of Behaviour (Ismail, S. A. and Alawdeen, S. S., Eds). Dept. Zool. The New College. Madras, pp: 150-153.
   brackish water oligochaete, Pontodrilus bermudensis Beddard in relation to salinity
4. Cathey, B. 1973. Some Morphological and Physiological Studies on the Effects of Carbaryl on the Earthworm *Lumbricus terrestris*, Diss. Abstr. mt., 34B: 3004.
5. Chio, H. and Sanborn, J. R. 1978. The metabolism of atrazine, chloramben and dicamba in Earth worms (*Lumbricus terrestris*) from treated and untreated plots. Weed Sci. 26, 331-335.
6. Doane, C.C. 1962. Effects of certain insecticides on earthworms. I Econ. Entomol. 55: 416-418.
7. Edwards, C.A., Thompson, A.R. and Beynon, K.I. 1968. Some effects of chiorfenvinfos, an organophosphorus insecticide, on populations of soil animals. Rev. Eco. Biol. Sol. 5: 199-224.
8. Edwards, C. A., Thompson, A. R., and Beynon, K. I. 1967. Some effects of chlorfenvinphos, an organophosphorus insecticide on populations of soil animals. *Rev. Ecol. Biol. Sol.* **5**: 199–214.
9. APHA, AWWA and WEF (1998) Standard methods for the examination of water and waste water, 20th edition, Clesceri, L.S. Greenberg, A.E. and Eaton, A.D. (Eds.), American Public Health Association, American Water Work Association, Water Environment Federation, Washington DC.
10. Finney. D.J. 1971. Probit analysis. Cambridge Univ. Press, Cambridge, 333 pp.
11. Gilman, A. and Vardanis, A.1974. Carbofuran comparative toxicity and metabolism in the worms *Lumbricus terrestris* L. and *Eisenia fetida.* S. I Agric. Food Chem. 22: 625-628.
12. Goven, A. J., Eyambe, G. S., Fitzpaatrick, L. C.,Venables, G.J. and Cooper, E. L. 1993. Cellular biomarkers for measuring toxicity of xenobiotics. Environ. Toxicol., Chem. 12 (5): 863-870.
13. Heungens, A. 1966. Bestrijding van Regenwormen in sparregrond on in vitro. Med. Rijksfak. Lanbd. W. Sch. Gent. 31, 329-342.
14. Heungens, A. 1969. L'Influence de la Fumure et des pesticides aldrine, Carbaaryl et DBCP Sur la Faune du Sol dans la culture des Azalees. Revue. Ecologic. El. Biologie. Du. sol.6(2): 131-145.
15. Hopkins A.R., Kirk V.M. 1957. Effects of several insecticides on the English red worm J Econ. Entomol. 1957; 50:699- 700.
16. Janardhana Rao. M. 1992. Effect of salinity and the pesticide endosulfan on the physiology of *Mytilopsis sallei*, Ph.D. Thesis, Andhra University, Visakhapatnam.
17. Kale, R.D. and Krishnamoorthy, R.V. 1979. Pesticidal effects of Sevin (ci-naphthyl-n-methyl carbamate) on the survival and abundance of the earthworm *Pentoscolex corethrurus*. Proc. Ind Acad. Sd. 88b(I): 391-396.
18. Kavitha, P. & Rao, J. V. 2007. Oxidative stress and locomotor behaviour response as biomarkers for assessing recovery status of mosquito fish, *Gambusia affinis* after lethal effect of an organophosphate pesticide, monocrotophos. Pesticide Biochemistry and Physiology, 87: 182–188.
19. Kring, J. B. 1969. Mortality of the earthworm *Lumbricus terrestris* following soil applications of insecticides to a tobacco field. J. Econ. Ent. 62, 963.
20. Kulkarni, V. D. 1989. Physiological studies on the earthworm *Lampito mauritii* (Kinberg, 1867) in relation to the impact of some environmental factors. Ph.D. Thesis, Marathwada University, Aurangabad, M. S. India.
21. Martin, L. N and Wiggans, S. C. 1959. The tolerance of earthworms to certain insecticides, herbicides and fertilizers. Oklahoma Agric. Exp. Stat. Proc. Ser. 334.

22. Patnaik, H. K. and Madhab, C. D. 1991. Monocrotophos toxicity and its effect on ammonia and urea excretion of some subtropical grassland earthworm species. Proc. Natn. Acad. Sci. India. B 61 (3): 273-282.
23. Rakesh, S. 2014. Studies on the effect of carbofuran and salinity variations on the physiology of a brakish water oligochaete,*Pontodrilus bermudensis* (Beddard) Ph.D., Thesis Andhra University, Visakhapatnam, pp.201.
24. Richards, A .G. and Cutkomp, L. K. 1946. Correlation between the possession of a chitinous cuticle and sensitivity of DDT. Biol. Bull. 90, 97-108.
25. Riepert, F. Römbke, J. and Moser, T. 2009. Eco toxicological Characterization of Waste, pp.3-25, Springer, New York, USA.
26. Rombke, J., Garcia, M. V. and Scheffczyk, A. 2007. Effects of the fungicide benomyl on earthworms in laboratory tests under tropical and temperate conditions," Archives of Environmental Contamination and Toxicology, vol. 53, no. 4, pp. 590–598.
27. Sattibabu, D. 2013. Studies on the effect of the pesticide Monocrotophos on the physiology of a brackish water oligochaete, *Pontodrilus bermudensis* Beddard in relation to salinity variations. Ph.D. Thesis, Andhra University, Waltair, Visakhapatnam.
28. Senapati, B. K., Pani, S. C. and Sahu, S. 1987. Impact of malathion on the population of earthworm biology and secondary production of *Drawida willsi* Michaelsen, a dominant earthworm in paddy field Proc. Nat. Con. Env. Imapact. On Biosystem. January, Madras.
29. Stenersen, J. 1979a. Action of pesticides on earthworms. Part I. The toxicity of cholinesterase worms as evaluated by laboratory tests. Pestic. Sci.10, 66-74.
30. Stenersen, J. and Oien, N. 1980. Action of pesticides on earthworms Part IV. Uptake and elimination of oxamyl compared with carbofuran. Pestic. Sci. 11, 396-400.
31. Stenersen, J. Gilman, A. and Vardanis, A. 1973. Carbofuran. Its toxicity to and metabolism by earthworm (Lumbricus terrestris). J. Agric. Food chem. 21, 166-171.
32. Stenersen, J., Guthenberg, C. and Mannervik, B. 1979. Glutathione S-transferase in earthworms (Lumbricus terrestris). Bio chem. J. 181, 47-50.
33. Thompson A.R. 1971. Effects of nine insectides on the numbers and biomass of earthworms in pasture. Bull. Environ. Contam. Toxicol. 5 (6) : 577-586
34. Thompson, A.R. 1973. Pesticide residues in soil invertebrates, in: C.A. Edwards, (ed.). Environmental Pollution by Pesticides. Plenum press, London, Pp. 87-133.
35. Vijayalakshmi, S. 1980. In vivo effects of sumithion on tissue respiration and enzyme activity in the fish, *Etroplus maculates*. Experientia (Switz.). 36, 1280.

ISSN 1070-3632, Russian Journal of General Chemistry, 2019, Vol. 89, No. 2, pp. 324–329. © Pleiades Publishing, Ltd., 2019.

Synthesis and Anticancer Activity of Amide Derivatives of 1,2-Isoxazole Combined 1,2,4-Thiadiazole

S. Shahinshavali[a], R. Sreenivasulu[b], V. R. Guttikonda[c], D. Kolli[d], and M. V. B. Rao[a]*

[a] *Department of Chemistry, Krishna University, Machilipatnam, Andhra Pradesh, 521001 India*
**e-mail: professormandava@gmail.com*

[b] *Department of Chemistry, University College of Engineering (Autonomous), Jawaharlal Nehru Technological University, Kakinada, Andhra Pradesh, 533003 India*

[c] *Department of Chemistry, SRR and CVR Government Degree College (Autonomous), Vijayawada, Andhra Pradesh, 520004 India*

[d] *Department of Chemistry, Koneru Lakshmaiah Education Foundation, Green Fields, Vaddeswaram, Andhra Pradesh, 522502 India*

Received November 26, 2018; revised February 15, 2019; accepted February 18, 2019

Abstract—A series of amide derivatives of 1,2-isoxazole combined with 1,2,4-thiadiazole are synthesized **11a–11j**. Their chemical structures are confirmed by ^{1}H and ^{13}C NMR, and mass spectra. The products are tested for their anticancer activity against four types of human cancer cell lines, including MCF-7 (breast), A549 (lung), Colo-205 (colon), and A2780 (ovarian). Etoposide is used as a positive control. Most of the compounds show good anticancer activity. The compounds **11b, 11c, 11d, 11e, 11g,** and **11j** demonstrate more potent activity than etoposide.

Keywords: Luminespib, Cefozopram, isoxazole, thiadiazole, anticancer activity

DOI: 10.1134/S1070363219020257

INTRODUCTION

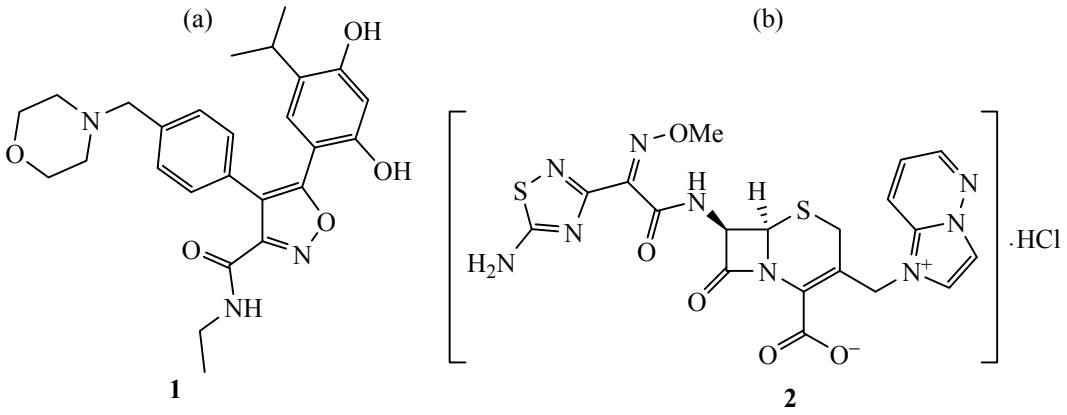
Different types of heterocyclic derivatives are used efficiently in anticancer chemotherapy [1–14]. Isoxazole derivatives are used extensively as agrochemicals and in medicine [15–18] due to a broad spectrum of activity, including anticancer [19], antifungal [20], anti-inflammatory [21], and antimicrobial [22]. Among these, Luminespib (**1**, NVP-AUY922) (see figure) is an FDA approved anticancer drug candidate. Thiadiazole derivatives are important functional components of molecules of many natural compounds [23] and drugs, for example, such as antibiotic Cefozopram (**2**) (see figure) which is used for treatment of CNS [24].

Based on the above information accumulated for isoxazole and thiadiazole and in continuation of our studies of heterocyclic compounds, we designed and synthesized a series of amide derivatives of 1,2-isoxazole combined with 1,2,4-thiadiazole **11a**–**11j**. Their structures were confirmed by ^{1}H and ^{13}C NMR and mass spectra. The compounds were tested for anticancer activity against four human cancer cell lines.

RESULTS AND DISCUSSION

Synthetic approach to the target compounds **11a**–**11j** (Scheme 1) started with introduction of compound **3** in the Claisen-Schmidt reaction with 4-cyano-benzaldehyde **4** which led to pure chalcone **5** with good yield. The following reaction of the intermediate **5** with 4-nitrobenzothioamide **6** in presence of $AlCl_3$ gave the product of cycloaddition **7**, which reacted with hydroxylamine hydrochloride to give isoxazole derivative **8**. The following reduction of compound **8** with Zn-dust in acetic acid with formation of amine **9**, and reaction of the latter with aromatic chloroanhydrides **10a**–**10j** led to the title compounds **11a**–**11j**.

Biological evaluation. *In vitro cytotoxicity.* The synthesized compounds **11a**–**11j** were screened for their anticancer activity against four human cancer cell lines such as MCF-7 (breast), A549 (lung), Colo-205 (colon), and A2780 (ovarian) by the MTT assay (see the table). Etoposide was used as a positive control. The products **11b**, **11c**, **11d**, **11e**, **11g**, and **11j** displayed higher activity than etoposide. The com-



1 **2**

Structures of (a) Luminespib and (b) Cefozopram.

pounds were examined for structure-activity relationship (SAR). The compound **11b** containing 3,4,5-trimethoxy substituents on the phenyl ring demonstrated high activity with IC_{50} values MCF-7 = 0.24±0.089 μM, A549 = 0.18±0.023 μM, Colo-205 = 0.11±0.05 μM, and A2780 = 0.55±0.072 μM, respectively. Compound **11c** with 3,5-dimethoxy substituents displayed lower activity (MCF-7 = 0.39±0.033, A549 = 1.33±0.45, Colo-205 = 0.93±0.065, and A2780 = 1.37±0.35 μM) than **11b**. The compound **11d** containing one 4-methoxy substituent exhibited the activity lower than the above two analogues. Replacement of 4-methoxy group by 4-chloro substituent on the phenyl ring **11e** resulted in its poorest activity. The compound **11g** with the 4-nitro group exhibited the highest activity. The compound **11h** with 3,5-dinitro substitution exhibited very poor activity. Compounds **11f** and **11i** with the 4-cyano substituent was of moderate activity.

EXPERIMENTAL

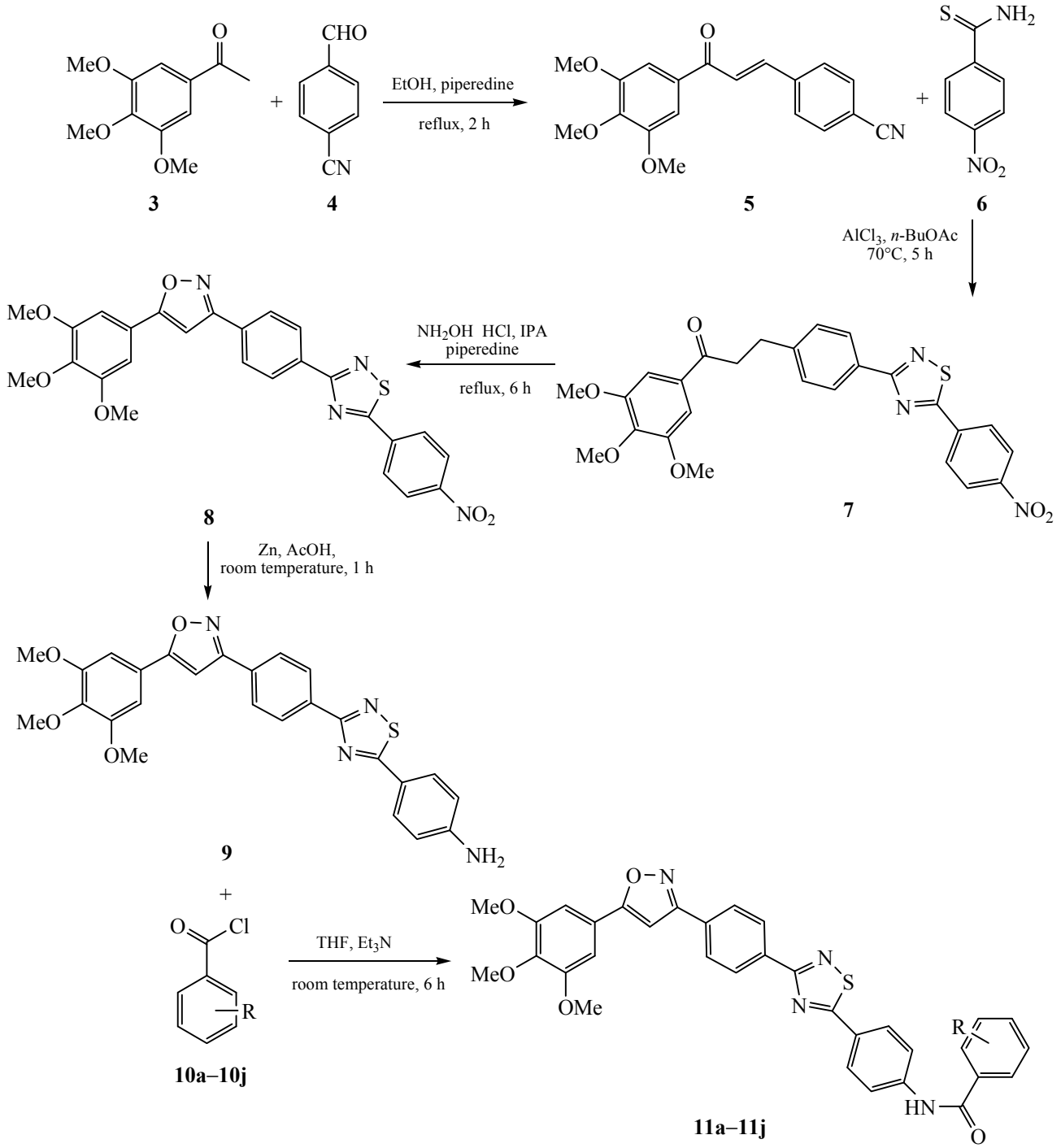
All chemicals and reagents were obtained from Aldrich (Sigma-Aldrich, St. Louis, MO, USA) and Lancaster (Alfa Aesar, Johnson Matthey Company, Ward Hill, MA, USA), and were used without further purification. Reactions were monitored by TLC, performed on silica gel glass plates containing 60 F-254, and visualized by UV light or iodine indicator. ^{1}H and ^{13}C NMR spectra were measured on a Gemini Varian-VXR-unity (300 MHz) spectrometer using DMSO-d_6 as a solvent ($CDCl_3$ for 5) and TMS as the internal standard. ESI spectra were recorded on a Micro mass,

Anticancer activity of the synthesized compounds **11a**–**11j** (IC_{50} μM)[a]

Compound	MCF-7[b]	A549[c]	Colo-205[d]	A2780[e]
11a	2.090±1.87	3.410±1.930	Not active	4.55±2.330
11b	0.240±0.089	0.180±0.023	0.11±0.050	0.55±0.072
11c	0.390±0.033	1.330±0.450	0.93±0.065	1.37±0.350
11d	1.990±0.540	1.830±0.560	1.44±0.880	2.43±1.880
11e	2.440±1.900	1.760±0.190	3.65±1.980	Not active
11f	4.110±2.400	9.670±5.100	Not active	8.34±5.090
11g	0.034±0.004	0.011±0.001	1.23±0.480	0.33±0.022
11h	2.170±1.230	2.880±1.990	7.33±4.100	5.60±4.300
11i	10.40±6.330	3.190±2.150	13.2±7.230	6.23±5.770
11j	1.460±0.320	1.670±0.450	1.42±0.360	Not active
Etoposide	2.110±0.024	3.080±0.135	0.13±0.017	1.31±0.270

[a] Each data is represented as mean ±S.D. of different experiments performed in triplicates. [b] (MCF-7) human breast cancer cell line. [c] (A549) human lung cancer cell line. [d] (Colo-205) human colon cancer cell line. [e] (A2780) human ovarian cancer cell line.

Scheme 1. Synthesis of amide derivatives of 1,2-isoxazole combined with 1,2,4-thiadiazole.



R = H (**10a, 11a**), 3,4,5-trimethoxy (**10b, 11b**), 3,5-dimethoxy (**10c, 11c**), 4-methoxy (**10d, 11d**), 4-cloro (**10e, 11e**), 4-bromo (**10f, 11f**), 4-nitro (**10g, 11g**), 3,5-dinitro (**10h, 11h**), 4-cyano, (**10i, 11i**), 4-methyl (**10j, 11j**).

Quattro LC using ESI+ software with capillary voltage 3.98 kV and ESI mode positive ion trap detector. Melting points were determined on an electrothermal melting point apparatus, and are uncorrected.

4-[(*E*)-3-(3,4,5-Trimethoxyphenyl)-3-oxoprop-1-enyl]benzonitrile (5). 3,4,5-Trimethoxyacetophenone **3** (20 g, 0.0951 mmol) was dissolved in 50 mL of ethanol, followed by addition of 4-cyanobenzaldehyde

4 (12.5 g, 0.0951 mmol) and 3 drops of piperdine base. The reaction mixture was refluxed for 2 h. After cooling the reaction mixture down, water (20 mL) was added slowly to it. The crystalline precipitate was filtered off and purified by column chromatography using ethyl acetate–hexane (1 : 1) as an eluent to afford pure compound **5**. Yield 73%. ^{1}H NMR spectrum, δ, ppm: 3.93 s (3H), 3.96 s (6H), 7.28 s (2H), 7.55 d (1H, J = 15.5 Hz), 7.68 d (2H, J = 7.23 Hz), 7.73 d (2H, J = 7.23 Hz), 7.78 d (1H, J = 15.5 Hz). MS (ESI): 325 $[M + H]^+$.

(*E*)-1-(3,4,5-Trimethoxyphenyl)-3-{4-[5-(4-nitrophenyl)-1,2,4-thiadiazol-3-yl]phenyl}prop-2-en-1-one (7). 4-[(*E*)-3-(3,4,5-Trimethoxyphenyl)-3-oxoprop-1-enyl]benzonitrile (**5**) (20 g, 0.0617 mmol) and $AlCl_3$ (8.2 g, 0.0617 mmol) were mixed in *n*-butyl acetate (50 mL), and then, upon stirring at 70°C, 4-nitrobenzothioamide **6** (3.9 mL, 0.030 mmol) was added dropwise. The mixture was stirred at 70°C for 5 h. After cooled down to room temperature and addition of 0.3 mL of water the reaction mixture was stirred at room temperature for 24 h. The organic and aqueous layers were separated, and the aqueous layer was extracted with ethyl acetate (3×20 mL). The combined organic layers were dried over anhydrous Na_2SO_4, concentrated and purified by column chromatography on silica gel, using ethyl acetate–petroleum ether (1 : 1) as an eluent to afford pure compound **7**. Yield 70%. ^{1}H NMR spectrum, δ, ppm: 3.93 s (3H), 3.96 s (6H), 7.28 s (2H), 7.57 d (1H, J = 15.6 Hz), 7.70 d (2H, J = 7.25 Hz), 7.75 d (2H, J = 7.25 Hz), 7.78 d (1H, J = 15.6 Hz), 7.83 d (2H, J = 7.27 Hz), 8.10 d (2H, J = 7.27 Hz). MS (ESI): 505 $[M + H]^+$.

3-{4-[5-(3,4,5-Trimethoxyphenyl)isoxazol-3-yl]-phenyl}-5-(4-nitrophenyl)-1,2,4-thiadia zole (8). A mixture of compound 7 (20 g, 0.039 mmol) with hydroxylamine hydrochloride (8.2 g, 0.117 mmol) was dissolved in 50 mL of 2-propanol, then 3 mL of pyridine were added and the reaction mixture was stirred upon refluxing for 6 h. After completion of reaction, according to TLC, the solvent was evaporated under reduced pressure. The precipitated product was washed with water (3×20 mL) and purified by column chromatography using ethyl acetate–hexane (7 : 3) as an eluent to afford pure compound **8**. Yield 70%. ^{1}H NMR spectrum, δ, ppm: 3.93 s (3H), 3.96 s (6H), 6.66 s (1H), 7.27 s (2H), 7.71 d (2H, J = 7.26 Hz), 7.77 d (2H, J = 7.26 Hz), 7.82 d (2H, J = 7.28 Hz), 8.11 d (2H, J = 7.28 Hz). MS (ESI): 518 $[M + H]^+$.

4-{3-(4-[5-(3,4,5-Trimethoxyphenyl)isoxazol-3-yl]phenyl)-1,2,4-thiadiazol-5-yl}benzenamine (9). To a solution of (*E*)-1-(3,4,5-trimethoxyphenyl)-3-{4-[5-(4-nitrophenyl)-1,2,4-thiadiazol-3-yl]phenyl}prop-2-en-1-one (**8**) (13 g, 0.0251 mmol) in acetic acid (40 mL) was added zinc powder (2.3 g, 0.0751 mmol). The reaction mixture was stirred at room temperature for 1 h. After completion of the process, according to TLC, the reaction mixture was filtered (Celite), and the filtrate was evaporated to dryness giving pure compound **9**. Yield 76%. ^{1}H NMR spectrum, δ, ppm: 3.93 s (3H), 3.96 s (6H), 5.51 br.s (2H), 6.66 s (1H), 7.28 s (2H), 7.70 d (2H, J = 7.25 Hz), 7.76 d (2H, J = 7.25 Hz), 7.80 d (2H, J = 7.27 Hz), 8.09 d (2H, J = 7.27 Hz). MS (ESI): 488 $[M + H]^+$.

General method of synthesis of amide derivatives 11a–11j. The compound 9 (500 mg, 0.0010 mmol) was dissolved in 10 mL of dry THF, and 0.0010 mmol of one of benzoyl chlorides **10a**–**10j** and 0.002 mmol of Et_3N were added. The reaction mixture was stirred at room temperature for 6 h, till completion of the process (TLC), then it was washed with water and extracted with CH_2Cl_2, dried over anhydrous Na_2SO_4. The crude product was purified by column chromatography using ethyl acetate–hexane (1 : 1) as an eluent to obtain the corresponding pure compound **11a**–**11j**.

***N*-(4-{3-(4-[5-(3,4,5-Trimethoxyphenyl)isoxazol-3-yl]phenyl)-1,2,4-thiadiazol-5-yl}phenyl)benzamide (11a).** Yield 51%, mp 300–302°C. ^{1}H NMR spectrum, δ, ppm: 3.93 s (3H), 3.96 s (6H), 6.66 s (1H), 7.28 s (2H), 7.52 t (1H), 7.56–7.66 m (2H), 7.70 d (2H, J = 7.24 Hz), 7.75 d (2H, J = 7.24 Hz), 7.78–7.88 m (4H), 8.07 d (2H, J = 7.26 Hz), 8.57 s (1H). ^{13}C NMR spectrum, δ, ppm: 57.4, 61.8, 96.4, 106.3, 123.8, 126.5, 128.3, 129.4, 129.7, 130.4, 131.2, 132.7, 133.4, 134.7, 140.5, 145.3, 156.7, 158.6, 159.5, 160.7, 168.4, 170.4. MS (ESI): 592 $[M + H]^+$.

3,4,5-Trimethoxy-*N*-(4-{3-(4-[5-(3,4,5-trimethoxyphenyl)isoxazol-3-yl]phenyl)-1,2,4-thiadiazol-5-yl}-phenyl)benzamide (11b). Yield 47%, mp 317–319°C. ^{1}H NMR spectrum, δ, ppm: 3.87 s (6H), 3.90 s (3H), 3.93 s (3H), 3.96 s (6H), 6.65 s (1H), 7.27 s (2H), 7.32 s (2H), 7.69 d (2H, J = 7.23 Hz), 7.76 d (2H, J = 7.23 Hz), 7.80 d (2H, J = 7.25 Hz), 8.08 d (2H, J = 7.25 Hz), 8.56 s (1H). ^{13}C NMR spectrum, δ, ppm: 56.5, 57.8, 61.2, 62.5, 96.3, 106.4, 107.8, 123.4, 126.5, 127.6, 129.8, 130.4, 130.8, 131.5, 133.6, 134.6, 139.6, 143.2, 145.6, 156.3, 157.8, 158.2, 160.5, 163.2, 169.3, 170.6. MS (ESI): 682 $[M + H]^+$.

3,5-Dimethoxy-*N*-(4-{3-(4-[5-(3,4,5-trimethoxyphenyl)isoxazol-3-yl]phenyl)-1,2,4-thiadiazol-5-yl}phenyl)benzamide (11c). Yield 62%, mp 312–314°C. ^{1}H NMR spectrum, δ, ppm: 3.77 s (6H), 3.92 s (3H), 3.95 s (6H), 6.66 s (1H), 7.27 s (2H), 7.30 s (2H), 7.68 d (2H, *J* = 7.24 Hz), 7.77 d (2H, *J* = 7.24 Hz), 7.81 d (2H, *J* = 7.26 Hz), 8.09 d (2H, *J* = 7.26 Hz), 8.57 s (1H). ^{13}C NMR spectrum, δ, ppm: 56.4, 57.3, 61.9, 96.4, 106.3, 107.4, 118.4, 123.4, 126.7, 127.4, 129.6, 130.4, 130.8, 133.5, 134.5, 135.2, 139.6, 145.6, 156.4, 158.6, 160.4, 161.5, 164.7, 169.5, 170.7. MS (ESI): 652 $[M + H]^+$.

4-Methoxy-*N*-(4-{3-(4-[5-(3,4,5-trimethoxyphenyl)-isoxazol-3-yl]phenyl)-1,2,4-thiadiazol-5-yl}phenyl)-benzamide (11d). Yield 59%, mp 307–309°C. ^{1}H NMR spectrum, δ, ppm: 3.79 s (3H), 3.93 s (3H), 3.95 s (6H), 6.65 s (1H), 7.27 s (2H), 7.55 d (2H, *J* = 7.20 Hz), 7.69 d (2H, *J* = 7.25 Hz), 7.73–7.80 m (4H), 7.84 d (2H, *J* = 7.27 Hz), 8.09 d (2H, *J* = 7.27 Hz), 8.57 s (1H). ^{13}C NMR spectrum, δ, ppm: 57.4, 58.3, 61.8, 96.4, 106.3, 115.7, 123.4, 126.5, 128.6, 129.5, 130.4, 130.7, 131.6, 132.4, 133.6, 134.2, 140.7, 145.6, 156.3, 158.7, 160.3, 161.5, 164.6, 169.6, 170.8. MS (ESI): 622 $[M + H]^+$.

4-Chloro-*N*-(4-{3-(4-[5-(3,4,5-trimethoxyphenyl)-isoxazol-3-yl]phenyl)-1,2,4-thiadiazol-5-yl}phenyl)-benzamide (11e). Yield 70%, mp 288–290°C. ^{1}H NMR spectrum, δ, ppm: 3.93 s (3H), 3.95 s (6H), 6.66 s (1H), 7.27 s (2H), 7.63 d (2H, *J* = 7.30 Hz), 7.68 d (2H, *J* = 7.26 Hz), 7.70–7.81 m (4H), 7.86 d (2H, *J* = 7.28 Hz), 8.10 d (2H, *J* = 7.28 Hz), 8.58 s (1H). ^{13}C NMR spectrum, δ, ppm: 57.6, 61.8, 96.4, 106.4, 123.7, 126.4, 127.6, 129.7, 130.6, 131.3, 132.7, 133.4, 134.2, 134.7, 135.2, 140.3, 140.7, 145.4, 156.4, 158.3, 160.5, 161.6, 169.6, 170.7. MS (ESI): 626 $[M + H]^+$.

4-Bromo-*N*-(4-{3-(4-[5-(3,4,5-trimethoxyphenyl)-isoxazol-3-yl]phenyl)-1,2,4-thiadiazol-5-yl}phenyl)-benzamide (11f). Yield 66%, mp 276–278°C. ^{1}H NMR spectrum, δ, ppm: 3.92 s (3H), 3.96 s (6H), 6.67 s (1H), 7.26 s (2H), 7.65 d (2H, *J* = 7.31 Hz), 7.69 d (2H, *J* = 7.27 Hz), 7.72–7.83 m (4H), 7.87 d (2H, *J* = 7.29 Hz), 8.10 d (2H, *J* = 7.29 Hz), 8.58 s (1H). ^{13}C NMR spectrum, δ, ppm: 57.3, 61.8, 96.5, 106.4, 123.4, 124.6, 126.5, 129.5, 130.3, 130.8, 131.4, 131.7, 133.4, 134.7, 135.4, 135.8, 140.4, 145.6, 156.3, 158.3, 160.4, 162.8, 168.9, 170.7. MS (ESI): 671 $[M + H]^+$.

***N*-(4-{3-(4-[5-(3,4,5-Trimethoxyphenyl)isoxazol-3-yl]phenyl)-1,2,4-thiadiazol-5-yl]phenyl)-4-nitro-benzamide (11g).** Yield 73%, mp 283–285°C. ^{1}H NMR spectrum, δ, ppm: 3.93 s (3H), 3.96 s (6H), 6.67 s (1H), 7.27 s (2H), 7.69 d (2H, *J* = 7.28 Hz), 7.73 d (2H, *J* = 7.28 Hz), 7.84–7.95 m (4H), 8.11 d (2H, *J* = 7.30 Hz), 8.20 d (2H, *J* = 7.32 Hz), 8.59 s (1H). ^{13}C NMR spectrum, δ, ppm: 57.4, 61.8, 96.7, 106.4, 123.4, 125.7, 126.5, 127.5, 129.7, 130.3, 130.8, 131.4, 133.6, 134.6, 136.5, 140.4, 145.6, 151.3, 156.7, 158.4, 160.5, 161.7, 169.5, 170.7. MS (ESI): 637 $[M + H]^+$.

***N*-(4-{3-(4-[5-(3,4,5-Trimethoxyphenyl)isoxazol-3-yl)phenyl)-1,2,4-thiadiazol-5-yl)phenyl)-3,5-dinitro-benzamide (11h).** Yield 71%, mp 309–311°C. ^{1}H NMR spectrum, δ, ppm: 3.93 s (3H), 3.96 s (6H), 6.68 s (1H), 7.27 s (2H), 7.70 d (2H, *J* = 7.28 Hz), 7.74 d (2H, *J* = 7.28 Hz), 7.83 d (2H, *J* = 7.31 Hz), 8.12 d (2H, *J* = 7.31 Hz), 8.30 s (1H), 8.36 s (2H), 8.59 s (1H). ^{13}C NMR spectrum, δ, ppm: 57.4, 61.9, 96.7, 106.8, 123.5, 124.7, 126.7, 128.4, 129.6, 130.7, 131.3, 131.7, 133.4, 134.5, 135.2, 136.5, 145.6, 148.3, 156.5, 158.6, 159.3, 160.4, 169.8, 171.8. MS (ESI): 682 $[M + H]^+$.

4-Cyano-*N*-(4-{3-(4-[5-(3,4,5-trimethoxyphenyl)-isoxazol-3-yl]phenyl)-1,2,4-thiadiazol-5-yl}phenyl)-benzamide (11i). Yield 82%, mp 269–271°C. ^{1}H NMR spectrum, δ, ppm: 3.93 s (3H), 3.96 s (6H), 6.68 s (1H), 7.27 s (2H), 7.68 d (2H, *J* = 7.26 Hz), 7.72 d (2H, *J* = 7.26 Hz), 7.81–7.94 m (4H), 8.10 d (2H, *J* = 7.28 Hz), 8.18 d (2H, *J* = 7.27 Hz), 8.57 s (1H). ^{13}C NMR spectrum, δ, ppm: 57.6, 61.8, 96.5, 106.8, 114.5, 119.6, 123.5, 126.8, 129.7, 130.3, 130.7, 131.4, 131.9, 133.5, 134.5, 135.7, 139.4, 140.3, 145.5, 156.4, 158.6, 160.7, 163.4, 169.8, 170.8. MS (ESI): 617 $[M + H]^+$.

***N*-(4-{3-(4-[5-(3,4,5-Trimethoxyphenyl)isoxazol-3-yl]phenyl)-1,2,4-thiadiazol-5-yl}phenyl)-4-methyl-benzamide (11j).** Yield 54%, mp 265–267°C. ^{1}H NMR spectrum, δ, ppm: 2.43 s (3H), 3.93 s (3H), 3.96 s (6H), 6.66 s (1H), 7.24 s (2H), 7.46 d (2H, *J* = 7.19 Hz), 7.55 d (2H, *J* = 7.19 Hz), 7.68 d (2H, *J* = 7.23 Hz), 7.72 d (2H, *J* = 7.23 Hz), 7.80 d (2H, *J* = 7.26 Hz), 8.09 d (2H, *J* = 7.26 Hz), 8.56 s (1H). ^{13}C NMR spectrum, δ, ppm: 24.8, 57.6, 61.8, 96.4, 106.8, 123.4, 126.5, 128.5, 129.6, 130.4, 131.3, 131.7, 132.4, 133.5, 134.2, 135.4, 140.6, 143.5, 145.6, 156.7, 158.6, 160.4, 163.6, 169.7, 170.9. MS (ESI): 606 $[M + H]^+$.

MTT assay. Individual wells of a 96-well tissue culture microtiter plate were inoculated with 100 μL of complete medium containing 1×10^4 cells. The plates were incubated at 37°C in a humidified 5% CO_2 incubator for 18 h prior to the experiment. After medium removal, 100 μL of fresh medium containing the test compounds and etoposide at different

concentrations (0.5, 1, 2 μM) were added to each well and incubated at 37°C for 24 h. The medium was discarded and replaced with 10 μL MTT dye. Plates were incubated at 37°C for 2 h. The resulting formazan crystals were solubilized in 100 μL extraction buffer. Optical density (O.D.) was measured at 570 nm with a micro plate reader (Multi-mode Varioskan Instrument-Themo Scientific). The percentage of DMSO in the medium never exceeded 0.25%.

CONCLUSIONS

A number of amide derivatives of 1,2-isoxazole combined with 1,2,4-thiadiazole **11a**–**11j** is synthesized. All the compounds are tested for their anticancer activity against four types of human cancer cell lines including MCF-7 (breast), A549 (lung), Colo-205 (colon) and A2780 (ovarian). Most of the compounds demonstrate significant anticancer activity, and **11b**, **11c**, **11d**, **11e**, **11g**, and **11j** exhibit more potent activity than etoposide. The compound **11g** demonstrates the superior activity.

CONFLICT OF INTEREST

No conflict of interest was declared by the authors.

REFERENCES

1. Madhavi, S., Sreenivasulu, R., and Raju, R.R., *Monatsh. Chem.,* 2017, vol. 148, p. 933. doi 10.1007/s00706-016-1790-y
2. Madhavi, S., Sreenivasulu, R., Jyotsna, Y., and Raju, R.R., *Saudi Pharm. J.,* 2017, vol. 25, p. 275. doi 10.1016/j.jsps.2016.06.005
3. Sreenivasulu, R., Sujitha, P., Jadav, S.S., Ahsan, M.J., Kumar, C.G., and Raju, R.R., *Monatsh. Chem*., 2017, vol. 148, p. 305. doi 10.1007/s00706-016-1750-6
4. Sreenivasulu, R., Durgesh, R., Jadav, S.S., Sujitha, P., Kumar, C.G., and Raju, R.R., *Chem. Pap.,* 2018, vol. 72, p. 1369. doi 10.1007/s11696-017-0372-8
5. Subramanyam, M., Sreenivasulu, R., Rambabu, G., Rao, M.V.B., and Rao, K.P., *Lett. Drug Des. Discov.,* 2018, vol. 15, p. 1299. doi 10.2174/1570180815666180219165119
6. Durgesh, R., Sreenivasulu, R., and Raju, R.R., *Asian J. Chem.,* 2018, vol. 30, p. 1201. doi 10.14233/ajchem.2018.21114
7. Durgesh, R., Sreenivasulu, R., Pinapati, S.R., and Raju, R.R., *J. Ind. Chem. Soc.,* 2018, vol. 95, p. 433.
8. Durgesh, R., Sreenivasulu, R., and Raju, R.R., *J. Pharm. Res.,* 2018, vol. 12, p. 42.
9. Spandana, Z., Sreenivasulu, R., Rekha, T.M., and Rao, M.V.B., *Lett. Drug Des. Discov.,* 2018, vol. 15. doi 10.2174/1570180816666181031125946
10. Mohamed, S.F., Abdel-Hafez, N.A., Amr, A.E., and Awad, H.M., *Russ. J. Gen. Chem.,* 2017, vol. 87, p. 1264. doi 10.1134/S1070363217060226
11. Chakrapani, B., Ramesh, V., Rao, G.P.C., Ramachandran, D., Reddy, T.M., and Chakravarthy, A.K., *Russ. J. Gen. Chem.,* vol. 88, p. 1020. doi 10.1134/S1070363218050304
12. Reddy, G.S., Mohanty, S., Kumar J., and Rao, B.V., *Russ. J. Gen. Chem.,* 2018, vol. 88, p. 2394. doi 10.1134/S1070363218110233
13. Ravikumar, P., Raolji, G.S.B., Sastry, K.V., Kalidasu, S., and Balaraju, T., *Russ. J. Gen. Chem.,* 2018, vol. 88, p. 2183. doi 10.1134/S1070363218100250
14. Rathod, A.S. and Biradar, J.S., *Russ. J. Gen. Chem.,* 2018, vol. 88, p. 2190. doi 10.1134/S1070363218100262
15. Dang, T.T., Dang, T.T., and Langer, P., *Synlett,* 2011, p. 2633. doi 10.1055/s-0031-1289550
16. Kumar, V., Aggarwal, R., and Singh, S.P., *Heterocycles,* 2008, vol. 75, p. 2893. doi 10.3987/REV-08-634
17. Giomi, D., Cordero, F., and Machetti, F., *Comprehensive Heterocyclic Chemistry III*; Katrizky, A.R., Ramsden, C.A., Scriven, E.F.V., Taylor, R.J.K., and Joule, J., Eds., Oxford: Elsevier, 2008, vol. 4.
18. Katritzky, A.R., Ostercamp, D.L., and Yousaf, T.I., *Tetrahedron,* 1987, vol. 43, p. 5171. doi 10.1016/S0040-4020(01)87693-6
19. Li, W., Hwang, D., Chen, D., Shen, C., Huang, C., Chen, T., Lin, C., Chang, Y., Lo, Y., Tseng, H., Lin, C., Song, J., Chen, H., Chen, S., Wu, S., and Chen, C., *J. Med. Chem.,* 2003, vol. 46, p. 1706. doi 10.1021/jm020471r
20. Santos, M.M.M., Faria, N., Iley, J., Coles, S.J., Hursthouse, M.B., Martins, M.L., and Moreira, R., *Bioorg. Med. Chem. Lett.,* 2010, vol. 20, p. 193. doi 10.1016/j.bmcl.2009.10.137
21. Daidone, G., Raffa, D., Maggio, B., Plescia, F., Cutuli, V.M.C., Mangano, N.G., and Caruso, A., *Arch. Pharm. Pharm. Med. Chem.,* 1999, vol. 332, p. 50. doi 10.1002/(SICI)1521-4184(19993)332:2%3C50::AID-ARDP50%3E3.0.CO;2-S
22. Al-Tel, T.H., Al-Qawasmeh, R.A., and Zaarour, R., *Eur. J. Med. Chem.,* 2011, vol. 46, p. 1874. doi 10.1016/j.ejmech.2011.02.051
23. Castro, A., Castano, T., Encinas, A., Porcal, W., and Gil, C., *Bioorg. Med. Chem.,* 2006, vol. 14, p. 1644. doi 10.1016/j.bmc.2005.10.012
24. Martınez, A., Fernandez, E., Castro, A., Conde, S., Rodrı-guez-Franco, I., Banos, J.E., and Badıa, A.E., *Eur. J. Med. Chem.,* 2000, vol. 35, p. 913. doi 10.1016/S0223-5234(00)01166-1

Indian Journal of Research in Pharmacy and Biotechnology (IJRPB)
ISSN: 2321-5674 (Print), 2320-3471 (Online)

CrossRef DOI: https://doi.org/10.31426/ijrpb **Indexed in CAS and CABI, Impact Factor: 0.64**

A Validated Reversed Phase HPLC Method Development for the Assay of Ciprofloxacin in Oral Suspension

Bathula Sivannarayana[1], Modugula Jyosthna[1], Dr Dasi Jeevan Mani Babu[1], Mekala Sunil[1], Choppavarapu Dorcas Anand[2], Dr M. Manoranjani[3]

[1]St.Xavier Institute of Pharmacy, Phirangipuram, Guntur. A.P., India
[2]SRR & CVR Govt. (A) Degree College, Vijayawada, A.P., India
[3]Dept. of Chemistry, PB Siddartha College of Arts and Sciences, Vijayawada, A.P., India

E-Mail: drjeevanbabu@gmail.com

Keywords:
Ciprofloxacin, RP-HPLC

ABSTRACT

A simple Reverse phase liquid chromatographic method has been developed and subsequently validated for the determination of Ciprofloxacin in oral suspension. The separation was carried out using a mobile phase consisting of buffer of pH 2.0 and Acetonitrile in the ratio of 87: 13. The column used was Inertsil ODS-3 4.6×250mm, 5µ. with a flow rate of 1.5 ml / min by detection at 278 nm. The described method was linear over a concentration range of 25-150%. The retention time of Ciprofloxacinwas found to be 9.4min. Results of analysis were validated statistically and by recovery studies. The results of the study showed that the proposed RP-HPLC method is simple, rapid, precise and accurate, which is useful for the routine determination of Ciprofloxacinin its pharmaceutical dosage forms.

1. INTRODUCTION

Ciprofloxacin is a broad-spectrum antimicrobial carboxyfluoroquinoline. The bactericidal action of ciprofloxacin results from inhibition of the enzymes topoisomerase II (DNA gyrase) and topoisomerase IV, which are required for bacterial DNA replication, transcription, repair, strand supercooling repair, and recombination. [1]

Indian Journal of Research in Pharmacy and Biotechnology (IJRPB)
ISSN: 2321-5674 (Print), 2320-3471 (Online)

CrossRef DOI: https://doi.org/10.31426/ijrpb **Indexed in CAS and CABI, Impact Factor: 0.64**

Ciprofloxacin is a broad-spectrum anti-infective agent of the fluoroquinolone class. Ciprofloxacin has in vitro activity against a wide range of gram-negative and gram-positive microorganisms. The mechanism of action of quinolones, including ciprofloxacin, is different from that of other antimicrobial agents such as beta-lactams, macrolides, tetracyclines, or aminoglycosides; therefore, organisms resistant to these drugs may be susceptible to ciprofloxacin. There is no known cross-resistance between ciprofloxacin and other classes of antimicrobials. Notably the drug has 100 times higher affinity for bacterial DNA gyrase than for mammalian. The bactericidal action of ciprofloxacin results from inhibition of the enzymes topoisomerase II (DNA gyrase) and topoisomerase IV, which are required for bacterial DNA replication, transcription, repair, strand supercooling repair, and recombination.

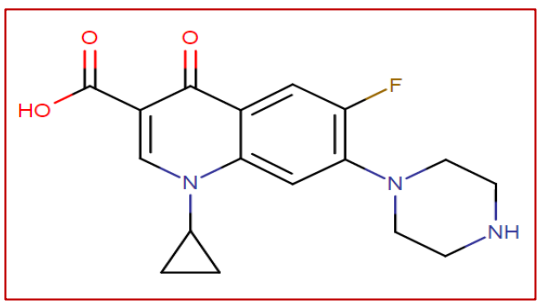


Figure. 1. Molecular structure of Ciprofloxacin

2. Materials and Methods:

2.1 Chemicals and Reagents:

Standard bulk drug sample Ciprofloxacin was provided by Chandra labs, Hyderabad. All the chemicals used were of analytical and HPLC grade procured from Qualigens, India Ltd. The chemicals used for this study were Acetonitrile (HPLC grade), Methanol (HPLC grade), Water (HPLC grade), Ortho phosphoric acid (Analytical grade). Waters HPLC 2695with UV detector was used for the analysis.

2.2. Preparation of Mobile Phase:

Mobile phase-A: (Buffer) Pipette out 10ml of Methanol in to 1000ml of and mix. Adjust to pH 2.0 with Orthophosphoric acid, then filter through 0.45µ filter paper and sonicate for 2minutes.

Mobile phase-B: Acetonitrile

Preparation of Mobile Phase:

Mix the mobile phase-A and mobile phase-B in the ratio in the ratio 87:13%v/v.

Indian Journal of Research in Pharmacy and Biotechnology (IJRPB)
ISSN: 2321-5674 (Print), 2320-3471 (Online)

CrossRef DOI: https://doi.org/10.31426/ijrpb **Indexed in CAS and CABI, Impact Factor: 0.64**

2.3. Preparation of Stock and Standard Solutions:

Preparation of Standard solution:

Weigh and transfer 25mg ciprofloxacin working standard into a 50mL volumetric flask. Add 7ml of acetonitrile andsonicate for 2minutes then add 30ml of pH2.00buffer, sonicate for 10minutes then make up to the mark with diluent. Further pipette out 5ml of the above solution in to 20ml volumetric flask, add 2.8ml of acetonitrile mix well, then add 12ml of pH2.00 buffer, then make up to the mark with diluent.

Preparation of Test Solution:

Shake the bottle 10minutes immediately prior to sampling in order to accomplish homogeneity of suspension. Weigh and transfer 5.5g ciprofloxacin suspension into a 500mL volumetric flask. Add 70ml of acetonitrile sonicate for 10 minutes, then add 250ml of pH 2.00 buffer, sonicate for 20minutes then make up to the mark with diluent. Further pipette out 5ml of the above solution in to 20ml volumetric flask, add 2.8ml of acetonitrile mix well, then add 12ml of pH2.00 buffer, then make up to the mark with diluent.

2.4. Optimized Chromatographic Conditions:

Column: Inertsil ODS-3 4.6×250mm, 5µ.

Flow rate : 1.5 mL /min.

Wavelength : 278 nm

Column temperature : 40°C

Injection Volume : 10 µL

Run Time : 15 minutes

Retention time: Ciprofloxacin, RT about 9.4min

3. Method Validation Parameters:

Linearity:

A series of Ciprofloxacin solutions were prepared in the concentration ranging from 25% to 150% of specification level and injected into the HPLC system as per the test method. The square of the correlation coefficient, intercept and residual sum of squares were calculated.

Indian Journal of Research in Pharmacy and Biotechnology (IJRPB)
ISSN: 2321-5674 (Print), 2320-3471 (Online)

CrossRef DOI: https://doi.org/10.31426/ijrpb **Indexed in CAS and CABI, Impact Factor: 0.64**

Accuracy:

A series of solutionswereprepared in triplicatetest preparation at the specification limit in the range of about 25%to 150% of test concentration and injected into HPLC system and analyzed as per the test method. Individual % recovery, mean % recovery, %RSD and linearity of the testmethodwere calculated at each level.

Intermediate Precision:

To evaluate the intermediate precision for assay method, six samples were prepared and analyzed as per test method by using different column, by different analysts on different days. Intermediate precision was calculated and found to be within the acceptable limits. The overall % RSD of six samples in method precision, intermediate precision (n=6 and n=12) were calculated.

Filter Validation:

A study was conducted to evaluate the filter suitability by using two different types of filters namely0. 45 µm PVDF and 0.45µm Nylon filters. Standard solution was prepared in single and test solution was prepared in duplicate as per the test method. Portion of standard and test solutions were filtered through 0.45 µm PVDF, 0.45 µm nylon filter and some portion of standard and sample solutions were centrifuged and analyzed as per test method.

Robustness:

Flow Rate Variation:

A study was conducted to determine the effect of variation in flow rate. Blank, Standard and sample (at the specification level) were prepared as per the test method and injected into the HPLC system with flow rates of 1.4ml/minute and 1.6ml/minute. The system suitability parameters sample was evaluated and found to be within the specified limits as per test method.

Column Oven Temperature Variation:

A study was conducted to determine the effect of variation in Column oven Temperature. Standard and test preparations (at the specification level) were prepared as per the test method and injected into the HPLC system with a column oven temperature of 35°C and 45°C. System suitability parameters and sample were evaluated and found to be within the specified limits as per test method.

Indian Journal of Research in Pharmacy and Biotechnology (IJRPB)
ISSN: 2321-5674 (Print), 2320-3471 (Online)
CrossRef DOI: https://doi.org/10.31426/ijrpb **Indexed in CAS and CABI, Impact Factor: 0.64**

Effect of Variation In Mobile Phase Composition:

A study was conducted to determine the effect of variation in mobile phase composition. Two different mobile phases of Buffer and Acetonitrile were prepared in the ratio of 855:145%v/v and 885:115%v/v as per the test method. Standard and test preparations with specification level were prepared as per the test method and injected into the HPLC system.

Effect of pH Variation in Mobile Phase:

A study was conducted to determine the effect of variation in pH in the mobile phase. Two mobile phases of pH 2.80 and 3.20 were prepared as per the test method. Blank, Standard and test preparations were prepared as per the test method and injected into the HPLC system with System suitability parameters and sample were evaluated and found to be within the specified limits as per test method.

The Effect of Wavelength Variation:

A study was conducted to determine the effect of variation in wavelength. Standard and test preparations (at the specification level) were prepared as per the test method and injected into the HPLC system with wavelength of -Ciprofloxacin280nm and 276nm.System suitability parameters and sample were evaluated and found to be within the specified limits as per test method.

4. Results and Discussion:

The solution of Ciprofloxacin was scanned in the range of 200-400nm and 278nm was selected as detection wavelength by RP-HPLC method with an isocratic elution technique. The optimization was done by changing the composition of the mobile phase, ratio and flow rate. Finally the mobile phase with buffer (pH 2): ACN in the ratio 87:13v/v% was optimized for the estimation of Ciprofloxacin and the column used for separation is Inertsil ODS-3 4.6×250mm,5µ. [2]

The chromatographicparameters of system suitability such as %RSD, standard recovery, Tailing factor, Theoretical plates were found to be satisfactory. The values of these parameters are tabulated in Table-1.

Indian Journal of Research in Pharmacy and Biotechnology (IJRPB)
ISSN: 2321-5674 (Print), 2320-3471 (Online)
CrossRef DOI: https://doi.org/10.31426/ijrpb **Indexed in CAS and CABI, Impact Factor: 0.64**

Table.1. System suitability data for Ciprofloxacin

System suitability parameters for Ciprofloxacin	Method Precision	Intermediate precision	Acceptance Criteria
%RSD	0.3	0.3	Not more than 2.0
Standard recovery (%)	101.4	99.5	Between 98.0 to 102.0
Tailing factor	1.1	1.1	Not more than 2.0
Theoretical plates	9925	9271	Not less than 2000

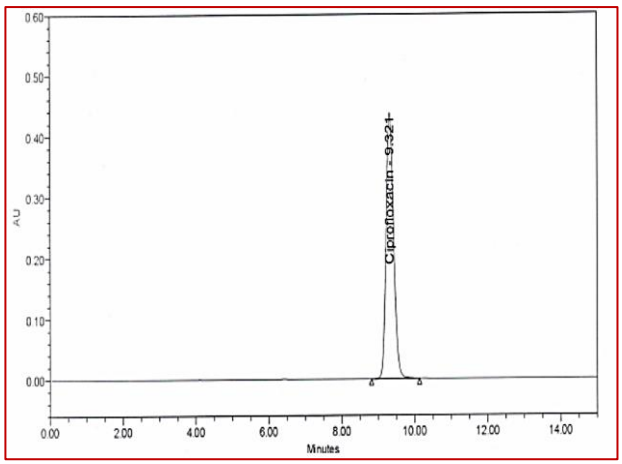


Figure.2.Typical chromatogram of Standard solution

The linearity of the developed method was determined by analyzing different concentrations of the standard solution containing a concentration range from 25% to 150%. The response factor of the standard solutions was calculated. The ratio of peak areas of ciprofloxacin was plotted against the concentration to obtain the calibration graph (Fig. 3) and was found to be linear over the concentration range from 25% to 150%. The data were analyzed by linear regression, least-squares method and the corresponding equation are given by Y = BX + c, where 'Y' is the ratio of the peak areas values of Ciprofloxacin, 'b' is the slope, 'c' is the intercept and 'X' is the concentration of the analyte. Linear regression, least squares fit data are given in (Table 2). [3] The percentage purity was found to be 99.3%. The precision of the method was confirmed by the repeatability of formulation for six times. The accuracy of the method was confirmed by recovery studies and the data was given by (Table 3). [4] Similarity factors were calculated for the filtered standards against unfiltered standard (Centrifuged) and found to be within the specified limit. The difference in the % between unfiltered (centrifuged) and filtered samples were calculated and found to be

Indian Journal of Research in Pharmacy and Biotechnology (IJRPB)
ISSN: 2321-5674 (Print), 2320-3471 (Online)
CrossRef DOI: https://doi.org/10.31426/ijrpb **Indexed in CAS and CABI, Impact Factor: 0.64**

meeting the acceptable limit. Both PVDF and Nylon filters were suitable for the intended purpose.

Table.2.Linearity of detector response for Ciprofloxacin

% Linearity level	Concentration (ppm)	Response	Acceptance criteria
25	31.0875	1536480	Square of Correlation co-efficient should not be less than 0.999
50	62.175	3107355	
75	93.2625	4623963	
100	124.35	6039873	
150	186.525	9110398	
Square of correlation coefficient : 0.999 Slope: 48483.76574 Intercept : 60448.78378 Residual sum of squares: 45710.56736			

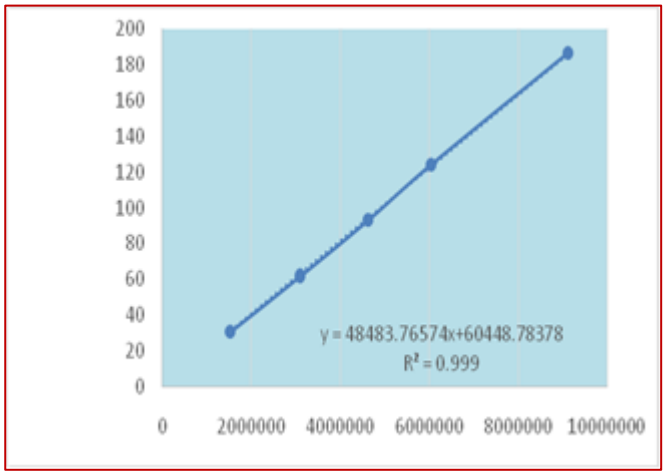


Figure.3.Linearity of detector response graph for Ciprofloxacin.

Indian Journal of Research in Pharmacy and Biotechnology (IJRPB)
ISSN: 2321-5674 (Print), 2320-3471 (Online)
CrossRef DOI: https://doi.org/10.31426/ijrpb **Indexed in CAS and CABI, Impact Factor: 0.64**

Table.3.Accuracy data of Ciprofloxacin

S. No.	% spike level	Amount added (%w/w)	Amount recovered (%w/w)	% Recovery	% Mean recovery	% RSD
1.	25%	62.1229	62.37308	100.4	99.8	0.6
2.		63.0287	62.40228	99.0		
3.		63.0885	62.62924	99.3		
4.		63.1979	62.72669	99.3		
5.		62.2424	62.36469	100.2		
6.		62.3220	62.55297	100.4		
1.	100%	250.8408	247.83270	98.8	99.3	0.4
2.		248.9894	247.87577	99.6		
3.		249.1088	247.78317	99.5		
1.	150%	378.5307	377.14133	99.6	100.6	0.5
2.		374.4894	377.08205	100.7		
3.		374.7781	377.28255	100.7		
4.		373.8921	377.45520	101.0		
5.		373.2252	376.76809	101.0		
6.		374.1609	376.10577	100.5		

Specificity:

Chromatogram of blank and placebo should not show any peak at the retention time of Ciprofloxacin peak and known impurity peaks.

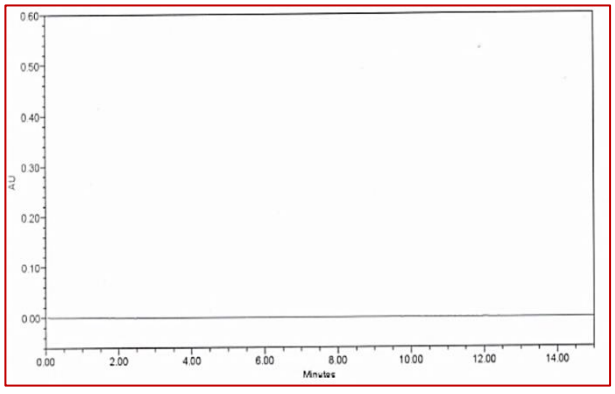


Figure.4.Typical chromatogram of Blank

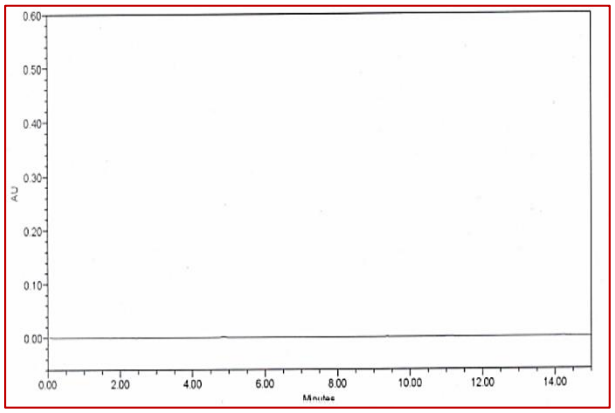


Figure.5.Typical chromatogram of placebo

Indian Journal of Research in Pharmacy and Biotechnology (IJRPB)
ISSN: 2321-5674 (Print), 2320-3471 (Online)

CrossRef DOI: https://doi.org/10.31426/ijrpb **Indexed in CAS and CABI, Impact Factor: 0.64**

Table.4.Method Precision data for Ciprofloxacin

Sample No.	Ciprofloxacin content (%)
1	100.9
2	100.2
3	100.0
4	99.4
5	101.1
6	100.5
Mean	**100.4**
% RSD	**0.6**

5. Conclusion:

This study showed that the antibiotic drug, Ciprofloxacin can be precisely and accurately determined in pure and pharmaceutical dosages. The proposed method is simple and requires less time for analysis. System performance parameters revealed that the method is ideal for the assay ofCiprofloxacin.

Hence, the developed chromatography method was applied for routine analysis and can be used for the intended purpose.

References:

1) Tripathi KD. Essentials of medical pharmacology; sixth edition 2008: 688
2) Abdel-Hay MH, Hassan EM, Gazy AA, Belal TS. Kinetic spectrophotometric analysis and spectrofluorimetric analysis of ciprofloxacin hydrochloride and norfloxacin in pharmaceutical preparations using 4-Chloro-7-nitrobenzo-2-oxa-1,3-diazole (NBD-Cl). J Chin ChemSoc 2008; 55(4): 818-827
3) Gummadi S, Thota D, Varri SV, Vaddi P, Jillella VLNSR. Development and validation of UV spectroscopic methods for simultaneous estimation of ciprofloxacin and tinidazole in tablet formulation.Intcurr Pharm j 2012; 1(10): 317-321
4) El-Brashy AM, El-Sayed MM, El-Sepai FA. Spectrophotometric determination of some fluoroquinoloneantibacterials through charge-transfer and ion-pair complexation reactions. Bul Korean ChemSoc2004; 25(3): 365
5) Safwan A, Mouhammed K. Kinetic Spectrophotometric method for the quantitative analysis of pravastatin sodium (PVS) in pure and pharmaceutical formulations. Arabian J Chem 2012; 4(3): 299-305
6) Chaudhari BG, Patel NM, Shah PB. Determination of simvastatin, pravastatin, rosuvastatin calcium in tablet

Indian Journal of Research in Pharmacy and Biotechnology (IJRPB)
ISSN: 2321-5674 (Print), 2320-3471 (Online)

CrossRef DOI: https://doi.org/10.31426/ijrpb **Indexed in CAS and CABI, Impact Factor: 0.64**

dosage form. Int j pharm sci 2007; 69(10): 130-132

7) Kadikar HK, Shah R. Simultaneous UV spectrophotometry of pravastatin and co-enzyme Q10 in their formulation combined dosage forms and synthetic mixtures. IJPR 2012; 1(4): 112-127
8) D'Silva T, Olivera MA, De'Oliveira RB, Soares CDV. Development and validation of a simple and fast hplc method for determination of lovastatin, pravastatin and simvastatin. J ChromatogrSci2010; 50(9): 831-832
9) Maha F, Abdel-Aziz O, Reham N, Abdel-Fattah L. Validated spectrophotometric methods for determination of some anti-hyperlipidemic drugs. J Med Res 2010; 2(3): 202-211
10) Safwan A, Husni N, Soulafa O. Quantitative determination of pravastatin in pharmaceutical dosage forms by high-performance liquid chromatography with ultraviolet detection. Int J Biomed sci 2011; 4(1): 84-90

S.R.R.&C.V.R. GOVT.DEGREE COLLEGE(A)

Department of Biochemistry

Training Program

CERTIFICATE COURSE IN MEDICAL CODING

Date: 10/12/2018 to 10/01/2019

Students participated: II, III BSc- MBC, BZC Program students

Resource person: Trainer from VAWE Institute of Technical Training Mrs. P. Swathi

---

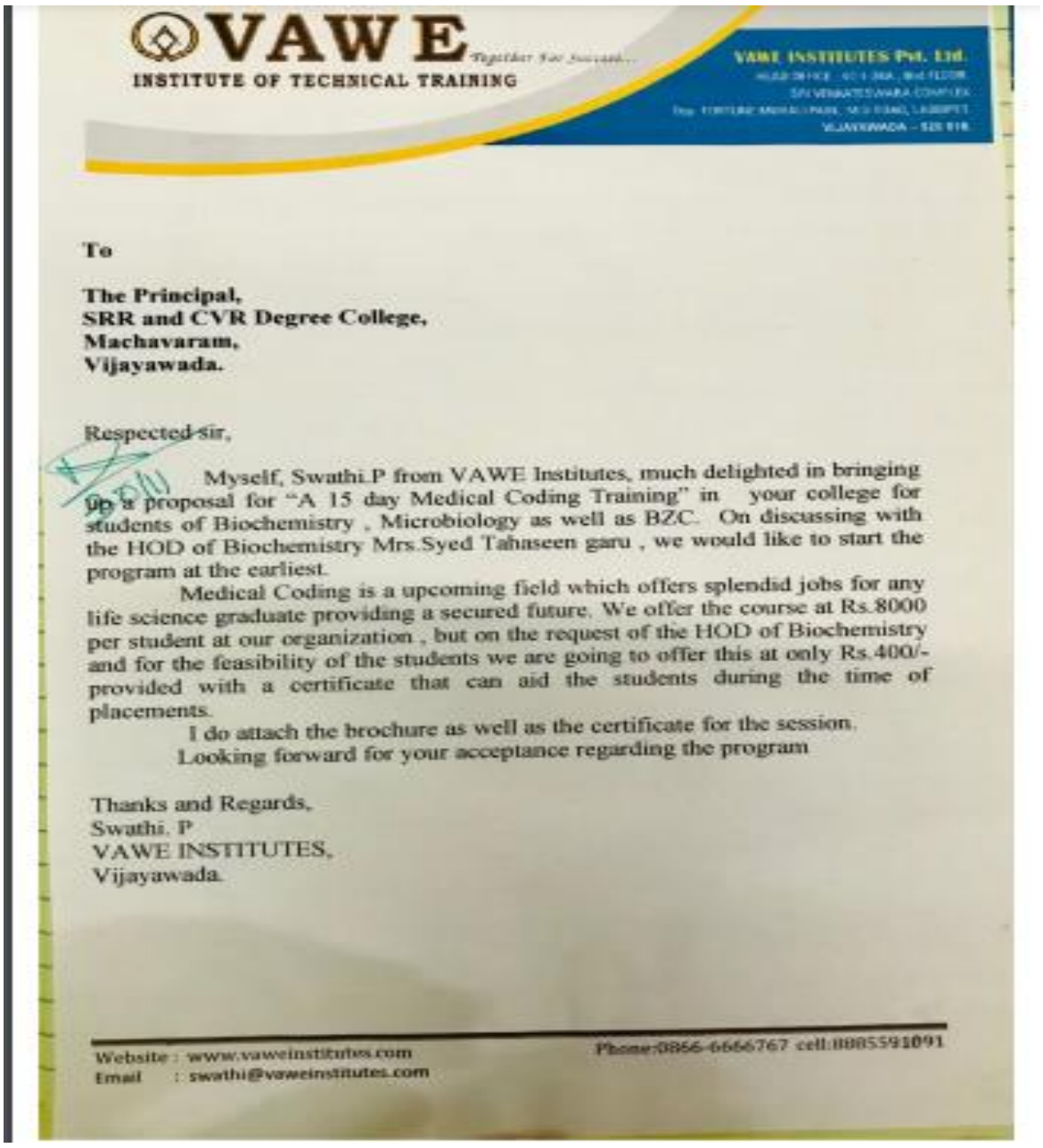
Reported by Syed Vaziha Tahaseen

The department of biochemistry has taken the initiative to start a training program in Medical coding. Medical coding is the **process of translating crucial medical information into simple codes to document medical records and for medical billing**. This standard medical coding system allows a more seamless transfer of medical records and more efficient analysis to track patients' health records. Many of the students, who are very interested in being selected in campus selections and getting immediate placements, need to be acquainted with the company's skills as Vijayawada city has many multispeciality hospitals and a massive need for medical translators. In this view, the department of biochemistry approached the **VAWE institute of technical** training to impart skills to students studying life sciences. Mrs. P.Swathi, the Trainer at the institute, came forward to provide training to our college students on the campus in addition to their regular college hours. The training program lasted for 30 days; students were introduced to all the technical knowledge required to work as a medical coder.

With the provided training, one of the students, Mr. Vishwanethtry Kanuru, of batch 2017-2019, was selected as a junior executive in medical coding at **PhyCare services, IT PARK, Mangalagiri (offer letter-page no.**

Acknowledgment: We thank our principal, Dr. Velaga Joshi, for encouraging and giving permission to organize the program.

We also show our gratitude for the VAWE institute of technical training for proving the Trainer P.Swathi for teaching the classes. We also thank our computer department, HOD, for providing the lab to organize the classes.



VAWE
INSTITUTE OF TECHNICAL TRAINING

VAWE INSTITUTES Pvt. Ltd.

To

The Principal,
SRR and CVR Degree College,
Machavaram,
Vijayawada.

Respected sir,

Myself, Swathi.P from VAWE Institutes, much delighted in bringing up a proposal for "A 15 day Medical Coding Training" in your college for students of Biochemistry , Microbiology as well as BZC. On discussing with the HOD of Biochemistry Mrs.Syed Tahaseen garu , we would like to start the program at the earliest.

Medical Coding is a upcoming field which offers splendid jobs for any life science graduate providing a secured future. We offer the course at Rs.8000 per student at our organization , but on the request of the HOD of Biochemistry and for the feasibility of the students we are going to offer this at only Rs.400/- provided with a certificate that can aid the students during the time of placements.

I do attach the brochure as well as the certificate for the session.

Looking forward for your acceptance regarding the program

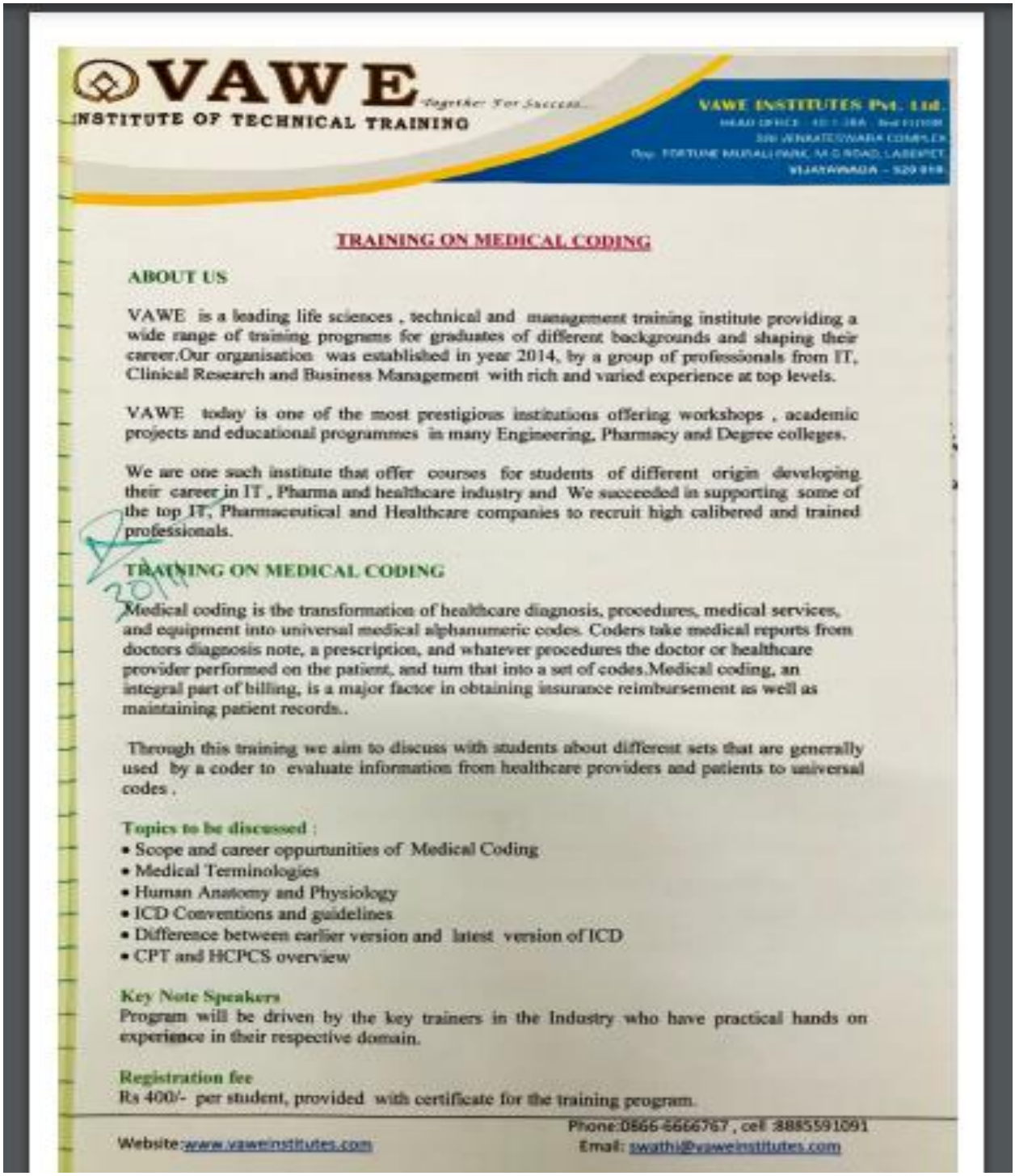
Thanks and Regards,
Swathi. P
VAWE INSTITUTES,
Vijayawada.

Website : www.vaweinstitutes.com
Email : swathi@vaweinstitutes.com
Phone:0866-6666767 cell:8885591091

Letter received from Trainer to the principal for organizing the classes in our college campus for 15 days initially, but the course was extended for another 15 days with

S.R.R.&C.V.R. GOVT.DEGREE COLLEGE(A)

Department of Biochemistry



VAWE
Together For Success...
INSTITUTE OF TECHNICAL TRAINING

VAWE INSTITUTES Pvt. Ltd.
HEAD OFFICE : 40-1-38A, 2nd FLOOR
320 VENKATESWARA COMPLEX
Opp: FORTUNE MURALI PARK, M G ROAD, LABBIPET
VIJAYAWADA – 520 010

TRAINING ON MEDICAL CODING

ABOUT US

VAWE is a leading life sciences , technical and management training institute providing a wide range of training programs for graduates of different backgrounds and shaping their career.Our organisation was established in year 2014, by a group of professionals from IT, Clinical Research and Business Management with rich and varied experience at top levels.

VAWE today is one of the most prestigious institutions offering workshops , academic projects and educational programmes in many Engineering, Pharmacy and Degree colleges.

We are one such institute that offer courses for students of different origin developing their career in IT , Pharma and healthcare industry and We succeeded in supporting some of the top IT, Pharmaceutical and Healthcare companies to recruit high calibered and trained professionals.

TRAINING ON MEDICAL CODING

Medical coding is the transformation of healthcare diagnosis, procedures, medical services, and equipment into universal medical alphanumeric codes. Coders take medical reports from doctors diagnosis note, a prescription, and whatever procedures the doctor or healthcare provider performed on the patient, and turn that into a set of codes.Medical coding, an integral part of billing, is a major factor in obtaining insurance reimbursement as well as maintaining patient records..

Through this training we aim to discuss with students about different sets that are generally used by a coder to evaluate information from healthcare providers and patients to universal codes .

Topics to be discussed :

- Scope and career oppurtunities of Medical Coding
- Medical Terminologies
- Human Anatomy and Physiology
- ICD Conventions and guidelines
- Difference between earlier version and latest version of ICD
- CPT and HCPCS overview

Key Note Speakers

Program will be driven by the key trainers in the Industry who have practical hands on experience in their respective domain.

Registration fee

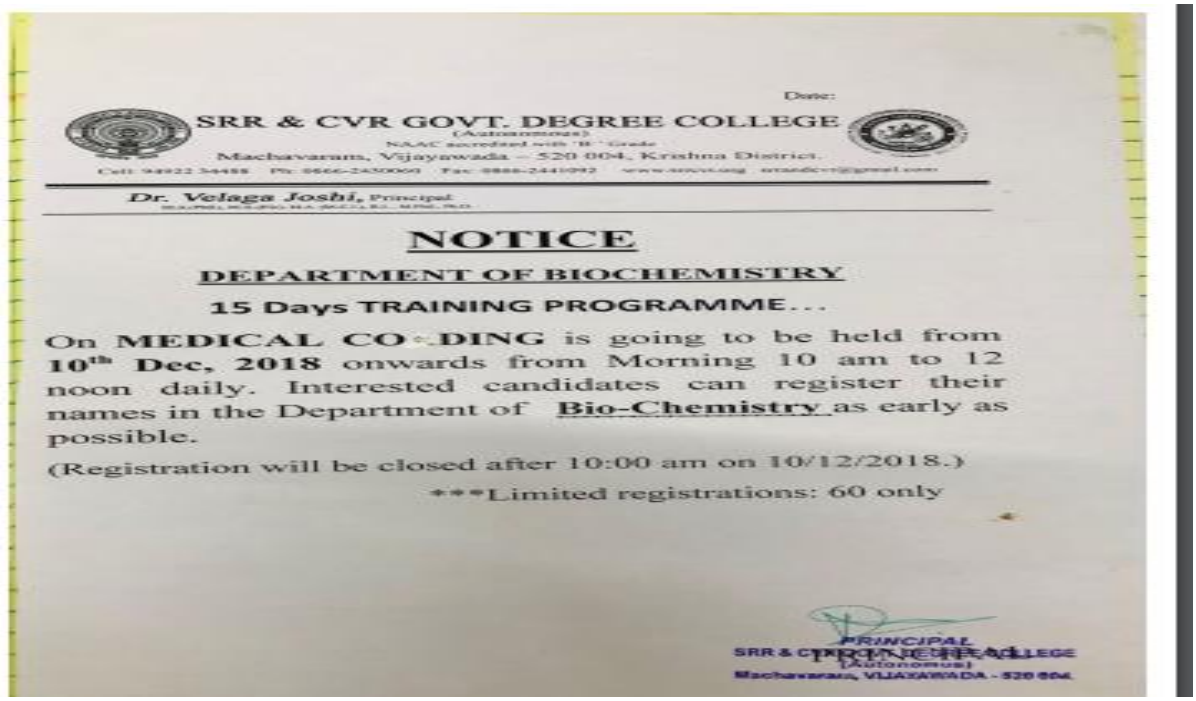
Rs 400/- per student, provided with certificate for the training program.

Website:www.vaweinstitutes.com

Phone:0866-6666767 , cell :8885591091
Email: swathi@vaweinstitutes.com

S.R.R.&C.V.R. GOVT.DEGREE COLLEGE(A)

Department of Biochemistry



Date:

SRR & CVR GOVT. DEGREE COLLEGE
(Autonomous)
NAAC accredited with 'B' Grade
Machavaram, Vijayawada – 520 004, Krishna District.
Cell: 94922 34488 Ph: 0866-2430069 Fax: 0866-2441092 www.srrcvr.org srrandcvr@gmail.com

Dr. Velaga Joshi, Principal

NOTICE

DEPARTMENT OF BIOCHEMISTRY

15 Days TRAINING PROGRAMME...

On **MEDICAL CO DING** is going to be held from **10th Dec, 2018** onwards from Morning 10 am to 12 noon daily. Interested candidates can register their names in the Department of **Bio-Chemistry** as early as possible.

(Registration will be closed after 10:00 am on 10/12/2018.)

***Limited registrations: 60 only

PRINCIPAL
SRR & CVR GOVT. DEGREE COLLEGE
(Autonomous)
Machavaram, VIJAYAWADA - 520 004.



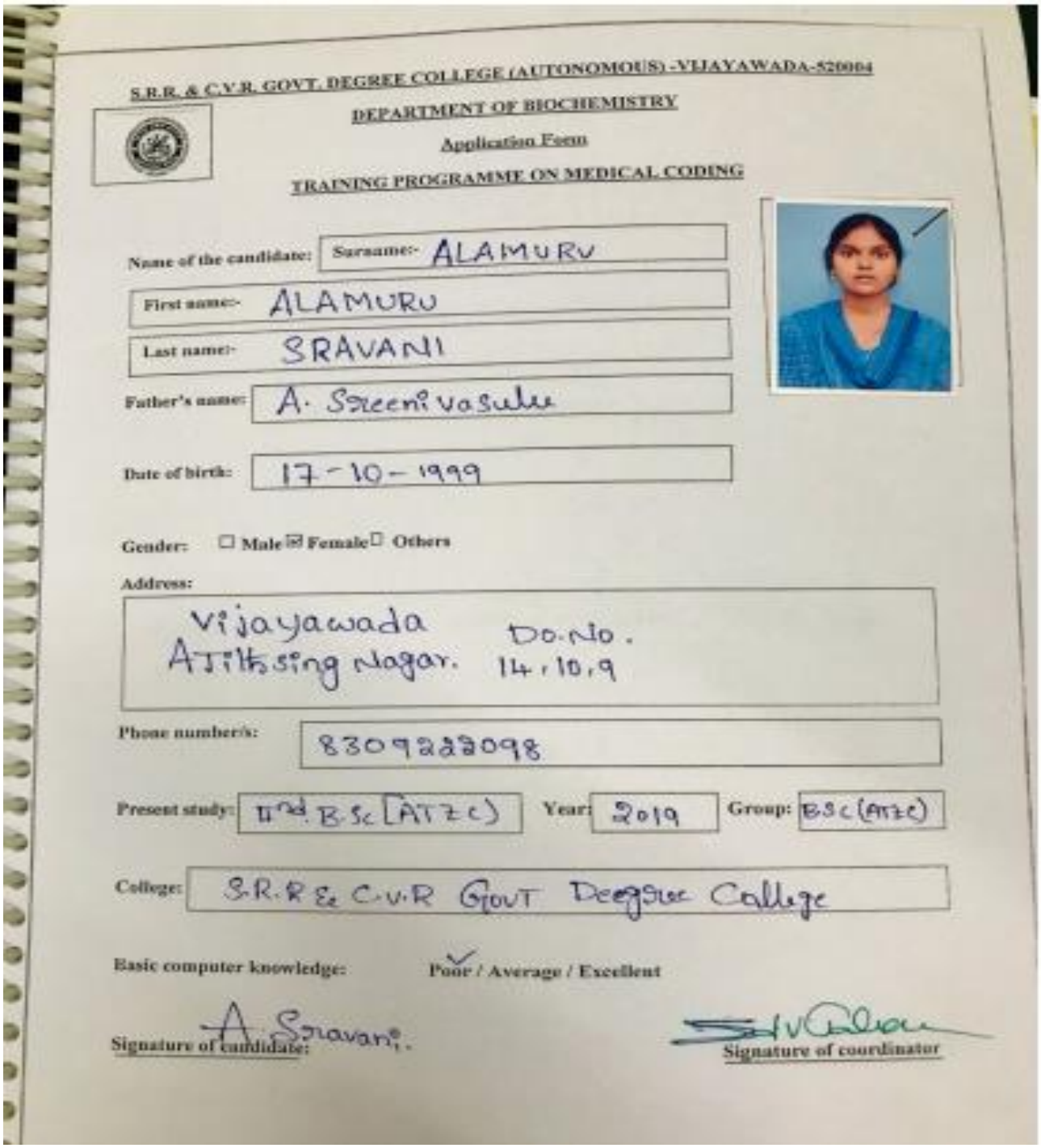
Madam P.Swathi took the medical coding classes at the computer lab at our colleg

S.R.R.&C.V.R. GOVT.DEGREE COLLEGE(A)

Department of Biochemistry



Our college principal Dr. Velaga Joshi awarded certificates to the students' for successfully completing the training program, appreciated the entire team for showing their efforts.



S.R.R. & C.V.R. GOVT. DEGREE COLLEGE (AUTONOMOUS) -VIJAYAWADA-520004

DEPARTMENT OF BIOCHEMISTRY

Application Form

TRAINING PROGRAMME ON MEDICAL CODING

Name of the candidate: Surname:- ALAMURU

First name:- ALAMURU

Last name:- SRAVANI

Father's name: A. Sreenivasulu

Date of birth: 17-10-1999

Gender: ☐ Male ☑ Female ☐ Others

Address:

Vijayawada
Ajithsing Nagar.
D.No. 14,10,9

Phone number/s: 8309222098

Present study: IInd B.Sc (AHZC) Year: 2019 Group: BSc (AHZC)

College: S.R.R & C.V.R Govt Degree College

Basic computer knowledge: Poor / Average / Excellent

Signature of candidate: A. Sravani.

Signature of coordinator

Application form to be filled by the student at the time of admission in this program. **Total 47 life sciences students from the program MBC, BZC** were enrolled.

S.R.R.&C.V.R. GOVT.DEGREE COLLEGE(A)

Department of Biochemistry



SRR & CVR GOVT. DEGREE COLLEGE

(Autonomous)

Machavaram, Vijayawada, Krishna Dist - 520 004

DEPARTMENT OF BIO-CHEMISTRY

in Collaboration with

VAWE GLOBAL TECHNOLOGIES PVT. LTD.

CERTIFICATE

This is to certify that Mr. / Ms. DUSSA SAI SREE

successfully completed the Certificate Course entitled

"MEDICAL CODING" with satisfactory attendance and performance during the period

from 10-12-2018 to 10-01-2019.

Mrs. Syed Vaziha Tahaseen
Course Co-ordinator

Mrs. P. Swathi
Life Science Sector Manager

Dr. VELAGA JOSHI
PRINCIPAL

Model copy of certificate awarded for the students who have completed their training.

S.R.R.&C.V.R. GOVT.DEGREE COLLEGE(A)

Department of Biochemistry

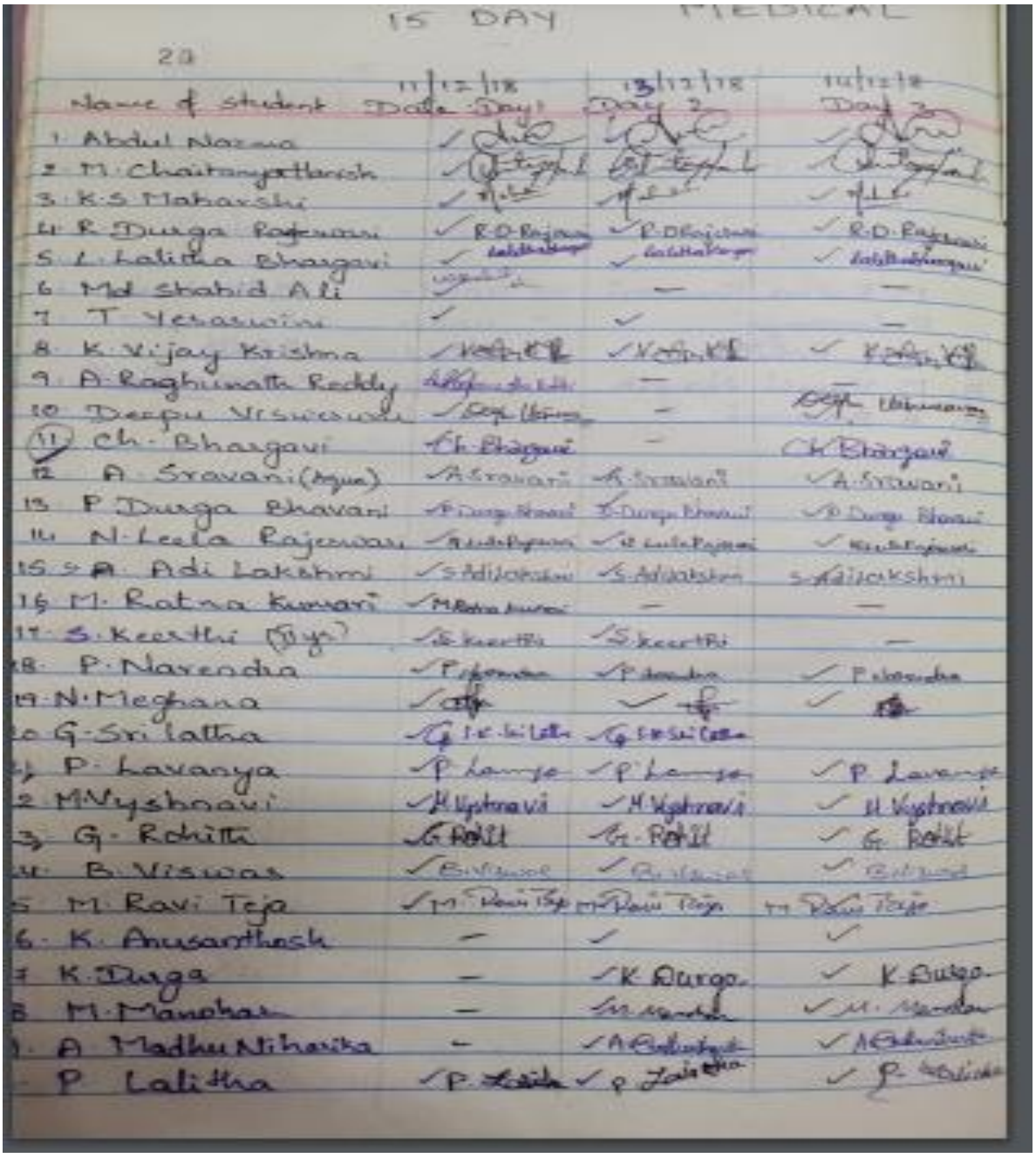


సర్టిఫికేషన్ కోర్సులతో ఉద్యోగ అవకాశాలు

- సుబ్బరం

S.R.R.&C.V.R. GOVT.DEGREE COLLEGE(A)

Department of Biochemistry



15 DAY MEDICAL

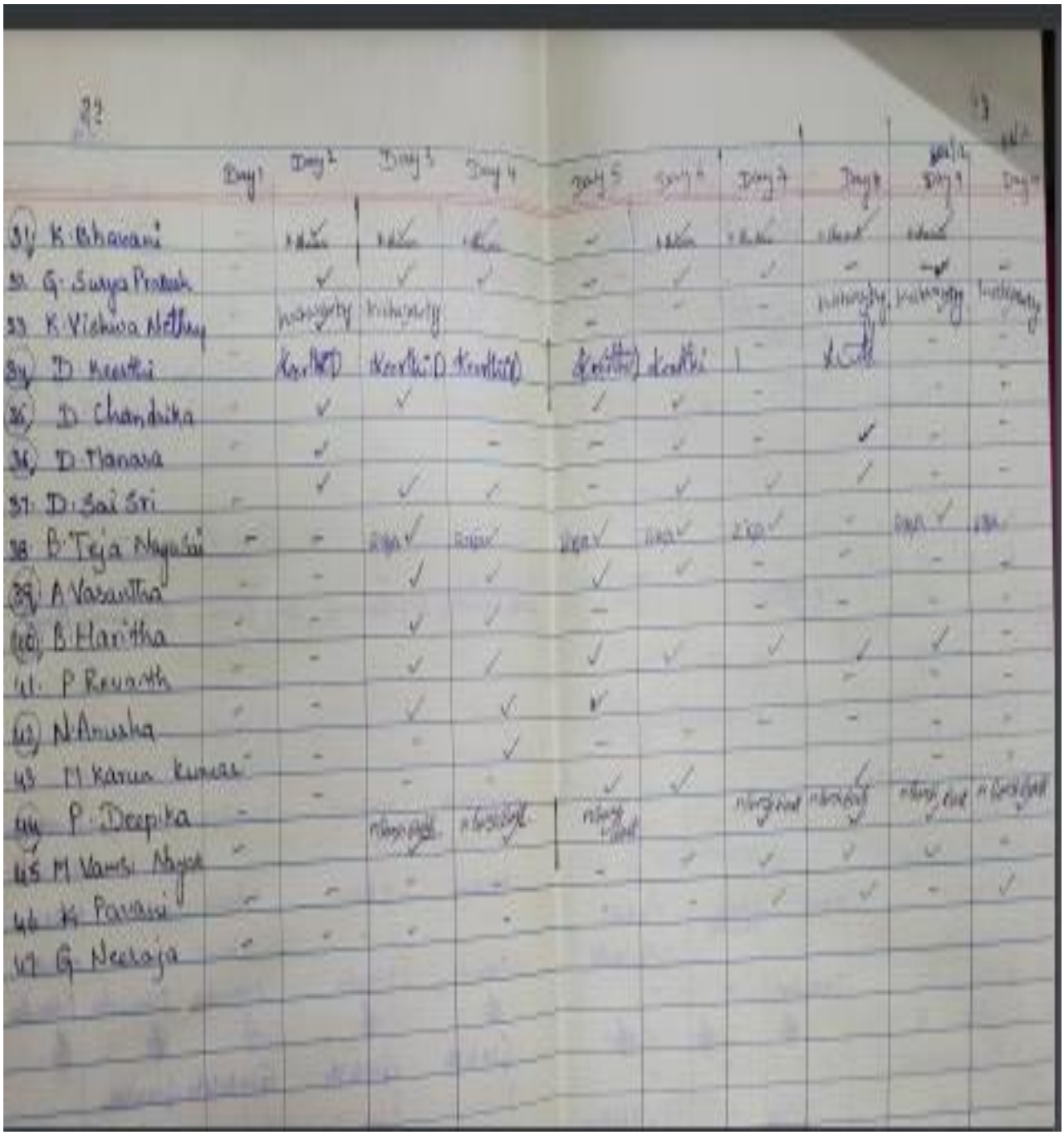
23

Name of student	11/12/18 Date Day 1	13/12/18 Day 2	14/12/18 Day 3
1 Abdul Nazeer	✓	✓	✓
2 M Chaitanyatharish	✓	✓	✓
3 K S Maharshi	✓	✓	✓
4 R Durga Rajeswari	✓ R.D.Rajeswari	✓ R.D.Rajeswari	✓ R.D.Rajeswari
5 L Lalitha Bhargavi	✓	✓	✓
6 Md Shahid Ali	✓	—	—
7 T Yesaswini	✓	✓	—
8 K Vijay Krishna	✓	✓	✓
9 A Raghunatha Reddy	—	—	—
10 Deepu Viswanath	✓	—	✓
11 Ch Bhargavi	✓ Ch Bhargavi	—	✓ Ch Bhargavi
12 A Sravani (Agua)	✓ A Sravani	✓ A Sravani	✓ A Sravani
13 P Durga Bhavani	✓ P Durga Bhavani	✓ P Durga Bhavani	✓ P Durga Bhavani
14 N Leela Rajeswari	✓ N Leela Rajeswari	✓ N Leela Rajeswari	✓ N Leela Rajeswari
15 A Adi Lakshmi	✓ S Adilakshmi	✓ S Adilakshmi	✓ S Adilakshmi
16 M Ratna Kumari	✓ M Ratna Kumari	—	—
17 S Keerthi (Jiya)	✓ S Keerthi	✓ S Keerthi	—
18 P Narendra	✓ P Narendra	✓ P Narendra	✓ P Narendra
19 N Meghana	✓	✓	✓
20 G Sri latha	✓ G Sri Latha	✓ G Sri Latha	
21 P Lavanya	✓ P Lavanya	✓ P Lavanya	✓ P Lavanya
22 M Vyshnavi	✓ M Vyshnavi	✓ M Vyshnavi	✓ M Vyshnavi
23 G Rohith	✓ G Rohith	✓ G Rohith	✓ G Rohith
24 B Viswas	✓ B Viswas	✓ B Viswas	✓ B Viswas
25 M Ravi Teja	✓ M Ravi Teja	✓ M Ravi Teja	✓ M Ravi Teja
26 K Anusanthosh	—	✓	✓
27 K Durga	—	✓ K Durga	✓ K Durga
28 M Manohar	—	✓ M Manohar	✓ M Manohar
29 A Madhu Niharika	—	✓ A Madhu Niharika	✓ A Madhu Niharika
30 P Lalitha	✓ P Lalitha	✓ P Lalitha	✓ P Lalitha

Enrolled students list

S.R.R.&C.V.R. GOVT.DEGREE COLLEGE(A)

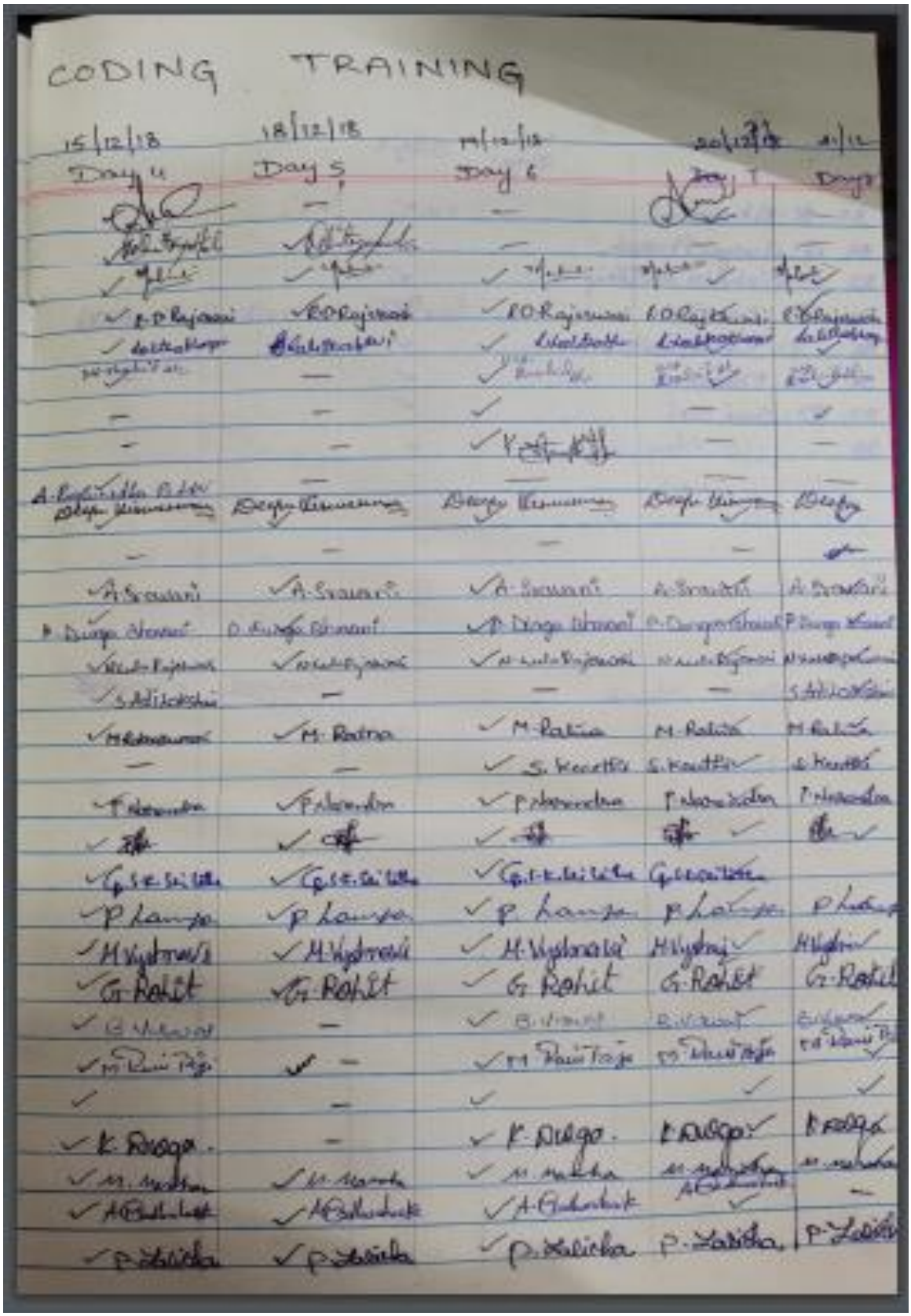
Department of Biochemistry



Student attendance

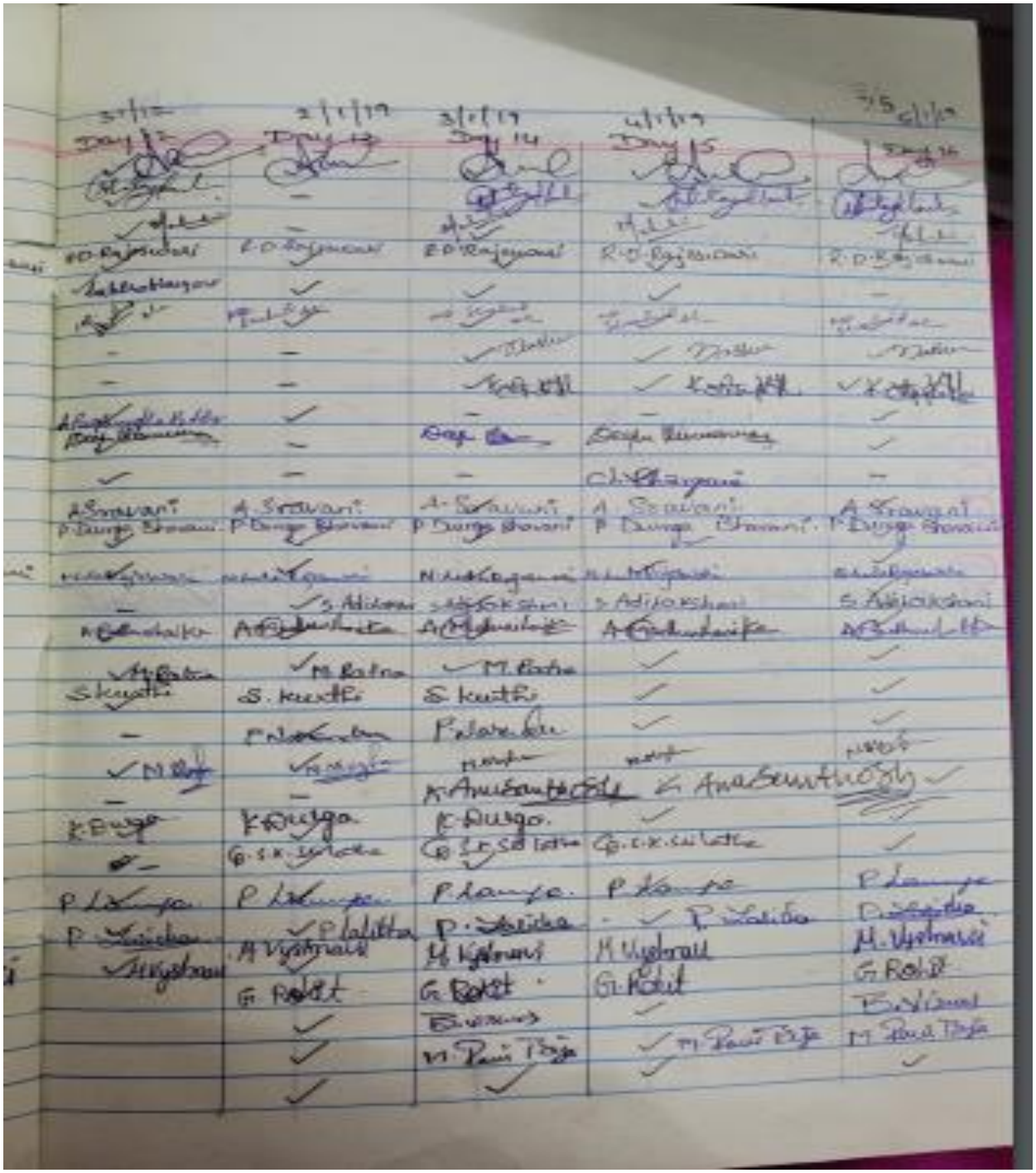
S.R.R.&C.V.R. GOVT.DEGREE COLLEGE(A)

Department of Biochemistry



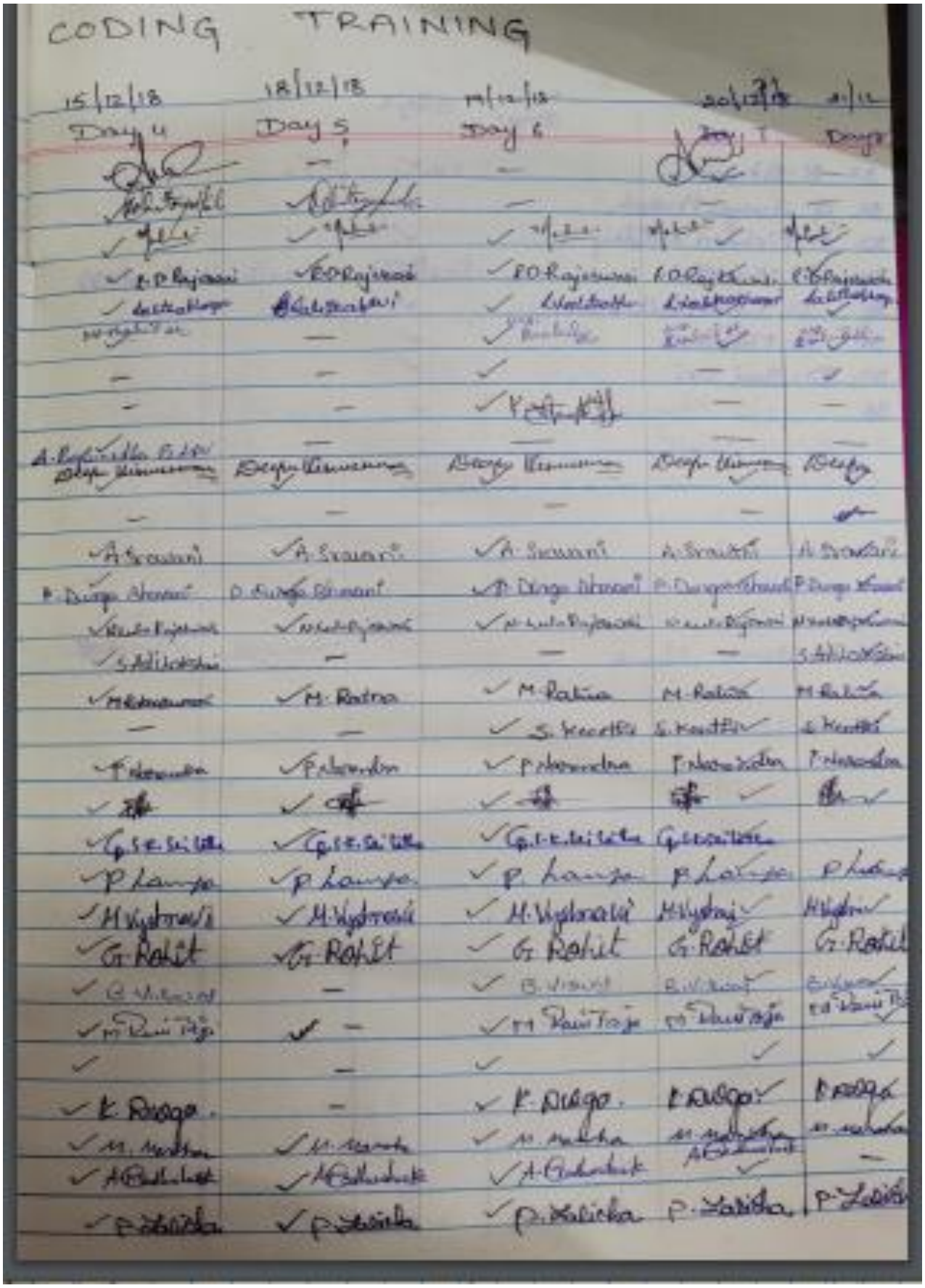
S.R.R.&C.V.R. GOVT.DEGREE COLLEGE(A)

Department of Biochemistry



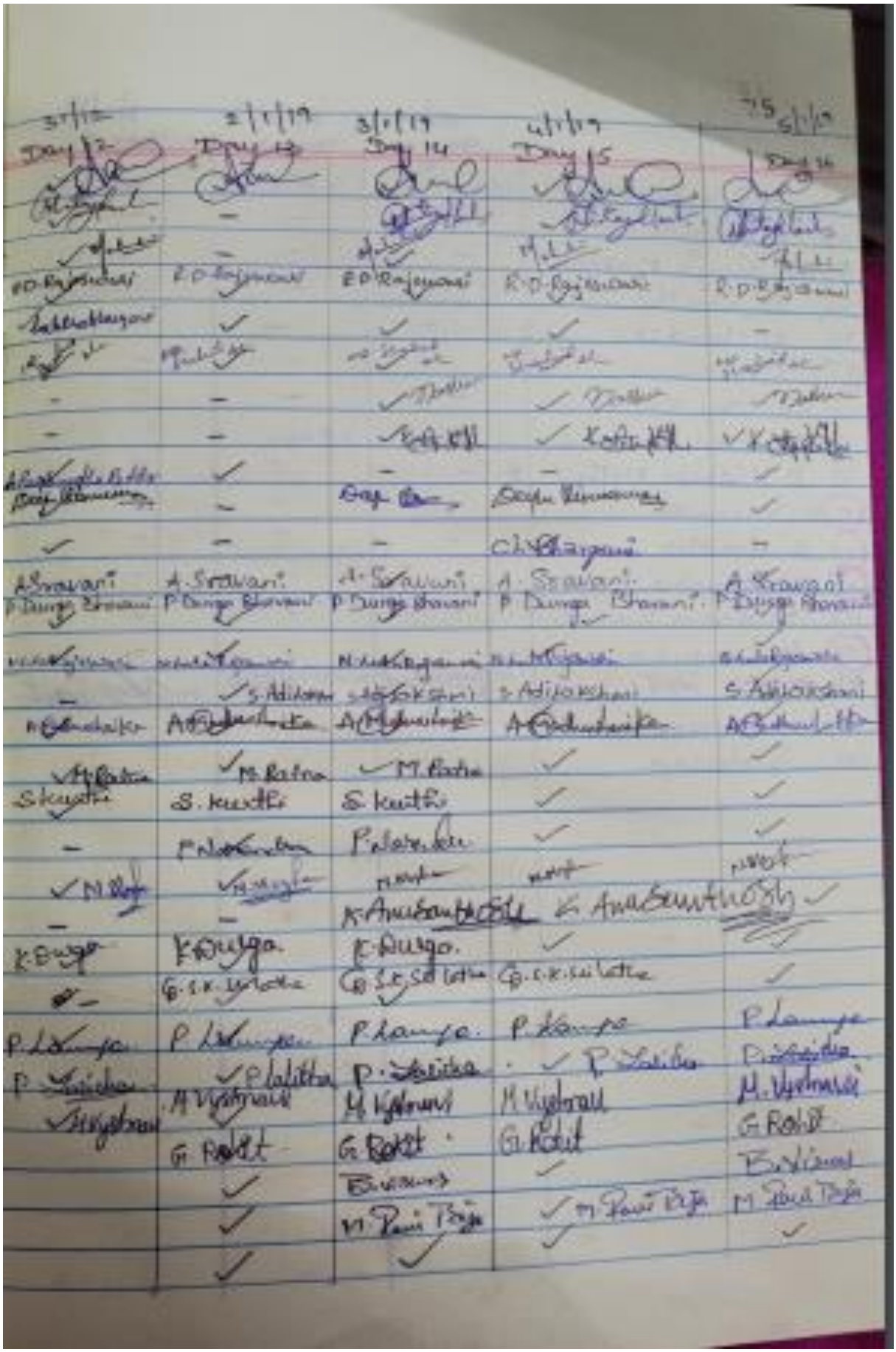
S.R.R.&C.V.R. GOVT.DEGREE COLLEGE(A)

Department of Biochemistry



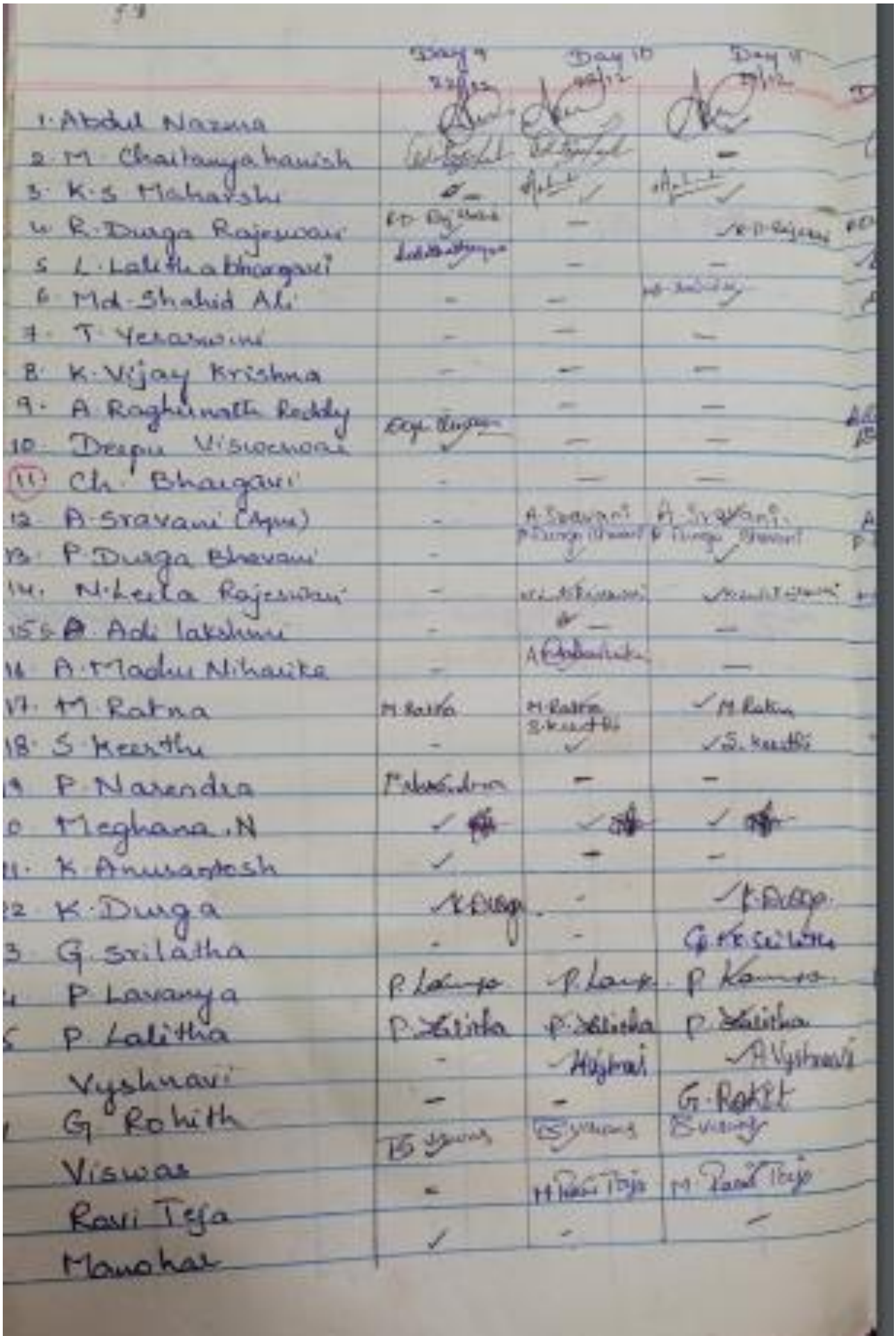
S.R.R.&C.V.R. GOVT.DEGREE COLLEGE(A)

Department of Biochemistry



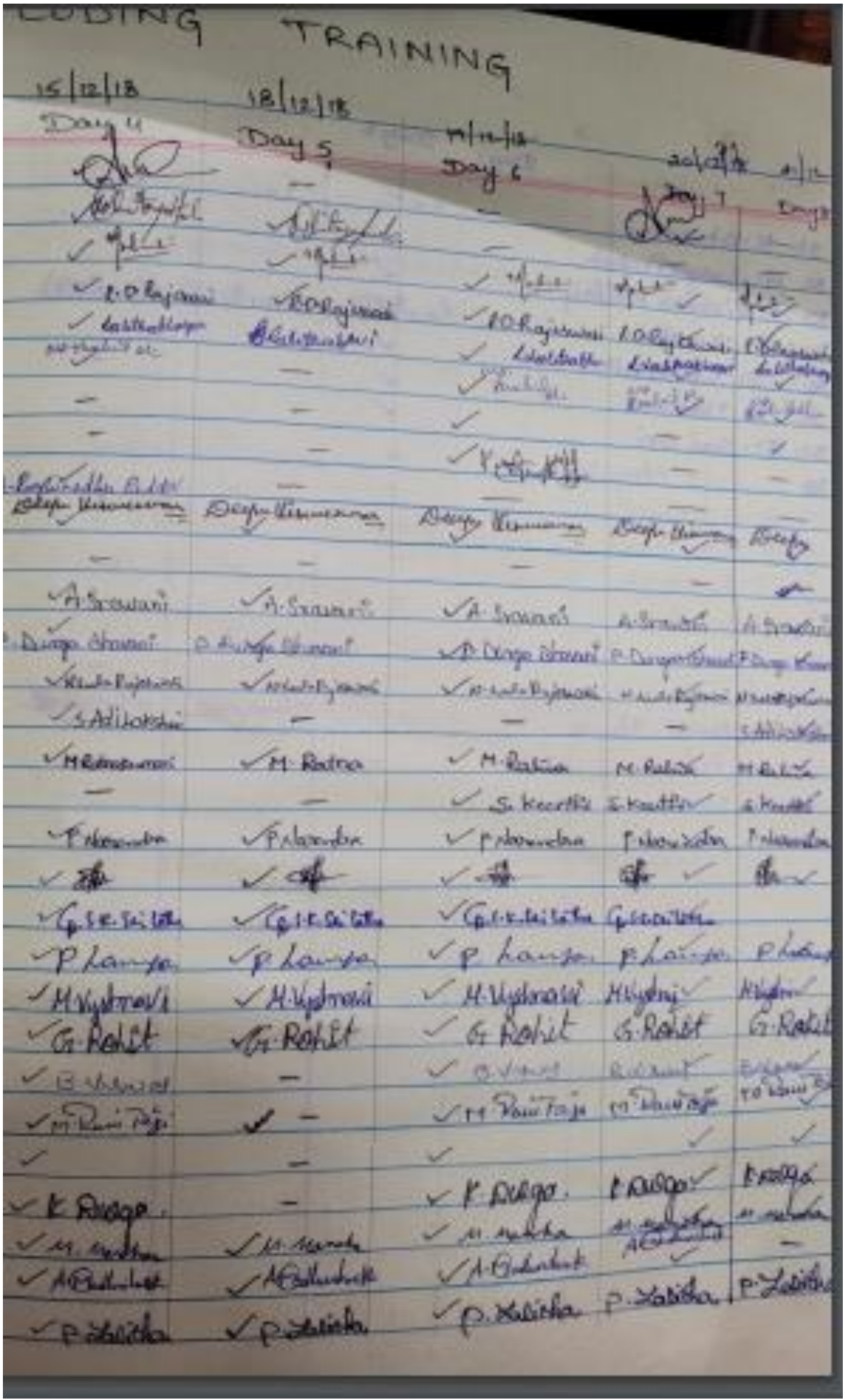
S.R.R.&C.V.R. GOVT.DEGREE COLLEGE(A)

Department of Biochemistry



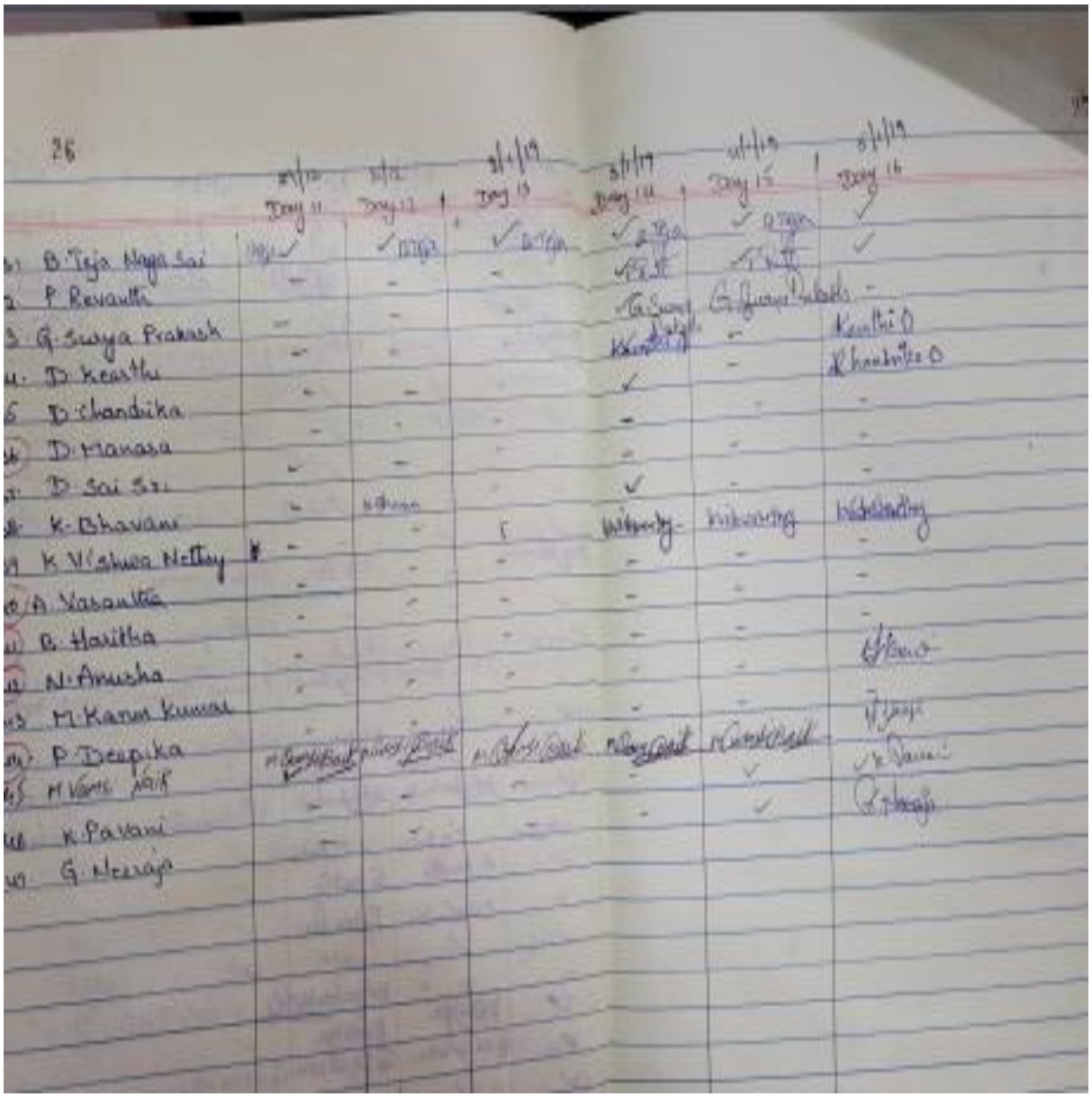
S.R.R.&C.V.R. GOVT.DEGREE COLLEGE(A)

Department of Biochemistry



S.R.R.&C.V.R. GOVT.DEGREE COLLEGE(A)

Department of Biochemistry



S.R.R.&C.V.R. GOVT.DEGREE COLLEGE(A)

Department of Biochemistry



Students successfully completed the

Medical coding program



PhyCare Services
(An ISO 9001:2008 & ISO 27001:2005 Company)

PhyCare Services India Pvt. Ltd.,
Plot No.9, Survey No.49,
IT Park, Mangalagiri,
Guntur District – 522 503
Andhra Pradesh, INDIA
Tel : +91 9394411007
www.phycaresolutions.com

Letter of Appointment

Date: 19 January, 2021
Ref: Appt./MC/HR/01/2021

Dear **Mr. Vishwanethry Kanuru,**

We are happy to offer you the letter of appointment with following position in our Organization under the terms and conditions indicated below:

Position: Junior - Executive

Department: Medical Coding - RCM

Date of Joining: 19 January, 2021

Your consolidated salary and other benefits (CTC) have been fixed at **INR. 10,000.00 (Rupees Ten Thousand Only)** per month payable on the 5th of the subsequent month. The payment of salary and other benefits will be subject to the deduction of Income Tax in accordance with the provisions of the Income Tax Act, 1961, and provisions of other applicable statutes, as at the time of payment.

All statutory deductions viz., PF, Professional Tax, IT, if applicable, will be done as per the prevailing rules of the Government and employers' contribution, where applicable, will be paid to the concerned department to the credit of your account. Gratuity and other benefits will be as per law. And annual performance incentives will be as per Company policy.

Income Tax Liability

The Income Tax Liability with regards to your salary and perks will be your liability, and will be governed by the tax laws of the country as applicable from time to time including TDS. You will have to work out your tax planning with us and advise us accordingly for IT TDS deduction failing which, the company will make the necessary calculations based on assumptions and deduct the TDS as shown above, in which case you will have to apply for refund of excess tax paid, if any, with IT Dept., on your own.

The cost to the company (CTC) of your employment works out to INR. 10,000.00.

Probationary Period: (IF mentioned as NIL in the period of probation, this section is not applicable to you).

You will be on probation for a period of **Six Months** from the date of joining. Upon satisfactory completion of this period & after the background verification which should be positive, you may be confirmed in the regular cadre of the Company.

During the period of probation, in the event of your resignation/leaving the company you will be required to give 60 days' notice to ensure smooth transition/takeover of duties without loss to the Company. In cases where adequate notice is not given, salary for the period of shortfall will be deducted while carrying out the full and final settlement. Also, during the period of probation, the Company may terminate the services of an individual without assigning any reasons, but with a minimum of one-weeks' notice or salary in lieu thereof. However, the management reserves the right to waive or reduce the notice period required to be given by the employee based on special circumstances of each case. Subsequently, on confirmation, you will have to give 60 working days notice. In the event that requisite period of notice is not being given by the employee, they will be liable to compensate proportionately to the extent of salary and allowances due for the period of shortfall in notice period or as mentioned in relieving point.

Professional Ethics

You are required to deal with the Company's money, material and documents with utmost honesty and professional ethics. If you are found guilty, at any point of time of moral turpitude or of dishonesty in dealing with the Company's money or material or documents or of theft or of misappropriation, regardless of the value involved your services would be terminated with immediate effect, not withstanding other terms and conditions mentioned in the appointment letter.

Performance Appraisal

Your next review of salary will be done on satisfactory completion of one-year service with us, subject to your appointment being confirmed as permanent, if you have been appointed on a probationary basis. Your performance appraisal will be conducted as per prevailing Company's policy. There shall be no automatic increments expect performance based incentives that may be given as per the Company policy for rewarding the performance of individuals after one year. The performance will

PhyCARE-HRD/2021-APL-4.0 Page 1 of 6 Confidential

in turn depend on the business prosperity appraisal of the whole business of the Company as conducted by the management. Your promotion to other positions or opportunities depends on your performance as mentioned above. And at point if your performance is not appreciated or not according to the standards then it can also be a negative appraisal or even no appraisal at all, until your performance is at par with others or as per the standards.

General

- You agree to devote your full time and ability to the Company and shall not engage yourself in other employment, business or vocation, whether part time or full time and whether with or without necessary benefits, without the prior written consent of the Company.
- You agree to comply with and abide by the policies, procedures, guidelines, code of conduct, standing orders and other rules and regulations of the Company that may currently be in-force or that may be issued or communicated to you from time to time, through the Employees' Manual, Circulars, Notices or otherwise.
- Any payment, not due to you, but made to you by the Company as a result of clerical/supervisory lapse, though may have recurred, will not entitle you to such payments as a matter of right. Management has the right not only to stop such payments, once detected, but will also recover such payments made earlier from amounts payable to you subsequently.

Offer letter received by Mr. Vishwanethtry Kanuru, of batch 2017-2019, was selected as a junior executive in medical coding at PhyCare services, IT PARK, Mangalagiri.

SRR & CVR GOVERNMENT DEGREE COLLEGE (A)
VIJAYAWADA

DRC conducted the Workshop on SVEEP 2019 March.in collaboration with District revenue administration

The SRR & CVR Degree College (A), Vijayawada, the District Resource Center, Krishna along with the Krishna, District revenue administration conducted the Systematic Voter Education Enrollment Program in the month of March 2019. The Principal of SRR & CVR Degree College (A), Vijayawada Dr.Velaga Joshi aired his views on the significance of vote in democracy. Activities under the Systematic Voters' Education and Electoral Participation (SVEEP) Programme are undertaken to educate the electors regarding procedures relating to registration of the name in Electoral Roll, correct of their existing particulars in Electoral Roll and deletion of the name of shifted and deceased family members.

Activities under the Systematic Voters' Education and Electoral Participation (SVEEP) Programme are undertaken to educate the electors regarding procedures relating to registration of the name in Electoral Roll, correct of their existing particulars in Electoral Roll and deletion of the name of shifted and deceased family members. SVEEP activities are also meant to inform about various online, and offline facilities available to voters regarding ethical voting like how to cast vote, how to help the election machinery prevent corrupt practices during elections etc. For awareness of general voters, following SVEEP activities have been initiated by the office of Chief Electoral Officer-Vijayawada.



Prayer by the students of SRR &CVR GDC(A) Vijayawada, during the SVEEP programme. Activities under the Systematic Voters' Education and Electoral Participation (SVEEP) Programme are undertaken to educate the electors regarding procedures relating to registration of the name in Electoral Roll, correct of their existing particulars in Electoral Roll and deletion of the name of shifted and deceased family members.

SRR& CVR GDC(A), student Miss V.Priyanka of IBSC(MECS) spoke on the importance of casting vote, voter registration and the importance of voting by the citizens.



Systematic Voters' Education and Electoral Participation program, better known as SVEEP, is the flagship program of the Election Commission of India for voter education, spreading voter awareness and promoting voter literacy in India. organisation registered under relevant Central or State Government Act can take part in the Institutional category. ➢ The participant shall give a brief description of the entry along with the name, address, and phone number. ➢ The participant shall email the entries along with the details to voter- contest@eci.gov.in.



The workshop was attended by District Collector, Krishna Sri Mohd.Imtiaz IAS and spoke to the SRR& CVR College students about the importance of vote and voter registration. Since 2009, Election has been working towards preparing electors and equipping them with basic knowledge related to the electoral process. SVEEP's primary goal is to build a truly participative democracy in India by encouraging all eligible citizens to vote and make an informed decision during the elections.



The rally took place in Vijayawada by the students of SRR & CVR GDC(A),Vijayawada. Specifically, this citizen-voter education module aims to: -acquaint the electorate with the basic concepts of democracy and the role of elections in democracy and governance; -stress the importance of one's vote; -encourage voters to participate in the whole electoral and governance process; and -eventually effect ...

By providing unbiased, non-partisan information, voters are able to connect directly with the facts so they can: Register to vote. Learn about the candidates and issues on their ballot. The law does not require citizens to vote, but voting is a very important part of any democracy. By voting, citizens are participating in the democratic process. Citizens vote for leaders to represent them and their ideas, and the leaders support the citizens' interests.





Rangavalli competitions were conducted in all colleges in the district and prizes were also distributed to the students. In order to encourage more young voters to take part in the political process, Government of India has decided to celebrate January 25 every year as "National Voters' Day". It has been started from 25 January 2011 to mark Commission's foundation day.





The students participated in Rangavalli Competitions in the college premises. Rangavalli reflects the theme of SVEEP means Systematic Voter Education and Enrollment Program. SVEEP's primary goal is to build a truly participative democracy in India by encouraging all eligible citizens to vote and make an informed decision during the elections. The programme is based on multiple general as well as targeted interventions which are designed according to the socio-economic, cultural and demographic profile of the state as well as the history of electoral participation in previous rounds of elections and learning thereof.

Essay writing competitions were conducted across the Krishna district and students enthusiastically participated from all colleges. Systematic Voters' Education and Electoral Participation program, better known as SVEEP, is the flagship program of the Election Commission of India for voter education, spreading voter awareness and promoting voter literacy in India. Since 2009, we have been working towards preparing India's electors and equipping them with basic knowledge related to the electoral process.







District level meetings were conducted at Kalakshetram, Vijayawada and all-district level heads of the departments participated. The Election Commission has declared 2019 as the 'year of the electoral roll'. The focus is on 'Purifying the electoral roll' by including more eligible voters particularly youth, women, and the Homeless' and deletion of non-existent with the due process of law. Summary Revision is done every year based on the qualifying date as of 1st January based on the Election Commission's directions and the time frame prescribed by them. There is a lot of gap between what the voters should know and what they actually

know in important areas related to Election function and management. This knowledge needs to be addressed by election Managers with a sense of urgency. Experience showed that even greater awareness does not necessarily get converted into greater Participation and the answer to this question has been found in voter education which is the most appropriate way to improve participation in a democracy in a country like India. We know that this is not a simple exercise though we have tried our level best to make this plan specific to our district and with this background; we are submitting our SVEEP Plan for Voter Registration of our District to achieve the goals and objective.

Overview - In the country like India, the legal age of casting the vote for assembly and parliamentary elections is 18 years and above. The Election Commission of India (ECI) has been consistently placing its indomitable efforts to encompass the entire citizen of India aiming that the eligible age group should be registered in the electoral list and must participate in the voting process. To a greater extent, these efforts have produced results but a lot of efforts need to be done in this direction and being done The issues like low understanding of the importance of the electoral process, thin participation of women at polling Booths, accessibility of ostracized sections of the society to polling booths and intimidated voters still pose challenges for the system. To address all such issues, the Election Commission of India has unfolded the strategy of SVEEP. When an assembly election in Andhra Pradesh is on the cards and the Parliamentary election is expected to be held in the year 2018, SVEEP adopts its vitality. SVEEP stands for Systematic Voters' Education for Electoral Participation, a process of concerted interventions to add people to the electoral process by sensitization and facilitation and ascertains increased participation of eligible age group people across all the sections and gender of society. When the electoral situation described in this report is seen, it is clear that certain polling booths have shown dismal turnout and poor participation of women voters. In such a context, the significance of SVEEP sounds relevant. SVEEP focuses on a targeted approach to bridge the gaps in enrolment.

SVEEP 2019 PROGRAMME SHEET

Calendar of SVEEP Activities

Krishna District

S. No	Date	Activity to be taken up
1	25-02-2019	• Roll-out of SVEEP Campaign • Flaging-off of the mobile awareness vehicles • Unveiling of Krishnayya Thatha
2	26-02-2019	• Slogan & Poster Making Competition- College Level
3	27-02-2019	• Human chain in all colleges • Voter Facilitation Counters in cinema halls & malls to be set up
4	28-02-2019	• Human chain in all schools • Slogan & Poster Making Competition- Inter College (Constituency Level)
5	01-03-2019	• Essay Writing & Debate Competitions in colleges • Know Your BLO Campaign kickstart
6	02-03-2019	• Drawing/ Painting Competition in all schools • Pledge to Vote Campaign starts
7	03-03-2019	• Street Plays • Slogan & Poster Making Competition- District Level
8	04-03-2019	• NCC Cadets rally
9	05-03-2019	• Essay Writing & Debate Competitions- Inter College (Constituency Level)
10	06-03-2019	• Rangoli Competitions for women
11	07-03-2019	• Technology Solutions for the voting process (Hackathon/ Competition in engineering colleges) • Essay Writing & Debate Competitions- District Level
12	08-03-2019	• Women Voters Walk • Rangoli Competitions Winners announcement
13	09-03-2019	• Campus Ambassadors announcement
14	10-03-2019	• Flash mobs by college students in malls
15	11-03-2019	• Meeting with all campus ambassadors
16	12-03-2019	• Campus Connect- Interaction of eminent speakers with college students • Cultural Programmes at Ghats
17	13-03-2019	• Campus Connect- Interaction of eminent speakers with college students • Cultural Programmes at Ghats
18	14-03-2019	• Campus Connect- Interaction of eminent speakers with college students • Cultural Programmes at Ghats
19	15-03-2019	• Human chain with PwDs
20	16-03-2019	• Campus Connect- Interaction of eminent speakers with college students • Cultural Programmes at Ghats
21	17-03-2019	• Collaborations with CSR/ Corporates to be finalized
22	18-03-2019	• Campus Connect- Interaction of eminent speakers with college students • Cultural Programmes at Ghats
23	19-03-2019	• Campus Connect- Interaction of eminent speakers with college students • Cultural Programmes at Ghats
24	20-03-2019	• Campus Connect- Interaction of eminent speakers with college students • Cultural Programmes at Ghats
25	21-03-2019	• NSS Volunteers rally
26	22-03-2019	• 2k Run
27	23-03-2019	• Street Play in a mall • Young Voters Festival (winners of all competitions to be given prizes)
28	24-03-2019	• Closing night of cultural programmes
29	25-03-2019	• SVEEP Campaign ends

Additional activities to be undertaken:

1. Voter Facilitation Counters in Cinema Halls & Malls: From 27-02-2019 to 25-03-2019 (to be set up at the entrance of the cinema hall/ mall)
2. Street Plays/ Kala Jathas: From 03-03-2019 to 25-03-2019 (will be scheduled constituency-wise)
3. Continuous engagement with all stakeholders through social media
4. Krishnayya Thatha (Campaign Mascot) will be created and used extensively to engage with the voters

S.R.R. and C.V.R. Govt. Degree College (A)
Machavarm, Vijayawada

Department of Microbiology in Association with WIPRO-GE HEALTHCARE, TATA TRUST AND GRAM TARANG

(CENTURION UNIVERSITY)

Certificate Course On

OPERATION THEATRE AND ANESTHESIA TECHNOLOGY

Course Duration: Six Months May 11th 2018 to Nov 15th 2018

Objectives:

The course is designed to meet the growing demand of experts in the fields of anaesthesia technology & operation theatre management, medical ethics, post operative care.

The course entails training of students in both theoretical and practical aspects of operating room technology. The student would be trained in various aspects of patient care, pre operative preparation, instrumentation, sterilization, operating room concepts, anesthesia, operating techniques and assistance to surgeons. On completion of the course the student would be able to perform as an operating theater nurse/ technologist in all aspects of surgical intervention in patient care.

They learn the utilization of numerous diagnostic equipments and also patient assessment abilities. Training also concentrates on the knowledge and skills of monitoring infection control policy and procedures in operation theatre.

List of Students: 22

S No	Name of the Student	Class
1	KAMABATTULA BHARGAVI	**III BSc MBC**
2	MERUGUMALA SRAVANI	
3	DEVULURI TONNY	
4	NETHALA JAYABABU	
5	MANDADAPU V VENUGOPAL	
6	MOHAMMED SOHAIL	
7	THOTA V S K MANIKANTA	
8	VALLURI LAKSHMINARAYANA	
9	GANDIKOTA NAGA PRATHYUSHA	
10	GUNTUR PRAVALLIKA	
11	GUBBALA NAVYASREE DURGA	
12	KOPPULA UDAY BHANU	
13	NEMALIKANTI SUDHAKAR	
14	ALLU INDU	
15	BOMMIDI PRASANTHI	
16	DEVADA SANTHOSI KUMARI	
17	PAPABATHINA ROJA	
18	BEZAWADA BLESSI	
19	BEJAWADA RANI PRAMILA	
20	BEVARA DIVYA	
21	RALI KALYANI	
22	BOGGAVARAPU RAJA KUMARI	







Student hands-on training in procedures










ప్రశాంత్ హాస్పిటల్

IN ASSOCIATION WITH

WIPRO-GE HEALTHCARE, TATA TRUST AND GRAM TARANG (CENTURION UNIVERSITY)

COURSE: OPERATION THEATRE AND ANESTHESIA TECHNOLOGY

CENTRE: SRR & CVR GDC (A), VIJAYAWADA

DATE OF EXAM- 27 AUGUST 2018 TIME- 10:15 AM TO 11:45 AM (90 MINS)

TOTAL MARKS- 80 PASS MARK- 50/80

INSTRUCTIONS

- EACH MODULE/SUBJECT WILL BE VALIDATED SEPARATELY. HENCE DONOT COMBINE ALL ANSWERS. USE SEPARATE PAPER FOR EACH SUBJECT WITH HEADING.
- NO MARKS FOR MISMATCHED QUESTION NUMBER TO ANSWER.
- DONOT WRITE QUESTIONS ON ANSWER SHEET. JUST MENTION QUESTION NUMBER TO ANSWER.
- NO COPIES ALLOWED.
- ANSWER ALL THE FOLLOWING QUESTIONS.

ALL THE BEST

ANATOMY AND PHYSIOLOGY – 25 MARKS

1. PARTS OF CELL
2. TYPES OF JOINTS
3. CONDUCTION SYSTEM OF HEART
4. MUSCLES OF RESPIRATION
5. NORMAL HR, BP, TEMP
6. TYPES OF BLOOD VESSELS
7. HORMONES PRODUCED BY PITUITARY GLANDS
8. PARTS OF NERVOUS SYSTEM (BOTH CNS AND PNS)
9. TYPES OF BLOOD CELLS
10. WHAT IS CSF? WHAT IS LUMBAR PUNCTURE?
11. PULSE POINTS
12. PARTS OF DIGESTIVE SYSTEM IN ORDER
13. WHAT IS COPD?
14. LIST SPECIAL SENSES
15. TYPES OF MUSCLE TISSUES
16. FUNCTIONS OF URINARY SYSTEM
17. MECHANISM OF VENTILATION
18. PARTS OF BRAIN
19. DIFFERENCE BETWEEN TENDONS AND LIGAMENTS

20. FUNCTIONS OF THE INTEGUMENTARY SYSTEM
21. SYSTEMIC AND PULMONARY CIRCULATION
22. WHAT IS BILE?
23. TYPES OF TISSUES
24. LIST SPINAL AND CRANIAL NERVES
25. DEFINE THE FOLLOWING
    A) HEMOLYSIS
    B) APNEA
    C) HYPOXIA
    D) HOMEOSTASIS

BASICS TO ANESTHETICS – 25 MARKS

1. WHAT IS ANESTHESIA?
2. WHAT IS CRITICAL FLOW?
3. PARTS OF ANESTHESIA MACHINE
4. BOYLE'S LAW
5. WHAT ARE MEDICAL GASES?
6. LIST EQUIPMENTS USED FOR GENERAL ANESTHESIA
7. PHASES OF ANESTHESIA CARE
8. STATES OF MATTER
9. INDICATIONS FOR OXYGEN THERAPY
10. WHAT IS HANGER YOLK ASSEMBLY?
11. PHASES OF GENERAL ANESTHESIA
12. TYPES OF HYPOXIA
13. ASA CLASSIFICATION
14. HAZARDS OF OXYGEN THERAPY
15. PIN INDEX SYSTEM
16. DIFFERENCE BETWEEN SPINAL AND EPIDURAL ANESTHESIA
17. NAME SOME GENERAL ANESTHETIC AGENTS
18. CONSIDERATIONS FOR CHOOSING A SPECIFIC TYPE OF ANESTHESIA
19. STANDARDS FOR BASIC ANESTHESIA MONITORING
20. STORAGE OF MEDICAL GASES
21. OXYGEN DELIVERY METHODS
22. FLUID FLOW TYPES
23. HYPOXEMIA
24. PREOPERATIVE EVALUATION OF ANESTHESIA
25. PREREQUISITES FOR ANESTHESIA

MICROBIOLOGY – 10 MARKS

1. WHAT IS MICROBIOLOGY?
2. WHAT IS IMMUNITY?
3. MICROORGANISMS ARE CLASSIFIED INTO HOW MANY TYPES?
4. TYPES OF IMMUNITY
5. NATURAL AND PASSIVE IMMUNITY
6. DIFFERENT TYPES OF BACTERIAL INFECTIONS
7. WHAT ARE VIRAL DISORDERS?
8. CELLS OF IMMUNE SYSTEM
9. DEFENSE MECHANISM OF NATURAL IMMUNITY
10. DIFFERENTIATE THE BACTERIA BASED ON THEIR CELLMEMBRANE

PATHOLOGY – 15 MARKS

1. WHAT IS PATHOLOGY?
2. WHAT IS PATHOGEN?
3. NEOPLASTIC DISORDERS
4. CARDIOVASCULAR DISORDERS
5. CYSTIC DISORDERS
6. SYMPTOMS OF CYSTIC DISORDERS
7. CAUSES OF MUSCULOSKELETAL DISORDERS
8. ATHEROSCLEROSIS
9. INFLAMMATORY HEART DISEASE
10. OSTEOPOROSIS
11. URINARY TRACT INFECTIONS
12. WHAT ARE SEXUALLY TRANSMITTED DISEASES?
13. VASCULAR DISORDERS
14. SYMPTOMS OF NERVOUS DISORDERS
15. CAUSES OF NEOPLASTIC DISORDERS

SOFT SKILLS – 05 MARKS

1. WHAT ARE INTERPERSONAL SKILLS?
2. SMILING FACE
3. WHAT ARE COMMUNICATION SKILLS?
4. HOW TO MANAGE TIME?
5. RESPONSIBILITY AS A HEALTHCARE PROFESSIONAL

Gram Tarang Employability Training Services (p) ltd.

Clearance Certificate

Employee Name	CHOPPAVARAPU DORCAS	Date of Join	11/05/2018
Reporting To	V. RAVI KUMAR	Date of Leaving	30/11/2018
Designation	ASSOCIATE TRAINER, SOFT SKILLS	Work Location	VIJAYAWADA.

Sl No	Department	Description	Comments	Signature
01	Department Head	Current Pending task	NONE	
		Documents	–	
		Files (Soft & Hard)	–	
02	Accounts & Finance	Company Loan	NA	
		Advance	NA	
		Financial liabilities	NA	
		Bill liabilities	NA	
03	HR	Stationary	–	
		Files	–	
		Company Assets	–	
		Salary	November Pending	
		Login ID	choppavarapu.anand@gramtarang.orgin	
		Laptop & Accessories	–	
04	Store/IT	–	–	

I hereby declared that I have handed over all my charge and company property to all respective departments.

C. Dorcas Anand	29-11-2018	
Employee Signature	**Date**	**Director/HR**

GRAM TARANG EMPLOYABILITY TRAINING SERVICES (GTETS) DATE 29/11 GTETS

WORKSHOP

SENSOR GUIDED ROBOT

DATE: 18-09- 2018 to 19-09-2018

No. of Participants : 47

Instructor: Mr. Tej Kumar Saka,

Engineer at Roboversity, Skyfi Labs

DEPARTMENT OF PHYSICS & ELECTRONICS

SRR & CVR GOVERNMENT DEGREE COLLEGE(A)

MACHAVARAM, VIJAYAWADA

Sensor Guided Robot

Robotics workshop is conducted to Physics & electronics students on 18th & 19th of September month 2018 with the collaboration of Sky- fi labs Bangalore run by IIT Kanpur, alumni affiliated to Angel's Organisation, Bangalore.. They had trained students to impart the skills of mechanics, electronics involved to make robots.

Workshop Outline: Students are trained to develop following projects using Ardunio programming with sensors.

Installation of Arduino Software in laptop & Programming to the Arduino UNO.

Explanation of that how the Programming language is stored in microcontroller as binary instructions.

Electrical Circuit Design for

Line Follower Robot
Obstacle Follower Robot
Obstacle Avoider Robot

Arduino based line follower robot, used IR Transmitters and IR receivers. They are used for sending and receiving light. IR transmits infrared lights. When infrared rays fall on the white surface, it's reflected back and caught by IR sensor which generate some voltage changes.

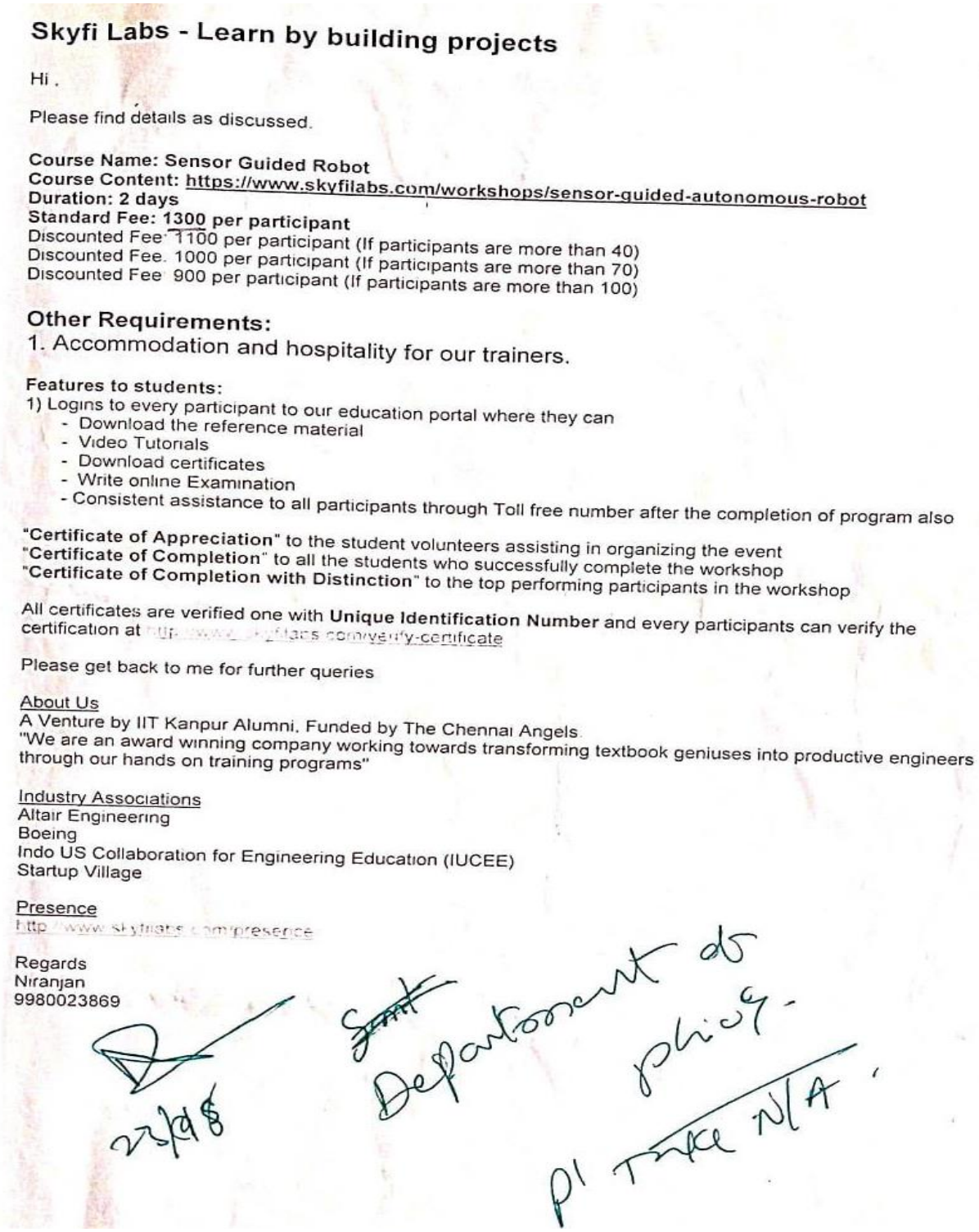
By using ultrasonic sensor, the line follower can detect an obstacle and can stop till the obstacle is removed. These robots can be used as automated equipment carriers in industries replacing traditional conveyer belts.
An obstacle avoiding robot is a fully autonomous robot which can be able to avoid any obstacle which it face when it move.

Action Plan

Department in charge Smt. P. Sailaja & Senior faculty Dr. R. Kameswari actively organised this training by proper Planning. They coordinated this training program with the Skifi Lab team, Bangalore through telephonic conservation & emails.

Skifi Lab accepted to train students & the fee amount to offer the course is sent through email.

Principal Dr. Velaga Joshi readily accepted the proposal forwarded by Department of Physics & Electronics Department & provided financial support required to conduct the Robotics Training. Principal Sir, also provided Computer systems in computer Lab to program the Ardunio.



Skyfi Labs - Learn by building projects

Hi ,

Please find details as discussed.

Course Name: Sensor Guided Robot
Course Content: https://www.skyfilabs.com/workshops/sensor-guided-autonomous-robot
Duration: 2 days
Standard Fee: 1300 per participant
Discounted Fee 1100 per participant (If participants are more than 40)
Discounted Fee. 1000 per participant (If participants are more than 70)
Discounted Fee 900 per participant (If participants are more than 100)

Other Requirements:
1. Accommodation and hospitality for our trainers.

Features to students:
1) Logins to every participant to our education portal where they can
- Download the reference material
- Video Tutorials
- Download certificates
- Write online Examination
- Consistent assistance to all participants through Toll free number after the completion of program also

"**Certificate of Appreciation**" to the student volunteers assisting in organizing the event
"**Certificate of Completion**" to all the students who successfully complete the workshop
"**Certificate of Completion with Distinction**" to the top performing participants in the workshop

All certificates are verified one with **Unique Identification Number** and every participants can verify the certification at http://www.skyfilabs.com/verify-certificate

Please get back to me for further queries

About Us
A Venture by IIT Kanpur Alumni, Funded by The Chennai Angels
"We are an award winning company working towards transforming textbook geniuses into productive engineers through our hands on training programs"

Industry Associations
Altair Engineering
Boeing
Indo US Collaboration for Engineering Education (IUCEE)
Startup Village

Presence
http://www.skyfilabs.com/presence

Regards
Niranjan
9980023869

23/9/8

Department of physics.
PI Trace N/A.

To

Dr.Velaga Joshi

Chairman of the Finance Committee (Autonomous)

SRR & CVR Government Degree College

Vijayawada.

Respected Sir,

Sub: Allotment and issue of check from UGC (Autonomous funds) to conduct Workshop on Robotics on 18th and 19th September 2018 and Projects with PCB formations in December 2018

With reference to the subject, we department of Physics and Electronics have taken permission to conduct workshop on Robotics on 18th & 19th September 2018 in our College with UGC Autonomous funds. We are collaborating with SkyfiLabs, Bangalore. A Venture by IIT Kanpur Alumni. Funded by The Chennai Angels.

Course Name: Sensor Guided Robot
Course Content: https://www.skyfilabs.com/workshops/sensor-guided-autonomous-robot
Duration: 2 days

Certificate of Appreciation" to the student volunteers assisting in organizing the event
"**Certificate of Completion**" to all the students who successfully complete the workshop
"**Certificate of Completion with Distinction**" to the top performing participants in the workshop

All certificates are verified one with **Unique Identification Number** and every participants can verify the certification at http://www.skyfilabs.com/verify_certificate

The Communications from Skyfi Labs, Objective and outcome of the project are attached to this letter. The workshop enables our student to create robotic projects and PCB based projects which carry marks in their internal assessments. Main aim of the Workshop is to give " Hands on " experience to our students in creation of Projects and lead them to skill based learning.

We need an amount of Rs.50,000/- to conduct the two workshops. So kindly direct the UGC Finance committee to arrange the check to conduct the workshop success fully.

Thanking You Sir,

Yours faithfully,

Smt.P.Sailaja
Lecturer in-charge
Dept. of Physics & Electronics
SRR & CVR Govt. Degree College
VIJAYAWADA-4

(In-charge of the Dept)



केनरा बैंक Canara Bank
VIJAYAWADA GOVERNORPET Branch
VIJAYAWADA ANDHRA PRADESH 520002
IFSC : CNRB0000680
2018/PSSKW
MULTI-CITY SB
Valid for three months only from the date of instrument
1 9 0 9 2 0 1 8
D D M M Y Y Y Y

Pay Skyfi Education labs pvt ltd
या धारक को Or Bearer
Rupees रुपये Fourty nine thousand five hundred Rupees only.
अदा करें ₹ 49,500/-
A/c. No. 0680101022174
Payable at par at all our branches in India
PRINCIPAL
SRR& CVR GOVT. DEGREE COLLEGE
(Autonomus)
Machavaram, VIJAYAWADA - 520 004.

Financial Support:

The financial support from UGC autonomous funds made this dream true. A cheque of Rs. 49,500 is paid to the Skyfi Education Labs, Pvt. Ltd by the SRR & CVR Government Degree college to get train Students in advanced Robotics.

To

Dr.Velaga Joshi

PRINCIPAL

SRR & CVR Government Degree College

Vijayawada.

Respected Sir,

Sub: Permission for Computer systems along with Computer Lab to conduct Workshop on Robotics on 18th and 19th September 2018

With reference to the subject, we department of Physics and Electronics have taken permission to conduct workshop on Robotics on 18th & 19th September 2018 in our College with UGC Autonomous funds. We are collaborating with SkyfiLabs, Banglore. They requested for 10 Computer Systems with High speed internet in Computer Lab itself, Smart board. So kindly direct the Computer Science Department to make the necessary arrangements to give the systems with internet and Windows 7.

Thanking You Sir,

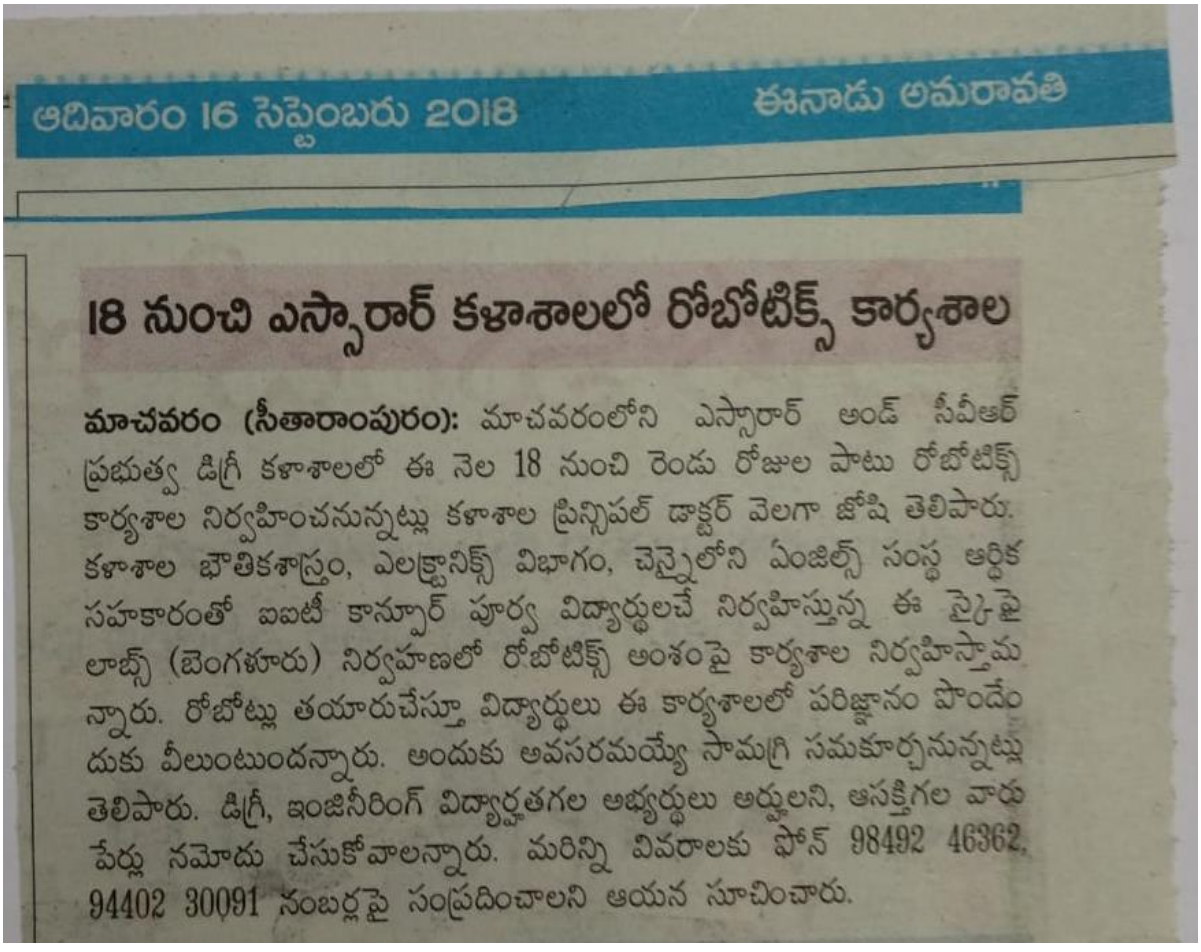
Yours faithfully,

P. Sailaja

(Smt.P.Sailaja)

(Incharge of the Dept)





ఆదివారం 16 సెప్టెంబరు 2018 ఈనాడు అమరావతి

18 నుంచి ఎస్సారార్ కళాశాలలో రోబోటిక్స్ కార్యశాల

మాచవరం (సీతారాంపురం): మాచవరంలోని ఎస్సారార్ అండ్ సీవీఆర్ ప్రభుత్వ డిగ్రీ కళాశాలలో ఈ నెల 18 నుంచి రెండు రోజుల పాటు రోబోటిక్స్ కార్యశాల నిర్వహించనున్నట్లు కళాశాల ప్రిన్సిపల్ డాక్టర్ వెలగా జోషి తెలిపారు. కళాశాల భౌతికశాస్త్రం, ఎలక్ట్రానిక్స్ విభాగం, చెన్నైలోని ఏంజిల్స్ సంస్థ ఆర్థిక సహకారంతో ఐఐటీ కాన్పూర్ పూర్వ విద్యార్థులచే నిర్వహిస్తున్న ఈ స్కైఫై లాబ్స్ (బెంగళూరు) నిర్వహణలో రోబోటిక్స్ అంశంపై కార్యశాల నిర్వహిస్తామన్నారు. రోబోట్లు తయారుచేస్తూ విద్యార్థులు ఈ కార్యశాలలో పరిజ్ఞానం పొందేందుకు వీలుంటుందన్నారు. అందుకు అవసరమయ్యే సామగ్రి సమకూర్చనున్నట్లు తెలిపారు. డిగ్రీ, ఇంజినీరింగ్ విద్యార్హతగల అభ్యర్థులు అర్హులని, ఆసక్తిగల వారు పేర్లు నమోదు చేసుకోవాలన్నారు. మరిన్ని వివరాలకు ఫోన్ 98492 46362, 94402 30091 నంబర్లపై సంప్రదించాలని ఆయన సూచించారు.

Learning Process

Interested students were selected from Science streams.30 students from III B.Sc , II B.Sc (MPCs, MECs) had enthusiastically participated in this workshop.

SRR & CVR GOVERNMENT DEGREE COLLEGE (A)

MACHAVARAM, VIJAYAWADA

TWO DAYS WORKSHOP ON ROBOTICS

September 18th & 19th

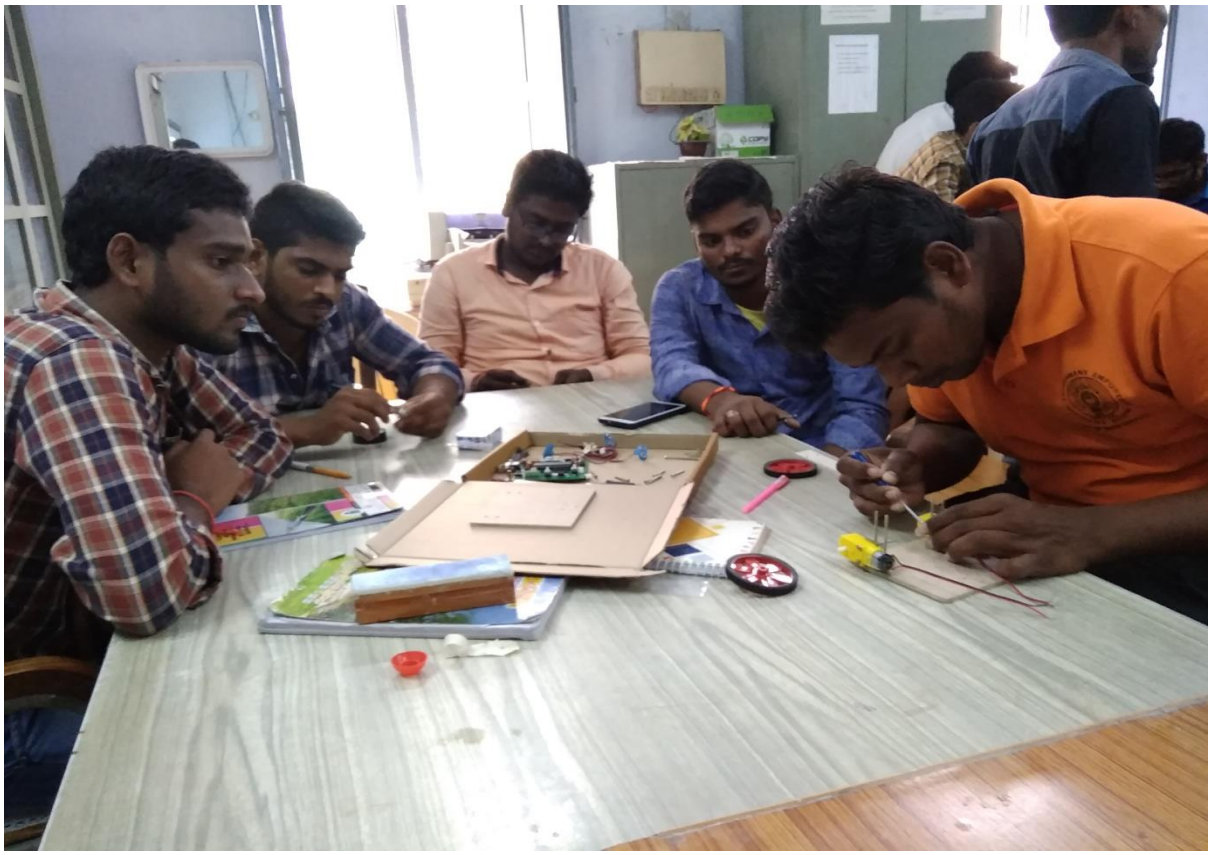
S.NO	NAME OF THE STUDENT	CLASS	COLLEGE NAME	E MAIL ID	MOBILE NO
1	E VENKATESWARA RAO	III BSC	SRR &CVR DEGREE COLLEGE	vaenkyerlla@gmail.com	7989583634
2	M SANDHYA	III BSC	SRR &CVR DEGREE COLLEGE	Sandhyasandi0001@gmail.com	7286813133
3	CH VASU	III BSC	SRR &CVR DEGREE COLLEGE	Vasuvicky00@gmail.com	7893343876
4	G S PRITHVI SAI	III BSC	SRR &CVR DEGREE COLLEGE	Prithvisai24@gmail.com	9493871663
5	D LOK MANOHAR	III BSC	SRR &CVR DEGREE COLLEGE	Lokmanoharkumar20@gmail.com	9701366639
6	R DURGA PRASAD	III BSC	SRR &CVR DEGREE COLLEGE	r.durgaprasad@gmail.com dsp903220	8885910208
7	V KALYAN KUMAR	III BSC	SRR &CVR DEGREE COLLEGE	kalyankumarkick@gmail.com	7794085191
8	T VENKATA SAI	III BSC	SRR &CVR DEGREE COLLEGE	Saivenkat71303@gmail.com	8886089120
9	M VIKRAM	III BSC	SRR &CVR DEGREE COLLEGE	Medavikram2017@gmail.com	9963192656
10	S SAI BHARGAV	III BSC	SRR &CVR DEGREE COLLEGE	Sbhargav626@gmail.com	8919991553
11	K NANDHINI	III BSC	SRR &CVR DEGREE COLLEGE	Nandhunandini79@gmail.com	9948809396

S.NO	NAME OF THE STUDENT	CLASS	COLLEGE NAME	E MAIL ID	MOBILE NO
12	J NIKHILA	III BSC	SRR &CVR DEGREE COLLEGE	Jonnalanikhila98@gmail.com	8328586453
13	CH VENKATA GANESH	III BSC	SRR &CVR DEGREE COLLEGE	Chintalaboinaganesh386@gmail.com	8464878023
14	D HANUMAN SANKAR	III BSC	SRR &CVR DEGREE COLLEGE	Hanumansankar57@gmail.com	9553404259
15	J BHASKAR	III BSC	SRR &CVR DEGREE COLLEGE	jonnakuribala@gmail.com	7285930718
16	P HARI KRISHNA	III BSC	SRR &CVR DEGREE COLLEGE	Haripydi5678@gmail.com	8179231510
17	K SUDHA RANI	III BSC	SRR &CVR DEGREE COLLEGE	Sudha99rani@gmail.com	9581508120
18	P JYOTSNA DEVI	III BSC	SRR &CVR DEGREE COLLEGE	Jyothsnadevi987@gmail.com	9154224493
19	G SUSMITHA	III BSC	SRR &CVR DEGREE COLLEGE	Susmithag95@gmail.com	9963996140
20	G HEMA LATHA	III BSC	SRR &CVR DEGREE COLLEGE	Hemadolly98@gmail.com	7901249772
21	D NEERAJA	III BSC	SRR &CVR DEGREE COLLEGE	Neerajadhanekula777@gmail.com	7095741676
22	M AKSHAY PAUL	I BSC	SRR &CVR DEGREE COLLEGE	bunnyakshaypaul@gmail.com	7036124373
23	S DINESH VENKATA SRI	III BSC	SRR &CVR DEGREE COLLEGE	Dineshnaidu48@gmail.com	7382325466
24	B SURYA PRAKASH	III BSC	SRR &CVR DEGREE COLLEGE	busasuryaprakash@gmail.com	9912824361
25	G SRI LAKSHMI	II BSC	SRR &CVR DEGREE COLLEGE	Srilakshmigaddam1234@gmail.com	8142491435
26	G DURGA BHAVANI	II BSC	SRR &CVR DEGREE COLLEGE	Durga9102000@gmail.com	9052882942
27	CH YASASVI	II BSC	SRR &CVR DEGREE COLLEGE	chintayasasvi@gmail.com	7288927266
28	S SATISH	III BSC	SRR &CVR DEGREE COLLEGE	Satish7prince@gmail.com	7032326993
29	K RAJESH	III BSC	SRR &CVR DEGREE COLLEGE	Katikalarajesh927@gmail.com	9553266856
30	R SITA MAHA LAKSHMI	II BSC	SRR &CVR DEGREE COLLEGE	Rseetha9k@gmail.com	8106175336

S.NO	NAME OF THE STUDENT	CLASS	COLLEGE NAME	E MAIL ID	MOBILE NO
31	S PUJITHA	II BSC	SRR &CVR DEGREE COLLEGE	poojithasanagasetti@gmail.com	9110562198
32	P SUREKHA	III BSC	SRR &CVR DEGREE COLLEGE	Pallipamusurekha98@gmail.com	9133436624
33	V RAJA NAIK	III BSC	SRR &CVR DEGREE COLLEGE	Naik3550@gmail.com	9133029432
34	L SAI KUMAR	III BSC	SRR &CVR DEGREE COLLEGE	Landasaikumar09@gmail.com	8639638588
35	MD MEHRAJUNNISA	III BSC	SRR &CVR DEGREE COLLEGE	Meharmehraj18@gmail.com	9550401265
36	CH PRATYUSHA	II BSC	SRR &CVR DEGREE COLLEGE	Chekurthipati1998@gmail.com	9505946291
37	K GOPI RAJU	III BSC	SRR &CVR DEGREE COLLEGE	Gopirajukorra0007@gmail.com	8688457573
38	N SAI MANEESA	III BSC	SRR &CVR DEGREE COLLEGE	Nsaimaneesha1988@gmail.com	7095165464
39	R MANI KANTA	III BSC	SRR &CVR DEGREE COLLEGE	Manikanta95r@gmail.com	7095387917
40	B V VARDHAN NAIDU	B TECH	SIR C R REDDY ENGG COLLEGE	Vivekavardhan12091999@gmail.com	9440231192
41	J DURGA PRASANTH	B TECH	SIR C R REDDY ENGG COLLEGE	jakkudurgaprasanth@gmail.com	6303838415
42	N MOHAN KUMAR	III BSC	SRR &CVR DEGREE COLLEGE	Nikkam.mohann599@gmail.com	8885833602
43	P SAMPATH	B TECH	NRI ENGG COLLEGE	Sampathprattipati5@gmail.com	9133219714
44	P A P BAGAT CHOWDARY	B TECH	NRI ENGG COLLEGE	Abishekchowdary434@gmail.com	9573662404
45	M GOPAL LAKSHMAN	B TECH	NRI ENGG COLLEGE	Lakshmanmarupilla1503@gmail.com	9491347438
46	U SURESH	III BSC	SRR &CVR DEGREE COLLEGE	Sureshu589@gmail.com	8522827882
47	J HEMANTH	III BSC	SRR &CVR DEGREE COLLEGE	Hemanthj7595@gmail.com	9700680652

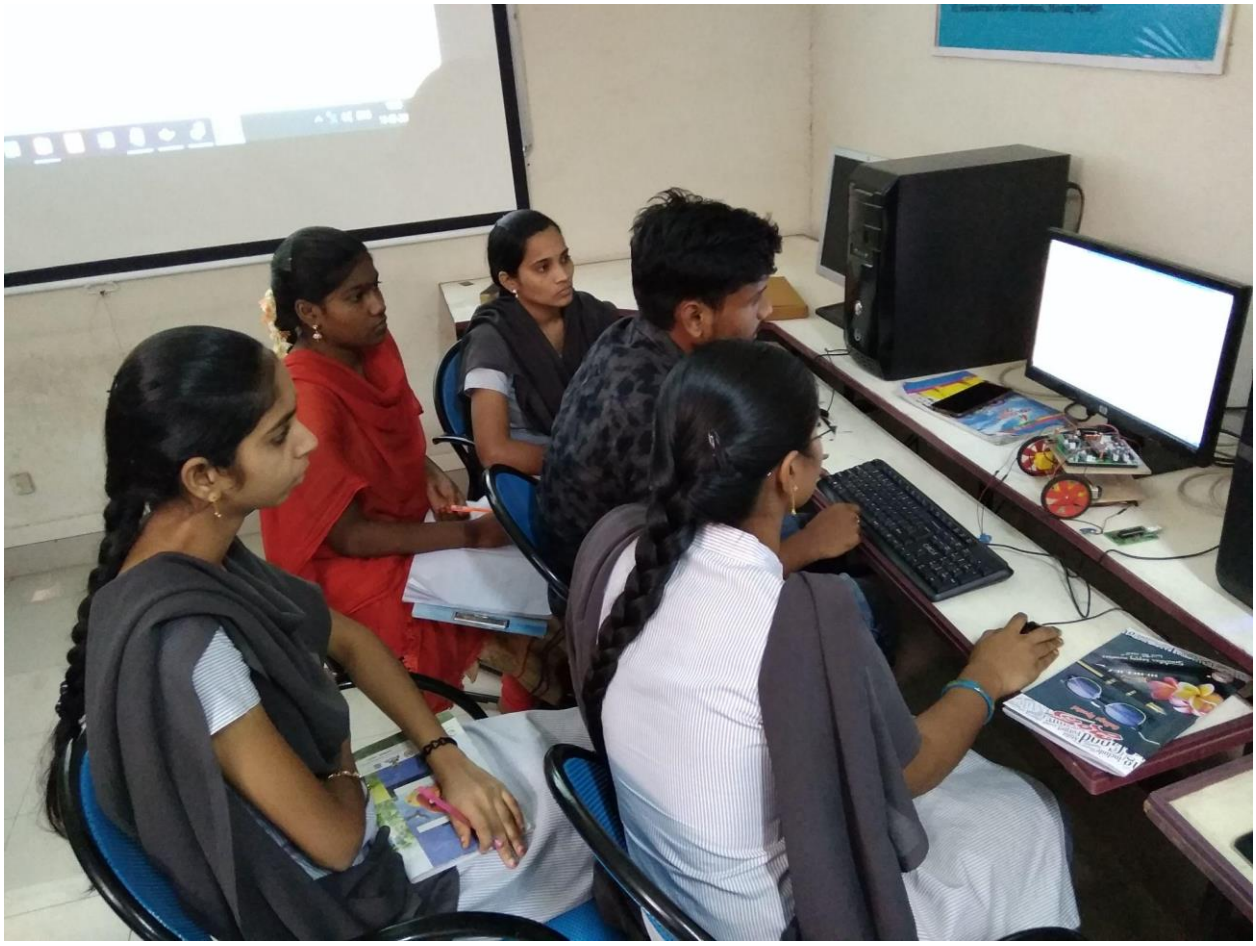
5 Students from NRI, Sir CR Reddy Engineering Colleges also joined in this workshop.

Students were trained theoretically about the programming concepts & had hands on experience to connect electrical circuit to Arduino pins.




S.R.R. & C.V.R. Government Degree College
UGC SPONSORED (AUTONOMOUS)
WORKSHOP ON ROBOTICS
"LEARN BY BUILDING PROJECTS"
Dr. VELAGA JOSHI





SRR & CVR GOVERNMENT DEGREE COLLEGE (A)

MACHAVARAM, VIJAYAWADA

TWO DAYS WORKSHOP ON ROBOTICS

September 18th & 19th

S NO	NAME OF THE STUDENT	18-SEPTEMBER		19 SEPTEMBER	
		FN	AN	FN	AN
1	E VENKATESWARA RAO				
2	M SANDHYA				
3	CH VASU				
4	G S PRITHVI SAI				
5	D LOK MANOHAR				
6	R DURGA PRASAD				
7	V KALYAN KUMAR				
8	T VENKATA SAI				
9	M VIKRAM				
10	S SAI BHARGAV				
11	K NANDHINI				
12	J NIKHILA				
13	CH VENKATA GANESH				
14	D HANUMAN SANKAR				
15	J BHASKAR				
16	P HARI KRISHNA				
17	K SUDHA RANI				
18	P JYOTSNA DEVI				
19	G SUSMITHA				
20	G HEMA LATHA				
21	D NEERAJA				
22	M AKSHAY PAUL				

23	S DINESH VENKATA SRI				
24	B SURYA PRAKASH				
25	G SRI LAKSHMI				
26	G DURGA BHAVANI				
27	CH YASASVI				
28	S SATISH				
29	K RAJESH				
30	R SITA MAHA LAKSHMI				
31	S PUJITHA				
32	P SUREKHA				
33	V RAJA NAIK				
34	L SAI KUMAR				
35	MD MEHRAJUNNISA				
36	CH PRATYUSHA				
37	K GOPI RAJU				
38	N SAI MANEESA				
39	R MANI KANTA				
40	B V VARDHAN NAIDU				
41	J DURGA PRASANTH				
42	N MOHAN KUMAR				
43	P SAMPATH				
44	P A P BAGAT CHOWDARY				
45	M GOPAL LAKSHMAN				
46	U SURESH				
47	J HEMANTH				

S.R.R & C.V.R Govt. Degree College (Autonomous)

Machavaram, Vijayawada-520 004, Krishna Dt. A.P

TWO DAYS WORKSHOP ON " ROBOTICS"

18-09-2018 & 19-09-2018, From 9.30 am to 5.00 pm

Conducted By

DEPARTMENT OF PHYSICS & ELECTRONICS

***in collaboration with* SKYFI LABS, Bangalore, A venture by IIT Kanpur Alumni,**

Funded by the Chennai Angels

REGISTRATION FORM



1. Name of the Applicant : J. Nikhila
2. Father's Name : J. Suresh
3. Date of Birth & Age : 27-09-1998
4. Address for Communication : DR.No. 32-26-62
   Sunkanavari street
   Machavaram. vijayawada
   Mobile No: 8328586453
   E-Mail ID: Jannalanikhila98@gmail.com
5. Educational Qualifications : Degree final year (pursuing)
6. Aadhar No. : 971040934245

7. Declaration: I hereby declare that the Information furnished above is ture to the the best of my knoledge. I will follow the rules and regulations of the College.

Date: - - 2018.

J. Nikhila

Signature of the Candidate

For Office Use Only

Fee paid Rs.....(Rupees.....only)

Vide Receipt No. : ....., Dt. - - 2018.

Office Staff **Incharge of Dept.** **Principal**

S.R.R & C.V.R Govt. Degree College (Autonomous)

Machavaram, Vijayawada-520 004, Krishna Dt. A.P

TWO DAYS WORKSHOP ON " ROBOTICS"

18-09-2018 & 19-09-2018, From 9.30 am to 5.00 pm

Conducted By

DEPARTMENT OF PHYSICS & ELECTRONICS

***in collaboration with* SKYFI LABS, Bangalore, A venture by IIT Kanpur Alumni,**

Funded by the Chennai Angels

REGISTRATION FORM



1. Name of the Applicant : G. Hemalatha
2. Father's Name : G. Srinadh
3. Date of Birth & Age : 23-7-1998, Age :-20y
4. Address for Communication : Sing nagar D.No:-77-137-1
   Sundharaiah nagar 4th Line
   Payakapuram, Vijayawada
   Mobile No: 7901204772
   E-Mail ID: Hemadolly98@gmail.com
5. Educational Qualifications : Degree 3rd year B.Sc.
6. Aadhar No. : 996887670984

7. Declaration: I hereby declare that the Information furnished above is ture to the the best of my knoledge. I will follow the rules and regulations of the College.

Date: 18-9-2018.

G. Hemalatha
Signature of the Candidate

For Office Use Only

Fee paid Rs.....(Rupees.....only)

Vide Receipt No. : ....., Dt. - - 2018.

Office Staff **Incharge of Dept.** **Principal**

Learning outcome:

Hands-on experience to students in creation of line follower Robot, obstacle avoiding Robot, obstacle follower robot using Ardunio coding. This leads them to skill based learning.

Students understand the structure and programming of microcontrollers and the techniques.

By using the same sensors and Learners enjoyed changing the programme login using the same sensor and how the function of Robot be modified .

Student participants come up with new ideas for further improvement of robots.

Impact:

The programme gave clear practical experience to students to understand the sensors and programming them with their own logic .

Students are able to develop the sensor Robots.

They got a way to opt Robotics as one of their career opportunities.

Students felt this course was fun with Knowledge.

Conclusion

Learners gave very positive feedback on this programme.

They got great satisfaction from designing their own robot with programming.

Students are issued digital verified e- certificates to their emails from Skifi labs, Bangalore.


VERIFIED CERTIFICATE

Skyfi labs
LEARN ENGINEERING. PRACTICALLY!

Roboversity

www.roboversity.com
www.skyfilabs.com

19 September 2018

SRR & CVR Govt. Degree College, Vijayawada

This is to certify that

SAILAJA PONNAM

has completed a 2-day project-based training program on

Sensor Guided Robotics

Unique Certificate Code: **48430044**

Verify at www.skyfilabs.com/verify-certificate/48430044

Pavan Kumar P
CEO, Skyfi Labs

SRR & CVR GOVERNMENT DEGREE COLLEGE (A)

MACHAVARAM, VIJAYAWADA

TWO DAYS WORKSHOP ON ROBOTICS

September 18th & 19th-2018

FEEDBACK FORM

1. **Name of the Trainee:** E. Venkateswara Rao
2. **Name of the College:** SRR & CVR Govt Degree college Vja(A)
3. **email-id:** : vaenkyesrlla@gmail.com
4. **How useful was workshop?**

(a) Beyond expectations (b) Satisfactory (c) Moderate

5. **How would you rate length of sessions?**

(a) Too long (b) Just right (c) Too short

6. **How would you rate this workshop?**

(a)Excellent (b) Very good (c) Good

7. **Trainer's knowledge of the subject**

(a) Excellent (b) Very good (c) Good

8. **Course materials/booklets**

(a) Excellent (b) Very good (c) Good

9. **The facilities**

(a) Excellent (b) Very good (c) Good

10. **Would you recommend this course to your friends?**

(a)Yes (b) No (c) Not sure

SRR & CVR GOVERNMENT DEGREE COLLEGE (A)

MACHAVARAM, VIJAYAWADA

TWO DAYS WORKSHOP ON ROBOTICS

September 18th & 19th-2018

FEEDBACK FORM

1. **Name of the Trainee:** E. Venkateswara Rao
2. **Name of the College:** SRR & CVR Govt Degree college Vja(
3. **email-id:** : Vaenkyeswa@gmail.com
4. **How useful was workshop?**

(a) Beyond expectations (b) Satisfactory (c) Moderate

5. **How would you rate length of sessions?**

(a) Too long (b) Just right (c) Too short

6. **How would you rate this workshop?**

(a)Excellent (b) Very good (c) Good

7. **Trainer's knowledge of the subject**

(a) Excellent (b) Very good (c) Good

8. **Course materials/booklets**

(a) Excellent (b) Very good (c) Good

9. **The facilities**

(a) Excellent (b) Very good (c) Good

10. **Would you recommend this course to your friends?**

(a)Yes (b) No (c) Not sure



ఈనాడు అమరావతి

గురువారం 20 సెప్టెంబరు 2018 .. 20 పేజీలు

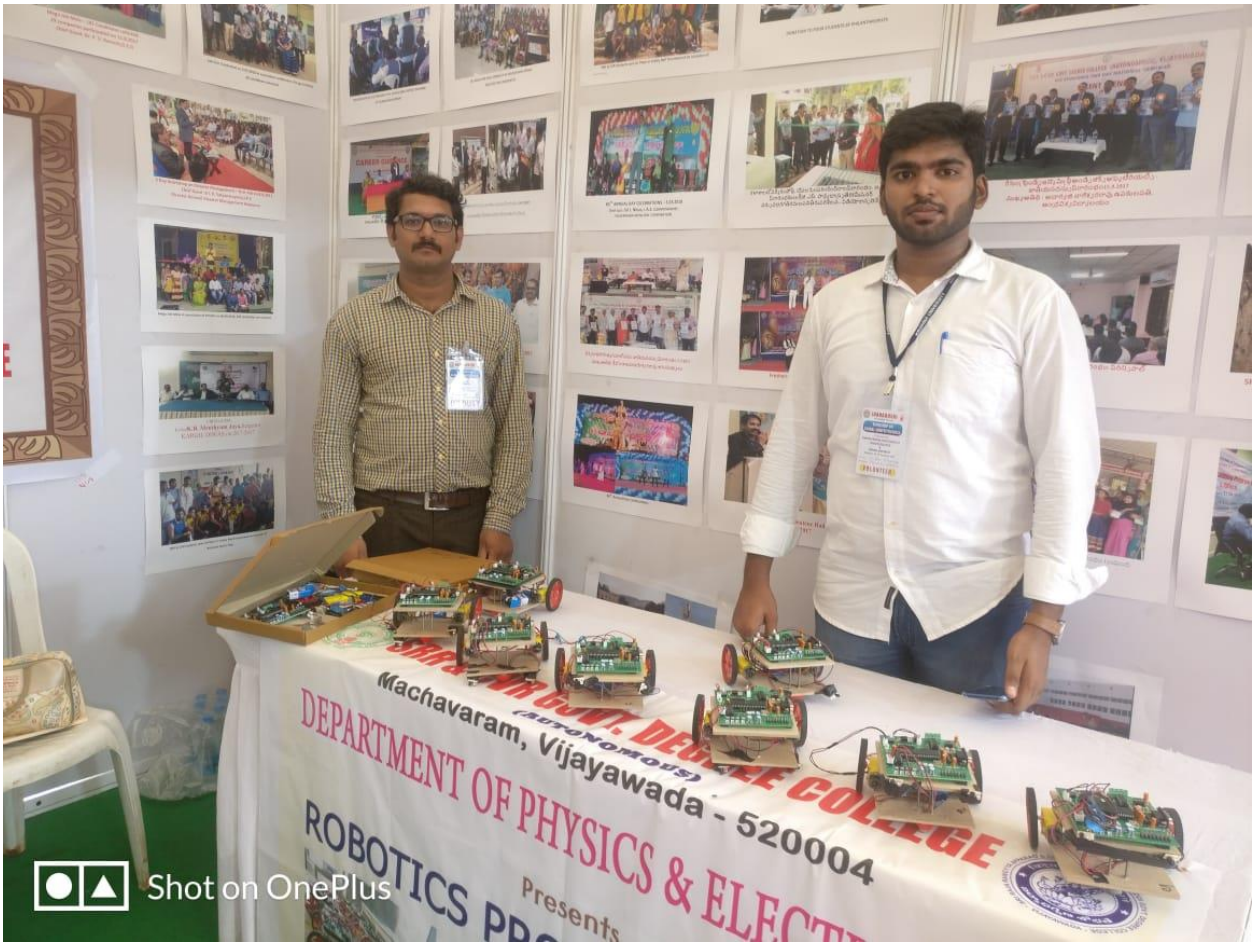
ముగిసిన రోబోటిక్స్ కార్యశాల

మాచవరం (సీతారాంపురం, న్యూస్‌టుడే): మాచవరంలోని ఎస్సారార్ అండ్ సీవీఆర్ ప్రభుత్వ డిగ్రీ కళాశాల ఫిజిక్స్, ఎలక్ట్రానిక్స్ విభాగం ఆధ్వర్యంలో రెండు రోజుల పాటు కళాశాలలో నిర్వహించిన రోబోటిక్స్ కార్యశాల బుధవారం ముగిసింది. ఎస్సారార్ అండ్ సీవీఆర్ ప్రభుత్వ డిగ్రీ కళాశాల బీఎస్సీ ఫైనల్ ఇయర్ విద్యార్థులతో పాటు ఇతర డిగ్రీ, ఇంజినీరింగ్ కళాశాలల నుంచి వచ్చిన 55 మంది అభ్యర్థులు కార్యశాలలో పాల్గొని ప్రత్యక్షంగా రోబోట్ తయారీ పరిజ్ఞానాన్ని పొందడమే కాకుండా స్వయంగా రోబోట్లను తయారుచేసి ప్రదర్శించారు. ఈ రోబోట్ల తయారీ కార్యశాలకు ఇంజినీరుగా తేజ్‌కుమార్ వ్యవహరించారు. చెన్నై ఏంజెల్స్ సంస్థచే ప్రాయోజితమైన స్కైపై ల్యాబ్స్ తరపున హాజరై రోబోట్ల తయారీ, పని తీరును విద్యార్థులకు నేర్పించారు. ఎస్సారార్ అండ్ సీవీఆర్ ప్రభుత్వ డిగ్రీ కళాశాల ప్రిన్సిపల్ డాక్టర్ వెలగా జోషి, భౌతికశాస్త్ర విభాగాధిపతి పి.శైలజ, సమన్వయకర్త డాక్టర్ ఆర్.కామేశ్వరి, డాక్టర్ సుజాత, బలరామ్, ఎండీ ఇక్బాల్ పాష, నయోమి పాల్గొన్నారు.

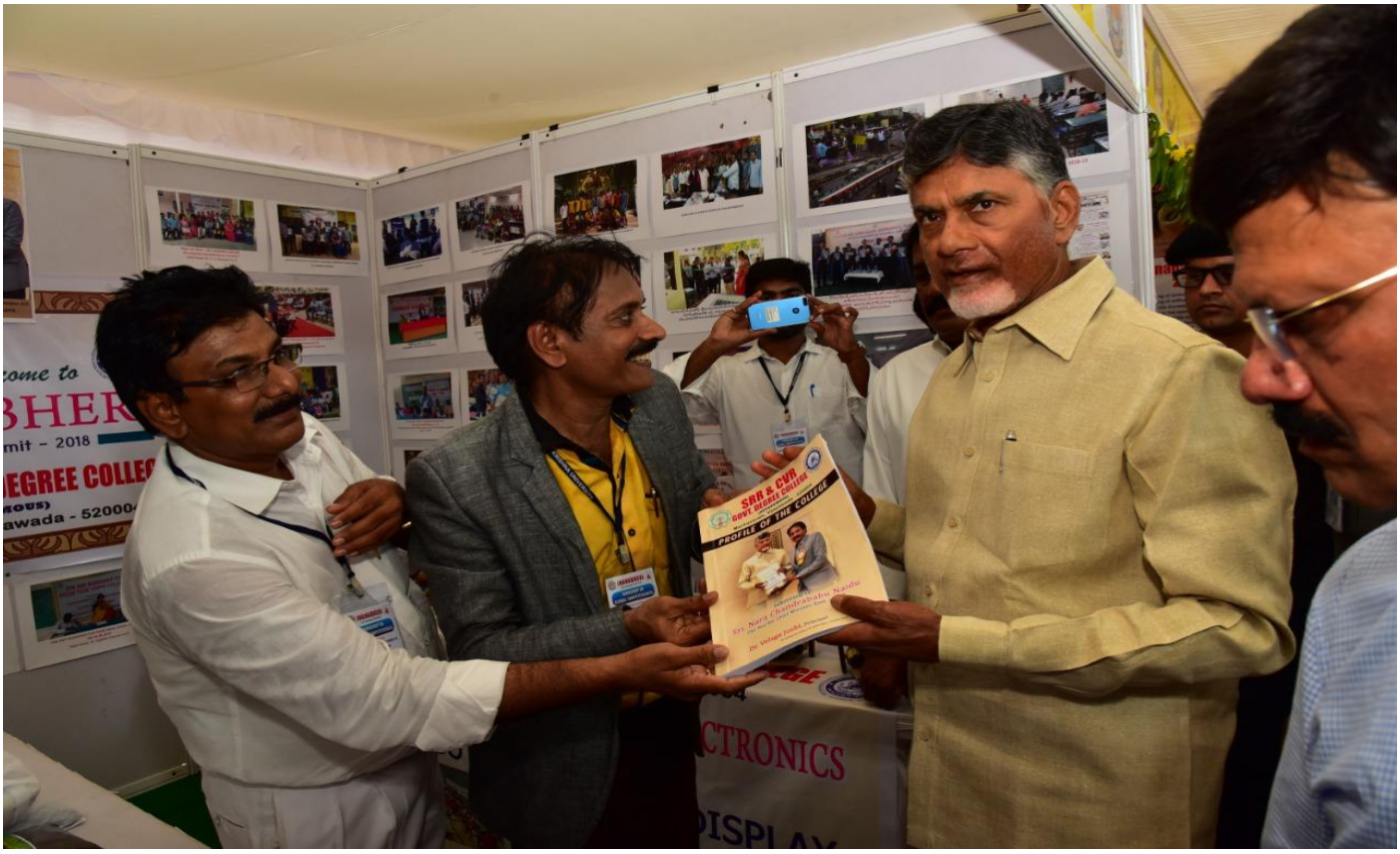
రోబోట్లను తయారుచేసిన విద్యార్థులతో అతిథులు

Students exhibited their robots at Gnanaberi program which is held to encourage innovation skills among the students in the state. The Chief Minister Nara Chandra babu Naidu visited Robotics stall, interacted and appreciated the student's creativity. Honourable APCCE Madam Sujatha Sarma also visited the stall & appreciated the efforts of students.




Machavaram, Vijayawada - 520004
DEPARTMENT OF PHYSICS & ELECTR
ROBOTICS
Presents
Shot on OnePlus

https://www.thehansindia.com/posts/index/Andhra-Pradesh/2018-08-21/Chandrababu-Naidu-to-take-part-in-Gnana-Bheri-on-August-23/406759





Scanned copy of Robotics Workshop Report

RSC Advances

PAPER

View Article Online
View Journal | View Issue

Open Access Article. Published on 02 February 2017. Downloaded on 18/03/2017 08:54:59.
This article is licensed under a Creative Commons Attribution-NonCommercial 3.0 Unported Licence.

Cite this: *RSC Adv.*, 2017, **7**, 9724

Unravelling the energy transfer mechanism in bismuth co-activation of $LaInO_3$:Sm^{3+}/Ho^{3+} nanophosphor for color-tunable luminescence†

Ch. Satya Kamal,[ac] T. K. Visweswara Rao,[ac] P. V. S. S. S. N. Reddy,[a] K. Sujatha,[a] Babajide Patrick Ajayi,[b] Jacek B. Jasinski[b] and K. Ramachandra Rao*[ab]

Received 26th December 2016
Accepted 19th January 2017

DOI: 10.1039/c6ra28719k

rsc.li/rsc-advances

A series of single-phased and color tunable $LaInO_3$:Bi^{3+},Ho^{3+}/Sm^{3+} nano phosphors were synthesized *via* a cost effective and low temperature chemical route. The crystal structure, morphology, photoluminescence (PL) and energy transfer mechanism between Bi^{3+} to Ho^{3+}/Sm^{3+} were investigated in detail. The considerable spectral overlap between the broad emission band of Bi^{3+} around 400–500 nm and the excitation band of Ho^{3+} and Sm^{3+} supports the efficient energy transfer from Bi^{3+} to Ho^{3+}/Sm^{3+}, which enhances the PL intensity remarkably. The energy transfer efficiency between Bi^{3+} and Ho^{3+}/Sm^{3+} in $LaInO_3$ was also calculated and the efficiency increased linearly with increasing concentration of Ho^{3+} and Sm^{3+}. The emission hue can be tuned from blue to green and pink by varying the content of Ho^{3+}/Sm^{3+}. This investigation will extend an understanding of interactions between Bi^{3+} and rare earth ions in semiconducting host $LaInO_3$ and show the potential applications of Bi^{3+}, Ho^{3+}/Sm^{3+} co-doped nanophosphors in displays and light emitting diodes.

Introduction

Owing to the gradual increase in energy consumption, light emitting diodes, as fourth generation lighting source, have been used widely in general illumination purposes and for display applications on account of their excellent characteristics. The manufacture of LEDs using inorganic phosphors or single-phase emitting phosphors excited by ultraviolet (UV) chips has received great attention. The single-phase phosphor-converted UV LEDs and phosphors with excellent red and green emission properties have become a vital part in the field of back lighting display applications. In the view of the above-mentioned reasons, research on rare earth (RE) activated luminescence materials plays a major technological role in lighting applications. Indeed, the absorption cross section of RE ions is small because of the parity forbidden character of 4f–4f transitions, and consequently RE ions cannot be excited directly by illuminating light.[1–8] Therefore, to improve the efficiencies and luminescence properties of RE ions, several methods are chosen, such as host absorption, f–d absorption, charge transfer state absorption, and energy transfer (ET).

Rare earth (RE) and transition ion-doped aluminates and gallates have been studied extensively for their display applications.[9–14] $SrAl_2O_4$:Dy^{3+},Eu^{2+} has been regarded to deliver a good green long persisting phosphorescence.[15] Furthermore, indates, being used as the host lattice for luminescence and being doped with rare-earth ions were also reported.[15–19] A few rare-earth doped $LaInO_3$ phosphors have been reported as an alternative luminescence material because of their high thermal and chemical stability. Silicon coated core–shell structured $LaInO_3$:Sm^{3+},Tb^{3+} phosphors have been used for their diverse luminescent properties.[20–23] Despite their use as a photoluminescent host, the energy transfer mechanism between sensitizer and activator is still unclear.

The semiconducting compound, $LaInO_3$, with a bandgap of 3.2 eV, belongs to the orthorhombically distorted perovskite-like structure with the space group *Pnma*[24] and is found to be a potential candidate for several applications in various fields, such as oxygen sensing,[25] solid oxide fuel cells (SOFC) and the presence of In^{3+} in the host lattice enhances its electrical conductivity, which can be used for display applications.[26] Semiconducting oxide-based phosphors like $LaInO_3$ are promising candidates with sufficient conductivity to overcome the charge build-up on the phosphor surfaces, in addition to their thermal and chemical stability.[27,28] L. I. van Steensel *et al.* showed that $LaInO_3$:Bi^{3+} is an efficient, blue-emitting photo luminescent material[29] and researchers have reported that on co-doping with Bi^{3+}, it acts as an excellent sensitizer to enhance

[a]*Crystal Growth and Nano-Science Research Center, Department of Physics, Government College (A), Rajamahendravaram, Andhra Pradesh, India-533105. E-mail: drkrcr@gmail.com*

[b]*Conn Center for Renewable Energy Research, University of Louisville, KY, USA*

[c]*Department of Physics, Adikavi Nannaya University, Rajamahendravaram, Andhra Pradesh, India*

† Electronic supplementary information (ESI) available. See DOI: 10.1039/c6ra28719k

This journal is © The Royal Society of Chemistry 2017

Open Access Article. Published on 02 February 2017. Downloaded on 18/03/2017 08:54:59.
This article is licensed under a Creative Commons Attribution-NonCommercial 3.0 Unported Licence.

the luminescence of RE ions in a wide variety of hosts.[30–38] The emission spectrum of Bi^{3+} contains a broad band, whose peak maximum varies from blue to green for different host lattices[39] because the outer $6s^2$ electronic configurations of Bi^{3+} depend strongly on their environmental conditions, such as covalence, coordination number and site symmetry.[40–42] Among the RE ions, Sm^{3+} and Ho^{3+} are important activators for producing significant orange-red and green emissions for wide applications in optical displays, remote sensing and medical purposes.[43,44] However, it is quite a challenge to select a proper host because doping and co-doping influence the optical properties of luminescence materials.

In this study, $LaInO_3$, a semiconducting luminescent material was used as the host material. To the best of our knowledge, no accurate information is available on Sm^{3+} or Ho^{3+}-doped $LaInO_3$ phosphor co-doped with Bi^{3+} ions. These phosphors were synthesized using the polyol route. The morphological structures, steady state conditions and decay times were investigated. Their luminescent properties as well as energy transfer (ET) process and efficiency (η_{ET}) from Bi^{3+} to Ho^{3+}/Sm^{3+}in $LaInO_3$:Bi^{3+},Sm^{3+} and Ho^{3+} phosphors were investigated systematically. Remarkably, the color tunability of $LaInO_3$:Bi^{3+},Sm^{3+} and Ho^{3+} phosphors varied with the doping concentration of Sm^{3+} and Ho^{3+}.

Experimental

Preparation of the nanoparticles

$La(NO_3)_3 \cdot 6H_2O$ [Merck, Germany], $In(NO_3)_3 \cdot H_2O$ [Alfa Aesar 99.99%], $Bi(NO_3) \cdot 5H_2O$ [BDH Laboratory Chemicals Division, India], $Sm(NO_3)_3 \cdot 5H_2O$ [Alfa Aesar 99.99%] and $Ho(NO_3)_3 \cdot 5H_2O$ [Sigma-Aldrich 99.9%] were used as starting materials. Herein, ethylene glycol was used as the capping agent and urea was used for hydrolysis. For the preparation of pure $LaInO_3$ nanoparticles, both $La(NO_3)_3 \cdot 6H_2O$ and $In(NO_3)_3 \cdot H_2O$ were dissolved in the required amount of distilled water. To this solution, ethylene glycol (25 mL) was added and the mixture was then transferred into a two-necked RB flask. The solution was slowly heated up to 100 °C, followed by the addition of 2 g of urea, and the temperature was increased to 120 °C. At this temperature, the solution became turbid. The temperature was maintained at this value for 2 hours. The precipitate was collected after the reaction by centrifugation and then washed two times with acetone and three times with methanol, followed by drying under ambient conditions. The samples thus prepared were finally heated to 700 °C, 900 °C and 1000 °C in air at a heating rate of 10 °C per minute. The temperature was maintained at the respective values for a duration of 5 hours. Subsequently, the furnace was switched off and the sample was subjected to natural cooling to room temperature. The same procedure was used to prepare $LaInO_3$:(1, 3, and 5 at%)Bi^{3+}, $LaInO_3$:3at%Bi^{3+},(0.5, 1, 1.5 at%)Ho^{3+} and $LaInO_3$:3at%Bi^{3+},(1, 1.5, 2, 2.5 at%)Sm^{3+} nanoparticles and were subjected to heating at 1000 °C in air at a heating rate of 10 °C per minute.

Characterization

X-ray diffraction (XRD) was carried out using a Philips powder X-ray diffractometer (model PW 1071) with Ni filtered Cu-Kα radiation. For calibration purposes, the diffraction peak corresponding to the (111) plane of Si at a 2θ value of 28.442° was employed. The XRD data was processed using POWDERX software. The average crystallite size was calculated from the diffraction line width based on Scherrer equation $D = 0.9\lambda/\beta \cos\theta$, where D is the average particle size, λ is the wavelength of X-rays and β is the corrected full width at half maximum (FWHM). All luminescence measurements were carried out at room temperature with a resolution of 5 nm using an Edinburgh Instruments FLSP 920 system attached with a 450 W Xe lamp as the excitation source. A micro second flash lamp and a nanosecond hydrogen flash lamp was used for the lifetime measurements. The SEM instrument used was from Seron Inc. (Model AIS 2100) having a standard tungsten filament. An accelerating voltage of 20 kV and magnification of 10k× was used to record the micrographs.

Results & discussion

XRD analysis

Fig. 1 shows the XRD patterns of $LaInO_3$:Bi^{3+}(3 at%), $LaInO_3$:(3 at%)Bi^{3+},(1 at%)Ho^{3+}, and $LaInO_3$:(3 at%)Bi^{3+},(2 at%)Sm^{3+} phosphors. The crystallinity, crystallite size and surface morphology have significant effects on the PL properties of

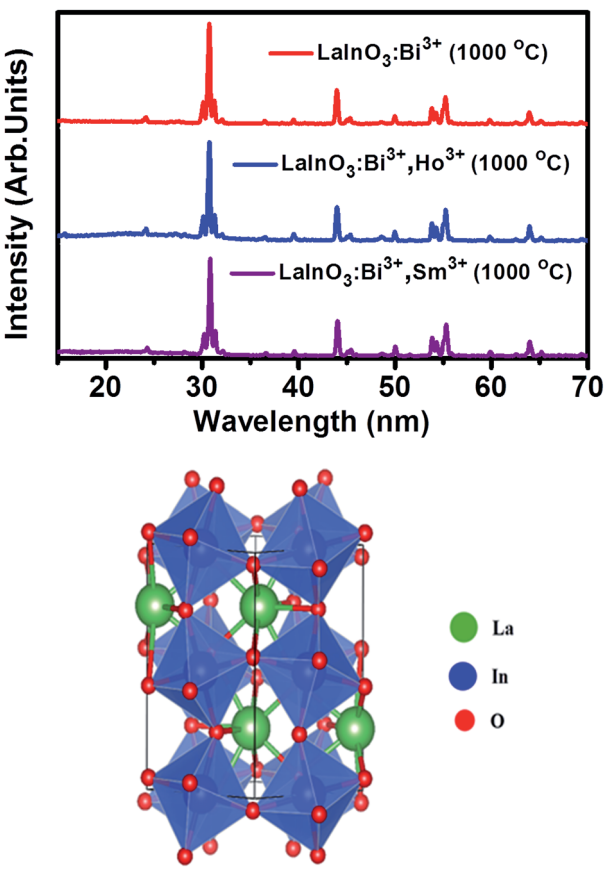


Fig. 1 XRD patterns corresponding to $LaInO_3$:Bi^{3+}(3 at%), $LaInO_3$:(3 at%)Bi^{3+},(1 at%)Ho^{3+}, $LaInO_3$:(3 at%)Bi^{3+},(2 at%)Sm^{3+} at 1000 °C and 3-D crystal structure of $LaInO_3$.

Open Access Article. Published on 02 February 2017. Downloaded on 18/03/2017 08:54:59.
This article is licensed under a Creative Commons Attribution-NonCommercial 3.0 Unported Licence.

phosphor materials. The XRD patterns of pure $LaInO_3$ calcined at three different temperatures (700 °C, 900 °C, 1000 °C) is shown in ESI Fig. 1a,† indicating that $LaInO_3$ began to crystallize at 700 °C. All the diffraction peaks of the doped and co-doped $LaInO_3$ samples annealed at 1000 °C are in agreement with the previously reported data,[26,45] indicating that the obtained samples are in a pure orthorhombic phase, where no impurity phase is detected, indicating that the dopants dissolved completely in the $LaInO_3$ host lattice.

In addition, it can be observed from ESI Fig. 1b† that the diffraction peak positions are shifted slightly to a higher angle, when Bi^{3+} or Bi^{3+}, Ho^{3+}/Sm^{3+} ions were doped into the $LaInO_3$ host, which can be due to the replacement of larger-size La^{3+} (1.16 Å) sites by the smaller-size trivalent Ho^{3+}, Sm^{3+} and Bi^{3+} ions (1.051 Å, 1.08 Å, and 1.03 Å), leading to lattice distortion, consequently contracting the lattice parameters, as illustrated in ESI Table S1.† The three-dimensional structure diagram shows the crystal structure of $LaInO_3$, the blue octahedrons represent the InO_6 units, whereas La^{3+} is in the center of the eight InO_6 octahedrons; hence, rare earth dopants Ho^{3+} or Sm^{3+} and Bi^{3+} will be replacing La^{3+} in the $LaInO_3$ structure. The crystallite size of all the samples was calculated from the Scherrer equation $D = 0.9\lambda/\beta \cos\theta$, where D is the average particles size, λ is the wavelength of X-rays and β is the corrected full width at half maximum (FWHM) of an observed peak.[46] The average crystallite size (D) of pure $LaInO_3$, doped and co-doped $LaInO_3$ particles, which are annealed at 1000 °C, were estimated to be around 35 nm.

SEM with energy dispersive X-ray analysis

Fig. 2a and b shows the Scanning Electron Microscopy (SEM) images of $LaInO_3$:(3 at%)Bi^{3+},(1 at%)Ho^{3+}, and $LaInO_3$:(3 at%) Bi^{3+},(2 at%)Sm^{3+} samples. Crystallization granules and agglomeration of particles were observed in the present phosphors. ESI Fig. 2a and b† shows an SEM image of pure $LaInO_3$, indicating irregular spherical particles with a size between 20 and 70 nm. This may be due to agglomeration among the phosphor particles during calcination. Compared to the Bi^{3+} single-doped sample, the Bi^{3+}, Ho^{3+}/Sm^{3+} co-doped phosphors have a smaller particle size distribution. Hence, the effect of coalescence could be decreased by single and co-doping in the host. The decrease in particle size is also explained as follows:

In poly synthesis, ethylene glycol acts as the capping agent for covering the nanoparticles and controlling the agglomeration. On the other hand, during annealing at 1000 °C, the ligand evaporates and nanoparticles due to high surface energy form a neck by solid state diffusion process, which leads to agglomeration and particle growth. The differences in ionic radii between La^{3+} and Bi^{3+}, Ho^{3+}, and Sm^{3+} ions lead to a lattice distortion, which encourages a decrease in particle size. Hence, crystallite and particle size reduces by co-doping due to a grain growth inhibition effect. Energy dispersive X-ray spectroscopy (EDS) was used to determine the composition of the samples and it shows good agreement with the nominal sample composition. (Refer to the inset of Fig. 3a and b.)

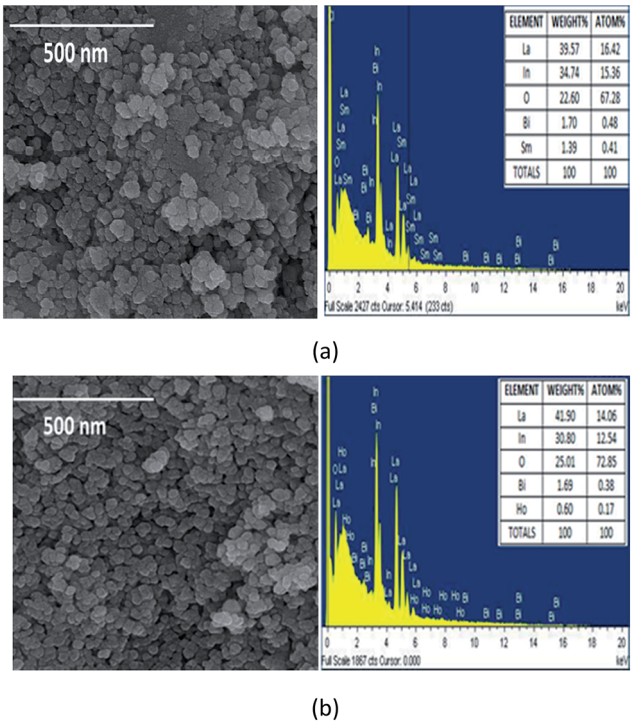


Fig. 2 (a and b) SEM images and EDAX spectra's of (a) Bi^{3+}, Ho^{3+} and (b) Bi^{3+}, Sm^{3+} doped $LaInO_3$.

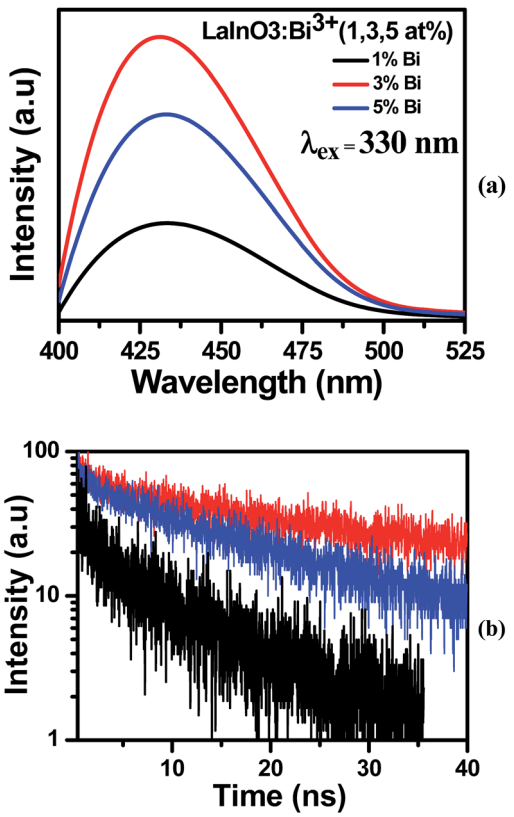


Fig. 3 (a and b) Emission and decay curves of the $LaInO_3$:Bi^{3+}(1, 3, 5 at%) samples heat at 1000 °C.

This journal is © The Royal Society of Chemistry 2017

Open Access Article. Published on 02 February 2017. Downloaded on 18/03/2017 08:54:59.
This article is licensed under a Creative Commons Attribution-NonCommercial 3.0 Unported Licence.

Photoluminescence and energy transfer mechanism

The emission and decay spectra of $LaInO_3$:Bi^{3+}(1, 3, and 5 at%) samples heated to 1000 °C are given in Fig. 3a and b respectively. From Fig. 3a, it can be observed that all samples have broad emission band centered at 432 nm, which can be attributed to the $^3P_1$–$^1S_0$ transition of Bi^{3+} ions upon excitation with 330 nm.[29] With increasing Bi^{3+} concentration, the intensity of the 432 nm emission band increases and reaches a maximum at 3 at% and then decreases remarkably when the Bi^{3+} content is increased further, which is due to concentration quenching. This is also confirmed by corresponding average bi-exponential life time value (295, 329, 273 ns) of decay curves shown in Fig. 3(b). In the excitation spectra (ESI Fig. 3†), a broad excitation band ranging from 300 to 350 nm with a maximum at about 330 nm was observed, arising from $^1S_0$–$^3P_1$ transition of Bi^{3+}.

The overlap spectra of the emission and allowed absorption create interest on the effective radiative energy transfer (ET) mechanism. Fig. 4 presents the excitation spectra of $LaInO_3$:Sm^{3+}(2 at%) $LaInO_3$:Ho^{3+}(1 at%) and emission spectra of $LaInO_3$:Bi^{3+}(3 at%) samples. The appearance of the excitation bands of Ho^{3+} and Sm^{3+} was clearly visible in the emission bands of Bi^{3+}. Therefore, it is expected that efficient energy transfer can occur from Bi^{3+} to Ho^{3+}/Sm^{3+}.

The excitation spectra of the Bi^{3+}, Ho^{3+}/Sm^{3+}-doped samples monitored at rare earth (RE) emission lines (544 nm and 603 nm) exhibited a broad excitation band arising from the $^1S_0$–$^3P_1$ transition of Bi^{3+} in the wavelength range of 300–350 nm, accompanying the Ho^{3+}/Sm^{3+} excitation lines. The same is shown in Fig. 5a–d, which represents the excitation and emission spectra of $LaInO_3$:3at%Bi^{3+},(0.5, 1, 1.5 at%)Ho^{3+} and $LaInO_3$:3at%Bi^{3+},(1, 1.5, 2, 2.5 at%)Sm^{3+} samples.

Under 330 nm and 333 nm excitation wavelengths, the samples consist of both blue-green emissions from Bi^{3+} and strong green emissions from Ho^{3+} and orange red emission from Sm^{3+}. By keeping Bi^{3+} at 3 at% and varying the Ho^{3+} and Sm^{3+} content, the intensity of Bi^{3+} emission decreases monotonously, whereas the intensity of Ho^{3+}/Sm^{3+} emission increases gradually and reaches a maximum at Ho^{3+} (1 at%) and Sm^{3+} (2 at%), and the Ho^{3+} and Sm^{3+} emissions then decrease with further increase in concentration, which can be rationalized as concentration quenching. The changes in emission intensity of Bi^{3+} as a function of Sm^{3+} and Ho^{3+} concentrations is clearly demonstrated in Fig. 5e–f. All abovementioned processes show that the emissions of Ho^{3+} and Sm^{3+} actually come from the ET process from Bi^{3+} to Ho^{3+}/Sm^{3+} ions. To investigate the effect of Bi^{3+} doping in enhancing the PL intensity, single doped Ho^{3+}/Sm^{3+}:$LaInO_3$ emission spectra are shown in ESI Fig. 4.† In addition, to support this ET process, the decay curves of all samples were measured, as shown in Fig. 6. For all samples, bi exponential luminescence decay curves were obtained and the lifetimes were characterized using the average lifetime (τ). The luminescence decay times (τ) of Bi^{3+} were obtained at 260, 228 and 192 ns for $LaInO_3$:Bi^{3+}(3 at%),Ho^{3+}(0.5, 1, 1.5 at%) and for $LaInO_3$:Bi^{3+}(3 at%),Sm^{3+}(1, 1.5, 2, 2.5 at%) 303, 291 and 211, 182 ns and also the corresponding decay times of Ho^{3+} 149, 179, and 122 μs, Sm^{3+} 1.22, 1.42, 1.73 and 1.13 ms, respectively. The increase in Ho^{3+}/Sm^{3+} content leads to the faster decay of Bi^{3+} emission, which was attributed to ET from Bi^{3+} to Ho^{3+}/Sm^{3+}. The corresponding energy level diagram of $LaInO_3$:Bi^{3+},Ho^{3+} and $LaInO_3$:Bi^{3+},Sm^{3+} with optical transitions and energy transfer process are displayed in Fig. 7. In this process, when excited by UV energy, the electrons of Bi^{3+} ions absorb energy and jump from the ground state $^1S_0$ to a higher level excited state $^3P_1$; the excited electrons then relax to the lower energy level (the bottom of parabola) by non-radiative relaxation. Hence, from the lower energy level of $^3P_1$, energy can be transferred to the $^4K_{11/2}$ level of Sm^{3+} and $^5F_1$ level of Ho^{3+} *via* an ET process (Cross relaxation) between these levels. Therefore, by co-doping with Bi^{3+} ions might improve the emission intensity of Sm^{3+} and Ho^{3+}. Finally, a part of the electrons of Bi^{3+} ions may radiate back to the ground state by emitting blue emission and can be reabsorbed by the ground state levels of Sm^{3+} and Ho^{3+} *i.e.* $^6H_{5/2}$ and $^5I_8$, which also leads to energy transfer (because spectral overlap is observed in both Sm^{3+} and Ho^{3+}), and can be subsequently excited to the respective high level excited state. The excited electrons relax to the $^5F_4$, $^5S_2$ level of Ho^{3+} and the $^4G_{5/2}$ level of Sm^{3+} by non-radiative transition, and finally electrons return to the ground states of Ho^{3+} and Sm^{3+} ions by emitting green and pink lines, respectively.

The ET efficiency η_T of Bi^{3+}–Ho^{3+} and Bi^{3+}–Sm^{3+} can be calculated using the following eqn (1)[35,36]

$$\eta_T = 1 - \frac{\tau_s}{\tau_{s_0}} \quad (1)$$

where τ_s and τ_{s_0} represent the life time values of the sensitizer Bi^{3+} in the presence and absence of Ho^{3+} and Sm^{3+}. The energy-transfer efficiency η_T values from Bi^{3+} to Sm^{3+} to Ho^{3+} for $LaInO_3$ are listed in Table 1. Generally, the ET mechanism consists of two main aspects;[39] one is exchange interaction and the other is an electric multipolar interaction. The exchange interaction from Bi^{3+} prevails when $R_c > R$ and an electric multipolar interaction from Bi^{3+} to Ho^{3+}/Sm^{3+} dominates when $R_c < R$. In this case, the critical distance (R) for the activators is restricted in the range of 5–8 Å.[47] When the value reaches the critical transfer distance, the electric multipolar interaction will take place.

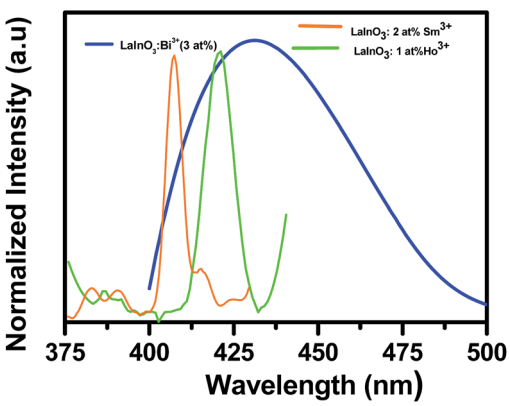


Fig. 4 Spectral overlap of excitation spectra of $LaInO_3$:Sm^{3+}(2 at%), $LaInO_3$:Ho^{3+}(1 at%) and emission spectra of $LaInO_3$:Bi^{3+}(3 at%) samples heated at 1000 °C.

Open Access Article. Published on 02 February 2017. Downloaded on 18/03/2017 08:54:59.
This article is licensed under a Creative Commons Attribution-NonCommercial 3.0 Unported Licence.

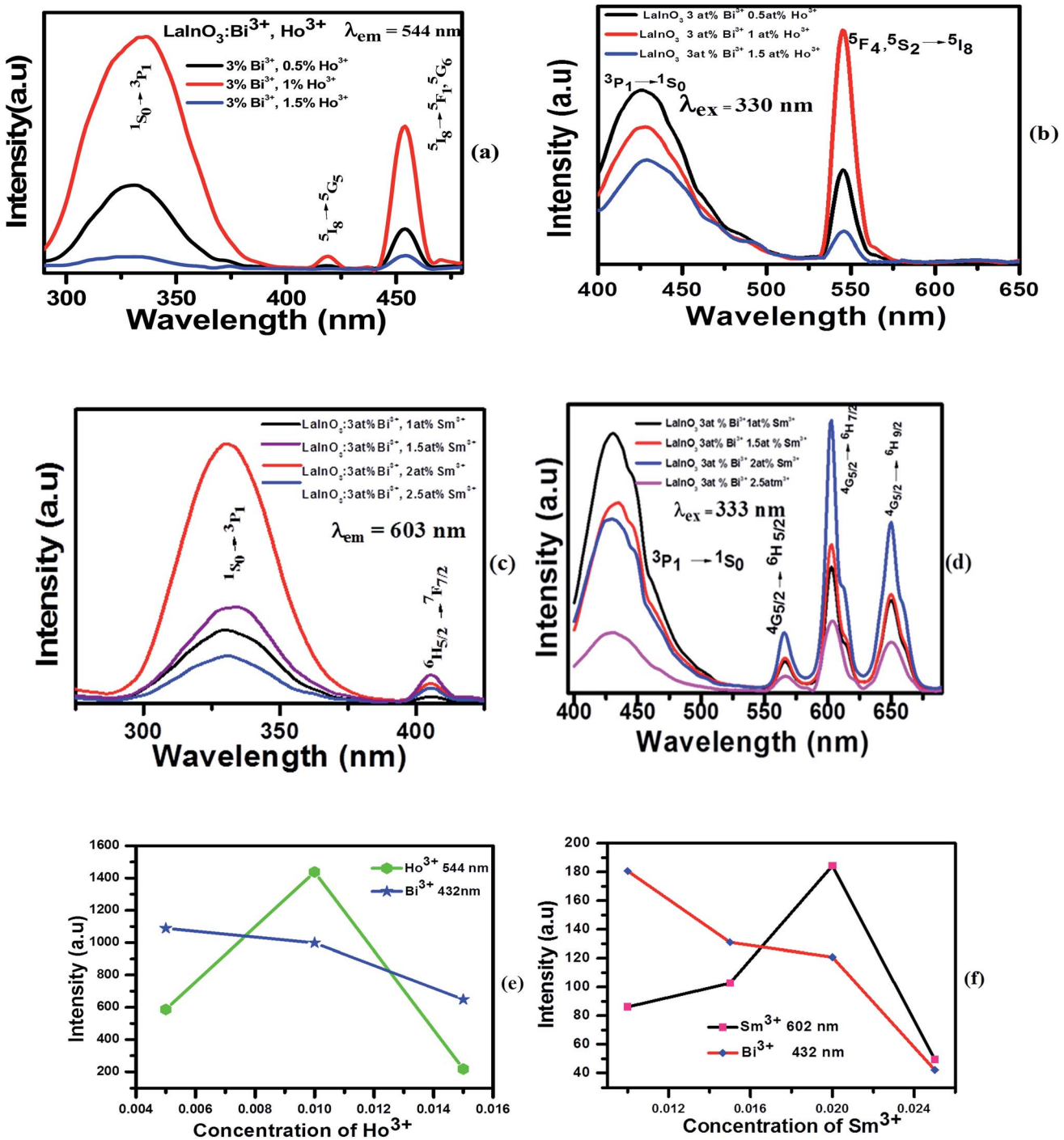


Fig. 5 Excitation and emission spectra of $LaInO_3$:3at%Bi^{3+},(0.5, 1, 1.5 at%)Ho^{3+} (a and b) and $LaInO_3$:3at%Bi^{3+},(1, 1.5, 2, 2.5 at%)Sm^{3+} (c and d) heated at 1000 °C. Variations in the emission intensity for Sm^{3+}/Ho^{3+} and Bi^{3+} with different (e) Sm^{3+}/Ho^{3+} (f) concentrations.

The critical distance R_c between Bi^{3+} and Ho^{3+}/Sm^{3+} in the $LaInO_3$ host can be estimated by the following equation:[48]

$$R_c \approx 2\left(\frac{3V}{4\pi\chi_c Z}\right)^{1/3} \quad (2)$$

where V is the volume of the unit cell, X_c is the total critical concentration of dopant ions, and Z represents the number of activator ions in the unit cell. Using the parameters of the $LaInO_3$ host (V = 289.63 Å, Z = 2) and the estimated critical concentration of dopant ions (Bi^{3+}–Ho^{3+}) (X_c = 0.04) and (Bi^{3+}–Sm^{3+}) (X_c = 0.05), the critical distance $R_{Bi-Ho/Sm}$ was calculated to be 11.99 Å and 11.14 Å. This value is much larger than 5 Å, suggesting the low probability of exchange interaction for energy transfer. Therefore, it is reliable to consider that the multipolar interaction is dominant for energy transfer from Bi^{3+} to Ho^{3+}/Sm^{3+} in $LaInO_3$.

To study the effect of the Ho^{3+}/Sm^{3+} ions doping content on the color of $LaInO_3$:3at%Bi^{3+}, we synthesized a series of samples

 This journal is © The Royal Society of Chemistry 2017

Open Access Article. Published on 02 February 2017. Downloaded on 18/03/2017 08:54:59.
This article is licensed under a Creative Commons Attribution-NonCommercial 3.0 Unported Licence.

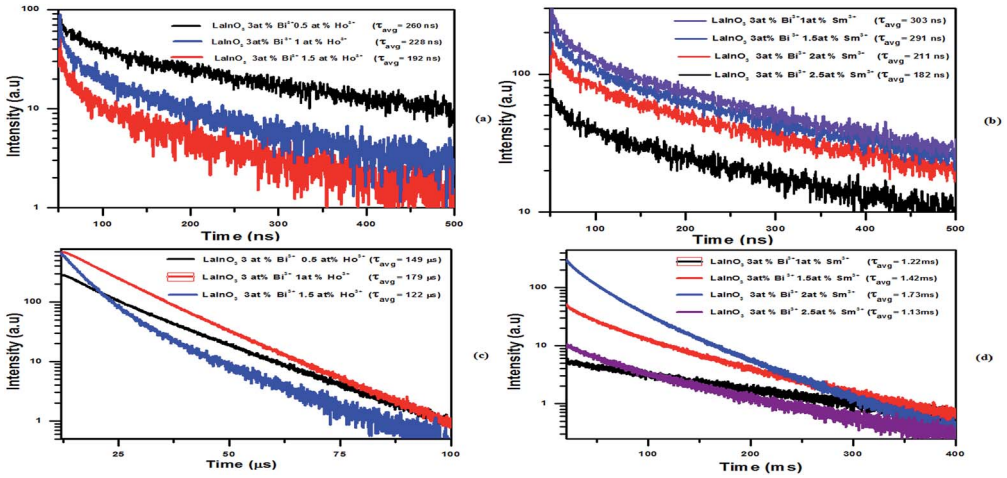


Fig. 6 Decay curves of Bi^{3+} (a and b) and Ho^{3+}, Sm^{3+} (c and d) in $LaInO_3$:3at%Bi^{3+},(0.5, 1, 1.5 at%)Ho^{3+} and $LaInO_3$:3at%Bi^{3+},(1, 1.5, 2, 2.5 at%)Sm^{3+}.

with the chemical compositions of $LaInO_3$:3at%Bi^{3+},Ho^{3+}(0.5, 1, 1.5 at%)/Sm^{3+}(1, 1.5, 2, 2.5 at%). The Commission International de L'Eclairage (CIE) chromaticity coordinates of the single-phased emission-tunable phosphors are presented in Fig. 8.

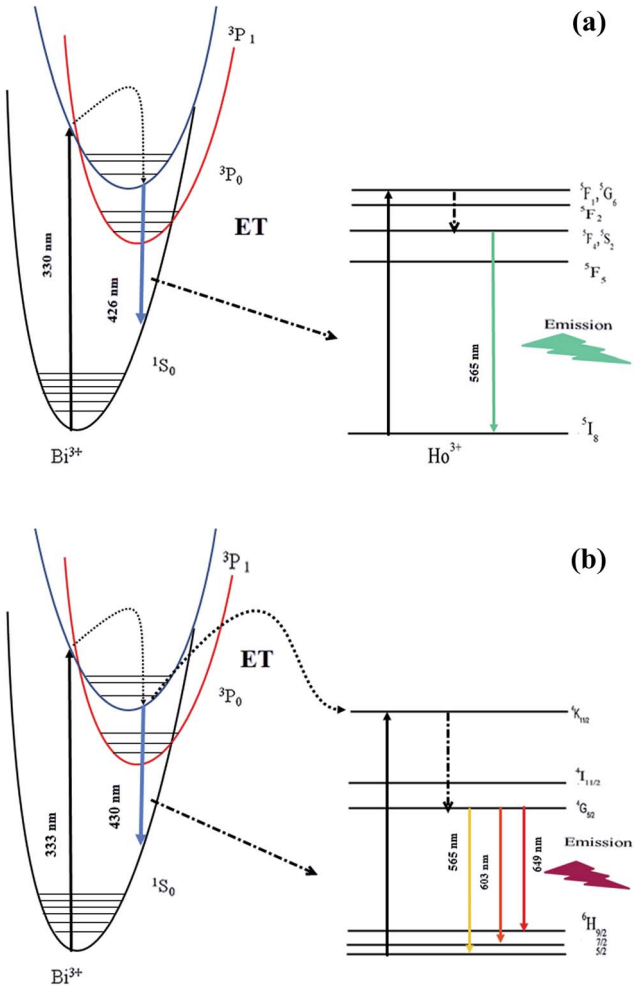


Fig. 7 Energy level diagram and ET schemes of $LaInO_3$:Bi^{3+},Ho^{3+} (a) Sm^{3+} (b).

The CIE chromaticity coordinates of pure 3 at% Bi^{3+}, 3 at% Bi^{3+}, 1 at% Ho^{3+} and 3 at% Bi^{3+}, 2 at% Sm^{3+} activated $LaInO_3$ phosphors were (0.15, 0.03), (0.21, 0.25), and (0.33, 0.17)

Table 1 ET efficiency (RE^{3+}) of the phosphors

Phosphors	Concentration (x)	Efficiency η_{ET} (%)
$LaInO_3$:3at%Bi^{3+},xHo^{3+}	0.5	39
	1.0	42
	1.5	59
$LaInO_3$:3at%Bi^{3+},xSm^{3+}	1.0	0.8
	1.5	12
	2.0	36
	2.5	45

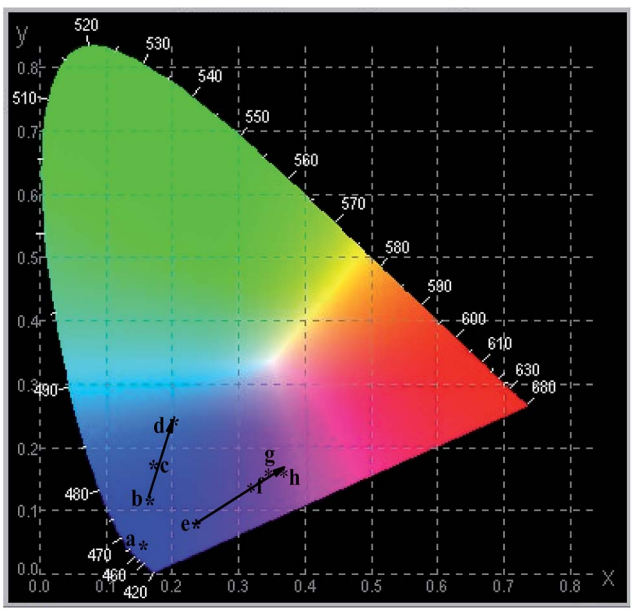


Fig. 8 CIE chromaticity diagram of the (point a) $LaInO_3$:3at%Bi^{3+}, (points b–d) $LaInO_3$:3at%Bi^{3+},(0.5, 1, 1.5 at%)Ho^{3+} and (points e–h) $LaInO_3$:3at%Bi^{3+},(1, 1.5, 2, 2.5 at%)Sm^{3+} phosphors.

Open Access Article. Published on 02 February 2017. Downloaded on 18/03/2017 08:54:59.
This article is licensed under a Creative Commons Attribution-NonCommercial 3.0 Unported Licence.

respectively. From the CIE diagram, it can be seen that the CIE chromaticity coordinates move from the bright blue to blue-green region and pink region as the amount of Ho^{3+}/Sm^{3+} varies, indicating that the developed phosphor may potentially be used as a single phase phosphor for UV light-emitting diodes and field display applications.

Conclusion

We synthesized a series of single phased and color-tunable $LaInO_3$:3at%Bi^{3+}, $LaInO_3$:3at%Bi^{3+},Ho^{3+}(0.5, 1, 1.5 at%)/Sm^{3+}(1, 1.5, 2, 2.5 at%) nanophosphors using the polyol method, and all the dopants were incorporated into the $LaInO_3$ lattice, as determined *via* the XRD patterns. The photoluminescence properties, life time studies and energy transfer process were investigated in detail. The energy transfer from Bi^{3+} to Ho^{3+}/Sm^{3+} and the energy transfer efficiency of $LaInO_3$:3at%Bi^{3+},Ho^{3+} and $LaInO_3$:3at%Bi^{3+},Sm^{3+} samples, which were calculated from the PL and decay curves, were 59 and 45%, respectively. Furthermore, the CIE diagram showed that the colors can be tuned from bright blue to blue-green and pink, indicating that the developed phosphor may potentially be used as a single phase phosphor for UV light-emitting diodes, VFD, FED, and other photoelectric fields.

Acknowledgements

The authors are grateful to Dr V. Sudarsan, Scientist-G, Bhabha Atomic Research Centre (BARC) for PL studies and Dr R. David Kumar, Principal, Government College (A), Rajamahendravaram, Andhra Pradesh for necessary lab facilities.

Notes and references

1 G. Blasse and B. Grabmaier, *Luminescent materials*, Springer Science & Business Media, 2012.
2 E. F. Schubert and J. K. Kim, *Science*, 2005, **308**, 1274–1278.
3 R. Wei, C. Ma, Y. Wei, J. Gao and H. Guo, *Opt. Express*, 2012, **20**, 29743–29750.
4 H. Guo, R. Wei and X. Liu, *Opt. Lett.*, 2012, **37**, 1670–1672.
5 W.-R. Liu, C. C. Lin, Y.-C. Chiu, Y.-T. Yeh, S.-M. Jang and R.-S. Liu, *Opt. Express*, 2010, **18**, 2946–2951.
6 A. Kuznetsov, A. Nikitin, V. Tikhomirov, M. Shestakov and V. Moshchalkov, *Appl. Phys. Lett.*, 2013, **102**, 161916.
7 S. Nigam, C. S. Kamal, K. R. Rao, V. Sudarsan and R. K. Vatsa, *J. Lumin.*, 2016, **178**, 219–225.
8 F. Wang, R. Deng, J. Wang, Q. Wang, Y. Han, H. Zhu, X. Chen and X. Liu, *Nat. Mater.*, 2011, **10**, 968–973.
9 A. Baszczuk, M. Jasiorski, M. Nyk, J. Hanuza, M. Mączka and W. Stręk, *J. Alloys Compd.*, 2005, **394**, 88–92.
10 Q. Shi, C. Wang, D. Zhang, S. Li, L. Zhang, W. Wang and J. Zhang, *Thin Solid Films*, 2012, **520**, 6845–6849.
11 C. S. Kamal, R. Mishra, D. K. Patel, K. R. Rao, V. Sudarsan and R. Vatsa, *Mater. Res. Bull.*, 2016, **81**, 127–133.
12 M. Yu, J. Lin, Y. Zhou and S. Wang, *Mater. Lett.*, 2002, **56**, 1007–1013.
13 X. Liu and J. Lin, *J. Appl. Phys.*, 2006, **100**, 124306.
14 T. Samuel, C. S. Kamal, K. Sujatha, V. Veeraiah, Y. Ramakrishana and K. R. Rao, *Optik*, 2016, **127**, 10575–10587.
15 X. Liu, R. Pang, Z. Quan, J. Yang and J. Lin, *J. Electrochem. Soc.*, 2007, **154**, J185–J189.
16 X. Liu and J. Lin, *J. Mater. Chem.*, 2008, **18**, 221–228.
17 X. Liu, C. Lin and J. Lin, *Appl. Phys. Lett.*, 2007, **90**, 081904.
18 X. Liu, C. Li, Z. Quan, Z. Cheng and J. Lin, *J. Phys. Chem. C*, 2007, **111**, 16601–16607.
19 X. Liu, C. Lin, Y. Luo and J. Lin, *J. Electrochem. Soc.*, 2007, **154**, J21–J27.
20 S. K. Chaluvadi, V. Aswin, P. Kumar, P. Singh, D. Haranath, P. K. Rout and A. Dogra, *J. Lumin.*, 2015, **166**, 244–247.
21 X. Liu, L. Yan and J. Lin, *J. Electrochem. Soc.*, 2009, **156**, P1–P6.
22 X. Liu and J. Lin, *Solid State Sci.*, 2009, **11**, 2030–2036.
23 Y. Shang, P. Yang, W. Wang, Y. Wang, N. Niu, S. Gai and J. Lin, *J. Alloys Compd.*, 2011, **509**, 837–844.
24 D. Rogers, J. Honig and J. Goodenough, *Mater. Res. Bull.*, 1967, **2**, 223–230.
25 V. Thangadurai and W. Weppner, *J. Electrochem. Soc.*, 2001, **148**, A1294–A1301.
26 H. He, X. Huang and L. Chen, *Solid State Ionics*, 2000, **130**, 183–193.
27 H. He, X. Huang and L. Chen, *Electrochim. Acta*, 2001, **46**, 2871–2877.
28 K. Sood, K. Singh and O. Pandey, *Trans. Indian Ceram. Soc.*, 2013, **72**, 32–35.
29 L. I. van Steensel, S. G. Bokhove, A. M. van de Craats, J. de Blank and G. Blasse, *Mater. Res. Bull.*, 1995, **30**, 1359–1362.
30 F. Angiuli, E. Cavalli and A. Belletti, *J. Solid State Chem.*, 2012, **192**, 289–295.
31 D. Chen, Y. Yu, P. Huang, H. Lin, Z. Shan, L. Zeng, A. Yang and Y. Wang, *Phys. Chem. Chem. Phys.*, 2010, **12**, 7775–7778.
32 Y. Zhydachevskii, L. Lipińska, M. Baran, M. Berkowski, A. Suchocki and A. Reszka, *Mater. Chem. Phys.*, 2014, **143**, 622–628.
33 E. Cavalli, F. Angiuli, A. Belletti and P. Boutinaud, *Opt. Mater.*, 2014, **36**, 1642–1648.
34 Z. Xia, D. Chen, M. Yang and T. Ying, *J. Phys. Chem. Solids*, 2010, **71**, 175–180.
35 L. Han, Y. Wang, J. Zhang and Y. Wang, *Mater. Chem. Phys.*, 2013, **139**, 87–91.
36 L. Chen, K.-J. Chen, S.-F. Hu and R.-S. Liu, *J. Mater. Chem.*, 2011, **21**, 3677–3685.
37 X. Wei, Y. Chen, X. Cheng, M. Yin and W. Xu, *Appl. Phys. B: Lasers Opt.*, 2010, **99**, 763–768.
38 H. Hara, S. Takeshita, T. Isobe, T. Sawayama and S. Niikura, *Mater. Sci. Eng., B*, 2013, **178**, 311–315.
39 P. Boutinaud, *Inorg. Chem.*, 2013, **52**, 6028–6038.
40 L. Wang, Z. Lv, W. Kang, X. Shangguan, J. Shi and Z. Hao, *Appl. Phys. Lett.*, 2013, **102**, 151909.
41 L. Wang, Q. Sun, Q. Liu and J. Shi, *J. Solid State Chem.*, 2012, **191**, 142–146.
42 H. Ju, W. Deng, B. Wang, J. Liu, X. Tao and S. Xu, *J. Alloys Compd.*, 2012, **516**, 153–156.

 This journal is © The Royal Society of Chemistry 2017

Open Access Article. Published on 02 February 2017. Downloaded on 18/03/2017 08:54:59.
This article is licensed under a Creative Commons Attribution-NonCommercial 3.0 Unported Licence.



43 Y. Zhang, Z. Zhu, W. Zhang and Y. Qiao, *J. Alloys Compd.*, 2013, **566**, 164–167.
44 H. H. T. Vu, T. S. Atabaev, H.-K. Kim and Y.-H. Hwang, *J. Nanosci. Nanotechnol.*, 2012, **12**, 5847–5851.
45 E. Ruiz-Trejo, G. Tavizon and A. Arroyo-Landeros, *J. Phys. Chem. Solids*, 2003, **64**, 515–521.
46 C. Hu, Z. Zhang, H. Liu, P. Gao and Z. L. Wang, *Nanotechnology*, 2006, **17**, 5983.
47 H. He, R. Fu, Y. Cao, X. Song, Z. Pan, X. Zhao, Q. Xiao and R. Li, *Opt. Mater.*, 2010, **32**(5), 632–636.
48 G. Blasse, *Philips Res. Rep.*, 1969, **24**(2), 131–144.

International Journal of ChemTech Research
CODEN (USA): IJCRGG, ISSN: 0974-4290, ISSN(Online):2455-9555
Vol.10 No.13, pp 119-127, 2017

Tunable luminescence properties and energy transfer behaviour in Bismuth sensitized $LaInO_3:Tb^{3+}$ phosphors

K. Sujatha[1], T.K.Visweswara Rao [2], Ch. SatyaKamal[3], K.Samatha[4], Y.Ramakrishna[5], K.RamachandraRao[6*]

[1,2,3,6]Crystal Growth and Nano-Science Research Center, Department of Physics, Government College (A), Rajamahendravaram, Andhra Pradesh, India-533105
[3,6]Department of Physics, Adikavi Nannaya University, Rajamahendravaram, Andhra Pradesh, India
[4]Department of Physics, Andhra University, Visakhapatnam, Andhra Pradesh-India-530003
[5]Department of Engg., Physics, Andhra University, Visakhapatnam, Andhra Pradesh-India-530003

Abstract : A series of Bi^{3+}:Tb^{3+} doped $LaInO_3$ phosphors were synthesized via Polyol method. The structure and luminescence properties were investigated. The optimum concentrations of Bi3+and Tb3+ were 3mol% and 3mol%, respectively. Furthermore, $LaInO_3$:3Bi^{3+} and$LaInO_3$:3at%Tb^{3+} phosphors emitted blue and green light and the emission color of $LaInO_3$:Bi3+, Tb3+could be tuned from blue to green through the energy transfer. This energy transfer from Bi^{3+} to Tb^{3+}wasconfirmed and investigated by photoluminescence spectrum and decay lifetime. With constantly increasing Tb^{3+}concentrations, the energy transfer efficiency from Bi^{3+} to Tb^{3+} in $LaInO_3$ host increased gradually and reached as high as 64%. The energy transfer mechanism (Bi^{3+}-Tb^{3+})was proved to be dipole–dipole mechanism. Moreover, the phosphor of LaInO3:3at% Bi^{3+}, 3at%Tb^{3+}could exhibited strong green emission with good CIE chromaticity coordinate. The results indicate thatLaInO3:3at% Bi^{3+}, 3at%$Tb^{3+}$is a potential green emitting phosphor for the application in LED and display field.
Keywords : Bi^{3+} Co-doping, $LaInO_3$:Tb^{3+}, Photoluminescence, Spectral overlap, Energy Transfer.

1. Introduction

Recently development of phosphor materials for field emission display (FED) technology is highly focused due to several interesting properties when compared to the traditional cathode ray tube (CRT) phosphors, such as high electric conductivity, low surface recombination velocities, vacuum compatibility, hazardlessness to cathodes, and theability to withstand high current densities[1]. However, highly efficient phosphors are desired for FEDs to have decrement in energy consumption, higher resistance to current saturation, and higher chemicalstability.Many reports [2–4] indicate that oxide based phosphors, which are semiconductor shave shown remarkable field emission properties. Among many semiconductor based oxidephosphors, Lanthanum Indium oxide ($LaInO_3$)with a bandgap of 3.2 eV have been found to be the promising candidate, with sufficient conductivity to overcome the charge build-up on the phosphor surfaces[5,6]. Rare-earth doped $LaInO_3$ phosphors have been reported as an alternative luminescence material

due to their high thermal and chemical stabilities. Silicon coated core-shell structured $LaInO_3$: Sm^{3+}, Tb^{3+} phosphors have been used for their diverse luminescent properties[7-9].LI.vanSteensel*et.al* showed that $LaInO_3$:Bi^{3+} is an efficient, blue-emitting phosphor material[10].

It is well-known that the Tb^{3+} ion is a most important green light emitting luminescent activator, the $^5D_4$–$^7F_5$ transition peaking around543 nm leads to the predominantly green emission. Nevertheless, due to the f–f forbidden transition, the intensities of Tb^{3+}absorptionpeaks in the NUV region are quite weak and the width is very narrowsoa sensitizer ion which strongly absorbs excitation energy in the NUV region is necessary [11–13]. In order to enhance Tb^{3+} absorption in the NUV region, one of the most feasible way is to introduce(such as Ce^{3+}, Eu^{2+}, Sb^{3+} and Bi^{3+}) sensitizer to transfer energy to Tb^{3+} effectively. The Bi^{3+} can serve as sensitizer in phosphors with their large cross- section to capture excitation energy efficiently and then transfer it to the activator ions (Tb^{3+} ions)[14-17].Moreover emission spectrum of Bi^{3+} ion varies from blue to green region for different host lattices[18]because outer $6s^2$ electronic configurations of Bi^{3+} depend strongly on their environmental conditions, such as covalence, coordination number and site symmetry[19-22].

In this study, Bi^{3+}, Tb^{3+} co-doped $LaInO_3$ phosphors have been prepared by polyol method, and their structural, morphological, luminescence properties, decay lifetime, energy transfer, color chromaticity have been systematically studied. Bi^{3+}, Tb^{3+} co-doped $LaInO_3$ phosphors can be effectively excited by NUV(Near Ultra-Violet) light and emit visible light from blue to green by changing the concentrations ratio of Bi^{3+}. The results show that it may have potential applications in white light-emitting phosphor for display applications.

2. Experimental details

2.1 Preparation of the particles

For preparation of pure and doped $LaInO_3$ samples, $La(NO_3)_3.6H_2O$ [Sigma-Aldrich 99.9%], $In(NO_3)_3.H_2O$ [Alfa Aesar 99.99%], $Bi(NO_3).5H_2O$[Sigma-Aldrich 99.9%], $Tb(NO_3)_3.6H_2O$ [Sigma-Aldrich 99.9%] were used as starting materials without any further purification. Polyol route was adopted for synthesis; ethylene glycol serves as the solvent and urea for hydrolysis. For preparing the undoped lanthanum indate ($LaInO_3$), initially Stoichiometric amounts of $La(NO_3)_3.6H_2O$ and $In(NO_3)_3.H_2O$ was transferred into a two-necked RB flask containing solution of 20ml ethylene glycol. The solution was kept under magnetic stirring and continuous heating. When the temperature was at 100^oC, around 2 gram urea was added and temperature was raised further to 120^oC and kept up at this temperature for 2 hours. The formed precipitate was cooled, centrifuged, washed thrice with methanol, twice with acetone and allowed to dry overnight at room temperature. Then the samples were sintered in a muffle furnace at a temperature of 1000 °C for 5h. Finally, the samples are naturally cooled down to room temperature and fully ground for further investigations. The above procedure was repeated for the preparation of Bi and Bi-Tb $LaInO_3$ samples by dissolving required amount of $Bi(NO_3)_3.5H_2O$ $Tb(NO_3)_3.6H_2O$ in ethylene glycol.

2.2 Characterization Techniques

X-ray diffraction (XRD) studies were carried out using a Philips powder X-ray diffractometer (model PW 1071) with Ni filtered Cu-Kα radiation. For calibration purpose, diffraction peak corresponding to the (111) plane of Si at a 2θ value of 28.442° was employed. The lattice parameters were obtained from the XRD patterns using POWDERX software. SEM instrument used was from Seron Inc. (Model AIS 2100) having standard tungsten filament. An accelerating voltage of 20 kV and magnification of 10 kx was used for recording the micrographs. All luminescence measurements were carried out at room temperature with a resolution of 5 nm, using Edinburgh Instruments FLSP 920 system attached with a 450 W Xe lamp as the excitation source. A micro second flash lamp and a nanosecond hydrogen flash lamp was used for lifetime measurements.

3. Results & Discussion

3.1 Phase identification, Structure and Morphology

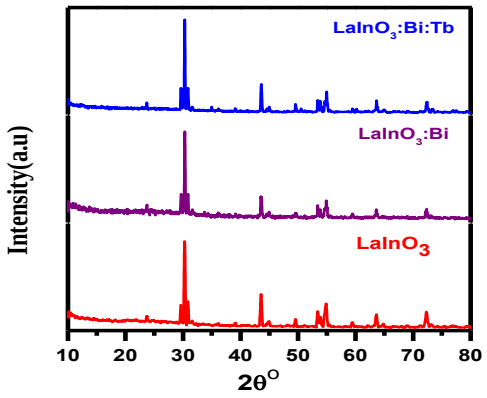


Fig 1. XRD patterns corresponding to pure $LaInO_3$, Bi^{3+} doped $LaInO_3$, $LaInO_3$: 3 at.% Bi^{3+}, 3at.% Tb^{3+}at 1000 ^oC

Fig. 1shows the diffraction patterns of the undoped and $LaInO_3$: 3 at.%Bi^{3+}, $LaInO_3$: 3 at.% Bi^{3+}, 3 at.% Tb^{3+}nanophosphors sintered at 1000 ^oC.All *X*-ray diffraction patterns are indexed to pure orthorhombic phase (JCPDS No. 08–0148) with ***Pnma*** space group and there are no formations of impurity phases. In general the crystallite size is estimated from the Scherrer's equation, $D_{h\,k\,l} = 0.9\lambda/\beta\cos\theta$, where D is the average crystallite size, λ is the X-ray wavelength (1.5406A˚), θ is the diffraction angle and β is the full-widths at half-maximum (FWHM) of observed peak (30.29^o). The strongest diffraction peaks are used to calculate the crystallite size of the samples. The calculated average crystallite size is 100 nm.The lattice parameters of the synthesized nanophosphors calculated by least square fitting using POWDERX software are illustrated in Table 1.

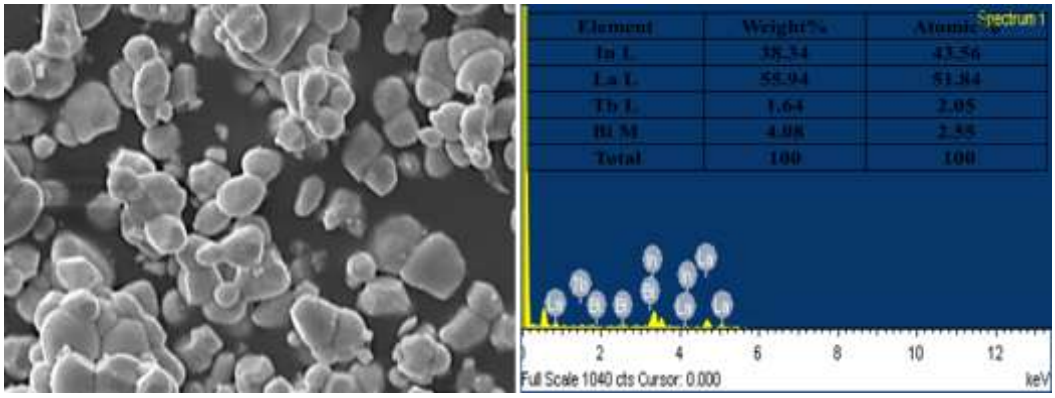


Fig. 2. SEM images and EDAX spectra's of Bi^{3+}, Tb^{3+} doped $LaInO_3$

Table.1 Unit cell parameters of $LaInO_3$, LaInO3:Bi^{3+}:Tb^{3+}

Composition	a(A^o)	b(A^o)	c(A^o)
$LaInO_3$	5.782	8.336	5. 999
$LaInO_3$:Bi^{3+}	5.775	8.245	5.928
$LaInO_3$: Bi^{3+}, Tb^{3+}	5.745	8.016	5. 799

Fig. 2shows the morphology and chemical composition of $LaInO_3$: 3 at.% Bi^{3+}, 3 at.% Tb^{3+} nanophosphors. The LIO (Lanthanum Indium oxide) powder particles are in nanometerrange and nearly all of the particles are spherical morphology, which agglomerate to larger material. The average particle size is between 100 and 200 nm. It is well known that, particles with spherical shaped (<2 µm) are of great importance because of their high packing density, lower scattering of light, brighter luminescent performance, high definition and more improved screen packing density [23].Energy dispersive X-ray spectrometroscopy (EDS) analysis was used to determine the composition of the samples and it shows good agreement with the nominal sample composition.

3.2 Photoluminescence and Lifetime measurements

1, 3 and 5 % bismuth doped $LaInO_3$ samples were heated at 1000 ^oC and also investigated for their emission, excitation and decay spectra. All samples have broad emission band centered at 432 nm which is attributed to $^3P_1$ - $^1S_0$ transition of Bi^{3+} ions on excitation with 330 nm [24] and observed the intensity of the 432 nm emission band with increasing Bi^{3+} concentration and reaches a maximum at 3 at.%, and then afterwards emission intensity decreases due to concentration quenching effect. The respective steady state, decay graphs and life time values were reported by our group previously[25].

Fig. 3 represents excitation spectra of $LaInO_3$:Tb^{3+}(3 at. %) (λ_{em} monitored at 543 nm)and emission spectra of (excited with 330nm) $LaInO_3$:Bi^{3+}(3 at%) samples. The considerable spectral overlap of an emission band and the excitation band indicates an effective radiative energy transfer (ET) is possible. Therefore, it was expected that an efficient energy transfer can occur from Bi^{3+} to Tb^{3+}. Apart from the spectral overlap, the evidence for the energy transfer occurring between Bi^{3+} to $Tb^{3+}$is been explained in the flowing section.

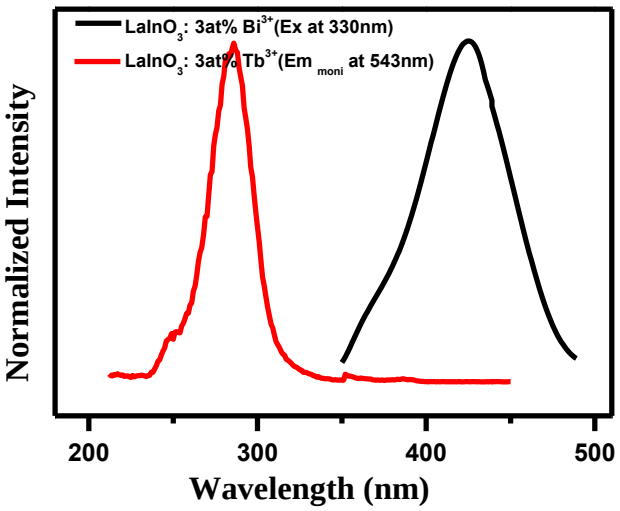
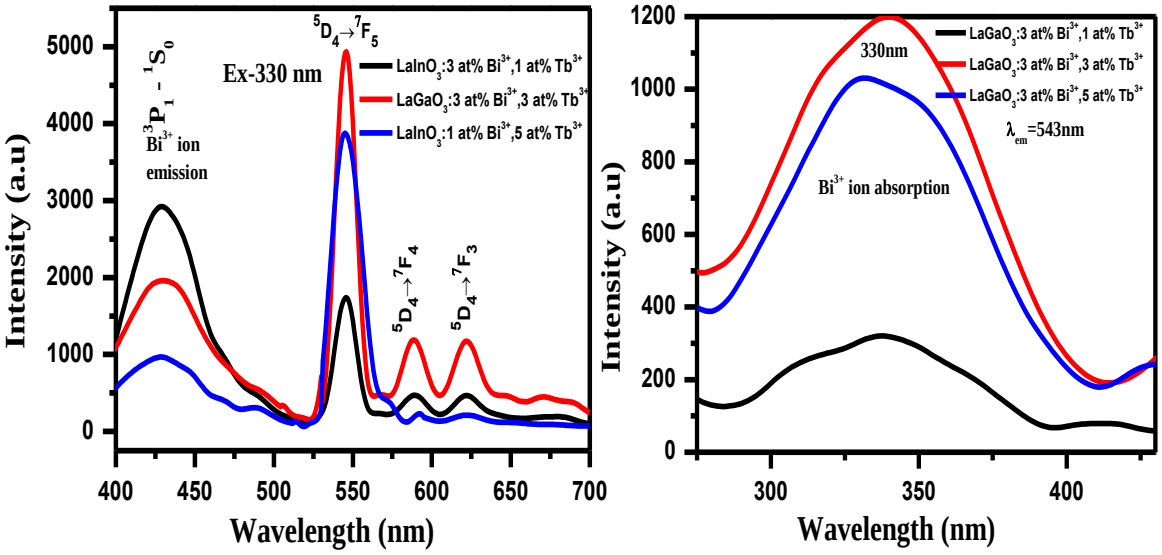


Fig. 3 Spectral overlap of excitation spectra of $LaInO_3$: Tb^{3+}(3at%) and emission spectra of $LaInO_3$:Bi^{3+}(3 at%) samples heated up to1000 ^oC

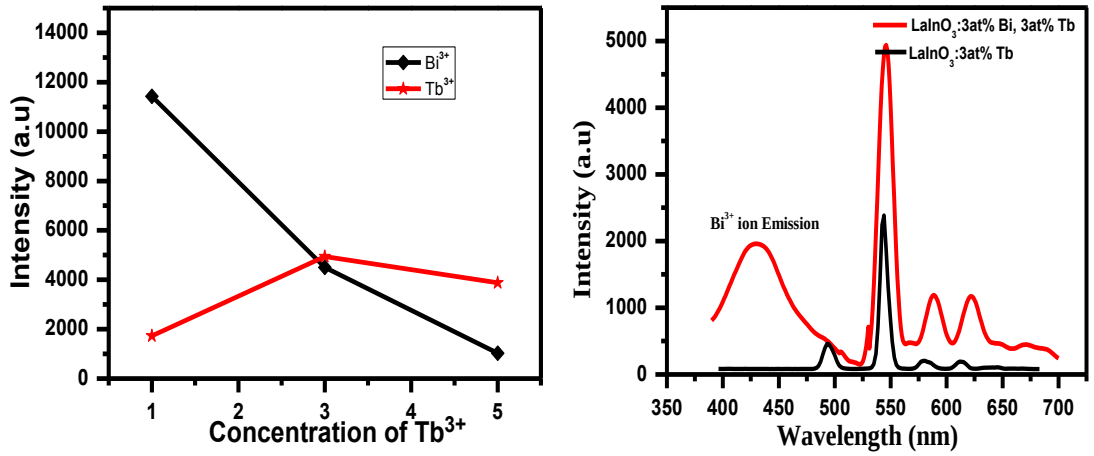
In order to further study the ET from Bi^{3+} to Tb^{3+}, a series of$LaInO_3$: 3 at.% Bi^{3+}, 1, 3, 5 at.% Tb^{3+} samples have been prepared. The PL emission spectra of samples sintered at 1000 ^oC, excitation with 330 nm were presented in Fig. 4(a). On increasing of Tb^{3+} ions concentrations, the Tb^{3+} emission intensity persistently increases until the Tb^{3+} concentration is above 0.03, and then decreases because of concentration quenching effect, while the intensity of the Bi^{3+} emission decreases although the content of Bi^{3+}wasfixed. As shown in Fig. 4(a), the emission intensity bands of Tb^{3+}were obviously enhanced as Bi^{3+} incorporated. The above variations in the emission intensities of the $Bi^{3+}$and Tb^{3+}ions strongly proved the occurrence of the ET from Bi^{3+} to Tb^{3+}ions.Theexcitationspectra (Fig.4(b)) of $LaInO_3$: Bi and Tb co-doped samples were wider than 3at% Tb doped $LaInO_3$ sample indicated that the absorption band of $LaInO_3$: 3 at.% Bi^{3+}, 1, 3, 5 at.% Tb^{3+} samples consist of a Bi^{3+}excitation band, which can predict that Bi^{3+} can transfer energy to Tb^{3+} in $LaInO_3$host.The relative emission intensities of Tb^{3+} ions at 543 nm and Bi^{3+}ions at 432 nm as a function of Tb^{3+} concentration

were shown in Fig. 5(a).In order to further verify the effect of Bi^{3+} doping in enhancing the PL intensity, single doped Tb^{3+}: $LaInO_3$ emission spectra are shown in Fig.5(b).



(a) **(b)**

Fig. 4. Plots representing intensity of the (a) emission and (b) excitation spectra of $LaInO_3$: 3 at.% Bi^{3+} (1, 3, 5 at.%) Tb^{3+}.



(a) **(b)**

Fig. 5.(a) Intensity variation of Bi^{3+} as a function of Tb^{3+} ions (b) Comparison of single doped (a) Tb^{3+} (Ex at 286 nm and monitored at 543 nm) and $LaInO_3$ Bi^{3+}: Tb^{3+} co-doping heated up to 1000 ^oC.

In order to certify and investigate the ET from Bi^{3+} to Tb^{3+}further,the decay curves of $Bi^{3+}$and Tb^{3+} emission of $LaInO_3$: 3 at.% Bi^{3+}, 1, 3, 5 at.% Tb^{3+} phosphors have been measured and shown in Fig. 6(a) and (b)respectively. The decay curves were well fitted with a double-exponential rule according to the following equation:

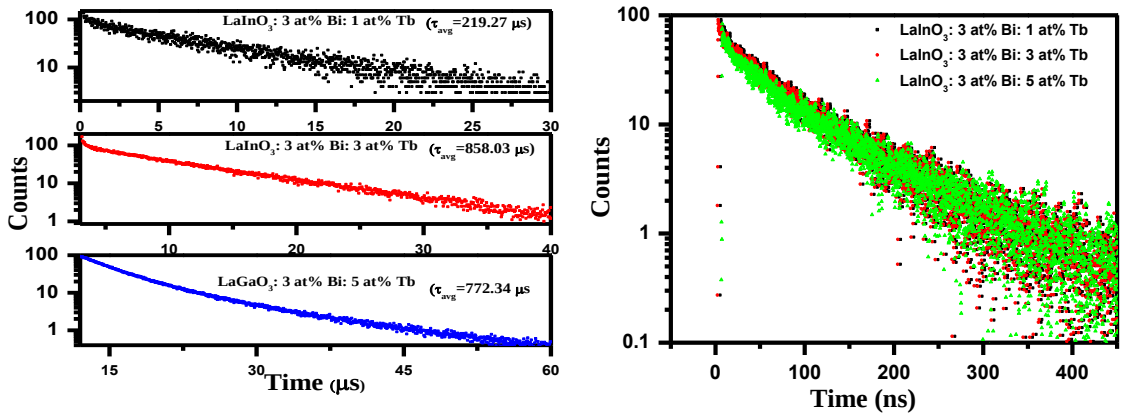
$$I = A_1 \exp\left(\frac{-t}{\tau_1}\right) + A_2 \exp\left(\frac{-t}{\tau_2}\right) (1)$$

where$I$ is the luminescence intensity at the time t, $\tau_1$and $\tau_2$are two components of the decay time, A_1 and A_2 are constants.

According to these parameters, the average decay times of $LaInO_3$: 3 at.% Bi^{3+}, 1, 3, 5 at.% Tb^{3+} can be calculated according to the following formula:

$$\tau = \frac{A_1\tau_1^2 + A_2\tau_2^2}{A_1\tau_1 + A_2\tau_2} \quad (2)$$

with increasing the concentrations of doped Tb^{3+}, there is a decreased life time of Bi^{3+} (from 181 to 126 ns)Fig.6(b).The decay times of corresponding Tb^{3+} are 219, 858, 772 µs shown in Fig. 6(a). The corresponding energy level diagram of $LaInO_3$:Bi^{3+}, Tb^{3+} with optical transitions and energy transfer process are displayed in Fig.7.



(a) **(b)**

Fig. 6(a & b). Decay curves of $Tb^{3+}$and Bi^{3+}in $LaInO_3$

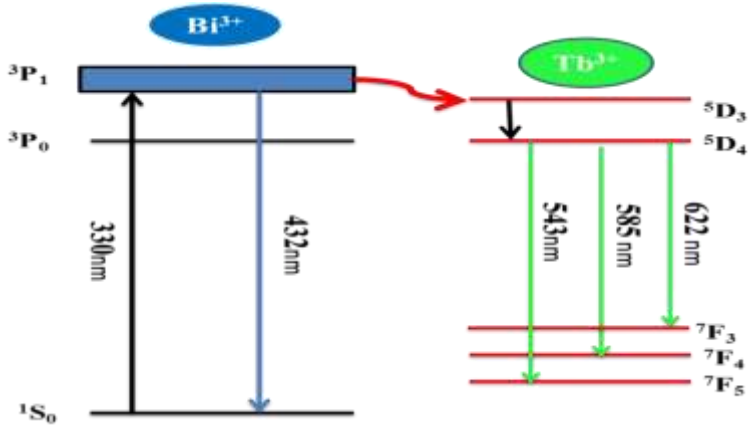


Fig 7. Energy level diagram of $LaInO_3$: Bi^{3+}, Tb^{3+}

3.3 Energy Transfer (ET) mechanism

The schematic diagram of ET between Bi^{3+} and $Tb^{3+}$was presented in Fig. 7. Firstly, the Bi^{3+} ion was excited by the UV light to a high erenergy level and then relaxes to a lower energy level $^3P_1$. Partial of the absorption energy has been released in the form of broad-band emission of 432 nm light; the other part was contributed by the energy transfer process from Bi^{3+} to the Tb^{3+}. Subsequently, the absorbed energy can be transferred to the $^5D_3$, which relaxed to $^5D_4$ later, or directly to the $^5D_4$ level of Tb^{3+}. Finally, the $^5D_4$ level gives the strong emission of Tb^{3+} ($^5D_4$-^7F_J).

The ET efficiency η_{ET} of Bi^{3+} - Tb^{3+} can be calculated using the following equation [26]

$$\eta_{ET} = 1 - \frac{\tau_S}{\tau_{S0}} \quad (3)$$

Where τ_s and τ_{s0} represent the life time values of sensitizer Bi^{3+} in the presence and absence of Tb^{3+}. The energy-transfer efficiency η_{ET} values from $Bi^{3+}$to Tb^{3+} for $LaInO_3$ are tabulated in Table 2.

Table 2. ET efficiency of the phosphors

Phosphor	*X*	η_{ET}(%)
$LaInO_3$: 3at.%Bi^{3+}, *x* Tb^{3+}	1	46
	3	55
	5	64

The resonant energy-transfer mechanism from a sensitizer (Bi) to an activator (Tb) in a phosphor consists of two interaction types: exchange and multipolar interaction. If energy transfer takes the exchange interaction, the critical distance between sensitizer and activator should be shorter than 5Å**.** When the value reaches the critical transfer distance, the electric multipolar interaction will take place. The critical distance R_c between Bi^{3+} and Tb^{3+} in the $LaInO_3$ host can be estimated by the following equation [27]**:**

$$R_c \approx 2\left(\frac{3V}{4\pi\chi_c Z}\right)^{1/3} \qquad (4)$$

where, *V* is the volume of the unit cell, $X_c$is the total critical concentration of dopant ions, while *Z* represents the number of the activator ions in the unit cell. Using the parameters of $LaInO_3$ host (*V* = 289.63 $Å^3$, *Z* = 2) and the estimated critical concentration of dopant ions (Bi^{3+}-Tb^{3+}) (X_c = 0.06 (As Bi^{3+} optimum is 3% written in decimal form 0.03, similarly for Tb^{3+} optimum is 0.03 adding together X_c = 0.06)), the critical distance R_{Bi-Tb} is calculated to be 16.64Å,which is much longer than 5 Å, implying that little possibility of ET via the exchange interaction nmechanism. Consequently, the transfer between the Bi^{3+} ions andTb^{3+} ions mainly takes place via electric multipolar interactions.

To further research the ET mechanism from Bi^{3+} to Tb^{3+} ions, it is well-know that the impurities can affect the luminescence properties, but it has the minute influence. Therefore, the interaction type between sensitizers or between sensitizer and activator can be calculated by the following equation[28]:

$$\frac{I}{x} = K[1+\beta(x)^{\theta/3}]^{-1} \qquad (5)$$

where x is the concentration of the activator ions (Bi^{3+} and Tb^{3+} ions), I is the emission intensity, K and β are constants for the same excitation condition for a given host lattice, and θ is a function of multipole–multipole interaction. When the value of θ is 6, 8, or 10, the interaction types correspond to dipole–dipole (d–d), dipole–quadrupole (d–q), and quadrupole– quadrupole (q–q) interactions, respectively. The dependence of log (I/x) on log (x) was found to be relatively linear, and it yields a straight line with a slope equal to θ/3, so we can obtain the θ value to study the energy-transfer process between Bi^{3+} and Tb^{3+} in $LaInO_3$ host. As shown in Fig. 7 the slope of the straight line is -θ/3 = -1.70 based on the PL data of this series of $LaInO_3$:3at%Bi^{3+}, (1, 3, 5 at %) Tb^{3+} samples. The calculated value of θ is 5.10, which is close to six, meaning that the dipole–dipole interaction is the dominant mechanism for the interaction of Bi^{3+} and Tb^{3+} in the $LaInO_3$ phosphors.

The color coordinates are shown in Fig. 9. With the increasing of Tb^{3+} concentrations, the chromaticity coordinates systematically change from A to C points which are shown in CIE diagram and point @ is representative of Bi single doped in $LaInO_3$ phosphor. Corresponding color can be changed gradually from blue to green by adjusting the doping concentrations of Tb^{3+}. The tuned luminous color with codoped Bi^{3+} provides a promising application of Tb^{3+} activated $LaInO_3$ phosphors in LEDs and FEDs applications.

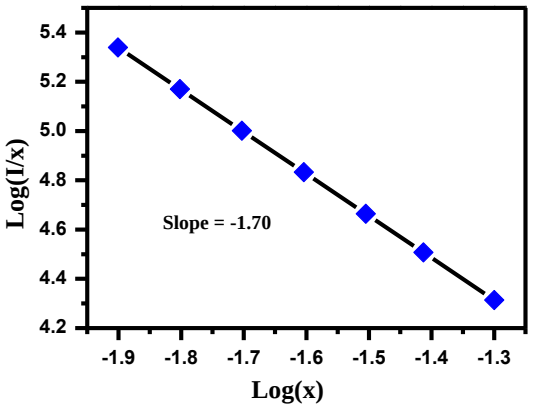


Fig. 8 The fitting line of log(I/x) vs. log(x) in LaInO3:3at% Bi^{3+}, 3at% Tb^{3+} phosphors beyond the quenching concentration.

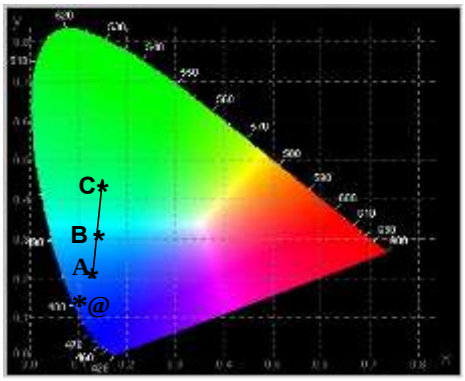


Fig.9 CIE chromaticity diagram

Conclusions

The novel green tunable phosphors, $LaInO_3$: Bi^{3+}:Tb^{3+}have been synthesized via polyol method and the structure, luminescence properties were investigated. TheET from Bi^{3+} to Tb^{3+} in $LaInO_3$ host was confirmed. The relativeintensity of $LaInO_3$:Tb^{3+} phosphor can be enhanced significantly withthe Bi^{3+} co-doping due to ET between Bi^{3+} and Tb^{3+} ions. Furthermore,the phosphor $LaInO_3$:3at% Bi^{3+}, 3at%Tb^{3+} exhibited a strong greenemission with good CIE chromaticity coordinate. After co-dopingBi^{3+}, Tb^{3+}, the color rendering, luminous intensity and the absorptionintensity in the ultraviolet area were improved through the ET. All theresults indicated that $LaInO_3$: Bi^{3+}:Tb^{3+} can be efficient green-emittingphosphors for field emission display device (FEDs) applications.

Acknowledgements

The authors are grateful to Chemistry Division, Bhabha Atomic Research Centre (BARC) for PL studies and Dr. R. David Kumar, Principal, Government College (A), Rajamahendravaram, Andhra Pradesh for necessary lab facilities.

References

1. Jing Y. D, Zhang F., SummersC. J., and WangZ. L., Appl. Phys. Lett., 1999,74, 1677
2. Robert P, Seisenbaeva G. A, WigluszR. J, KepinskiL and KesslerV. G., Inorg. Chem. 2011,50, 2966.
3. LiuX and LinJ., Solid State Sci. 2009,11, 2030.
4. Lakshminarasimhan N and Varadaraju U.V., Mater. Res. Bull. 2006,41 724.
5. He H, Huang X and Chen L., Electrochimica acta, 2001, 46, 2871-2877.
6. SoodK, Singh Kand PandeyO., Transactions of the Indian Ceramic Society, 2013, **72**, 32-35.
7. Chaluvadi S. K, Aswin V, Kumar P, SinghP, HaranathD, Rout P. K and DograA, Journal of Luminescence, 2015, 166, 244-247.
8. LiuX, Yan L. and J. Lin., Journal of The Electrochemical Society, 2009, 156, P1-P6.
9. LiuX.and Lin J., Solid state sciences, 2009, 11, 2030-2036.
10. Shang Y, Yang P, Wang W, Wang Y, Niu N, GaiS. and Lin J., Journal of Alloys and Compounds, 2011, 509, 837-844.
11. van Steensel L. I, Bokhove S. G, van de Craats A. M, de Blank J. and Blasse G., Materials Research Bulletin, 1995, 30, 1359-1362.
12. XuM, Wang L, Jia D, LeF., J. Lumin. 2015,158, 125–129.
13. ZhangQ, NiH, Wang L, Xiao F., Ceram. Int. 2016,42 (5), 6115–6120.
14. ZhangW, HuangY, SeoH.J., Ceram. Int. 2013,39(4), 4313–4319.
15. BlasseG, Grabmaier B.C., Lumin. Mater., Springer press, Berlin, 1994, 91.

16. Samuel T, Satya Kamal Ch, Sujatha K, Veeraiah V, Ramakrishana Y, Ramachandra Rao K., *Optik* 2016, 127, 10575–10587.
17. Samuel T, Satya Kamal Ch, Ravipati S, Ajayi B. P, VeeraiahV, SudarsanV, Ramachandra Rao K., Optical Materials 2017, 69, 230-237
18. Satya Kamal Ch, Visweswara RaoT. K, ReddyP. V. S. S. S. N, SujathaK, AjayiB.P, JasinskiJ. B, Ramachandra RaoK., RSC Adv.,2017, **7**, 9724
19. BoutinaudP., Inorganic chemistry, 2013, 52, 6028-6038.
20. WangL, LvZ, KangW, Shangguan X, Shi J. and HaoZ., Applied Physics Letters, 2013, 102, 151909.
21. WangL, SunQ, Liu Qand ShiJ., Journal of Solid State Chemistry, 2012, 191, 142-146.
22. JuH, Deng W, Wang B, Liu J, Tao Xand XuS., Journal of alloys and compounds, 2012, 516, 153-156.
23. S. R. R.G, BuddhuduS, Mater. Lett. 2008,62, 1259.
24. Hu C, Zhang Z, Liu H, Gao P, Wang Z. L., Nanotechnology, 2006,17, 5983.
25. L. Chen, K.J. Chen, S.F. Hu, R. S. LiuJ. Mater. Chem, 2011,21, 3677-3685.
26. H. He, R. Fu, Y. Cao, X. Song, Z. Pan, X. Zhao, Q. Xiao, R. Li, Opt. Mater, 2010, 32, 632-636.
27. G. Blasse, Philips Res. Rep, 1969,24131-144.
28. T. Miyakawa, D.L. Dexter, Phys.Rev.B1, 1970, 2961.

*****

Structural and luminescent properties of Fe^{3+} doped tin oxide thin films by spray pyrolysis

M. C. RAO[a,*], K. RAVINDRANADH[b], T. SATYANARAYANA[c], G. NAGARJUNA[d], R. K. N. R. MANEPALLI[e]
[a]*Department of Physics, Andhra Loyola College, Vijayawada - 520 008, India*
[b]*Physics Division, Department of Basic Sciences & Humanities, Chirala Engineering College, Chirala-523 157, India*
[c]*Department of EIE, Lakireddy Bali Reddy College of Engineering, Mylavaram- 521230, India*
[d]*Department of Chemistry, S. R. R. & C. V. R. Govt. College, Vijayawada-520 004, India*
[e]*Department of Physics, The Hindu College, Krishna University, Machilipatnam-521001, India*

The study and application of thin film technology is entirely entered in to almost all the branches of science and technology. Semiconductor oxide thin films are materials with numerous applications in electronic and optoelectronic devices as well as some other applications such as protective coatings, heat mirrors and catalysis. Transparent conducting oxide films have been widely used in the fields of flat panel displays, solar cells, touch panels and other optoelectronic devices owing to their high electrical conductivity and optical transmittance in visible region. Fe^{3+} doped tin oxide thin films were prepared by chemical spray pyrolysis synthesis and characterized by different spectroscopic techniques. The morphologies of prepared sample were analyzed by using SEM and TEM studies. Functional groups of the prepared sample were observed in the FT-IR spectrum. PL studies of Fe^{3+} doped SnO_2 thin films exhibit ultraviolet and blue emission bands. CIE chromaticity coordinates were also calculated from emission spectrum of Fe^{3+} doped SnO_2 thin films.

(Received October 21, 2015; accepted April 6, 2017)

Keywords: SnO_2, Thin films, Spray pyrolysis, SEM, TEM, FT-IR and Photoluminescence

1. Introduction

The interest in the surface structures with their special properties has increased considerably due to extensive applications in micro and optoelectronics. It is known that the properties of films of submicron size can be different from those of structures having macroscopic dimensions [1]. The parameters that change the properties of films are the thickness, number of layers, uniformity of the films, size of clusters and nanocrystals [2]. The presence of small particles and nano-sized elements leads to changes in material properties such as electrical conductivity, refractive index, band gap, magnetic properties, strength and others [3-5]. Metal oxides play a very important role in many areas of chemistry, physics and materials science. The metal elements are able to form a large diversity of oxide compounds. In technological applications, oxides are used in the fabrication of microelectronic circuits, sensors, piezoelectric devices and fuel cells, coatings for the passivation of surfaces against corrosion and as catalysts [6-9]. One of the most promising materials in this regard is tin dioxide (SnO_2). Semiconducting tin oxide thin films with suitable catalysts in the form of nanoparticles, overlayers, clusters etc. are known to exhibit enhanced sensitivity, better selectivity and fast response speeds to various reducing gases. SnO_2 sensors are invariably anion deficient and oxygen vacancies are mainly responsible for making available free electrons for the conduction process. In addition, the surface morphology of the sensing layer is also important for realization of sensor with enhanced response characteristics, which in turn depend on the growth kinetics [10, 11].

SnO_2 films have a wide range of applications because of their excellent performance along with high mechanical, chemical and environmental stability and low cost material [12, 13]. By volume, the most deposited transparent conductive oxide (TCO) today is SnO_2, which is used in IR-efficient architectural window application. In addition, it is receiving more attention for photovoltaic devices, especially for the heterojunction with intrinsic thin layer cells and related cells Si [14]. Another major application of intrinsic tin oxide is using it as gas sensors [15, 16]. Doped tin oxide, especially fluorine doped tin oxide, can be used as an ideal TCO layer in different applications such as transparent electrode in the solar cells. SnO_2 is a special oxide material because it has a low electrical resistance with high optical transparency in the visible range. Due to these properties, apart from gas sensors, SnO_2 is being used in many other applications, such as electrode materials in solar cells, light-emitting diodes, flat-panel displays and other optoelectronic devices where an electric contact needs to be made without obstructing photons from either entering or escaping the optical active area and in transparent electronics, such as transparent field effect transistors [17]. SnO_2 owing to a wide bandgap is an insulator in its stoichiometric form. However, due to the high intrinsic defects, that are oxygen deficiencies, tin oxide possesses a high conductivity. It has been shown that the formation energy of oxygen vacancies and tin interstitials in SnO_2 is very low. Therefore, these defects

form readily, which explains the high conductivity of pure, but nonstoichiometric, tin oxide [18, 19].

SnO_2 thin films have been deposited using different techniques, such as spray pyrolysis [20], sol-gel process [21], chemical vapour deposition [22], sputtering [23] and pulsed laser deposition [24]. Rao et al. successfully explained transition metal oxides with diverse structures, properties and phenomena have been the focus of much attention in recent years in view of their scientific and technological applications. These transition metal oxides, exhibit interesting structural, chemical, electrical and optical properties [25-28]. Ravindranadh et al. successfully prepared Co^{2+} doped SnO_2 thin films and the crystal system is indexed to tetragonal rutile phase. PL spectrum of prepared samples shows strong yellow emission with suppressed blue emission and these materials are useful for display and LED devices [29]. Among these, spray pyrolysis is the most convenient method because of its simplicity, low cost, easy to add doping materials and the possibility of varying the film properties by changing composition of starting solution. In the present work, Fe^{3+} doped (0.01 mol %) SnO_2 thin films were prepared by using chemical spray pyrolysis method. The prepared thin films were characterized by FT-IR, SEM with EDS, TEM and PL studies to collect the information about the luminescent properties of the prepared sample.

2. Experimental

All the chemicals used in the work were of analytical grade. Fe^{3+} doped SnO_2 thin films were prepared by chemical spray pyrolysis. Spray solution was prepared by mixing 0.1 M aqueous solutions of SnO_2 and Fe_2O_3 (0.01 mol %) using magnetic stirrer. The automated spray solution was then transferred to the hot substrate kept at the normalized deposition temperature of 673 K using filtered air as carrier gas at a flow rate normalized to approximately 1.8 ml/min. To prevent the substrate from excessively cooling, the prepared solution was sprayed on the substrate for 10 s with 15 s intervals. The films deposited onto micro-glass slides were first cleaned with detergent water and then dipped in acetone. Scanning electron microscope (SEM) and energy dispersive spectrum (EDS) images are taken on ZEISS EVO 18. Transmission electron microscope (TEM) images are recorded on HITACHI H-7600 and CCD CAMERA system AMTV-600 by dispersing samples in ethanol. Bruker FT-IR spectrophotometer is used for recording FT-IR spectrum of the prepared samples in the region 400-4000 cm^{-1}. Photoluminescence (PL) spectrum is taken at room temperature on Horiba Jobin-Yvon Fluorolog-3 spectrofluorimeter with Xe continuous (450 W) and pulsed (35 W) lamps as excitation sources.

3. Results and discussion

Fe^{3+} doped (0.01 mol %) SnO_2 thin films were prepared by using chemical spray pyrolysis method. The prepared thin films were characterized by FT-IR, SEM with EDS, TEM and PL studies to collect the information about the luminescent properties of the prepared sample. The analysis of X-ray diffraction pattern revealed that the prepared tin oxide films are pure crystalline in nature.

3.1. Morphological studies

The morphology and chemical composition of as synthesized thin film was investigated by SEM and EDS analysis. Fig. 1 shows the SEM micrographs of Fe^{3+} doped SnO_2 thin films taken with different magnifications. It can be clearly observed from low resolution SEM images that, the prepared sample show many agglomerates with an irregular morphology. The agglomeration could be induced by densification resulting from the narrow space between particles. SEM images reveal that the sample consists of irregular shaped sphere like structures. The incorporation of iron into the host material was confirmed by EDS measurements. The observed EDS pattern was shown in Fig. 2. The pattern showed the elemental compositions of Sn, O and iron. From this it was confirmed that the prepared sample contains doped iron species. TEM measurements were performed to confirm the nanocrystalline nature of the samples and to study the morphology of the particles. The TEM images of Fe^{3+} doped SnO_2 thin films are depicted in Fig. 3. The particles are more or less uniformed in size and of irregular shape [30].

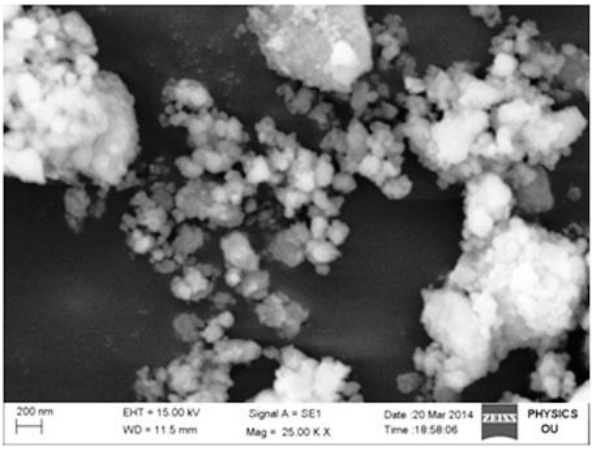


Fig. 1. SEM image of Fe^{3+} doped SnO_2 thin films

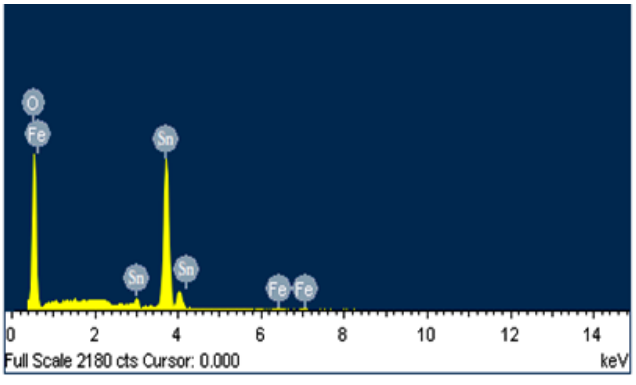


Fig. 2. EDS spectrum of Fe^{3+} doped SnO_2 thin films

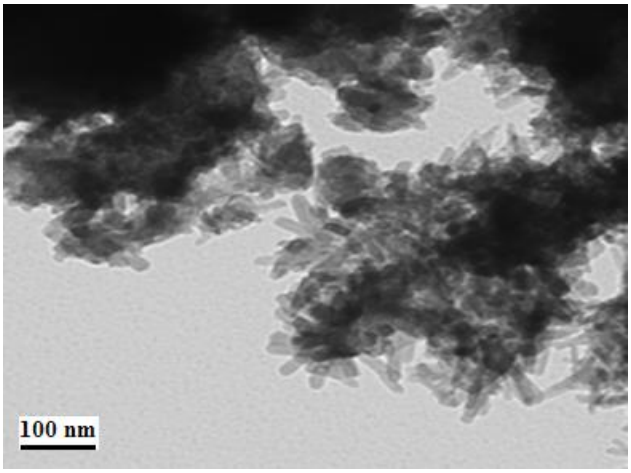


Fig. 3. TEM image of Fe^{3+} doped SnO_2 thin films

3.2. FT-IR studies

FT-IR spectrometry was used for the determination of existing surface species. The FT-IR spectrum of Fe^{3+} doped SnO_2 thin films was illustrated in Fig. 4. The bands at the low wavenumbers (500-1000 cm^{-1}) could be attributed to SnO_2. The peaks at 677, 786 and 965 cm^{-1} were assigned to O–Sn–O, Sn–O–Sn stretching vibrations and lattice vibrations, while the peaks at 569 and 864 cm^{-1} were due to Sn–OH bonds of the SnO_2 crystalline phase [31]. The bands observed in the region 2500-1640 cm^{-1} are due to symmetric and asymmetric vibrations of hydroxyl ions situated at different sites in the lattice.

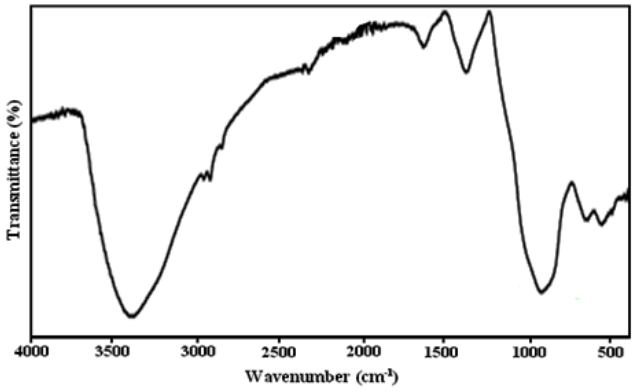


Fig. 4. FT-IR spectrum of Fe^{3+} doped SnO_2 thin films

3.3. Photoluminescence studies

Fig. 5 shows the room temperature PL spectrum of Fe^{3+} doped SnO_2 thin films under the excitation wavelength of 280 nm. The spectrum exhibits two emission bands: a strong UV emission band at 374 nm and a weak blue emission band at 452 nm.

The emission bands of Fe^{3+} doped SnO_2 thin films 374 and 452 nm are assigned to the transition $^4T_{2g}(D) \rightarrow {}^6A_{1g}(S)$ and $^4A_{1g}(G) \rightarrow {}^6A_{1g}(S)$ [32]. The emission spectrum of Fe^{3+} doped SnO_2 thin films exhibits near band edge (NBE) emission in UV region and the deep level emission in visible regions [33]. By doping Fe^{3+} in SnO_2 the emission bands are blue shifted and the quenching of visible luminescence and enhancement of UV emission was observed. The strong UV emission is observed for materials with better crystal quality [34]. In this study, a sharp and dominated UV emission at 374 nm and a suppressed blue emission at 452 nm in Fe^{3+} doped SnO_2 thin films indicate that the prepared samples have better crystal quality and good optical properties with less defect states [35].

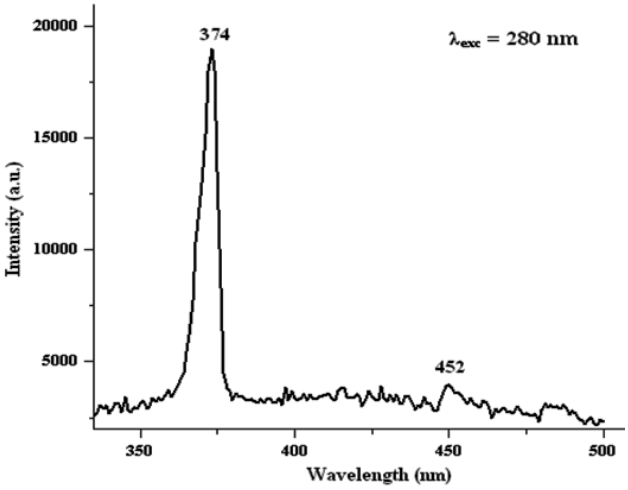


Fig. 5. PL spectrum of Fe^{3+} doped SnO_2 thin films

3.4. Chromaticity properties

Most lighting specifications refer to colour in terms of the Commission Internationale deI'Eclairage (CIE) 1931chromatic colour coordinates which recognize that the human visual system uses three primary colours: red, green and blue [36]. In general, the colour of any light source can be represented on the (x, y) coordinate in colour space. Colour purity was compared to the 1931 CIE Standard Source C (illuminant Cs). The chromatic coordinates (x, y) was calculated using the CIE coordinate calculator. The CIE chromaticity coordinates of Fe^{3+} doped SnO_2 thin films were calculated from the emission spectrum. The location of the colour coordinates for Fe^{3+} doped SnO_2 thin films in the CIE chromaticity diagram is shown in Fig. 6 by a solid circle sign (•). From this figure, one can see that the colour of Fe^{3+} doped SnO_2 thin films located in the blue region and the CIE coordinates are (x = 0.145, y = 0.116). These characteristic features may represent the possible applications in the fields of UV back lights, UV LEDs and display devices.

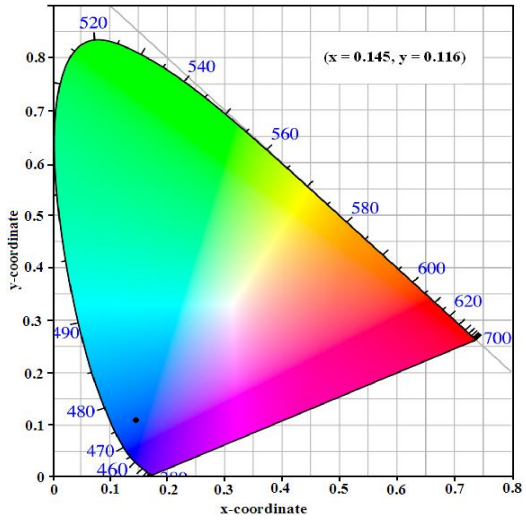


Fig. 6. CIE diagram of Fe^{3+} doped SnO_2 thin films

4. Conclusion

Fe^{3+} doped SnO_2 thin films were prepared successfully by chemical spray pyrolysis method. SEM micrographs shows irregular shaped sphere like structures and EDS analysis confirms the presence of constituent elements of the prepared material. TEM images clearly show the formation of nano rods. FT-IR spectrum showed the characteristic vibrational modes of host lattice. PL spectrum of Fe^{3+} doped SnO_2 thin films shows strong UV emission with suppressed blue emission. From CIE diagram, Fe^{3+} doped SnO_2 thin films emits blue colour light and the corresponding coordinates are (x = 0.145, y = 0.116) and these materials may be useful for UV and display devices.

References

[1] K. L. Chopra, S. Major, D. K. Pandya, Thin Solid Films **102**(1), 1 (1983).
[2] J. Kennedy, P. P. Murmu, J. Leveneur, A. Markwitz, J. Futter, Appl. Surf. Sci. **367**, 52 (2016).
[3] J. Kennedy, A. Markwitz, Z. Li, W. Gao, C. Kendrick, S. M. Durbin, R. Reeves, Cur. Appl. Phys. **6**(3), 495 (2006).
[4] P. P. Murmu, J. Kennedy, Inter. J. Chem. Tech. Res. **7**(3), 1651 (2015).
[5] J. Kennedy, B. Sundrakannan, R. S. Katiyar, A. Markwitz, Z. Li, W. Gao, Cur. Appl. Phys. **8**(3-4), 291 (2008).
[6] M. C. Rao, Int. J. Chem. Sci. **10**(2), 1111 (2012).
[7] M. C. Rao, Optoelectron. Adv. Mat. **6**(3-4), 511 (2012).
[8] M. C. Rao, O. M. Hussain, Ind. J. Eng. Mater. Sci. **16**(5), 335 (2009).
[9] M. C. Rao, O. M. Hussain, Res. J. Chem. Sci. **1**(7), 92 (2011).
[10] H. Hosono, Thin Solid Films **515**(15), 6000 (2007).
[11] K. Ravindranadh, D. Sridhar Kumar, K. Durga Venkata Prasad, M. C. Rao, Inter. J. Chem. Tech. Res. **9**(4), 598 (2016).
[12] C. G. Granqvist, Thin Solid Films **515**, 7025 (2007).
[13] H. L. Hartnagel, A. L. Dawar, A. K. Jain, C. Jagadish, Semiconducting Transparent Thin Films, IOP Publ. Ltd., London (1995).
[14] E. Fortunato, D. Ginly, H. Hosono, D. C. Paine, MRS Bull. **32**(3), 242 (2007).
[15] J. W. Bae, S. W. Lee, G. Y. Yeom, J. Electrochem. Soc. **154**(1), D34 (2007).
[16] M. R. Vaezi, S. K. Sadrnezhaad, Mater. Sci. Eng. B **140**(1-2), 73 (2007).
[17] J. F. Wager, Science **300**(5623), 1245 (2003).
[18] R. L. Hoffman, B. J. Norris, J. F. Wager, Appl. Phys. Lett. **82**(5), 733 (2003).
[19] M. C. Rao, K. Ravindranadh, T. Satyanarayana, Y. Dasaradhudu, G. Nagarjuna, K. Srinivas, M. S. Shekhawat, Der Pharma Chem. **8**, 243 (2016).
[20] S. D. Shinde, G. E. Patil, D. D. Kajale, V. B. Gaikwad, G. H. Jain, J. Alloys Compd. **528**, 109 (2012).
[21] C. Cobianu, C. Savaniu, P. Siciliano, S. Capone, M. Utriainen, L. Niinisto, Sens. Actuators B **77**(1-2), 496 (2001).
[22] R. Larciprete, E. Borsella, P. De Padova, P. Perfetti, G. Faglia, G. Sberveglieri, Thin Solid Films **323**(1-2), 291 (1998).
[23] G. Sberveglieri, G. Faglia, S. Groppelli, P. Nelli, Sens. Actuators B **8**(1), 79 (1992).
[24] R. Dolbec, M. A. El Khakani, A. M. Serventi, R. G. Saint-Jacques, Sens. Actuators B **93**(1-3), 566 (2003).
[25] M. C. Rao, AIP Conf. Proc. **1447**(1), 613 (2012).
[26] M. C. Rao, J. Optoelectron. Adv. M. **12**(12), 2433 (2010).
[27] M. C. Rao, AIP Conf. Proc. **1728**(1), 020077 (2016).
[28] M.C. Rao, AIP Conf. Proc. **1536**, 27 (2013).
[29] K. Ravindranadh, K. Durga Venkata Prasad, M. C. Rao, AIMS Mater. Sci. **3**, 796 (2016).
[30] K. Kaviyarasu, Prem Anand Devarajan, S. Stanly John Xavier, S. Augustine Thomas, S. Selvakumar, J. Mater. Sci. Technol. **28**(1), 15 (2012).
[31] A. F. Khan, M. Mehmood, M. Aslam, M. Ashraf, Appl. Surf. Sci. **256**(7), 2252 (2010).
[32] K. Srinivasulu, I. Omkaram, H. Obeid, A. Suresh Kumar, J. L. Rao, J. Alloys Compd. **546**, 208 (2013).
[33] S. L. Cho, J. Ma, Y. K. Kim, Y. Sun, G. K. L. Wong, J. B. Ketterson, Appl. Phys. Lett. **75**(18), 2761 (1999).
[34] A. Umar, Y. B. Hahn, Nanotech. **17**(9), 2174 (2006).
[35] H. Hao, M. Qin, P. Li, J. Alloys Compd. **515**, 143 (2012).
[36] S. Shionoya, W. M. Yen, Phosphor Handbook, Phosphor Research Society, CRC Press, 459 (1998).

*Corresponding author: raomc72@gmail.com

International Journal of
Life Sciences
International Peer Reviewed Open Access Refereed Journal

Int. J. of Life Sciences, 2018; 6 (1):194-204
ISSN:2320-7817(p) | 2320-964X(o)
UGC Approved Journal No 48951

Original Article Open Access

Medicinal plants of tribal traditional system from Guntur district, Andhra Pradesh, India

Vishnuvardhan Z[1], Jyothirmayi GLV[1] and Jyothi D[2]

[1]Department of Botany & Microbiology, Acharya Nagarjuna University, Guntur- 522 510, AP. India
[2]Department of Botany, SRR & CVR Govt. College, Vijayawada-522508, AP, India

Manuscript details:

Received : 27.11.2017
Accepted : 07.02.2018
Published : 14.03.2018

Editor: Dr. Arvind Chavhan

Cite this article as:
Vishnuvardhan Z, Jyothirmayi GLV and Jyothi D (2018) Medicinal plants of tribal traditional system from Guntur district, Andhra Pradesh, India, *Int. J. of Life Sciences*, Volume 6(1): 194-204.

Copyright: © Author, This is an open access article under the terms of the Creative Commons Attribution-Non-Commercial - No Derives License, which permits use and distribution in any medium, provided the original work is properly cited, the use is non-commercial and no modifications or adaptations are made.

Available online on
http://www.ijlsci.in

ISSN: 2320-964X (Online)
ISSN: 2320-7817 (Print)

ABSTRACT

Objective: To enumerate the medicinal plants used by the tribals of Guntur district in their traditional system for the cure of various human ailments. Very few ethnobotanical studies are reported from Guntur district.

Methods: The data on ethnobotanical and ethnomedicinal plant species was collected during 2015-2016 through regular intensive field trips of 2-3 weeks duration to the tribal habitats. The standard ethnobotanical methods of Jain were followed for the data collection. First-hand information on tribal medicine was recorded and repeated enquiries were made to ascertain tribal knowledge, method of disease diagnosis and treatment. Data on plant local name, part of plant used in the drug, method of administration and dosage along with precautions to be followed were collected. The identification of plant species was made with the help of authentic published flora.

Results: The present study provides information on 67 ethnomedicinal plant species used by tribals of Guntur district for the treatment of 69 human ailments. Plant species such as *Alternanthera sessilis, Annona squamosa, Carica papaya* and *Givotia moluccana* were used each in the treatment of five diseases. The literature search on tribal ethnomedicine revealed striking coincidences in the ailment and plant species used by various tribes and provides ethnobotanical lead that makes *Gymnema sylvestre, Aristolochia indica, Calatropis gigantia* and *Phyllanthus amarus* a valuable source of a raw materials for further critical evaluation by the pharmacologists and phytochemists.

Keywords: Ethnic Tribes, Guntur district, Ethnomedicines, Ethnobotanical leads, Traditional practices.

INTRODUCTION

In India the aboriginal tribes use 8000 wild plant species for medicinal purposes (Pushpangadan and Pradeep 2005). These communities depend mostly on plants as source of medicine to treat their ailments since modern medicines are out of their reach and unaffordable by them. In recent times the

importance of traditional knowledge in drug development is much appreciated and even developed countries are inclined to the use of traditional medicinal system that involves the use of herbal drugs and remedies (Lanfranco 1992).

The leads of traditional knowledge system help to reduce the three main hurdles (time, money and toxicity) in drug development. The information obtained through traditional medicine helps a useful pre-screen to select plants for experimental pharmacological studies (Bigoniya 2008). Moreover, the success rate of finding an useful bioactive molecule through selective screening based on ethnobotanical leads is 50 times greater than it was through random screening (Pushpangadan et al 2016). Hence, an inquiry into documentation of medicinal plants used in the traditional health practices of tribals in Guntur district becomes very pertinent study.

METHODOLOGY

The Guntur district is one out of the eight coastal districts of Andhra Pradesh. It is in the centre of the state arched over either sides by the 12 districts of AP state. The Guntur district is bounded on the east by the Bay of Bengal, on the west by Mahaboobnagar and Kurnool districts on the south by Prakasam district and on north Krishna and Nalgonda districts. The district lies between 15^0 18^1 and 16^0 50^1 of northern latitudes and 79^0 10^1 and 80^0 55^1 of eastern longitudes. The major tribes of the district are Sugali, Chenchu, Koya, Yerukala and Yanadi. The three tribal villages considered for data collection are part of Achampet mandal in Guntur district.

The information on plants used in medicinal practices of tribals has been collected during 2015-2016. The field trips of 2-3 weeks duration were made to the tribal villages (Neeleswarapalem, Putlagudem and Talvay Thanda) in Achampet mandal, Guntur district, AP. The local knowledgeable people and tribal medicine-men were asked to explain how different plants were used in the cure of diseases. Their narration about local plants has been on spot recorded and subsequently they have been accompanied to locate the plants in their natural habitat.

The data on plant part used, preparation of drug, dosage and method of administration were noted down. The plants were photographed and plant specimen were collected to keep them as herbarium voucher specimen. The plants were identified with the help of floras published by Gamble & Fischer (1935) and Pullaiah et al (2000).

RESULTS

The present study reports 67 medicinal plant species used in the therapeutic practices by the tribals in Achampeta mandal (Guntur district, Andhra Pradesh) to cure 72 ailments (Tables 1and 2).

Table 1: Enumeration of Ethnomedicinal Plants used by the tribals of Achampet Mandal, Guntur District (AP) India**.**

S.No	Plant name	Plant Local Name	Family	Ailment treated	Plant parts used in the preparation of drug and mode of administration
1.	*Acacia intsia*	Korinda Teega	Mimosoideae	1. Whooping cough	The fibre of the plant is wear around the neck as necklace for the relief from whooping cough.
2.	*Acacia leucophloea (Rosob,) Willd*	Thella Thumma	Mimosoideae	2. Dental Problems	The decoction made from the bark of this plant *Pentaptera arjuna* and along with dried ginger is gargled.
				3. Leucorrhea	The bark is ground with sugar and taken orally.
3.	*Acacia catechu*	Chandra thumma	Mimosoideae	4. Bone fractures	The leaves and flowers are ground with sesame (Sesamum indicum) oil and massaged over the fractured area.
4.	*Achyranthes aspera. L*	Uttareni	Amaranthaceae	5. Eye-infection in* cattle	Leaf paste made with butter milk and table salt is put in the eyes of cattle.
5.	*Aegle marmelos Corr.Serr.*	Maredu	Rutaceae	6. Diarrhoea 7. Dysentery 8. Fevers	Half ripe fruit is eaten to get relief from these ailments.
6.	*Aerva lanata (L.)*	Kondapindi	Amaranthaceae	9. Kidney Stones	The leaves are made into with jaggery and eaten to get relief.

Table 1: Continued…

S.No	Plant name	Plant Local Name	Family	Ailment treated	Plant parts used in the preparation of drug and mode of administration
7.	*Aloe vera (L.) Burm.f.*	Kalabanda	Liliaceae	10. Diabetes	The gel of the leaf is orally administered
				11. Burns	The gel is applied externally on burns
				12. Purgative 13. Abortifacient	The gel is a powerful purgative. In small does it clears constipation and larger does act as abortifacient.
8.	*Alternanthera sessilis (L.) R.Br.Ex.Dc*	Ponnaganti kura	Amaranthaceae	14. Insect bites 15. Snake bites 16. Dyspepsia 17. Anaemia 18. Constipation	The leaf juice is applied orally to get relief.
9.	*Andrographis paniculata (Burm.f) Wallich Ex Ness*	Nallavemu	Acanthaceae	19. Stomach ache	Leaf paste is mixed with honey is administered.
10.	*Annona squamosa l.*	Seethaphalam	Annonaceae	20. Abortifacient	Excess fruit eating by pregnant women leads to abortion
				21. Insect repellant	Leaves act as insect repellants
				22. Lice Killer 23. Sores 24. Boils	Seed paste applied to hair kills lice Sores and boils: leaf paste is applied on sores and boils
11.	*Aristolochia indica (L.)*	Nalla eswari	Aristolochiaceae	25. Snake bite 26. Scorpion bite	The leaf paste is applied locally on the place of bite
				27. Round worms	The plant juice is orally given to kill worms in stomach.
12.	*Asparagus racemosus Willd.*	Pillipeechara	Liliaceae	28. Impotency	The powder of dried bulbs is used in the treatment of impotency.
13.	*Atlantia monophylla (Roxb.)DC*	Adavi nimma	Rutacease	29. Skin diseases	The leaf paste mixed with leaves of *Aegle marrmelos* (Neredu) is applied over the effected skin.
14.	*Balanites eagyptiaca (L.) Del*	Gara chettu	Balanitaceae	30. Leprosy 31. Vitiligo	The leaf paste is externally applied to the effected parts.
				32. Sperm production	Intake of leaf juice improves sperm count
15.	*Bauhinia racemosa*	Are chettu	Caesalpinioideae	33. Dysentery 34. Fevers	The powder of dried flowers mixed with water and taken orally to control dysentery and fevers.
16.	*Biophytum nervifoilum Th.w*	Attapathi	Oxalidaceae	35. Impotency	Leaves of this plant and fruits of banyan tree are made into paste and mixed with sugar taken orally to get relief from impotency.
17.	*Butea monosperma (Roxb.) Taubert.*	Moduga	Faboideae	36. Snake bite:	The wood of this tree is ground with ginger and is given as an antidote for snake bite.
				37. Sperm production	The gum of the plant is orally taken to improve sperm count.
				38. Skin diseases 39. Gonorrhea	The leaf juice is applied externally to control skin diseases and taken orally to treat gonorrhea.
18.	*Caesalpinia decapetala (Roxb.)*	Chegudicha aku	Caesalpinioideae	40. Migraine	A few drops of leaf juice is put into eyes to get relief from migraine.
19.	*Canthium parviflorum Lam*	Balusu chettu	Rubiaceae	41. Dysentery	The decoction of root bark and leaf is orally administered to control dysentery

Table 1: Continued…

S.No	Plant name	Plant Local Name	Family	Ailment treated	Plant parts used in the preparation of drug and mode of administration
20.	*Calatropis gigantia (L.) Ait.t.*	Tella jilledu	Asclepiadaceae	42. Snake bite 43. Sores 44. Boils 45. Skin diseases	The leaf paste is orally applied on the place of snake bite. The latex of the plant is applied externally. The leaf paste controls skin diseases
21.	*Capparis zeylanica L.*	Are donda	Capparaceae	46. Bone fractures	Leaf paste mixed with castor oil is used in the bandages over fractured bones.
				47. Piles	Leaf paste is applied as poultice in treating piles
22.	*Carica papaya L.*	Boppayi	Caricaceae	48. Abortifacient:	Fruit induces abortion in pregnant women
				49. Laxative	Un-ripe fruit is a laxative.
				50. Dyspepsia	Ripe fruit is eaten to control dyspepsia
				51. Piles	The poultice of leaf is applied over piles.
				52. Galactogogue	The latex of the plant is applied over breasts for increased milk secretion of mothers.
23.	*Cassia fistula L.*	Rela	Caesalpinioideae	53. Haematorrhoea 54. Rheumatism	The leaf juice is orally administered to cure haematorrhea and externally applied in case of rheumatism.
24.	*Catunaregam spinosa (Thunb.)*	Manga chettu	Rutaceae	55. Headache	Root paste is applied on forehead to get relief from headache.
25.	*Chloroxylon swietenia DC*	Billudu	Rutaceae	56. Numbness 57. Haughtiness	The leaf juice is massaged on the body to get relief from the ailments.
26.	*Cissus quadrangularis L.*	Nalleru	Vitaceae	58. Diabetes 59. Stomach disorders 60. Paralysis	The Plant is dried powdered and taken orally with honey.
27.	*Coculus hirsutus (L.)Diels*	Duseti teega	Menispermaceae	61. Gout	The leaf juice mixed with curd and sugar is orally administered.
28.	*Corchorus aestuans L .*	Kalasakura	Tiliaceae	62. Sores	Leaf paste is locally applied on sores
				63. Rinderpest* 64. Tympanites*	The leaves are crushed in butter milk and orally given to cattle to control veterinary diseases (Rinderpest Tympanitis) in cattle.
29.	*Cymbopogon colaratus (Nees) stapf.*	Bodagaddi	Poaceae	65. Menstrual pains	Leaf juice is orally given to control menstrual pains.
				66. Fertility restorer	Leaves of this plant are crushed along with pepper seed and garlic into paste and orally given to restore fertility in women.
30.	*Datura stramonium L.*	Tella ummetha	Solanaceae	67. Asthma	The smoke of dried flowers is inhaled to get relief from asthma
31.	*Diospyros chloroxylon (Roxb.)*	Ullinda	Ebenaceae	68. Urinary problem:	The powder of dried flowers is mixed with water and orally administered.
				69. Ulcers	Leaf paste is locally applied on ulcers
32.	*Elytraria acaulis (L.f) Lindau*	Nelamarri / cheppuattaku	Convolvulaceae	70. Wounds 71. Boils	The paste of leaves is externally applied on wounds and boils.
33.	*Euphorbia nivulia Buch. Ham*	Akugemudu	Euphorbiaceae	72. Gout:	The decoction of root is orally given to treat gout.
34.	*Euphorbia tirucalli L.*	Kada gemudu / Chemudu kada	Euphorbiaceae	73. Cough:	The latex of this plant is applied on the throat and turmeric powder is sprinkled on it to control cough.
				74. Ear-ache	A few drops are sequeezed from gently heated ripe stem and put in affected ear.

Table 1: Continued…

S.No	Plant name	Plant Local Name	Family	Ailment treated	Plant parts used in the preparation of drug and mode of administration
35.	*Ficus mollis Vahl.*	Banda Junsi	Moraceae	75. Easy delivery of women	The gum of this plant is mixed in hot water and given to effect easy delivery in women.
36.	*Gardenia gummifera L.f.*	Bikki chettu	Rubiaceae	76. Sciatica 77. Rheumatism	The leaf juice is orally administered.
37.	*Givotia moluccana (L.) Seemann.*	Ponki / Poliki	Euphorbiaceae	78. Eczema 79. Skin diseases	The powder of dried seeds mixed with coconut oil and applied on effected parts externally
				80. Emetic 81. Laxative 82. Purgative	The leaf juice is orally administered to effect vomiting and motions.
38.	*Gymnema sylvestre (Retz.) R. Br.*	Podapatri	Asclepiadaceae	83. Jaundice 84. Diabetes	Leaf juice is orally taken to control jaundice and diabetes.
39.	*Helicteres isora L.*	Gubathada	Stereuliacease	85. Gout 86. Dyspepsia	The juice made with leaves of this plant + *Cassia lanceolata, Pterospermum suberifolium* + Palm candy +seeds of *Butea monosperma* is orally taken to cure gout and dyspepsia.
40.	*Hemidesmus indicus (L.) R. Br.*	Sugandhipala	Asclepiadaceae	87. Dyspepsia 88. Flatulence	The root paste mixed with a few drops of castrol oil and breast milk is orally given to infants with empty stomach to treat dyspepsia and flatulence in children.
41.	*Ichnocarpus frutescens L.*	Nalla teega	Apocynaceae	89. Snake bite 90. Scorpion bite 91. Insect bite 92. Sores:	The root paste is applied on the bitten spot The leaf paste is applied on sores and pustules
				93. Diuretic	The decoction of root is a diuretic.
42.	*Indigofera tinctoria L.*	Neeli mokka	Faboideae	94. Dental pain	The leaves are chewed for the relief from pain.
43.	*Ipomoea mauritiana Jacq.*	Bellapaku	Convolvulaceae	95. Bone fractures	The leaf paste mixed with egg yolk is applied externally on the part of fractured bone.
44.	*Jatropha glandulifera (Roxb.)* Red	Yerra dundiga	Euphorbiaceae	96. Pimples	Leaf paste made with warm water and turmeric powder is externally applied.
45.	*J.glandulifera (Roxb.)* White	Tella dundiga	Euphorbiaceae	97. Mouth Ulcers 98. Tonsilitis	The leaf juice mixed with water is gargled to got relief.
46.	*Kydia calycina Roxb.*	Kondapathi	Malvaceae	99. Atrabilis 100. Gout	Paste prepared with leaves of this plant and Cassia auriculata mixed with dates is orally given to get relief.
47.	*Lawsonia inermis L.*	Gorintaku	Lythraceae	101. Ulcers 102. Boils 103. Wounds	Leaf paste is externally applied on effected parts.
48	*Mitragyna Parvifolia (Roxb.) Korth.*	Battaganapu	Rubiaceae	104. Burns:	The Leaves are roasted, powdered, mixed with coconut oil and applied on burns with feathers.
49.	*Moringa oleifera Lam*	Munaga	Moringaceae	105. Factures	Leaves are boiled and poultice is applied on fractures.
				106. Anaemia	The leaf juice is orally given in treatment of anemia.
50.	*Pergularia daemia (Forsik.) Chior.*	Juttupaku	Asclepiadaceae	107. Sciatica	Leaf paste is externally applied.
				108. Rheumatic	Leaf paste is massaged over the affected parts.
				109. Pains 110. Asthma	Leaf juice is orally given to treat asthma

Table 1: Continued…

S.No	Plant name	Plant Local Name	Family	Ailment treated	Plant parts used in the preparation of drug and mode of administration
51.	*Phyllanthus amarus Schum & Thonn.*	Nela usiri	Euphorbiaceae	111. Jaundice	Leaf juice is orally administered to cure Jaundice.
				112. Menstrual pains	Leaf paste made with butter milk is orally taken to get relief from menstrual pains.
52.	*Phyllanthus reticulatus Poiret.*	Nallapulicheru	Euphorbiaceae	113. Carminative 114. Neuralgic	The leaf juice acts as carminative and neuralgic.
53.	*Piper betle L*	Tamalapaku	Piperaceae	115. Pyorrhea 116. Dyspepsia 117. Expectorant	The fresh leaves are chewed to get relief from pyorrhea and dyspepsia
54.	*Pterospermum, xylocarpum (Garrner).*	Tada Chettu	Sterculiaceae	118. Haughtiness 119. Gout 120. Dyspepsia	The leaves of this plant along with leaves of *Cassia lanceolata, Helicteres isora* and seeds of *Butea frondosa* are mixed with palm candy and made into a paste. It is administered orally to get relief from haughtiness, gout and dyspepsia.
55.	*Senna occidentalis (L.) Link*	Kasinda	Caesalpinioideae	121. Skin diseases 122. Paralysis	The leaf paste is externally applied to treat skin diseases. The leaf paste is mixed with butter and massaged over the affected parts
56.	*Strebulus aspera Lour.*	Palabarinka	Moraceae	123. Leprosy 124. Skin diseases	The decoction of the bark and dried leaves is orally given to treat leprosy. The leaf juice controls skin diseases.
57.	*Striga gesnerioides*	Nakkapeetaku	Acanthaceae	125. Piles:	The leaf paste is externally applied to cure piles.
58.	*Strychnos nux-vomica L.*	Mushti chettu	Loganiaceae	126. Neuralgia 127. Dysentery	Leaf juice is given orally in low dose to treat neuralgia and dysentery. Large doses are toxic.
59.	*Strychnos potatorum L.f.*	Chilla chettu	Loganiaceae	128. Spermatorrhoea	Seeds soaked for 12hrs in cow milk are eaten to treat spermatorrhoea.
60.	*Tabernaemontana divaricata (L.) R.Br.*	Nandivardhanam	Apocynaceae	129. Toothache 130. Conjunctivitis	The milky juice of leaf cures conjunctivitis and bark chewed controls toothache.
61.	*Tarenna asiatica (L.) Kuntze ex Schum*	Kommi	Rubiaceae	131. Stomach ulcers	The leaf juice controls stomach ulcers.
62.	*Tephrosia pupurea (L) pers.*	Vempali	Faboideae	132. Stomachache 133. Antihelmintic	The dried roots powder is mixed with hot water and is given orally to control stomachache and acts also as antihelmintic
63.	*Tribulus terrestris L.*	Palleru	Zygophyllaceae	134. Kidney problems 135. Impotency	The leaf juice is orally given to control kidney problems and to remove impotency.
64.	*Tridax procumbens*	Gaddi chamanthi	Asteraceae	136. Wounds 137. Boils	The juice is externally applied to heal wounds and boils
65.	*Urgenia indica (Roxb.) Kunth.*	Adavi vulli / Verri vulli	Liliaceae	138. Epilepsy 139. Boils	The paste of the bulb is externally applied on fore head and on affected part to treat epilepsy and boils.
66.	*Vitex negundo L.*	Vavili	Verbinaceae	140. Pain relief	The leaves are boiled in water along with leaves of Eucalyptus and Neem leaves and turmeric powder is added. This water is used for bathing of delivered women to get relief from delivery pains.
				141. Antihelmintic	The leaf juice is orally taken that acts as antihelmintic.
67.	*Ziziphus xylopyrus (Retz.) willd.*	Gotti	Rhamnaceae	142. Sores 143. Boils	The leaf paste is externally applied on boils and sores.

*Veterinary diseases

Table 2. Names of different ailments and plant species used to cure them

S. No	Name of the ailment	No. of plant species useful in the treatment	Names of plant species used in the treatment
1.	Abortifacient	2	*Aloe vera, Carica papaya*
2.	Anaemia	1	*Moringa oleifera*
3.	Anti-helmintic	2	*Tephrosia pupurea, Vitex negundo*
4.	Asthama	2	*Datura stramonium, Pergularia daemia*
5.	Atrabilis	1	*Kydia calycina*
6.	Boils	7	*Lawsonia inermis, Urgenia indica,Tridax procumbens, Ziziphus Xylopyrus, Elytraria acaulis, Annona squamosa, Calatropis gigantia.*
7.	Bone fractures	3	*Acacia catechu, Carica papaya, Ipomoea mauritiana*
8.	Burns	2	*Aloe vera, Mitragyna Parvifolia*
9.	Carminative	1	*Phyllanthus reticulates*
10.	Conjunctivitis	1	*Tabernaemontana divaricata*
11.	Constipation	1	*Alernanthera sessilis*
12.	Cough	1	*Euphorbia tirucalli*
13.	Dental pain or problem	1	*Acacia leucophloea*
14.	Diabetes	3	*Aloe vera, Gymnema sylvestre, Cissus quadrangularis*
15.	Diarrhea	1	*Aegle marmelos*
16.	Diuretic	1	*Ichnocarpus frutescens*
17.	Dysentery	4	*Bauhinia racemosa, Canthium parviflorum, Strychnos nux-vomica, Aegle marmelos.*
18.	Dyspepsia	5	*Alernanthera sessilis, Carica papaya, Pterospermu xylocarpum, Piper betle, Hemidesmus indicus.*
19.	Ear ache	1	*Euphorbia tirucalli*
20.	Eazy delivery	1	*Ficus mollis*
21.	Eczema	1	*Givotia moluccana*
22.	Emetic	1	*Givotia moluccana*
23.	Epilepsy	1	*Urgenia indica*
24.	Expectorant	1	*Piper betle*
25.	Eye infection in cattle*	1	*Achyranthes aspera*
26.	Flatulance	1	*Hemidesmus indicus*
27.	Fertility restorer	1	*Cymbopogon colaratus*
28.	Fever	2	*Aegle marmelos, Bauhinia racemosa*
29.	Galactogogue	1	*Carica papaya*
30.	Gonorrhea	1	*Butea monosperma*
31.	Gout	6	*Coculus hirsutus, Euphorbia nivulia, Helicteres isora, Kydia calycina, Pterospermum, xylocarpum, Andrographis paniculata*
32.	Haughtiness	2	*Chloroxylon swietenia, Pterospermum, xylocarpum*
33.	Head ache	1	*Catunaregam spinosa*
34.	Hematorrhea	1	*Cassia fistula*
35.	Impotency	3	*Asparagus racemosus, Tribulus terrestris, Biophyture nervifolium*
36.	Insect bite	2	*Alernanthera sessilis, Ichnocarpus frutescens*
37.	Insect repellent		*Annona squamosa*
38.	Jaundice	2	*Phyllanthus amarus , Gymnema sylvestre*
39.	Kidney stones	2	*Aerva lanata, Tribulus terrestris*

Table 2. Continued…

S. No	Name of the ailment	No. of plant species useful in the treatment	Names of plant species used in the treatment
40.	Laxative	2	*Carica papaya, Givotia moluccana Seemann.*
41.	Leprosy	2	*Balanites eagyptiaca, Strebulus aspera*
42.	Leucorrhoea	1	*Acacia leucophloea*
43.	Lice killer	1	*Annona squamosa*
44.	Menstrual pains	2	*Phyllanthus amarus , Cymbopogon colaratus*
45.	Migraine	1	*Caesalpinia decapetala*
46.	Neuralgia	2	*Phyllanthus reticulates Poiret, Strychnos nux-vomica*
47.	Pain relief	1	*Viter negundo*
48.	Paralysis	2	*Senna occidentalis, Cissus quadrangularis*
49.	Piles	3	*Carica papaya, Capparis zeylanica, Striga gesnerioides*
50.	Pimples	1	*Jatropha glandulifera*
51.	Purgative	2	*Givotia moluccana, Aloe vera*
52.	Pyorrhoea	1	*Pipper betle*
53.	Rinder pest*	1	*Corchorus aestuans*
54.	Ring worm control	1	*Aristolochia indica*
55.	Rheumatism	2	*Cassia fistula, Gardenia gummifera, Pergularia daemia*
56.	Sciatica	2	*Gardenia gummifera, Pergularia daemia*
57.	Scorpion bite	2	*Aristolochia indica, Ichnocarpus frutescens*
58.	Skin diseases	5	*Atlantia monophylla, Butea monosperma, Senna accidentails, Givotia moluccana, Strebulus terrestris*
59.	Snake bite	5	*Alernanthera sessilis, Aristolochia indica, Calatropis gigantia, Butea monosperma, Ichnocarpus frutescens*
60.	Sperm production	2	*Balanites eagyptiaca, Butea monosperma*
61.	Spermatorrhea	1	*Strychnos potatorum*
62.	Stomach ache	2	*Andrographis paniculata, Tephrosia pupurea*
63.	Stomach disorders	1	*Cissus quadrangularis*
64.	Sores	5	*Annona squamosa , Calatropis gigantia, Corchorus aestuans, Ichnocarpus frutescens, Ziziphus xylopyrus*
65.	Tonsillitis	1	*Jatropha glandulifera (white form)*
66.	Tooth ache / decay	3	*Corchorus aestuans, Indigofera tinctoria, Tabernaemontana divaricate*
67.	Timpanites*	1	*Corchorus aestuans*
68.	Ulcers	4	*Diospyros chloroxylon, Lawsonia inermis, Jatropha glandulifera (white form)*
69.	Urinary problems	1	*Diospyros chloroxylon*
70.	Vitiligo	1	*Balanites eagyptiaca*
71.	Whooping cough	1	*Acacia intsia*
72.	Wounds	2	*Lawsonia inermis, Tridax procumbens*

*Veterinary diseases

Table 3. Similarity exhibited in the different tribal phyto-therapeutic practices in respect of medicinal plant species.

S. No	Plant Name & its medicinal use	Used by the tribals of the area / District / State	Reference
1.	*Gymnema sylvestre* Antidiabetic plant	i. Tribes of Achampet Mandal, Guntur district Andhra Pradesh	Present study
		ii. Yanadi tribe of Sheshachalam hills, Kadapa & Chittoor district, Andhra Pradesh	Reddy et al (2009)
		iii. Sugalis tribe of Yerramalalais, Kurnool district, Andhra Pradesh	Basha & Sudarsanam (2010)
		iv. Yandi tribe of Penchalakona Forest, Nellore district Andhra Pradesh	Savithramma et al (2012)
		v. Tribe of Adilabad district Andhra Pradesh	Rama Krishna et al (2014)
		vi. Traditional healers West Godavari district Andhra Pradesh	Kadali & Sandeep (2015)
2.	*Phyllanthus amarus* Hepato-protective effect	i. Tribes of Achampet Mandal Guntur district Andhra Pradesh	Present study
		ii. Tribes of Khammam district, Andhra Pradesh	Manjula et al (2011)
		iii. Chenchu tribes of Nallamalais in Eastern Ghats Andhra Pradesh	Sabjan et al (2014)
		iv. Tribes of Achampet forest division, Telangana state	Reddy (2015)
3.	*Aristolochia indica* Anti-dote for snake bite	i. Tribes of Achampet Mandal, Guntur district, Andhra Pradesh	Present study
		ii. Tribes of Srikakulam district Andhra Pradesh	Rao & Sreeramulu (1985)
		iii. Bagata tribe of Eastern Ghats, Andhra Pradesh	Sandhya Sri & Reddy (2011)
		iv. Gonds tribe of Adilabad district Andhra Pradesh	Murthy (2012)
		v. Konda Reddi tribe of West Godavari district Andhra Pradesh	Prasanna Kumari & Vishnuvardhan (2017)
		vi. Sugali tribe of Krishna district, Andhra Pradesh	Nageswara Rao Naik et al (2017)
	Calotropis gigantia Anti-dote for snake bite	i. Tribes of Achampet Mandal, Guntur district, Andhra Pradesh	Present study
		ii. Tribes of Kotia hills, Vizianagaram district, Andhra Pradesh	Babu et al (2011)
		iii. Sugali tribe of Yerramalais, Kurnool district, Andhra Pradesh	Basha & Sudarsanam (2012)
		iv. Koya tribe of Warangal North forest division, Telangana state	Suthari et al (2014)
		v. Tribes of Achampet forest division Telangana state	Reddy (2015)

Out of the 72 ailments, three are of veterinary diseases and 68 are human ailments. The 68 plant species belong to 33 families. Fabaceae is the most dominant family with 10 species followed by Euphorbiaceae (7 sp), Rubiaceae (4sp), Rutaceae (4 sp), Asclepiadaceae (4 sp), Amaranthaceae (3 sp) and Liliaceae (3 sp). The families such as Acanthaceae, Apocynaceae, Convolvulaceae, Loganiaceae, Moraceae and Sterculiaceae are represented each with 2 species. Twenty families are represented by one species each. Many plants of present study are used in the treatment of more than one ailment. *Alternanthera sessilis* is used in the cure of anaemia, constipation, dyspepsia, snake bite and insect bite. Similarly, *Annona squamosa, Carica papaya* and *Givotia moluccana* are also used each in the treatment of five different ailments. Of the 67 species, seven species are used in the treatment of boils. The ailments such as dyspepsia, gout, snake bite, sores and skin diseases are treated with five species each (Table 2).

DISCUSSION

The Guntur is an important district being located in the capital region of Andhra Pradesh state and also centrally placed arched over on either sides by the remaining 12 districts. The district was floristically rich with 495 genera and 891 species (Pullaiah et al 2000). In 2001, Muralidhar Rao & Pullaiah made an attempt to study ethnomedicinal plants from Guntur district. Although Andhra Pradesh state was well studied ethnobotanically, the Guntur district received very little attention.

The resemblance between the health practices of different tribes in respect of ailment and plant species has been assessed and presented in Table-3. The tribals of Achampet mandal used *Gymnema sylvestre* plant in the treatment of diabetes. The Yanadi tribes of Seshachalam hills in Kadapa and Chittoor districts, Penchalakona forest area in Nellore district, Sugalis of Kurnool district and tribes of Adilabad district also used this plant in the cure of diabetes (Reddy et al 2009; Savithramma et al 2012; Basha & Sudarsanam 2012; Ramakrishna et al 2014). Also the traditional healers in West Godavari district used it in diabetes treatment (Kadali & Sandeep 2015).

The tribals of Achampet mandal (Guntur district, Andhra Pradesh) used *Phyllanthus amarus* to cure jaundice. Manjula et al (2011) Sabjan et al (2014) and Reddy (2015) reported that the tribes of Khammam district, Nallamalais in Eastern Ghats and Achampet forest division in Telangana region also use this plant to cure liver disorders.

The tribals of Srikakulam district, Bagatas of Eastern Ghats, Gonds of Adilabad district, Konda reddis of West Godavari district and Sugalis of Krishna district use *Aristolochia indica* in the treatment of snake bite similar to the tribal practice reported now from Achampet mandal, Guntur district (Rao & Sreeramulu 1985; Sandhya Sri & Reddy 2011; Murthy 2012; Prasanna Kurmari & Vishnuvardhan 2017; Nageswara Rao Naik et al 2017). In the present study *Calotropis gigantia* is another plant species used in the snake bite treatment similar to the practice of the tribes of Kotia hills Vizianagaram district, Yerramalais of Kurnool district, Achampet forest division and Warangal North forest division in Telangana (Babu et al 2011; Basha & Sudarsanam 2012; Suthari et al 2014; Reddy 2015).

The similarity in the use of particular plant species for a particular ailment by different, ethnic tribes signifies its profound medicinal value. Hence, Pharmacognostic and Phytochemical analyses in *Phyllanthus amarus, Gymnema sylvestre, Aristolochia indica* and *Calotropis gigantia* will result in useful bioactive molecules to treat diabetes, jaundice and snakebites.

CONCLUSION

In the Guntur district the tribals used 67 medicinal plants in their health care practices to treat 60 different human ailments. They depend mostly on plants in their vicinity and used them in curde drugs preparation to cure a broad spectrum of diseases. Some practices of the present study exactly resembled with the tribal practices from other districts of Andhra Pradesh and Telangana states. Such similarity between plant species and disease therapy can be considered as on useful lead in ethnobotanical research to provide a rich source of plant materials for bioactive compounds screening by pharmacologists.

REFERENCES

Babu CN, Naidu MT, Venkaiah M (2011) Ethnomedicinal plants of Kotia hills of Vizianagaram District, A.P, *India. J. Phytomed*. 2(6):76-82.

Basha SK, Sudarsanam G (2012) Traditional use of plants against snakebite in Sugali tribes of Yerramalais of Kurnool district, Andhra Pradesh, *India. Asian Pac. J.Trop. Biomed*. 2:S575-S579.

Bigoniya P (2008) Ethnopharmacological approach in herbal drug development. The Pharma Review: New Delhi. Kongposh Publications.

Gamble J, Fischer CEC (1915-1936) Flora of the Presidency of Madras. Vol. I-III (Adlard & son Ltd. London)

Kadali VN, Sandeep BV (2015) Antihyper glycemic plants used by the traditional healers of West Godavari district, Andhra Pradesh. *India. Int. J. Pharmacognesy*. 2:473-477.

Lanfranco G (1992). Popular use of medicinal plants in the Maltese Islands. Insula. 1:34-35.

Manjula RR, Koteswara Rao J, Seetharami Reddy TVV (2011) Ethnomedicinal plants used to cure jaundice in Kammam district of Andhra Pradesh. *Journal of Phytology.* 3:33-35.

Muralidhar Rao D, Pullaiah T (2001) Ethno-medico-botanical studies in Guntur district of Andhra Pradesh, *India. Ethnobotany.* 13:40-44.

Murthy EN (2012) Ethno medicinal plants used by Gonds of Adilabad district, Andhra Pradesh. *Int. J. Pharma. Life. Sci.* 3(10):2034-2043.

Nageswara Rao Naik B, Vishnuvardhan Z, Rosaiah G (2017) Traditional phytotherapentic practices among Sugalis of Krishna district, Andhra Pradesh, *India. Int. J. Res. Sci. Res.* 8(9):20393-20402.

Prasanna Kumari P, Vishnuvardhan Z (2017) A survey on the ethnomedicinal practices of Konda reddi tribe from Polavaram mandal, Andhra Pradesh, *India. Int. J. Computl. Engg. Res.(IJCER)* 7:51-62.

Pullaiah T, Rama Krishnaiah V, Sandhya Rani S, Rao PN (2000) Flora of Guntur district, New Delhi Regency Publications.

Pushpangadan P, George V, Ijinu TP. Rajasekharan S (2016) Ethnobotany, ethnobiology, ethnopharmacology, bioprospecting of traditional knowledge and evolution of benefit sharing In: Indian Ethnobotany: Emerging trends Editor, AK Jain, Scientific Publishers, Jodhpur – 342001 (India):1-23.

Pushpangadan P, Pradeep PRJ (2005) A glimpse at tribal India – An Ethnobotanical enquiry. Joint publication of Amity Institute for herbal and biotech products development Thiruvanthapuram and forests, Govt. of India;1-167.

Rama Krishna N, Varma YNR Saidulu CH. (2014) Ethnomedicinal Studies of Adilabad district, Andhra Pradesh, *India. Journal of Pharmacognosy and Phytochemistry* 3(1):18-36.

Rao KP, Hara Sreeramulu S (1985) Ethnobotany of selected medicinal plants of Srikakulam district, Andhra Pradesh. *Ancient Sciences of Life*. 4:238-244.

Reddy CS, Reddy KN, Murthy EN, Raju VS (2009) Traditional Medicinal Plants in Seshachalam hills, Andhra Pradesh. *Indian. J. Med. Plants Res*. 3(5):408-412.

Reddy DS (2015) Ethnomedicinal plants used by the tribals of Achampet forest division in Nallamalais, Telangana, *India. Int. J. Plant.Animal and Environ. Sci.* (IJPAES) 5:65-73.

Sabjan G, Sudarsanam G, Reddy DD, Muralidhara Rao D (2014) Ethnobotanical crude drugs used in treatment of liver diseases by Chenchu tribes in Nallamalais, Andhra Pradesh, *India. Ame. J. Ethnomed* 1(3):115-121.

Sandhya Sri B, Reddy TVV (2011) Traditional Phytioantdotes used for snake bite by Bagata tribe of Eastern Ghats of Visakhapatnam district, Andhra Pradesh. *Int. Multidisci. Res. Journal* 1(6):42-45.

Savithramma N, Linga Rao M, Yugandhar P, Hari Babu R. (2012) Ethonobotanical study of Penchalakona forest area of Nellore district, Andhra Pradesh, *India. International Journal of Phytomedicine* 4:333-339.

Suthari S, Sreemulu N, Omkar K, Reddy CS, Raju VS. (2014) Intercultural cognizance of medicinal plants of Warangal North Forest division, Northern Telangana, India. Ethnobotany Research &Applications 12:211-235.

© 2018 | Published by IJLSCI

Annals of Pure and Applied Mathematics
Vol. 14, No. 3, 2017, 497-508
ISSN: 2279-087X (P), 2279-0888(online)
Published on 13 November 2017
www.researchmathsci.org
DOI: http://dx.doi.org/10.22457/apam.v14n3a17

Annals of
Pure and Applied Mathematics

r-Relatively Prime Sets and *r*-Generalization of *Phi* Functions for Subsets of {1,2,…,n}

***G. Kamala*[1] and *G. Lalitha*[2]**

[1]Department of Mathematics, Osmania University, Hyderabad (TS), India
[2]Department of Mathematics, SRR & CVR Govt. Degree College
Vijayawada (AP) India
Email: [1]gkamala369@gmail.com, [2]lalitha.secpg@gmail.com
[1]Corresponding author.

Received 24 October 2017; accepted 9 November 2017

Abstract. A non-empty subset A of positive integers {1,2,…,*n*} is said to be relatively prime if $\gcd(A)=1$. Let r be a positive integer ≥ 1. A nonempty subset $A \subseteq \{1,2,...,n\}$ is r-relatively prime if greatest r^{th} power common divisor of elements of A is 1. In this case we write $\gcd_r(A)=1$. Note that $\gcd(A)=1$ implies $\gcd_r(A)=1$ but the converse need not be true. Let $f^{(r)}(n)$ denotes the number of *r*-relatively prime subsets of $\{1, 2, ..., n\}$ and $f_k^{(r)}(n)$ denotes the number of *r*-relatively prime subsets of $\{1, 2, ..., n\}$ of Cardinality *k*. $\Phi(n)$ denotes the number of non empty subsets A of $\{1, 2, ..., n\}$ such that $\gcd(A)$ is relatively prime to *n*. $\Phi_k(n)$ denotes the number of non-empty subsets A of Cardinality *k* of {1,2,…,*n*} such that $\gcd(A)$ is relatively prime to *n*. We define $\Phi^{(r)}(n)$ to be the number of non-empty subsets *A* of $\{1, 2, ..., n\}$ such that greatest r^{th} power common divisor of elements of *A* and *n* is 1. $\Phi_k^{(r)}(n)$ is defined as the number of subsets *A* of $\{1, 2, ..., n\}$ such that $\mathrm{Card}(A)=k$ and $\gcd_r(A)$ is *r*-relatively to *n*. $\Phi^{(r)}(n)$ and $\Phi_k^{(r)}(n)$ are *r*-generalizations of $\Phi(n)$ and $\Phi_k(n)$ defined by Nathanson [2]. Exact formulas and asymptotic estimates are obtained for these functions. These results are extensions of results of Nathanson [2]. Some of our proofs use the r-Generalization of Mobius inversion formula.

Keywords: *r*-relatively prime sets, *r*-generalization of Euler *Phi* function.

AMS Mathematics Subject Classification (2010): 1BXX, 11B75

1. Introduction

For a nonempty subset A of {1,2,…,n } let $\gcd(A)$ denote the gcd of the elements of A. Nathanson [2] defined a non empty subset A of {1,2,…,n} is relatively prime if $\gcd(A)$=1.Let $f(n)$ denote the number of relatively prime subsets of {1,2,…,n} and for $k \geq 1$, $f_k(n)$ denote the number of relatively prime subsets of {1,2,…,n} of cardinality k. Let $\Phi(n)$ denote the number of non empty subsets A of {1,2,…,n} such that $\gcd(A)$ is relatively prime to n and for integer $k \geq 1$, $\Phi_k(n)$ denote the number of non empty subsets A of {1,2,…,n} such that $\gcd(A)$ is relatively prime to n and card (A)=k. Nathanson[2] obtained the exact formulas and Asymptotic estimates for these four fuctions. In this paper ,we define the functions $f^{(r)}(n)$, $f_k^{(r)}(n)$, $\Phi^{(r)}(n)$ and $\Phi_k^{(r)}(n)$ and obtain exact formulas and Asympotic estimates for these four functions. We derive Mobius Inversion Formula r- Generalized Version to obtain Exact formulas.

Definition 1.

Mobius function r-analogue

$$\mu_r(n) = \begin{cases} 1 & \text{if } n = 1 \\ (-1)^s & \text{if } n = p_1^r p_2^r \ldots p_s^r \text{ where } p_1, p_2, \ldots, p_s \text{ are distinct primes} \\ 0 & \text{otherwise.} \end{cases}$$

Theorem 1. For all positive integers $n \geq 2^r$,

$$f^{(r)}(n) \leq 2^n - 2^{\left\lfloor \frac{n}{2^r} \right\rfloor}. \tag{1}$$

For positive integers $n \geq 2^r$ and k,

$$f_k^{(r)}(n) \leq \binom{n}{k} - \binom{\left\lfloor \frac{n}{2^r} \right\rfloor}{k}. \tag{2}$$

Proof: The set $\{1, 2, 3, \ldots, 2^r, \ldots, n\}$ contains the set $\{2^r, 2\times 2^r, \ldots, \left\lfloor \frac{n}{2^r} \right\rfloor 2^r\}$ which has no subset that is r-relatively prime. Therefore among the $2^n - 1$ non-empty subsets of $\{1, 2, .., n\}$ those which contain any one of the $2^{[n/2^r]} - 1$ non-empty subsets of $\{2^r, 2\times 2^r, \ldots, \left\lfloor \frac{n}{2^r} \right\rfloor 2^r\}$ are not r-relatively prime. Hence

$f^{(r)}(n) \le \left(2^n-1\right)-\left(2^{\left\lfloor \frac{n}{2^r} \right\rfloor}-1\right) = 2^n-2^{\left\lfloor \frac{n}{2^r} \right\rfloor}$ which proves (1). Similarly, $f_k^{(r)}(n) \le \binom{n}{k}-\binom{\left\lfloor \frac{n}{2^r} \right\rfloor}{k}$. We now find a lower bound for $f^{(r)}(n)$ and $f_k^{(r)}(n)$.

If $1\in A$, $A\subseteq\{1,\ 2,\ ..,\ n\}$ then A is r-relatively prime. There are 2^{n-1} sets $A\subseteq\{1,\ 2,\ ..,\ n\}$ with $1\in A$. Hence $f^{(r)}(n) \ge 2^{n-1}$. (3)

Let $n\ge 3^r$. If $1\notin A,\ 2^r\in A,\ 3^r\in A$ then A is r-relatively prime and hence

$$f^{(r)}(n) \ge 2^{n-1}+2^{n-3}. \tag{4}$$

Let $n\ge 5^r$. If $1\notin A,\ 3^r\in A$, but $2^r\in A,\ 5^r\in A$ then A is r-relatively prime and there are 2^{n-4} such subsets. Again $1\notin A,\ 2^r\in A$, but $3^r\in A,\ 5^r\in A$ then A is r-relatively prime and there are 2^{n-4} such subsets. Hence

$$f^{(r)}(n) \ge 2^{n-1}+2^{n-3}+2\times 2^{n-4} = 2^{n-1}+2^{n-2}. \tag{5}$$

Similarly

$$f_k^{(r)}(n) \le \binom{n-1}{k-1}+\binom{n-3}{k-2}+2\binom{n-4}{k-2}. \tag{6}$$

Exact formulas and asymptotic estimates

Let $\lfloor x\rfloor$ denotes the greatest integer less than or equals to *x*. If $x\ge 1$ and $n=\lfloor x\rfloor$ then $\left\lfloor \frac{x}{d} \right\rfloor=\left\lfloor \frac{\lfloor x\rfloor}{d} \right\rfloor=\left\lfloor \frac{n}{d} \right\rfloor$ for all positive integers *d*.

2. Mobius inversion formula r- generalized version

Theorem 2. Let $F^{(r)}(x)$ be a function defined for $x\ge 1$ and define the function $G^{(r)}(x)$ for $x\ge 1$ as $G^{(r)}(x)=\sum_{1\le d^r\le x} F^{(r)}\left(\frac{x}{d^r}\right)$ where the summation is over all positive integers *d* where $d^r\le x$

and $F^{(r)}(x)=0=G^{(r)}(x)$ if $x\in(0,\ 1)$. Then for all inters *d* where $d^r\le x$,

$$G^{(r)}(x)=\sum_{1\le d^r\le x} F^{(r)}\left(\frac{x}{d^r}\right) \Leftrightarrow F^{(r)}(x)=\sum_{1\le d^r\le x} \mu_r\left(d^r\right)G^{(r)}\left(\frac{x}{d^r}\right) \tag{6a}$$

Proof: Assume $G^{(r)}(x) = \sum_{1 \le d^r \le x} F^{(r)}\left(\frac{x}{d^r}\right)$.

Consider

$$G^{(r)}(x) = \sum_{1 \le d^r \le x} \mu_r\left(d^r\right) G^{(r)}\left(\frac{x}{d^r}\right) = \sum_{1 \le d^r \le x} \mu_r\left(d^r\right)\left[\sum_{1 \le t^r \le \frac{x}{d^r}} F^{(r)}\left(\frac{x}{t^r d^r}\right)\right]$$

$$= \sum_{1 \le u^r \le x} F^{(r)}\left(\frac{x}{u^r}\right)\left[\sum_{d^r / u^r} \mu_r\left(d^r\right)\right] = F^{(r)}(x).$$

Conversely, Assume $F^{(r)}(x) = \sum_{1 \le d^r \le x} \mu_r\left(d^r\right) G^{(r)}\left(\frac{x}{d^r}\right)$.

Consider $\sum_{1 \le d^r \le x} F^{(r)}\left(\frac{x}{d^r}\right) = \sum_{1 \le d^r \le x} \mu_r\left(d^r\right)\left[\sum_{1 \le t^r \le \frac{x}{d^r}} \mu_r\left(d^r\right) G^{(r)}\left(\frac{x}{t^r d^r}\right)\right]$

$$= \sum_{1 \le u^r \le x} G^{(r)}\left(\frac{x}{u^r}\right)\left[\sum_{t^r / u^r} \mu_r\left(t^r\right)\right]$$

$$= G^{(r)}(x).$$

Theorem 3. For all positive integers $n \ge 2^r$,

$$\text{(i)} \quad \sum_{1 \le d^r \le n} f^{(r)}\left(\left[\frac{n}{d^r}\right]\right) = 2^n - 1 \tag{7}$$

and $$\text{(ii)} \quad f^{(r)}(n) = \sum_{1 \le d^r \le n} \mu_r\left(d^r\right)\left(2^{\left[\frac{n}{d^r}\right]} - 1\right). \tag{8}$$

For all positive integers $n \ge 2^r$, k and $r \ge 1$,

$$\text{(i)} \quad \sum_{1 \le d^r \le n} f_k^{(r)}\left(\left[\frac{x}{d^r}\right]\right) = \binom{n}{k} \tag{9}$$

and $$\text{(ii)} \quad f_k^{(r)}(n) = \sum_{1 \le d^r \le n} \mu_r\left(d^r\right)\binom{\left[\frac{n}{d^r}\right]}{k} \tag{10}$$

Proof: Let A be a non-empty subset of $\{1,\ 2,\ ..,\ n\}$ and greatest r^{th} power common divisor of A is d^r. Then $A^1 = \frac{1}{d^r} * A = \left\{ \frac{a}{d^r} \Big/ a \in A \right\}$ is r-relatively prime subset of $\left\{1,\ 2,\ ..,\ \left[\frac{n}{d^r}\right]\right\}$. Conversely, if A^1 is r-relatively prime subset of $\left\{1,\ 2,\ ..,\ \left[\frac{n}{d^r}\right]\right\}$, then $A = d^r * A^1 = \left\{ d^r \cdot a \Big/ a \in A^1 \right\}$ is a non-empty subset of $\{1,\ 2,\ ..,\ n\}$ with greatest r^{th} power common divisor of A equals to d^r. Therefore it follows that there are exactly $f^{(r)}\left(\left[\frac{n}{d^r}\right]\right)$ subsets of $\{1,\ 2,\ ..,\ n\}$ with greatest r^{th} power common divisor d^r and hence $\sum_{1 \le d^r \le n} f^{(r)}\left(\left[\frac{n}{d^r}\right]\right) = 2^n - 1$ which proves (7). We apply Theorem (2) to the function $F^{(r)}(x) = f^{(r)}([x])$ for all $x \ge 1$ we define $G^{(r)}(x) = \sum_{1 \le d^r \le x} F^{(r)}\left(\frac{x}{d^r}\right)$

$$= \sum_{1 \le d^r \le x} f^{(r)}\left(\left[\frac{x}{d^r}\right]\right) = 2^{[x]} - 1.$$

By Theorem (2) $f^{(r)}([x]) = F^{(r)}(x) = \sum_{1 \le d^r \le x} \mu_r\left(d^r\right) G^{(r)}\left(\left[\frac{x}{d^r}\right]\right)$

$$= \sum_{1 \le d^r \le x} \mu_r\left(d^r\right)\left(2^{\left[\frac{x}{d^r}\right]} - 1\right)$$

$$f^{(r)}(n) = n \sum_{1 \le d^r \le n} \mu_r\left(d^r\right)\left(2^{\left[\frac{n}{d^r}\right]} - 1\right)$$ which proves (8).

We now prove (9) and (10).

Note that $f_k^{(r)}(n) = \#\left\{A \subseteq \{1,\ 2,\ ...,\ n\} : \text{Card } A = k,\ \gcd_r(A) = 1\right\}$.

Let $A \subseteq \{1,\ 2,\ ...,\ n\}$ with $\text{Card } A = k$ and greatest r^{th} power common divisor of A is equals to d^r. Let $A^1 = \frac{1}{d^r} * A = \left\{ \frac{a}{d^r} \Big/ a \in A \right\}$. Then $A^1 \subseteq \left\{1,\ 2,\ ...,\ \left[\frac{n}{d^r}\right]\right\}$,

Card $A^1 = \text{Card}\, A = k$ and $\gcd_r\left(A^1\right) = 1$. Conversely ,if $A^1 \subseteq \left\{1,\ 2,\ ...,\ \left[\frac{n}{d^r}\right]\right\}$ and $\text{Card}\, A^1 = k, \gcd_r\left(A^1\right) = 1$ then $A = d^r * A^1$ is such that Card $A = k$ and $\gcd_r(A) = d^r$.

There is $1-1$ correspondence between r-relatively prime subsets $A^1 \subseteq \left\{1,\ 2,\ ...,\ \left[\frac{n}{d^r}\right]\right\}$ of Cardinality k and the non-empty subsets A of $\{1,\ 2,\ ...,\ n\}$ with $\gcd_r(A) = d^r$ and $\text{Card}\, A = k$. Hence $\sum_{1 \le d^r \le n} f_k^{(r)}\left(\left[\frac{n}{d^r}\right]\right) = \binom{n}{k}$ which proves (9).

By Theorem (1) we have $f_k^{(r)}(n) = \sum_{1 \le d^r \le n} \mu_r\left(d^r\right)\binom{\left[\frac{n}{d^r}\right]}{k}$ which proves (10).

Theorem 4. For all positive integers $n \ge 2^r$, r we have

$$2^n - 2^{\left[\frac{n}{2^r}\right]} - n \cdot 2^{\left[\frac{n}{3^r}\right]} \le f^{(r)}(n) \le 2^n - 2^{\left[\frac{n}{2^r}\right]}. \tag{11}$$

Proof: For $n \ge 2^r$ we have by equation (7) $2^n - 1 = \sum_{1 \le d^r \le n} f^{(r)}\left(\left[\frac{n}{d^r}\right]\right)$

This implies $2^n = f^{(r)}([n]) + f^{(r)}\left(\left[\frac{n}{2^r}\right]\right) + \sum_{3 \le d^r \le n} f^{(r)}\left(\left[\frac{n}{d^r}\right]\right) + 1$

$$\le f^{(r)}(n) + 2^{\left[\frac{n}{2^r}\right]} + n \cdot 2^{\left[\frac{n}{3^r}\right]}$$

combining this with equality (1), $2^n - 2^{\left[\frac{n}{2^r}\right]} - n \cdot 2^{\left[\frac{n}{3^r}\right]} \le f^{(r)}(n) \le 2^n - 2^{\left[\frac{n}{2^r}\right]}$.

Theorem 5. For all positive integers $n \ge 2^r$, k and r

$$\binom{n}{k} - \binom{\left[\frac{n}{2^r}\right]}{k} - n\binom{\left[\frac{n}{3^r}\right]}{k} \le f_k^{(r)}(n) \le \binom{n}{k} - \binom{\left[\frac{n}{2^r}\right]}{k}. \tag{12}$$

Proof: By equation (9) $\sum_{1 \le d^r \le n} f_k^{(r)}\left(\left[\frac{n}{d^r}\right]\right) = \binom{n}{k}$

$$\text{Therefore } \binom{n}{k} = f_k^{(r)}([n]) + f_k^{(r)}\left(\left[\frac{n}{2^r}\right]\right) + \sum_{3^r \le d^r \le n} f_k^{(r)}\left(\left[\frac{n}{d^r}\right]\right)$$

$$\le f_k^{(r)}(n) + \binom{\left[\frac{n}{2^r}\right]}{k} + n\binom{\left[\frac{n}{3^r}\right]}{k}.$$

$$\text{Therefore } \binom{n}{k} - \binom{\left[\frac{n}{2^r}\right]}{k} - n\binom{\left[\frac{n}{3^r}\right]}{k} \le f_k^{(r)}(n) \le \binom{n}{k} - \binom{\left[\frac{n}{2^r}\right]}{k} \text{ by equation (2).}$$

3. A Phi function for sets and its *r*-generalization

Nathanson [2] defined Phi function for sets, denoted by $\Phi(n)$ to be the number of non-empty subsets A of $\{1, 2, 3, ..., n\}$ such that $\gcd(A)$ is relatively prime to n. For example for distinct primes p and q we have

$$\Phi(p) = 2^p - 2, \quad \Phi\left(p^2\right) = 2^{p^2} - 2^p, \quad \Phi(pq) = 2^{pq} - 2^p - 2^q + 2.$$

Note that $\Phi_1(n) = \varphi(n)$ for all $n \ge 1$. We define, for a positive integer $r \ge 1$, $\Phi^{(r)}(n)$ to be the number of non-empty subsets A of $\{1, 2, ..., n\}$ such that greatest r^{th} power common divisor of A and n is 1. For example for distinct primes p and q,

$$\Phi^{(r)}\left(p^r\right) = 2^{p^r} - 2$$

$$\Phi^{(r)}\left(p^{2r}\right) = 2^{p^{2r}} - 2^{p^r}$$

$$\Phi^{(r)}\left(p^r q^r\right) = 2^{p^r q^r} - 2^{q^r} - 2^{p^r} + 2.$$

Corollary 6. If $F^{(r)}(n)$ and $G^{(r)}(n)$ are arithmetic functions, then

$$G^{(r)}(n) = \sum_{d^r / n} F^{(r)}\left(\frac{n}{d^r}\right) \Leftrightarrow F^{(r)}(n) = \sum_{d^r / n} \mu_r\left(d^r\right) G^{(r)}\left(\frac{n}{d^r}\right).$$

Proof: Assume $G^{(r)}(n) = \sum_{d^r / n} F^{(r)}\left(\frac{n}{d^r}\right)$.

$$\text{Consider } \sum_{d^r / n} \mu_r\left(\frac{n}{d^r}\right) = \sum_{d^r / n} \mu_r\left(d^r\right) \left(\sum_{t^r / \frac{n}{d^r}} F^{(r)}\left(\frac{n}{t^r d^r}\right) \right)$$

$$= \sum_{u^r/n} F^{(r)}\left(\frac{n}{u^r}\right) \sum_{d^r/u^r} \mu_r\left(d^r\right) = F^{(r)}(n).$$

Conversely, assume $F^{(r)}(n) = \sum_{d^r/n} \mu_r\left(d^r\right) G^{(r)}\left(\frac{n}{d^r}\right)$.

Consider $$\sum_{d^r/n} F^{(r)}\left(\frac{n}{d^r}\right) = \sum_{d^r/n} \left(\sum_{t^r/\frac{n}{d^r}} \mu_r\left(t^r\right) G^{(r)}\left(\frac{n}{t^r d^r}\right) \right)$$

$$= \sum_{u^r/n} G^{(r)}\left(\frac{n}{u^r}\right) \left(\sum_{t^r/u^r} \mu_r\left(t^r\right) \right) = G^{(r)}(n).$$

Theorem 7. For all positive integers n, $r \geq 1$,

$$\sum_{d^r/n} \Phi^{(r)}\left(\frac{n}{d^r}\right) = 2^n - 1. \tag{13}$$

Also $\Phi^{(r)}(1) = 1$ and for $n \geq 2^r$, $\Phi^{(r)}(n) = \sum_{d^r/n} \mu_r\left(d^r\right)\left(2^{\frac{n}{d^r}} - 1\right)$. (14)

Proof: For every r^{th} power divisor d^r of n we define the function $\psi^{(r)}(n, d)$ to be the number of non-empty subsets A of $\{1, 2, ..., n\}$ such that greatest r^{th} power common divisor of A and n is d^r, i.e.

$$\psi^{(r)}(n, d) = \#\left\{A \subseteq \{1, 2, ..., n\} : A \neq \phi, \text{ and } \gcd_r\left(A \cup \{n\}\right) = d^r\right\}.$$

Then $\psi^{(r)}(n, d) = \Phi^{(r)}\left(\frac{n}{d^r}\right)$ and hence $2^n - 1 = \sum_{d^r/n} \psi^{(r)}(n, d) = \sum_{d^r/n} \Phi^{(r)}\left(\frac{n}{d^r}\right)$.

which proves (13). This implies $\Phi^{(r)}(n) = \sum_{d^r/n} \mu_r\left(d^r\right)\left(2^{\frac{n}{d^r}} - 1\right)$ (by using corollary (6)) which proves (14).

Theorem 8. For positive integers $n \geq 2^r$, k and r

$$\sum_{d^r/n} \Phi_k^{(r)}\left(\frac{n}{d^r}\right) = \binom{n}{k} \tag{15}$$

and $$\Phi_k^{(r)}(n) = \sum_{d^r/n} \mu_r\left(d^r\right)\binom{\frac{n}{d^r}}{k}. \tag{16}$$

Proof: For every r^{th} power divisor d^r of n we define $\psi_k^{(r)}(n,\ d)$ to be number of subsets A of $\{1,\ 2,\ ...,\ n\}$ of Cardinality k such that greatest r^{th} power common divisor of A and n is d^r.

That is

$$\psi_k^{(r)}(n,\ d) = \#\left\{A \subseteq \{1,\ 2,\ ...,\ n\}\ :\ \#A = k \text{ and } \left(\gcd_r(A) \cup \{n\}\right)_r = d^r\right\}.$$

Note that $\psi_k^{(r)}(n,\ d) = \Phi_k^{(r)}\left(\frac{n}{d^r}\right)$

$\sum_{d^r/n} \psi_k^{(r)}(n,\ d) = \binom{n}{k} = \sum_{d^r/n} \Phi_k^{(r)}\left(\frac{n}{d^r}\right)$ which proves (15).

Using Corollary (6), we get $\Phi_k^{(r)}(n) = \sum_{d^r/n} \mu_r\left(d^r\right)\binom{\frac{n}{d^r}}{k}$ which proves (16).

Theorem 9. Let $n \geq 2^r$ **.** If n is odd then $\Phi^{(r)}(n) = 2^n + \mathrm{O}\left(n.2^{\left\lfloor \frac{n}{3^r} \right\rfloor}\right)$. (17)

If $2^r \mid n$, $\Phi^{(r)}(n) = 2^n - 2^{\frac{n}{2^r}} + \mathrm{O}\left(n.2^{\left\lfloor \frac{n}{3^r} \right\rfloor}\right)$. (18)

Proof: We have $\Phi^{(r)}(n) = \sum_{\substack{d^r=1 \\ \gcd_r\left(d^r,\ n\right)=1.}}^{n} \#\left\{A \subseteq \{1,\ 2,\ ...,\ n\} / A \neq \phi,\ \gcd_r(A) = d^r\right\}$ where

the summation is over r^{th} power of integer d which satisfy the condition $1 \leq d^r \leq n$

$$= \sum_{\substack{d^r=1 \\ \gcd_r\left(d^r,\ n\right)=1.}}^{n} f^{(r)}\left(\left\lfloor \frac{n}{d^r} \right\rfloor\right)$$

If n is odd, then $\Phi^{(r)}(n) = f^{(r)}(n) + f^{(r)}\left(\left[\frac{n}{2^r}\right]\right) + \sum_{\substack{3^r \le d^r \le n \\ \gcd_r(d^r, n)=1}} f^{(r)}\left(\left[\frac{n}{d^r}\right]\right)$

$$= 2^n - 2^{\left[\frac{n}{2^r}\right]} + O\left(n.2^{\left[\frac{n}{3^r}\right]}\right) + 2^{\left[\frac{n}{2^r}\right]} + O\left(2^{\left[\frac{n}{4^r}\right]}\right) + O\left(n.2^{\left[\frac{n}{3^r}\right]}\right)$$

$$= 2^n + O\left(n.2^{\left[\frac{n}{3^r}\right]}\right) \text{ (Using equation (11)) which proves (17).}$$

If $2^r \mid n$, then $\Phi^{(r)}(n) = f^{(r)}(n) + f^{(r)}\left(\frac{n}{2^r}\right) + \sum_{\substack{3^r \le d^r \le n \\ \gcd_r(d^r, n)=1}} f^{(r)}\left(\left[\frac{n}{d^r}\right]\right)$

$$= \left(2^n - 2^{\frac{n}{2^r}} + O\left(n.2^{\left[\frac{n}{3^r}\right]}\right)\right) + O\left(n.2^{\left[\frac{n}{3^r}\right]}\right)$$

$$= 2^n - 2^{\frac{n}{2^r}} + O\left(n.2^{\left[\frac{n}{3^r}\right]}\right) \text{ which proves (18)}$$

Theorem 10. If $2^r \nmid n$ and n is sufficiently large then

$$\Phi_k^{(r)}(n) = \binom{n}{k} + O\left(n\binom{\left[\frac{n}{3^r}\right]}{k}\right). \tag{19}$$

If $2^r \mid n$ then $\Phi_k^{(r)}(n) = \binom{n}{k} - \binom{\frac{n}{2^r}}{k} + O\left(n\binom{\left[\frac{n}{3^r}\right]}{k}\right)$. (20)

Proof: We have

$$\Phi_k^{(r)}(n) = \sum_{\substack{1 \le d^r \le n \\ \gcd_r(d^r, n)=1}} \#\left\{A \subseteq \{1, 2, ..., n\} : \#A = k,\ \gcd_r(A) = d^r\right\}$$

$$= \sum_{\substack{1\le d^r\le n \\ \gcd_r\left(d^r,\, n\right)=1}} f_k^{(r)}\left(\left[\frac{n}{d^r}\right]\right).$$

By theorem (4), $f_k^{(r)}(n)=\binom{n}{k}-\left(\left[\frac{n}{2^r}\right]\right)+\mathrm{O}\left(n\left(\left[\frac{n}{3^r}\right]\right)\right)$

Therefore $\Phi_k^{(r)}(n)=\binom{n}{k}-\left(\frac{n}{2^r}\right)+\mathrm{O}\left(n\left(\left[\frac{n}{3^r}\right]\right)\right)$

$$+\left(\frac{n}{2^r}\right)-\left(\left[\frac{n}{4^r}\right]\right)+\mathrm{O}\left(n\left(\left[\frac{n}{6^r}\right]\right)\right)+\mathrm{O}\left(n\left(\left[\frac{n}{3^r}\right]\right)\right)$$

$$= \binom{n}{k}-\left(\frac{n}{2^r}\right)+\mathrm{O}\left(n\left(\left[\frac{n}{3^r}\right]\right)\right) \text{ if } 2^r \mid n.$$

If $2^r \nmid n$ $\Phi_k^{(r)}(n)=\binom{n}{k}+\mathrm{O}\left(n\left(\left[\frac{n}{3^r}\right]\right)\right)$.

4. Conclusion

In conclusion we have obtained effective formulas to get the exact number of r-relatively prime subsets of {1,2,…,n} and number of non empty subsets *A* of {1,2,…,n} such that *A* is r-relatively prime to n by deriving Mobius inversion formula r- generalised version.

Acknowledgement. We are grateful to the referees for suggesting some corrections and valuable comments.

REFERENCES

1. M.B.Nathanson, Elementary Methods in Number Theory, Graduate Texts in Mathematics, Vol. 195. Springer-Verlag, New York, (2000).
2. Melvyn B.Nathanson, Affine invariants, relatively prime sets, and a Phi function for subsets of {1,2,…,n}, *Integers*, 7(2007), A1, 7pp.
3. V.Kavitha and R.Govindarajan, A study on Ramsey numbers and its bounds, *Annals of Pure and Applied Mathematics*, 8(2) (2014) 227-236.
4. M.Ayad and O.Kihel, The number of relatively prime subsets of {1,2,…,n}, *Integers*, 9 (2009) 163-166.

5. M.El.Bachraoui, On relatively prime subsets, combinatorial identities, and diaphontine equations, *J. Integers Seq.*, 15 (2012) Article 12.3.6, 9 pp.
6. C.Jayasekaran and A.Jancy Vini, Results on relatively prime dominating sets in graphs, *Annals of Pure and Applied Mathematics*, 14(3) (2017) 359-369.

Annals of Pure and Applied Mathematics
Vol. 14, No. 3, 2017, 581-592
ISSN: 2279-087X (P), 2279-0888(online)
Published on 5 December 2017
www.researchmathsci.org
DOI: http://dx.doi.org/10.22457/apam.v14n3a25

Annals of
Pure and Applied Mathematics

The Number of *r*-Relatively Prime Subsets and *Phi* Functions for $\{m,m+1, \ldots, n\}$- its *r*-Generalization

G. Kamala[1] **and** ***G. Lalitha***[2]

[1]Department of Mathematics, Osmania University, Hyderabad (TS), India
[2]Department of Mathematics, SRR & CVR Govt. Degree College
Vijayawada (AP), India.
Email: [1]gkamala369@gmail.com; [2]lalitha.secpg@gmail.com
[2]Corresponding author.

Received 15 November 2017; accepted 30 November 2017

Abstract. A nonempty finite set A of positive integers is relatively prime if $\gcd(A)=1$ and it is relatively prime to n if $\gcd(A\cup\{n\})=1$. For $k\geq 1$, the number of nonempty subsets A of {1,2,…,n} which are relatively prime is $f(n)$ and the number of such subsets of cardinality k, is $f_k(n)$. The number of nonempty subsets A of {1,2,…,n} which are relatively prime to n is $\Phi(n)$ and the number of such subsets of cardinality k is $\Phi_k(n)$. A nonempty finite set A of positive integers is r-relatively prime if greatest r th power common divisor of elements of A is 1. In this case we write $\gcd_r(A)=1$. The number of r-relatively prime subsets of {1,2,…,n} is $f^{(r)}(n)$ and the number of such subsets of cardinality k is $f_k^{(r)}(n)$. The number of nonempty subsets A of {1,2,…,n} which are r-relatively prime to n is $\Phi^{(r)}(n)$ and the number of such subsets of cardinality k is $\Phi_k^{(r)}(n)$. In this paper we generalize the four functions $f^{(r)}(n)$, $f_k^{(r)}(n)$, $\Phi^{(r)}(n)$ and $\Phi_k^{(r)}(n)$ for the set $\{m,\ m+1,\ \ldots,\ n\}$ where $m\leq n$, as follows **:**

$$f^{(r)}(m,\ n)=\#\{A\subseteq\{m,\ m+1,\ \ldots,\ n\}\ :\ A\neq\phi,\ \gcd_r(A)=1\}$$
$$f_k^{(r)}(m,\ n)=\#\{A\subseteq\{m,\ m+1,\ \ldots,\ n\}\ :\ \#A=k,\ \gcd_r(A)=1\}$$
$$\Phi^{(r)}(m,\ n)=\#\{A\subseteq\{m,\ m+1,\ \ldots,\ n\}\ :\ A\neq\phi,\ \gcd_r(A\cup\{n\})=1\}$$

$$\Phi_k^{(r)}(m,\ n) = \#\left\{A \subseteq \{m,\ m+1,\ ...,\ n\}\ : \#A = k\ ,\ \gcd_r\left(A \cup \{n\}\right) = 1\right\}.$$

We obtain the exact formulae for the above four functions. We use r-Generalized Mobius inversion formula for two variables.

Keywords: *r*-relatively prime sets, *r*-Generalization of *Phi* functions, *r*-Generalized Mobius inversion for two variables.

AMS Mathematics Subject Classification (2010): 11BXX, 11B75

1. Introduction

A nonempty finite set A of positive integers is relatively prime if $\gcd(A) = 1$ and it is relatively prime to n if $\gcd(A \cup \{n\}) = 1$. The number of nonempty subsets of {1,2,…,n} which are relatively prime is $f(n)$ and the number of such subsets of cardinality k is $f_k(n)$. The number of nonempty subsets A of {1, 2 ,…, n} which are relatively prime to n is $\Phi(n)$ and the number of such subsets of cardinality k is $\Phi_k(n)$. A nonempty finite set A of positive integers {1, 2 ,…, n} is r-relatively prime if greatest r^{th} power common divisor of elements of A is 1. In this case, we write $\gcd_r(A) = 1$. The number of r-relatively prime subsets of {1, 2,…, n} is $f^{(r)}(n)$ and the number of such subsets of cardinality k is $f_k^{(r)}(n)$. The number of nonempty subsets *A* of {1, 2 ,…, n} which are r-relatively prime to n is $\Phi^{(r)}(n)$ and the number of such subsets of cardinality k is $\Phi_k^{(r)}(n)$. Nathanson [2] obtained the exact formulae for the functions $f(n)$, $f_k(n)$, $\Phi(n)$ and $\Phi_k(n)$. Inspired by the work of Nathanson [2] , we obtained the exact formulae for $f^{(r)}(n)$, $f_k^{(r)}(n)$, $\Phi^{(r)}(n)$ and $\Phi_k^{(r)}(n)$ in [1]. Bachraoui [3] generalized the results of Nathanson [2]. In this paper we generalize the results obtained in [1] and derive the explicit formulae for the functions $f^{(r)}(m,\ n)$, $f_k^{(r)}(m,\ n)$, $\Phi^{(r)}(m,\ n)$ and $\Phi_k^{(r)}(m,\ n)$ by using r-Generalized Mobius inversion formula for two variables.

Definition 1**.** Let r ≥ 1 be a positive integer. $F^{(r)}$ and $G^{(r)}$ are generalized arithmetical functions of two variables with domain $(0,\ \infty)^2$ such that

$G^{(r)}(y_1,\ y_2) = 0 = F^{(r)}(y_1,\ y_2)$ whenever $0 < y_2 < 1$.

Definition 2. *r* - Relatively prime subsets of {m, m+1, …, n}. Let $r \geq 1,\ k \geq 1$ be fixed integers .Then we define,

$$g^{(r)}(m,\ n) = \#\{A \subseteq \{m,\ m+1,\ ...,\ n\}\ :\ m \in A,\ \gcd_r(A) = 1\}$$

$$g_k^{(r)}(m,\ n) = \#\{A \subseteq \{m,\ m+1,\ ...,\ n\}\ :\ m \in A,\ \#A = k,\ \gcd_r(A) = 1\}$$

$$f^{(r)}(m,\ n) = \#\{A \subseteq \{m,\ m+1,\ ...,\ n\}\ :\ A \neq \phi,\ \gcd_r(A) = 1\}$$

$$f_k^{(r)}(m,\ n) = \#\{A \subseteq \{m,\ m+1,\ ...,\ n\}\ :\ A \neq \phi,\ \#A = k,\ \gcd_r(A) = 1\}.$$

Note that $f^{(r)},\ f_k^{(r)},\ g^{(r)},\ g_k^{(r)}$ are counting sets on nonempty subsets.

$f^{(r)}(n) =$ Number of *r* - relatively prime subsets of $\{1,\ 2,\ ...,\ n\} = f^{(r)}(1,\ n)$.

Definition 3. Let $n \geq m$ be positive integers. We define

$$\psi^{(r)}(m,\ n) = \#\{A \subseteq \{m,\ m+1,\ ...,\ n\}\ :\ m \in A,\ \gcd_r(A \cup \{n\}) = 1\}$$

$$\psi_k^{(r)}(m,\ n) = \#\{A \subseteq \{m,\ m+1,\ ...,\ n\}\ :\ m \in A,\ \#A = k,\ \gcd_r(A \cup \{n\}) = 1\}$$

$$\Phi^{(r)}(m,\ n) = \#\{A \subseteq \{m,\ m+1,\ ...,\ n\}\ :\ A \neq \phi,\ \gcd_r(A \cup \{n\}) = 1\}$$

$$\Phi_k^{(r)}(m,\ n) = \#\{A \subseteq \{m,\ m+1,\ ...,\ n\}\ :\#A = k\ ,\ \gcd_r(A \cup \{n\}) = 1\}.$$

Note that the four functions defined above count the sets that are nonempty.

$\Phi^{(r)}(\ n)$ =Number of non empty subsets of $\{1,\ 2,\ ...,\ n\}$ that are *r*-relatively prime to n

$= \quad \Phi^{(r)}(1,n)$

2. r-Generalized Mobius inversion formula for two variables

Theorem 1. Let $F^{(r)}$ and $G^{(r)}$ be generalized arithmetical functions with domain $(0,\ \infty)^2$ then

$$G^{(r)}(m,\ n) = \sum_{1 \leq d^r \leq m} F^{(r)}\left(\frac{m}{d^r},\ \frac{n}{d^r}\right) \Leftrightarrow F^{(r)}\left(\frac{m}{d^r},\ \frac{n}{d^r}\right) = \sum_{1 \leq d^r \leq m} \mu_r(d^r)\, G^{(r)}\left(\frac{m}{d^r},\ \frac{n}{d^r}\right) \quad (1)$$

where the summation is over all integers *d* such that $d^r \leq m$.

Proof: Assume $G^{(r)}(m,\ n) = \sum_{1 \leq d^r \leq m} F^{(r)}\left(\frac{m}{d^r},\ \frac{n}{d^r}\right)$

Consider

$$\sum_{1\le d^r\le m}\mu_r\left(d^r\right)G^{(r)}\left(\frac{m}{d^r},\ \frac{n}{d^r}\right)=\sum_{1\le d^r\le m}\mu_r\left(d^r\right)\left[\sum_{1\le t^r\le\frac{m}{d^r}}F^{(r)}\left(\frac{m}{t^rd^r},\ \frac{n}{t^rd^r}\right)\right]$$

$$=\sum_{1\le u^r\le m}F^{(r)}\left(\frac{m}{u^r},\ \frac{n}{u^r}\right)\left[\sum_{d^r/u^r}\mu_r\left(d^r\right)\right]$$

$$=F^{(r)}(m,\ n).$$

Conversely, assume $F^{(r)}(m,\ n)=\sum_{1\le d^r\le m}\mu_r\left(d^r\right)G^{(r)}\left(\frac{m}{d^r},\ \frac{n}{d^r}\right).$

Consider

$$\sum_{1\le d^r\le m}F^{(r)}\left(\frac{m}{d^r},\ \frac{n}{d^r}\right)=\sum_{1\le d^r\le m}\left[\sum_{1\le t^r\le\frac{m}{d^r}}\mu_r\left(d^r\right)G^{(r)}\left(\frac{m}{t^rd^r},\ \frac{n}{t^rd^r}\right)\right]$$

$$=\sum_{1\le u^r\le m}G^{(r)}\left(\frac{m}{u^r},\ \frac{n}{u^r}\right)\left[\sum_{t^r/u^r}\mu_r\left(t^r\right)\right]$$

$$=G^{(r)}(m,\ n).$$

Corollary 2. Suppose $F^{(r)}(x,\ y)$ and $G^{(r)}(x,\ y)$ are generalized arithmetical functions such that $F^{(r)}(x,\ y)=0=G^{(r)}(x,\ y)$ if x is not an integer and $F^{(r)}(x,\ y)=0=G^{(r)}(x,\ y)$ if $0<y<1,$ then Mobius inversion formula for such functions reduces to the following form

$$G^{(r)}(m,\ n)=\sum_{d^r\mid m}F^{(r)}\left(\frac{m}{d^r},\ \left[\frac{n}{d^r}\right]\right)\Leftrightarrow F^{(r)}(m,\ n)=\sum_{d^r\mid m}\mu_r\left(d^r\right)\left(\frac{m}{d^r},\ \left[\frac{n}{d^r}\right]\right)\quad(2)$$

Proof: Suppose $G^{(r)}(m,\ n)=\sum_{d^r\mid m}F^{(r)}\left(\frac{m}{d^r},\ \left[\frac{n}{d^r}\right]\right)$ holds.

Consider

$$\sum_{d^r \mid m} \mu_r\left(d^r\right) G^{(r)}\left(\frac{m}{d^r}, \left[\frac{n}{d^r}\right]\right) = \sum_{d^r \mid m} \mu_r\left(d^r\right)\left(\sum_{t^r \mid \frac{m}{d^r}} F^{(r)}\left(\frac{m}{t^r d^r}, \left[\frac{n}{t^r d^r}\right]\right)\right)$$

$$= \sum_{u^r \mid m} F^{(r)}\left(\frac{m}{u^r}, \left[\frac{n}{u^r}\right]\right)\left(\sum_{d^r \mid u^r} \mu_r\left(d^r\right)\right)$$

$$= F^{(r)}(m,\ n).$$

Conversely, suppose $F^{(r)}(m,\ n) = \sum_{d^r \mid m} \mu_r\left(d^r\right) G^{(r)}\left(\frac{m}{d^r}, \left[\frac{n}{d^r}\right]\right)$

Consider $$\sum_{d^r \mid m} F^{(r)}\left(\frac{m}{d^r}, \left[\frac{n}{d^r}\right]\right) = \sum_{d^r \mid m}\left(\sum_{t^r \mid \frac{m}{d^r}} \mu_r\left(t^r\right) G^{(r)}\left(\frac{m}{t^r d^r}, \left[\frac{n}{t^r d^r}\right]\right)\right)$$

$$= \sum_{u^r \mid m} G^{(r)}\left(\frac{m}{u^r}, \left[\frac{n}{u^r}\right]\right)\left(\sum_{t^r \mid u^r} \mu_r\left(t^r\right)\right)$$

$$= G^{(r)}(m,\ n).$$

3. Exact formulae

To find the exact formulas we use the following theorems proved in [1].

Theorem 3. For all positive integers $n \geq 2^r \quad r \geq 1$, *k*,

(i) $$f^{(r)}(n) = \sum_{1 \leq d^r \leq n} \mu_r\left(d^r\right)\left(2^{\left[\frac{n}{d^r}\right]} - 1\right) = f^{(r)}(1,\ n) \tag{3}$$

(ii) $$f_k^{(r)}(n) = \sum_{1 \leq d^r \leq n} \mu_r\left(d^r\right)\binom{\left[\frac{n}{d^r}\right]}{k} = f_k^{(r)}(1,\ n). \tag{4}$$

Theorem 4. For all positive integers $n, r \geq 1$, *k*,

(i) $\Phi^{(r)}(n) = \sum_{d^r/n} \mu^r\left(d^r\right)\left(2^{\frac{n}{d^r}} - 1\right) = \Phi^{(r)}(1, n).$ (5)

(ii) $\Phi_k^{(r)}(n) = \sum_{d^r/n} \mu^r\left(d^r\right)\binom{\frac{n}{d^r}}{k} = \Phi_k^{(r)}(1, n).$ (6)

Lemma 5. If $n \geq m$, we have

(i) $g^{(r)}(m, n) = \sum_{d^r \mid m} \mu_r\left(d^r\right) 2^{\left[\frac{n}{d^r}\right] - \frac{m}{d^r}}$ (7)

(ii) $g_k^{(r)}(m, n) = \sum_{d^r \mid m} \mu_r\left(d^r\right)\binom{\left[\frac{n}{d^r}\right] - \frac{m}{d^r}}{k-1}.$ (8)

Proof: (i) Let $P(m, n)$ denotes the set of subsets of $\{m, m+1, ..., n\}$ containing *m*. Then # $P(m, n) = 2^{n-m}$. We define a relation on $P(m, n)$ as follows:

For $A, B \in P(m, n)$ we say that $A \cong B$ if and only if $\gcd_r(A) = d^r = \gcd_r(B)$. Note that $d^r \mid m$ and $1 \leq d^r \leq m$. Then $\cong$ is an equivalence relation on $P(m, n)$. If *m* is *r*-free then $\gcd_r(A) = 1 = \gcd_r(B)$. Hence the elements of $P(m, n)$ can be partitioned using the relation "$\cong$" of having the same r^{th} power gcd d^r. Also the mapping $A \to \frac{1}{d^r} A$ is a 1-1 correspondence between the subsets of $P(m, n)$ having r^{th} power gcd d^r and *r*-relatively prime subsets of $\left\{\frac{m}{d^r}, ..., \frac{n}{d^r}\right\}$ which contain $\frac{m}{d^r}$. Then we have the following identity $2^{n-m} = \sum_{d^r \mid m} g^{(r)}\left(\frac{m}{d^r}, \left[\frac{n}{d^r}\right]\right)$.

By Corollary (2) $g^{(r)}(m, n) = \sum_{d^r \mid m} \mu_r\left(d^r\right) 2^{\left[\frac{n}{d^r}\right] - \frac{m}{d^r}}$ which proves (7).

(ii) Note that the correspondence $A \to \frac{1}{d^r} A$ preserves the Cardinality and hence

$$\binom{n-m}{k-1} = \sum_{d^r \mid m} g_k^{(r)}\left(\frac{m}{d^r},\ \left[\frac{n}{d^r}\right]\right).$$

By Corollary (2), we have

$$g_k^{(r)}(m,\ n) = \sum_{d^r \mid m} \mu_r\left(d^r\right)\binom{\left[\frac{n}{d^r}\right]-\frac{m}{d^r}}{k-1}. \quad \text{which proves (8).}$$

Theorem 6. If $n \geq m$, then the following two identities are true.

(i) $$f^{(r)}(m,\ n) = \sum_{1\leq d^r \leq n} \mu_r\left(d^r\right)\left(2^{\left[\frac{n}{d^r}\right]}-1\right) - \sum_{i=1}^{m-1}\sum_{d^r \mid i} \mu_r\left(d^r\right)2^{\left[\frac{n}{d^r}\right]-\frac{i}{d^r}} \tag{9}$$

(ii) $$f_k^{(r)}(m,\ n) = \sum_{1\leq d^r \leq n} \mu_r\left(d^r\right)\binom{\left[\frac{n}{d^r}\right]}{k} - \sum_{i=1}^{m-1}\sum_{d^r \mid i} \mu_r\left(d^r\right)\binom{\left[\frac{n}{d^r}\right]-\frac{i}{d^r}}{k-1}. \tag{10}$$

Proof: (i) Repeatedly applying Lemma (5) and equations (7) and (3)

$$\begin{aligned} f^{(r)}(m,\ n) &= f^{(r)}(m-1,\ n) - g^{(r)}(m-1,\ n) \\ &= f^{(r)}(m-2,\ n) - \left[g^{(r)}(m-2,\ n) + g^{(r)}(m-1,\ n)\right] \\ &\ \ \vdots \\ &= f^{(r)}(1,\ n) - \sum_{i=1}^{m-1} g^r(i,\ n) \\ &= \sum_{1\leq d^r \leq n} \mu_r\left(d^r\right)\left(2^{\left[\frac{n}{d^r}\right]}-1\right) - \sum_{i=1}^{m-1}\left(\sum_{d^r \mid i} \mu_r\left(d^r\right)2^{\left[\frac{n}{d^r}\right]-\frac{i}{d^r}}\right) \end{aligned}$$

(ii) From equation (4), we have $$f_k^{(r)}(1,\ n) = \sum_{1\leq d^r \leq n} \mu_r\left(d^r\right)\binom{\left[\frac{n}{d^r}\right]}{k}.$$

By equation (8), we have

$$g_k^{(r)}(m,\ n) = \sum_{d^r \mid m} \mu_r\left(d^r\right) \binom{\left[\frac{n}{d^r}\right] - \frac{m}{d^r}}{k-1}$$

Therefore $f_k^{(r)}(m,\ n) = f_k^{(r)}(m-1,\ n) - g_k^{(r)}(m-1,\ n)$

$$= f_k^{(r)}(m-2,\ n) - \left[g_k^{(r)}(m-2,\ n) + g_k^{(r)}(m-1,\ n) \right]$$

$$\vdots$$

$$= f_k^{(r)}(1,\ n) - \sum_{i=1}^{m-1} g_k^{(r)}(i,\ n)$$

$$= \sum_{1 \le d^r \le n} \mu_r\left(d^r\right) \binom{\left[\frac{n}{d^r}\right]}{k} - \sum_{i=1}^{m-1} \sum_{d^r \mid i} \mu_r\left(d^r\right) \binom{\left[\frac{n}{d^r}\right] - \frac{i}{d^r}}{k-1}.$$

Note : $\gcd_r\left(A \cup \{n\}\right) = 1 \Leftrightarrow \left(\gcd_r(A),\ n\right)_r = 1.$

Proof: Assume $\gcd_r\left(A \cup \{n\}\right) = 1.$

Let $\left(\gcd_r(A),\ n\right)_r = d^r$

$\Rightarrow\ d^r \mid n$ and $d^r \mid \gcd_r(A)$ (since $\gcd_r(A) \mid a$ for all $a \in A$)

$\Rightarrow\ d^r \mid n$ and $d^r \mid a$ for all $a \in A$

$\Rightarrow\ d^r \mid \gcd_r\left(A \cup \{n\}\right) \Rightarrow\ d^r \mid 1 \Rightarrow\ d = 1.$

Conversely, let $\left(\gcd_r(A),\ n\right)_r = 1$ and $\gcd_r\left(A \cup \{n\}\right) = d^r$

$\Rightarrow\ d^r \mid a$ for all $a \in A$ and $d^r \mid n$

$\Rightarrow\ d^r \mid a$ and $d^r \mid n$ for all $a \in A$

$\Rightarrow\ d^r \mid \gcd_r(A)$ and $d^r \mid n$

$\Rightarrow\ d^r \mid \left(\gcd_r(A),\ n\right)_r$

$\Rightarrow\ d^r \mid 1 \Rightarrow\ d = 1.$

Lemma 7. If $n_2 \ge n_1$ are natural numbers and $G^{(r)}$, $F^{(r)}$ are generalized arithmetical functions with domain $(0,\ \infty)^2$. Then

$$G^{(r)}(n_1,\ n_2) = \sum_{d^r \left| \gcd_r(n_1,\ n_2) \right.} F^{(r)}\left(\frac{n_1}{d^r},\ \frac{n_2}{d^r}\right)$$

$$\Leftrightarrow F^{(r)}(n_1,\ n_2) = \sum_{d^r \left| \gcd_r(n_1,\ n_2) \right.} \mu_r\left(d^r\right) G^{(r)}\left(\frac{n_1}{d^r},\ \frac{n_2}{d^r}\right)$$

Proof: Assume $G^{(r)}(n_1,\ n_2) = \sum_{d^r \left| \gcd_r(n_1,\ n_2) \right.} F^{(r)}\left(\frac{n_1}{d^r},\ \frac{n_2}{d^r}\right)$

Consider $\sum_{d^r \left| \gcd_r(n_1,\ n_2) \right.} \mu_r\left(d^r\right) G^{(r)}\left(\frac{n_1}{d^r},\ \frac{n_2}{d^r}\right)$

$$= \sum_{d^r \left| \gcd_r(n_1,\ n_2) \right.} \mu_r\left(d^r\right) \left(\sum_{t^r \left| \gcd_r\left(\frac{n_1}{d^r},\ \frac{n_2}{d^r}\right) \right.} F^{(r)}\left(\frac{n_1}{t^r d^r},\ \frac{n_2}{t^r d^r}\right) \right)$$

$$= \sum_{u^r \left| \gcd_r(n_1,\ n_2) \right.} F^{(r)}\left(\frac{n_1}{u^r},\ \frac{n_2}{u^r}\right) \left(\sum_{d^r \left| u^r \right.} \mu_r\left(d^r\right) \right) \quad = F^{(r)}(n_1,\ n_2).$$

Conversely, assume $F^{(r)}(n_1,\ n_2) = \sum_{d^r \left| \gcd_r(n_1,\ n_2) \right.} \mu_r\left(d^r\right) G^{(r)}\left(\frac{n_1}{d^r},\ \frac{n_2}{d^r}\right)$

Consider

$$\sum_{d^r \left| \gcd_r(n_1,\ n_2) \right.} F^{(r)}\left(\frac{n_1}{d^r},\ \frac{n_2}{d^r}\right) = \sum_{d^r \left| \gcd_r(n_1,\ n_2) \right.} \left(\sum_{t^r \left| \gcd_r\left(\frac{n_1}{d^r},\ \frac{n_2}{d^r}\right) \right.} \mu_r\left(t^r\right) G^{(r)}\left(\frac{n_1}{t^r d^r},\ \frac{n_2}{t^r d^r}\right) \right)$$

$$= \sum_{u^r \left| \gcd_r(n_1,\ n_2) \right.} G^{(r)}\left(\frac{n_1}{u^r},\ \frac{n_2}{u^r}\right) \left(\sum_{t^r \left| u^r \right.} \mu_r\left(t^r\right) \right) = \ G^{(r)}(n_1,\ n_2).$$

Theorem 8. If $n \geq m$, then we have the following two identities

(i) $\psi^{(r)}(m,\ n) = \sum_{d^r \mid \gcd_r(m,\ n)} \mu_r\left(d^r\right) 2^{\frac{n-m}{d^r}}$ (11)

(ii) $\psi_k^{(r)}(m,\ n) = \sum_{d^r \mid \gcd_r(m,\ n)} \mu_r\left(d^r\right) \binom{\frac{n-m}{d^r}}{k}$. (12)

Proof: (i) Let $P(m,\ n)$ denotes the set of subsets of $\{m,\ m+1,\ ...,\ n\}$ containing m. Then $\#\ P(m,\ n) = 2^{n-m}$. We define the set

$$P\left(m,\ n,\ d^r\right) = \left\{A \subseteq \{m,\ m+1,\ ...,\ n\} : m \in A \text{ and } \gcd_r\left(A \cup \{n\}\right) = d^r\right\}$$

The set $P(m,\ n)$ can be partitioned using the equivalence relation "$\cong$" for having the same r^{th} power gcd, that is , $A \cong B \Leftrightarrow A,\ B \in P\left(m,\ n,\ d^r\right)$ for some $d^r \mid \gcd_r(m,\ n)$. Further, the mapping $A \to \frac{1}{d^r} A$ is a $1-1$ correspondence between $P\left(m,\ n,\ d^r\right)$ and the set of subsets B of $\left\{\frac{m}{d^r},\ \frac{m}{d^r}+1,\ \frac{m}{d^r}+2,\ ...,\ \frac{n}{d^r}\right\}$ such that $\frac{m}{d^r} \in B$ and $\gcd_r\left(B \cup \left\{\frac{n}{d^r}\right\}\right) = 1$.

Then we have $\#P\left(m,\ n,\ d^r\right) = \psi^{(r)}\left(\frac{m}{d^r},\ \frac{n}{d^r}\right)$.

Thus we have $2^{n-m} = \sum_{d^r \mid \gcd_r(m,\ n)} \#P\left(m,\ n,\ d^r\right) = \sum_{d^r \mid \gcd_r(m,\ n)} \psi^{(r)}\left(\frac{m}{d^r},\ \frac{n}{d^r}\right)$

Therefore $2^{n-m} = \sum_{d^r \mid \gcd_r(m,\ n)} \psi^{(r)}\left(\frac{m}{d^r},\ \frac{n}{d^r}\right)$.

Applying Lemma (7) we have

$$\psi^{(r)}(m,\ n) = \sum_{d^r \mid \gcd_r(m,\ n)} \mu_r\left(d^r\right) 2^{\frac{n-m}{d^r}} \quad \text{which proves (11).}$$

(ii) Note that the correspondence $A \to \frac{1}{d^r} A$ defined above preserves the Cardinality and hence using an argument similar to the one in part (i) , we have

$$\binom{n-m}{k-1} = \sum_{d^r \mid \gcd_r(m,\, n)} \psi_k^{(r)}\left(\frac{m}{d^r},\ \frac{n}{d^r}\right)$$

is equivalent to which proves (12).

$$\psi_k^{(r)}(m,\ n) = \sum_{d^r \mid \gcd_r(m,\, n)} \mu_r\left(d^r\right)\binom{\frac{n-m}{d^r}}{k-1}$$

Theorem 9. If $n \geq m$, then the following two identities are true.

(i) $$\Phi^{(r)}(m,\ n) = \sum_{d^r \mid n} \mu_r\left(d^r\right)\left(2^{\frac{n}{d^r}} - 1\right) - \sum_{i=1}^{m-1} \sum_{d^r \mid \gcd_r(i,\, n)} \mu_r\left(d^r\right) 2^{\frac{n-i}{d^r}} \tag{13}$$

(ii) $$\Phi_k^{(r)}(m,\ n) = \sum_{d^r \mid n} \mu_r\left(d^r\right)\binom{\frac{n}{d^r}}{k} - \sum_{i=1}^{m-1} \sum_{d^r \mid \gcd_r(i,\, n)} \mu_r\left(d^r\right)\binom{\frac{n-i}{d^r}}{k-1}. \tag{14}$$

Proof: (i) Applying theorem (8) repeatedly and using the equation (5) we have

$$\begin{aligned}
\Phi^{(r)}(m,\ n) &= \Phi^{(r)}(m-1,\ n) - \psi^{(r)}(m-1,\ n) \\
&= \Phi^{(r)}(m-2,\ n) - \left[\psi^{(r)}(m-2,\ n) + \psi^{(r)}(m-1,\ n)\right] \\
&\ \ \vdots \\
&= \Phi^{(r)}(1,\ n) - \sum_{i=1}^{m-1} \psi^{(r)}(i,\ n) \\
&= \sum_{d^r \mid n} \mu_r\left(d^r\right)\left(2^{\frac{n}{d^r}} - 1\right) - \sum_{i=1}^{m-1}\left(\sum_{d^r \mid \gcd_r(i,\, n)} \mu_r\left(d^r\right) 2^{\frac{n-i}{d^r}}\right)
\end{aligned}$$

which proves (13)**.**

(ii) Applying theorem (8) repeatedly and using equation (6)

$$\begin{aligned}
\Phi_k^{(r)}(m,\ n) &= \Phi_k^{(r)}(m-1,\ n) - \psi_k^{(r)}(m-1,\ n) \\
&= \Phi_k^{(r)}(m-2,\ n) - \left[\psi_k^{(r)}(m-2,\ n) + \psi_k^{(r)}(m-1,\ n)\right] \\
&\ \ \vdots
\end{aligned}$$

$$= \Phi_k^{(r)}(1,\ n) - \sum_{i=1}^{m-1} \psi_k^{(r)}(i,\ n)$$

$$= \sum_{d^r \mid n} \mu_r\left(d^r\right) \binom{\frac{n}{d^r}}{k} - \sum_{i=1}^{m-1} \left(\sum_{d^r \mid \gcd_r(i,\ n)} \mu_r\left(d^r\right) \binom{\frac{n-i}{d^r}}{k-1} \right).$$

which proves (14)**.**

4. Conclusion

We count the exact number of nonempty subsets of { m , m+1 ,…, n} which are
(i) r-relatively prime
(ii) r-relatively prime of cardinality k.
(iii) r-relatively prime to n
(iv) r-relatively prime to n of cardinality k.
by using r-Generalized version of Mobius inversion formula for two variables.

Acknowledgements. The authors are grateful to the referee for valuable comments and interesting suggestions.

REFERENCES

1. G.Kamala and G.Lalitha, r-Relatively prime sets and r-Generalization of phi functions for subsets of {1, 2 , … , n}, *Annals of Pure and Applied Mathematics*, 14(3) (2017) 497-508.
2. M.B.Nathanson, Affine invariants, relatively prime sets, and a phi function for subsets of {1, 2 , … , n}, *Integer*, 7 (2007) #A1,7pp. (electronic).
3. M.El.Bachraoui, The Number of relatively prime subsets and phi functions for {*m, m+1, … n*}, *Integer*, **7 (**2007), #A43, 8pp. (electronic).
4. M.B.Nathanson, *Elementary Methods in Number Theory*, *Graduate Texts in Mathematics*, Vol. 195. Springer- New York, 2000.
5. M.Ayad and O.Kihel, *The number of relatively prime subsets of* {1, 2 , … ,n}, *Integers*, 9 (2009) 163-166.
6. C.Jayasekaran and A. Jancy Vini, Results on relatively prime dominating sets in graphs, *Annals of Pure and Applied Mathematics*, 14(3) (2017) 359-369.
7. N.Burshtein, A note on the diaphontine equation $p^3 + q^4 = z^4$ when *p* is prime, *Annals of Pure and Applied Mathematics*, 14(3) (2017) 509-511.
8. A.Sugumaran and V.Mohan, Further results on prime cordial labeling, *Annals of Pure and Applied Mathematics*, 14(3) (2017) 489-496.
9. A.Sugumaran and K.Rajesh, Some new results on sum divisor cordial graphs, *Annals of Pure and Applied Mathematics*, 14(1) (2017) 45-52.

Research maGma

An International Multidisciplinary Journal

ISSN NO- 2456-7078 IMPACT FACTOR- 4.520

VOL-1, ISSUE-9, NOV-2017 UGC JOURNAL ID- 63465

INFLUENCE OF DEMONETISATION ON SMALL BUSINESSMEN- A STUDY IN VIJAYAWADA CITY, ANDHRA PRADESH

[1]Mrs. B. Prathima and [2]Dr. M. Trimurthi Rao

[1]Lecturer in Commerce, SRR & CVR Govt. Degree & PG College, Vijayawada, Krishna Dist., A.P.

[2]Asst. Professor, Dept. of Sociology & Social Work, Acharya Nagarjuna University, Nagarjuna Nagar, Guntur Dist. A.P.

ABSTRACT

In November 2016, Indian Government decided to demonetize Rupees 1000/- and 500/- notes, the two biggest denominations in its currency system; these notes accounted for 86% of the country's circulating cash. With little warning, India's Prime Minister Narendra Modi announced to the citizenry on 8th November 2016 that those notes were worthless, effective immediately and they had until the end of the year to deposit or exchange them for newly introduced 2000 Rupees and later 500 Rupees notes.

The Government's restriction on daily withdrawal amounts added to the misery, though a waiver on transaction fees did help a bit. Small businesses, vendors and households struggled to find cash and reports of daily wage workers not receiving their dues surfaced. The rupee fell sharply against the dollar. The government's goal was to combat India's thriving underground economy on several fronts, eradicate counterfeit currency, fight tax evasion, eliminate black money gotten from money laundering and terrorist financing activities, and to promote a cashless economy. The present study discusses the influences of demonetisation on small business vendors and shops in Vijayawada city.

KEYWORDS:

Currency, Demonetization, Indian Economy, Small and Medium Enterprises.

INTRODUCTION:

Demonetization is the act of stripping a currency unit of its status as legal tender. It occurs whenever there is a change of national currency. The current form or forms of money is pulled from circulation and retired, often to be replaced with new notes or coins. Sometimes, a country completely

www.aensi.in /Index in Cosmos ISSN 0025-1348 UGC APPROVED

Received: 2 November Revised: 7 November Accepted: 17 November

Women empowerment through NGOS - a study of self help groups in Guntur district, Andhra Pradesh

Dr. M. Trimurthi Rao
Asst. Professor,
Dept. Of Sociology & Social Work
Acharya Nagarjuna University
Nagarjuna Nagar – 522 510, A.P.

B. Prathima
Lecturer, Dept. Of Commerce
SRR & CVR Govt. Degree & P.G College (A),
Vijayawada, Krishna DT., A.P.

ABSTRACT: This paper seeks to highlights the importance of Non-Governmental Organizations (NGOs) and participation of NGOs in promoting sustainable community development through micro-finance, capacity building and self-reliance women in Guntur District of Andhra Pradesh. NGOs through the micro-finance empower women, help members of community to access jobs, income generation and improve economic situation, and then they would become empowered economically. NGOs highlight how these programmes would affect women empowerment, community empowerment, and finally contribute to sustainable community development. NGO by name AMG (Advanced Ministry of Gospel) India International, Chilakaluripet, Guntur District its Rural Project was selected to conduct the study on empowerment of self-help group women in Guntur district of Andhra Pradesh.

KEY WORDS: AMG India International, Community Development, Empowerment, Non-Governmental Organizations (NGOs), Self Help Groups (SHGs).

INTRODUCTION

The concept of women empowerment is the modern context; it is increasingly discussed and promoted by third world feminists and women's organizations. Women's empowerment forms a theoretical framework that emphasizes addressing the issues of subordination of women. Empowerment of women has become a relevant issue due to the magnitude of women's powerlessness and subordination in the contemporary social context. At times the term is reduced to a jargon through over use and lack of clarity.

The popular meaning of the term 'empowerment of women' is enjoyment of certain rights by women, but generally signifies a little more than feeling better or more powerful. There are self-help, liberation, professional, managerial and market models of empowerment *(Davies, 2000)*. Women empowerment has a regulatory function with regard to the control exercised by men over women. By regulating the power distribution among men and women, the process of empowerment liberates women from the age old culture of submission and subjugation to the practical forces.

Empowerment is essentially a transition from a position of enforced powerlessness to one of power. It promotes women's inherent strengths and positive self-image. It should not be misunderstood that empower women; men have to give women more power to dominate others, to

Scanned with CamScanner

Journal of Innovations in Pharmaceutical and Biological Sciences (JIPBS)
ISSN: 2349-2759
Available online at www.jipbs.com

Research article

Haematological changes induced in the fish *Ctenopharyngodon idella* (Valenciennes) exposed to organophosphate Dichlorvos both technical and 76% EC (Nuvan)

Swarna Kumari. R[1], Vijaya Kumar. M[2*], Gopala Rao. N[1]

[1]*Department of Zoology and Aquaculture, Acharya Nagarjuna University, Nagarjunanagar-522510. A.P India.*
[2]*Department of Zoology, SRR & CVR Government Degree College, Vijayawada-520004. A.P India.*

Key words: *Ctenopharyngodon idella*, Dichlorvos, 76% EC (Nuvan) RBC, WBC, Hb, Haematocrit, PCV, MCH and MCHC, lethal and sublethal.

***Corresponding Author: M. Vijaya Kumar,** SRR & CVR Government Degree College, Vijayawada-520 004.

Abstract

Defilement of anthropogenic xenobiotic chemicals Viz., pesticides as organophosphate–the dichlorvos alter the circulatory fluid, blood in the heterotrophic, cold blooded nektonic culturableexotic fish, *Ctenopharyngodon idella*. The fish were exposed to both lethal and sublethal concentrations of technical grade and 76% EC (Nuvan). In both the concentrations the branchial single circuit blood pumped through venous blood, right from the early point showed imbalance of homeostasis with a dire consequence of haemostasis. The alterations studied were RBC, WBC, Hb, Haematocrit, PCV, MCV and MCHC. A decrement and increment of the parameters studied were reported herewith.

Introduction

All pollutants are not toxicants but all toxicants are pollutants. The toxicants cause the death if it is in lethal where as in sublethal concentration; render the animal not suitable to maintain its life, the active buoyant swimmers especially the fish, heterotrophic cold blooded animals. Due to the presence even in low concentrations bring changes and in aquatic toxicology any variations in the blood serve as biomarker. Such rapid changes in the characteristics of the fish blood measured are used as indices of pollution by pesticides. The provide assessment of pollution and will be warning sign of the inhabiting organism.Such alterations either increase or decreases in the blood were studied and reported [1-6] and even mentioned in the review articles [7-11].

Different chemicals of the four classes of pesticides organochlorines, organophosphates, carbamates and synthetic pyrethroids are reported and such changes in the fish are varied being species specific. Howeverpaucity of information is available for the grass carp *Ctenopharyngodon idella,* for the pesticide dichlorvos. Hence the present study is contemplated to assess the effects of the toxicant dichlorvos both in lethal and sublethal concentration using technical grade as well as 76% EC as Nuvan.

Experimental

Materials and methods

Collection and maintenance of test organism

The freshwater fish *Ctenopharyngodon idella* 3 to 5cm in length 4 to 5 gms in weight irrespective of their sex, have been chosen as the test organisms for the present investigation. Healthy and active fish were obtained from Ratna Singh Hatcheries, Nandivelugu, Guntur district, Andhra Pradesh, India. The fish were acclimatized to the laboratory conditions in large plastic water tanks for three weeks at a room temperature of 28±1°C. Water was renewed every day with 12-12h dark and light cycle. The water used for acclimatization and conducting experiments was clear unchlorinated ground water and the hydrographical conditions as physical and chemical properties of water were: Turbidity-8 silica units, Electrical conductivity at 28°C -816 Micro ohms/cm, pH at 28°C-8.1, Alkalinity: Phenolphthalein-Nil mg/l, Alkalinity: Methyl orange-172mg/l, Total Hardness (as $CaCO_3$-232mg/l, Carbonate Hardness (as $CaCO_3$)-232mg/l, Non Carbonate Hardness (as $CaCO_3$)-Nil mg/l, Calcium Hardness (as $CaCO_3$)-52mg/l, Magnesium Hardness-40mg/l, Nitrite Nitrogen (as N)-Nil mg/l, Sulphate (as $SO4_2^-$)-Trace mg/l, Chloride (as Cl^-)-40mg/l, Fluoride (as F^-)-1.8mg/l, Iron (as Fe)-Nil mg/l, Dissolved Oxygen- 8–10ppm, Temperature-28±2°C.

During the period of acclimatization, the fish were fed *(ad libitum*) with groundnut oil cake and rice bran. Feeding was stopped one day prior to the acute toxicity test. All the precautions laid by committee on toxicity tests to aquatic organism [11-13] were followed and such acclimatized fish only were used for experimentation. If mortality exceeded 5% in any batch of fish during

©JIPBS, All rights reserved

acclimatization, the entire batch of that fish were discarded. Such acclimatised fish were selected for experimentation. The technical grade which was 95-98% pure which was supplied by the Syngenta India Ltd, Mumbai-400 020. The pesticide 76%EC Nuvan is locally purchased manufactured by Hikal Limited 629/630 GIDC Industrial estate Panoli Bharuch Gujarat marked by Syngenta India., 14, J. Tata Road, Mumbai. The organophosphate pesticide was introduced into water from where the pesticide entered into the fish through gill. A total of 50 fish were taken each in sublethal and lethal concentrations for both technical grade and 76%EC Nuvan. The 96hrs LC_{50} values are determined by Finneysprobit analysis [12] as mentioned in APHA [13-15]**.**Haematological changes were determined at the end period of 96hrs LC_{50} value (9.841 ppm for Technical and 11.238 ppm for 76 % EC Nuvan) and $1/10^{th}$ of LC_{50} of 96hrs exposed for 10 days for both technical grade and 76%EC Nuvan.50% of the organisms were dead for lethal concentrations and the remaining organisms were sacrificed for the experimentation.

Ctenopharyngodon and *idella* are both Greek words, meaning "comb-like throat-teeth" and "distinct" respectively. The grass carp is one of the largest members of the minnow family. The body is oblong with moderately large scales, while the head has no scales. There are three simple and seven branched rays on the dorsal fin. Grass carp are silvery to olive in color, lacking the golden hue of common carp, and they have no barbels.

Sampling of blood

Fish were euthanized by an overdose of MS-222 and then weighed and measured. Blood sample was collected by caudal severance from the disease free test fish during early hours of the day and stabilized with 50 IU sodium heparin (anticoagulant)/ml blood.

Haematological examination

The haematological variables analyzed were red blood cells count (RBC), haemoglobin (Hb), white blood cells count (WBC), haematocrit (Ht), mean corpuscular volume (MCV), mean corpuscular haemoglobin(MCH) and mean corpuscular haemoglobin concentration(MCHC).

Determination of red blood corpuscles (RBC) count

RBC count was determined with an improved Neubauer crystalline counting chamber [16]. The blood was sucked up to 0.5mark on the RBC pipette and immediately, Hayem's solution as a diluent stain was drawn up to 101 mark and the pipette was rotated between the thumb and the forefinger to facilitate adequate mixing of the solution (dilution: 1:200). The counting chamber and the cover glass were cleaned thoroughly and cover glass was placed in position over the ruled area. The fluid from the stem of the pipette was expelled as it contains only the diluting fluid. The pipette was then held at an angle of 45^0 with the tip of the pipette at the junction of the edge of cover glass and the counting chamber. A drop of blood was placed from the tip of the pipette on the central platform near the edge of the cover slip, so that the drop was sucked up between the central platform and cover slip by the capillary force. The cells were allowed to settle for 2 to 3 min. The ruled area of the counting chamber was focused under the microscope and the numbers of RBC were counted in 80 small squares (4 squares of 16 at the four corners and one of 16 at the centre). The cells touching the upper and left hand lines were counted. The cells touching the lower and the right hand lines were omitted.

The numbers of RBC per sq mm were calculated as follows

The area of Small Square: 1/400 sq mm
The depth of the counting chamber: 1/10 mm
Therefore the volume of a small square is: 1/400 x 1/10 = 1/4000 cu mm
The dilution of blood is 1:200
Total number of RBC = n x 4000 x 200/80
n =Number of cells counted in 80 small squares

Determination of white blood corpuscles (WBC) count

WBC count was determined [17]. The blood was drawn up to 0.5 mark of WBC pipette and immediately the diluting fluid was drawn up to the 101 mark above the bulb (the dilution fluid consists of 1.5ml of glacial acetic acid and 1 ml of aqueous gentian violet solution and made up to 100 ml with distilled water). The solution was mixed thoroughly by shaking gently and allowed to stand for 3 min. Cleaned Neubauer counting chamber and cover glass were placed over the ruled area. Excess solution was expelled and a drop of fluid was allowed to flow under the cover slip by holding the pipette at an angle of 40^o and allowed to stand for 2 to 3 min. The WBC was counted in the four corner square millimetres and the number of WBC per cubic millimetre was calculated.

Estimation of haemoglobin (Hb)

Hb concentration in the blood was estimated by cyanmethaemoglobin method [18].Hb is converted into cyanmethaemoglobin by the addition of potassium ferricyanide (KCN) and the colour was read in a spectrophotometer at 540 nm against a reagent blank.

Determination of packed cell volume (PCV) or Haematocrit value

Packed cell volume was determined by micro haematocrit method [19]. The heparinised blood was filled up to the

mark 100 of the haematocrit tube with the help of Pasteur pipette and centrifuged at 3000 rpm for 30min. The relative volume of the height of the RBC's packed at the bottom of the haematocrit tube was recorded as packed cell volume in terms of percentage of total blood column taken in the haematocrit tube.

Determination of mean corpuscular volume (MCV)

MCV indicates the average size of the blood cell in a given sample of blood. MCV was calculated by the following formula and expressed as femtoliter (fL).

MCV = Haematocrit (%) x10/RBC count.

Determination of mean corpuscular haemoglobin (MCH)

MCH represents the average content of the HB in each red blood cell. MCH is influenced by the HB concentration and the number of RBC. MCH was calculated by the following formula and expressed in picogram (pg).

MCH = haemoglobin (g/dL) x 10/ RBC count

Mean corpuscular haemoglobin concentration (MCHC)

MCHC reflects the average concentration of the haemoglobin in the red blood cells in a given of the blood. MCHC was obtained by the following formula and expressed in terms of gram percent (g%).

MCHC = haemoglobin (g/dL) x 100/ haemoglobin (%)

Result and discussion

The blood parameters in both lethal and sublethal concentration of technical grade as well as 76% EC Nuvan are presented in the Figure-1 and represented as graph in Figure-1. Marked changes are observed in exposed fish in the commercial formulation experimented fish resulted more percentage of changes rather than the technical grade, because of the ingredients mixed imparting additive toxicity. The RBC count decreased in both lethal and sublethal concentration and more percentage of decrement in 76% EC. The WBC count increased in both lethal and sublethal more in 76% EC.The haemoglobin content decreased in both lethal and sublethal concentration more in 76% EC. The haematocrit value altered accordingly to the RBC count. Accordingly the calculated values of MCV, MCH and MCHC also showed changes.

The review article mentioned about organochlorines organophosphates, carbamates and synthetic pyrethroids alter the haematological changes as effects in fish [6]. The work of organophosphates was reviewed and gave a thought that the pesticides do effect the biochemical changes in the blood and also parameters of the blood change [20-22]. In the opinion of [7] the review articles on toxicity of pesticides in fish documented the work where pesticide induce alteration in blood parameters and stressed the impact of such changes [23-24]. Haematobiochemical changes induced by pyrethroid insecticides in avian, fish and mammalian species [25]. The effects of pesticides in the blood of fish serve as indices of toxicity. The review on dichlorvos toxicity in fish indirectly opined that the toxic action result in fish alteration are likely [9] and that is mentioned. The dichlorvos toxicity on fish, a review published and commented on the toxic effect of biochemical nature of the circulating fluid [26]. The review mentioned that the haematological parameters are important in toxicological research and indicative of toxic stress. After exposure to two sublethal concentration 203 µg/L and 68.0 µg/L of chlorpyrifos for 1, 3, 7, 14 and 21 days a decreased erythrocyte count, leucocyte count, haemoglobin and haematocrit mean values in *Channa punctatus* (Bloch) [27] was also in support of present research. Toxication altered the haematological parameters in *Cyprinus carpio* particularly ESR count due to chlorpyrifos toxicity which is another organophosphate [28-29]. The same was opined, for the same chlorpyrifos to *Cyprinus carpio* [30]. In bony fish *Tilapia guineensis* exposed to common pesticides produced characteristic alteration in the blood [31]. The review on the toxicity and other effects of dichlorvos an organophosphates pesticides to freshwater fish, documented exposure of *Orieochromis niloticus* to dichlorvos for 96 hours duration marked changes of packed cell volume (PCV), haemoglobin (Hb), Red Blood cell (RBC), neutrophil, monocyte and lymphocytes count [8]. The review also mentioned the work done on the fish *Cyprinus carpio* exposed to dichlorvos [32]. The other works also emphasized the haematological changes are no doubt serve indices of toxicity [33-36].

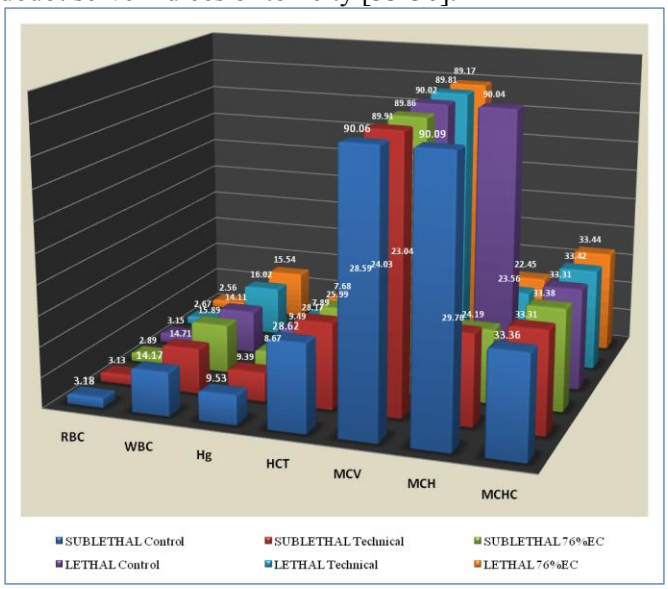


Figure 1. Haematological alterations of *Ctenopharyngodon idella* (Valenciennes) exposed to lethal and sub lethal concentrations of technical grade Dichlorvos and 76% EC (Nuvan).

Haematological changes of silver carp *Hypophthalmichthys molitrix* in response to diazonin pesticide after the exposed to half of the lethal concentration was reported [37]. The results showed that leucocytes (WBC), haematocrit (Ht) haemoglobin (Hb), MCHC and lymphocyte cortisol and glucose increased where MCV and MCH were significantly decreased. They also reported to significant differences in RBC Monocyte and Eosinophils among the fish exposed to the toxicant which are derivative changes. Haematological parameters of *Cyprinus carpio* exposed to Monocrotophosan organophosphate exposed to 4.5 ppm, 6.7 ppm and 13.5 ppm was studied and found that a significant decrease in all the sublethal concentrations and maximum decrease at 12.5 ppm RBC content, ESR PCV and a significant increase in RBC and WBC count was reported [38]. The effect of Glyphosite (Roundup 41%) on the haematology of the freshwater fish *Catla catla* was studied and the RBC, WBC, haemoglobin and haematocrit value showed marked decline while MCV, MCH and MCHC showed fluctuating pattern [39]. The present work can be correlated with this work, but both of them belong to same group of pesticides i.e., organophosphate.

Changes in haematology of the freshwater fish *Channa punctatus* (Bloch) exposed to delta methrin for 45 days was reported [40], where there was a significant decrease in haemoglobin content, total erythrocyte count, PCV, MCV and MCHC. On the other hand a significant increase in total leucocyte count and MCH which coincides the present work. Toxic impact of pesticide trichlorofon on the morphological characteristics of blood cells of fish *Channa punctatus* (Bloch) and opined not only the quantitative aspects of the blood parameters are altered but also the morphological aspects of the fish where compared with control are altered. Anisocytosis deformed erythrocytes and large bulged nucleus, deformed cells are clumped and finally cell lysis, an increase in the size of MCV has been associated in response to stress[41].Haematological changes induced by pyrethroid insecticide fenvalerate in cat fish *Clarias gariepinus* was reported [42], a significant decrease in the haemoglobin content haematocrit value and erythrocytes whereas the leukocyte was increased. The work is similar of the present report even though both of them belong to two different classes of pesticides. Haematological response of grass carp *Ctenopharyngodon idella* after exposed to endosulphan was studied [43]. The fish were exposed to two sublethal concentrations for 15, 30 and 45 days. The RBC, haemoglobin content and hematocrit values showed declined trend and MCH, MCHC also showed declined trend while MCV showed an increasing trend. She opined variation in erythrocyte count is the indices of polluted aquatic environment. The present study also showed similar results but both of them belong to different class of pesticides.

The effects of Deltamethrin on haematological indices of Indian major carp *Cirrhinus mrigala* (Hamilton) was studied by exposing the fish to lethal and sublethal concentrations and the results showed that the RBC, HB and Haematocrit values decreased in both lethal and sublethal concentration. WBC, MCV and MCH were increased consequently [44]. An increase in WBC revealed haematological toxicity coincide the present work. Haematological changes in African catfish *Clarias gariepinus* exposure to mixture of Atrazine and metolachlor in the laboratory was studied [45]. Because of mixture, the two chemicals behaved differently when compared with the present result. A significant reduction in Hb, RBC, PCV and MCV were observed. The MCHC of result showed an increase. The haematological parameters are used in monitoring health status of the fish in the wild and culture medium. Even the present study fish is a culturable one and stringent steps have to be taken not to use the pesticides in disease management of culture practices. Haematological changes in the fish *Channa punctatus* (Bloch) exposed to fenvalerate. The percentage of haemoglobin PCV, RBC showed a gradual increase while WBC showed are increase [46]. The result showed similar trend of the present study. Haematological effects of commonly used fungicide on fish *Clarias batrachus* was studied [47] where they exposed the fish to sublethal concentration and blood was assayed for selected haematological parameters. A decrease in the Hb, MCV, MCHC, RBC levels and an increase in WBC level was observed. The report in strictly different owing to chemical nature of the two toxicants i.e., Chloropyrifos and Mancozeb.

Haematological changes in the fish *Cyprinus carpio* exposed to permethrin, a synthetic pyrethroid of class I type was reported [48]. Where in a decrease in RBC, Hb, PCV was found but an increase in WBC, MCV, MCH, MCHC was observed when the fish is exposed to technical grade and 25% ECin both lethal and sublethal concentrations. Commercial formulation concentration was causing more alteration because of the ingredients present which shows similar result of the present study even though both belong to different classes. A similar report was observed in sublethal effects of dichlorvos on the freshwater fish *Cyprinus carpio* var. Communis [49]**.** The fish were exposed to three sublethal concentrations 50% 60% and 70% and the results showed changes of the RBC and WBC count, Hb and haematocrit and PCV. Since osmoregulatory dysfunction was the cause for increase in the rate of destructions in hematopoietic organs [50]. The same is reiterated [51]. Studies on freshwater fish *Channa punctatus* (Bloch) in sublethal toxicity of Deltemethrin in relation to sex was reported [52]. The fish exposed to different concentrations of Deltemethrin ranging from 0.02ppm and 0.2ppm of 5 exposure periods 24, 7, 15,20 and 30 days in sub lethal concentrations and due to long duration exposure , due to

change in haemostatic mechanisms the fish showing leucocytosis initially and fish might have evoked a changed and neutralized the toxicant effects of deltemethrin. However the present study cannot be compared with this result because of a different methodology. Haematological alterations in *Cyprinus carpio* as biomarkers of cypermethrin toxicity exposed to lethal and 1/10th of 96h LC_{50} values as sublethal for 5, 10, 15 days. RBC count, Hb content, PCV showed decrement at both lethal sublethal concentrations. WBC count and MCHC exhibited increasing trend at sublethal and decreasing trend at lethal concentrations whereas MCH increased in both concentrations [10]. The presence of the toxicant disturbs the balance in the echo systems and the fish is definitely not comfortable.

Conclusion

Hence it may be concluded that, even the *Ctenopharyngodon idella* a grass carp cultured along with the other major carps, when pesticides contaminate the culture medium, alter the blood parameters and such alterations are more severe in EC due to the ingredients mixed. Hence stringent measures have to be taken for quality control before giving pesticide representativeness for environmental usage.

Acknowledgement

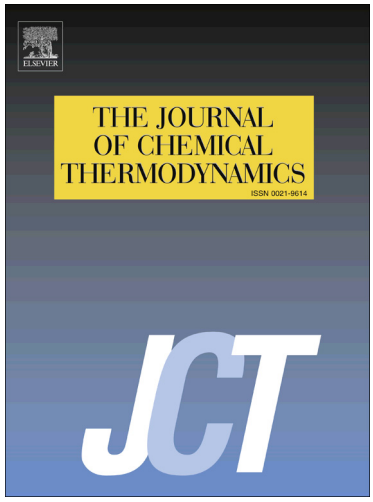
The authors are thankful to Department of Zoology, Acharya Nagarjuna University for providing laboratory facilities and Instrumentation. One of the authors R. Swarna Kumari acknowledges UGC New Delhi for the financial help received through RJNF in research period as JRF and SRF scholar.

References

1. SahanA, AltunT, CevikF, CengizlerI, NevsatE, GencE: Comparative study of some haematological parameters in Europeaneel (*Anguilla anguilla* L., 1758) caught from different regions of Ceyhan River (Adana,Turkey). E.U. Journal of Fisheries and Aquatic Sciences 2007; 24 (1-2): 167–171.
2. Di Giulio RT, Hinton DE: The toxicology of fishes. Taylor & Francis Group 2008; 1101.
3. Li ZH, Velisek J, Zlabek V, Grabic R, Machova J, Kolarova J, Randak T: Hepatic antioxidant status and hematological parameters in rainbow trout, *Oncorhynchus mykiss*, after chronic exposure to carbamazepine. Chemico-Biological Interactions 2010; 183: 98–104.
4. Velisek J, Stara A, SvobodovaZ: The effects of pyrethroid and trazine pesticides on fish physiology. In: Pesticides in the Modern World–Pests Control and Pesticides Exposure and Toxicity Assessment, Stoytcheva, M., (Ed.). InTech Open Access Publisher 2011; 377–402.
5. Shinde BR, Borane VR, Zambare SP: Ascorbate effect on endosulfan and cypermethrin induced alterations in the RBC of the fresh water fish, *Channa orientalis* (scheinder). Journal of Environmental Research and Development 2014; 8(3A), 673-675.
6. Ullah S, Zorriehzahra MJ: Ecotoxicology: A review of pesticides induced toxicity in fish.Advances in Animal and Veterinary Sciences 2015; 3(1): 40-57.
7. Shankar Murthy K, Kiran BR, Venkateshwarlu M: A review on toxicity of pesticides in fish. International journal of open scientific research 2013; 1(1):15-36.
8. Chandra SekharaRao J, Neelima P, GovindaRao K: A review on the toxicity and other effects of Dichlorvos, an organophosphate pesticide to the freshwater fish. Bioscience Discovery 2017; 8(3):402- 415.
9. Das S: A review of dichlorvos toxicity in fish. Current world environment 2013; 8 (1): 143-149.
10. Neelima P, Sunitha K, GopalaRao N, Chandra S, Rao J: Haematological alterations in *Cyprinus carpio* as biomarkers of cypermethrin toxicity. International journal of current research 2015; 7(8): 18864-18870.
11. HomairaAfreen, Toufiq-Ul Amin, Siddiqul Islam. Md, Salma Parvin, Rayhanus Salam: In vitro phytochemical analysis and cytotoxic assay of leaves of *Solanum lycopersicum* Linn by brine shrimp bioassay. Journal of Innovations in Pharmaceuticals and Biological Sciences 2016; 3 (3):81-85.
12. Finney DJ: Probit analysis 3rd Ed., Cambridge University Press, London, New York, 333p.
13. APHA, AWWA and WEF: Standard methods for the examination of water and waste water, 20th Edition, Clesceri, L.S. Greenberg, A.E. and Eaton, A.D. (Eds.), 1998; American Public Health Association, American Water Work Association, Water Environment Federation, Washington DC. USA.
14. APHA: Standard Methods for the Examination of Water and Wastewater. 21st Edition, 2005; American Public Health Association/American Water Works Association/Water Environment Federation, Washington DC. USA.
15. APHA, AWWA and WEF: Standard Methods for examination of water and wastewater. 22nd Edition. 2012; Washington: American Public Health Association; 1360.
16. ShaperclausW: Fish Diseases, vol. 1. AkademieVerlag, Berlin.1979; 570.
17. Donald H and Bonford RR: Hutchinson Clinical Methods. 14thEdtion. London.1963; 145.
18. Blaxhall PC, Daisley KW: Routine haematological methods for use with fish blood. Journal of fish biology 1973; 5: 771- 781.
19. Schalm OW, Jain NC, Carroll EJ: Veterinary Haematology, 3rd Edition.1975; Lea and Febiger, Philadelphia.
20. Saeedi FM, Roodsari HV, Zamini A, Mirrasooli E, Kazemi R: The Effects of Diazinon on Behavior and Diazinon on Behaviour and Some Haematological Parameters of Fry Rainbow. Trout (*Oncorhynchus mykiss*). World Journal of Fisheries and Marine Sciences 2012; 4(4): 369-375.
21. Sampath K, James R, Velammal S: Effect of methyl parathion on blood parameters and its recovery in a catfish, *Mystus keletius*. Indian Journal of Fisheries. 2003; 50(2): 191-197.
22. Svoboda M, Luskova V, Drastichova J, Zlabek V: The effect of diazinon on haematological indices of common carp (*Cyprinus carpio* L.). Acta Vetrinary Bruno 2001; 70: 457-465.
23. Satyanarayan S, Bejankiwar RS, Chaudhari PR, Kotangale JP, Satyanarayan A: Impact of some chlorinated pesticides on the haematology of the fish *Cyprinus carpio* and *Puntius ticto*. Journal of Environmental Science 2004; 16(4): 631-634.
24. Geyer HJ, Steinberg CE, Scheunert I, Brüggemann R, Schütz W, Kettrup A, Rozman K: A review of the relationship between acute toxicity (LC50) of gamma-hexachlorocyclohexane. (gamma-HCH, Lindane) and total lipid content of different fish species. Toxicology 1993; 83 (1-3):169-179.
25. Ahrar khan, Latif Ahmad and Muhammad Zargham Khan: Review article, Hemoto -Biochemical changes induced by pyrethroid insecticides in Avian, fish and mammalian species. International Journal of agriculture & biology 2012; 14(5):834-842.
26. Deka S, Mahanta R: Dichlorvos toxicity on fish –A review. European Journal of Biological Research 2015; 5 (3):78-85.
27. Sunanda M, Chandra SekharaRao J, Neelima P, GovindaRao K, Simhachalam G: Effects of Chlorpyrifos (an Organophosphate Pesticide) in Fish. International Journal of Pharmaceutical Sciences Review and Research 2016; 39(1): 299-305.
28. Ali D, Kumar S: Study on the effect of chlorpyrifos on acetylcholinesterase and hematological response in *Channa punctatus* (Bloch), IIOAB Journal 2012; 3(5): 12-18.
29. Malla FA, Sharma G, Singh S: Chlorpyrifos pesticide toxicity on erythrocyte sedimentation rate in fish, *Channa punctatus* (Bloch.) Biology and Medicine 2009; 1(2): 54-55.
30. Ramesh M, Saravanan M: Haematological and biochemical responses in a freshwater fish *Cyprinus carpio* exposed to chlorpyrifos. International Journal of Integrative Biology 2008; 3(1): 80-83.
31. Chindah AC, Sikoki FD, Vincent-Akpu I: Changes in haematological characteristics of a bony fish, *Tilapia guineensis* (Bleeker, 1862), exposed to common pesticides in the Niger Delta Wetland, Nigeria, Ghana Journal of Agricultural Science 2004; 37: 59-67.

32. Tak AM, Bhat FA, Jan U, Shah GH: Sublethal haematological effects of dichlorvos on the freshwater fish, *Cyprinus carpio* var. communis. International Journal of Recent Scientific Research 2014; 5(7): 1334-1337.
33. Lakshmanan SA, Rajendran C, Sivasubramaniyan: Studies on impact of Dichlorvos on selected haematological parameters of freshwater fish, *Orechromis mossambicus* (Peters). International Research Journal of Biological Sciences 2013; 3(1): 28-33.
34. Ashade OO, Ashiru AW, Obiri CM: The comparative study of the toxic effects of 2-3 diclorovinyl dimethyl phosphate (DDVP) and chlorpyrifos on the behaviour and haematology of african- (*Clarias gariepinus*). International Journal of Science and Society Yabatech 2011; 1(1): 38-47.
35. Sobhana KS, George KC, Sanil NK, Surendran KK, Paul Raj R: Immunosuppressive action of nuvan (dichlorvos) in the banded pearl spot, *Etroplus suratensis* - evaluation of effect on haematology and humoral immune response. Journal of the Marine Biological Association of India 2006; 48(1): 29-34
36. Das BK, Mukherjee SC: Sublethal effect of quinalphos on selected blood parameters of *Labeo rohita* (Ham.) fingerlings. Asian Fisheries Science 2000; 13: 225-233.
37. Hedayati A, Hassan NatajNiazie E: Hematological changes of silver carp in response to Diazinon pesticide. Journal of Environmental Health Science and Engineering 2015;13 (52): 1-5.
38. Vaiyanan V, Sridharan G, Raveendran S, Chairman K: Impact of pesticide on haematological parameters of *Cyprinus carpio*. World Journal of pharmacy and pharmaceutical sciences 2015; 4(8): 1424-1430.
39. Jerald Felix F, Saradhamani N: Impact of the herbicide glyphosate roundup (41%) on the haematology of the freshwater fish, *Catla catla* (Hamilton). IOSR Journal of Environmental Science, Toxicology and Food Technology 2015; 9 (4) 3: 56-60.
40. Jayaprakash C, Shettu N: Changes in the hematology of the freshwater fish, Channa punctatus (Bloch) exposed to the toxicity of deltamethrin. Journal of Chemical & Pharmaceutical Research 2013; 5(6):178-183.
41. Mishra A: Toxic impact of pesticides on the morphological characteristics of blood cells of fish *Channa punctatus* (Bloch) Indian Journal of scientific Research 2017; 12 (2): 068-072.
42. Sheikh Jamal AL: Haematological changes induced by a pyrethroid insecticide fenvalerate in catfish *Clarias gariepinus*. Sci. J. Fac. Sci. Minufa Univ. 2006; 20: 89 - 100.
43. RenuBalaSingla: Morphometric alterations in exotic freshwater fish, *Ctenopharyngodon idella* (Cuv. and Val.) upon exposure to endosulfan International Journal of Fisheries and Aquatic Studies 2016; 4(3): 590-593.
44. David M, Sangeetha J, Shrinivas J, Harish ER, Naik VR Effects of deltamethrin on haematological indices of indian major carp, *Cirrhinus mrigala* (Hamilton) International Journal of Pure and Applied Zoology 2015; 3 (1): 37-43.
45. George ADI, Akinrotimi OA, Nwokoma UK: Haematological changes in African Catfish (*Clarias gariepinus*) exposed to mixture of Atrazine and Metolachlor in the laboratory. Journal of Fisheries Sciences 2017; 11(3): 048-054.
46. Tilak K S, Satyavardhan K: Effect of feneveralate on oxygen consumption and haematological parameters in the fish, *Channa punctatus* (Bloch). Journal of Aquatic Biology 2002; 17:81-86.
47. Jaya Shahi, Ajay Singh: Genotoxic and haematological effect of commonly used fungicide on fish *Clarias batracus*. Journal of Biology and Earth Sciences 2014; 4 (2): B137-B143.
48. GopalaRao N, Bala Krishna Naik R, SrinivasaRao G: Haematological changes in the fish *Cyprinus carpio* exposed to a synthetic pyrethroid [Class I], Permethrin and its 25% EC. Current Trends in Technology and Science 2017; 6 (5): 759-763.
49. Abdul MajidTak, Bhat FA, UlfatJan, Mustafa Shah G: Sublethal haematological effects of dichlorvos on the fresh water fish, *Cyprinus carpio* var. Communis. International Journal of Recent Scientific Research Research 2014; 5 (7): 1334-1337.
50. Jenkins F, SmithJ, Rajanna B, Shameem U, Umadevi K, Sandhya V, Mahadevi R: Effect of sublethal concentration of endosulfan on haematological and serum biochemical parameters in the carp *Cyprinus carpio*. Bulletin of Environmental Contamination and Toxicology 2003; 70:993-997.
51. Seth N, Saxena KK: Hematological responses in a freshwater fish, *Channa punctatus* due to fenvalerate. Bulletin of Environmental Contamination and Toxicology 2003; 71: 1192-1199.
52. Venkata Ramudu M, Nagabhushan Reddy M, Chennaiah K, Indira P: Carbohydrate metabolism in freshwater fish *Channa punctatus* (Bloch) during sublethal toxicity of deltamethrin in relation to sex . Bulletin of Pure & Applied Sciences Section A 2008; 27(1): 7-16.

Accepted Manuscript



Investigation of solute-solvent interactions in {1-butyl-3-methyl imidazolium-Bis(trifluoromethylsulfonyl)imide+dimethylcarbonate} mixture using physico-chemical properties

V. Srinivasa Rao, M. Srinivasa Reddy, Sk. MdNayeem, K. Thomas S.S. Raju, K. Bala Murali Krishna, B. Hari Babu

PII: S0021-9614(17)30238-0
DOI: http://dx.doi.org/10.1016/j.jct.2017.07.013
Reference: YJCHT 5131

To appear in: *J. Chem. Thermodynamics*

Received Date: 25 April 2017
Revised Date: 20 June 2017
Accepted Date: 6 July 2017

Please cite this article as: V. Srinivasa Rao, M. Srinivasa Reddy, Sk. MdNayeem, K.T.S.S. Raju, K. Bala Murali Krishna, B. Hari Babu, Investigation of solute-solvent interactions in {1-butyl-3-methyl imidazoliumBis(trifluoromethylsulfonyl)imide+dimethylcarbonate} mixture using physicochemical properties, *J. Chem. Thermodynamics* (2017), doi: http://dx.doi.org/10.1016/j.jct.2017.07.013

This is a PDF file of an unedited manuscript that has been accepted for publication. As a service to our customers we are providing this early version of the manuscript. The manuscript will undergo copyediting, typesetting, and review of the resulting proof before it is published in its final form. Please note that during the production process errors may be discovered which could affect the content, and all legal disclaimers that apply to the journal pertain.

ACCEPTED MANUSCRIPT

Investigation of solute-solvent interactions in {1-butyl-3-methyl imidazoliumBis(trifluoromethylsulfonyl)imide+dimethylcarbonate} mixture using physicochemical properties

V. SrinivasaRao[a,d], M. SrinivasaReddy[b], Sk.MdNayeem[c], K.Thomas S S Raju[d], K. BalaMuraliKrishna[c], B. HariBabu[e*]

[a]*Department of Chemistry, SRR& CVR Govt. Degree College , Vijayawada-520008, A.P., India.*

[b]*Department of Chemistry, KRK Govt. Degree College , Addanki-523201, A.P., India.*

[c]*Department of Physics, KRK Govt. Degree College , Addanki-523201, A.P., India.*

[d] *Department of Chemistry, Andhra Loyola College, Vijayawada-520008, A.P., India.*

[e]*Department of Chemistry, AcharyaNagarjuna University, Nagarjunanagar–522510, A.P.,India.*

ABSTRACT:

Physical properties, such as density (ρ), speed of sound (u) and refractive index of [Bmim][NTf_2], DMC and their binary mixtures are measured over the whole composition range as a function of temperature between (303.15 - 323.15) K at atmospheric pressure. Experimental values are used to calculate excess values of molar volumes (V_m^E)/partial molar volumes ($\overline{V}_m^E$)/ partial molar volumes at infinite dilution ($\overline{V}_m^{E,\infty}$)/isentropic compressibility (κ_s^E)/free length (L_f^E), speed of sound (u^E) and isobaric thermal expansion coefficient (α_P^E) for the binary mixture. These excess properties are fitted to the Redlich-Kister equation to obtain the binary coefficients and the standard deviations. A qualitative analysis of these parameters indicates strong intermolecular interactions and the interaction increases with the increase in temperature. Further, through physicochemical properties, an attempt for calorimetric excess chemical potential using different equations is computed at T=308.15K. The present investigation also comprises of evaluation of the acoustic non-linearity parameter (B/A) in the mixtures and calculation of cohesive energy (ΔA), Van der Wall's constants (a, b), distance of closest approach (d). The presence of strong interactions is further supported by IR spectroscopy and the Prigogine–Flory–Patterson (PFP) theory.

Key words: [Bmim][NTf_2]; DMC; density; speed of sound; refractive index; excess thermodynamic parameters.

* Corresponding Author:dr.b.haribabu@gmail.com

Phone: +91-8500338866

ACCEPTED MANUSCRIPT

1. Introduction

Substances that are entirely composed of ions with melting temperatures around 373 K are a family of Ionic liquids (ILs). Present days they attracted considerable attention because of their distinctive properties such as thermal stability, non-volatility and reusability [1,2]. Ionic liquids can be selected to have different anions and cations, so that one can form ionic liquid with the desired properties. ILs with special functional groups has been designed for application in many industrial processes. ILs are utilized for different purposes like extraction, separation and alternative solvents in catalytic reactions, synthesis, catalysis, biocatalyst, electro chemical devices, separation technology, reaction media, green solvents and in bio degradable materials.

Mixtures of ILs and molecular organic solvents are gaining interest of researchers as resultant liquid mixtures containing the advantages over both IL and molecular organic solvents. The properties of these mixtures are based on the mixing ratio. Mixing of the ILs with molecular solvents is one of the alternative steps to minimize the usage of expensive ILs and to save time for preparing new ILs [3]. From an economic and ecological perspective, the mixtures of ILs and traditional organic solvents may be gaining a tremendous amount of attention from both the researchers and the industries. Ionic liquids are more viscous than conventional organic solvents, which may hamper their application. Fortunately, their mixtures with molecular solvents show reduced viscosity without affecting their advantages as green solvents. In particular, the addition of polar co-solvents can strongly influence the physical and chemical properties of ILs such as viscosity, reactivity and electrical conductivity as well as solubility and solvation properties [4]. Recently, several binary IL+ molecular solvent systems have been shown to perform better than the pure ILs, and such systems have been used in numerous applications such as biocatalyzed reactions, as super capacitors, as reaction media, medium for dissolution of biopolymers etc. [5-17]. Hence, IL + molecular solvent mixtures have received growing attention in the past few years. The potential of these new substances can be exploited with experimental methods that can reliably predict the thermodynamic properties. Most of these novel media are characterized by their volumetric, acoustic and refractive index properties, since this data is important for industrial applications. To predict molecular interactions between binary liquids, speed of sound and refractive index along with experimental data of density plays vital role.

ACCEPTED MANUSCRIPT

The choice of the investigated Ionic liquid, 1-butyl-3-methylimidazoliumbis (trifluoromethylsulfonyl)imide ([Bmim][NTf_2]) was on the basis of its ability to act as extracting solvent for the removal of many organic compounds through liquid-liquid extraction [18,19]. It is also widely used in catalysis [20] and chromatography [21]. On the other hand, dimethyl carbonate (DMC) can be a replacement of conventional organic solvents that damage the atmosphere. Moreover, DMC has been favoured as a green replacement for halogenated solvents due to its similarity with these types of liquids as well as ethers and esters [22]. Thus, one of the main properties of DMC is its ability to dissolve salts and particularly lithium ions. It contains high concentration of $LiPF_6$ and also used for high power density double-layer capacitors [23,24] and thus it represents a viable alternative to acetate esters and ketones in most applications, from paints to adhesives, taking advantage of its good solvency power [25]. Further, it is the file leader of many derived carbonic esters, available by transesterification reactions, whose properties can be tailored according to the target applications, like in the field of lubricating oils [26]. It is a non-aqueous electrolyte component and is finding increasing applications in the field of lithium rechargeable batteries, as witnessed by the number of patents in the area [27]. Additionally, it is used as a blowing agent in polyurethane foam after CFC ban [28].

Systematic investigation of the physicochemical properties of [Bmim][NTf_2] with molecular organic solvents including water have been reported. Alfonsina *et al* [29] reported the physicochemical properties such as density, refractive index, viscosity of [Bmim][NTf_2] binary mixture with ethanol orethyl acetate. Zarrougui *et al* [30] reported the density, viscosity and conductivity and thermal expansivities of propylene carbonate with [Bmim][NTf_2], where as Widowati *et al* [31] reported pressure-volume-temperature properties of binary mixtures of the [Bmim][NTf_2]with anisole or acetophenone at elevated pressures. Vranes *et al* [32] reported density and excess properties of [Bmim][NTf_2]+Propylene carbonate binary mixtures, Monika *et al* [33] reported acoustic and volumetric properties of binary mixtures of [Bmim][NTf_2] with acetonitrile or tetrahydrofuran, Vranes *et al* [34] reported density, electrical conductivity and viscosity of binary liquid mixtures of [Bmim][NTf_2] with γ-butyrolactone (GBL), Salinas *et al* [35] reported densities, speed of sound, viscosity and excess properties of binary mixtures formed by ethanol and [Bmim][NTf_2], Jacquemin *et al* [36] reported the density and viscosity of several pure and water-saturated ionic liquids including [Bmim][NTf_2], Kassim *et al* [37]

ACCEPTED MANUSCRIPT

reported the experimental densities and viscosities of binary mixture of [Bmim][NTf_2] with glycerol or sulfolane and their molecular interaction by COSMO-RS, Krishna *et al* [38] reported densities, speeds of sound and refractive indexes of the binary mixture of [Bmim][NTf_2] with pyrrolidin-2-one. But the thermo acoustic, volumetric and refractive index data of [Bmim][NTf_2] with DMC was not reported.

On the basis of our initial experiments, [Bmim][NTf_2] is found to be totally miscible with DMC in all proportions. Hence, in the present study, it is proposed to measure the densities, speeds of sound and refractive indexes of the binary mixtures of [Bmim][NTf_2] with DMC in the temperature range between (303.15-323.15) K in the entire composition range and at atmospheric pressure. On the basis of the measured values, we calculated the excess/deviation properties for their potential application in industrial processes. Here we reported the excess properties such as molar volumes ($V_{\mathrm{m}}^{\mathrm{E}}$), isentropic compressibilities (κ_s^E), free length (L_f^E), speeds of sound (u^E) and isobaric thermal expansion coefficient (α_P^E) along with $\left(\frac{\partial V_m^E}{\partial T}\right)_P$ and $\left(\frac{\partial H_m^E}{\partial P}\right)_T$. Besides, the deviation of refractive index on volume fraction basis ($\Delta_\phi n_D$) reported for the binary mixture and fitted using Redlich-Kister polynomial equation. Calorimetric excess chemical potential is also estimated through these physicochemical properties using 3-parameter Morgules, Porter, Wilson and Van Laar equations at T=308.15K. In addition, non-linearity parameter using two different models is also evaluated along with certain molecular properties. Lastly, an attempt has been made to understand the interaction behavior between the two liquids in the mixture using IR spectroscopy. In addition, analysis of $V_{\mathrm{m}}^{\mathrm{E}}$ data of the present mixture was done through the Prigogine-Flory-Patterson (PFP) theory.

2. Experimental

2.1. Materials

The ionic liquid, [Bmim][NTf_2] (CAS174899-83-3) with purity 0.99 in mass fraction used in this work. It was purchased from Iolitec GmBH (Germany), while DMC (CAS616-38-6) with purity 0.995 in mass fraction was supplied by Sigma Aldrich. The chemicals used in the present investigation were purified by the methods described in literature [39,40]. The water

ACCEPTED MANUSCRIPT

content in investigated IL and DMC was determined using a Karl Fisher titrator (Mtrohm,890Titrando). Before any measurements, all samples were dried for at least 72h under a vacuum (0.1Pa) and moderate temperature (beginning at room temperature and increasing it gradually over a 6 h period up to 333K). The water content of all the samples were further checked and found to be in the range of less than 150 ppm, a value much lower than the original pre-evacuation analysis, which typically showed values in the range of less than 210×10^{-6}. DMC is further purified by distillation. List of chemicals with details of Provenance, CAS number, and mass fraction purity are given in **Table 1**. The purities were verified by comparing the measured density, speed of sound and refractive index of the pure liquids with the literature at atmospheric pressure are given in **Table 2.** Figures S1–S6 of the supplementary material represent comparison of pure values of densities, speeds of sound and refractive indices of [Bmim][NTf_2] and DMC of this work with the reported literature [31,32,35,38,41-44,46–66]. The experimental refractive index data show much discrepancy with the literature. With regards to refractive index of the [Bmim][NTf_2], our data show deviation of -0.05 %, -0.04% and -0.11% with the data of Krishna *et al.* [38], Montalban *et al.* [54] at 303.15 K and Tariq *et al.* [55] at 313.15 K respectively. Moreover, the refractive index data of DMC have deviations of +0.05%, +0.06% with the data of Rodriguez [62[, Shin *et al.* [43] and -0.03% of Moosavi *et al.* [66] at 303.15 K and -0.23 % from Pal *et al.* [65] at 308.15 K respectively. The observed deviations may be due to variation of percentage of purity and instruments. We used latest version of Anton Paar DSA 5000M/ Anton Paar Dr Krenchen Abbemat (WR-HT) having automatic viscosity corrector giving high accurate values. Further, our samples, [Bmim][NTf_2] and DMC have 99% and 99.5% purity respectively. We have taken utmost care to remove water content.

2.2 Apparatus and procedure

2.2.1. Sample preparation

All samples are freshly prepared in amber colour glass vials with screw caps having PFE septa, and a secure sealed with parafilm to prevent absorption of moisture from the atmosphere, and is then stirred for more than 30 min to ensure total dissolution of the mixtures. Samples are taken from the vials with a syringe through the PFE septum. Samples are prepared by weighing

ACCEPTED MANUSCRIPT

with a precision of ±0.01 mg, using a Sartorius electronic balance (CPA225D). The uncertainty of the resulting mole fractions of the mixtures was estimated as being $\pm 5\times10^{-4}$.

2.2.2. Measurement of density and speed of sound

Densities and speed of sound are measured with an Anton Paar DSA-5000M vibrating tube density and sound velocity meter. The density meter is calibrated with doubly distilled degassed water, and with dry air at atmospheric pressure. The temperature of the apparatus is controlled to within ±0.01 K by a built-in Peltier device. Measured density and speed of sound values (at frequency approximately 3 MHz) are precise to 5×10^{-3} kg·m^{-3} and 5×10^{-1}m·s^{-1} respectively. The standard uncertainties associated with the measurements of temperature, density and speed of sound are estimated to be ±0.01 K, 1 kg·m^{-3} and ±0.5 m·s^{-1} respectively.

2.2.3 Measurement of refractive index

The refractive indices are determined using an automatic refractometer (Anton Paar Dr Krenchen Abbemat (WR-HT)) which has also a temperature controller that keeps the samples at working temperature. The uncertainties in the temperature and refractive index values are ±0.01K and $\pm 5\times10^{-4}$ respectively. The apparatus is calibrated by measuring the refractive index of Millipore quality water and tetrachloroethylene (supplied by the company) before each series of measurements according to manual instructions. The calibration is checked with pure liquids by known refractive index.

2.2.4 Measurement of infrared spectra

Infrared transmittance is measured by using Shimadzu Fourier transform infrared (FT-IR) spectrometer (IR Affinity-1S) equipped with attenuated total reflectance (ATR) accessories. The spectral region is (650-4000) cm^{-1} with resolution of 2 cm^{-1} and 100 scans. At least five repeated measurements are performed for each sample.

3. Results and Discussion

The experimentally measured density (ρ), speed of sound (u) and refractive index (n_D) for the binary mixture of [Bmim][NTf$_2$] with DMC over the region of complete miscibility as a function of temperature between (303.15-323.15) K in steps of 5 K under atmospheric pressure are given in the **Table 3**. The changes in values of ρ, u and n_D with respect to temperature and mole fraction are linear and non-linear respectively. This trend specifies that molecular interactions definitely exist at all temperature between liquids in study. The excess and deviation

ACCEPTED MANUSCRIPT

parameters are calculated from the experimental data according to well-known thermodynamic expressions given below.

The excess molar volume is given by

$$V_m^E = \frac{x_1 M_1 + x_2 M_2}{\rho} - \left(\frac{x_1 M_1}{\rho_1} + \frac{x_2 M_2}{\rho_2} \right) \quad (1)$$

where, M_1 & M_2 represent molar mass, x_1 & x_2 the mole fractions of [Bmim][NTf_2] and DMC respectively, while ρ_1, ρ_2 & ρ the densities of [Bmim][NTf_2], DMC and the mixture respectively.

The isentropic compressibility, κ_S, is computed directly from the measured values of speed of sound and density using the Newton-Laplace equation

$$\kappa_S = -\frac{1}{V_m}\left(\frac{\partial V_m}{\partial P}\right)_s = \left(\frac{1}{\rho u^2}\right) = \left(\frac{V_m}{M u^2}\right) \quad (2)$$

Excess isentropic compressibility is given by

$$\kappa_s^E = \kappa_s - \kappa_s^{id} \quad (3)$$

where, κ_S, is the isentropic compressibility and κ_S^{id}, is the isentropic compressibility of the ideal mixture, which is calculated in the manner as suggested by Benson and Kiyohara [67].

$$\kappa_S^{id} = \sum_{i=1}^{2} \phi_1 \left[\kappa_{S,i} + \frac{T V_i \alpha_i^2}{C_{p,i}} \right] - \left\{ T \frac{\left(\sum_{i=1}^{2} x_i V_i \right) \left(\sum_{i=1}^{2} \phi_i \alpha_i \right)^2}{\left(\sum_{i=1}^{2} x_1 C_{p,i} \right)} \right\} \quad (4)$$

where, ϕ_i, is the volume fraction of the i^{th} component and is given by, $\phi_i = \frac{x_i V_i}{\sum_{i=1}^{2} x_i V_i}$, T is the temperature, $\kappa_{s,i}$ is the isentropic compressibility, V_i is the molar volume, α_i is the isobaric thermal expansion coefficient and $C_{P,i}$ is heat capacity of the i^{th} component.

Free length is given by

ACCEPTED MANUSCRIPT

$$L_f = \kappa_j (\kappa_S)^{1/2} \tag{5}$$

where, κ_j is the temperature dependent Jacobson's constant which is equal to κ_j = (93.875+0.375T) 10^{-8}

The excess intermolecular free length is given by

$$L_f^E = L_f - L_f^{id} = \kappa_j (\kappa_S)^{1/2} - \kappa_j (\kappa_S^{id})^{1/2} \tag{6}$$

The excess speeds of sound, u^{E} is estimated in binary and ternary mixtures using the following expression [68].

$$u^{\mathrm{E}} = u - u^{id} = u - (\rho^{id} k_S^{id})^{-1/2} \tag{7}$$

where $\rho^{id} = \sum_{i=1}^{2} \phi_i \rho_i$

Isobaric thermal expansion coefficient, α_p, of the pure components is calculated from the measured densities by the relation,

$$\alpha_p = \frac{1}{V_m}\left(\frac{\partial V_m}{\partial T}\right)_p = -\frac{1}{\rho}\left(\frac{\partial \rho}{\partial T}\right)_p = -\left(\frac{\partial \ln \rho}{\partial T}\right) \tag{8}$$

The values of α_p are derived by taking differentiation of second order polynomial fit [69] between density and temperature (R^2>0.999).

Excess isobaric thermal expansion coefficient, α_P^E is calculated from the following equation

$$\alpha_P^E = \alpha_P - \alpha_P^{id} = \frac{\left(\frac{\partial V_m^E}{\partial T}\right)_P - V_m^E \alpha_P^{id}}{V_m^{id} + V_m^E} \tag{9}$$

where, $\alpha_P^{id} = \sum_{i=1}^{2} \phi_i \alpha_{P,i}^*$

The dependence of the excess molar enthalpy of mixing with pressure at fixed temperature $\left(\frac{\partial H_m^E}{\partial P}\right)_T$ can be derived indirectly from accurate measurement of V_m^E, as a function

ACCEPTED MANUSCRIPT

of the temperature and composition by application of the following exact thermodynamic expression

$$\left(\frac{\partial H_m^E}{\partial P}\right)_T = V_m^E - T\left(\frac{\partial V_m^E}{\partial T}\right)_P \tag{10}$$

If the difference between the refractive indices of the two components is small then deviation in refractive index of binary mixtures containing ILs

$$\Delta_\phi n_D = n_D - n_D^{id} \tag{11}$$

$$n_D^{id} = \phi_1 n_{D,1} + \phi_2 n_{D,2}$$

The excess/deviation properties are fitted to a Redlich-Kister polynomial equation given by

$$Y^E = x_1 x_2 \sum_{i=o}^{j} A_i \left(x_1 - x_2\right)^i \tag{12}$$

Where $Y^E = V_m^E$, κ_s^E, L_f^E, $\mathcal{U}^E$, α_P^E, $\Delta_\phi n_D$, $\left(\frac{\partial V_m^E}{\partial T}\right)_P$ and $\left(\frac{\partial H_m^E}{\partial P}\right)_T$. x_1 and x_2 are the mole fraction of [Bmim][NTf_2] and DMC respectively. Further, A_i are the adjustable parameters of the function; and are determined using the least square method. In the present investigation '*i*' values are taken from 0 to 4. The corresponding standard deviations $\sigma(Y^E)$ are calculated using the following expression.

$$\sigma(Y^E) = \left[\frac{\sum\left(Y_{\text{exp}}^E - Y_{\text{cal}}^E\right)^2}{\left(m - n\right)}\right]^{1/2} \tag{13}$$

where 'm' is the total number of experimental points and 'n' is the number of coefficients in equation (12). The Redlich-Kister polynomial coefficients and correspondingstandard deviations are presented in **Table 4**.

The variations as observed in these excess/deviation parameters indicate the strength of interactions that exist between the component molecules of the binary mixture under study and their further dependence on the composition, molecular size, shape and temperature. The effects which influence these thermodynamic functions may be the resultant contribution from several opposing effects, namely chemical, structural, and physical [70,71]. The chemical or specific

ACCEPTED MANUSCRIPT

interactions include the formation of hydrogen bonding between component molecules, charge-transfer complexes. The structural contributions arise from several effects such as interstitial accommodation and geometrical fitting of one component into another. Excess molar volumes for the binary mixture of [Bmim][NTf_2] with DMC as a function of composition from T = (303.15-323.15) K are shown in **Figure 1**. Excess molar volumes are found to be negative in the entire composition at all temperatures. The variations of excess molar volumes are found to be negative in the whole composition range at all temperatures which may be credited to the hydrogen bonding between solute and solvent molecules and also favourable fitting of smaller DMC molecules (at T=303.15K, V_m=85.24 $\times 10^{-6}$ $m^3 \cdot mol^{-1}$) into the voids created by larger [Bmim][NTf_2] molecules (at T=303.15K, V_m=293.48 $\times$ 10^{-6} $m^3 \cdot mol^{-1}$) is definitely contributing to interactions. The similar variations in V_m^E values are also observed for the rest of studied temperatures. Moreover, the variation of V_m^E for the present system as a function of temperature becomes more negative with rise in temperature. This is because of the fact that, more favourable fitting of smaller DMC molecules into the voids created by larger IL molecules, thereby, shrinkage of the volume of the mixture to a larger extent, resulting in more negative V_m^E values with rise in temperature. Therefore, order of strength of interaction enhances with rise in temperature.

The existing molecular interactions in the current binary system are properly reflected on the properties of partial molar volumes of the constituent molecules. Partial molar volume is the contribution that a component of a mixture makes to the total volume of the solution. Therefore, the partial molar volume is a function of mixture composition. The partial molar volumes $\overline{V}_{m,1}$ of component 1 ([Bmim][NTf_2]) and $\overline{V}_{m,2}$ of component 2 (DMC) in the mixtures over the whole composition range have been computed using the following relationships.

$$\overline{V}_{m,1} = V_m^E + V_1^* + x_2\left(\frac{\partial V_m^E}{\partial x_1}\right)_{T,P} \tag{14}$$

$$\overline{V}_{m,2} = V_m^E + V_2^* - x_1\left(\frac{\partial V_m^E}{\partial x_1}\right)_{T,P} \tag{15}$$

ACCEPTED MANUSCRIPT

where V_1^* and V_2^* are the molar volumes of pure components of [Bmim][NTf_2] and DMC respectively. The derivatives in the above equations are obtained by differentiating Redlich-Kister eqn. (14) that leads to the following equations for $\overline{V}_{m,1}$ and $\overline{V}_{m,2}$.

$$\overline{V}_{m,1} = V_1^* + x_2^2 \sum_{i=0}^{4} A_i (x_1 - x_2)^i - 2x_1 x_2^2 \sum_{i=1}^{4} A_i (i)(x_1 - x_2)^{i-1} \quad (16)$$

$$\overline{V}_{m,2} = V_2^* + x_1^2 \sum_{i=0}^{4} A_i (x_1 - x_2)^i + 2x_2 x_1^2 \sum_{i=1}^{4} A_i (i)(x_1 - x_2)^{i-1} \quad (17)$$

using the above equations $\overline{V}_{m,1}^E$ and $\overline{V}_{m,2}^E$ have been calculated using,

$$\overline{V}_{m,1}^E = \overline{V}_{m,1} - V_1^* \quad (18)$$

$$\overline{V}_{m,2}^E = \overline{V}_{m,2} - V_2^* \quad (19)$$

The calculated values of $\overline{V}_{m,1}$ and $\overline{V}_{m,2}$ for the studied binary system are represented in **Table 5**. On visualizing the values of $\overline{V}_{m,1}$ and $\overline{V}_{m,2}$ for the two components in the mixtures (**Table 5**), it is evident that the values are lower than their individual molar volumes in the pure state, which reveals contraction of volume occurs on mixing [Bmim][NTf_2] with DMC at all examined temperatures. **Figure 2** and **Figure 3** represent the disparity of excess partial molar volumes of $\overline{V}_{m,1}^E$ ([Bmim][NTf_2]) and $\overline{V}_{m,2}^E$ (DMC) respectively in the binary mixture at *T*= (303.15, 308.15, 313.15, 318.15 and 323.15) K. The **Figure 2** and **Figure 3** not only show the existence of strong forces between the unlike molecules but also supports the inferences drawn from excess molar volume.

The excess partial molar volumes at infinite dilution of component 1 ($\overline{V}_{m,1}^{E,\infty}$) and component 2 ($\overline{V}_{m,2}^{E,\infty}$) have been calculated using

$$\overline{V}_{m,1}^{E,\infty} = A_0 - A_1 + A_2 - A_3 + \ldots\ldots\ldots = \overline{V}_{m,2}^{\infty} - V_2^* \quad (20)$$

$$\overline{V}_{m,2}^{E,\infty} = A_0 + A_1 + A_2 + A_3 + \ldots\ldots\ldots = \overline{V}_{m,1}^{\infty} - V_1^* \quad (21)$$

The partial molar volumes ($\overline{V}_{m,1}^{\infty}$, $\overline{V}_{m,2}^{\infty}$) and excess partial molar volumes at infinite dilution ($\overline{V}_{m,1}^{E,\infty}$, $\overline{V}_{m,2}^{E,\infty}$) of [Bmim][$NTf_2$]and DMC are calculated using the equations (18-21).The pertinent

ACCEPTED MANUSCRIPT

data of $\overline{V}_{m,1}^{\infty}$, $\overline{V}_{m,2}^{\infty}$ and $\overline{V}_{m,1}^{E,\infty}$, $\overline{V}_{m,2}^{E,\infty}$ is presented in **Table 6** at T = (303.15, 308.15, 313.15, 318.15 and 323.15) K. The values of $\overline{V}_{m,1}^{E,\infty}$ and $\overline{V}_{m,2}^{E,\infty}$ are found to be negative and become more negative with increase of temperature. This indicates that the association effect is greater than the dissociation effect for both the components in the present system. The excess partial molar volumes at infinite dilution for [Bmim][NTf_2] ($\overline{V}_{m,1}^{E,\infty}$) are more negative than those of DMC ($\overline{V}_{m,2}^{E,\infty}$) at all studied temperatures. This is because for more concentrated DMC solution, no hydrogen bonds exist among DMC molecules. Hence we conclude that strong interactions increase among the unlike molecules of the mixtures with increase in temperature [72]. These are noticed in the case of V_m^E values in the binary system which are well reproduced from the evaluated properties of partial molar volumes at infinite dilution as well as at all investigated temperatures.

In **Figure 4**, the κ_s^E values for [Bmim][NTf_2]+DMC are negative over the whole composition range at all investigated temperatures. The negative κ_s^E values attributed to the strong attractive interactions between the molecules of the components [73]. This supports the inference drawn from V_m^E. The intermolecular free length indicates closer approach of unlike molecules. The trends of L_f^E values (**Figure 5**) are negative at all investigated temperatures. The negative values of L_f^E are generally observed due to the dominance of specific interactions between unlike molecules in the liquid mixture and also due to the structural readjustments in the liquid mixture towards a less compressible phase of fluid and closer packing of molecules [74]. **Figure 6** shows that the u^E values are positive for the system over the entire range of composition at all temperatures studied. Positive deviations indicate the increasing strength of interaction between component molecules of binary liquid mixtures. In general, strong interactions among the components of a mixture lead to the formation of molecular aggregates and more compact structures; then sound will travel faster through the mixture [75]. According to Ali *et al.* [76], more positive values mean much more strong interactions between the molecules.

The refractive indices (n_D) for the binary mixtures at the studied temperatures over the whole composition range are given in **Table 3** which increases with increase in the concentration of the ILs in the mixture and decreases as the temperature increases for a particular concentration

ACCEPTED MANUSCRIPT

of [Bmim][NTf_2]. The values of $\Delta_\phi n_D$ are positive over the studied range of composition for the binary mixtures (**Figure 7**) which may be attributed to the non-availability of the free volume in the mixture in comparison with the ideal mixtures. As the mole fraction of the [Bmim][NTf_2] increases, V_m^E becomes more negative because the free space available decreases in the mixtures and speed of the light travel with lesser velocity than that in the ideal mixtures [77,78]. This gives increase in refractive index (n_D) causing $\Delta_\phi n_D$ positive. Further, as temperature increases, V_m^E found to become more negative consequently $\Delta_\phi n_D$ become more positive. Thus the inference of $\Delta_\phi n_D$ also supports the increase of strength of strong interactions with increase in temperature.

The negative values of α_P^E are due to strong interactions between solute and solvent molecules [79]. **Figure 8** shows negative values of α_P^E in the whole composition range and at all investigated temperatures for the binary mixture in study. This further supports the existence of strong interactions between the constituent molecules in binary liquid solution. In **Figure 9** and **Figure 10**, the values of excess functions $\left(\frac{\partial V_m^E}{\partial T}\right)_P$ and $\left(\frac{\partial H_m^E}{\partial P}\right)_T$ are plotted against mole fraction of [Bmim][NTf_2]**.** The variation of $\left(\frac{\partial V_m^E}{\partial T}\right)_P$ and $\left(\frac{\partial H_m^E}{\partial P}\right)_T$ is similar with the mole fraction and temperature but with opposite sign. The negative values of $\left(\frac{\partial V_m^E}{\partial T}\right)_P$ for the studied mixture may be due to strong interactions existing between the unlike molecules of the mixture [80]. The isothermal pressure coefficient of excess molar enthalpy $\left(\frac{\partial H_m^E}{\partial P}\right)_T$ has positive values in the whole composition range. This reflects increase in attraction forces between two components of this mixture by increasing pressure. Hence, contraction in the volume of the mixture is still possible by increasing pressure [81].

Phase equilibria are essential for chemical separation process design. The imperfectness of the liquid phase is accounted by liquid-phase excess chemical potential by way of thermodynamic models. Experimental data are frequently unavailable over the range of conditions of interest; for this reason, the required data must be estimated using one of a variety

ACCEPTED MANUSCRIPT

of approaches. In this paper an attempt has been made to predict excess chemical potentials using 3-parameter Margules (Standard error: 0.0113), Porter (Standard error: 0.0904), Wilson (Standard error: 0.0404) and Van Laar (Standard error: 0.0340) equations at *T*=308.15 K rather calorimetric method. For the present scenario, estimated excess chemical potentials using various theories are plotted in **Figure 11** with composition of [Bmim][NTf_2] at T=308.15K. Further, it is worthy to note that the curved lines emanated from four theories show non-ideal deviation from the ideal case [82] supporting the presence of molecular interactions between the hetero molecules in study.

The non-linearity parameter (B/A) is a gauge of the non-linearity of the equation of state for a fluid. It shows a significant position in acoustics, from underwater acoustics to biology and medicine. The non-linearity parameter indicates deformation of a finite amplitude wave spreading in the liquid. Further, it can be correlated to the molecular dynamics of the medium and it can bestow information concerning structural properties of medium, internal pressure, clustering, and inter-molecular spacing, etc. Significance of the B/A parameter rises with the advancement of high-pressure technologies of food processing and preservation. Therefore, an effort has been made to assess the values of molecular properties of the liquid mixtures using non-linearity parameter (B/A) values from semi empirical relations proposed by Hartmann – Balizar (H&B) [83] and Ballou [84] with the use of Sehgal's relations [85]. The microscopic parameters pertinent to the binary liquid system like cohesive energy (**ΔA**), Van der Waal's constants (***a&b***) and the distance of closest approach (***d***) are estimated and tabulated in **Table 7**. The relevant equations pertinent to excess chemical potentials are provided in the supplementary material. It is to be noted that excess values of (B/A) are found to be negative at all temperatures. Negative/positive values of $(B/A)^E$ indicate the presence of strong/relatively weak interactions between unlike molecules [86] respectively. Thus negative values of $(B/A)^E$ also supports the existence of strong interactions in the present binary system under study.

3.1. Infrared spectral studies

The existence of strong interactions in the system which were drawn from the above inferences of derived excess/deviation parameters are well supported by IR spectral studies. The unique properties of imidazolium cations are found in their electronic structure. The electronic structure of imidazolium cations (**Figure 12**) contains delocalized 3-center-4-electron

ACCEPTED MANUSCRIPT

configuration across the N_1-C_2-N_3 moiety, a double bond between C_4 and C_5 at the opposite side of the ring, and a weak delocalization in the central region [87]. The hydrogen in C_2-H is more acidic than C_4-H, and C_5-H due to the electron deficiency in the C=N bond. The resultant acidity of the hydrogen atoms is key to understand the properties of these ionic liquids. The hydrogen on the C_2 carbon (C_2–H) has been shown to bind typically with solute molecules [88, 89].

In order to study the effects of molecular interactions, infrared absorbance are recorded from 650 cm^{-1} to 4000 cm^{-1} (**Figure 13 and Table 8**). In $[Bmim]^+$cation, the C-H stretching region from (2800 to 3200) cm^{-1} is investigated. For [Bmim][NTf_2], the signals in this region can be separated into two parts: signals between 3000 cm^{-1} and 3200 cm^{-1} can be attributed to C-H vibrational modes mainly arising from the aromatic imidazolium ring, from C_2-H and $C_{4,5}$-H stretching frequencies [90]. The signals between 2800 cm^{-1} and 3000 cm^{-1} are due to aliphatic C-H groups in the methyl and butyl moieties [91-93]. The C_2-H vibrational frequency (3120.7 cm^{-1}) is shifted to lower frequencies by about 36.5 cm^{-1} when compared to the C_4-H and C_5-H stretches (3157.2 cm^{-1}) because of its stronger acidic character. In [Bmim][NTf_2], there exist hydrogen bond between aromatic C-H hydrogen's of the cation and oxygen, fluorine atoms of the anion [94]. In the present mixtures, C_2-H and $C_{4,5}$-H stretching frequencies of the cation and SO_2 Sym Stretch, CF_3 Sym Stretch of the anion are analysed where there is no overlap from peaks of DMC. As mole fraction of IL (x_1) changes from 1.0000 to 0.7006, not very much change in the frequencies indicating the existence of ionic clusters. Further, in the region between x_1=0.7006 and $x_{1=}$0.4158, the significant change in $[NTf_2]^-$ ion frequencies indicated the formation of ion pairs from clusters. Furthermore, in DMC rich region (x_1<0.4158), complete solvation of individual ions take place. There is a slight red shift in C_2-H and $C_{4,5}$-H stretching frequencies indicating the formation of hydrogen bond between $[Bmim]^+$ and DMC. Simultaneously, a clear blue shift in SO_2 Sym Stretch, CF_3 Sym Stretch frequencies is observed because of the breakup of hydrogen bond between cation and anion of the ionic liquid. The shifts are predominant at DMC rich region.

By examining ATR-FTIR, it can be accomplished that hydrogen bonds exist extensively in such systems which play a key role towards the miscibility and stability of the [Bmim][NTf_2]+DMC binary system. Additionally, the hydrogen bonding interactions are also accountable in the present system to get complete miscibility and solvation. Hence, it can be

ACCEPTED MANUSCRIPT

assumed that the hydrogen bonds between the ionic liquid [Bmim][NTf_2] and DMC are also responsible to make a remarkable contraction in the volume of the mixture.

3.2. Prigogine-Flory-Patterson statistical theory for excess molar volume V_m^E

The Prigogine-Flory-Patterson (PFP) theory may be used to analyse and correlate the experimental excess molar volumes of binary mixtures [95-98]. We have correlated V_m^E of presently studied binary mixture using PFP theory over the entire range of mole fractions at T = (303.15-323.15) K. The PFP theory considered V_m^E for three different contributions [99]: (i) interaction contribution V_{int}^E, which is associated with intermolecular specific interaction with sign of H_m^E (ii) free volume contribution V_{fv}^E, which is associated with reduced volume to reducedtemperature ratio with negative sign (iii) internal pressure contribution,$V_{P^*}^E$, which is associated with breaking of IL structure with introduction of molecular organic solvents and changes in reduced volume of components with positive or negative sign. The detailed equations of PFP theory are given in supplementary material.

The pure components parameters for the PFP theory are included in **Table 9**. **Figure 14** indicates the composition dependence of values calculated from PFP theory for [Bmim][NTf_2]+DMC mixture compared with experimental at 303.15K. The Flory contact interaction parameter χ_{12}, the only adjustable parameter, needed in the PFP theory was obtained by experimental V_m^E values in absence of the experimental excess molar enthalpy (H_m^E). The Flory contact interaction parameter χ_{12} was found to be negative for all the investigated temperatures. The values of three contributions:V_{int}^E,V_{fv}^E and $V_{P^*}^E$, to V_m^E(PFP) at equimolar composition are summarized in **Table 10.** The first term V_{int}^E is negative which suggests that the strong interactions take place in the binary mixture. The interactional contributions are negative at all calculated temperatures. The second term V_{fv}^E was found to be negative for the system studied (**Table 10**) as V_{fv}^E is proportional to $-(\tilde{v}_1 - \tilde{v}_2)^2$ [96]. The magnitude of negative values for V_{fv}^E depends upon difference in Flory's reduced volumes ofinvolved components. Negative values of V_{fv}^E increases in magnitude as the temperatureincreases which shows that as the temperature increases, more free volume in the [Bmim][NTf_2] becomes available to accommodate the smaller DMC molecules which resulted in more negative V_m^E. The third term,

ACCEPTED MANUSCRIPT

i.e. characteristic pressure $V_{P^*}^E$, the P^* effect which depends on the relative cohesive energy of the expanded and less expanded component is found to be positive at all investigated temperatures. It is proportional to $(\tilde{V}_1 - \tilde{V}_2)(P_1^* - P_2^*)$ and can have both the negative and positive sign depending upon the magnitude of P_i^* and $\widetilde{V_i^*}$ of unlike components [104]. For the system [Bmim][NTf_2] + DMC, $V_{P^*}^E$ is positive which is related to the structure-braking effect of the DMC on the electrostatic interactions between the ions of [Bmim][NTf_2] and so the DMC molecules can be placed around the $[Bmim]^+$ and $[NTf_2]^-$ ions [96,104]. In the present system, V_{int}^E and V_{fv}^E were found to be negative while $V_{P^*}^E$ was found to be positive which shows that the interaction and free volume contributions are responsible for the overall strong interactions between solute and solvent molecules. From **Figure 14**, the V_m^E values calculated from PFP theory are in good agreement with the experimental values particularly at IL rich region. We can conclude that, it is possible to explain the volumetric behavior of [Bmim][NTf2] + DMC binary mixture by the application of the PFP theory quite successfully.

4. Conclusions

Densities, ultrasonic speed of sounds and refractive indices for binary liquids of [Bmim][NTf_2] with DMC have been measured experimentally at atmospheric pressure over the entire composition range at temperature 303.15 K, 308.15 K, 313.15 K, 318.15 K and 323.15 K. From the experimental data, excess/ deviation properties such as V_m^E, κ_S^E, L_f^E, u^E, α_P^E and $\Delta_\phi n_D$ have been evaluated. The excess and deviation parameters have been fitted to Redlich-Kister type polynomial and also corresponding standard deviations have been computed. In the present binary liquid systems of [Bmim][NTf_2] with DMC, the observed excess values clearly reflecting the dominance of strong attractive forces. The order of strong interactions follows (303.15< 308.15 <313.15 <318.15 < 323.15) K. The observed lower partial molar volumes in the liquid mixture when compared to the molar volumes of respective pure components also support the existence of strong interactions in the system. An attempt for the estimation of excess chemical potentials is made using 3-parameter Morgules, Porter, Wilson and Van Laar at T=308.15 K. Non-linear parameter (B/A) is evaluated using semi empirical relations and certain molecular properties are calculated from Sehgal's equations. Negative values of $(B/A)^E$ also support the existence of strong interaction between the components of mixture at all temperatures. The IR

ACCEPTED MANUSCRIPT

spectral studies also supported the presence of strong interaction between molecules in study. PFP theory was able to explain the volumetric behaviour of the system quite successfully.

References

[1] T.L.Greaves, C.J.Drummond, Chem.rev., 115 (2015) 11379-11448.

[2] F.Guo, S.Zhang, J.Wang, B.Teng, T.Zhang, M.Fan, Curr. Org.Chem. 19 (2015) 455-468.

[3] A.A.Shamsuri, R.Daik, Rev. Adv.Mat.Sci. 40 (2015) 45-59.

[4] C. Comminges, R. Barhdadi, M. Laurent, M. Troupel, J. Chem. Eng. Data2006, 51, 680–685.

[5] M. D. Bhatt, C. O'Dwyer, Phys. Chem. Chem. Phys. 2015, 17, 4799–4844.

[6] C. J. Allen, S. Mukerjee, E. J. Plichta, M. A. Hendrickson, K. M. Abraham, J. Phys. Chem. Lett. 2011, 2, 2420–2424.

[7] S. Park, R.J. Kazlauskas, Curr. Opin. Biotechnol. 14 (2003) 432.

[8] M. Sureshkumar, C.-K. Lee, J. Mol. Catal. B Enzym. 60 (2009) 1.

[9] M. Moniruzzaman, K. Nakashima, N. Kamiya, M. Goto, Biochem. Eng. J. 48 (2010) 295.

[10] J.V. Rodrigues, D. Ruivo, A. Rodríguez, F.J. Deive, J.M.S.S. Esperança, I.M. Marrucho, C.M. Gomes, L.P.N. Rebelo, Green Chem 16 (2014) 4520.

[11] M.N. da Graça, J.M.R. da Silva, , J.C. da Silva, M.M. Alves, , J. Mol. Catal. B Enzym. 112 (2015) 1-8.

[12] P. Lozano, T. Diego, D. Carrie, M. Vaultier, J. Iborra. Chem.Comm. 7 (2002) 692–693.

[13] M.B. Turner, S.K. Spear, J.D. Holbrey, R.D. Rogers. Biomacromolecules 5(2004)1379–1384.

[14] M.B. Turner, S.K. Spear, J.D. Holbrey, D.T. Daly, R.D. Rogers. Biomacromolecules 6 (2005) 2497–2502.

[15] S.S.Y. Tan, D.R. MacFarlane, J. Upfal, Edye LA, W.O. Doherty, A.F. Patti, J.M. Pringle, J.L. Scott. Green Chem 11 (2009) 339–345.

[16] M. Gericke, T. Liebert, T. Heinze. Macromol Biosci. 9 (2009) 343–353.

[17] M. Gericke, J. Schaller, T. Liebert, P. Fardim, F. Meister, T. Heinze. Carbohydr Polym. 89 (2012) 526–536

[18] C. Yao, J.L. Anderson, Anal. Bioanal. Chem. 395 (2009) 1491–502.

ACCEPTED MANUSCRIPT

[19] D. Hameister, S. Illner, C. Vogel, D. Michalik, U. Kragl, Sep. Purif. Technol. 132 (2014) 438-445.

[20] D. Betz, A. Raith, M. Cokoja, F.E. Kuehn, ChemSusChem. 3 (2010) 559-562.

[21] T.D. Ho, P.M. Yehl, N.P. Chetwyn, J. Wang, J.L Anderson, Q. Zhong, J. Chromatogr. A, 1361 (2014) 217-228.

[22] A. Kokorin, Ionic liquids: applications and perspectives, InTech (2011).

[23] M.H. Mabaso, G.G. Redhi, K.G. Moodley, S. African J.Chem.65 (2012) 145-149.

[24] J. Barthel, R. Neueder, H. Poepke, H. Wittmann, J. Solution Chem. 28 (1999) 489-503.

[25] A. Laheaar, H Kurig,A. Janes, E. Lust, Electrochim. Acta. 54 (2009) 4587-4594.

[26] F. Rivetti, in: P.T. Anastas, P. Tundo (Eds.), Green Chemistry: Challenging Perspectives, Oxford University Press, Oxford (2001) 201.

[27] G. Gerbaz, G. Fisicaro, in: R.L. Shubkin (Ed.), Synthetic Lubricants and High Performance Functional Fluids,Marshall Dekker, NewYork (1993) 229.

[28] B. Scrosati, Nanocomposite polymer electrolytes for lithium batteries,Chim. Ind. (Milan) 79 (1997) 463.

[29] E. Alfonsina, Andreatta, A. Alberto, E. Rodil, A. Soto, J. Solution Chem. 39 (2010) 371-383

[30] R. Zarrougui, M. Dhahbi, D. Lemordant, J. Solution Chem. 39 (2010) 921-942.

[31] E. Widowati, M. J Lee, J. Chem. Thermodyn. 63 (2013) 95-101.

[32] M. Vranes, N. Zec, A. Tot, S. A. Papovic, S. Dozic, S.Gadzuric, J. Chem. Thermodyn. 68 (2014) 98-108.

[33] M. Geppert-Rybczynska, M. Sitarek, J. Chem. Eng. Data 59 (2014) 1213-1224.

[34] M. Vranes, S. AnaPapovic, A. Tot, N. Zec, S.Gadzuric, J. Chem.Thermodyn. 76 (2014) 161-171.

[35] R. Salinas, J. Pla-Franco, E. Lladosa,Juan B. Monto, J. Chem. Eng. Data 60(2015) 525-540.

[36] J. Jacquemin, P. Husson, A.A. Padua, V. Majer, Green Chem. 8 (2006) 172-180.

[37] M. AzlanKassim, N. AsrinaSairi, R. Yusoff, A. Ramalingam, Y. Alias, M. K. Aroua, Thermochim. Acta 639 (2016) 130-147

[38] T. Srinivasa Krishna, Anil K. Nainb, S. Chentilnathc, D. Punyaseshadud, B. Munibhadrayyae, J. Chem. Thermodyn. 101 (2016) 103-114.

ACCEPTED MANUSCRIPT

[39] W. L. Armarego, C. L. L. Chai, Purification of laboratory chemicals. Butterworth-Heinemann (2013).

[40] E. Scholz, Karlfisher titration, Springer-Verlag: Berlin (1984).

[41] R. Ren, Y. Zuo, Q. Zhou, H. Zhang, S. Zhang, Density, J. Chem. Eng. Data 56 (2010) 27-30.

[42] A. B. Pereiro, A. Rodriguez, J. Canosa, J.Tojo, J. Chem. Eng. Data 2004, 49, 1392-1399

[43] S. H. Shin, I. Y. Jeong, Y. S. Jeong, S. J. Park, Fluid Phase Equilib. 376 (2014) 105-110.

[44] J. Troncoso, C.A. Cerdeirin, Y.A. Sanmamed, L. Roman, L. Paulo, N. Rebelo, J. Chem. Eng. Data 51 (2006) 1856-1859.

[45] B.R.Arbad, M.K.Lande, N. N. Wankhede, D.S.Wankhede, J. Chem. Eng. Data51 (2006) 68-72.

[46] R. Hamidova, I. Kul, J. Safarov, A. Shahverdiyev, E. Hassel, 2015. Braz. J. Chem. Eng. 32 (2015) .303-316.

[47] Y. Hiraga, A. Kato, Y. Sato, R.L. Smith Jr, J. Chem. Eng. Data, 60 (2015).876-885.

[48] M. Kanakubo, K.R. Harris, J. Chem. Eng. Data. 60 (2015) 1408-1418.

[49] C.A.N. de Castro, E. Langa, A.L. Morais, M.L.M. Lopes, M.J. Lourenço, F.J. Santos, M.S.C. Santos, J.N.C. Lopes, H.I. Veiga, M. Macatrão, J.M. Esperança, Fluid Phase Equilib., 294 (2010).157-179.

[50] J. Jacquemin, P. Husson, V. Mayer, I. Cibulka, J. Chem. Eng. Data, 52 (2007) 2204-2211.

[51] M.R. Currás, P. Husson, A.A. Pádua, M.F. Costa Gomes, J. García, Ind.Eng.Chem. Res., 53 (2014) 10791-10802.

[52] R.G. De Azevedo, J.M.S.S. Esperanca, J. Szydlowski, Z.P. Visak, P.F. Pires, H.J.R. Guedes, L.P.N. Rebelo, J. Chem. Thermodyn., 37 (2005) 888-899.

[53] N.I. Malek, S.P. Ijardar, J. Chem. Thermodyn., 93 (2016) 75-85.

[54] M.G. Montalban, C.L. Bolivar, F.G. Díaz Baños, G. Villora, J. Chem. Eng. Data, 60 (2015) 1986-1996.

[55] M. Tariq, P.A.S. Forte, M.C. Gomes, J.C. Lopes, L.P.N. Rebelo, J. Chem. Thermodyn., 41 (2009) 790-798.

[56] M.J.P. Comuñas, A. Baylaucq, C. Boned, J. Fernández, Int. J. thermophy., 22 (2001) 749-768.

ACCEPTED MANUSCRIPT

[57] J. Troncoso, D. Bessières, C.A. Cerdeiriña, E. Carballo, L. Romaní, J. Chem. Eng. Data, 49 (2004) 923-927.

[58] J. Zhou, R. Zhu, H. Xu, Y. Tian,. J. Chem. Eng. Data, 55 (2010) 5569-5575.

[59] A. Gayol, L.M. Casás, R.E. Martini, A.E. Andreatta, J.L. Legido, J. Chem. Thermodyn., 58 (2013) 245-253.

[60] W.V. Steele, R.D. Chirico, S.E. Knipmeyer, A. Nguyen J. Chem. Eng. Data, 42 (1997) 1008-1020.

[61] F. Chen, Z. Yang, Z. Chen, J. Hu, C. Chen, J. Cai, J. Mol. Liq., 209 (2015) 683-692.

[62] A. Rodriguez, J. Canosa, J. Tojo, J. Chem. Eng. Data, 46 (2001) 1476-1486.

[63] J.M. Pardo, D. González-Salgado, C.A. Tovar, C.A. Cerdeiriña, E. Carballo, L. Romaní, Can. J. Chem., 80 (2002).370-378.

[64] L. Mosteiro, A.B. Mariano, L.M. Casás, M.M. Piñeiro, J.L. Legido, J. Chem. Eng. Data, 54 (2009) 1056-1062.

[65] A. Pal, A. Kumar, J. Chem. Eng. Data, 43 (1998) 143-147.

[66] M. Moosavi, A. Motahari, A. Vahid, V. Akbar, A.A. Rostami, A. Omrani, J. Chem. Eng. Data, 61 (2016) 1981-1991.

[67] G.C. Benson, O. Kiyohara, J. Chem. Eng. Data 21 (1976) 362-365.

[68] G. Douheret, M.I. Davis, J.C.R. Reis, M.J. Blandamer, Chem.Phys.Chem. 2 (2001) 148-161.

[69] A.J. Costa, J. M. Esperanca I.M. Marrucho, L.P.N. Rebelo, J. Chem. Eng. Data 56 (2011) 3433-3441.

[70] M.S. Reddy, Sk. Md Nayeem, C. Soumini, K.T.S.S. Raju, B.H. Babu, Thermochim. Acta. 630 (2016) 37-39.

[71] S.M. Nayeem, M. Kondaiah, K. Sreekanth, M.S. Reddy, D.K. Rao, J. Therm. Anal. Calorim. 123 (2016) 2241-2255.

[72] M.S. Reddy, K.T.S.S. Raju, A.S. Rao, N. Sharmila, B.H. Babu, J. Chem. Thermodyn. 101 (2016) 139-149.

[73] P.K. Chhotaray, S. Jella, R.L. Gardas, J. Mol. Liq. 219 (2016) 829-844.

[74] M.S. Reddy, Sk.Md. Nayeem, K.T.S.S. Raju, B.H. Babu, J. Therm. Anal. Calorim. 124 (2016) 959-971.

ACCEPTED MANUSCRIPT

[75] M. S. Reddy, K.T.S.S. Raju, Sk.Md. Nayeem, I. Khan, K.B.M. Krishna, B.H. Babu, J. Solution Chem. 45 (2016) 675-701.

[76] A. Ali, F. Nabi, M. Tariq , Int. J. Thermophy. 30 (2009) 464-474.

[77] E. Vercher, J.L. Francisco, A. Vicenta Gonzalez, J.M. Pablo, O. Vicent, M.A. Antoni, J. Chem.Thermodyn. 90 (2015) 174-184.

[78] Z. Vaid, U.U. More, R.L. Gardas, N.L. Malek, S.P. Ijardar, J. Solution Chem. 44(2015) 718-741.

[79] A. Ali, M. Tariq, J. Pure. App. Ultrason. 28 (2006) 99.

[80] M.S. Reddy, Sk.Md. Nayeem, K.T.S.S. Raju, A.S. Rao, B.H. Babu, J. Mol. Liq. 218 (2016) 83-94.

[81] C. Roth, A. Appelhagen, N. Jobst, R. Ludwig, Chem. Phys. Chem. 13 (2012) 1708-1717.

[82] Sk.Md. Nayeem, I. Khan, Sk. Nyamathulla, D.S. Rao, P. Indira, M.S. Reddy, J. Mythri, P.N. Kumari. Procg of National seminar on 20-21 of Dec, 2016; ISBN: 978-93-85132-12-4.

[83] B. Hartmann. J. Acoust. Soc. Am. 65 (1979) 1392-1396.

[84] A.B. Copens, R.T. Beyer, J. Ballou. . J. Acoust. Soc. Am. 41 (1967) 1443-1448.

[85] J. Jugan, M.A. Khadar. J Mol Liq. 100 (2002) 217-227.

[86] Sk.Md. Nayeem, S. Nyamathulla, I. Khan, D.K. Rao. J Mol Liq. 218 (2016) 676–85.

[87] P.A. Hunt, B. Kirchner, T. Welton, Chemi. A Europ. J. 12 (2006) 6762-6775.

[88] A. Aggarwal, N.L. Lancaster, A.R. Sethi, T. Welton, Green Chem. 4 (2002) 517-520.

[89] V. Znamenskiy, M.N. Kobrak, J. Phys. Chem. B. 108 (2004) 1072-1079.

[90] N.R. Dhumal, H.J. Kim, J. Kiefer, J. Phys. Chem. A. 115 (2011) 3551-3558.

[91] J. C. Lassegues, J. Grondin, D. Cavagnat, P. Johansson, New interpretation of the CH stretching vibrations in imidazolium-based ionic liquids,J. Phys. Chem. A. 113 (2009) 6419-6421.

[92] J. C. Lassegues, J. Grondin, D. Cavagnat, P. Johansson, J. Phys. Chem. A. 114 (2009) 687-688.

[93] J. Grondin, J. C. Lassegues, D. Cavagnat, T. Buffeteau, P. Johansson, R. Holomb, J. Raman Spectro. 42 (2011) 733-743.

[94] N. Kristina, P. S. Schulz, P. Natalia, K. Johannes, P. Wasserscheid, A. Leipertz, Phys. Chem. Chem. Phys., 12(2010) 14153-14161

ACCEPTED MANUSCRIPT

[95] E. Vercher, F. J. Llopis, M. V. Gonzalez-Alfaro, A. M. Andreu, J. Chem. Eng. Data 55(2010) 1377-1388 .

[96] D. Patterson, G. Delmas, Discuss. Faraday Soc. 49(1970) 98-105.

[97] M. T. Zafarani-Moattar, H. Shekaari, J. Chem. Thermodyn. 38(2006) 1377-1384.

[98] F. Kermanpour, H. Z. Niakan, J. Chem. Thermodyn. 48(2012) 129-139 .

[99] R.B. Torres, M.I. Ortolan, P.L.O. Volpe, J. Chem. Thermodyn. 40 (2008) 442-459.

[100] P. J. Flory, J. Am. Chem. Soc. 87(1965) 1833-1838 .

[101] A. Abe, P. J. Flory, J. Am.Chem. Soc. 87 (1965) 1838-1846.

[102] E. Vercher, A. V. Orchilles, P. J. Miguel, A. M. Andreu, J. Chem. Eng. Data 52(2007) 1468-1482.

[103] A. Kumar, T. Singh, R. L. Gardas, J.A. Coutinho, J. Chem. Thermodyn. 40 (2008) 32-39.

[104] Z. S. Vaid, U. U More,S. B. Oswal, N.I. Malek, Thermochim.Acta, 634 (2016) 38-47.

ACCEPTED MANUSCRIPT

ACCEPTED MANUSCRIPT

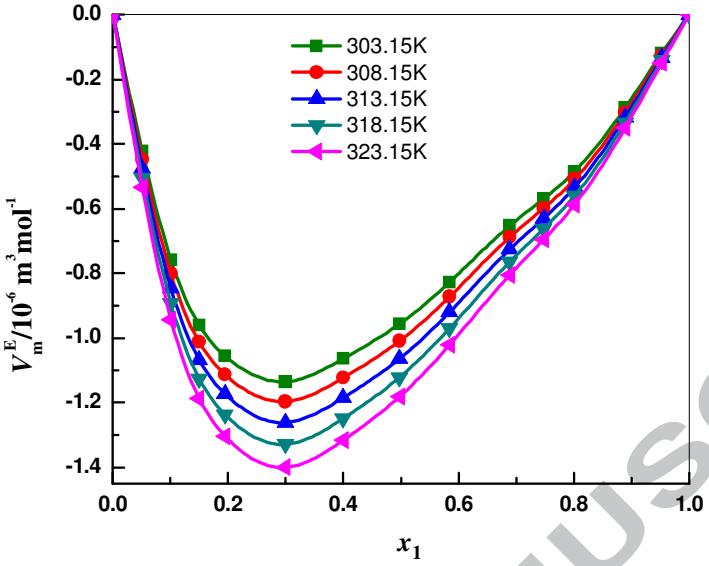


Fig. 1 Plots of excess molar volume (V_m^E) against mole fraction of [Bmim][NTF_2] in the mixture with DMC at different temperatures**.**

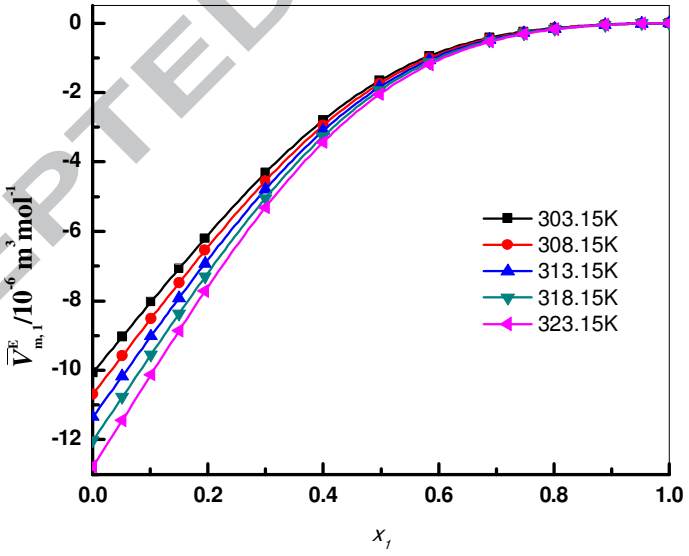


Fig.2 Plots of excess partial molar volume ($\overline{V}_{m,1}^E$) against mole fraction of [Bmim][NTF_2] in the mixture with DMC at different temperatures.

ACCEPTED MANUSCRIPT

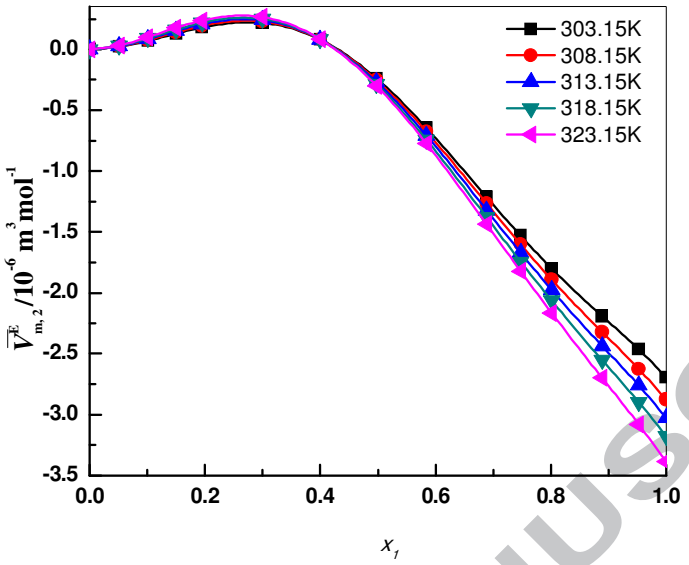
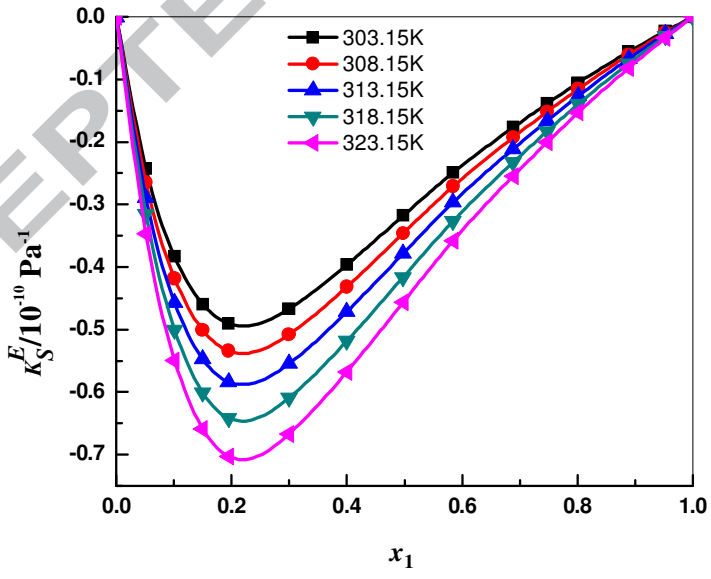


Fig. 3 Plots of excess partial molar volume ($\overline{V}^{E}_{m,2}$) against mole fraction of [Bmim][NTF_2] in the mixture with DMC at different temperatures.



c

Fig. 4 Plots of excess isentropic compressibility (κ_S^E) against mole fraction of [Bmim][NTF_2] in the mixture with DMC at different temperatures.

ACCEPTED MANUSCRIPT

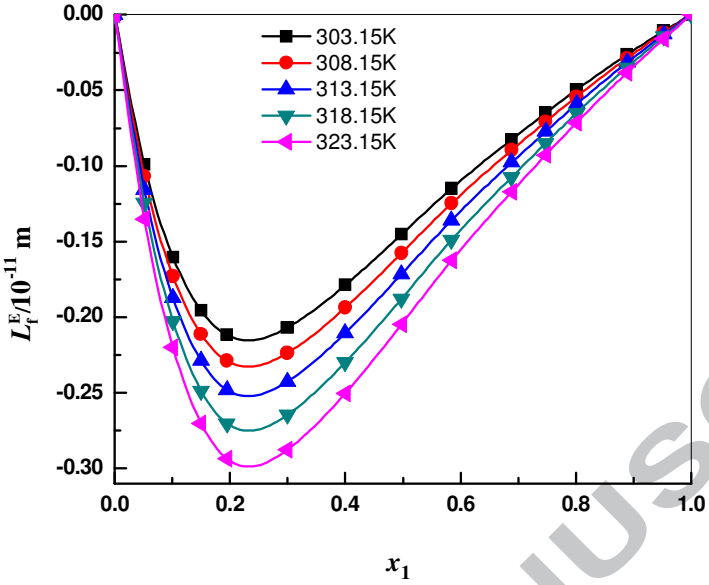


Fig. 5 Plots of excess free length (L_f^E) against mole fraction of [Bmim][NTF_2] in the mixture with DMC at different temperatures.

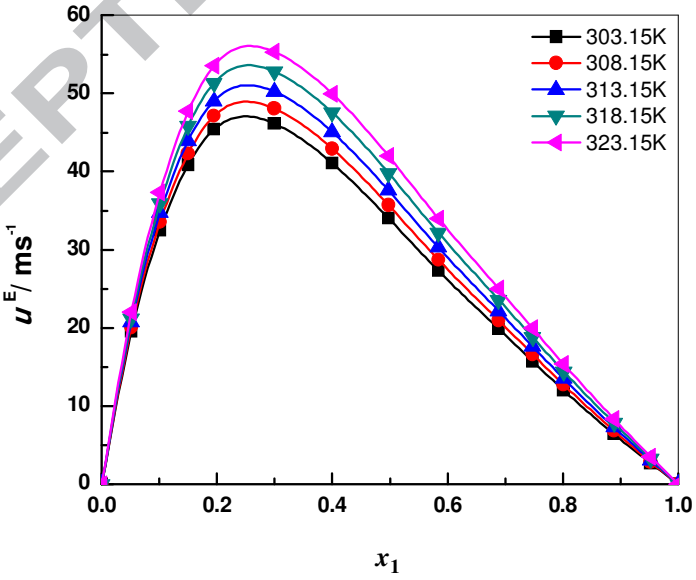


Fig.6 Plots of Excess ultrasonic speed of sounds (u^E) against mole fraction of [Bmim][NTF_2] in the mixture with DMC at different temperatures.

ACCEPTED MANUSCRIPT

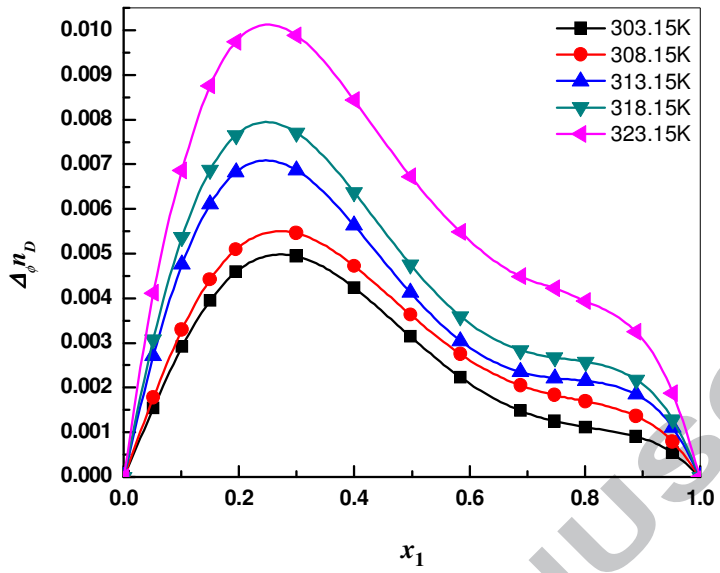


Fig. 7 Plots of deviation in refractive index ($\Delta_\phi n_D$) against mole fraction of [Bmim][NTF_2] in the mixture with DMC at different temperatures.

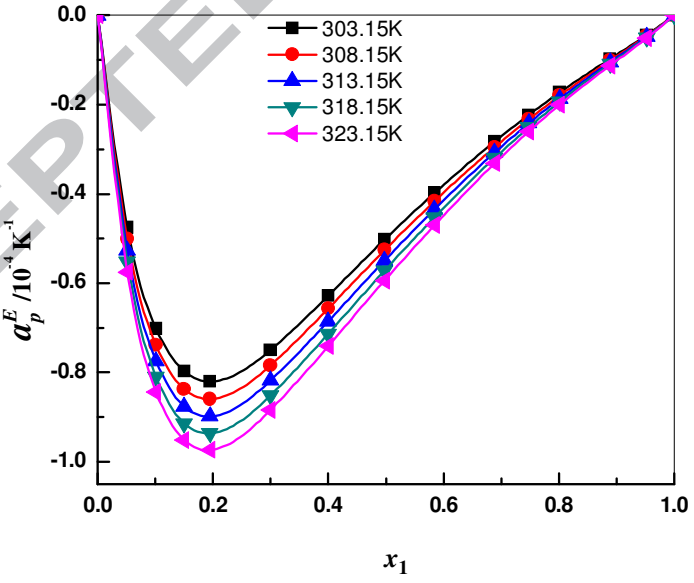


Fig. 8 Plots of Excess isobaric thermal expansion coefficient (α_P^E) against mole fraction of [Bmim][NTF_2] in the mixture with DMC at different temperatures.

ACCEPTED MANUSCRIPT

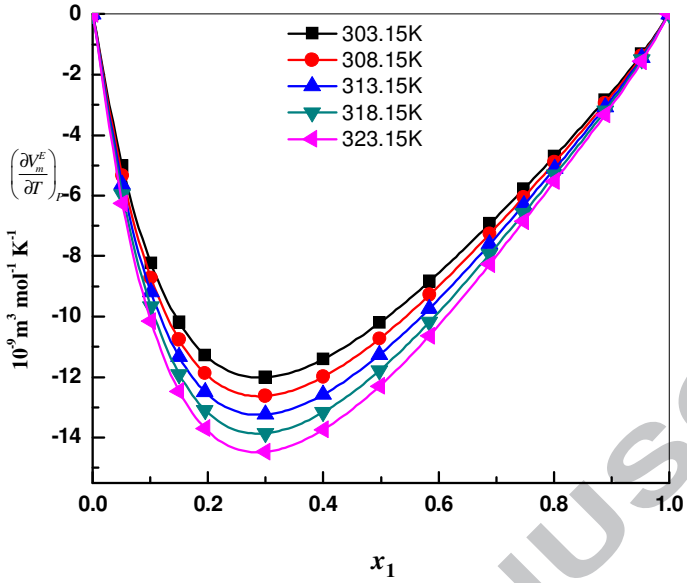


Fig. 9 Plots of $\left(\frac{\partial V_m^E}{\partial T}\right)_P$ against mole fraction of [Bmim][NTF_2] in the mixture with DMC at different temperatures.

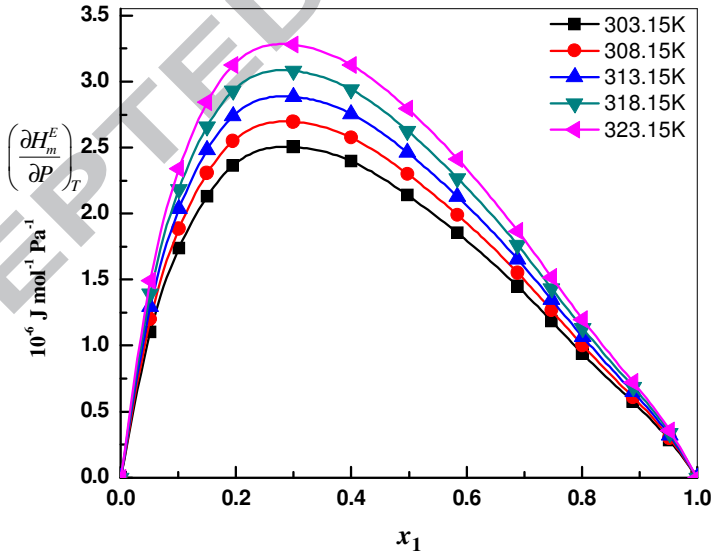


Fig. 10 Plots of $\left(\frac{\partial H_m^E}{\partial P}\right)_T$ against mole fraction of [Bmim][NTF_2] in the mixture with DMC at different temperatures.

ACCEPTED MANUSCRIPT

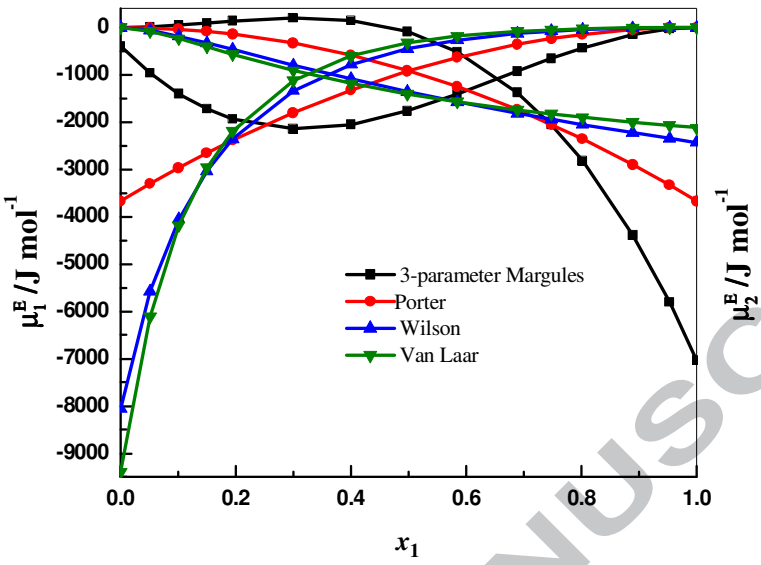
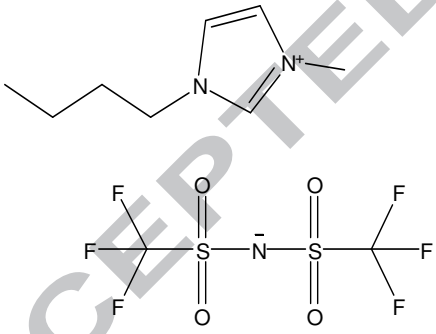
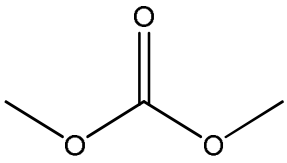


Fig.11 Variation of excess chemical potentials μ_1^E ([Bmim][NTF_2]) and μ_2^E (DMC) with mole fraction, x_1 of [Bmim][NTf_2] for 3-parameter Margules, Porter, Wilson and Van Laar at T=308.15 K.



1-Butyl-3-methylimidazolium bis(trifluoromethylsulfonyl)imide



dimethylcarbonate

Fig.12 Chemical Structures of ([Bmim][NTf_2]) and DMC.

ACCEPTED MANUSCRIPT

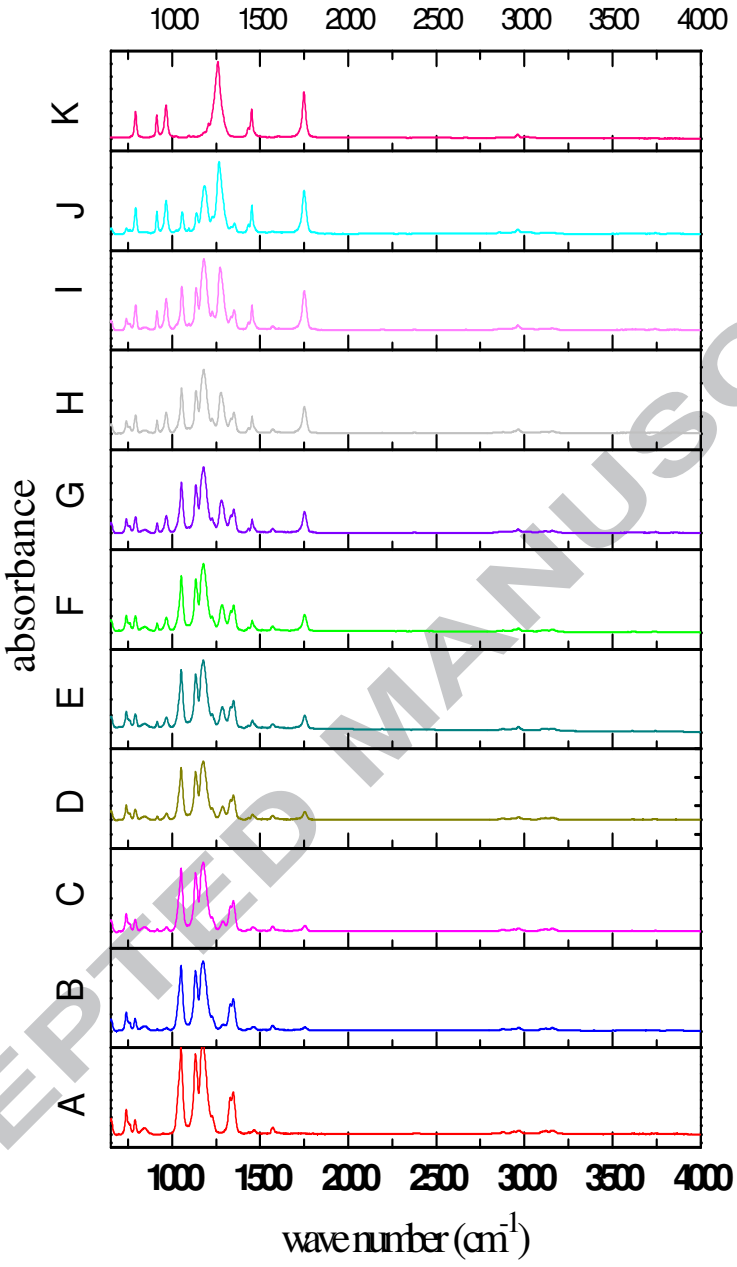


Fig.13 Infrared spectra of (A) Pure IL [Bmim][NTf_2], (B) 0.8990; (C) 0.8055; (D) 0.7006; (E) 0.6001; (F) 0.5024; (G) 0.4158; (H) 0.3114; (I) 0.2525; (J) 0.1110 and (K) Pure DMC. (B), (C), (D), (E), (F), (G), (H), (I), (J) represents mole fraction of [Bmim][NTf_2] in the mixture with DMC.

ACCEPTED MANUSCRIPT

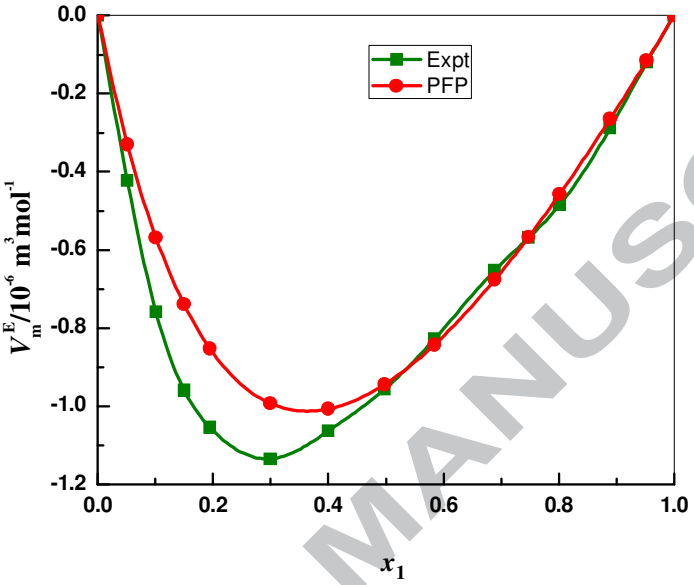


Fig. 14 Plots of excess molar volumes (V_m^E) of experimental and calculated from PFP theory against mole fraction of [Bmim][NTf_2] in the mixture with DMC at 303.15K**.**

ACCEPTED MANUSCRIPT

ACCEPTED MANUSCRIPT

Table 1 List of chemicals with details of Provenance, CAS number, and mass fraction purity.

Chemical name (CAS number)	Provenance	Purification method	Mass fraction purity	Analysis method	Final water mass fraction	Water Analysis method
1-butyl-3-methylimidazoliumbis (trifluoromethylsulfonyl)imide (174899-83-3)	Io-Li-Tec, Germany	Vacuum treatment	0.99*	NA	$<1.5\times10^{-4}$	K.F
Dimethyl carbonate (616-38-6)	Sigma Aldrich	Distillation	0.995	GC	$<1.5\times10^{-4}$	K.F

*Purity as given by the suppliers, K.F= Karl Fisher Titrator, GC= Gas Chromatography.

ACCEPTED MANUSCRIPT

ACCEPTED MANUSCRIPT

Table 2 Comparison of experimental values of density, ρ, speed of sound, u, refractive index, n_D, and specific heat, C_p, of pure liquids with the corresponding literature values at different temperatures and at atmospheric pressure P = 101.3 kPa.

Liquid	T / K	ρ /kg·m^{-3}		u/m·s^{-1}		n_D		C_p/J·K^{-1}·mol^{-1}
		Expt.	Lit.	Expt.	Lit.	Expt.	Lit.	Lit.
[Bmim][NTF_2]	303.15	1428.9	1429.40[32] 1429.31[44] 1430.81[54]	1216.8	1216.77[38] 1217.5[53]	1.4245	1.42523[38] 1.4250[54]	569.74[44]
	308.15	1424.1	1424.57[32] 1424.54[44]	1205.8	1205.80[38] 1205.23[53]	1.4231	1.42374[38]	572.82[44]
	313.15	1419.4	1419.61[32] 1419.78[44] 1420.16[54]	1195.0	1194.95[38] 1194.36[53]	1.4210	1.42225[38] 1.4214[54]	575.56[44]
	318.15	1414.6	1414.67[32] 1415.04[44]	1184.2	1184.23[38] 1184.54[53]	1.4195	1.42076[38]	578.49[44]
	323.15	1409.9	1409.65[32] 1410.31[44] 1411.55[54]	1173.6	1173.61[38] 1171.35[53]	1.4173	1.41923[38] 1.4185[54]	581.68[44]
Dimethyl carbonate	303.15	1056.8	1056.719[41] 1056.632[61]	1177.3	1177[42] 1177[62] 1173.5[64]	1.3648	1.3640[43] 1.36414[62]	159.8[45]
	308.15	1050.2	1050.071[41] 1049.983[61]	1155.6	1155[42] 1151.5[64]	1.3629	1.3618[43] 1.3661[64]	161.7[45]
	313.15	1043.5	1043.388[41] 1043.307[61]	1134.2	1134[42] 1135[62]	1.3626	1.3595[43] 1.35932[62]	162.9[45]
	318.15	1036.8	1036.687[41] 1036.59[61]	1113.1	-	1.3601	1.3570[43] 1.3629[64]	163.0[45]
	323.15	1030.0	1029.939[41] 1029.843[61]	1092.2	-	1.3586	-	163.6[45]

Standard uncertainties u are: u (ρ) = 1 kg·m^{-3},u (u) = 0.5 m·s^{-1}, u (n_D) = 0.0005,u (T) = 0.01 K and u(P)=0.5 kPa

ACCEPTED MANUSCRIPT

ACCEPTED MANUSCRIPT

Table 3 Experimental density (ρ), speed of sound (u), refractive index (n_D), molar volume (V_m),Isentropic compressibility(κ_s),free length (L_f)and isobaric thermal expansion coefficient (α_p) with mole fraction (x_1) of [Bmim][NTF_2] in the binary liquid mixture of {[Bmim][NTF_2]+Dimethyl Carbonate} from T/K = 303.15 to 323.15 at pressure P = 101.3 kPa.

x_1	ρ / kg·m^{-3}	u / m·s^{-1}	n_D	V_m/ 10^{-6} m^3·mol^{-1}	κ_s / 10^{-10}Pa^{-1}	L_f /10^{-11}m	α_p /10^{-4} K^{-1}
303.15 K							
0.0000	1056.8	1177.3	1.3648	85.24	6.83	5.423	12.54
0.0512	1120.1	1187.0	1.3757	95.48	6.34	5.225	11.15
0.1010	1168.9	1196.1	1.3844	105.51	5.98	5.076	10.21
0.1495	1207.1	1203.7	1.3913	115.41	5.72	4.963	9.54
0.1945	1236.1	1209.2	1.3965	124.69	5.53	4.882	9.07
0.2994	1288.3	1215.4	1.4053	146.45	5.25	4.758	8.32
0.3999	1324.3	1217.4	1.4106	167.44	5.09	4.685	7.85
0.4976	1351.4	1217.7	1.4141	187.90	4.99	4.637	7.53
0.5842	1370.7	1217.4	1.4165	206.06	4.92	4.605	7.31
0.6886	1389.7	1217.4	1.4191	227.99	4.86	4.573	7.11
0.7475	1399.0	1217.2	1.4204	240.33	4.82	4.559	7.01
0.8014	1406.6	1217.0	1.4216	251.65	4.80	4.547	6.93
0.8890	1417.4	1216.8	1.4233	270.09	4.76	4.531	6.82
0.9526	1424.2	1216.8	1.4242	283.49	4.74	4.520	6.75
1.0000	1428.9	1216.8	1.4245	293.48	4.73	4.513	6.71
308.15 K							
0.0000	1050.2	1155.6	1.3629	85.78	7.13	5.592	12.68
0.0512	1113.8	1167.2	1.3741	96.01	6.59	5.377	11.25
0.1010	1163.0	1177.7	1.3830	106.05	6.20	5.215	10.28
0.1495	1201.3	1186.5	1.3900	115.96	5.91	5.093	9.60
0.1945	1230.5	1192.9	1.3953	125.26	5.71	5.005	9.12
0.2994	1282.9	1200.7	1.4042	147.06	5.41	4.870	8.35
0.3999	1319.1	1203.8	1.4095	168.10	5.23	4.790	7.87
0.4976	1346.3	1204.9	1.4131	188.61	5.12	4.737	7.54

ACCEPTED MANUSCRIPT

ACCEPTED MANUSCRIPT

0.5842	1365.6	1205.0	1.4155	206.82	5.04	4.703	7.32
0.6886	1384.8	1205.5	1.4181	228.80	4.97	4.669	7.11
0.7475	1394.1	1205.6	1.4195	241.17	4.94	4.653	7.01
0.8014	1401.8	1205.6	1.4207	252.52	4.91	4.640	6.93
0.8890	1412.6	1205.6	1.4223	271.01	4.87	4.622	6.82
0.9526	1419.4	1205.7	1.4230	284.45	4.85	4.610	6.75
1.0000	1424.1	1205.8	1.4231	294.47	4.83	4.602	6.71
313.15 K							
0.0000	1043.5	1134.2	1.3626	86.33	7.45	5.767	12.83
0.0512	1107.5	1147.5	1.3744	96.56	6.86	5.533	11.35
0.1010	1157.0	1159.4	1.3836	106.60	6.43	5.358	10.36
0.1495	1195.5	1169.4	1.3907	116.52	6.12	5.226	9.65
0.1945	1224.9	1176.8	1.3959	125.83	5.90	5.131	9.16
0.2994	1277.6	1186.2	1.4042	147.68	5.56	4.984	8.37
0.3999	1313.9	1190.3	1.4089	168.77	5.37	4.897	7.89
0.4976	1341.2	1192.1	1.4119	189.32	5.25	4.840	7.55
0.5842	1360.7	1192.8	1.4140	207.58	5.17	4.803	7.33
0.6886	1379.8	1193.7	1.4166	229.62	5.09	4.765	7.11
0.7475	1389.2	1194.0	1.4180	242.02	5.05	4.748	7.01
0.8014	1396.9	1194.2	1.4193	253.40	5.02	4.734	6.93
0.8890	1407.8	1194.5	1.4208	271.93	4.98	4.715	6.82
0.9526	1414.6	1194.8	1.4213	285.41	4.95	4.702	6.75
1.0000	1419.4	1195.0	1.4210	295.46	4.93	4.694	6.71
318.15 K							
0.0000	1036.8	1113.1	1.3601	86.88	7.78	5.948	12.98
0.0512	1101.2	1127.6	1.3724	97.11	7.14	5.697	11.45
0.1010	1151.0	1141.0	1.3819	107.15	6.67	5.507	10.43
0.1495	1189.8	1152.4	1.3892	117.09	6.33	5.363	9.71
0.1945	1219.3	1160.8	1.3946	126.41	6.09	5.260	9.21
0.2994	1272.2	1171.7	1.4030	148.30	5.73	5.101	8.40
0.3999	1308.8	1176.9	1.4077	169.43	5.52	5.007	7.91

ACCEPTED MANUSCRIPT

0.4976	1336.2	1179.5	1.4107	190.04	5.38	4.945	7.56
0.5842	1355.7	1180.6	1.4128	208.34	5.29	4.904	7.33
0.6886	1374.9	1182.1	1.4154	230.43	5.20	4.864	7.12
0.7475	1384.3	1182.6	1.4168	242.87	5.16	4.845	7.02
0.8014	1392.1	1183.0	1.4181	254.28	5.13	4.830	6.93
0.8890	1403.0	1183.6	1.4196	272.86	5.09	4.809	6.81
0.9526	1409.9	1184.0	1.4199	286.38	5.06	4.795	6.74
1.0000	1414.6	1184.2	1.4195	296.45	5.04	4.786	6.70
323.15 K							
0.0000	1030.0	1092.2	1.3586	87.45	8.14	6.135	13.13
0.0512	1094.9	1108.3	1.3719	97.67	7.44	5.864	11.56
0.1010	1145.0	1123.0	1.3817	107.72	6.92	5.659	10.51
0.1495	1184.0	1135.6	1.3893	117.66	6.55	5.504	9.77
0.1945	1213.7	1144.9	1.3948	127.00	6.29	5.392	9.26
0.2994	1266.9	1157.4	1.4033	148.92	5.89	5.220	8.44
0.3999	1303.6	1163.6	1.4078	170.11	5.67	5.119	7.93
0.4976	1331.1	1166.9	1.4106	190.76	5.52	5.051	7.58
0.5842	1350.7	1168.6	1.4126	209.10	5.42	5.008	7.34
0.6886	1370.1	1170.5	1.4149	231.26	5.33	4.964	7.12
0.7475	1379.5	1171.3	1.4162	243.73	5.28	4.943	7.02
0.8014	1387.3	1171.8	1.4172	255.16	5.25	4.927	6.93
0.8890	1398.2	1172.7	1.4185	273.79	5.20	4.904	6.81
0.9526	1405.1	1173.3	1.4183	287.34	5.17	4.890	6.74
1.0000	1409.9	1173.6	1.4173	297.44	5.15	4.880	6.70

Standard uncertainties u are: u (x_1) = 0.0005, u (ρ) = 1 kg·m^{-3},u (u) = 0.5 m·s^{-1}, u (n_D) = 0.0005, u (T) = 0.01 K and $u(P)$=0.5kPa Combined uncertainties (Confidence level, 95%).: $U_c(V_m) = \pm 0.01 \times 10^{-6}$ m^3·mol^{-1},$U_c(\kappa_S) = \pm 0.01\times10^{-10}$ Pa^{-1},$U_c(L_f) = \pm 0.004\times10^{-11}$ m, $U_c(\alpha_p) = \pm 0.02\times10^{-4}$ K^{-1}. All the experiments were carried out at atmospheric pressure.

ACCEPTED MANUSCRIPT

ACCEPTED MANUSCRIPT

Table 4 Redlich-Kister coefficients of deviation/excess properties and corresponding standard deviations (σ) for the systems at different temperatures

	T/K	A_0	A_1	A_2	A_3	A_4	σ
V_m^E /10^{-6} m^3·mol^{-1}	303.15	-3.7691	2.7718	-3.1693	0.9125	0.5598	0.0116
	308.15	-3.9776	2.9260	-3.2755	0.9779	0.4746	0.0116
	313.15	-4.1973	3.0796	-3.3947	1.0777	0.4088	0.0116
	318.15	-4.4264	3.2397	-3.5207	1.1823	0.3486	0.0118
	323.15	-4.6667	3.4168	-3.6344	1.2738	0.2268	0.0118
κ_s^E /10^{-10} Pa^{-1}	303.15	-1.2590	1.6018	-1.5522	1.1085	-0.3642	0.0009
	308.15	-1.3716	1.7399	-1.6863	1.2149	-0.4139	0.0010
	313.15	-1.4992	1.8959	-1.8365	1.3357	-0.4696	0.0011
	318.15	-1.6475	2.0902	-2.0444	1.4293	-0.4468	0.0016
	323.15	-1.8056	2.2819	-2.2271	1.5892	-0.5319	0.0017
u^E/ m·s^{-1}	303.15	134.83	-155.38	131.88	-47.51	-17.82	0.19
	308.15	141.47	-161.03	135.73	-46.27	-20.48	0.20
	313.15	148.90	-167.28	139.80	-44.99	-23.30	0.21
	318.15	157.59	-175.62	147.18	-40.03	-33.20	0.27
	323.15	166.23	-182.49	151.30	-39.45	-34.95	0.29
L_f^E/(10^{-11} m)	303.15	-0.5757	0.7055	-0.6564	0.3768	-0.0557	0.0005
	308.15	-0.6244	0.7609	-0.7064	0.4041	-0.0616	0.0006
	313.15	-0.6793	0.8228	-0.7615	0.4346	-0.0678	0.0007
	318.15	-0.7429	0.8996	-0.8382	0.4507	-0.0399	0.0010
	323.15	-0.8100	0.9741	-0.9033	0.4909	-0.0533	0.0010
α_P^E 10^{-4} K^{-1}	303.15	-2.0062	2.3457	-2.2104	2.9501	-2.3566	0.0058
	308.15	-2.0998	2.4468	-2.2782	3.1473	-2.5624	0.0062
	313.15	-2.1919	2.5464	-2.3451	3.3387	-2.7621	0.0066

ACCEPTED MANUSCRIPT

ACCEPTED MANUSCRIPT

	318.15	-2.2829	2.6448	-2.4102	3.5244	-2.9575	0.0070
	323.15	-2.3725	2.7411	-2.4742	3.7052	-3.1455	0.0074
	303.15	0.01245	-0.02333	0.01845	0.01435	-0.00846	0.00002
	308.15	0.01069	-0.01352	0.03020	-0.02158	-0.00363	0.00059
	313.15	0.01634	-0.02940	0.03592	0.01380	-0.00810	0.00002
$\Delta_{\phi} n_D$	318.15	0.01884	-0.03157	0.04000	0.01390	-0.00815	0.00002
	323.15	0.02677	-0.03442	0.04592	0.01220	-0.00213	0.00005
	303.15	-40.7100	29.0818	-22.2609	15.2811	-11.9823	0.00002
$\left(\frac{\partial V_m^E}{\partial T}\right)_P$	308.15	-42.7938	30.5777	-22.8838	16.9091	-13.9121	0.00002
	313.15	-44.8774	32.0734	-23.5063	18.5380	-15.8427	0.00001
/10^{-9} m^3·mol^{-1}·K^{-1}	318.15	-46.9612	33.5688	-24.1286	20.1673	-17.7740	0.00001
	323.15	-49.0449	35.0647	-24.7526	21.7959	-19.7029	0.00002
	303.15	8.5721	-6.0444	3.5792	-3.7197	4.1920	0.0116
$\left(\frac{\partial H_m^E}{\partial P}\right)_T$	308.15	9.2093	-6.4965	3.7762	-4.2328	4.7616	0.0116
	313.15	9.8560	-6.9642	3.9665	-4.7275	5.3698	0.0116
/10^{-6} J·mol^{-1}·Pa^{-1}	318.15	10.5142	-7.4404	4.1562	-5.2338	6.0028	0.0118
	323.15	11.1822	-7.9144	4.3643	-5.7694	6.5939	0.0118

ACCEPTED MANUSCRIPT

ACCEPTED MANUSCRIPT

Table 5 Partial molar volumes of component-1 ($\overline{V}_{m,1}$) ([Bmim][NTF_2])and component-2($\overline{V}_{m,2}$) (Dimethyl Carbonate) with mole fraction (x_1) of [Bmim][NTF_2] in the binary liquid mixture from T/K =303.15 to 323.15 at pressure P = 101.3 kPa.

x_1	303.15 K		308.15 K		313.15 K		318.15 K		323.15 K	
	$\overline{V}_{m,1}$	$\overline{V}_{m,2}$	$\overline{V}_{m,1}$	$\overline{V}_{m,2}$	$\overline{V}_{m,1}$	$\overline{V}_{m,2}$	$\overline{V}_{m,1}$	$\overline{V}_{m,2}$	$\overline{V}_{m,1}$	$\overline{V}_{m,2}$
	/ 10^{-6} $m^3 \cdot mol^{-1}$		/ 10^{-6} $m^3 \cdot mol^{-1}$		/ 10^{-6} $m^3 \cdot mol^{-1}$		/ 10^{-6} m^3 mol^{-1}		/ 10^{-6} $m^3 \cdot mol^{-1}$	
0.0000	283.42	85.24	283.79	85.78	284.12	86.33	284.43	86.88	284.68	87.45
0.0512	284.45	85.26	284.88	85.80	285.29	86.35	285.68	86.91	286.01	87.48
0.1010	285.45	85.31	285.95	85.85	286.43	86.41	286.90	86.98	287.32	87.55
0.1495	286.41	85.37	286.99	85.92	287.54	86.48	288.08	87.05	288.59	87.63
0.1945	287.28	85.42	287.92	85.97	288.53	86.53	289.14	87.10	289.72	87.69
0.2994	289.16	85.45	289.92	86.00	290.67	86.56	291.40	87.14	292.13	87.72
0.3999	290.69	85.32	291.52	85.86	292.36	86.41	293.19	86.97	294.01	87.54
0.4976	291.82	85.00	292.72	85.52	293.61	86.06	294.51	86.60	295.39	87.15
0.5842	292.53	84.59	293.46	85.10	294.39	85.62	295.33	86.14	296.25	86.68
0.6886	293.06	84.02	294.02	84.51	294.98	85.00	295.94	85.50	296.90	86.01
0.7475	293.23	83.71	294.20	84.17	295.18	84.65	296.15	85.14	297.13	85.63
0.8014	293.34	83.44	294.32	83.88	295.29	84.35	296.28	84.82	297.26	85.29
0.8890	293.43	83.04	294.42	83.45	295.41	83.89	296.40	84.33	297.39	84.75
0.9526	293.47	82.77	294.46	83.15	295.45	83.56	296.44	83.99	297.43	84.37
1.0000	293.48	82.54	294.47	82.90	295.46	83.30	296.45	83.71	297.44	84.07

Standard uncertainties u are $u(x_1) = 0.0005$, $u(\rho) = 1$ kg·m^{-3},$u(T) = 0.01$ K and $u(P)$=0.5 kPa

Combined uncertainties (Confidence level, 95%):$U(\overline{V}_{m,1}) = \pm 0.02 \times 10^{-6}$ $m^3 \cdot mol^{-1}$, $U(\overline{V}_{m,2}) = \pm 0.02 \times 10^{-6}$ $m^3 \cdot mol^{-1}$

ACCEPTED MANUSCRIPT

ACCEPTED MANUSCRIPT

Table 6 Partial molar volumes atinfinite dilution ($\overline{V}_{m,1}^{\infty}$, $\overline{V}_{m,2}^{\infty}$) and excess partial molar volumes atinfinite dilution ($\overline{V}_{m,1}^{E,\infty}$, $\overline{V}_{m,2}^{E,\infty}$) of [Bmim][$NTF_2$] and Dimethyl CarbonateatT = (303.15, 308.15, 313.15, 318.15 and 323.15) K.

T/ K	$\overline{V}_{m,1}^{\infty}$	$\overline{V}_{m,1}^{E,\infty}$	$\overline{V}_{m,2}^{\infty}$	$\overline{V}_{m,2}^{E,\infty}$
	/10^{-6} $m^3 \cdot mol^{-1}$		/10^{-6} $m^3 \cdot mol^{-1}$	
303.15	283.42	-10.06	82.55	-2.69
308.15	283.79	-10.68	82.91	-2.87
313.15	284.12	-11.34	83.30	-3.03
318.15	284.43	-12.02	83.70	-3.18
323.15	284.68	-12.76	84.07	-3.38

Combined uncertainties (Confidence level, 95%):$U(\overline{V}_{m,1}^{E,\infty}) = \pm 0.02\times10^{-6}$ $m^3 \cdot mol^{-1}$, $U(\overline{V}_{m,2}^{E,\infty}) = \pm 0.02\times10^{-6}$ $m^3 \cdot mol^{-1}$

ACCEPTED MANUSCRIPT

ACCEPTED MANUSCRIPT

Table 7

Computed excess values of $(B/A)^E$, cohesive energy (ΔA), Van der Waal's constants (a & b), distance of closest approach (d), from non-linear parameters proposed by Hartmann–Balizar (*B&H*) and Ballou relations

$(B/A)^E$	ΔA	a	b	d	$(B/A)^E$	ΔA	a	b	d
	/J·mol^{-1}	/N·m^4·mol^{-1}	/10^{-3} m^3·mol^{-1}	/10^{-10} m		/ J·mol^{-1}	/N·m^4·mol^{-1}	/10^{-3} m^3·mol^{-1}	/10^{-10} m
Hartmann-Balizar					**Ballou**				
***T*=303.15 K**									
0.0000	-188292.0015	0.9338	0.0656	3.7338	0.0000	-199408.6326	0.9890	0.0667	3.7544
-0.0545	-229412.5970	1.2710	0.0774	3.9448	-0.0667	-243395.2996	1.3485	0.0784	3.9624
-0.1033	-270796.2088	1.6545	0.0886	4.1259	-0.1265	-287780.0498	1.7583	0.0896	4.1413
-0.1423	-311827.4368	2.0808	0.0993	4.2861	-0.1742	-331851.9850	2.2144	0.1002	4.3001
-0.1670	-349807.5325	2.5190	0.1091	4.4235	-0.2045	-372646.3641	2.6835	0.1101	4.4364
-0.1801	-435268.5564	3.6739	0.1317	4.7100	-0.2206	-464216.9518	3.9183	0.1327	4.7209
-0.1664	-514746.7969	4.9608	0.1532	4.9530	-0.2037	-549184.4722	5.2927	0.1541	4.9626
-0.1420	-590547.5032	6.3802	0.1740	5.1673	-0.1739	-630092.2220	6.8074	0.1748	5.1759
-0.1167	-656969.1007	7.7782	0.1923	5.3429	-0.1429	-700924.3264	8.2987	0.1932	5.3509
-0.0883	-737512.2039	9.6542	0.2144	5.5404	-0.1082	-786851.9245	10.3001	0.2153	5.5477
-0.0713	-782634.4973	10.7958	0.2268	5.6454	-0.0873	-834966.8813	11.5177	0.2277	5.6524
-0.0553	-823857.5219	11.8964	0.2382	5.7383	-0.0678	-878912.5186	12.6914	0.2391	5.7450
-0.0304	-890984.1988	13.8031	0.2568	5.8834	-0.0372	-950490.1335	14.7250	0.2576	5.8898
-0.0129	-939846.3372	15.2789	0.2702	5.9845	-0.0158	-1002606.4218	16.2992	0.2711	5.9906
0.0000	-976342.1751	16.4287	0.2803	6.0577	0.0000	-1041537.4309	17.5258	0.2811	6.0636
***T*=308.15 K**									
0.0000	-179133.0308	0.8988	0.0648	3.7181	0.0000	-188946.8254	0.9481	0.0659	3.7388
-0.0657	-219270.2249	1.2273	0.0768	3.9341	-0.0805	-231779.7091	1.2973	0.0778	3.9518
-0.1230	-259813.0869	1.6022	0.0881	4.1183	-0.1506	-275171.1391	1.6970	0.0891	4.1339
-0.1680	-300095.5321	2.0198	0.0989	4.2808	-0.2057	-318355.7598	2.1427	0.0999	4.2949
-0.1965	-337437.0551	2.4498	0.1089	4.4197	-0.2406	-358394.1605	2.6020	0.1098	4.4327
-0.2129	-421473.6884	3.5839	0.1316	4.7084	-0.2607	-448294.1925	3.8119	0.1325	4.7194

ACCEPTED MANUSCRIPT

-0.1983	-499662.4223	4.8488	0.1532	4.9527	-0.2428	-531759.8887	5.1603	0.1541	4.9624
-0.1709	-574208.5057	6.2447	0.1740	5.1679	-0.2093	-611212.7531	6.6471	0.1749	5.1766
-0.1416	-639467.9287	7.6195	0.1924	5.3441	-0.1734	-680700.2884	8.1108	0.1933	5.3522
-0.1080	-718694.2379	9.4661	0.2146	5.5422	-0.1322	-765102.5937	10.0774	0.2155	5.5496
-0.0877	-763076.5675	10.5901	0.2271	5.6475	-0.1074	-812361.2896	11.2741	0.2280	5.6546
-0.0684	-803592.8396	11.6735	0.2385	5.7407	-0.0838	-855489.6602	12.4274	0.2394	5.7475
-0.0379	-869575.9858	13.5508	0.2571	5.8861	-0.0465	-925744.2793	14.4260	0.2580	5.8926
-0.0162	-917574.4702	15.0037	0.2706	5.9875	-0.0198	-976861.0838	15.9731	0.2715	5.9936
0.0000	-953399.3579	16.1355	0.2807	6.0608	0.0000	-1015015.6349	17.1783	0.2815	6.0668
***T*=313.15 K**									
0.0000	-170284.8837	0.8594	0.0637	3.6978	0.0000	-178896.9490	0.9029	0.0648	3.7187
-0.0771	-209410.9805	1.1781	0.0760	3.9201	-0.0945	-220547.1074	1.2407	0.0770	3.9379
-0.1430	-249077.5447	1.5430	0.0874	4.1083	-0.1751	-262906.3476	1.6287	0.0884	4.1240
-0.1944	-288616.5739	1.9507	0.0984	4.2735	-0.2381	-305210.9693	2.0628	0.0994	4.2877
-0.2270	-325311.4235	2.3710	0.1084	4.4142	-0.2780	-344485.0280	2.5108	0.1094	4.4273
-0.2468	-407926.6262	3.4808	0.1314	4.7055	-0.3022	-432720.1667	3.6924	0.1323	4.7167
-0.2314	-484831.9858	4.7202	0.1531	4.9515	-0.2834	-514693.3541	5.0109	0.1540	4.9613
-0.2009	-558132.7394	6.0885	0.1740	5.1677	-0.2460	-592704.6321	6.4656	0.1749	5.1765
-0.1675	-622269.9982	7.4364	0.1925	5.3447	-0.2051	-660896.4061	7.8980	0.1934	5.3528
-0.1284	-700178.9073	9.2484	0.2148	5.5434	-0.1572	-743775.8743	9.8242	0.2156	5.5509
-0.1046	-743812.3862	10.3515	0.2273	5.6491	-0.1281	-790169.9457	10.9967	0.2282	5.6562
-0.0820	-783647.4653	11.4150	0.2388	5.7425	-0.1004	-832512.2900	12.1268	0.2396	5.7494
-0.0458	-848501.0593	13.2578	0.2574	5.8883	-0.0560	-901463.0830	14.0854	0.2583	5.8948
-0.0196	-895667.5272	14.6842	0.2710	5.9899	-0.0241	-951619.2411	15.6016	0.2718	5.9962
0.0000	-930831.3233	15.7949	0.2811	6.0635	0.0000	-989010.7055	16.7821	0.2819	6.0695
***T*=318.15 K**									
0.0000	-161805.4271	0.8215	0.0626	3.6750	0.0000	-169314.5044	0.8596	0.0637	3.6960
-0.0864	-199750.5098	1.1295	0.0750	3.9041	-0.1058	-209592.7116	1.1851	0.0761	3.9220
-0.1617	-238544.1825	1.4845	0.0867	4.0968	-0.1980	-250924.9450	1.5616	0.0877	4.1127
-0.2210	-277405.0909	1.8828	0.0978	4.2652	-0.2706	-292424.3676	1.9847	0.0988	4.2795
-0.2587	**-313539.4257**	**2.2943**	**0.1080**	**4.4080**	-0.3168	**-331032.8021**	**2.4223**	**0.1090**	**4.4212**
-0.2821	-394744.7597	3.3802	0.1311	4.7022	-0.3455	-417617.8569	3.5761	0.1320	4.7135

ACCEPTED MANUSCRIPT

ACCEPTED MANUSCRIPT

-0.2659	-470388.0325	4.5945	0.1529	4.9498	-0.3256	-498124.3414	4.8654	0.1538	4.9598
-0.2323	-542492.4455	5.9362	0.1739	5.1672	-0.2844	-574751.8323	6.2892	0.1749	5.1761
-0.1945	-605505.6083	7.2576	0.1925	5.3449	-0.2381	-641647.5164	7.6907	0.1934	5.3532
-0.1497	-682140.7266	9.0359	0.2149	5.5444	-0.1833	-723056.2924	9.5778	0.2158	5.5520
-0.1223	-725042.7620	10.1186	0.2275	5.6504	-0.1497	-768607.0219	10.7266	0.2283	5.6576
-0.0962	-764212.6984	11.1626	0.2390	5.7441	-0.1178	-810182.9556	11.8341	0.2398	5.7511
-0.0540	-827982.7786	12.9722	0.2577	5.8904	-0.0661	-877884.8679	13.7540	0.2585	5.8970
-0.0233	-874318.1901	14.3724	0.2713	5.9923	-0.0285	-927083.2029	15.2398	0.2721	5.9986
0.0000	-908837.1818	15.4624	0.2814	6.0659	0.0000	-963731.7598	16.3963	0.2823	6.0721
***T*=323.15 K**									
0.0000	-153663.7313	0.8152	0.0613	3.6492	0.0000	-160160.0427	0.8287	0.0623	3.6702
-0.0989	-190614.3122	1.1215	0.0740	3.8865	-0.1212	-199280.9732	1.1457	0.0750	3.9044
-0.1838	-228540.6163	1.4749	0.0859	4.0843	-0.2251	-239595.1127	1.5137	0.0869	4.1002
-0.2500	-266639.9866	1.8715	0.0972	4.2560	-0.3061	-280196.0389	1.9285	0.0982	4.2704
-0.2921	-302121.1458	2.2815	0.1075	4.4010	-0.3576	-318034.0969	2.3581	0.1085	4.4143
-0.3192	-381921.1857	3.3638	0.1308	4.6984	-0.3909	-402976.1005	3.4922	0.1317	4.7097
-0.3021	-456312.4649	4.5744	0.1527	4.9478	-0.3699	-482028.9263	4.7612	0.1536	4.9578
-0.2650	-527216.6415	5.9120	0.1739	5.1664	-0.3245	-557269.7824	6.1633	0.1748	5.1754
-0.2228	-589152.7388	7.2295	0.1925	5.3449	-0.2728	-622925.0504	7.5438	0.1934	5.3532
-0.1719	-664508.1158	9.0028	0.2150	5.5452	-0.2105	-702858.4292	9.4037	0.2159	5.5528
-0.1408	-706708.3162	10.0826	0.2276	5.6515	-0.1724	-747600.9464	10.5365	0.2285	5.6588
-0.1110	-745226.1882	11.1238	0.2391	5.7456	-0.1360	-788426.6079	11.6286	0.2400	5.7526
-0.0625	-807915.7855	12.9284	0.2579	5.8922	-0.0766	-854885.1145	13.5217	0.2588	5.8989
-0.0270	-853456.2278	14.3249	0.2716	5.9944	-0.0331	-903168.6157	14.9870	0.2724	6.0008
0.0000	-887343.7008	15.4119	0.2817	6.0683	0.0000	-939090.9440	16.1272	0.2826	6.0745

ACCEPTED MANUSCRIPT

ACCEPTED MANUSCRIPT

Table 8 Infrared absorbance wave numbers (cm^{-1}) between 2800 to 3200 of [Bmim][NTf_2] in DMC at room temperature and atmospheric pressure P = 101.3 kPa.

		Infrared absorbance wave numbers / cm^{-1}			
Mole fraction of [Bmim][NTf_2]	Mole fraction of DMC	C_2-H stretching	$C_{4,5}$-H stretching	SO_2 Sym Stretch	CF_3 Sym Stretch
1.0000	0.0000	3120.7	3157.2	1131.5	1226.1
0.8990	0.1010	3120.7	3157.5	1131.7	1226.4
0.8055	0.1945	3120.7	3157.7	1132.0	1226.6
0.7006	0.2994	3120.7	3158.0	1132.3	1226.7
0.6001	0.3999	3119.5	3157.0	1132.5	1226.9
0.5024	0.4976	3120.2	3157.0	1133.0	1226.9
0.4158	0.5842	3120.2	3157.0	1133.8	1227.0
0.3114	0.6886	3119.9	3157.8	1134.1	1227.1
0.2525	0.7475	3118.3	3156.7	1135.1	1227.2
0.1110	0.8890	3118.1	3156.3	1137.0	1227.2
0.0000	1.0000	-	-	-	-

ACCEPTED MANUSCRIPT

ACCEPTED MANUSCRIPT

Table 9 Characteristic and reduced parameters for the pure components used in PFP theory at various temperatures.

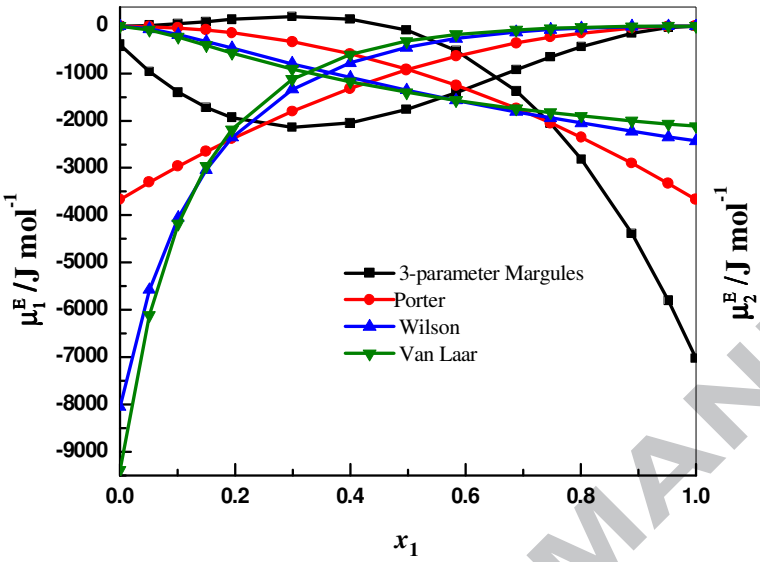
T/K	$\tilde{V}$	V_1^* /10^{-6}m^3·mol^{-1}	P_1^* /10^6 J·mol^{-1}
[Bmim][NTf$_2$]			
303.15	1.1788	248.97	520.66
308.15	1.1813	249.28	520.50
313.15	1.1838	249.59	520.16
318.15	1.1862	249.91	519.73
323.15	1.1887	250.23	519.19
DMC			
303.15	1.3015	65.491	687.24
308.15	1.3082	65.569	685.34
313.15	1.3149	65.651	682.36
318.15	1.3217	65.737	677.89
323.15	1.3285	65.828	673.69

Table 10 PFP interaction parameter, χ_{12}, and calculated values of the three contributions from the PFP theory at equimolar composition for ([Bmim][NTf$_2$] + DMC) system at T=(303.15-323.15)K

T	χ_{12}	V_m^E/int	V_m^E/fv	V_m^E/ip
/K	/10^6 J·m^{-3}	/10^{-6} m^3·mol^{-1}		
303.15	-63.1996	1.2105	-0.6834	0.9516
308.15	-63.1190	-1.2405	-0.7298	0.9758
313.15	-62.7714	-1.2664	-0.7780	0.9951
318.15	-61.9954	-1.2847	-0.8278	1.0058
323.15	-61.3045	-1.3047	-0.8800	1.0181

ACCEPTED MANUSCRIPT

Graphical abstract



ACCEPTED MANUSCRIPT

ACCEPTED MANUSCRIPT

Highlights

- The studied binary system is {**[Bmim][NTf_2]+DMC**}
- Density, speed of sound and refractive index are measured at various temperatures
- Derived excess/deviation parameters indicated the existence of strong interactions
- Acoustic non-linearity parameter , cohesive energy etc., are evaluated
- IR spectra and PFP theory also support the existence of strong interactions

ACCEPTED MANUSCRIPT

ARTICLE IN PRESS

+ MODEL

Available online at www.sciencedirect.com

ScienceDirect

Karbala International Journal of Modern Science xx (2017) 1–8
http://www.journals.elsevier.com/karbala-international-journal-of-modern-science/

Investigation of intermolecular interactions in binary liquid mixtures of [Bmim][NTf_2] and propylene carbonate at different temperatures using ultrasonic, optical and FT-IR studies

V. Srinivasa Rao [a,d], M. Srinivasa Reddy [b], K. Thomas S.S. Raju [c], B. Hari Babu [d,*]

[a] *Department of Chemistry, SRR & CVR Govt. Degree College, Vijayawada, 520008, A.P., India*
[b] *Department of Chemistry, KRK Govt. Degree College, Addanki, 523201, A.P., India*
[c] *Department of Chemistry, Andhra Loyola College, Vijayawada, 520008, A.P., India*
[d] *Department of Chemistry, Acharya Nagarjuna University, Nagarjuna Nagar, 522510, A.P., India*

Received 11 May 2017; revised 7 July 2017; accepted 19 July 2017

Abstract

Speeds of sound and refractive indices of [Bmim][NTf_2]+propylene carbonate mixtures have been measured experimentally over the entire composition range at 303.15, 308.15, 313.15, 318.15 and 323.15 K, under 101.3 kPa pressure. Semi empirical relations of speed of sound and refractive index have been applied for the liquid mixtures in terms of the pure components proposed by different investigators. The deviation of refractive index on volume fraction basis ($\Delta_\phi n_D$) reported for the binary mixture and fitted using Redlich-Kister polynomial equation. The measured and computed data have been used to interpret intermolecular interactions between unlike molecules upon mixing. This was further supported by FTIR spectroscopy.
© 2017 The Authors. Production and hosting by Elsevier B.V. on behalf of University of Kerbala. This is an open access article under the CC BY-NC-ND license (http://creativecommons.org/licenses/by-nc-nd/4.0/).

Keywords: Bmim][NTf_2]; Propylene carbonate; Speed of sound; Refractive index; FTIR spectroscopy

1. Introduction

Recently, Ionic Liquids attracted considerable attention because of their distinctive properties which are desirable for the field of green chemistry such as thermal stability, non-volatility and reusability [1,2]. Ionic liquids can be selected to have different anions and cations, so that one can form ionic liquid with the desired properties. Mixing of the ILs with molecular solvents is one of the alternative steps to minimize the usage of expensive ILs and to save time for preparing new ILs of desired properties [3]. Fortunately, their mixtures with molecular solvents show reduced viscosity without affecting their advantages as green solvents. Mixtures of ILs and molecular organic solvents are gaining interest of researchers as resultant liquid mixtures containing the advantages over both IL and molecular organic solvents. The measurement and interpretation of physical properties of ionic liquids and their mixtures are necessary to develop those applications and to explain the physical and chemical behavior of ILs. The properties of these mixtures are based on the mixing ratio. The importance of these

* Corresponding author.
E-mail address: dr.b.haribabu@gmail.com (B.H. Babu).
Peer review under responsibility of University of Kerbala.

http://dx.doi.org/10.1016/j.kijoms.2017.07.002
2405-609X/© 2017 The Authors. Production and hosting by Elsevier B.V. on behalf of University of Kerbala. This is an open access article under the CC BY-NC-ND license (http://creativecommons.org/licenses/by-nc-nd/4.0/).

Please cite this article in press as: V. Srinivasa Rao et al., Investigation of intermolecular interactions in binary liquid mixtures of [Bmim][NTf_2] and propylene carbonate at different temperatures using ultrasonic, optical and FT-IR studies, Karbala International Journal of Modern Science (2017), http://dx.doi.org/10.1016/j.kijoms.2017.07.002

new substances can be exploited by studying their properties like acoustic and refractive index which provide vital information about solute–solute and solute–solvent interactions occurring in mixtures.

The choice of the investigated Ionic liquid, 1-butyl-3-methylimidazolium bis(trifluoromethylsulfonyl) imide ([Bmim][NTf_2]) was on the basis of its ability to act as extracting solvent for the removal many organic compounds through liquid–liquid extraction [4,5]. It is also widely used in catalysis [6] and chromatography [7]. The molecular organic solvent, Propylene carbonate (PC) used in extractions, in the production of many synthetic and natural resins and polymers [8], in the synthesis of pharmaceuticals [9], in agricultural chemistry, and as fuel additive [10]. Particularly, there is high interest in the propylene carbonate applications as storage batteries [11,12], such batteries can be recharged thermally at relatively low temperatures.

Systematic investigation of the physicochemical properties of [Bmim][NTf_2] with molecular organic solvents like ethanol or ethyl acetate [13], anisole or acetophenone [14], acetonitrile or tetrahydrofuran [15], γ-butyrolactone [16], ethanol [17], water [18] and pyrrolidin-2-one [19] have been reported. Vranes et al. [20] reported density and excess properties of [Bmim][NTf_2]+Propylene carbonate binary mixtures. However, the literature review indicates that the systematic acoustic, optical and spectroscopic properties of binary mixtures of [Bmim][NTf_2] with propylene carbonate (PC) have not been reported earlier.

On the basis of our initial experiments, [Bmim][NTf_2] is found to be totally miscible with PC in all proportions. Hence, in the present study, it is proposed to measure the speeds of sound and refractive indices of the binary mixtures of [Bmim][NTf_2] with PC in the temperature range between 303.15 and 323.15 K for the entire composition range and at atmospheric pressure. An attempt has been made to understand the interaction behavior between the two liquids in the mixture using FTIR spectroscopy. On the basis of the measured and calculated properties, molecular interactions in the binary mixtures have been interpreted for their potential application in industrial processes.

2. Experimental section

2.1. Materials

The ionic liquid, [Bmim][NTf_2] (CAS 174899-83-3) with purity 0.99 in mass fraction used in this work. It was purchased from Iolitec GmBH (Germany), while PC (CAS 108-32-7) with purity 0.995 in mass fraction was supplied by Sigma Aldrich. The chemicals used in the present investigation were purified by the methods described in literature [21,22]. The water content in investigated IL and DEC was determined using a Karl Fisher titrator (Metrohm, 890 Titrando). The water content of all the samples were further checked and found to be in the range of less than 150 ppm, a value much lower than the original pre-evacuation analysis, which typically showed values in the range of less than 210 ppm. [Bmim][NTf_2] is used without further purification; PC is further purified by distillation. List of chemicals with details of Provenance, CAS number and mass fraction purity along with the purities verified by comparing the measured speed of sound and refractive index of the pure liquids with the literature at atmospheric pressure are given in Table 1.

2.2. Procedure

Samples are prepared by weighing with a precision of ±0.01 mg, using a Sartorius electronic balance

Table 1
List of chemicals with details of Provenance, Comparison of experimental values of speed of sound, u and refractive index, n_D, of pure liquids with the corresponding literature values including density, ρ, at different temperatures and at atmospheric pressure P = 101.3 kPa.

Liquid	Provenance	Mass fraction purity	Temp/K	ρ/(kg m^{-3})	u/m s^{-1}		n_D	
				Lit.	Lit.	Lit.	Expt.	Lit.
[Bmim][NTf_2]	Io-Li-Tec, Germany	0.99	303.15	1429.40 [20]	1216.8	1216.77 [19]	1.42451	1.42523 [19]
			308.15	1424.57 [20]	1205.8	1205.80 [19]	1.42309	1.42374 [19]
			313.15	1419.61 [20]	1195.0	1194.95 [19]	1.42104	1.42225 [19]
			318.15	1414.67 [20]	1184.2	1184.23 [19]	1.41951	1.42076 [19]
			323.15	1409.65 [20]	1173.6	1173.61 [19]	1.41728	1.41923 [19]
Propylene carbonate	Sigma Aldrich	0.995	303.15	1194.00 [20]	1414.9	–	1.41802	1.4174 [23]
			308.15	1188.57 [20]	1397.9	–	1.41602	1.4155 [23]
			313.15	1183.11 [20]	1381.1	–	1.41402	
			318.15	1177.55 [20]	1364.4	–	1.41198	
			323.15	1171.96 [20]	1347.9	–	1.40995	–

Please cite this article in press as: V. Srinivasa Rao et al., Investigation of intermolecular interactions in binary liquid mixtures of [Bmim][NTf_2] and propylene carbonate at different temperatures using ultrasonic, optical and FT-IR studies, Karbala International Journal of Modern Science (2017), http://dx.doi.org/10.1016/j.kijoms.2017.07.002

(CPA225D). The uncertainty of the resulting mole fractions of the mixtures was estimated as being $\pm 2 \times 10^{-4}$. Speeds of sound are measured with an Anton Paar DSA-5000 M vibrating tube density and sound velocity meter. The density meter is calibrated with doubly distilled degassed water, and with dry air at atmospheric pressure. The temperature of the apparatus is controlled to within ±0.01 K by a built-in Peltier device. Measured density and speed of sound values (at frequency approximately 3 MHz) are precise to 5×10^{-1} m s^{-1} respectively. The standard uncertainties associated with the measurements of temperature, density and speed of sound are estimated to be ±0.01 K and ±0.5 m s^{-1} respectively. The refractive indices are determined using an automatic refractometer (Anton Paar Dr Krenchen Abbemat (WR-HT)). The uncertainties in the temperature and refractive index values are ±0.01 K and $\pm 5 \times 10^{-5}$ respectively. Infrared transmittance is measured by using Shimadzu Fourier transform infrared (FT-IR) spectrometer (IR Affinity-1S) equipped with attenuated total reflectance (ATR) accessories.

3. Theory

3.1. Theoretical calculation of ultrasonic sound velocities

3.1.1. Nomoto's relation

Nomoto [24] derived the following relation for sound velocity based on the assumption of the linearity of the molecular sound velocity and the additivity of molar volume.

$$U_N = \{(\Sigma x_i R_i)/(\Sigma x_i V_i)\}^3, \quad (1)$$

where 'x_i'is mole fraction, 'R_i' is the molar sound speed and V_i is the molar volume of the ith component.

3.1.2. Van Dael and Vangeel's equation

Van Dael and Vangeel [25] obtained the ideal mixture relation

$$\sum \left(x_i M_i / u_i^2\right) = \left\{1 \Big/ \sum x_i M_i\right\}\{1/U_V\}^2, \quad (2)$$

where 'M_i' is molecular weight of ith component in the liquid mixture and U_V is the Van Dael's velocity.

3.1.3. Impedance relation

Impedance dependence relation [26] is given by

$$U_{imp} = \Sigma x_i Z_i / \Sigma x_i \rho_i, \quad (3)$$

where 'Z_i' is the acoustic impedance and 'ρ_i' is the density of the ith component of the mixture.

3.2. Refractive index mixing rules

A number of mixing rules of refractive index have been proposed for liquid mixtures in terms of the refractive indices of the pure components such as Arago−Biot (A−B) [27], Gladstone−Dale (G−D) [28], Newton (N) [29], Eyring and John (E−J) [30], Lorentz−Lorenz (L−L) [31], Heller (H) [32], Eykman (EK) [33], Oster (Os) [34] and Weiner (W) [35] were examined for present [Bmim][NTf_2]+PC mixture.

$$n = \sum_{i=1}^{2} n_i \phi_i \quad \text{Arago} - \text{Biot} \quad (4)$$

$$n - 1 = \sum_{i=1}^{2} (n_i - 1)\phi_i \quad \textit{Gladstone} - \textit{Dale} \quad (5)$$

$$n^2 - 1 = \sum_{i=1}^{2} \left(n_i^2 - 1\right)\phi_i \quad \textit{Newton} \quad (6)$$

$$n = n_1 \phi_1^2 + 2(n_1 n_2)^{1/2} \phi_1 \phi_2 + n_2 \phi_2^2 \quad \textit{Eyring} - \textit{John} \quad (7)$$

$$\frac{n^2 - 1}{n^2 + 2} = \sum_{i=1}^{2} \left(\frac{n_i^2 - 1}{n_i^2 + 2}\right)\phi_i \quad \textit{Lorentz} - \textit{Lorenz equation} \quad (8)$$

$$\frac{n - n_1}{n_1} = \frac{3}{2}\left(\frac{n_2^2 - n_1^2}{n_2^2 + 2n_1^2}\right)\phi_2 \quad \textit{Heller} \quad (9)$$

$$\frac{n^2 - 1}{n^2 + 0.4} = \sum_{i=1}^{2} \left(\frac{n_i^2 - 1}{n_i^2 + 0.4}\right)\phi_i \quad \textit{Eykman} \quad (10)$$

$$\frac{(n^2 - 1)(2n^2 + 1)}{n^2} = \sum_{i=1}^{2} \left(\frac{\left(n_i^2 - 1\right)\left(2n_i^2 + 1\right)}{n_i^2}\right)\phi_i \quad \textit{Oster} \quad (11)$$

$$\frac{n^2 - n_1^2}{n^2 + 2n_1^2} = \left(\frac{n_2^2 - n_1^2}{n_2^2 + 2n_1^2}\right)\phi_2 \quad \textit{Wiener} \quad (12)$$

where, ϕ_i, is the volume fraction of the ith component and is given by $\phi_i = \frac{x_i V_i}{\sum_{i=1}^{2} x_i V_i} n_i$ and n are the refractive indices of each component and mixture respectively.

The Absolute Percentage Deviation (APD) of experimental refractive index is calculated by the relation

$$AAD = \frac{100}{n} \sum_{i=1}^{n} \left(\left| \frac{n_{cal}}{n_{\exp}} - 1 \right| \right) \quad (13)$$

where n_{exp} is experimental refractive index and n_{cal} is the value calculated from various mixing rules and 'n' is the number of data points.

Please cite this article in press as: V. Srinivasa Rao et al., Investigation of intermolecular interactions in binary liquid mixtures of [Bmim][NTf_2] and propylene carbonate at different temperatures using ultrasonic, optical and FT-IR studies, Karbala International Journal of Modern Science (2017), http://dx.doi.org/10.1016/j.kijoms.2017.07.002

The Maximal deviation (M Dev) is given by

$$MDev = 100*\max\left|\frac{n_{cal}}{n_{\exp}} - 1\right| \quad (14)$$

3.3. Deviations in refractive index

$$n_D^{id} = \phi_1 n_{D,1} + \phi_2 n_{D,2} \quad (15)$$

$$\Delta_\phi n_D = n_D - n_D^{id} \quad (16)$$

The deviation in refractive index is fitted to the following Redlich-Kister polynomial equation and the corresponding values are represented in Table 3.

$$Y^E = x_1 x_2 \sum_{i=o}^{j} A_i (x_1 - x_2)^i \quad (17)$$

4. Results and discussion

The values of the experimental speed of sound, u, and refractive index, n_D for the binary mixtures of [Bmim][NTf_2] with PC as a function of mole fraction, x_1 of [Bmim][NTf_2] at investigated temperatures are given in Table 2. The speeds of sound of [Bmim][NTf_2]+PC binary system is decreasing as the concentration of IL increases and decreases with rise in temperature. The trend indicates that the mixtures become more compressible at IL rich region and also the mixtures become more compressible at higher temperatures. However, theoretical formulations based on Nomoto, Van Dael and Vangeel, Impedance equations are widely used to calculate speeds of sound in binary systems of nonelectrolyte mixtures. Therefore, we in the present work attempt to extend these formulations for calculating the speeds of sound in [Bmim][NTf_2]+PC mixtures. The pertinent relations are summarized in theory section. The calculated ultrasonic speeds along with the experimental speeds are represented in Fig. 1 and deviations in the calculated values from the experimental values are listed in Table 4. The results indicate that Nomato's and Impedance relations provide the best results for ultrasonic speeds of the system under study when compared to Van Deal and Vangeel's relations. The large deviations for Van Deal and Vangeel's relation is expected, as this formulation is applicable for nonassociating binary

Table 2
Experimental speed of sound (u), refractive index (n_D mole fraction (x_1) of [Bmim][NTf_2] in the binary liquid mixture of {[Bmim][NTf_2]+Propylene Carbonate} from T/K = 303.15 to 323.15 at pressure P = 101.3 kPa.

x_1	303.15 K		308.15 K		313.15 K		318.15 K		323.15 K	
	u/m s^{-1}	n_D	u/m s^{-1}	n_D	u/m s^{-1}	n_D	u/m s^{-1}	n_D	u/m s^{-1}	n_D
0.0000	1414.91	1.41802	1397.92	1.41602	1381.10	1.41402	1364.43	1.41198	1347.93	1.40995
0.0522	1392.42	1.41892	1376.13	1.41697	1360.02	1.41502	1344.05	1.41305	1328.24	1.41109
0.0903	1376.93	1.41955	1361.14	1.41762	1345.50	1.41571	1330.02	1.41378	1314.68	1.41187
0.1422	1357.09	1.42034	1341.92	1.41845	1326.90	1.41658	1312.04	1.41471	1297.31	1.41286
0.1963	1337.96	1.42110	1323.39	1.41924	1308.97	1.41742	1294.70	1.41560	1280.55	1.41381
0.3000	1305.68	1.42237	1292.11	1.42057	1278.68	1.41882	1265.41	1.41709	1252.24	1.41540
0.3959	1280.98	1.42332	1268.18	1.42157	1255.51	1.41987	1242.98	1.41820	1230.56	1.41658
0.4993	1259.91	1.42410	1247.75	1.42240	1235.71	1.42074	1223.81	1.41912	1212.02	1.41755
0.6001	1244.92	1.42462	1233.20	1.42297	1221.60	1.42133	1210.14	1.41974	1198.79	1.41819
0.7112	1234.73	1.42492	1223.29	1.42331	1211.97	1.42168	1200.79	1.42010	1189.71	1.41856
0.7826	1231.69	1.42496	1220.31	1.42337	1209.07	1.42174	1197.94	1.42015	1186.93	1.41860
0.8290	1229.69	1.42499	1218.29	1.42337	1207.02	1.42177	1195.88	1.42017	1184.84	1.41860
0.8736	1227.30	1.42504	1215.87	1.42337	1204.58	1.42183	1193.41	1.42022	1182.36	1.41863
0.9432	1222.29	1.42514	1210.96	1.42348	1199.77	1.42200	1188.71	1.42042	1177.75	1.41884
1.0000	1216.77	1.42523	1205.80	1.42374	1194.95	1.42225	1184.23	1.42076	1173.61	1.41924

Table 3
Redlich-Kister coefficients of deviation of refractive indices and corresponding standard deviations (σ) for the systems at different temperatures.

	T/K	A_0	A_1	A_2	A_3	A_4	σ
$(\Delta_\phi n_D)$	303.15	0.00202	0.00227	−0.00479	0.00097	−0.00007	0.00001
	308.15	0.00186	0.00238	−0.00523	0.00089	0.00011	0.00002
	313.15	0.00173	0.00239	−0.00539	0.00089	0.00002	0.00002
	318.15	0.00162	0.00236	−0.00590	0.00098	0.00049	0.00003
	323.15	0.00151	0.00237	−0.00643	0.00120	0.00107	0.00003

Please cite this article in press as: V. Srinivasa Rao et al., Investigation of intermolecular interactions in binary liquid mixtures of [Bmim][NTf_2] and propylene carbonate at different temperatures using ultrasonic, optical and FT-IR studies, Karbala International Journal of Modern Science (2017), http://dx.doi.org/10.1016/j.kijoms.2017.07.002

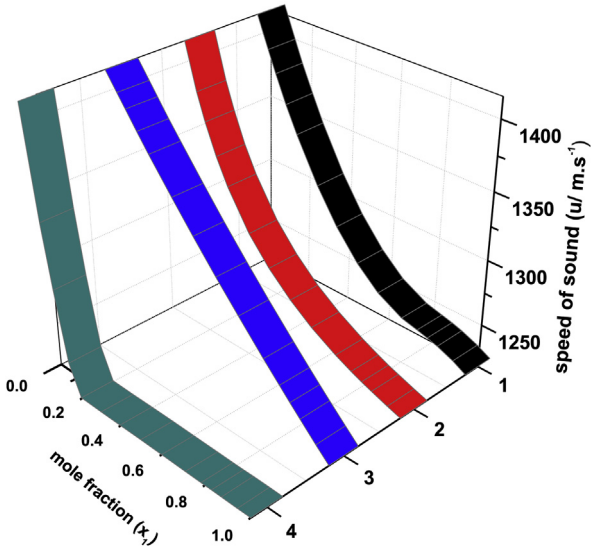


Fig. 1. Plots of speeds of sound (u) calculated from various theories along with experimental values against mole fraction of [Bmim][NTf_2] in the mixture with PC at 303.15 K. 1- Expt. 2- Nomato 3- Imped 4- Vand-Vang.

Table 4
Average percentage deviation of calculated speeds of sound compared to experimental values at various temperatures of [Bmim][NTf_2] and propylene carbonate binary mixture at T = (303.15, 308.15, 313.15, 318.15 and 323.15) K.

T/K	Nomato	Imped	Vand-Vang
303.15	0.46	−1.73	8.20
308.15	0.45	−1.69	8.28
313.15	0.44	−1.65	8.35
318.15	0.43	−1.61	8.42
323.15	0.42	−1.57	8.50
Average	0.44	−1.65	8.35

systems, while [Bmim][NTf_2]+PC binary mixture displays strong nonideal deviations.

The refractive indices (n_D) for the binary mixtures at the studied temperatures over the whole composition range were given in Table 2. Refractive index increases as the concentration of the ILs in the mixture increases. For the fixed concentration of [Bmim][NTf_2], as the temperature increases, n_D decreases which may be due to the non availability of free volume which leads to more compressible structure in the mixture as compared to the ideal mixtures [36]. The values of $\Delta_\phi n_D$ are positive at $x_1 > 0.3$ for the binary mixtures (Fig. 2) which may be attributed to the non-availability of the free volume in the mixture in comparison with the ideal mixtures. It is very similar to the V_m^E reported in the literature for the binary mixture [20].

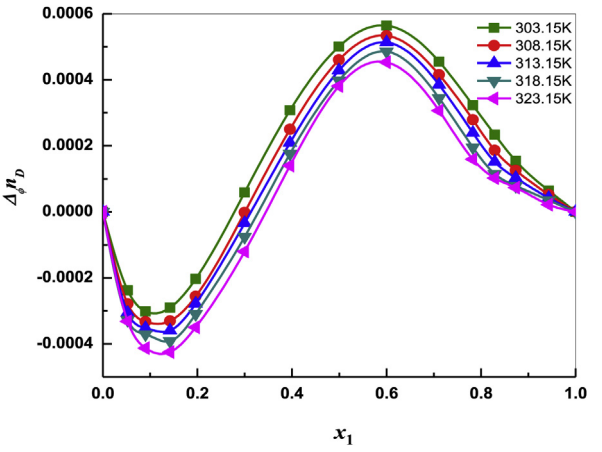


Fig. 2. Plots of deviation in refractive index ($\Delta_\varnothing n_D$) against mole fraction of [Bmim][NTf_2] in the mixture with PC at different temperatures.

A number of mixing rules of refractive index (n_D) have been proposed by different investigators were examined for present [Bmim][NTf_2]+PC mixture. The refractive indices values calculated from various theories along with experimental values at different temperatures are represented in Fig. 3. The absolute percentage deviation is obtained as described in eq (13) are represented at Table 5. From these calculations, we conclude that the Newton equation is the one that best fitted our experimental results.

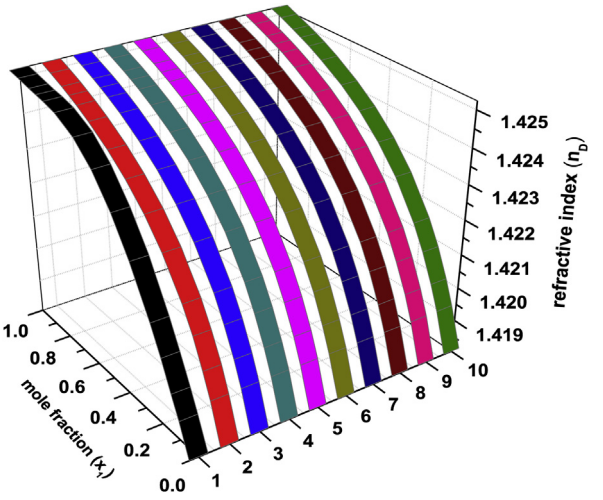


Fig. 3. Plots of refractive indices (n_D) calculated from various theories along with experimental values against mole fraction of [Bmim][NTf_2] in the mixture with PC at 303.15 K. 1- Expt. 2- Ara–Biot 3- Gla–Dale 4- Newton 5- Eyri–John 6- Lor–Lor 7- Heller 8- Eykman 9- Oster 10-Wiener.

Please cite this article in press as: V. Srinivasa Rao et al., Investigation of intermolecular interactions in binary liquid mixtures of [Bmim][NTf_2] and propylene carbonate at different temperatures using ultrasonic, optical and FT-IR studies, Karbala International Journal of Modern Science (2017), http://dx.doi.org/10.1016/j.kijoms.2017.07.002

Table 5
Average percentage deviation of calculated refractive indices compared to experimental values at various temperatures of [Bmim][NTf_2] and propylene carbonate binary mixture at T = (303.15, 308.15, 313.15, 318.15 and 323.15) K.

T/K	A–B	G–D	N	E–J	L–L	H	EK	Os	W
303.15	0.008	0.008	0.007	0.008	0.008	0.008	0.008	0.008	0.008
308.15	0.005	0.005	0.005	0.005	0.005	0.005	0.006	0.006	0.005
313.15	0.003	0.003	0.003	0.004	0.004	0.004	0.004	0.004	0.004
318.15	0.002	0.002	0.001	0.002	0.002	0.002	0.002	0.002	0.002
323.15	0.000	0.000	0.000	0.000	0.000	0.000	0.001	0.001	0.000
Average	0.004	0.004	0.003	0.004	0.004	0.004	0.004	0.004	0.004

4.1. Infrared spectral studies

The existence of interactions in the system which were drawn from the above inferences of derived excess/deviation parameters are well supported by IR spectral studies. The unique properties of imidazolium cations are found in their electronic structure. The hydrogen in C_2-H is more acidic than C_4-H, and C_5-H due to the electron deficiency in the C=N bond. The resultant acidity of the hydrogen atoms is the key to understand the properties of these ionic liquids. The hydrogen on the C_2 carbon (C_2-H) has been shown to bind typically with solute molecules [37].

In order to study the effects of molecular interactions, infrared absorbance is recorded from 650 cm^{-1} to 4000 cm^{-1} (Fig. 4 and Table 6). In $[Bmim]^+$ cation, the C-H stretching region from 2800 to 3200 cm^{-1} is investigated. For [Bmim][NTf_2], the signals in this region can be separated into two parts: signals between 3000 cm^{-1} and 3200 cm^{-1} can be attributed to C-H vibrational modes mainly arising from the aromatic imidazolium ring, from C_2-H and $C_{4,5}$-H stretching frequencies [38]. The signals between 2800 cm^{-1} and 3000 cm^{-1} are due to aliphatic C-H groups in the methyl and butyl moieties [39–41]. The C_2-H vibrational frequency (3121.4 cm^{-1}) is

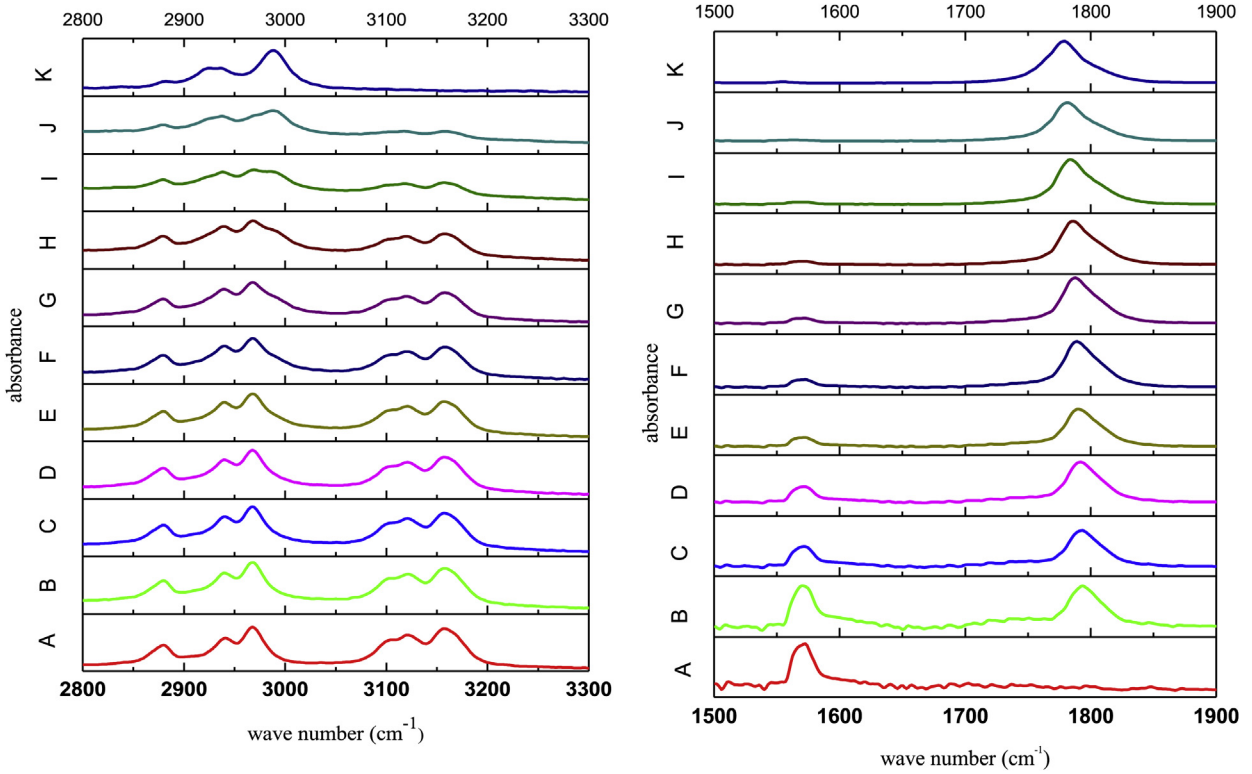


Fig. 4. Infrared spectra (1500 cm^{-1}–1900 cm^{-1} and 2800 cm^{-1}–3300 cm^{-1}) of (A) Pure IL [Bmim][NTf_2]; (B) 0.8736; (C) 0.7826; (D) 0.7112; (E) 0.6001; (F) 0.4993; (G) 0.3959; (H) 0.3000; (I) 0.1963; (J) 0.0903and (K) Pure PC. (B), (C), (D), (E), (F), (G), (H), (I), (J) represents mole fraction of [Bmim][NTf_2] in the mixture with PC.

Please cite this article in press as: V. Srinivasa Rao et al., Investigation of intermolecular interactions in binary liquid mixtures of [Bmim][NTf_2] and propylene carbonate at different temperatures using ultrasonic, optical and FT-IR studies, Karbala International Journal of Modern Science (2017), http://dx.doi.org/10.1016/j.kijoms.2017.07.002

Table 6
Infrared absorbance wave numbers (cm^{-1}) between 2800 and 3200 of [Bmim][NTf_2] in PC at room temperature and atmospheric pressure P = 101.3 kPa.

Mole fraction of [Bmim][NTf_2]	Mole fraction of PC	C_2-H stretching	$C_{4,5}$-H stretching	C=O sym stretch
0.0000	1.0000	–	–	1778.7
0.0903	0.9097	3118.1	3157.5	1781.4
0.1963	0.8037	3118.6	3157.8	1783.7
0.3000	0.7000	3119.2	3157.8	1785.8
0.3959	0.6041	3119.3	3157.5	1787.5
0.4993	0.5007	3120.2	3157.5	1788.9
0.6001	0.3999	3120.5	3156.5	1790.0
0.7112	0.2888	3120.7	3156.8	1792.1
0.7826	0.2174	3120.9	3157	1793.3
0.8736	0.1264	3121.2	3157.2	1793.6
1.0000	0.0000	3121.4	3157.5	–

shifted to lower frequencies by about 36.1 cm^{-1} when compared to the C_4-H and C_5-H stretches (3157.5 cm^{-1}) because of its stronger acidic character. In the present mixtures, C_2-H and $C_{4,5}$-H stretching frequencies of the cation is analyzed (Fig. 4). The experimental ATR-IR spectra for PC for the C=O stretching (Fig. 4) spectral regions are reported. A peak at 1778.7 cm^{-1} corresponding C=O stretching region of pure PC [42,43]. The band around 1575 cm^{-1} belongs to ring in-plane symmetric/anti-symmetric stretch, CH_2(N) and CH_3(N) CN stretch of pure [Bmim][NTf_2] [44].

As mole fraction of PC increases a blue shift in C_2-H and $C_{4,5}$-H stretching frequencies indicating the formation of hydrogen bond between $[Bmim]^+$ and PC. The blue shift is very predominant in C_2-H frequencies when compared to $C_{4,5}$-H stretching frequencies which indicates that more acidic C_2-H plays major role in the formation of hydrogen bond with carbonyl oxygen of PC (Fig. 4). Simultaneously, as mole fraction of IL increases a clear red shift in C=O Sym Stretch frequencies is observed in PC. This clearly indicates the formation of intermolecular hydrogen bond between hydrogens of aromatic imidazolium ring and carbonyl oxygen of PC.

By examining ATR-FTIR, it can be accomplished that hydrogen bonds exist extensively in such systems which play a key role towards the miscibility and stability of the [Bmim][NTf_2]+PC binary system. Additionally, the hydrogen bonding interactions are also accountable in the present system to get complete miscibility and solvation. Hence, it can be assumed that contraction in volumes of the mixtures are because of hydrogen bonds between the ionic liquid [Bmim][NTf_2] and PC.

5. Conclusions

Ultrasonic speed of sounds and refractive indices for binary liquids of [Bmim][NTf_2] with PC have been measured experimentally at atmospheric pressure over the entire composition range at temperature 303.15 K, 308.15 K, 313.15 K, 318.15 K and 323.15 K. In the present binary liquid system, the observed excess values clearly reflecting the dominance of strong attractive forces. The IR spectral studies also supported the inferences drawn from excess properties.

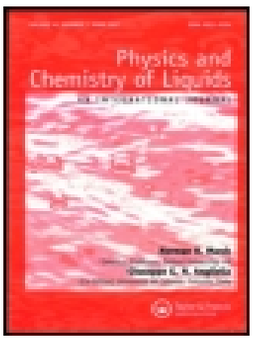
References

[1] T.L. Greaves, C.J. Drummond, Chem. Rev. 115 (2015) 11379–11448.
[2] F. Guo, S. Zhang, J. Wang, B. Teng, T. Zhang, M. Fan, Curr. Org.Chem. 19 (2015) 455–468.
[3] A.A. Shamsuri, R. Daik, Rev. Adv.Mat.Sci. 40 (2015) 45–59.
[4] C. Yao, J.L. Anderson, Anal. Bioanal. Chem. 395 (2009) 1491–2150.
[5] D. Hameister, S. Illner, C. Vogel, D. Michalik, U. Kragl, Sep. Purif. Technol. 132 (2014) 438–445.
[6] D. Betz, A. Raith, M. Cokoja, F.E. Kuehn, ChemSusChem. 3 (2010) 559–562.
[7] T.D. Ho, P.M. Yehl, N.P. Chetwyn, J. Wang, J.L. Anderson, Q. Zhong, J. Chromatogr. A 1361 (2014) 217–228.
[8] The Merck Index, thirteenth ed., Merck & Co., Inc., Whitehouse Station, NJ, 2001.
[9] M.C. Annesini, R. De Sanctis, I. Kikic, R. Marrelli, J. Chem. Eng. Data 29 (1984) 39–41.
[10] J.M. Pardo, C.A. Tovar, C.A. VCerdeireina, E. Carballo, L. Romani, J. Chem. Thermodyn. 31 (1999) 787–796.
[11] G. Pistoia, Industrial Chemical Library vol. 5, Elsevier, Amsterdam, 1994.
[12] S. Tobishima, M. Arakawa, E. Yamaki, Electrochim. Acta 33 (1988) 239–244.
[13] A.E. Andreatta, A. Arce, E. Rodil, A. Soto, J. Solut. Chem. 39 (2010) 371–383.
[14] E. Widowati, M.J. Lee, J. Chem. Thermodyn. 63 (2013) 95–101.
[15] M. Geppert-Rybczynska, M. Sitarek, J. Chem. Eng. Data 59 (2014) 1213–1224.
[16] M. Vranes, S. AnaPapovic, A. Tot, N. Zec, S. Gadzuric, J. Chem.Thermodyn 76 (2014) 161–171.
[17] R. Salinas, J. Pla-Franco, E. Lladosa, Juan B. Monto, J. Chem. Eng. Data 60 (2015) 525–540.
[18] J. Jacquemin, P. Husson, A.A. Padua, V. Majer, Green Chem. 8 (2006) 172–180.
[19] T.S. Krishna, A.K. Nain, S. Chentilnath, D. Punyaseshadu, B. Munibhadrayya, J. Chem. Thermodyn. 101 (2016) 103–114.
[20] M. Vranes, N. Zec, A. Tot, S.A. Papovic, S. Dozic, S. Gadzuric, J. Chem. Thermodyn. 68 (2014) 98–108.
[21] W.L. Armarego, C.L.L. Chai, Purification of Laboratory Chemicals, Butterworth-Heinemann, 2013.
[22] E. Scholz, Springer-Verlag Berlin (1984).
[23] G. Moumouzias, G. Ritzoulis, J. Chem. Eng. Data 45 (2000) 202–206.
[24] O. Nomoto, J. Phys. Soc. Jpn. 13 (1958) 1528–1532.

Please cite this article in press as: V. Srinivasa Rao et al., Investigation of intermolecular interactions in binary liquid mixtures of [Bmim][NTf_2] and propylene carbonate at different temperatures using ultrasonic, optical and FT-IR studies, Karbala International Journal of Modern Science (2017), http://dx.doi.org/10.1016/j.kijoms.2017.07.002

[25] W. Van Dael, E. Vangeel, in: Proc. Int. Conf. On Calorimetry and Thermodynamics,Warsa, 1955, p. 555.
[26] S. Baluja, P.H. Parsania, Asian J. Chem. 7 (1995) 417.
[27] D.F.J. Arago, J.B. Biot, Mem. Aced. Fr. (1806) 7.
[28] D. Dale, F. Gladstone, Trans. R. Soc. Lond. 148 (1858) 887–894.
[29] P. Baraldi, M.G. Giorgini, D. Manzini, A. Marchetti, L. Tassi, J. Solut. Chem. 31 (2002) 873–973.
[30] H. Eyring, M.S. John, Significant Liquid Structures, John Wiley, New York, 1969.
[31] H.A. Lorentz, The Theory of Electrons and its Applications to the Phenomena of Light and Radiant Heat, Leipzig, 1906.
[32] W.J. Heller, J. Phys. Chem. 69 (1965) 1123–1129.
[33] J.F. Eykman, Rec. Trav. Chim. Pays-Bas 14 (1895) 185–202.
[34] G. Oster, Chem. Rev. (1948) 319–365.
[35] O. Weiner, Berichte Leipz. 62 (1910) 256–260.
[36] M.S. Reddy, K.T.S.S. Raju, SkMd Nayeem, I. Khan, K.B.M. Krishna, B.H. Babu, J. Solut. Chem. 45 (2016) 675–701.
[37] A. Aggarwal, N.L. Lancaster, A.R. Sethi, T. Welton, Green. Chem. 4 (5) (2002) 517–520.
[38] V. Znamenskiy, M.N. Kobrak, J. Phys. Chem. B 108 (2004) 1072–1079.
[39] N.R. Dhumal, H.J. Kim, J. Kiefer, J. Phys. Chem. A 115 (2011) 3551–3558.
[40] J.C. Lassègues, J. Grondin, D. Cavagnat, P. Johansson, J. Phys. Chem. A 113 (2009) 6419–6421.
[41] J.C. Lassègues, J. Grondin, D. Cavagnat, P. Johansson, J. Phys. Chem. A 114 (2009) 687–688.
[42] B. Zhang, Y. Zhou, X. Li, X. Ren, H. Nian, Y. Shen, Q. Yun, Spectrochimi. Acta Part A Mol. Biomol. Spectros. 122 (2014) 59–64.
[43] D. Battisti, G.A. Nazri, B. Klassen, R. Aroca, J. Phys. Chem. 97 (1993) 5826–5830.
[44] K. Noack, P.S. Schulz, N. Paape, J. Kiefer, P. Wasserscheid, A. Leipertz, Phys. Chem. Chem. Phys. 12 (2010) 14153–14161.

Please cite this article in press as: V. Srinivasa Rao et al., Investigation of intermolecular interactions in binary liquid mixtures of [Bmim][NTf_2] and propylene carbonate at different temperatures using ultrasonic, optical and FT-IR studies, Karbala International Journal of Modern Science (2017), http://dx.doi.org/10.1016/j.kijoms.2017.07.002



Taylor & Francis
Taylor & Francis Group

Physics and Chemistry of Liquids
An International Journal

ISSN: 0031-9104 (Print) 1029-0451 (Online) Journal homepage: http://www.tandfonline.com/loi/gpch20

Volumetric, acoustic, optical and spectroscopic studies of binary mixtures of the ionic liquid, 1-butyl-3-methyl imidazolium bis(trifluoromethylsulfonyl)imide and diethyl carbonate

V. Srinivasa Rao, M. Srinivasa Reddy, A. Srinivasa Rao, G. Pushpa Raju, K. Thomas S. S. Raju & B. Hari Babu

To cite this article: V. Srinivasa Rao, M. Srinivasa Reddy, A. Srinivasa Rao, G. Pushpa Raju, K. Thomas S. S. Raju & B. Hari Babu (2017): Volumetric, acoustic, optical and spectroscopic studies of binary mixtures of the ionic liquid, 1-butyl-3-methyl imidazolium bis(trifluoromethylsulfonyl)imide and diethyl carbonate, Physics and Chemistry of Liquids, DOI: 10.1080/00319104.2017.1337766

To link to this article: http://dx.doi.org/10.1080/00319104.2017.1337766

View supplementary material

Published online: 22 Jun 2017.

Submit your article to this journal

View related articles

View Crossmark data

Full Terms & Conditions of access and use can be found at
http://www.tandfonline.com/action/journalInformation?journalCode=gpch20

Download by: [The UC San Diego Library] **Date:** 23 June 2017, At: 01:14

PHYSICS AND CHEMISTRY OF LIQUIDS, 2017
https://doi.org/10.1080/00319104.2017.1337766

Taylor & Francis
Taylor & Francis Group

ARTICLE

Check for updates

Volumetric, acoustic, optical and spectroscopic studies of binary mixtures of the ionic liquid, 1-butyl-3-methyl imidazolium bis (trifluoromethylsulfonyl)imide and diethyl carbonate

V. Srinivasa Rao[a,d], M. Srinivasa Reddy[b], A. Srinivasa Rao[a,e], G. Pushpa Raju[e], K. Thomas S. S. Raju[c] and B. Hari Babu[d]

[a]Department of Chemistry, SRR Govt. Degree College, Vijayawada, India; [b]Department of Chemistry, KRK Govt. Degree College, Addanki, India; [c]Department of Chemistry, Andhra Loyola College, Vijayawada, India; [d]Department of Chemistry, Acharya Nagarjuna University, Nagarjunanagar, India; [e]Department of Chemistry, C.R. College, Guntur, India

ABSTRACT

The properties, density, speed of sound and refractive index of 'IL' [Bmim][NTf2], diethyl carbonate and their binary mixtures are measured over the whole composition range as a function of temperature between 303.15 and 323.15 K at atm. pressure. These values are used to calculate the excess molar volumes, excess partial molar volumes, partial molar volumes at infinite dilution, excess isentropic compressibility, free length, speeds of sound and isobaric thermal expansion coefficient for the mixture. Various rules were used to predict the refractive indices and the data have been compared with the experimental results. These excess properties are fitted to the Redlich–Kister type equation to obtain the binary coefficients and the standard deviations. A qualitative analysis of these parameters indicates strong intermolecular interactions and the interaction increases with the increase in temperature. This was further supported by IR spectroscopy. In addition, analysis of data of the mixture was done through the Prigogine–Flory–Patterson theory.

ARTICLE HISTORY
Received 7 February 2017
Accepted 31 May 2017

KEYWORDS
Ionic liquid [Bmim][NTf2]; DEC; density; speed of sound; excess thermodynamic parameters; PFP theory

1. Introduction

Substances that are entirely composed of ions and in liquid state are called ionic liquids (ILs). In present days, they attracted considerable attention because of their distinctive properties such as thermal stability, non-volatility and reusability [1–5]. ILs can be selected to have different anions and cations so that one can form IL with the desired properties. ILs with special functional groups have been designed for application in many industrial processes [6,7]. ILs are utilised for different purposes like extraction, separation and alternative solvents in catalytic reactions, synthesis, catalysis, biocatalyst, electro chemical devices, separation technology, reaction media, green solvents and in biodegradable materials.

Mixtures of ILs and molecular organic solvents are gaining interest of researchers as resultant liquid mixtures containing the advantages over both IL and molecular organic solvents. The properties of these mixtures are based on the mixing ratio. Mixing of the ILs with molecular solvents is one of the alternative steps not only to minimise the usage of expensive ILs and also to save time for preparing new ILs [8]. From an economic and ecological perspective, the mixtures of ILs and traditional organic solvents may be gaining a

CONTACT B. Hari Babu dr.b.haribabu@gmail.com
Supplementary data for this article can be accessed here.

© 2017 Informa UK Limited, trading as Taylor & Francis Group

tremendous amount of attention from both the researchers and the industries. ILs are more viscous than conventional organic solvents, which may hamper their application. Fortunately, their mixtures with molecular solvents show reduced viscosity to exploit their potential applications. In particular, the addition of polar co-solvents can strongly influence the physical and chemical properties of ILs such as viscosity, reactivity and electrical conductivity as well as solubility and solvation properties [9]. Recently, several binary IL+ molecular solvent systems have been shown to perform better than the pure ILs, and such systems have been used in numerous applications such as biocatalysed reactions, as super capacitors, as reaction media, medium for dissolution of biopolymers etc. [10–22]. Hence, IL+ molecular solvent mixtures have received growing attention in the past few years. The potential of these new substances can be exploited with experimental methods. Most of these novel media are characterised by their volumetric, acoustic and refractive index properties, since these data are important for industrial applications. To predict molecular interactions between binary liquids, speed of sound and refractive index along with experimental data of density plays vital role.

The choice of the investigated IL, 1-butyl-3-methylimidazolium bis(trifluoromethylsulfonyl) imide ([Bmim][NTf_2]), was on the basis of its ability to act as extracting solvent for the removal of many organic compounds through liquid–liquid extraction [23,24]. It is also widely used in catalysis [25] and chromatography [26]. The molecular organic liquid, diethyl carbonate (DEC), has been chosen because of its wide range of applications such as fuel additive, as green solvent for the replacement to conventional organic solvents and in organic synthesis [27]. It is also widely used in pesticides, fertiliser, manufacture of dyes and pharmaceutical products. DEC is expansively investigated as an electrolyte for lithium ion batteries [28,29].

Systematic investigation of the physicochemical properties of [Bmim][NTf_2] with molecular organic solvents including water has been reported. Alfonsina *et al.*[30] reported the physicochemical properties such as density, refractive index, viscosity of [Bmim][NTf_2] binary mixture with ethanol or ethyl acetate. Zarrougui *et al.* [31] reported the density, viscosity and conductivity and thermal expansivities of propylene carbonate with [Bmim][NTf_2], whereas Widowati *et al.* [32] reported pressure–volume–temperature properties of binary mixtures of the [Bmim][NTf_2] with anisole or acetophenone at elevated pressures. Vranes *et al.* [33] reported density and excess properties of [Bmim][NTf_2] + Propylene carbonate binary mixtures, Monika *et al.* [34] reported acoustic and volumetric properties of binary mixtures of [Bmim][NTf_2] with acetonitrile or tetrahydrofuran, Vranes *et al.* [35] reported density, electrical conductivity and viscosity of binary liquid mixtures of [Bmim][NTf_2], with γ-butyrolactone, Salinas *et al.* [36] reported densities, speed of sound, viscosity and excess properties of binary mixtures formed by ethanol and [Bmim][NTf_2], Jacquemin *et al.*[37] reported the density and viscosity of several pure and water-saturated ILs including [Bmim][NTf_2], Kassim *et al.* [38] reported the experimental densities and viscosities of binary mixture of [Bmim][NTf_2] with glycerol or sulfolane and their molecular interaction by COSMO-RS and Krishna *et al.*[39] reported densities, speeds of sound and refractive indices of the binary mixture of [Bmim][NTf_2] with pyrrolidin-2-one. But the thermo-acoustic, volumetric and refractive index data of [Bmim][NTf_2] with DEC were not reported.

On the basis our initial experiments, [Bmim][NTf_2] is found to be totally miscible with DEC in all proportions. Hence, in the present study, it is proposed to measure the densities, speeds of sound and refractive indices of the binary mixtures of [Bmim][NTf_2] with DEC in the temperature range between 303.15 and 323.15 K in the entire composition range and at atmospheric pressure. On the basis of the measured values, we calculated the excess/deviation properties for their potential application in industrial processes. Here, we reported the excess properties such as molar volumes (V_m^E), isentropic compressibilities (κ_s^E), free length (L_f^E), speeds of sound (u^E) and isobaric thermal expansion coefficient (α_P^E) along with $\left(\partial V_m^E/\partial T\right)_P$

and $\left(\partial H_{\mathrm{m}}^{\mathrm{E}}/\partial P\right)_T$. Also, the deviation of refractive index on volume fraction basis ($\Delta_\phi n_{\mathrm{D}}$) reported for the binary mixture and fitted using Redlich–Kister polynomial equation. Lastly, an attempt has been made to understand the interaction behaviour between the two liquids in the mixture using IR spectroscopy. In addition, analysis of $V_{\mathrm{m}}^{\mathrm{E}}$ data of the present mixture was done through the Prigogine–Flory–Patterson (PFP) theory.

2. Experimental section

2.1. *Materials*

The IL, [Bmim][NTf_2] (CAS 174899-83-3) with purity 0.99 in mass fraction used in this work. It was purchased from Io-Li-Tec GmBH (Germany), while DEC (CAS 105-58-8) with purity 0.995 in mass fraction was supplied by Sigma Aldrich. The chemicals used in the present investigation were purified by the methods described in literature [40,41]. The water content in investigated IL and DEC was determined using a Karl Fisher titrator (Mtrohm, 890 Titrando). Before any measurement, all samples were dried for at least 72 h under a vacuum (0.1 Pa) and moderate temperature (beginning at room temperature and increasing it gradually over a 6-h period up to 333 K). The water content of all the samples was further checked and found to be in the range of less than 150 ppm, a value much lower than the original pre-evacuation analysis, which typically showed values in the range of less than 210 ppm. [Bmim][NTf_2] is used without further purification; DEC is further purified by distillation. List of chemicals with details of provenance, CAS number and mass fraction purity is given in Table 1. The purities were verified by comparing the measured density, speed of sound and refractive index of the pure liquids with the literature at atmospheric pressure are given in Table 2.

Table 1. List of chemicals with details of provenance, CAS number and mass fraction purity.

Chemical	Provenance	CAS number	Purification method	Mass fraction purity	Final water mass fraction	Analysis method
1-Butyl-3-methylimidazoliumbis (trifluoromethylsulfonyl) imide	Io-Li-Tec, Germany	174899-83-3	Vacuum treatment	0.99	$<1.5 \times 10^{-4}$	NA
Diethyl carbonate	Sigma Aldrich	105-58-8	Distillation	0.995	$<1.5 \times 10^{-4}$	Gas liquid chromatography

Table 2. Comparison of experimental values of density, ρ, speed of sound, u, refractive index, n_{D}, and specific heat, C_{p}, of pure liquids with the corresponding literature values at different temperatures and at atmospheric pressure P = 101.3 kPa.

		ρ (kg m^{-3})		u (m s^{-1})		n_{D}		C_{p} (J K^{-1} mol^{-1})
Liquid	Temp (K)	Expt.	Lit.	Expt.	Lit.	Expt.	Lit.	Lit.
[Bmim][NTf_2]	303.15	1428.9	1429.40 [35]	1216.8	1216.77 [39]	1.42451	1.42523 [39]	569.74 [39]
	308.15	1424.1	1424.57 [35]	1205.8	1205.80 [39]	1.42309	1.42374 [39]	572.82 [39]
	313.15	1419.4	1419.61 [35]	1195.0	1194.95 [39]	1.42104	1.42225 [39]	575.56 [39]
	318.15	1414.6	1414.67 [35]	1184.2	1184.23 [39]	1.41951	1.42076 [39]	578.49 [39]
	323.15	1409.9	1409.65 [35]	1173.6	1173.61 [39]	1.41728	1.41923 [39]	581.68 [39]
Diethyl carbonate	303.15	963.7	963.5 [43]	1156.6	1156.9 [43]	1.37991	1.3802 [43]	213.82 [44]
	308.15	958.1	957.8 [43]	1136.3	1136.6 [43]	1.37755	1.3779 [43]	214.88 [44]
	313.15	952.4	952.1 [43]	1116.1	1116.5 [43]	1.37526	1.3756 [43]	215.82 [44]
	318.15	946.7	946.4 [43]	1096.2	1096.5 [43]	1.37290	1.3733 [43]	218.54 [44]
	323.15	941.0	940.7 [43]	1076.4	1076.7 [43]	1.37055	1.3710 [43]	220.31 [44]

Standard uncertainties u are $u(\rho) = 5 \times 10^{-2}$ kg m^{-3}, $u(u) = 0.5$ m s^{-1}, $u(n_{\mathrm{D}}) = 0.00005$, $u(T) = 0.01$ K and $u(P) = 0.5$ kPa.

2.2. *Apparatus and procedure*

2.2.1. *Sample preparation*

All samples are freshly prepared in amber colour glass vials with screw caps having PFE septa, and a secure seal with parafilm to prevent absorption of moisture from the atmosphere and are then stirred for more than 30 min to ensure total dissolution of the mixtures. Samples are taken from the vials with a syringe through the PFE septum. Samples are prepared by weighing with a precision of ±0.01 mg, using a Sartorius electronic balance (CPA225D). The uncertainty of the resulting mole fractions of the mixtures was estimated as being $\pm 2 \times 10^{-4}$.

2.2.2. *Measurement of density and speed of sound*

Densities and speed of sound are measured with an Anton Paar DSA-5000M-vibrating tube density and sound velocity meter. The density meter is calibrated with doubly distilled degassed water, and with dry air at atmospheric pressure. The temperature of the apparatus is controlled to within ±0.01 K by a built-in Peltier device. Measured density and speed of sound values (at frequency approximately 3 MHz) are precise to 5×10^{-3} kg m^{-3} and 5×10^{-1}m s^{-1}, respectively. The standard uncertainties associated with the measurements of temperature, density and speed of sound are estimated to be ±0.01 K, 5×10^{-2} kg m^{-3} and ±0.5 m s^{-1}, respectively.

2.2.3. *Measurement of refractive index*

The refractive indices are determined using an automatic refractometer (Anton Paar Dr Krenchen Abbemat (WR-HT)) that has also a temperature controller that keeps the samples at working temperature. The uncertainties in the temperature and refractive index values are ±0.01K and $\pm 5 \times 10^{-5}$, respectively. The apparatus is calibrated by measuring the refractive index of Millipore quality water and tetrachloroethylene (supplied by the company) before each series of measurements according to manual instructions. The calibration is checked with pure liquids by known refractive index.

2.2.4. *Measurement of infrared spectra*

Infrared transmittance is measured by using Shimadzu Fourier transform infrared spectrometer (IR Affinity-1S) equipped with attenuated total reflectance (ATR) accessories. The spectral region is 650–4000 cm^{-1} with resolution of 2 cm^{-1} and 100 scans. At least five repeated measurements are performed for each sample.

3. Results and discussion

The experimentally measured density (ρ), speed of sound (u) and refractive index (n_D) for the binary mixture of [Bmim][NTf$_2$] with DEC over the region of complete miscibility as a function of temperature between 303.15 and 323.15 K in steps of 5 K under atmospheric pressure are given in Table 3. The changes in values of ρ, u and n_D with respect to temperature and mole fraction are linear and non-linear, respectively. This trend specifies that molecular interactions definitely exist at all temperature between liquids in study. The excess and deviation parameters are calculated from the experimental data according to well-known thermodynamic expressions given below.

The excess molar volume is given by

$$V_m^E = \frac{x_1 M_1 + x_2 M_2}{\rho} - \left(\frac{x_1 M_1}{\rho_1} + \frac{x_2 M_2}{\rho_2} \right) \tag{1}$$

where M_1 and M_2 are the molecular weights, x_1 and x_2 are the mole fractions of [Bmim][NTf$_2$] and DEC, respectively, while ρ_1, ρ_2 and ρ are the densities of [Bmim][NTf$_2$], DEC and the mixture, respectively.

Table 3. Experimental density (ρ), speed of sound (u), refractive index (n_D), molar volume (V_m), isentropic compressibility (κ_s), free length (L_f) and isobaric thermal expansion coefficient (a_p) with mole fraction (x_1) of [Bmim][NTf_2] in the binary liquid mixture of {[Bmim][NTF_2] + diethyl carbonate} from T (K) = 303.15–323.15 at pressure P = 101.3 kPa.

x_1	ρ (kg m^{-3})	u (m s^{-1})	n_D	V_m ($10^{-6}m^3$ mol^{-1})	$k_s(10^{-10}Pa^{-1})$	$L_f(10^{-11}m)$	$a_p(10^{-4}$ $K^{-1})$
303.15 K							
0.0000	963.7	1156.6	1.37991	122.58	7.76	5.780	11.81
0.0542	1023.8	1159.2	1.38693	131.33	7.27	5.596	10.81
0.1108	1077.1	1167.9	1.39318	140.66	6.81	5.415	10.02
0.1522	1111.7	1173.8	1.39679	147.51	6.53	5.303	9.57
0.2084	1153.3	1181.1	1.40116	156.85	6.22	5.175	9.08
0.2886	1203.8	1190.0	1.40600	170.35	5.87	5.027	8.54
0.3927	1256.9	1199.0	1.41107	188.10	5.53	4.883	8.06
0.4805	1293.5	1204.5	1.41434	203.23	5.33	4.791	7.79
0.5887	1331.1	1208.9	1.41724	221.96	5.14	4.706	7.54
0.7043	1364.9	1211.5	1.41988	241.99	4.99	4.637	7.29
0.8009	1389.2	1213.0	1.42179	258.70	4.89	4.591	7.05
0.8586	1402.1	1213.9	1.42278	268.71	4.84	4.566	6.89
0.9127	1413.2	1215.1	1.42382	278.15	4.79	4.544	6.76
0.9521	1420.4	1216.3	1.42448	285.08	4.76	4.528	6.69
1.0000	1428.9	1216.8	1.42523	293.48	4.73	4.513	6.66
308.15 K							
0.0000	958.1	1136.3	1.37755	123.30	8.08	5.955	11.88
0.0542	1018.3	1139.3	1.38470	132.04	7.57	5.761	10.88
0.1108	1071.7	1149.6	1.39102	141.36	7.06	5.565	10.09
0.1522	1106.3	1156.5	1.39478	148.22	6.76	5.444	9.64
0.2084	1148.1	1164.9	1.39931	157.57	6.42	5.306	9.14
0.2886	1198.6	1174.9	1.40417	171.09	6.04	5.149	8.60
0.3927	1251.8	1185.0	1.40935	188.86	5.69	4.995	8.11
0.4805	1288.4	1191.1	1.41264	204.02	5.47	4.898	7.83
0.5887	1326.2	1196.2	1.41564	222.80	5.27	4.808	7.58
0.7043	1360.0	1199.5	1.41837	242.87	5.11	4.735	7.32
0.8009	1384.3	1201.4	1.42028	259.61	5.00	4.685	7.08
0.8586	1397.3	1202.6	1.42130	269.64	4.95	4.659	6.92
0.9127	1408.3	1203.9	1.42234	279.10	4.90	4.635	6.78
0.9521	1415.6	1205.2	1.42301	286.04	4.86	4.619	6.71
1.0000	1424.1	1205.8	1.42374	294.47	4.83	4.602	6.68
313.15 K							
0.0000	952.4	1116.1	1.37526	124.03	8.43	6.135	11.96
0.0542	1012.8	1121.1	1.38269	132.76	7.86	5.923	10.95
0.1108	1066.3	1132.1	1.38935	142.08	7.32	5.716	10.16
0.1522	1101.0	1139.5	1.39306	148.93	7.00	5.589	9.70
0.2084	1142.8	1148.6	1.39758	158.29	6.63	5.442	9.20
0.2886	1193.5	1159.7	1.40246	171.82	6.23	5.274	8.66
0.3927	1246.8	1170.9	1.40763	189.63	5.85	5.111	8.16
0.4805	1283.4	1177.9	1.41096	204.82	5.62	5.008	7.88
0.5887	1321.2	1183.7	1.41405	223.64	5.40	4.911	7.62
0.7043	1355.0	1187.6	1.41688	243.75	5.23	4.834	7.36
0.8009	1379.4	1189.9	1.41884	260.54	5.12	4.782	7.11
0.8586	1392.4	1191.2	1.41988	270.58	5.06	4.754	6.95
0.9127	1403.5	1192.8	1.42085	280.05	5.01	4.729	6.81
0.9521	1410.9	1194.2	1.42155	287.01	4.97	4.711	6.74
1.0000	1419.4	1195.0	1.42225	295.46	4.93	4.694	6.71
318.15 K							
0.0000	946.7	1096.2	1.37290	124.78	8.79	6.321	12.03
0.0542	1007.2	1102.3	1.38101	133.49	8.17	6.094	11.02
0.1108	1060.9	1114.4	1.38807	142.81	7.59	5.873	10.23
0.1522	1095.6	1122.5	1.39200	149.66	7.24	5.737	9.77
0.2084	1137.6	1132.5	1.39635	159.03	6.85	5.581	9.27
0.2886	1188.4	1144.7	1.40129	172.56	6.42	5.402	8.71
0.3927	1241.8	1157.1	1.40626	190.39	6.01	5.228	8.21
0.4805	1278.5	1164.8	1.40929	205.62	5.77	5.119	7.92
0.5887	1316.2	1171.3	1.41249	224.49	5.54	5.017	7.66
0.7043	1350.0	1175.8	1.41531	244.66	5.36	4.935	7.39
0.8009	1374.5	1178.5	1.41734	261.46	5.24	4.879	7.13
0.8586	1387.6	1180.1	1.41843	271.53	5.18	4.850	6.97

(*Continued*)

Table 3. (Continued).

x_1	ρ (kg m^{-3})	u (m s^{-1})	n_D	V_m (10^{-6}m^3 mol^{-1})	k_s(10^{-10}Pa^{-1})	L_f(10^{-11}m)	a_p(10^{-4} K^{-1})
0.9127	1398.7	1181.9	1.41940	281.02	5.12	4.823	6.84
0.9521	1406.2	1183.4	1.42008	287.97	5.08	4.804	6.76
1.0000	1414.6	1184.2	1.42076	296.45	5.04	4.786	6.73
323.15 K							
0.0000	941.0	1076.4	1.37055	125.54	9.17	6.513	12.10
0.0542	1001.7	1083.6	1.37982	134.23	8.50	6.271	11.10
0.1108	1055.5	1096.9	1.38670	143.55	7.87	6.035	10.30
0.1522	1090.3	1105.8	1.39066	150.40	7.50	5.890	9.84
0.2084	1132.3	1116.6	1.39515	159.77	7.08	5.724	9.33
0.2886	1183.1	1129.9	1.40046	173.32	6.62	5.534	8.77
0.3927	1236.5	1143.3	1.40501	191.20	6.19	5.349	8.26
0.4805	1273.1	1151.8	1.40778	206.48	5.92	5.233	7.97
0.5887	1311.0	1159.1	1.41101	225.37	5.68	5.124	7.69
0.7043	1345.0	1164.1	1.41379	245.57	5.49	5.037	7.42
0.8009	1369.6	1167.2	1.41582	262.40	5.36	4.979	7.16
0.8586	1382.7	1169.0	1.41692	272.48	5.29	4.947	7.00
0.9127	1394.0	1171.0	1.41787	281.97	5.23	4.919	6.86
0.9521	1401.6	1172.7	1.41855	288.91	5.19	4.899	6.79
1.0000	1409.9	1173.6	1.41924	297.44	5.15	4.880	6.75

Standard uncertainties u are: $u(x_1) = 0.0001$, $u(\rho) = 5 \times 10^{-2}$ kg m^{-3}, $u(u) = 0.5$ m s^{-1}, $u(n_D) = 0.00005$, $u(T) = 0.01$ K and $u(P) = 0.5$ kPa. Combined uncertainties (confidence level, 95%): $U_c(V_m) = \pm 0.05 \times 10^{-6}$ m^3 mol^{-1}, $U_c(\kappa_s) = \pm 0.01 \times 10^{-10}$ Pa^{-1}, $U_c(L_f) = \pm 0.007 \times 10^{-11}$m, $U_c(\alpha_p) = \pm 0.04 \times 10^{-4}$ K^{-1}. All the experiments were carried out at atmospheric pressure.

The isentropic compressibility, κ_S, is computed directly from the measured values of speed of sound and density using the Newton–Laplace equation:

$$\kappa_s = -\frac{1}{V_m}\left(\frac{\partial V_m}{\partial P}\right)_s = \left(\frac{1}{\rho u^2}\right) = \left(\frac{V_m}{M u^2}\right) \tag{2}$$

Excess isentropic compressibility is given by

$$\kappa_S^{\mathrm{E}} = \kappa_S - \kappa_S^{\mathrm{id}} \tag{3}$$

where κ_S is the isentropic compressibility and κ_S^{id} is the isentropic compressibility of the ideal mixture, which is calculated in the manner as suggested by Benson and Kiyohara [45].

$$\kappa_S^{\mathrm{id}} = \sum_{i=1}^{2} \phi_i \left[\kappa_{S,i} + \frac{T V_i \alpha_i^2}{C_{p,i}}\right] - \left\{ T \frac{\left(\sum_{i=1}^{2} x_i V_i\right)\left(\sum_{i=1}^{2} \phi_i \alpha_i\right)^2}{\left(\sum_{i=1}^{2} x_i C_{p,i}\right)} \right\} \tag{4}$$

where ϕ_i is the volume fraction of the ith component and is given by, $\phi_i = x_i V_i / \sum_{i=1}^{2} x_i V_i$, T is the temperature, $\kappa_{s,i}$ is the isentropic compressibility, V_i is the molar volume, α_i is the isobaric thermal expansion coefficient and $C_{P,i}$ is heat capacity of the ith component.

Free length is given by

$$L_{\mathrm{f}} = \kappa_j (\kappa_S)^{1/2} \tag{5}$$

where κ_j is the temperature-dependent Jacobson's constant which is equal to $\kappa_j = (93.875 + 0.375T) \times 10^{-8}$.

The excess intermolecular free length is given by

$$L_f^E = L_f - L_f^{id} = \kappa_j(\kappa_S)^{1/2} - \kappa_j\left(\kappa_S^{id}\right)^{1/2} \tag{6}$$

The excess speeds of sound, u^E is estimated in binary and ternary mixtures using the following expression [42]:

$$u^E = u - u^{id} = u - \left(\rho^{id}k_S^{id}\right)^{-1/2} \tag{7}$$

where $\rho^{id} = \sum_{i=1}^{2}\phi_i\rho_i$

Isobaric thermal expansion coefficient, α_p, of the pure components is calculated from the measured densities by the relation,

$$\alpha_p = \frac{1}{V_m}\left(\frac{\partial V_m}{\partial T}\right)_p = -\frac{1}{\rho}\left(\frac{\partial \rho}{\partial T}\right)_p = -\left(\frac{\partial \ln \rho}{\partial T}\right) \tag{8}$$

The values of α_p are derived by taking differentiation linear regression between density and temperature.

Excess isobaric thermal expansion coefficient, α_P^E is calculated from the following equation:

$$\alpha_P^E = \alpha_P - \alpha_P^{id} = \frac{\left(\partial V_m^E/\partial T\right)_p - V_m^E\alpha_P^{id}}{V_m^{id} + V_m^E} \tag{9}$$

where $\alpha_P^{id} = \sum_{i=1}^{2}\phi_i\alpha_{P,i}^*$.

The dependence of the excess molar enthalpy of mixing with pressure at fixed temperature $\left(\partial H_m^E/\partial P\right)_T$ can be derived indirectly from accurate measurement of V_m^E, as a function of the temperature and composition by application of the following exact thermodynamic expression:

$$\left(\frac{\partial H_m^E}{\partial P}\right)_T = V_m^E - T\left(\frac{\partial V_m^E}{\partial T}\right)_P. \tag{10}$$

If the difference between the refractive indices of the two components is small, then deviation in refractive index of binary mixtures containing ILs:

$$\Delta_\phi n_D = n_D - n_D^{id} \tag{11}$$

$$n_D^{id} = \phi_1 n_{D,1} + \phi_2 n_{D,2}$$

The excess/deviation properties are fitted to a Redlich–Kister polynomial equation given by

$$Y^E = x_1x_2\sum_{i=o}^{j} A_i(x_1 - x_2)^i \tag{12}$$

where $Y^E = V_m^E$, κ_s^E, L_f^E, u^E, α_P^E, $\Delta_\phi n_D$, $\left(\partial V_m^E/\partial T\right)_P$ and $\left(\partial H_m^E/\partial P\right)_T$. x_1 and x_2 are the mole fraction of [Bmim][NTf_2] and DEC, respectively. Further, A_i are the adjustable parameters of the function and are determined using the least square method. In the present investigation 'i' values are taken from 0 to 4. The corresponding standard deviations $\sigma(Y^E)$ are calculated using the following expression and represented in Table S1 of the supplementary material.

$$\sigma\left(Y^E\right) = \left[\frac{\sum\left(Y_{exp}^E - Y_{cal}^E\right)^2}{(m-n)}\right]^{1/2} \tag{13}$$

where m is the total number of experimental points and n is the number of coefficients in Equation (12).

The variations as observed in these excess/deviation parameters indicate the strength of interactions that exist between the component molecules of the binary mixture under study and their further dependence on the composition, molecular size, shape and temperature. The effects which influence these thermodynamic functions may be the resultant contribution from several opposing effects, namely chemical, structural and physical [46,47]. The chemical or specific interactions include the formation of hydrogen bonding between component molecules, charge-transfer complexes. The structural contributions arise from several effects such as interstitial accommodation and geometrical fitting of one component into another. Excess molar volumes for the binary mixture of [Bmim][NTf_2] with DEC as a function of composition from T = 303.15 to 323.15 K are shown in Figure 1. The variations of excess molar volumes are found to be negative in the whole composition range at all temperatures which may be credited to the hydrogen bonding between solute and solvent molecules and also favourable fitting of smaller DEC molecules (at T = 303.15 K, V_m = 122.58 × 10^{-6} m^3 mol^{-1}) into the voids created by larger [Bmim][NTf_2] molecules (at T = 303.15 K, V_m = 293.48 × 10^{-6} m^3 mol^{-1}) is definitely contributing to interactions. The similar variations in V_m^E values are also observed for the rest of studied temperatures. Moreover, the variation of V_m^E for the present system as a function of temperature becomes more negative with rise in temperature. This is because of the fact that, more favourable fitting of smaller DEC molecules into the voids created by larger IL molecules, thereby, shrinkage of the volume of the mixture to a larger extent, resulting in more negative V_m^E values with rise in temperature. Therefore, order of strength of interaction enhances with rise in temperature.

The existing molecular interactions in the current binary system are properly reflected on the properties of partial molar volumes of the constituent molecules. Partial molar volume is the contribution that a component of a mixture makes to the total volume of the solution. Therefore, the partial molar volume is a function of mixture composition. The partial molar volumes $\bar{V}_{m,1}$ of component **1** ([Bmim][NTf_2]) and $\bar{V}_{m,2}$ of component **2** (DEC) in the mixtures over the whole composition range have been computed using the following relationships:

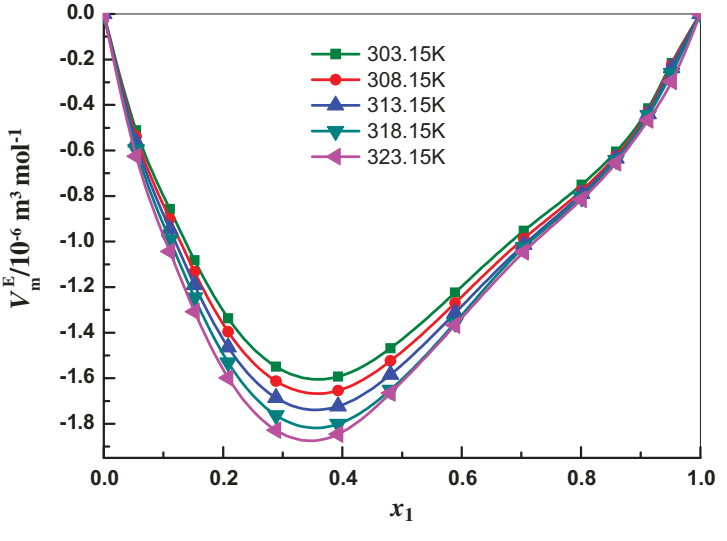


Figure 1. Plots of excess molar volume (V_m^E) against mole fraction of [Bmim][NTf_2] with DEC at different temperatures.

$$\bar{V}_{\mathrm{m},1} = V_{\mathrm{m}}^{\mathrm{E}} + V_1^* + x_2\left(\frac{\partial V_{\mathrm{m}}^{\mathrm{E}}}{\partial x_1}\right)_{T,P} \tag{14}$$

$$\bar{V}_{\mathrm{m},2} = V_{\mathrm{m}}^{\mathrm{E}} + V_2^* - x_1\left(\frac{\partial V_{\mathrm{m}}^{\mathrm{E}}}{\partial x_1}\right)_{T,P} \tag{15}$$

where V_1^* and V_2^* are the molar volumes of pure components of [Bmim][NTf_2] and DEC, respectively. The derivatives in the above equations are obtained by differentiating Redlich–Kister equation (12) which leads to the following equations for $\bar{V}_{\mathrm{m},1}$ and $\bar{V}_{\mathrm{m},2}$.

$$\bar{V}_{m,1} = V_1^* + x_2^2\sum_{i=0}^{4} A_i(x_1 - x_2)^i - 2x_1x_2^2\sum_{i=1}^{4} A_i(i)(x_1 - x_2)^{i-1} \tag{16}$$

$$\bar{V}_{m,2} = V_2^* + x_1^2\sum_{i=0}^{4} A_i(x_1 - x_2)^i + 2x_2x_1^2\sum_{i=1}^{4} A_i(i)(x_1 - x_2)^{i-1} \tag{17}$$

Using the above equations, $\bar{V}_{\mathrm{m},1}^{\mathrm{E}}$ and $\bar{V}_{\mathrm{m},2}^{\mathrm{E}}$ have been calculated using,

$$\bar{V}_{\mathrm{m},1}^{\mathrm{E}} = \bar{V}_{\mathrm{m},1} - V_1^* \tag{18}$$

$$\bar{V}_{\mathrm{m},2}^{\mathrm{E}} = \bar{V}_{\mathrm{m},2} - V_2^* \tag{19}$$

The calculated values of $\bar{V}_{\mathrm{m},1}$ and $\bar{V}_{\mathrm{m},2}$ for the studied binary system are represented in Table 4. On visualising the values of $\bar{V}_{\mathrm{m},1}$ and $\bar{V}_{\mathrm{m},2}$ for the two components in the mixtures (Table 4), it is evident that the values are lower than their individual molar volumes in the pure state, which reveals contraction of volume occurs on mixing [Bmim][NTf_2] with DEC at all examined temperatures. Figures 2 and 3 represent the disparity of excess partial molar volumes of $\bar{V}_{\mathrm{m},1}^{\mathrm{E}}$ ([Bmim][NTf_2]) and $\bar{V}_{\mathrm{m},2}^{\mathrm{E}}$ (DEC), respectively, in the binary mixture at T = 303.15, 308.15, 313.15, 318.15 and 323.15 K. Figures 2 and 3 not only show the existence of strong forces between the unlike molecules but also support the inferences drawn from excess molar volume.

The excess partial molar volumes at infinite dilution of component **1** ($\bar{V}_{\mathrm{m},1}^{\mathrm{E},\infty}$) and component **2** ($\bar{V}_{\mathrm{m},2}^{\mathrm{E},\infty}$) have been calculated using:

$$\bar{V}_{\mathrm{m},1}^{\mathrm{E},\infty} = A_0 - A_1 + A_2 - A_3 + \ldots = \bar{V}_{\mathrm{m},2}^{\infty} - V_2^* \tag{20}$$

$$\bar{V}_{\mathrm{m},2}^{\mathrm{E},\infty} = A_0 + A_1 + A_2 + A_3 + \ldots = \bar{V}_{\mathrm{m},1}^{\infty} - V_1^* \tag{21}$$

The partial molar volumes ($\bar{V}_{\mathrm{m},1}^{\infty}$, $\bar{V}_{\mathrm{m},2}^{\infty}$) and excess partial molar volumes at infinite dilution ($\bar{V}_{\mathrm{m},1}^{\mathrm{E},\infty}$, $\bar{V}_{\mathrm{m},2}^{\mathrm{E},\infty}$) of [Bmim][$NTf_2$] and DEC are calculated using Equations (18–21). The pertinent data of $\bar{V}_{\mathrm{m},1}^{\infty}$, $\bar{V}_{\mathrm{m},2}^{\infty}$ and $\bar{V}_{\mathrm{m},1}^{\mathrm{E},\infty}$, $\bar{V}_{\mathrm{m},2}^{\mathrm{E},\infty}$ is presented in Table 5 at T = (303.15, 308.15, 313.15, 318.15 and 323.15) K. The values of $\bar{V}_{\mathrm{m},1}^{\mathrm{E},\infty}$ and $\bar{V}_{\mathrm{m},2}^{\mathrm{E},\infty}$ are found to be negative and become more negative with increase of temperature. This indicates that the association effect is greater than the dissociation effect for both the components in the present system. The excess partial molar volumes at infinite dilution for [Bmim][NTf_2] ($\bar{V}_{\mathrm{m},1}^{\mathrm{E},\infty}$) are more negative than those of DEC ($\bar{V}_{\mathrm{m},2}^{\mathrm{E},\infty}$) at all studied temperatures. This is because for more concentrated DEC solution, no hydrogen bonds exist among DEC molecules. Hence, we conclude that strong interactions increase among the unlike molecules of the mixtures with increase in temperature [48]. These are noticed in the case of $V_{\mathrm{m}}^{\mathrm{E}}$ values in the binary system which are well reproduced from the evaluated properties of partial molar volumes at infinite dilution as well as at all investigated temperatures.

Table 4. Partial molar volumes of component-1 ($\bar{V}_{m,1}$) ([Bmim][NTf_2]) and component-2 ($\bar{V}_{m,2}$) (diethyl carbonate) with mole fraction (x_1) of [Bmim][NTf_2] in the binary liquid mixture from T (K) = 303.15–323.15 at pressure P = 101.3 kPa.

	303.15 K		308.15 K		313.15 K		318.15 K		323.15 K	
	$\bar{V}_{m,1}$	$\bar{V}_{m,2}$	$\bar{V}_{m,1}$	$\bar{V}_{m,2}$	$\bar{V}_{m,1}$	$\bar{V}_{m,2}$	$\bar{V}_{m,1}$	$\bar{V}_{m,2}$	$\bar{V}_{m,1}$	$\bar{V}_{m,2}$
x_1	(10^{-6} m^3 mol^{-1})		(10^{-6} m^3 mol^{-1})		(10^{-6} m^3 mol^{-1})		(10^{-6} m^3 mol^{-1})		(10^{-6} m^3 mol^{-1})	
0.0000	284.14	122.58	284.53	123.30	284.93	124.03	285.27	124.78	285.56	125.54
0.0542	285.09	122.56	285.55	123.29	286.02	124.02	286.45	124.77	286.81	125.54
0.1108	285.98	122.53	286.52	123.26	287.07	124.00	287.60	124.75	288.04	125.52
0.1522	286.59	122.51	287.18	123.24	287.78	123.98	288.38	124.73	288.88	125.51
0.2084	287.38	122.48	288.04	123.22	288.70	123.96	289.38	124.70	289.95	125.49
0.2886	288.45	122.45	289.20	123.18	289.93	123.92	290.68	124.66	291.34	125.47
0.3927	289.80	122.36	290.63	123.08	291.43	123.83	292.22	124.57	293.00	125.41
0.4805	290.87	122.17	291.75	122.88	292.60	123.63	293.41	124.41	294.28	125.24
0.5887	292.03	121.64	292.95	122.34	293.85	123.10	294.72	123.92	295.68	124.72
0.7043	292.94	120.61	293.90	121.28	294.85	122.01	295.80	122.82	296.81	123.51
0.8009	293.36	119.36	294.34	119.98	295.33	120.65	296.33	121.34	297.35	121.88
0.8586	293.47	118.48	294.46	119.07	295.45	119.68	296.46	120.25	297.48	120.69
0.9127	293.50	117.63	294.49	118.18	295.48	118.72	296.49	119.17	297.50	119.51
0.9521	293.49	117.02	294.48	117.55	295.47	118.05	296.47	118.41	297.47	118.68
1.0000	293.48	116.37	294.47	116.87	295.46	117.33	296.45	117.61	297.44	117.82

Standard uncertainties u are $u(x_1)$ = 0.0001, $u(\rho)$ = 5 × 10^{-2} kg m^{-3}, $u(T)$ = 0.01 K and $u(P)$ = 0.5 kPa.
Combined uncertainties (confidence level, 95%): $U(\bar{V}_{m,1}) = \pm 0.05 \times 10^{-6}$ m^3 mol^{-1} and $U(\bar{V}_{m,2}) = \pm 0.05 \times 10^{-6}$ m^3 mol^{-1}.

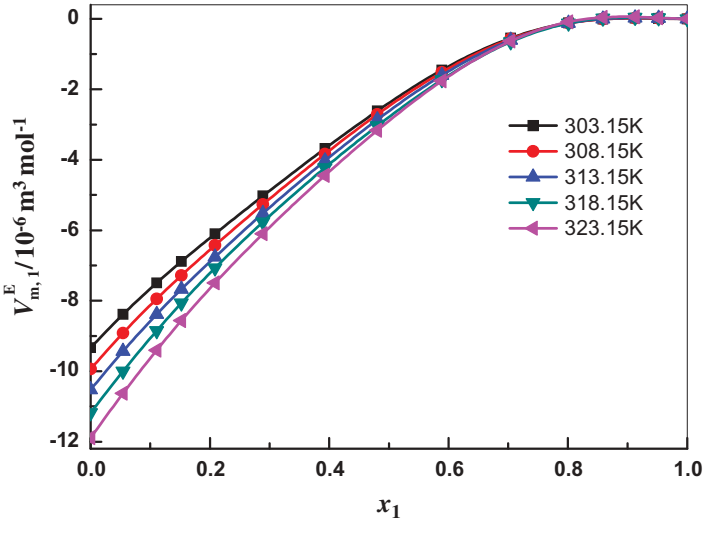


Figure 2. Plots of excess partial molar volume ($V^E_{m,1}$) against mole fraction of [Bmim][NTf_2] with DEC at different temperatures.

In Figure 4, the κ_s^E values for [Bmim][NTf_2] + DEC are negative in the whole composition range at all investigated temperatures. The negative κ_s^E values attributed to the strong attractive interactions between the molecules of the components [49]. This supports the inference drawn from V_m^E. The intermolecular free length indicates closer approach of unlike molecules. The trends of L_f^E values (Figure S1 of the supplementary material) are negative at all investigated temperatures. The negative values of L_f^E are generally observed due to the dominance of specific interactions between unlike molecules in the liquid mixture and also due to the structural readjustments in the liquid mixture towards a less compressible phase of fluid and closer packing of molecules [50]. Figure S2 of the supplementary material shows that the u^E values are positive for the system

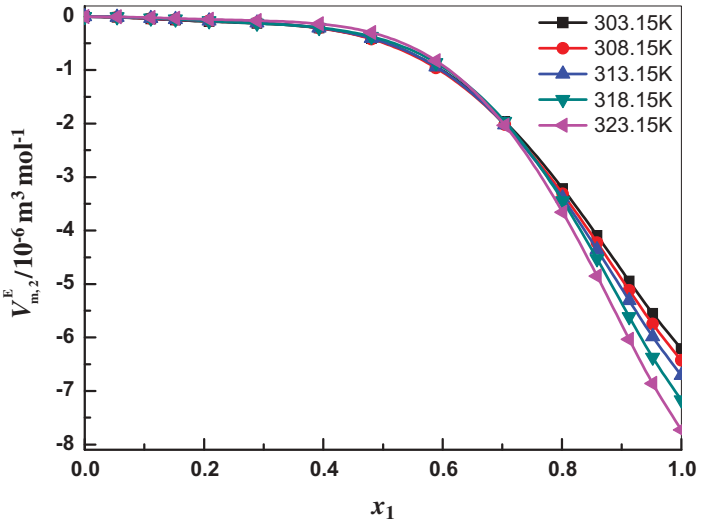


Figure 3. Plots of excess partial molar volume ($V^E_{m,2}$) against mole fraction of [Bmim][NTf_2] with DEC at different temperatures.

Table 5. Partial molar volumes at infinite dilution ($\bar{V}^{\infty}_{m,1}$,$\bar{V}^{\infty}_{m,2}$) and excess partial molar volumes at infinite dilution ($\bar{V}^{E,\infty}_{m,1}$, $\bar{V}^{E,\infty}_{m,2}$) of [Bmim][NTf_2] and diethyl carbonate at T = (303.15, 308.15, 313.15, 318.15 and 323.15) K.

	$\bar{V}^{\infty}_{m,1}$	$\bar{V}^{E,\infty}_{m,1}$	$\bar{V}^{\infty}_{m,2}$	$\bar{V}^{E,\infty}_{m,2}$
Temp (K)	(10^{-6} m^3 mol^{-1})		(10^{-6} m^3 mol^{-1})	
303.15	284.14	−9.34	116.37	−6.21
308.15	284.53	−9.94	116.87	−6.43
313.15	284.93	−10.53	117.32	−6.71
318.15	285.27	−11.18	117.61	−7.17
323.15	285.55	−11.89	117.81	−7.73

Combined uncertainties (confidence level, 95%): $U\left(\bar{V}^{E,\infty}_{m,1}\right) = \pm 0.05 \times 10^{-6}\ m^3\ mol^{-1}$ and $U\left(\bar{V}^{E,\infty}_{m,2}\right) = \pm 0.05 \times 10^{-6}\ m^3\ mol^{-1}$.

over the entire ranges of composition at all the studied temperatures. Positive deviations indicate the increasing strength of interaction between component molecules of binary liquid mixtures. In general, strong interactions among the components of a mixture lead to the formation of molecular aggregates and more compact structures; then, sound will travel faster through the mixture [51]. According to Ali *et al.* [52], more positive values mean much more strong interactions between the molecules.

The refractive indices (n_D) for the binary mixtures at the studied temperatures over the whole composition range were given in Table 3 which increases with increase in the concentration of the ILs in the mixture and decreases as the temperature increases for a particular concentration of [Bmim][NTf_2]. The values of $\Delta_\phi n_D$ are positive over the studied range of composition for the binary mixtures (Figure 5) which may be attributed to the non-availability of the free volume in the mixture in comparison with the ideal mixtures. As the mole fraction of the [Bmim][NTf_2] increases, V^E_m becomes more negative because the free space available decreases in the mixtures and speed of the light travel with lesser velocity than that in the ideal mixtures [53,54]. This gives increase in refractive index (n_D) causing $\Delta_\phi n_D$ positive. Further, as temperature increases, V^E_m found to become more negative and consequently $\Delta_\phi n_D$ become more positive. Thus, the inference of $\Delta_\phi n_D$ also supports the increase of strength of strong interactions with increase in temperature. A number of mixing rules of refractive index (n_D) have been proposed for liquid mixtures in terms of the refractive indices of the pure components proposed by different investigators such as Arago–Biot (A–B) [55], Gladstone–Dale

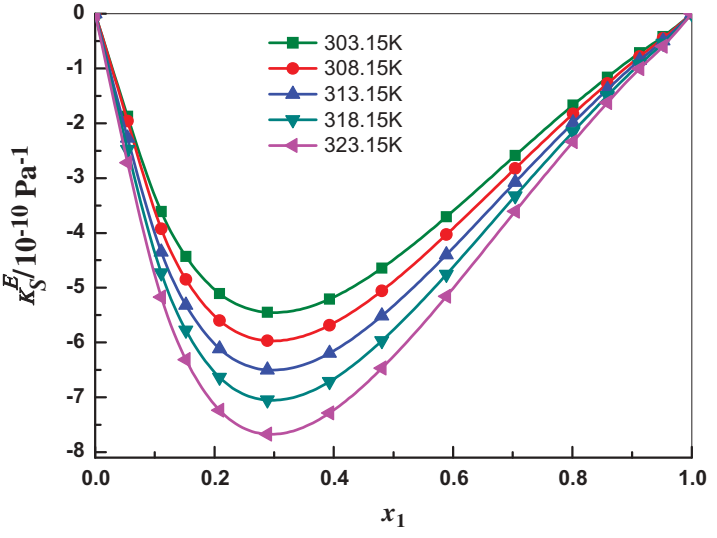


Figure 4. Plots of excess isentropic compressibility (κ_s^E) against mole fraction of [Bmim][NTf_2] with DEC at different temperatures.

(G–D) [56], Newton (N) [57], Eyring and John (E–J) [58], Lorentz–Lorenz (L–L) [59], Heller (H) [60], Eykman (EK) [61], Oster (Os) [62] and Weiner (W) [63] which were examined for present [Bmim][NTf_2] + DEC mixture. The refractive indices values calculated from various theories along with experimental values at different temperatures are represented in Figure 6. The absolute percentage deviation (APD) of experimental refractive index is calculated by Equation (22) and represented in Table 6.

$$\mathrm{APD} = \frac{100}{n}\sum_{i=1}^{n}\left(\left|\frac{n_{\mathrm{cal}}}{n_{\mathrm{exp}}} - 1\right|\right) \tag{22}$$

where n_{exp} is experimental refractive index and n_{cal} is the value calculated from various mixing rules and n is the number of data points.

The negative values of α_P^E are due to strong interactions between solute and solvent molecules [64]. Figure 7 shows negative values of α_P^E in the whole composition range and at all investigated temperatures for the binary mixture in study. This further supports the existence of strong interactions between the constituent molecules in binary liquid solution. In Table 7, the values of excess functions $\left(\partial V_m^E/\partial T\right)_P$ and $\left(\partial H_m^E/\partial P\right)_T$ are represented. The variation of $\left(\partial V_m^E/\partial T\right)_P$ and $\left(\partial H_m^E/\partial P\right)_T$ is similar with the mole fraction and temperature but with opposite sign. The negative values of $\left(\partial V_m^E/\partial T\right)_P$ for the studied mixture may be due to strong interactions existing between the unlike molecules of the mixture [65]. The isothermal pressure coefficient of excess molar enthalpy $\left(\partial H_m^E/\partial P\right)_T$ has positive values in the whole composition range. This reflects increase in attraction forces between two components of this mixture by increasing pressure. Hence, contraction in the volume of the mixture is still possible by increasing pressure [48,66].

3.1. *Infrared spectral studies*

The existence of strong interactions in the system which were drawn from the above inferences of derived excess/deviation parameters is well supported by IR spectral studies. The unique properties of imidazoliumcations are found in their electronic structure. The electronic structure of

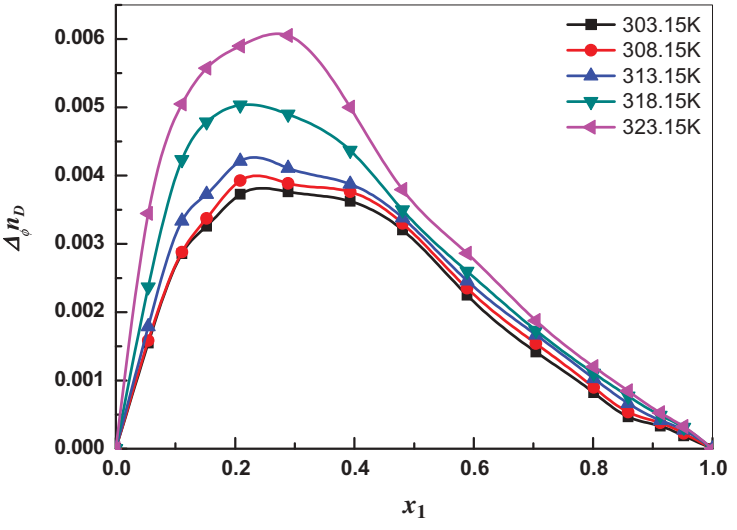


Figure 5. Plots of deviation in refractive index ($\Delta_{\emptyset} n_D$) against mole fraction of [Bmim][NTf_2] with DEC at different temperatures.

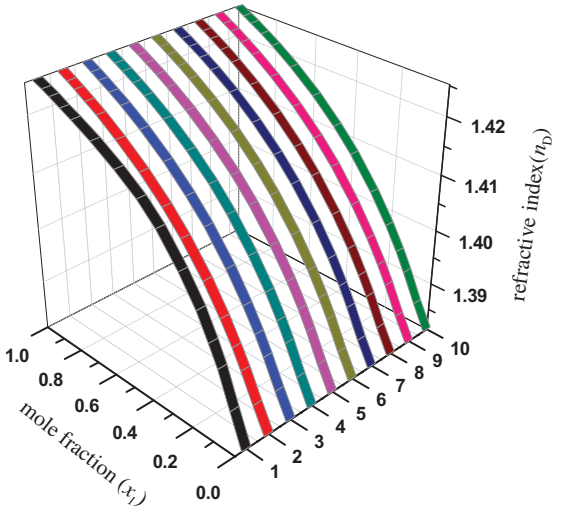


Figure 6. Plots of deviations in refractive index ($\Delta_{\phi_{n_D}}$) calculated from various theories along with experimental values against mole fraction of [Bmim][NTf_2] with DEC at 303.15 K.

(1) Expt., (2) Ara–Biot, (3) Gla–Dale, (4) Newton, (5) Eyri–John, (6) Lor–Lor, (7) Heller, (8) Eykman, (9) Oster, (10) Wiener.

Table 6. Average percentage deviation of calculated refractive indices compared to experimental values at various temperatures of [Bmim][NTf_2] and diethyl carbonate binary mixture at T = (303.15, 308.15, 313.15, 318.15 and 323.15) K.

T (K)	A–B	G–D	N	E–J	L–L	H	EK	Os	W
303.15	0.13	0.13	0.12	0.13	0.14	0.14	0.15	0.15	0.13
308.15	0.14	0.14	0.13	0.14	0.14	0.14	0.15	0.16	0.14
313.15	0.15	0.15	0.14	0.15	0.15	0.15	0.16	0.17	0.15
318.15	0.17	0.17	0.16	0.18	0.18	0.18	0.19	0.20	0.17
323.15	0.20	0.20	0.19	0.21	0.21	0.21	0.22	0.23	0.20
Average	0.16	0.16	0.15	0.16	0.16	0.16	0.17	0.18	0.16

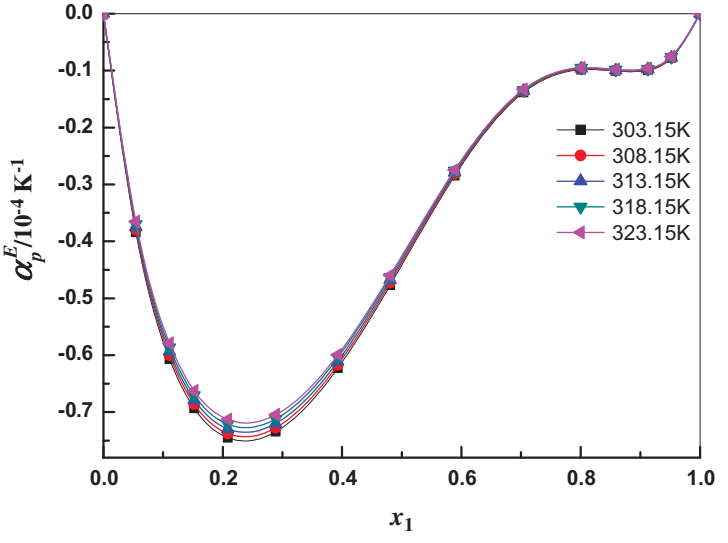


Figure 7. Plots of excess isobaric thermal expansion coefficient (α_p^E) against mole fraction of [Bmim][NTf_2] with DEC at different temperatures.

Table 7. The values of excess functions $\left(\partial V_m^E/\partial T\right)_P$ and $\left(\partial H_m^E/\partial P\right)_T$ at 298.15 K against mole fraction of [Bmim][NTf_2].

	$\left(\partial V_m^E/\partial T\right)_P$	$\left(\partial H_m^E/\partial P\right)_T$
x_1	(10^{-9} m^3 mol^{-1} K^{-1})	(10^{-6} J mol^{-1} Pa^{-1})
0.0000	0.0	0.00
0.0542	−5.62	1.19
0.1108	−9.45	2.01
0.1522	−11.34	2.36
0.2084	−13.00	2.60
0.2886	−13.95	2.68
0.3927	−13.10	2.38
0.4805	−10.90	1.84
0.5887	−7.27	0.98
0.7043	−4.06	0.28
0.8009	−3.08	0.18
0.8586	−3.13	0.35
0.9127	−3.04	0.51
0.9521	−2.37	0.50
1.0000	0.00	0.00

Standard uncertainties u are $u(x_1) = 0.0002$, $u(T) = 0.01$ K and $u(P) = 0.5$ kPa. Combined uncertainties (confidence level, 95%): $U\left(\partial V_m^E/\partial T\right)_P = \pm 0.1 \times 10^{-9}$ m^3 mol^{-1} K^{-1} and .

$U\left(\partial H_m^E/\partial P\right)_{T=298.15\,K} = \pm 0.06 \times 10^{-6}$ J mol^{-1} Pa^{-1}

imidazolium cations (Figure 8) contains delocalised 3-centre-4-electron configuration across the N_1–C_2–N_3 moiety, a double bond between C_4 and C_5 at the opposite side of the ring, and a weak delocalisation in the central region [67]. The hydrogen in C_2–H is more acidic than C_4–H, and C_5–H due to the electron deficiency in the C=N bond. The resultant acidity of the hydrogen atoms is key to understand the properties of these ILs. The hydrogen on the C_2 carbon (C_2–H) has been shown to bind typically with solute molecules [68,69].

In order to study the effects of molecular interactions, infrared absorbance is recorded from 650 to 4000 cm^{-1} (Figure 9 and Table 8). In [Bmim]$^+$ cation, the C–H stretching region from 2800 to 3200 cm^{-1} is investigated. For [Bmim][NTf_2], the signals in this region can be separated into

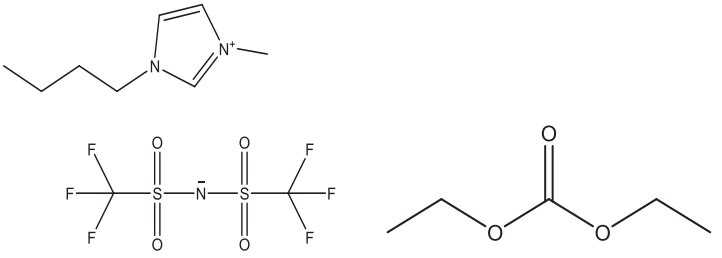


Figure 8. Chemical Structures of ([Bmim][NTf_2]) and DEC.

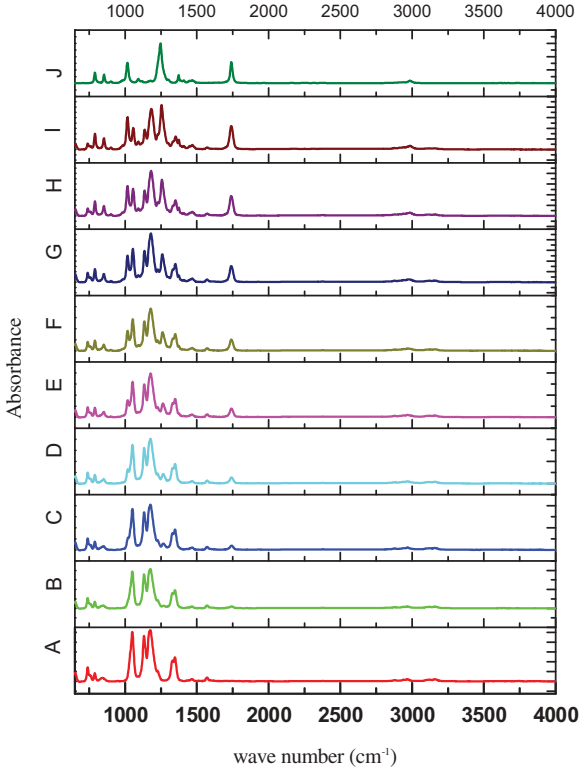


Figure 9. Infrared spectra of (A) pure IL [Bmim][NTf_2], (B) 0.8892, (C) 0.7916, (D) 0.7114, (E) 0.6073, (F) 0.5195, (G) 0.4113, (H) 0.2957, (I) 0.1991, (J) 0.0873 and (K) pure DEC. (B–J) represents mole fraction of [Bmim][NTf_2] in DEC.

two parts: signals between 3000 and 3200 cm^{-1} can be attributed to C–H vibrational modes mainly arising from the aromatic imidazolium ring, from C_2–H and $C_{4,5}$–H stretching frequencies [70]. The signals between 2800 and 3000 cm^{-1} are due to aliphatic C–H groups in the methyl and butyl moieties [71–73]. The C_2–H vibrational frequency (3120.7 cm^{-1}) is shifted to lower frequencies by about 36.5 cm^{-1} when compared to the C_4–H and C_5–H stretches (3157.2 cm^{-1}) because of its stronger acidic character. In [Bmim][NTf_2], there exist hydrogen bond between aromatic C–H hydrogen's of the cation and oxygen, fluorine atoms of the anion [74]. In the present mixtures, C_2–H and $C_{4,5}$–H stretching frequencies of the cation and SO_2 Sym. stretch, CF_3 Sym. stretch of the anion are analysed where there is no overlap from peaks of DEC. As mole fraction of IL (x_1) changes from 1.0000 to 0.7916, not very much change in the frequencies

Table 8. Infrared absorbance wave numbers (cm^{-1}) between 2800 and 3200 of [Bmim][NTf_2] in DEC at room temperature and atmospheric pressure P = 101.3 kPa.

Mole fraction of [Bmim][NTf_2]	Mole fraction of DEC	C_2–H stretching	$C_{4,5}$–H stretching	SO_2 Sym. stretch	CF_3 Sym. stretch
1.0000	0.0000	3120.7	3157.2	1131.5	1226.1
0.8892	0.1108	3120.7	3157.5	1131.6	1226.6
0.7916	0.2084	3120.7	3157.5	1131.6	1226.6
0.7114	0.2886	3120.2	3156.9	1132.2	1226.6
0.6073	0.3927	3120.2	3156.9	1133.4	1226.6
0.5195	0.4805	3119.6	3156.3	1134.0	1226.6
0.4113	0.5887	3119.3	3156.1	1134.6	1226.6
0.2957	0.7043	3119.0	3156.0	1135.2	1227.2
0.1991	0.8009	3118.8	3155.8	1136.5	1228.4
0.0873	0.9127	–	–	1138.2	1228.8
0.0000	1.0000	–	–	–	–

indicates the existence of ionic clusters. Further, in the region $x_1 < 0.7916$, the significant change in $[NTf_2]^-$ ion frequencies indicated the formation of ion pairs from clusters. Furthermore, in DEC-rich region, complete solvation of individual ions takes place. There is a slight red shift in C_2–H and $C_{4,5}$–H stretching frequencies indicating the formation of hydrogen bond between $[Bmim]^+$ and carbonyl oxygen atoms of DEC. Simultaneously, a clear blue shift in SO_2 Sym. stretching frequencies is observed because of the breakup of hydrogen bond between cation and anion of the IL. The shifts are predominant at DEC-rich region. But, not much variation in CF_3 Sym. stretching frequencies is observed.

By examining ATR-FTIR, it can be accomplished that hydrogen bonds exist extensively in such systems which play a key role towards the miscibility and stability of the [Bmim][NTf_2] + DEC binary system. Additionally, the hydrogen bonding interactions are also accountable in the present system to get complete miscibility and solvation. Hence, it can be assumed that the hydrogen bonds between the IL [Bmim][NTf_2] and DEC are also responsible to make a remarkable contraction in the volume of the mixture.

3.2. *PFP statistical theory for excess molar volume* V_m^E

The PFP theory may be used to analyse and correlate the experimental excess molar volumes of binary mixtures [75–78]. We have correlated V_m^E of presently studied binary mixture using PFP theory over entire range of mole fractions at T = 303.15–323.15 K. The PFP theory considered V_m^E in three different contributions [79]: (1) interaction contribution V_{int}^E, which is associated with intermolecular-specific interaction with sign of ; H_m^E (2) free volume contribution V_{fv}^E, which is associated with reduced volume to reduced temperature ratio with negative sign and (3) internal pressure contribution, $V_{P^*}^E$, which is associated with breaking of IL structure with introduction of molecular organic solvents and changes in reduced volume of components with positive or negative sign. The calculation of various parameters of the theory based on relevant equations is given elsewhere [80–83].

The pure components parameters for the PFP theory are included in Table S2 of the supplementary material. The Flory contact interaction parameter χ_{12}, the only adjustable parameter, needed in the PFP theory was obtained by experimental V_m^E values in absence of the experimental excess molar enthalpy (H_m^E). The Flory contact interaction parameter χ_{12} was found to be negative for all the investigated temperatures. The values of three contributions V_{int}^E, V_{fv}^E and $V_{P^*}^E$, to V_m^E (PFP) at equimolar composition, are summarised in Table 9. The first term V_{int}^E is negative which suggests that the strong interactions take place in the binary mixture. The interactional contributions are negative at all calculated temperatures. The second term V_{fv}^E was found to be negative for the system studied (Table 9) as V_{fv}^E is proportional to $-\left(\tilde{V}_1 - \tilde{V}_2\right)^2$ [76]. The magnitude of negative values for

Table 9. PFP interaction parameter, χ_{12}, and calculated values of the three contributions from the PFP theory at equimolar composition for ([Bmim][NTf_2] + DEC) system at T = (303.15–323.15) K.

T (K)	χ_{12} (10^6 J m^{-3})	V_m^E(int)	V_m^E(*fv*)	V_m^E(ip)
		(10^{-6} m^3 mol^{-1})		
303.15	−51.8174	−1.2439	−0.6509	0.4628
308.15	−50.2984	−1.2387	−0.6724	0.4252
313.15	−48.8677	−1.2349	−0.6942	0.3846
318.15	−44.9035	−1.2392	−0.7170	0.3487
323.15	−44.9035	−1.1939	−0.7398	0.3055

V_{fv}^E depends upon difference in Flory's reduced volumes of involved components. Negative values of V_{fv}^E increase in magnitude as the temperature increases which shows that as the temperature increases, more free volume in the [Bmim][NTf_2] becomes available to accommodate the smaller DEC molecules which resulted in more negative V_m^E. The third term, i.e. characteristic pressure $V_{P^*}^E$, the P^* effect which depends on the relative cohesive energy of the expanded and less expanded component, is found to be positive at all investigated temperatures. It is proportional to $\left(\tilde{V}_1 - \tilde{V}_2\right)\left(P_1^* - P_2^*\right)$ and can have both the negative and positive sign depending upon the magnitude of P_i^* and $\widetilde{V_i^*}$ of unlike components [76]. For the system [Bmim][NTf_2] + DEC, $V_{P^*}^E$ is positive which is related to the structure-braking effect of the DEC on the electrostatic interactions between the ions of [Bmim][NTf_2] and so, the DEC molecules can be placed around the $[Bmim]^+$ and $[NTf_2]^-$ ions [76,84]. In the present system, V_{int}^E and V_{fv}^E were found to be negative while $V_{P^*}^E$ was found to be positive which shows that the interaction and free volume contributions are responsible for the overall strong interactions between solute and solvent molecules. Figure 10 indicates the composition dependence of V_m^E (PFP) values calculated from PFP theory for [BMIM][NTf_2] + DEC mixture compared with experimental V_m^E at 303.15 K. From the Figure, the V_m^E values calculated from PFP theory are in good agreement with the experimental values at whole composition range. We can conclude that it is possible to explain the volumetric behaviour of [Bmim][NTf_2] + DEC binary mixture by the application of the PFP theory quite successfully.

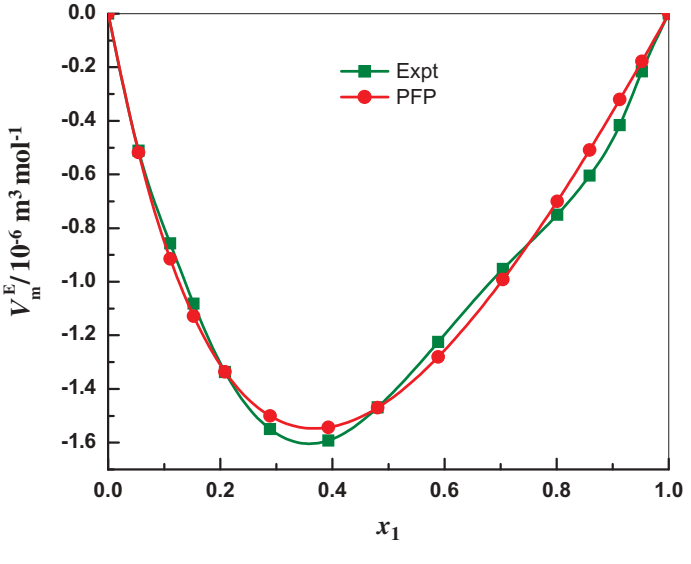


Figure 10. Plots of excess molar volumes (V_m^E) of experimental and calculated from PFP theory against mole fraction of [Bmim][NTf_2] with DEC at 303.15 K.

4. Conclusions

Densities, ultrasonic speed of sounds and refractive indices for binary liquids of [Bmim][NTf_2] with DEC, have been measured experimentally at atmospheric pressure over the entire composition range at temperature 303.15, 308.15, 313.15, 318.15 and 323.15 K. From the experimental data excess/deviation properties such as V_S^E, κ_S^E, L_f^E, u^E, α_P^E and $\Delta_\phi n_D$ have been evaluated. The excess and deviation parameters have been fitted to Redlich–Kister-type polynomial and also corresponding standard deviations have been computed. In the present binary liquid systems of [Bmim][NTf_2] with DEC, the observed excess values clearly reflect the dominance of strong attractive forces. The observed lower partial molar volumes in the liquid mixture when compared to the molar volumes of respective pure components also support the existence of strong interactions in the system. Various mixing rules were used to predict the refractive indices and the data have been compared with the experimental results. The IR spectral studies also supported the presence of strong interaction between molecules in study. PFP theory was able to explain the volumetric behaviour of the system quite successfully.

Disclosure statement

No potential conflict of interest was reported by the authors.

References

[1] Rebelo LPN, Canongia Lopes JN, Esperança JMSS, et al. On the critical temperature, normal boiling point, and vapor pressure of ionic liquids. J Phys Chem B. 2005;109:6040–6043.
[2] Huddleston JG, Visser AE, Reichert WM, et al. Characterization and comparison of hydrophilic and hydrophobic room temperature ionic liquids incorporating the imidazolium cation. Green Chem. 2001;3:156–164.
[3] Nishida T, Tashiro Y, Yamamoto M. Physical and electrochemical properties of 1-alkyl-3-methylimidazolium tetrafluoroborate for electrolyte. J Fluorine Chem. 2003;120:135–141.
[4] Holbrey JD, Seddon KR, Chem J. The phase behaviour of 1-alkyl-3-methylimidazolium tetrafluoroborates; ionic liquids and ionic liquid crystals. Soc Dalton Trans. 1999;13:2133–2140.
[5] Law G, Watson PR. Surface tension measurements of N-alkylimidazolium ionic liquids. Langmuir. 2001;17:6138–6141.
[6] Wilkes JS. A short history of ionic liquids—from molten salts to neoteric solvents. Green Chem. 2002;4:73–80.
[7] Fujita K, Macfarlane DR, Forsyth M. Protein solubilising and stabilising ionic liquids. Chem Commun. 2005;38:4804–4806.
[8] Shamsuri AA, Daik R. Rev Advmatsci. Applications Of Ionic Liquids And Their Mixtures For Preparation Of Advanced Polymer Blends And Composites: A Short Review. 2015;40:45–59.
[9] Comminges C, Barhdadi R, Laurent M, et al. Determination of viscosity, ionic conductivity, and diffusion coefficients in some binary systems: ionic liquids + molecular solvents. J Chem Eng Data. 2006;51:680–685.
[10] Bhatt MD, Dwyer CO. Recent progress in theoretical and computational investigations of Li-ion battery materials and electrolytes. Phys Chem Chem Phys. 2015;17:4799–4844.
[11] Allen CJ, Mukerjee S, Plichta EJ, et al. Oxygen electrode rechargeability in an ionic liquid for the Li–air battery. J Phys Chem Lett. 2011;2:2420–2424.
[12] Park S, Kazlauskas RJ. Biocatalysis in ionic liquids – advantages beyond green technology. Curr Opin Biotechnol. 2003;14:432–437.
[13] Sureshkumar M, Lee CK. Biocatalytic reactions in hydrophobic ionic liquids. J Mol Catal B Enzym. 2009;60:1–12.
[14] Moniruzzaman M, Nakashima K, Kamiya N, et al. Recent advances of enzymatic reactions in ionic liquids. Biochem Eng J. 2010;48:295–314.
[15] Rodrigues JV, Ruivo D, Rodríguez A, et al. Structural–functional evaluation of ionic liquid libraries for the design of co-solvents in lipase-catalysed reactions. Green Chem. 2014;16:4520–4523.
[16] Da Graca MN, Da Silva JMR, Da Silva JC, et al. The use of organic solvents/ionic liquids mixtures in reactions catalyzed by lipase from Burkholderia cepacia immobilized in different supports. J Mol Catal B.Enzym. 2015;112:1–8.
[17] Lozano P, Diego T, Carrie D, et al. Continuous green biocatalytic processes using ionic liquids and supercritical carbon dioxide. J Iborra Chem Comm. 2002;7:692–693.

[18] Turner MB, Spear SK, Holbrey JD, et al. Production of bioactive cellulose films reconstituted from ionic liquids. Biomacromolecules. 2004;5:1379–1384.
[19] Turner MB, Spear SK, Holbrey JD, et al. Ionic liquid-reconstituted cellulose composites as solid support matrices for biocatalyst immobilization. Biomacromolecules. 2005;6:2497–2502.
[20] Tan SSY, MacFarlane DR, Upfal J, et al. Extraction of lignin from lignocellulose at atmospheric pressure using alkylbenzenesulfonate ionic liquid. Green Chem. 2009;11:339–345.
[21] Gericke M, Liebert T, Heinze T. Interaction of ionic liquids with polysaccharides, 8 - synthesis of cellulose sulfates suitable for polyelectrolyte complex formation. Macromol Biosci. 2009;9:343–353.
[22] Gericke M, Schaller J, Liebert T, et al. Studies on the tosylation of cellulose in mixtures of ionic liquids and a co-solvent, CarbohydrPolym. CarbohydrPolym. 2012;89:526–536.
[23] Yao C, Anderson JL. Dispersive liquid–liquid microextraction using an in situ metathesis reaction to form an ionic liquid extraction phase for the preconcentration of aromatic compounds from water. Anal Bioanal Chem. 2009;395:1491–1502.
[24] Hameister D, Illner S, Vogel C, et al. Application and mechanism of carrier facilitated carbohydrate extraction from aqueous solution. Sep Purif Technol. 2014;132:438–445.
[25] Betz D, Raith A, Cokoja M, et al. Olefin epoxidation with a new class of ansa-molybdenum catalysts in ionic liquids. ChemSusChem. 2010;3:559–562.
[26] Ho TD, Yehl PM, Chetwyn NP, et al. Determination of trace level genotoxic impurities in small molecule drug substances using conventional headspace gas chromatography with contemporary ionic liquid diluents and electron capture detection. J Chromatogr. 2014;1361:217–228.
[27] Huang S, Yan B, Wang S, et al. Recent advances in dialkyl carbonates synthesis and applications. Chemical Society Reviews. 2015;44(10):3079–3116.
[28] Selva M, Caretto A, Noè M, et al. Carbonate phosphonium salts as catalysts for the transesterification of dialkyl carbonates with diols. The competition between cyclic carbonatesand linear dicarbonate products. Org Biomol Chem. 2014;12(24):4143–4155.
[29] Haregewoin AM, Leggesse EG, Jiang JC, et al. Comparative study on the solid electrolyte interface formation by the reduction of alkyl carbonates in lithium ion battery. Electrochim Acta. 2014;136:274–285.
[30] Andreatta AE, Alberto A, Rodil E, et al. Physico-chemical Properties of Binary and Ternary Mixtures of Ethyl Acetate plus Ethanol+1-Butyl-3-methyl-imidazolium bis(trifluoromethylsulfonyl)imide at 298.15 K and Atmospheric Pressure. J Solution Chem. 2010;39:371–383.
[31] Zarrougui R, Dhahbi M, Lemordant D. Effect of temperature and composition on the transport and thermodynamic properties of binary mixtures of ionic liquid N-butyl-N-methylpyrrolidinium bis (Trifluoromethanesulfonyl)imide and propylene carbonate. J Solution Chem. 2010;39:921–942.
[32] Widowati E, Lee MJ. P–V–T properties of binary mixtures of the ionic liquid 1-butyl-3-methylimidazolium bis(trifluoromethylsulfonyl)imide with anisole or acetophenone at elevated pressures. J Chem Thermodyn. 2013;63:95–101.
[33] Vranes M, Zec N, Tot A, et al. Density, electrical conductivity, viscosity and excess properties of 1-butyl-3-methylimidazolium bis(trifluoromethylsulfonyl)imide+propylene carbonate binary mixtures. J Chem Thermodyn. 2014;68:98–108.
[34] Geppert-Rybczynska M, Sitarek M. Acoustic and volumetric properties of binary mixtures of ionic liquid 1-butyl-3-methylimidazolium bis(trifluoromethylsulfonyl)imide with acetonitrile and tetrahydrofuran. J Chem Eng Data. 2014;59:1213–1224.
[35] Vranes M, AnaPapovic S, Tot A, et al. Density, excess properties, electrical conductivity and viscosity of 1-butyl-3-methylimidazolium bis(trifluoromethylsulfonyl)imide+γ-butyrolactone binary mixtures. J Chem. Thermodyn. 2014;76:161–171.
[36] Salinas R, Pla-Franco J, Lladosa E, et al. Density, speed of sound, viscosity, and excess properties of binary mixtures formed by ethanol and bis(trifluorosulfonyl)imide-based ionic liquids. J Chem Eng Data. 2015;60:525–540.
[37] Jacquemin J, Husson P, Padua AA, et al. Density and viscosity of several pure and water-saturated ionic liquids. Green Chem. 2006;8:172–180.
[38] AzlanKassim M, AsrinaSairi N, Yusoff R, et al. Experimental densities and viscosities of binary mixture of 1-butyl-3-methylimidazolium bis(trifluoromethylsulfonyl)imide or glycerol with sulfolane and their molecular interaction by COSMO-RS. Thermochim.Acta. 2016;639:130–147.
[39] SrinivasaKrishna T, Nainb AK, Chentilnathc S, et al. Densities, ultrasonic speeds, refractive indices, excess and partial molar properties of binary mixtures of imidazolium based ionic liquid with pyrrolidin-2- one at temperatures from 298.15 L to 323.15 K T. J Chem Thermodyn. 2016. DOI:10.1016/j.jct.2016.05.021
[40] Armarego WL, Chai CLL. Purification of laboratory chemicals. Seventh edition. Amsterdam: Butterworth-Heinemann; 2013.
[41] Scholz E. Karl Fischer Titration: Determination of Water Chemical Laboratory Practice. Berlin: Springer-Verlag; 1984.

[42] Douheret G, Davis MI, Reis JCR, et al. Isentropic compressibilities—experimental origin and the quest for their rigorous estimation in thermodynamically ideal liquid mixtures. Chem Phys Chem. 2001;2:148–161.
[43] Narendra K, Srinivasa Krishna T, Sudhamsa B, et al. Thermophysical and optical studies of molecular interactions in binary mixtures of diethyl carbonate with aromatic compounds at temperatures from 298.15 to 323.15K. J Chem Thermodyn. 2016;103:17–29.
[44] Comelli F, Bigi A, Vitalini D, et al. Densities, Viscosities, Refractive Indices, and Heat Capacities of Poly (ethylene glycol-ran-propylene glycol)+ Esters of Carbonic Acid at (293.15 and 313.15) K and at Atmospheric Pressure. J Chem Eng Data. 2009;55:205–210.
[45] Benson GC, Kiyohara O. Thermodynamic properties of some cycloalkane-cycloalkanol systems at 298.15 K. 4. Excess volumes. J Chem Eng Data. 1976;21:362–365.
[46] Reddy MS, MdNayeem SK, Soumini C, et al. Study of molecular interactions in binary liquid mixtures of [Emim][BF4] with 2-methoxyethanol using thermo acoustic, volumetric and optical properties. Thermochim Acta. 2016;630:37–39.
[47] Nayeem SM, Kondaiah M, Sreekanth K, et al. Thermoacoustic, volumetric, and viscometric investigations in the binary mixtures of 1,4-dioxane with n-hexane or n-heptane or n-octane. J Therm Anal Calorim. 2016;123:2241–2255.
[48] Reddy MS, Raju KTSS, Rao AS, et al. Study of thermophysical properties of the binary mixtures of ionic liquid 1-ethyl-3-methylimidazolium ethylsulfate and 2-propoxyethanol from T=(298.15 to 328.15)K at atmospheric pressure. J Chem Thermodyn. 2016;101:139–149.
[49] Chhotaray PK, Jella S, Gardas RL. Structural and compositional effect on the acoustic and volumetric properties of ammonium based ionic liquids with water and N -methyl-2-pyrrolidone. J Mol Liq. 2016;219:829–844.
[50] Reddy MS, MdNayeem SK, Raju KTSS, et al. The study of solute–solvent interactions in 1-ethyl-3-methylimidazolium tetrafluoroborate + 2-ethoxyethanol from density, speed of sound, and refractive index measurements. J Therm Anal Calorim. 2016;124:959–971.
[51] Reddy MS, Raju KTSS, MdNayeem SK, et al. Excess Thermodynamic Properties for Binary Mixtures of Ionic Liquid 1-Ethyl-3-methylimidazolium Ethyl Sulfate and 2-Methoxyethanol from T = (298.15 to 328.15) K at Atmospheric Pressure. J Solution Chem. 2016;45:675–701.
[52] Ali A, Nabi F, Tariq M. Volumetric, viscometric, ultrasonic, and refractive index properties of liquid mixtures of benzene with industrially important monomers at different temperatures. Int J Thermophy. 2009;30:464–474.
[53] Vercher E, Francisco JL, Vicenta González A, et al. Volumetric properties, viscosities and refractive indices of binary liquid mixtures of tetrafluoroborate-based ionic liquids with methanol at several temperatures. J Chem. Thermodyn. 2015;90:174–184.
[54] Vaid Z, More UU, Gardas RL, et al. Composition and temperature dependence of excess properties of binary mixtures of imidazolium based ionic liquids: II ([C n mim][PF6]) + propylamine. J Solution Chem. 2015;44:718–741.
[55] Arago DFJ, Biot JB. Mem Aced Fr. 1806:7.
[56] Dale D, Gladstone F. On the influence of temperature on the refraction of light. Trans R Soc London. 1858;148:887–894.
[57] Baraldi P, Giorgini MG, Manzini D, et al. Density, Refractive Index, and Related Properties for 2-Butanone + n- Hexane Binary Mixtures at Various Temperatures. J Solution Chem. 2002;31:873–973.
[58] Eyring H, John MS. Significant Liquid Structures. New York: John Wiley; 1969.
[59] Lorentz HA. The theory of electrons and its applications to the phenomena of light and radiant heat. Leipzig: B.G.Teubner; 1906.
[60] Heller WJ. Remarks on refractive index mixture rules. J Phys Chem. 1965;69:1123–1129.
[61] Eykman JF. Recherches réfractométriques (suite). Rec Trav Chim Pays-Bas. 1895;14:185–202.
[62] Oster G. The scattering of light and its applications to chemistry. Chem Rev. 1948;43:319–365.
[63] Weiner O. Berichte (Leipzig). Refractive index mixing rule in higher alkanes and alkanol systems. 1910;62:256–260.
[64] Ali A, Tariq M. J Pure App Ultrason. Thermal expansivity and isothermal compressibility of binary liquid mixtures from ultrasonic velocity: a comparison to Flory's theory andhard sphere models. 2006;28:99.
[65] Reddy MS, MdNayeem SK, Raju KTSS, et al. The study of solute–solvent interactions in 1-ethyl-3-methylimidazolium ethylsulfate+2-ethoxyethanol from density, speed of sound and refractive index measurements. J Mol Liq. 2016;218:83–94.
[66] Roth C, Appelhagen A, Jobst N, et al. Microheterogeneities in ionic-liquid-methanol solutions studied by FTIR spectroscopy, DFT calculations and molecular dynamics simulations. Chem Phys Chem. 2012;13:1708–1717.
[67] Hunt PA, Kirchner B, Welton T. Chemi Europ J. Characterising the Electronic Structure of Ionic Liquids: An Examination of the 1-Butyl-3-Methylimidazolium Chloride Ion Pair.2006;12:6762–6775.

[68] Aggarwal A, Lancaster NL, Sethi AR, et al. The role of hydrogen bonding in controlling the selectivity of diels–alder reactions in room-temperature ionic liquids. Green Chem. 2002;4:517–520.
[69] Znamenskiy V, Kobrak MN. Molecular dynamics study of polarity in room-temperature ionic liquids. J Phys Chem B. 2004;108:1072–1079.
[70] Dhumal NR, Kim HJ, Kiefer J. Electronic structure and normal vibrations of the 1-ethyl-3-methylimidazolium ethyl sulfate ion pair. J Phys Chem A. 2011;115:3551–3558.
[71] Lassegues JC, Grondin J, Cavagnat D, et al. New interpretation of the CH stretching vibrations in imidazolium-based ionic liquids. J Phys Chem A. 2009;113:6419–6421.
[72] Lassegues JC, Grondin J, Cavagnat D, et al. Reply to the "Comment on" new interpretation of the CH stretching vibrations in imidazolium-based ionic liquids. J Phys Chem A. 2009;114:687–688.
[73] Grondin J, Lassegues JC, Cavagnat D, et al. Revisited vibrational assignments of imidazolium-based ionic liquids. J Raman Spectro. 2011;42:733–743.
[74] Kristina N, Schulz PS, Natalia P, et al. The role of the C2 position in interionic interactions of imidazolium based ionic liquids: a vibrational and NMR spectroscopic study. Phys Chem Chem Phys. 2010;12:14153–14161.
[75] Vercher E, Llopis FJ, Gonzalez-Alfaro MV, et al. Density, speed of sound, and refractive index of 1-ethyl-3-methylimidazolium trifluoromethanesulfonate with acetone, methyl acetate, and ethyl acetate at temperatures from (278.15 to 328.15) K. J Chem Eng Data. 2010;55:1377–1388.
[76] Patterson D, Delmas G. Corresponding states theories and liquid models. Discuss Faraday Soc. 1970;49:98–105.
[77] Zafarani-Moattar MT, Shekaari H. Application of Prigogine–Flory–Patterson theory to excess molar volume and speed of sound of 1-n-butyl-3-methylimidazolium hexafluorophosphate or 1-n-butyl-3-methylimidazolium tetrafluoroborate in methanol and acetonitrile. J Chem Thermodyn. 2006;38:1377–1384.
[78] Kermanpour F, Niakan HZ. Measurement and modeling the excess molar properties of binary mixtures of {[C6mim][BF4]+3-amino-1-propanol} and {[C6mim][BF4]+isobutanol}: application of Prigogine–Flory–Patterson theory. J Chem Thermodyn. 2012;48:129–139.
[79] Torres RB, Ortolan MI, Volpe PLO. Volumetric properties of binary mixtures of ethers and acetonitrile: experimental results and application of the Prigogine–Flory–Patterson theory. J Chem Thermodyn. 2008;40:442–459.
[80] Flory PJ. Statistical thermodynamics of liquid mixtures. J Am Chem Soc. 1965;87:1833–1838.
[81] Abe A, Flory PJ. The thermodynamic properties of mixtures of small, nonpolar molecules. J Am Chem Soc. 1965;87:1838–1846.
[82] Vercher E, Orchilles AV, Miguel PJ, et al. Volumetric and ultrasonic studies of 1-ethyl-3-methylimidazolium trifluoromethanesulfonate ionic liquid with methanol, ethanol, 1-propanol, and water at several temperatures. J Chem Eng Data. 2007;52:1468–1482.
[83] Kumar A, Singh T, Gardas RL, et al. Non-ideal behaviour of a room temperature ionic liquid in an alkoxyethanol or poly ethers at T=(298.15 to 318.15)K. J Chem Thermodyn. 2008;40:32–39.
[84] Vaid ZS, More UU, Oswal SB, et al. Experimental and theoretical excess molar properties of imidazolium based ionic liquids with isomers of butanol. Thermochimica Acta. 2016;634:38–47.

J Solution Chem
https://doi.org/10.1007/s10953-018-0729-9

The Study of Solute–Solvent Interactions in 1-Butyl-3-Methylimidazolium Hexafluorophosphate + 2-Pyrrolidone from Volumetric, Acoustic, Optical and Spectral Properties

V. Srinivasa Rao[1,5] · M. Srinivasa Reddy[2] · K. Thomas S. S. Raju[3] · B. L. Rani[4] · B. Hari Babu[5]

Received: 31 March 2017 / Accepted: 16 October 2017
© Springer Science+Business Media, LLC, part of Springer Nature 2018

Abstract The density (ρ), speed of sound (u) and refractive index (n_D) of [Bmim][PF_6], 2-pyrrolidone and their binary mixtures were measured over the whole composition range as a function of temperature between (303.15 and 323.15) K at atmospheric pressure. Experimental values were used to calculate the excess molar volumes $\left(V_m^E\right)$, excess partial molar volumes $\left(\overline{V}_m^E\right)$, partial molar volumes at infinite dilution $\left(\overline{V}_m^{E,\infty}\right)$, excess values of isentropic compressibility $\left(\kappa_S^E\right)$, free length $\left(L_f^E\right)$ and speeds of sound $\left(u^E\right)$ for the binary mixtures. The calculated properties are discussed in terms of molecular interactions between the components of the mixtures. The results reveal that interactions between unlike molecules take place, particularly through intermolecular hydrogen bond formation between the C_2–H of [Bmim][PF_6] and the carbonyl group of pyrrolidin-2-one. An excellent correlation between thermodynamic and IR spectroscopic measurements was observed. The observations were further supported by the Prigogine–Flory–Patterson (PFP) theory of excess molar volume.

Keywords [Bmim][PF_6] · 2-Pyrrolidone · Density · Speed of sound · Refractive index · Excess thermodynamic parameters

Electronic supplementary material The online version of this article (https://doi.org/10.1007/s10953-018-0729-9) contains supplementary material, which is available to authorized users.

✉ B. Hari Babu
dr.b.haribabu@gmail.com

[1] Department of Chemistry, SRR & CVR Govt. Degree College, Vijayawada 520008, AP, India

[2] Department of Chemistry, TRR Govt. Degree College, Kandukur 523105, AP, India

[3] Department of Chemistry, Andhra Loyola College, Vijayawada 520008, AP, India

[4] Department of Chemistry, Chalapathi Institute of Engineering and Technology, Guntur 522034, AP, India

[5] Department of Chemistry, Acharya Nagarjuna University, Nagarjunanagar 522510, AP, India

Published online: 16 March 2018

1 Introduction

In recent times, ionic liquids (ILs) have attracted considerable attention because of their distinctive properties such as thermal stability, non-volatility and reusability [1, 2]. ILs can be selected with different anions and cations, so that one can form an ionic liquid with the desired properties. Moreover, ILs had been known for a long time, but their extensive use as solvents in chemical processes for synthesis and catalysis has recently became significant. Two main disadvantages of ILs are that they are very expensive when compared to molecular organic solvents and more viscous than conventional organic solvents, which may hamper their applications. Mixtures of ILs and molecular organic solvents have been gaining the interest of researchers because the resultant liquid mixtures possess advantages over both IL and molecular organic solvents. The properties of these mixtures depend on the mixing ratio. Mixing of the ILs with molecular solvents is one of the steps to minimize the usage of expensive ILs and to save time for preparing new ILs with desired properties [3]. Fortunately, their mixtures with molecular solvents show reduced viscosity without affecting their advantages as green solvents. In particular, the addition of polar co-solvents can strongly influence the physical and chemical properties of ILs such as viscosity, reactivity and electrical conductivity as well as solubility and solvation properties [4]. Hence, IL + molecular solvent mixtures have received growing attention in the past few years. The potential of these new substances can be exploited by studying their properties like volumetric, acoustic and refractive index, etc., because this data is important for industrial applications.

The choice of the ionic liquid, 1-butyl-3-methylimidazolium hexafluoro phosphate ([Bmim][PF_6]), was on the basis of its ability as a green plasticizer for poly(L-lactide) [5], in sequential application in Tussah silk dyeing [6], in RP HPLC [7], in organic synthesis [8], in separation technology [9] and also used in enzymatic catalysis [10]. On the other hand, 2-pyrrolidone (PY) was chosen because of its wide use in applied chemistry, industry and participation in biological processes [11, 12]. A variety of drugs are 2-pyrrolidone derivatives including Cotinine, Doxapram, Piracetam, Povidone, and Ethosuximide. It is also used in inkjet cartridges. Sustainable production of 2-pyrrolidone, used as a building block for active pharmaceutical ingredients, a solvent found in water-based ink and used as a solvent for membrane filters, polymer precursor, etc., is important. The study of the molecular interactions in the binary mixtures of two industrially important solvents, 1-butyl-3-methylimidazolium hexafluoro phosphate and 2-pyrrolidinone can be useful in many industrial applications like organic synthesis, separation technology, etc.

Systematic investigations of the physicochemical properties of [Bmim][PF_6] with molecular organic solvents like *N*,*N*-dimethylformamide [13], methyl methacrylate [14], butanol, acetone [15], THF, DMSO, methanol, acetonitrile [16], ethanol, benzene [17] and 2-propoxyethanol [18] have been reported. However, a literature review indicates that a systematic study of the volumetric, acoustic, optical and spectroscopic properties of binary mixtures of [Bmim][PF_6] with 2-pyrrolidone has not been previously reported. In the present work, we investigate the molecular interactions of [Bmim][PF_6] with 2-pyrrolidone and their affect on the volumetric, acoustic, optical, spectroscopic properties and their derived parameters of [Bmim][PF_6] + 2-pyrrolidone binary mixtures.

On the basis of our initial experiments, [Bmim][PF_6] was found to be totally miscible with PY in all proportions. Hence, in the present study, we measured the densities, speeds of sound and refractive indices of the binary mixtures of [Bmim][PF_6] with PY in the temperature range between 303.15 and 323.15 K over the entire composition range at

atmospheric pressure. Based on the measured values, we calculated the excess/deviation properties needed for their potential application in industrial processes. Here we report excess properties such as molar volumes $\left(V_m^{\mathrm{E}}\right)$, isentropic compressibilities $\left(\kappa_S^{\mathrm{E}}\right)$, free length $\left(L_{\mathrm{f}}^{\mathrm{E}}\right)$, and speeds of sound $\left(u^{\mathrm{E}}\right)$ along with $\left(\frac{\partial V_m^{\mathrm{E}}}{\partial T}\right)_p$ and $\left(\frac{\partial H_m^{\mathrm{E}}}{\partial p}\right)_T$. Also, the deviations of refractive index on the volume fraction basis $(\Delta_\phi n_{\mathrm{D}})$ are reported for the binary mixtures and fitted with the Redlich–Kister polynomial equation. Finally, an attempt has been made to understand the interaction behavior between the two liquids in the mixtures using IR spectroscopy. In addition, analysis of $V_{\mathrm{m}}^{\mathrm{E}}$ data of the present mixtures was done through the Prigogine–Flory–Patterson (PFP) theory.

2 Experimental Section

2.1 Materials

The ionic liquid, [Bmim][PF_6] (CAS174501-64-5), with mass fraction purity 0.99 was used in this work. It was purchased from Iolitec GmBH (Germany), while PY (CAS616-45-5) with mass fraction purity 0.995 was supplied by Sigma–Aldrich. The chemicals used in the present investigation were purified by methods described in the literature [19, 20]. The water content in the IL and PY was determined using a Karl Fisher titrator (Metrohm, 890 Titrando). Before taking any measurement, all samples were dried for at least 72 h under a vacuum (0.1 Pa) and moderate temperature (beginning at room temperature and increasing it gradually over a 6 h period up to 333 K). The water content of all the samples was further checked and found to be less than 150 ppm, a value much lower than the original pre-evacuation analysis, which typically showed values in the range of less than 210 ppm. [Bmim][PF_6] was thus used without further purification, while PY was further purified by distillation. A list of chemicals with details of their provenance, CAS number, and mass fraction purity are given in Table S1 of the supplementary information. The purities were verified by comparing the measured density, speed of sound and refractive index of the pure liquids with the literature values at atmospheric pressure and the results are given in Table 1.

2.2 Apparatus and Procedure

2.2.1 Sample Preparation

lL samples were freshly prepared in amber colored glass vials with screw caps having PFE septa, and were secured sealed with parafilm to prevent absorption of moisture from the atmosphere, and were then stirred for more than 30 min to ensure total dissolution of the mixtures. Samples were taken from the vials with a syringe through the PFE septum. Samples were prepared by weighing with a precision of $\pm$ 0.01 mg, using a Sartorius electronic balance (CPA225D). The uncertainty of the resulting mole fractions of the mixtures was estimated as being $\pm\ 2 \times 10^{-4}$.

Table 1 Comparison of experimental values of density, ρ, speed of sound, u, refractive index, n_D, and specific heat, C_p, of pure liquids with the corresponding literature values at different temperatures and at atmospheric pressure p = 101.3 kPa

Liquid	T (K)	ρ (kg·m^{-3})		u (m·s^{-1})		n_D		C_p (J·K^{-1}·mol^{-1})
		Expt.	Lit.	Expt.	Lit.	Expt.	Lit.	Lit.
[Bmim][PF_6]	303.15	1364.588	1363.277 [14]	1431.66	1430.6 [22]	1.40779	1.40746 [18]	410.33 [23]
	308.15	1360.409	1359.191 [14]	1419.82	1419.00 [22]	1.406474	1.40585 [18]	413.14 [23]
	313.15	1356.239	1355.087 [14]	1408.22	1406.4 [22]	1.405118	1.40468 [18]	415.98 [23]
	318.15	1352.085	1350.980 [14]	1396.84	1395.50 [21]	1.403706	1.40352 [18]	418.91 [23]
	323.15	1347.953	1346.874 [14]	1385.63	1385.155 [21]	1.402342	1.40243 [18]	421.88 [23]
2-Pyrrolidinone	303.15	1103.073	1103.07 [25] 1103.17 [26]	1617.97	1617.71 [25]	1.484032	1.48403 [25]	171.33 [24]
	308.15	1098.989	1098.99 [25] 1099.13 [26]	1601.62	1601.32 [25]	1.482177	1.48218 [25]	172.57 [24]
	313.15	1094.903	1094.90 [25] 1095.18 [26]	1585.44	1585.44 [25]	1.48033	1.48033 [25]	173.91 [24]
	318.15	1090.823	1090.82 [25] 1091.01 [26]	1569.39	1570.39 [25]	1.47412	1.47841 [25]	175.10 [24]
	323.15	1086.745	1086.75 [25]	1553.48	1553.48 [25]	1.476486	1.47649 [25]	176.31 [24]

Standard uncertainties u are: $u(\rho)$ = 1.0 kg·m^{-3}, $u(u)$ = 0.5 m·s^{-1}, $u(n_D)$ = 0.00005, $u(T)$ = 0.01 K and $u(p)$ = 0.5 kPa

2.2.2 Measurement of Density and Speed of Sound

Densities and speed of sound were measured with an Anton Paar DSA-5000 M vibrating-tube density and sound velocity meter. The density meter was calibrated with doubly distilled degassed water, and with dry air at atmospheric pressure. The temperature of the apparatus was controlled to within ± 0.01 K by a built-in Peltier device. Measured density and speed of sound values (at a frequency of approximately 3 MHz) are precise to 5×10^{-3} kg·m^{-3} and 5×10^{-1} m·s^{-1}, respectively. The standard uncertainties associated with the measurements of temperature, density and speed of sound are estimated to be ± 0.01 K, 5×10^{-2} kg·m^{-3} and ± 0.5 m·s$^{-1,}$ respectively.

2.2.3 Measurement of Refractive Index

The refractive indices were determined using an automatic refractometer (Anton Paar Dr Krenchen Abbemat (WR-HT)) which also has a temperature controller that keeps the samples at working temperature. The uncertainties in the temperature and refractive index values are ± 0.01 K and ± 5×10^{-5}, respectively. The apparatus was calibrated by measuring the refractive index of Millipore quality water and tetrachloroethylene (supplied by the company) before each series of measurements according to the manual instructions. The calibration was checked with pure liquids having known refractive indices.

2.2.4 Measurement of Infrared Spectra

Infrared transmittance was measured using a Shimadzu Fourier transform infrared (FT-IR) spectrometer (IRAffinity-1S) equipped with attenuated total reflectance (ATR) accessories. The spectral region was 650–4000 cm^{-1} with resolution of 2 cm^{-1} and 100 scans were taken. At least five repeated measurements were performed for each sample.

3 Results and Discussion

The experimentally measured density (ρ), speed of sound (u) and refractive index (n_D) results for the binary mixtures of [Bmim][PF_6] with PY at different temperatures are given in Table 2. The IR spectral data was recorded at room temperature. The changes in values of ρ, u and n_D with respect to mole fraction are non-linear at all studied temperatures, whereas the changes in their values with respect to temperature are linear. This trend indicates the existence of molecular interactions between the liquids under study at all studied temperatures. The excess and deviation parameters were calculated from the experimental data using well-known thermodynamic expressions given elsewhere [27]. The Redlich–Kister polynomial coefficients of the computed excess properties and corresponding standard deviations are presented in Table S2 of the supporting information.

The variations observed in these excess/deviation parameters are due to the resultant contribution of several opposing effects, namely chemical, structural, and physical [28]. The chemical or specific interactions include hydrogen bonding between component molecules and charge-transfer complexes. The structural contributions are such as interstitial accommodation and geometrical fitting of one component into another. Excess molar volumes for the binary mixtures of [Bmim][PF_6] with PY as a function of composition from T = 303.15–323.15 K are shown in Fig. 1. The curves in the figure have a sigmoid

Table 2 Experimental density (ρ), speed of sound (u), refractive index (n_D), molar volume (V_m), isentropic compressibility (κ_s), free length (L_f) and isobaric thermal expansion coefficient (α_p) with mole fraction (x_1) of [Bmim][PF_6] in the binary liquid mixture of {[Bmim][PF_6] + 2-pyrrolidinone} from T/K = 303.15–323.15 at pressure p = 101.3 kPa

x_1	ρ (kg·m^{-3})	u (m·s^{-1})	n_D	V_m (10^{-6} m^3·mol^{-1})	κ_s (10^{-10} Pa^{-1})	L_f (10^{-11} m)	α_p (10^{-4} K^{-1})
303.15 K							
0.0000	1103.07	1617.97	1.48403	77.16	3.463	3.862	7.41
0.0494	1134.15	1584.68	1.47539	83.72	3.511	3.889	6.54
0.1025	1161.46	1575.15	1.46743	90.84	3.470	3.866	6.17
0.1503	1182.17	1566.55	1.46088	97.31	3.447	3.853	6.06
0.2215	1209.05	1553.76	1.45232	106.86	3.426	3.842	6.03
0.3376	1249.12	1532.89	1.44097	121.95	3.407	3.831	6.00
0.4502	1281.92	1512.66	1.43229	136.30	3.409	3.832	5.91
0.5654	1309.38	1491.96	1.42521	150.96	3.431	3.845	5.82
0.6527	1326.07	1476.26	1.42077	162.17	3.460	3.861	5.76
0.7421	1339.46	1460.19	1.41683	173.84	3.501	3.884	5.68
0.8295	1348.94	1446.49	1.41345	185.51	3.543	3.907	5.63
0.8622	1351.84	1442.61	1.41227	189.93	3.554	3.913	5.63
0.9019	1355.19	1438.47	1.41089	195.30	3.566	3.920	5.67
0.9495	1359.38	1434.92	1.40932	201.66	3.573	3.923	5.81
1.0000	1364.59	1431.66	1.40779	208.26	3.575	3.925	6.14
308.15 K							
0.0000	1098.99	1601.62	1.48218	77.44	3.547	3.944	7.43
0.0494	1130.43	1569.09	1.47367	83.99	3.593	3.970	6.64
0.1025	1157.89	1560.04	1.46577	91.12	3.549	3.945	6.30
0.1503	1178.59	1551.84	1.45925	97.60	3.523	3.931	6.20
0.2215	1205.38	1539.60	1.45075	107.19	3.500	3.918	6.16
0.3376	1245.37	1519.50	1.43947	122.31	3.478	3.906	6.10
0.4502	1278.13	1499.87	1.43084	136.70	3.478	3.906	6.00
0.5654	1305.56	1479.62	1.42380	151.40	3.499	3.917	5.91
0.6527	1322.25	1464.16	1.41939	162.64	3.528	3.934	5.85
0.7421	1335.64	1448.25	1.41547	174.34	3.570	3.957	5.77
0.8295	1345.14	1434.60	1.41211	186.04	3.612	3.980	5.70
0.8622	1348.02	1430.72	1.41094	190.47	3.624	3.987	5.69
0.9019	1351.33	1426.56	1.40956	195.86	3.636	3.994	5.71
0.9495	1355.39	1422.97	1.40800	202.26	3.644	3.998	5.83
1.0000	1360.41	1419.82	1.40647	208.90	3.646	3.999	6.14
313.15 K							
0.0000	1094.90	1585.44	1.48033	77.73	3.633	4.028	7.46
0.0494	1126.64	1553.66	1.47197	84.27	3.677	4.052	6.74
0.1025	1154.21	1545.09	1.46409	91.41	3.629	4.025	6.43
0.1503	1174.91	1537.31	1.45761	97.91	3.601	4.010	6.34
0.2215	1201.61	1525.63	1.44916	107.52	3.576	3.996	6.29
0.3376	1241.54	1506.30	1.43795	122.69	3.550	3.981	6.20
0.4502	1274.25	1487.28	1.42937	137.12	3.548	3.980	6.09

Table 2 continued

x_1	ρ (kg·m^{-3})	u (m·s^{-1})	n_D	V_m (10^{-6} m^3·mol^{-1})	κ_s (10^{-10} Pa^{-1})	L_f (10^{-11} m)	α_p (10^{-4} K^{-1})
0.5654	1301.66	1467.48	1.42237	151.86	3.567	3.991	6.00
0.6527	1318.34	1452.26	1.41798	163.12	3.597	4.007	5.94
0.7421	1331.75	1436.50	1.41408	174.85	3.639	4.031	5.86
0.8295	1341.27	1422.91	1.41074	186.58	3.682	4.055	5.77
0.8622	1344.17	1419.03	1.40956	191.02	3.695	4.062	5.75
0.9019	1347.47	1414.85	1.40820	196.42	3.707	4.069	5.76
0.9495	1351.47	1411.21	1.40665	202.84	3.715	4.073	5.86
1.0000	1356.24	1408.22	1.40512	209.54	3.718	4.074	6.13
318.15 K							
0.0000	1090.82	1569.39	1.47841	78.02	3.722	4.113	7.48
0.0494	1122.77	1538.38	1.47018	84.56	3.763	4.136	6.83
0.1025	1150.44	1530.28	1.46234	91.71	3.712	4.107	6.56
0.1503	1171.13	1522.90	1.45591	98.22	3.682	4.090	6.48
0.2215	1197.78	1511.76	1.44752	107.87	3.653	4.075	6.42
0.3376	1237.66	1493.20	1.43638	123.08	3.624	4.058	6.30
0.4502	1270.34	1474.77	1.42786	137.54	3.619	4.056	6.17
0.5654	1297.74	1455.43	1.42089	152.31	3.638	4.066	6.08
0.6527	1314.42	1440.46	1.41651	163.61	3.667	4.082	6.03
0.7421	1327.83	1424.85	1.41263	175.36	3.710	4.106	5.95
0.8295	1337.36	1411.33	1.40930	187.12	3.754	4.130	5.84
0.8622	1340.28	1407.45	1.40814	191.57	3.766	4.137	5.81
0.9019	1343.59	1403.26	1.40678	196.98	3.780	4.145	5.81
0.9495	1347.53	1399.57	1.40523	203.44	3.789	4.149	5.88
1.0000	1352.09	1396.84	1.40371	210.19	3.791	4.150	6.13
323.15 K							
0.0000	1086.75	1553.48	1.47649	78.32	3.813	4.199	7.50
0.0494	1118.92	1523.19	1.46840	84.86	3.852	4.221	6.93
0.1025	1146.67	1515.58	1.46059	92.01	3.797	4.190	6.70
0.1503	1167.36	1508.60	1.45419	98.54	3.764	4.172	6.62
0.2215	1193.93	1498.02	1.44588	108.22	3.732	4.155	6.55
0.3376	1233.75	1480.24	1.43483	123.47	3.699	4.136	6.40
0.4502	1266.40	1462.42	1.42635	137.97	3.692	4.132	6.26
0.5654	1293.77	1443.55	1.41943	152.78	3.709	4.142	6.17
0.6527	1310.45	1428.83	1.41508	164.11	3.738	4.158	6.12
0.7421	1323.87	1413.40	1.41122	175.89	3.781	4.182	6.04
0.8295	1333.43	1399.96	1.40791	187.67	3.826	4.207	5.91
0.8622	1336.36	1396.09	1.40676	192.13	3.839	4.214	5.87
0.9019	1339.68	1391.89	1.40541	197.56	3.853	4.221	5.85
0.9495	1343.57	1388.17	1.40386	204.04	3.862	4.226	5.90

Table 2 continued

x_1	ρ (kg·m^{-3})	u (m·s^{-1})	n_D	V_m (10^{-6} m^3·mol^{-1})	κ_s (10^{-10} Pa^{-1})	L_f (10^{-11} m)	α_p (10^{-4} K^{-1})
1.0000	1347.95	1385.63	1.40234	210.83	3.864	4.227	6.12

Standard uncertainties u are: $u(x_1) = 0.0001$, $u(\rho) = 1$ kg·m^{-3}, $u(u) = 0.5$ m·s^{-1}, $u(n_D) = 0.00005$, $u(T) = 0.01$ K and $u(p) = 0.5$ kPa. Combined uncertainties (confidence level, 95%): U_c (V_m) = $\pm$ 0.01 $\times$ 10^{-6} m^3·mol^{-1}, U_c (κ_s) = $\pm$ 0.01 $\times$ 10^{-10} Pa^{-1}, U_c (L_f) = $\pm$ 0.004 $\times$ 10^{-11} m, U_c (α_p) = $\pm$ 0.02 $\times$ 10^{-4} K^{-1}. All the experiments were carried out at atmospheric pressure

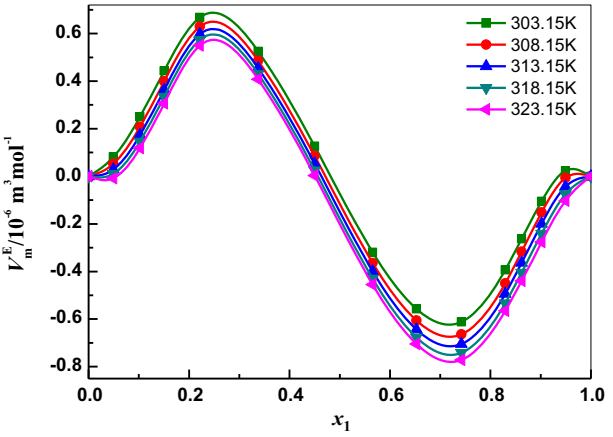


Fig. 1 Plots of excess molar volume $\left(V_m^E\right)$ against mole fraction of [Bmim][PF_6] with PY at different temperatures

shape at all temperatures with positive V_m^E values in the PY rich region and negative V_m^E values in the IL rich region. The present observations of V_m^E can be explained based on microscopic structural changes in the binary system. In the pure state, PY molecules exist as cyclic dimers due to intermolecular hydrogen bonding. This prevents fitting of PY molecules (dimers) into the voids of [Bmim][PF_6], which leads to positive excess molar volumes in the PY rich region. In the IL rich region, the dimeric structure of PY molecules is disturbed in such a way that breakage of intermolecular H bond occurs and consequently more favorable fitting of the smaller PY molecules (monomers) takes place into the voids created by the larger [Bmim][PF_6] molecules, giving rise to negative V_m^E values. In addition to the geometrical fitting, inter molecular hydrogen bond formation between the carbonyl oxygen of PY and C_2-H/$C_{4,5}$-H of $[Bmim]^+$ is also responsible for the strong interactions between solute and solvent in the IL rich region. A similar type of behavior for V_m^E is observed for the rest of studied temperatures. Moreover, the variation of V_m^E for the present system as a function of temperature becomes more negative with rise in temperature in the IL rich region. This is because of the fact that there is more favorable fitting of the smaller PY molecules into the voids created by larger IL molecules, thereby resulting in shrinkage of the volume of the mixture to a larger extent, resulting in more negative V_m^E values with rise in temperature. Therefore, the strength of interaction is enhanced with rise in temperature.

The existing molecular interactions in the current binary system are properly reflected in the properties of partial molar volumes of the constituent molecules. A partial molar volume is the contribution that a component of a mixture makes to the total volume of the solution. Therefore, the partial molar volume is a function of mixture composition. The partial molar volumes $\overline{V}_{m,1}$ of component 1 ([Bmim][PF_6]) and $\overline{V}_{m,2}$ of component 2 (PY) in the mixtures over the whole composition range have been computed using the relationships given elsewhere [29].

The calculated values of $\overline{V}_{m,1}$ and $\overline{V}_{m,2}$ for the studied binary system are presented in Table S3 of the supporting information. From the table, it is evident that the values of $\overline{V}_{m,1}$ ([Bmim][PF_6]) are bigger in the PY rich region than its individual molar volumes in the pure state, which reveals expansion of the volume in the PY rich region and contraction of the volume in the IL rich region when [Bmim][PF_6] is mixed with PY. In the case of $\overline{V}_{m,2}$ (PY), the values are bigger than its individual molar volumes over the entire composition range, which reveals expansion of the volume of PY upon mixing with [Bmim][PF_6]. Figures 2 and 3 illustrate the disparity of excess partial molar volumes of $\overline{V}^{\mathrm{E}}_{m,1}$ ([Bmim][PF_6]) and $\overline{V}^{\mathrm{E}}_{m,2}$ (PY), respectively, in the binary mixtures at T = (303.15, 308.15, 313.15, 318.15 and 323.15) K. These figures not only show the variation of attractive forces between the unlike molecules but also support the inferences drawn from the excess molar volume.

The partial molar volumes $\left(\overline{V}^{\infty}_{m,1},\ \overline{V}^{\infty}_{m,2}\right)$ and excess partial molar volumes at infinite dilution $\left(\overline{V}^{\mathrm{E},\infty}_{m,1},\ \overline{V}^{E,\infty}_{m,2}\right)$ of [Bmim][PF_6] and PY were calculated. The pertinent $\overline{V}^{\infty}_{m,1}$, $\overline{V}^{\infty}_{m,2}$ and $\overline{V}^{\mathrm{E},\infty}_{m,1}$, $\overline{V}^{\mathrm{E},\infty}_{m,2}$ values are presented in Table 3 at T = (303.15, 308.15, 313.15, 318.15 and 323.15) K. Excess partial molar volumes at infinite dilution are of specific interest to understand the solute–solvent interactions, as solute–solute interactions are assumed to have disappeared at infinite dilution. Positive values of $\overline{V}^{\mathrm{E},\infty}_{m,1}$ (at 303.15 K) in the mixtures suggest weaker interactions between ions of [Bmim][PF_6] and PY molecules because of the existence of inter molecular hydrogen bonds in PY. Positive $\overline{V}^{\mathrm{E},\infty}_{m,2}$ values for PY at (303.15, 308.15, 313.15) K are attributed to an ion solvation process and termination of

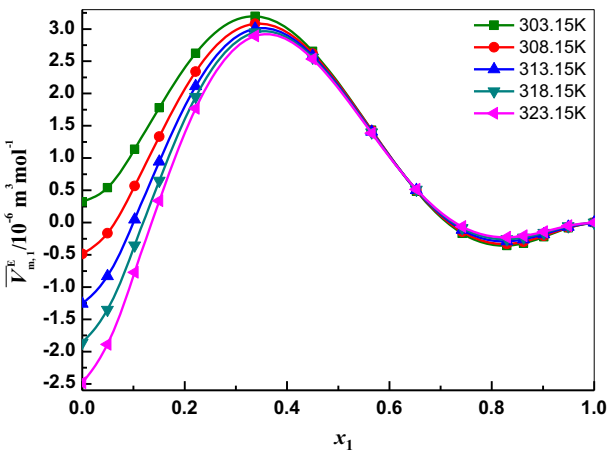


Fig. 2 Plots of excess partial molar volume $\overline{V}^{\mathrm{E}}_{m,1}$ against mole fraction of [Bmim][PF_6] with PY at different temperatures

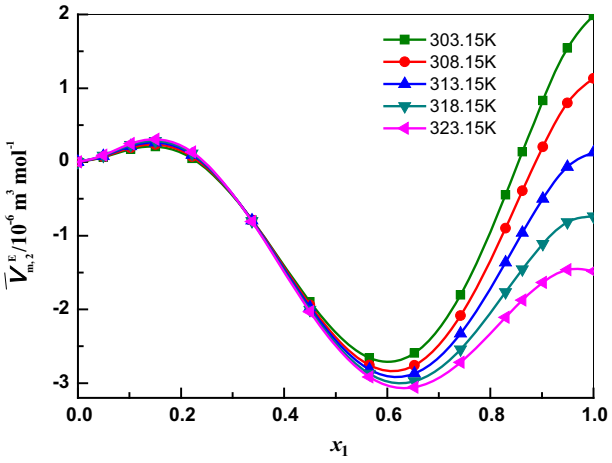


Fig. 3 Plots of excess partial molar volume $\overline{V}^{E}_{m,2}$ against mole fraction of [Bmim][PF_6] with PY at different temperatures

Table 3 Partial molar volumes at infinite dilution ($\overline{V}^{\infty}_{m,1}$, $\overline{V}^{\infty}_{m,2}$) and excess partial molar volumes at infinite dilution ($\overline{V}^{E,\infty}_{m,1}$, $\overline{V}^{E,\infty}_{m,2}$) of [Bmim][$PF_6$] and 2-pyrrolidinone T = (303.15, 308.15, 313.15, 318.15 and 323.15) K

Temp (K)	$\overline{V}^{\infty}_{m,1}$ (10^{-6} m^3·mol^{-1})	$\overline{V}^{E,\infty}_{m,1}$	$\overline{V}^{\infty}_{m,2}$ (10^{-6} m^3·mol^{-1})	$\overline{V}^{E,\infty}_{m,2}$
303.15	208.58	0.32	79.14	1.98
308.15	208.41	− 0.49	78.58	1.13
313.15	208.28	− 1.26	77.86	0.13
318.15	208.32	− 1.86	77.29	− 0.74
323.15	208.35	− 2.49	76.83	− 1.48

Combined uncertainties (confidence level, 95%): $U\left(\overline{V}^{E,\infty}_{m,1}\right) = \pm 0.02 \times 10^{-6}$ m^3·mol^{-1}, $U\left(\overline{V}^{E,\infty}_{m,2}\right) = \pm 0.02 \times 10^{-6}$ m^3·mol^{-1}

ion–ion interactions in [Bmim][PF_6]. As the temperature increases, both $\overline{V}^{E,\infty}_{m,1}$ and $\overline{V}^{E,\infty}_{m,2}$ values decrease and become negative. The decrease in $\overline{V}^{E,\infty}_{m,1}$ and $\overline{V}^{E,\infty}_{m,2}$ values with rise in temperature indicates an increase in the strength of attractions between solute and solvent molecules, which further supports the observed trends in V^{E}_{m} values for the binary system.

In Fig. 4 the κ^{E}_{S} values for [Bmim][PF_6] + PY are seen to be negative except in the PY rich region at all investigated temperatures. The negative κ^{E}_{S} values are attributed to the strong attractive interactions between the molecules of the components [29]. This supports the inference drawn from V^{E}_{m}. The intermolecular free length indicates closer approach of unlike molecules. The trends of the L^{E}_{f} values (Fig. 5) are similar to κ^{E}_{S} at all investigated temperatures. Negative values of L^{E}_{f} are generally explained as being due to the dominance of specific interactions between unlike molecules in the liquid mixture and also due to the structural readjustments in the liquid mixtures towards a less compressible phase of fluid and closer packing of the molecules [29]. Figure 6 shows that the u^{E} values are positive for

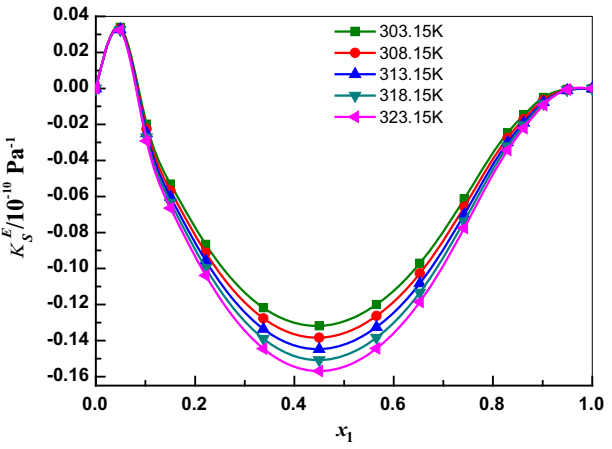


Fig. 4 Plots of excess isentropic compressibility K_S^E against mole fraction of [Bmim][PF_6] with PY at different temperatures

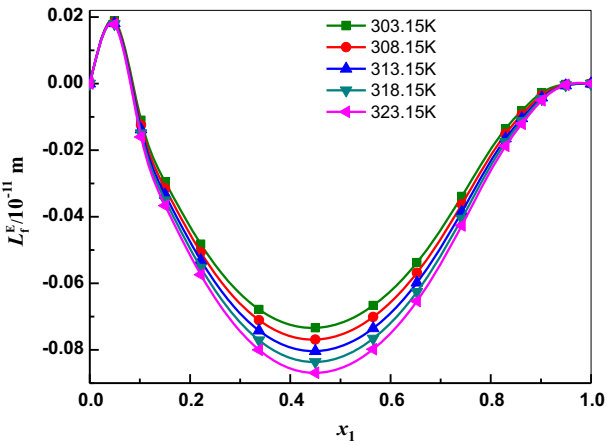


Fig. 5 Plots of excess free length L_f^E against mole fraction of [Bmim][PF_6]with PY at different temperatures

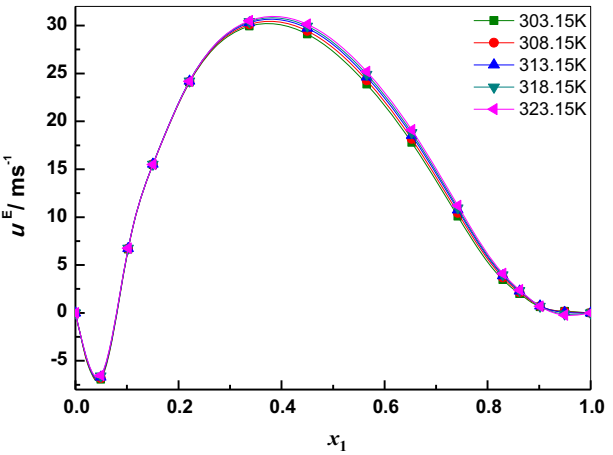


Fig. 6 Plots of excess ultrasonic speed of sounds (u^E) against mole fraction of [Bmim][PF_6] with PY at different temperatures

the system except in the PY rich region at all the studied temperatures. Positive deviations indicate an increasing strength of interaction between the component molecules of the binary liquid mixtures [30]. The refractive indices (n_D) for the binary mixtures at the studied temperatures over the whole composition range are given in Table 2; the values increase with increase in the concentration of the ILs in the mixtures and decrease as the temperature increases for a particular concentration of [Bmim][PF_6]. The values of $\Delta_\phi n_D$ are positive over the range of composition (Fig. 7), which may be attributed to the non-availability of the free volume in the mixture in comparison with the corresponding ideal mixtures [31].

This further supports the existence of strong interactions between the constituent molecules in the binary liquid solutions. The values of the excess functions $\left(\frac{\partial V_m^E}{\partial T}\right)_p$ and $\left(\frac{\partial H_m^E}{\partial p}\right)_T$ are given in Table 4. The variation of $\left(\frac{\partial V_m^E}{\partial T}\right)_p$ and $\left(\frac{\partial H_m^E}{\partial p}\right)_T$ are similar with mole fraction and temperature but with opposite sign. The negative values of $\left(\frac{\partial V_m^E}{\partial T}\right)_p$ for the studied mixtures may be due to the strong interactions existing between the unlike molecules of the mixtures [31]. The isothermal pressure coefficient of excess molar enthalpy $\left(\frac{\partial H_m^E}{\partial p}\right)_T$ has positive values over the whole composition range. This reflects an increase in attraction forces between the two components of these mixtures caused by increasing pressure. Hence, contraction in the volume of the mixture is still possible by increasing the pressure [29, 32].

3.1 Infrared Spectral Studies

The existence of interactions in the system, which were inferred from the above excess/deviation parameters, is well supported by the IR spectral studies. The unique properties of imidazolium cations are found in their electronic structure. The hydrogen in C_2-H is more acidic than for C_4-H and C_5-H due to the electron deficiency in the C=N bond. The resultant acidity of the hydrogen atoms is key to understanding the properties of these ionic

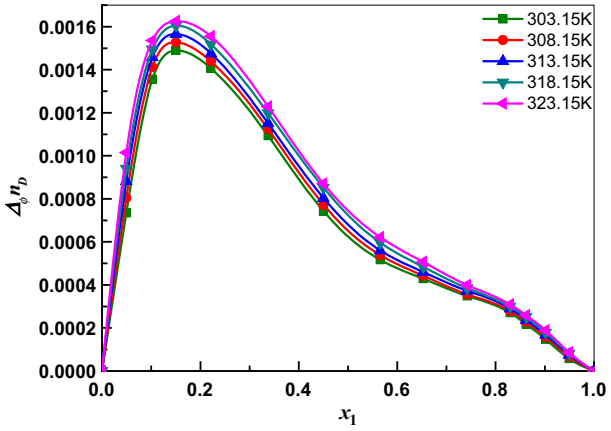


Fig. 7 Plots of deviation in refractive index $\Delta_\phi n_D$ against mole fraction of [Bmim][PF_6] with PY at different temperatures

Table 4 The values of excess functions $\left(\frac{\partial V_m^E}{\partial T}\right)_p$ and $\left(\frac{\partial H_m^E}{\partial p}\right)_T$ at 298.15 K as a function of mole fraction of [Bmim][PF_6]

x_1	$\left(\frac{\partial V_m^E}{\partial T}\right)_p$ (10^{-9} $m^3 \cdot mol^{-1} \cdot K^{-1}$)	$\left(\frac{\partial H_m^E}{\partial p}\right)_T$ (10^{-6} $J \cdot mol^{-1} \cdot Pa^{-1}$)
0.0000	0.00	0.00
0.0494	− 5.92	1.88
0.1025	− 8.42	2.80
0.1503	− 8.89	3.14
0.2215	− 8.46	3.23
0.3376	− 7.94	2.93
0.4502	− 8.47	2.69
0.5654	− 9.32	2.50
0.6527	− 9.99	2.47
0.7421	− 10.86	2.68
0.8295	− 11.47	3.08
0.8622	− 11.27	3.15
0.9019	− 10.27	3.01
0.9495	− 7.16	2.19
1.0000	0.00	0.00

Standard uncertainties u are: $u(x_1) = 0.0002$, $u(T) = 0.01$ K and $u(p) = 0.5$ kPa

Combined uncertainties (confidence level, 95%): $U\left(\left(\frac{\partial V_m^E}{\partial T}\right)_p\right) = \pm\ 0.1 \times 10^{-9}$ $m^3 \cdot mol^{-1} \cdot K^{-1}$, $U\left(\left(\frac{\partial H_m^E}{\partial p}\right)_{T=298.15K}\right) = \pm\ 0.06 \times 10^{-6}$ $J \cdot mol^{-1} \cdot Pa^{-1}$

liquids. The hydrogen on the C_2 carbon (C_2-H) has been shown to bind typically with solute molecules [33, 34].

In order to study the effects of molecular interactions, the infrared absorbance was recorded from 650 to 4000 cm^{-1} (Fig. S1 of the supporting information and Table 5). In the $[Bmim]^+$ cation, the C–H stretching region from 2800 to 3200 cm^{-1} was investigated. The signals in this region can be separated into two parts: signals between 3000 and 3200 cm^{-1} can be attributed to C–H vibrational modes mainly arising from the aromatic imidazolium ring, from the C_2–H and $C_{4,5}$–H stretching frequencies [35]. The signals between 2800 and 3000 cm^{-1} are due to aliphatic C–H groups in the methyl and butyl moieties [36–38]. The C_2–H vibrational frequency (3124.5 cm^{-1}) is shifted to lower frequencies by about 45.4 cm^{-1} when compared to the C_4–H and C_5–H stretches (3169.9 cm^{-1}) because of its stronger acidic character. In the present mixtures, the C_2–H and $C_{4,5}$–H stretching frequencies of the cation are analyzed (Fig. 8). The experimental ATR-IR spectra for PY for the N–H stretching and C=O stretching (Fig. 8) of the amide spectral regions are reported. A wide peak with a maximum at 3228.0 cm^{-1} for the N–H stretching (hydrogen bonded) and a narrower peak at 1688.2 cm^{-1}, corresponding C=O stretching of the amide region of pure PY, are observed. The absence of a peak around 3430.0 cm^{-1} (free N–H) shows that there is no presence of monomeric, nonassociated, PY molecules in its pure state. PY molecules are self-associated through hydrogen bonding and exist as a cyclic dimer (Fig. 9) in its pure state [39].

Table 5 Infrared absorbance wave numbers between 2800 and 3200 cm^{-1} of [Bmim][PF_6] in PY at room temperature and atmospheric pressure p = 101.3 kPa

Mole fraction of [Bmim][PF_6]	Mole fraction of PY	C_2–H stretching	$C_{4,5}$–H stretching	Free N–H stretch	C=O stretch
1.0000	0.0000	3124.5	3169.9	–	–
0.9019	0.0981	3123.5	3169.2	–	1666.1
0.8295	0.1705	3123.2	3168.8	3433.8	1667.8
0.7421	0.2579	3122.8	3168.7	3432.1	1674.8
0.6527	0.3473	3122.3	3168.5	3432.5	1678.8
0.5654	0.4346	3121.2	3168.4	3431.2	1681.1
0.4502	0.5498	3119.8	3167.8	3430.9	1683.7
0.3376	0.6624	3118.2	3167.2	3430.6	1685.3
0.2215	0.7785	3115.1	3167.1	3428.7	1686.5
0.1025	0.8975	–	–	3428.1	1687.1
0.0000	1.0000	–	–	3424.9	1688.2

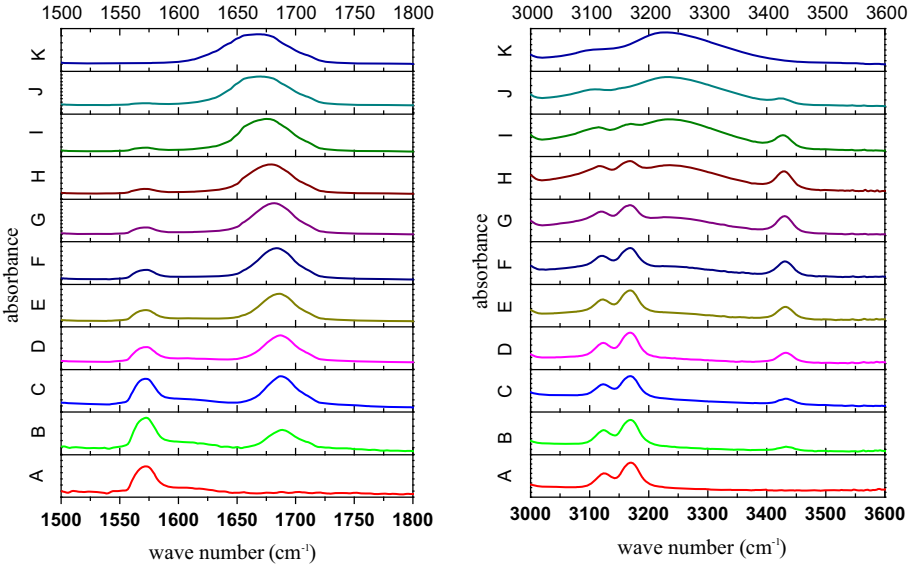
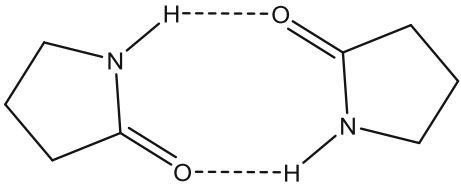


Fig. 8 Infrared spectra between 1500 and 1800 cm^{-1} and between 3000 and 3600 cm^{-1} of: (A) pure IL [Bmim][PF_6]; (B) 0.9019; (C) 0.8295; (D) 0.7421; (E) 0.6527; (F) 0.5654; (G) 0.4502; (H) 0.3376; (I) 0.2215; (J) 0.1025 and (K) pure PY where. (B–J) are the the mole fraction of [Bmim][PF_6] in PY

As the mole fraction of PY increases, an observed red shift in the C_2–H and $C_{4,5}$–H stretching frequencies indicates the formation of a hydrogen bond between $[Bmim]^+$ and PY. The red shift is very predominant in the C_2–H frequencies when compared to the $C_{4,5}$–H stretching frequencies, which indicates that the more acidic C_2–H plays a major role in the formation of a hydrogen bond with the carbonyl oxygen of PY (Fig. 10). Simultaneously, a clear blue shift in C=O Sym Stretch frequencies is observed because of

Fig. 9 Dimeric structure of PY



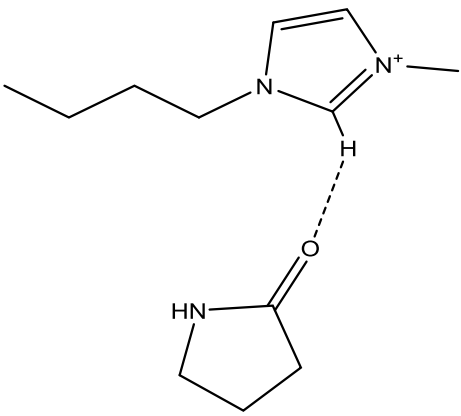
the breakup of strong hydrogen bonds in the cyclic dimeric PY. A wide peak with a maximum at 3228.0 cm^{-1} for the N–H stretching belonging to the cyclic dimer appears in the PY rich region only. As the mole fraction of IL increases it gradually disappears and a sharp peak around 3430.0 cm^{-1} appears that is assigned to free N–H. This also indicates that the N–H proton has no role in the formation of hydrogen bonds in the mixtures.

By examining the ATR-FTIR, it can be concluded that hydrogen bonds exist extensively in such systems which play a key role towards the miscibility and stability of the [Bmim][PF_6] + PY binary system. Hence, it can be assumed that the cyclic dimer in the PY rich region is responsible for the expansion of volume and contraction in the IL rich region because of hydrogen bond formation between the ionic liquid [Bmim][PF_6] and PY.

3.2 Prigogine–Flory–Patterson Statistical Theory for Excess Molar Volume V_m^E

The Prigogine–Flory–Patterson (PFP) theory may be used to analyze and correlate the experimental excess molar volumes of binary mixtures [40, 41]. We have correlated V_m^E of the binary mixtures using PFP theory over the entire range of mole fractions at T = 303.15–323.15 K. The PFP theory considers V_m^E as having three different contributions [42–44]: (i) an interaction contribution V_{int}^E, which is associated with intermolecular specific interactions according to the sign of H_m^E, (ii) a free volume contribution V_{fv}^E, which is associated with the reduced volume-to-reduced temperature ratio with a negative sign, and (iii) an internal pressure contribution,$V_{p^*}^E$, which is associated with breaking of the IL structure upon introduction of molecular organic solvents and changes in the reduced

Fig. 10 Inter molecular hydrogen bonded structure between [Bmim][PF_6] and PY



volume of components and has positive or negative sign. The method of calculation of various parameters of the theory based on relevant equations are given elsewhere [45].

The pure components parameters for the PFP theory are included in Table 6. The Flory contact interaction parameter χ_{12}, the only adjustable parameter needed in the PFP theory, was obtained from the experimental V_m^E values in the absence of the experimental excess molar enthalpies $\left(H_m^E\right)$. The Flory contact interaction parameter χ_{12} was found to be negative for all of the investigated temperatures. The values of three contributions: V_{int}^E, V_{fv}^E and V_p^E to V_m^E (PFP), at equimolar compositions are summarized in Table 7. The first term V_{int}^E is negative, which suggests that strong interactions take place in the binary mixtures. The interactional contributions are negative at all temperatures. The second term V_{fv}^E was found to be negative for the system studied (Table 7) as V_{fv}^E is proportional to $-\left(\tilde{V}_1 - \tilde{V}_2\right)^2$ [41]. The magnitude of negative values for V_{fv}^E depends upon difference between Flory's reduced volumes of the components. Negative values of V_{fv}^E increase in magnitude as the temperature increases, which shows that as the temperature increases, more free volume in [Bmim][PF_6] becomes available to accommodate the smaller PY molecules that resulted in the more negative V_m^E values. For the third term, the characteristic pressure effect $V_{p^*}^E$, the P^* effect which depends on the relative cohesive energy of the expanded and less expanded component, is found to be positive at all investigated temperatures. It is proportional to $\left(\tilde{V}_1 - \tilde{V}_2\right)\left(p_1^* - p_2^*\right)$ and can have both the negative and positive sign depending upon the magnitude of p_i^* and $\tilde{V}_i^*$ of the unlike components [45]. For the system [Bmim][PF_6] + PY, V_{p*}^E is positive which is related to the structure-braking effect of PY on the electrostatic interactions between the ions of [Bmim][PF_6], and so the PY molecules can be placed around the $[Bmim]^+$ and $[PF_6]^-$ ions [41, 45]. In the present system, V_{int}^E and V_{fv}^E are found to be negative while $V_{p^*}^E$ is found to be positive which shows that the interaction and free volume contributions are responsible for the overall strong interactions between solute and solvent molecules. We can conclude that it is possible to explain the volumetric behavior of [Bmim][PF_6] + PY binary mixtures quite successfully by application of the PFP theory.

Table 6 Characteristic and reduced parameters for the pure components, used in PFP theory, at various temperatures

T (K)	$\tilde{V}$	V_1^* (10^{-6} $m^3 \cdot mol^{-1}$)	p_1^* (10^{-6} $J \cdot mol^{-1}$)
[Bmim][PF_6]			
303.15	1.1653	178.71	608.45
308.15	1.1676	178.91	609.14
313.15	1.1699	179.11	609.77
318.15	1.1722	179.31	610.35
323.15	1.1745	179.51	610.82
PY			
303.15	1.1949	64.57	761.40
308.15	1.1982	64.63	762.79
313.15	1.2015	64.70	764.08
318.15	1.2048	64.76	765.04
323.15	1.2081	64.83	765.82

Table 7 PFP interaction parameter, χ_{12}, and calculated values of the three contributions from the PFP theory at equimolar composition for the ([Bmim][PF_6] + PY) system at T = (303.15–323.15) K

T (K)	χ_{12} (10^6 J·m^{-3})	V_m^E(int)	$V_m^E(fv)$ (10^{-6} m^3·mol^{-1})	V_m^E(ip)
303.15	− 61.8168	− 0.6938	− 0.0371	0.1754
308.15	− 63.2611	− 0.7233	− 0.0396	0.1820
313.15	− 64.8821	− 0.7556	− 0.0423	0.1888
318.15	− 66.5222	− 0.7890	− 0.0451	0.1954
323.15	− 68.1638	− 0.8233	− 0.0480	0.2021

4 Conclusions

In this study, measured densities, ultrasonic speeds of sound and refractive indices for binary liquids of [Bmim][PF_6] with PY over the entire composition range at temperatures (303.15, 308.15, 313.15, 318.15 and 323.15) K at atmospheric pressure have been used to compute excess/deviation properties. The observed excess values clearly reflect the dominance of strong attractive forces in IL rich region. The attractive forces are further increased with rise in temperature. The IR spectral studies also support inferences drawn from the excess properties. The more acidic C_2–H of the imidazolium cation plays a major role in the formation of hydrogen a bond with the carbonyl oxygen of PY. It was observed that the cyclic dimer in the PY rich region is responsible for the expansion of volume and contraction in the IL rich region because of hydrogen bond formation between the ionic liquid [Bmim][PF_6] and PY. The PFP theory was able to explain the volumetric behavior of the system quite successfully.

References

1. Greaves, T.L., Drummond, C.J.: Proticionic liquids: evolving structure–property relationships and expanding applications. Chem. Rev. **115**, 11379–11448 (2015)
2. Guo, F., Zhang, S., Wang, J., Teng, B., Zhang, T., Fan, M.: Synthesis and applications of ionic liquids in clean energy and environment: a review. Curr. Org. Chem. **19**, 455–468 (2014)
3. Shamsuri, A.A., Daik, R.: Applications of ionic liquids and their mixtures for preparation of advanced polymer blends and composites: a short review. Rev. Adv. Mat. Sci. **40**, 45–59 (2015)
4. Comminges, C., Barhdadi, R., Laurent, M., Troupel, M.: Determination of viscosity, ionic conductivity, and diffusion coefficients in some binary systems: ionic liquids + molecular solvents. J. Chem. Eng. Data **51**, 680–685 (2006)
5. Zhang, P., Peng, L., Li, W.: Application of ionic liquid [bmim]PF_6 as green plasticizer for poly(L-lactide). e-Polymers **172**, 8 (2008)
6. Lin, J., Teng, Y., Lu, Y., Lu, S., Hao, X., Cheng, D.: Usage of hydrophobic ionic liquid [BMIM][PF_6] for recovery of acid dye from wastewater and sequential application in Tussah silk dyeing clean. Soil Air Water **42**, 799–803 (2014)
7. Flieger, J.: Effect of ionic liquids as mobile-phase additives on chromatographic parameters of neuroleptic drugs in reversed-phase high-performance liquid chromatography. Anal. Lett. **42**(11), 1632–1649 (2009)
8. Zhao, H., Sanjay, M.: Applications of ionic liquids in organic synthesis. Aldrichimica Acta **35**(3), 75–83 (2002)
9. Han, D., Ho Row, K.: Recent applications of ionic liquids in separation technology. Molecules **15**, 2405–2426 (2010)

10. Markus, E., Anita, J.M., Alan, J.R.: Enzymatic catalysis of formation of Z-aspartame in ionic liquid—an alternative to enzymatic catalysis in organic solvents. Biotechnol. Prog. **16**, 1129–1131 (2000)
11. Mehta, S.K., Ram, G., Bhasin, K.K.: Effect of placement of hydroxyl groups in isomeric butanediol on the behaviour of thermophysical and spectroscopic properties of pyrrolidin-2-one. J. Chem. Thermodyn. **37**, 791–801 (2005)
12. Garcia, B., Alcalde, R., Leal, J.M., Matos, J.S.: Solute–solvent interactions in amide–water mixed solvents. J. Phys. Chem. **101**, 7991–7997 (1997)
13. Geng, Y., Wang, T., Yu, D., Peng, C., Liu, H., Hu, Y.: Densities and viscosities of the ionic liquid [C4mim][PF6]–*N*, *N*-dimethylformamide binary mixtures at 293.15 to 318.15 K. Chin. J. Chem. Eng. **16**, 256–262 (2008)
14. Fan, W., Zhou, Q., Sun, J., Zhang, S.: Density, excess molar volume, and viscosity for the methyl methacrylate-1-butyl-3methylimidazolium hexafluorophosphate ionic liquid binary system at atmospheric pressure. J. Chem. Eng. Data **54**, 2307–2311 (2009)
15. Zhu, A., Wang, J., Han, L., Fan, M.: Measurements and correlation of viscosities and conductivities for the mixtures of imidazolium ionic liquids with molecular solutes. Chem. Eng. J. **147**, 27–33 (2009)
16. Taghi Zafarani-Moattar, M., Majdan-Cegincara, R.: Viscosity, density, speed of sound, and refractive index of binary mixtures of organic solvent + ionic liquid, 1-butyl-3-methylimidazolium hexafluorophosphate at 298.15 K. J. Chem. Eng. Data **52**, 2359–2364 (2007)
17. Qiao, Y., Fangyou, Y., Xia, S., Shen, Y., Peisheng, M.: Densities and viscosities of [Bmim][PF_6] and binary dystems [Bmim][PF6]–ethanol, [Bmim][PF_6]–benzene at several temperatures and pressures: determined by the falling-ball method. J. Chem. Eng. Data **56**, 2379–2385 (2011)
18. Srinivasa Krishna, K.T., Raju, K.T.S.S., Gowrisankar, M., Anil, K.N., Munibhadrayya, B.: Volumetric, ultrasonic and spectroscopic studies of molecular interactions in binary mixtures of 1-butyl-3-methylimidazolium hexafluorophosphate with 2-propoxyethanol at temperatures from 298.15 to 323.15. J. Mol. Liquids **216**, 484–495 (2016)
19. Armarego, W.L., Chai, C.L.L.: Purification of Laboratory Chemicals. Butterworth-Heinemann publisher, Oxford (2013)
20. Scholz, E.: Karl Fisher Titration. Springer, Berlin (1984)
21. Costa, A.J., Esperanca, I.M., Marrucho, J.M., Rebelo, L.P.N.: Densities and viscosities of 1-ethyl-3-methylimidazolium *n*-alkyl sulfates. J. Chem. Eng. Data **56**, 3433–3441 (2011)
22. Pereiro, A.B., Legido, J.L., Rodriguez, A.: Physical properties of ionic liquids based on 1-alkyl-3-methylimidazolium cation and hexafluorophosphate as anion and temperature dependence. J. Chem. Thermodyn. **39**, 1168–1175 (2007)
23. Troncoso, J., Cerdeiriña, C.A., Sanmamed, Y.A., Romani, L., Lui Rebelo, L.P.N.: Thermodynamic properties of imidazolium-based ionic liquids: densities, heat capacities, and enthalpies of fusion of [bmim][PF_6] and [bmim][NTf_2]. J. Chem. Eng. Data **51**, 1856–1859 (2006)
24. Reid, R.C., Prausnitz, J.M., Poling, B.E.: The Properties of Gases and Liquids, 4th edn, p. 139. McGraw Hill Inc, New York (1987)
25. Srinivasa Krishnaa, T., Anil, K.N., Chentilnathc, S., Punyaseshadud, D., Munibhadrayya, B.: Densities, ultrasounds, refractive indices, excess and partial molar properties of binary mixtures of imidazolium based ionic liquid with pyrrolidin-2-one at temperatures from 298.15 L to 323.15 K. J. Chem. Eng. (2016). https://doi.org/10.1016/j.jct.2016.05.021
26. García, B., Hoyuelos, F.J., Alcalde, R., Leal, J.M.: Molar excess volumes of binary liquid mixtures: 2-pyrrolidinone with C6–C10 *n*-alkanols. Can. J. Chem. **74**, 121–127 (1996)
27. Reddy, M.S., Md Nayeem, S., Soumini, C., Raju, K.T.S.S., Babu, B.H.: Study of molecular interactions in binary liquid mixtures of [Emim][BF_4] with 2-methoxyethanol using thermo acoustic, volumetric and optical properties. Thermochim. Acta **630**, 37–39 (2016)
28. Reddy, M.S., Raju, K.T.S.S., Rao, A.S., Sharmila, N., Babu, B.H.: Study of thermophysical properties of the binary mixtures of ionic liquid 1-ethyl-3-methylimidazolium ethylsulfate and 2-propoxyethanol from T = (298.15 to 328.15) K at atmospheric pressure. J. Chem. Thermodyn. **101**, 139–149 (2016)
29. Reddy, M.S., Md Nayeem, S., Raju, K.T.S.S., Babu, B.H.: The study of solute–solvent interactions in 1-ethyl-3-methylimidazolium tetrafluoroborate + 2-ethoxyethanol from density, speed of sound, and refractive index measurements. J. Therm. Anal. Calorim. **124**, 959–971 (2016)
30. Ali, A., Nabi, F., Tariq, M.: Volumetric, viscometric, ultrasonic, and refractive index properties of liquid mixtures of benzene with industrially important monomers at different temperatures. Int. J. Thermophys. **30**, 464–474 (2009)
31. Reddy, M.S., Raju, K.T.S.S., Md Nayeem, S., Khan, I., Krishna, K.B.M., Babu, B.H.: Excess thermodynamic properties for binary mixtures of ionic liquid 1-ethyl-3-methylimidazolium ethyl sulfate and 2-methoxyethanol from T = (298.15 to 328.15) K at atmospheric pressure. J. Solution Chem. **45**, 675–701 (2016)

32. Roth, C., Appelhagen, A., Jobst, N., Ludwig, R.: Microheterogeneities in ionic-liquid–methanol solutions studied by FTIR spectroscopy, DFT calculations and molecular dynamics simulations. Chem. Phys. Chem. **13**, 1708–1717 (2012)
33. Aggarwal, A., Lancaster, N.L., Sethi, A.R., Welton, T.: The role of hydrogen bonding in controlling the selectivity of Diels–Alder reactions in room-temperature ionic liquids. Green Chem. **4**, 517–520 (2002)
34. Znamenskiy, V., Kobrak, M.N.: Molecular dynamics study of polarity in room-temperature ionic liquids. J. Phys. Chem. B **108**, 1072–1079 (2004)
35. Dhumal, N.R., Kim, H.J., Kiefer, J.:Electronic structure and normal vibrations of the 1-ethyl-3-methylimidazolium ethyl sulfate ion pair. J. Phys. Chem. A **115**, 3551–3558 (2011)
36. Lassegues, J.C., Grondin, J., Cavagnat, D., Johansson, P.: New interpretation of the CH stretching vibrations in imidazolium-based ionic liquids. J. Phys. Chem. A **113**, 6419–6421 (2009)
37. Lassegues, J.C., Grondin, J., Cavagnat, D., Johansson, P.: Reply to the comment on 'New interpretation of the CH stretching vibrations in imidazolium-based ionic liquids'. J. Phys. Chem. A **114**, 687–688 (2009)
38. Grondin, J., Lassegues, J.C., Cavagnat, D., Buffeteau, T., Johansson, P., Holomb, R.: Revisited vibrational assignments of imidazolium-based ionic liquids. J. Raman Spectrosc. **42**, 733–743 (2011)
39. Maria, J.D.V., Rafael, A., Santiago, A.: Pyrrolidone derivatives in water solution: an experimental and theoretical perspective. Ind. Eng. Chem. Res. **48**, 1036–1050 (2009)
40. Vercher, E., Llopis, F.J., Gonzalez-Alfaro, M.V., Andreu, A.M.: Density, speed of sound, and refractive index of 1-ethyl-3-methylimidazolium trifluoromethanesulfonate with acetone, methyl acetate, and ethyl acetate at temperatures from (278.15 to 328.15) K. J. Chem. Eng. Data **55**, 1377–1388 (2010)
41. Patterson, D., Delmas, G.: Corresponding states theories and liquid models. Discuss. Faraday Soc. **49**, 98–105 (1970)
42. Torres, R.B., Ortolan, M.I., Volpe, P.L.O.: Volumetric properties of binary mixtures of ethers and acetonitrile: experimental results and application of the Prigogine–Flory–Patterson theory. J. Chem. Thermodyn. **40**, 442–459 (2008)
43. Flory, P.J.: Statistical thermodynamics of liquid mixtures. J. Am. Chem. Soc. **87**, 1833–1838 (1965)
44. Abe, A., Flory, P.J.: The thermodynamic properties of mixtures of small, nonpolar molecules. J. Am. Chem. Soc. **87**, 1838–1846 (1965)
45. Vaid, Z.S., More, U.U., Oswal, S.B., Malek, N.I.: Experimental and theoretical excess molar properties of imidazolium based ionic liquids with isomers of butanol. Thermochim. Acta **634**, 38–47 (2016)

S.R.R.& C.V.R. Government Degree College (A), Vijayawada.

MATLAB Training Programme
at ANDHRA LOYOLA ENGINEERING COLLEGE,
Vijayawada

Vijayawada,

17/11/2017.

To

The Principal
S.R.R & C.V.R Govt Degree College (A)
Vijayawada.

Sir,

Sub: Permission to send faculty and **B.Sc and M.Sc Mathematics students** to attend **MAT LAB training programme at Andhra Loyola college by ECE Department.**

I bring to kind notice the faculty members along with B.Sc and M.Sc Mathematics students are attending the **MAT LAB training programme at Andhra Loyola college by ECE Department** from 17/11/2017 to 18/11/2017 that is two days programme, hence I request you kindly to permit them to the above programme and treat the faculty members as on duty.

Thanking you Sir.

Yours faithfully

K.V. Naga Lakshmi

In charge of the Mathematics Department.

PRINCIPAL
SRR & CVR GOVT. DEGREE COLLEGE
(Autonomous)
Mechavaram, VIJAYAWADA-520 004.


ANDHRA LOYOLA INSTITUTE OF ENGINEERING AND
SRR & CVR GOVT. DEGREE COLLEGE
[NAAC accredited 'B' Grade College]
Welcome
to
Department of Mathematics & Statistics

MATLAB is a programming platform designed specifically for engineers and scientists to analyze and design systems and products that transform our world. The heart of MATLAB is the MATLAB language, a matrix-based language allowing the most natural expression of computational mathematics.

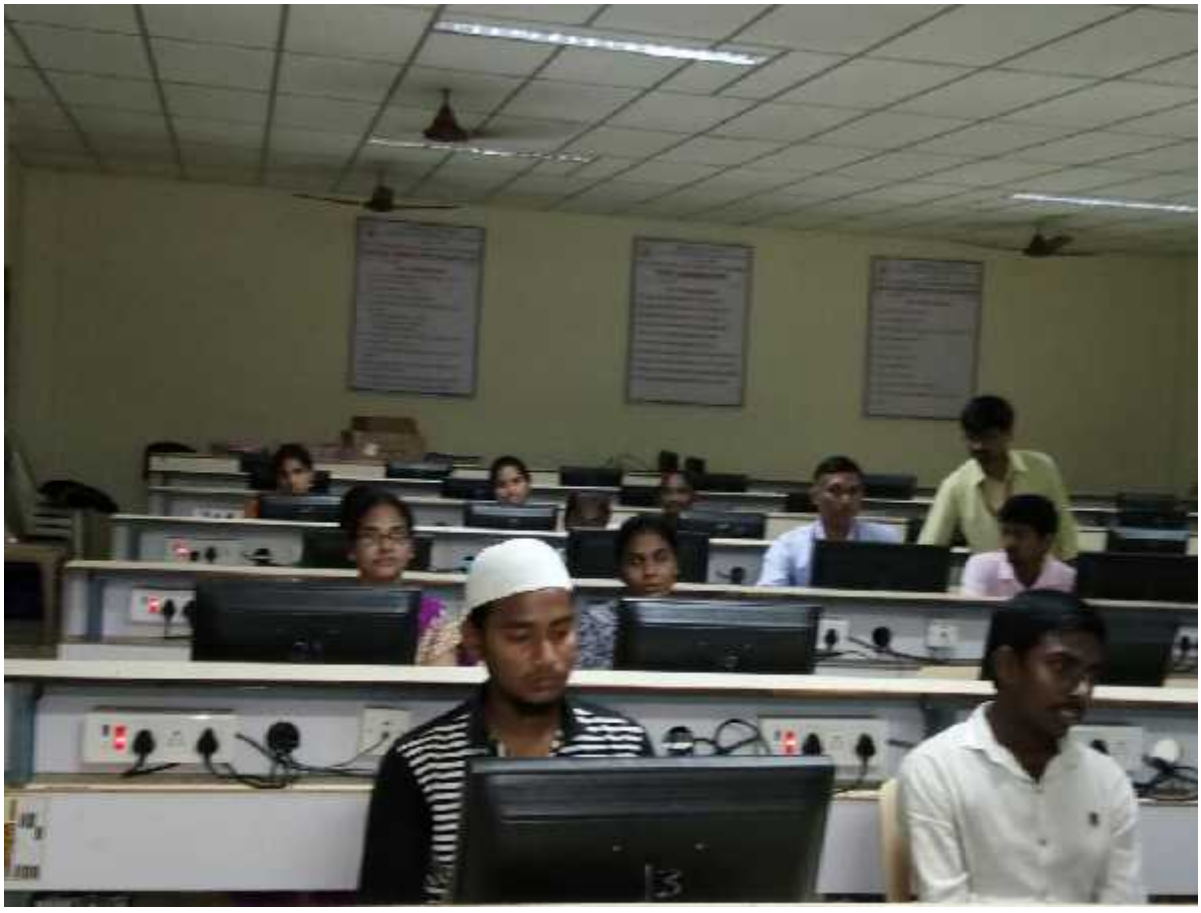
MATLAB lets you take your ideas from research to production by deploying to enterprise applications and embedded devices, as well as integrating with Simulink and Model-Based Design.

Millions of engineers and scientists worldwide use MATLAB for a range of applications, in industry and academia, including deep learning and machine learning, signal processing and communications, image and video processing, control systems, test and measurement, computational finance, and computational biology.

SYLLABUS: Computational Mathematics Laboratory. Numerical algorithms for Eigenvalue problems. Laplace and Fourier transforms. Linear, integer, and non-linear optimization problems. Necessary theoretical background of above subjects, and using the following software: Mathematica, MATLAB, MathCAD, LINDO, etc, following practicals are to be done in the Computer Laboratory.

NUMBER OF PARTICIPANTS :28

FACULTY MEMBERS :7






LOYOLA INSTITUTE OF ENGINEERING AND TECHNOLO



ANDHRA LOYOLA INSTITUTE OF ENGINEERING & TECHNOLOGY

ALC Campus, VIJAYAWADA - 520 008. An ISO 9001:2008 Certified Institute

(Approved by AICTE, Affiliated to JNTUK, Kakinada)

Certificate of Training

This is to certify that

Mr./Ms. B. RATNA KUMARI

has successfully completed a training course in

INTRODUCTION TO MATLAB

from 17-11-2017 to 18-11-2017

Organized by

Department of Electronics & Communication Engineering

in association with

Dr. APJ ABDUL KALAM RESEARCH FORUM

Trainer

Head of the Department

Principal / Director

Out Comes:

1. Students got awareness on Matrix operations and Eigenvalue problems using MAT LAB.
2. Students got awareness on Laplace and Fourier transforms using MAT LAB.
3. Students got awareness on Two and three dimensional graphics using MAT LAB.
4. Students got awareness on Linear, integer, and quadratic programming using MAT LAB.

MAT LAB Training Programme

Date: 17-11-2017

With the permission of the Principal, B.Sc. & M.Sc. Mathematics Students along with the Faculty of Mathematics attended **MAT LAB Training Programme** at **Andhra Layola Engineering College,** Vijayawada organized by the Department of E.C.E. HOD, Ramakrishna on 17-11-2017 and 18-11-2017.

Signature of the Faculty members attended.

1. K.V. Naga Lakshmi
2. K. Shanmukha
3. CHOACARSA
4. K. V RAMA RAO
5. Sk. Parveen
6. D. Swarna Kumari
7. N. Srinivas

Principal

SNO	Name of the student	Section	Signature
1.	P. Shameem	II B.Sc [MPCS]	P. Shayeem
2.	MD. Mehaboojunnisa	II BSc [MPCS]	MD. Mehaboojunnisa
3.	P. Surakha	II BSc [MPCS]	P. Surakha.
4.	D. Neeraja	II B.S.c (MPCS)	D. Neeraja.
5.	N. Sai Maneesha	II BSc (MPCS)	N. Sai Maneesha.
6	P. RAMBABU	II B.Sc [M.P.C.S]	P. Rambabu
7	J Bhaskar	II Bsc [M.P.C.S]	J. Bhaska.
8.	P. Hari krishna	II BSc [MPCS]	P. Harikrishna.
9.	V. SURESH	II B.Sc [MPCS]	V. Suresh
10	R. Manikanta	II BSc (M.P.C.S)	R. Manikanta
11.	J. RAVINDRA	II BSc (MPCS)	J Ravindra.
12.	L. Saikumar	II BSc (M.P.C.S)	L. Saikumar
13.	K. Gopiraju	II nd B.S.c (MPCS)	K. Gopiraju

(Next page)

SNO	Name of the Student	Section	signature
14.	R. Renuka	III rd BSC (MSCS)	R. Renuka
15	ch. v. v. Nirilakshmi	III rd BSC (MSCS)	ch. v. v. Nirilakshmi
16	K. padmavathi	III rd BSc (MSCS)	K. Padmavathi
17	L. suma Durga	B.Sc (MSCS)	L. Suma Durga
18	M. Aruna	B.Sc (MSCS)	M. Aruna
19	P. prakash	B.Sc (MSCS)	P. Prakash
20	P. Swetha	B.Sc (MSCS)	P. Swetha
21	S. Bhavani	B.Sc (MSCS)	S. Bhavani
22	Ch. vijaya	B.Sc (MSCS)	ch. Vijaya
23	Ch. Mani Kanta	B.Sc (MSCS)	Ch. Manikanta
24	A. Mohan	B.Sc (MSCS)	A. Mohan
25	G. Surendra	B.Sc (MSCS)	G. Surendra
26	Ch. Sailaja	B.Sc (MSCS)	Ch. Sailaja
27	B. Srinu	B.Sc (MSCS)	B. Srinu
28	A. Rama Krishna	B.Sc (MSCS)	A. Ramakrishna

SRR & CVT GOVERNMENT DEGREE COLLEGE (A), VIJAYAWADA

DISTRICT RESOURCE CENTER, KRISHNA

WITH THE COLLABORATION OF SAMACHARA HAKKU PRACHARA IKYA VEDIKA, KRISHNA DISTRICT

CONDUCTED

WORKSHOP ON RTI ACT 2005 ON 12 OCTOBER 2017

SRR & CVR Government Degree College, Vijayawada celebrated 12 years of the Right to Information Act 2005 on 12 October 2017. DRDA Project Director Sri Chandrasekhar Raju, attended as chief guest of the function. Samachara Hakku ikya Vedika President Yerramsetti JaganMohan Rao and Secretary P.Satyanarayana also attended the function as speakers. They discussed the importance of RTI Act 2005. An applicant who desires to obtain any information under the RTI Act can make a request through this Web Portal to the Ministries/Departments of Government of India. On clicking a "Submit Request", the applicant has to fill in the required details on the page that will appear.



The chief guest of the meeting discussed the RTI importance. This right includes inspection of work, documents and records; taking notes, extracts or certified copies of documents or records; and taking certified samples of material held by the public authority or held under the control of the public authority.



If the applicant does not receive the response for the RTI, within 30 days (or 35 days in case the application was transferred to another department or was submitted to APIO) of submitting the application, then the applicant can file for an appeal. You may only ask for specific information under RTI Act, 2005 rather than questioning the action of public authority. ' The RTI act does not state that queries must not be answered, nor does it stipulate that prefixes such as 'why, what, when and whether' cannot be used.



RTI applications may now be limited to 250 words and to only one topic if the rules for processing of such applications suggested by the department of personnel may find their way through. “Section 8 (of RTI Act) has categorically mentioned that personal information cannot be supplied … which has no relation to any public activity,” said the court. The court said that the personal information of the candidates has no relationship to any public activity or interest.



This law empowers people to ask for information about central, state governments including non-governmental organizations which are substantially funded by the government. The law gives citizens of India the tools to fight against corruption.





Abstract: Transparency and accountability in administration is the sine qua non of participatory democracy. Information is the oxygen that any citizen needs to live in the social structure of the society and maintain its democratic balance. Right to Information (RTI) in India was developed through Judicial pronouncements thereby distinguishing itself as a Fundamental Right under Article 19 (1) (a). After a gradual period of time, realizing the importance of this right to know, this right was established in 2005 as a full-fledged statute in the name of "The Right to Information Act, 2005". This RTI Act became a pioneer tool to the citizens of India for promoting, protecting and defending their Right to know. Good Governance may be termed as a synonym for the work carried out by a Government where the maximum benefit is given to the maximum number of people. India being a huge democracy needs participation from every front to implement the objective of good governance. The scenario often turns out that laws of public interest and benefit are mostly used by the elite section of the society. However, this piece of legislation stands as an exception as it has reached its extent to the remote corner of the country. The paper will study the implementation and extent of this prominent law to the grass root level of India through the participation and activeness of common people who thrive to promote good governance through their extraordinary works. In addition, the paper also highlights the need to amend the Act so as to protect the activists who often risk their lives for public interest.

Keywords: Right to Information, Participatory Democracy, grass root level, Fundamental Right Implementation, Good governance, RTI Activists.

"Where a society has chosen to accept democracy as its creedal faith, it is elementary that the citizens ought to know what their government is doing." -Justice P N Bhagwati

RTI is inherent in democratic functioning and a precondition to good governance and realization of all other human rights. The main objectives of the law on RTI are:

a. To operationalise the fundamental right to information;

b. To set up systems and mechanisms that facilitate people's easy access to information; to promote transparency, and

c. Accountability in governance; to minimize corruption and inefficiency in public offices and to ensure people's participation in governance and decision making.

Important Features of the Right to Information Act, 2005:

- **Every citizen possesses the right to information.**
- **The term information includes any mode of information in any form of record, document, email, circular, press release, contract sample or electronic data etc.**
- **Right to information covers inspection of work, document, record and its certified copy and information in any other electronic mode.**

- **Applicant can obtain information within 30 days from the date of request in a normal case. Information can be obtained within 48 hours from time of filing the request if it is a matter of life or liberty of a person.**
- **Every public authority is under obligation to provide information on written request or request by electronic means.**
- **Certain information is prohibited for security reasons. Penalty for not providing information is Rs. 250/ per day but the total amount of penalty should not exceed Rs. 25,000.**
- **Central Information Commission and State Information Commission are to be constituted by the Central Government and the respective State Governments.**
- **No Court can entertain any suit, application or other proceedings in respect of any order made under the Act.**



The End